Advanced Topics in Science and Technology in China

Hao Zhou et al. *Editors*

Ultra-high Voltage AC/DC Power Transmission

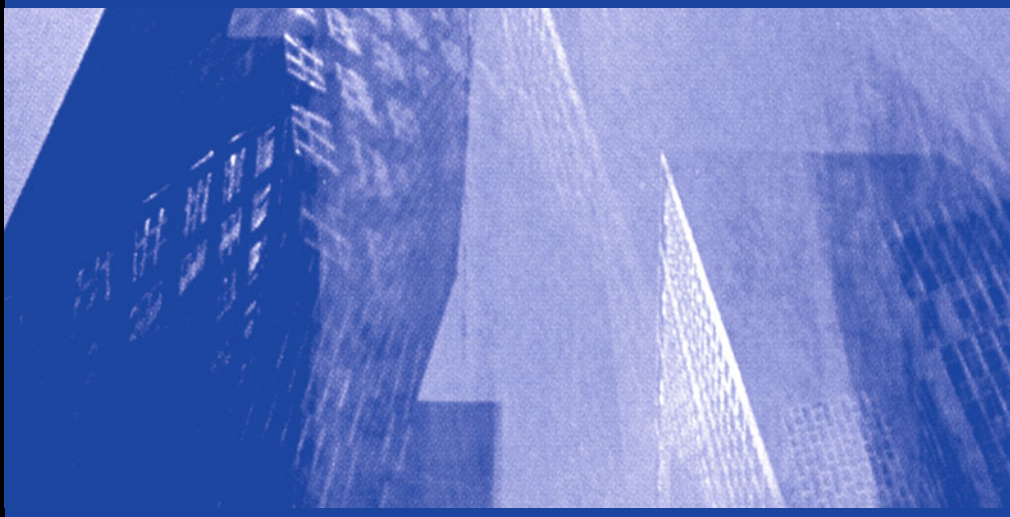

ZHEJIANG UNIVERSITY PRESS
浙江大学出版社

Springer

Advanced Topics in Science and Technology in China

www.FreeEngineeringBooksPdf.com

Zhejiang University is one of the leading universities in China. In Advanced Topics in Science and Technology in China, Zhejiang University Press and Springer jointly publish monographs by Chinese scholars and professors, as well as invited authors and editors from abroad who are outstanding experts and scholars in their fields. This series will be of interest to researchers, lecturers, and graduate students alike. Advanced Topics in Science and Technology in China aims to present the latest and most cutting-edge theories, techniques, and methodologies in various research areas in China. It covers all disciplines in the fields of natural science and technology, including but not limited to, computer science, materials science, life sciences, engineering, environmental sciences, mathematics, and physics.

More information about this series at http://www.springer.com/series/7887

www.FreeEngineeringBooksPdf.com

Hao Zhou · Wenqian Qiu
Ke Sun · Jiamiao Chen · Xu Deng
Feng Qian · Dongju Wang
Bincai Zhao · Jiyuan Li · Sha Li
Yuting Qiu · Jingzhe Yu
Editors

Ultra-high Voltage AC/DC Power Transmission

ZHEJIANG UNIVERSITY PRESS
浙江大学出版社

Springer

www.FreeEngineeringBooksPdf.com

Editors

Hao Zhou
College of Electrical Engineering
Zhejiang University
Hangzhou
China

Wenqian Qiu
China Energy Engineering Group
Zhejiang Electric Power Design Institute Co., Ltd.
Hangzhou
China

Ke Sun
Zhejiang Electric Power Company
Hangzhou
China

Jiamiao Chen
China Energy Engineering Group
Zhejiang Electric Power Design Institute Co., Ltd.
Hangzhou
China

Xu Deng
Guangzhou Municipal Commission of Commerce
Guangzhou
China

Feng Qian
China Energy Engineering Group
Zhejiang Electric Power Design Institute Co., Ltd.
Hangzhou
China

Dongju Wang
College of Electrical Engineering
Zhejiang University
Hangzhou
China

Bincai Zhao
State Grid Weifang Power Supply Company
Weifang
China

Jiyuan Li
College of Electrical Engineering
Zhejiang University
Hangzhou
China

Sha Li
College of Electrical Engineering
Zhejiang University
Hangzhou
China

Yuting Qiu
College of Electrical Engineering
Zhejiang University
Hangzhou
China

Jingzhe Yu
College of Electrical Engineering
Zhejiang University
Hangzhou
China

ISSN 1995-6819 ISSN 1995-6827 (electronic)
Advanced Topics in Science and Technology in China
ISBN 978-3-662-54573-7 ISBN 978-3-662-54575-1 (eBook)
https://doi.org/10.1007/978-3-662-54575-1

Jointly published with Zhejiang University Press, Beijing, China

The print edition is not for sale in China Mainland. Customers from China Mainland please order the print book from: Zhejiang University Press.

Library of Congress Control Number: 2017935388

© Zhejiang University Press, Hangzhou and Springer-Verlag GmbH Germany 2018
This work is subject to copyright. All rights are reserved by the Publishers, whether the whole or part of the material is concerned, specifically the rights of translation, reprinting, reuse of illustrations, recitation, broadcasting, reproduction on microfilms or in any other physical way, and transmission or information storage and retrieval, electronic adaptation, computer software, or by similar or dissimilar methodology now known or hereafter developed.
The use of general descriptive names, registered names, trademarks, service marks, etc. in this publication does not imply, even in the absence of a specific statement, that such names are exempt from the relevant protective laws and regulations and therefore free for general use.
The publishers, the authors and the editors are safe to assume that the advice and information in this book are believed to be true and accurate at the date of publication. Neither the publishers nor the authors or the editors give a warranty, express or implied, with respect to the material contained herein or for any errors or omissions that may have been made. The publishers remains neutral with regard to jurisdictional claims in published maps and institutional affiliations.

Printed on acid-free paper

This Springer imprint is published by Springer Nature
The registered company is Springer-Verlag GmbH Germany
The registered company address is: Heidelberger Platz 3, 14197 Berlin, Germany

www.FreeEngineeringBooksPdf.com

Preface

Viewed from the distribution of the energy resources throughout China, though the total reserves are abundant, the resource distribution and productivity distribution are rather unbalanced. The coal resource is mostly located in the North and Northwest China, the hydropower resource is mainly located in the Southwest China, the onshore wind energy and solar energy resources are mainly located in the Northwest China, while the energy demands are mainly concentrated in the Central China and China's east coastal areas. The distance between the energy base and the load center is up to 1000 km. The energy resources used for power generation are mainly coal and water, and the energy resources and productivity development are reversely distributed, which is the basic national condition of China. Since the reform and opening-up, the electricity demand of China has been continuously and rapidly increased, and the scale and capacity of the newly built power sources have been increased. Subject to the energy transmission capacity and environmental protection requirements, China will inevitably develop the long-distance and large-capacity power transmission technology to improve the development and utilization rate of the resources, alleviate the pressure in the energy transmission, and meet the requirements of the environmental protection.

The UHV power transmission technology is the power transmission technology with the highest voltage level in the world presently, and the most prominent characteristic thereof is the large-capacity, long-distance, and low-loss power transmission. The transmission capacity of the 1000 kV UHVAC system is about 4–5 times that of the 500 kV extra-high voltage (EHV) AC system. The development of the UHVAC and UHVDC power transmission can effectively solve the issue of large-scale power transmission. In addition, compared with the EHV power transmission line, the UHV line occupies less land resource and achieves quite prominent economic and social benefits under the same power transmission capacity. The building of the national-level power grid in which the UHV grid acts as the backbone and the grids of all levels develop in a coordinated manner, meeting the basic national condition of China that the energy resources and economic development are reversely distributed and according with the China's overall arrangement for energy-saving and emission reduction, is the effective way to

www.FreeEngineeringBooksPdf.com

realize the coordinated development of grids and power sources and the urgent demand for the construction of the resource-saving and environment-friendly society.

In the world, a few countries such as the former Soviet Union, Japan, America, Italy, and Canada have ever conducted tests and researches on the UHVAC power transmission technology. During 1981–1994, the former Soviet Union successfully built a total of 2364 km 1150 kV power transmission lines, among which, the Ekibastuz–Kokshetau line (495 km in length) put into operation at 1150 kV in 1985 was the first UHV power transmission line put into actual operation in the world. Japan built the 1000 kV UHVAC double-circuit power transmission line in the 1990s , which, however, was under the 500 kV reduced voltage operation all the time. The overseas DC power transmission project with the highest voltage level that has been built and put into operation is the Itapúa Power Transmission Project in Brazil, which includes double-circuit DC line with voltage level of ±600 kV and rated transmission power of 3600 MW. The Soviet Union ever planned to build a ±750 kV UHVDC power transmission line project from Ekibastuz to Tambovskaya Oblast, the first engineering practice of the UHVDC power transmission technology in the world, and commenced the construction in 1980, but finally ceased the construction due to the political and economic reasons, after the completion of the construction of 1090 km-long line.

The research on the UHV power transmission was started relatively late in China. Since 1986, the research on the UHV power transmission has been successively included in the key science and technology research programs during China's "Seventh Five-Year Plan," "Eighth Five-Year Plan," and "Tenth Five-Year Plan". During 1990–1995, the Significant Project Office of the State Council organized the "Demonstration of Long-distance Transmission Modes and Voltage Levels"; and during 1990–1999, the State Scientific and Technological Commission organized the monographic researches such as the "Preliminary Demonstration of UHV Power Transmission" and "Feasibility of Application of AC Megavolt Ultra-high Voltage for Power Transmission". State Grid Corporation of China put forward for the strategic concept of "establishment of the UHV-based robust state grid" in 2004 the first time to focus on the construction of a network system in which the UHV grid acts as the backbone and the grids of all levels develop in a coordinated manner. China Southern Power Grid Co., Ltd. also began to study the feasibility in the construction of ±800 kV DC power transmission project in 2003. In 2006, the National Development and Reform Commission formally approved the 1000 kV UHVAC Demonstration Project from Southeast Shanxi through Nanyang to Jingmen connecting the North China grid and Central China grid. In 2007 and 2010, China respectively completed and put into operation the 1000 kV Southeast Shanxi–Nanyang–Jingmen UHVAC Power Transmission Demonstration Project and ±800 kV Yunnan–Guangdong and Xiangjiaba–Shanghai UHVDC Power Transmission Projects. Since then, the UHV power transmission has accomplished a rapid development in China. Up to August 2017, six 1000 kV UHVAC power transmission lines and nine ±800 kV UHVDC power transmission lines have been built and put into operation. There is still another 1000

www.FreeEngineeringBooksPdf.com

kV UHVAC power transmission line and the other four ±800 kV UHVDC power transmission lines will be put into operation at the end of 2017. Moreover, one ±1100 kV UHVDC power transmission line is being built and will be put into operation in 2018..

The UHV power transmission is the engineering technology leading the world's power transmission technology. Its rapid and successful development in China has fully proven the tremendous achievement accomplished by China in the technological aspect of the electric power system. Meanwhile, the complexity of the UHV power transmission technology and the urgency of its development in China require that the professional personnel engaging in the work related to the electric power system have a deeper understanding and mastery of it. Based on the significant research results obtained by Zhejiang University High Voltage Laboratory in the field of UHVAC and UHVDC power transmission in the last decade and the abundant practical experience accumulated by Zhejiang Electric Power Design Institute in the field of UHV power transmission engineering over the years, and in combination with the relevant research results in the aspect of UHVAC and UHVDC power transmission technology and the actual operation experience in China and abroad, this book systematically introduces the key technical issues existing in the UHVAC and UHVDC power transmission.

This book consists of four sections containing a total of 28 chapters, and focuses on the study of the overvoltage, insulation coordination and design of the UHV power grid. Section I, consisting of three chapters provides an overview of the development of the UHV power transmission and the system characteristics and economy thereof. Section II, consisting of ten chapters discusses the UHVAC system. Section III, consisting of ten chapters discusses the UHVDC system. Section IV, consisting of four chapters discusses the design of the UHVAC substation and UHVDC converter station as well as UHVAC and DC power transmission lines. Hao Zhou is responsible for the final compilation and editing of the whole book, and Wenqian Qiu, Xu Deng, Jiyuan Li and Jingzhe Yu act as the chief reviewers.

We sincerely hope that this book can better help the readers understand the UHVAC and UHVDC power transmission technology and can provide reference for the research work carried out by the technicians engaging in the work related to the electric power system. This book is jointly edited by the relevant researchers from Zhejiang University, Zhejiang Electric Power Design Institute, State Grid Zhejiang Electric Power Company, China Electric Power Research Institute, China Southern Power Grid Corporation, East China Grid Company Limited, Southwest Electric Power Design Institute, and North China Electric Power University. The editing of this book has received the guidance and help from numerous experts. Gratitude is hereby expressed to Academician Han Zhenxiang, Academician Chen Weijiang, Professor Zhao Zhida, Professorate Senior Engineer Zhou Peihong, Professorate Senior Engineer Zhang Cuixia, Professorate Senior Engineer Li Yongwei, Professorate Senior Engineer Gu Dingxie, Professorate Senior Engineer Nie Dingzhen, Professorate Senior Engineer Tian Jie, Professor Kang Chongqing, Professor Cui Xiang, Professor Li Chengrong, Professor Wen Fushuan, Professor

www.FreeEngineeringBooksPdf.com

Xu Zheng, Professorate Senior Engineer Su Zhiyi, Professorate Senior Engineer Wu Xiong, Professorate Senior Engineer Wan Baoquan, Professorate Senior Engineer Sun Zhaoying, Professorate Senior Engineer Chen Jiahong, Professorate Senior Engineer Dai Min, Professorate Senior Engineer Li Zhibing, Professorate Senior Engineer Wang Xinbao, Senior Engineer Huang Ying, Senior Engineer Shen Haibin, etc., for their support and help.

The editing of this book had been in progress for nearly 8 years and agglomerates the research results of the authors. Nevertheless, due to the authors' limited theoretical level and practical experience, inappropriateness and errors are unavoidable. Any comment will be highly appreciated.

Hangzhou, China Hao Zhou
August 2017

www.FreeEngineeringBooksPdf.com

Contents

Part I Overview

1 Development of UHV Power Transmission 3
Ke Sun, Dongju Wang, Sha Li and Haifeng Qiu
1.1 UHV Power Transmission 4
1.1.1 Development of Power Transmission Voltage Level 4
1.1.2 Voltage Level Sequence in Power Grid 6
1.1.3 Selection of UHV Transmission Voltage Levels 11
1.2 Development of UHV Power Transmission Technology 16
1.2.1 The Former Soviet Union (Russia) 16
1.2.2 Japan 17
1.2.3 United States 19
1.2.4 Canada 20
1.2.5 Italy 20
References 21

2 Development of UHV Power Transmission in China 23
Ke Sun, Shichao Yuan and Yuting Qiu
2.1 Necessity in the Development of UHV Power Transmission in China 24
2.1.1 Objectively Required by the Sustained and Rapid Growth in Electricity Demands 24
2.1.2 Objectively Required by the Long-Distance and Large-Capacity Power Transmission 24
2.1.3 Objectively Required by the Basic Law of Power Grid Development 26
2.1.4 Required to Ensure Safe and Reliable Energy Transmission 26
2.2 Development Process of UHV Power Transmission in China 27

www.FreeEngineeringBooksPdf.com

2.2.1 Preliminary Study of UHV 27
2.2.2 Construction of UHV Test Base 28
2.2.3 China's UHV Transmission Projects 31
References 37

3 Analysis on System Characteristics and Economy of UHV Power Transmission 39
Guang Chen, Hao Zhou, Jiyuan Li and Jingzhe Yu
3.1 System Characteristics of UHVAC Power Transmission 40
3.1.1 Reliability and Stability 40
3.1.2 Transmission Characteristics and Transmission Capacity 41
3.2 System Characteristics of UHVDC Power Transmission 48
3.2.1 Reliability and Stability 48
3.2.2 Transmission Characteristics and Transmission Capacity 51
3.3 Analysis on Economy of UHV Power Transmission 52
3.3.1 Comparison of Economy for UHVAC/EHVAC Power Transmission 52
3.3.2 Comparison of Economy for UHVDC/EHVDC Power Transmission 55
3.4 Applicable Occasions of UHVAC/UHVDC Power Transmissions 57
3.4.1 Technical Characteristics of UHVAC/UHVDC Power Transmissions 57
3.4.2 Technical Advantages of UHV Power Transmission 57
3.4.3 Interconnection of UHV Power Grids 58
3.4.4 Applicable Occasions of UHVAC/UHVDC Power Transmissions 60
References 65

Part II Alternating Current

4 Power Frequency Overvoltage of UHV Power Transmission Lines 69
Hao Zhou, Qiang Yi, Sha Li and Jingzhe Yu
4.1 Mechanisms of Power Frequency Overvoltage 70
4.1.1 No-Load Long-Line Capacitance Effect 70
4.1.2 Asymmetrical Short-Circuit Fault of the Line 73
4.1.3 Power Frequency Overvoltage due to Three-Phase Load Shedding 74
4.2 Characteristics of UHV Power Frequency Overvoltage 77
4.3 Categories of UHV Power Frequency Overvoltage 78

www.FreeEngineeringBooksPdf.com

4.3.1 Classification of UHV Power Frequency Overvoltage . . . 78
4.3.2 Systematic Comparison of Various Power Frequency Overvoltage . . . 82
4.4 Requirements on Restriction of UHV Power Frequency Overvoltage . . . 92
4.5 Influence Factors of UHV Power Frequency Overvoltage . . . 93
4.5.1 Line Length . . . 93
4.5.2 Equivalent Impedance of Power Supply . . . 94
4.5.3 Location of the Ground Fault Point . . . 97
4.5.4 Transmission Power . . . 102
4.5.5 Tower Structures of the Line . . . 103
4.6 Restrictive Measures for UHV Power Frequency Overvoltage . . . 104
4.6.1 Fixed High-Voltage Shunt Reactor . . . 104
4.6.2 Controllable High-Voltage Shunt Reactor . . . 110
4.6.3 Relay Protection Restriction Scheme . . . 118
4.6.4 Selection of Restrictive Measures . . . 120
4.7 Determination of the Upper and Lower Limits of Compensation Degree of High-Voltage Shunt Reactor . . . 121
4.7.1 Determination of the Upper Limit of Compensation Degree of High-Voltage Shunt Reactor . . . 122
4.7.2 Determination of the Lower Limit of Compensation Degree of High-Voltage Shunt Reactor . . . 149
References . . . 162

5 Secondary Arc Current of UHVAC System . . . 163
Qiang Yi, Hao Zhou and Sha Li
5.1 Generation Mechanism of Secondary Arc Current . . . 164
5.2 Measures to Extinguish the Secondary Arc . . . 165
5.2.1 Connection of Small Reactance at the Shunt Reactor's Neutral Point for Compensation . . . 165
5.2.2 Extinguish of the Secondary Arc by Adding HSGS . . . 181
5.2.3 Comparison and Discussion on the Two Methods to Restrict the Secondary Arc Current . . . 185
5.3 Simulation of the Secondary Arc Current and the Recovery Voltage . . . 188
5.3.1 Modeling . . . 188
5.3.2 Analysis of Effect on Inhibiting the Secondary Arc by Connecting Small Reactance at the Neutral Point of Shunt Reactors . . . 188
5.3.3 Analysis of the Effect of HSGS on the Inhibition of Secondary Arc . . . 192
References . . . 196

www.FreeEngineeringBooksPdf.com

6 Switching Overvoltage of UHVAC Systems 199
Rongrong Ji, Hao Zhou and Xiujuan Chen
6.1 Switching Overvoltage Classification and Limiting Methods of UHVAC Systems 200
6.1.1 Switching Overvoltage Classification of UHVAC Systems 200
6.1.2 Common Methods for Limiting Switching Overvoltage in the UHVAC System 203
6.1.3 New Methods for Limiting Switching Overvoltage in the UHVAC System 207
6.2 Single-Phase Ground Fault Overvoltage 209
6.2.1 Mechanism for Generation 209
6.2.2 Modeling and Simulation 211
6.2.3 Analysis of Influence Factors 213
6.2.4 Limitation Measures 224
6.3 Closing Overvoltage 239
6.3.1 Mechanism for Generation 239
6.3.2 Modeling and Simulation 244
6.3.3 Analysis of Influence Factors 248
6.3.4 Limitation Measures 262
6.3.5 Research on Applicability of Closing Resistors for EHV and UHVAC Transmission Line Circuit Breakers 262
6.4 Opening Overvoltage 277
6.4.1 Load Shedding Overvoltage 278
6.4.2 Fault Clearing Overvoltage 285
6.5 Influence on the Electromagnetic Transient Characteristics by Series Compensation Device 293
6.5.1 Composition of Series Compensation Device 293
6.5.2 Influence on the Closing Switching Overvoltage by Series Compensation Device 294
6.5.3 Influence on Power Frequency Overvoltage by Series Compensation Device 294
6.5.4 Influence on Secondary Arc Current by Series Compensation Device 295
6.5.5 Linkage Between Series Compensation Device and Circuit Breaker 296
References 296

7 Very Fast Transient Overvoltage of UHVAC System 299
Yang Li, Guoming Ma and Hao Zhou
7.1 Generation Mechanism and Characteristics of VFTO 300
7.2 Harm of VFTO 303
7.2.1 Harm of VFTO to GIS Main Insulation 304

www.FreeEngineeringBooksPdf.com

7.2.2 Influence of VFTO on Power Transformer 304
7.2.3 Influence of VFTO on the Secondary Equipment 307
7.2.4 Cumulative Effect of VFTO. 307
7.3 VFTO in 1000 kV GIS Substation Under Different Operation Conditions 307
7.3.1 VFTO Generated Due to Operation with Main Transformer 309
7.3.2 VFTO Generated Due to Operation with Outgoing Line 309
7.3.3 VFTO Generated Due to Operation with Busbar 310
7.4 Influence Factors of VFTO 311
7.4.1 Influence of the Residual Voltage at Load Side on the Amplitude of VFTO 312
7.4.2 Influence of the Capacitance at Inlet of Transformer on VFTO 312
7.4.3 Influence of Arc Resistance on the Amplitude of VFTO 313
7.4.4 Influence of Zinc Oxide Arrester on VFTO 314
7.5 Comparison of VFTO in 500 and 1000 kV GIS Substations . . 314
7.5.1 Switch Operation Sequence in Substation Under Typical Disconnector Operating Mode 315
7.5.2 VFTO Restriction Level by Equipment in 500/1000 kV GIS Substation 318
7.5.3 Comparison of VFTO in Typical 500 and 1000 kV GIS Substations 319
7.5.4 Conclusions on Influences on the 500 and 1000 kV GIS Substations by VFTO 324
7.5.5 Discussion on Whether to Install Parallel Resistance of Disconnector in the 500 and 1000 kV GIS Substations 325
7.6 Comparison of Characteristics of VFTO in Substation and Power Plant 325
7.6.1 Comparison of Wiring Diagrams for Substation and Power Plant. 325
7.6.2 Comparison of Characteristics of VFTO in the UHV GIS Substation and the Power Plant. 327
7.6.3 Conclusions on Comparison of VFTO in UHV GIS Substation and Power Plant 332
7.7 Restriction and Protection Measures 333
7.7.1 Rational Arrangement of Operation Sequence of Circuit Breakers and Disconnectors. 333
7.7.2 Installation of Generator Outlet Circuit Breaker in the Power Plant 334

www.FreeEngineeringBooksPdf.com

7.7.3 Additional Installation of Parallel Resistance on the Disconnector . . . 336
7.7.4 Ferrite Toroid . . . 337
7.7.5 Overhead Line . . . 338
7.7.6 Other Measures . . . 339
7.8 Quantitative Study on the Restriction of Wave Front Steepness of VFTO Invading the Main Transformer Port by the Overhead Line . . . 339
7.8.1 Experimental Study of the Influence on the VFTO Wave Front Steepness by the Overhead Line Length . . . 340
7.8.2 Simulation Analysis of the Influence on the VFTO Wave Front Steepness by Overhead Line Length . . . 343
7.8.3 Further Discussion on Restriction of Wave Front Steepness of VFTO Invading the Main Transformer by Means of Overhead Line in the 1000 kV Power Plant . . . 350
7.9 Study on Transient Enclosure Voltage (TEV) of GIS in Substation and Power Plant . . . 354
7.9.1 Principle for Its Generation . . . 355
7.9.2 TEV Calculation Method . . . 355
7.9.3 Measures to Reduce the Transient Enclosure Voltage . . . 357
7.10 Experimental Investigation on VFTO Characteristics in the UHV GIS System in China . . . 358
7.10.1 VFTO Characteristic Test Circuit . . . 358
7.10.2 VFTO Generation Mechanism and Waveform Characteristics . . . 360
7.10.3 Tests on the Effect of Operating Speed of Disconnectors on VFTO . . . 362
7.10.4 Tests and Studies on the Effect of Branch Busbar Length on VFTO . . . 368
7.10.5 Effect of Connection Direction of Disconnector Contacts on VFTO . . . 371
7.11 Conclusions on VFTO Characteristics in the 500/1000 kV GIS Substation and Power Plant . . . 377
References . . . 380

8 Lightning Protection of UHVAC System . . . 383
Bincai Zhao, Hao Zhou, Yuchuan Han and Jingzhe Yu
8.1 Lightning Protection of the UHVAC Lines . . . 384
8.1.1 Overview . . . 384
8.1.2 Calculation Methods for Assessment of Lightning Withstand Performance . . . 390

www.FreeEngineeringBooksPdf.com

8.1.3 Assessment for Lightning Withstand Performance of 1000 kV UHV Lines in China . . . 416
8.1.4 Lightning Protection Measures for the UHVAC Lines . . . 422
8.1.5 Analysis of Sideward Lightning Rod in Lightning Protection of UHVAC Line . . . 427
8.2 Lightning Protection of the UHV Substations (Switch Stations) . . . 435
8.2.1 Overview . . . 435
8.2.2 Assessment Methods for the Lightning Withstand Performance of the UHV Substation . . . 436
8.2.3 Lightning Intruding Overvoltage Protection of the UHV Substations . . . 451
8.2.4 Lightning Invasion Wave Protection Measures for the UHV Substations . . . 456
References . . . 459

9 Insulation Coordination of UHV Substations . . . 461
Fei Su, Hao Zhou and Yang Li
9.1 Basic Concept and Principles of Insulation Coordination . . . 462
9.2 Insulation Coordination Methods for UHV Power Grid . . . 463
9.3 Insulation Coordination of the UHV Substation . . . 467
9.3.1 Determination of Air Clearance of the UHV Substation . . . 467
9.3.2 Selection of Insulation for the UHV Equipment . . . 475
References . . . 484

10 Insulation Coordination of UHVAC Transmission Lines . . . 485
Hao Zhou, Fei Su and Jingzhe Yu
10.1 Selection of Type and Form of UHV Insulator Strings . . . 485
10.1.1 Comparison Among Three Different UHV Transmission Line Insulators . . . 486
10.1.2 Selection of Type and Form of the UHV Transmission Line Insulator Strings . . . 491
10.2 Methods to Determine the Number of the UHV Transmission Line Insulators . . . 492
10.2.1 Selection of the Number of Insulators Based on Power Frequency Voltage . . . 492
10.2.2 Selection of the Number of Insulators as Per Switching Overvoltage . . . 508
10.2.3 Checking of the Number of Insulators as per Lightning Overvoltage Requirements . . . 509
10.3 Determination of Air Clearances of the UHV Line . . . 509
10.3.1 Determination of Air Clearance Under Power Frequency Voltage . . . 515

www.FreeEngineeringBooksPdf.com

10.3.2 Determination of Air Clearance Under Switching Impulse Voltage. 520
10.3.3 Determination of Air Clearance Under Lightning Impulse Voltage. 537
10.3.4 Selection of Line's Air Clearance of the UHV System Under Three Types of Overvoltage 542
10.3.5 Selection of Air Clearance of the UHV Lines in Various Countries 543
References. 544

11 UHVAC Electrical Equipment 547
Xiande Hu, Yang Li and Xiujuan Chen
11.1 UHV Transformer. 547
11.1.1 Status Quo of the UHV Transformers in China and Other Countries. 548
11.1.2 Characteristics and Type Selection of the UHV Transformer 549
11.1.3 Main Parameters of the UHV Transformers Used for the UHVAC Demonstration Project 553
11.2 UHV Shunt Reactor 554
11.2.1 Structural Design 556
11.2.2 Insulation Design. 558
11.2.3 Cooling Mode 558
11.2.4 Noise Control 559
11.2.5 UHV Controllable Shunt Reactor 560
11.3 UHV Instrument Transformer 561
11.3.1 Status Quo of the UHV Voltage Transformers and Current Transformers in China and Other Countries 561
11.3.2 UHV Voltage Transformer 562
11.3.3 UHV Current Transformer. 564
11.3.4 Photoelectric UHV Instrument Transformer. 565
11.4 UHV Arrester 566
11.4.1 Status Quo of the UHV Arresters in China and Other Countries. 566
11.4.2 Characteristics of the UHV Arrester 566
11.4.3 Main Parameters of the UHV Arresters Used in the UHVAC Demonstration Projects 568
11.4.4 UHVAC Controllable Arrester. 568
11.5 UHV Switchgear. 572
11.5.1 Status Quo of the UHV Switchgear in China and Other Countries. 572
11.5.2 Characteristics of UHV Switchgear 573

www.FreeEngineeringBooksPdf.com

11.6 UHV Bushing . . . 576
11.6.1 Status Quo of UHV Bushing in China and Other Countries . . . 576
11.6.2 Characteristics of the UHV Bushing . . . 577
11.7 UHV Series Compensation Device . . . 578
11.7.1 Status Quo of the UHV Series Compensation Device in China and Other Countries . . . 578
11.7.2 Protection Mode of the UHV Series Compensation Device . . . 579
References . . . 579

12 UHV Power Frequency Electromagnetic Induction . . . 581
Baoju Li, Jidong Shi and Yijing Su
12.1 Induced Voltage and Current of the 1000 kV Double-Circuit Line on the Same Tower . . . 582
12.1.1 Generation Mechanism and Four Different Induction Parameters . . . 582
12.1.2 Simulation Calculation of Induced Voltage and Current . . . 585
12.1.3 Analysis on Influence Factors of Induced Voltage and Induced Current . . . 588
12.2 Induced Voltage and Induced Current on Overhead Ground Wires of 1000 kV AC Transmission Line . . . 589
12.2.1 Induced Voltage and Induced Current on Overhead Ground Wires of the UHV Single-Circuit Line . . . 591
12.2.2 Induced Voltage and Induced Current on Overhead Ground Wires of the UHV Double-Circuit Line on the Same Tower . . . 593
12.2.3 Selection of Insulation Gap and Withstand Voltage of the UHV Overhead Insulated Conductors . . . 594
12.3 Power Frequency Electromagnetic Induction Influence of the AC Line on the UHVDC Line Erected in Parallel with It . . . 595
12.3.1 Power Frequency Electromagnetic Induction by the UHVAC Line to the UHVDC Line Erected in Parallel with It . . . 596
12.3.2 Influence Factors of the Electromagnetic Induction by the AC Line to the DC Line Erected in Parallel with It . . . 599
12.3.3 Comparative Analysis on Parallel Erection of the UHV Single-Circuit and Double-Circuit on the Same Tower of AC Line and the UHVDC Line . . . 606

www.FreeEngineeringBooksPdf.com

12.3.4 Comparative Analysis on Parallel Erection of the EHV/UHVAC Transmission Line and UHVDC Line 608
References 610

13 Electromagnetic Environment of UHVAC System 611
Xiao Zhang, Haiqing Lu, Yang Shen and Chuan He
13.1 Comparison Between Electromagnetic Environment of UHV and EHV Transmission Lines 612
13.2 Electromagnetic Environment of the UHVAC Transmission Line 614
13.2.1 Power Frequency Electric Field 614
13.2.2 Power Frequency Magnetic Field 622
13.2.3 Corona Loss 625
13.2.4 Radio Interference 629
13.2.5 Audible Noise 639
13.3 Optimized Phase Sequence Arrangement of the UHV Double-Circuit Transmission Line 645
13.3.1 Impact on Electromagnetic Environment 647
13.3.2 Impact on Natural Power 648
13.3.3 Impact on Unbalance Degree of Line 649
13.3.4 Impact on Lightning Withstand Performance 651
13.3.5 Impact on Induced Voltage and Current of Ground Wire 652
13.3.6 Recommended Optimal Phase Sequence for UHV Double-Circuit Line on the Same Tower 653
13.4 Safe Distance of UHV Transmission Line Over Buildings 654
13.4.1 Necessity of Research on Safe Distance 654
13.4.2 Calculation Methods and Simulation Models 655
13.4.3 Discussion on Influence Factors of Distorted Electric Field 658
13.4.4 Calculation of Safe Distance for UHV Transmission Line Over Building 666
13.5 Electromagnetic Environment of UHVAC Substation 667
13.5.1 Power Frequency Electric Field 667
13.5.2 Power Frequency Magnetic Field 668
13.5.3 Radio Interference 669
13.5.4 Noise 669
References 670

14 Principles and Configurations of UHVAC Protection 671
Laqin Ni, Jiyuan Li and Zhiyong Qiu
14.1 Basic Overview of UHVAC Protection 671

www.FreeEngineeringBooksPdf.com

14.1.1 Basic Requirements of UHVAC Protection 671
14.1.2 Setting Principles of the UHVAC Protection 672
14.1.3 Characteristics of UHVAC Protection 674
14.2 Principles and Configurations of UHVAC Protection 683
14.2.1 Principles and Configurations of Line Protection 684
14.2.2 Principles and Configurations of CB Protection 695
14.2.3 Principles and Configurations of Busbar Protection 699
14.2.4 Principles and Configurations of Transformer Protection 703
14.2.5 Principles and Configurations of HV Shunt Reactor Protection 716
14.2.6 Principles and Configurations of LV Shunt Reactor and LV Capacitor Protection 722
References 725

Part III Direct Current

15 Basic Information and Calculation of Main Parameters for UHVDC Transmission System 729
Yang Shen, Xilei Chen and Yuting Qiu
15.1 Operating Principle of Converter 729
15.1.1 6-Pulse Converter 731
15.1.2 12-Pulse Converter 738
15.1.3 Double 12-Pulse Converter Connected in Series 739
15.2 Operating Modes of the UHVDC Transmission System 740
15.2.1 Selection of Voltage Level of UHVDC Converters 741
15.2.2 Operating Modes of UHVDC System 742
15.3 Calculation of Main Circuit Parameters of UHVDC System 748
15.3.1 Main Connection and Operation Modes of UHVDC Transmission Project 750
15.3.2 Rated Operating Parameters of DC System 751
15.3.3 Rated Operating Parameters of AC System 752
15.3.4 Parameters of DC Line 752
15.3.5 Equipment Parameters 753
15.3.6 Operating Parameters of DC System 763
References 765

16 Switching Overvoltage of UHVDC System 767
Dongju Wang, Hao Zhou and Jiyuan Li
16.1 Classification and Characteristics of Switching Overvoltage in UHVDC System 768

www.FreeEngineeringBooksPdf.com

16.1.1 Classification of Switching Overvoltage 768
16.1.2 Characteristics of UHVDC Switching Overvoltage 769
16.1.3 Type of Faults Resulting in Switching Overvoltage 771
16.2 Simulation Model of DC System 772
16.2.1 Model for Main Circuit of DC System 772
16.2.2 Model of DC Control System 773
16.2.3 Scheme for Arrangement of Arresters in Converter Station. 777
16.3 Switching Overvoltage at AC Side 778
16.3.1 Three-Phase Ground Fault and Clearing 780
16.3.2 Loss of AC Power Supply at the Inverter Side 782
16.3.3 Internal Overvoltage of AC Filters 786
16.4 Switching Overvoltage in Valve Hall 793
16.4.1 Switching Overvoltage on Valve Arrester V11/V1 795
16.4.2 Switching Overvoltage on Valve Arrester V12/V2 801
16.4.3 Switching Overvoltage on Valve Arrester V3 804
16.4.4 Switching Overvoltage on DC Converter Busbar Arrester 808
16.5 Switching Overvoltage in DC Field 811
16.5.1 Overvoltage on DC Pole Line 811
16.5.2 Overvoltage on Neutral Busbar 818
16.5.3 Internal Overvoltage of DC Filter 830
16.6 Monopolar Ground Fault Overvoltage of DC Line 836
16.6.1 Conditions for Simulation 837
16.6.2 Simulation Calculation Results 840
16.6.3 Analysis of Overvoltage Mechanism 847
16.6.4 Overvoltage Control and Protection Measures 854
References. 855

17 Lightning Overvoltage of UHVDC Transmission System 857
Pan Dai, Hao Zhou and Bincai Zhao
17.1 Lightning Protection of UHVDC Transmission Line 858
17.1.1 Main Differences in Lightning Protection of AC and DC Lines 858
17.1.2 Characteristics of Lightning Withstand Performance for UHVDC Line 861
17.1.3 Analysis of Lightning Protection for the ±800 kV UHVDC Transmission Line. 862
17.2 Lightning Protection of UHVDC Converter Station 866

www.FreeEngineeringBooksPdf.com

17.2.1 Protection Characteristics of Lightning Invasion Wave for DC Converter Station. 866
17.2.2 Calculation Method for Lightning Intruding Overvoltage in DC Converter Station 868
17.2.3 Analysis for Overvoltage Protection of Lightning Invasion Wave in ±800 kV DC Converter Station 874
References. 886

18 Insulation Coordination of UHVDC Converter Station 887
Xilei Chen, Hao Zhou and Xu Deng
18.1 Basic Procedures for Determining the Insulation Level of Equipment 888
18.2 Overview of UHVDC Arrester 889
18.2.1 Characteristics of UHVDC Arrester. 889
18.2.2 Definition of Basic Parameters of UHVDC Arrester 890
18.3 Configuration of Arresters in Converter Station 891
18.3.1 Basic Principles for Configuration of Arresters 891
18.3.2 Configuration Scheme of Arresters in Converter Station 892
18.3.3 Characteristics for Configuration of Arresters in UHVDC Converter Station 897
18.4 Selection of Parameters for UHVDC Arresters 898
18.4.1 Basic Principles for Selection of Parameters for Arresters. 898
18.4.2 Arresters at AC Side 899
18.4.3 Arresters at DC Side 901
18.4.4 Difference in Parameters of Arresters for Converter Stations at Both Terminals. 911
18.5 Determination for Insulation Level of Converter Station's Equipment. 913
18.5.1 Method for Insulation Coordination of Converter Station's Equipment. 913
18.5.2 Insulation Margin 913
18.5.3 Protection Level and Insulation Level 915
18.6 Scheme for Separate Arrangement of Smoothing Reactors 916
18.6.1 Economic and Technical Advantages of Separate Arrangement of Smoothing Reactors 918
18.6.2 Necessity for Adoption of Separate Arrangement of Smoothing Reactors in UHVDC System. 923
18.7 Minimum Air Clearance in Converter Station. 924
18.7.1 Air Clearance Discharge Characteristic Test of Pole Busbar in Converter Station 927

www.FreeEngineeringBooksPdf.com

18.7.2 Equation Method for Design of Minimum Air Clearance . . . 930
18.7.3 Non-standard Atmospheric Correction Method . . . 933
18.8 Polluted External Insulation of Converter Station . . . 942
18.8.1 Operation Experience of Polluted External Insulation of Chinese ±500 kV Converter Stations . . . 942
18.8.2 Selection of Post Insulators in Converter Stations . . . 946
18.8.3 External Insulation Design of Post Insulators in Converter Station . . . 947
18.8.4 Creepage Distance of DC Wall Bushing in Converter Station . . . 954
References . . . 956

19 Insulation Coordination of UHVDC Transmission Line . . . 959
Jidong Shi, Hao Zhou and Xu Deng
19.1 Selection of Type and Number of Insulators for UHVDC Transmission Line . . . 960
19.1.1 Selection of Material and Umbrella Type of Insulators . . . 960
19.1.2 Type Selection of Insulator Strings . . . 963
19.1.3 Determination of the Insulators' Number . . . 964
19.1.4 Selection of Insulators in Icing Area . . . 974
19.2 Determination of Air Clearance for UHVDC Transmission Line . . . 978
19.2.1 Determination of Air Clearance Under DC Voltage . . . 983
19.2.2 Determination of Air Clearance Under Switching Impulse . . . 984
19.2.3 Determination of Air Clearance Under Lightning Impulse . . . 985
19.2.4 Code-Recommended Value and Engineering-Applied Value for Air Clearance of UHVDC Line . . . 986
References . . . 987

20 Overvoltage Characteristics and Insulation Coordination of UHVDC Converter Valves . . . 989
Kunpeng Zha, Xiaoguang Wei and Jie Liu
20.1 Analysis on Overvoltage Characteristics of Converter Valves Under the Effect of Impulse Voltage . . . 990

www.FreeEngineeringBooksPdf.com

20.1.1 Extraction of Parasitic Capacitance of Converter Valve System. 990
20.1.2 Analysis Model for Impulse Transient of Converter Valve System 994
20.1.3 Characteristics of Impulse Transient Overvoltage of Converter Valve System 994
20.2 Analysis on Overvoltage Characteristics of Converter Valve Under Operating Condition. 996
20.2.1 Analysis on Turn-off Transient Overvoltage of Converter Valve 998
20.2.2 Physical Simulation Method 1000
20.2.3 Classical Method 1001
20.2.4 Time-Domain Circuit Method 1002
20.3 Overvoltage Protection of DC Transmission Converter Valve and Its Design 1004
20.3.1 Strategy Selection for Insulation Coordination of Converter Valves. 1005
20.3.2 Overvoltage Protection Function of Gate Electronic Circuit. 1005
20.4 Study on Insulation Coordination for DC Transmission Converter Valves 1007
20.4.1 Calculation Method for Creepage Distance 1007
20.4.2 Calculation Method for Air Clearance 1008
References. 1008

21 UHVDC Electrical Equipment 1009
Xu Deng, Anwen Xu and Yuting Qiu
21.1 Arrangement of UHVDC Equipment 1009
21.2 UHV Converter Valve 1012
21.2.1 Structure of UHV Converter Valve 1013
21.2.2 Characteristics of UHV Converter Valve. 1016
21.2.3 Tests of UHV Converter Valve 1018
21.2.4 Manufacturing Level of UHV Converter Valve. 1018
21.3 UHV Converter Transformer 1019
21.3.1 Structure of UHV Converter Transformer 1020
21.3.2 Characteristics of UHV Converter Transformer. 1021
21.3.3 Tests of UHV Converter Transformer 1024
21.3.4 Manufacturing Level of UHV Converter Transformer. 1025
21.4 UHV Smoothing Reactor 1026
21.4.1 Structure of UHV Smoothing Reactor 1026
21.4.2 Characteristics of UHV Smoothing Reactor. 1028
21.4.3 Tests of UHV Smoothing Reactor 1030

www.FreeEngineeringBooksPdf.com

21.4.4 Manufacturing Level of UHV Smoothing Reactor . . . 1030
21.5 UHVAC and DC Filters . . . 1031
21.5.1 UHVAC Filter . . . 1031
21.5.2 UHVDC Filter . . . 1033
21.5.3 Tests of UHVAC/DC Filters . . . 1036
21.5.4 Manufacturing Level of UHVAC/UHVDC Filters . . . 1036
21.6 UHVDC Arrester . . . 1037
21.6.1 Type of UHVDC Arrester . . . 1037
21.6.2 Characteristics of UHVDC Arrester . . . 1038
21.6.3 Tests of UHVDC Arrester . . . 1041
21.6.4 Manufacturing Level of UHVDC Arrester . . . 1042
21.7 UHV Bushing . . . 1042
21.7.1 Structure of UHV Bushing . . . 1043
21.7.2 Characteristics of UHV Bushing . . . 1045
21.7.3 Tests of UHV Bushing . . . 1047
21.7.4 Manufacturing Level of UHV Bushing . . . 1047
21.8 UHVDC Switchgear . . . 1047
21.8.1 UHVDC Transfer Switch . . . 1048
21.8.2 UHVDC Disconnector and Grounding Switch . . . 1052
21.8.3 UHVDC Bypass Switch . . . 1052
21.8.4 Tests of UHVDC Switchgear . . . 1054
21.9 UHVDC Measuring Equipment . . . 1054
21.9.1 UHVDC Voltage Measuring Equipment . . . 1054
21.9.2 UHVDC Current Measuring Equipment . . . 1055
References . . . 1056

22 Electromagnetic Environment of UHVDC System . . . 1059
Yiru Wan, Xiao Zhang and Jiyuan Li
22.1 Electromagnetic Environmental Issues of UHVDC Transmission Line . . . 1060
22.1.1 Electric Field Intensity and Ion Flow Density . . . 1061
22.1.2 DC Magnetic Field . . . 1064
22.1.3 Surface Electric Field Intensity of Conductor . . . 1065
22.1.4 Radio Interference . . . 1074
22.1.5 Audible Noise . . . 1077
22.1.6 Corona Loss . . . 1081
22.2 Electromagnetic Environmental Assessment of UHVDC Transmission Lines . . . 1084
22.2.1 Electric Field Intensity and Ion Flow Density . . . 1085
22.2.2 Magnetic Induction Intensity . . . 1087
22.2.3 Radio Interference . . . 1087
22.2.4 Audible Noise . . . 1089

www.FreeEngineeringBooksPdf.com

22.3 Analysis on Electromagnetic Environmental Impact Factors of UHVDC Transmission Line 1090
22.3.1 Influence of the Pole Conductor Height Above the Ground 1090
22.3.2 Influence of the Interpolar Distance 1090
22.3.3 Influence of Bundling Spacing of Pole Conductors 1092
22.3.4 Influence of the Number of Bundled Sub-conductors 1092
22.3.5 Influence of Cross-Sectional Area of Pole Conductors 1094
22.3.6 Influence of Altitude 1096
22.4 Measures for Improving the Electromagnetic Environment of DC Transmission Lines 1096
22.5 Electromagnetic Environment of UHVDC Converter Station 1098
22.5.1 Noise Sources of Converter Station 1100
22.5.2 Noise Control Indicators of Converter Station 1103
22.5.3 Noise Control Measures of Converter Station 1103
References 1106

23 Comparison of Overvoltage and Insulation Coordination of ±800 kV and ±1100 kV UHVDC Systems 1107
Wenqian Qiu, Hao Zhou and Dongju Wang
23.1 System Parameters 1108
23.2 Configuration and Parameters of Arresters in Converter Station 1109
23.2.1 Configuration of Arresters in Converter Station 1109
23.2.2 Basic Parameters of Arresters 1111
23.3 Analysis and Contrast of Overvoltage in Converter Station 1111
23.3.1 Overvoltage at AC Side 1111
23.3.2 Overvoltage in Valve Hall 1114
23.3.3 Overvoltage at DC Line Side 1121
23.3.4 Neutral Busbar Overvoltage 1122
23.4 Insulation Coordination of ±1100 kV UHVDC Power Transmission System 1125
23.4.1 Configuration Scheme for Arresters in Converter Station 1125
23.4.2 Influence of Short Circuit Impedance on Insulation Level of Equipment 1128
23.4.3 Insulation Level of Equipment 1129
23.5 Discussion on Converter Combination for ±1100 kV UHVDC System 1132

www.FreeEngineeringBooksPdf.com

23.5.1 Discussion on Combination of ±1100 kV Converters . . . 1132
23.5.2 Selection of Combination Scheme for Converters of ±1100 kV UHVDC System . . . 1137
References . . . 1138

24 Principles and Configurations of UHVDC Protection . . . 1139
Taoxi Zhu
24.1 Overview of UHVDC Protection . . . 1139
24.1.1 Basic Requirements of UHVDC Protection . . . 1139
24.1.2 Action Result of UHVDC Protection . . . 1140
24.1.3 Zone of UHVDC Protection . . . 1143
24.1.4 Measuring Points of UHVDC Protection . . . 1144
24.2 Principles and Configurations for UHVDC Protection . . . 1147
24.2.1 Protection of Converter Area . . . 1147
24.2.2 Protection of Polar Area . . . 1163
24.2.3 Bipolar Area Protection . . . 1170
24.2.4 Protection of DC Line Area . . . 1177
24.2.5 Protection of DC Filter Area . . . 1182
24.2.6 Protection of DC Switch . . . 1188
24.2.7 Coordination Relation of DC Protection . . . 1192
24.3 Difference Between UHVDC Protection and Conventional DC Protection . . . 1195
24.3.1 Configuration of Protective Devices . . . 1195
24.3.2 Protection Configuration and Principle . . . 1195
References . . . 1197

Part IV Design of UHV Power System

25 Design of Ultra-High-Voltage Alternating Current (UHVAC) Substation . . . 1201
Feng Qian, Wenqian Qiu, Jian Ding, Chunxiu An, Hongbo Liu, Jianhua Chen and Yang Shen
25.1 Design Depth Requirements and Main Standards . . . 1202
25.1.1 Design Depth Requirements . . . 1202
25.1.2 Main Standards . . . 1202
25.1.3 Key and Difficult Issues of Design . . . 1203
25.2 Site Selection and General Layout . . . 1203
25.2.1 Site Selection . . . 1203
25.2.2 General Planning and Layout . . . 1205
25.3 Main Electrical Connection . . . 1206
25.4 Overvoltage Protection . . . 1207
25.5 Minimum Air Clearance . . . 1210
25.6 Insulation Level of Electrical Equipment . . . 1210

www.FreeEngineeringBooksPdf.com

25.7 Selection of Main Electrical Equipment 1212
25.7.1 Electrical Calculation 1212
25.7.2 Main Transformer 1212
25.7.3 Switchgear 1215
25.7.4 Voltage Transformer 1215
25.7.5 UHV Shunt Reactor 1216
25.8 UHV Distribution Equipment 1217
25.8.1 Classification and Design Principle of UHV Distribution Equipment 1217
25.8.2 Minimum Safety Clearance Values *A*, *B*, *C*, and *D* 1225
25.8.3 Main Features of UHV Distribution Equipment 1227
25.8.4 Size Determination of 1000 kV Distribution Equipment 1227
25.9 Connection and Layout of Shunt Compensation Device 1230
25.9.1 Classification of Shunt Compensation Devices 1232
25.9.2 Grouping Capacity of Shunt Compensation Devices 1232
25.9.3 Shunt Compensation Devices 1234
25.9.4 Layout of Shunt Compensation Devices 1235
25.10 Connection and Layout of Station-Service Power 1236
25.10.1 Main Design Principles 1236
25.10.2 Connection of Station-Service Power 1236
25.10.3 Station-Service Equipment and Layout 1236
25.10.4 Lighting and Maintenance 1237
25.11 General Plan and Vertical Layout 1237
25.11.1 General Layout Plan 1237
25.11.2 Vertical Layout 1240
25.11.3 Roads of Substation 1241
25.12 Main Buildings (Structures) 1241
25.12.1 Buildings of Substation 1241
25.12.2 UHV Substation Framework 1245
25.12.3 UHV GIS Equipment Foundation 1255
25.13 Secondary Electrical Connection 1258
25.13.1 Main Design Principles 1258
25.13.2 Computer-Based Monitoring System 1259
25.13.3 Element Protection 1261
25.13.4 System Protection 1263
25.13.5 System Communication 1267
25.13.6 Dispatching Automation System 1268
25.13.7 Electric Energy Metering and Billing System 1268

www.FreeEngineeringBooksPdf.com

25.13.8 Operating Power Supply System and Others 1269
25.13.9 Equipment Status On-Line Monitoring System 1270
References 1271

26 Design of UHVDC Converter Station 1273
Zhichao Zhou, Xiaofei Ding, Wenqian Qiu, Jianhua Chen, Chunxiu An and Sheng Liu
26.1 Site Selection and General Layout 1274
26.1.1 General Requirements 1274
26.1.2 General Layout 1274
26.1.3 Heavy-Duty Equipment Transport 1275
26.1.4 Water Supply to Converter Station 1276
26.1.5 Environmental Impact 1277
26.2 Main Electrical Connection 1278
26.2.1 Connection of Converter Unit 1278
26.2.2 Connection of DC Switchyard 1278
26.2.3 AC Switchyard Connection 1285
26.2.4 AC Filter Connection 1285
26.3 Overvoltage Protection of Converter Station 1286
26.4 Insulation Levels of Equipment 1287
26.5 Minimum Air Clearance Distance 1291
26.6 Selection of Main Electrical Equipment 1296
26.6.1 Calculation of Short-Circuit Current 1296
26.6.2 Converter Valve 1303
26.6.3 Converter Transformer 1306
26.6.4 Smoothing Reactor 1308
26.6.5 AC Filter and Shunt Capacitor 1309
26.6.6 DC Filter 1310
26.6.7 Other DC Equipment 1310
26.6.8 Wall Bushing 1314
26.7 Vertical Layout Design 1315
26.7.1 Main Tasks and Design Principles 1315
26.7.2 Vertical Layout with Slight Slope and Slope Selection 1316
26.7.3 Vertical Layout with Terrace 1316
26.7.4 Vertical Layout of Buildings and Structures 1317
26.8 Power Distribution Device of UHVDC Converter Station 1317
26.8.1 Converter Area Layout 1318
26.8.2 DC Switchyard Arrangement 1329
26.8.3 Layout of AC Filter Yard 1332
26.8.4 Layout of AC Power Distribution Devices 1340
26.8.5 Summary of Electrical General Layout 1340
26.9 Buildings in Converter Station 1341
26.9.1 Main Buildings and Structures 1341

www.FreeEngineeringBooksPdf.com

26.9.2 Valve Hall . . . 1342
26.9.3 Control Building and Auxiliary Equipment Building . . . 1343
26.9.4 Indoor DC Yard . . . 1344
26.9.5 GIS House . . . 1344
26.9.6 Other Buildings . . . 1344
26.9.7 Type of Structure . . . 1344
26.10 Connection and Layout of Substation-Service Power . . . 1345
26.11 Secondary System . . . 1346
26.11.1 Control and Protection of AC and DC Systems . . . 1346
26.11.2 AC Protection System and Safety and Stabilizing Devices . . . 1356
26.11.3 Dispatching Automation . . . 1357
26.11.4 System Communication . . . 1359
References . . . 1360

27 Design of Ultra-High-Voltage Alternating Current (UHVAC) Power Transmission Lines . . . 1361
Jiamiao Chen, Wenqian Qiu, Feng Pan and Gang Song
27.1 Design Basis . . . 1363
27.2 Line Routes . . . 1363
27.3 Design Meteorological Conditions . . . 1364
27.3.1 Principles of Selection . . . 1364
27.3.2 Basic Wind Speed . . . 1364
27.3.3 Design Icing . . . 1366
27.4 Selection of Conductor and Ground Wire of AC Lines . . . 1367
27.4.1 Main Parameters for Conductor Selection . . . 1368
27.4.2 Conductor Cross-Section and Bundled Configuration . . . 1372
27.4.3 Phase-Sequence Arrangement of the Double-Circuit Conductors . . . 1374
27.4.4 Application of Expanded Conductors . . . 1376
27.4.5 Selection of Ground Wire and OPGW Optical Cable . . . 1379
27.5 Insulation Coordination Design of AC Transmission Line . . . 1382
27.5.1 Type Selection of Insulators . . . 1383
27.5.2 Selection of the Number of Pieces of Insulator Strings . . . 1387
27.5.3 Air Clearance at Tower Head . . . 1390
27.5.4 Lightning Protection and Grounding Design . . . 1392
27.6 Design of AC Line Insulator Strings and Fittings . . . 1394
27.6.1 Basic Principles . . . 1394
27.6.2 Safety Factor . . . 1395
27.6.3 Suspension Insulator String of Conductor . . . 1396

www.FreeEngineeringBooksPdf.com

27.6.4 Strain Insulator String of Conductor 1398
27.6.5 Jumper Fitting String of Strain Tower 1399
27.6.6 Main Fittings 1402
27.7 Conductor Transposition Design for AC Line 1406
27.7.1 Main Content of Conductor Transposition Design 1407
27.7.2 Determination of Unbalance Factor Limits 1407
27.7.3 Calculation of Unbalance Factor for Power Transmission Line 1408
27.7.4 Selection of Transposition Ways 1410
27.8 Tower Design for UHV Transmission Line 1412
27.8.1 Types and Characteristics of Tower 1412
27.8.2 Tower Loads and Combinations 1417
27.8.3 Materials of Tower 1418
27.8.4 Optimization Design of Tower Structure 1421
27.8.5 Issues to Be Noticed in the Design of Tower Structure 1425
References 1427

28 Design of UHVDC Transmission Lines 1429
Jiamiao Chen, Wenqian Qiu, Jia Tao, Yong Guo and Jianfei Chen
28.1 Selection of Conductors for DC Line 1430
28.1.1 Main Principles for Conductor Selection 1430
28.1.2 Conductor Section and Bundle Configuration 1431
28.1.3 Main Electrical Properties of Conductor 1433
28.1.4 Selection of Ground Wire Types 1440
28.2 Insulation Coordination Design of DC Line 1440
28.2.1 Pollution Investigation and Polluted Area Classification 1441
28.2.2 Insulator Types 1442
28.2.3 Selection of the Number of Insulators for the Insulator Strings 1445
28.2.4 Air Clearance of Tower Head 1452
28.3 Design of Insulator Strings and Fittings of DC Line 1453
28.3.1 Insulator String of Conductor 1453
28.3.2 Selection of Main Fittings 1457
28.4 Clearance of Conductor to Ground for DC Line 1459
28.4.1 Minimum Clearance of Conductor to Ground 1459
28.4.2 Relation Between Clearance of Conductor to Ground and Environmental Climate 1460
28.5 Tower Design of DC Line 1461
28.5.1 Tower Types of DC Line 1461
28.5.2 Structural Characteristics of Towers for DC Line 1463

www.FreeEngineeringBooksPdf.com

28.5.3 Tower Load and Combination 1465
28.5.4 Tower Materials of DC Line 1465
28.5.5 Issues to Be Noticed in Tower Design 1467
28.6 Foundation Design for DC Line 1469
28.6.1 Common Foundation Types 1469
28.6.2 Issues to Be Noticed in Foundation Design 1470
28.6.3 Treatment Measures for Foundations Under Special Geological Conditions 1473
28.6.4 Mechanical Construction of Foundations 1474
References 1475

www.FreeEngineeringBooksPdf.com

Introduction

This book systematically introduces the key technical issues existing in the ultra-high-voltage (UHV) AC and DC power transmission. The whole book consists of four parts, among which, Part I provides an overview of the development of the UHV power transmission and the system characteristics and economy thereof. Part II mainly elaborates the key technical issues involved in the UHVAC system, including power frequency overvoltage of UHV lines, secondary arc current of UHVAC system, switching overvoltage of UHVAC system, very fast transient overvoltage (VFTO) of UHVAC system, lightning protection of UHVAC system, insulation coordination of UHV substation, insulation coordination of UHVAC transmission line, UHVAC electrical equipment, UHV power frequency electromagnetic induction and electromagnetic environment of UHVAC system, protection principles, and configuration of UHVAC system. Part III mainly elaborates the key technologies for the UHVDC system, including UHVDC system foundation and main parameter calculation, switching overvoltage of UHVDC system, lightning overvoltage of UHVDC transmission system, insulation coordination of UHVDC converter station, external insulation coordination of UHVDC transmission line, overvoltage characteristics and insulation coordination of UHVDC converter valve, UHVDC electrical equipment, electromagnetic environment of UHVDC system and comparison of overvoltage and insulation coordination of $\pm$800 kV and $\pm$1100 kV UHVDC systems, protection principles, and configuration of UHVDC system. Part IV gives a main introduction to the design of the UHVAC substation and UHVDC converter station as well as AC and DC power transmission lines.

This book not only can be applied as the specialized course material and reference book for the electrical discipline undergraduates and postgraduates of senior colleges to allow the teachers and students of senior colleges to understand the UHVAC and UHVDC power transmission technology, but also can be applied as the reference book for the technicians engaging in the UHV power transmission theoretical research, planning and design, operation and maintenance, and other works.

www.FreeEngineeringBooksPdf.com

This book is supported by the *Basic Research on Electromagnetic and Insulation Characteristics of UHVAC and DC Power Transmission System* (2011CB209400), a major project under the National Key Basic Research Development Program of China (973 Program), and also supported by the National Science and Technology Academic Publication Fund and Zhejiang University—Zhejiang Electric Power Design Institute Cooperation Center.

www.FreeEngineeringBooksPdf.com

Part I
Overview

The UHV power transmission system refers to the transmission system at voltage level of AC 1000 kV, DC ±750 kV and above. The fast growth of electrical load and the urgent needs in high-capacity and long-distance power transmission directly promote the rapid planning and construction of the UHV power transmission projects in China. Up to august 2017, six 1000 kV UHVAC power transmission lines and nine ±800 kV UHVDC power transmission lines have been built and put into operation. There are still another 1000 kV UHVAC power transmission line and the other four ±800 kV UHVDC power transmission lines will be put into operation at the end of 2017. Moreover, one ±1100 kV UHVDC power transmission line is being built and will be put into operation in 2018. The UHV power transmission technology will greatly promote the sustainable development of China's power industry and energy industry, and have a positive and profound impact on the construction of power technology innovation, energy guarantee system and global energy internet in the world.This section first discusses the selection of voltage levels of the UHVAC and UHVDC power grid and the development of UHV power transmission technology around the world, and then introduces the UHV planning and development in China, and finally conducts discussion on the characteristics and economy of UHV system.

www.FreeEngineeringBooksPdf.com

Chapter 1
Development of UHV Power Transmission

Ke Sun, Dongju Wang, Sha Li and Haifeng Qiu

With the rapid development of China's economy and the rapid increase in the demand for electricity by the whole society, the power transmission technology of the conventional EHV voltage level cannot meet the growing demand for electricity, thus it is necessary to develop the power transmission technology of higher voltage level. The adoption of the UHV power transmission technology not only can effectively solve the rapid growth of China's growing demand for electricity, but also makes the long-distance and high-capacity power transmission become more economic. China's existing UHVAC and UHVDC power transmission projects are all developed under this background. This chapter begins with the introduction of the development of the AC and DC power grid's voltage level from low voltage to high, and, additionally, focuses on the selection of UHVAC and UHVDC power transmission voltage levels and the development of UHV power transmission technology in the world.

K. Sun (✉)
Zhejiang Electric Power Corporation, Hangzhou, Zhejiang, People's Republic of China
e-mail: ssunke@sina.com

D. Wang · S. Li
College of Electrical Engineering, Zhejiang University, Xihu District, Hangzhou, Zhejiang, People's Republic of China
e-mail: wangdongju@zju.edu.cn

S. Li
e-mail: lisha1210@zju.edu.cn

H. Qiu
State Grid Hangzhou Power Supply Company, Hangzhou, Zhejiang, People's Republic of China
e-mail: 21713778@qq.com

© Zhejiang University Press, Hangzhou and Springer-Verlag GmbH Germany 2018

H. Zhou et al. (eds.), *Ultra-high Voltage AC/DC Power Transmission*,
Advanced Topics in Science and Technology in China,
https://doi.org/10.1007/978-3-662-54575-1_1

www.FreeEngineeringBooksPdf.com

1.1 UHV Power Transmission

1.1.1 Development of Power Transmission Voltage Level

In 1882, Deprez, a French physicist, by making use of a DC generator in a coal mine under DC voltage of 2 kV, and power of 1.5 kW and along the telegraph line of 57 km, successfully sent the electrical energy to an international exhibition held in Munich, completing the long-distance power transmission first ever in human history by the way of DC power transmission. This DC power transmission mode was once very popular. But because of the DC motor's complex structure, poor reliability, and the great difficulty in the design and manufacturing technology of large-capacity and high-voltage DC motor, under the circumstances at that time, the power transmission voltage, capacity, and distance could only be increased by connecting multiple generators in series. In 1889, in France, a high voltage was obtained by connecting DC generators in series, and a 230 km DC power transmission line was built from Moutiers to Lyon, whose transmission voltage and transmission power were 125 kV and 20 MW, respectively. Under the technical conditions at that time, it was quite difficult to achieve the power transmission with longer distance and larger capacity using the DC power transmission mode. So the people began to turn to study the use of AC power transmission mode, by which the transmission voltage could be more easily and rapidly improved, thus achieving the power transmission with longer distance and larger capacity.

In 1888, on the River Thames in London, the large-scale AC power station designed by Ferranti began to transmit power. The copper-core cables were used by the power station to send the 10 kV single-phase AC power to the urban substation 10 km away, where the power was transformed from 10 kV to 2500 V and then distributed to the secondary transformers in all blocks, where the power was once more transformed to 100 V for lighting by users. In 1889, Dolivo–Dobrovolsky of Russia had developed the first three-phase AC generator with power of 100 W, which was used widely in Germany and the US. In this context, the three-phase high-voltage AC power transmission mode got rapid promotion worldwide. Through the AC power transmission mode, the transformer could be used to improve the transmission voltage to achieve power transmission with longer distance and larger capacity easily. So the AC power transmission, with obvious economic and technical advantages displayed, got continued rapid development, gradually became common and replaced the original DC power transmission, and eventually became the transmission mode with absolute dominance in the field of electric energy transmission. Since the 10 kV AC transmission mode was used by scientists in 1888, the transmission voltage was increased to 33 kV with the help of AC transformer in 1898, increased to the high voltage of 110 and 230 kV in 1907 and 1923, respectively, increased to the extra high voltage of 380, 500, and 735 kV, respectively, in 1952, 1959, and 1965, and even increased to the ultrahigh voltage of 1150 kV by the former Soviet Union in 1985 [1–3]. Since the first 500 kV EHVAC power transmission line in China, Pingdingshan–Wuhan 500 kV EHVAC

www.FreeEngineeringBooksPdf.com

power transmission line, was put into operation in 1981, the 500 kV EHV power grid had gradually become the main grid framework of the major regions; the first 750 kV EHV power transmission line from Guanting, Qinghai to Lanzhou, Gansu in China was built in the northwest power grid in 2005, and now the 750 kV power grid is becoming the main grid framework in the northwest power grid; in 2009, the 1000 kV Southeast Shanxi–Nanyang–Jingmen power transmission line, China's first UHVAC demonstration project, was put into operation. In 2013, the Huainan–Shanghai 1000 kV UHV double-circuit AC power transmission line project was completed. Subsequently, in December 2014, the North Zhejiang–Fuzhou 1000 kV UHV double-circuit AC power transmission line project was put into operation. In addition, a number of other 1000 kV UHVAC power transmission projects are under planning and construction.

Since the AC power transmission was applied in 1890, the development of DC power transmission had been nearly halted for more than half a century until the Sweden Gotland DC power transmission project, the DC submarine cable power transmission system adopting mercury arc valve conversion mode, was put into operation in 1954. However, due to the poor reliability of mercury arc valve conversion mode, it did not effectively promote the DC power transmission mode to move forward. Since the 1970s, with the rapid development of power electronics and microelectronics technologies, new high-voltage and large-power thyristor emerged. Because the thyristor valve had no inverse arc faults and was much easier and more convenient than the mercury arc valve in manufacturing, testing, operation, maintenance and repair, it effectively improved the operating performance and reliability of DC power transmission and quickly got good application in the DC power transmission projects, greatly promoting the development of DC power transmission technology [4]. In 1970, based on the original Gotland DC power transmission project, Sweden first expanded it by the construction of the thyristor valve demonstration project with DC voltage of 50 kV and transmission power of 10 MW. In 1972, the Eel River DC Back-to-Back Project (2×80 kV, 2×160 MW), the first project fully adopting thyristor conversion in the world, was put into operation in Canada. Because the DC power transmission has prominent and special advantages in such fields as the long-distance and large-capacity overhead power transmission line, submarine cable power transmission and AC system back-to-back link, with the help of the new thyristor valves, the DC power transmission, thereafter, once again got rapid development in the whole world. The new DC power transmission projects making use of thyristor valves constantly emerged and the DC transmission voltage constantly was increased. By 2003, a total of 65 thyristor valve projects were constructed and put into operation in the world, among which a considerable part was important long-distance EHVDC power transmission projects with transmission voltage of ± 500 to ± 600 kV and a few were multi-terminal DC power transmission projects. In China, since the Gezhouba–Shanghai ± 500 kV DC power transmission project was put into operation in 1990, several ± 500 kV EHVDC power transmission projects had been successively built and put into operation. China built the Yunnan (Chuxiong)–Guangzhou (Suidong) ± 800 kV DC power transmission project and

www.FreeEngineeringBooksPdf.com

the Xiangjiaba (Fulong)–Shanghai (Fengxian) ±800 kV DC power transmission project in 2010, completed the Ningxia (Ningdong)–Shandong (Qingdao) ±660 kV DC power transmission project in 2011, completed the Sichuan Jinping (Yulong)–Jiangsu Sunan (Tongli) ±800 kV DC power transmission project in 2012, completed the Yunnan (Puer)–Guangdong (Jiangmen) ±800 kV DC power transmission project (or called as Nuozadu DC power transmission project) in 2013, and completed the South Hami (South Hami)–Zhengzhou (Zhengzhou) and Xiluodu (Shuanglong)–West Zhejiang (Jinhua) ±800 kV DC power transmission projects in 2014. Currently, China has several ±800 kV UHVDC power transmission projects under construction and preparation. The bipolar single-circuit DC power transmission project with voltage grade of ±1100 kV has been researched and demonstrated, and the design preparation of the pre-phase engineering has been conducted depending on the East Junggar Basin–East China project.

1.1.2 Voltage Level Sequence in Power Grid

The basic purpose of the development of power transmission technology is to improve transmission capacity and reduce line losses. Increasing the transmission voltage is an effective way to improve the transmission capacity and also an effective way to reduce line losses. Thus, the whole history of the development of power transmission technology is almost the process to continuously improve the transmission voltage level so as to constantly increase the transmission power and constantly extend the transmission distance. For the division of transmission voltage levels, there are many different methods prescribed. For AC power transmission, in combination with scientific researches and practical applications, the voltage levels are currently often divided as follows: the voltage level of 10, 20, and 35 kV is referred to as the distribution voltage or medium voltage (including the voltage level of 66 kV which, however, is applied only in a few countries and regions); the voltage level of 110–220 kV is referred to as high voltage; the voltage level above 220 kV and below 1000 kV is referred to as extra-high voltage (EHV), mainly including 330, 500, and 750 kV; the voltage level of 1000 kV and above is referred to as ultrahigh voltage (UHV). The situation for DC power transmission is different to some extent. According to the American National Standards, the voltage level above ±100 kV is referred to as high voltage, the voltage level of ±500 and ±600 kV is referred to as EHV and the voltage level above ±600 kV is referred to as UHV; the Soviet studies suggest that the voltage level of ±750 kV and above is referred to as UHV; in China, the voltage level of ±800 kV and above is normally deemed as UHV.

Table 1.1 shows the overview of the development of AC transmission voltage levels, and Table 1.2 shows the overview of the development of DC transmission voltage levels.

The emergence of new transmission voltage levels depends on many factors: first, the need for long-distance and large-capacity transmission, and second the

www.FreeEngineeringBooksPdf.com

Table 1.1 Development of AC transmission voltage levels

1890	10 kV	UK	Medium voltage
1898	33 kV	USA	
1906	110 kV	USA	High voltage
1923	220 kV	USA	
1937	287 kV	USA	EHV
1952	380 kV	Sweden	
1959	500 kV	Former Soviet Union	
1965	735 kV	Canada	
1985	1150 kV	Former Soviet Union	UHV

consideration in such aspects as transmission technology, economic efficiency and environmental impact. The development of a new voltage level needs the completion of many works, such as selection of voltage values, determination of insulation levels, development of equipment and construction of test lines, so that it can be compatible with the original voltage levels and can adapt to the needs for power development in the next two decades or longer. Each country has different economic conditions, resource distribution and geographical conditions, so the voltage level sequence applied is different, resulting in the formation of different AC and DC transmission voltage level sequences.

The different AC transmission voltage level sequences used in some of the major countries in the world are as shown in Table 1.3.

Since Sweden's Gotland DC power transmission project was put into operation in 1954, hundreds of DC power transmission projects had been built and put into operation around the world. Currently, the rated voltage of DC power transmission project has not yet formed into standard voltage level sequence as same as AC power transmission, and the rated voltage of each specific DC power transmission project is determined according to the actual situations, which causes that the equipment design, production and selection cannot be generalized and scaled, increasing the project cost, reducing the maintainability of equipment and bringing difficulties for production and operation. The DC power transmission projects include overhead lines, cable lines and back-to-back projects and many other types. During the conversion of mercury arc valves prior to the industrial application of thyristor products, the rated voltage of DC power transmission projects is also limited by the withstand voltage of mercury arc valve and other factors. After the emergence of thyristor converters, they commonly adopt the structure of elements connected in series. It is theoretically allowable to use any rated voltage, which does not increase the difficulty in design and manufacture of the converter, resulting in the various rated voltages involved in current DC power transmission projects. At present, the DC rated voltages (kV) of DC power transmission projects in the world having been put into operation include: ±17, ±25, ±50, ±70, ±80, ±82, ±85, ±100, ±120, ±125, ±140, ±150, ±160, ±180, ±200, ±250, ±266, ±270, ±350, ±400, ±500, ±600, ±660, ±800, etc.

www.FreeEngineeringBooksPdf.com

Table 1.2 Development of DC power transmission and its voltage levels

1882	DC 2 kV	Germany, Miesbach Coal Mine to Munich International Exhibition	Single DC generator
1890	DC 125 kV	France, Moutiers to Lyon	Multiple DC generators connected in series
1954	±100 kV (Gotland DC Project, Sweden) (The first mercury arc valve conversion project)	From 1954 to 1977, a total of 12 DC projects applying mercury arc valve conversion were put into operation in the world, of which the maximum transmission capacity was 1440 MW (US Pacific Intertie Phase 1 Project); the maximum transmission voltage was ±450 kV (Nelson River Phase 1 Project); the longest transmission distance was 1362 km (Pacific Intertie)	Large-power mercury arc valve converter
1977	±450 kV (Nelson River Phase 1 project) (The last mercury arc conversion valve project)		
1970	±50 kV, 10 MW (The first thyristor valve demonstration project)	Sweden, Gotland DC project expansion works	Large-power thyristor valve conversion
1972	2 × ±80 kV, 2 × 160 MW (Eel River DC Back-to-Back Project, Canada) (The first formal thyristor valve project)	After the project, almost all new DC power transmission projects in the world adopted the thyristor valves	
1978	±533 kV (EHV) (Cahora Bassa Project, Mozambique–South Africa)	By the end of 2003, a total of 65 thyristor valve projects were constructed and put into operation in the world, among which a considerable part was important long-distance EHVDC power transmission projects with transmission voltage of ±500 to ±600 kV and a few were multi-terminal DC power transmission projects	
1981	±500 kV (EHV) [Inga–Sabah Project, Congo (DRC)]		
1986–1987	±600 kV (EHV) (Itaipu Phase 1 and 2 Projects, Brazil)		
1990	±500 kV (EHV) (Gezhouba–Shanghai Project, China)		
1986/90/92	±500 kV (EHV) (Quebec Multi-Terminal DC Project, Canada–US)		
2002	±500 kV (EHV) (Southeast Link Project, India)		

(continued)

www.FreeEngineeringBooksPdf.com

Table 1.2 (continued)

2010	±800 kV (UHV) (Yunnan–Guangzhou Project, China)	The Xiangjiaba–Shanghai ±800 kV UHVDC power transmission demonstration project was put into operation in 2010. The Changji–Guquan ±1100 kV UHVDC power transmission project was put into construction in Jan 2016 and is expected to be put into operation in 2018, with total line length of 3324 km and rated transmission power of 12,000 MW	
2010	±800 kV (UHV) (Xiangjiaba–Shanghai Project, China)		
2012	±800 kV (UHV) (Jinping–Sunan Project, China)		
2013	±800 kV (UHV) (Nuozadu–Guangdong Project, China)		
2014	±800 kV (UHV) (South Hami–Zhengzhou Project, China)		
2014	±800 kV (UHV) (Xiluodu–West Zhejiang Project, China)		
2018	±1100 kV (UHV) (Changji–Guquan Project, China)		
1997	±10 kV, 3 MW, Hellsjon Pilot Project, Sweden	The light DC power transmission, also known as HVDC Light, was a new power transmission technology developed by ABB Company in the 80s and 90s of last century. The HVDC Light technology takes voltage source converter (VSC) as the core, uses IGBT and other turn-off devices as the hardware and applies pulse width modulation (PWM) technology for control to achieve the purpose of DC power transmission with a high controllability	Conversion by voltage source converter composed of IGBT (VSC-HVDC)
1999	±80 kV, 50 MW, Gotland Light Project, Sweden		
2002	±250 kV, 200 MW, Hellsjon Pilot Project, Sweden		
2010	±350 kV, 300 MW, Caprivi Link Project, Namibia	As of 2010, more than ten HVDC Light projects had been put into operation all over the world	

www.FreeEngineeringBooksPdf.com

Table 1.3 Main AC transmission voltage level sequences used in some countries

Country		Sequence
USA		765/345/138 kV, 500/220/115 kV
Former Soviet Union		750/330/110(150) kV, 500/220/110 kV
UK, France, Germany, Sweden		400(380)/220/110(150) kV
China	Most regions	1000/500/220/110 kV
	Northwest region	750/330/220/110 kV

According to the distribution of China's energy and the characteristics of the development of power grid, the scale of DC power transmission in China will be far larger than other countries in the future. If a specific rated voltage is still determined based on each project, it will inevitably lead to a huge waste in research and engineering construction investment. To improve the efficiency, save the costs and achieve generalization of devices, it is necessary to form a sequence of voltage levels for DC transmission system.

The main considerations for the formation of China's DC transmission voltage level sequence are: production and manufacturing scale having been formed and operating experience; equipment research, development and manufacturing capacity and transportation conditions; scale of power development and demand for delivering and receiving power by the system; DC power transmission distance; impact by DC system on the natural environment and the safe and stable operation of the power system; project investment and economy of power transmission, etc.

For the traditional DC power transmission mode using thyristor valves, the State Grid Corporation proposed a DC transmission voltage level sequence: ±500, ±660, ±800, and ±1000 kV (±1100 kV). Among them, the early technical demonstration of the voltage levels above ±800 kV was conducted as ±1000 kV. The Xinjiang (Zhundong)–Sichuan (Chengdu) DC power transmission project is planned as the first UHVDC power transmission project with voltage level above ±800 kV, having transmission distance over 2500 km and transmission capacity up to 10,000 MW and above. To meet the requirements for power transmission, the voltage level of the project may be determined as ±1000 or ±1100 kV, so here ±1000 or ±1100 kV is temporarily included in the sequence of DC transmission voltage. The issue that whether the voltage level of ±1000 or ±1100 kV shall be used for the UHVDC power transmission with voltage level higher than ±800 kV deserves further discussion. The transmission capacity and economic transmission distance of the DC power transmission system with the above-mentioned four voltage levels basically cover the demand by China's medium- and long-term power planning for long-distance and large-capacity DC power transmission.

www.FreeEngineeringBooksPdf.com

1.1.3 Selection of UHV Transmission Voltage Levels

1.1.3.1 UHVAC Voltage Levels

The voltage level (nominal voltage) is the basic parameter of power grid. To determine the nominal voltage of UHVAC power grid, not only the maximum transmission capacity and transmission distance shall be taken into consideration, but also the impacts by the nominal voltage on the system dispatching operation and the cost and difficulty in manufacturing UHV power transmission and transformation equipment need to be considered. After the nominal voltage of UHV power grid is determined, the corresponding maximum operating voltage is to be determined. The determination of the UHVAC maximum operating voltage is related to many factors, such as the grid structure, nominal voltage of power grid, reactive power compensation and voltage regulation methods, line corridor altitude and overvoltage level of power transmission and transformation equipment. Comprehensively considering from the technical and economic aspects, the UHV nominal voltage in China is determined as 1000 kV, with the maximum voltage of 1100 kV. Table 1.4 shows the voltage selection and designed power transmission value for the UHV in some countries around the world [5, 6].

1. Selection of nominal voltage for UHVAC lines

(1) Saturation characteristic of air insulation clearance

For the selection of UHV transmission voltage level, the saturation characteristic of the air clearance insulation is an important factor to be considered. As with the increase of the voltage, the dielectric strength of gas media will show an obvious nonlinear saturation trend as the distance increases. Figure 1.1 shows the discharge voltage characteristic curves under rod–rod and rod–plane clearances with different clearance distances, from which the saturation relation between the dielectric strength of gas media and the insulation clearance distance can be seen [7, 8].

Table 1.4 UHV voltage levels in different countries

Country		Voltage/kV		Design transmission power/MW	Distance/km
		Nominal	Maximum		
USA	BPA	1100	1200	6000–8000	300–400
	AEP	1500	1600	>5000	400–500
Japan		1000	1100	5000–13000	About 200
Italy		1000	1050	5000–6000	300–400
Former Soviet Union		1150	1200	5000	2500
China		1000	1100	4000–6000	–[a]

[a]The Southeast Shanxi–Nanyang–Jingmen UHVAC transmission demonstration project that has been built has an overall length of 640 km (put into operation in January 2009); the Huainan–West Shanghai UHVAC double-circuit transmission project has an overall length of 642.7 km (put into operation in September 2013)

www.FreeEngineeringBooksPdf.com

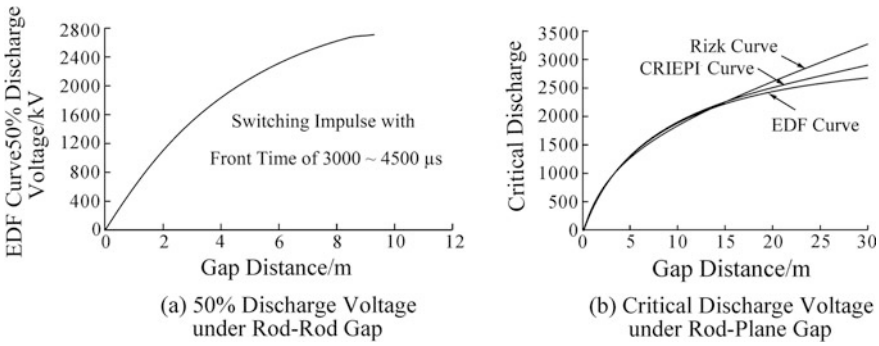

Fig. 1.1 Discharge voltage characteristic curves under rod–rod and rod–plane clearances with different clearance distances, reprinted from Ref. [7], copyright 2014, with permission from Power System Technology

Figure 1.1b is drawn based on a lot of experiments and researches and according to the regression formula for the relation between rod–plane clearance distance and critical discharge voltage raised by different scholars, and the formulas corresponding to the curves are known as EDF formula, CRIEPI formula and Rizk formula, respectively. It can be seen from Fig. 1.1b that, when the clearance distance <17 m, these three curves are close. But when the clearance distance is more than 17 m, they gradually separate from each other. Among the three curves, the saturation trend of EDF curve is more obvious and that of CRIEPI curve is between EDF and Rizk curves. Among the three curves, the CRIEPI formula has been accepted by IEC and is used in the calculation for obtaining the clearance coefficient. The formula is as follows:

$$U_{50.\mathrm{crit}} = 1080 \times \ln(0.66d + 1), \quad 1 \le d \le 25. \tag{1.1}$$

Table 1.5 shows the phase-to-phase insulation air clearance distance used in the implemented transmission line projects with three different voltage levels of 800, 1000, and 1150 kV.

It can be seen from Table 1.5 that the phase-to-phase distance of 1000 kV UHV power transmission lines is nearly as same as that of 800 kV EHV power transmission lines, which basically increases linearly as the voltage increases, while the phase-to-phase insulation distance of 1150 kV UHV lines is much greater than that of 1000 kV lines. Within 1000–1150 kV voltage range, the insulation clearance may have shown a relatively obvious nonlinear saturation trend with the increase of voltage. Once it enters into the obvious nonlinear saturation stage, even a small increase in the rated voltage of the lines leads to significantly increase of the air clearance insulation distance, which not only results in a substantial increase in UHV line corridor width, volume of equipment and substation land coverage, but also increases the technical difficulty and the total investment, while the transmission capacity is not increased much. In summary, in terms of the economy and

www.FreeEngineeringBooksPdf.com

Table 1.5 Phase-to-phase insulation clearance for the used voltage levels

Voltage level (kV)	Phase-to-phase insulation clearance (m)
800	8–10
1000	9–12
1150	24–29[a]

[a]The voltage level of 1150 kV was selected for the UHV lines of former Soviet Union. Its large insulation clearance was not only due to the insulation requirements, but also because of the abundant land resources and less consideration in the limits of line corridors. In case the voltage level of 1150 kV is to be developed in China, the design insulation clearance may be less than the value listed

technology, the selection of 1000 kV as the voltage level of UHV power transmission lines is relatively reasonable.

(2) Consideration based on power transmission capacity

The selection of UHVAC power transmission voltage levels is often related to the outward transmission power of large-scale power sources. The higher the voltage is, the larger the transmission power will be. The maximum transmission capacity of UHV power grid is mainly determined by the capacity of the power source at sending end, and the transmission distance is dependent on the geographical distribution of power source and load center. The single-circuit transmission capacity of the 1000 kV lines in Japan is about 5000–6000 MW. For the lines planned to be constructed by BPA in USA, the rated voltage is selected as 1100 kV and the transmission capacity as 6000–8000 MW. The former Soviet Union had a vast territory and was rich in energy, making the power transmission distance very long and the power transmission capacity very high. It once planned to construct several power plants with capacity in the range of 4000–6000 MW to jointly feed power to some of its load centers in Europe. The transmission capacity could be as high as tens of thousands MW grade. The corresponding voltage level was selected at 1150 kV since almost no limits to the line corridor needed to be considered.

Based on the analysis of China's power grid interconnection, the normal transmission power of the UHVAC lines is mostly around 4000–6000 MW and the transmission distance of UHVAC lines is usually around 600–1500 km. The relation among the optimal voltage U_{optimal}, transmission distance L and transmission power P of power grid as recommended by Г.А. Илларионов is as follows:

$$U_{U_{\text{optimal}}} = \frac{1000}{\sqrt{\frac{500}{L} + \frac{2500}{P}}} \tag{1.2}$$

Using this expression, the optimal voltage of China's UHV power transmission lines can be estimated. In the estimation, the transmission power of UHV transmission line is considered as 5000 MW and the transmission distance as 1000 km. By putting the corresponding figures in the above expression, the optimal voltage

www.FreeEngineeringBooksPdf.com

can be obtained as $U_{optimal}$ = 1000 kV. In combination with the actual conditions of power grid in China, the transmission capacity and transmission distance of UHVAC lines are normally around the above calculated values, and hence 1000 kV is selected as the nominal voltage of UHVAC power grid, which can meet the requirements of power transmission scale.

(3) Development law of voltage level and structure of China's power grid

According to the development laws of voltage levels around the world, the voltage ratio of adjacent levels is normally around 2–3. New voltage level cannot be selected as too low; otherwise, it will cause such problems as many electromagnetic loop networks, difficulty in tidal current control and large loss of power grid. It cannot be selected as too high, either; otherwise, the transmission capacity cannot be adequately utilized, leading to waste. Currently, 154–345–765–1500 kV voltage level and 110–220–500–1000 kV voltage level are the two voltage levels internationally recognized as reasonable. In view of the current conditions of China's power grid structure, the 500 kV grid structure is widely used in Northeast, North, Central, East and South China except for Northwest China where 330 kV grid structure is used. The aim of construction of the UHV power grid in China is to build a powerful UHVAC grid structure in North China, Central China and East China, which will gradually extend to the peripheral areas and form, jointly with the UHVAC and UHVDC systems fed from hydropower in Southwest China, the UHV power grid covering the large-scale power bases and load centers. Since the 330 and 750 kV EHV power grids have already formed in the Northwest region, the use of 330 and 750 kV AC power transmission already can meet the demands. Therefore, in the current planning, it is not necessary to construct UHVAC power transmission lines in the Northwest region of China. However, construction of UHVDC lines can be planned in the area to be connected with the grids nationwide. Therefore, the voltage level of China's UHV power transmission is selected at 1000 kV, i.e., it is suitable for the main grid framework to develop based on 110–220–500–1000 kV voltage level series.

(4) Other factors to be considered

Some UHVAC power transmission lines in China will have to pass through the west region where average altitude is about 1000–2000 m. High-altitude area has a higher requirement on the external insulation of equipment. Selection of a proper nominal voltage can mitigate the external insulation level of power transmission and transformation equipment thus reducing the equipment investment. In addition, the corona loss under severe weather is proportional to the operating voltage, under the same critical corona voltage, the higher the operating voltage is, the higher the corona loss of circuit line will be. When the same type of steel towers is used in the same area, the application of 1000 kV nominal voltage can reduce the height of steel towers and save the number of insulators as compared to 1150 kV nominal voltage. In addition, the construction cost of UHV transformer is mainly affected by external insulation level. Therefore, the construction cost of UHV transformer with

www.FreeEngineeringBooksPdf.com

higher nominal voltage will be higher than that with lower nominal voltage. In addition, UHV power grid with lower nominal voltage can reduce the cost of investment of reactive compensation equipment.

2. Selection of the maximum operating voltage for UHVAC system

The maximum operating voltage of system will affect the required capacity of phase-modulated and voltage-regulated equipment, the operation of generator and power transmission lines, the control standard of system operation as well as the manufacture and cost of equipment.

The upper limit of maximum operating voltage of the system is limited by altitude, corona loss and equipment manufacturing codes and standards. Therefore, the maximum operating voltage should not be determined as too high. Viewing the actual conditions of the manufacturing level of UHV equipment both in China and other countries, the maximum operating voltage of 1000 kV system should not exceed 1100 kV.

1.1.3.2 UHVDC Voltage Levels

The selection of UHVDC transmission voltage level is mainly determined by power transmission distance and transmission capacity. In terms of the basic principles and structure of engineering equipment, it is similar with the one of ±500 kV DC transmission, but due to the higher DC voltage to be withstood, the requirements of its inner and outer insulation are more stringent. Currently, the maximum DC voltage level that has been put into operation in the world is ±800 kV.

Since the 1970s, the study of UHVDC transmission has begun abroad, and a series of research results have been drawn. From the economy and environment points of view, in case of 1000–3000 km transmission distance, the DC power transmission of voltage level above ±600 kV is the preferred way; the technical difficulty of design, construction and operation of ±800 kV DC power transmission system is relatively small, and it has been successfully built and put into operation in China. Based on the current technologies and foreseeable developments, ±1000 kV DC power transmission system is feasible in theory, but the process must go through extensive research and development works in practice; the development of DC power transmission system with voltage level of ±1200 kV and above still needs a larger technical breakthrough.

Construction of ±800 kV UHVDC transmission project can achieve large-capacity and long-distance power transmission, reducing coal transportation and environmental pressure, while significantly reducing construction costs, reducing the occupation of land resources and reducing the network losses. Therefore, determining the rated voltage of China's UHVDC transmission as ±800 kV is reasonable from the technical and economic points of view. With the increase of power transmission demand and transmission distance and the continual maturing of ±1000 kV (±1100 kV) DC transmission technology, there will be more space for the development of ±1000 kV (±1100 kV) DC power transmission system in the future.

www.FreeEngineeringBooksPdf.com

1.2 Development of UHV Power Transmission Technology

Since the 1960s, due to the increased transmission capacity, the layout of transmission line corridor becomes more and more difficult, and the short-circuit current is close to the limit of switches, so the US, the Soviet Union, Canada, Japan, Italy and other countries have begun to study the UHV transmission technology, and after long working time, they have made many important research results in this field. Currently, India, Brazil, South Africa, and other countries are actively studying the UHV transmission technology.

US, the former Soviet Union, Italy, and Japan are the first countries to start on the research of UHV transmission technology. Among them, the former Soviet Union and Japan have built the critical UHVAC transmission lines; especially the former Soviet Union is the sole country having operating experience of UHVAC transmission project before China.

The research of UHV transmission technology in China started late, but with rapid development. Since January 2009, China has built many UHVAC and UHVDC transmission projects, such as Southeast Shanxi–Jingmen 1000 kV AC Transmission Project, Huainan–Shanghai 1000 kV AC Transmission Project, North Zhejiang–Fuzhou 1000 kV AC Transmission Project, Yunnan–Guangzhou ±800 kV DC Transmission Project, Xiangjiaba–Shanghai ±800 kV DC Transmission Project, Sichuan Jinping–Jiangsu Sunan ±800 kV DC Transmission Project, Yunnan Puer to Guangdong Jiangmen ±800 kV UHVDC Transmission Project, South Hami–Zhengzhou ±800 kV DC Transmission Project, and Xiluodu–Zhexi ±800 kV DC Transmission Project, for which the safe operation has remained, and the safety, economy and environmental friendliness of UHVDC transmission have fully been verified.

Up to August 2017, six 1000 kV UHVAC power transmission lines and nine ±800 kV UHVDC power transmission lines have been built and put into operation. There are still another 1000 kV UHVAC power transmission line and the other four ±800 kV UHVDC power transmission lines will be put into operation at the end of 2017. Moreover, one ±1100 kV UHVDC power transmission line is being built and will be put into operation in 2018.

The following will briefly describe the development process and major research items about the UHV power transmission technology of former Soviet Union (Russia), Japan, USA, Canada, Italy, and other countries.

1.2.1 The Former Soviet Union (Russia)

The former Soviet Union was one of the first countries to conduct the research of UHVAC and UHVDC transmission technology internationally, and has a wealth of experience in the actual operation of UHVAC transmission project.

The energy resource center is far from the load center in the former Soviet Union. It is not only rich in water resources but also contains a lot of coal in eastern

www.FreeEngineeringBooksPdf.com

Siberia. It also has a lot of coal resources in Kazakhstan region, while most of its power load was located in the west. So to ensure the electricity supply, the long-distance and large-capacity power transmission from east to west must be implemented.

The former Soviet Union had conducted comprehensive study on the basic technology of UHV transmission before 1972, mainly focusing on the key technologies of UHV transmission, such as insulation, systems, lines and equipment as well as the impact on the environment and other issues. During the period of 1972–1978, the former Soviet Union carried out the technical research of equipment, conducted trial run of prototype, and transferred it to full production in 1978–1980, and the prototype devices were put into trial operation for performance test.

In the period of 1973–1974, the former Soviet Union built a three-phase UHV test line section with length of 1.17 km at Beily Rast substation, to carry out the experimental study of UHV. In 1978, an industrial test line with length of 270 km was built for carrying out on-site assessment test to a variety of UHV equipment. In 1981, the former Soviet Union constructed UHV transmission line consisting of five sections, with a total length of 2344 km. In August 1985, the world's first 1150 kV line was put into operation at rated working voltage with load in the former Soviet Union. However, after the disintegration of the former Soviet Union, due to a number of reasons, such as the substantial reduction in transmission capacity, financial difficulties and political factors, the Kazakhstan central scheduling department reduced the voltage of 1150 kV line to 500 kV for operation.

The UHV transmission lines and substation equipment at both ends in the Former Soviet were actually operated for total cumulative running time of 4 years during 1985–1991 with the rated working voltage. During this period, the UHV power transformation equipments were running in good condition, and no major accidents such as power outage caused by tower collapse, line breakage and insulator damage took place, which not only proved high operational reliability of UHV technology, but also fully demonstrated the feasibility of UHV power transmission.

In terms of UHVDC power transmission, in 1980, the former Soviet Union began the construction of UHVDC power transmission project for transmitting the coal power generated at Ekibastuz coal-producing areas of the central territory of Kazakhstan to the load centers in its European part. The power transmission solution of ±750 kV, 6000 MW was used in this project. The DC equipment used in this project was developed by the former Soviet Union, and had passed the type test. But due to various reasons, the project was not actually put into operation (Fig. 1.2).

1.2.2 Japan

Japan is the second country in the world to conduct engineering practices in the field of UHVAC transmission. The construction of UHVAC transmission line in the

www.FreeEngineeringBooksPdf.com

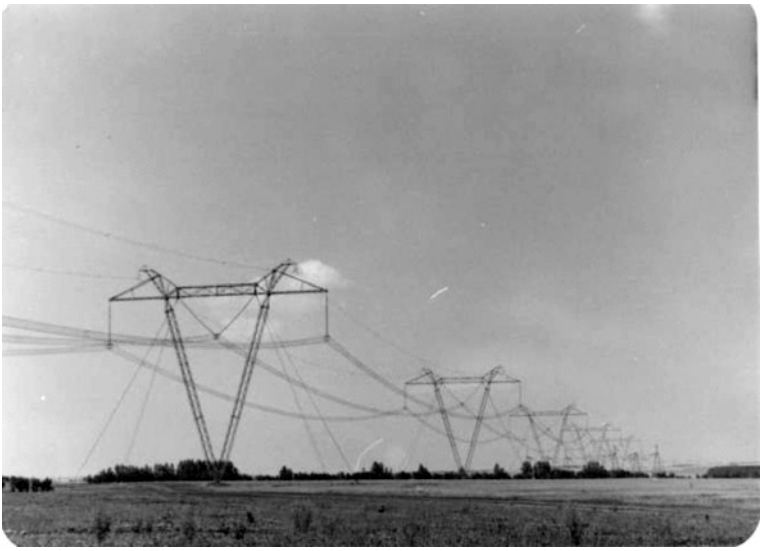

Fig. 1.2 UHVAC power transmission lines of the Former Soviet Union

Tokyo area is mainly to solve the difficulties of the transmission line corridors, the short-circuit current exceedance, etc. To obtain a stable power supply, Tokyo Electric Power Company (TEPCO) plans to build a series of coastal nuclear power plants, with a total capacity of over 17 million kilowatts. Because it is not far from Tokyo, through certification, the most economic scheme is using 1000 kV UHVAC transmission.

In 1980, the Central Research Institute of Electric Power Industry of Japan established a 1000 kV test line section with length of 600 m, double circuits and two spans at Akagi. On this test line section, the characteristic tests of 8-bundled conductor, 10-bundled conductor and 12-bundled conductor and towers in a strong wind and under earthquake conditions were carried out, and the researches on UHV construction and maintenance techniques, audible noise, radio interference, television interference, and ecological effects of electromagnetic fields and other aspects were conducted. Tokyo Electric Power Company researched and technically developed the mechanical properties of bundled conductors and insulator strings in the Takayama test line section, such as galloping and icing performance. Tokyo Electric Power Company uses NGK's corona test equipment and 1000 kV pollution test equipment for the radio interference and audible noise test of insulator strings under pollution conditions. In addition, the characteristics tests, such as the operation of line, lightning, power frequency overvoltage and phase-to-phase air clearance, as well as the flashover characteristic of prototype sleeves and string insulator under pollution conditions were also carried out on the line (Fig. 1.3).

Japan is the second country to successfully build the UHV lines in the world. In 1993, Tokyo Electric Power Company built the Kashiwazaki Kariwa–West Gunma–Higashiyamanashi UHV north–south transmission line, with length of

www.FreeEngineeringBooksPdf.com

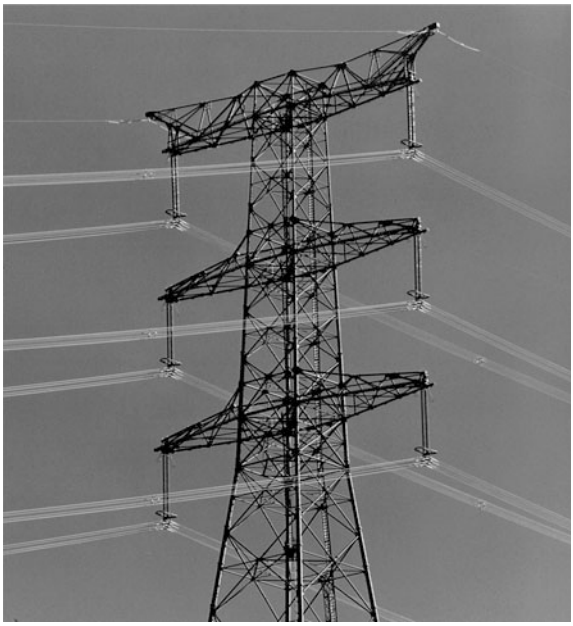

Fig. 1.3 UHV transmission lines in Japan

about 190 km, and in 1999, built South Iwaki–East Gunma UHV east–west transmission line, with a length of about 240 km. These UHV transmission lines were erected using double circuits on the same tower.

After the completion of the UHVAC lines, due to the slow growth of electricity demand in Japan and the postponement of construction plan of nuclear power, that line has been running at a reduced voltage of 500 kV.

1.2.3 United States

To reduce the land for transmission corridor, American Electric Power (AEP) has ever planned to build several 1500 kV AC transmission lines on the 765 kV grid. To transmit the electricity from the eastern coal base to the west load center, and to meet the needs of long-distance and large-capacity power transmission, US Bonneville Power Authority (BPA) also plans to build the transmission lines with 1000 kV voltage level.

The US has built Reno UHV testing ground (with line length of 523 m), in which the experimental study began in 1974. On Lyons UHV test line section (2.1 km) and Monroe mechanical test line (1.8 km), the experimental study began in 1976. In Renault test base, a number of test line sections have been built, including ±600 kV DC bipolar test line, on which AC environmental test, DC environmental test, AC and DC test in the same corridor, magnetic field trials under special arrangement of wires, etc., are carried out, respectively.

www.FreeEngineeringBooksPdf.com

Subsequently, the US does not put the research results of UHV transmission into project practice, mainly due to the slowdown in the growth of electricity demand since then, as well as implementation of a new energy development strategy, through which power plants were built at the load center, and the distributed power supplies were developed, thereby reducing the requirements of long-distance and large-capacity power transmission.

1.2.4 Canada

Canada Quebec Hydropower Bureau built an outdoor test site and studied the line conductor corona. The test lines and corona cage within the test site were used for the bundled conductor corona test of AC system up to 1500 kV and DC system up to 1800 kV. The air insulation tests of 1500 kV lines and substations were conducted in Quebec high-voltage test chamber. The study on four bundled conductors, i.e., 8×41.4 mm, 6×46.53 mm, 8×46.53 mm, and 6×50.75 mm were conducted in the outdoor test site of Quebec Hydro Bureau. Quebec Hydropower Bureau also studied the characteristics of corona, electric field and ion flow of ± 600 to ± 1200 kV DC transmission lines.

1.2.5 Italy

In the mid-1970s, to send the nuclear power under planning in the southern region to the load center in north region, and saving line corridor area meanwhile, Italian National Electricity Company (ENEL) started the experimental study of UHV transmission project. Entrusted by Western European International Power Generation Federation, Italy, and France also had ever done the demonstration works of the selection of AC 800 and 1000 kV transmission schemes in the European continent.

After establishing the research program of 1000 kV, Italian National Electricity Company carried out relevant researches at different test stations and laboratories. Italian National Electricity Company tested the switching and the lightning impact, including switching impulse characteristics of air clearance, the surface insulating properties of UHV system under atmospheric contamination, SF6 gas-insulated properties, the development and test of unconventional insulators. On the testing line sections at Sava Reto, audible noise, radio noise, and corona losses were measured. In corona test cages, symmetrical bundling structure was tested for up to 14 conductors, asymmetric bundling structure was tested for 6, 8, and 10 sub-conductors and the tubular conductors with a diameter of 0.2, 0.4, and 0.6 m. The experimental research has also been carried out on the interference levels of UHV insulators and fittings and the mechanical structure of line vibration dampers,

www.FreeEngineeringBooksPdf.com

spacers, suspension fittings, and connections. In addition, the ecological effects of electromagnetic fields had been studied in Sava Reto UHV test line and corona cage.

The development of UHV transmission in other countries provides experience and lessons for the development of UHV transmission in China. Through the research and development of UHV technology by these countries, the technical issue was no longer a limiting factor to UHV development. Now the development of UHV transmission is mainly determined by the demands of large-capacity transmission. After entering into the 1990s, UHVAC transmission was becoming quiet in the international arena, its engineering applications were at a standstill, and even the projects that have been built were operated at a reduced voltage. The main reason lies in the fact that the growth rates of the economy and the power consumption of the countries are much lower than the expected ones, reducing the need for long-distance and large-capacity power transmission. But with the growth of electricity demand in the future, this situation will change. For example, the basic distribution pattern of the power resources and the load centers in Russia has not been changed yet, so it is still possible to develop UHVAC and UHVDC transmission systems in the future. For the UHVAC transmission lines in Japan, it was also planned to increase to 1000 kV for operation after the transmission needs were increased, but an earthquake/tsunami/nuclear disaster occurred in 2011 which had a tremendous impact on the construction of nuclear power plants group at Fukushima area in the future. Therefore, whether the issue of "voltage step-up" will be finally realized or not still remains to be seen.

References

1. Zhou H. Recommendation for the development of AC UHV power transmission in China. High Volt Eng. 1996;22(1):25–7.
2. Zhao Z. Brief on characteristics of EHV and UHV transmission and segmentation of voltage levels. High Volt Eng. 1982;2:19–25.
3. Huang X. Compendium of the history of the development of power technology. Beijing: China Water Power Press; 1986.
4. Li L. Technical characteristics and engineering applications of UHV DC power transmission. Electr Equip. 2006;7(3):1–4.
5. Xiang L, Wang L, Li T. Overview and analysis of development of foreign UHV transmission. Power Syst Technol. 1987;1:59–63.
6. Xiang L. Speed up earlier UHV transmission research in China. Power Syst Technol. 1996;20 (2):54–8.
7. Zhou H, Yu Y. Discussion on several important problems of developing UHV AC transmission in China. Power Syst Technol. 2005;29(12):1–9.
8. Wan Q, Huo F, Xie L, Xu T. Summary of research on flashover characteristics of long air-gaps. High Volt Eng. 2012;38(10):2499–505.

www.FreeEngineeringBooksPdf.com

Chapter 2
Development of UHV Power Transmission in China

Ke Sun, Shichao Yuan and Yuting Qiu

The objective requirements for the development of UHV transmission in China are raised based on the continued rapid growth in electricity demand, unevenly distributed energy resources, and lagged development of power grid. For long-distance and large-capacity power transmission, compared with the use of low-voltage level power transmission technology, UHV has obvious advantages in improving the transmission capacity, conservation of land resources, and reduction of transmission losses and savings of investment, etc. In addition, the development of UHV power transmission is of great significance for improving China's technological innovation ability and promoting the upgrading and development of the equipment manufacturing industry and other aspects.

This chapter first discusses the necessity of the development of UHV power transmission in China, and then the development planning and development process of UHV power grid in China, and finally provides a brief introduction of 1000 kV UHVAC and ±800 kV UHVDC projects that have been completed or under construction.

K. Sun (✉)
Zhejiang Electric Power Corporation, Hangzhou, Zhejiang
People's Republic of China
e-mail: ssunke@sina.com

S. Yuan
State Grid Ningbo Power Supply Company, Ningbo, Zhejiang
People's Republic of China
e-mail: 87221678@qq.com

Y. Qiu
State Grid Shanghai Power Supply Company, Shanghai, Zhejiang
People's Republic of China
e-mail: ytqiu0927@163.com

© Zhejiang University Press, Hangzhou and Springer-Verlag GmbH Germany 2018

H. Zhou et al. (eds.), *Ultra-high Voltage AC/DC Power Transmission*,
Advanced Topics in Science and Technology in China,
https://doi.org/10.1007/978-3-662-54575-1_2

www.FreeEngineeringBooksPdf.com

2.1 Necessity in the Development of UHV Power Transmission in China

2.1.1 Objectively Required by the Sustained and Rapid Growth in Electricity Demands

Since the reform and opening up policy of China, with the sustained and rapid development of China's national economy, the electric power industry is under accelerating development. By the end of 2006, the national power generation capacity reached 620 million kW, and the total electricity consumption reached 2.8 trillion kWh. It is expected that the installed capacity will reach up to 1.3 billion kW in 2020, and the electricity consumption will reach 6.6 trillion kWh [1, 2]. The electricity demand and power construction scale are huge. Figure 2.1 shows the growth of China's installed capacity and electricity consumption since the reform and opening up (Figs. 2.2, 2.3; Table 2.1).

2.1.2 Objectively Required by the Long-Distance and Large-Capacity Power Transmission

China's basic national conditions are: the energies for power generation are mainly based on coal and water, and the energy resources and the development of productive forces were in reverse distribution. China is bound to develop long-distance and large-capacity power transmission due to these conditions, which are referred as of three "2/3" conditions hereafter [3].

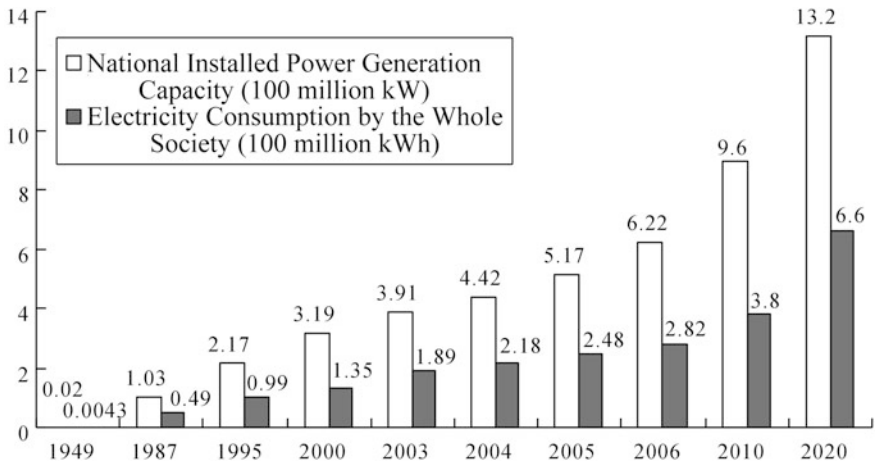

Fig. 2.1 Growth of China's installed power generation capacity and electricity consumption by the whole society

www.FreeEngineeringBooksPdf.com

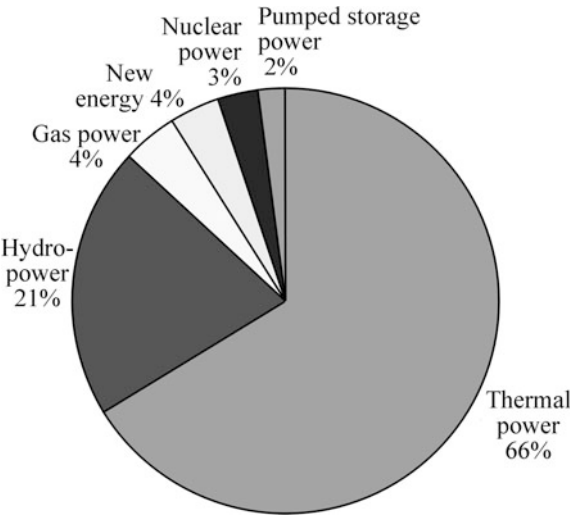

Fig. 2.2 Proportion of various power generation energies in China by 2020

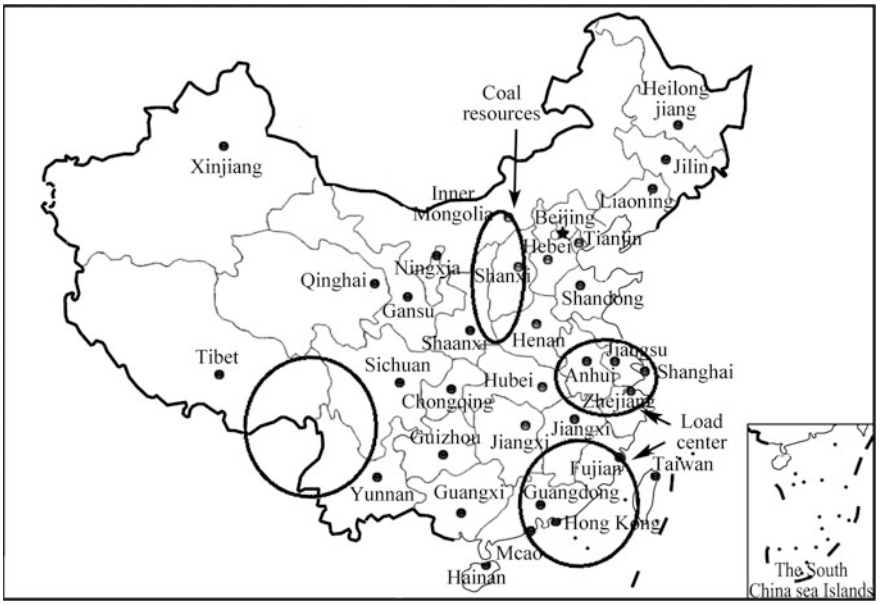

Fig. 2.3 Extremely uneven energy and load distribution in China

1. China's exploitable hydropower resources rank first in the world (about 395 million kW). By the end of 2008, the national total installed hydropower capacity (170 million kW) ranked first in the world, and the world's largest running hydropower station (Three Gorges Hydropower Station) by far is also in

www.FreeEngineeringBooksPdf.com

Table 2.1 Distances from China's power bases to load centers

Starting point	Terminal point	Distance (km)
Northwest coal power base	Load centers in Central and East China	800–1700
Southwest hydropower base	Load centers in Central and East China	1500–2500
Xinjiang coal power base	Load center in East China	>3000

China. However, about 2/3 of the hydropower resources that can be developed are located in southwest of China, such as Sichuan, Yunnan, and Tibet Provinces, which are far from the load centers.

2. China's coal reserves are about 1 trillion tons, ranking the third in the world, but there are about 2/3 located in the "Three West Regions" of the northwest provinces (Shanxi, Shanxi, and western part of Inner Mongolia), which are far from the load centers.
3. About 2/3 of China's electricity load is located at the east coast and the economically developed areas to the east of Beijing–Guangzhou railway.

The distances between the above-mentioned energy resources and load centers are mostly between 800 and 3000 km. These basic conditions decide the necessity of using UHV power transmission in China, and the basic pattern of the power flow is necessarily large-capacity and long-distance power transmission, which is known as "West to East Power Transmission Project".

2.1.3 Objectively Required by the Basic Law of Power Grid Development

The development process of power systems from small scale to large scale, from low voltage to high voltage, from isolation system to interconnected system reflects the basic laws of power industry development. Using high-voltage level and developing large-scale power grid are the general trend of the development of the world's electricity. The construction of national grid with UHV power grid as the backbone and the coordinated development of power grid at all levels are in line with the basic national conditions of energy resources and economic development of reverse distribution, are in line with the overall deployment of the national energy saving, can change the lagging behind in development of Chinese grid, and are effective ways to achieve a coordinated development of the power grid and power sources, as well as the urgent need to build a resource-saving and environment-friendly society.

2.1.4 Required to Ensure Safe and Reliable Energy Transmission

The transportation of coal has a very high reliability under normal circumstances, but under specific conditions, this energy transmission is also affected by external factors, of which the most obvious one is the impact of the snow disaster weather. Due

www.FreeEngineeringBooksPdf.com

to the snow in winter weather coupled with the pressure of passenger transport during the Spring Festival in China, the rail and road freight transmission will be severely affected. A large number of coal-fired electricity generating units that far from coal producing areas are suffering from the shortage of adequate electricity coal supply, resulting in a wide range of power shortage phenomenon appearing in winter season in China, bringing inconvenience to people's lives, and posing the enormous threat to the safety of production. Although the safety of the power transmission has ever affected by the snow disaster, with improved transmission technology, the anti-ice capacity of grid will be growing, and the issue of melting ice will be considered as a key technical problem for the UHV transmission line at the beginning of the design, to ensure that the impact of disasters to the line is as small as possible, and to improve the safety and reliability of power supply. Therefore, locally converting the primary energy in the rich region into electricity, and having it efficiently delivered to the load-intensive areas by means of UHV lines, to achieve simultaneous development of power transmission and coal transportation, as well as coordinate with and complement each other, thus improving the reliability of energy supply, have become an important problem to be solved urgently in China.

2.2 Development Process of UHV Power Transmission in China

The research of UHV transmission technology in China started relatively late. Since 1986, the UHV power transmission research had successively been included in China's "Seventh Five-Year Plan", "Eighth Five-Year Plan", and "Tenth Five-Year Plan" key science and technology research programs. During 1990–1995, Significant Project Office of the State Council organized "argumentation on long-distance transmission mode and voltage levels"; during 1990–1999, the thematic studies on "UHV early demonstration" and "feasibility of million volts AC high voltage transmission" were organized by the Science and Technology Commission of China.

It is proven by the practical experience of the development of EHV and UHVAC and UHVDC transmission in different countries that, whenever it is necessary to adopt a new transmission of one higher voltage level, it generally must go through three stages: First, build a new experimental research base to conduct the test and research on the various basic characteristics of the transmission systems of the new voltage level and related equipment; second, construct an industrial test project; third, construct an official commercial transmission systems. In general, these three stages will take 10–20 years [4–6].

2.2.1 Preliminary Study of UHV

Since 1986, China Electric Power Research Institute, Wuhan High Voltage Research Institute, Electric Power Research Institute, and related universities have

www.FreeEngineeringBooksPdf.com

carried out the basic research on UHV power transmission, including the discharge characteristics of UHV external insulation, environmental impact of UHV, power frequency, and operating over-voltage, etc. In 1994, Wuhan High Voltage Research Institute constructed a test line section at 1000 kV voltage level, with length of 200 m, and 8 bundled conductors. At the tower experimental station constructed by Electric Power Research Institute in 2004, the prototype strength test can be carried out for the UHV single circuit, 8 × 800 mm bundled conductor, 30°–60° angle tower, and the shockproof design for power transmission lines can be tested. China Wuhan High Voltage Research Institute started the construction of UHV outdoor test site as early as in 1988. By 1996, China's first true class type 1000 kV UHV test line had been formally completed, and therefore, China had its first large-scale UHV test and research unit.

2.2.2 Construction of UHV Test Base

2.2.2.1 UHVAC Test Base of Wuhan High Voltage Research Institute

To fully meet the requirements of comprehensive study of UHVAC and UHVDC transmission technology and the electrified assessment of UHV power transmission equipment etc., the State Grid Corporation has constructed two new larger and more modern UHV research bases. The UHVAC test base was started in September 2006, and the double-circuit test line was fully charged in June 15, 2007; the UHVDC test base was started in March 2007, and the test line was fully charged in June 28, 2007. The construction of UHV test bases plays a role in optimizing the design of UHV construction by creating the conditions for providing empirical evidence and technical support, and it also tested the ability of Chinese design, manufacture, and construction of UHV projects to some extent.

The UHVAC test base is located in Wuhan City, including UHVAC single-circuit and double-circuit test lines on the same tower, electromagnetic environment measurement laboratory, environment and climate laboratory, charged assessment courses for UHV equipment, and other test equipment. The transmission line and towers at the base are as shown in Figs. 2.4 and 2.5.

The UHVAC test base covers an area of 133,400 m^2, and the equipment is developed and provided by more than 20 manufacturers in China. Its comprehensive testing capabilities create a number of world firsts, including:

1. adjustable geometry of UHV test lines and functions of tower optimization test;
2. having the devices to simulate the external insulating properties of the test conditions at altitude up to 5500 m;
3. all-weather electromagnetic environmental monitoring system;
4. pollution flashover testing capabilities of full-size UHVAC insulator string;
5. function of UHV GIS/AIS full-voltage and full-current live examination field;

www.FreeEngineeringBooksPdf.com

Fig. 2.4 Single-circuit test lines

Fig. 2.5 Double-circuit test lines

www.FreeEngineeringBooksPdf.com

6. voltage levels and capacity of power frequency resonance test device;
7. comprehensive training function and conditions of UHV operation, maintenance, and live working.

2.2.2.2 Beijing UHVDC Test Base of China Electric Power Research Institute

UHVDC test base is located in Beijing, consisting of the UHVDC test line section, outdoor test field, test hall, pollution and environmental test chambers, line electromagnetic environment simulation testing site, corona cage, insulators laboratory, and arresters test chamber. Experimental studies can be fully carried out to test UHVDC up to ±1000 kV electromagnetic environment, insulating properties, etc., and the charged assessment of the device for a long time. Currently, the line test in the base has successfully been boosted to ±1100 kV and started a stable operation, which can provide valuable design basis and strong technical support for the engineering design of new voltage level.

The transmission lines and towers in the UHVDC test base are as shown in Fig. 2.6.

Fig. 2.6 UHVDC test lines and towers

www.FreeEngineeringBooksPdf.com

2.2.2.3 Yunnan Kunming High-Altitude UHV Test Base of China Southern Power Grid

China Southern Power Grid built a UHV test base in Kunming, Yunnan, with the study objects also are 1000 kV AC and ±800 kV DC, and the research focuses on the outer insulation at high altitudes.

2.2.2.4 High-Current Switching Test Base of Xi'an High Voltage Apparatus Research Institute

The test site has the ability to conduct 1100 kV/120 kA AC equipment capacity test, 1100 kV AC equipment insulation test, ±1100 kV DC converter valve insulation, and run tests, which have reached the world advanced level, and some of which are in the international leading level.

Whenever a new voltage level is used, many new problems will occur. Because the research at test base is often not sufficient, and if it is not assessed through the actual test run, the result may not be cautious and conservative enough, likely to cause serious damage. Therefore, it is an appropriate and prudent practice to build an industrial test project first to find problems, accumulate operating experience, and improve the mastering of new technologies. The undertaking of costly and unprecedented UHV power transmission project is even an essential step.

2.2.3 China's UHV Transmission Projects

Up to August 2017, six 1000 kV UHVAC power transmission lines and nine ±800 kV UHVDC power transmission lines have been built and put into operation. There is still another 1000 kV UHVAC power transmission line and the other four ±800 kV UHVDC power transmission lines will be put into operation at the end of 2017. Moreover, one ±1100 kV UHVDC power transmission line is being built and will be put into operation in 2018.

2.2.3.1 Southeast Shanxi–Nanyang–Jingmen 1000 kV UHVAC Transmission Demonstration Project

The project started from Shanxi Changzhi Substation (Jindongnan Substation), through Henan Nanyang Switchyard, and ended at Hubei Jingmen Substation, with total line length of approximately 640 km, rated transmission power of 5000 MW, and total static investment of 5.688 billion Yuan. The project was commenced in August 2006 and put into operation at the end of 2008. After the completion of 168-h trial run at 22:00 on January 6, 2009, it was officially put into commercial operation. The project scale covered: a bank of 3000 MVA transformers and a bank of 960 Mvar high-voltage shunt reactors installed at Jindongnan Substation; two banks of 720 Mvar high-voltage

www.FreeEngineeringBooksPdf.com

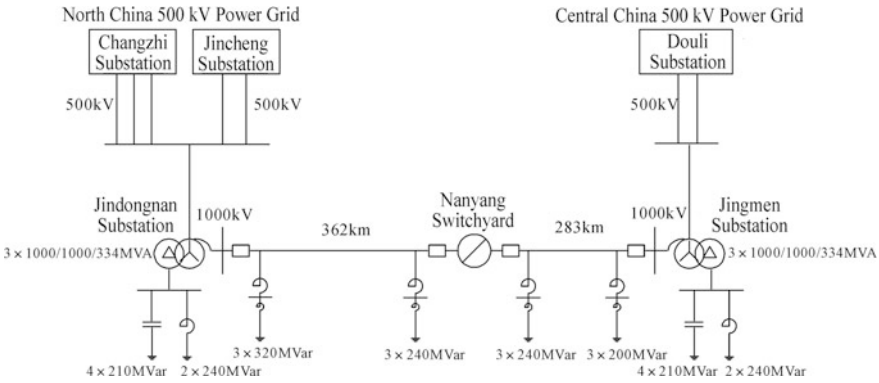

Fig. 2.7 Sketch of UHVAC project

shunt reactors installed at Nanyang Station which was a switchyard; and a bank of 3000 MVA transformers and a bank of 600 Mvar high-voltage shunt reactors installed at Jingmen Substation. All these three stations adopted the 3/2 circuit breaker wiring method, with incomplete strings applied at the initial stage of construction and two circuit breakers installed, as shown in Fig. 2.7.

The State Grid Corporation expanded the project in 2011, with a bank of 3000 MVA UHV transformers additionally installed at Jindongnan Substation and Jingmen Substation, respectively, and two banks of 3000 MVA UHV transformers additionally installed at Nanyang Switchyard. The supporting primary and secondary electrical equipments such as switches are installed ether. The UHV series compensators with 40% compensation degree (20% on each side) were installed in the line section from Southeastern Shanxi to Nanyang, and the UHV series compensators with 40% compensation degree [concentrated at Nanyang side] were installed in the line section from Nanyang to Jingmen. The UHV series compensators, large-capacity UHV switches, two-legged UHV transformers, and other new UHVAC devices were successfully used in this project, with integrated localization rate of over 90%.

The 1000 kV Southeast Shanxi–Nanyang–Jingmen UHVAC Demonstration Project Expansion Works was officially put into production on December 16, 2011. After the expansion, the three stations, i.e., Jindongnan Substation, Nanyang Switchyard, and Jingmen Substation, were installed with two banks of UHV main transformers with capacity of 3 million kW and the maximum transmission capacity up to 5 million kW.

2.2.3.2 Huainan–Shanghai 1000 kV UHVAC Transmission Project (Power Transmission Project from Anhui to Eastern China)

This project was commenced in October 2011 and completed in August 2013. The Power Transmission Project from Anhui to Eastern China started from Anhui 1000 kV Huainan Substation, through Anhui 1000 kV Wannan Substation and Zhejiang 1000 kV Zhebei Substation, and ended at Shanghai 1000 kV Huxi Substation, with

www.FreeEngineeringBooksPdf.com

transformation capacity of 21 million kVA, overall line length of 2 × 648.7 km, and total investment of about 18.6 billion Yuan. The system had a nominal voltage of 1000 kV and the maximum operating voltage of 1100 kV, using the large-capacity UHV transformer with rated capacity of 3 million kVA and the sulfur hexafluoride gas insulated metal enclosed switchgear with rated interrupting current of 63 kA, erected on the same tower in double circuits for the full line. This project was completely and independently designed, manufactured, and constructed by China.

The Power Transmission Project from Anhui to Eastern China, connecting the coal power bases in Anhui Huainan and Huaibei and the load centers of East China power grid, undertook the outward power transmission task of the coal bases in Anhui Huainan and Huaibei. After the project is completed, the scale of electricity transmission from Anhui to East China will be expanded and the safe and reliable outward power transmission from the coal power bases in Huainan and Huaibei will be ensured, and further to meet the electricity demand by north Zhejiang and Shanghai, having important economic and social significances.

2.2.3.3 Yunnan–Guangdong ±800 kV UHVDC Transmission Project

The Yunnan–Guangdong ±800 kV UHVDC Transmission Project is not only the independent UHVDC transmission demonstration project in China, but also the first UHVDC transmission project put into commercial operation in the world. This project started from Chuxiong Converter Station in Lufeng County, Chuxiong Prefecture, Yunnan Province in the west and went to Suidong Converter Station in Zengcheng District, Guangzhou City, Guangdong Province in the east, through Yunnan, Guangxi, and Guangdong provinces, with transmission distance of 1373 km and transmission power of 5000 MW. The project was put into monopolar operation on December 28, 2009 and put into bipolar operation on June 18, 2010. The total investment was about 13.2 billion Yuan.

2.2.3.4 Xiangjiaba–Shanghai ±800 kV UHVDC Power Transmission Demonstration Project

The Xiangjiaba–Shanghai ±800 kV UHVDC Demonstration Project was officially put into operation in July 2010. The project started from Sichuan Fulong Converter Station, through eight provinces and cities, i.e., Sichuan, Chongqing, Hunan, Hubei, Anhui, Zhejiang, Jiangsu, and Shanghai, and ended at Shanghai Fengxian Converter Station, with overall line length of approximate 1907 km.

The project had a rated current of 4000 A, rated transmission power of 6400 MW, and the maximum continuous transmission power of 7200 MW. The project adopted the main wiring method of double 12-pulse converters connected in series (400 + 400 kV) for each pole. The capacity of converter transformers was (24 + 4) × 297.1 (321.1) MVA (with four for standby); the type of converter transformer was the single-phase double-winding transformers fitted with on-load

www.FreeEngineeringBooksPdf.com

tap-changer; the ±800 kV DC switchyard adopted bipolar wiring and was provided with bypass circuit breaker and disconnector circuit for each 12-pulse valve bank; Fulong Converter Station had nine circuits of 500 kV AC outgoing lines, and Fengxian Converter Station had three circuits of 500 kV AC outgoing lines.

2.2.3.5 Jinping–Sunan ±800 kV UHVDC Transmission Project

This project started from Yulong Converter Station in Xichang City, Sichuan in the west, through eight provinces and cities, i.e., Sichuan, Yunnan, Chongqing, Hunan, Hubei, Anhui, Zhejiang, and Jiangsu, and ended at Tongli Converter Station in Suzhou City, Jiangsu Province, with overall line length of 2059 km and total investment of 22 billion Yuan. On December 12, 2012, the Jinping–Sunan ±800 kV UHVDC Power Transmission Project was officially put into commercial operation after the full completion of system commissioning and trail operation.

The project increased the UHVDC transmission capacity from 6400 to 7200 MW, and broke through 2000 km in the power transmission distance for the first time, creating a new record in UHVDC power transmission. After the project was fully put into operation, the electricity of about 36 billion kWh could be transmitted to East China annually.

2.2.3.6 Yunnan Puer–Guangdong Jiangmen ±800 kV DC Power Transmission Project (Nuozhadu DC Project)

This project started from Yunnan Puer Converter Station and ended at Guangdong Jiangmen Converter Station, with overall line length of 1413 km and rated transmission capacity of 5 million kW. On September 3, 2013, the Yunnan Puer–Guangdong Jiangmen ±800 kV DC Power Transmission Project began to send power to Guangdong, which was the second UHVDC transmission line constructed by China Southern Power Grid Company after the Yunnan–Guangdong ±800 kV UHVDC Transmission Project. Yunnan has abundant hydropower resource, with economic and exploitable capacity of 95.7 million kW in far future. By the later period of the "Twelfth Five-Year Plan", in addition to meeting its own electricity demand, there will be a lot of surplus hydropower for outward transmission. The completion and operation of this project are of important significance for optimizing the configuration of resources in East and West China, transmitting the clean power in West China and meeting the rapidly growing demand for electricity by Guangdong and other provinces.

2.2.3.7 Northern Zhejiang–Fuzhou 1000 kV UHVAC Transmission Project

The construction of the project was commenced on April 11, 2013, officially put into operation in December 2014. The Northern Zhejiang–Fuzhou UHVAC Transmission

www.FreeEngineeringBooksPdf.com

Project starts from Zhejiang 1000 kV Zhebei Substation, goes through 1000 kV Zhezhong Substation and Zhenan Substation, and ends at Fujian 1000 kV Fuzhou Substation, with overall line length of 2 × 603 km, transformation capacity of 18 million kVA, and newly built lines of 2 × 603 km. The total investment is more than 18 billion Yuan. The Northern Zhejiang–Fuzhou UHVAC Transmission Project is an important part of the UHV main grid framework in East China, which has important significance for improving the transmission capacity of Zhejiang and Fujian networking, meeting the needs to send out the surplus electricity of Fujian power grid during the peak load period in near future and getting such benefits from the interconnection between the main power grids of Fujian and East China as peak load shifting and regulation, interbasin compensation, and surplus and deficiency regulation.

The Northern Zhejiang–Fuzhou UHV Transmission Project is the third UHVAC transmission project built in China after the Southeast Shanxi–Nanyang–Jingmen Project and the Huainan–North Zhejiang–Shanghai Project.

2.2.3.8 South Hami–Zhengzhou ±800 kV UHVDC Transmission Project

This project, with total line length of 2210 km and project investment of 23.39 billion Yuan, is the UHVDC transmission project with the highest voltage level, the largest transmission capacity, and the longest transmission distance in the current world, passing through six provinces, i.e., Xinjiang, Gansu, Ningxia, Shaanxi, Shanxi, and Henan, and ending at Zhongzhou Converter Station in Zhongmu County, Zhengzhou. The project, approved for construction commencement in May 2012, is the major measure to further promote the strategies of "Development of West China" and "Power Transmission from West to East", promote conversion of Xinjiang resource advantages, serve the local economic and social development, and ease the contradiction between power supply and demand in Central China.

This project was formally put into operation in January 2014. It will provide annually more than 40 billion kWh of electricity to Henan, which is equivalent to the energy produced by more than 20 million tons of coal annually transmitted to Henan in a clean and efficient way. It can effectively alleviate the contradiction between the rapid growth of load and the inadequate total amount of resources and short supply of coal in Henan Province.

The six bundled conductors with large section of 1000 mm^2 were used in this project for the first time, and a number of innovation achievements in application of large-size angle steels and large-tonnage insulators were made.

2.2.3.9 Xiluodu–West Zhejiang ±800 kV UHVDC Transmission Project

The Xiluodu–West Zhejiang project was formally approved in July 2012 and put into operation in July 2014. The project started from Shuanglong Converter Station

www.FreeEngineeringBooksPdf.com

in Yibin, Sichuan, goes through 48 cities in five provinces, i.e., Sichuan, Guizhou, Hunan, Jiangxi, Zhejiang, and ended at Zhexi Converter Station in Jinhua, Zhejiang, with overall line length of 1728 km and transmission capacity of 8 million kW, which is the renewable energy key project during the "Twelfth Five-Year Plan" in China.

This project is significant to ensure the power outward transmission of the Sichuan hydropower and relieve power utility pressure in Zhejiang, which is beneficial to optimizing allocation of clean energy in a larger scope, has great importance to achieving balanced regional economic development, and is the embodiment of implementing the western development strategy and converting the western resource advantage into the economic advantage, a strategy move to implement the scientific concept of development in electric power industry and the concrete measure of State Grid Corporation to implement the strategic planning of UHV power grid with four huge resources and take the road of sustainable development.

Some of the UHVAC and UHVDC transmission projects that have been built or under construction in China are shown in Tables 2.2 and 2.3.

Table 2.2 UHVAC transmission projects in China

S/N	Project Name	Time Put into Operation	Rated Voltage /kV	Length /km	Transmission Capacity /MW
1	South Shanxi-Nanyang-Jingmen	2009	1000	640	5000
2	Huainan-North Zhejiang-Shanghai	2013	1000	2×648.7	6500
3	North Zhejiang-Fuzhou	2014	1000	2×603	4000–6000
4	Ximeng-Shandong	2016	1000	2×730	6500
5	Huainan-Nanjing-Shanghai	2016	1000	2×759	6500
6	West Inner Mongolia-South Tianjin	2016	1000	2×608	6500
7	Yuheng-Weifang	under construction	1000	2×1048.5	6500

www.FreeEngineeringBooksPdf.com

Table 2.3 UHVDC transmission projects in China

S/N	Project Name	Time Put into Operation	Rated Power /MW	DC Voltage /kV	Length /km
1	Chuxiong-Guangzhou	2010	5000	±800	1373
2	Xiangjiaba-Shanghai	2010	6400	±800	1907
3	Jinping-Sunan	2012	7200	±800	2059
4	Nuozadu-Guangdong	2013	5000	±800	1413
5	South Hami-Zhengzhou	2014	8000	±800	2192
6	Xiluodu-West Zhejiang	2014	7500	±800	1653
7	East Ningxia-Zhejiang	2016	8000	±800	1720
8	Jiuquan-Hunan	2017	8000	±800	2383
9	Shanxi-Jiangsu	2017	8000	±800	1119
10	Ximeng-Jiangsu	under construction	10000	±800	1620
11	Shanghai-Shandong	under construction	10000	±800	1238
12	Northwest Yunnan-Guangdong	under construction	5000	±800	1959
13	Jarud-Qingzhou	under construction	10000	±800	1234
14	Zhundong-South Anhui	under construction	12000	±1100	3324

References

1. Qingyun Y. Development planning and research achievements of UHVDC transmission in China. Electr Equip. 2007;8(3):1–4.
2. Zhao X, Zhang X. Application and development of UHV power transmission technology in China. Symposium Proceedings on Protection and Control of China's Electric Power System. 2006.
3. Shen Y, Peng X, Mao X, et al. Comprehensive evaluation indexes framework and evaluation method on location layout of UHV substations. Power Syst Technol. 2012;36(12):44–53.
4. Yonghua Y. A study of large UHV electric power grid development planning. Power Syst Clean Energy. 2009;25(10):1–3.
5. Yunzhou Z. Exploration of several problems of UHV transmission planning in China. Power Syst Technol. 2005;29(19):19–22.
6. Xu B. Proposals concerning interconnection of regional power systems. Power Syst Technol. 1999;23(9):32–4.

www.FreeEngineeringBooksPdf.com

Chapter 3
Analysis on System Characteristics and Economy of UHV Power Transmission

Guang Chen, Hao Zhou, Jiyuan Li and Jingzhe Yu

This chapter will first discuss the system characteristics of UHVAC and UHVDC power transmission, mainly including the parameter characteristics of the transmission lines and the main transformer, the transmission characteristics, and transmission capacity of power grid and the reliability and stability of the system as well as the characteristics of the transmission and transformation equipment, such as high-voltage shunt reactors and series capacitors. Then, the analysis on economy will be made for UHV power transmission, mainly including the comparison of economy of UHVAC and EHVAC power transmission, the comparison of economy of UHVDC and EHVDC power transmission, etc. Finally, the technical characteristics and applicable occasions of UHVAC and UHVDC power transmission will be discussed.

G. Chen (✉)
State Grid Jiangsu Electric Power Research Institute, Nanjing, Jiangsu, People's Republic of China
e-mail: 416797015@qq.com

H. Zhou · J. Li · J. Yu
College of Electrical Engineering, Zhejiang University, Xihu District, Hangzhou, Zhejiang, People's Republic of China
e-mail: zhouhao_ee@zju.edu.cn

J. Li
e-mail: lijiyuan_ee@zju.edu.cn

J. Yu
e-mail: 21510213@zju.edu.cn

© Zhejiang University Press, Hangzhou and Springer-Verlag GmbH Germany 2018

H. Zhou et al. (eds.), *Ultra-high Voltage AC/DC Power Transmission*,
Advanced Topics in Science and Technology in China,
https://doi.org/10.1007/978-3-662-54575-1_3

www.FreeEngineeringBooksPdf.com

3.1 System Characteristics of UHVAC Power Transmission

3.1.1 Reliability and Stability

1. Reliability

The reliability of UHV power transmission and transformation project is the system characteristic representing the magnitude of the system's safe operating risk, and its evaluation is carried out through analysis on and calculation of the following reliability indexes. These indexes mainly include the probability of failures resulting from the factors of power transmission and transformation project itself and the atmospheric environmental factors in the place where the project locates, the impact of such failures on the capacity of power transmission and the economic losses incurred, etc. No matter for AC or DC power transmission system, an appropriate reliability model shall be established to build the reliability index system and establish the perfect safe operation system; besides, the key elements that affect the system reliability shall be analyzed and the necessary measures shall be taken to improve the reliability of UHV power transmission.

In consideration of the failure probability, repair rate summarized from various equipment of AC transmission and transformation project and the N-1 criteria, the major indexes of reliability of UHVAC project consist of line average disconnection rate/[times·(100 km·a)$^{-1}$] and line average transmission interruption rate/[times·(100 km·a)$^{-1}$]. Table 3.1 gives the statistical data on the operating reliability of lines with three voltage levels in the former Soviet Union during 1985–1992 [1].

It can be seen from the operating experience of the former Soviet Union that the statistical failure rate of 1150 kV UHV transmission line is significantly lower than that of 500 and 750 kV EHV lines, with an extremely high reliability in power supply. In addition, the statistics show that 80% of the transmission interruption failures of the UHV lines in the former Soviet Union are due to the line tripping caused by lightning and most of the failures result from lightning shielding failure. Therefore, it is necessary to take preventive measures against lightning shielding failure for the UHV transmission lines to improve the operating reliability of UHV transmission lines.

Table 3.1 Statistical failure rates of 500, 750, and 1150 kV lines of the Former Soviet Union

Voltage level (kV)	Total line length (km)	Line average disconnection rate [times·(100 km·a)$^{-1}$]	Line average transmission interruption rate [times·(100 km·a)$^{-1}$]
500	57,314	0.574	0.201
750	15,519	0.206	0.097
1150	11,112	0.144	0.045

Note The total line length refers to the sum of the line lengths that are involved in the annual statistics. The line average disconnection rate and line average transmission interruption rate are obtained based on the total times of failures of each year divided by the total line length

www.FreeEngineeringBooksPdf.com

2. Stability

Because of the large transmission power of the UHVAC line, its transmission power may have a high proportion in the load power of the receiving-end system, and the tripping and outage due to line failure may endanger the safe operation of the receiving-end power grid, especially when the power base sends power through multi-circuit UHV large-capacity transmission lines to the same region, in the event of the simultaneous tripping of multi-circuit UHV transmission lines on the same corridor caused by multiple failures, it will have a serious impact on the safe operation of the power grid of the entire region. Therefore, in case that multi-circuit UHV transmission lines are used to supply power to the load centers, the mode of transmission by power supplies, lines, and locations shall be taken to avoid the fatal impact on the entire receiving-end system by the simultaneous failure of multi-circuit UHV lines, so as to ensure, from the aspect of structure, the safe, and stable operation of the power grid.

In the early days of UHV power grid construction, the interconnection between regional power grids through UHV lines was relatively weak, and the internal EHV system networks within the regional power grids were complex, which might form into a very large-scale electromagnetic ring grid that can cause serious safety hazards. For example, serious power transfer may occur in case of certain accidents in the power grid and may spread the accidents resulting in serious consequences. With the ongoing construction of UHV power grids, the capacity of interconnected grids to withstand severe accidents will be greatly improved, with higher safety and stability. However, due to the formation of a synchronous grid with greater scale, more complicated structure, and more difficulty in control and management after the interconnection, more and more complex safety and stability issues will be faced, so it must be closely paid attention to and be carefully studied.

3.1.2 Transmission Characteristics and Transmission Capacity

1. Basic Electrical Parameters of Transmission Lines

The basic electrical parameters of AC transmission line include resistance (R_0), reactance (X_0), conductance (G_0), and susceptance (B_0). Compared with the EHV lines, the unit length of UHV transmission line has significantly reduced R_0, slightly reduced X_0 and increased B_0 To reduce the impact of the corona on the environment, make the current in the conductor evenly distributed as far as possible, and reduce the line resistance, UHV transmission lines usually use the bundled conductors with more bundles than the EHV lines. The impedance of transmission line depends on the number of sub-conductors of each phase, diameter of bundled conductors, and spacing of sub-conductors and phase-to-phase distance. When the cross-sectional areas of phase conductors are approximately the same, with the

www.FreeEngineeringBooksPdf.com

increase in the bundles, the line impedance will decrease gradually, and the transmission capacity will enhance.

2. Transmission Loss

Compared with the EHV transmission lines, the loss of UHV transmission line is greatly reduced. According to the typical design of the used line, for the power transmission with the same capacity, the comprehensive loss of 1000 kV line is about half of that of the 500 kV line.

3. Impact of System Stability and Line Thermal Stability on the Transmission Capacity

When determining the power transmission capacity of transmission lines, it is necessary to consider the limitations of system stability and line thermal stability on the transmission capacity. In fact, the power angle stability and reactive power control are the two basic factors limiting the transmission capacity of EHVAC and UHVAC transmission systems, while the heating and resistance loss generally will not become the factors that limit the transmission capacity. The reason is that the line design and conductor selection for the EHV and UHV transmission lines need to meet the corresponding standards on environmental impact (power frequency electric field, audible noise and electromagnetic interference, etc.), but the conductors meeting these standards usually have a large thermal capacity which is much higher than the system's allowable stability limits. Therefore, the transmission capacity of the line is determined primarily by the system stability limits during the line operation, such as the system static stability margin, transient stability and dynamic stability limits, line voltage drop percentage limit, and line maximum operating voltage limit. The stability of the system is not only related to the parameters of the line itself, but is also affected by the transformer parameters, generator parameters, sending-end and receiving-end system strengths, line shunt reactors and series capacitors, etc. It is deemed in the reference document [2] that, for the UHV lines with long transmission distance (300 km and above), its transmission capacity is mainly limited by the power angle stability, including static stability, dynamic stability, and transient stability; for the lines with medium transmission distance (80–300 km), the transmission capacity is mainly limited by the voltage stability; for the lines with short transmission distance (less than 80 km), the transmission capacity is mainly limited by thermal stability limits. Therefore, the stability requirement of the system is a key factor that limits the transmission capacity of UHV lines.

The line thermal stability limit refers to the maximum current-carrying capacity of the line I_{max}. The operation current exceeding this current-carrying capacity may cause overheating of the line, increasing the line sag, drooping of conductors, resulting in the discharge to ground, and leading to line accidents. I_{max} corresponds to the maximum transmission power to ensure thermal stability. Since the multiple-bundled and large-section conductors are used for the UHV line, its thermal stability limit may reach up to 10,000 MW. Therefore, the thermal stability

www.FreeEngineeringBooksPdf.com

limit of UHV line does not limit much to the transmission capacity of the line, unless it is a very short transmission line (for example, less than 80 km).

4. Impact of the Sending-End and Receiving-End System Strengths on the Transmission Capacity

The UHV sending-end and receiving-end system strengths have a great impact on the transmission capacity of UHVAC lines, calculated from the following system power angle equation:

$$P = \frac{E_S E_D \sin(\theta_S - \theta_D)}{Z_L + Z_{TS} + Z_{TD} + Z_S + Z_D}, \tag{3.1}$$

where

E_S and E_D	respectively the sending-end and receiving-end system voltages;
θ_s and θ_D	respectively the sending-end and receiving-end system phase angles;
Z_L, Z_{TS} *and* Z_{TD}	respectively the line impedance and the sending-end and receiving-end transformer impedances;
Z_S and Z_D	respectively the sending-end and receiving-end system equivalent impedances.

According to Eq. (3.1), when the sending-end and receiving-end systems become from weak to strong, their system equivalent impedances Z_S and Z_D decrease gradually, and the line transmission capacity will be raised. Especially, for the UHV transmission lines with medium and short transmission distances, since the sending-end and receiving-end system impedances account for a large proportion of the total line impedance, the sending-end and receiving-end system strengths have a more obvious impact on the line transmission capacity. In the early period of UHV transmission construction, since the sending-end and receiving-end systems are not strong, the actual UHV transmission capacity was significantly constrained.

With the fixed sending-end and receiving-end system strengths, the transmission capacity of UHV line will reduce rapidly as the increase of transmission distance. If drop points are not set in the middle of a long line to divide the long-length line into short-length lines and voltage support is not enhanced, the transmission capacity of the entire line will be significantly limited.

Therefore, to achieve the long-distance and large-capacity UHV power transmission, the drop points must be set every 300–500 km in the middle of the line and voltage support must be provided. In fact, when the single section of a line is longer than 500 km, the overvoltage on the lines is difficult to be effectively controlled, either. Therefore, considering from this aspect, an appropriate segmentation of the long line in the middle is necessary.

www.FreeEngineeringBooksPdf.com

5. Impact of Transformer Impedance on the Transmission Capacity

The transformer impedance is a very important factor that limits the UHV power transmission capacity. In fact, the total system impedance limiting the transmission capacity of the line mainly consists of the sending-end and receiving-end equivalent transformer impedance, source impedance, and line impedance. With the increase of transmission voltage, the ratio of equivalent transformer impedance to the total system impedance increases, and the impact on the transmission capacity also increases, so the impact of the transformer impedance of UHV system on the transmission capacity is even greater. Especially, for the UHV transmission lines with medium and short distances, the transformer impedance becomes a major factor limiting the transmission capacity of the entire transmission system. Therefore, in such case, the simply increase of the number of circuits of transmission lines cannot effectively improve the transmission capacity of the line, and the transmission capacity of line that can be increased by the addition of circuits will be limited by the transformer impedance and the receiving-end system strength. Obviously, for the UHV transmission lines with medium and short distances, when the line is increased from single circuit to multiple circuits, the total transmission capacity will not increase much.

It can be known from Eq. (3.1) that the system transmission capacity is inversely proportional to the impedances at its beginning and ending ends, and the impedances include the line impedance and transformer impedance. For UHV lines, because of the more number of the bundles of conductors and the larger equivalent diameter, the impedance of line Z_L of the same length will be less than that of the EHV transmission line. However, the impedance of UHV transformer Z_T is more than that of EHV transmission line; this is because that, in general, with the increase of the rated voltage, the impedance of transformer usually will be increased to reduce the short-circuit current. For example, the short-circuit impedance of 500 kV transformer is 12%, while that of 1000 kV transformer will be up to 18% or even higher. According to the short-circuit impedance of 18%, the calculated total reactance at the primary and secondary sides of UHV transformer is about 75 Ω, which is equivalent to the resistance of about 350 km line. Therefore, for the point-to-point line connected through UHV transformer and a lower voltage level of 500 kV at both terminals, its transformer impedance Z_T at both terminals is equivalent to the impedance of 700 km line, and such a high impedance will significantly limit the transmission capacity of the line.

For the selection of UHV transformer impedance, there are two different viewpoints: one requires to lower down the transformer impedance to reduce its impact on the transmission capacity of the line; while the other, based on the consideration in the safety of high-voltage level, deems that the transformer impedance shall be increased to reduce the short-circuit current level. Both viewpoints have their reasons and shall be taken into account comprehensively, without completely leaning to any one; otherwise, the advantage of UHV line in high transmission capacity cannot be given full play, or the system cannot operate due to the excessive short-circuit current.

www.FreeEngineeringBooksPdf.com

6. Impact of High-Voltage Shunt Reactor on the Transmission Capacity

The UHV lines are characterized by long lines, large transmission capacity, and large charging power. The charging power of long-distance UHV transmission line is very large, approximately 4.4 times of the 500 kV line. The capacitive rise effect of transmission line may cause very serious power frequency overvoltage, which will seriously affect the reliability of the transmission. The addition of shunt reactors in line is an important measure to limit the power frequency overvoltage. To limit the power frequency overvoltage within the required range, the high-voltage shunt reactor with large capacity will usually be installed in the UHV line, with a capacity of up to 80–90% of the charging power of the line. However, the high-voltage shunt reactor with such a large capacity will affect the balance of reactive power of the line when in heavy load.

Figure 3.1 shows a sketch of line distribution parameter model. The line reactive power mainly consists of two aspects: the reactive power Q_L consumed by line inductance L_0 and the reactive power Q_C provided by line capacitance C_0. If the effective values of line voltage and current are U_N and I, respectively, then: $Q_C = j\omega C_0 U_N^2$, $Q_L = j\omega L_0 I^2$. It can be seen that the reactive power Q_C generated by line capacitance is only related to the line voltage and basically has nothing to do with the transmission power. Considering that the voltage fluctuation of the line under normal operation is normally small, it can be considered that Q_C is constant. The reactive power loss Q_L of transmission line reactance has a square relation with the line current I, i.e., it is proportional to the square of the transmission power.

During the no-load operation for the UHV long transmission line, the high-voltage shunt reactors need to provide the line with a lot of inductive reactive power to balance the lots of capacitive reactive power generated by the capacitance to ground of UHV long line; while during the large-capacity power transmission of the UHV long line, the reactive power Q_L consumed by the line inductance L_0 itself can be basically balanced with the reactive power Q_C provided by the line capacitance C_0. Therefore, in case of high power transmission by a UHV long line,

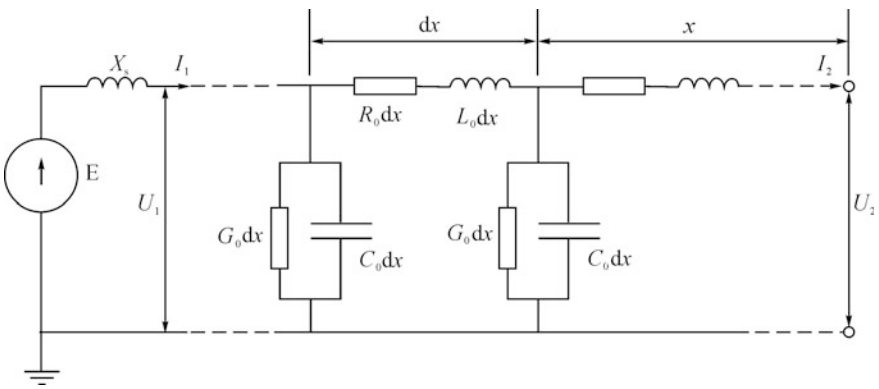

Fig. 3.1 Sketch of line distribution parameter model

www.FreeEngineeringBooksPdf.com

the high-voltage shunt reactor does not need to further provide the inductive reactive power of high capacity; otherwise, it will cause the difficulty in balancing the reactive power and thereby depress the system voltage, resulting in severe impact on the stable operation of the system. At this point, the following three methods can be considered to solve the problem: removal of the high-voltage shunt reactors; placement of a bank of capacitors in the UHV transformer's third coil winding (usually with rated voltage of 110 kV) to compensate the high-voltage shunt reactors; or change of the high-voltage shunt reactors into controllable and adjustable modes (controllable reactor), i.e., the high-voltage shunt reactors themselves can be adjusted; during no load of the line, the reactance value shall be adjusted to the maximum, while under the maximum load conditions, the reactance value shall be adjusted to the minimum (or zero). In fact, the first method is often difficult to do, because the existing circuit breaker switching technology is difficult to realize the removal of high-current and high-voltage shunt reactors. Currently, the second method is more widely used in UHV practices. However, the third method shall be the most promising way, which is under active research by some research units and has got good application in the EHV transmission projects. The 1000 kV and 200 Mvar controllable reactors have also been successfully trial made in China, and will be applied in the future UHV projects. Actually, considering that the reactive power regulation is very difficult in the UHV transmission, and there is lots of surplus reactive power during the light load of the line, but the surplus reactive power of the line is little or even deficient during the heavy load, to better adapt to the changes in the transmission capacity of UHV line; the controllable method by the shunt reactor compensation is more needed compared to 500 kV.

7. Impact of Line Impedance on the Power Transmission

Because the UHV transmission lines have a long distance and a large line impedance, it will cause a large voltage drop at the line ends, which is also a major factor that limits its transmission capacity. Therefore, similar to the EHV transmission, the transmission capacity of UHV lines will also decrease with the increase of transmission distance.

In a comprehensive consideration of the impacts of the system stability, high-voltage shunt reactors, and other factors on the transmission capacity of the UHV lines, the impact of the transmission line length on the power transmission is shown in Fig. 3.2.

L_1 and L_2 in Fig. 3.2 are 80–300 km, respectively. It can be seen from the above figure that, when the line is short (L less than 80 km), the line transmission capacity is mainly limited by the thermal stability limit, i.e., the maximum transmission capacity may be up to 10,000 MW; for the medium-distance line (80–300 km), it is mainly limited by the reactive power balance, and normally, the transmission capacity can be up to 3000–5000 MW; for the long-distance line (above 300 km), it is mainly limited by the power angle stability, and its transmission capacity is normally lower than 4000 MW.

www.FreeEngineeringBooksPdf.com

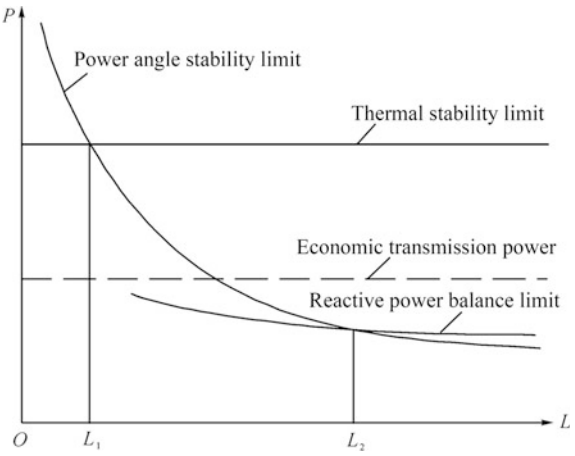

Fig. 3.2 Impact of the transmission line length on the power transmission

8. Impact of the Series Capacitor on the Transmission Capacity

Different from the effect of shunt reactors, the effect of series capacitor compensation is equivalent to the reduction of the length of the transmission line. The series capacitor compensation is to have the capacitors connected in series in the transmission lines of power grid to improve the line parameters and improve the transmission capacity of the line. The series capacitor compensation for the UHV transmission lines can greatly improve the transmission capacity of UHV lines. However, this measure may lead to resonance and other problems; therefore, normally, the series capacitor with compensation degree greater than 80% is inadvisable to be used in the practical projects.

In view of the above factors, the UHVAC transmission line does not have a very uniform transmission capacity standard; instead, there are different levels of transmission capacity depending on the actual situations, but, in general, the UHVAC transmission has a very strong capacity in power transmission, which can reach up to four to five times the transmission capacity of 500 kV EHV lines. In addition, the UHV transmission lines not only have long economic transmission distance to meet the requirements in realizing the optimal configuration of China's energy resources in a wide range, but can also achieve the networking at multiple points provided with voltage support, with good flexibility in grid design.

9. Measures to Improve the Transmission Capacity of UHV lines

(1) Using double-circuit line on the same tower

The benefits of using double-circuit line on the same tower are that the diversion area of the line is increased, which, as a result, increases the carrying current and enhances the line transmission capacity accordingly as well, and significantly reduces the line corridor. In fact, the development direction of UHV is double-circuit line on the same tower. The Southeast Shanxi–Nanyang–

www.FreeEngineeringBooksPdf.com

Jingmen UHV single-circuit demonstration line that has been built has also reserved the space for future upgrade to double circuits, and after the demonstration line, all China's UHV lines under planning or construction adopt the double-circuit lines.

(2) Research and application of controllable high-voltage shunt reactors

Since serious power frequency overvoltage with high amplitude may occur to the UHV line in case of no-load operation of the line, there must be high-voltage shunt reactors with large capacity for limitation; while in case of heavy load of the line, the line inductance itself will consume large amount of reactive power. At this time, the reactive power consumed by the inductance of the line itself is basically equilibrium with the reactive power produced by the line capacitance. In such case, the inductive reactive power generated by high-voltage shunt reactor will be in great surplus, which will seriously affect the normal line voltage levels, endangering the system safety. Therefore, in case of no-load operation of the UHV line, there must be high-voltage shunt reactors to control the overvoltage; while in case of heavy load of the line, the high-voltage shunt reactors must be reduced in number or even removed. This is self-contradictory, and the measure most likely to resolve the contradiction is controllable high-voltage shunt reactor.

(3) Series compensation

The line impedance will largely affect the transmission capacity, and the series compensation capacitor can effectively solve this problem. The principle of series compensation capacitor is to compensate part of the line inductive reactance through the capacitive reactance of series capacitors in the line to shorten the electrical distance, so as to achieve the purpose of improving the transmission capacity of the line. The series compensation for UHV transmission line involves the technologies in stability, high voltage, power electronics, and many other aspects, and is extremely difficult, but the UHV series compensation devices have been successfully developed in China, and have got good application in the Southeast Shanxi–Nanyang–Jingmen UHV demonstration line.

3.2 System Characteristics of UHVDC Power Transmission

3.2.1 Reliability and Stability

1. Reliability

To reflect the levels of all aspects of the DC system such as the system design, equipment manufacturing, engineering construction, and operation management, the reliability indexes of UHVDC projects are mainly as follows: forced energy unavailability, planned energy unavailability, converter forced outage rate, mono-pole forced outage rate, and bi-pole forced outage rate. Among these indexes, the

www.FreeEngineeringBooksPdf.com

forced energy unavailability and planned energy unavailability are collectively referred to as energy unavailability, expressing the decrease in energy transmission capacity of DC power transmission system resulting from planned outages, unplanned outages, or operation under a reduced voltage during the statistical time. Table 3.2 shows the reliability indexes recommended for the Sanxia–Changzhou, Sanxia–Guangdong, and Sanxia–Shanghai ±500 kV DC projects and ±800 kV UHVDC projects [3].

The converter of UHVDC system will produce harmonic voltage and current at both AC and DC sides, unfavorable to the stability control of grid system. Meanwhile, the analysis on the causes of failures of the existing domestic ±500 kV DC projects reveals that the probability of the system forced outage resulting from DC control and protection is relatively high, the operation control of the secondary equipment of UHVDC system is more complicated, so the failure rate of the system may be higher. In general, the reliability of the UHVDC transmission system is not as good as that of the UHVAC transmission system.

In combination with the existing operation experience in the conventional HVDC power transmission, the application of technical measures enabling independence from each other and dismantling of the mutual coupling can significantly improve the design, manufacturing, operation, and maintenance performance of UHVDC transmission systems and avoid the frequent occurrence of some typical faults in the UHVDC transmission systems. Specifically:

(1) In terms of the converter system, for the AC power feeding bay, valve chamber, AC and DC power systems, and air conditioning cooling system, etc, the reliability of power transmission project can be enhanced by such measures as keeping them independent from each other as far as possible, dismantling their mutual couplings and designing highly independent control systems for them. In addition, a converter bypass switch shall be used, so that each individual converter can start, shut down, and exit to maintenance without affecting the operation of other converters, thereby reducing the probability of monopole outage.

Table 3.2 Reliability indexes of DC power transmission system

Project	P_1 (%)	P_2 (%)	P_3 [times·(converter·a)$^{-1}$]	P_4 (times·a^{-1})	P_5 (times·a^{-1})
Sanxia–Changzhou system	0.5	1	–[a]	6	0.1
Sanxia–Guangdong system	0.5	1	–	5	0.1
Sanxia–Shanghai system	0.5	1	–	5	0.1
UHV system	0.5	1	3	2	0.05

Note P_1–P_5 represents in turn the forced energy unavailability, planned energy unavailability, converter forced outage rate, monopole forced outage rate and bi-pole forced outage rate

[a]The 500 kV systems have only one bank of converters at one pole, so their converter forced outage rate is equivalent to the monopole forced outage rate

www.FreeEngineeringBooksPdf.com

(2) In terms of the system design, to improve the reliability of the bipolar system operation, the two poles shall be kept independent as far as possible to avoid bipolar coupling caused by control system coupling or grounding electrode coupling and eliminate the possibility in the outage of one pole resulting from the failure, outage, or maintenance error of another pole.

2. Stability

When the UHVDC transmission mode is used for large-capacity power transmission, the problem in stability may also occur. As the transmission capacity of UHVDC transmission line is large, when the transmission capacity of the line accounts for a larger ratio with respect to the capacity of the receiving-end system, if the line is de-energized, it will have a serious impact on the safety and stability of the grids at the sending and receiving ends. In fact, the impact of a large-capacity UHVDC line on the stability of the AC system of the sending-end and receiving-end grids can be simulated by the loss of a large load and the loss of a large power source.

For the Yunnan–Guangdong ±800 kV DC power transmission project of China Southern Power Grid, its rated capacity of power transmission accounted for about 1/4 of the west-to-east electricity transmission capacity of China Southern Power Grid in 2010, about 1/3 of the electricity load of Yunnan power grid and 2/3 of the outward transmission power. When the project's sending-end power supply or line fails, it will have a relatively serious impact on the safe and stable operation of the receiving-end grid.

The stability of UHVDC power transmission is directly related to the electrical strength of the receiving-end grid. When the electrical distance of the receiving-end drop points of multiple UHVDC transmission lines is in close proximity, leading to the formation of a multi-infeed DC transmission system, since the DC inverter station is prone to be subject to commutation failure due to the receiving-end voltage fluctuation, one fault may cause simultaneous or successive commutation failure of multiple inverter stations, and even lead to the interruption of DC power transmission, bringing a huge impact to the entire multi-infeed DC transmission system. Research shows that in the multi-infeed UHVDC receiving-end grid, when a number of DC lines interact with AC system at the same time, the problem of system transient and dynamic power angles and voltages stability may be very serious and shall be paid with close attention to. Currently, China Southern Power Grid has had a number of EHV ±500 kV DC lines with drop points in Guangdong Power Grid. It is expected that the number of EHVDC transmission lines with drop points in Guangdong Power Grid will reach up to 7 by the year of 2015. Meanwhile, with the construction of ±800 kV UHVDC transmission line taken into consideration, by then, China Southern Power Grid will become one of the grids containing the largest "multi-infeed DC transmission system" in the world. For the multi-infeed DC transmission system, the failure of AC system or DC systems is likely to be a factor causing instability of the system, and may even lead to the collapse of the entire system. Therefore, in consideration of the complex interaction

www.FreeEngineeringBooksPdf.com

between AC and DC systems, appropriate targeted measures must be taken to ensure the safety and stability of multi-infeed DC power transmission system.

3.2.2 Transmission Characteristics and Transmission Capacity

Due to the special system structure of DC power transmission, it is basically not affected by the distributed capacitance and distributed inductance of the line. In the calculation of transmission capacity and line loss, the equivalent circuit of DC transmission lines has a big difference from AC lines. The concept of natural power does not exist for DC transmission line, and there are no particular problems such as capacitance effect in the long-distance AC transmission line. Therefore, there is no need to additionally install series capacitors to improve the transmission capacity or to additionally install shunt reactors to limit the power frequency overvoltage.

The losses of DC transmission consist of three parts, i.e., line loss, the loss of converter stations at both terminals, and the loss of grounding electrode system. The loss of the DC grounding electrode system is very small and can be negligible basically, so the losses of DC transmission are mainly composed of line loss and the loss of converter stations at both terminals. Due to the "shielding effect" of space charge, the corona loss in DC line is much smaller than that in AC line with the same voltage level; besides, since no skin effect exists in the DC lines, basically, the efficiency of use of the conductor is very high. Therefore, its line loss is much smaller than AC transmission line. The loss of converter stations is an important part of the losses of the entire DC transmission project, but because there are many types of equipment in the converter stations at both terminals and their loss mechanisms are different, it is, actually, often difficult to specify them precisely.

In DC transmission system, the converter that consists of thyristor valves will absorb a lot of reactive power. To compensate for this part of reactive power, in addition to AC filters, sometimes, it is necessary to install such reactive power compensation devices as power capacitors, condenser, or static reactive power compensator.

Both the active power transmitted by the DC transmission system and the reactive power absorbed by converter can be quickly and easily controlled, and therefore, the DC power transmission is characterized by flexibility.

The DC power transmission is ideally suited for long-distance, large-capacity and point-to-point transmission, and its transmission capacity and distance will not be limited by the synchronous operation of the AC systems at both terminals. The transmission capacity of DC power transmission is determined by the allowable current value of converter valve and line voltage level. Currently, the four major domestic DC voltage levels are ±500, ±660, ±800, and ±1000/±1100 kV; and the two available DC converter valves are 5-in. converter valve with flow capacity

www.FreeEngineeringBooksPdf.com

Table 3.3 Transmission capacities, line loss rates and economic distances of DC transmission lines with different voltage levels

Voltage level (kV)	Transmission capacity (MW)	Line loss rate (%)	Economic distance (km)
±500	3000 (5-in. converter valve)	4.49–7.48	Below 1100
±660	3960 (5-in. converter valve)	5.85–7.58	900–1700
±800	7200 (6-in. converter valve)	5.98–9.50	1200–2700
±1100	9000 (6-in. converter valve)	6.54–10.58	Above 1800

of 3000 A and 6-in. converter valve with flow capacity of 4500 A, which are used, respectively, in the ±500, ±660 kV lines and ±800, ±1000/±1100 kV lines. The corresponding transmission capacities and economic distances are shown in Table 3.3 [4]. It can be predicted that with the continuous improvement of converter valve technology and flow capacity, the transmission capacity of the DC transmission lines will also be improved considerably.

3.3 Analysis on Economy of UHV Power Transmission

3.3.1 Comparison of Economy for UHVAC/EHVAC Power Transmission

1. Line Corridor and Covered Land Cost

Now, the issue of line corridor has become more and more important. The land resources of corridor have also become more and more limited, and the costs required have become higher and higher, as well. The cost of land used by line corridor accounts for about 5–10% of the total costs of the line. Therefore, the saving of corridor can save considerable investment, and more importantly, in some special terrain conditions, it is impossible to have a wide line corridor. With UHV transmission technology, the floor space of line corridors and substations can be greatly saved compared with the existing voltage level.

In general, the transmission capacity of one circuit of 1000 kV transmission lines can replace 4–5 circuits of normal 500 kV lines. The corridor width of 1000 kV UHV transmission lines in accordance with the environmental requirements is about 65 m, while the corridor width of 4–5 circuits of 500 kV lines is about 140–175 m, which shows that the corridor of 1000 kV UHV line is only about one third of the corridor required by 500 kV lines with equal transmission capacity.

www.FreeEngineeringBooksPdf.com

2. Transmission Costs

It is shown by a large number of researches that when the transmission distance and transmission capacity reach a certain value, the use of UHV is more economic than other voltage levels.

USA had ever compared the costs of 1100 and 500 kV power transmission and transformation equipment [5]. Except for the unit capacity cost of generator step-up transformers, which was higher in 1100 kV than in 500 kV by 40–50%, the unit capacity costs of 1100 kV transmission lines, circuit breakers and their frameworks and shunt reactors were all lower than that of 500 kV (as shown in Table 3.4).

During the determination of the target voltage of UHV transmission, Japan compared the costs of 1100 and 800 kV by a mathematical model [5], assuming that the 1100 kV line was a double-circuit 1500 km-long line and that the lines and substations accounted for 68 and 29.8% of the project, respectively. It was deemed that the former could save 3% of the construction costs compared with the later (as shown in Table 3.5). If the line loss and increase of land price in future are taken into consideration, the application of UHV will have higher economic benefits.

It was deemed by the former Soviet Union that, in case of transmission distance of more than 700 km and transmission capacity of more than 4500 MW, the use of 1150 kV was the most economic. In its opinions: in case of transmission of the same capacity, the use of 1150 kV can save 1/3 steel materials, 1/2 conductors, 1/2 construction costs and 10–15% construction costs of lines and substations compared with the use of 500 kV. The former Soviet Union conducted comparison and analysis on the economy of Siberia-Ural Transmission Project by voltage levels of 1150, 750, and 500 kV (as shown in Table 3.6) [5], from which it concluded that the investment in UHV transmission unit capacity was smaller.

It is indicated by the above figures that UHVAC transmission has more advantages in the economy of construction investment than other EHVAC voltage levels.

In addition to the consideration of construction investment, in actual operation, the line loss, also as an important part of transmission costs, shall be considered for the transmission costs, as well. Considering the line loss, the US had ever compared the transmission costs of 500 and 1100 kV [6]. With the 322 km-long transmission line taken as an example, assuming the same line loss for 1100 and 500 kV lines,

Table 3.4 Cost comparisons of 1100 kV UHV and 500 kV EHV equipment

Equipment	Capacity factor	Cost ratio	Cost ratio for unit capacity
Transmission line	4.3–6.1	2.9–3.4	0.6–0.7
Circuit breaker and its framework	4.3–6.1	2.9–3.1	0.5–0.7
Shunt reactor	5.0	4.3–4.6	0.9
Generator step-up transformer	1.0	1.4–1.5	1.4–1.5
Step-up or step-down autotransformer	2.0–3.0	2.1–3.0	1.0

www.FreeEngineeringBooksPdf.com

Table 3.5 Economy comparison of Japan's line costs (prices in 1978 in trillion yen)

Voltage (kV)	Line	Substation	Transmission loss	Total cost
800	2.52	0.83	0.07	3.43
1100	2.26	0.99	0.06	3.32

Table 3.6 Economic comparison of Siberian-ural transmission line in different voltage level

Voltage (kV)	Line length (km)	Line materials (10,000 tons)	Tower materials (10,000 tons)	Total investment (0.1 billion rubles)
500	11,955	16.5	55.6	5.98
750	5140	13.3	20.5	5.06
1150	2570	7.6	17.7	3.97

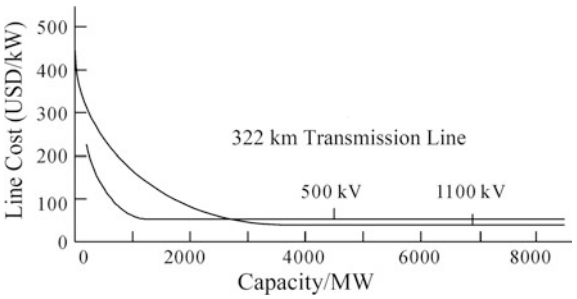

Fig. 3.3 Comparison of transmission costs of UHV 1100 kV and EHV 500 kV

the economic conversion point of the transmission power at this time is 2400 MW, as shown in Fig. 3.3, and when the transmission power is more than this point, the use of UHV transmission is more economic; in consideration that the line loss of 1100 kV is often much smaller than that of 500 kV, the economic conversion point of the transmission powers of the 1100 and 500 kV shall be lower than 2400 MW. In consideration that the transmission capacity of the UHVAC transmission line planned in China is much larger than 2400 MW, the transmission capacity of a normal single-circuit line can reach 5000–6000 MW, the line length is far greater than 322 km, and the line loss of 1100 kV line is much smaller than that of 500 kV line (the former is usually about 50% or less of the latter), so the UHV transmission has obvious economic advantages.

In the early demonstration process of UHV construction, China also analyzed and compared the economy of UHVAC and EHVAC lines. It was shown by the analysis that, from economic considerations, the contrast relationship between UHVAC transmission technology and 500 kV AC transmission technology was related to the transmission capacity and transmission distance, rather than unchanged. Besides, in terms of technology, the 500 kV AC transmission was limited by the system stability, with transmission distance normally not be more than 1000 km, while the 1000 kV AC transmission distance could be more than

www.FreeEngineeringBooksPdf.com

2000 km. In consideration of China's demands in long-distance and large-capacity transmission, a detailed model was set up for calculation and comparison in the analysis by taking the same large-capacity and long-distance electricity transmission as an example. It was deemed that the use of UHVAC transmission line had lower costs and smaller loss, with higher economic and technical advantages.

3.3.2 Comparison of Economy for UHVDC/EHVDC Power Transmission

Currently, no standard voltage level sequence like that for AC transmission system has been established for DC transmission system. The DC project design and construction lack uniform standards, and the parameters are all separately selected for each practical project. Such idea can realize the optimization of DC project design and operation in a local small scope. However, in the long run, it is not conducive to the planning of large-scale DC transmission and manufacturing of converter station equipment. For this reason, the State Grid has organized its subordinates to carry out research work and proposed the recommendation in establishing the DC voltage sequence of ±1000 (±1100 kV), ±800, ±660, and ±500 kV.

To maximize the overall efficiency of DC power transmission, a comparative study is made on the economy of DC lines with different voltage levels [4]. The results show that: ① the unit capacity investment increases with the increase of voltage level, the unit investments of different voltage levels are close when the transmission distance is long, and the capacity investment has a lower growth rate with the distance; ② the lower the voltage level, the higher the cost in line loss, and when the transmission distance is increased, the cost in line loss of DC transmission at a lower voltage level has a higher growth rate; and ③ in case of short-distance transmission, the annual cost of DC transmission at a lower voltage level is lower, but, with the increase of transmission distance, the economy of DC transmission at a higher voltage level gradually reveals. Based on the consideration of the changes in investment, feed-in tariff, utilization hours, and operation period, the economic transmission distances of DC transmission at all voltage levels are obtained as follows: the economic transmission distance of ±500 kV DC transmission is less than 1100 km, the economic transmission distance of ±660 kV DC transmission is 900–1700 km, the economic transmission distance of ±800 kV DC transmission is 1200–2700 km, and the economic transmission distance of ±1000 kV (±1100 kV) DC transmission is more than 1800 km.

www.FreeEngineeringBooksPdf.com

3.3.2.1 Comparison of Economy for UHVAC/UHVDC Power Transmissions

The UHVAC and UHVDC transmissions are applicable to different occasions. In case both UHVAC and UHVDC transmission modes can be achieved technically, an economic comparison of these two different transmission modes shall be made to select a reasonable transmission scheme.

In case of long-distance and large-capacity power transmission, the cost of DC transmission line is lower than that of AC transmission line. In general, the DC transmission is structured by two poles, two wires and one ground system, with only two polar conductors needed, while three-phase conductors are required for the three-phase AC line. In terms of transmission capacity, with the same conductor section and insulation level, the transmission power of ±800 kV DC transmission lines with two polar conductors is basically equal to the active power that can be transmitted by the single-circuit 1000 kV AC line with three-phase conductors, both of which can reach above 5000 MW. Therefore, in case of transmission of the same capacity, the DC transmission can save one conductor and its corresponding supporting line facilities compared with the AC transmission. For example, the number of insulators and fittings of ±800 kV DC line is about 2/3 of that of 1000 kV AC line. The least corridor width of one 1000 kV AC transmission line is generally around 50–60 m, while the least corridor width of ±800 kV DC transmission line is generally around 30–40 m. Today, with the growing shortage of transmission corridors, the DC transmission has revealed obvious advantages in this regard. However, the DC transmission needs to add one more converter station and its corresponding converter equipment respectively at the power sending and receiving ends, so the cost of DC transmission converter stations is much higher than that of AC substations. Therefore, for the same transmission capacity, only when the transmission distance is more than a certain length, the cost saved from DC lines can cover the extra cost spent in converter stations. The transmission distance mentioned here is usually referred to as the equivalent distance for AC and DC power transmission. For a given transmission capacity, when the transmission distance is greater than the equivalent distance, the adoption of DC transmission mode will be more economic.

Related researches around the world have shown that [7], the equivalent transmission distance for 1000 kV UHVAC transmission and ±800 kV DC transmission is 800–1000 km, as shown in Table 3.7. In fact, for different regions and countries, due to their different circumstances, the equivalent distances are not the same, even

Table 3.7 Applicable economic distances of UHVAC and UHVDC power transmissions

Transmission distance (km)	<800	800–1000	>1000
Economy dominant scheme	UHVAC	Unfixed (depending on specific project)	UHVDC

www.FreeEngineeringBooksPdf.com

for different transmission projects in the same country; due to the different implementation conditions of projects, there will be difference in the equivalent distances.

3.4 Applicable Occasions of UHVAC/UHVDC Power Transmissions

3.4.1 Technical Characteristics of UHVAC/UHVDC Power Transmissions

The outstanding advantages of UHVDC power transmission include: high transmission voltage, large transmission capacity, narrow line corridor, and suitable for large-capacity and long-distance power transmission. The utilization of UHVDC power transmission for interconnection of large regions, also with advantages, can reduce or avoid a lot of penetration power, change the tidal current according to the change in operation modes of the sending and receiving ends, and facilitate the control of direction and magnitude of tidal current.

The highlighted advantages of UHVAC power transmission are as follows: the UHVAC transmission is economically competitive when used in extra-large-power and mid-range transmission occasions or large-capacity, long-distance, and multi-point transmission occasions; and the construction of UHVAC transmission backbone grid to replace the EHVAC power grid has advantages of optimizing the allocation of resources, protecting the environment, conserving the land used by line corridors, reducing construction costs, and effectively lowering transmission losses and so on.

3.4.2 Technical Advantages of UHV Power Transmission

The UHV power transmission refers to the three-phase AC transmission mode with rated voltage of 1000 kV and above and the bipolar DC transmission mode with rated voltage of ±750 kV and above. Compared with the EHV power transmission, it has the following main technical advantages.

1. Large Transmission Capacity and Long Transmission Distance

It can be used for extra-long-distance and large-capacity power transmission, making it possible to make use of the energy resources (water and coal, etc) in remote locations (1500–3000 km). The long-distance and large-capacity transmission can also reduce the pressure on railway and highway transportation, reduce the scale of construction of thermal power fleet in load centers, and reduce the environmental pollution caused by thermal power, etc.

www.FreeEngineeringBooksPdf.com

2. Significant Saving in Line Corridor Land

The UHV large-capacity and long-distance power transmission can reduce the number of circuits of transmission lines and save line corridors. By the use of UHV transmission technology, a lot of conductors and tower materials can be saved, achieving the same scale in transmission with relatively less input, thereby reducing the construction costs and investment.

3. Limiting the Short-Circuit Current of System

With the development of the power system and the increase of installed capacity, the problem that the system short-circuit fault current exceeds the limit has become very prominent. The results of researches around the world show that, when the development of UHV power grid is strong enough, the system short-circuit current level can be effectively reduced through 500 kV looping-off operation.

4. Low Transmission Loss

Compared with EHV power transmission, the loss of UHV transmission line is greatly reduced. The loss of 1000 kV AC line is 1/4 of that of 500 kV line; and the loss of ±800 kV DC line is 39% of that of ±500 kV DC line. In case of long-distance and large-capacity transmission, the UHV power transmission technology can effectively reduce the operating costs of the grid.

5. High Overall Benefits

The development of UHV power grid can enhance the grid structure, realizing peak load regulation and shifting, complementation of hydropower and thermal power, regional mutual aid, and mutual backup, thereby improving the power grid's capability in anti-interference and achieving the optimal use of resources and other overall benefits from grid connection.

3.4.3 Interconnection of UHV Power Grids

With a vast territory, China's energy distribution and regional economic development are very uneven. With the application of UHVAC and UHVDC transmission technologies, the transmission distance is longer and the transmission power is larger, which will significantly expand the scale of cross-region and long-distance power transmission in the coming period. Meanwhile, with the development of China's power industry, the interconnection of major regional power grids has become an inevitable trend. The interconnection of China's major regional and separate provincial grids has entered the implementation phase.

The AC and DC transmission modes have their own strengths and are mutually complementary. The access of large-scale DC transmission to the receiving end needs to rely on a strong AC power grid to ensure safe and reliable operation. During the planning and construction of power grid, measures shall be taken to

www.FreeEngineeringBooksPdf.com

maximize the strengths of these two transmission modes, so as to meet the needs in safe and economic operation of the large power grids.

If two power grid systems are interconnected by DC mode, the synchronous operation between them needs not to be considered. If they are connected through multi-circuit DC transmission lines and the power of each DC transmission line can be effectively controlled, the transmission power can be reduced accordingly in case of failure of DC transmission line, and the power balance can be maintained by the adjustments made by these two power grid systems, respectively. The DC transmission system is mainly based on power transmission, and the stability at both sides of the system needs not to be considered. For the systems at both sides, it may be considered as power supply or load. When the system is disconnected, it can be considered as losing the power or load. In such case, only the issue of safety and stability of the respective system needs to be considered, and the measures are simple, feasible, and effective. If the interconnection is made through AC transmission lines, in addition to transmission of electricity, the synchronous operation of the systems at both sides must be considered. If it is the connection from power points to grid, the tidal current is relatively fixed and easy to control. If the transmission line is cutoff directly after a failure occurs, the situation is similar to the interconnection by DC transmission system. However, if the connection is made grid to grid, the distribution of tidal current depends on the system status. For the connection through multi-circuit AC transmission lines, the faults of some networked lines may cause the overload of other networked lines. Since the tidal current of the networked lines is determined by the power supplies, load distribution, and network parameters of the two systems, it is difficult to adjust. If it cannot be effectively adjusted and controlled, it will result in the spreading of an accident. Therefore, during the arrangement of operation modes, the consequences of the failure of part of the networked lines must be considered. For this reason, the transmission power of the networked lines must be limited, which, as a result, affects the effectiveness of networked lines. This is why the DC networked lines can run under full load, but the AC networked lines must leave sufficient safety margin.

The advantages in such aspects as technology, economy, and safety for asynchronous interconnection by DC power transmission have been proven in the worldwide. Therefore, the DC power transmission technology, with its unique technical and economic advantages, will certainly play a very important role in the development of the power industry in China in the two aspects of long-distance and large-capacity transmission and nation-wide grid interconnection. Because of the large transmission capacity of UHV lines, the method of grid interconnection has more options, which will accelerate the formation of the national uniform grid. The major regional power grids may form into a synchronous grid through UHVAC interconnection, or form into a non-synchronous grid through UHVDC interconnection. For the interconnection of large regional power grids, there are different opinions on whether to use UHVAC or UHVDC. The different technical characteristics of AC and DC transmissions determine their applicable scopes. For instance, the occasions, such as long-distance submarine DC cables, back-to-back, and onshore long-distance transmission, are the traditional application fields of DC

www.FreeEngineeringBooksPdf.com

transmission system. The UHVAC and UHVDC technologies have their own different positioning. The UHVAC technology, having network function and can being used for flexible collection, transmission, and distribution of electricity, is the basis for the construction and safe operation of the power grid, while the UHVDC technology mainly has power transmission function and has economic advantages in large-capacity and extra-long-distance power transmission. In many cases, both AC and DC power transmission schemes are feasible, but there will be difference in the technical and economic aspects of the schemes. The interconnection of large regional grids has high requirements in safe operation, so it shall be determined after a comprehensive technical and economic comparison.

With the gradual advance of UHV power grid construction in China, several large sending-end and receiving-end power grids relying on UHV power grids will be formed, especially after the North China, East China, and Central China are interconnected by UHVAC, a very massive synchronous grid will be formed. In such an extra-large UHVAC synchronous grid, great attention shall be paid to such issues as system stability and short-circuit current increase, which still need further intensive research.

3.4.4 *Applicable Occasions of UHVAC/UHVDC Power Transmissions*

The use of UHVAC transmission mode is based on the need in large-capacity transmission, and it can be divided into two specific cases, i.e., medium-distance and long-distance transmissions. For Russia, due to its vast land, the energy bases are far from the load centers. With the transmission distance of above 2400 km, it belongs to the typical long-distance and large-capacity UHV transmission mode; while for other countries, the transmission distance of UHV transmission projects is usually in the range of 200–500 km or even shorter, but its transmission capacity is very large (TEPCO, 5000–13,000 MW; BPA, 8000–10,000 MW), it is more appropriate to refer to it as UHV medium-distance and large-capacity or extra-large-capacity transmission mode. It can be seen that most countries in the world that have ever researched and developed the UHVAC transmission belong to the latter case. The main reason is to solve the critical technical issues, such as difficult transmission corridor layout and constrained short-circuit capacity. Table 3.8 lists the relevant information on the development plans of UHVAC power transmission in some countries.

China, with special situations, is one of the few countries in the world that most need the development of UHVAC and UHVDC transmission technologies. The main occasions in which UHV power transmission may be applied in China include: medium-distance and large-capacity or extra-large-capacity transmission, long-distance and large-capacity transmission, large regional backbone grid and large regional grid interconnection, etc.

www.FreeEngineeringBooksPdf.com

Table 3.8 Relevant information on the development plans of UHVAC power transmission in different countries

Country	Department	Voltage level (kV)	Transmission power (MW)	Transmission distance (km)	Adoption reason
Soviet Union/Russia	Power electrification department	1150	5500	2400	Large capacity and long distance
Japan	TEPCO	1000	5000–13,000	200–250	Extra-large-capacity, large short-circuit current, difficult corridor layout
USA	BPA	1100	6000–8000	300–400	Extra-large-capacity, difficult corridor layout, reduction in transmission loss
	AEP	1500	>5000	400–500	Large capacity, difficult corridor layout
Italy	ENEL/CESI	1000	5000–6000	300–400	Large capacity, difficult corridor layout

1. Medium-Distance and Large-Capacity Transmission

With the rapid development of China's economy and power industry, the construction and development of power grid are facing a series of challenges and problems. In the economically developed coastal areas where electricity utilization is concentrated, the technical problems such as difficulties in layout of power transmission corridors and control of short-circuit current have begun to appear, and the critical problem that needs to solve is how to improve the utilization rate of transmission corridors. The UHVAC transmission mode can achieve the medium-distance and large-capacity or extra-large-capacity transmission, which can meet the needs in power transmission by large-capacity plants in the receiving-end power grid.

2. Long-Distance and Large-Capacity Transmission

With the formation of China's hydropower base in the southwestern region and coal-power base in the northwestern region, the power system shows a main pattern of "West-to-East Electricity Transmission" and "North-to-South Electricity Transmission", with the transmission distance mostly within 800–3000 km and transmission capacity within 4000–20,000 MW. For example, the installed capacities of Xiluodu and Xiangjiaba Hydropower Stations of Jinsha River Phase I Project are 12.6 and 6 GW, respectively, with total installed capacity of 18.6 GW in Phase I and total installed capacity of 19.4 GW in Phase II. The transmission

www.FreeEngineeringBooksPdf.com

distance from the hydropower stations to Central China is 1000 km, and the transmission distance to East China is 2000 km. For the newly planned and constructed "West-to-East Electricity Transmission" projects, no matter it is Jinsha River downstream hydropower or Sichuan hydropower or Yunnan hydropower, and they all have the characteristics of long transmission distance and large capacity. Because of the transmission capacity is up to 4000–20,000 MW and transmission distance is 1000–2000 km, the use of UHVDC transmission has obvious economic advantages. As for the "North-to-South Electricity Transmission" projects, it is also suitable to use UHVDC transmission to transmit, in a long distance, the large amount of electric energy produced by the large-scale mine-mouth thermal power plant fleet in North China to Central China and East China. Meanwhile, some large-capacity and long-distance UHV transmission lines may require to drop points in multiple places, to promote the UHV power system interconnection, in this case, the UHVAC transmission has to be selected, because the cost in dropping points halfway for power distribution of DC transmission is unacceptable.

3. Large Regional Backbone Grid

In addition to the lack of transmission capacity of the existing 500 kV regional grids, which requires the development of UHV transmission to meet the requirements for medium-distance and large-capacity transmission, the excessive short-circuit current in the power load concentrated region is also an outstanding technical issue. To solve the problem of excessive short-circuit current caused by the increase of power grid transmission capacity, it may be considered to build a main grid framework with higher voltage level. It can be predicted that the formation of the main UHVAC power grid will go through two stages. In the early construction of UHV lines, as the main grid framework cannot yet be formed and the load capacity of the line is low, it is mainly used for centralized outward power transmission of the large power supplies, and it may bring impact to system stability due to the fault tripping of UHV line. In this case, the 500 kV grids of a lower level cannot yet go into looping-off operation, and the short-circuit current cannot yet be effectively reduced. However, with the continued strengthening of the power grid with voltage level of 1000 kV, the UHVAC lines will eventually form into a sufficiently strong backbone ring grid, and at that time, the hierarchical and regional operation method can be adopted to solve the problem of excessive grid short-circuit current fundamentally.

4. Large Regional Power Grid Interconnection

At present, China has established six large trans-provincial and trans-regional power grids: East China Grid, North China Grid, Northeast China Grid, Central China Grid, Northwest China Grid, and China Southern Power Grid. The main grid framework of 500 kV (750 and 330 kV for Northwest China Grid) in each power grid is gradually formed and growing. In 1989, Gezhouba–Shanghai ±500 kV DC line was put into operation, which achieved the non-synchronous interconnection of the grids in the two large regions of Central China and East China, marking China's

www.FreeEngineeringBooksPdf.com

entry into the era of large regional power grid interconnection. The use of UHV power grid to achieve the interconnection of large regional power grids (including the three transmission modes of AC, DC, and AC–DC in parallel) can, in addition to meeting the requirements for long-distance and large-capacity power transmission, also realize the mutual aid of hydropower and thermal power across large regions and basins, optimize the allocation of nation-wide energy resources, meet the requirements for flexible trade in China's power market, and promote the development of the electricity market. For the non-synchronized interconnected operation of large regions realized by the UHVDC transmission mode, the AC grids at both terminals independently operate according to their own frequencies and voltages, and the power can be controlled as required without transmission of short-circuit power, which will help to improve the stability of the system. The use of UHVAC transmission mode to achieve synchronous interconnected operation requires a high synchronizing capacity of the two interconnected grids. In addition, it will cause the increase of AC short-circuit capacity, and may lead to the system safety and stability problems such as low-frequency oscillation among the large regional power grids, which need to be given with special attention, and must be analyzed and demonstrated with extreme caution and care, to avoid the hidden dangers in safety and stability of the grid system.

From the practical experience in the world, for the interconnection of the large regional grids, the UHVDC has more technical advantages than the UHVAC. However, in terms of the economy, the direct use of UHVDC back-to-back interconnection between large regions is not economic. Therefore, the interconnection of large regional grids with long distance can be made between two large regions at the two points that are relatively distant and appropriate, which will be better if the long-distance power transmission and the mutual interconnection can both be realized. In such a case, the advantages of UHVDC will become more apparent.

5. Grid Structure Development of China's Power Grid in the future

At present, the China's backbone grid structure has developed from 220 to 500 kV, and the more dense the 500 kV power grids become, the more prominent the resulting problems of three-phase short-circuit current exceeding standard will be, which will threaten the safe and stable operation of power grid. Meanwhile, in areas of load center with tense power transmission corridor, the construction scale of 500 kV transmission channel of large-capacity power transmission is also limited accordingly. Therefore, the construction of power grid with higher voltage level can fundamentally solve the issue of 500 kV short-circuit current exceeding standard, also help to achieve power balance of a larger scale, and meet the requirements of large-capacity transmission. At present, the west and north of East China have been formed 1000 kV UHVAC half-ring network structure. Realization of UHVAC ring network in East China as the primary grid structure in East China power grid is in plan. Furthermore 1000 kV UHVAC ring network in North China is also in plan. In general, the UHVDC and EHVDC transmission lines are used as transmission and link lines of regional power grid. Therefore, it can be predicted that the ring network of 1000 kV UHVAC power grid in the large region and the interconnection

www.FreeEngineeringBooksPdf.com

of ±800 or ±1100 kV UHVDC power grid will be China's main power grid structure in the future.

In addition, with the rapid development of HVDC and UHVDC transmission in recent years, a centralized multi-infeed DC system has been formed in East China power grid. In accordance with the planning of State Grid Corporation of China, by 2020, the State Grid will build 19 UHVDC projects and there will be more multi-infeed DC systems forming in regional power grid, while the "strong DC and weak AC" issue in existing grid will be more prominent. Considering the very large capacity of UHVDC transmission, when the bipolar blocking fault occurs in UHVDC systems, the impact on the receiving-end AC grid is very large. If the receiving-end AC grid is not strong enough, it will be seriously affected. For example, a certain UHVDC bipolar block occurred in East China power grid in 2015, the East China power grid instantaneously lost power of 5400 MW, and its frequency fell to the lowest 49.56 Hz (drop below 49.8 Hz for the first time in recent 10 years) and exceeded the limit value lasting up to hundreds of seconds, resulting in great risk to safe operation of power grid [8].

In addition, considering that stable operation of DC transmission is also directly related to electrical strength of the receiving-end grid; when a single-phase or three-phase short-circuit fault occurs in the AC line near the inverter station, it could trigger simultaneous commutation failure of multi-circuit DC lines, causing that the receiving-end AC system will withstand the impact of the instantaneously decrease of DC-input active power and the instantaneously increase of absorbed reactive power, which kind of fault conditions has already occurred in the East China power grid. Therefore, the construction of UHV backbone grid needs to be strengthened, so as to match the DC capacity and scale, forming a large power grid pattern of "strong AC and strong DC". Furthermore, UHVAC transmission has capacity of interconnection between large regional power grids, which can provide a strong voltage and reactive power support for receiving-end grids with DC multi-infeed. Based on the above considerations, State Grid has considered achieving the interconnection of more regional power grids through UHVAC transmission in the future on the basis of the present. For example, the existing "North, East and Central China" power grid and Northeast power grid interconnect through UHVAC transmission, forming the eastern UHV synchronous power grid (referred to as "Eastern Grid"); the existing Northwest Power Grid and Sichuan, Chongqing, Tibet Power Grid interconnect through the networking of UHVAC transmission, forming the western UHV synchronous power grid (referred to as "Western Grid"). Among them, UHVAC transmission is mainly used in the main grid construction and the network transmission in synchronous power grid and UHVDC transmission is used in long-distance power transmission crossing between eastern and western power grid and within the synchronous power grid, so as to form two UHV synchronous power grid patterns with clear structure of sending-end and receiving-end and coordinated development between AC and DC systems. Some of the key technical issues possibly existing in large-scale synchronous power grid still need to be further studied carefully.

www.FreeEngineeringBooksPdf.com

Table 3.9 Applicable occasions of UHVAC and UHVDC transmissions

Transmission mode	Applicable occasions
1000 kV AC transmission	Medium-distance and large-capacity or extra-large-capacity transmission Long-distance, large-capacity and multi-point transmission Main grid framework of regional grids Large regional power grid synchronous interconnection (required to be prudently demonstrated)
±800 kV DC transmission	Long-distance and large-capacity transmission
±1100 kV DC transmission	Large regional power grid asynchronous interconnection

In applications of UHV power transmission, for the UHV lines mainly positioned in power transmission, the first consideration is its economy, while for the UHV lines to be used for interconnection of systems, the stability of the systems shall be fully considered, and after the comprehensive consideration of the economy, appropriate project scheme shall be selected properly. The application of UHVAC and UHVDC power transmission is complementary mutually. Based on the actual situations of China's power grids, the UHVAC transmission is mainly positioned in medium-distance and large-capacity or extra-large-capacity power transmission and long-distance, large-capacity, and multi-point power transmission, as well as the construction of the main grid framework of large regional grids. In case that it is to be applied to the synchronous interconnection of large regional grids, the system short-circuit current and the system stability will need to be analyzed and demonstrated in detail to avoid any problem regarding to the safety and stability of the system. The UHVDC transmission is mainly positioned in the long-distance and large-capacity transmission with a clear sending–receiving relationship, and the interconnection of some large regional and provincial grids. In summary, the applicable occasions of UHVAC and UHVDC transmissions can be represented, as shown in Table 3.9 [3].

References

1. Zhao Z, Wan Q, Wan Y. Analysis on superiority of UHV power transmission[C]. Chinese Society for Electrical Engineering Annual Conference Proceedings. ZhengZhou, China, December, 2006;123–27.
2. Zhenya L. UHV power grid. Beijing: China Economic Press; 2005.
3. Hao Z, Yijun Z. Applicable occasions of UHVAC/UHVDC transmission and their technology comparisons in China. Electr Power Autom Equip. 2007;27(15):6–12.
4. Yunzhou Z, Feng H, Biao Z, Le W. Economic comparison of HVDC voltage class sequence. Power Syst Technol. 2008;32(9):37–41.
5. Dingxie G. The prospect of developing UHV transmission system in China. High Volt Eng. 2002;28(3):28–30.

www.FreeEngineeringBooksPdf.com

6. Ling P. The prospect of application of UHVAC transmission in China. Water Resour Power. 1998;16(3):68–72.
7. Minghai Z. Energy recourses, integrated interconnection network, UHV transmission. High Volt Eng. 2000;26(2):28–30.
8. Mingjie L. Characteristic analysis and operational control of large-scale hybrid UHV AC/DC power grids. Power Syst Technol. 2016;40(4):985–91.

www.FreeEngineeringBooksPdf.com

Part II
Alternating Current

Compared to the EHVAC power transmission system, the UHVAC power transmission system has longer transmission line, larger transmission capacity, larger reactive charging power of the line and more prominent problems such as power-frequency overvoltage and secondary arc current. In addition, the switching overvoltage is the most important basis to determine the UHVAC transmission system's insulation level. Meanwhile, due to the reduced switching overvoltage limit but higher and stricter standards for the UHVAC system, some types of the switching overvoltage which will not jeopardize the EHVAC system may, however, pose a threat to the safety of UHVAC system. The high-amplitude and steep-front very fast transient overvoltage (VFTO) is possible to pose a threat to the important equipment such as UHV GIS equipment and main transformer, especially the UHV main transformer, the turn-to-turn insulation of which may be jeopardized by the steep-front VFTO. Along with the rise of the system voltage level, the electromagnetic environment of the line is more prominent, and, therefore, research on this field is required. In consideration of the large transmission capacity of the UHV transmission system and that it is more important than the EHV transmission system, the lightning protection thereof shall be attached with sufficient importance. In addition, the UHV relay protection differs from the EHV relay protection. The issues mentioned above are all worthy of deep research and analysis.This section will focus on discussion of the issues such as various important overvoltage mechanisms and limiting measures for the UHVAC transmission, insulation coordination of substations and lines involved in the UHVAC system, electromagnetic environment and the relay protection of UHVAC system.

www.FreeEngineeringBooksPdf.com

Chapter 4
Power Frequency Overvoltage of UHV Power Transmission Lines

Hao Zhou, Qiang Yi, Sha Li and Jingzhe Yu

The UHV transmission lines are featured by large transmission capacity, large charging power, and long transmission distance. Compared to the EHV transmission lines, the power frequency overvoltage of the UHV transmission lines is usually more serious, and seriously affecting the power transmission reliability. Therefore, the deep research on the characteristics of power frequency overvoltage of the UHV transmission lines, analyzing the various influence factors and verifying the feasibility in restricting the power frequency overvoltage of the UHV lines, does not only have significance on theoretical research, but can also provide reference value for the construction of UHV transmission lines in China [1–3].

This chapter first discusses the mechanisms, characteristics, classification, and main influence factors of power frequency overvoltage of the UHVAC transmission line, and then focuses on the discussion of two restrictive measures for power frequency overvoltage, namely, high-voltage shunt reactor and controllable high-voltage shunt reactor, and finally carries out detailed discussion on the determination of the upper and lower limits of the compensation degree of high-voltage shunt reactor.

H. Zhou (✉) · S. Li · J. Yu
College of Electrical Engineering, Zhejiang University,
Xihu District, Hangzhou, Zhejiang, People's Republic of China
e-mail: zhouhao_ee@zju.edu.cn

S. Li
e-mail: lisha1210@zju.edu.cn

J. Yu
e-mail: 21510213@zju.edu.cn

Q. Yi
SIEMENS Power Automation Co., Ltd., Nanjing, Jiangsu, People's Republic of China
e-mail: 307289798@qq.com

© Zhejiang University Press, Hangzhou and Springer-Verlag GmbH Germany 2018

H. Zhou et al. (eds.), *Ultra-high Voltage AC/DC Power Transmission*,
Advanced Topics in Science and Technology in China,
https://doi.org/10.1007/978-3-662-54575-1_4

www.FreeEngineeringBooksPdf.com

4.1 Mechanisms of Power Frequency Overvoltage

The power frequency overvoltage mainly consists of the following three basic modes [4]:

(1) no-load long-line capacitance effect;
(2) asymmetrical ground fault;
(3) three-phase load shedding (or three-phase opening).

The mechanisms of the power frequency overvoltage under the above three cases are, respectively, analyzed as follows.

4.1.1 No-Load Long-Line Capacitance Effect

In the lumped parameter LC circuit, when the capacitive reactance is larger than the inductive reactance, there will be capacitive current in the circuit. At this time, the voltage on the capacitance is equal to the sum of the potential voltage of power supply and voltage of the inductance, higher than the potential of power supply. The distributed parameter line can be considered to be composed of numerous LC circuits connected in series, and the total capacitive reactance of the line under power frequency is usually larger than the inductive reactance, and therefore, the voltage on the line is gradually increased along the direction away from the power supply terminal, and this is the increase of power frequency voltage resulting from no-load line capacitance effect.

The model of evenly distributed parameter line is shown in Fig. 4.1, where R_0, L_0, G_0, and C_0 are, respectively, resistance, inductance, conductance, and capacitance of the unit length of conductor.

In the power frequency steady-state analysis, for simplify and convenient purposes, the model of lossless uniform transmission line is usually used, namely, $R_0 = 0$:

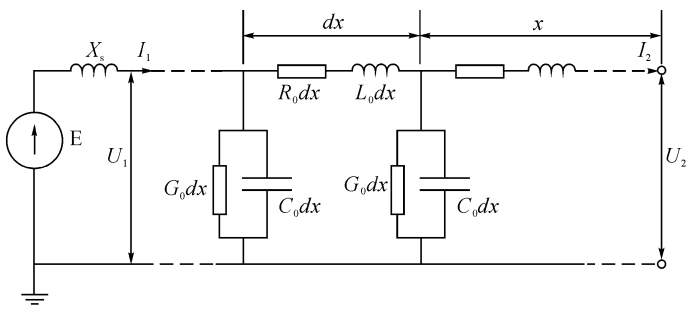

Fig. 4.1 Model of evenly distributed parameter line

www.FreeEngineeringBooksPdf.com

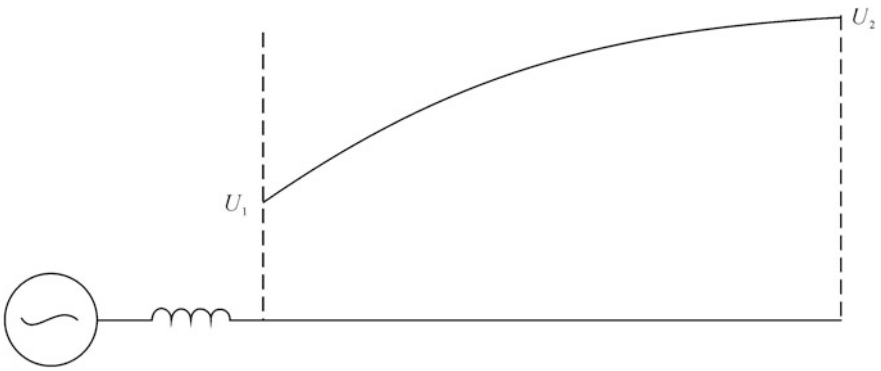

Fig. 4.2 Voltage distribution along the no-load long line

$$\begin{bmatrix} \dot{U}(x) \\ \dot{I}(x) \end{bmatrix} = \begin{bmatrix} \cos(\alpha x) & jZ_c \sin(\alpha x) \\ j\frac{1}{Z_c} \sin(\alpha x) & \cos(\alpha x) \end{bmatrix} \begin{bmatrix} \dot{U}_2 \\ \dot{I}_2 \end{bmatrix}, \tag{4.1}$$

where

Z_C the wave impedance of conductor;
x the distance from the point to the tail end of line.

In the equation $\alpha = \frac{\omega}{\upsilon}$, ω is the angular frequency of power supply and υ is the velocity of light. Supposing there is a lossless line with no load at the tail end and with length of l, then (Fig. 4.2)

$$\dot{U}_1 = \dot{U}_2 \cos \alpha l, \tag{4.2}$$

$$\dot{U}_x = \dot{U}_2 \cos(\alpha l) = \frac{\dot{U}_1}{\cos(\alpha l)} \cos(\alpha x). \tag{4.3}$$

In case of the tail end of the line is open, namely, $\dot{I}_2 = 0$, the coefficient of voltage transmission from the power supply terminal to the end of the no-load line will be

$$\frac{\dot{U}_2}{\dot{U}_1} = \frac{1}{\cos(\alpha l)}. \tag{4.4}$$

When the equivalent reactance of the system power supply is considered, it will be

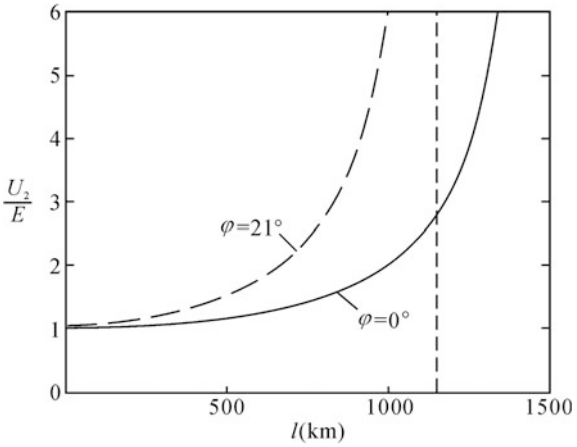

Fig. 4.3 Relation curve between voltage at the end of line and line length. $\varphi = 0°$ means that the impedance of power supply is neglected, and $\varphi = 21°$ means that the impedance of power supply is considered

$$\frac{U_2}{E} = \frac{\cos\varphi}{\cos(\alpha l + \varphi)}, \tag{4.5}$$

where

E the system power supply voltage.

In the equation $\varphi = \arctan\frac{X_s}{Z}$, X_s is the equivalent reactance of the system power supply.

From the above equations, it can be seen that the voltage of the line is gradually increased from the power supply terminal, and the line length has a large influence on such power frequency overvoltage. The impedance of power supply corresponds to the increase of line length, and therefore, it also has a large influence on the amplitude of such overvoltage. Figure 4.3 shows the relation curve between the voltage at the end of line and the line length.

The UHV line can be up to approximately 500 km in length, far above the EHV line. Meanwhile, both the terminals thereof are usually connected with the EHV system through UHV transformer and the impedance of power supply is relatively large. In case no restrictive measures are taken, the voltage at the tail end will be up to around 1.5 p.u. when the line is under no load, exceeding the limit value in the procedures.

4.1.2 Asymmetrical Short-Circuit Fault of the Line

The asymmetrical short-circuit fault mainly refers to single-phase ground fault and two-phase ground fault, in which the single-phase ground fault is most common and the rise amplitude in power frequency voltage caused by it is generally more serious. Therefore, only the case of single-phase ground fault is discussed here.

In case of asymmetrical fault of the system, the voltage and current of various phases at the fault point are asymmetrical and can be analyzed through symmetrical component method and compound sequence network. Supposing the single-phase ground fault is occurred to phase A of the system and its boundary conditions are: $\dot{U}_A = 0$, $\dot{I}_B = \dot{I}_C = 0$, then the compound sequence network can be worked out, as shown in Fig. 4.4.

In case it is approximately considered that $Z_1 = Z_2$ and the resistance component of the impedance is neglected, then the voltage rise coefficient of the sound phase under single-phase ground fault will be

$$K^{(1)} = \sqrt{3}\frac{\sqrt{\left(\frac{X_0}{X_1}\right)^2 + \left(\frac{X_0}{X_1}\right) + 1}}{\frac{X_0}{X_1} + 2}. \tag{4.6}$$

Obviously, such power frequency overvoltage has much relation to X_0/X_1 of single-phase ground point towards the power supply side; in case the rise of X_0/X_1 will result in the rise trend of voltage of the sound phase under asymmetrical

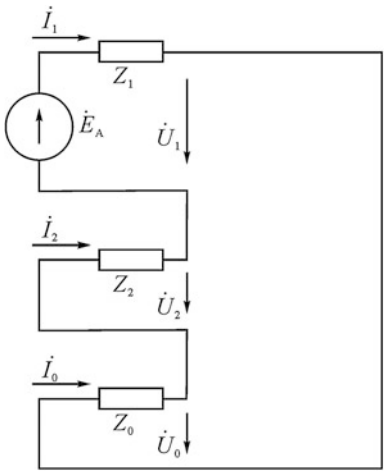

Fig. 4.4 Diagram of the compound sequence network under single-phase earthing fault

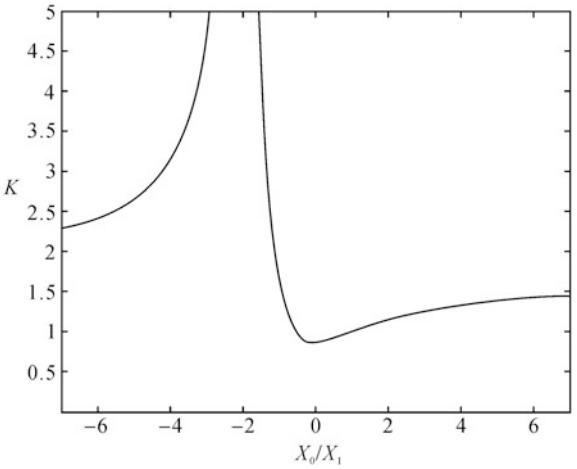

Fig. 4.5 Relation curve between power frequency voltage rise and X_0/X_1 under single-phase ground fault

short-circuit fault, the relation curve between power frequency voltage rise and X_0/X_1 under single-phase ground fault is shown in Fig. 4.5.

For the UHV transmission line, in general, $X_0/X_1 \approx 2.6$, as shown in Fig. 4.5, the power frequency voltage rise coefficient resulting from asymmetrical fault is larger than 1, that is, the power frequency overvoltage resulting from asymmetrical fault is generated.

4.1.3 Power Frequency Overvoltage due to Three-Phase Load Shedding

4.1.3.1 Principles

When the power transmission line is under heavy-load operation, the load shedding caused by the sudden tripping of circuit breaker at the tail end of the line due to certain reasons is also one of the reasons for power frequency voltage rise. Usually, it is called load shedding effect.

Analysis is carried out by the simplified electric power system, as shown in Fig. 4.6a, and the influence of reactive power equipment is tentatively not considered. The load shedding at the receiving end is taken as the example for analysis. Before the load shedding, since the power supply will transmit power flow (including active power flow and reactive power flow) to the line, as a result, voltage drop will be formed on the equivalent impedance of the power supply at the sending end, resulting in the potential of power supply E_m higher than the voltage of busbar U_{bar}; since the magnetic linkage of generator cannot be subject to sudden change before and after the load shedding, the potential of power supply E_m will be maintained unchanged basically within a short time after the load shedding, but the

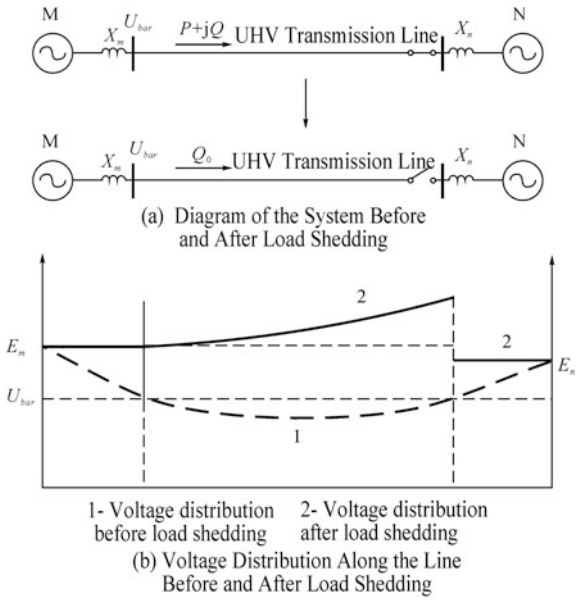

Fig. 4.6 Voltage distribution along the line under load shedding overvoltage

voltage drop on the equivalent impedance of the power supply will disappear after load shedding, resulting in the increase of the voltage of busbar and the formation of relatively high overvoltage in the line. The variation process of voltage along the line before and after the load shedding is shown in Fig. 4.6b, in which P and Q are, respectively, the active power and reactive power transmitted in the line during normal operation, and Q_0 is the reactive power output by the capacitance of the line when the line with open circuit at the tail end is unloaded.

4.1.3.2 Influence Factors

During normal operation, the relationship between the potential of power supply and the voltage of busbar can be expressed as follows:

$$\dot{E}_{\mathrm{m}} = \dot{U}_{\mathrm{bar}} + \Delta U + j\delta U = \dot{U}_{\mathrm{bar}} + \frac{QX}{U_{\mathrm{bar}}} + j\frac{PR}{U_{\mathrm{bar}}}, \tag{4.7}$$

where

P and Q the active power and reactive power transmitted by the power supply to the line;
U_{bar} the voltage of busbar;
R the equivalent resistance of power supply system;
X the equivalent impedance of power supply system.

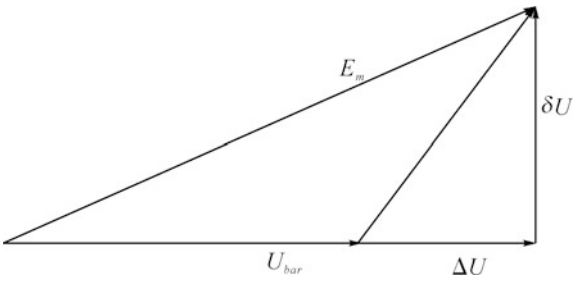

Fig. 4.7 Vector relation between the potential voltage of power supply and voltage of busbar during normal operation

Considering that the equivalent resistance of the system is usually very small, it can be neglected. X is usually used to indicate the positive sequence impedance of the power supply hereunder. The vector relation between the potential of power supply and the voltage of busbar during normal operation is shown in Fig. 4.7. In general, as the fluctuation amplitude of the voltage of busbar U_{bar} is small, the voltage drop on the equivalent impedance of power supply determines the amplitude of voltage rise of busbar; however, the voltage drop on the impedance of power supply is mainly depended upon the magnitude of the impedance of power supply and the magnitude of power flow from power supply to busbar. Therefore, after the load shedding, the amplitude of voltage rise of busbar is mainly depended upon the impedance of power supply and the power flow from power supply to busbar.

The overvoltage amplitude resulting from load shedding effect is mainly influenced by the following five factors:

(1) Transmission power of the line before load shedding
The line transmission power and high-voltage shunt reactor directly determine the magnitude of active power and reactive power transmitted from power supply to busbar, thus to influence the load shedding effect.
(2) High-voltage reactor
When the line transmission power is relatively large, the inductive reactive power required by the line will be relatively small. In case there is high-voltage shunt reactor nearby the power supply, the power supply will transmit large amount of capacitive reactive power to the busbar to offset the excessive inductive reactive power generated by the high-voltage shunt reactor, resulting in relatively large voltage drop on the impedance of power supply and leading to relatively large voltage rise of the busbar after load shedding.
(3) Equivalent impedance of the power supply
The smaller the capacity of power supply is, the larger the equivalent impedance will be. When the voltage of busbar is maintained unchanged and the same power is transmitted, the larger the electromotive force E of power supply is, the higher the power frequency overvoltage will be.
(4) Line length
The longer the line is, the more serious the capacitance effect of no-load line after load shedding and the higher the power frequency overvoltage will be.

(5) Generator speed characteristics
In the actual electric power system, due to the inertia of speed governor and braking equipment of the generator set, the due speed governing effect cannot be achieved immediately after load shedding, resulting in the speed rise of generator and the increase in electromotive force and frequency, which makes the power frequency overvoltage of the no-load line become more serious. However, since the electromechanical transient response speed is usually much slower than the electromagnetic transient response speed, the influence due to this factor is in general relatively small and not considered in the overvoltage simulation.

4.2 Characteristics of UHV Power Frequency Overvoltage

In the UHV system, the power frequency overvoltage directly determines the selection of the rated voltage of arrester and influences the level of switching overvoltage. In case the amplitude rise of power frequency voltage is excessive, to avoid the power frequency overvoltage, the rated voltage of arrester will be required to be high and the impulse flashover voltage and residual voltage thereof will also be increased; correspondingly, the insulation strength of the protected equipment shall also be increased, which will increase the insulation costs of the UHV system greatly. Meanwhile, the high power frequency overvoltage will directly uplift the level of switching overvoltage, making it more difficult to restrict the switching overvoltage; therefore, the power frequency overvoltage of the UHV system must be restricted.

Similar to EHV system, the power frequency overvoltage of the UHV system is also mainly generated due to the three factors, namely, no-load long-line capacitance effect, asymmetrical ground fault, and three-phase load shedding (or three-phase opening). However, the intrinsic characteristics of UHV transmission line determine that its power frequency overvoltage is more serious than that of other voltage levels [1, 5–9].

(1) The UHV line has long transmission distance, which makes the capacitance effect more obvious. Table 4.1 lists the proportions of 1000 kV transmission lines with different lengths according to the China's planned UHV grid framework. The statistical results show that, among the China's planned UHV lines, most are within the length of 100–500 km, and the UHV lines with length

Table 4.1 Proportion of the UHV lines with different lengths

Length range (km)	Proportion (%)
(0, 100)	1.5
[100, 200]	16.9
[200, 300]	32.3
[300, 400]	20.0
[400, 500]	29.2

of 300–500 km account for 49.2% (nearly a half). It can be seen that the average length of single section of UHV lines is far above that of the lines at 500 kV voltage level, and the capacitance effect will be more serious.

(2) The transmission power flow is large and the load shedding overvoltage is large. The natural power of single-circuit 1000 kV UHV transmission line is about 5000 MW; for the UHV core ring grid with relatively strong power grid structure, the transmission capacity of the UHVAC transmission line is strong, and each circuit thereof can transmit the power approximating to or exceeding 4000 MW; even if the line with a long transmission distance is sent out from the power supply of weak sending-end power grid, such as the lines sent out from the two independent thermal power bases in west Inner Mongolia and north Shaanxi, the transmission power of each circuit of line can be up to about 2000 MW. The transmission power is greatly larger than that of the 500 kV EHV transmission line, and compared to the EHV lines, the load shedding overvoltage is more serious.

(3) The UHV power frequency overvoltage is usually generated by the combined action of these three factors, namely, no-load long-line capacitance effect, asymmetrical ground fault and three-phase load shedding (or three-phase opening), and therefore, the amplitude is higher and the hazard is more serious. Here, the single-phase grounding load shedding overvoltage in the UHV system is taken as an example for analysis. First, the asymmetrical grounding effect resulting from the single-phase grounding of the line will cause the voltage rise of the sound phase of the line; then, the relay protection equipment will detect the ground fault and send out command to open the three phases at one end of the line, and thus, the load shedding effect will further result in the rise in voltage of busbar of the UHV system; meanwhile, because at this time, one end of the line is open and suspended, the no-load capacitance effect will further result in overvoltage rise. Actually, at this time, it is the combined action of these three factors, namely, no-load long-line capacitance effect, asymmetrical ground fault, and three-phase load shedding, that cause the overvoltage to be far above that generated by only one factor.

In conclusion, the power frequency overvoltage of UHV power grid, which is usually more serious than that of HV and EHV power grids, is more difficult to be restricted than other voltage levels. Therefore, sufficient importance must be attached to the issue.

4.3 Categories of UHV Power Frequency Overvoltage

4.3.1 Classification of UHV Power Frequency Overvoltage

The power frequency overvoltage of UHV system can be generated by the action of one factor or the combined action of multiple factors of the three factors, namely,

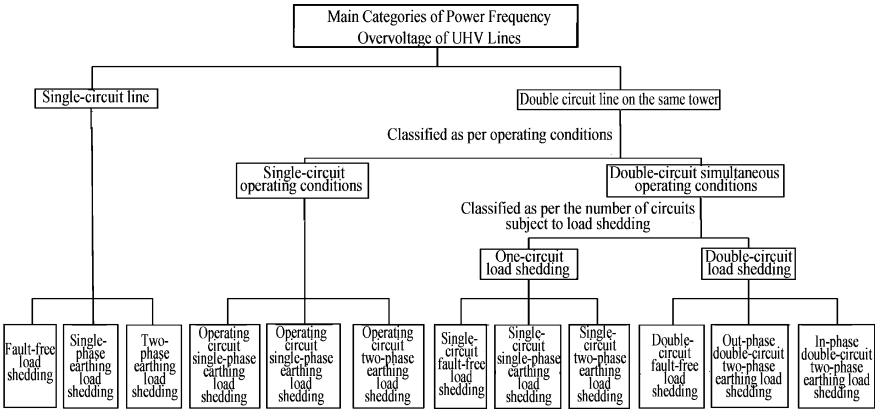

Fig. 4.8 Main categories of power frequency overvoltage of UHV lines

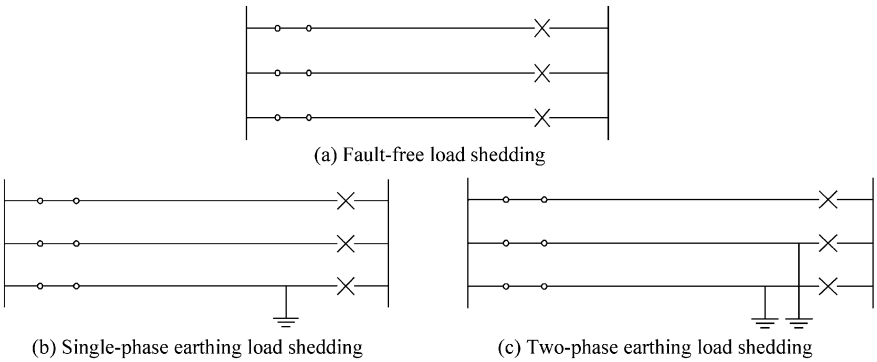

Fig. 4.9 Power frequency overvoltage of single-circuit UHV line

no-load long-line capacitance effect, asymmetrical ground fault, and three-phase load shedding (or three-phase opening). The main categories of power frequency overvoltage of UHV system are shown in Fig. 4.8. The overvoltage level resulting from the single action of no-load long-line capacitance effect or asymmetrical ground fault is low and, therefore, generally not considered.

1. Single-circuit UHV line

The power frequency overvoltage of single-circuit UHV transmission line mainly includes that generated under fault-free load shedding, single-phase grounding load shedding, and two-phase grounding load shedding. The sketch thereof is shown in Fig. 4.9.

According to the provisions in the procedures, the power frequency overvoltage under the two fault conditions, namely, load shedding under the normal power transmission state and load shedding after the ground fault of line, is usually mainly

considered. The probability of the occurrence of the three-phase opening fault at one end of the line resulting from the two-phase grounding of single-circuit line is very small and usually can be considered properly according to the actual conditions. In general, the single-phase grounding load shedding overvoltage is higher than the fault-free load shedding overvoltage. Therefore, the single-phase grounding load shedding overvoltage is often taken as the main research object for power frequency overvoltage of single-circuit UHV line.

2. Double-circuit UHV line on the same tower

For the double-circuit UHV transmission line on the same tower, the power frequency overvoltage under the two fault conditions, namely, load shedding under the normal power transmission state and load shedding after the ground fault of line, is also considered.

However, the double-circuit transmission line on the same tower needs to be studied under two operating conditions, namely, single-circuit operating condition and double-circuit operating condition. Similar to the single-circuit UHV transmission line, during the single-circuit operation of the double-circuit line on the same tower, the power frequency overvoltage under operating circuit fault-free load shedding, single-phase grounding load shedding, and two-phase grounding load shedding must be considered. While under the double-circuit operating condition,

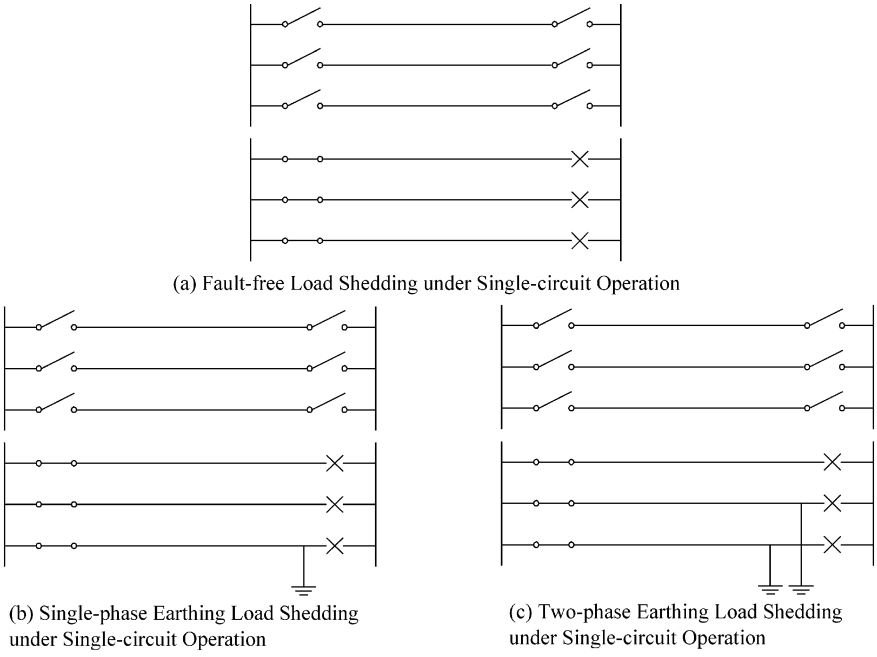

Fig. 4.10 Power frequency overvoltage of the double-circuit UHV line on the same tower under single-circuit operating conditions

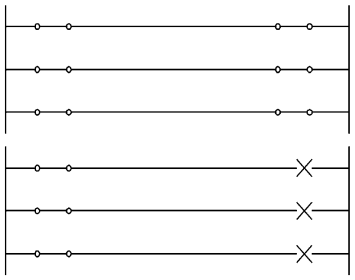

(a) Single-circuit Fault-free Load Shedding under Double-circuit Operation

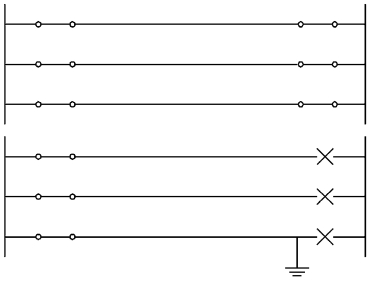

(b) Single-phase Earthing Single-phase Load Shedding under Double-circuit Operation

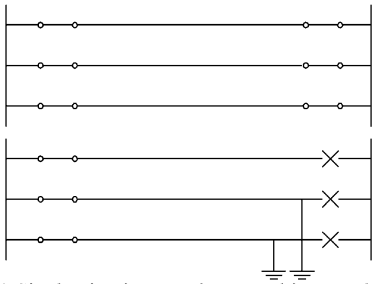

(c) Single-circuit Two-phase Earthing Load Shedding under Double-circuit Operation

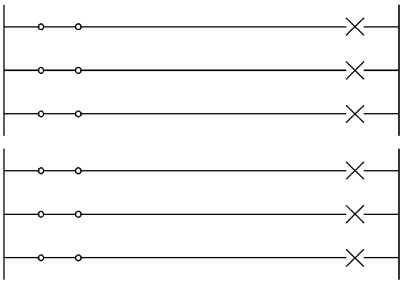

(d) Double-circuit Fault-free Load Shedding under Double-circuit Operation

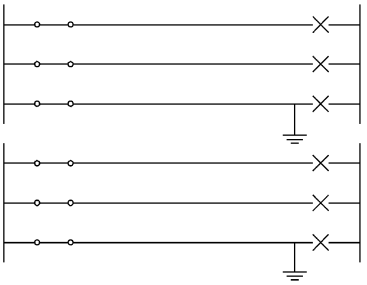

(e) In-phase Two-phase Earthing Load Shedding

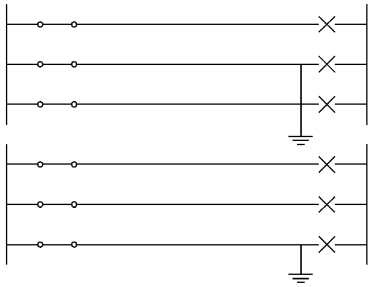

(f) Out-phase Two-phase Earthing Load Shedding

Fig. 4.11 Power frequency overvoltage of the double-circuit UHV line on the same tower under double-circuit operating conditions

the single-circuit load shedding and double-circuit load shedding need to be considered. The single-circuit load shedding includes single-circuit fault-free load shedding and single-circuit grounding (including single-phase grounding and two-phase grounding) load shedding; the double-circuit load shedding includes double-circuit fault-free load shedding and double-circuit load shedding after ground fault, in which the double-circuit load shedding after ground fault can be divided into in-phase two-phase grounding load shedding and out-phase grounding load shedding according to the difference in the phases subject to ground fault. The fault states of power frequency overvoltage of the double-circuit UHV line on the same tower under the single-circuit and double-circuit operating conditions are, respectively, shown in Figs. 4.10 and 4.11.

Same as the single-circuit line, the probability of the occurrence of the two-phase ground fault under the single-circuit operation of the double-circuit line on the same tower is extremely small; besides, the practical experience in operation of the double-circuit line on the same tower shows that the probability of the occurrence of the double-circuit in-phase and out-phase ground faults is also very small. Therefore, for the double-circuit line on the same tower, the fault-free load shedding overvoltage and the load shedding overvoltage resulting from single-phase earthing are generally mainly considered, while the power frequency overvoltage resulting from single-circuit line's two-phase ground fault and double-circuit in-phase and out-phase ground faults shall also be considered properly according to the actual conditions.

4.3.2 Systematic Comparison of Various Power Frequency Overvoltage

There are many kinds of power frequency overvoltage resulting in that the amount of calculation thereof is very large. Therefore, it is necessary to compare the amplitudes of different power frequency overvoltage to obtain the power frequency overvoltage with higher amplitude, which shall be given main consideration in the study and calculation, to simplify the calculation of power frequency overvoltage.

1. Single-circuit UHV line

The fault-free load shedding, with certain probability in occurrence, mainly results from misoperation and unwanted operation of relays; the single-phase ground fault is relatively common and accounts for more than 80% of the total line faults [10]. The two-phase grounding load shedding overvoltage only results from lightning back flashover, and the two-phase ground fault resulting from back flashover is never found in the 500 kV system with back-flashover lightning withstanding level of 150–175 kA. The calculations show that the 1000 kV system has a back-flashover lightning withstanding level of exceeding 250 kA, and hence, the two-phase ground fault resulting from back flashover is more impossible to occur. Therefore, the

two-phase ground fault can be considered to be nearly impossible to occur and shall not be treated as the focus in research. From the perspective of probability of the occurrence, the fault-free load shedding overvoltage and the single-phase grounding load shedding overvoltage shall be mainly considered.

The difference between fault-free load shedding overvoltage and grounding load shedding overvoltage is caused by ground fault. The ground fault makes the voltage of the sound phase change. The ratio of power frequency voltage of the sound phase before and after single-phase grounding can be expressed by the following equation [11]:

$$K_{j1} = \frac{U}{U_0} = \frac{\sqrt{3(1+K+K^2)}}{K+2} \tag{4.8}$$

$$K = \frac{Z_0}{Z_1}$$

where

K zero-positive sequence impedance ratio;
K_{j1} the single-phase ground fault coefficient;
U_0 and U the power frequency voltage of the sound phase before and after the single-phase grounding, respectively.

It can be seen from Eq. (4.8) that, in case the zero-positive sequence impedance ratio viewed from the fault point to the system is larger than 1, the ground fault will make voltage of the sound phase increase. When viewed from the fault point to the system, it is first the line and then the power supply. Therefore, the zero-positive sequence impedance ratio viewed from the fault point to the system is mainly influenced by the line impedance. Since the zero-positive sequence impedance ratio of the UHV line is about 2.6, far above 1, the zero-positive sequence impedance ratio viewed from the fault point to the system is also generally larger than 1, resulting in the amplitude of the grounding load shedding overvoltage larger than that of the fault-free load shedding overvoltage. Therefore, from the perspective of amplitude of overvoltage, for the single-circuit UHV line, the main consideration shall be given to the load shedding overvoltage after ground fault when research.

The result of simulation for the single-circuit line with length of 400 km is shown in Fig. 4.12.

It can be seen from the figure that the single-phase grounding load shedding overvoltage has larger amplitude than the fault-free load shedding overvoltage in all cases. Therefore, the single-phase grounding load shedding overvoltage is the most important calculation object of the power frequency overvoltage for single-circuit line.

2. Double-circuit UHV line on the same tower

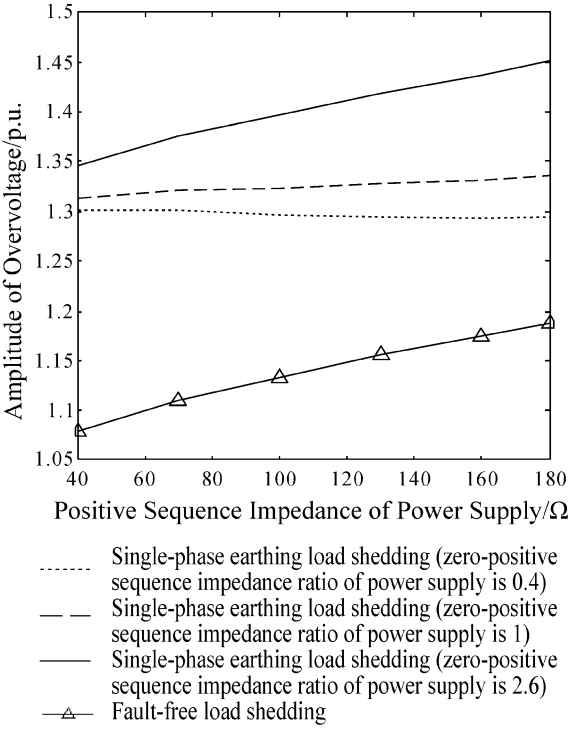

Fig. 4.12 Power frequency overvoltage of single-circuit UHV line

Table 4.2 Types of power frequency overvoltage with large probability of the occurrence in the UHV double-circuit line

		Types of overvoltage		
		Single-circuit fault-free load shedding	Single-phase grounding, single-circuit load shedding	Double-circuit fault-free load shedding
Operating mode	Single circuit	Single-circuit fault-free load shedding under single-circuit operating mode	Single-phase grounding and single-circuit load shedding under single-circuit operating mode	–
	Double circuit	Single-circuit fault-free load shedding under double-circuit operating mode	Single-phase grounding and single-circuit load shedding under double-circuit operating mode	Double-circuit fault-free load shedding

Similar to the single-circuit line, the single-circuit two-phase ground fault and the in-phase and out-phase ground faults of the double-circuit line on the same tower can only be caused by lightning back flashover. Since the back-flashover lightning withstanding level of the 1000 kV system exceeds 250 kA, the occurrence

probability of these three faults resulting from lightning back flashover is very small. Hence, according to the provisions in the procedures, the load shedding overvoltages resulting from the above three faults only need to be considered properly according to the actual conditions. Therefore, in the actual calculation of power frequency overvoltage, the single-circuit load shedding overvoltage resulting from single-circuit two-phase grounding and the overvoltage resulting from in-phase and out-phase grounding load shedding shall not be treated as the focus in research.

Apart from the above-mentioned types of overvoltage to be excluded from the perspective of probability of the occurrence, there are still five types of power frequency overvoltage for the double-circuit line on the same tower: single-circuit fault-free load shedding and single-phase grounding single-circuit load shedding under single-circuit operating mode, and single-circuit fault-free load shedding, single-phase grounding single-circuit load shedding, and double-circuit fault-free load shedding under double-circuit operating mode, as shown in Table 4.2.

To determine the overvoltage, as shown in Table 4.2, that can be categorized as per fault types or operating modes, the comparison of the same type of overvoltage is taken as the breakthrough point to compare the various types of power frequency overvoltage, as shown in Table 4.2.

(1) Comparison of different types of power frequency overvoltage under the same operating mode

Similar to the single-circuit line, in consideration that the asymmetrical earthing will make the voltage of the sound phase increase, the amplitude of single-phase grounding load shedding overvoltage of the double-circuit line on the same tower will be higher than that of the fault-free load shedding overvoltage under the same operating mode, as shown in Fig. 4.13.

The double-circuit line with length of 400 km is taken as an example for simulation. The amplitudes of load shedding overvoltage under three cases are calculated. During the calculation, the variations of positive sequence impedance and zero-positive sequence impedance ratio of power supply are considered. The results are shown in Fig. 4.14.

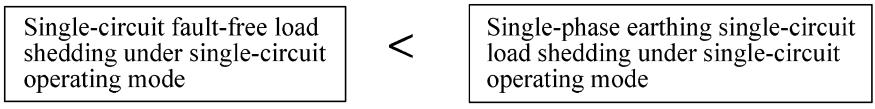

(a) Single-circuit operating mode

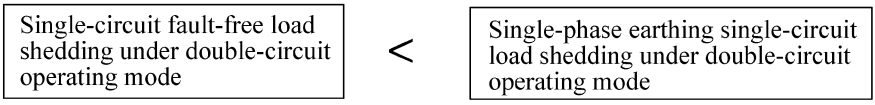

(b) Double-circuit operating mode

Fig. 4.13 Relationship between different types of power frequency overvoltage of double-circuit line under the same operating mode

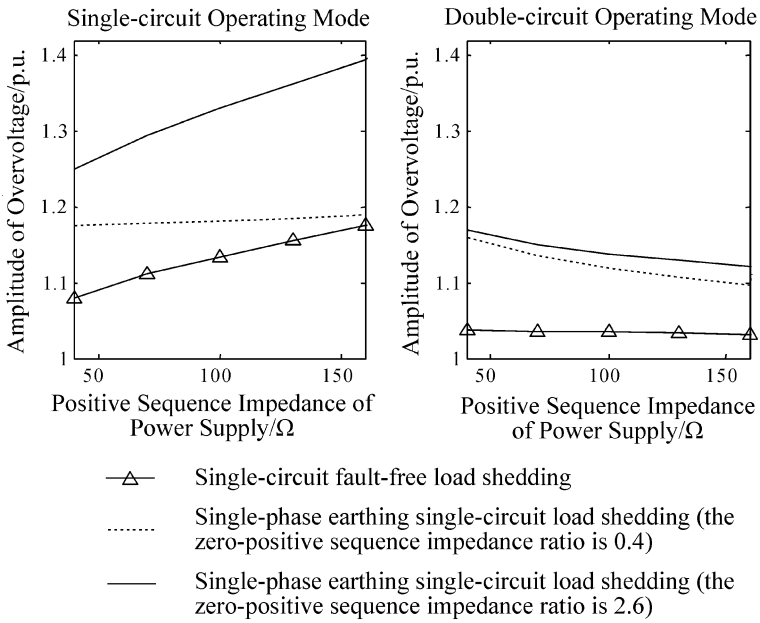

Fig. 4.14 Comparison of different types of power frequency overvoltage of double-circuit line under the same operating mode

It can be seen from Eq. (4.1) that the single-phase grounding load shedding overvoltage increases with the increase of zero-positive sequence impedance ratio of the system. The zero-positive sequence impedance ratio of the system is determined by the line and power supply. Since the zero-positive sequence impedance ratio of the line is generally unchanged, the zero-positive sequence impedance ratio of the system is mainly influenced by the zero-positive sequence impedance ratio of the power supply. The smaller the zero-positive sequence impedance ratio of the power supply is, the smaller the zero-positive sequence impedance ratio of the system will be, and the lower the overvoltage will be. In consideration of the extreme condition, the minimum zero-positive sequence impedance ratio of the power supply is 0.4, so when the zero-positive sequence impedance ratio of the power supply is 0.4, the single-phase grounding load shedding overvoltage will be the minimum. In Fig. 4.14, even if the zero-positive sequence impedance ratio of the power supply is down to 0.4, the single-phase grounding load shedding overvoltage is still larger than the fault-free load shedding overvoltage. In fact, the zero-positive sequence impedance ratio of the power supply rarely lowers to 0.4; for the point-to-point line with small zero-positive sequence impedance ratio of the power supply, the equivalent zero-positive sequence impedance ratio of the power supply is generally around 1; at this time, the single-phase grounding single-circuit load shedding overvoltage will be even higher than the single-circuit fault-free load shedding overvoltage.

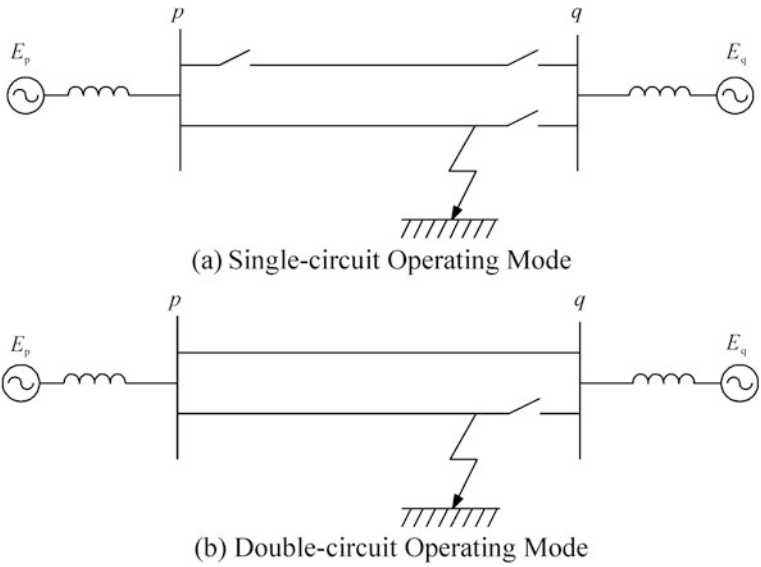

Fig. 4.15 Sketch of single-phase grounding load shedding of double-circuit UHV line

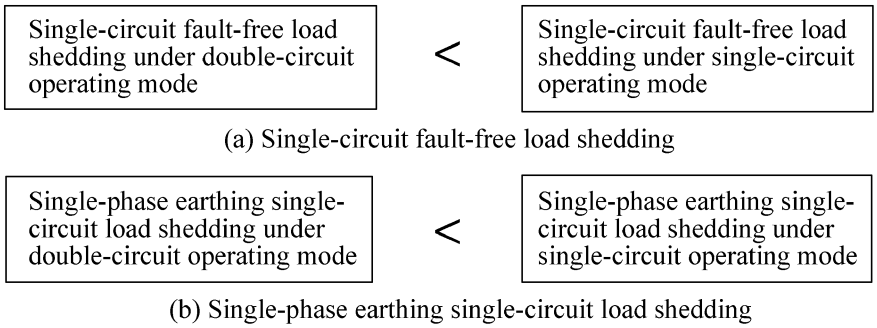

Fig. 4.16 Relationship between power frequency overvoltage of double-circuit line under different operating modes

(2) Comparison of the same type of power frequency overvoltage under different operating modes

Before and after the load shedding under two operating modes, the difference in the line structures determines the relative magnitude of overvoltage amplitude under the two operating modes. Under single-circuit operating mode (as shown in Fig. 4.15a), after load shedding, the operating circuit is only connected with the power supply at the head end; while under double-circuit operating mode (as shown in Fig. 4.15b), the circuit subject to load shedding is not only connected with the

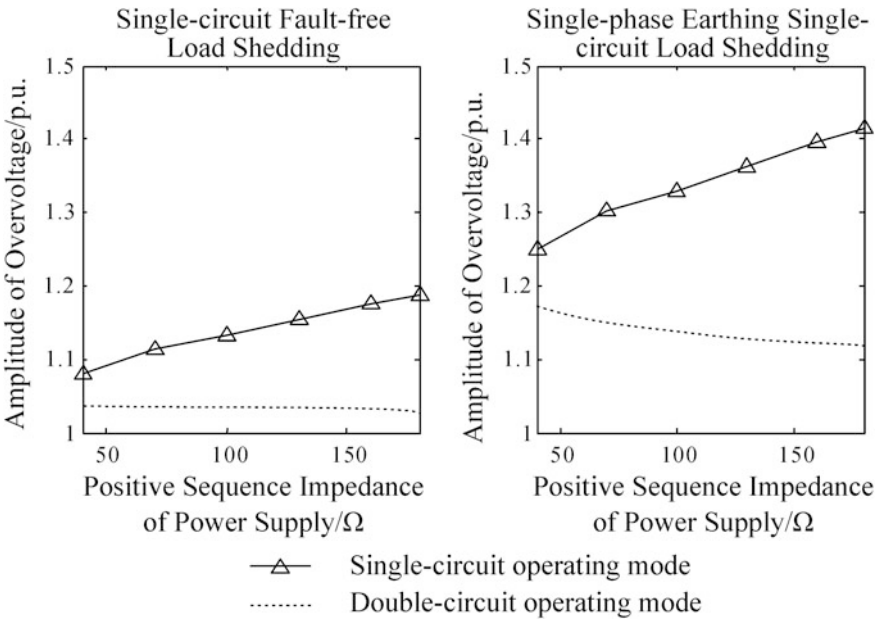

Fig. 4.17 Comparison of power frequency overvoltage of double-circuit line under different operating modes

power supply at the head end, but also connected with the power supply at the tail end through the other circuit, equivalent to the connection between two parallel connected power supplies and the no-load line after load shedding. The equivalent impedance of the power supply under double-circuit operating mode is smaller than that under single-circuit operating mode. Therefore, the single-circuit load shedding power frequency overvoltage under double-circuit operating mode is smaller than that under single-circuit operating mode. Similarly, for the single-phase grounding and single-circuit load shedding, the increase amplitude of voltage of the sound phase due to asymmetrical ground fault under the double-circuit operating mode is not as large as that under single-circuit operating mode, resulting in the power frequency overvoltage thereof smaller than that of the latter, as well. For the power frequency overvoltage resulting from single-circuit fault-free load shedding and single-phase grounding single-circuit load shedding, the relationship between the relative magnitudes of power frequency overvoltage of double-circuit line under different operating modes is shown in Fig. 4.16.

For the double-circuit line with different positive sequence impedances of the power supply, the amplitudes of power frequency overvoltage resulting from single-circuit fault-free load shedding and single-phase grounding and single-circuit load shedding under different operating modes are shown in Fig. 4.17.

It can be seen from Fig. 4.17 that, for the single-circuit fault-free load shedding overvoltage and the single-phase grounding and single-circuit load shedding

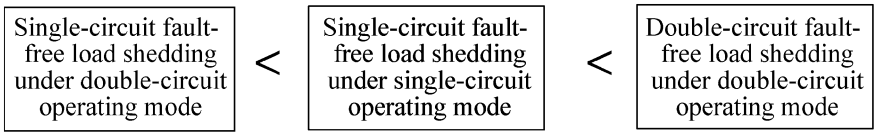

Fig. 4.18 Relationship among the three types of fault-free load shedding overvoltage of double-circuit line

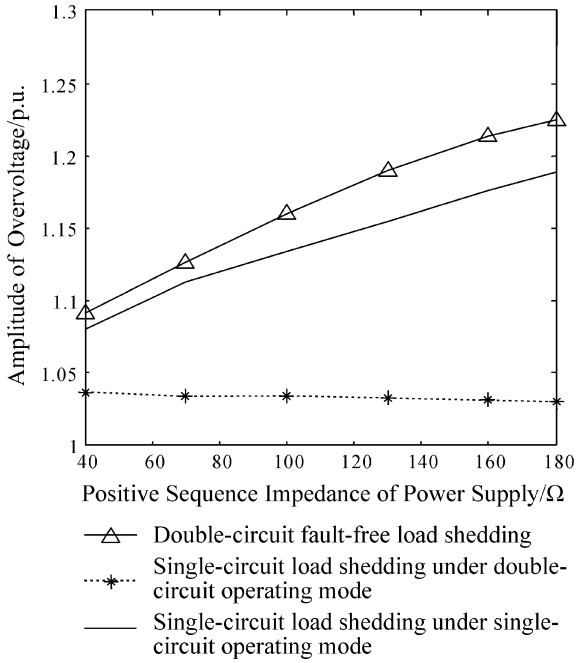

Fig. 4.19 Comparison of the three types of fault-free load shedding overvoltage

overvoltage, the amplitudes under double-circuit operating mode are less than that under single-circuit operating mode in all cases.

(3) Comparison of the three types of fault-free load shedding overvoltage

It is the difference in capacities rejected during the three types of fault-free load shedding that causes difference in overvoltage. In general, the larger the capacity rejected is, the more serious the overvoltage generated will be. Since the transmission capacity of single-circuit line under double-circuit operating mode is less than the transmission capacity of the line under single-circuit operating mode, and the transmission capacity of the line under single-circuit operating mode is less than the total capacity under double-circuit operating mode, as a result, the amplitudes of power frequency overvoltage under the three fault conditions, namely, single-circuit fault-free load shedding under double-circuit operating mode, fault-free load shedding under single-circuit operating mode, and double-circuit fault-free load

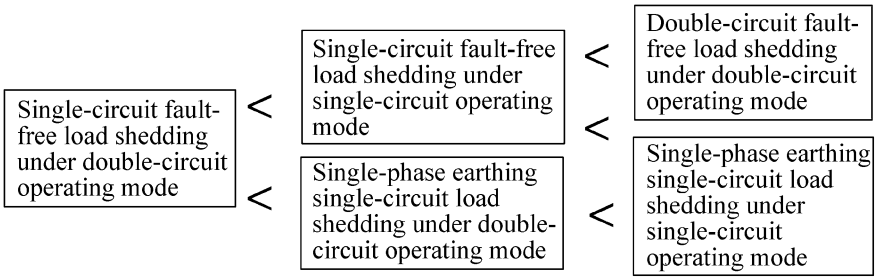

Fig. 4.20 Relative relationship of various types of power frequency overvoltage of double-circuit line

shedding under double-circuit operating mode, increase sequentially. The relationship among them is shown in Fig. 4.18.

The double-circuit line with length of 400 km is taken as an example for simulation calculation. For the calculation of the amplitudes of the above three types of fault-free load shedding overvoltage, since the fault-free load shedding has nothing to do with the zero-positive sequence impedance ratio but is influenced by the positive sequence impedance, only the influence due to variation of the positive sequence impedance of the power supply is considered. The results are shown in Fig. 4.19.

It can be seen from Fig. 4.19 that the three types of the fault-free load shedding overvoltage with amplitudes in a descending order are the double-circuit fault-free load shedding overvoltage under double-circuit operating mode, fault-free load shedding overvoltage under single-circuit operating mode and single-circuit fault-free load shedding overvoltage under double-circuit operating mode.

Based on the above analysis, the relationship between relative magnitudes of various types of power frequency overvoltage of the double-circuit line on the same tower can be obtained, as shown in Fig. 4.20.

It can be seen that, for the four types of overvoltage, namely, the single-circuit fault-free load shedding and single-phase grounding single-circuit load shedding under single-circuit operating mode and the single-circuit fault-free load shedding and single-phase grounding and single-circuit load shedding under double-circuit operating mode, the single-phase grounding and single-circuit load shedding overvoltage under single-circuit operating mode is the largest. However, only through Fig. 4.20, it is still impossible to judge the magnitude relationship between double-circuit fault-free load shedding overvoltage and single-phase grounding and single-circuit load shedding overvoltage under single-circuit operating mode. The magnitude relationship between the two will be further compared below, so as to determine the type of power frequency overvoltage with the largest amplitude.

(4) Comparison between single-phase grounding and load shedding overvoltage under single-circuit operating mode and double-circuit fault-free load shedding overvoltage under double-circuit operating mode

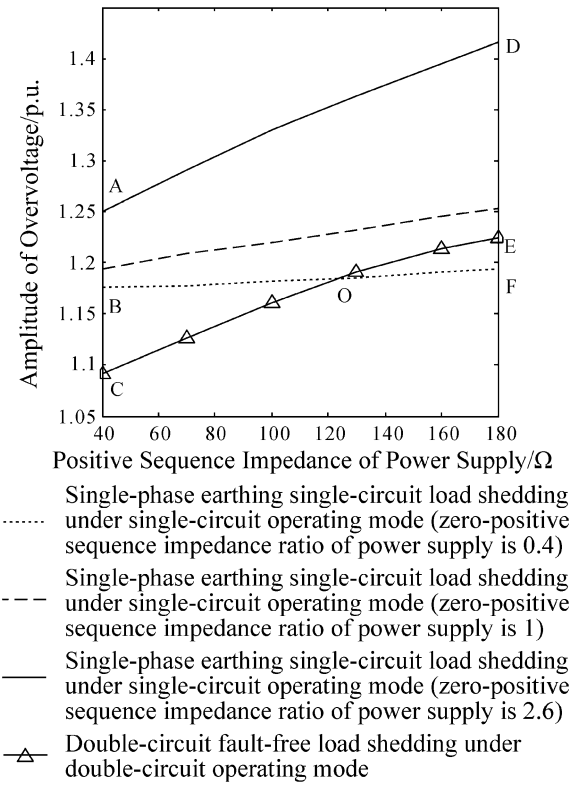

Fig. 4.21 Comparison between single-phase grounding load shedding overvoltage under single-circuit operating mode and double-circuit fault-free load shedding overvoltage under double-circuit operating mode

The single-phase grounding and load shedding overvoltage under single-circuit operating mode and the double-circuit fault-free load shedding overvoltage under double-circuit operating mode are compared through calculation with the influence of the positive sequence impedance of power supply considered. The zero-positive sequence impedance ratio of power supply which has influence on the single-phase grounding and load shedding overvoltage is also considered during the calculation. In consideration of the variation of zero-positive sequence impedance ratio, the results are shown in Fig. 4.21.

It can be seen from the figure that the double-circuit fault-free load shedding overvoltage increases with the increase of positive sequence impedance of the power supply. The single-phase grounding and load shedding overvoltage under single-circuit operating mode is influenced by both the power supply's positive sequence impedance and zero-positive sequence impedance ratio. The larger the positive sequence impedance of power supply is and the larger the zero-positive sequence impedance ratio of power supply is, the larger the single-phase grounding and load shedding overvoltage under single-circuit operating mode will be.

In Fig. 4.21, the trapezium ABFD is the area of amplitude of single-phase grounding and single-circuit load shedding overvoltage under single-circuit operating mode. Within the area covered by ABOED, the single-phase grounding and single-circuit load shedding overvoltage under single-circuit operating mode is larger than the double-circuit fault-free load shedding overvoltage in all cases. Only

within the area covered by the triangle EFO, the single-phase grounding and single-circuit load shedding overvoltage under single-circuit operating mode is smaller than the double-circuit fault-free load shedding overvoltage.

That is to say, the magnitude relationship between the single-phase grounding and load shedding overvoltage under single-circuit operating mode and double-circuit fault-free load shedding overvoltage shall be determined according to the actual conditions: for the lines with large positive sequence impedance of power supply and small zero-positive sequence impedance ratio, the double-circuit fault-free and load shedding overvoltage will be larger; for the lines with large zero-positive sequence impedance ratio of power supply, the single-phase grounding and load shedding overvoltage under single-circuit operating mode will be larger. However, in most cases, the zero-positive sequence impedance ratio of power supply is rarely obviously lower than 1. Therefore, usually, the single-phase grounding and load shedding overvoltage under single-circuit operating mode is larger than the double-circuit fault-free load shedding overvoltage under double-circuit operating mode.

4.4 Requirements on Restriction of UHV Power Frequency Overvoltage

Due to the different restrictive measures of power frequency overvoltage of UHV transmission line, various countries have different requirements on restriction of power frequency overvoltage of UHV system. The particular requirements are shown in Table 4.3 [1]. According to China's procedures, the overvoltage at the busbar side of substation shall be not higher than 1.3 p.u. and that at the line side shall be not higher than 1.4 p.u.; in addition, the time under power frequency overvoltage at the line side shall be not higher than 0.5 s. In Russia, the power frequency overvoltage limit is relatively high due to the long line, high voltage level and great difficulty in restriction. In Japan, although the double-circuit UHV line on the same tower is relatively short, since no high-voltage shunt reactors have yet been used to restrict the power frequency overvoltage, the overvoltage resulting from the double-circuit simultaneous load shedding of the double-circuit line is

Table 4.3 Power frequency overvoltage limits of UHV system in various countries

Country	Japan	Former Soviet Union	Italy	USA BPA	China
Maximum operating voltage U_m/kV	1100	1200	1050	1200	1100
Multiple of power frequency transient overvoltage (p.u.)	1.3/1.5[a]	1.44	1.35	1.3	1.3 (busbar side)/1.4[b] (line side)

[a]Overvoltage duration is less than 0.2 s; [b]overvoltage duration is less than 0.5 s

relatively large; therefore, the power frequency overvoltage limit in Japan is relatively high and the short-duration power frequency overvoltage limit is up to 1.5 p.u.

4.5 Influence Factors of UHV Power Frequency Overvoltage

The first section of this chapter has analyzed the causes for generation of power frequency overvoltage. It can be seen that the amplitude of UHV power frequency overvoltage is influenced by many factors, such as fault type, line length, equivalent impedance of power supply, location of ground fault point, and transmission power. Hereunder, these factors will be, respectively, discussed. In consideration that these main influence factors basically have similar influence on the single-circuit and double-circuit UHV lines, thus the power frequency overvoltage of single-circuit line is taken as an example for discussion when these influence factors are studied.

4.5.1 Line Length

As the UHV line cannot only be used for long-distance and large-capacity power transmission, but can also be used for short-distance and large-power transmission to save the line corridors which are highly scarcity in the economically developed

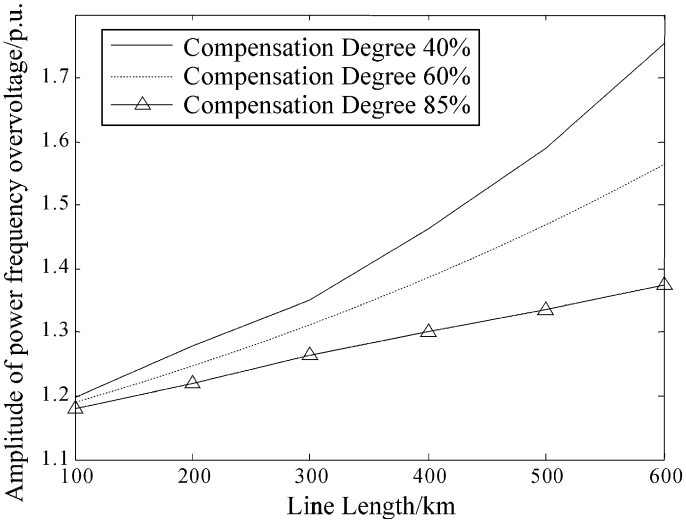

Fig. 4.22 Power frequency overvoltage of lines with different lengths

regions, the line length thereof varies a lot (which can also be seen from Table 4.1). The power frequency overvoltage of UHV lines with different lengths is simulated and the results are shown in Fig. 4.22. During simulation, to avoid the influence due to other factors, the impedance of power supply and voltage of busbar and transmission power are maintained unchanged, and the compensation degree is 40, 60, and 85%, respectively [12, 13]. It can be seen that the amplitude of power frequency overvoltage of UHV line gradually increases with the increase of line length.

4.5.2 Equivalent Impedance of Power Supply

1. Influence law of impedance of power supply on the power frequency overvoltage

Since the UHV line can undertake the power transmission tasks with different purposes, the conditions of power grid at the access point of UHV line have large difference, that is, the variation range of power supply characteristics of UHV line is large. Different power supplies will have large influence on the UHV power frequency overvoltage; therefore, it is necessary to compare and study the power frequency overvoltage of UHV line under different power supply characteristics,

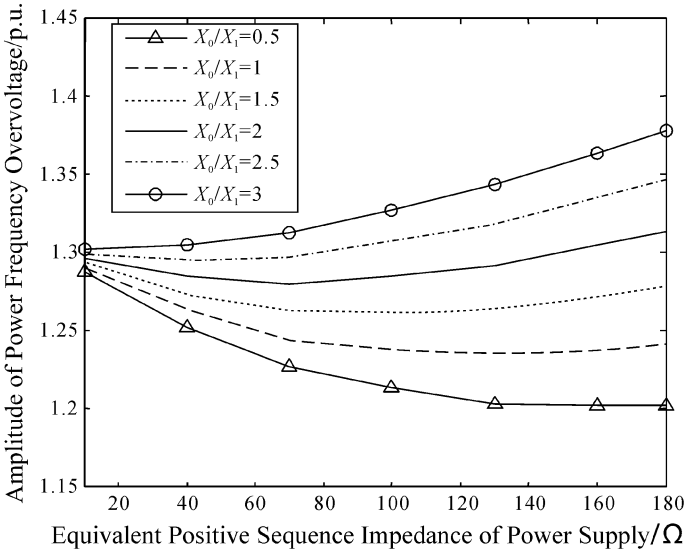

Fig. 4.23 Power frequency overvoltage corresponding to different equivalent positive sequence impedances of power supply

thus to obtain the influence law of impedance of power supply on the power frequency overvoltage.

The power supply mainly influences the power frequency overvoltage in two aspects, namely, the power supply's equivalent positive sequence impedance and zero-positive sequence impedance ratio X_0/X_1. The power frequency overvoltage of single-circuit UHV line with length of 400 km is calculated. During calculation, the power supply's positive sequence impedance and zero-positive sequence impedance ratio are changed and other conditions are maintained unchanged. The results are shown in Fig. 4.23.

From the above figure, the following two laws can be obtained:

(1) The larger the zero-positive sequence impedance ratio of power supply X_0/X_1 is, the more serious the power frequency overvoltage will be. The larger the equivalent zero-positive sequence impedance ratio of power supply is, the larger the zero-positive sequence impedance ratio of the entire UHV system will be, the more obvious the increase of voltage of the sound phase will be when single-phase ground fault occurs to the UHV line, and the larger the power frequency overvoltage will be.
(2) When the zero-positive sequence impedance ratio of power supply X_0/X_1 is larger than 2.5, the larger the positive sequence impedance of power supply is, the higher the amplitude of power frequency overvoltage will be; however, when the zero-positive sequence impedance ratio of power supply X_0/X_1 is smaller than 2.5, along with the increase of the positive sequence impedance of power supply, the amplitude of power frequency overvoltage will decrease first and then increase.

2. Analysis of principles

When the transmission power is maintained unchanged, the power frequency overvoltage is influenced by both the X_0/X_1 value and the magnitude of the positive sequence impedance of power supply. The X_0/X_1 value influences the increase of voltage of the sound phase due to ground fault. The larger the X_0/X_1 value is, the more increase of voltage of the sound phase and the more serious the overvoltage will be after the ground fault. The positive sequence impedance of power supply determines the strength of load shedding effect. When the transmission power is maintained unchanged, the larger the positive sequence impedance of power supply is, the increase amplitude of voltage for busbar after load shedding will be, and the higher the amplitude of system overvoltage will be.

In general, the zero-positive sequence impedance ratio of the UHV transmission line is about 2.6. When the zero-positive sequence impedance ratio of power supply is larger than 2.6, the increase of positive sequence impedance will result in the increase of zero-positive sequence impedance ratio of the entire system, thus to present more obvious increase of voltage of the sound phase due to ground fault. At the same time, the increase of positive sequence impedance will result in more obvious presentation of load shedding effect of the system, and thus, the power

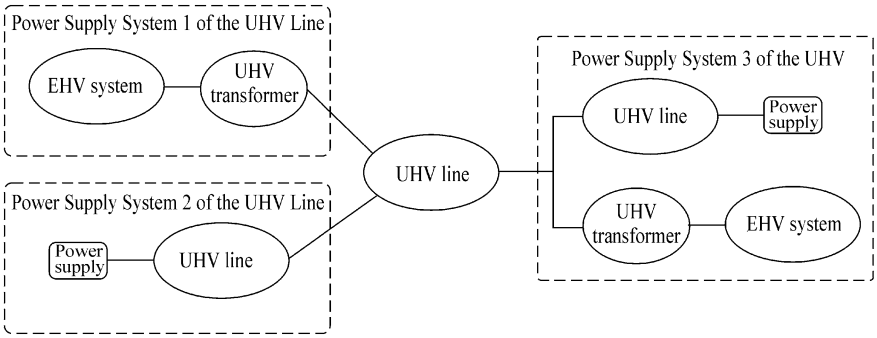

Fig. 4.24 Types of power supplies of the UHV line

frequency overvoltage will be increased significantly. However, when the zero-positive sequence impedance ratio of power supply is smaller than 2.6, the increase of positive sequence impedance will intensify the load shedding effect, but the zero-positive sequence impedance ratio of entire system will be decreased, thus to relatively weaken the increase of voltage of sound phase due to ground fault. As for the case that zero-positive sequence impedance ratio is smaller than 2.6, when positive sequence impedance of the power supply is relatively small, the weakening on the increase of voltage of sound phase due to ground fault will take the advantage along with the increase of positive sequence impedance; therefore, at this time, overvoltage level will be decreased along with the increase of positive sequence impedance; when positive sequence impedance is relatively large, the strengthening of load shedding effect will start to take the advantage; therefore, at this time, power frequency overvoltage will be increased along with the increase of the positive sequence impedance.

3. Power supply system of the UHV line

The power supply system of the UHV transmission line is divided into three major types, as shown in Fig. 4.24. The first type of power supply consists of the EHV system and UHV transformer, and the power supply of point-to-point UHV line is of this type; the second type of power supply consists of one or several adjacent UHV lines and power supply thereof after the UHV line is networked; and the third type of power supply is that the above two types of power supplies are paralleled and connected to the UHV line at the same time.

During the initial development period of UHV, the point-to-point line played the leading role, and the power supply was in general the first type. This type of power supply is connected with the EHV line through UHV transformer. Since the UHV transformer's positive sequence impedance is large and zero-positive sequence impedance ratio is small, so the first type of power supply system, as a result, has large equivalent positive sequence impedance and small zero-positive sequence impedance ratio. The second type of power supply is formed after the UHV line is networked. At this time, the grid structure of UHV system is strong and its

equivalent impedance of the power supply is relatively small; however, since it is connected with the line, the zero-positive sequence impedance ratio of such power supply is approximate to the zero-positive sequence impedance ratio of the UHV line and larger than that of the first type of power supply. To obtain more voltage support, the UHV line will be connected with EHV system generally through UHV transformer at the nodes, and thus, the third type of power supply system is generated. Actually, it is the combination of the above two types of power supply systems; therefore, the impedance and zero-positive sequence impedance ratio of power supply are also between those of the above two types of power supply systems.

4. Power frequency overvoltage of the UHV line of islanding power supply

As mentioned above, during the initial construction period of the UHV system, the power supply systems, including such islanding coal power bases in west Inner Mongolia and Shanxi, were weak. The islanding power supply, simple in structure, is connected with the main grid framework only through the UHV line and its equivalent impedance is large. During the transmission of large power, it can cause a very serious power frequency overvoltage in case of three-phase load shedding fault. Therefore, it must be attached with sufficient importance.

The power frequency overvoltage of such a type of UHV line is very serious, but not unrestricted. Since the impedance of islanding power supply is large, the transmission power of the line is usually relatively small; when high-voltage shunt reactor with large capacity is additionally installed, the reactive power balance can be more easily met, providing favorable conditions to additionally install high-voltage shunt reactor with large capacity. In such a way, it is more favorable to restrict the power frequency overvoltage.

4.5.3 Location of the Ground Fault Point

When ground fault points are different, the amplitudes of power frequency overvoltage are also generally different. Therefore, it is necessary to study the influence law of ground fault point location on the amplitude of power frequency overvoltage, thus to determine the location of that ground fault point generating high-amplitude power frequency overvoltage, to which the main consideration shall be given.

1. Calculation example

For single circuit UHV line with length of 400 km, the load shedding overvoltage is calculated when single-phase grounding is occurred in various points along the line according to three cases, that is, the high-voltage shunt reactor is, respectively, mounted at sending end, receiving end, and even distributed at both ends; the compensation degree of high-voltage shunt reactor is taken as 85%, and the zero-positive sequence impedance ratio of power supply is taken as 1.4. Such

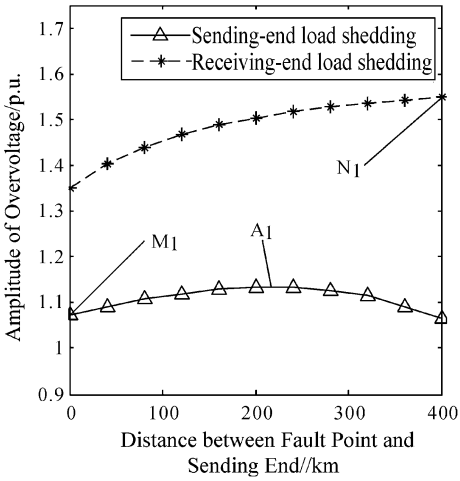

Fig. 4.25 Power frequency overvoltage of the whole line in case of single-phase ground fault occurred to the points along the line under sending-end compensation

overvoltage is mainly related to several factors: first, the compensation modes of high-voltage shunt reactor (compensation at sending end, receiving end, and both ends) and their compensation degree of high-voltage shunt reactor; then the modes of load shedding (sending-end load shedding or receiving-end load shedding); and finally single-phase ground fault location along the line (sending end, receiving end, or other position of the line). In addition, it is also related to the impedance characteristics of power supply (zero-positive sequence impedance ratio).

(1) Compensation at sending end

In case of compensation at sending end, when the single-phase ground fault is occurred to the points along the line, the variation of the maximum overvoltage of the whole line under sending-end load shedding and receiving-end load shedding is shown in Fig. 4.25. It can be seen from Fig. 4.25 that, in case of receiving-end load shedding of the line, along with the movement of the fault point to load shedding end, the overvoltage will be increased gradually; the ground fault point that generating the maximum overvoltage will be located at the line end after load shedding of the line (receiving end, at point N_1 in Fig. 4.25). In case of sending-end load shedding of the line, along with the movement of the fault point to load shedding end, sending-end load shedding overvoltage will present the trend of initial increase and subsequent decrease, and the ground fault point that generating the maximum overvoltage will be located in the middle of the line (at point A_1), instead of load shedding end (sending end, at point M_1).

(2) Compensation at receiving end

In case of compensation at receiving end, when the single-phase ground fault is occurred to the points along the line, the variation of the maximum overvoltage of the whole line under sending-end load shedding and receiving-end load shedding is shown in Fig. 4.26. It can be seen from Fig. 4.26 that, in case of sending-end load

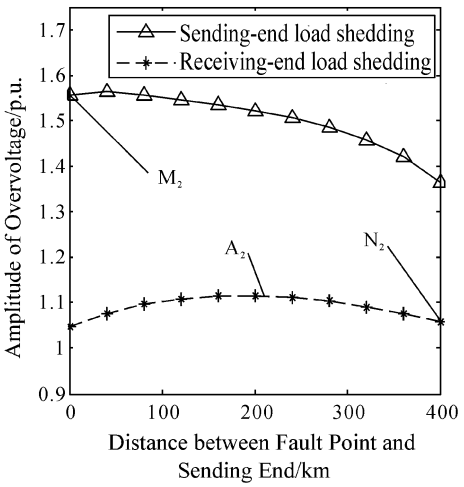

Fig. 4.26 Power frequency overvoltage of the whole line in case of single-phase ground fault occurred to the points along the line under receiving-end compensation

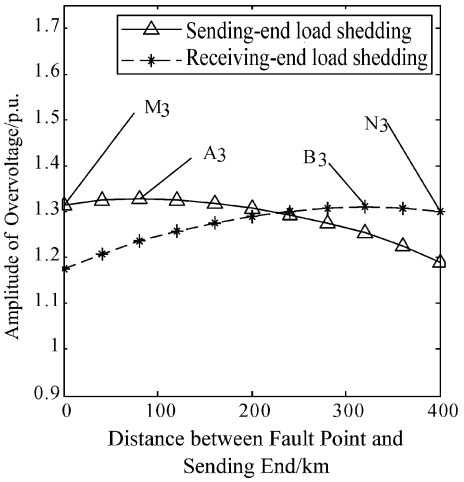

Fig. 4.27 Power frequency overvoltage in case of grounding of the points along the line under compensation at both ends

shedding of the line, along with movement of fault point to load shedding end, the overvoltage will be increased gradually; the ground fault point generating maximum overvoltage will be located at load shedding end of the line (sending end, at point M_2 in Fig. 4.26). In case of receiving-end load shedding of the line, along with movement of fault point to load shedding end, sending-end load shedding overvoltage will present the trend of initial increase and subsequent decrease, and the ground fault point generating maximum overvoltage will be located in the middle of the line (at point A_2).

(3) Compensation at both ends

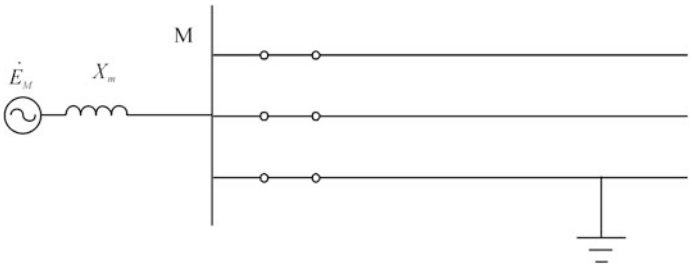

Fig. 4.28 Sketch of the line after load shedding

In case of average compensation at both ends, when the single-phase ground fault is occurred to the points along the line, the variation of the maximum overvoltage of the whole line under sending-end load shedding and receiving-end load shedding is shown in Fig. 4.27. The amplitude of power frequency overvoltage is the maximum when single-phase ground fault is occurred to at the point with a distance of about 80 km to the load shedding end (the maximum values under the two modes, respectively, emerge at the points A_3 and B_3 in the two curves, as shown in Fig. 4.27).

2. Influence of the relative position of power supply, high-voltage shunt reactor and ground point on the power frequency overvoltage

After load shedding, the secondary steady-state structure connected with power supply and grounding line that unloaded, as shown in Fig. 4.28, will be formed in short time. At this time, the position of ground point that generating higher overvoltage will be mainly influenced by the following factors: the impedance characteristics of the power supply, and the relative position of the high-voltage shunt reactor and load shedding end.

The closer to the power supply of the fault point is, the larger the influence of impedance of the power supply on the impedance characteristics will be (when viewed from the fault point to the system); usually, the equivalent zero-positive sequence impedance ratio of power supply will be smaller than that of the line; therefore, the closer to the power supply of the fault point is, the smaller the zero-positive sequence impedance ratio will be (when viewed from the fault point to the system), and the smaller the amplitude of overvoltage will be.

After grounding load shedding, the maximum overvoltage is in general emerged on the sound phase adjacent to ground point. The high-voltage shunt reactor can perfect inhibit such maximum overvoltage; in addition, the closer to the high-voltage shunt reactor of the fault is, and the larger the capacity of high-voltage shunt reactor will be, the better the inhibition results will be. When ground point is close to load shedding end and load shedding end is mounted with high-voltage shunt reactor, the overvoltage on the sound phase nearby the fault point will be inhibited greatly; otherwise, the inhibition results of the high-voltage shunt reactor on the overvoltage of the sound phase nearby the fault point will be weakened.

Thus, the position of fault point generating maximum grounding load shedding overvoltage will be moved to the direction away from high-voltage shunt reactor.

3. Determination of the ground fault point

In the calculation of power frequency overvoltage, some researchers take the ground point at load shedding end as the condition for calculation of the maximum grounding load shedding overvoltage, namely, only calculating the sending-end load shedding overvoltage in case of sending-end grounding and receiving-end load shedding overvoltage in case of receiving-end grounding. This condition is used to calculate the line with compensation at single end, and in general, the maximum overvoltage can be obtained.

Taking the line with compensation at the receiving end as an example, the sending-end load shedding overvoltage in case of sending-end single-phase grounding and receiving-end load shedding overvoltage in case of receiving-end single-phase grounding are calculated according to the above condition, where sending-end load shedding overvoltage in case of sending-end single-phase-to-ground fault is the maximum value of sending-end load shedding overvoltage after fault. However, sending-end load shedding overvoltage after fault is far above receiving-end load shedding overvoltage after fault; therefore, the maximum value of sending-end load shedding overvoltage after fault is the maximum value of single-phase grounding load shedding overvoltage, that is, sending-end load shedding overvoltage in case of sending-end single-phase grounding is the maximum value of single-phase grounding load shedding overvoltage. However, for the line with compensation at both ends, the sending-end load shedding overvoltage level after fault is equivalent to the receiving-end load shedding overvoltage level after fault; in addition, both sending-end load shedding overvoltage in case of sending-end single-phase-to-ground fault and receiving-end load shedding overvoltage in case of receiving-end single-phase-to-ground fault are not the respective maximum values; therefore, at this time, the condition for calculation of the maximum grounding load shedding overvoltage while locating the ground point at load shedding end (tail end) is not rational. Therefore, in the new procedures (about overvoltage and insulation coordination in the 1000 kV UHV transmission projects), the provisions on ground fault point location in terms of grounding load shedding overvoltage are canceled.

According to the above discussions, it is recommended to use the following calculation conditions for single-phase grounding load shedding overvoltage: in case of no high-voltage shunt reactor mounted at the load shedding end, calculating the tail end grounding load shedding overvoltage is enough; in case of high-voltage shunt reactor mounted at the load shedding end of the line, the load shedding power

Table 4.4 Power frequency overvoltage under different load flow

Power (MW)	1000	2000	3000	4000
Overvoltage of busbar (kV)	940	952	968	1011
Overvoltage of line (kV)	1133	1145	1164	1214

frequency overvoltage when single-phase grounding is occurred to various points along the line shall be calculated, thus to determine the power frequency overvoltage level according to its maximum value when single-phase grounding load shedding is occurred to the line.

4.5.4 Transmission Power

The variation of transmission power will have large influence on the power frequency overvoltage of the UHV line; therefore, in the overvoltage design of the UHV line, it shall be given sufficient consideration. Taking the single circuit UHV line with length of 400 km as example, the magnitude of power frequency overvoltage when transmitting different power flow is calculated and the results are shown in Table 4.4. Considering that the natural power of each circuit of the UHV line is approximate to 5000 MW, and the load flow of the line will be taken as 1000–4000 MW and the operating voltage of busbar under different load flow will be maintained unchanged.

It can be seen from Table 4.4 that, on the condition that the voltage of busbar during normal operation is maintained identical, the larger the power transmitted on the same line is, the more serious the power frequency overvoltage will be.

It can be seen through analysis that this mainly results from the causes in the following two aspects:

(1) When the transmission power is large, the load shedding effect will be more obvious. The larger the transmission power is, the higher the equivalent voltage of the power supply during normal operation will be, then the larger the increase amplitude of voltage of busbar after load shedding will be, and the more serious the overvoltage will be.
(2) When the transmission power is large, the inductive reactive power required in the line will be smaller, to achieve the reactive power balance, the LV capacitance on the third winding of UHV transformer is necessary to put into

Table 4.5 Power frequency overvoltage under different nominal heights of tower

Nominal height (m)	Capacitance (MΩ/km)		100 km charging power (Mvar)	High-voltage shunt reactor (H)	Overvoltage (kV)	
	Positive sequence	Zero sequence			Line	Busbar
49	0.2283	0.3526	530	4.2747	1180	991
59	0.2301	0.3812	526	4.3084	1181	991
69	0.231	0.4023	524	4.3253	1181	991
79	0.2315	0.4198	523	4.3346	1181	991

Table 4.6 Power frequency overvoltage under different outer conductor spaces

Outer conductor space (m)	Capacitance (MΩ/km)		100 km charging power (Mvar)	High-voltage shunt reactor (H)	Overvoltage (kV)	
	Positive sequence	Zero sequence			Line	Busbar
21.4	0.2201	0.4224	550	4.1212	1195	993
31.4	0.231	0.4023	524	4.3253	1181	991
41.4	0.24	0.3869	504	4.4938	1171	990

use. The larger the power is, the larger the capacity of the LV capacitance put into use will be, the more obvious the weakening effect on the high-voltage shunt reactor will be, and the higher the load shedding overvoltage will be.

4.5.5 Tower Structures of the Line

Since the area through which the UHV line passes has complex topographic conditions and requirements on the conductor height and position are different under different circumstances, the tower parameters thereof are also different to certain extent. In the overvoltage design, whether the influence of variation of tower parameters on the amplitude of power frequency overvoltage is necessary to consider will be discussed in this section. Taking the cathead-type tower used in Chinese single circuit UHV line as reference (in the typical design scheme, nominal height is 69 m and distance from outer conductor to conduct center axis is 15.7 m), the power frequency overvoltage when tower height and outer conductor space are changed is calculated, and the results are shown in Tables 4.5 and 4.6.

According to the provisions as specified in the procedures, the minimum conductor to ground distance of single circuit UHV line is 19 m (for non-agricultural cropped location with less population); considering 11 m insulator length and 15 m arc sag, the minimum nominal height of tower is 45 m; large nominal height is not favorable to lightning protection and also enlarge the size of tower and the cost; therefore, in general, the nominal height will not have significant increase in comparison with typical design value; therefore, in Table 4.5, the upper limit of nominal height is taken as 69 m. The outer conductor spacing is mainly determined by the air clearance between conductor and tower and has a small variation in general; the range of 21.4–41.4 m, as shown in Table 4.6, has completely included the possible variation range of outer conductor spacing.

The calculation results show that the variation of the nominal height nearly has no influence on the power frequency overvoltage of the line. Along with the decrease of outer conductor spacing, the amplitude of power frequency overvoltage is increased slightly; however, changing the outer conductor spacing will have certain influence on the charging power of the line: when the outer conductor spacing is decreased from 41.4 to 21.4 m, the power frequency overvoltage will be

increased by 24 kV. However, in a whole, changing the nominal height and the outer conductor spacing will have small influence on the power frequency overvoltage of the UHV line; the influence of tower variation on the power frequency overvoltage cannot be considered.

The influence of the nominal height and the outer conductor spacing on the power frequency overvoltage can be explained from the perspective of line capacitance. The larger the line capacitance is, the more obvious the capacitance effect will be, and the more serious the power frequency overvoltage will be. However, under the same compensation degree, the line with larger charging power also has larger capacitance capacity that not being compensated, and therefore, the amplitude of power frequency overvoltage thereof is also larger. Changing the nominal height and the outer conductor spacing will have small influence on the charging power of the UHV line; therefore, in case of change to the nominal height and the outer conductor spacing, the variation amplitude of power frequency overvoltage will be very small.

4.6 Restrictive Measures for UHV Power Frequency Overvoltage

4.6.1 Fixed High-Voltage Shunt Reactor

The compensating line capacitance with high-voltage shunt reactor can effectively restrict the power frequency overvoltage. In the UHV lines having been constructed in both the former Soviet Union and China, the fixed high-voltage shunt reactors are all used to restrict the power frequency overvoltage.

Research on the compensation with high-voltage shunt reactor mainly involves the determination of compensation degree and compensation mode. The higher the compensation degree of the high-voltage shunt reactor is, the better the results on restriction of the power frequency overvoltage will be. The UHV transmission line has a large charging power, especially the long-distance UHV transmission line; therefore, the high-voltage shunt reactor with higher compensation degree shall be mounted to achieve compensation. However, to avoid difficulties in the reactive power balance and voltage control during normal operation and prevent the occurrence of open-phase operation resonance overvoltage, the compensation degree of the high-voltage shunt reactor shall not be too high. During the initial construction period of UHV power grid, the compensation degree of the high-voltage shunt reactor is in general considered to be controlled at 80–90% [1]. For areas with strong power grid or short UHV transmission line, the compensation degree can be appropriately reduced.

In case the compensation degree is fixed, the compensation mode will have large influence on the UHV power frequency overvoltage. According to the difference in quantities of compensation points, it can be divided into compensation at single

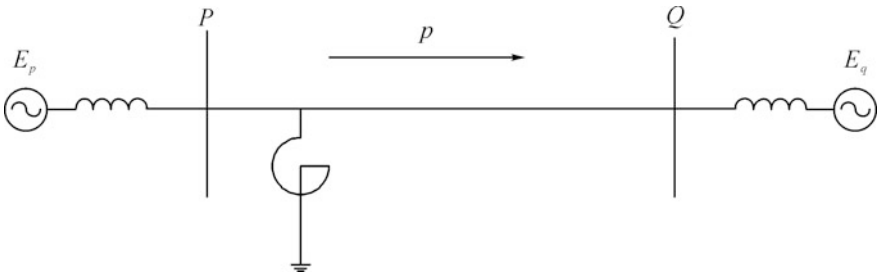

Fig. 4.29 Sketch of the line with compensation at sending end

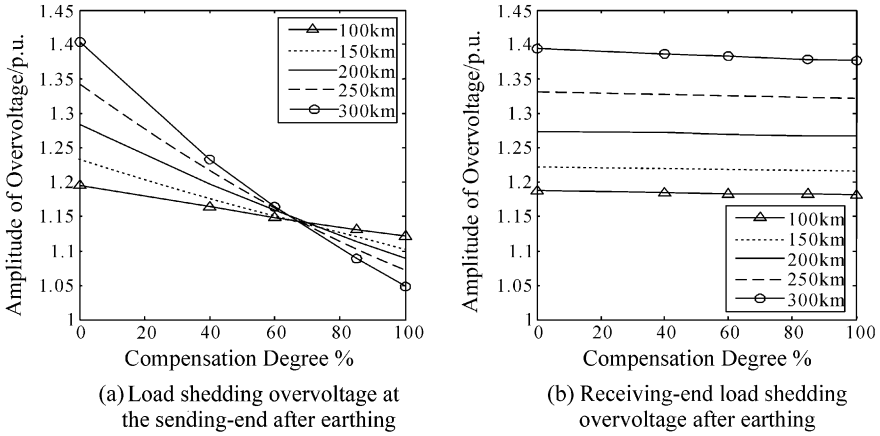

Fig. 4.30 Load shedding power frequency overvoltage of the line with compensation at sending end in case of single-phase ground fault

end, compensation at both ends, and sectional multi-point compensation [14]. Here, the results on restriction of power frequency overvoltage through three compensation modes are, respectively, studied.

4.6.1.1 Compensation at Single End

For any line, the both ends can be divided into sending end and receiving end through power flow. Therefore, the compensation at single end consists of two cases, that is, the high-voltage shunt reactor is, respectively, mounted at sending end or receiving end.

1. Compensation at sending end

The line with compensation at sending end is shown in Fig. 4.29, where the power is transmitted from P end to Q end. Here, the line with length of 100–300 km

subject to compensation at sending end is studied. Considering the conditions of common power supply (namely, impedance characteristics of power supply are the same at both ends), for load shedding at sending end and receiving end, the power frequency overvoltage after single-phase ground fault is calculated under different compensation degrees and the results are shown in Fig. 4.30.

It can be seen from Fig. 4.30 that:

(1) Compensation at sending end has good restriction effect on the sending-end load shedding overvoltage in case of single-phase ground fault; in addition, along with the increase of compensation degree, the longer the line is, the quicker the decrease of overvoltage level will be. For the UHV line with length of 300 km, when the compensation degree is increased from 0 to 100%, the decrease amplitude of overvoltage will be up to 0.35 p.u.

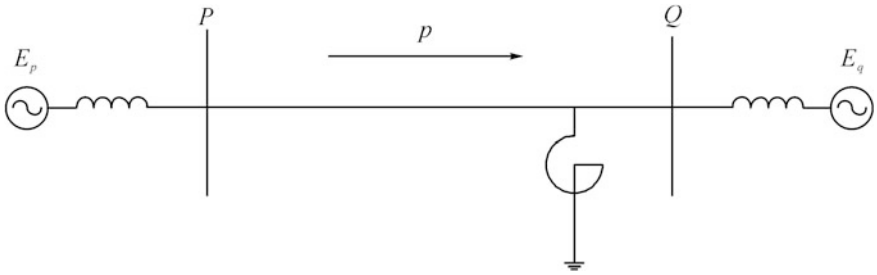

Fig. 4.31 Sketch of the line with compensation at receiving end

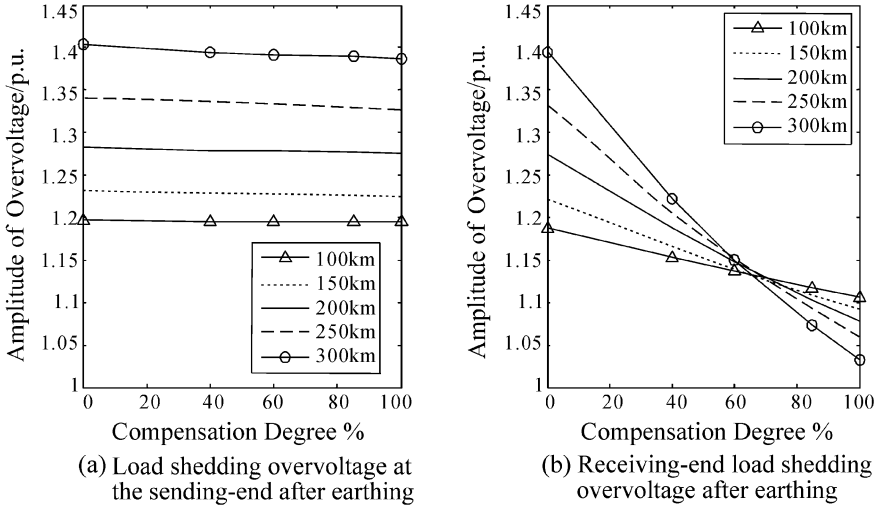

Fig. 4.32 Load shedding power frequency overvoltage of the line with compensation at receiving end after single-phase ground fault

(2) The restriction effect of compensation at sending end on receiving-end load shedding overvoltage in case of single-phase ground fault is not obvious, and the decrease of overvoltage is small along with the increase of compensation degree. For the lines with the lengths as shown in the figure, when the compensation degree is increased from 0 to 100%, the decrease amplitude of overvoltage is not larger than 0.03 p.u.

2. Compensation at receiving end

The line with compensation at the receiving end is shown in Fig. 4.31. Similar to the line with compensation at the sending end, the line with length of 100–300 km is studied. The single-phase grounding load shedding power frequency overvoltage of the line with compensation at sending end is calculated under different compensation degrees, and the results are shown in Fig. 4.32.

It can be seen from the calculation results that:

(1) Compensation at the receiving end has not obvious restriction effect on the sending-end load shedding overvoltage in case of single-phase ground fault; the decrease of overvoltage is small along with the increase of compensation degree. For the lines with the lengths as shown in the figure, when the compensation degree is increased from 0 to 100%, the decrease amplitude of overvoltage is small and not larger than 0.03 p.u. in all cases.

(2) Compensation at the receiving end has good restriction effect on the receiving-end load shedding overvoltage in case of single-phase ground fault; in addition, along with the increase of the compensation degree, the longer the line is, the quicker the decrease of overvoltage level will be. For the UHV line with length of 300 km, when the compensation degree is increased from 0 to 100%, the decrease amplitude of overvoltage will exceed 0.35 p.u.

From the summarized calculation results for the lines with compensation at sending end and the lines with compensation at receiving end, it can be seen that: the compensation at sending end and the compensation at receiving end both have obvious restriction effect on load shedding overvoltage at the end with high-voltage shunt reactor and very small restriction effect on load shedding overvoltage at the end without high-voltage shunt reactor.

In consideration that the compensation at single end will only have obvious restriction effect on the load shedding overvoltage at one end of the line, the position at which the high-voltage shunt reactor is to be additionally installed shall be rationally selected when the mode of compensation at single end is adopted. Supposing the two ends of a line are, respectively, named *A* and *B*, due to the different power supply characteristics at both ends of the line, the load shedding power frequency overvoltage at end *A* before the additional installation of high-voltage shunt reactor is obviously higher than the load shedding power frequency overvoltage at end *B*. In such a case, the compensation at single end shall be mainly considered to restrict the load shedding overvoltage at end *A*, and hence, the high-voltage shunt reactor shall be additionally mounted at end *A*.

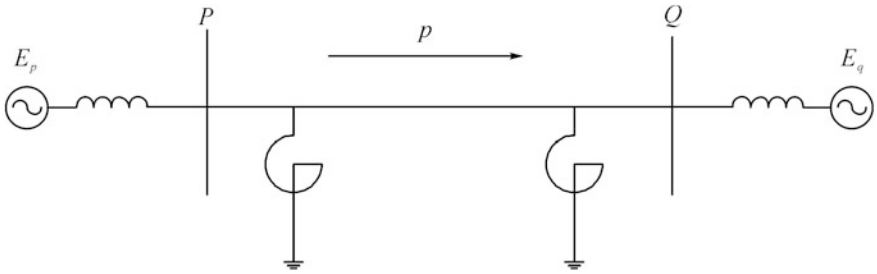

Fig. 4.33 Sketch of the line with compensation at both ends

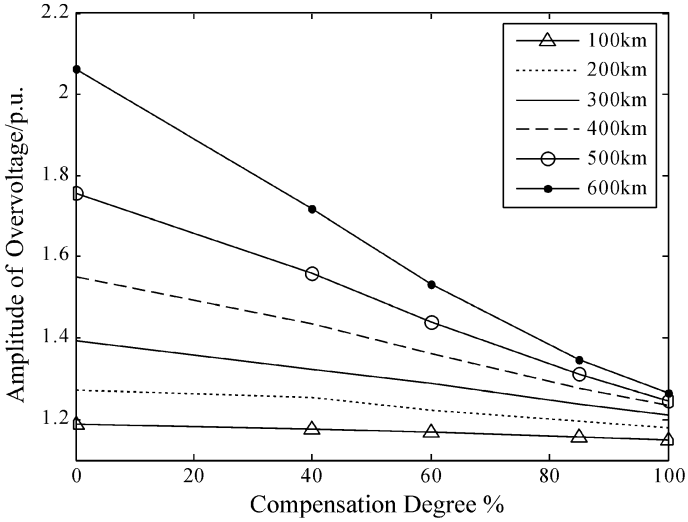

Fig. 4.34 Power frequency overvoltage of the line with compensation at both ends

4.6.1.2 Compensation at Both Ends

The system with compensation at both ends is shown in Fig. 4.33. Compared to the compensation at single end, the compensation at both ends has the following advantages: no matter which end of the line is subject to load shedding, there will be partial high-voltage shunt reactor at the load shedding end, and hence, it is able to well restrict the maximum value of the power frequency overvoltage. The UHV lines with different lengths subject to compensation at both ends are simulated and the results are shown in Fig. 4.34.

It can be seen from the figure that the high-voltage shunt reactor under-compensation at both ends has a very obvious restriction effect on power frequency overvoltage. In addition, the longer the line is, the quicker the decrease of over-voltage level along with the increase of compensation degree will be. When the

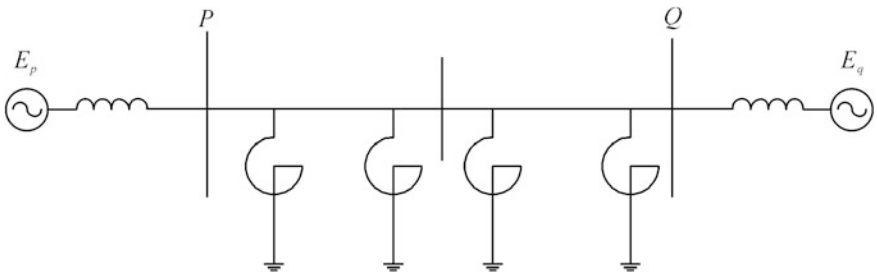

Fig. 4.35 Sketch of the line with two-section compensation at three points

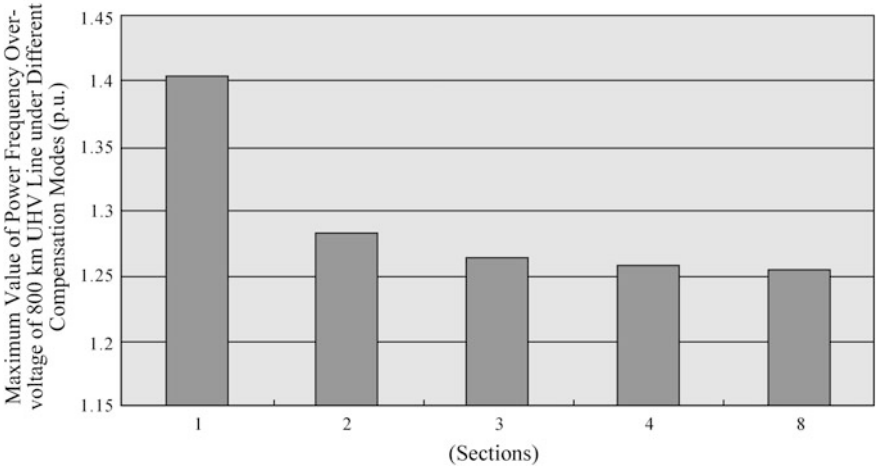

Fig. 4.36 Power frequency overvoltage under different compensation modes. *Note* The abscissa refers to the number of sections. The capacity of high-voltage shunt reactors at both ends of each line section is identical

compensation degree is high, the power frequency overvoltage of the lines with different lengths can always be restricted to a low level.

4.6.1.3 Sectional Compensation at Multiple Points

For the long-distance UHV transmission line (with length longer than 600 km), even if the capacity of high-voltage shunt reactor reaches the upper limit, the power frequency overvoltage under-compensation at both ends may still exceed the range as specified in the procedures. At this time, in case to decrease the maximum value of power frequency overvoltage, it is necessary to add compensation points at the middle of the line to more evenly distribute the capacity of high-voltage shunt reactor on the line, namely, adopting the mode of sectional compensation at multiple points. Figure 4.35 shows the mode of two-section compensation at three

points. At both ends of each line section, the capacity of high-voltage shunt reactor is identical.

The point-to-point UHV line with length of 800 km is taken as an example for calculation. The line is, respectively, divided into 1–4 and 8 sections for compensation and the total compensation degree is 85% for all cases. The calculation results are shown in Fig. 4.36.

It can be seen from Fig. 4.36 that: ① the more the compensation points are, the lower the power frequency overvoltage will be. When the number of sections is increased from 1 to 8, the decrease amplitude of power frequency overvoltage is approximate to 0.15 p.u. and ② when the number of sections is increased to a certain extent and the space between adjacent compensation points is decreased to a certain extent, the continuous increase of sections and decrease of space between adjacent compensation points cannot significantly decrease the level of power frequency overvoltage. For example, when the number of sections is increased from 3 to 8, the decrease amplitude of the maximum value of power frequency overvoltage is only 0.01 p.u.

4.6.1.4 Selection of Compensation Modes for High-Voltage Shunt Reactors

From the perspective of restriction of power frequency overvoltage, the more the compensation points are, the better the restriction effect will be. With the increase of line length, or in case the grid structure of power supply is weak, the compensation at single end, compensation at both ends and sectional compensation at multiple points will be considered in turn to restrict the power frequency overvoltage. However, from the perspective of economy, the less the compensation points are, the better the economy will be. Therefore, in the practical projects, both the restriction effect on power frequency overvoltage and the economy shall be considered to rationally select the compensation mode and the number of sections. On the premise that the restriction requirements for power frequency overvoltage are met, the number of compensation points shall be minimized to reduce the costs for compensation with high-voltage shunt reactors.

4.6.2 Controllable High-Voltage Shunt Reactor

The largest advantage of the UHV transmission line is that it is suitable for long-distance and large-capacity power transmission. However, at present, to restrict the power frequency overvoltage, the long-distance UHV transmission line will in general be mounted with high-voltage shunt reactor with large capacity, which will greatly reduce the transmission capacity of the line. However, this problem can be well solved by means of controllable high-voltage shunt reactor. Starting from the function of reactive power compensation equipment, this section will describe the

insufficiency of fixed high-voltage shunt reactor and demonstrate the necessity of controllable high-voltage shunt reactor; in addition, the principles and development process of controllable high-voltage shunt reactor will also be introduced.

4.6.2.1 Necessity of Controllable High-Voltage Shunt Reactor

The reactive power compensation equipment of power grid must have two functions: (1) restricting the power frequency overvoltage and (2) facilitating to achieve reactive power balance during normal operation of the system [1].

1. Restricting the power frequency overvoltage

As one type of reactive power compensation equipment, high-voltage shunt reactor has good restriction effect on the power frequency overvoltage; for long-distance transmission line, in general, the high-voltage shunt reactor shall be mounted to restrict the power frequency overvoltage to be within the range as specified in the procedures.

The capacity of the high-voltage shunt reactor is determined through restriction on the power frequency overvoltage. The UHV transmission line features long distance, large transmission capacity, and large charging power, and thus, the amplitude of power frequency overvoltage is large; to restrict the power frequency overvoltage to a range as specified in the procedures, its capacity can be up to 80–90% of charging power of the line.

2. Reactive power balance

To ensure the operating voltage of the system within the rational range, and reduce the reactive power transmission and network loss, the reactive power provided by the reactive power compensation equipment shall be balanced with the reactive power consumed by the system. The principles of reactive power balance are layered, zoned, and local balance. Therefore, the reactive power compensation equipment of the UHV transmission line is mainly used to balance the reactive power consumed by the UHV system.

In the UHV system, the equipment consuming the reactive power mainly includes UHV transformer and UHV line. The reactive power consumed by both of them is closely related to the transmission power.

(1) Transformer

The larger the transmission power is, the larger the current passing through the transformer will be, and the larger the reactive power consumed by the transformer impedance will be.

(2) Transmission line

Figure 4.37 shows the sketch of line distribution parameter model. It can be seen from the figure that the reactive power of the line mainly includes two aspects: the

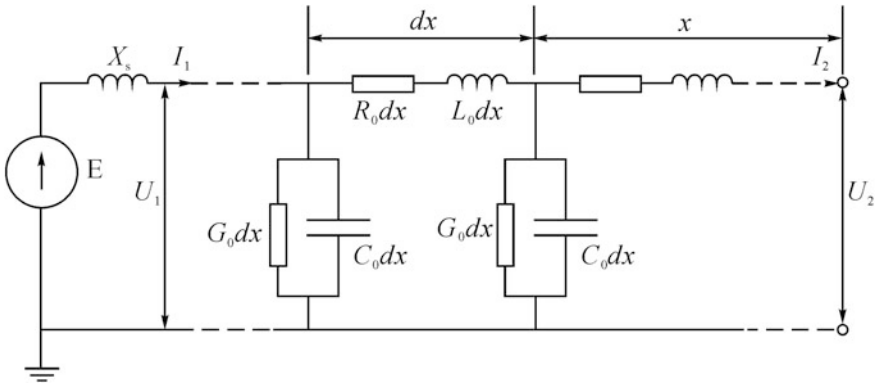

Fig. 4.37 Sketch of line distribution parameter model

reactive power Q_L consumed by unit-length line inductance L_0 and the reactive power Q_C provided by unit-length line capacitance C_0. In case the effective values of the rated operating voltage and current of the line are, respectively, U_N and I, thus $Q_C = j\omega C_0 U_N^2$, $Q_L = j\omega L_0 I^2$. It can be seen that the reactive power Q_C generated by line capacitance is only related to the line voltage and has nothing to do with the transmission power; on the line under normal operation, the voltage fluctuation is small in general; therefore, Q_C can be considered unchanged. The reactive power Q_L consumed by transmission line reactance presents square relation with the line current I, namely, presenting direct proportion relation with square of transmission power.

In case of different load flow, the reactive power required by the system is different.

When the transmission power of the line is small, for example, the unloaded UHV line under extreme conditions, the line current will be zero ($I = 0$) and line reactance will not consume reactive power, namely, $Q_L = 0$; however, the line capacitance will generate large quantities of excess reactive power, $Q_C = j\omega C_0 U_N^2$; thus, it is necessary to provide high-voltage shunt reactor at both ends of the line to generate inductive reactive power and balance large quantities of excess capacitive reactive power on the no-load line. For full compensation under which the compensation degree of high-voltage shunt reactor is 100%, $\omega C U_N^2 = \frac{U_N^2}{\omega L}$, where L is the value of high-voltage shunt reactor of the line and C is the capacitance to ground of the whole line.

When the transmission power of the line is large, for example, for the UHV line of which transmission power is natural power, the reactive power consumed on the line reactance is justly equal to the reactive power generated by the line capacitance ($Q_L = Q_C$); the reactive power on the line achieves the balance by itself; therefore, it is not necessary to provide high-voltage shunt reactor at both ends of the line to compensate capacitive reactive power; at this time, it is necessary to cutoff the high-voltage shunt reactor. When the transmission power of the line is less than the

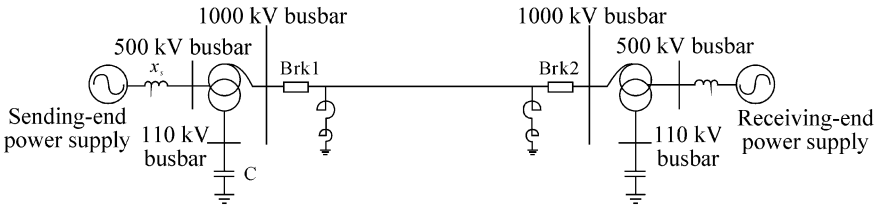

Fig. 4.38 Diagram of the UHV system

natural power, it is necessary to cutoff the partial high-voltage shunt reactor corresponding to such transmission power; therefore, to achieve reactive power balance of the system under different transmission power, the capacity of the high-voltage shunt reactor shall be changed along with the variation of transmission power. Therefore, along with the variation of transmission power of the line, the value of high-voltage shunt reactor mounted at both ends of the line is better to be changed. This is the controllable high-voltage shunt reactor equipment required in the UHV transmission line, and it is usually mounted at both ends of the line.

Before the emergence of the controllable high-voltage shunt reactor, the method used on the UHV transmission line is to mount fixed high-voltage shunt reactor and LV reactive power compensation equipment at the same time (as shown in Fig. 4.38); the two equipments shall be coordinated to use, thus to meet the requirements of reactive power balance and power frequency overvoltage on the reactive power compensation equipment. The main task of fixed high-voltage shunt reactor is to inhibit power frequency overvoltage; it has large capacity and its compensation degree can be up to 80–90%; since the capacity at HV side is very difficult to adjust, it cannot be arbitrarily switched. The main task of LV reactive power compensation equipment is to maintain the reactive power balance; it is mounted at the third winding of UHV transformer and consists of LV capacitance and LV reactance; due to lower voltage level, it can be switched in planned manner. Based on the above description, the capacity of reactive power compensation equipment at HV side is usually difficult to adjust, and the capacity of reactive power compensation equipment at LV side is usually easier to adjust relatively; therefore, through coordinated adjustment of them, the goal of controllable reactive power compensation can be achieved.

However, due to the capacity restriction of LV winding of the UHV transformer, the adjustment range of LV reactive power compensation equipment is limited. In case the transmission capacity of the line is large, the adjustment of LV reactive power compensation equipment cannot counteract that of large-capacity high-voltage shunt reactor, so that the line cannot achieve reactive power balance, that is, it is difficult to coordinate the contradiction between reactive power balance and restriction of power frequency overvoltage. At this time, it is usually only possible to reduce the transmission power of the line; thus, the transmission capacity of the UHV transmission line cannot be fully played. Therefore, this

reactive power compensation mode still cannot solve the problem of controllable reactive power adjustment perfectly.

To solve the above problems, the concept of controllable reactor is presented. First, in case of the occurrence of power frequency overvoltage, the controllable reactor can rapidly increase the compensation degree, thus to reduce the amplitude of overvoltage; second, the controllable high-voltage shunt reactor can adjust its reactive power compensation capacity according to the operating mode of the system, thus to meet the reactive power balance under different operating modes. It can be seen that the controllable high-voltage shunt reactor has two major advantages: ① fully playing the transmission capacity on the condition that power frequency overvoltage is restricted and ② saving the cost of LV reactive power compensation equipment.

4.6.2.2 Development Process of Controllable Reactor

1. Spark gap switched reactor

The controllable reactor was originally appeared in the former Soviet Union; it is actually one kind of fixed capacity reactor switched in manner of spark gap. It is mainly purposed to coordinate the contradiction between reactive power balance and restriction of power frequency overvoltage. When the line is under heavy duty, to maintain the line voltage, the circuit breaker shall be used to exit the operation of shunt reactor. In case the load shedding power frequency overvoltage of the line exceeds the spark gap discharge voltage, the spark gap will be broken down, thus to quickly put the shunt reactor into use to restrict the overvoltage. The shunt reactor switched in manner of spark gap is not the controllable reactor in its true sense.

The shunt reactor switched in manner of spark gap had been used in both 500 and 750 kV systems in the former Soviet Union. Since the shunt reactor switched in manner of spark gap has complex structure, the dispersibility of spark gap discharge voltage is large, its reliability is not high, and it is very hard to use in the UHV system; therefore, what was used in the UHV system in the former Soviet Union is still the fixed parallel high-voltage shunt reactor. Since the transmission power flow is always low after completion of the UHV system in the former Soviet Union, the contradiction between reactive power balance and restriction of power frequency overvoltage is not very serious.

2. Controllable high-voltage shunt reactor

Considering the demand for UHV transmission, the research on controllable shunt reactor has been started since 1970s in the countries of the former Soviet Union represented by Russia, and such reactor has been used in the projects with relatively low voltage level, thus to accumulate engineering experiences for UHV application.

At present, there are two types of controllable high-voltage shunt reactors that can be used for EHV and UHV system, namely, magnetic-valve type (MCSR) and

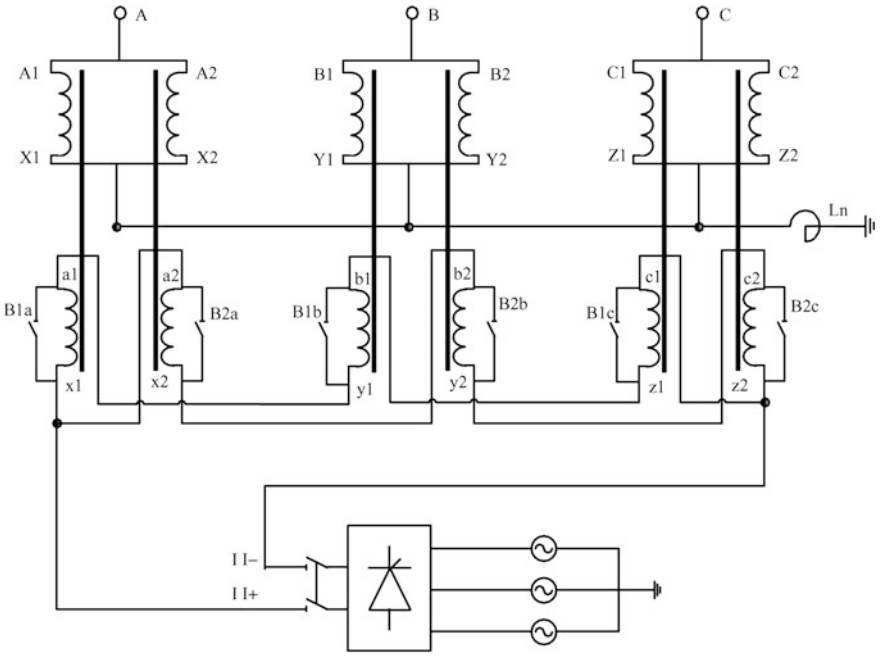

Fig. 4.39 Wiring diagram of magnetic-valve-type controllable shunt reactor

transformer type (TCSR); both of them can adjust the reactor capacity quickly in continuous or stepped manner. Emergence of them provides the possibility to solve the contradiction between reactive power balance and the restriction of power frequency overvoltage, and achieves the controllable reactive power compensation of the UHV system.

(1) Magnetic-valve-type controllable shunt reactor [15]

The wiring of magnetic-valve type (also called magnetic control type) controllable shunt reactor is shown in Fig. 4.39. It mainly consists of two parts, namely, reactor proper and control system. The operating winding of the main part is of star connection, with neutral point grounded by means of small reactance. The control winding can be applied with triangle connection, thus to reduce the content of third harmonic and frequency tripling harmonic in the output current. The reactor has two iron cores in each phase, and each iron core is, respectively, wound with one operating winding and one control winding. The section area of certain section of core limb is very small; in case of small magnetic flux, it will not be saturated and reluctance is small; in case of large magnetic flux, it will be saturated and reluctance is large. During normal operation of the line, the thyristor trigger angle will be real-time changed according to the variation of transmission capacity, thus to adjust the DC magnetic field supporting current, so as to control the magnetic saturation degree of iron core and finally achieve continuous capacity adjustment of operating

winding. The larger the DC magnetic field supporting current is, the higher the saturation degree will be, the larger the excitation current of operating winding will be, and the larger the reactive power capacity generated by the reactor will be; contrarily, the smaller the reactive power capacity generated by the reactor will be. When fault is occurred to the line, through bypass circuit breakers B1a, B2a, B1b, B2b, B1c, and B2c, the control winding is shorted; at this time, controllable reactor is equivalent to a transformer with secondary side shorted; then, the rapid increase of secondary current will saturate the iron core, thus to rapidly increase the reactor capacitance to maximum and achieve the goal to restrict the power frequency overvoltage.

The magnetic-valve-type controllable reactor has the following features:

① The reactor capacity is controlled in manner of adjustment of trigger angle; therefore, the capacity can be adjusted continuously.
② Both ends of thyristor for magnetic-valve-type controllable reactor are only applied with low voltage and there is only small DC current instead of the main current pass through the reactor; therefore, the requirements thereof on voltage withstand and capacity are relatively low and the control and maintenance thereof are relatively convenient.
③ The magnetic saturation phenomenon of iron core and corresponding flux leakage will enlarge eddy current loss of edge core limb and magnetic yoke; therefore, you must face the problems such as inhibition of temperature rise and vibration.
④ The magnetic saturation phenomenon will generate harmonic current in the winding; however, appropriate parameter design can inhibit it to a relatively low level.

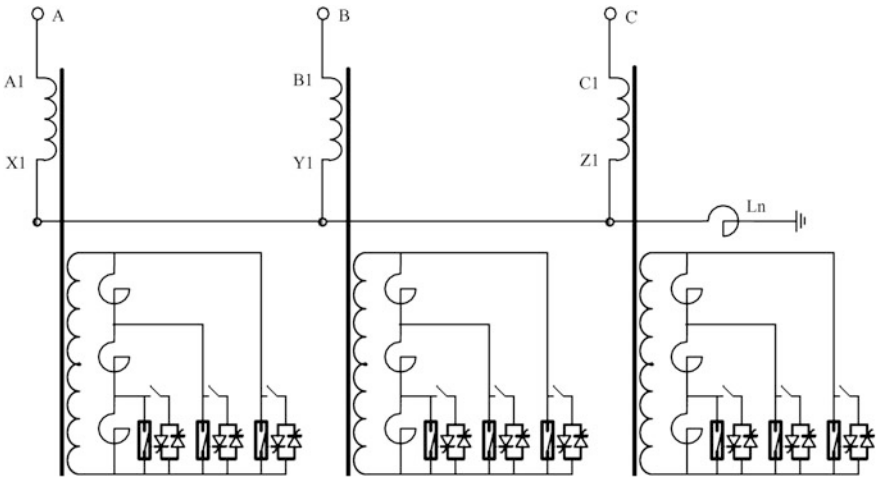

Fig. 4.40 Wiring diagram of impedance-type controllable shunt reactor

⑤ Response speed is relatively slow. For the purpose of rectification, the time constant of control circuit is relatively long; therefore, the time required for the change of control current is also relatively long, thus to cause slow capacity adjustment of such type of controllable reactor. At the same time, due to different control circuit response modes in case of steady-state response and transient-state response (respectively, as control thyristor trigger angle and mechanical switch), the response time is also different.

(2) Impedance-type controllable shunt reactor

The impedance-type controllable reactor is also called transformer-type controllable reactor, with the structure, as shown in Fig. 4.40. Actually, it is the step-down transformer bank with secondary impedance controllable, for which the capacity is controlled through adjustment of the secondary impedance. The larger the secondary impedance is, the smaller the reactive power capacity will be; contrarily, the larger the reactive power capacity will be.

The impedance-type controllable reactor has the following features:

① The impedance-type controllable reactor controls its capacity in manner of changing secondary operating impedance; therefore, its reactive power capacity can be adjusted in stepless manner.

② During operation, the iron core of the impedance-type controllable reactor is in general not statured; therefore, the harmonic problem is not serious.

③ The operating current after step-down will be increased as per transformation ratio and flow through thyristor completely, thus to generate relatively large heat on the thyristor; therefore, the corresponding heat radiation control device must be provided similarly as converter substation; hence, the floor space and operation and maintenance workload will be large.

④ Partial flux leakage will penetrate through lateral iron shell, or penetrate through the upper and lower iron yokes in the vertical direction, thus to form the circuit, and this will cause serious local heating and generate large vibration.

⑤ For the secondary control circuit, the inductance is relative small and the current change is relative quick; therefore, the response speed is quick.

4.6.2.3 Status Quo of Use

China witnessed rapid development in terms of research on controllable reactor. In September 2006, the 500 kV step-switched impedance-type controllable high-voltage shunt reactor, first of its kind in the world, was put into operation in Shanxi Xinzhou 500 kV Switch station; it had the functions of both busbar controllable reactor and line controllable reactor, and had the design capacity of 150 Mvar. In September 2007, the 500 kV magnetic-control-type controllable reactor,

first of its kind in the world, was put into operation in Hubei Jingzhou 500 kV Converter Substation, and the operation performance thereof was very good.

In June 2011, China XD Group Corporation successfully developed the 750 kV and 100 Mvar AC stepped controllable shunt reactor, first of its kind in the world, and achieved its application in the 750 kV Dunhuang Substation. In August 2011, China XD Group Corporation once again successfully developed the 1000 kV and 200 Mvar AC stepped controllable shunt reactor, first of its kind in the world; it passed all test at one time and the technical performances thereof are up to international advance level. This product will be used in the Xuzhou Substation of "Xilin Gol League—Nanjing" UHV power transformation and transmission project. The 1000 kV and 200 Mvar AC stepped controllable shunt reactor successfully developed at this time features rational structure, free of local overheat, less loss, less noise, less vibration, less local discharge, and safe and reliable insulation.

4.6.3 Relay Protection Restriction Scheme

In Japan, the scheme with combination of high-performance metal-oxide arrester and relay protection is used to restrict short-term and high-amplitude power frequency overvoltage. The increased performance of metal-oxide arrester makes it possible for application of this method.

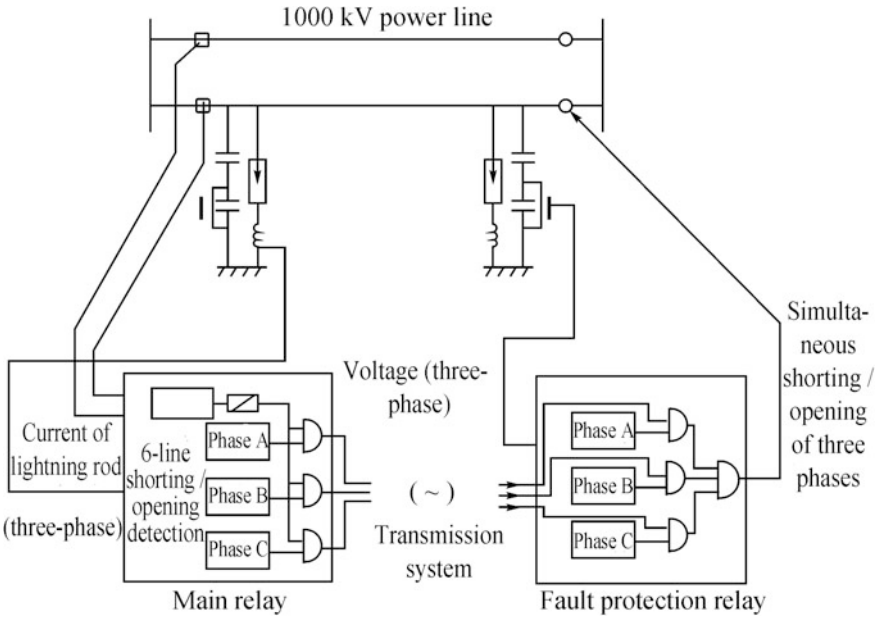

Fig. 4.41 Relay protection restriction scheme for power frequency overvoltage

Taking the UHV line in Japan as example, the length of single line section having been completed (not passing through switch station or substation) does not exceed 150 km in all cases. In addition, the line is not transposed and three-phase parameters of the line are not symmetrical completely. The restriction effect on power frequency overvoltage by means of reactor is not obvious, and the power frequency overvoltage is not as serious as that of long line; therefore, HV reactor is not used, but the power frequency overvoltage restriction scheme with combination of arrester and relay protection is proposed. When this scheme is adopted, due to the effect of MOA, the overvoltage waveform is no longer in manner of sine wave; strictly speaking, it shall be called temporary overvoltage, or power frequency temporary overvoltage (TOV).

To avoid thermal runaway of the arrester due to absorption of energy from TOV, in general, the TOV shall be deemed as the basis for selection of rated voltage of the arrester. The absorbed energy of the arrester is closely related to the amplitude and duration of overvoltage; in case the amplitude of power frequency overvoltage is not restricted and TOV duration is restricted, it is also able to reduce thermal load of the arrester and ensure safe operation of the arrester.

In Japan, relay protection scheme is used to restrict the duration of the power frequency overvoltage, with the principles, as shown in Fig. 4.41. Considering simultaneous load shedding for double-circuit UHV line (opening of switch at left side), the end of the line at switching-off side (left side) will present higher TOV (since the high-voltage shunt reactor is not installed, the power frequency overvoltage generated on the line due to load shedding effect and no-load capacitance effect will be relatively high, with the amplitude up to 1.5 p.u.). At this time, both amplitude and duration of overcurrent on the grounding lead of the arrester will exceed the setting values, the arrester current signal and the circuit breaker breaking signal will be delivered to the main relay at the same time, and it will be judged as high-amplitude TOV resulting from load shedding; thus, it will send the command (to trip the circuit breaker at opposite side) to fault protection relay at opposite side; so that, the circuit breaker at opposite side will be quickly tripped to cutoff the fault and restrict the maximum duration of high amplitude of power frequency overvoltage within 0.2 s. During duration of power frequency overvoltage, the restriction is mainly achieved by relying on MOA (the MOA-rated voltage of the UHV line in Japan is selected as 826 kV, equivalent to 1.3 p.u.).

This scheme is focused to restrict the duration of the power frequency overvoltage, thus to reduce the energy flowing through MOA. Therefore, it has higher requirements on the maximum energy capacity of MOA; at the same time, the relay protection system required is more complex. As for long line, due to higher power frequency overvoltage, even if the duration is short, it is also possible to pose threat to the arrester. Therefore, this scheme is only suitable for the line for which it is not long and the power frequency overvoltage is not serious and applied in smaller scope.

4.6.4 Selection of Restrictive Measures

For different UHV transmission lines, different measures shall be taken to restrict the power frequency overvoltage reasonably. For the UHV transmission lines having been constructed, the former Soviet Union and China mainly use parallel high-voltage shunt reactor to restrict the power frequency overvoltage; for the short-distance UHV transmission lines in Japan, the relay and MOA are used to restrict the power frequency overvoltage. Combined with the characteristics of various UHV transmission lines, it can be seen that the main factors that determining restrictive measures of power frequency overvoltage are line length and whether the line is transposed.

For the UHV transmission lines with short distance, the restriction effect of power frequency overvoltage with high-voltage shunt reactor is not obvious; at the same time, since the line is not transposed, the use of high-voltage shunt reactor will cause resonance overvoltage; therefore, it is not suitable for use of high-voltage shunt reactor. However, the amplitude of power frequency overvoltage for the short-distance UHV transmission lines is relatively low; when the protection measures with combination of relay and MOA are taken, the energy absorbed by MOA will not exceed the maximum allowable value; therefore, the protection measures with combination of relay and MOA are suitable to restrict the power frequency overvoltage. For the UHV transmission lines with long distance, the amplitude of power frequency overvoltage is relatively high, even if the duration is very short, it is also possible to pose threat to MOA, and therefore, it is not suitable to restrict it with MOA. For the UHV transmission lines with long distance, the restriction effect of the power frequency overvoltage with high-voltage shunt reactor is obvious; at the same time, due to the restriction requirements on three-phase unbalance degree, the long-distance lines will in general use transposition to reduce three-phase unbalance degree, so that resonance is not easy to happen even if the high-voltage shunt reactor is mounted on the line; therefore, for the long-distance lines, it is more suitable to restrict power frequency overvoltage with high-voltage shunt reactor.

In the actual engineering, apart from the above-mentioned several common special measures to restrict the power frequency overvoltage, application of good grounding conductor and rational operation mode are also favorable to the reduction of power frequency overvoltage level. The good grounding conductor can reduce the zero-positive sequence impedance ratio of the line to certain extent, thus to reduce the power frequency overvoltage related to asymmetrical grounding; during the initial period after completion of the UHV transmission line, the selection of the operation mode under which the short-circuit impedance is large will achieve low transmission power of the line, thus to effectively reduce load shedding overvoltage.

4.7 Determination of the Upper and Lower Limits of Compensation Degree of High-Voltage Shunt Reactor

The use of high-voltage shunt reactor is the most common measure to restrict the power frequency overvoltage, and the compensation degree of the high-voltage shunt reactor has the decisive influence on the restriction effect. In general, the higher the compensation degree is, the better the restriction effect will be. However, in case it is only considered to increase the compensation degree of the high-voltage shunt reactor for the purpose of restriction of the power frequency overvoltage, it is possible to cause high-amplitude resonance overvoltage under the operation mode of open phase, which is possible to occur such a case on the open-phase switching of the line. Therefore, in the design of the UHV transmission line, it is necessary to determine the upper limit of the compensation degree of the high-voltage shunt reactor. In case it is still unable to restrict the power frequency overvoltage within the range as specified in the procedures when the compensation degree of the high-voltage shunt reactor has arrived the upper limit, it shall be restricted through other measures, such as changing the compensation mode.

In the references both around the world, the researches on the high-voltage shunt reactor mainly focus on the restriction of the power frequency overvoltage, including researches on restriction effect of the power frequency overvoltage with different compensation modes, restriction effect of the power frequency overvoltage with increased compensation degree of the high-voltage shunt reactor, and restriction of the power frequency overvoltage on the long-distance transmission line. However, the researches and discussions related to the upper limit of the compensation degree of the high-voltage shunt reactor are very less. At present, the design upper limit of the compensation degree of the high-voltage shunt reactor is mainly based to the previous design experiences, short of the support of theoretical analysis and actual calculation results.

In terms of the above problems, this section will analyze the relation between open-phase operation resonance overvoltage and the compensation degree of the high-voltage shunt reactor from the perspective of principles, present the theoretical method to determine the upper limit of the compensation degree of the high-voltage shunt reactor, and work out the upper limit of the compensation degree of the high-voltage shunt reactor determined with such method for the single- and double-circuit UHV transmission lines, thus to provide a sufficient theoretical basis for the compensation design of high-voltage shunt reactor for the UHV transmission line.

To restrict the power frequency overvoltage within the range as specified in the procedures, the high-voltage shunt reactor must not only have sufficient compensation capacity, but also meet the requirements on restriction of the secondary arc current and the control of no-load line voltage. Especially, for the line for which power frequency overvoltage is not very serious, the compensation degree of the high-voltage shunt reactor is even mainly determined by restriction of the

secondary arc current and the control of no-load line voltage; therefore, it is quite necessary to carry out research.

At present, in the references both around the world, the researches on the high-voltage shunt reactor mainly focus on restriction of the power frequency overvoltage. The deep research on requirements on compensation capacity of high-voltage shunt reactor by means of restriction of the secondary arc current and the control of no-load line voltage is rarely involved. Even if it is involved, it is rarely to analyze the relation between different factors and compensation capacity of high-voltage shunt reactor from the perspective of principles and the quantitative conclusions are less. Thus, the research results may be not complete and are short of guiding significance to the engineering practices. In terms of the above problems, this section will analyze the requirements on the compensation degree of the high-voltage shunt reactor by means of restriction of the secondary arc current and the control of no-load line voltage from the perspective of principles, and present the theoretical method to determine the lower limit of the compensation degree of the high-voltage shunt reactor by means of restriction of secondary arc current and control of no-load line voltage.

4.7.1 Determination of the Upper Limit of Compensation Degree of High-Voltage Shunt Reactor

4.7.1.1 Research on the Upper Limit of Compensation Degree of High-Voltage Shunt Reactor in Single-Circuit UHV Line

The high-voltage shunt reactor is the important electrical equipment in the UHV power grid. It is better able to compensate the dynamic capacitive reactive power on the line, and effectively inhibit the power frequency overvoltage. However, when high-voltage shunt reactor is mounted as the reactive power compensation equipment of the line, the resonance possibility of the system will be increased. Actually, in case the parallel high-voltage shunt reactor is applied with neutral point grounding method (namely, neutral point is not grounded through small reactance) to compensate, the parallel high-voltage shunt reactor is possible to witness power frequency resonance phenomenon on the open-phase cut-in line. For small reactance mounted at neutral point of the high-voltage shunt reactor, in case the value of small reactance is selected appropriately, it is able to block the phase-to-phase relation of the transmission line perfectly, and obviously reduce the influence of "sound phase" and "fault phase" in the open-phase operation, thus to effectively inhibit the occurrence of power frequency resonance overvoltage. However, the design value and actual value of neutral point small reactance usually have certain deviation, and the system frequency also have certain deviation with the reference frequency 50 Hz; these factors will result in the possibility of power frequency resonance of the system in case the compensation degree of the parallel

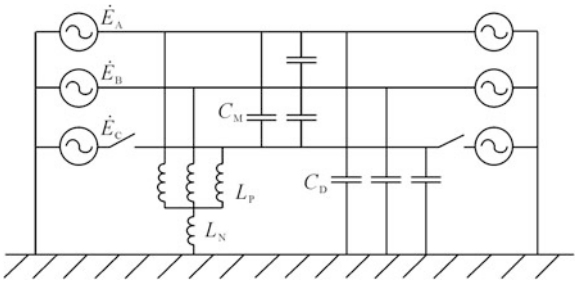

Fig. 4.42 Sketch of open-phase operation

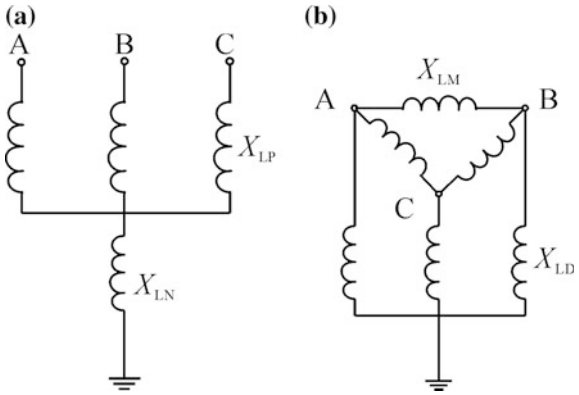

Fig. 4.43 Equivalent sketch of small reactance connected at neutral point of shunt reactor

high-voltage shunt reactor is too high. Therefore, it is necessary to carry out detailed research on the upper limit of the compensation degree of the high-voltage shunt reactor, thus to avoid power frequency resonance occurred to the system.

1. Mechanism for the occurrence of open-phase operation resonance overvoltage

The open-phase operation resonance overvoltage is generated when resonance circuit is formed on the sound phase of the line through phase-to-phase capacitance and high-voltage shunt reactor after one phase of the line is tripped and suspended due to fault [16, 17]. Figure 4.42 shows the sketch of open-phase operation; where, supposing both sides thereof are infinite power supply systems, and three-phase potentials are $\dot{E}_A$, $\dot{E}_B$, and $\dot{E}_C$, respectively; C_M is phase-to-phase capacitance; C_D is ground capacitance of each phase; L_P is high-voltage shunt reactor; and L_N is the neutral point ground capacitance of high-voltage shunt reactor, namely, so-called "small reactance". The phase C of the line opened due to fault is also called "suspended phase", and phase A and phase B of the line are called "sound phase".

To restrict the secondary arc current, one small reactance X_{LN} is mounted at the neutral point of high-voltage shunt reactor. At this time, the compensation capacity of the high-voltage shunt reactor will be distributed to phase-to-phase reactance and

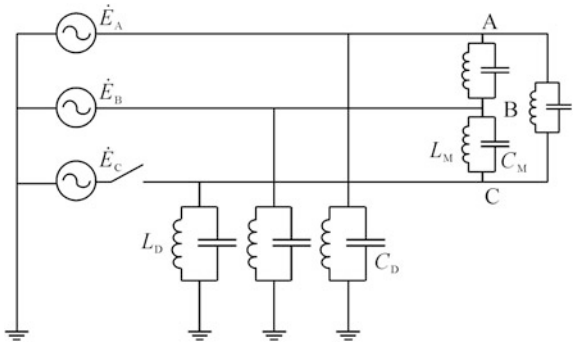

Fig. 4.44 Equivalent circuit diagram of line under open-phase operation

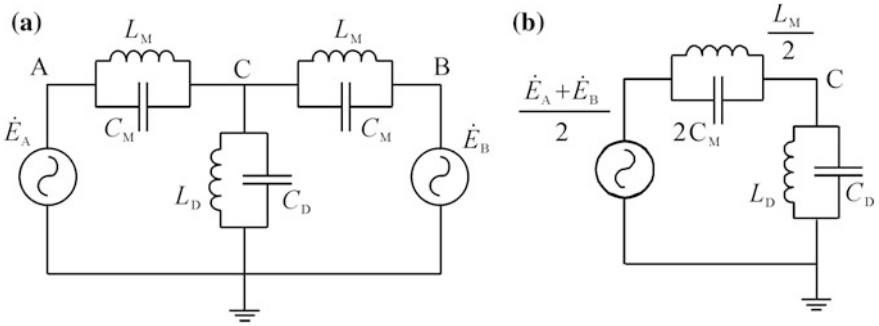

Fig. 4.45 Simplified diagram of line under open-phase operation

phase-to-ground reactance; where, X_{LM} is the equivalent phase-to-phase reactance and X_{LD} is the equivalent phase-to-ground reactance, as shown in Fig. 4.43.

The corresponding relations of parameters in Fig. 4.43a, b are shown as follows:

$$\begin{cases} X_{LD} = 3X_{LN} + X_{LP} \\ X_{LM} = X_{LP}^2 / X_{LN} + 3X_{LP}. \end{cases} \tag{4.9}$$

After conversion of Fig. 4.42, the circuit as shown in Fig. 4.44 can be obtained. The ground capacitances of phase A and phase B and phase-to-phase capacitance between these two phases are directly connected to the power supply of the sound phase; therefore, they shall not be considered. Thus, the circuit as shown in Fig. 4.45a can be obtained. After further simplification, the equivalent circuit, as shown in Fig. 4.45b, can be obtained upon merging of phase A and phase B, where the potential at point C is the potential of suspended phase C.

According to circuit as shown in Fig. 4.45b, the voltage U_C of open phase is

$$\begin{aligned} U_{\mathrm{C}} &= \frac{jX_{\mathrm{LD}}//(-jX_{\mathrm{CD}})}{jX_{\mathrm{LD}}//(-jX_{\mathrm{CD}}) + \frac{jX_{\mathrm{LM}}//(-jX_{\mathrm{CM}})}{2}} \left| \frac{\dot{E}_{\mathrm{A}} + \dot{E}_{\mathrm{B}}}{2} \right| \\ &= \frac{jX_{\mathrm{LD}}//(-jX_{\mathrm{CD}})}{jX_{\mathrm{LD}}//(-jX_{\mathrm{CD}}) + \frac{jX_{\mathrm{LM}}//(-jX_{\mathrm{CM}})}{2}} \frac{U_{0\mathrm{N}}}{2} \end{aligned} \tag{4.10}$$

where

$U_{0\mathrm{N}}$ the effective value of phase voltage;

$$X_{\mathrm{LM}} = \omega L_{\mathrm{M}}, \quad X_{\mathrm{LD}} = \omega L_{\mathrm{D}}, \quad X_{\mathrm{CM}} = \frac{1}{\omega C_{\mathrm{M}}}, \quad X_{\mathrm{CD}} = \frac{1}{\omega C_{\mathrm{D}}}.$$

Under certain parameter coordination of high-voltage shunt reactor and small reactance, in case that the phase-to-phase impedance $\frac{X_{\mathrm{LM}}}{2}//\frac{X_{\mathrm{LM}}}{2}$ and phase-to-ground impedance $X_{\mathrm{LD}}//X_{\mathrm{CD}}$ meet the following series resonance conditions:

$$jX_{\mathrm{LD}}//(-jX_{\mathrm{CD}}) + \frac{jX_{\mathrm{LM}}//(-jX_{\mathrm{CM}})}{2} = 0 \tag{4.11}$$

or

$$\frac{\frac{L_{\mathrm{D}}}{C_{\mathrm{D}}}}{\frac{1}{j\omega C_{\mathrm{D}}} + j\omega L_{\mathrm{D}}} + \frac{1}{2}\frac{\frac{L_{\mathrm{M}}}{C_{\mathrm{M}}}}{\frac{1}{j\omega C_{\mathrm{M}}} + j\omega L_{\mathrm{M}}} = 0. \tag{4.12}$$

The phase-to-phase impedance and phase-to-ground impedance are under series resonance, thus to generate high-amplitude resonance overvoltage on suspended phase C (namely, $U_{\mathrm{C}} \to \infty$).

2. Causes for the occurrence of resonance overvoltage

Theoretically, in case neutral point grounded by small reactance is selected in accordance with the principle of full phase-to-phase compensation, it will not generate high amplitude of open-phase operation resonance overvoltage under any compensation degree of the high-voltage shunt reactor (namely, $\frac{X_{\mathrm{LM}}}{2}//\frac{X_{\mathrm{LM}}}{2} \to \infty, U_{\mathrm{C}} \to 0$). However, the actual parameters and design parameters of the equipment usually have certain difference, so that it may have the risk to generate resonance overvoltage. The particular causes are shown in the following:

(1) Deviation in Impedance Value of Small Reactance
The deviation in impedance value of small reactance can cause error on compensation capacity distribution of the high-voltage shunt reactor; this is possible to generate resonance on the line.

(2) Frequency Deviation
The configuration of the high-voltage shunt reactor and the small reactance of the line is obtained according to power frequency of 50 Hz; however, under fault conditions, the system frequency is usually deviating from power frequency of 50 Hz; thus, it is possible to generate open-phase operation resonance overvoltage on the line.

3. Conditions for the occurrence of resonance overvoltage

(1) Deviation in impedance value of small reactance

Here, the research will be focused on the conditions for resonance overvoltage resulting from deviation of impedance value of small reactance (supposing the frequency is equal to power frequency and maintained unchanged).

To generate series resonance in the circuit, as shown in Fig. 4.45b, the two parts in series must be capacitive and inductive, respectively; in case both of them are capacitive or inductive, it is impossible to generate series resonance. Therefore, it is only possible to generate open-phase operation resonance overvoltage under two conditions: phase-to-phase over-compensation, phase-to-ground under-compensation; or phase-to-phase under-compensation, phase-to-ground over-compensation.

The following research is carried out in two steps: first, study the actual possibility of these two cases, and then, present the relation between resonance overvoltage and deviation of impedance value of small reactance under different compensation degrees of the high-voltage shunt reactor.

The compensation degree of the high-voltage shunt reactor (k) is the percentage between compensation capacity of the high-voltage shunt reactor and reactive power of positive sequence capacitance of the line under power frequency, as shown in Eq. (4.13):

$$k = \frac{Q_{\mathrm{LP}}}{Q_{\mathrm{C1}}} = \frac{\frac{3U_{0\mathrm{N}}^2}{X_{\mathrm{LP}}}}{\frac{3U_{0\mathrm{N}}^2}{X_{\mathrm{C1}}}} = \frac{X_{\mathrm{C1}}}{X_{\mathrm{LP}}}, \tag{4.13}$$

where

$U_{0\mathrm{N}}$ the phase voltage;
X_{LP} the impedance of the high-voltage shunt reactor;
X_{C1} the impedance of positive sequence capacitance of the line, $X_{\mathrm{C1}} = 3X_{\mathrm{CM}} + X_{\mathrm{CD}}$.

(a) Analysis of the deviation source of impedance value of small reactance and analysis of the maximum deviation

In the design of the UHV transmission line, the impedance value of small reactance can be determined as follows:

① Create the model according to geometric parameters of the tower and conductor of the UHV transmission line, and calculate the sequence parameters of the line.
② Based on restriction of the power frequency overvoltage, determine the compensation capacity of the high-voltage shunt reactor and order the high-voltage shunt reactor from its manufacturer.
③ Obtain the impedance value of small reactance according to the design value of the high-voltage shunt reactor (the high-voltage shunt reactor has not been delivered at this time, and actual parameters of the high-voltage shunt reactor cannot be got) and theoretical calculation parameters of the line (the line project has not been completed at this time, and actual parameters of the line cannot be got), which is defined as the design impedance value of small reactance, and order the small reactance from its manufacturer.
④ After delivery of the small reactance, determine the connecting method of tap joint of the small reactance according to the actual parameters of the line, the high-voltage shunt reactor, and the small reactance.

The impedance value of small reactance at the time of delivery (step ④) is defined as the impedance value of the finished product of the small reactance. For any line having been completed, there is one optimum impedance value of the small reactance that can restrict the secondary arc current to minimum, which is simplified to the actual demand value of the small reactance.

The resonance research is targeted to resonance overvoltage on the actual line; therefore, the deviation of small reactance to be considered is the deviation between the impedance value of the finished product of the small reactance and actual demand value of the small reactance, expressed with P. According to the design and manufacturing process of the small reactance, it can be seen that the deviation of the impedance value of the small reactance lies in two causes, as shown in Fig. 4.46.

① In the design of the impedance value of the small reactance, the line has not been completed yet; therefore, the impedance value of the small reactance can only be calculated through theoretically calculated

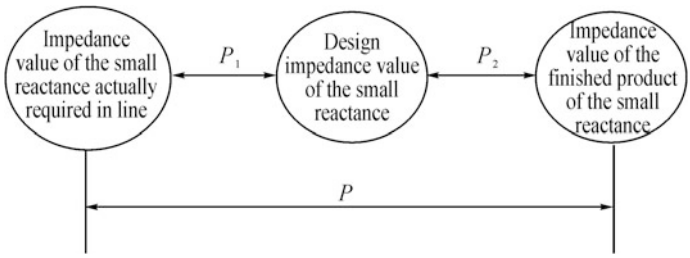

Fig. 4.46 Diagram of deviation relationship of impedance value of the small reactance. *Note* The theoretically calculated impedance value of small reactance is taken as the basis

parameters of the line and high-voltage shunt reactor; however, a certain difference exists between actual parameters and theoretical calculation parameters of the line and high-voltage shunt reactor, which will present deviation between design impedance value and actual demand value of the small reactance. Such deviation is called design deviation, namely, $P_{1,}$ as shown in Fig. 4.46; supposing that design impedance value of the small reactance is larger than actual demand value, P_1 will be larger than 0; contrarily, P_1 will be smaller than 0.

② It is the deviation in impedance value of the small reactance generated during manufacturing process, namely, the deviation between the design impedance value of the small reactance and the impedance value of the finished product of the small reactance. Such deviation is called manufacturing deviation, namely, $P_{2,}$ as shown in Fig. 4.46; supposing that impedance value of the finished product of the small reactance is larger than design value, P_2 will be larger than 0; contrarily, P_2 will be smaller than 0.

The resonance research shall consider the possible maximum P. For the purpose of strictness, considering the deviation between theoretical calculation parameters and actual parameters of the line and high-voltage shunt reactor, usually, P_1 does not exceed ±15% (the percentage of each deviation is based on the design value); considering the manufacturing deviation of neutral point small reactance, P_2 does not exceed ±5% (based on the manufacturing ability of the manufacturer, the manufacturing error of neutral point small reactance can be controlled within ±5% in general). To sum up, considering the least favorable conditions, the design impedance value of the small reactance according to theoretical calculation is taken

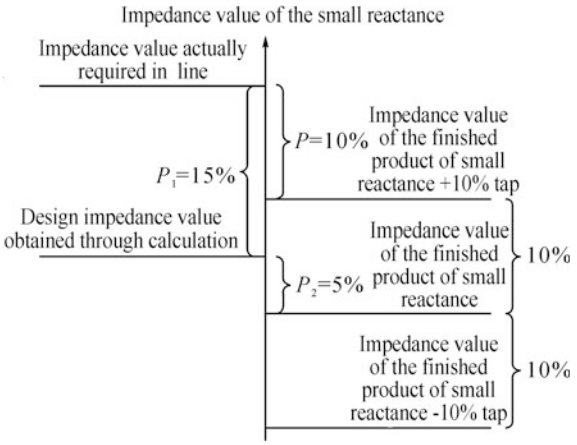

Fig. 4.47 Calculation diagram of the maximum negative deviation of small reactance. *Note* The theoretically calculated impedance value of small reactance is taken as the basis

as a reference, the impedance value of the finished product of the small reactance is taken as −5% deviation, and the impedance value of the small reactance required on actual line is taken as +15% deviation; thus, the deviation P between the impedance value of the finished product of the small reactance and the impedance value of the small reactance required on actual line will not exceed 20%. Considering that UHV neutral point small reactance is also provided with two taps in general, its impedance adjustment range is ±10% of the rated impedance; for the purpose of strictness, in case +10% tap is selected, the maximum deviation P of the small reactance will also not exceed 10%. Figure 4.47 presents the calculation diagram of maximum negative deviation of the small reactance (after considering the tap, the maximum negative deviation between the impedance value of the finished product of the small reactance and the impedance value of the small reactance required on actual line will be −10%).

(b) Analysis on resonance overvoltage resulting from the deviation of impedance value of small reactance

Supposing that after installation of the high-voltage shunt reactor, the impedance between two phases of the line is X_M, the impedance to ground of each phase of the line is X_D, and the reactive power of X_M and X_D is Q_M and Q_D, respectively. Supposing that the inductive reactive power is positive, thus:

$$\begin{cases} Q_M = \frac{(\sqrt{3}U_{0N})^2}{X_M} = \frac{(\sqrt{3}U_{0N})^2}{X_{LM}} - \frac{(\sqrt{3}U_{0N})^2}{X_{CM}} \\ Q_D = \frac{U_{0N}^2}{X_D} = \frac{U_{0N}^2}{X_{LD}} - \frac{U_{0N}^2}{X_{CD}}. \end{cases} \tag{4.14}$$

In case phase-to-phase capacitance is of under-compensation, X_M shall be capacitive and Q_M shall be less than zero; in case phase-to-phase capacitance is of over-compensation, X_M shall be inductive and Q_M shall be larger than zero. In case ground capacitance is of under-compensation, X_D shall be capacitive and Q_D shall be less than zero; in case ground capacitance is of over-compensation, X_D shall be inductive and Q_D shall be larger than zero.

First, simplify Figs. 4.45a, 4.46, 4.47, and 4.48a, and then merge phase A and phase B, thus to obtain the equivalent circuit, as shown in Fig. 4.48b.

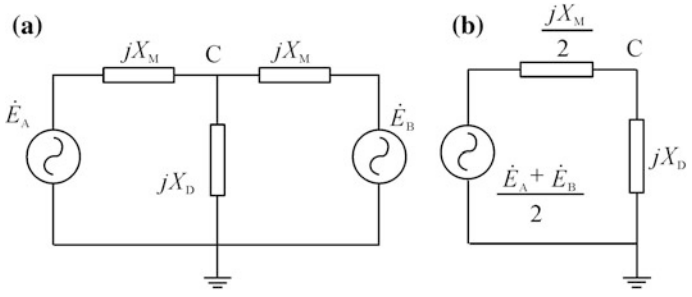

Fig. 4.48 Impedance of line under open-phase operation

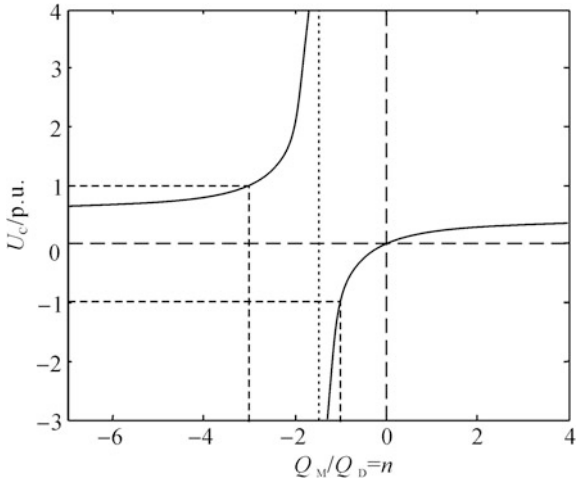

Fig. 4.49 Relationship between the opened phase voltage and n

According to Fig. 4.48b, the voltage on Phase C can be obtained:

$$\dot{U}_C = \frac{X_D}{\frac{X_M}{2} + X_D} \times \frac{\dot{E}_A + \dot{E}_B}{2}. \tag{4.15}$$

From Eq. (4.14), obtain the ratio

$$n = \frac{Q_M}{Q_D} = \frac{3X_D}{X_M}. \tag{4.16}$$

Substitute Eq. (4.16) for Eq. (4.15); thus, the amplitude of overvoltage on Phase C will be

$$U_C = \frac{X_D}{\frac{X_M}{2} + X_D} \times \frac{U_{0N}}{2} = \frac{n}{3 + 2n} U_{0N}. \tag{4.17}$$

According to Eq. (4.17), the relation curve between the open-phase voltage and ratio n is shown in Fig. 4.49.

Between the phase-to-phase compensation and phase-to-ground compensation, when one is under-compensation and the other is over-compensation, n will be negative; when both of them are under-compensation or over-compensation, n will be positive. When n is within the range of $(-\infty, -3)$ and $(-1, +\infty)$, the voltage of suspended phase C will be lower than the normal operating voltage. When n is within the range of $(-3, -1)$, the voltage of suspended phase C has exceeded the normal operating voltage; where in case of $n = -1.5$, the phase-to-phase and phase-to-ground impedance will generate full resonance ($0.5X_M + X_D = 0$), at this time, the amplitude of overvoltage will be trended toward infinite theoretically.

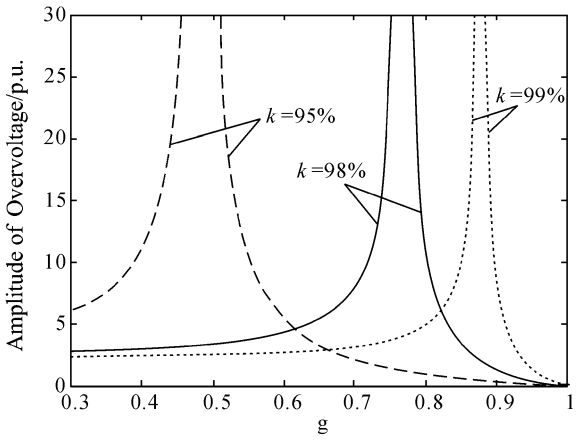

Fig. 4.50 Relationship between the amplitude of resonance overvoltage on suspended phase and the deviation confident g of impedance value of small reactance under different compensation degrees of high-voltage shunt reactor

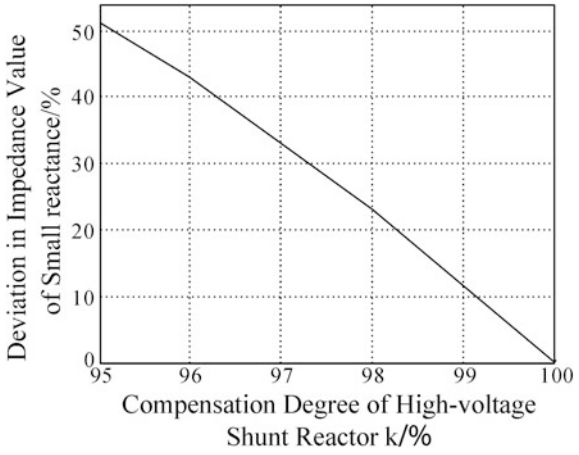

Fig. 4.51 Corresponding deviation in impedance value of small reactance in case of resonance under different compensation degrees of high-voltage shunt reactor

(c) Relationship between the deviation in impedance value of small reactance and the amplitude of resonance voltage

It can be calculated from Eqs. (4.9), (4.10), (4.12), and (4.13) that, under the three compensation degrees of the high-voltage shunt reactor, the relation curve between the deviation degree of impedance value of the small reactance and the amplitude of overvoltage is shown in Fig. 4.50.

It can be seen from Fig. 4.50 that, when the impedance value of the small reactance is ideal value (phase-to-phase capacitance is fully compensated, and $g = 1$), the voltage on suspended phase is 0; along with gradual decrease of the impedance value of the small reactance, the voltage on suspended phase is increased gradually; when the impedance value of the small reactance is a certain value lower than the ideal value, the resonance overvoltage on suspended phase can

be up to infinite. Actually, even if full resonance (for which the resonance overvoltage on suspended phase is infinite) is not emergent, the resonance overvoltage generated is also sufficient to endanger the equipment safety.

(d) Deviation in impedance value of small reactance resulting in resonance under different compensation degrees of high-voltage shunt reactor

Change the magnitude of the compensation degree k of the high-voltage shunt reactor, and calculate the deviation of the impedance value of the small reactance resulting in resonance under different compensation degrees of the high-voltage shunt reactor.

Figure 4.51 presents the corresponding deviation of the impedance value of the small reactance resulting in resonance under different compensation degrees of the high-voltage shunt reactor. In Fig. 4.51, abscissa refers to the compensation degree of high-voltage shunt reactor of the line, and the ordinate refers to the percent that the impedance value of small reactance is smaller than the actual demand value when resonance overvoltage is generated.

It can be seen from Fig. 4.51 that the closer to 100% that the compensation degree of the high-voltage shunt reactor is, the smaller the deviation of the impedance value of the small reactance resulting in resonance will be, that is, the easier to generate resonance it will be. Therefore, to avoid generation of resonance overvoltage, the compensation degree of the high-voltage shunt reactor that is too close to 100% shall be avoided.

(2) Frequency deviation

In case of system fault, the system frequency is usually has certain change, thus to possibly result in resonance overvoltage.

(a) System frequency deviation and resonance voltage

Here, Fig. 4.45b is used for analysis. In consideration of the condition that the compensation degree of high-voltage shunt reactor is less than 100%, the small reactance is configured according to the principle that the phase-to-phase capacitance is fully compensated. Then, ground capacitance is under-compensation, thus:

$$\begin{cases} \frac{(\sqrt{3}U_{0N})^2}{\frac{1}{2\pi f_n C_M}} = \frac{(\sqrt{3}U_{0N})^2}{2\pi f_n L_M} \\ \frac{U_{0N}^2}{\frac{1}{2\pi f_n C_D}} > \frac{U_{0N}^2}{2\pi f_n L_D}, \end{cases} \tag{4.18}$$

where f_n is 50 Hz.

Under certain fault conditions, the frequency will be down to $f_g < 50$ Hz, thus to increase the compensation capacity of phase-to-phase reactance, and decrease the reactive power of phase-to-phase capacitance, so that the situation of phase-to-phase capacitance over-compensation and ground capacitance under-compensation is possible to generate, as shown in Eq. (4.19); at this time, it is possible to generate resonance. When the frequency is larger than 50 Hz, both

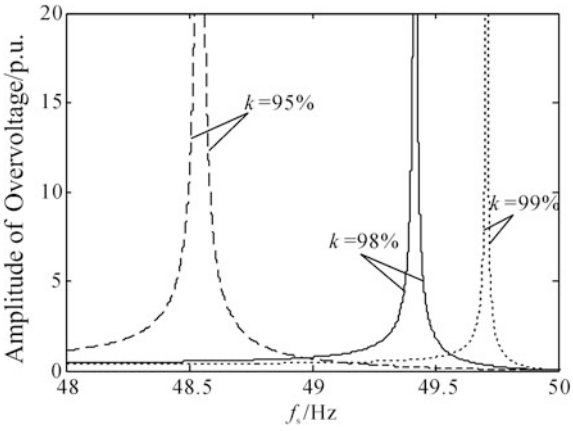

Fig. 4.52 Resonance voltage of suspended phase under different system frequencies

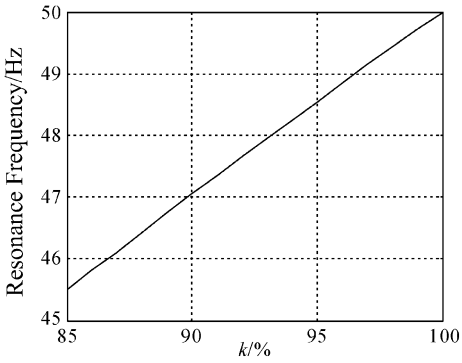

Fig. 4.53 Resonance frequency under different compensation degrees of high-voltage shunt reactor

phase-to-phase capacitance and ground capacitance are in under-compensation state, and thus, it will not generate resonance:

$$\begin{cases} \dfrac{(\sqrt{3}U_{0N})^2}{\frac{1}{2\pi f_g C_M}} = \dfrac{(\sqrt{3}U_{0N})^2}{2\pi f_g L_M} \\ \dfrac{U_{0N}^2}{\frac{1}{2\pi f_g C_D}} > \dfrac{U_{0N}^2}{2\pi f_g L_D}, \end{cases} \tag{4.19}$$

(b) Relationship between system frequency and amplitude of resonance overvoltage

From Eqs. (4.9), (4.10), (4.12), and (4.13), the voltage on suspended phase C under three compensation degrees of the high-voltage shunt reactor and different system frequencies can be calculated, and the results are shown in Fig. 4.52.

It can be seen from Fig. 4.52 that when system frequency is power frequency, the voltage on suspended phase C is very small; along with the decrease of the system frequency, the amplitude of the voltage on suspended phase C will be increased gradually; when system frequency is a certain value lower than the power

frequency ($f_s < 50$ Hz), the resonance overvoltage with very high amplitude may be emergent on suspended phase C; in addition, the system frequency at which resonance overvoltage is generated is related to the compensation degree of the high-voltage shunt reactor.

(c) Resonance frequency under different compensation degrees of high-voltage shunt reactor

According to Eq. (4.4), calculate the frequency at which resonance is generated; then, change the magnitude of k, and calculate the resonance frequency under different compensation degrees of the high-voltage shunt reactor; the results are shown in Fig. 4.53. In Fig. 4.53, abscissa is the compensation degree k of the high-voltage shunt reactor of the line, and ordinate is the system frequency at which resonance overvoltage is generated.

In Fig. 4.53, it is able to find the system frequency at which resonance is generated according to the compensation degree of the high-voltage shunt reactor. In a whole, the closer to 100% the compensation degree of the high-voltage shunt reactor is, the closer to power frequency the frequency at which resonance is generated will be, that is, the easier to happen the resonance will be. Therefore, to avoid the occurrence of resonance overvoltage, the compensation degree of the high-voltage shunt reactor that is too close to 100% shall be avoided.

4. Determination of the upper limit of compensation degree of high-voltage shunt reactor in single-circuit UHV line

In the actual system, resonance overvoltage may be jointly caused by two factors, namely, deviation of the impedance value of the small reactance and fluctuation of system frequency; therefore, these two factors shall be considered comprehensively.

It can be seen from the above analysis that, to avoid the occurrence of resonance overvoltage, the compensation degree of the high-voltage shunt reactor that is too close to 100% shall be avoided. The maximum compensation degree of the high-voltage shunt reactor is mainly dependent on the possible deviation degree of both impedance value of the small reactance and frequency. In case the possible maximum deviations of impedance value of the small reactance and system frequency are known or can be estimated, the appropriate maximum compensation degree of the high-voltage shunt reactor can be determined through the magnitude of such deviation.

(1) Method

The specific steps are as follows:

① Calculate various sequence parameters of the line, thus to obtain phase-to-phase capacitance C_M and phase-to-ground capacitance C_D; then, according to the compensation degree k of the high-voltage shunt reactor required for line design, calculate and obtain high-voltage shunt reactor L_P of the line.

② When phase-to-phase capacitance is fully compensated ($X_{LM} = X_{CM}$), calculate the design impedance value X_{LN} of the small reactance under power frequency from Eq. (4.9).

③ Derive the possible maximum deviation between the impedance value of finished product of the small reactance after the adjustment of the tap under power frequency and the impedance value of the small reactance actually required in the line, and assume the inductance value of the small reactance as X_{LNs} when the deviation is maximum; in general, it is considered as the maximum negative deviation of −10%.

④ Combined with line parameters, calculate phase-to-phase reactance X_{LMs} and phase-to-ground reactance X_{LDs} (under power frequency) when deviation of the small reactance is maximum, and further calculate the corresponding phase-to-phase inductance L_{Ms} and ground inductance L_{Ds}; then, substitute L_{Ms} and L_{Ds} in Eq. (4.11) and calculate the frequency at which resonance is occurred to the line, as shown in Fig. 4.45b; change the compensation degree k of the high-voltage shunt reactor.

⑤ Calculate resonance frequency under different compensation degrees of the high-voltage shunt reactor, and obtain relation diagram between compensation degree k of the high-voltage shunt reactor (abscissa) and resonance frequency (ordinate).

⑥ According to the requirements of resonance frequency (less than the certain value), obtain the upper limit of the compensation degree of the high-voltage shunt reactor from the above relation curve between the

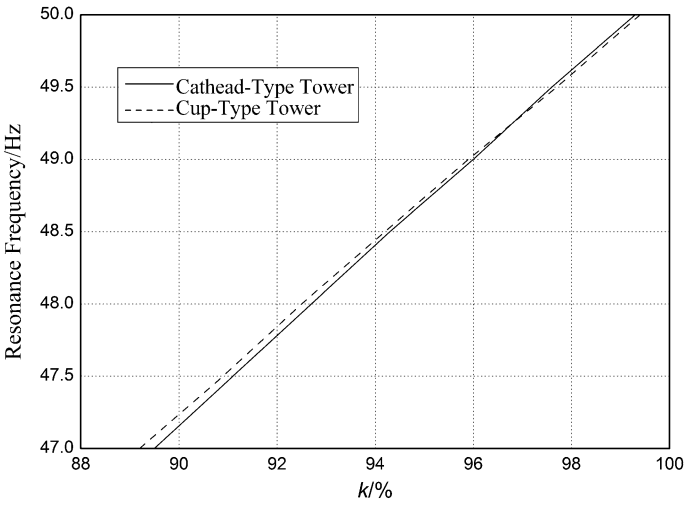

Fig. 4.54 Resonance frequencies under different compensation degrees of high-voltage shunt reactor

Table 4.7 Relationship between compensation degrees of high-voltage shunt reactor and resonance frequencies for single-circuit UHV line

		Resonance frequency/Hz						
		47	47.5	48	48.5	49	49.5	50
k/%	Cathead-type tower	89.5	91.1	92.7	94.3	96.0	97.6	99.3
	Cup-type tower	89.2	90.9	92.5	94.2	95.9	97.7	99.4

compensation degree k of the high-voltage shunt reactor and resonance frequency.

(2) Calculation examples

Considering the extreme conditions that the impedance value of finished product of the small reactance is 10% less than actual demand value, then calculate the frequency of single circuit UHV transmission line at which resonance is generated under different compensation degrees of the high-voltage shunt reactor. The calculation is carried out for cathead-type tower and cup-type tower with typical nominal height, and the results are shown in Fig. 4.54.

According to Fig. 4.54, the corresponding compensation degree of the high-voltage shunt reactor at which full resonance is generated under typical frequency is obtained, while both deviations of the impedance value of the small reactance and deviation of the high-voltage shunt reactor are considered (as shown in Table 4.7).

For system frequency fluctuation, the national standard GB/T 15945-1995 (*Quality of electric energy supply Permissible deviation of frequency for power system*) [18] specifies that the permissible deviation of normal frequency for power system is 0.2 Hz; when system capacity is small, the deviation can be widened to 0.5 Hz. For fault frequency, the dispatching procedures in each province mostly have the following provisions: in case of system frequency beyond 50 ± 0.2 Hz, the duration shall not exceed 60 min; in case of system frequency beyond 50 ± 1.0 Hz, the duration shall not exceed 15 min; and the system frequency shall not exceed 50 ± 3 Hz under all circumstances. At the same time, the standard of electric power industry DL/T 428-2010 (*Technical rules for power system automatic under-frequency load shedding*) [19] specifies that: "under other common conditions, in order to ensure the continuous safe operation of the thermal power plant, the duration shall not exceed 0.5 s in case of the frequency lower than 47.0 Hz, thus to avoid further worsening of the accident".

Based on the above, the system frequency shall be rarely less than 49 Hz. Considering certain allowance, at this time, the corresponding design value of upper limit of the compensation degree for the high-voltage shunt reactor is about 95%; in addition, it is considered that system frequency must not be lower than 47 Hz, that is,when compensation degree of the high-voltage shunt reactor is less than 89.2%, it must not generate resonance.

Therefore, for the single-circuit lines, in general, the corresponding design value of upper limit of the compensation degree for the high-voltage shunt reactor can be chosen as not more than 95%; for the purpose of strictness, the corresponding design value of upper limit of the compensation degree for the high-voltage shunt reactor is better to be about 90%.

4.7.1.2 Research on the Upper Limit of Compensation Degree of High-Voltage Shunt Reactor in Double-Circuit UHV Line

For double-circuit UHV line, here, two operation modes, namely, single-circuit operation mode and double-circuit operation mode, are considered. Under different operation modes, the capacitances that be able to provide secondary arc current are different, and thus, the identical reactors required for the compensation of these capacitances are also different, thus to result in the difference in the most suitable impedance value of the small reactance under different modes; comprehensive consideration between the two is required, thus to determine the relatively rational final small reactance. After determining the small reactance, then the resonance conditions under these two operation modes will be considered at the same time, thus to determine the upper limit of the compensation degree of the high-voltage shunt reactor.

1. Calculation of impedance value of the small reactance of double-circuit UHV line

(1) Single-circuit operation mode

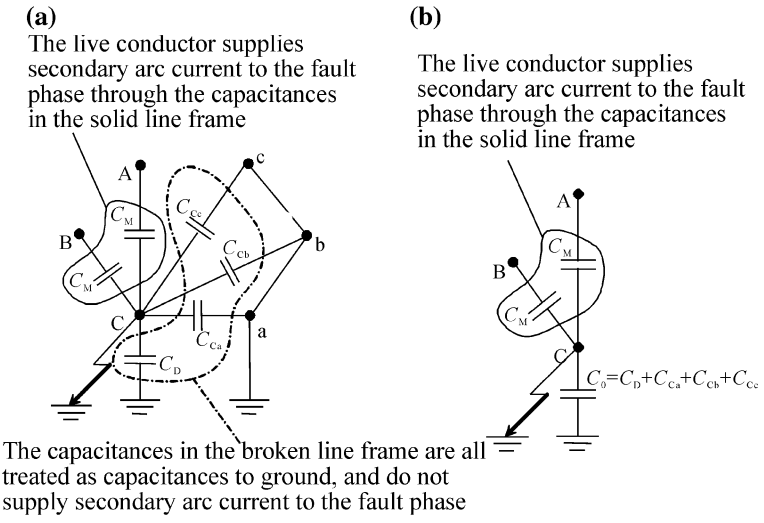

Fig. 4.55 Sketch of capacitance distribution under single-circuit operation mode

In case of single-circuit operation mode, the other circuit is usually grounded at both ends. At this time, the principles of the secondary arc current are shown in Fig. 4.55a. In Fig. 4.55a, phase C on the left circuit is the fault phase, with the circuit breakers at both ends having been tripped open; phase A and phase B are live sound phases; phase a, phase b, and phase c on the right circuit are grounded; and the potential thereof is 0; where C_{Ca}, $C_{Cb,}$ and C_{Cc} are the inter-circuit coupling capacitances between fault phase C and phase a, phase b, and phase c of the other circuit having been shut down; and C_M is the phase-to-phase coupling capacitance between sound phases A and B and fault phase C.

After simplifying Fig. 4.55a, b can be obtained. It can be seen from this figure that the secondary arc current is all supplied through phase-to-phase capacitance of this circuit. The capacitance between circuits will not supply secondary arc current to the suspended phase; in addition, it will also diverge partial secondary arc current that shall be flowed to ground through ground capacitance C_D of the line. Therefore, to achieve minimum secondary arc current under single-circuit operation mode when single circuit is grounded, it is only necessary to fully compensate the phase-to-phase capacitance of this circuit. That is to say, the impedance of both phase-to-phase reactance and phase-to-phase capacitance shall be equal at this time:

$$X_{LM1} = X_{CM}. \tag{4.20}$$

According to the positive and zero sequence capacitances C_1 and C_0 on the whole line, the phase-to-phase capacitance C_M on the line can be obtained:

$$C_M = \frac{1}{3}(C_1 - C_0). \tag{4.21}$$

Correspondingly, the impedance of phase-to-phase capacitance is

$$X_{CM} = \frac{1}{\frac{1}{3}\omega(C_1 - C_0)}. \tag{4.22}$$

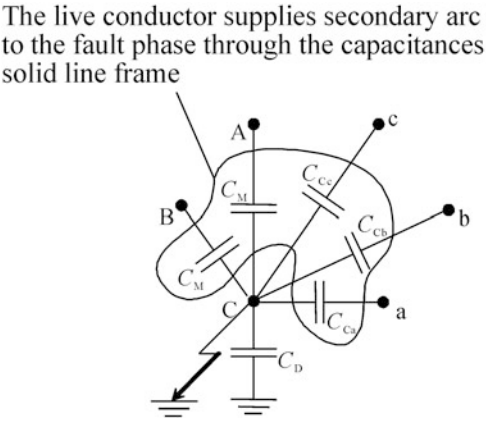

Fig. 4.56 Sketch of line capacitance distribution under double-circuit operation mode

Therefore, according to Eq. (4.20), there is

$$X_{\mathrm{LM1}} = \frac{1}{\frac{1}{3}\omega(C_1 - C_0)}. \tag{4.23}$$

Substitute Eq. (4.23) in Eq. (4.9), then the ideal impedance value of the small reactance under single-circuit operation mode can be obtained:

$$X_{\mathrm{LN1}} = \frac{X_{\mathrm{LP}}^2}{\frac{1}{\frac{1}{3}\omega(C_1 - C_0)} - 3X_{\mathrm{LP}}}. \tag{4.24}$$

Actually, the solution of the ideal impedance value of the small reactance for double-circuit UHV line under single-circuit operation mode is completely the same as that of single circuit UHV line.

(2) Double-circuit operation mode

The sketch of capacitance distribution under double-circuit operation mode is shown in Fig. 4.56. In Fig. 4.56, phase C on the left circuit is the fault phase, phase A and phase B are live sound phases; and phase a, phase b, and phase c on the right circuit are operating normally.

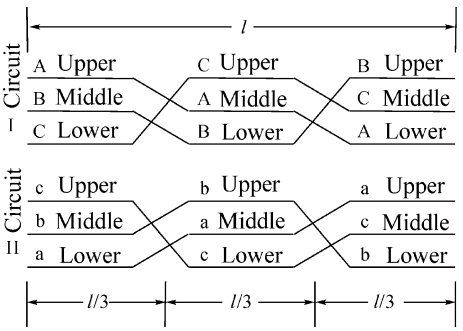

Fig. 4.57 Sketch of negative phase sequence reverse transposition

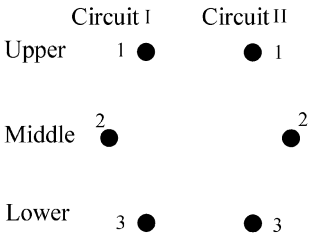

Fig. 4.58 Conductor number

Table 4.8 Capacitances between phase conductors among different circuits

		Circuit I		
		A	B	C
Circuit II	a	$(c_{13}+c_{22}+c_{31})l/3$	$(c_{23}+c_{32}+c_{11})l/3$	$(c_{33}+c_{12}+c_{21})l/3$
	b	$(c_{12}+c_{21}+c_{33})l/3$	$(c_{22}+c_{31}+c_{13})l/3$	$(c_{32}+c_{11}+c_{23})l/3$
	c	$(c_{11}+c_{23}+c_{32})l/3$	$(c_{21}+c_{33}+c_{12})l/3$	$(c_{31}+c_{13}+c_{22})l/3$

It can be seen from Fig. 4.56 that, in comparison with single-circuit operation mode, during double-circuit operation mode, the inter-circuit coupling capacitances C_{Ca}, $C_{Cb,}$ and C_{Cc} will also supply secondary arc current to fault phase.

Although the line transposition makes the three-phase voltage of each line circuit symmetrical ($\dot{U}_a + \dot{U}_b + \dot{U}_c = 0$); however, at present, the double-circuit UHV line in China is applied with negative phase sequence transposition method, as shown in Fig. 4.57, thus to cause the unequal the inter-circuit coupling capacitances C_{Ca}, $C_{Cb,}$ and C_{Cc}, asymmetrical among three phases, and always not equal to zero of the current supplied to suspended phase C through phase a, phase b, and phase c. Thus, the phase-to-phase reactance will not only compensate phase-to-phase capacitance of this line circuit, but also compensate the inter-circuit coupling capacitance.

Here, the magnitude of coupling capacitance between adjacent circuit and fault phase will be studied in case of transposition of negative phase sequence. First, the conductor will be numbered as per Fig. 4.58.

Supposing that the capacitance between two conductors in different circuits is, respectively, c_{11}, c_{12}, c_{13}, c_{21}, c_{22}, c_{23}, c_{31}, c_{32}, and c_{33} (the unit is μF/km). Obviously, $c_{12} = c_{21}$, $c_{13} = c_{31}$, and $c_{23} = c_{32}$. Combined with Figs. 4.57 and 4.58, the capacitances between conductors of each phase for different circuits are shown in Table 4.8. In Table 4.8, l is the line length.

It can be seen from Table 4.8 that the capacitance between conductors of any phase on one circuit and other conductors of the other circuit is different. In addition, the capacitance between in-phases is $(c_{13}+c_{22}+c_{31})l/3$ in all cases, and the capacitance between out-phases is $(c_{12}+c_{21}+c_{33})l/3$ and $(c_{11}+c_{23}+c_{32})l/3$, respectively.

In general, the capacitance between conductors is inversely proportional to the spacing thereof. Therefore, from the conductor distribution of double-circuit UHV line, the relation of inter-circuit capacitances can be obtained as follows:

$$\begin{cases} c_{12} \approx c_{23} > c_{32} \\ c_{11} \approx c_{33} > c_{22}. \end{cases} \tag{4.25}$$

Therefore

$$\begin{cases} (c_{12}+c_{21}+c_{33})l/3 \approx (c_{11}+c_{23}+c_{32})l/3 \\ (c_{12}+c_{21}+c_{33})l/3 > (c_{13}+c_{22}+c_{31})l/3 \\ (c_{11}+c_{23}+c_{32})l/3 > (c_{13}+c_{22}+c_{31})l/3. \end{cases} \tag{4.26}$$

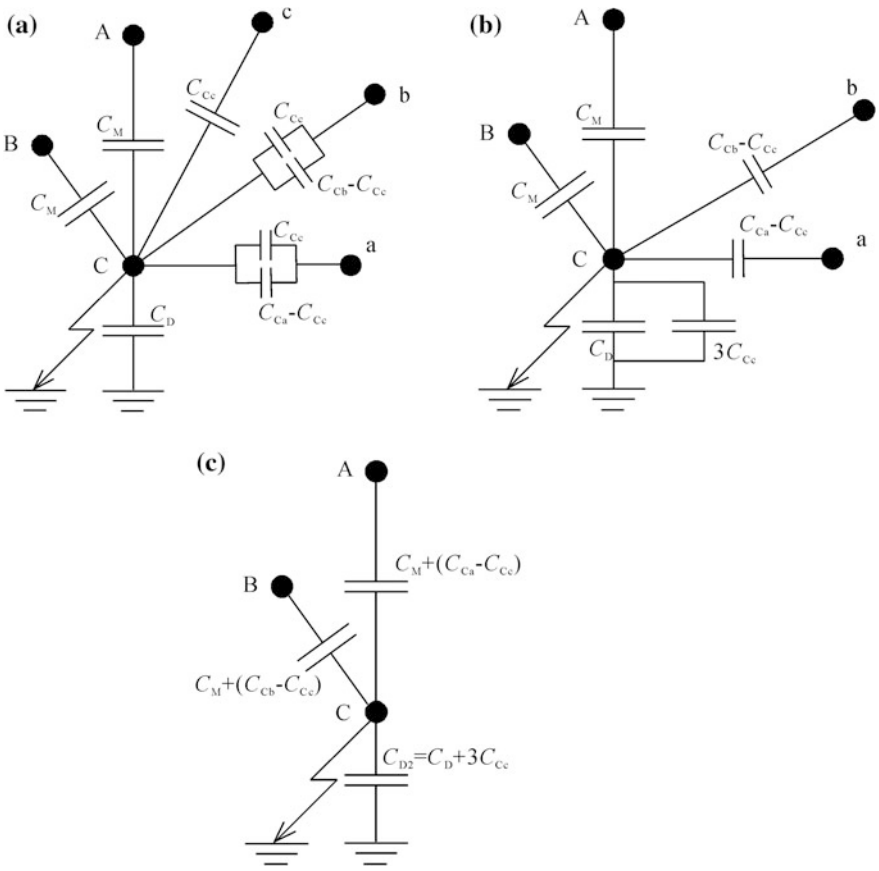

Fig. 4.59 Simplification of capacitances between circuits

Namely, the magnitudes of the two capacitances between out-phases are close, and are all larger than the capacitance between in-phases. Here, the calculation is carried out for one of Chinese double-circuit UHV lines under construction; the inter-circuit capacitance between phase C and phase a, phase b, and phase c is, respectively, 9.94×10^{-4}, 10.41×10^{-4}, and 5.80×10^{-4} μF/km.

Simplify the capacitances, as shown in Fig. 4.59:

① First, respectively, decompose the capacitances C_{Ca} and C_{Cb} between out-phases, as shown in Fig. 4.59a, into two parts, in which one part thereof is equal to the capacitance C_{Cc} between in-phases. At this time, there is, respectively, one capacitance C_{Cc} between phase C and phase a, phase b, and phase c, then merge the three sub-circuits containing C_{Cc}. The power voltage of the three sub-circuits is three-phase symmetry; therefore, the power voltage will be zero after merging; therefore, the

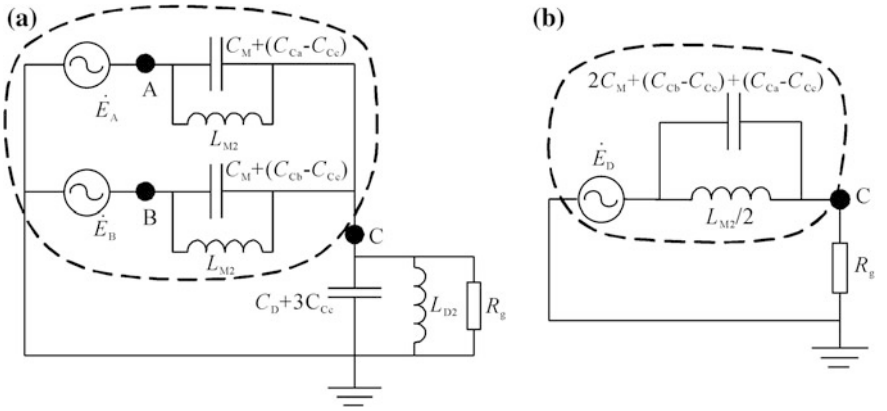

Fig. 4.60 Simplification of circuit with reactance considered

three capacitances C_{Cc} can be directly transferred to a point between phase C and ground, thus to obtain the circuit, as shown in Fig. 4.59b.

② The voltage for phase A and phase a and the voltage for phase B and phase b are basically the same. Therefore, the remaining capacitances $C_{Ca} - C_{Cc}$ and $C_{Cb} - C_{Cc}$ (between phase a and phase C, and between phase b and phase C) are, respectively, transferred to a point between phase A and phase C and between phase B and phase C, thus to merge with phase-to-phase capacitance and obtain the circuit, as shown in Fig. 4.59c.

It can be seen from Fig. 4.59c that, to restrict the secondary arc current to the minimum level, it is necessary to, respectively, compensate the capacitances $C_M + (C_{Ca} - C_{Cc})$ and $C_M + (C_{Cb} - C_{Cc})$ between phase A and phase C and between phase B and phase C. Add reactance in the circuit, as shown in Fig. 4.59c, and carry out research, as shown in Fig. 4.60a, where L_{M2} and L_{D2} are, respectively, equivalent phase-to-phase inductance and ground inductance, and R_g is arc resistance.

The arc resistance R_g is far less than the impedance of equivalent ground capacitance $C_D + 3C_{Cc}$ and ground inductance L_{D2}; therefore, for the purpose of simplification, the influence on secondary arc current of the arc resistance due to equivalent ground capacitance and ground inductance is neglected. At the same time, according to Thevenin Theorem, the two parallel sub-circuits within broken line area, as shown in Fig. 4.60a, is equalized into one power voltage source $\dot{E}_D$ in series with one impedance, as shown in Fig. 4.60b, where $\dot{E}_D$ is equal to the pen potential when point C is open, as shown in Fig. 4.60a.

It can be seen from Fig. 4.60b that, to fully compensate the capacitive secondary arc current, it is necessary to achieve parallel resonance for parallel circuit between $2C_M + (C_{Ca} - C_{Cc}) + (C_{Cb} - C_{Cc})$ and $L_{M2}/2$; at this time, the impedance of phase-to-phase inductance is

$$X_{\mathrm{LM2}} = \omega L_{\mathrm{M2}} = \frac{2}{\omega(2C_{\mathrm{M}} + (C_{\mathrm{Ca}} - C_{\mathrm{Cc}}) + (C_{\mathrm{Cb}} - C_{\mathrm{Cc}}))}. \tag{4.27}$$

Substitute Eq. (4.27) into Eq. (4.9), and obtain the ideal value X_{LN2} of the impedance value of the neutral point small reactance:

$$X_{\mathrm{LN2}} = \frac{X_{\mathrm{LP}}^2}{\frac{2}{\omega(2C_{\mathrm{M}} + (C_{\mathrm{Ca}} - C_{\mathrm{Cc}}) + (C_{\mathrm{Cb}} - C_{\mathrm{Cc}}))}} - 3X_{\mathrm{LP}}. \tag{4.28}$$

(3) Selection of the impedance value of the small reactance

Under single-circuit operation mode and double-circuit operation mode, the ideal impedance value of the small reactance is different; in general, the ideal impedance value of the small reactance under double-circuit operation mode is higher than that under single-circuit operation mode, namely

$$X_{\mathrm{LN1}} < X_{\mathrm{LN2}}. \tag{4.29}$$

This is because that, to restrict the secondary arc current to the minimum level, the phase-to-phase reactance under double-circuit operation mode will compensate phase-to-phase capacitance of this circuit and partial inter-circuit capacitance at the same time; however, under single-circuit operation mode, phase-to-phase reactance is only necessary to compensate phase-to-phase capacitance of the circuit. That is to say, under double-circuit operation mode, the ideal phase-to-phase reactance shall be smaller. Therefore, it can be seen from Eq. (4.29) that the ideal impedance value of the small reactance under double-circuit operation mode is in general larger than that under single-circuit operation mode.

After obtaining the ideal impedance value of the small reactance under both single-circuit operation mode and double-circuit operation mode, it is necessary to consider the possibility of the occurrence of two operation modes. The ideal impedance value of the small reactance under both single-circuit operation mode and double-circuit operation mode will be used to obtain the final impedance value of the small reactance through weighted mean. It is particularly:

$$X_{\mathrm{LN}} = p_1 X_{\mathrm{LN1}} + p_2 X_{\mathrm{LN2}}, \tag{4.30}$$

where

p_1 and p_2 the possibility of the occurrence of single-circuit operation mode and double-circuit operation mode;

X_{LN} the final impedance value of the small reactance.

In general, to fully play the transmission capability of double-circuit UHV line, the line is usually under simultaneous double-circuit operation mode and it is under

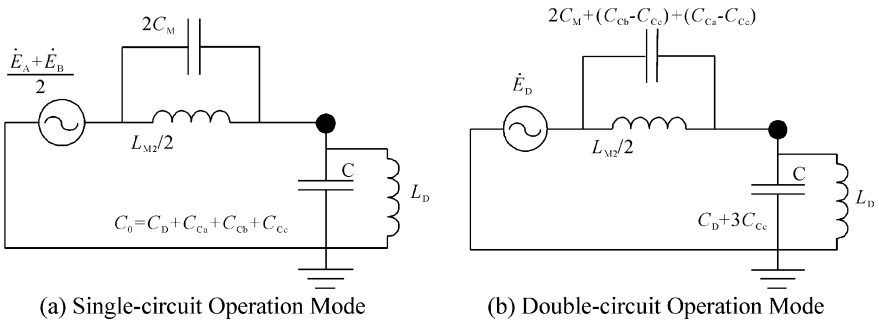

Fig. 4.61 Resonance circuit of double-circuit line

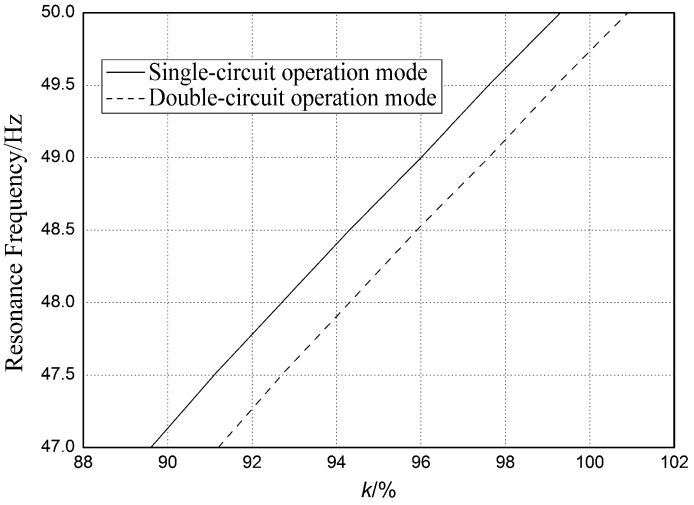

Fig. 4.62 Relationship between compensation degree of high-voltage shunt reactor and resonance frequency for double-circuit line

single-circuit operation mode only in case of special conditions (such maintenance). Therefore, p_2 is far above p_1 in most of time.

2. Determination of the upper limit of compensation degree of high-voltage shunt reactor in double-circuit line

(1) Calculation of the upper limit of compensation degree of high-voltage shunt reactor in double-circuit line

When studying resonance conditions for double-circuit UHV line, it is still required to consider the following three factors resulting in resonance: ① the impedance value of the small reactance is less than the ideal impedance value of the small reactance under this operation mode; ② system frequency is less than power

Table 4.9 Corresponding relationship between compensation degree of high-voltage shunt reactor and resonance frequency

Resonance frequency/Hz	47	47.5	48	48.5	49	49.5	50
Single-circuit operation mode (k/%)	89.6	91.1	92.7	94.3	96.0	97.6	99.3
Double-circuit operation mode (k/%)	91.2	92.7	94.3	95.9	97.6	99.2	100.9

frequency 50 Hz; and ③ the compensation degree of the high-voltage shunt reactor is close to 100%.

The research method for the upper limit of the compensation degree of the high-voltage shunt reactor in double-circuit line under single-circuit operation mode and double-circuit operation mode is completely the same as that for single-circuit line, and the only difference is resonance circuit. According to the above analysis in calculation of the impedance value of the small reactance for double-circuit UHV line, it can be seen that the resonance circuit under single-circuit operation mode and double-circuit operation mode for double-circuit UHV line is shown in Fig. 4.61.

After determining the resonance circuit, the determination method of upper limit of the compensation degree of the high-voltage shunt reactor for double-circuit UHV line is completely the same as that for single-circuit UHV line.

The calculation is carried out for drum-type tower used in Chinese UHV transmission line. The relation between compensation degree of the high-voltage shunt reactor and resonance frequency under single-circuit operation mode and double-circuit operation mode is obtained, while deviation of the impedance value of the small reactance is considered, as shown in Fig. 4.62.

According to the curve as shown in Fig. 4.62, the corresponding compensation degree of the high-voltage shunt reactor at which full resonance is generated under typical frequency is obtained, while both deviations of the impedance value of the small reactance and deviation of the high-voltage shunt reactor are considered, as shown in Table 4.9.

It can be seen from Table 4.9 that, for certain resonance frequency, the upper limit of the compensation degree of the high-voltage shunt reactor allowed for double-circuit UHV line under single-circuit operation mode is lower than that under double-circuit operation mode. For example, when resonance frequency is 48 Hz, the upper limit of the compensation degree of the high-voltage shunt reactor allowed for double-circuit UHV line under single-circuit operation mode is 90.1%; however, the upper limit of the compensation degree of the high-voltage shunt reactor allowed under double-circuit operation mode is 91.7%. Therefore, in the actual application, the upper limit of the compensation degree of the high-voltage shunt reactor for double-circuit UHV line shall be determined according to the situation that double-circuit UHV line is under single-circuit operation mode. By referring to the above analysis, system frequency is less than 49 Hz rarely; at this time, the upper limit of the design compensation degree of the high-voltage shunt

reactor can be chosen as not more than 95%; at the same time, the system frequency is considered to be not less than 47 Hz in all cases, that is to say, when design compensation degree of the high-voltage shunt reactor is less than 89.6%, the resonance will not be generated in all cases.

Therefore, for the double-circuit lines, in general, the corresponding design value of upper limit of the compensation degree for the high-voltage shunt reactor can be chosen as not more than 95%; for the purpose of strictness, the corresponding design value of upper limit of the compensation degree for the high-voltage shunt reactor is better to be about 90%.

(2) Analysis on the calculation results of the upper limit of compensation degree of high-voltage shunt reactor in double-circuit line

It can be seen from Fig. 4.62 that the relation curve between compensation degrees of the high-voltage shunt reactor and resonance frequency under double-circuit operation mode is located below the curve under single-circuit operation mode; that is to say, under the same compensation degree of the high-voltage shunt reactor, the resonance frequency under single-circuit operation mode is higher and it is easier to generate resonance under single-circuit operation mode.

This results from the different charging powers of the line under single-circuit operation mode and double-circuit operation mode.

It can be seen from Fig. 4.56 that, under single-circuit operation mode, inter-circuit coupling capacitances C_{Cc}, C_{Cb}, and C_{Ca} are all ground capacitance; at this time, phase-to-phase capacitance and phase-to-ground capacity thereof are, respectively, C_{M} and $C_{\mathrm{D}} + C_{\mathrm{Ca}} + C_{\mathrm{Cb}} + C_{\mathrm{Cc}}$; therefore, the charging power is

$$Q_1 = \frac{3(\sqrt{3}U_{0\mathrm{N}})^2}{\frac{1}{\omega C_{\mathrm{M}}}} + \frac{3U_{0\mathrm{N}}^2}{\frac{1}{\omega(C_{\mathrm{D}} + C_{\mathrm{Ca}} + C_{\mathrm{Cb}} + C_{\mathrm{Cc}})}}. \tag{4.31}$$

It can be seen from Fig. 4.59 that, under double-circuit operation mode, the equivalent ground capacitance is changed to $C_{\mathrm{D}} + 3C_{\mathrm{Cc}}$ and both ends are applied with phase voltage; for this circuit, the voltage applied on both ends of phase-to-phase capacitance C_{M} and capacitances between out-phases (with magnitude of $(C_{\mathrm{Ca}} - C_{\mathrm{Cc}}) + (C_{\mathrm{Cb}} - C_{\mathrm{Cc}})$) are the line voltage; at this time, the charging power is

$$Q_2 = \frac{3(\sqrt{3}U_{0\mathrm{N}})^2}{\frac{1}{\omega(2C_{\mathrm{M}} + (C_{\mathrm{Ca}} - C_{\mathrm{Cc}}) + (C_{\mathrm{Ca}} - C_{\mathrm{Cc}}))}} + \frac{3U_{0\mathrm{N}}^2}{\frac{1}{\omega(C_{\mathrm{D}} + 3C_{\mathrm{Cc}})}}. \tag{4.32}$$

That is to say, when it is switched from single-circuit operation mode to double-circuit operation mode, the voltage applied on both ends of the inter-circuit capacitance (with magnitude of $(C_{\mathrm{Ca}} - C_{\mathrm{Cc}}) + (C_{\mathrm{Cb}} - C_{\mathrm{Cc}})$) will be transformed from phase voltage to line voltage. Therefore, when the total capacitance is the same, the charging power under double-circuit operation mode will be larger than

that under single-circuit operation mode. When taking the typical drum-type tower as example, the charging power under double-circuit operation mode is about 1.03 times of that under single-circuit operation mode (547 Mvar per 100 km), up to 563 Mvar. That is to say, under single-circuit operation mode, the reactive charging power for compensation with the high-voltage shunt reactor has larger proportion, thus the actual compensation degree of the high-voltage shunt reactor is higher, and it is easier to generate resonance.

Table 4.10 Parameters of single-circuit line

	Nominal height/m	Positive sequence capacitance/μF/km	Zero sequence capacitance/μF/km
Cathead-type tower	50	0.0141	0.0091
	60	0.0139	0.0083
	70	0.0138	0.0078
Cup-type tower	50	0.0137	0.0101
	60	0.0134	0.0091
	70	0.0133	0.0085

Table 4.11 Parameters of double-circuit line

	Nominal height/m	Capacitance between circuits/10^{-4} μF/km			Positive sequence capacitance/μF/km	Zero sequence capacitance/μF/km
		C_{Ca}	C_{Cb}	C_{Cc}		
Drum-type tower	50	5.60	9.47	10.11	0.0141	0.0091
	60	6.03	10.49	10.76	0.0139	0.0083
	70	6.40	11.23	11.28	0.0138	0.0078

Table 4.12 Corresponding relationship between compensation degree of high-voltage shunt reactor and resonance frequency for single-circuit line

		Nominal height/m	Resonance frequency/Hz						
			47	47.5	48	48.5	49	49.5	50
k/%	Cathead-type tower	50	89.4	91.0	92.6	94.3	95.9	97.6	99.3
		60	89.5	91.1	92.7	94.3	96.0	97.6	99.3
		70	89.6	91.2	92.8	94.4	96.0	97.6	99.3
	Cup-type tower	50	89.1	90.8	92.5	94.2	95.9	97.7	99.5
		60	89.2	90.9	92.5	94.2	95.9	97.7	99.4
		70	89.4	91.0	92.6	94.3	95.9	97.6	99.3

Table 4.13 Corresponding relationship between compensation degree of high-voltage shunt reactor and resonance frequency for double-circuit line under single-circuit operation mode

	Nominal height/m	Resonance frequency/Hz						
		47	47.5	48	48.5	49	49.5	50
k/%	50	89.5	91.1	92.7	94.3	96.0	97.6	99.3
	60	89.6	91.1	92.7	94.3	96.0	97.6	99.3
	70	89.6	91.2	92.8	94.4	96.0	97.6	99.3

Table 4.14 Corresponding relationship between compensation degree of high-voltage shunt reactor and resonance frequency for double-circuit line under double-circuit operation mode

	Nominal height/m	Resonance frequency/Hz						
		47	47.5	48	48.5	49	49.5	50
k/%	50	91.0	92.6	94.2	95.8	97.4	99.1	100.8
	60	91.2	92.7	94.3	95.9	97.6	99.2	100.9
	70	91.5	93.0	94.6	96.2	97.8	99.4	101.1

4.7.1.3 Research on the Generality of the Upper Limit of Compensation Degree of High-Voltage Shunt Reactor and Comparison Between the Upper Limits of Compensation Degree of High-Voltage Shunt Reactors for Single-Circuit Line and Double-Circuit Line

The above analysis and calculation are based on typical parameters, and the conclusions therefrom are necessary to verify the generality. Therefore, this section will carry out research on the influence on line parameters on the upper limit of the compensation degree of the high-voltage shunt reactor.

According to provisions as specified in the procedures, the minimum conductor ground distance of single circuit UHV line and double-circuit UHV line is 19 and 18 m, respectively (for non-agricultural cropped location with less population); considering 20 m sag for single-circuit UHV line, and 12.5 m length for insulator and hardware, the minimum nominal height for single-circuit and double-circuit UHV lines is 51.5 and 50.5 m, respectively. At the same time, excessive nominal height and tower height will result in the increase in cost; in general, it shall not exceed 70 m. Therefore, this document will consider the nominal height with range of 50–70 m, and the capacitance parameters thereof are shown in Tables 4.10 and 4.11.

Under different line parameters, while deviation of the impedance value of the small reactance and deviation of the high-voltage shunt reactor are considered, the relation between compensation degree of the high-voltage shunt reactor and resonance frequency for single circuit UHV line is shown in Table 4.12, and the relation between compensation degree of the high-voltage shunt reactor and resonance frequency for double-circuit UHV line is shown in Tables 4.13 and 4.14.

It can be seen from Tables 4.12, 4.13, and 4.14, parameter change has a very small influence on the resonance frequency of both single-circuit UHV line and double-circuit UHV line, thus to have a very small influence on the upper limit of the compensation degree of the high-voltage shunt reactor. Therefore, the upper limit obtained above is suitable for common parameters of the UHV transmission line.

The upper limit of compensation degree of high-voltage shunt reactor in double-circuit line is mainly considered in terms of single-circuit operation mode. Through comparison of Tables 4.12 and 4.13, it can be seen that upper limits of the compensation degree of the high-voltage shunt reactor for both single-circuit UHV line and double-circuit UHV line are very close; this is because that for double-circuit UHV line under single-circuit operation mode, the determination method of the upper limit of the compensation degree of the high-voltage shunt reactor is completely corresponding to that for single-circuit UHV line. From the above analysis on the upper limit of the compensation degree of the high-voltage shunt reactor for single circuit UHV line, it can be seen that line parameter change has a very small influence on the upper limit of the compensation degree of the high-voltage shunt reactor (even it can be neglected), thus to result in basically the same upper limit of the compensation degree of the high-voltage shunt reactor for both single-circuit UHV line and double-circuit UHV line.

In summary, for both the single-circuit lines and the double-circuit lines, in general, the corresponding design value of upper limit of the compensation degree for the high-voltage shunt reactor can be chosen as not more than 95%; for the purpose of strictness, the corresponding design value of upper limit of the compensation degree for the high-voltage shunt reactor is better to be about 90%.

Moreover, if neutral point small reactance is provided with more taps and larger impedance adjustment range (>±10%), UHV line can increase the corresponding design value of upper limit of the compensation degree for the high-voltage shunt reactor properly.

4.7.2 Determination of the Lower Limit of Compensation Degree of High-Voltage Shunt Reactor

This chapter will, respectively, analyze the requirements of restriction of secondary arc current and the control of no-load line voltage on the compensation degree of the high-voltage shunt reactor from the perspective of principles, and present determination method of the lower limit of the compensation degree of the high-voltage shunt reactor through restriction of secondary arc current and control of no-load line voltage, thus to provide basis for compensation design of the high-voltage shunt reactor for the UHV transmission line.

4.7.2.1 Basis for Determination of the Lower Limit of Compensation Degree of High-Voltage Shunt Reactor

Apart from meeting the requirements of restriction of power frequency overvoltage, the compensation capacity of the high-voltage shunt reactor shall also meet the following two requirements:

1. In China, the EHV and UHV transmission lines mainly use the neutral point of the high-voltage shunt reactor grounded by small reactance to restrict of secondary arc current; the principles are: through small reactance, partial reactive compensation power of the high-voltage shunt reactor is distributed to phase-to-phase of the line, thus to generate parallel resonance with phase-to-phase capacitance and block the path of capacitive component of secondary arc current. Therefore, the compensation capacity of the high-voltage shunt reactor must be at least higher than the capacity of phase-to-phase capacitance of the line, thus to ensure that it is able to restrict secondary arc current.
2. The UHV reactive power compensation equipment can meet the requirement for switching of no-load line; that is to say, when the line is of no load, the voltage at both ends of the line can be ensured lower than 1100 kV. Therefore, the reactive power compensation design of the line shall be in general determined according to the principles that charging power of the line is fully compensated with inductive reactive power; that is to say, the total compensation degree of the high-voltage reactor and low-voltage reactor on the third winding of the UHV transformer shall be up to or exceed 100%. However, due to the capacity restriction of third winding of the UHV transformer, the compensation capacity of LV reactive power compensation equipment has an upper limit; therefore, the requirements on lower limit of the compensation capacity of the high-voltage shunt reactor are also presented.

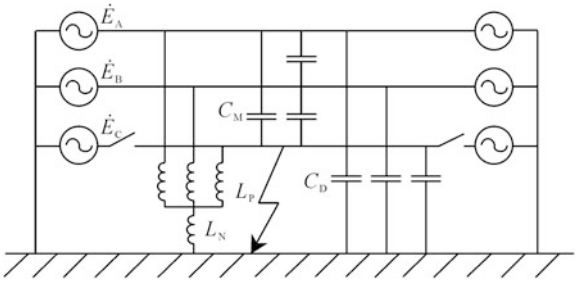

Fig. 4.63 Schematic diagram of secondary arc current

4.7.2.2 Determination of the Lower Limit of Compensation Degree of High-Voltage Shunt Reactor

1. Restriction of secondary arc current

(1) Single-circuit line

Due to causes, such as lightning, after transient single-phase ground fault is occurred to certain phase of the operation line, the automatic single-phase recloser will break the circuit breaker at both ends of the fault phase. At this time, the sound phase and possible adjacent lines will supply current, namely, secondary arc current to the fault point by means of electrostatic coupling and electromagnetic coupling. Thereinto, the component of electrostatic coupling accounts for large proportion. The high-voltage shunt reactor and neutral point small reactance will achieve the goal of restricting the secondary arc current through restricting the component of electrostatic coupling.

The single-circuit UHV line is taken as example for the purpose of analysis. After eliminating the fault, the simplified system structure is shown in Fig. 4.63; after fault phase C is grounded, the single phase will be tripped and suspended,

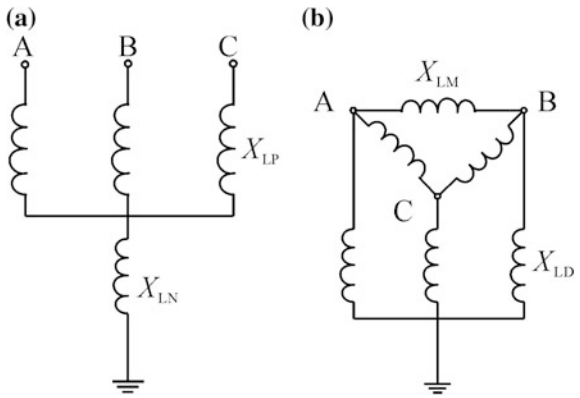

Fig. 4.64 Equivalent sketch of shunt reactor with neutral point connected with small reactance

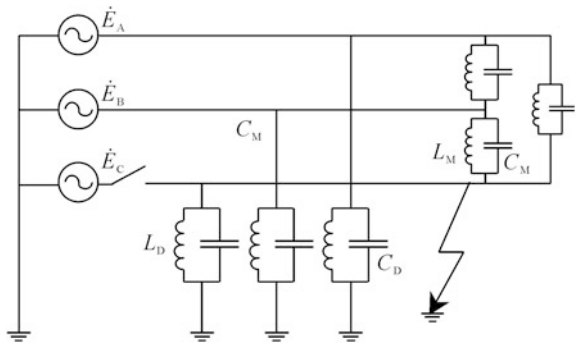

Fig. 4.65 Equivalent schematic diagram of secondary arc current

while phase A and phase B are still connected on the power supply; through phase-to-phase capacitance, phase A and phase B will supply secondary arc current to phase C. Supposing that it is infinite bus system at both sides of the line and the potential on three phases is $\dot{E}_a$, $\dot{E}_b$, and $\dot{E}_c$; the phase-to-phase capacitance and ground capacitance used for the line are, respectively, C_M and C_D. The line is connected with the high-voltage shunt reactor L_P with compensation degree of k, and the neutral point of the high-voltage shunt reactor is grounded through small reactance L_N. It can be seen from Fig. 4.63 that the generation of secondary arc current and open-phase operation resonance overvoltage are actually the same process, and the only difference is the emphasis involved.

The circuit, as shown in Fig. 4.63, can be converted through Fig. 4.64, thus to obtain Fig. 4.65, where X_{LD} and X_{LM} are shown in Eq. (4.33):

$$\begin{cases} X_{LD} = 3X_{LN} + X_{LP} \\ X_{LM} = X_{LP}^2/X_{LN} + 3X_{LP}. \end{cases} \tag{4.33}$$

To restrict the secondary arc current, it is necessary to select the small reactance X_{LN} rational, so that its equivalent phase-to-phase reactance X_{LM} is equal to phase-to-phase capacitive reactance X_{CM}, namely, the inductive reactive power of equivalent phase-to-phase reactance X_{LM} is equal to the capacitive reactive power of phase-to-phase capacitive reactance X_{CM} of the line, as shown in Eq. (4.34):

$$\frac{(\sqrt{3}U_{0N})^2}{X_{LM}} = \frac{(\sqrt{3}U_{0N})^2}{X_{CM}}. \tag{4.34}$$

Through Eq. (4.33), it can be seen that the inductive reactive power of high-voltage shunt reactor $X_{LP,}$ and phase-to-ground reactance X_{LD} and phase-to-phase reactance X_{LM} have the following relation:

$$\frac{U_{0N}^2}{X_{LD}} + \frac{(\sqrt{3}U_{0N})^2}{X_{LM}} = \frac{U_{0N}^2}{X_{LP}}, \tag{4.35}$$

where

U_{0N} the effective value of phase voltage;

$\frac{U_{0N}^2}{X_{LP}}$, $\frac{U_{0N}^2}{X_{LD}}$ and $\frac{(\sqrt{3}U_{0N})^2}{X_{LM}}$ the inductive reactive power of single-phase high-voltage shunt reactor X_{LP} and the inductive reactive power of ground reactance X_{LD} and phase-to-phase reactance X_{LM}.

From the above equation, the compensation capacity of high-voltage shunt reactor X_{LP} is equal to the sum of inductive reactive power of both ground reactance X_{LD} and phase-to-phase reactance X_{LM}. From Eqs. (4.33) and (4.35), it can be seen that the small reactance does not change the compensation capacity of high-voltage shunt reactor, and its purpose is to distribute compensation capacity of high-voltage shunt reactor to phase-to-phase part and ground part.

From Eqs. (4.34) and (4.35), it can be seen that, to fully compensate the reactive power of phase-to-phase capacitance, compensation capacity of high-voltage shunt reactor shall be at least larger than or equal to the reactive power of phase-to-phase capacitance, namely

$$\frac{U_{0N}^2}{X_{LP}} \geq \frac{\left(\sqrt{3}U_{0N}\right)^2}{X_{CM}}. \tag{4.36}$$

In addition, due to

$$\frac{U_{0N}^2}{X_{LP}} = k\frac{U_{0N}^2}{X_{C1}}, \tag{4.37}$$

where

X_{C1} the positive sequence capacitive reactance of the line.

Substitute Eq. (4.37) into Eq. (4.36), the compensation degree of the high-voltage shunt reactor obtained shall meet the following conditions:

$$k \geq \frac{3X_{C1}}{X_{CM}}, \tag{4.38}$$

or

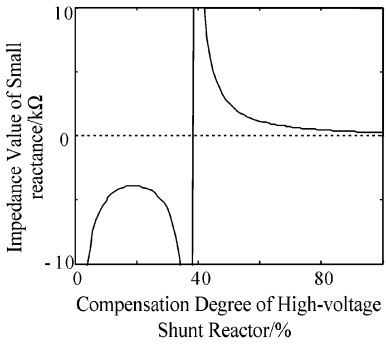

Fig. 4.66 Relationship between the impedance value of the small reactance in shunt reactors and the compensation degree of high-voltage shunt reactor

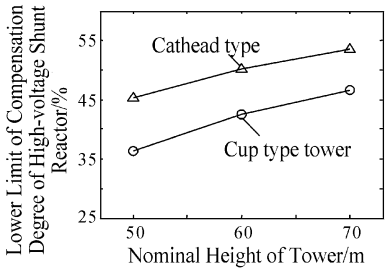

Fig. 4.67 Lower limit of compensation degree of high-voltage shunt reactor determined based on the restriction of secondary arc current for single-circuit line

$$k \geq \frac{3C_{\mathrm{M}}}{C_1}. \tag{4.39}$$

When the compensation capacity of high-voltage shunt reactor is very close to the reactive power of phase-to-phase capacitance, to fully compensate the phase-to-phase capacitance, the impedance value of the small reactance will be very large, and it can be derived from Eqs. (4.33) and (4.35). According to Eq. (4.33), the relation between the impedance value of the small reactance and the compensation degree of the high-voltage shunt reactor for single-end compensation line (cathead-type tower) with the length of 200 km can be obtained, as shown in Fig. 4.66.

It can be seen from Fig. 4.66 that when compensation degree of the high-voltage shunt reactor is very close to the reactive power of phase-to-phase capacitance, the impedance value of the small reactance will be very large; however, excessive impedance value of the small reactance will make it difficult for manufacturing. Therefore, certain margin shall be provided between the compensation capacity of the high-voltage shunt reactor and reactive power of phase-to-phase capacitance, thus to achieve the impedance value of the small reactance within rational range; usually, the margin of 10% is considered relatively rational.

Considering that the margin is 10% and nominal height of tower is within the range of 50–70 m, the lower limit of the compensation degree of the high-voltage shunt reactor is shown in Fig. 4.67. From Fig. 4.67, it can be seen that there are three characteristics: ① along with the increase of nominal height of tower, the ground capacitance of the line is decreased, and the proportion of phase-to-phase capacitance in the line capacitance is increased, thus to result in the increase of the lower limit of the compensation degree of the high-voltage shunt reactor; ② in comparison with cathead-type tower, the difference in three-phase conductor height of the cup-type tower is relative small, and under the same nominal height, the average ground distance of three conductors is smaller, the ground capacitance is larger, and the conductor space is large, and the phase-to-phase capacity is smaller, thus to result in that lower limit of the compensation degree of the high-voltage shunt reactor for line erected in manner of cup-type tower is lower than that for line erected in manner of cathead-type tower under the condition of the same height; ③ within possible variation range of nominal height, for single-circuit UHV line, the lower limit of the compensation degree of the high-voltage shunt reactor determined by means of restriction of secondary arc current will not exceed 54% maximally (55% after rounding).

(2) Double-circuit line

Here, the capacitance structure of double-circuit UHV line is analyzed to study the lower limit of the compensation degree of the high-voltage shunt reactor that must be achieved to meet the requirements for restriction of secondary arc current.

The discussion is carried out in manner of both single-circuit operation mode and double-circuit operation mode.

(a) Single-circuit operation mode

It can be seen from the analysis in previous section that, in case of single-circuit operation mode, phase-to-phase reactance is only required to compensate phase-to-phase capacitance of this circuit; at this time, the determination method of the lower limit of the compensation degree of the high-voltage shunt reactor is completely the same as that for single-circuit UHV line; that is to say, the lower limit of the compensation degree of the high-voltage shunt reactor can be calculated with the following equation:

$$k \geq \frac{3C_{\mathrm{M}}}{C_1}. \tag{4.40}$$

(b) Double-circuit operation mode

It can be seen from Fig. 4.60b that, in case of double-circuit operation mode, to restrict the secondary arc current to minimum level, the magnitude of capacitance requiring compensation for each phase-to-phase reactance will be $C_{\mathrm{M}} + 0.5(C_{\mathrm{Ca}} - C_{\mathrm{Cc}} + C_{\mathrm{Cb}} - C_{\mathrm{Cc}})$.

At this time, the compensation degree of the high-voltage shunt reactor shall meet the following conditions:

$$k \geq \frac{3(C_{\mathrm{M}} + 0.5(C_{\mathrm{Ca}} - C_{\mathrm{Cc}} + C_{\mathrm{Cb}} - C_{\mathrm{Cc}}))}{C_1}. \tag{4.41}$$

(c) Research on the lower limit of compensation degree of high-voltage shunt reactor.

From analysis of the upper limit of the compensation degree of the high-voltage shunt reactor, it can be seen that, in case of single-circuit operation mode,

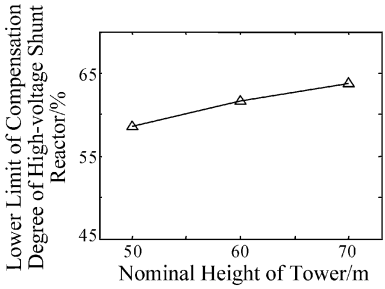

Fig. 4.68 Lower limit of compensation degree of high-voltage shunt reactor determined based on the restriction of secondary arc current for double-circuit line

phase-to-phase reactance is only required to compensate phase-to-phase capacitance C_M of this circuit; in case of double-circuit operation mode, apart from compensating phase-to-phase capacitance C_M, each phase-to-phase reactance will also compensate the capacitance with magnitude of $(C_{Ca} - C_{Cc} + C_{Cb} - C_{Cc})/2$. After determining the small reactance through comprehensive consideration of these two operation modes, the capacitance compensated with phase-to-phase reactance shall be between C_M and $C_M + 0.5(C_{Ca} - C_{Cc} + C_{Cb} - C_{Cc})$. For the purpose of strictness, the phase-to-phase reactance for double-circuit UHV line is necessary to fully compensate the capacitance with the magnitude of $C_M + 0.5(C_{Ca} - C_{Cc} + C_{Cb} - C_{Cc})$; based on this, the lower limit of the compensation degree of the high-voltage shunt reactor for double-circuit UHV line will be determined, and the calculated equation is given in Eq. (4.34).

Considering that the allowance is 10% and the nominal height of tower is within the range of 50–70 m, the lower limit of the compensation degree of the high-voltage shunt reactor is shown in Fig. 4.68.

From Fig. 4.68, it can be seen that: ① similar to the single circuit UHV line, along with the increase of nominal height of tower for double-circuit UHV line, the ground capacitance of the line is decreased, and the proportion of phase-to-phase capacitance in the line capacitance is increased, thus to result in the increase of the lower limit of the compensation degree of the high-voltage shunt reactor and ② within possible variation range of nominal height, for double-circuit UHV line, the lower limit of the compensation degree of the high-voltage shunt reactor determined based on the restriction of secondary arc current will not exceed 64% maximally (65% after rounding).

2. Control on the voltage of switched no-load line

During switching of no load line, to control line voltage, the compensation capacity of inductive reactive power compensation equipment shall be sufficiently large. At present, during reactive power compensation design of the line, the inductive reactive power compensation capacity shall be determined according to the principles that charging power of the line can be fully compensated with inductive reactive power at least; that is to say, the total compensation degree of the high-voltage reactor and low-voltage reactor shall be up to or exceed 100%. However, the compensation capacity of low-voltage reactor is restricted by the capacity of the third winding of the UHV transformer and the compensation capacity has an upper limit; therefore, the requirements on the minimum compensation capacity of the high-voltage shunt reactor are also presented. At present, for common transformers used on the Chinese UHV transmission line, the capacity at LV side of each phase is all at 334 Mvar; this means that maximum compensation capacity of low-voltage reactor enabled on each transformer is only 1002 Mvar [20, 21].

After meeting the principles that charging power of the line is fully compensated with inductive reactive power, the compensation degree of the high-voltage shunt reactor shall be at least

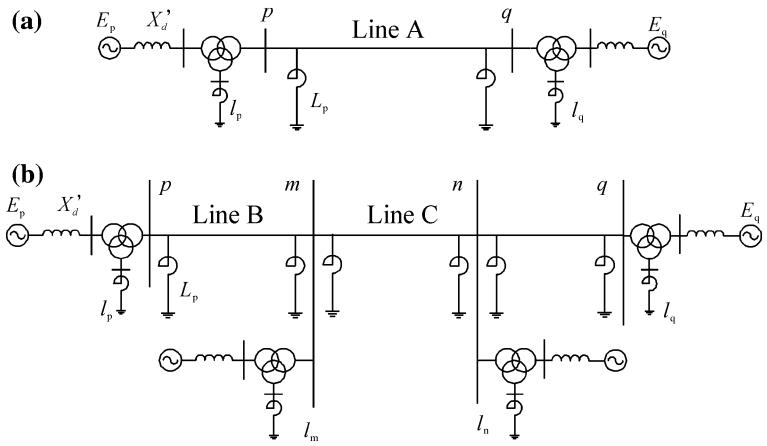

Fig. 4.69 Sketch of classification of UHV lines

$$k \geq \frac{Q_C \times l - (Q_{TL1} + Q_{TL2})}{Q_C \times l}, \tag{4.42}$$

where

Q_C	the charging power per 100 km of the line, in Mvar;
l	the line length, in 100 km;
Q_{TL1} and Q_{TL2}	the reactive power provided to the line through LV reactive power reactance equipment of the transformer at the tail end and head end of the line, in Mvar.

The drop points of the UHV transmission line are mainly divided into terminal drop point and intermediate drop point. In case of terminal drop point, there is only one outgoing UHV line connected with EHV power grid by means of UHV transformer; for the line in manner of point-to-point UHV transmission, the placement at both ends is the terminal drop point. In case of intermediate drop point, there are two outgoing UHV lines, which are placed with UHV line connected with EHV power grid by means of transformer. For different lines, the placement type at both ends is different, thus the inductive reactive power compensation capacities Q_{TL1} and Q_{TL2} that can be provided to the line by means of transformer are also different; therefore, the line can be divided into three types:

(1) Type A line: Point-to-point line for which it is terminal drop point at both ends, as shown line A in Fig. 4.69a. The third winding of the UHV transformer at both ends of the line can all be used to provide reactive power to the line. According to the current practices that each end of the line is connected with one transformer, for each circuit of type A line, the maximum reactive power that can be obtained through LV reactor at both ends of the line is $2 \times 3 \times 334$ Mvar $= 2004$ Mvar.

(2) Type B line: the line for which one end is terminal drop point and one end is intermediate drop point, as shown line B in Fig. 4.69b. The LV reactive power compensation equipment on the third winding of the transformer at intermediate drop point of the line is necessary to provide reactive power for line B and line C at both ends simultaneously; therefore, the compensation capacity shall be designed to be distributed to the line at both ends, and distributed equally in general. Thereinto, reactive power of the LV reactor at p end will be completely provided to line B, and reactive power of the LV reactor at m end will be distributed to line B and line C; thus, each circuit of type B line can obtain maximum reactive power of $(1+0.5) \times 3 \times 334$ Mvar $= 1503$ Mvar from the LV reactor at both ends of the line.

(3) Type C line: the line for which both ends are intermediate drop point, as shown line C in Fig. 4.69b. Reactive power of the LV reactor at both ends of the line will be distributed to adjacent two lines; therefore, each circuit of type C line can obtain the reactive power of $(0.5+0.5) \times 3 \times 334$ Mvar $= 1002$ Mvar from the LV reactor at both ends of the line.

The above classification method only considers the distribution of compensation capacity of LV reactive power compensation equipment at both ends of the line and it does not consider the influence due to number of the circuit of the line and compensation capacity of the high-voltage shunt reactor; therefore, this classification method is suitable to single-circuit UHV line and double-circuit UHV line under different compensation modes.

During the construction period of the UHV transmission line at present, the outgoing UHV line with three or more placements is very less; therefore, it is not considered here. The research method is the same as that mentioned above.

The lower limit of the compensation degree of the high-voltage shunt reactor for type A line, type B line, and type C line, determined through the control of no-load line voltage, is calculated. For single-circuit UHV line and double-circuit UHV line,

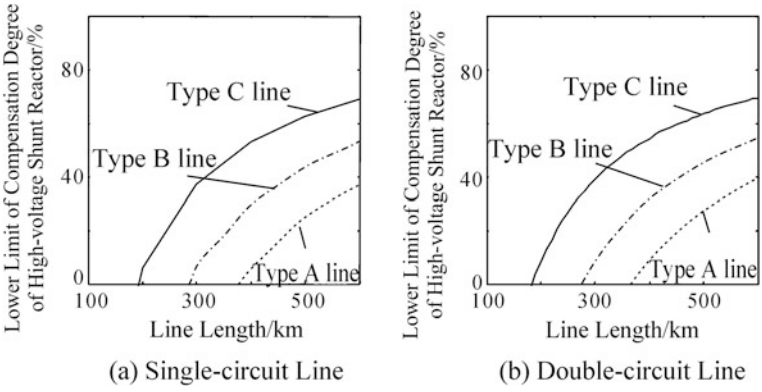

Fig. 4.70 Lower limits of compensation degree of high-voltage shunt reactor determined based on the control of no-load line voltage

the charging power per 100 km is, respectively, 533 and 547 Mvar, as shown in Fig. 4.70.

It can be seen from Fig. 4.70 that:

(1) The longer the line is, the higher the compensation degree of the high-voltage shunt reactor required will be. This is because that longer line requires larger inductive reactive power; however, the reactive power provided by the LV reactor is limited, and thus, it requires the high-voltage shunt reacor having higher compensation capacity.
(2) When it is considered in terms of the control of no-load line voltage, type A line (point-to-point line) has the minimum requirements on the compensation degree of the high-voltage shunt reactor, it is followed by type B line, and type C line has the maximum requirements on the compensation degree of the high-voltage shunt reactor. The reason is that, according to the sequence of type A line, type B line, and type C line, the reactive power provided by LV reactor is in turn decreased, so that the requirements on compensation capacity of the high-voltage shunt reactor are increased gradually.

3. Characteristics of the lower limit of compensation degree of high-voltage shunt reactor

Combining with the above analysis of the lower limit of compensation degree of high-voltage shunt reactor from the perspective of both restriction of secondary arc current and control of no-load line voltage, it can be seen that:

(1) The lower limit of the compensation degree of the high-voltage shunt reactor determined through restriction of secondary arc current is mainly determined by sequence parameters of the line, while the lower limit of the compensation degree of the high-voltage shunt reactor determined through the control of no-load line voltage is influenced by types of placements at both ends and line length. These factors are varied a lot, and therefore, the variation range of the lower limit of the compensation degree of the high-voltage shunt reactor is also large; in addition, the longer the line is, the smaller the inductive reactive power provided by the LV inductive reactive power compensation equipment at power supply side will be, and the higher the lower limit of the compensation degree of the high-voltage shunt reactor will be.
(2) The capacitance parameters and length of the line are different for real line; therefore, the lower limit of the compensation degree of the high-voltage shunt reactor shall be calculated, respectively, from the perspective of the above two aspects according to the actual parameters, and then, the larger one between the two shall be considered as the final lower limit of the compensation degree of the high-voltage shunt reactor.
(3) When the line is short, the lower limit of the compensation degree of the high-voltage shunt reactor determined through restriction of secondary arc current is higher than the lower limit of the compensation degree of the high-voltage shunt reactor determined through the control of no-load line voltage; while when the line is long, the lower limit of the compensation degree

of the high-voltage shunt reactor determined through restriction of secondary arc current is lower than the lower limit of the compensation degree of the high-voltage shunt reactor determined through control of no-load line voltage.

4.7.2.3 Summary of the Upper and Lower Limit of Compensation Degree of the High-Voltage Shunt Reactor

According to the above analysis, the research results on upper and lower limits of the compensation degree of the high-voltage shunt reactor for the UHV transmission line can be summarized as follows:

For the upper limit:

1. Deviation of the impedance value between manufactured small reactance and small reactance actually required in the line and system frequency fluctuation is the main causes for resonance overvoltage. In case of resonance occurred to the line with compensation degree of the high-voltage shunt reactor less than 100%, it either results from phase-to-phase capacitance under-compensation and ground capacitance over-compensation due to low impedance value of the small reactance, or results from phase-to-phase capacitance over-compensation and ground capacitance under-compensation due to low frequency.
2. The solution of ideal impedance value of the small reactance of double-circuit UHV line under single-circuit operation mode is completely the same as that of single circuit UHV line. It is only necessary to consider that phase-to-phase capacitance of this circuit is fully compensated by phase-to-phase reactance. However, under double-circuit operation mode, apart from compensating phase-to-phase capacitance, phase-to-phase reactance shall also compensate partial inter-circuit capacitance.
3. This chapter proposed the theoretical method to determine the upper limit of the compensation degree of the high-voltage shunt reactor through line parameters, while deviation of the impedance value of the small reactance, system frequency deviation, and deviation of compensation capacity of the high-voltage shunt reactor are considered.
4. The resonance frequency for double-circuit UHV line under single-circuit operation mode is slightly higher than that under double-circuit operation mode; that is to say, it is easier to generate resonance under single-circuit operation mode.
5. The difference for the upper limit of the compensation degree of the high-voltage shunt reactor for both single-circuit UHV line and double-circuit UHV line is relatively small. The line parameters have a very small influence on the upper limit of the compensation degree of the high-voltage shunt reactor for both single-circuit UHV line and double-circuit UHV line.
6. For both the single-circuit lines and the double-circuit lines, in general, the corresponding design value of upper limit of the compensation degree for the high-voltage shunt reactor can be chosen as not more than 95%; for the purpose

of strictness, the corresponding design value of upper limit of the compensation degree for the high-voltage shunt reactor is better to be about 90%.

Moreover, if neutral point small reactance is provided with more taps and larger impedance adjustment range (>±10%), UHV line can increase the corresponding design value of upper limit of the compensation degree for the high-voltage shunt reactor properly.

For the lower limit:

1. To achieve the goal to restrict secondary arc current, the compensation degree of the high-voltage shunt reactor for single-circuit UHV line shall be larger than the reactive power of phase-to-phase capacitance of the line; however, for double-circuit UHV line, apart from phase-to-phase capacitance of the line, it is also necessary to compensate partial inter-circuit capacitance.
2. When determining the lower limit of the compensation degree of the high-voltage shunt reactor from the perspective of restriction of secondary arc current, certain allowance shall be reserved; otherwise, the impedance value of the small reactance will be very large, and thus, it is not favorable for manufacturing.
3. The lower limit of the compensation degree of the high-voltage shunt reactor determined through restriction of secondary arc current will be under obvious influence of the line parameters. Within possible range of the parameters, such lower limit for single-circuit UHV line and double-circuit UHV lines shall be, respectively, 55 and 65% maximally.
4. The lower limit of the compensation degree of the high-voltage shunt reactor determined through the voltage control of switching no-load line is increased along with the increase of line length, and in turn increased according to the sequence of type A line, type B line, and type C line.
5. When the line is short, the lower limit of the compensation degree of the high-voltage shunt reactor determined through the restriction of secondary arc current is higher than the lower limit of the compensation degree of the high-voltage shunt reactor determined through the control of no-load line voltage; when the line is long, the lower limit of the compensation degree of the high-voltage shunt reactor determined through the restriction of secondary arc current is lower than the lower limit of the compensation degree of the high-voltage shunt reactor determined through the control of no-load line voltage. As the actual line has different capacitance parameters and lengths, therefore, the lower limit of the compensation degree of the high-voltage shunt reactor shall be calculated from the above two aspects according to the actual parameters, and the larger one shall be taken as the final lower limit of the compensation degree of the high-voltage shunt reactor.

The research in this chapter shows that the compensation of high-voltage shunt reactor will influence the stable operation of the UHV transmission line directly. Therefore, the selection of high-voltage shunt reactor shall be scientific and cautious, thus to ensure that high-voltage shunt reactor can effectively restrict the

power frequency overvoltage and at the same time will not present negative influence on the restriction of secondary arc current and reactive power balance.

References

1. Liu Z. UHV power grid. Beijing: China Economic Press; 2005.
2. Sun K, Yi Q, Dong C, Zhou H. Research on power frequency over-voltage in UHV AC transmission lines. Power Syst Technol. 2010;34(12):30–5.
3. China Electric Power Research Institute. UHV transmission technology—volume of AC transmission. Beijing: China Electric Power Press; 2012.
4. Guangrun X. Overvoltage of electric power system. Beijing: Water Resources and Electric Power Press; 1985.
5. Gu D, Zhou P, Xiu M, Wang S, Dai M, Lou Y. Study on overvoltage and insulation coordination for 1000 kV AC transmission system. High Volt Eng. 2006;3(12):1–6.
6. Caixin S, Wenxia S, Jie Z, Hong R, Mi Z. Overvoltage in UHV transmission system. Electric Power Autom Equip. 2005;25(9):5–9.
7. Huang J, Wang G, Li H, Han F. Study on simulation of fundamental frequency overvoltage for UHV AC transmission lines. Relay. 2007;35(4):32–9.
8. Yesheng J. Analysis and restriction research on overvoltage of UHV transmission system. Guiyang: Guizhou University; 2007.
9. Kun S, Yongli L, Bin L, Zhiyu M. Research and simulation of over-voltage in UHV transmission lines. Proc CSU EPSA. 2003;15(6):13–8.
10. Du Z, Niu L, Zhao J. Developing UHV AC transmission and constructing strong state power grid. Electric Power Autom Equip. 2007;27(5):1–5.
11. Li H, Huang Y, Shi W. Effect of ACSR on suppressing power frequency overvoltage of EHV transmission system. High Volt Appar. 2004;40(3):186–8.
12. Yi Q, Zhou H, Ji R, Su F, Sun K, Chen J. Upper limit of compensation degree of high voltage shunt reactor for UHVAC transmission lines. Power Syst Technol. 2011;35(7):6–18.
13. Yi Q, Zhou H, Ji R, Su F, Sun K, Chen J. Research on lower limit of compensation degree of high voltage shunt reactor for UHVAC transmission lines. Power Syst Technol. 2011;35 (8):18–25.
14. Yi Q, Ji R. PSCAD/EMTDC-based research on compensation mode of UHV AC shunt reactor. East China Electric Power. 2011;39(2):257–61.
15. Zhou Q, Guo Q, Bu G, Ban L. Application of controllable reactors in China's power grid at extra and ultra voltage level. Proc CSEE. 2007;27(7):1–6.
16. Linghui Y, Xuhang Z, Renming Ma, Jiamin Z. Resonance simulation for 500 kV double-circuit lines on the same tower. East China Electric Power. 2008;36(7):31–3.
17. Xiaodong L, Bingjun Z, Haidong J, Xiongwei Z. Calculation and analysis on resonance overvoltage in non-full phase operation for 500 kV transmission line. Hebei Electric Power. 2007;26(6):16–24.
18. GB/T15945-1995. Quality of electric energy supply: permissible deviation of frequency for power system. 1995.
19. DL/T 428-2010. Technical rules for power system automatic under-frequency load shedding. 1991.
20. Yinsheng T. A design method for reactive power compensation in UHV network. Power Syst Technol. 1996;20(4):38–9.
21. Guquan Z. Balance and compensation of reactive power in power system. Electric Power Autom Equip. 1997;2:16–8.

Chapter 5
Secondary Arc Current of UHVAC System

Qiang Yi, Hao Zhou and Sha Li

The study shows that the success in single-phase auto-reclosure depends much on the magnitudes of the secondary arc current and the recovery voltage at the fault point. Compared with EHV lines, the UHV transmission lines have high voltage, long transmission line, large phase-to-phase capacitance, and mutual inductance values, which make it to have larger secondary arc current and higher recovery voltage, causing longer burning time of the secondary arc, requiring measures to be taken to control the secondary arc current and recovery voltage, or the success rate of the single-phase auto-reclosure will be significantly reduced, which is very harmful to the system. Therefore, to improve the success rate of the UHV line single-phase auto-reclosure, the corresponding measures shall be taken to shorten the burning time of the secondary arc. Currently, there are two major methods for extinguishing the UHV secondary arc: one is to add the shunt reactor and connect small reactance at the neutral point; the other is to install the high-speed grounding switch (HSGS). The nature of these two methods is to shorten the arc burning time through reducing the amplitudes of the secondary arc current and recovery voltage, and thereby improve the success rate of the single-phase auto-reclosure.

In this chapter, the secondary arc current generation mechanism and the secondary arc extinguishing measures are discussed first, and then, the impacts on secondary arc current by the two measures, i.e., additional installation of small

Q. Yi (✉)
SIEMENS Power Automation Co., Ltd., Nanjing, Jiangsu, People's Republic of China
e-mail: 307289798@qq.com

H. Zhou · S. Li
College of Electrical Engineering, Zhejiang University, Xihu District,
Hangzhou, Zhejiang, People's Republic of China
e-mail: zhouhao_ee@zju.edu.cn

S. Li
e-mail: lisha1210@zju.edu.cn

© Zhejiang University Press, Hangzhou and Springer-Verlag GmbH Germany 2018

H. Zhou et al. (eds.), *Ultra-high Voltage AC/DC Power Transmission*,
Advanced Topics in Science and Technology in China,
https://doi.org/10.1007/978-3-662-54575-1_5

reactance at the neutral point of shunt reactor and additional installation of HSGS, are discussed, and finally, the calculation is carried out for the two methods based on simulation modeling.

5.1 Generation Mechanism of Secondary Arc Current

The generation mechanism of secondary arc current is shown in Fig. 5.1 [1]. Due to some reasons such as lightning strike, one phase of the operating line has transient single-phase ground fault, and then, the short-circuit current passes through the fault point. The burning arc at the fault point is known as primary arc. Then, the single-phase auto-reclosing device acts immediately, which makes the circuit breakers at both ends of the fault phase line break, and the short-circuit current is cutoff. At this moment, the sound phase and some adjacent lines possibly existing shall supply current to the fault point through the electrostatic coupling of phase-to-phase capacitance and the electromagnetic coupling of phase-to-phase mutual inductance, and this current is called the secondary arc current. The arc with low energy existing on the arcing channel is referred to the secondary arc. After the secondary arc extinguished, the induction between lines will make the voltage of the disconnected phase increase immediately, and thereby make the arc rekindle, and the arc light grounding fault occurs again. Therefore, the voltage of the disconnected phase to ground which might cause the arc to rekindle at the fault point is referred to as the recovery voltage.

The secondary arc current consists of capacitive component and inductive component. The capacitive component refers to the current provided by the voltage on the sound phase line through phase-to-phase capacitance C_M (including C_{m1} and C_{m2} on both sides). The magnitude of the capacitive component depends on the voltage of the sound phase line at fault time, independent of fault point position. The inductive component refers to the current at the fault point, which is caused by the induced electromotive force generated by the current on the sound phase line through phase-to-phase mutual inductance M (including M_1 and M_2 on both sides).

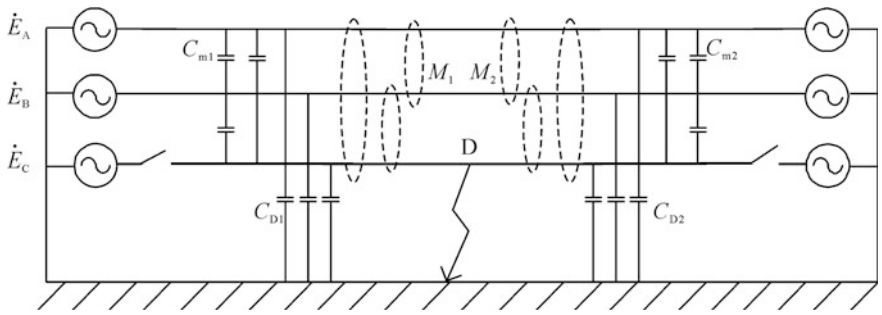

Fig. 5.1 Sketch of the generation mechanism of the secondary arc current

The induced electromotive force generates the current at the fault point through the loop formed by ground and the capacitance of fault phase. The current is closely related to the magnitude of the sound phase current and fault position.

5.2 Measures to Extinguish the Secondary Arc

5.2.1 Connection of Small Reactance at the Shunt Reactor's Neutral Point for Compensation

5.2.1.1 Restriction Principle and Selection of Small Reactance for Single-Circuit Line

The connection of small reactance at the shunt reactor's neutral point, as shown in Fig. 5.2, is adopted for EHV and UHV lines in most countries to restrict the secondary arc. Its idea is to restrict the capacitive component of the secondary arc current through compensating the phase-to-phase capacitance. The system in which the small reactance is connected at the shunt reactor's neutral point is shown in Fig. 5.3a. Assuming that the infinite power systems are on both sides, triphasic potentials are $\dot{E}_A$, $\dot{E}_B$ and $\dot{E}_C$, and X_{LP} is high-voltage shunt reactor, X_{LN} is the small reactance connected at the neutral point [1], C_{m1} and C_{m2} are phase-to-phase capacitance, M_1 and M_2 are phase-to-phase mutual inductance, and C_{D1} and C_{D2} are phase-to-ground capacitances.

The high-voltage shunt reactor additionally installed with small reactance can obtain the circuit, as shown in Fig. 5.3b, through conversion, with the relationship of each parameter as follows [1]:

$$\begin{cases} X_{LD} = 3X_{LN} + X_{LP} \\ X_{LM} = X_{LP}^2 / X_{LN} + 3X_{LP} \end{cases} \tag{5.1}$$

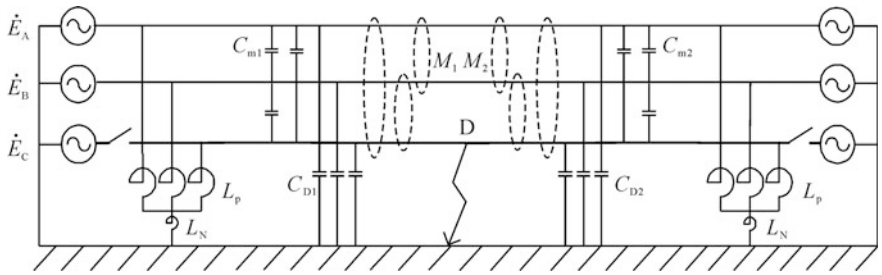

Fig. 5.2 Sketch of line with small reactance connected at the shunt reactor's neutral point for compensation

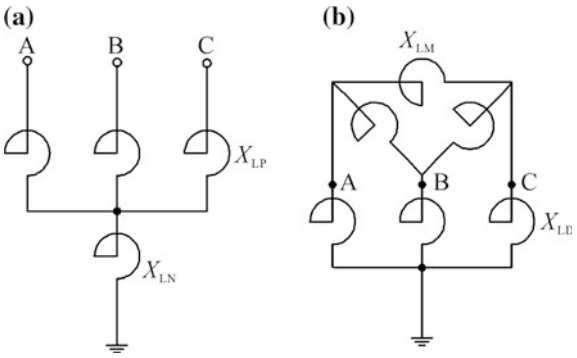

Fig. 5.3 Sketch for adding small reactance at shunt reactor's neutral point

where X_{LD} and X_{LM}: equivalent reactance to ground and phase-to-phase reactance, respectively.

Equation (5.1) shows the relationship among the capacities of high-voltage shunt reactor X_{LP} and phase-to-ground reactance X_{LD} and phase-to-phase reactance X_{LM} as follows:

$$\frac{U_{0N}^2}{X_{LD}} + \frac{\left(\sqrt{3}U_{0N}\right)^2}{X_{LM}} = \frac{U_{0N}^2}{X_{LP}} \tag{5.2}$$

where

U_{0N} the effective value of phase voltage.

Equation (5.2) shows that the capacity of the high-voltage shunt reactor X_{LP} equals to the sum of the capacities of the phase-to-ground reactance X_{LD} and phase-to-phase reactance X_{LM}. The small reactance does not change the compensating capacity. Its role is to distribute the capacity of the high-voltage shunt reactor reasonably to the phase-to-phase reactance and phase-to-ground reactance.

The analysis on the principle that the small reactance connected at the neutral point to restrict the secondary arc current is carried out as follows. The schematic diagram for restricting the secondary arc current by small reactance is shown in Fig. 5.4, in which, after the single-phase ground fault being occurred to phase C, the single-phase circuit breakers on both ends trip, and the sound phases A and B supply the secondary arc current to the fault point through capacitive coupling and inductive coupling, i.e., the secondary arc current consists of capacitive component and inductive component. The No. 1 path in Fig. 5.4 is the flow path of the capacitive component of the secondary arc current. The currents I_1' and I_1'' flow from the sound phases through the phase-to-phase capacitances (C_{m1} and C_{m2}) and the equivalent phase-to-phase reactances (L_{m1} and L_{m2}) to the suspended fault phase, and then flow to the ground through the fault point. In addition, $I_1' + I_1''$ is the capacitive component of the secondary arc current that flowing past the fault point. The No. 2 path in Fig. 5.4 is the flow path of the inductive component of the secondary arc current. The induced electromotive force on the fault phase is caused

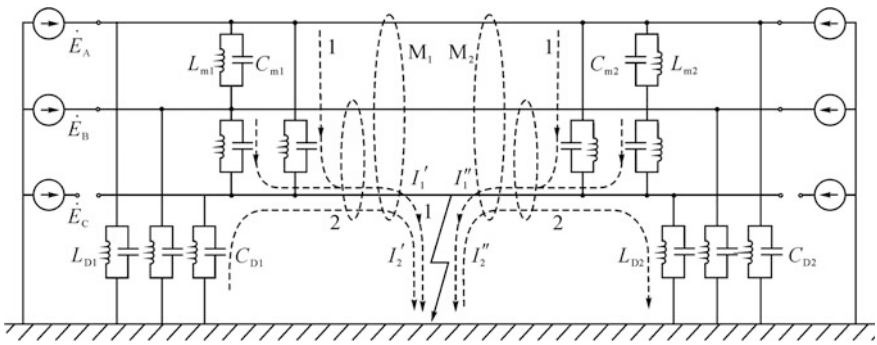

Fig. 5.4 Sketch of line with small reactance connected at neutral point of the shunt reactor

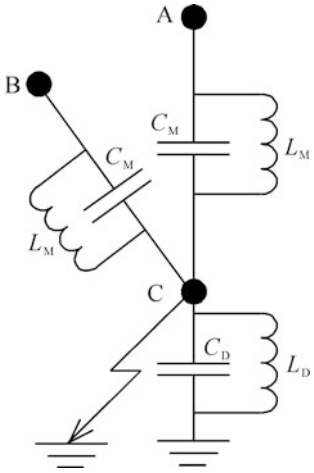

Fig. 5.5 Schematic diagram for restricting the secondary arc current by connecting small reactance at the neutral point of the shunt reactor

by the sound phase current through the phase-to-phase mutual inductances M_1 and M_2. The circuits on left and right sides are formed with the fault point through the fault phase's capacitances to ground (C_{D1} and C_{D2}) and equivalent phase-to-ground reactances (L_{D1} and L_{D2}). Then, the induced electromotive force generates circular currents I_2' and I_2'' in the circuits on both sides. $I_2' - I_2''$ is the inductive component of the secondary arc current that flowing past the fault point.

The additional installation of small reactance at the neutral point of high-voltage shunt reactor in the single-circuit line is mainly to restrict the capacitive component of the secondary arc current. Its flow loop is shown in Fig. 5.5. The equivalent circuit diagram is shown in Fig. 5.6. In the figures, C_M is the total phase-to-phase capacitance ($C_{m1} + C_{m2}$), L_M is the total equivalent phase-to-phase reactance (L_{m1}// L_{m2}), C_D is the total phase-to-ground capacitance ($C_{D1} + C_{D2}$), and L_D is the total equivalent phase-to-ground reactance (L_{D1} //L_{D2}).

As the arc resistance R_g is far less than the impedances of the equivalent capacitance to ground C_D and reactance to ground L_D, for the purpose of

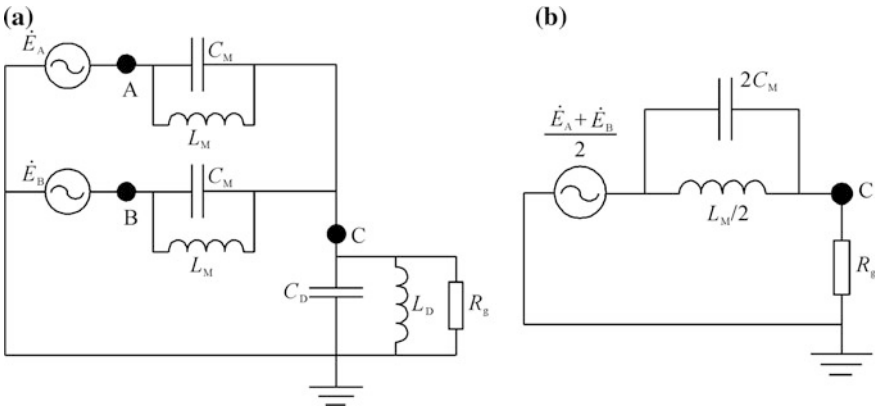

Fig. 5.6 Equivalent schematic diagram for restricting the secondary arc current by connecting small reactance at the neutral point of the shunt reactor

simplification, Fig. 5.6b ignores the impact of the capacitance to ground and the equivalent reactance to ground on the secondary arc current through the arc resistance.

It is observed that to minimize the secondary arc current flowing past the arc channel, it is required to make the impedance of $2C_M$ and $L_M/2$ are equal and form parallel resonance. Thereby, it is concluded that

$$X_{LM} = X_{CM}. \tag{5.3}$$

According to the positive and zero sequence capacitances of the whole line C_1 and C_0, the line's phase-to-phase capacitance C_M can be calculated as follows:

$$C_M = \frac{1}{3}(C_1 - C_0). \tag{5.4}$$

Then, the obtained impedance of phase-to-phase capacitance is

$$X_{CM} = \frac{1}{\frac{1}{3}\omega(C_1 - C_0)}. \tag{5.5}$$

Therefore

$$X_{LM} = \frac{1}{\frac{1}{3}\omega(C_1 - C_0)}. \tag{5.6}$$

Assuming that the compensation degree of the line is k, then $X_{LP} = X_{C1}/k$ may be obtained through Eq. (4.13) and the optimal impedance value of the small reactance may be calculated in combination with Eqs. (5.1) and (5.4):

$$X_{\mathrm{LN}} = \frac{X_{\mathrm{LP}}^2}{X_{\mathrm{LM}} - 3X_{\mathrm{LP}}} = \frac{X_{\mathrm{LP}}^2}{\frac{1}{3\omega(C_1 - C_0)} - 3X_{\mathrm{LP}}} = \frac{1}{\omega C_1 k(kC_1/C_{\mathrm{M}} - 3)}. \tag{5.7}$$

The capacitive component of the recovery voltage, in fact, results by the voltage division of the phase-to-phase impedance (shunt connection between equivalent phase-to-phase reactance and phase-to-phase capacitance) and the impedance to ground of the fault phase (shunt connection between equivalent reactance to ground and capacitance to ground of the fault phase); after the small reactance is selected as per Eq. (5.7), a resonant state is formed between the phases of the line giving rise to a large phase-to-phase impedance, while the phase-to-ground capacitance is only partially compensated and the phase-to-ground impedance appears to be relatively small, thus making the voltage of the impedance to ground of the fault phase low, meaning that the capacitive component of the recovery voltage of the fault phase is small. As the capacitive component always plays a leading role in the recovery voltage, the restriction of the capacitive component will significantly reduce the amplitude of the recovery voltage to achieve the purpose of rapid arc extinction.

Meanwhile, as the capacitance to ground is also partially compensated by the equivalent reactance to ground, the impedance of the inductive component circuit of the secondary arc current is significantly increased, but there is no change to its inductive potential, thus resulting in a large decrease of the amplitude of the inductive component of the secondary arc current. However, it is necessary to point out that the small reactance connected at the neutral point is primarily used to restrict the capacitive component of the secondary arc current by fully compensating the phase-to-phase capacitance; though the equivalent inductance to ground has a certain restriction effect on the inductive component, but it is not the main purpose. In general, it is not recommended to restrict the inductive component of the secondary arc current by intentionally increasing the compensation degree of high-voltage shunt reactor to make the capacitance to ground receive greater compensation, because the excessively high compensation degree may result in the danger of resonance. For example, if the compensation degree is 100% and the small reactance is appropriate, the phase-to-phase capacitance and capacitance to ground will be fully compensated and the line's capacitance to ground and equivalent phase-to-ground reactance will also give rise to shunt resonance, resulting in a great increase in the recovery voltage which is not advantageous to the extinction of the secondary arc.

5.2.1.2 Restriction Principle for Double-Circuit Line and Selection of Small Reactance

When the small reactance is used to restrict the secondary arc current of the double-circuit UHV line on the same tower, the small reactance is still installed at the neutral point of high-voltage shunt reactors in each circuit of line, just as installed in the single-circuit line. However, due to the fact that the effect of

coupling capacitance between the circuits of the double-circuit line on the same tower causes the secondary arc current to present different characteristics in case of different operation modes and fault types, the restriction of the secondary arc current in the double-circuit line is more complicated than that in the single-circuit UHV line and such complication is mainly reflected in the more complex selection of the impedance value of the small reactances connected at the neutral points.

Based on the probability of occurrence, the following two operation modes are mainly considered for a double-circuit line:

(1) single-circuit operation mode;
(2) double-circuit operation mode.

Under different operation modes, as different phase-to-phase reactances are required to compensate the different capacitances which may supply secondary arc current, the impedance value of the most appropriate small reactance under different operation modes and the final small reactance needs to be determined by taking a comprehensive consideration. After the small reactance scheme is determined, it is also necessary to take the resonance situations under these two operation modes into consideration to determine the upper limit of the high-voltage shunt reactor.

1. Single-circuit operation mode

When the transmission line is under single-circuit operation, the two ends of the other circuit are generally grounded. The capacitance structure of the line at this time is shown in Fig. 5.7a, in which the reactance is temporarily not considered. In this figure, the phase C in the left circuit is the fault phase, whose circuit breakers on both ends have tripped, phases A and B are live sound phases, and phases a, b, and c in the right circuit are grounded with the electric potential of 0.

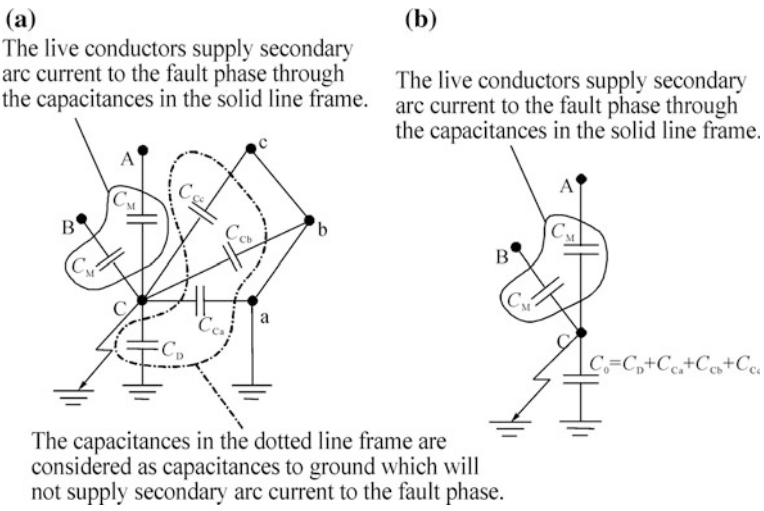

Fig. 5.7 Sketch of capacitances under single-circuit operation mode

Figure 5.7a may be simplified to Fig. 5.7b [2], from which it can be seen that the secondary arc current is completely supplied by the phase-to-phase capacitances in this circuit. The capacitance between the circuits will not only supply secondary arc current to the suspended phase, but will also shunt part of the secondary arc current which is supposed to flow to the ground from the line's capacitance to ground C_D. Therefore, to minimize the secondary arc current under the single-circuit operation mode when a single circuit is grounded, it only needs to fully compensate the phase-to-phase capacitance of this circuit, which is the same to that in the single-circuit line.

Fig. 5.8 shows the equivalent circuit for the flow loop of the capacitive component of the secondary arc current after the reactance has been taken into account.

As the arc resistance R_g is much less than the impedances of the equivalent capacitance to ground C_D and the reactance to ground L_{D1}, for the purpose of simplification, Fig. 5.8b neglects the effect of the equivalent capacitance to ground and the reactance to ground on the arc resistance's secondary arc current.

It can be seen that, equal to the single-circuit line, to restrict the secondary arc current to its minimum, it is required that the impedance of phase-to-phase reactance be identical to the impedance of phase-to-phase capacitance, that is

$$X_{LM1} = X_{CM}. \tag{5.8}$$

Assuming that the line compensation degree is k and the method similar to the single-circuit line is used, according to the whole-line positive and zero sequence capacitances C_1 and C_0 of the whole line as well as the high-voltage shunt reactor, the ideal impedance value of the small reactance under the single-circuit operation mode is calculated as follows [2]:

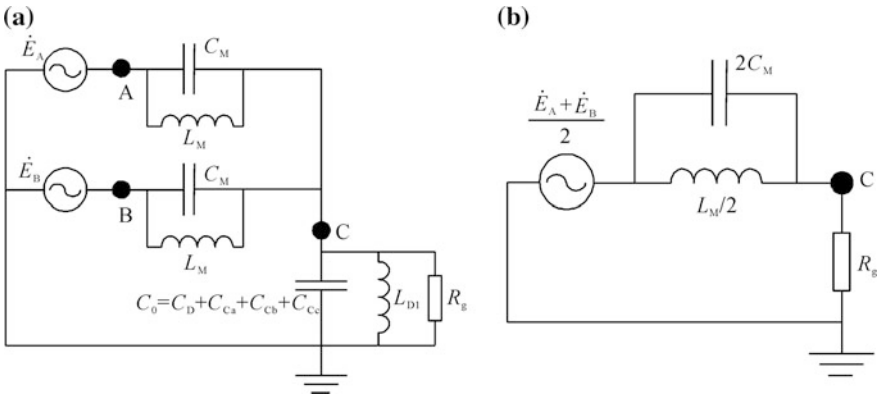

Fig. 5.8 Sketch for the capacitive component circuit of the secondary arc current under single-circuit operation mode

$$X_{\mathrm{LN1}} = \frac{X_{\mathrm{LP}}^2}{\frac{1}{\frac{1}{3}\omega(C_1 - C_0)} - 3X_{\mathrm{LP}}} = \frac{1}{\omega C_1 k(kC_1/C_{\mathrm{M}} - 3)}. \tag{5.9}$$

From the above equation, it can be seen that the method for calculating the ideal small reactance for the double-circuit line under single-circuit operation mode is completely consistent with that for the single-circuit line.

2. Double-circuit operation mode

The capacitances under the double-circuit operation mode are shown in Fig. 5.9, in which the reactance is temporarily not considered. In this figure, phase C in the left circuit is the fault phase, phases A and B are live sound phases, and phases a, b, and c operate normally.

By reference to the analysis in Chap. 4, the simplified capacitance circuit with small reactors additionally installed at the neutral point of high-voltage shunt reactors in the double-circuit line under double-circuit operation mode is shown in Figs. 5.10 and 5.11 shows the equivalent circuit diagram thereof [2].

From Fig. 5.10, it can be seen that, to restrict the secondary arc current to its minimum, it is necessary to compensate the capacitances with respective values of $C_{\mathrm{M}} + (C_{\mathrm{Ca}} - C_{\mathrm{Cc}})$ and $C_{\mathrm{M}} + (C_{\mathrm{Cb}} - C_{\mathrm{Cc}})$ between the two phases of A and B and the phase of C. In consideration of the effects of the parallel high-voltage shunt reactors and the small reactances connected at the neutral points, the equivalent circuit is shown in Fig. 5.11a, in which L_{M2} and L_{D2} are, respectively, the equivalent phase-to-phase reactance and the reactance to ground obtained by taking into account the equivalent conversion of the high-voltage shunt reactor and the small reactance. Besides, R_{g} is the arc resistance.

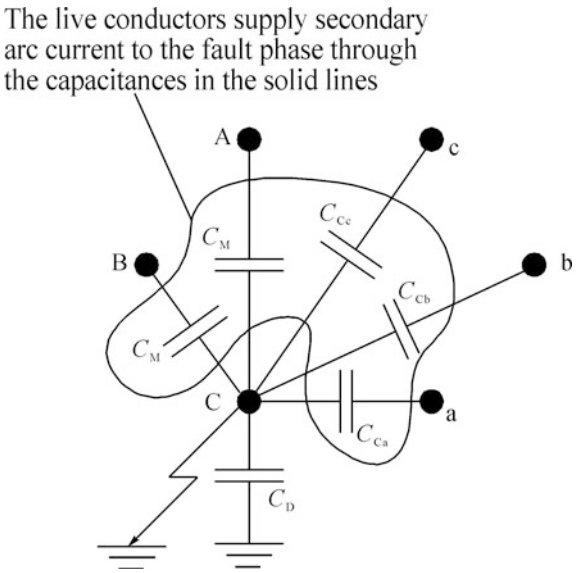

Fig. 5.9 Sketch for capacitors in the line under double-circuit operation mode

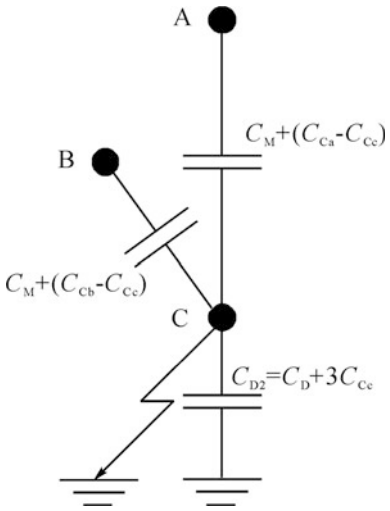

Fig. 5.10 Simplified capacitance circuit for double-circuit line under double-circuit operation mode

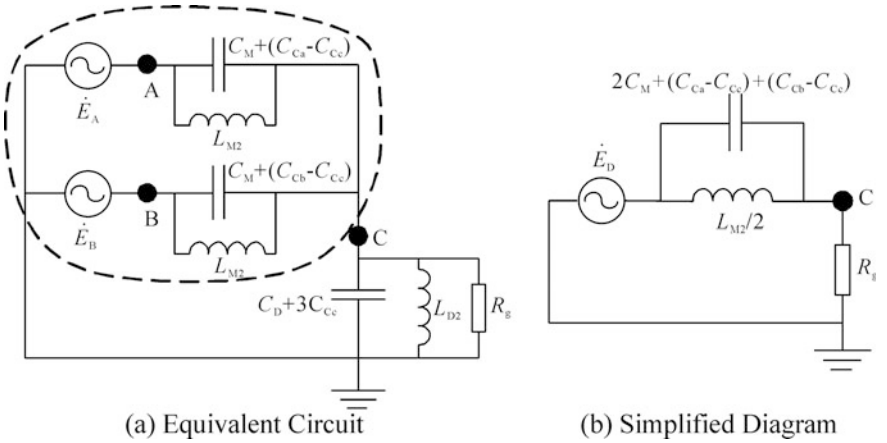

Fig. 5.11 Equivalent circuit and its simplified diagram after considering the parallel high-voltage shunt reactors and the small reactance that connected at the neutral points

According to the Thevenin Theorem, the two shunt branches in the area of dotted lines in Fig. 5.11a are made equivalent to a voltage source $\dot{E}_D$ with an impedance connected in series (as shown in Fig. 5.11b), where $\dot{E}_D$ is equal to the open-circuit electric potential when point C in Fig. 5.11a is disconnected; in addition, as the arc resistance R_g is far less than the impedances of the equivalent capacitance to ground $C_D + 3C_{Cc}$ and the reactance to ground L_{D2}, for the purpose

of simplification, Fig. 5.11b neglects the effect of the equivalent capacitance to ground and reactance to ground on the arc resistance's secondary arc current.

From Fig. 5.11b, it can be known that, to fully compensate the capacitive secondary arc current, it is necessary to achieve parallel resonance in the shunt circuits of $2C_{\mathrm{M}} + (C_{\mathrm{Ca}} - C_{\mathrm{Cc}}) + (C_{\mathrm{Cb}} - C_{\mathrm{Cc}})$ and $L_{\mathrm{M2}}/2$, and then the impedance of the phase-to-phase inductance is as follows:

$$\begin{aligned} X_{\mathrm{LM2}} &= \omega L_{\mathrm{M2}} \\ &= \frac{2}{\omega(2C_{\mathrm{M}} + (C_{\mathrm{Ca}} - C_{\mathrm{Cc}}) + (C_{\mathrm{Cb}} - C_{\mathrm{Cc}}))} \\ &= \frac{2}{\omega(\frac{2(C_1 - C_0)}{3} + (C_{\mathrm{Ca}} - C_{\mathrm{Cc}}) + (C_{\mathrm{Cb}} - C_{\mathrm{Cc}}))} \end{aligned} \tag{5.10}$$

By substituting the Eq. (5.10) into Eq. (5.1), the ideal value X_{LN2} of the small reactor connected at the neutral point during double-circuit operation can be obtained:

$$X_{\mathrm{LN2}} = \frac{X_{\mathrm{LP}}^2}{\frac{2}{\omega(\frac{2(C_1 - C_0)}{3} + (C_{\mathrm{Ca}} - C_{\mathrm{Cc}}) + (C_{\mathrm{Cb}} - C_{\mathrm{Cc}}))}} - 3X_{\mathrm{LP}} \tag{5.11}$$

3. Method for choosing the final small reactance

The value of the ideal small reactance varies under the single-circuit and double-circuit operation modes and the impedance value of the ideal small reactance under the double-circuit operation mode is generally higher than that in the single-circuit operation mode, i.e.

$$X_{\mathrm{LN1}} < X_{\mathrm{LN2}} \tag{5.12}$$

This is because to restrict the secondary arc current to its minimum, the phase-to-phase reactance under the double-circuit operation mode needs to compensate the phase-to-phase capacitance of the circuit and part of the inter-circuit capacitance at the same time, while under the single-circuit operation mode, the phase-to-phase reactance only needs to compensate the phase-to-phase capacitance of the circuit, i.e. the impedance of the ideal phase-to-phase reactance under the double-circuit operation mode is supposed to be lower. Therefore, according to Eq. (5.1), it can be known that the ideal small reactance under the double-circuit operation mode is generally higher than that under the single-circuit operation mode.

After the ideal small reactances X_{LN1} and X_{LN2} under the single-circuit and double-circuit operation modes are obtained, it needs to consider the probabilities of occurrence of the two operation modes, and then determine the final small reactance scheme by weighted averaging the ideal small reactances under the single-circuit and double-circuit operation modes.

$$X_{LN} = p_1 X_{LN1} + p_2 X_{LN2} \tag{5.13}$$

where

p_1 and p_2 respectively, the probabilities of occurrence of the single-circuit and double-circuit operation modes;

X_{LN} the impedance value of the final small reactance.

Under ordinary circumstances, to fully realize the transmission capacity of the UHV double-circuit line, the two circuits of the line are generally running simultaneously and the line is only subject to the single-circuit operation under the special circumstances such as maintenance, so p_2 is generally far greater than p_1.

At present, there are two main methods to obtain the ideal small reactances X_{LN1} and X_{LN2} under the single-circuit and double-circuit operation modes. One is the direct analysis method and the other is the trial-and-error method.

(1) Direct analysis method

Based on the detailed theoretical analysis in the previous chapter and the preceding part of this section, the ideal small reactances under single-circuit and double-circuit operation modes may be directly calculated through Eqs. (5.9) and (5.11). In addition, then, the scheme for the value of the final small reactance may be obtained using the weighted average method through Eq. (5.13). The workload arising from the use of this method is significantly less than that arising from the trial-and-error method.

(2) Trial-and-error method

In case of lacking the theoretical analysis on the secondary arc current in the double-circuit line, the trial-and-error method is generally used to determine the impedance value of the small reactance at the neutral point of the double-circuit line. This method is to calculate the secondary arc currents with different small reactances one by one under each mode and the small reactance corresponding to the minimum secondary arc current under a certain mode is deemed as the ideal small reactance under this mode.

The exact steps of the trial-and-error method can be described as follows by taking a 400 km-long double-circuit UHV line with the drum-type towers adopted along the whole line and the compensation degree of the high-voltage shunt reactor being 85% as an example.

Step one: Under the single-circuit and double-circuit operation modes, change the impedance values of the small reactances to calculate the amplitude of the secondary arc current under each of the impedance values of small reactances and take the maximum value of the secondary arc current in case of three-phase failure to plot the diagram representing the relationship between the small reactance and the secondary arc current, as shown in Fig. 5.12.

Step two: According to Fig. 5.12, under the case of one circuit is grounded, for single-circuit operation mode, the secondary arc current is the minimum when the

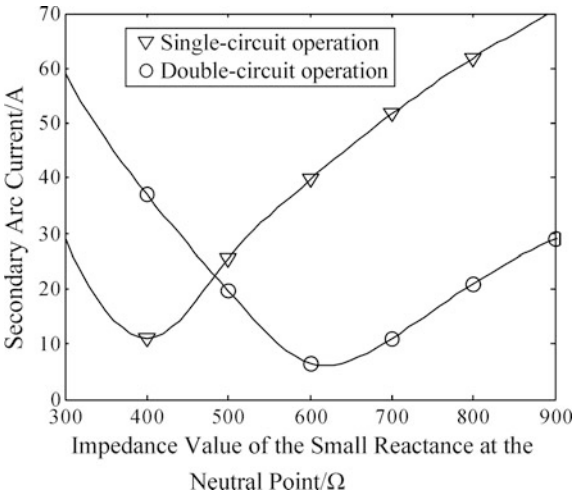

Fig. 5.12 Calculation results by trial-and-error method

impedance value of the small reactance at the neutral point is 400 Ω; and for the double-circuit operation mode, the secondary arc current is the minimum when the impedance value is 600 Ω.

Step three: Conduct the weighted average of the two values and have the impedance value of the small reactance at the neutral point of this line taken as 500 Ω.

The disadvantages of this method lie in that it is required to calculate the secondary arc currents with different impedances of the small reactance under each operation mode one by one, which involves a very large calculation amount.

5.2.1.3 Methods for Measuring the Parameters of the Power Transmission Lines Required for the Calculation of Small Reactance [3]

1. Line's positive sequence capacitance C_1

The wiring shall be carried out, as shown in Fig. 5.13, when the line's positive sequence capacitance C1 is to be measured. Open the tail end of the line, and add a three-phase power supply at the head end, measure the three-phase current at the head end, and measure the three-phase voltage and power at both ends. When the positive sequence capacitance of the double-circuit line is measured, the both ends of the other circuit shall be subject to three-phase ground to reduce the impact on the measurement results.

The positive sequence parameters of the conductor of each phase shall be obtained by the following equation.

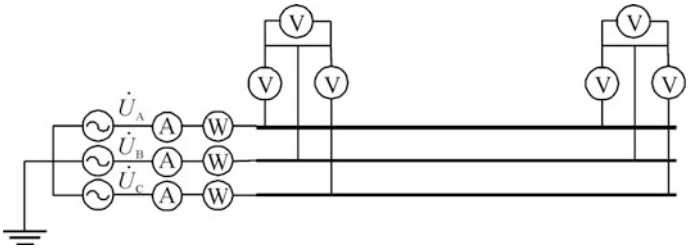

Fig. 5.13 Wiring diagram for measuring the positive sequence capacitance

Positive sequence admittance of unit length:

$$y_1 = \frac{\sqrt{3} I_{av1}}{U_{av1} l} (\text{S/km}) \tag{5.14}$$

Positive sequence conductance of unit length:

$$g_1 = \frac{P_1}{U_{av1}^2 l} (\text{S/km}). \tag{5.15}$$

Positive sequence capacitance of unit length:

$$c_1 = \frac{b_1 \times 10^6}{2\pi f} (\mu\text{F/km}) \tag{5.17}$$

Positive sequence capacitance of the whole line:

$$C_1 = c_1 \times l (\mu\text{F}). \tag{5.18}$$

where

P_1 the total three-phase loss power (MW);
U_{av1} the average value of voltage on the three-phase conductors at the head and tail ends (effective value, kV);
I_{av1} the average value of the three-phase current (effective value, kA);
l the length of the line (km); and
f the frequency of the power supply (Hz).

2. Line's zero sequence capacitance C_0

The wiring shall be carried out, as shown in Fig. 5.14, when the line's zero sequence capacitance C_0 is to be measured. Open the tail end of the line, shorten the three phases' conductors at the head end and add a single-phase power supply, then

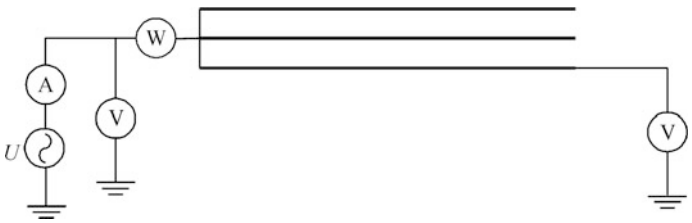

Fig. 5.14 Wiring diagram for measuring zero sequence capacitance

measure the sum of the three-phase zero sequence currents at the head end, and measure the average value of the voltage at the head and tail ends and the total three-phase zero sequence power. When the zero sequence capacitance of the double-circuit line is measured, the both ends of the other circuit shall be subject to three-phase ground to reduce the impact on the measurement results.

The zero sequence parameters of the conductor of each phase conductor shall be obtained by the following equations.

Zero sequence admittance of unit length:

$$y_0 = \frac{I_0}{3U_{\text{av0}}l}(\text{S/km}). \tag{5.19}$$

Zero sequence conductance of unit length:

$$g_0 = \frac{P_0}{3U_{\text{av0}}^2 l}(\text{S/km}). \tag{5.20}$$

Zero sequence susceptance of unit length:

$$b_0 = \sqrt{y_0^2 - g_0^2}(\text{S/km}). \tag{5.21}$$

Zero sequence capacitance of unit length:

$$c_0 = \frac{b_0 \times 10^6}{2\pi f}(\mu\text{F/km}). \tag{5.22}$$

Zero sequence capacitance of the whole line:

$$C_0 = c_0 \times l(\mu\text{F}). \tag{5.23}$$

where

P_0 the total zero sequence power loss of the three-phase conductors (MW);
U_{av0} the average value of phase voltages at the head and tail ends (effective value, kV);

I_0 the total three-phase zero sequence current (the effective value, kA);
l the length of the line (km); and
f the frequency of the power supply (Hz).

3. Inter-circuit coupling capacitance of the double-circuit line

During the calculation of the small reactance at the neutral point in the double-circuit line, it needs to know the inter-circuit capacitance parameters of the double-circuit line. The wiring shall be carried out, as shown in Fig. 5.15, when the coupling capacitance between two phases of the different circuits is to be measured (the measurement of the capacitance between phases A and c is taken as an example), with one phase of the circuit I connected with the voltage source, one phase of the measurement circuit II grounded through ampere meter, and the other four phases are grounded.

The capacitance between two conductors of the different circuits shall be calculated according to the following equation:

$$C_{\mathrm{Ac}} = \frac{I \times 10^6}{2\pi f U} (\mu\mathrm{F}) \tag{5.24}$$

where

I the current measured by the ampere meter;
U the applied voltage; and
f the frequency of the power supply.

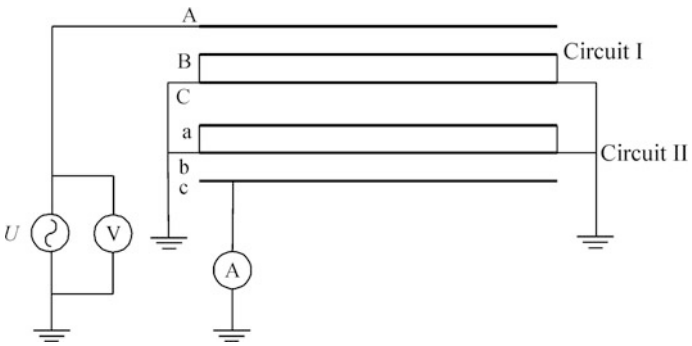

Fig. 5.15 Wiring diagram for measuring inter-circuit capacitance

5.2.1.4 Requirements on Restriction

The single-phase reclosing time is defined as the time from the response made by the line protection device in case of system failure to the completion of reclosure, mainly including the time of protection and switch actions, the time of arc path ionization and recovery, and the duration of secondary arc (or the self-extinguishing time). For the line with high-voltage shunt reactor for compensation, the distribution process of the reclosing time is shown in Fig. 5.16. In the EHV/UHV system, the single-phase reclosing time is generally taken as 1 s, on the basis of which it may be calculated that the self-extinguishing time of the secondary arc at the grounding point is approximately within 0.67 s, based on which the requirement to complete the single-phase reclosure in 1 s can only be met.

North China Electric Power Research Institute (NCEPRI) has conducted a lot of researches on the self-extinguishing characteristics of the secondary arc and obtained the fitting equation between the extinction time t and the secondary arc current magnitude I_C under the conditions that the probability for extinction of secondary arc is 90% in case the wind speed is greater than 1.5 m/s, the arcing potential gradient is less than 13.5 kV/m, and there is high-voltage shunt reactor for compensation [4]:

$$t_{90\%} = 3.3333 \times 10^{-4} I_C^2 + 6.6968 \times 10^{-3} I_C + 6.5105 \times 10^{-2}. \tag{5.25}$$

Using Eq. (5.25), it can obtain that the self-extinguishing time of the secondary arc (with probability of 90%) with the amplitude of secondary arc current of 35 A (effective value) is 0.71 s. Therefore, for the line with high-voltage shunt reactor for compensation, when the reclosing time of about 1 s is used, the value of the

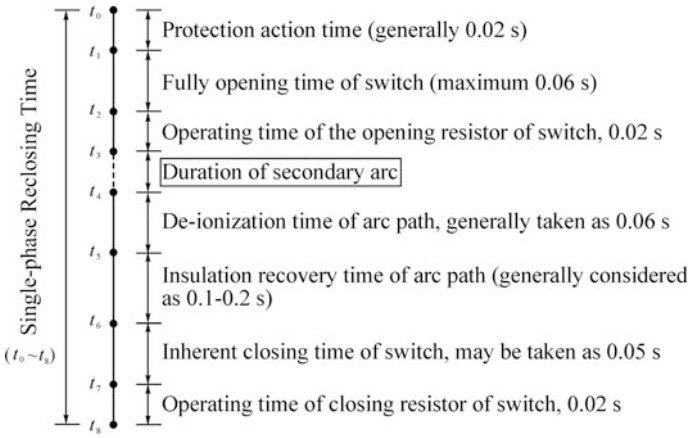

Fig. 5.16 Sketch for distribution process of the single-phase reclosing time of the line with high-voltage shunt reactor for compensation

Table 5.1 Recommended values for self-extinguishing time of secondary arc under normal compensation

Recovery voltage gradient (kV/m)	Secondary arc current (effective value A)	Self-extinguishing time (under probability of 90%) (s)
12	28	Self-extinction in 0.2 s
	35	Self-extinction in 0.2 s
	40	0.636–0.837
20	28	Around 0.2 s
	35	Around 0.2 s
	40	0.704–0.827

secondary arc current during the single-phase reclosing process shall be controlled within 35 A.

To satisfy the construction needs of the UHV project, China Electric Power Research Institute (CEPRI) has conducted further research on the self-extinguishing characteristics of the secondary arc in the normally compensated line. For the line with high-voltage shunt reactor for compensation, the recommended values for the self-extinguishing time limits of the secondary arc under various secondary arc currents when the recovery voltage gradient is 12 and 20 kV/m, respectively, in case the wind speed ranges from 1.5 to 2.0 m/s are shown in Table 5.1 [5].

Table 5.1 shows that, under normal compensation, when the recovery voltage gradient is 20 kV/m or below and the secondary arc current is 35 A or below, the secondary arc can rapidly self-extinguish in around 0.2 s and the self-extinguishing time of the secondary arc rises to around 0.7 s when the secondary arc current reaches 40 A. CEPRI reckons that a certain value exists between the secondary arc current of 35 and 40 A, at which the secondary arc and the self-extinguishing time are rapidly increased. In combination with the research results from the above two research institutes, it can be known that, for the line with small reactance installed at the neutral point of high-voltage shunt reactor, the valid value of the secondary arc current shall be limited to 35 A or below to meet the requirement that the reclosing time be 1 s.

5.2.2 Extinguish of the Secondary Arc by Adding HSGS

5.2.2.1 Principle of Restriction

The HSGS, as an effective method to extinguish the secondary arc (as shown in Fig. 5.17) [1], is applied in the UHV lines in Japan and the EHV lines in some countries.

The HSGS reduces the duration of the secondary arc by shunting the secondary arc current and inhibiting the recovery voltage at the fault points, and its operating sequence and principle are shown in Figs. 5.17 and 5.18, respectively. When the

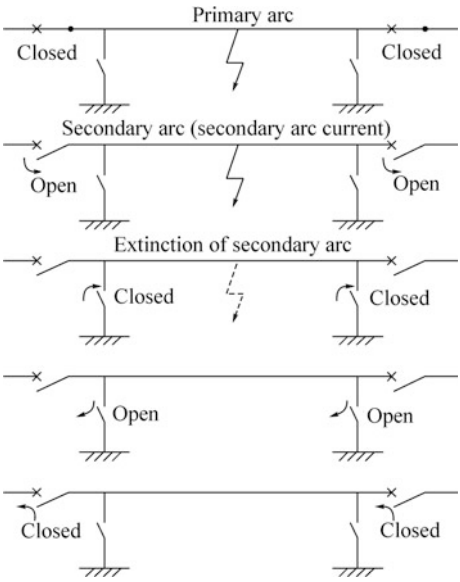

Fig. 5.17 Sketch for operation of HSGS

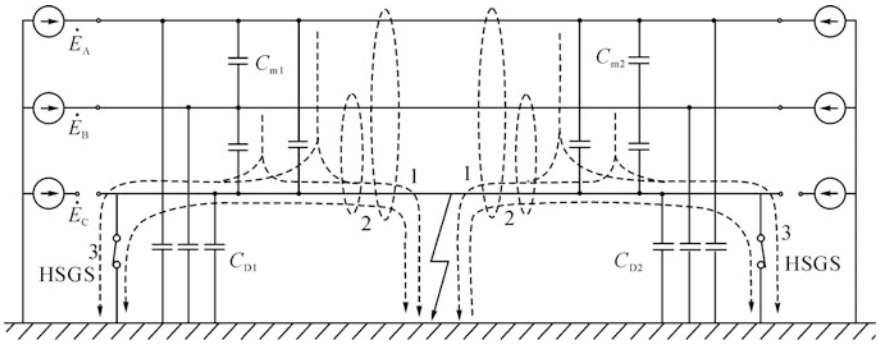

Fig. 5.18 Sketch for the line added with HSGS

single-phase ground fault occurs to the UHV line, after the short-circuit current flows through the fault point and the relay protection devices detect the fault, the circuit breakers on both sides of the fault phase rapidly trip to cutoff the short-circuit current and the sound phase supplies secondary arc current to the fault point through the phase-to-phase capacitance coupling and inductive coupling. Paths 1 and 2, as shown in Fig. 5.18, are the paths by which the capacitive component and inductive component of the secondary arc current are circulated. The HSGS is then immediately put into operation, and the generally low grounding resistance of HSGS enables a substantial part of the capacitive component of the secondary arc current to flow to the ground through HSGS which would have flowed through the fault point (as shown in path 3 in Fig. 5.18), thus reducing the capacitive

component of the secondary arc current flowing through the fault point to some extent. The HSGS which is directly grounded and has low resistance enables the amplitude of the recovery voltage at the fault point to be limited to a very low level, which is advantageous to the extinction of the secondary arc within a short time. After the extinction of the secondary arc, the arc in the HSGS switch is forcibly extinguished by the ability of the HSGS switch to extinguish arc, and then, the fault phase is reclosed by opening the HSGS.

Before the HSGS is put into operation, the inductive component of the secondary arc mainly flows through the circulation path of the capacitance to ground. Figure 5.18 shows that, for the lines with HSGS put into operation, as the grounding resistance of HSGS is very small compared to the capacitance to ground of fault phase, the inductive component of the secondary arc current primarily forms a circuit with the fault point through the HSGS, i.e., ground–grounding point–line–HSGS–ground. However, this also means that the impedance of the inductive component circuit is greatly reduced and the inductive component of the secondary arc current is likely to be greater than that without HSGS. But, in general, because the capacitive component accounts for a greater percentage in the secondary arc current, the HSGS still has restriction effect on the secondary arc current. Moreover, the closed HSGS which reduces the recovery voltage at the fault point to an extremely low level will make it easier to extinguish the secondary arc and the reignition is not prone to occur.

The grounding resistance of HSGS, fault grounding resistance, and the position of the fault point greatly affect the magnitude of the secondary arc current. First, the grounding resistance of HSGS and the fault grounding resistance will directly affect the shunting effect of the capacitive component of the secondary arc current. The greater the HSGS resistance, the lower the current flowing through the HSGS and the greater the current flowing through the fault point; the greater the fault grounding resistance, the greater the current shunted to HSGS and the lower the current flowing through the fault point. The capacitive component of the secondary arc current is substantially shunted to HSGS, which results in the rise of percentage of the inductive component of the secondary arc current flowing through the fault point. The grounding resistance of HSGS and the fault grounding resistance impose a certain impact upon the inductive component of the secondary arc current which directly flows through HSGS and the fault point. The fault point divides the circuit into two sections and the directions of potentials inducted by the sound phase on both sections of the fault phase are identical, while the currents formed by the two potentials flow the fault point in reverse directions, so the inductive component of the secondary arc current flowing through the fault point shall be the difference value between the two currents. When the fault points is at the middle of the line, the currents formed by the inductive potentials on both sections of the line are substantially equivalent, so the inductive component of secondary arc current at the fault point is very minor; however, when the fault point is at both ends of the line, the difference between the amplitudes of currents formed by the inductive potentials at both sections of the line is great, and the inductive component of the secondary arc current is relatively great.

5.2.2.2 Requirements of Restriction

For HSGS, to extinguish the arc rapidly and effectively, it is crucial to realize the close matching between HSGS and the closing and opening time of the circuit breakers. The time control of HSGS during its operating process is shown in Fig. 5.19 [1], where QF represents the circuit breakers on both sides of the line. From Fig. 5.19, it can be obtained that it takes about 0.5 s for HSGS to open from its closure, and considering that the recovery time of the medium in the arcing channel is more than 0.04 s after the secondary arc is extinguished, 0.1 s may be generally selected [1], so the secondary arc must be blown out within 0.4 s after the HSGS is put into operation. According to the experimental statistics of CEPRI, reference may be generally made to the following values, as shown in Table 5.2 [5], in terms of the self-extinguishing time of the uncompensated secondary arc (by the probability of 90%) when the wind speed ranges from 1.5 to 2.5 m/s. Therefore, it may be generally believed that for lines adopting HSGS, reclosure may be done in 1 s after fault occurs as long as the secondary arc is extinguished within 0.4 s.

Due to the fact that the EHV lines in China generally restrict the secondary arc current by connecting small reactance at the neutral point, the present research on HSGS is not mature and no systematic research has been conducted on the self-extinguishing characteristics of the secondary arc when HSGS is used in China. However, as CEPRI has ever conducted some research on the extinguishing characteristics of the secondary arc in the lines without compensation by high-voltage shunt reactor, this section will refer to the research results thereof to judge the extinction time of the secondary arc in the line added with HSGS. CEPRI gives the recommended values for the self-extinguishing time of the secondary arc current with various amplitudes when the wind speed is less than 2.0 m/s in case of no compensation by high-voltage shunt reactor, as shown in Table 5.2 [5].

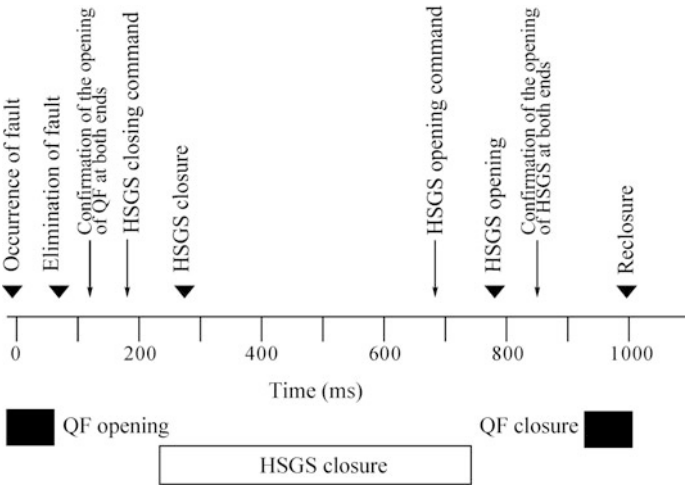

Fig. 5.19 Sketch for operating process of HSGS

Table 5.2 Recommended values for the self-extinguishing time of the secondary arc without high-voltage shunt reactor for compensation

Recovery voltage gradient (kV/m)	Effective values of the secondary arc current/A	Self-extinguishing time (with probability of 90%)/s
10	18.4	0.25–0.4
	21	0.31–0.49
	42	0.52–0.65
20	18.4	0.6–0.8
	21	0.8111–0.955
	42	1.172–1.417
30	18.4	1.27–1.48
	21	1.391–1.536
	42	Not extinguished within 2 s

From Table 5.2, it can be seen that, under most circumstances, for a specific value of the secondary arc current, the extinction time of the arc rises or falls at linear speeds (or even faster) with the rise or fall in the recovery voltage gradients. For example, for a secondary arc current of 42 A, when the recovery voltage gradient is 10 kV/m, the self-extinguishing time of the arc ranges from 0.52 to 0.65 s; when the recovery voltage gradient is 20 kV/m, the self-extinguishing time of the arc is 1.17–1.42 s. Then, it can be deduced that for a secondary arc current of 42 A, when the recovery voltage gradient is equal to or less than 5 kV/m, the self-extinguishing time of the arc is less than 0.4 s.

Under normal circumstances, the UHV line which uses HSGS to restrict the secondary arc current is short and its recovery voltage is generally low. For example, for a typical short UHV line with length of 200 km, after it is equipped with HSGS, its recovery voltage is only around 3 kV and its secondary arc current is approximately 41.2 A. Assuming that the insulator string of the 1000 kV UHVAC line is approximately 8 m in length, then the recovery voltage gradient shall be far less than 5 kV/m, and if the secondary arc current is approximately 41.2 A, the self-extinguishing time of the arc shall certainly be less than 0.4 s.

5.2.3 Comparison and Discussion on the Two Methods to Restrict the Secondary Arc Current

By comparing the two methods to restrict the secondary arc current, it can be seen that the major differences exist between them, which are described in details as follows:

(1) The use of the method to connect small reactance at the neutral point of high-voltage shunt reactor cannot only restrict the capacitive component of the secondary arc current, but also inhibits its inductive component; while HSGS

can only restrict its capacitive component but fails to restrict its inductive component.

(2) The method to connect small reactance at the neutral point of high-voltage shunt reactor may generally reduce the recovery voltage of the line significantly, while the effect of HSGS on the restriction of recovery voltage is distinctly superior to that in the mode of small reactance connected at the neutral point of high-voltage shunt reactors. As the grounding resistance of HSGS is usually very small (below 1 Ω), once grounded the recovery voltage of the fault phase may be reduced to a very low level (several kV), thus compelling the recovery voltage gradient to fall to very low values, which is very advantageous to the extinguish of the secondary arc.

(3) Applicable occasions of the two restriction methods.

As for the method to restrict the secondary arc current by connecting small reactance at the neutral point of high-voltage shunt reactor, its aim is to restrict the secondary arc current effectively by realizing the complete compensation between the phase-to-phase reactance and the phase-to-phase capacitance through the reasonable distribution of the capacity of high-voltage shunt reactor to the phase-to-phase reactance and reactance to ground by the effect of small reactance. As the phase-to-phase reactance is three-phase symmetry, if the phase-to-phase capacitance itself is not three-phase symmetry, the full compensation between the phase-to-phase reactance and the phase-to-phase capacitance cannot be realized, nor can the secondary arc current be well restricted. Therefore, if the secondary arc current is to be restricted by connecting a small reactance at the neutral point of high-voltage shunt reactor, the UHV line must be subject to good transposition and the capacitances among the lines of the three phases must be symmetrical; otherwise, the secondary arc current of the lines cannot be well restricted. In consideration that a line has good transposition, the restriction of secondary arc current by connecting small reactance at the neutral point of high-voltage shunt reactors is generally applicable to the UHV power transmission line with long length and good transposition.

As for the restriction of the secondary arc current by means of HSGS, the very low grounding resistance of HSGS provides a circulation circuit for the inductive component of the secondary arc current, and thus, one flaw that exists of HSGS is that the inductive component of the secondary arc current cannot be well controlled. In fact, the inductive component of the secondary arc current is directly related to the position of the fault point along the line, the length of the line, and the load of the line. Under the circumstances where the fault points of the line are located at the ends of the line and the line is under heavy load, the inductive component of the secondary arc current will also be great, and if the whole line is also very long, the inductive component of the secondary arc current along the line is likely to reach a very high value, thus difficult to extinguish the secondary arc. Therefore, the HSGS mode is generally applicable only to short UHV power transmission lines.

Furthermore, the lines using HSGS will not use transposition mode generally, as shown in Fig. 5.20. For the lines with transposition, after the both ends of the fault

phase are opened upon the occurrence of the single-phase ground fault in the middle of the line, the mutual inductance of each sound phase at various positions to the fault phase varies, as shown in Fig. 5.20a. By reference to the analytical method in the previous section, it may follow that the inductive components in the circuits on both sides of the fault point are not equal and will give rise to a great inductive component of the secondary arc current at the fault point. Under the circumstances where the line is not transposed, if a single-phase ground fault occurs in the middle of the line, the mutual inductance at both sides of the fault point is substantially symmetrical and the inductive component of the secondary arc current at the fault point approximates zero. Therefore, if HSGS is used, the line will not use the transposition mode generally, and then, the secondary arc current will be even smaller.

In summary of the above analysis, the mode of connecting small reactances at the neutral point of shunt reactors is appropriate for lines with long length, requiring compensation of the high-voltage shunt reactors and with good transposition. While HSGS is appropriate for short lines which require no compensation of high-voltage shunt reactors and transposition; it is recommended to consider restricting the secondary arc by adding HSGS in lines with length ranging from 100 to 200 km. In fact, for UHV lines with long length which have not been transposed and have multiple drop points and whose single sections are short (their total length is long, but each section is short and a switching station is added in the middle of the line), if the secondary arc is restricted by means of HSGS, the restricting effect is identical to that for HSGS in UHV short lines.

Given the fact that China is very experienced in the use of the small reactance connected at the neutral point of shunt reactors along the 500 kV lines and that the current UHV lines in China are all transposed, and having long distance and equipped with shunt reactors; therefore, the current UHV power transmission lines

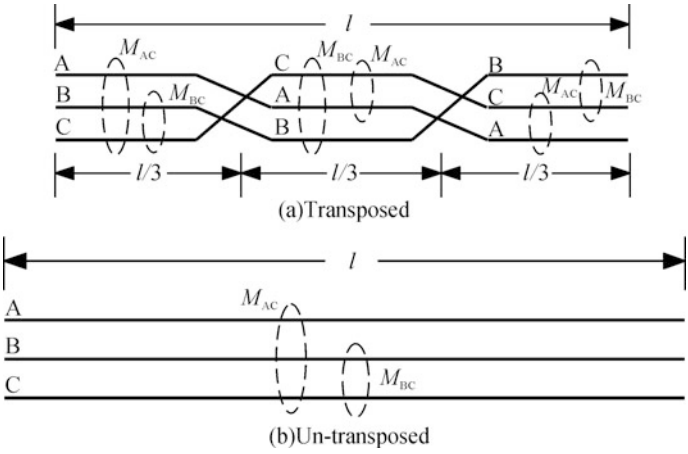

Fig. 5.20 Sketch of single-circuit line transposed and un-transposed

in China mainly adopt the method to parallel the high-voltage shunt reactors and add small reactances at the neutral point of high-voltage shunt reactors to restrict the secondary arc current and the recovery voltage.

5.3 Simulation of the Secondary Arc Current and the Recovery Voltage

5.3.1 Modeling

Establish a model of power transmission lines with power supplies at both ends, as shown in Fig. 5.21, and the power flow flows from M to N. The tower shape is the M-shape cathead-type tower with triangular arrangement, as shown in Fig. 5.22, the selected conductors are aluminum conductors steel reinforced 8 × LGJ-500, and the bundled conductor spacing is 400 mm.

5.3.2 Analysis of Effect on Inhibiting the Secondary Arc by Connecting Small Reactance at the Neutral Point of Shunt Reactors

The model shown in Fig. 5.21 is used and the line is 350 km long. Shunt reactors are added to the power supplies at both ends of the line, the capacity of the HV reactors at the sending end is 960 and is 720 Mvar at the receiving end with a compensation degree of 88%, and the neutral point is grounded through the small reactance, whose value is 150 Ω. The values of the small reactances at the neutral point depend upon the parameters and compensation degrees, and can be obtained by the following equation:

$$X_{\mathrm{LN}} = \frac{1}{\omega C_1 k(kC_1/C_{\mathrm{M}} - 3)}. \tag{5.26}$$

where

K the compensation degree of the high-voltage shunt reactor;
C_1 the line's positive sequence capacitance; and
C_{M} the line's phase-to-phase capacitance.

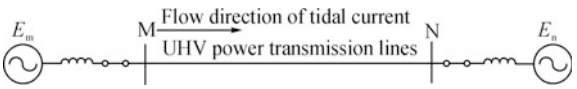

Fig. 5.21 Simulation model of 1000 kV power transmission line

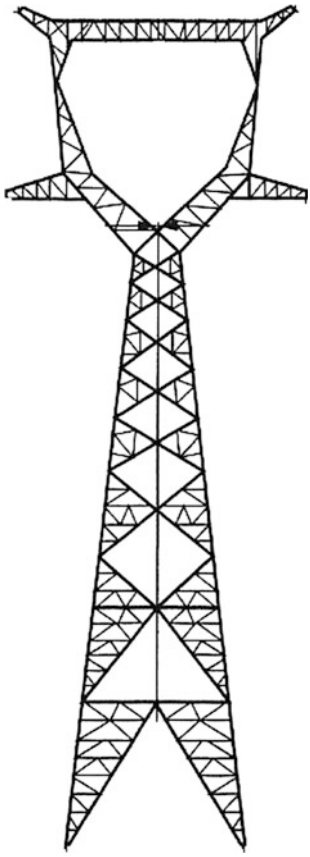

Fig. 5.22 M-shape cathead-type tower with triangular arrangement

After the shunt reactors with small reactance are connected to the neutral point, the secondary arc current and the recovery voltage are simulated by EMTP. Assuming that the ground fault occurs at the second *t*, the circuit breakers on both sides are opened after 0.08 s.

Under the two circumstances that before and after the shunt reactors with small reactance are connected to the neutral point, simulated calculations of different fault points are conducted and the results from the simulated calculations of the corresponding secondary arc currents and recovery voltages are shown in Table 5.3.

From Table 5.3, it can be seen that the secondary arc current and recovery voltage obviously drop after the shunt reactors with small reactance are installed at the neutral points, particularly for the secondary arc current which falls to be within 10 A, while, at this time, the recovery voltage gradient falls to about 10 kV/m and below (assuming the insulator string of the UHV line is 8 m in length). Combined with the results from Table 5.1, it can be concluded that the rapid arc extinction can be realized under this circumstance.

Table 5.3 Secondary arc current and recovery voltage under two different circumstances

Position of fault point/km		30	75	175	275	320
Secondary arc current/A	Before shunt reactors with small reactance are installed	121.4	117.2	107.9	102.8	99.9
	After shunt reactors with small reactance are installed	5.9	3.3	5.2	6.2	5.9
Recovery voltage/kV	Before shunt reactors with small reactance are installed	239.1	232.5	218.1	205.2	198.2
	After shunt reactors with small reactance are installed	42.4	32.3	83.4	84.4	42.4

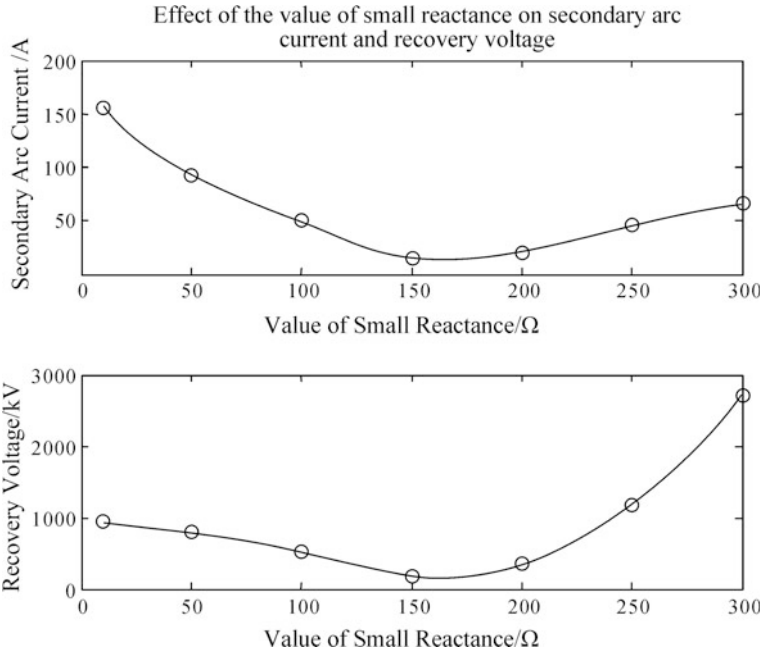

Fig. 5.23 Effect of the value of small reactance on the secondary arc current and recovery voltage

Moreover, for the purpose of studying the effect of the values of small reactance on the secondary arc current and the recovery voltage, the shunt reactors are added at the both ends of the line with the compensation degree of 88%, the value of the small reactance at the neutral point is changed, and the simulated calculation of the circumstance where the fault point is located at the position of 175 km is carried out. The results from the analysis are shown in Fig. 5.23.

It can be found out from Fig. 5.23 that the value of small reactance affects the secondary arc current and recovery voltage significantly and the selection of a proper value will result in the minimum value of the secondary arc current and

recovery voltage, which appears when the value of small reactance is around 150 Ω as shown in the figure, consistent with the calculation results from Eq. (5.26).

The above simulated calculations are based on a 350 km-long 1000 kV UHV power transmission line model. To study the secondary arc current in the 1000 kV short line (150 km) and long line (1000 km) models, the model, as shown in Fig. 5.21, is still adopted. Based on the condition that the compensation degree of the shunt reactor is 88%, the small reactance connected at the neutral point is obtained by Eq. (5.26), and other conditions keep unchanged, the simulated calculations for the two circumstances which before and after the installation of shunt reactors with small reactance connected at the neutral point are carried out. The obtained values of the secondary arc current are shown in Fig. 5.4.

From Table 5.4, it can be seen that before the shunt reactors are installed, the amplitude of the secondary arc current on the 1000 km-long line is generally far greater than that on the 150 km-long line, because the phase-to-phase capacitance and mutual inductance on the longer line are much greater than those on the shorter line and the current supplied by the sound phase through electrostatic coupling and electromagnetic coupling to the fault point is also much greater. However, after the shunt reactors with small reactance are installed at the neutral point, the secondary arc current on the longer or shorter line is obviously inhibited, thus making it smooth to blow out the secondary arc.

Table 5.4 Simulated calculations of the secondary arc current in short and long lines

Secondary arc current/A	150 km-long line	Position of fault point/km	20	40	75	110	130
		Before shunt reactors with small reactance are installed	67.5	66.4	63.7	60.1	57.6
		After shunt reactors with small reactance are installed	3.8	2.9	2.0	3.2	3.8
	1000 km-long line	Position of fault point/km	100	400	500	600	900
		Before shunt reactors with small reactance are installed	800.2	670.2	652.3	641.1	645.1
		After shunt reactors with small reactance are installed	38.6	30.4	30.1	30.8	37.6

5.3.3 *Analysis of the Effect of HSGS on the Inhibition of Secondary Arc*

Using the model, as shown in Fig. 5.21, assuming that the transposition mode of the line is ideal, HSGS are installed at the power supplies at both sides of the power transmission line and the grounding resistance of HSGS is taken as 1.65 Ω. The secondary arc current and recovery voltage are simulated using EMTP simulation software, and the single-phase reclosure operating process is shown in Fig. 5.19; assuming that an ground fault occurs at the second *t*, the circuit breakers on both sides are opened after 0.08 s, and then, HSGS are put into after another 0.2 s.

5.3.3.1 Impact of the Towers' Transposition Modes on the Restriction Effect of HSGS

To study the impact of the towers' transposition modes on the restriction effect of HSGS on the secondary arc, the model, as shown in Fig. 5.21, is adopted, and the length of line is taken as 150 km. The simulated calculation for the power transmission lines before and after the transposition is carried out based on the transposition modes, as shown in Fig. 5.24. The obtained values of the secondary arc current *I* and the recovery voltage *U* are shown in Table 5.5.

From Table 5.5, it can be seen that the restriction effect of HSGS in the lines not transposed is much better. Because under the circumstance in which HSGS is used, for the lines not transposed and those transposed are compared, the maximum value

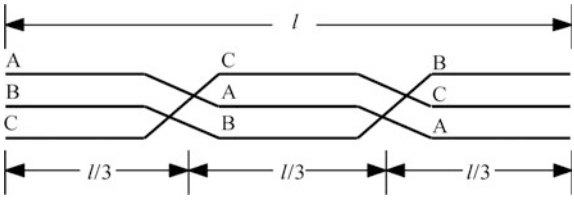

Fig. 5.24 Transposition modes of towers

Table 5.5 Impact of the transposition modes on the restriction effect of HSGS

Fault phase	Transposition mode	*d* = 10		*d* = 30		*d* = 75		*d* = 120		*d* = 140	
		I/A	*U*/kV	*I*/A	*U*/kV	*I*/A	*U*/kV	*I*/A	*U*/kV	*I*/A	*U*/kV
Phase A	Un-transposed	21.1	1.6	24.2	1.6	29.1	2.1	24.2	1.6	5.3	1.2
	Transposed	16.9	1.6	16.4	1.6	63.4	3.2	49.3	1.7	22.7	1.5
Phase B	Un-transposed	15.8	1.6	25.6	1.5	29.5	2.1	20.4	1.6	6.1	1.2
	Transposed	14.5	1.6	15.3	1.6	50.0	2.7	64.1	2.0	23.1	1.6
Phase C	Un-transposed	20.1	1.6	25.9	1.5	30.2	1.7	22.0	1.6	7.3	1.6
	Transposed	36.2	1.5	64.8	2.0	56.6	3.0	36.7	1.5	13.4	1.6

of the secondary arc current rises from 30.2 to 64.8 A, and the value of the recovery voltage also climbs from 2.1 to 3.2 kV. Therefore, the HSGS is appropriate for the lines which require no transposition.

For the simulated calculations hereinafter contained in this chapter, the transposition mode of towers is selected as un-transposed mode.

5.3.3.2 Impact of the Grounding Resistance of HSGS on the Restriction Effect of HSGS

The value of the grounding resistance of HSGS directly affects the shunting effect of HSGS. To study the impact of the grounding resistance on the restriction effect of HSGS, the length of line is taken as 150 km, various values are taken for the grounding resistance of HSGS, and the simulated calculations for various fault point positions are carried out. The obtained values of the secondary arc currents are shown in Fig. 5.25.

Figure 5.25 shows that the grounding resistance greatly affects the restriction effect of HSGS. In a line installed with HSGS, when the grounding resistance is less than 0.5 Ω, the values of the secondary arc current are greatly reduced, and when the grounding resistance is further reduced, the secondary arc current only drops by a small margin; however, when the grounding resistance is greater than 1.5 Ω, the secondary arc current at some fault points of the line is still great, indicating that the restriction effect of HSGS is not good. Hence, the grounding resistance of HSGS is recommended to be less than 0.5 Ω and its maximum value shall not exceed 1.5 Ω.

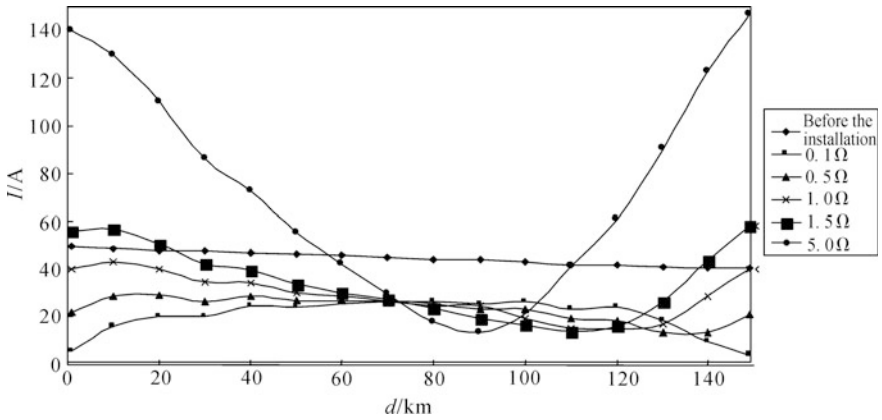

Fig. 5.25 Impact of HSGS's grounding resistance on HSGS's restriction effect on secondary arc current

5.3.3.3 Effect of HSGS on the Inhibition of Secondary Arc

The model, as shown in Fig. 5.21, is adopted and the length of line is taken as 350 km. The simulated calculations for various fault point positions are carried out under the two circumstances that before and after HSGS is installed. The obtained secondary arc current and recovery voltage are shown in Table 5.6, in which the resistance value of HSGS is taken as 0.1 Ω.

Table 5.6 shows that for this line, the installation of HSGS obviously inhibits the recovery voltage, and while there is a significant drop in the amplitude of the secondary arc current, however, its value is still so great that the rapid blow-out of arc within 0.4 s may not be fulfilled; thus, the reclosure of the circuit breakers within 1 s cannot be guaranteed.

In addition, the effect of HSGS on the inhabitation of the secondary arc current in the 1000 kV UHV short line (taken as 150 km) and long line (taken as 1000 km) models is studied hereinafter. Based on the condition that the model, as shown in Fig. 5.21, is still adopted, the length of line is, respectively, taken as 150 and 1000 km, and changing the resistance value of HSGS, the simulated calculations for various fault point positions are carried out. The obtained values of the secondary arc current are shown in Figs. 5.26 and 5.27.

Figures 5.26 and 5.27 show that after HSGS is installed, the secondary arc currents in the two power transmission lines drop significantly. However, for the 1000 km-long line, even after HSGS is installed, the amplitude of the secondary arc current is still large (>250 A) and the secondary arc cannot successfully self-extinguish at all. However, for the 150 km-long line, the installation of HSGS is quite effective. In particular, when the grounding resistance value is less than 0.5 Ω, HSGS can effectively restrict the secondary arc current (≤ 30 A) to enable the secondary arc to self-extinguish successfully.

To further study the effect of HSGS on the extinction of the secondary arc, the model, as shown in Fig. 5.21, is adopted and the simulated calculations of the changes in the maximum values of the secondary arc current I and recovery voltage U along the power transmission lines of various lengths before and after HSGS is installed are carried out. In the calculation, the grounding resistance of HSGS is taken as 0.1 Ω and the grounded transition resistance is taken as 10 Ω. The calculation results are shown in Fig. 5.28.

Table 5.6 Secondary arc current and recovery voltage under two different circumstances

Position of fault point/km		30	75	175	275	320
Secondary arc current/A	Before HSGS is installed	121.4	117.2	107.9	102.8	99.9
	After HSGS is installed	82.6	80.2	71.1	52.5	21.1
Recovery voltage/kV	Before HSGS is installed	239.1	232.5	218.1	205.2	198.2
	After HSGS is installed	2.6	4.2	6.7	3.0	1.6

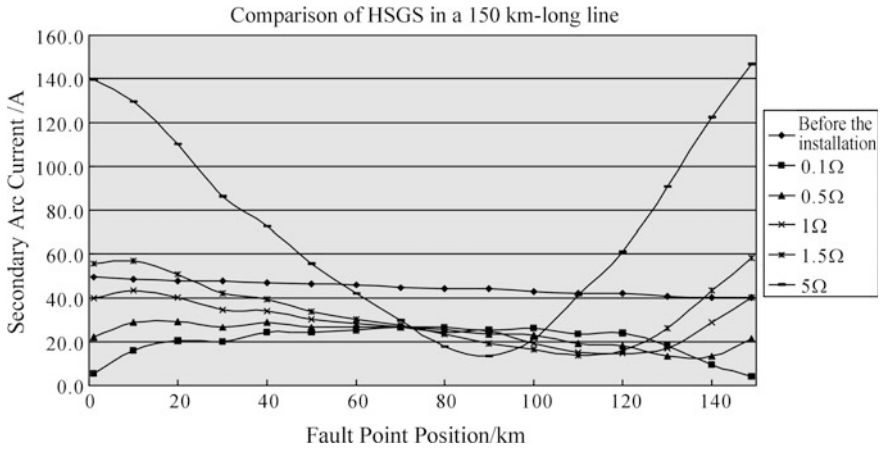

Fig. 5.26 Effect of HSGS on inhibition of the secondary arc current in a 150 km-long line

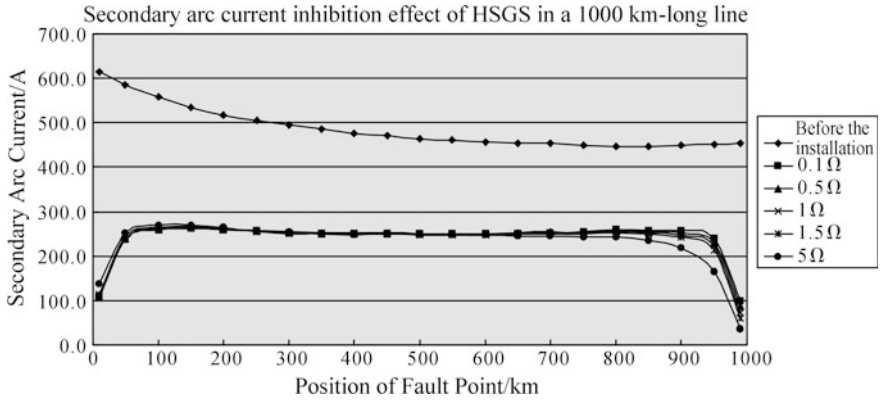

Fig. 5.27 Effect of HSGS on inhibition of the secondary arc current in a 1000 km-long line

Figure 5.28 shows that, before HSGS is installed, the longer the line is, the greater the secondary arc current and the recovery voltage are. After HSGS is installed, they are reduced significantly, but for longer lines, the secondary arc current is still great.

Figure 5.28 also shows that, after HSGS is installed, the recovery voltage for the 200 km-long line is 3 kV and the secondary arc current is 41.2 A when its recovery voltage gradient is far less than 5 kV/m. By consult with the relevant data in Table 5.2, it can be found that the secondary arc can be extinguished within 0.4 s under this circumstance. Hence, the extinction time of the secondary arc current in lines whose length is not greater than 200 km may be shortened by installing HSGS to meet the requirement that the reclosing time be 1 s; however, for longer lines, the

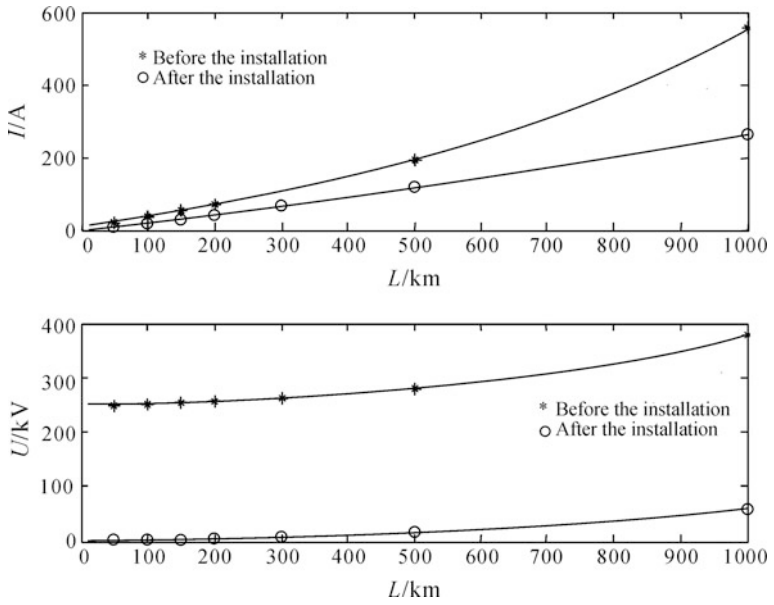

Fig. 5.28 Restriction effect of HSGS in lines with various lengths

greater values of the secondary arc currents and recovery voltages are likely to result in the circumstances, where the arc cannot be extinguished smoothly.

In summary, the conclusions on the method to restrict the secondary arc current by HSGS are mainly as follows:

(1) In the UHV lines, the method to restrict the secondary arc current by HSGS is applicable to the lines without transposition.
(2) The grounding resistance of HSGS affects the secondary arc current restriction effect of HSGS greatly and is generally required to be less than or equal to 0.5 Ω, with the maximum value not exceeding 1.5 Ω;
(3) HSGS is generally applicable to the short lines with length generally less than 200 km.

References

1. Liu Z. UHV power grid. Beijing: China Economic Press; 2005.
2. Yi Q, Zhou H, Ji R, Su F, Sun K, Chen J. Restriction on secondary arc current on ultra-high voltage ac double circuit transmission lines on the same tower. Autom Electr Power Syst. 2011;35(10):83–8.
3. Sun P. The design of measure system for power frequency parameters of power transmission line. Baoding: Hebei University; 2006.

4. Sun Q. Research on dynamic physical characteristics and suppressing technology of secondary arcs of uhv transmission lines. Jinan: Shandong University; 2012.
5. Research Report on Key Technologies in the 1000 kV-level AC UHV power transmission and transformation project. Beijing: Electric Power Research Institute; 2008.

Chapter 6
Switching Overvoltage of UHVAC Systems

Rongrong Ji, Hao Zhou and Xiujuan Chen

The UHV system is featured by high-voltage level and large switching overvoltage amplitude. The allowable switching overvoltage is relevant to the rated voltage of the system. For example, it is required that the switching overvoltage multiple of the 330 kV system shall not exceed 2.2 p.u., and that of the 500 kV system shall not exceed 2.0 p.u., that is, the higher the rated voltage of the grid is, the stricter the limitation requirement for the switching overvoltage is. According to the research data from the former Soviet Union, Japan, and Italy, etc., the allowable overvoltage multiple of the 1000 kV transmission line is 1.6–1.8, obviously lower than that of the 500 kV system [1]. The increase of the rated voltage and the decrease of the limit standard put forward more rigorous requirements for the limitation measures for the switching overvoltage of the UHV system, and the preventive measures for the EHV system are no longer completely applicable. Besides, the overvoltage which does not jeopardize the system in other voltage levels may also become prominent in the UHV system. The UHV system does not only require to specifically limit the closing overvoltage (the overvoltage to be specifically limited in the HV and EHV systems), but also to attach importance to the ground fault overvoltage and opening overvoltage, etc. (due to such characteristics as high source

R. Ji (✉)
State Grid Zhejiang Maintenance Branch Company,
Hangzhou, Zhejiang, People's Republic of China
e-mail: 397563569@qq.com

H. Zhou
College of Electrical Engineering, Zhejiang University,
Xihu District, Hangzhou, Zhejiang, People's Republic of China
e-mail: zhouhao_ee@zju.edu.cn

X. Chen
China Electric Power Research Institute, Haidian District,
Beijing, People's Republic of China
e-mail: xjchen@epri.sgcc.com.cn

© Zhejiang University Press, Hangzhou and Springer-Verlag GmbH Germany 2018

H. Zhou et al. (eds.), *Ultra-high Voltage AC/DC Power Transmission*,
Advanced Topics in Science and Technology in China,
https://doi.org/10.1007/978-3-662-54575-1_6

impedance, long line distance, and large transmission power of the UHV system, the switching overvoltage thereof also shows some characteristics different from the overvoltage of the EHV system) [1–4]. Therefore, the problem of the switching overvoltage of the UHVAC systems is one of the important research tasks in the construction and development of UHV lines.

This chapter first discusses the main types of switching overvoltage of the UHVAC system and their limitation methods, and then details the mechanisms, simulation and influencing factors, and the limitation measures for such main switching overvoltage as single-phase grounding overvoltage, closing overvoltage, and opening overvoltage, and gives a study on the influence of the series compensation device on the electromagnetic transient characteristic of the UHV line in final.

6.1 Switching Overvoltage Classification and Limiting Methods of UHVAC Systems

6.1.1 Switching Overvoltage Classification of UHVAC Systems

The research on the switching overvoltage is closely linked with the development of the electric power system. In the early period of the electric system development, as the neutral point of the grid was not directly grounded, the overvoltage caused by single-phase intermittent arc grounding seriously jeopardized the electric system. Because of this, the research on it became the focus. From then on, as the power grid's rated voltage, line length and transmission capacity increased and the neutral point of the system was grounded directly, the overvoltage resulting from switch-off of the no-load transformer and the no-load line had become prominent, among which, for the reason that the overvoltage energy resulting from switch-off of the no-load transformer is lower and can be prevented by use of arresters, the overvoltage resulting from switch-off of the no-load line had become the research focus for the switching overvoltage in the high-voltage power grid. In recent years, with the building and development of the EHV and long-distance transmission lines, the switching overvoltage has shown new conditions. For example, the capacitance effect of the no-load long transmission line causes a significant increase in the power frequency overvoltage, based on which a very high no-load line closing (including reclosing) overvoltage is probable to occur. As the performance of the circuit breakers is improved and the shunt reactors are used, both the amplitude of the overvoltage resulting from switch-off of the no-load line and the probability of its occurrence are decreased significantly. Therefore, the no-load line closing (including reclosing) overvoltage in the EHV power grid and UHV power grid, as one of the most typical and serious switching overvoltages, has become the research object which needs to be emphasized and concerned most. In addition, the less

prominent overvoltage such as ground fault overvoltage and opening overvoltage, etc. in the EHV power grid have become more serious in the UHV power grid, which also have become the research objects required to attach importance to.

The research suggests that the following types of switching overvoltage mainly need to be considered in the UHV system [1, 3]: ① ground fault overvoltage, mainly the single-phase grounding overvoltage; ② closing overvoltage, including no-load line closing overvoltage and single-phase reclosing overvoltage; ③ opening overvoltage, including load shedding overvoltage and fault clearing overvoltage.

6.1.1.1 Ground Fault Overvoltage

For the ground fault overvoltage, the practical operation experience of EHV and UHV systems around the world shows that the single-phase ground fault accounts for most of the proportion, and that the probability of two-phase and three-phase ground faults is thin, so it is required to pay great attention to the single-phase ground fault overvoltage in the study on the overvoltage.

As the single-phase ground fault overvoltage occurs at random and it is often difficult to predict the occurrence time and grounding position, etc., it is difficult to take preventive measures, and the circuit breaker fails to activate in time in the continuous process, so that the opening and closing resistor does not have restriction effect. Therefore, no better limitation measures are available, except that MOA and high-voltage shunt reactor compensation have a certain limitation effect.

Now, the limitation measures for the single-phase ground fault overvoltage taken in China are compared with that in other countries.

The UHV transmission line is short in Japan, with single section not more than 200 km, so it is often understood that the single-phase grounding overvoltage phenomenon is not severe. However, no high-voltage shunt reactor compensation device is used in the whole transmission line in Japan, only a bank of MOA is used for power protection at each end of the transmission line, so that the overvoltage can reach 1.6 p.u. in this case. In addition, a closing/opening resistor is used in the circuit breaker in Japan to limit the opening overvoltage and closing overvoltage to a lower level when the resistor is activated, so that the single-phase ground fault overvoltage becomes prominent among all of the overvoltage. Hence, the single-phase ground fault overvoltage of the UHV system in Japan plays a decisive role in the insulation coordination of the system.

The former Soviet Union's UHV transmission lines cross the Eurasia continent for thousands of miles, with long single section line. For the purpose of limiting the switching overvoltage, the measures adding MOAs and high-voltage shunt reactors with high compensation degree are adopted, and the compensation is made section by section at an interval of 150 km. In this case, the single-phase grounding overvoltage can be effectively limited to the allowable range.

China is a country with a vast territory. The UHV transmission line often bears a long distance and large capacity transmission task. The lines are usually long,

of which the Southeast Shanxi–Nanyang–Jingmen UHV transmission line established is 636 km long in total. In this case, MOAs and high-voltage shunt reactors with high compensation degree are used at both ends of the transmission line in China, and switch stations are built in the middle segment of the transmission line of which MOAs and sectional compensation are set up, enabling the single-phase grounding overvoltage to be limited effectively and be less than other overvoltage, and not to control the insulation coordination of the transmission line.

In a word, the use of MOA and rational high-voltage shunt reactor compensation is the main measure to limit the single-phase ground fault overvoltage in the UHV system. To limit the single-phase ground fault overvoltage of a long transmission line, the use of high-voltage shunt reactor compensation and installation of MOA by means of dividing the line appropriately and setting up switch stations in the middle of transmission line is the most efficient way.

6.1.1.2 Closing Overvoltage

The closing overvoltage is the overvoltage produced at the time of closing operation in the electric system, and can be fallen into no-load line closing overvoltage and reclosing overvoltage in terms of the operations that producing overvoltage. Among them, the no-load line closing overvoltage means the overvoltage produced when carrying out the scheduled closing operation in the no-load transmission line, and the reclosing overvoltage means the overvoltage produced during reclosure after a transient arc extinguishing time in case of fault trip of the operation transmission line.

As described above, it is desirable to carry out single-phase reclosure operation due to high probability of occurrence of single-phase ground fault of the UHV system. No residual electric charge exists in the faulted phase line in this case and the damping action of the zero-sequence circuit of the system is larger than that of the positive sequence circuit, enabling the single-phase reclosing overvoltage to be much lower than the three-phase reclosing overvoltage and can be controlled easily. From the perspective of controlling the overvoltage, single-phase reclosure is often used in the UHV system. Therefore, it is required to limit the overvoltage primarily produced by no-load line closing and single-phase reclosure in the UHV system.

6.1.1.3 Opening Overvoltage

The opening overvoltage is the overvoltage produced during opening operation of the electric power system. The common overvoltage in the electric system includes overvoltage resulting from switching-off of the no-load line and transformer, which are classified into the opening overvoltage needing to be mainly prevented. Unlike the high-voltage system, the overvoltage resulting from switching-off of the no-load line is not high, because the circuit breaker uses SF_6 as the insulation medium in the EHV and UHV systems to obtain excellent arc extinguishing performance and low

reignition probability at the break-point, as well as the high-voltage shunt reactors on the line can limit the break-point voltage of the circuit breaker. Moreover, with the improvement of the EHV and UHV transformers and under restriction of the arrester at the inlet of the transformer, the overvoltage resulting from switching-off of the no-load transformer becomes very small. Hence, the overvoltage resulting from switching-off of the no-load line and transformer in the UHV system is not serious. However, the limit standards are reduced in the UHV system, and some opening overvoltage that does not severely impair the HV and EHV systems can jeopardize the insulation equipment in the UHV system, such as load shedding and fault clearing overvoltage, etc.

It is required to attach importance to consider the fault clearing overvoltage and load shedding overvoltage in the UHVAC system. The load shedding overvoltage can be divided into fault-free load shedding overvoltage and load shedding overvoltage under single-phase ground fault, which are caused in the system by sudden tripping and load shedding of three phases of the circuit breaker due to a fault or other reasons during operation of the UHV line. The fault clearing overvoltage means, after a fault occurs in a line, the transfer overvoltage produced at the sound phase and its neighboring sound lines when the circuit breaker of the fault line cuts off the fault line. The overvoltage can be divided into single-phase ground fault clearing overvoltage, two-phase ground fault clearing overvoltage, three-phase ground fault clearing overvoltage, and phase-to-phase short-circuit fault clearing overvoltage in terms of type of faults, of which the single-phase ground fault clearing overvoltage is the most common one, while the probability of the later three ones is extremely thin; therefore, it is usually required to attach importance to analyze the single-phase ground fault clearing overvoltage during overvoltage analysis.

6.1.2 Common Methods for Limiting Switching Overvoltage in the UHVAC System

At present, several countries in the world have carried out research on the overvoltage control of the UHV system and promoted practical application of their respective research results. Some common limitation measures adopted by individual countries are as shown in Table 6.1.

It can been seen from Table 6.2 that MOA, high-voltage shunt reactor compensation, and closing resistor are the main limitation measures for the switching overvoltage of the UHV system, and the use of the opening resistor depends on specific condition.

The following introduces the main limitation measures for the switching overvoltage.

Table 6.1 Common measures for limiting switching overvoltage in UHV systems around the world

Limitation measures	Japan	Italy	Former Soviet Union	America BPA	China
High-voltage shunt reactor	Not used	Not used	Used	Used	Used
MOA	Used	Used	Used	Used	Used
Closing resistor	700 Ω	500 Ω	378 Ω	300 Ω	400–600 Ω
Opening resistor	700 Ω	500 Ω	Not used	Not used	Not used

Table 6.2 Parameters of UHV MOA used in China

Rated voltage (kV)	Continuous operating voltage (kV)	Allowable energy absorption value (MJ)	Switching impulse residual voltage (kV, peak value)		Lightning impulse residual voltage (kV, peak value)	
828	636	40	1 kA	2 kA	10 kA	20 kA
			1430	1460	1553	1620

6.1.2.1 High-Voltage Shunt Reactor Compensation

The power frequency overvoltage is the base for the generation of the switching overvoltage, so the switching overvoltage can be effectively suppressed by reducing the power frequency overvoltage.

Due to the long-distance transmission line, the charging power for the EHV and UHV transmission lines is very huge. For example, the reactive power consumption of the 500 kV transmission line exceeds 100 Mvar/100 km, the reactive power consumption of the 1000 kV UHV transmission line can exceed 500 Mvar/100 km, and the capacitive effect of the transmission line is also very remarkable, which is able to cause switching overvoltage with a high amplitude. Therefore, in case of impossibility to efficiently solve the reactive power problem of the line, it will result in significant increase in power frequency and switching overvoltage along the line, which is very adverse to the safety and stability of the power grid. For the purpose of solving this problem, it is required to install shunt reactors in the transmission line to compensate the reactive power consumption, so as to stabilize the line voltage. First, the compensation degree is usually between 60 and 90% by use of the fixed high-voltage reactor (the high-voltage shunt reactor) to compensation most reactive power of the line, and the high-voltage shunt reactor is installed at each side of the line; second, the reactive compensation can be adjusted in a real-time manner through the reactor (low impedance) or capacitor (low capacitance) at the LV side of the transformer, so as to meet the line's reactive power requirement to achieve the aim of stabilizing the voltage.

Due to the existence of the high-voltage shunt reactor of the UHV line, the problem of the switching overvoltage differs from that of the low-voltage grid. For the single-phase reclosure, the use of the high-voltage shunt reactor reduces the induced voltage of the non-fault phases in the fault line, and the overvoltage can be efficiently suppressed just by proper coordination between the high-voltage shunt reactor and the small reactor connected to its neutral point; for the no-load line closing overvoltage and load shedding overvoltage, the high-voltage shunt reactor at the end of the line, to some extent, suppresses the terminal voltage increase after the operation, improving the overvoltage distribution along the line and reducing the overvoltage amplitude.

In addition, the UHV controllable high-voltage shunt reactor has successfully been developed in China at first, but its application effect still needs further verification and improvement in practical application.

6.1.2.2 Metal Oxide Arrester (MOA)

The MOA with excellent performance is the key device to control the overvoltage level of the UHV transmission line. The former Soviet Union's 1150 kV transmission line adopts valve type arrester with a clearance during early construction, with switching overvoltage being 1.8 p.u., and after using ZnO arrester instead, the overvoltage can be reduced to 1.6 p.u.; ZnO arrester is used in Japan, with switching overvoltage being 1.6 p.u.; the residual voltage of the arrester developed by the America-based BPA is 1.83 p.u. at the current of 26 kA, and the residual voltage of the arrester developed by America-based AEP is equivalent to 1.72 p.u. at the current of 40 kA.

In recent years, China lays great emphasis on the development of MOA, and continuously improving the ability to limit the overvoltage. At present, the MOA has become the main equipment to limit overvoltage of the UHVAC grid in China. Table 6.2 shows main parameters of UHV MOA used in China [5, 6].

6.1.2.3 Closing Resistor of Circuit Breaker

It is proven from the practical EHV and UHV operation that the closing resistor can reach very ideal voltage limitation effect, which is one of the key devices to control the switching voltage of the UHV system. Therefore, at present, the closing resistor is adopted in the UHV circuit breaker in individual countries across the world, without exception.

The operating process of closing resistor can be divided into two parts, with diagram, as shown in Fig. 6.1. First, close the switch Q_2 to connect the resistor R in the circuit, thus to absorb energy and reduce the line impulse; after a period, re-close the switch Q_1 to enable the resistor R to be shorted. The switch-on and switch-off of the closing resistor will produce overvoltage. It is hoped that the closing resistance is as maximum as possible during switch-on, and, however,

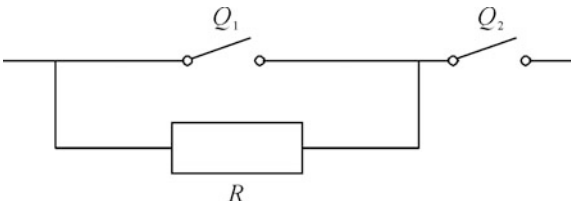

Fig. 6.1 Sketch for the closing resistor of circuit breaker

the closing resistance is as minimum as possible during switch-off. Therefore, it is required to obtain an appropriate resistance value after comprehensive analysis, so as to minimize the overvoltage produced.

Due to the imperfect manufacturing process of the early produced closing resistor, it is reported around the world that the closing resistor has an accident, influencing the safe operation of the system. For example, according to the statistics in 1994, the number of damaged phases has reached 15 phase time for 500 kV closing resistor in China. To some extent, this phenomenon enables the people to doubt the reliability of the closing resistor, so as to eliminate the use of the closing resistor in partial EHV projects. However, as the manufacturing level of the circuit breaker is improved in recent years, and especially the manufacturing requirement for the UHV circuit breaker is harsher, the performance thereof is gradually optimized and improved, and the accident caused by the closing resistor has been very rarer than before. Up to now, no explosion accident in connection with the UHV closing resistor occurs around the world.

The key problem to be solved for use of the closing resistor is to control the energy absorbed by the resistor within specified standard, so as to ensure the proper closing and safe operation of the circuit breaker. The allowable maximum energy absorption value of the closing resistor is calculated as per Eq. (6.1), which is specified as follows:

$$W = \frac{U^2 t}{R}, \tag{6.1}$$

where

U the maximum break-point voltage, and considering the reverse phase closing possibility, it is two times of the phase-to-ground operating voltage;
R the closing resistance value;
t the switch-on time of the closing resistor, which is usually between 8–12 ms, and considering dispersibility of the parameter, a strict value should be taken during design, as well as considering a proper margin, the switch-on time of the closing resistor can be 13 ms

Thus, the maximum energy absorbed considers the extremely rare severest conditions in practical operation to ensure the reliability and stability of the closing resistor of the circuit breaker during design.

The content discussed above covers the condition when the circuit breaker adds a one-stage closing resistor. Over years, a multistage closing resistor that has better

limitation effect is also researched in some literatures. The multistage closing resistor, considering different resistance value requirement during switch-on and switch-off of the closing resistor in overvoltage condition, reduces the closing impact through high resistance switch-on, medium resistance transition, and low resistance switch-off, so as to better limit the overvoltage [7]. However, due to the complexity of its structure, high difficulty in manufacture, high cost, and other problems, these measures are difficultly to be promoted in practical applications in EHV and UHV systems.

6.1.2.4 Opening Resistor of Circuit Breaker

In the UHV system, some opening overvoltage will result in serious consequence, and the opening resistor is a method to limit this overvoltage. At present, the opening resistor is adopted together with the closing resistor in Japan and Italy.

The sketch for the principle of the opening resistor is as shown in Fig. 6.2. The opening process is divided into two parts: first, open the switch Q_1, and switch-on the opening resistor R in the circuit to absorb the energy and reduce the line impulse; after a while, open the switch Q_2 to cut off the line. In these two processes of the opening, considering reducing recovery voltage between the contacts, it is desired to obtain a small R value during switch-off of the Q_1, and it is desired to obtain a large R value during switch-off of the Q_2, so it is also required to comprehensively consider the value of the opening resistor.

The opening resistor of circuit breaker can limit the opening overvoltage, but it has such problems as high fault rate and high heat capacity, so it is worthwhile to carry out a further discussion for the use of opening resistor in UHV circuit breaker.

6.1.3 New Methods for Limiting Switching Overvoltage in the UHVAC System

6.1.3.1 Necessity for Deeply Limiting Switching Overvoltage

As the voltage level of the transmission system increases, the switching overvoltage's influence on the insulation level of the transmission and transformation equipment keep growing, and thus, the switching overvoltage multiple must be limited at a lower and lower value. The allowable switching overvoltage multiples

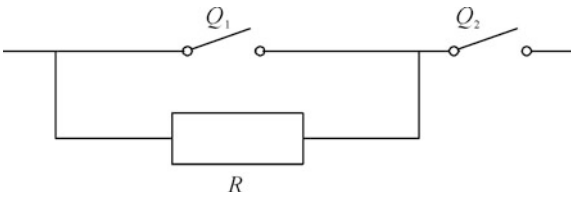

Fig. 6.2 Sketch for the opening resistor of circuit breaker

Table 6.3 Allowable switching overvoltage multiples of systems at various voltage levels

Voltage level/kV	10–66	110/220	330	500	750	1000
Switching overvoltage multiple/p.u.	4.0	3.0	2.2	2.0	1.8	1.6–1.7

1.0 p.u. $= \sqrt{2}U_m/\sqrt{3}$, where U_{m} is the maximum system voltage

Table 6.4 Influence of switching overvoltage multiple on air clearance in the UHV transmission system

	Switching overvoltage multiple/p.u.	Air clearance at different altitudes/m	
		1000	2000
Tower window's intermediate-phase V-type string	1.6	6.5	8.2
	1.7	7.3	9.2
Tower window's side-phase V-type string	1.6	6.2	7.7
	1.7	6.9	8.6
Tower window's side-phase I-type string	1.6	5.0	6.1
	1.7	5.5	6.8

of the systems at various voltage levels in China are as listed in Table 6.3 [1, 8]. From the voltage level of EHV 330 kV, the switching overvoltage starts to control the insulation level of the transmission and transformation equipment. In the UHV transmission system, the saturation characteristic of the air clearance's switching impulse flashover voltage is more distinct, and the deep reduction of the switching overvoltage level plays a crucial role in the reduction of the lines' air clearance. Table 6.4 shows the reduction in the air clearance of the tower window's intermediate-phase V-type string, side-phase V-type string, and side-phase I-type string at different altitudes when the switching overvoltage drops from 1.7 to 1.6 p.u. It can be seen from Table 6.4 that the air clearance reduces by 0.6 m on an average when the switching overvoltage reduces by only 0.1 p.u. Besides, the switching overvoltage level has certain influence on the manufacturing of the transmission and transformation equipment, as well [9]. Therefore, it is quite necessary to deeply reduce the switching overvoltage multiple.

6.1.3.2 Common Methods for Limiting Switching Overvoltage and Their Shortcomings

Currently, the following two schemes are mainly adopted to reduce the switching overvoltage:

(1) The combined utilization of both metal oxide arrester and circuit breaker with closing resistor can limit the system's maximum phase-to-ground 2% statistical switching overvoltage at 1.6–1.7 p.u. However, as the closing resistor has some major shortcomings in the operating reliability and economy, the installation of

closing resistor in the circuit breaker will complicate the structure of the circuit breaker, greatly increase the operating risk of the circuit breaker and, meanwhile, largely increase the cost; therefore, both the power system operation department and the manufacturers tend to use the circuit breaker without closing resistor when the system condition permits.

(2) In case of a short line between two UHV substations, the reduction of the arrester's rated voltage can also limit the system's switching overvoltage at 1.6–1.7 p.u. Take the Huainan–Nanjing–Shanghai UHVAC Power Transmission Project for example, its shortest line section—Suzhou–Shanghai section has a line length of only 60 km; for such line section, if only the metal oxide arrester is utilized without the utilization of the circuit breaker with closing resistor, the rated voltage of the metal oxide arrester must be reduced from the current 828 to 804 kV (by 3%), leading to the increase of the arrester's chargeability from the current 0.77 to 0.79. However, for a longer line, even if the rated voltage of the arrester is reduced to 804 kV, the requirement cannot be met. Take the Ya'an–Wuhan UHVAC Power Transmission Project under planning stage for example, its shortest line section—Ya'an–Leshan section—has a line length of 85.5 km; for such line section, the utilization of 804 kV arrester can only reduce the overvoltage along the line to 1.74 p.u. which cannot meet the requirement yet; to meet the requirement, the rated voltage of the arrester must be reduced to a lower value and may even need to be reduced to 762 kV (by 8%), at which the long-term operation chargeability of the arrester will be increased from the current 0.77 to 0.83, resulting in the accelerated aging of the arrester's varistor under normal operation and greatly lowered reliability margin. Moreover, the precondition for the utilization of the 762 kV arrester is that the system's power frequency overvoltage must be limited at 1.2 p.u. at the busbar side and at 1.3 p.u. at the line side, which extremely limit the utilization of the arrester.

Therefore, a flexible method to limit the switching overvoltage in a manner that is adaptive to the operating condition changes can well solve the problems existing in the above methods [10]. The core content of such method is to combine the utilization of controllable arrester installed at the substation's line side and the conventional arrester installed at the middle of the line to deeply reduce the switching overvoltage and eliminate the circuit breaker closing resistor, as shown in Fig. 6.3.

6.2 Single-Phase Ground Fault Overvoltage

6.2.1 Mechanism for Generation

The single-phase ground fault overvoltage is the transient overvoltage produced on a sound phase when a single-phase ground fault occurs in a line, and the circuit

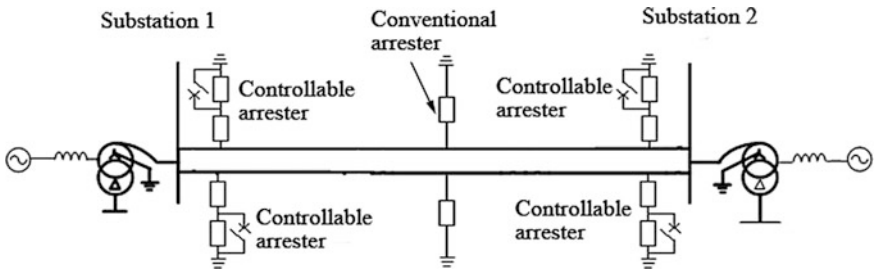

Fig. 6.3 Flexible method to limit the switching overvoltage

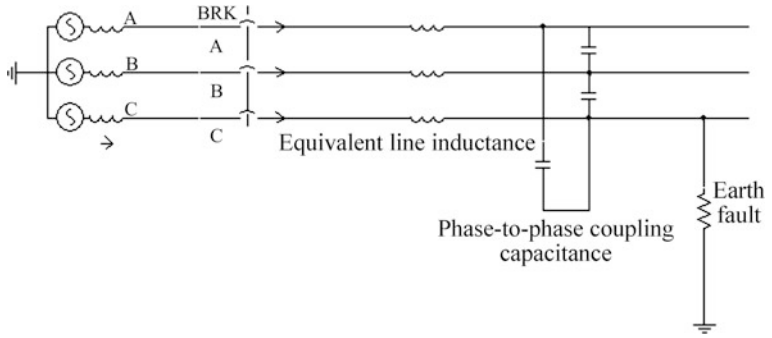

Fig. 6.4 Schematic diagram for single-phase ground fault overvoltage

breakers on both ends of the fault phase are still not disconnected, which differs from the power frequency single-phase grounding overvoltage in steady state. Figure 6.4 shows the equivalent circuit diagram for the single-phase ground fault circuit in the electric system with neutral point directly grounded. In case of single-phase ground fault on phase C, the voltage at the grounding point is suddenly reduced to a voltage after being grounded from the initial voltage prior to fault. As the coupling capacitance exists between phase C and A and between phase C and B and the capacitance voltage cannot be changed suddenly, the voltage of phase A and B in the vicinity of the fault point is changed in a forced manner and the sudden voltage wave is refracted and reflected in the line for several times. When the sound phase voltage reaches the peak or valley value, the refraction and reflection waves with the same polarity are superposed to produce a serious overvoltage. The maximum value of the overvoltage often appears in oscillation of the first power frequency cycle, and at this moment, the circuit breakers are not activated.

If the neutral point of the power supply is grounded through an impedance, then the neutral point impedance will bear a certain voltage drop and rise the voltage on the sound phase when a single-phase ground fault occurs, resulting in a serious overvoltage.

As the single-phase ground fault overvoltage is a transient process caused by reducing the initial voltage of the fault phase by the ground fault in a forced manner, it is possible to cause the most severe ground fault overvoltage if the single-phase ground fault occurs when the fault phase neighbors the peak value.

6.2.2 Modeling and Simulation

As the switching overvoltage has statistic characteristics, the 2% statistic switching overvoltage in the insulation coordination is used as its description in engineering. Its probability is defined as follows: $P(U > U_{2\%}) = 0.02$, i.e., the overvoltage value within confidence probability of 98%.

In the statistic calculation of the switching overvoltage, the Monte Carlo method is widely used. The Monte Carlo method is also called statistical simulation method, whose basic thought is that the probability distribution of the random quantity can be obtained by random sampling. When sampling times is sufficient, it is possible to use the statistics result as an approximate answer of the random experiment. When analyzing the switching overvoltage by use the Monte Carlo method, it is required to take different sample values for the random variables in terms of the distribution law of the random variables, and obtain a 2% statistic value through sampling calculation with proper times at an calculation accuracy acceptable by the project.

For the reason that it is difficult to predict the position of the ground fault occurrence and that the grounding time is random, the software simulation should comprehensively consider the influence of these factors. First, it is required to simulate the ground fault at different time for the fixed ground fault point, calculate the statistic overvoltage, and take the line fault time as the random variable during simulation, enabling the variables to be distributed uniformly in a cycle; then, it is required to calculate the statistic overvoltage at different positions along the line, and take the maximum value from all of the calculated values.

This section gives a systematic and comprehensive study on the single-phase ground fault overvoltage by use of PASCAD software, making reference to the parameters of the Southeast Shanxi–Nanyang–Jingmen UHVAC demonstration line and based on a great amount of simulation calculations.

It is required to build a double-end power transmission model for the UHVAC system with the transmission line length of 600 km, and MOAs and high-voltage

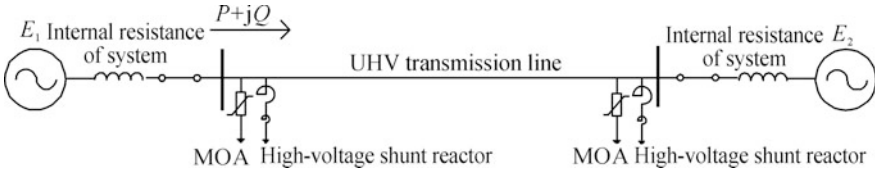

Fig. 6.5 Sketch for UHVAC transmission line

Table 6.5 Parameters of UHVAC line

Sequence parameter	Resistance/Ω	Reactance/Ω	Capacitive reactance/Ω
Positive sequence	0.00805	0.25913	0.22688
Zero sequence	0.20489	0.74606	0.35251

Table 6.6 Parameters of MOA in UHVAC system in China

Rated voltage (kV)	Continuous operating voltage (kV)	Switching impulse residual voltage (peak)/kV)		Lightning impulse residual voltage (peak)/kV	
828	636	1 kA	2 kA	10 kA	20 kA
		1430	1460	1553	1620

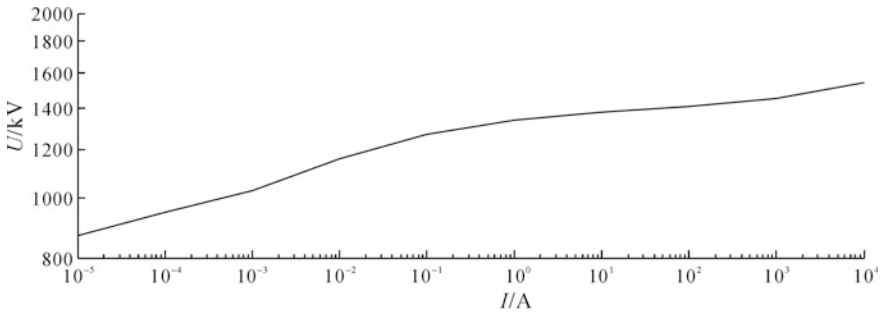

Fig. 6.6 MOA volt–ampere characteristic curve

shunt reactors being arranged on both ends of the line, which is as shown in Fig. 6.5. For the parameters of the lines and poles and towers, refer to those of the Southeast Shanxi–Nanyang–Jingmen UHVAC demonstration line established: the conductor type is steel-cored aluminum strand wire 8× LGJ-500/35, the splitting spacing is 400 mm, and the tower is a cat-head type tower. The sequence parameters of the line are as shown in Table 6.5 [11].

Use the 1000 kV MOA parameters provided by the China Electric Power Research Institute, which is as shown in Table 6.6.

The volt–ampere characteristic curve for this type of arrester is as shown in Fig. 6.6, in which logarithmic coordinates are used for the abscissa.

The production process of the single-phase ground fault overvoltage is simple, and the calculation model is as shown in Fig. 6.7. For the parameters of the lines and poles and towers in this figure, refer to those of the Southeast Shanxi–Nanyang–Jingmen UHVAC demonstration line established. When the voltage, power, and other indexes of the system model meet requirements, it can be obtained the waveform and amplitude of the overvoltage by set a ground fault (action of the circuit breaker is not considered), which is as shown in Fig. 6.8.

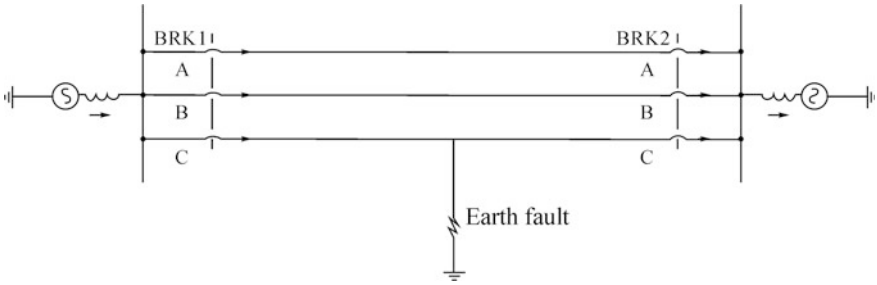

Fig. 6.7 Sketch for single-phase ground fault overvoltage model

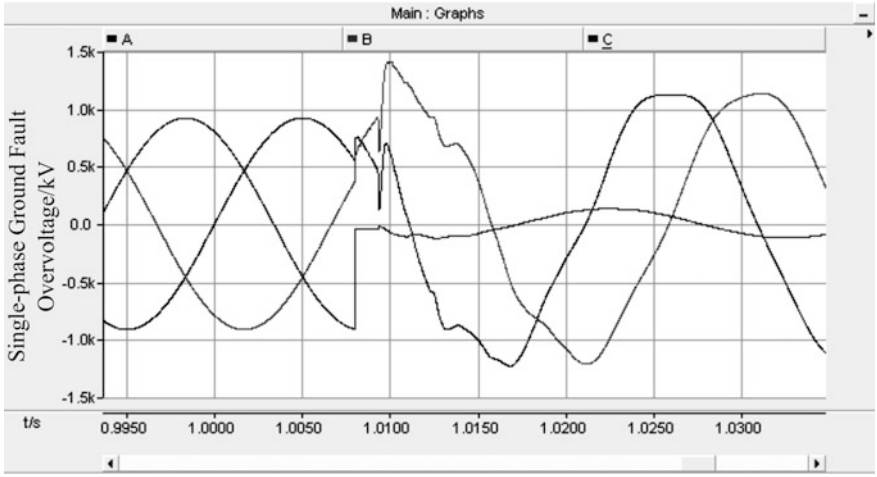

Fig. 6.8 Sketch for single-phase ground fault overvoltage waveform

6.2.3 Analysis of Influence Factors

The single-phase ground fault overvoltage is the transient overvoltage produced on the sound phase when a single-phase ground fault occurs in the line (the circuit breakers on both ends of the fault phase are not open). Although the process is very simple, the influence factors are complicated. Such factors as ground (including grounding resistance and grounding position), transmission power of the line, parameters of poles and towers, compensation degree of high-voltage shunt reactor, impedance characteristics of power supplies at both ends, etc., can influence the single-phase ground fault overvoltage. Among them, such factors as ground, transmission power of the line, parameters of poles and towers and compensation degree of high-voltage shunt reactor, etc., are basic influence factors, having a simple and small influence on the overvoltage; the impedance characteristic of the equivalent power that supplies at both ends of the line is the key influence factor, which has a great influence on the single-phase ground fault overvoltage.

In the following chapters, we will carry out the analysis on the influence factors of the overvoltage.

6.2.3.1 Basic Influence Factors

1. Analysis on the influence of the grounding resistance and grounding position

The single-phase ground fault overvoltage is produced by ground fault. The ground fault factors mainly include grounding position and resistance value R_g at the grounding position. The following analyzes the influence of the factors on the overvoltage, respectively. When the ground fault factor varies, the calculation results of the single-phase ground fault overvoltage are as shown in Table 6.7.

The results show that:

(1) At the same grounding point, the overvoltage amplitude increases with the value of the resistance R_g at grounding position decreasing, because when the grounding resistance becomes small, the grounding transient process becomes violent, resulting in the increase of the overvoltage.

Based on the principle of strictness, the grounding resistance value can be chosen as 0.1 Ω in the following research.

(2) When the grounding resistances are same, the overvoltage amplitudes at different grounding points differ from each other, which is caused by the existing difference of the impedance distribution from the grounding point to the line when the single-phase ground fault occurs at different position.

Therefore, it is required to take into account the influence of the grounding position change on the overvoltage when study the single-phase ground fault overvoltage.

2. Analysis on the influence of the transmission power

Before the ground fault occurs, the line may be in operating state in which the transmission power differs. The following analyzes whether the transmission power

Table 6.7 Calculation results of single-phase ground fault overvoltage under various grounding factors

Grounding point position/km		100	200	300	400	500	600
Overvoltage level/p.u.	R_g = 0.1 Ω	1.522	1.532	1.496	1.501	1.557	1.497
	R_g = 1 Ω	1.509	1.521	1.487	1.496	1.531	1.485
	R_g = 5 Ω	1.491	1.514	1.477	1.489	1.509	1.461
	R_g = 10 Ω	1.458	1.491	1.463	1.481	1.489	1.459
	R_g = 20 Ω	1.411	1.455	1.439	1.473	1.441	1.449
	R_g = 50 Ω	1.271	1.303	1.276	1.334	1.257	1.332

Table 6.8 Calculation results of single-phase ground fault overvoltage under different transmission powers

Grounding point position/km		100	200	300	400	500	600
Overvoltage level/p.u.	P = 0 MW	1.556	1.555	1.569	1.533	1.58	1.614
	P = 1000 MW	1.563	1.56	1.573	1.536	1.569	1.611
	P = 2000 MW	1.555	1.554	1.563	1.524	1.572	1.613
	P = 3000 MW	1.550	1.552	1.558	1.519	1.57	1.610

Table 6.9 Calculation results of single-phase ground fault overvoltage under different conductor models

Common conductor types	Outer diameter/mm	DC resistance/$\Omega \cdot km^{-1}$	Overvoltage/p.u.
LGJ-400/35	26.82	0.07389	1.531
LGJ-400/50	27.63	0.07232	1.531
LGJ-500/35	30	0.05812	1.533
LGJ-500/45	30	0.05912	1.537
LGJ-630/45	33.6	0.04633	1.533

in the line has an influence on the overvoltage. During calculation, it is required to ensure that the busbar voltage at both ends of the line at different power is identical, as shown in Table 6.8.

It is known from Table 6.8 that, as the line transmission power is varied, the overvoltage amplitude at the same grounding point is changed slightly in the line. When the transmission power increased to 3000 MW from 0, the difference in the overvoltage amplitude at the same grounding point does not exceed 0.02 p.u., which can be neglected.

Thus, the transmission power adopts the no-load state of the 0 MW in the following study.

3. Analysis on the influence of the line and tower parameters

It is required to analyze the influence of the different type of conductors and tower parameters on the single-phase ground fault overvoltage, and during calculation, ensure that other conditions of the model are identical. The results are as shown in Tables 6.8 and 6.9, and the overvoltage values in the said table are the maximum ones when the ground fault occurs at different position in the whole line under the condition (Table 6.10).

The results show that: as the conductor type is changed, the single-phase ground fault overvoltage amplitude is changed slightly, with the maximum difference not more than 0.006 p.u., which can be neglected; after the pole and tower parameters are changed apparently, the overvoltage amplitude is changed slightly, with maximum difference not more than 0.04 p.u., which has no substantial influence on the calculation results.

Table 6.10 Calculation results of single-phase ground fault overvoltage under different tower parameters

Change in tower parameters	Nominal height (m)	Horizontal spacing between two neighboring phases/m	Vertical spacing between middle and side phases/m	Overvoltage/p.u.
Dimension of common cat-head type towers	57	15.7	19.6	1.543
Nominal height decreased	37	15.7	19.6	1.569
Nominal height increased	77	15.7	19.6	1.557
Spacing among three phases decreased	57	5.7	9.6	1.573
Spacing among three phases increased	57	25.	29.6	1.586

Table 6.11 Calculation results of single-phase ground fault overvoltage under different high-voltage shunt reactor compensations

Compensation degree (%)	0	10	30	50	70	90
Overvoltage/p.u.	1.697	1.595	1.568	1.563	1.562	1.557

Thus, in the following research, the conductor type of LGJ-500/35 is adopted, and the pole and tower of the line is the commonly used cat-head type for UHV system.

4. Analysis on the influence of the high-voltage shunt reactor compensation

It is required to analyze the influence of different high-voltage shunt reactor compensation degree on the single-phase ground fault overvoltage, and during calculation, ensure that other conditions of the model are identical. The results are as shown in Table 6.11.

The results show that the high-voltage shunt reactor compensation shows certain inhibition effect on the single-phase ground fault overvoltage, and the single-phase ground fault overvoltage decreases as the compensation degree is increased. When the compensation degree is lower than 30%, the overvoltage decreases significantly with the compensation degree increased; when the compensation degree is more than 30%, the increase of the compensation degree has a small influence on the overvoltage, and at this moment, the overvoltage decreases slightly with the compensation degree further increased. At present, the high-voltage shunt reactor compensation degree of the UHV line is often between 80 and 90%, and based on the principle of strictness, the 80% high-voltage shunt reactor compensation degree is used in the following study.

6.2.3.2 Analysis on the Characteristics of Power Supply Impedance

1. Definition of the range of power supply impedance

In practice, the power supply impedance characteristics have a substantial influence on the single-phase ground fault overvoltage. At present, calculation of some typical conditions such as the maximum, minimum, and normal operation mode is insufficient during engineering calculation of the single-phase ground fault overvoltage. Because they mainly reflect the load change, however, the analysis mentioned above shows that the load change has a small influence on the single-phase grounding overvoltage, while the power supply impedance characteristics have a significant influence on the single-phase ground fault overvoltage. Therefore, it is required to define the range of the equivalent power supply impedance of the UHVAC system, and to study its influence on the single-phase ground fault overvoltage.

At present, the construction of the UHVAC grid is at early construction period in China, and the main mode used in China is to erect the UHV line on the basis of two EHV grids to realize point-to-point transmission. Hence, this section mainly gives the study on the equivalent power supply impedance for this case. In the model shown in Fig. 6.6, the power supply impedance often includes the equivalent power supply impedance at the 500 kV side grid, impedance of the transformer, and capacitive impedance at LV of the third winding side, etc. Its calculation is complicated and it is difficult to define them accurately. This section, after comprehensively considering the equivalent case of the EHV grid, and distribution of the capacitive impedance of the UHV transformer and the LV side, gives an equivalent power supply impedance range with the equivalent method, as shown in Fig. 6.9.

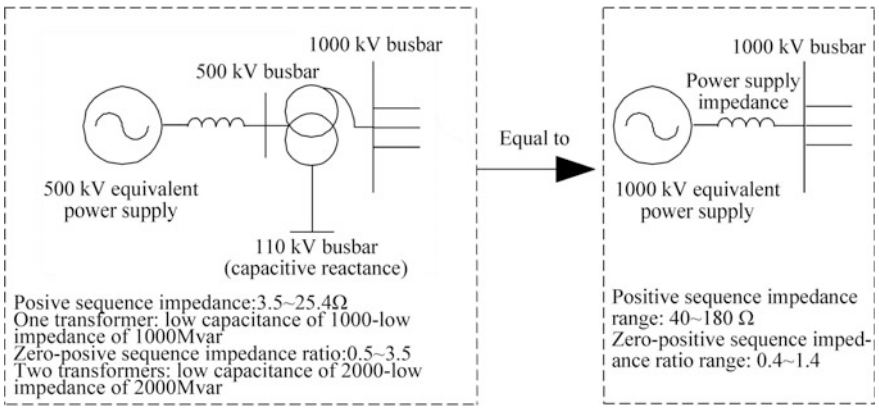

Fig. 6.9 Sketch for calculation of 1000 kV equivalent power supply impedance

The following presents a specific analysis on the range of the three factors that influencing the equivalent power supply impedance [12].

First, analyze the X_1 (positive sequence impedance) range of the 500 kV equivalent power supply. The data show that the short-circuit current is usually between 12.5 and 75 kA in a 500 kV system, and it can be inferred from the short-circuit current calculation Eq. (6.2) that the equivalent X_1 is approx. between 3.85 and 23.1 Ω. This section takes an error of 10% from the stricter consideration, and then, the X_1 is between 3.5 and 25.4 Ω.

$$X_1 = \frac{U_1}{\sqrt{3} I_k}, \tag{6.2}$$

where

X_1 the positive sequence reactance;
U_1 line voltage of the system, taken as 500 kV;
I_k the short-circuit current.

Second, analyze the X_0/X_1 (zero-sequence impedance/positive sequence impedance) relation of the 500 kV equivalent power supply. The ratio of the 500 kV line and transformer is taken fully into account. Adhering to the principle of strictness, the ratio range is defined between 0.5 and 3.5 [10, 11].

Finally, using the transformer parameters of the UHV demonstration line in China and considering the two conditions where one transformer operates or two transformers operate in parallel, the capacitive impedance at LV side of the transformer is defined as follows: in case of one transformer, low capacitance of 1000 Mvar–low reactance of 1000 Mvar; in case of two transformers: low capacitance of 2000 Mvar–low reactance of 2000 Mvar.

Within the range of parameters mentioned above, the single-phase and three-phase short-circuit current amplitude can be obtained by simulation, and then, it is inferred from the short-circuit current equation by inverse calculation and proper expansion and rounding that the X_1 of the equivalent UHV power supply is between 40 and 180 Ω, and the X_0/X_1 is between 0.4 and 1.4, as shown in Fig. 6.9.

The range of the three parameters mentioned above with adequate margin includes power supply impedance conditions of most UHVAC systems. Therefore, it can be argued that the equivalent power supply impedance of the UHV system obtained based on the above range is ample, and the maximum overvoltage amplitude obtained is also stricter during the research on the maximum value of the overvoltage within the above range.

2. Determination of the power supply impedance under the maximum overvoltage

In accordance with the model shown in Fig. 6.6 and within the power supply impedance range obtained above, it is required to study the influence of the power supply impedance on the single-phase ground fault overvoltage, then find out the power supply impedance characteristics under the maximum overvoltage, and acquire the method to calculate the maximum single-phase ground fault overvoltage.

Table 6.12 Calculation results of single-phase ground fault overvoltage in case of change in power supply impedance at E_2 end

X_1/Ω	Overvoltage level/p.u.		
	$X_0/X_1 = 0.4$	$X_0/X_1 = 1.0$	$X_0/X_1 = 1.4$
40	1.644	1.701	1.728
60	1.574	1.613	1.648
100	1.531	1.580	1.638
140	1.543	1.615	1.635
180	1.568	1.626	1.664

(1) Relationship between the single-phase ground fault overvoltage and power supply's zero-positive sequence impedance ratio

It is required to keep the power supply impedance at E_1 end unchanged, but change the power supply impedance at E_2 end, obtaining the calculation results, as shown in Table 6.12. During calculation, 20 grounding points are set up at an equal spacing along the line, and then, it is required to calculate the maximum overvoltage value along the line when a fault occurs at each grounding point. Then, the maximum overvoltage value selected from the 20 maximum overvoltage values corresponding to the 20 grounding points is taken as the single-phase ground fault overvoltage value in such power supply impedance condition.

It can be known from Table 6.12 that the change in the power supply impedance has a significant influence on the single-phase ground fault overvoltage, and the overvoltage increases as the impedance ratio X_0/X_1 increases. Meanwhile, the further calculation shows that, when the power supply impedance is unchanged at E_2 end and the power supply impedance at E_1 end is changed, this law is also applicable. Therefore, it can be believed that the single-phase ground fault overvoltage reaches the maximum value when the X_0/X_1 impedance ratio reaches the maximum value of 1.4. The reason can be analyzed as follows.

The single-phase ground fault overvoltage is produced based on the single-phase ground power frequency overvoltage after the ground fault occurs in the line, so it is closely related to the single-phase ground power frequency voltage value. From the research results of the power frequency overvoltage, it can be known that the voltage rise coefficient K of the sound phase is substantially related to the X_0/X_1 ratio (zero-positive sequence impedance ratio from the grounding point to the whole system) of the system at the time of occurrence of single ground fault, which is as shown in Eq. (6.3), while the X_0/X_1 ratio of the system is also closely related to the power supply impedance. Apparently, the X_0/X_1 ratio of the system increases as the X_0/X_1 of the power supply impedance increases, so the voltage rise coefficient of the sound phase increases accordingly, which is as shown in Fig. 6.10. Hence, the switching overvoltage also increases when the single-phase ground fault occurs, accordingly.

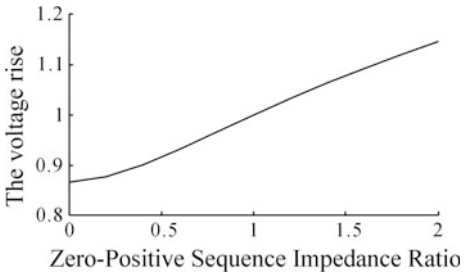

Fig. 6.10 Relation curve between the voltage rise coefficient K and system's X_0/X_1 ratio

Table 6.13 Calculation results of single-phase ground fault overvoltage under different power supply positive sequence impedances

X_{1E2}/Ω		40	60	100	140	180
Overvoltage level/p.u.	X_{1E1} = 40 Ω	1.728	1.648	1.638	1.635	1.664
	X_{1E1} = 60 Ω	1.647	1.585	1.579	1.554	1.567
	X_{1E1} = 100 Ω	1.639	1.580	1.516	1.527	1.530
	X_{1E1} = 140 Ω	1.635	1.553	1.529	1.520	1.540
	X_{1E1} = 180 Ω	1.662	1.564	1.530	1.542	1.576

$$K = \sqrt{3}\frac{\sqrt{\left(\frac{X_0}{X_1}\right)^2 + \left(\frac{X_0}{X_1}\right) + 1}}{\frac{X_0}{X_1} + 2}. \tag{6.3}$$

(2) Relationship between the single-phase ground fault overvoltage and power supply positive sequence impedance

Under the circumstance that the impedance ratio of X_0/X_1 at both ends of power supply is all 1.4, it is required to vary the positive sequence impedance X_{1E1} and X_{1E2} of the power supply E_1 and E_2 at both ends, and calculate the overvoltage, whose results are shown in Table 6.13. The overvoltage values in the table are the maximum overvoltage values when the ground fault occurs at different positions of the whole line in such condition.

It is known from Table 6.13 that the single-phase ground fault overvoltage value presents a V trend decreasing first and increasing later as the positive sequence impedance of the power supply increases to 180 from 40 Ω gradually, so the maximum overvoltage value appears at the boundary of the impedance range. The analysis is as follows:

On one hand, the single-phase ground fault overvoltage increases as the X_0/X_1 ratio increases, which is as shown in Fig. 6.10, while the X_0/X_1 of the system is related to that of the power supply and line. The $X_{0\ \text{supply}}$ represents the zero-sequence impedance of the power supply, the $X_{1\ \text{supply}}$ represents the positive sequence impedance of the power supply, a represents the zero-positive sequence impedance ratio of the power supply, the $X_{0\ \text{line}}$ represents the zero-sequence

impedance of the transmission line, the $X_{1\ \text{line}}$ represents the positive sequence impedance of the transmission line, b represents the zero-positive sequence impedance ratio of the transmission line, and the a is less than b; therefore, the zero-positive sequence impedance ratio $X_{0\ \text{system}}/X_{1\ \text{system}}$ of the whole system from the fault point is as follows:

$$\frac{X_{0\ \text{system}}}{X_{1\ \text{system}}} = \frac{X_{0\ \text{supply}} + X_{0\ \text{line}}}{X_{1\ \text{supply}} + X_{1\ \text{line}}} = \frac{aX_{1\ \text{supply}} + bX_{1\ \text{line}}}{X_{1\ \text{supply}} + X_{1\ \text{line}}} = a + (b-a)\frac{X_{1\ \text{line}}}{X_{1\ \text{supply}} + X_{1\ \text{line}}}. \tag{6.4}$$

As the zero-positive sequence impedance ratio b of the UHV line is about 2.6, under the circumstance of keeping the power supply zero-positive sequence impedance ratio unchanged, it can be known from Eq. (6.4) that the X_0/X_1 of the system decreases as the X_0 and X_1 of the power supply increase proportionally, so the overvoltage amplitude decreases.

On the other hand, it is analyzed from the perspective of the switching voltage that the existence of X_1 is equivalent to extend the line length, so that the overvoltage increases with the line length increased; therefore, the single-phase ground fault overvoltage increases with the X_1 increased.

Under the effect of such two factors together, when the X_1 is smaller, the former one's effect is dominant, while the X_1 is larger, the later one's effect stands out. Therefore, with the X_1 increased, the overvoltage amplitude presents a V trend decreasing first and increasing later.

(3) Conclusion on the method to calculate the maximum value of the single-phase ground fault overvoltage

The conclusion for the two sections described above is the result obtained for the line with length of 600 km. The further calculation shows that the influence of power supply impedance characteristics on the single-phase ground fault overvoltage presents a same law as this line in case of change in length of the line, namely that the overvoltage increases as the zero-positive sequence impedance ratio of the power supply increases; under the circumstance where the zero-positive sequence impedance ratio of the power supply keeps unchanged, the overvoltage presents a V trend as positive sequence impedance of the power supply increases. For ordinary UHV lines, therefore, the maximum amplitude of the single-phase ground fault overvoltage appears when the X_0/X_1 reaches the maximum value and the X_1 reaches the boundary value.

The positive sequence impedance of the power supply E_1 and E_2 corresponds to X_{1E1} and X_{1E2}, and its upper and lower boundary values is 180 and 40 Ω, respectively. The boundary value (i.e., $X_{1\ \text{upper boundary}}$, $X_{1\ \text{lower boundary}}$) of the positive sequence impedance X_1 for the equivalent power supply of the UHV system should be taken as the following four conditions: ($X_{1E1} = X_{1\ \text{upper boundary}}$, $X_{1E2} = X_{1\ \text{upper boundary}}$), ($X_{1\text{E1}} = X_{1\ \text{lower boundary}}$, $X_{1\text{E2}} = X_{1\ \text{lower boundary}}$), ($X_{1E1} = X_{1\ \text{upper boundary}}$, $X_{1E2} = X_{1\ \text{lower boundary}}$), and ($X_{1\text{E1}} = X_{1\ \text{lower boundary}}$, $X_{1\text{E2}} =$

$X_{1\,\text{upper boundary}}$). In case of each of the power supply impedance values mentioned above, it is required to fully take into account the influence by the grounding factor, and assume that n single-phase grounding points are set up at an equal interval along the line, as well as calculate the maximum overvoltage value when a fault occurs at each grounding point along the line, so that the maximum value selected from the n maximum overvoltage values taken along the line is the single-phase ground fault overvoltage value in such power supply impedance condition. It is required to calculate the single-phase ground fault overvoltage values $U_{1\max}$, $U_{2\max}$, $U_{3\max}$, and $U_{4\max}$ in such four power supply impedance conditions, respectively, and select the maximum value as the maximum single-phase ground fault overvoltage value $U_{\max}$ of the line from the four ones. Figure 6.11 shows the steps for calculating the maximum single-phase ground fault overvoltage value for a specific length of the UHV line.

Actually, under most conditions, in case of that $X_{1E1} = 40\ \Omega$ and $X_{1E2} = 40\ \Omega$, and that zero-positive sequence impedance ratio is all 1.4 for power supplies at both ends of the line, the single-phase ground fault overvoltage amplitude reaches the maximum value. Therefore, for the convenience, it can also take into account such condition to carry out estimation of the maximum single-phase ground fault overvoltage.

From the analyses above, it is required to take the line transmission power of 0 MW, line compensation degree of 80%, and grounding resistance of 0.1 Ω first when calculating the maximum single-phase ground fault overvoltage of a line, and then to select the above four conditions for positive sequence impedance boundary value under the premise of ensuring the maximum zero-positive sequence impedance ratio for power supplies at both ends of the line. By such four conditions, it is possible to change the grounding points and then calculate the single-phase ground fault overvoltage for each condition. The maximum single-phase ground fault overvoltage obtained from such four conditions is considered as the maximum single-phase ground fault overvoltage when the impedance value for power supplies at both ends of the line is any impedance value within the impedance range.

6.2.3.3 Comparison of the Overvoltage in Single-Circuit and Double-Circuit Lines

The line parameters of single-circuit model and double-circuit model refer to the Southeast Shanxi–Nanyang–Jingmen UHV single-circuit demonstration line and Huainan–Anhui–Zhejiang–Shanghai UHV double-circuit line, respectively. Meanwhile, it is required to maintain the same parameters for both lines, such as power supply characteristics, high-voltage shunt reactor compensation degree, etc., and carry out comparative analysis on the single-phase ground fault overvoltage of the single- and double-circuit lines.

Considering that the double-circuit line can be put into operation in two modes, i.e., one circuit is grounded (one circuit for operation), or two circuits are put into

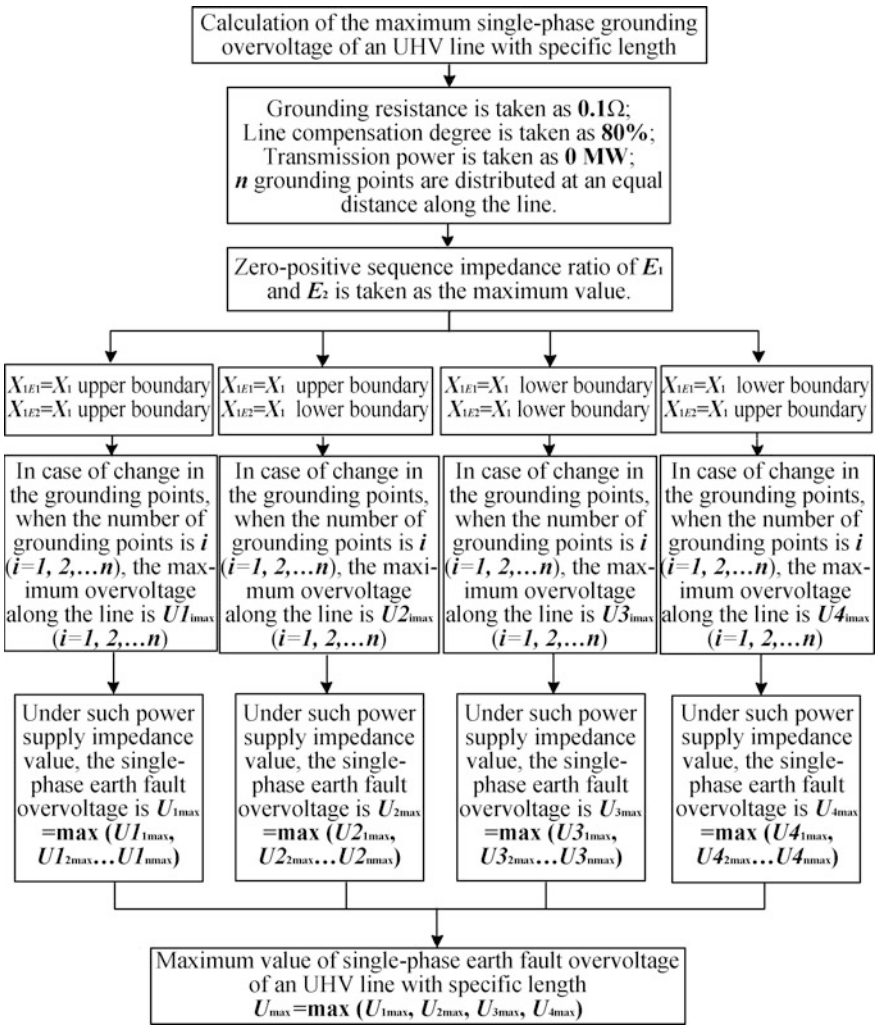

Fig. 6.11 Steps for calculating the maximum value of single-phase ground fault overvoltage

operation, the following analyzes the overvoltage condition in different operating modes through calculation. The results are as shown in Table 6.14.

It can be known from Table 6.14 that the single-phase ground fault overvoltage of the single-circuit line is more severe than the double-circuit line in the same condition. This is because, compared to the single-circuit line system with same line length, the double-circuit line system features better contact and stability, being not liable to intensify overvoltage fluctuation. Moreover, under the circumstance where the line length keeps the same, the consumption of the overvoltage wave increases with the quantity of the circuits increased, so the overvoltage amplitude of the

Table 6.14 Comparison of the single-phase ground fault overvoltage in single-circuit and double-circuit lines

Different line length/km		200	400	600
Overvoltage level/p.u.	Single-circuit line	1.407	1.600	1.728
	Double-circuit line with one circuit grounded	1.291	1.462	1.703
	Double-circuit line with two circuits under operation	1.276	1.396	1.573

Table 6.15 Single-phase ground fault overvoltage amplitudes for lines with different lengths

Line length/km	100	200	300	400	500	600
Overvoltage/p.u.	1.379	1.418	1.498	1.542	1.633	1.728

double-circuit line is lower than the single-circuit line [4]. Accordingly, it can be inferred that, if the single-phase ground fault overvoltage of the single-circuit line can be controlled effectively, the overvoltage of the double-circuit line can also be effectively controlled in the same condition.

6.2.4 Limitation Measures

6.2.4.1 Overvoltage Limitation for Lines with Different Lengths

1. High-voltage shunt reactor compensation and MOA protection are adopted at both ends of the line

With respect to the point-to-point UHV transmission line, it is required to analyze the controllable line length for the single-phase ground fault overvoltage by use of the method obtained in the previous section for calculating the maximum single-phase ground fault overvoltage of the UHV line, with the busbar voltage at both ends of the line keeping 1100 kV (to be considered as a strict value). In the model calculation, the common limitation measure (i.e., one group of MOAs and high-voltage shunt reactor compensation are used at both ends of the line) is adopted, and the compensation degree of the line amounts to 80%.

By following the calculation steps shown in Fig. 6.11, it is possible to calculate the maximum single-phase grounding switching overvoltage amplitudes for the line with length ranging from 100 to 600 km. The results are as shown in Table 6.15.

It can be known from Table 6.15 that, using the method shown in Fig. 6.15 and in case of line length of 500 km, the overvoltage is 1.633 p.u., meeting the limitation requirement; in case of line length of 600 km, the overvoltage is more than 1.7 p.u., exceeding the requirements set forth in the specification. Hence,

considering that the severity of conditions selected, it can be believed that the single-phase ground fault overvoltage also meets the limitation requirements set forth in the specification, only when the line length does not exceed 500 km, even in the most severest condition; and the single-phase ground fault overvoltage is difficultly controlled within the allowable range when the line length exceeds 600 km.

For a longer UHV line, the single-phase ground fault overvoltage is usually limited by several groups of MOAs and multi-point high-voltage shunt reactor sectional compensation measures, which are analyzed, respectively, as follows.

2. Research on the limitation by several groups of MOAs

A 800 km transmission line is selected and adopts an 80% high-voltage shunt reactor compensation at both ends of the line [2]. The following analyzes the limitation effect obtained by use of several groups of MOAs (several groups of MOAs are distributed evenly in the line).

(1) Research on overvoltage limitation by even groups of MOAs

2, 4, and 6 groups of MOAs are arranged along the line, respectively. In case of change in fault position, the maximum overvoltage along the line is as shown in Fig. 6.12. "Two groups of MOAs" in Fig. 6.12 means that both ends of the line have one group of MOAs setup, respectively; where "four groups of MOAs" are provided, the other two groups of MOAs are set up at 1/3 and 2/3 of the line length, respectively; where "six groups of MOAs" are provided, the other four groups of MOAs are set up at 1/5, 2/5, 3/5, and 4/5 of the line length, respectively.

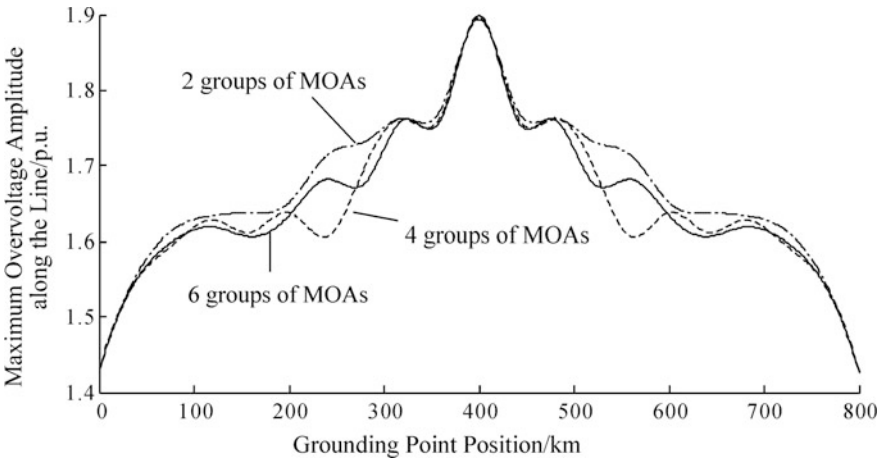

Fig. 6.12 Single-phase ground fault overvoltage amplitudes under limitation by even groups of MOAs

Comparison of the overvoltage amplitudes obtained in the three conditions in Fig. 6.12, it can be found that the maximum overvoltage amplitudes along the line are closely related to the fault position, and the ground fault overvoltage can be limited only at the place where the MOA is set up. As no arresters are set up at middle point of the line, the ground fault overvoltage at the middle of the line cannot be effectively limited. In case of a single-phase ground fault at the middle of the line, the overvoltage amplitude is the maximum value. In these three conditions, the maximum overvoltage amplitude exceeds 1.85 p.u., and the difference thereof is very small.

(2) Research on overvoltage limitation by odd groups of MOAs

3, 5, and 7 groups of MOAs are arranged along the line. In case of change in fault position, the maximum overvoltage along the line is as shown in Fig. 6.13. "Two groups of MOAs" in Fig. 6.13 means that both ends of the line have one group of MOAs, respectively; where "three groups of MOAs" are provided, the other one group of MOAs are set up at the middle of the line; where "five groups of MOAs" are provided, the other three groups of MOAs are set up at 1/4, 2/4, and 3/4 of the line length, respectively; where "seven groups of MOAs" are provided, the other five groups of MOAs are set up at 1/6, 2/6, 3/6, 4/6, and 5/6 of the line length, respectively.

It can be known from Fig. 6.13 that the maximum overvoltage is limited, obviously because one group of MOAs are installed at the middle of the line if odd numbers of MOAs are arranged along the line. However, where 3, 5, or 7 groups of MOAs are provided to limit the overvoltage, the maximum overvoltage of the line reaches approx. 1.74 p.u. and fails to meet the limitation requirement. The maximum overvoltage obtained by use of different groups of MOAs is shown in Table 6.16, and it can be found that the maximum overvoltage decreases slightly, with the increase in group numbers of the MOAs.

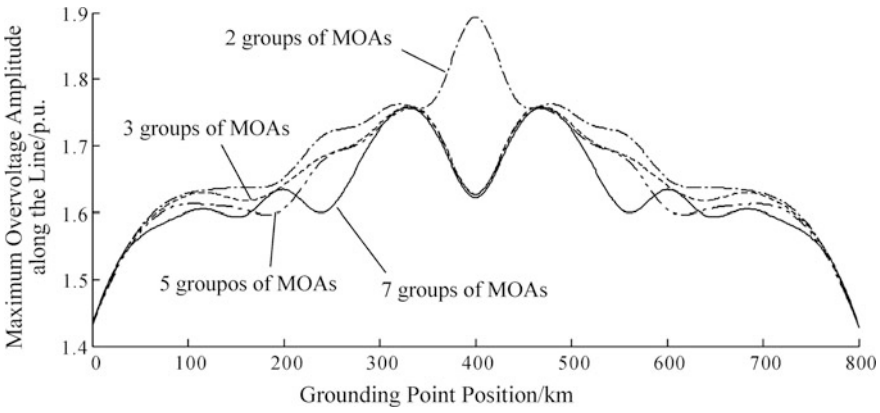

Fig. 6.13 Single-phase ground fault overvoltage amplitudes under limitation by odd groups of MOAs

Table 6.16 Effect on single-phase ground fault overvoltage limitation by 2, 3, 5, and 7 groups of MOAs

Groups of MOAs	2	3	5	7
Overvoltage/p.u.	1.885	1.745	1.744	1.740

(3) Conclusions

From Figs. 6.12, 6.13, and 6.16, it can be found that the ground fault overvoltage can be limited effectively only at the place where MOAs are set up, and the MOAs limit the single-phase ground fault overvoltage only at the place neighboring the installation location thereof (approx. within 80 km), but do not have obvious limitation of the ground fault overvoltage at a farther place. With the increase in the quantity of MOAs, the maximum overvoltage value decreases slightly. When the line is long, many more MOAs cannot achieve excellent limitation effect, but increase the economic expenditure as well. Moreover, through comparison between Figs. 6.12 and 6.13, it can be known that the installation of MOAs at the middle of the line can reduce the overvoltage value significantly for the long line.

In summary, installing one group of MOAs at the middle of a long UHV line adopting double-end compensation measures can significantly reduce the single-phase ground fault overvoltage. Furthermore, when the single-phase ground fault overvoltage is limited only by MOAs, it is required to arrange more groups of MOAs along the line to control the overvoltage. Therefore, this method has a certain limitation.

3. Research on overvoltage limitation by sectional high-voltage shunt reactor compensation

The high-voltage shunt reactor compensation has certain limitation effect on the single-phase ground fault overvoltage. In general, the higher the compensation degree is, the better the limitation effect is. Different arrangement patterns of the high-voltage shunt reactors with same compensation degree have different overvoltage limitation effect, which is analyzed as follows.

Select an 800 km line with both ends of the line arranging a group of MOA, and maintain a high-voltage shunt reactor compensation degree of 80% unchanged and change the number of compensation points (the compensation capacity at each point is distributed evenly), as well as analyze the limitation effect on the single-phase ground fault overvoltage by different number of compensation points. The results are as shown in Fig. 6.14.

It can be found from Fig. 6.14 that under the same high-voltage shunt reactor compensation degree, the more the compensation points are, the better the overvoltage limitation is. As shown in the figure, the three-point distribution of the high-voltage shunt reactor compensation (i.e., a compensation is also available at the middle part of the line) apparently has better limitation effect than the two-point distribution (i.e., compensation at both ends of the line); in case of the increase of compensation points, the overvoltage limitation tends to reach the maximum effect gradually. Hence, the installation of high-voltage shunt reactor compensation at the

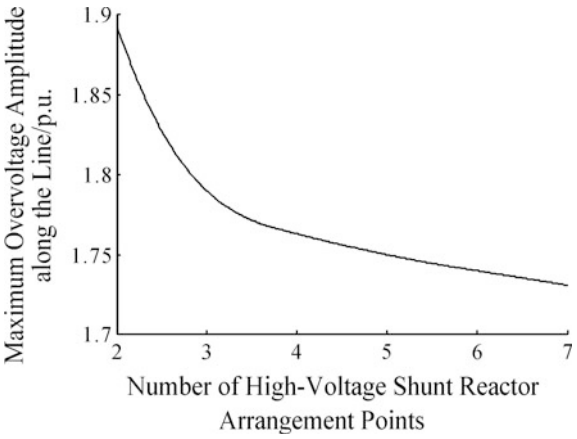

Fig. 6.14 Single-phase ground fault overvoltage under compensation by high-voltage shunt reactors evenly arranged at multiple points

Table 6.17 Single-phase ground fault overvoltage under different compensation capacity distribution

Compensation capacity ratio	Head end:middle part:tail end of line				
	1:0:1	2:1:2	1:1:1	1:2:1	1:4:1
Overvoltage/p.u.	1.907	1.827	1.783	1.718	1.696

middle part of the line is good for limitation of overvoltage for the long line. Meanwhile, it is found that the maximum overvoltage under three-point compensation for the 800 km line still exceeds the allowable value of 1.7 p.u. which sets forth in the specification.

The following analyzes the influence of different distribution patterns of the high-voltage shunt reactor capacity on the overvoltage under three-point compensation. In addition, select an 800 km line for the analysis, and maintain a high-voltage shunt reactor compensation degree of 80% unchanged, and adopt three-point compensation; however, the compensation capacity distribution at both ends of the line is not identical to the middle part of the line. The calculation results are as shown in Table 6.17. The compensation capacity ratio in Table 6.17 is 1:1:1, namely average three-point compensation.

It can be known from Table 6.17 that, with the increase in high-voltage shunt reactor compensation capacity proportion at the middle part of the line, a better overvoltage limitation effect can be obtained. This is because the voltage at the middle part of the line often remains high and it is difficult to control the overvoltage, and due to the reason that the line is long, a high overvoltage amplitude can be caused easily by the violent voltage change at this place. Through installation of high-voltage shunt reactors at the middle of the line, the voltage fluctuation is weaken, and the overvoltage distribution over the whole line is improved, either; hence, the higher the compensation degree at this place is, the better the limitation effect is. With respect to the long line, therefore, installation of high-voltage shunt

reactors with high compensation degree at the middle part of the line is beneficial to the limitation of the overvoltage.

However, the further calculation shows that for a longer UHV line and from the perspective of limiting power frequency overvoltage, the high-voltage shunt reactor compensation capacity at the middle part of the line should always keep at an appropriate value. Taking the UHV line with 800 km length as an example, the maximum power frequency overvoltage values are as shown in Table 6.18 below when a load shedding power frequency overvoltage after single-phase ground fault appears at both ends of the line.

From Tables 6.17 and 6.18, it can be known that, with respect to a long UHV line with three-point compensation, because of the reason that the maximum load shedding power frequency overvoltage often appears at the parts close to both ends of the line, the single-phase grounding load shedding power frequency overvoltage increases as the high-voltage shunt reactor compensation capacity increases at the middle part of the line, so that the power frequency overvoltage may exceed the limitation requirement when more high-voltage shunt reactors are installed at the middle part of the line; however, for the single-phase ground fault overvoltage in a long line, the maximum overvoltage value along the line often appears at the middle part of the line, so the single-phase ground fault overvoltage will decrease as the high-voltage shunt reactor compensation capacity increases in the middle part of the line. Therefore, for a long line and from the perspective of limiting the power frequency overvoltage and single-phase ground fault overvoltage, it is required to install appropriate quantity of high-voltage shunt reactors at the middle part of the line, and it can be known from Tables 6.17 to 6.18 that it is beneficial to the limitation of the two overvoltage when the high-voltage shunt reactor compensation capacity at the middle part of the line remains about 50%.

At present, the high-voltage shunt reactor compensation capacity at the middle part of the common sectionalized UHV line which adopting three-point compensation remains about 50% [1]. It can be known from Table 6.17 that the overvoltage of an 800 km line may exceed the limitation requirement set forth in the specification, so it is required to take further limitation measures.

4. Research on combined limitation by several groups of MOAs and sectionalized high-voltage shunt reactor compensation

It can be known from the previous two subsections that, for a long UHV line, the overvoltage value decreases significantly when MOA or the high-voltage shunt reactor is arranged at the middle part of the line, but it is impossible to meet the limitation requirement set forth in the specification only by means of arrangement

Table 6.18 Power frequency overvoltage under different compensation capacity distribution

Compensation capacity ratio	Head end:middle part:tail end of line			
	2:1:2	1:1:1	1:2:1	1:4:1
Overvoltage/p.u.	1.371	1.377	1.380	1.435

Table 6.19 Single-phase ground fault overvoltage under combined limitation by MOAs and high-voltage shunt reactors under the three-point limitation mode

Compensation capacity ratio	Head end:middle part:tail end of line		
	2:1:2	1:1:1	1:2:1
Overvoltage/p.u.	1.704	1.642	1.604

of arresters or high-voltage shunt reactors along the line. For the long line which adopting three-point limitation mode (i.e., MOA and high-voltage shunt reactor compensation are arranged at the head end, middle part and tail end of the line, respectively), this section conducts a research on the effect of limiting overvoltage jointly obtained by arranging several groups of MOAs and sectionalized high-voltage shunt reactor compensation.

By selecting an 800 km line and adopting three-point limitation mode, the overvoltage calculation results are as shown in Table 6.19.

It can be known from Table 6.19 that the single-phase ground fault overvoltage is effectively limited for the 800 km line under three-point limitation mode, meeting the requirements set forth in the specification. Hence, it can be inferred that, for a long line with length of 500–800 km, it is possible to limit the overvoltage effectively when sectionalizing the line at the middle part of the line (the divided line section is about 400 km long) and setting up MOAs and appropriate high-voltage shunt reactor compensation.

In fact, in view of difficulty in limiting the single-phase ground fault overvoltage of the long line, the Southeast Shanxi–Nanyang–Jingmen UHV demonstration line and Huainan–Anhui–Zhejiang–Shanghai UHV double-circuit line established in China adopt switch station sectionalization technology. The maximum distance of each section line is approx. 400 km, and MOAs and high-voltage shunt reactor compensation measures are provided to jointly limit the overvoltage at the sectionalized place.

Therefore, it is possible to better meet the limitation requirements of the power frequency overvoltage and switching overvoltage simultaneously by adopting three-point limitation mode and several groups of MOAs and sectionalized high-voltage shunt reactor compensation measures to jointly limit the overvoltage, so as to reduce the quantity of MOAs to be installed along the line. For this reason, it is a technically feasible and economically advantageous limitation method.

6.2.4.2 Further Research on the Single-Phase Ground Fault Overvoltage in the Long Lines

It can be known from the previous analysis that, for a shorter UHV line, the single-phase ground fault switching overvoltage often does not exceed the restriction level of 1.7 p.u., which is not the decisive factor to determine the system insulation level [1]. When the line is long (more than 600 km), the single-phase

ground fault overvoltage also may exceed the restriction level of 1.7 p.u., jeopardizing the safety of the UHV system. For a longer UHV line, however, from the perspective of limiting the power frequency overvoltage and voltage stabilization, it is required to sectionalize the line, and install parallel high-voltage shunt reactors at both ends of each line section to decrease the single-phase ground fault overvoltage. For this reason, in case of being able to sectionalize the long line properly (provide appropriate MOA protection and high-voltage shunt reactor compensation) to ensure that the single-phase ground fault overvoltage does not exceed limitation level set forth in the specification, the line sectionalizing method can be directly referenced for the line planning, design and overvoltage protection calculation, so as to avoid a great amount of simulation calculation for the single-phase ground fault overvoltage (because there are many overvoltage influence factors and the operating condition is too complicated), saving much time and efforts.

For this reason, this section conducts a detailed research on the single-phase ground fault overvoltage of the sectionalized UHV line with the help of the PSCAD-EMTDC software simulation, based on a great amount of simulation calculations. In the condition of calculating the severest single-phase ground fault overvoltage, this section studies the single-phase ground fault overvoltage problem for a long UHV line divided into 3–5 sections, discusses the maximum length that can be reached in the line when the overvoltage does not exceed the limitation requirements by different line sectionalizing methods, and proposes the maximum length for which the single-phase ground fault overvoltage of the whole line cannot exceed the limitation requirements by different sectionalizing methods and gives corresponding line sectionalizing methods which can provide direct reference to the construction of the UHV transmission projects.

Based on the previous discussion of the single-phase ground fault overvoltage influence factors, the following discusses the single-phase ground fault overvoltage level under the circumstance where the line is divided into three, four, and five sections, respectively, and calculates the maximum length of the whole line and each section of the line that can be reached in the line divided into 3–5 sections when the single-phase ground fault overvoltage does not exceed the limitation level.

1. Research on the single-phase ground fault overvoltage in the long line divided into three sections

(1) Research on the overvoltage in the line equally divided into three sections

For a UHV line that is divided into three sections, with 400 km length for each section, the ordinary limitation measure, such as installation of high-voltage shunt reactors and MOAs, is as shown in Fig. 6.15. The high-voltage shunt reactor compensation capacity ratio for point A, B, C and D is 1:2:2:1.

To research the MOA's overvoltage limitation effect, the MOA arrangement along the line can be varied as follows: the first MOA arrangement method is to install six groups of MOAs along the line, which is as shown in Fig. 6.15, and is usually adopted when the MOAs are arranged along the sectionalized line, of which

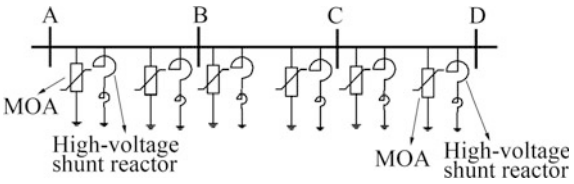

Fig. 6.15 UHVAC line divided into three sections

Table 6.20 Single-phase ground fault overvoltage in a line equally divided into three sections

Compensation degree (%)	Single-phase ground fault overvoltage level/p.u.			
	a1	b1	c1	d1
80	1.667	1.667	1.667	1.669
85	1.646	1.647	1.648	1.649
90	1.623	1.624	1.624	1.624

one group of MOAs is set up at A and D, respectively, and two groups of MOAs at B and C, respectively, represented by a1; the second MOA arrangement method is to arrange four groups of MOAs along the line, of which one group of MOAs is set up at A, B, C, and D, respectively, represented by b1; the third MOA arrangement method is to arrange two groups of arresters along the line, of which one group of arresters are set up at B and C, respectively, represented by c1; the fourth arrangement method is that no arresters are set up along the line, represented by d1. The maximum single-phase ground fault overvoltage levels along the line are as shown in Table 6.20.

It can be known from Table 6.20 that, with the increase in the numbers of the MOAs along the line, the single-phase ground fault overvoltage value keeps basically the same when the line compensation degree keeps unchanged; when the arrangement condition of the MOAs is not changed, the single-phase ground fault overvoltage decreases obviously with the increase in the line compensation degree. Hence, the high-voltage shunt reactor compensation is better to limit the single-phase ground fault overvoltage of the long line, compared to the MOA. For the UHV line with length of 3×400 km, the single-phase ground fault overvoltage does not exceed the limitation level of 1.7 p.u. when the compensation degree changes between 80 and 90%, so that such overvoltage will not endanger the UHV line that is equally divided into three sections, with length of 400 km for each section.

The single-phase ground fault overvoltage presents positive correlation with the line length, i.e., the longer the line length is, the greater the overvoltage is. Thus, it is inferred that, for a UHV line whose total length is less than 1200 km and equally divided into three sections or whose total length is less than 1200 km and section length is less than 400 km, the single-phase ground fault overvoltage does not exceed the limitation level, without need to take into account the danger to the insulation by such overvoltage.

Table 6.21 single-phase ground fault overvoltage in a three-section line in case of change in the length of a single line section

Line sectionalizing method/km	Overvoltage/p.u.		
	Compensation degree 80%	Compensation degree 85%	Compensation degree 90%
400-400-400	1.667	1.648	1.624
200-600-400	1.725	1.699	1.677
300-500-400	1.708	1.689	1.660
500-400-400	1.694	1.679	1.654
400-500-400	1.719	1.699	1.677
500-400-500	1.762	1.734	1.704
500-500-500	1.785	1.742	1.712

(2) Research on the overvoltage in the three-section long line in case of change in the length of a single line section

In case of change in the section length, the single-phase ground fault overvoltage is as shown in Table 6.21. The arresters are arranged symmetrically at both ends of each line section; the high-voltage shunt reactors are also arranged symmetrically at both ends of each line section, with capacity thereof proportional to the line section length.

It can be known from Table 6.21 that, for a UHV line that is not equally divided, the single-phase ground fault overvoltage produced when the longer line section is at either of the ends of the whole line should be less than that produced when the said line is at the middle part of the whole line. When the number of the line sections is fixed, the more equal the line sections are, the smaller the overvoltage is. Based on the consideration of general conclusion, the line length is represented in 100 km in the following simulation calculation. In case of adopting the ordinary overvoltage limitation measures, the maximum length of the whole line can be up to 1300 km, and the maximum length of each line section can be up to 500 km, provided that the compensation degree is varied between 80 and 90% and that the single-phase ground fault overvoltage of the line divided into three sections does not exceed the limitation level. Moreover, the line can be divided by either of following methods to produce a lower overvoltage: 500-400-400 km or 400-400-500 km.

2. Research on the Single-Phase Ground Fault Overvoltage in the Long Line Divided into Four Sections

(1) Research on the overvoltage in the line equally divided into four sections

For a UHV line that is equally divided into four sections with length of 400 km for each section, ordinary limitation measures are taken, such as installation of high-voltage shunt reactors and MOAs, as shown in Fig. 6.16. In the figure below,

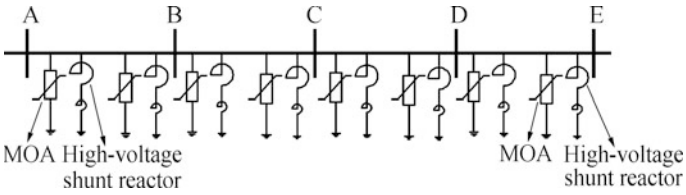

Fig. 6.16 UHVAC line divided into four sections

Table 6.22 Single-phase ground fault overvoltage in the line equally divided into four sections

Compensation degree (%)	Single-phase ground fault overvoltage level/p.u.				
	a2	b2	c2	d2	e2
80	1.820	1.828	1.828	1.837	1.847
85	1.781	1.785	1.785	1.790	1.794
90	1.732	1.734	1.734	1.735	1.737

the high-voltage shunt reactor compensation capacity ratio of point A, B, C, D, and E is 1:2:2:2:1.

To research the MOA's overvoltage limitation effect, the MOA arrangement along the line can be varied as follows: the first MOA arrangement method is to install eight groups of MOAs along the line, which is as shown in Fig. 6.16, and is usually adopted when the MOAs are arranged along the sectionalized line, of which one group of MOAs is set up at A and E, respectively, and two groups at B, C, and D, respectively, represented by a2; the second MOA arrangement method is to arrange five groups of MOAs along the line, of which one group of MOAs is set up at A, B, C, D, and E, respectively, represented by b2; the third MOA arrangement method is to arrange three groups of arresters along the line, of which one group of arresters is set up at B, C, and D, respectively, represented by c2; the fourth MOA arrangement method is to arrange only one group of arresters at C, represented by d2; the fifth MOA arrangement method is that no arresters are set up along the line, represented by e2. The maximum single-phase ground fault overvoltage along the line is as shown in Table 6.22.

It can be known from Table 6.22 that the MOA has weak limitation effect on the single-phase ground fault overvoltage. When the line compensation degree is varied between 80 and 90%, the overvoltage exceeds the limitation level of 1.7 p.u. Thus, for a long UHV line equally divided into four sections, it is impossible to meet the condition in which the single-phase ground fault overvoltage is less than the limitation level in case that the length of a single line section is 400 km by taking ordinary limitation measures.

(2) Research on the overvoltage in the four-section long line in case of change in the length of a single line section

Table 6.23 Single-phase ground fault overvoltage in the four-section line in case of change in the length of a single line section

Line sectionalizing method/km	Overvoltage/p.u.		
	Compensation degree 80%	Compensation degree 85%	Compensation degree 90%
400-400-400-400	1.820	1.783	1.732
400-500-300-400	1.885	1.831	1.778
400-400-400-300	1.807	1.769	1.724
300-400-400-300	1.795	1.753	1.711
400-300-300-400	1.712	1.704	1.681
300-400-300-300	1.759	1.726	1.694
400-300-300-300	1.691	1.662	1.646
300-300-300-300	1.683	1.654	1.623
300-200-400-300	1.698	1.669	1.645

In case of change in the length of a single line section, the single-phase ground fault overvoltage is as shown in Table 6.23. The arresters take the conventional method of being arranged at both ends of a single line section. The arresters are arranged symmetrically at both ends of each line section and the high-voltage shunt reactors are also arranged symmetrically at both ends of each line section, with capacity proportional to the line section length.

It can be known from Table 6.23 that, when the number of the line sections is fixed, the more equal the line sections are, the smaller the overvoltage is. The higher the compensation degree is, the smaller the overvoltage is. For the UHV line divided into four sections, when the line compensation degree is between 80 and 85%, the maximum length of the whole line can reach 1300 km and the maximum line length of a single line section can reach 400 km when the single-phase ground fault overvoltage of the whole line cannot exceed the limitation level, with reasonable line sectionalizing method of 400-300-300-300 km; when the compensation degree is 90%, the overvoltage level is further decreased, and the maximum length of the whole line increases to 1400 km, and the maximum length of a line section can reach 400 km when the single-phase ground fault overvoltage of the whole line cannot exceed the limitation level, with reasonable line sectionalizing method of 400-300-300-400 km.

In addition, comparing Tables 6.20 and 6.22, it can be known that different line sectionalizing methods have a huge influence on the single-phase ground fault overvoltage when the line length keeps the same. The increase in number of the line sections and decrease in the line section length have a certain effect on impairing the overvoltage. When the number of the line sections is fixed, the shorter the middle line sections are, the smaller the single-phase ground fault overvoltage usually is.

3. Research on the single-phase ground fault overvoltage in the long line divided into five sections

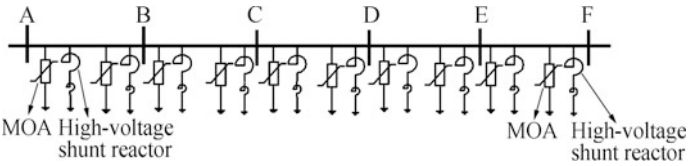

Fig. 6.17 UHVAC line divided into five sections

Table 6.24 Single-phase ground fault overvoltage in the line equally divided into five sections

Compensation degree (%)	Single-phase ground fault overvoltage level/p.u.				
	a3	b3	c3	d3	e3
80	1.725	1.730	1.730	1.730	1.768
85	1.715	1.719	1.719	1.724	1.739
90	1.665	1.668	1.668	1.668	1.674

(1) Research on the overvoltage in the line equally divided into five sections

For a UHV line that is equally divided into five sections with length of 300 km for each section, ordinary limitation measures are taken, such as installation of high-voltage shunt reactors and MOAs, as shown in Fig. 6.17. In the figure below, the high-voltage shunt reactor compensation capacity ratio of A, B, C, D, E, and F is 1:2:2:2:2:1.

To research the MOA's overvoltage limitation effect, the MOA arrangement along the line can be varied as follows: the first MOA arrangement method is to install ten groups of MOAs along the line, which is as shown in Fig. 6.17, and is usually adopted when the MOAs are arranged along the sectionalized line, of which one group of MOAs is set up at A and F, respectively, and two groups at B, C, D, and E, respectively, represented by a3; the second MOA arrangement method is to arrange six groups of MOAs along the line, of which one group of MOAs is set up at A, B, C, D, E, and F, respectively, represented by b3; the third MOA arrangement method is to arrange four groups of MOAs along the line, of which one group of MOAs is set up at B, C, D, and E, respectively, represented by c3; the fourth MOA arrangement method is to arrange two groups of MOAs, of which one group of MOAs is set up at C and D, respectively, represented by d3; the fifth arrangement method is that no MOAs are set up along the line, represented by e3. The maximum single-phase ground fault overvoltage along the line is as shown in Table 6.24.

It can be known from Table 6.24 that the MOAs do not have apparent overvoltage limitation effect, and the single-phase ground fault overvoltage exceeds the limitation level when the line compensation degree is 80 or 85%; and the overvoltage value decreases below 1.7 p.u. when the compensation degree is 90%.

(2) Research on the overvoltage in the five-section long line in case of change in the length of a single line section

Table 6.25 Single-phase ground fault overvoltage in the five-section line in case of change in the length of a single line section

Line sectionalizing method/km	Overvoltage/p.u.		
	Compensation degree 80%	Compensation degree 85%	Compensation degree 90%
300-300-300-300-300	1.725	1.710	1.665
300-200-400-300-300	1.756	1.725	1.688
300-200-500-200-300	1.773	1.730	1.695
300-300-300-300-400	1.758	1.718	1.672
300-300-300-400-300	1.773	1.746	1.708
300-300-400-300-300	1.820	1.782	1.731
400-300-300-300-400	1.787	1.751	1.714
300-300-400-400-300	1.828	1.794	1.738

When the line sectionalizing method is varied, the single-phase ground fault overvoltage values are as shown in Table 6.25. The arresters take the conventional method of being arranged at both ends of the single line section. The arresters are arranged symmetrically at both ends of each line section and the high-voltage shunt reactors are arranged symmetrically at both ends of each line section, with capacity proportional to the line section length.

It can be known from Table 6.25 that, when the number of the line sections is fixed, the shorter the middle line sections are, the smaller the overvoltage is, and the more equal the line sections are, the smaller the overvoltage is. For a UHV line divided into five sections, when the compensation degree is 80–85%, the overvoltage values under several line sectionalizing methods listed in the table exceed the limitation level; when the compensation degree is 90%, the overvoltage decreases within the limitation level under partial line sectionalizing methods, and the maximum line length can reach 1600 km and the maximum length of a single line section can reach 400 km in the condition in which the single-phase ground fault overvoltage along the line does not exceed the limitation level. To minimize the overvoltage, a reasonable line sectionalizing method is as follows: 300-300-300-300-400 km.

4. Condition under which there are drop points in the middle of the line

For a longer UHV line, except for the condition of direct point-to-point transmission, the condition where one or more drop point load or drop point equivalent power supplies are provided in the middle part of the line also exists, as shown in Fig. 6.18 where the sectionalization of the line is omitted.

Where drop point power supplies are provided in the middle part of a longer UHV line, on one hand, the voltage at the busbar (points A and B in Fig. 6.18) which is at the outlet of the drop point power supply is limited to the power frequency voltage value during normal operation, and when the single-phase ground fault occurs in the whole line, the overvoltage decreases; on the other hand, shortening the transmission line between power supplies can result in the decrease

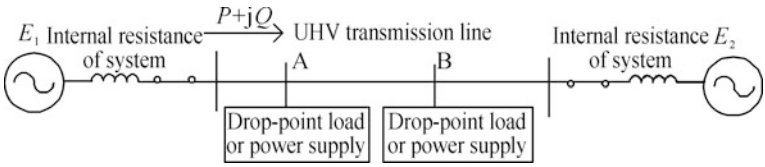

Fig. 6.18 UHV long line with drop point loads or power supplies

Table 6.26 Line sectionalizing methods by which the single-phase ground fault overvoltage will not exceed the limitation level in case of change in the line length

Maximum line length/km	Reasonable line sectionalizing method/km	Compensation degree (%)
1200	400-400-400	80–90
1300	400-400-500	80–90
1400	400-300-300-400	90
1500	300-300-300-300-300	90
1600	300-300-300-300-400	90

in overvoltage. Where drop point load is provided in the middle part of the longer UHV line, the damping action of the load on the overvoltage also results in the decrease in the overvoltage level. Therefore, for the single-phase ground fault overvoltage of the long line, the drop point power supplies or loads provided in the middle part of the line can result in the decrease in the single-phase ground fault overvoltage. With development of the UHV grid, the long-distance UHVAC transmission becomes a trend, and drop point power supplies or loads are usually provided in the middle part of the line. Therefore, the single-phase ground fault overvoltage is lower than that of long line in which no drop point load or power supply is provided in its middle part.

5. Conclusions

It can be known from the previous four subsections that, for a long UHV line with different lengths, when the number of the line sections is fixed, the overvoltage produced when the longer line section is in the middle part of the whole line is higher than that produced when it is at the both ends of the whole line; meanwhile, the more equal the line sections are, the smaller the single-phase ground fault overvoltage is. Therefore, from the perspective of limiting the single-phase ground fault overvoltage and in case of the adoption of ordinary overvoltage limitation measures, the adoption of the line sectionalizing methods listed in Table 6.26 below when the length of the UHV line varies will not cause the single-phase ground fault overvoltage to exceed the limitation level. Based on the consideration to make a general conclusion, the line length is shown in 100 km. The overvoltage will further decrease when drop point loads or power supplies are provided in the middle part of the long line.

It can be known from Table 6.26 that the line sectionalizing methods listed are based on the general conclusion to obtain a low overvoltage, i.e., for a UHV line divided into 3–5 sections, the single-phase ground fault overvoltage does not exceed the limitation level of 1.7 p.u. if the length of each line section is not more than that in the line sectionalizing methods listed in the table and the compensation degree is not less than that listed in the right column of the table.

In addition, considering that the practical limitation of drop point and difficulty in implementation of the project, a certain line sectionalizing method listed in Table 6.26 is difficult to implement in the practical construction, so it is required to, combining the results listed in Tables 6.21, 6.23 or 6.25, and actual drop point condition and difficulty in implementation of the construction, re-determine a reasonable line sectionalizing method based on the overvoltage limitation level. For example, when the line high-voltage shunt reactor compensation degree is 90%, for the long UHVAC transmission line with length of 1500 km, the line sectionalizing method of 300-300-300-300-300 km may be inconvenient to implement in the practical construction, and combining Table 6.25, it is possible to select the line sectionalizing method of 300-200-400-300-300 km, by which the overvoltage does not exceed 1.7 p.u. either. Therefore, it is possible to consider use of the line sectionalizing method of 300-200-400-300-300 km only if such method is better to facilitate construction, compared to the equal line sectionalization method.

6.3 Closing Overvoltage

6.3.1 Mechanism for Generation

6.3.1.1 No-Load Line Closing Overvoltage

When closing the no-load line, there is not any abnormality (no fault and residual charge) in the line before closing, so the initial voltage of the line is zero; after closing, the voltage at each point in the line transits from zero to the power frequency steady-state voltage considering the capacitance effect, and in the transient process, the overvoltage appears [12, 13]. Assuming that the wiring of three phases is fully symmetrical to each other, and is closed simultaneously, it is possible to analyze the single-phase model under lumped parameters equivalent to the three-phase line model. As shown in Fig. 6.19, the line adopts a T type equivalent circuit, in which the L_T and C_T are equivalent inductance and capacitance of the line, respectively; the electromotive force of the power supply is $e(t)$, and the equivalent inductance of the power supply is L_s.

The circuit is further simplified, as shown in Fig. 6.20, in which $L = L_S + L_T/2$.

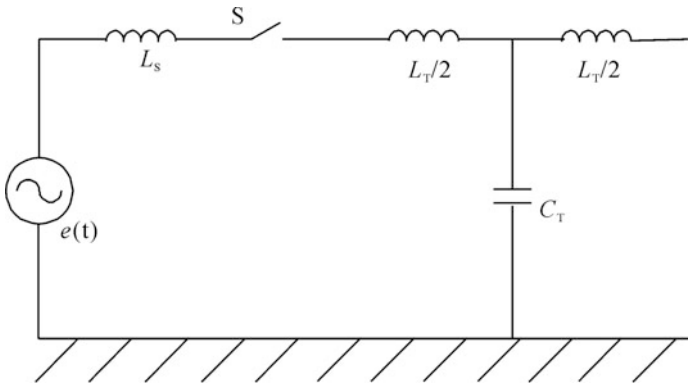

Fig. 6.19 Equivalent circuit of single-phase model

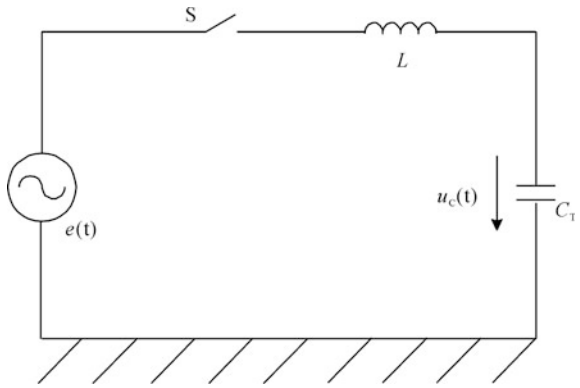

Fig. 6.20 Simplified equivalent circuit

Assuming that the electromotive force of the power supply $e(t) = E_m \cos\omega t$, when closing, it is possible to calculate the voltage on the capacitor:

$$U_c(t) = U_{cm}(\cos\omega t - \cos\omega_0 t) \tag{6.5}$$

$$U_{cm} = E_m / \left[1 - \left(\frac{\omega}{\omega_0}\right)^2\right] \tag{6.6}$$

$$\omega_0 = 1/\sqrt{LC_1}, \tag{6.7}$$

where

U_{cm} the phase voltage peak at tail end of the line, which considering the capacitance rise effect;

ω_0 the natural frequency of vibration for the equivalent circuit, which is often 1.5–3.0 times ω in the EHV and UHV systems

It can be known from Eq. (6.6) that the maximum value can reach two times U_{cm}, and U_{cm} is larger than E_m. In practice, this reflects the capacitance rise effect; hence, theoretically, the maximum overvoltage produced in the line can exceed two times the electromotive force of the power supply. However, due to power consumption in the line, the actual overvoltage amplitude is often lower than the maximum value mentioned above.

The actual no-load line closing process is more complicated than that described for the single-phase model. During closing, actually, the three phases of the circuit breaker are difficulty to be synchronized completely, resulting in a time difference between actual closing time of three phases, which is referred to closing non-synchronism of three phases of the circuit breaker. For a reason that the three phases are non-synchronized, the line is in an asymmetrical operation state instantaneously, and after one phase or two phases are closed, a homopolar induced voltage is produced in an isolated and opening conductor under the influence of the voltage in the transition process of the closed phases, mainly through the coupling of the phase-to-phase capacitance. When such phase is closed, the polarity of the power supply voltage may be reverse to the polarity of the induced voltage, and this will intensify the transient oscillation process of the line, resulting in a more severe overvoltage. Hence, even when a short line with unobvious capacitance rise effect is switched on without load, the maximum overvoltage value is probable to exceed two times the electromotive force of the power supply due to non-synchronism of three phases switch during closing.

6.3.1.2 Single-Phase Reclosing Overvoltage

The single-phase reclosure is a common operation in the electric power system. When a single-phase ground fault occurs in a line, the relay protection is activated to disconnect the fault phase, and at this moment, the sound phase is still in operation, resulting in a secondary arc current at fault phase under the influence of the phase-to-phase coupling. In addition, after the secondary arc current decreases and disappears gradually, the fault phase is reclosed, and at this moment, a reclosing overvoltage produces in the line.

The following specifically analyzes the principle for the generation of overvoltage during single-phase reclosure of the line.

The UHV line is usually provided with shunt reactors with compensation. After the arc at the fault point extinguishes, a recovery voltage exists at the opening phase, including the electrostatic coupling component of phase-to-phase capacitance and the electromagnetic coupling component of phase-to-phase mutual inductance from the sound phase to the fault phase, of which the electrostatic coupling component plays the major role.

Figure 6.21 shows the equivalent diagram of the actual circuit before reclosure of the UHV line, in which L_R and L_N are high-voltage shunt reactor value and small reactor value, respectively; C_m and C_o are phase-to-phase capacitance and phase-to-ground capacitance of the line, respectively.

Then, it is required to further carry out equivalence of the high-voltage shunt reactor and small reactor, of which the L_m and L_0 are phase-to-phase compensation inductance and phase-to-ground compensation inductance after calculating the equivalent values of the high-voltage shunt reactor and small reactor, as shown in Fig. 6.22.

The equivalence of the power supply at sound phase is further carried out, as shown in Fig. 6.23.

As it is difficult to fully compensate the phase-to-phase capacitance by use of the reactors of the line, a recovery voltage $\dot{U}_h$ exists at the opening phase. Where only the steady-state process is considered, the recovery voltage only includes the power frequency component, with steady-state value as follows:

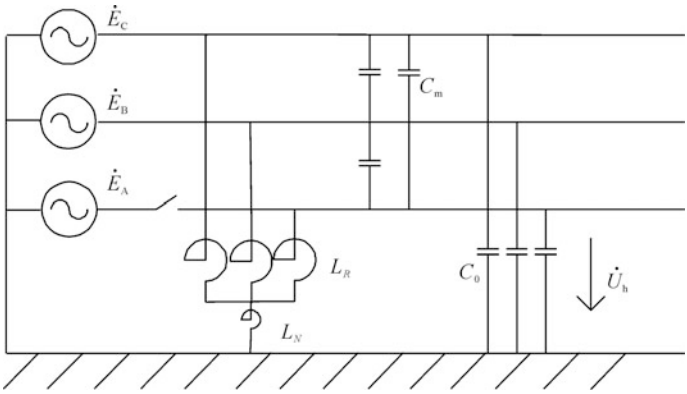

Fig. 6.21 Actual equivalent circuit diagram of the line

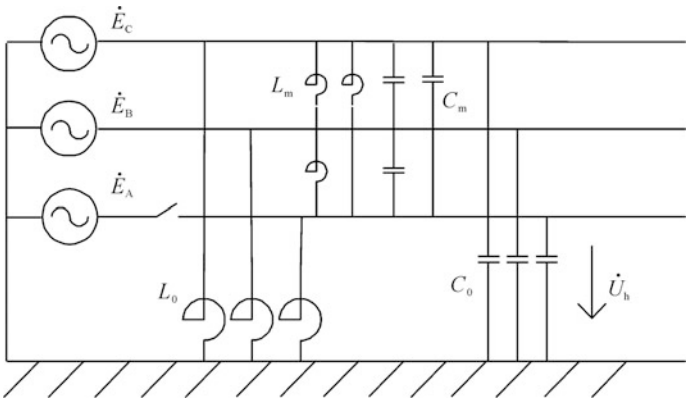

Fig. 6.22 Equivalent circuit diagram (I)

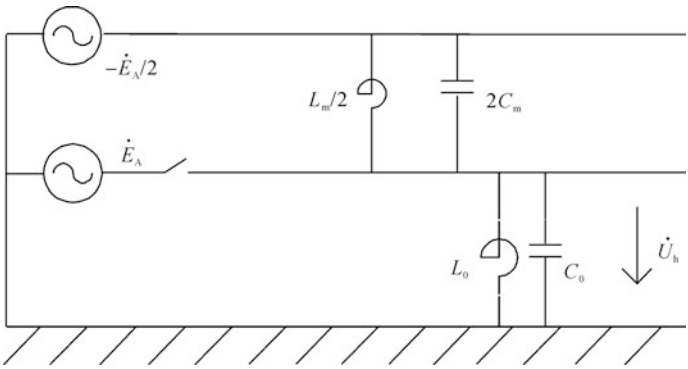

Fig. 6.23 Equivalent circuit diagram (II)

$$\dot{U}_h = -\dot{E}_A \frac{X_0}{2(X_m + 2X_0)}, \tag{6.8}$$

where

X_0 the reactance obtained after the L_0 and C_0 are paralleled ($L_0//C_0$);
X_m the reactance obtained after the $L_m/2$ and $2C_m$ are paralleled ($L_m/2//2C_m$)

Practically, due to the variation of the transition process after the line fault is cleared, the recover voltage $\dot{U}_h$ at the opening phase also includes the free oscillation component. It is mainly composed of several signals with different frequency, whose amplitude is varied as time varies, enabling the recovery voltage to present beat-frequency characteristic.

Therefore, if the line is reclosed when the break voltage difference (i.e., $\left|\dot{E}_A - \dot{U}_h\right|$) of the circuit breaker is close to the maximum value, it will result in a violent oscillation process and produce the most severe overvoltage.

The previous contents discuss the mechanism for generation of the no-line closing overvoltage and single-phase reclosing overvoltage, respectively. During single-phase reclosure, two sound phases are in steady state, and the voltage inducted at the third phase also tends to steady state, so the transient process is not very violent during closing of the third phase. By comparison, the transient characteristics in the no-load line closing process are more apparent. The existence of non-synchronism results in a voltage inducted at the third phase by the two previously closed phases under the influence of the phase-to-phase coupling, and at this moment three phases are in transient state, so closing of the third phase is a transient superposition process based on the transient state, being probable to produce a more severe overvoltage. Therefore, the single-phase reclosing overvoltage may be less than the no-load line closing overvoltage, especially when the line transmission power is small, and the transient state process while reclosing is

not severe, because the voltage component inducted by the two sound phases at the third fault phase is also small.

6.3.2 Modeling and Simulation

6.3.2.1 Simulation of No-Load Line Closing Overvoltage

The no-load line closing process is not complicated, but the line is in asymmetrical operation state transiently due to the non-synchronism of the circuit breaker during closing, aggravating the severity of the overvoltage. Hence, the simulation of no-load line closing overvoltage should consider the influence of the non-synchronism.

The references show that the probability model of non-synchronism can be represented by the mean time T_0 for contact closing of three phases and deviation ΔT_j of actual closing time T_j for contact of phases A, B, and C from T_0.

$$T_j = T_0 + \Delta T_j, j = A, B, C, \tag{6.9}$$

where

T_0 depends on the performance parameters of the circuit breaker;
ΔT_j normal distribution within the range $(-\Delta T_m, \Delta T_m)$.

In the software model, it is possible to take the mean time for contact closing of three phases as a random variable, enabling it to be distributed in a power frequency cycle and simulating the randomness of the overall closing time. Then, the random time offset of each phase is added to make an adjustment for the actual closing time of each phase of the circuit breaker and simulate the non-synchronism. Finally, through several times of simulation, it is possible to calculate 2% statistical overvoltage and take the maximum value from the statistical overvoltage of each point along the line.

The model of the no-load closing line is as shown in Fig. 6.24, and the overvoltage waveform produced is as shown in Figs. 6.25 and 6.26. For parameters of the line, poles and towers, etc., refer to that of the Southeast Shanxi–Nanyang–Jingmen demonstration line established in our country.

The synchronous closing is an ideal closing method, by which the three phases of circuit breaker are connected simultaneously during closing and the voltage at three phases of the line is varied simultaneously, so that no severe overvoltage occurs, which is as shown in Fig. 6.25.

As shown in Fig. 6.26, in case of non-synchronous closing, after phase A first closes, the homopolar induced voltage is produced on phases B and C (still without load) by phase A due to the phase-to-phase coupling effect. When phase B and C are closed, if the power supply voltage polarity is reverse to the induced voltage polarity, it is possible to aggravate the transient oscillation process of the line,

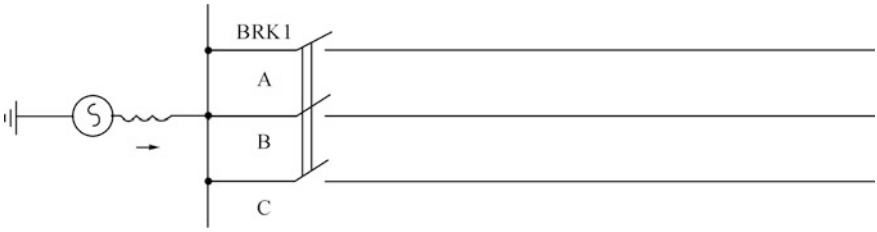

Fig. 6.24 Sketch for no-load line closing overvoltage model

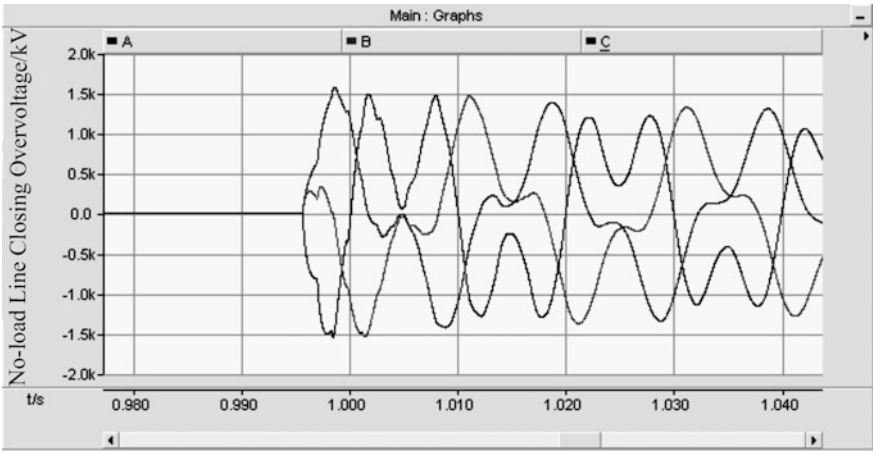

Fig. 6.25 Overvoltage waveform of the no-load line closing (synchronous closing)

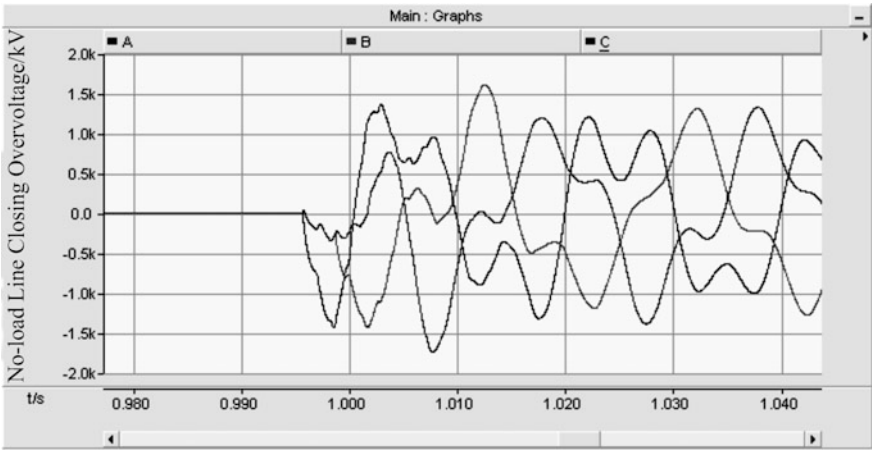

Fig. 6.26 Overvoltage waveform of the no-load line closing (non-synchronous closing)

producing a more severe overvoltage. In the closing sequences as shown in Figs. 6.27 and 6.28, the overvoltage is the most severe. In the simulation, 0.1 ms is taken as the unit time difference to simulate the asynchrony of the three phases.

It can be found out that phase A closes first shortly after the peak, and then, about 3.4 ms later, phase C closes shortly after the trough, and finally, about another 1.9 ms later, phase B closes near the peak, resulting in the most severe overvoltage in the line.

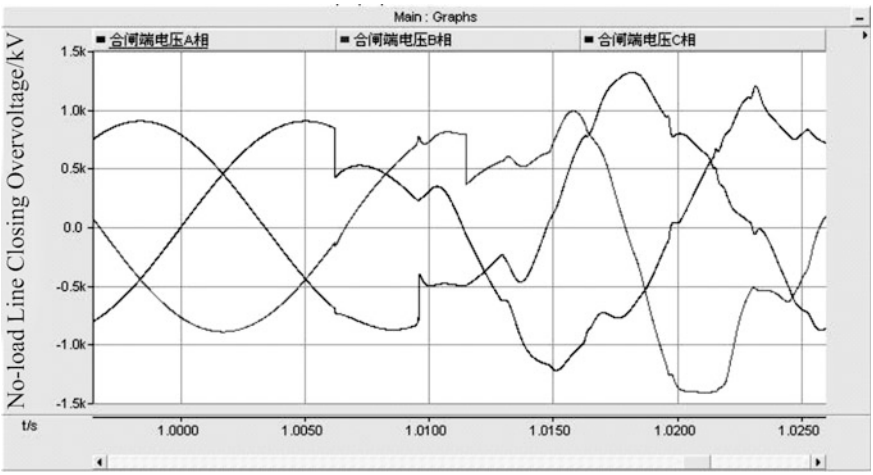

Fig. 6.27 Terminal voltage in closing sequence under the maximum no-load line closing overvoltage (phase A closes at 1.0062 s, phase B closes at 1.0115 s, and phase C closes at 1.0096 s)

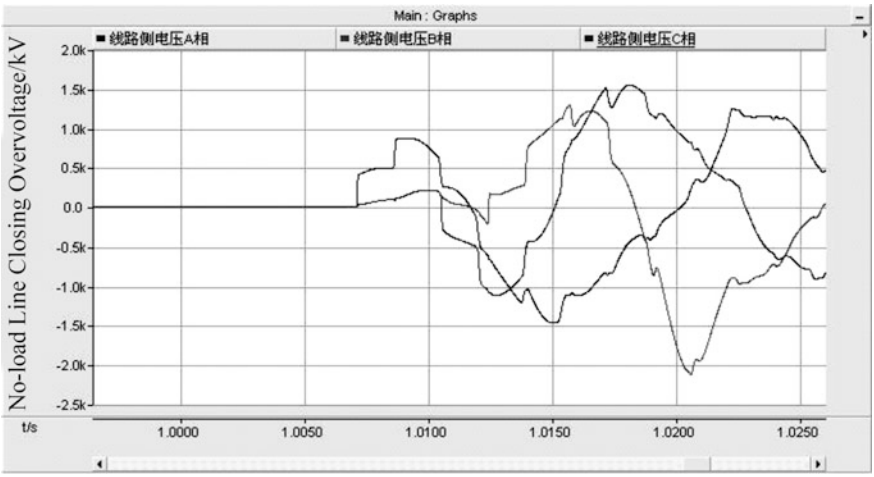

Fig. 6.28 Voltage at the line side in closing sequence under the maximum no-load line closing overvoltage

6.3.2.2 Simulation of the Single-Phase Reclosing Overvoltage

Unlike the closing of no-load line, the operating sequence of the single-phase reclosure is complicated, with model diagram, as shown in Fig. 6.29. For the parameters of line and tower, etc., refer to that of Southeast Shanxi–Nanyang–Jingmen demonstration line established in China.

When a single-phase ground fault occurs at phase C of the line, the phase C connected with the circuit breaker BRK1 and BRK2 opens early or late to interrupt the fault current after a short while (usually tens of milliseconds or over hundred milliseconds), while phase A and B are still operated normally. The phase C becomes a no-load phase with ground fault, and there is a secondary arc current at the place where the fault occurs; with the secondary arc current extinguished gradually, the fault disappears and there is an oscillatory induced voltage at phase C; the phase C of BRK1 and BRK2 automatically recloses in about 1 s after occurrence of the fault, respectively (a time difference in millisecond exists instantly at the time of the actual closing of these two circuit breakers), an overvoltage appears in the line, and the single-phase reclosure process finishes. During reclosure, if the induced voltage polarity of phase C is reverse to the power supply polarity, a high amplitude overvoltage will appears. In the software simulation, it is possible to take the closing time of the fault phase as a random variable distributed in a cycle, so that it is possible to obtain a 2% statistical overvoltage by numerous calculations and take the maximum value from the statistical overvoltage of each point along the line.

The single-phase reclosing overvoltage waveform is as shown in Fig. 6.30.

The high-voltage shunt reactor compensation has a huge influence on the induced voltage at fault phase. Figures 6.31 and 6.32 show the decay waveform and beat-frequency waveform at compensation degree of 80%, respectively.

For a line with high-voltage shunt reactor compensation, the induced voltage of the fault phase can be minimized by accurate coordination of the high-voltage shunt reactor and small reactor. This has a certain effect in limiting the single-phase reclosing overvoltage. However, without high-voltage shunt reactor compensation, a certain induced voltage always exists at fault phase, which is unbeneficial to effectively limiting the reclosing overvoltage.

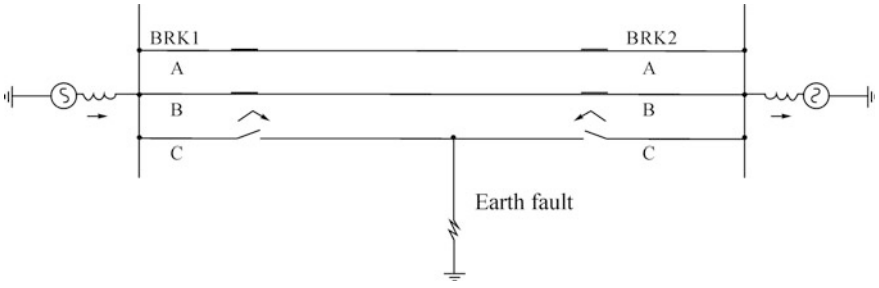

Fig. 6.29 Sketch for single-phase reclosing overvoltage

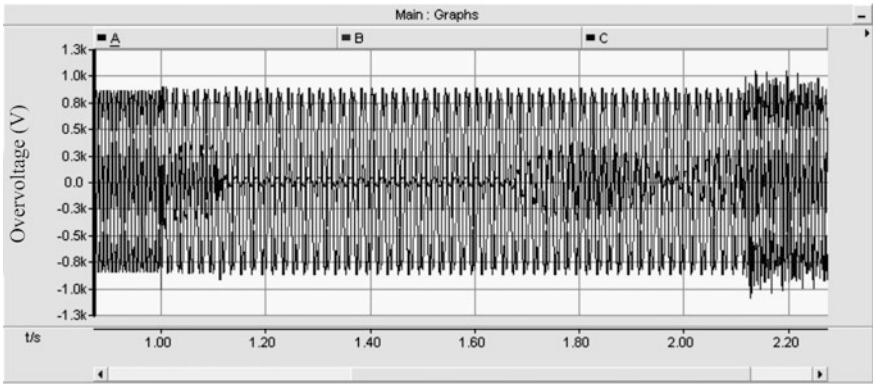

Fig. 6.30 Sketch for single-phase reclosing overvoltage waveform

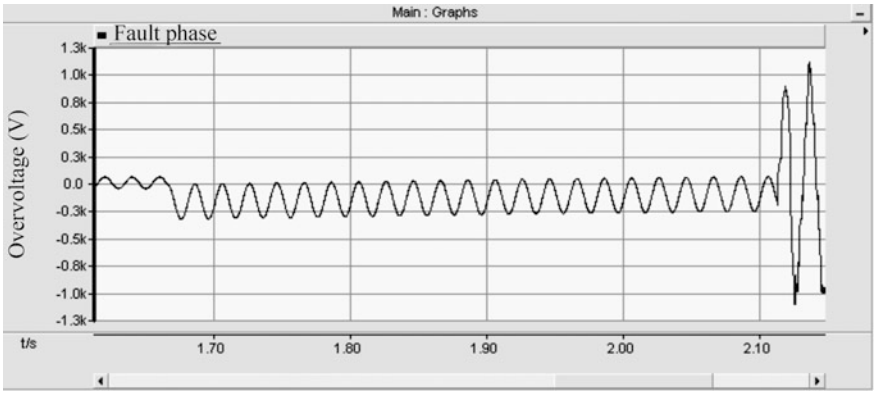

Fig. 6.31 Induced voltage of fault phase without the high-voltage shunt reactor

6.3.3 Analysis of Influence Factors

6.3.3.1 General

The closing overvoltage amplitude is influenced by many factors, such as line length, system reactance, transmission power, closed break-point voltage difference, three-phase non-synchronism, line loss, and etc.

1. Line length

For an overvoltage amplitude, with the increase in the line length, the voltage of the line tail end rises rapidly due to capacitance effect, and the overvoltage amplitude increases accordingly, so the closing overvoltage of a long line is more severe than the short line.

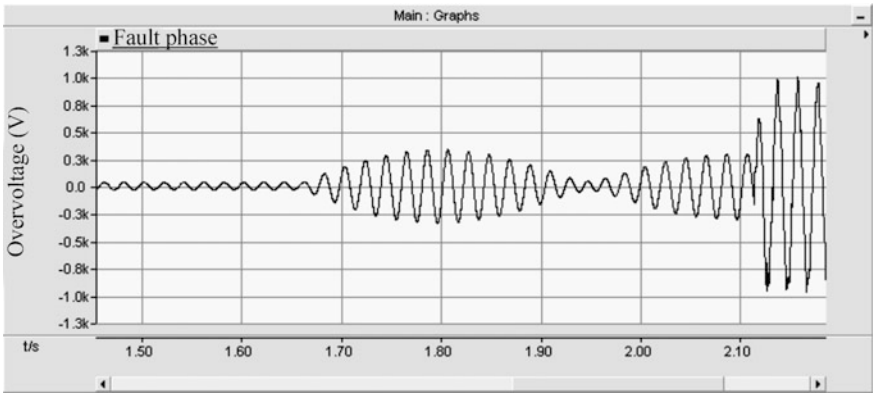

Fig. 6.32 Induced voltage of fault phase under 80% compensation

2. System reactance

For a no-load closing overvoltage, when the circuit breaker closes, the positive sequence impedance of the system is equivalent to the extension of the line length, so it enlarges the no-load line closing overvoltage. In general, the greater the positive sequence impedance is, the greater the overvoltage is.

3. Transmission power

For the single-phase reclosing overvoltage, the sound phase can, through phase-to-phase coupling, exert an influence on the fault phase, so the transmission power of the line is also one of the factors that influencing the overvoltage. The higher the transmission power is, the greater the overvoltage is.

4. Three-phase non-synchronism

During closing of the circuit breaker, a certain degree of non-synchronism always exists between three phases. For a 500 kV circuit breaker, the non-synchronism can be between 10 and 20 ms. The UHV circuit breaker also has a certain non-synchronism, about 5 ms. The simulation test shows that the non-synchronism results in the increase in overvoltage amplitude by 10–30%.

5. Closed break-point voltage difference

In an instant of line closing, the larger the break-point voltage difference of the circuit breaker is, the more violent the closing transition process is, and often the higher the overvoltage amplitude produced in the oscillation process is.

6. Line loss

The resistance and corona loss of the transmission line, to a great extent, can reduce the closing overvoltage amplitude. The higher the overvoltage amplitude is,

the smaller the conductor diameter is, the lower the initial natural frequency of vibration is (the longer the overvoltage duration is), and the more obvious the effect on voltage drop is.

6.3.3.2 Analysis of Single-Circuit Line

1. No-load line closing overvoltage

Calculation of the closing overvoltage amplitude in the no-load line under different line lengths is as shown in Table 6.27.

It can be known from Table 6.27 that, with the increase in the line length, the no-load line closing overvoltage increases obviously, and after the use of closing resistor, the overvoltage is limited significantly.

2. Single-phase reclosing overvoltage

The following analyzes main influence factors (including grounding factor and line transmission power, etc.) of the single-phase reclosing overvoltage.

(1) Analysis on the influence by grounding fault

The ground fault has a certain influence on the single-phase reclosing overvoltage. The ground fault factor mainly includes ground fault position and resistance at the grounding position. The following first analyzes their influential degree on the overvoltage.

As the UHVAC lines in China are often long, e.g., Southeast Shanxi–Nanyang–Jingmen demonstration line that is composed of two line sections, approx. 300 km for each section, and Huainan–Anhui–Zhejiang–Shanghai double-circuit line, of which Huainan–Anhui section is 326 km, so here takes the 300 km UHV line as an example for analysis. The calculation results are as shown in Tables 6.28 and 6.29.

The results show that the ground fault position and grounding resistance value have a small influence on the single-phase reclosing overvoltage, and with closing resistor adopted to limit overvoltage, the maximum difference should not exceed 0.004 p.u. The difference does not have substantial influence can be neglected. This is because the ground fault has disappeared before the single-phase reclosure, and the voltage of the fault line has stabilized, so the grounding factor has an unobvious influence on the reclosing overvoltage.

Table 6.27 No-load line closing overvoltage under different line lengths

Line length/km	No-load line closing overvoltage/p.u.				
	100	200	300	400	500
Without closing resistor	1.794	1.834	1.921	2.048	2.144
With closing resistor	1.139	1.145	1.151	1.257	1.427

Thus, the ground fault position is placed in the middle part of the line for the research below, with grounding resistance being 50 Ω.

(2) Analysis on the influence by line length and transmission power

During single-phase reclosure, the other two phases of the line are still in operation state, so the value of the transmission power may influence the overvoltage. The following analyzes the influential degree of the transmission power on the reclosing overvoltage in the case of different line lengths. During calculation, it is required to ensure that the busbar voltage keeps the same at different transmission power levels, as shown in Fig. 6.33.

It can be known from Fig. 6.33 that:

① With the increase in the line length, the single-phase reclosing overvoltage increases obviously. It can be know from the contents above that, according to the lumped parameter model of closing overvoltage, the longer the line is, the larger the equivalent line inductance is, so that the line inductance rise effect should be stronger, resulting in a greater closing overvoltage.

② With the increase in the line transmission power, the single-phase reclosing overvoltage rises obviously, and the overvoltage rise amplitude of the long line is larger than that of the short line.

Table 6.28 Influence on single-phase reclosing overvoltage by ground fault positions

Distance from fault point to head end/km		Single-phase reclosing overvoltage/p.u.				
		0	75	150	225	300
Single-circuit line	Without closing resistor	1.996	2.004	2.014	2.023	2.027
	With closing resistor of 300 Ω	1.276	1.276	1.276	1.276	1.276
Double-circuit line	Without closing resistor	1.716	1.716	1.715	1.713	1.710
	With closing resistor of 300 Ω	1.264	1.265	1.265	1.266	1.266

Table 6.29 Influence on single-phase reclosing overvoltage by resistance at grounding points

Grounding resistance/Ω		Single-phase reclosing overvoltage/p.u.				
		10	20	50	100	200
Single-circuit line	Without closing resistor	2.011	2.014	2.014	2.014	2.014
	With closing resistor of 300 Ω	1.276	1.276	1.276	1.276	1.276
Double-circuit line	Without closing resistor	1.727	1.720	1.715	1.714	1.714
	With closing resistor of 300 Ω	1.269	1.267	1.265	1.265	1.265

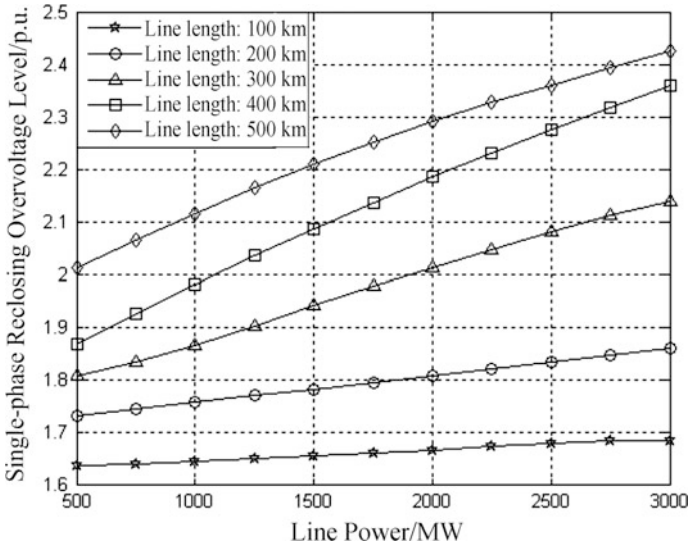

Fig. 6.33 Single-phase reclosing overvoltage under different transmission powers

It can be known from the previous analysis that, for the single-phase reclosing overvoltage, its amplitude mainly depends on the voltage difference between both ends of the circuit breaker in an instant of reclosing, while the difference depends on the induced voltage U_h of the line and power supply voltage E of the reclosure ends. When the line bears different power levels, the induced voltage amplitude U_h of the sound phase voltage at the fault phase does not vary obviously, while the busbar voltage E varies apparently.

This is because, for the purpose of meeting the long-distance and high-power transmission requirements in the UHV line, the LV reactive power compensation is often used to maintain stable voltage of the line. Thus, the higher the transmission power is, the larger the LV capacitive reactive power capacity needing to be compensated is, and when a single-phase fault appears in the line and the fault is cleared subsequently, the LV capacitive reactive power capacity cannot respond to it in time, so that the busbar voltage E at closing end undergoes a greater increase. Especially where a high resistance type UHV transformer is used, its large leakage reactance causes a higher voltage E at outlet side of the transformer in case of a large transmission power in the UHV system (equivalent to the increase in power supply voltage at the closing end). In this case, a more severe reclosing overvoltage produces [5, 6].

3. Comparative research on no-load line closing overvoltage and single-phase grounding reclosing overvoltage

For a UHV line with a certain length, when the line transmission power is small, the no-load line closing overvoltage often exceeds the single-phase grounding

reclosing overvoltage. And when the transmission power further increases, the single ground reclosing overvoltage increases accordingly, being probable to exceed the no-load line closing overvoltage. Table 6.30 gives an amplitude comparison between the no-load line closing overvoltage and single-phase reclosing overvoltage under the circumstance of different line lengths and transmission power levels, and Table 6.30 gives the corresponding line transmission power levels when the no-load line closing overvoltage value of a line with different line lengths is the same to the single-phase reclosing overvoltage value.

It can be known from Tables 6.30 and 6.31 that, when the line is short, the no-load line closing overvoltage is usually more severe than the single-phase reclosing overvoltage. If the line length is 200 km and the line transmission power is less than 2500 MW, the no-load line closing overvoltage is more severe. While the line is longer, the single-phase reclosing overvoltage is usually more severe than the no-load line closing overvoltage. If the line length is 400 km and the line transmission power is more than 1100 MW, the reclosing overvoltage is more severe.

This is because the total reactive power for compensation of the line is proportional to the line length, and when the line is short, even if the transmission power is large, its reactive power compensation is small; therefore, the upgrading effect on the reclosing overvoltage is unobvious. In this case, the no-load line closing overvoltage will result in more severe danger due to the combination of violent transient process in an instant of closing and three-phase non-synchronism during closing and other factors [1]. Hence, the no-load closing overvoltage is more than the reclosing overvoltage when the line is shorted.

When the line is long, a great amount of reactor power is required to be compensated during power transmission, and the upgrading effect on the reclosing overvoltage is obvious, and the overvoltage will become more severe. Furthermore, as the no-load line closing operation is a planned operation and when the longer line is closed, it is often required to limit the busbar-end voltage, enabling the line voltage not to exceed the maximum voltage of the system after the line is closed and stabilized. Therefore, under the circumstance of long line and high power, the single-phase reclosing overvoltage is more severe than the no-load line overvoltage.

Table 6.30 Comparison between no-load line closing overvoltage and single-phase reclosing overvoltage under different line lengths and transmission powers

Line length/km		100	200	300	400	500
No-load line closing overvoltage/p.u.		1.794	1.834	1.921	2.048	2.144
Single-phase reclosing overvoltage (p.u.)	1000 MW[a]	1.646	1.758	1.856	1.983	2.128
	3000 MW[a]	1.686	1.862	2.141	2.362	2.429

[a]Denotes the single-phase reclosing overvoltage amplitude of the line at this transmission power level

Table 6.31 Corresponding line transmission power when the no-load line closing overvoltage is identical to the single-phase reclosing overvoltage under different line lengths

Line length/km	100	200	300	400	500
No-load line closing overvoltage/p.u.	1.794	1.834	1.921	2.048	2.144
[a]Corresponding transmission power of single-phase reclosing overvoltage/MW	>3000	2500	1400	1100	1000

[a]Denotes that, in the condition of the equivalent line length, the no-load line closing overvoltage is equivalent to the corresponding power of the single-phase reclosing overvoltage amplitude

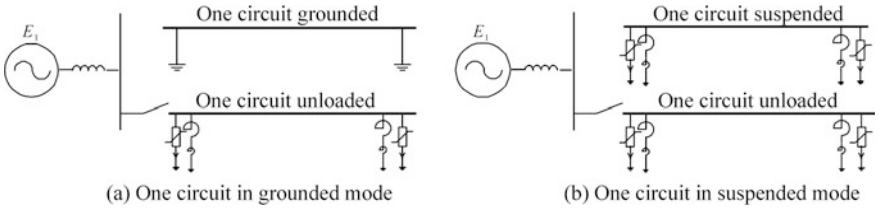

Fig. 6.34 Single-circuit operating mode

6.3.3.3 Double-Circuit Line Analysis

1. No-load line closing overvoltage

(1) Single-circuit operating mode

The single-circuit operating mode means that one circuit of the double-circuit line is grounded or in suspension state, and the other circuit is subject to the no-load line closing operation, as shown in Fig. 6.34.

The following calculates and analyzes the influential degree of both operation states on the no-load line closing overvoltage, as shown in Table 6.32.

The results show that, in both modes, the difference of no-load line closing overvoltage is relatively small, and with a closing resistor adopted, the maximum difference is only 0.006 p.u., which can be neglected.

This is because, with respect to the no-load line closing overvoltage, the factors that having significant influence mainly include closing-end busbar voltage, three-phase non-synchronism, and internal resistance of the system. However, both single-circuit operating modes mentioned above differ only by the coupling between both circuits, and the difference has a little influence on the equivalent parameters of the no-load line. Moreover, the research shows that the difference between the line towers has a little influence on the no-load line closing overvoltage. Hence, the no-load line closing overvoltage in both modes differs slightly, and it is possible to only calculate the overvoltage in one of both modes.

(2) Double-circuit operating mode

The double-circuit operating mode means that one circuit of the double-circuit line is in switch-on operation state, and the other circuit of the double-circuit is subject to no-load line closing operation, as shown in Fig. 6.35.

Table 6.32 No-load line closing overvoltage in different single-circuit operating modes

Single-circuit operating mode			One circuit grounded	One circuit suspended
Line length	100 km	Without closing resistor	1.78	1.798
		With closing resistor	1.12	1.118
	300 km	Without closing resistor	1.901	1.883
		With closing resistor	1.155	1.153
	500 km	Without closing resistor	2.23	2.218
		With closing resistor	1.423	1.429

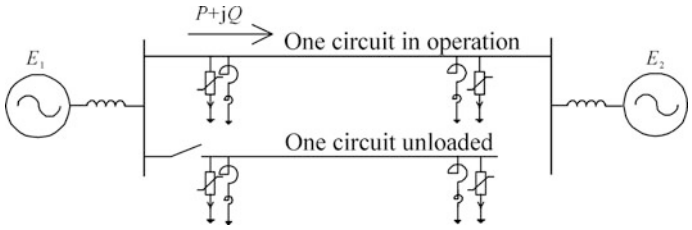

Fig. 6.35 Double-circuit operating mode

In this operating mode, as one circuit has been in steady state before closing and the line voltage and current are symmetrical at three phases, the operating line will not produce induced voltage in the no-load line. Hence, the initial voltage of no-load line is also zero. Therefore, the following specifically analyzes the influence on the closing overvoltage of the no-load line due to difference in transmission power of the operating line. The research should be carried out by selecting 100, 300, and 500 km line, respectively, and when calculating, it is required to ensure the busbar voltage keeps unchanged, as shown in Fig. 6.36.

The results show that the difference in transmission power of one circuit has a little influence on the no-load line closing overvoltage of other circuit, with difference not more than 0.01 p.u. Therefore, the overvoltage difference is small at different transmission power levels, and it is possible to only calculate the overvoltage in one of these modes.

The cause is analyzed as follows: when one circuit of the double-circuit line is subject to power transmission in the power transmission mode of the power supplies at both ends of the line, the different transmission power has no influence on the structure of the electric power grid, so the power supply characteristics are fully consistent at the busbar side of the closing end after the equivalent of the internal. Moreover, as the operating line with different power levels is in steady state before and after closing, no inductive influence is exerted on the closing line. Hence, the transmission power level of this circuit line has a little influence on the no-load line closing overvoltage.

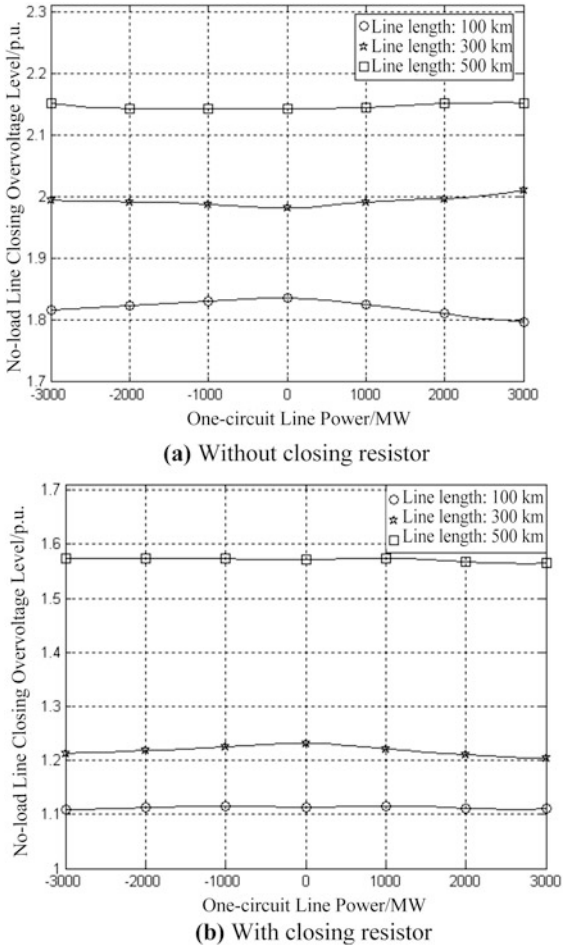

Fig. 6.36 No-load line closing overvoltage in one circuit line with different transmission powers. *Note* The minus sign of the power denotes a reverse transmission direction

In fact, if spacing between two circuit lines increases artificially, it also has a little influence on the no-load line closing overvoltage, and the calculation results are as shown in Table 6.33.

The results show that, under the influence of the operating circuit on the no-load line closing overvoltage of the other circuit line through the spacing between circuits, the maximum voltage difference is less than 0.03 p.u. without closing resistor adopted, and does not exceed 0.05 p.u. with closing resistor adopted, having a small influence, generally speaking. If this difference is neglected, the no-load line closing overvoltage model in double-circuit operating mode can be equivalent as

Table 6.33 Influence on no-load line closing overvoltage by spacing between two circuits of lines

Line length (km)	Closing resistor	Spacing between two circuits of lines/km				
		Normal	0.5	1	10	50
100	No	1.826	1.831	1.83	1.831	1.83
	Yes	1.116	1.109	1.107	1.109	1.109
300	No	1.982	1.968	1.962	1.96	1.961
	Yes	1.202	1.16	1.158	1.157	1.157
500	No	2.146	2.121	2.117	2.116	2.116
	Yes	1.575	1.597	1.596	1.595	1.595

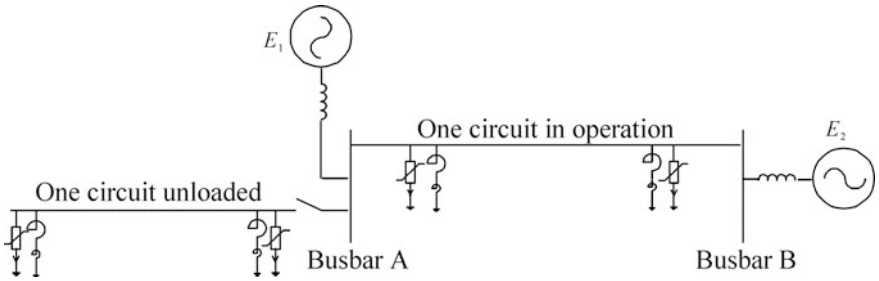

Fig. 6.37 Equivalent double-circuit no-load line closing model

shown in Fig. 6.37, and at this moment, there is not any coupling effect due to a large spacing between circuits.

For no-load line closing operation of one circuit line of the double-circuit line, where the internal resistance at one end of power supply E_1 is infinite (equivalent to disconnection of E_1 from busbar A), the closing process of the no-load line is to close the other line section based on one line section, being equivalent to closing a line with two times of length. This enables the no-load line closing overvoltage to be more severe, compared to closing purely based on the power supply. Especially when the line is very long, the no-load line closing overvoltage is difficult to be controlled. Similarly, when the internal resistance of the power supply is larger (i.e., the power supply capacity is small), the influence of power supply E_1 on the voltage at busbar A is not strong, the closing of the no-load line also aggravates the no-load line closing overvoltage of this line at this moment. To effectively limit the short-circuit current, the UHVAC system adopts a high resistance transformer, resulting in a large power supply internal resistance in most conditions. Therefore, the no-load line closing overvoltage is too high when one circuit of the double-circuit line in the UHVAC system is put into operation, where should provide an effective protection. The following takes a 500 km line as an example to carry out analysis. During calculation, it is required to maintain the busbar voltage at both ends and transmission power of one circuit line unchanged, but only change the internal resistance of E_1 power supply. The results are as shown in Table 6.34.

Table 6.34 Influence on no-load line closing overvoltage of double-circuit line by power supply capacity

No-load line closing overvoltage of one circuit of line when the other circuit of line is in operation for the double-circuit line/p.u.					
Internal resistance of E_1 power supply/Ω		50	100	150	200
Closing resistor	No	1.330	1.595	1.643	1.664
	Yes	1.378	1.526	1.608	1.692

Table 6.35 Single-phase reclosing overvoltage under double-circuit operating mode

Line length (km)	Closing resistor	Transmission power/MW			
		2 × 500	2 × 1000	2 × 1500	2 × 2000
100	No	1.732	1.734	1.720	1.717
	Yes	1.169	1.174	1.175	1.170
300	No	1.832	1.839	1.836	1.824
	Yes	1.261	1.267	1.284	1.290
500	No	1.899	1.927	1.968	2.009
	Yes	1.335	1.323	1.322	1.339

The results show that the larger the internal resistance of E_1 power supply (i.e., the smaller the power supply capacity is), the more severe the no-load line closing overvoltage is, which is consistent with the analysis given previously.

2. Single-Phase Reclosing Overvoltage

For the single-circuit operating mode in a double-circuit line, the change law of the single-phase reclosing overvoltage is identical to the single-circuit line, which is not repeated here.

For the double-circuit operating mode in a double-circuit line, the following takes 100, 300, and 500 km line for analysis, and conducts a research on the influential degree of the line transmission power on the overvoltage. During calculation, it is required to maintain a same busbar voltage, and the results are as shown in Table 6.35.

The results show that the voltage difference of the single-phase reclosing overvoltage is small at different line transmission power levels for the double-circuit line, and with a closing resistor adopted, the maximum voltage difference does not exceed 0.03 p.u., having a small influence.

Unlike the single-circuit line, when the double-circuit line is in operation and after a fault occurs at one phase of one circuit and is cleared, the most part of the power that should have been borne by this phase can be equivalently transferred to other five phases, so the requirement for LV reactive power capacity is varied slightly. Therefore, the busbar voltage at the closing ends does not rise significantly, and the change in overvoltage is not apparent.

6.3.3.4 Analysis on the High-Voltage Shunt Reactor and Small Reactor

1. Influence by high-voltage shunt reactor compensation degree

Due to large reactive power consumption, the UHV line is often compensated by the high-voltage shunt reactor, with compensation degree usually more than 60%. The following analyzes its influence on the closing overvoltage of a 300 km line. The results are as shown in Table 6.36.

Table 6.36 No-load line closing overvoltage under different compensation degrees

High-voltage shunt reactor compensation degree (%)		60	70	80	90
No-load line closing overvoltage/p.u.	Without closing resistor	1.912	1.902	1.892	1.881
	300 Ω	1.276	1.223	1.174	1.154
Single-phase reclosing overvoltage/p.u.	Without closing resistor	1.912	1.890	1.867	1.844
	300 Ω	1.264	1.249	1.239	1.233

It can be known from the results that the larger the high-voltage shunt reactor compensation degree is, the smaller the closing overvoltage is, but the overvoltage amplitude increases slightly when the compensation degree increases from 60 to 90%, so the compensation degree has a small influence on the closing overvoltage, and an excessively high compensation degree has an unobvious limitation on the closing overvoltage.

2. Analysis on Small Reactor Selection

The following analyzes the influence of the small reactor on the closing overvoltage through single-circuit line and double-circuit line.

(1) Analysis on single-circuit line

For the single-circuit line, the induction is produced by the sound phase at fault phase through phase-to-phase coupling during single-phase reclosure, so that a circuit is formed at open phase through the phase-to-ground capacitance and high-voltage shunt reactor with compensation. At this moment, the line is in open-phase operation state. The beat-frequency voltage amplitude of the open-phase depends on the phase-to-ground and phase-to-phase compensation of this circuit, while the small reactor is used to coordinate the phase-to-ground and phase-to-phase compensation. Under the influence of the high-voltage shunt reactor and small reactor, the steady-state induced voltage at the open phase is as shown in the following equation:

$$\dot{U}_{\mathrm{h}} = -\dot{E}_{\mathrm{A}} \times \frac{X_0}{2(X_{\mathrm{m}} + X_0)}, \tag{6.10}$$

where

X_0 the impedance produced after L_0 and C_0 are paralleled ($L_0//C_0$);
X_m the impedance produced after the $L_m/2$ and $2C_m$ are paralleled ($L_m/2//2C_m$), as shown in Fig. 6.23.

Improper coordination of the parameters enables X_m and X_0 approximated to each other in the size and opposite to each other in the sign, resulting in resonance. Figure 6.38 shows the resonance overvoltage at fault position when the small reactor differs.

Theoretically, where parameters of the line can be accurately determined, it is possible to better compensate phase-to-phase and phase-to-ground capacitance and no resonance overvoltage occurs at any compensation degree when the small reactor is determined by the principle of full phase-to-phase compensation at HV reactor compensation degree. However, the investigation and determination of the small reactor are carried out usually before the project construction. At the moment, parameters of the UHV line are not measured accurately, but they are calculated according to the theoretical parameter values and high-voltage shunt reactor compensation degree of the HV line to be constructed, so as to result in a certain difference between the small reactor value obtained by research and actual resistance required by the line. Furthermore, considering manufacturing error of the small reactor and compensation error of the high-voltage shunt reactor, the difference further increases. Meanwhile, the three-phase imbalanced difference of the line parameters also has an influence on the accurate value of the high-voltage shunt reactor and small reactor. Moreover, the fault system will also present a certain deviation for the reference frequency thereof due to instantaneous change in the power. The combined action of those factors results in the increase in probability of resonance occurrence in practical operation of the line.

Therefore, the selection of the high-voltage shunt reactor and small reactor is directly related to the open-phase resonance overvoltage of the line. To avoid the influence by the factors above, the high-voltage shunt reactor compensation degree should not be high, enabling these deviations to be covered in a large margin. The research shows that the high-voltage shunt reactor compensation degree should not exceed 90%, and when the compensation degree is larger, especially approximating to 100%, the danger resulted from resonance of the line increases significantly, being unbeneficial to effectively limiting the single-phase reclosing overvoltage [14, 15]. Meanwhile, it is possible to calculate an appropriate small reactor value through line parameters once the high-voltage shunt reactor compensation degree is determined.

(2) Analysis on double-circuit line

For the single-phase reclosure of double-circuit lines, the condition is more complicated. At this moment, the induction is produced at fault phase through phase-to-phase coupling under the influence of the sound phase. The selection of the small reactor of the double-circuit line should comprehensively consider these factors.

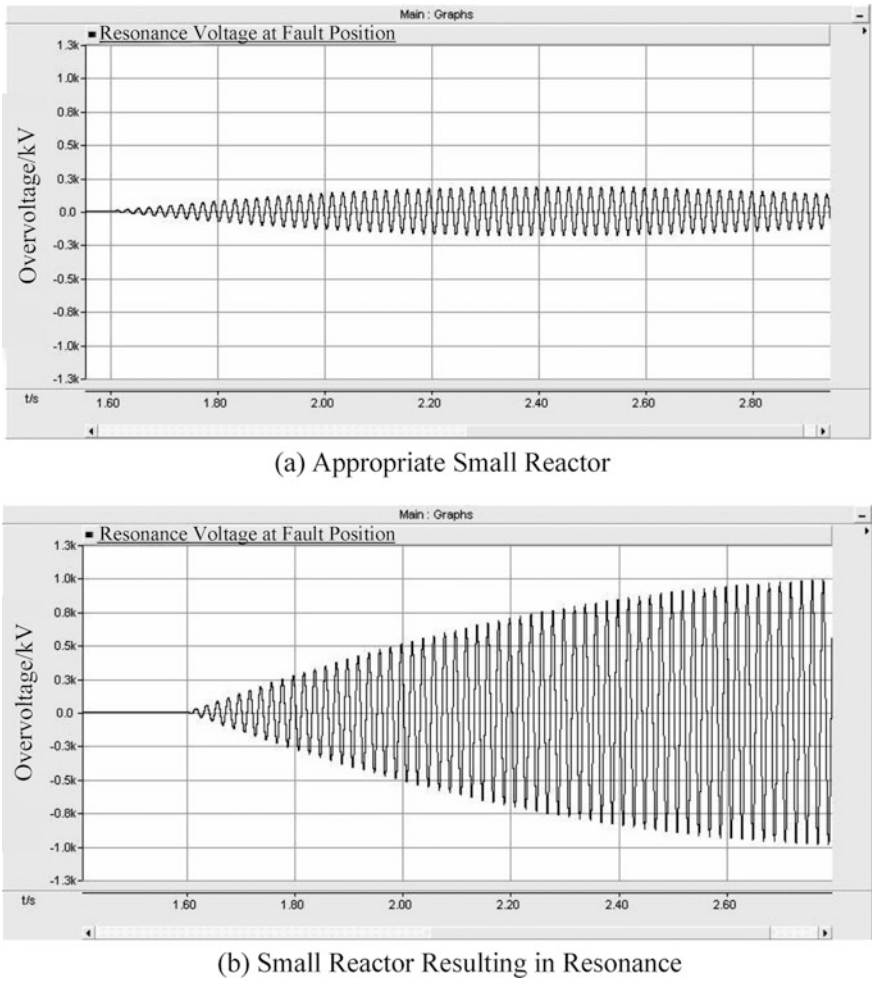

Fig. 6.38 Resonance overvoltage at fault position in case of use of different small reactors

The equivalent phase-to-ground and phase-to-phase capacitance of the open phase are varied (because the other circuit influences the positive and zero-sequence parameters of the fault circuit in different modes) in different operating modes (including one circuit grounded, one circuit suspended, and one circuit operated), so the calculated value of the small reactor that most appropriate to each operating modes differs significantly, resulting in a different reclosing overvoltage. In this case, the small reactor of the double-circuit line should be selected by comprehensively considering several operating modes.

6.3.4 Limitation Measures

Through the analysis mentioned above, the closing overvoltage of the UHVAC system is usually limited by the following measures.

(1) Avoiding resonance

First, adopt an appropriate high-voltage shunt reactor compensation degree being not more than 90% where the power frequency overvoltage conditions are met; then, select an appropriate small reactor to avoid a large resonance and limit the single-phase reclosing overvoltage effectively.

(2) Adopting closing resistor

With closing resistor adopted, it is possible to achieve better limitation effect. Moreover, a longer line should be provided with a closing resistor with lower resistance, and a shorter line should be provided with a closing resistor with higher resistance, being more beneficial to limiting the no-load line closing overvoltage. Meanwhile, as the double-circuit line can be operated in several modes, the selection of closing resistor does not only should meet the requirements for limiting the no-load line closing overvoltage and single-phase reclosing overvoltage, but also should meet the requirements for limiting the closing overvoltage in several operation modes [1, 3].

For the no-load line closing overvoltage, if the power supply capacity is small (the internal resistance is large), the overvoltage produced by the other circuit line is more severe when closing under the condition that one circuit line has been put into operation. Therefore, it is required to close the busbar at larger power supply capacity side first during closing. For the single-phase reclosing overvoltage, it is required to attach importance to limiting the overvoltage when the transmission power is very large.

6.3.5 Research on Applicability of Closing Resistors for EHV and UHVAC Transmission Line Circuit Breakers

In EHV and UHVAC grids, in view of controlling the overvoltage, they are usually operated by single-phase reclosure method. Therefore, the closing overvoltage mainly includes no-load line closing overvoltage and single-phase reclosing overvoltage, of which no-load line closing overvoltage has more severe impairment due to consideration of violent transient process in an instant of closing, capacitance rise effect of the line, and three-phase synchronism during closing and other factors. The overvoltage amplitude can reach 2.0 p.u. or more when without limitation measures, and does not meet the specification that the allowable switching overvoltage value of the EHV and UHV systems should not be more than 2.0 and 1.7 p.u.,

respectively. Therefore, reasonable and effective limitation of no-load line closing overvoltage is the key in the research of switching overvoltage. At present, the closing resistor is usually used to limit the no-load line closing overvoltage; in addition, some literatures also report the research results on limitation of this overvoltage by use of MOAs in place of closing resistor.

Generally speaking, the circuit breaker with closing resistor, due to its complicated structure, is prone to accident, and having a certain safety risk. Practically, even without closing resistor adopted, the no-load line closing overvoltage is approx. 2.0 p.u. Considering that the allowable overvoltage is limited to 2.0 p.u. in a 500 kV AC system and the 500 kV line in China presents a trend of short distance power transmission and the capacitance rise effect thereof is in a low level, and hence, the overvoltage may also meet the limitation requirements specified in the 500 kV system specification under protection of MOAs at both ends of the line. In fact, closing resistors are canceled in partial lines around the world, without overvoltage out-of-specification problems caused accordingly. Therefore, cancelation of closing resistor has a practical feasibility. At present, the problems on closing resistor, discussed in published literatures, are subject to qualitative analysis, and up to now, no quantitative conclusion about how long the 500 kV transmission line can cancel the closing resistor has been made in any research. Therefore, this section lays an emphasis on quantitative analysis with respect to closing resistor of EHV and UHVAC transmission line circuit breakers, and from the perspective of limiting the no-load line closing overvoltage, the software simulation technique is used to discuss the applicability of the closing resistor in the 500 kV system, and give a quantitative range of a line length for cancelation of the closing resistor, which is for reference in engineering practice [15]. Furthermore, a feasibility research is carried out for cancelation of closing resistors in the 1000 kV UHV system. The results show that the difficulty in limitation of the UHV system increases significantly as the allowable limit value of the switching overvoltage is decreased to 1.7 p.u., and due to the long line in normal condition and large capacitance rise effect, it is difficult to meet the overvoltage limitation requirement only by use of MOAs, so it is usually required to adopt closing resistors.

6.3.5.1 Analysis on 500 kV AC Line

1. Simulation model

Figure 6.39 shows the no-load line closing overvoltage model in three-phase, which is composed of power supply, non-synchronous circuit breaker, no-load line, and MOA, etc. During the simulation of 500–1000 kV line, due to the use of different poles and towers and conductors for lines at different voltage levels, the model parameters must be adjusted, but its structure is not changed.

2. MOA parameters

The 500 kV transmission line simulation model adopts the typical 500 kV line MOAs in the specification, with specific parameters as shown in Table 6.37.

3. Line parameters

Many types of conductors and poles and towers are used for 500 kV AC line in China, it is possible to exert the influence on the no-load line closing overvoltage. With respect to several common types of conductors and poles and towers, the following calculates and analyzes their influential degree of the overvoltage amplitude. To ensure other conditions are consistent, the only parameter of the conductors or poles and towers is changed during calculation, and the results are shown in Tables 6.38 and 6.39.

The calculation results show that the difference in conductor types and tower parameters has a small influence on the no-load line closing overvoltage, and the maximum voltage difference is only 0.008 p.u. for the former, and only 0.006 p.u. for the latter, with no substantial influence on the calculation results, so their influence can be neglected.

In the research given in this section, the conductor type used is steel-cored aluminum strand 4× LGJ-400/35, with splitting spacing of 450 mm, the pole and tower of the line used are ZM1 cat-head tower. Such type of conductors and poles and towers and their parameters have widely been used for typical design of 500 kV system in China.

4. System conditions

The system conditions that will influence the no-load line closing overvoltage mainly include busbar voltage at the closing end, three-phase non-synchronism, and

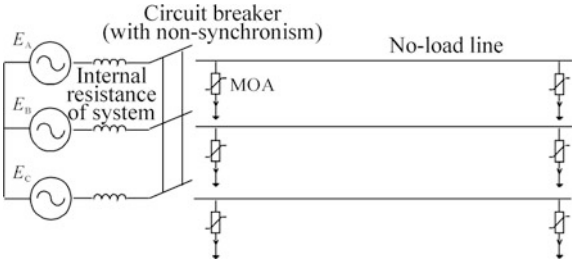

Fig. 6.39 Simulation model of no-load line closing overvoltage

Table 6.37 Typical characteristic parameters of MOA in 500 kV AC system

Rated voltage/kV	Continuous operating voltage/kV	DC 1 mA reference voltage (Peak)/kV	Switching impulse residual voltage (Peak)/kV	Lightning impulse residual voltage (Peak)/kV
444	324	597	907	1106

Table 6.38 Influence on no-load line closing overvoltage by different conductor models

Specifications of common conductors	Outer diameter/mm	DC resistance/Ω· km^{-1}	Overvoltage/p.u.
LGJ-400/35	26.82	0.073 89	1.908
LGJ-400/50	27.63	0.072 32	1.902
LGJ-500/35	30	0.058 12	1.909
LGJ-500/45	30	0.059 12	1.909
LGJ-630/45	33.6	0.046 33	1.910

Table 6.39 Influence on no-load line closing overvoltage by different types of towers

Specifications of common towers	Nominal height/m	Horizontal spacing between two neighboring phases/m	Vertical spacing between middle and side phases/m	Overvoltage/p.u.
Cat-head type tower ZM1	36.0	7.5	9.0	1.908
Cat-head type tower ZM2	39.0	8.0	9.3	1.905
Cat-head type tower ZM3	42.0	8.75	11.25	1.903
Cup type tower ZB1	42.0	11.0	0	1.905
Cup type tower ZB2	48.0	11.6	0	1.904
Cup type tower ZB3	48.0	12.0	0	1.902

internal resistance of the system. In the research, these three parameters are selected on the basis of conditions that producing the most severe no-load line closing overvoltage.

(1) The busbar voltage is the basis of grid overvoltage amplitude. This means that the higher the voltage level is, the larger the absolute value of the overvoltage is. Therefore, the voltage at each node is usually controlled within a certain range in a forced manner to maintain safe stability of the grid in the electric power system. Adhering to the principle of strictness, the busbar voltage is set to the maximum line voltage, i.e., 550 kV, during calculation.
(2) The three-phase non-synchronism means when the no-load line closes, there is a certain difference between the actual closing time of each phase of the circuit breaker after reception of closing signal. The simulation test and simulation research show that the no-load line closing overvoltage tends to be severe under the influence of three-phase non-synchronism, and the overvoltage amplitude can increase by 10–30%, while the non-synchronism difference has a small

influence on the overvoltage. The non-synchronism of 500 kV circuit breaker can reach 10 ms, and this value is taken for calculation in this section.

(3) The internal resistance of the system means the positive sequence impedance of the power supply being subject to equivalency, including resistance and inductance. The damping action exerted on the overvoltage increases as the resistance intensifies, so the overvoltage becomes smaller; the transient process becomes more violent as the inductance part intensifies, so the overvoltage becomes higher. Considering that a certain resistance usually exists in the positive sequence impedance after the 500 kV system is subject to equivalency, the positive sequence impedance thereof usually does not exceed 86°. The larger the impedance angle is, the weaker the resistance becomes, and the stronger the inductance becomes, and the higher the overvoltage becomes. Based on the principle of strictness, the positive sequence impedance angle taken in this section is 88°, and it can be deemed that the overvoltage in this condition is more severe than that in a real system.

The statistical data show that the short-circuit current of the 500 kV system in China is within 12.5–75 kA, and it can be known from the short-circuit current calculation equation that the equivalent positive sequence impedance range of the system is approximately within 3–24 Ω. It can be deemed that this range nearly includes the equivalent internal resistance of all 500 kV systems. This section takes the 500 kV line with 100 km length as an example to carry out research on the influence of the internal resistance of the system on the no-load line closing overvoltage, with results as shown in Table 6.40.

It can be known from Table 6.40 that, with the internal resistance of the system increasing, the overvoltage varies without significant law, and this phenomenon occurs for the reason that the resistance and inductance part are increased with the increase in the internal resistance, while their influence trend in the overvoltage is contrary. As the internal resistance of the system within the range above has a little influence on the overvoltage, which is only within 0.03 p.u., without substantial influence on the calculation results. An internal resistance of 10 Ω as typical value is used in the following analysis and calculation.

5. Overvoltage research

(1) Analysis on high-voltage shunt reactor compensation degree

Due to the requirement for reactive power stabilization, the EHVAC line is often installed with high-voltage shunt reactors for compensation. As a limitation measure for the power frequency overvoltage, the high-voltage shunt reactor has a certain limitation on the switching overvoltage of the line. At present, considering that there are many short distance transmission lines with length less than 100 km

Table 6.40 Influence on no-load line closing overvoltage by 500 kV system internal resistance

Internal resistance of system/Ω	3	5	10	15	20	25
Overvoltage/p.u.	1.774	1.757	1.776	1.762	1.766	1.752

Table 6.41 No-load line closing overvoltage of a 100 km-long 500 kV transmission line with high-voltage shunt reactor compensation

Compensation degree/%	0	20	40	60	80	100
Overvoltage/p.u.	1.908	1.906	1.905	1.903	1.902	1.902

in 500 kV systems, a 500 kV line with length of 100 km is taken as an example to research the influence of the high-voltage shunt reactor compensation degree on the no-load line closing overvoltage, with results as shown in Table 6.41.

It can be known from Table 6.41 that the increase in the high-voltage shunt reactor compensation degree can result in the decrease in the no-load line closing overvoltage, but the decrease amplitude is small; when the line is longer, the decrease amplitude increases slightly. Therefore, the high-voltage shunt reactor has a certain limitation on the no-load line closing overvoltage, but its effect is not apparent as a whole.

Based on the principle of strictness, the high-voltage shunt reactor compensation measures are not taken in the following research.

(2) Analysis on line length

The line length is a main factor influencing the overvoltage, whose severity is mainly reflected by the capacitance rise effect. For the no-load line closing overvoltage, in case of no influence of the line capacitance rise effect and three-phase non-synchronism, even without any limitation measures, the maximum theoretical overvoltage value is only 2.0 p.u., and the actual value is less than 2.0 p.u. due to line loss and other influences. In a 500 kV system, MOAs are usually installed at both ends of the line for protection, so the overvoltage is usually not more than 2.0 p.u., and the limitation requirement has been met. If, however, the long line capacitance rise effect is more apparent, it is possible to exceed the limitation requirement. Figure 6.40 shows a curve for the measured capacitance rise effect of a 500 kV line.

It can be known from the results that the severity of the capacitance rise effect increases in exponent law with the increase of the line length, and the longer the line is, the more apparent the effect becomes. According to the estimation equation for the maximum closing overvoltage amplitude (i.e., $U_{\mathrm{MAX}} = 2U_{\text{steady state}} - U_{\text{initial}}$), if the steady-state value after closing (namely the steady-state voltage after the capacitance rise effect considered) becomes higher, the oscillation in the transient process becomes more violent, and the produced overvoltage peak also becomes higher. Therefore, due to the influence of the capacitance rise effect, the closing overvoltage of a shorter line can be easily limited, and however, the closing overvoltage of a longer line is difficult to limit.

To carry out the calculation analysis on the closing overvoltage of lines with different length, the results are as shown in Fig. 6.41.

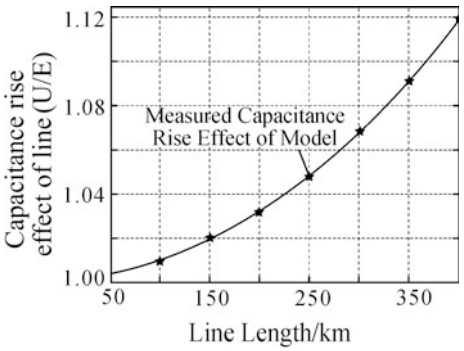

Fig. 6.40 Measured capacitance rise effect of a 500 kV line

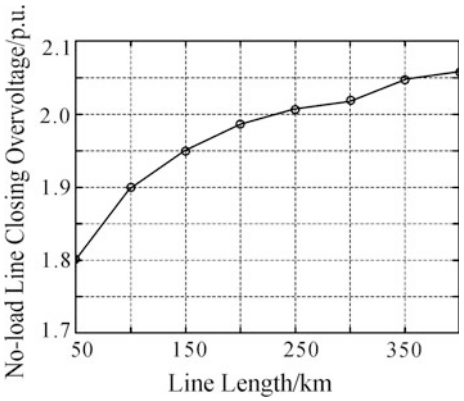

Fig. 6.41 Amplitudes of no-load line closing overvoltage in lines with different lengths

It can be known from Fig. 6.41 that the closing overvoltage amplitude increases with the increase of the line length. The no-load line closing overvoltage for a line with length less than 200 km is less than 2.0 p.u. specified in the specification, and for a line more than 300 km, exceeds the requirement specified in the specification.

(3) Analysis on short-line overvoltage

The distribution of no-load line closing overvoltage along 100 and 200 km 500 kV lines is calculated, respectively, in a "severe" condition that given in this section and without closing resistor adopted, with results as shown in Fig. 6.42.

The following results can be obtained from the calculation:

① When the line length is 100 km, the maximum no-load line closing overvoltage is only 1.91 p.u., which is less than 2.0 p.u. specified in the specification, and has been controlled within the required range with a certain margin. Considering that the no-load line closing overvoltage increases with the increase of the line length due to the capacitance rise effect, so it can be deemed that, even in the most severe system condition and without closing resistor adopted, the no-load line closing

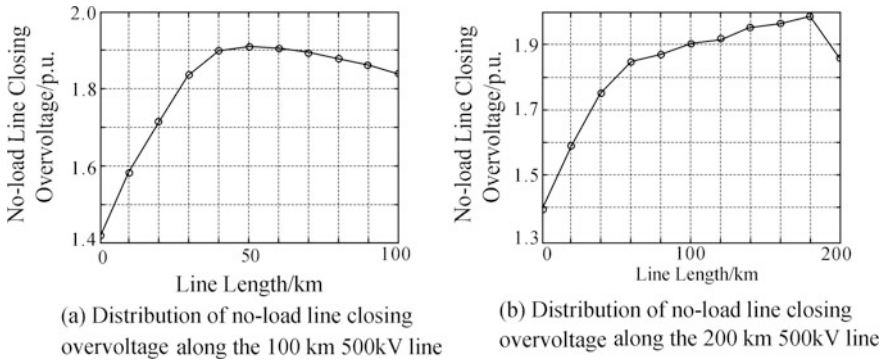

Fig. 6.42 No-load line closing overvoltage of a 500 kV short line

overvoltage of the line with length less than 100 km also cannot exceed the range specified in the standards.

② When the line length is 200 km, the maximum no-load line closing overvoltage is 1.98 p.u., being close to 2.0 p.u. Considering that the calculation condition is severe, it can be deemed that the no-load line closing overvoltage for a line with length between 100 and 200 km usually does not exceed the range set forth in the standards, but the margin is very small. It seems prudent to carry out calculation verification for actual line condition to confirm whether the closing resistor is canceled during the construction process of the lines.

When the line is longer, the no-load line closing overvoltage may exceed 2.0 p.u., and at this moment, it is required to take other measures to limit the overvoltage.

(4) Analysis on long line overvoltage

For a longer line with length between 200 and 400 km, it is required to limit the overvoltage by installing closing resistor or taking several groups of MOAs along the line, because the capacitance rise effect has been apparent at this moment. Here, a 400 km-long line is selected to carry out the calculation in a severe condition, with results, as shown in Figs. 6.43 and 6.44.

The calculation results show that the no-load line closing overvoltage amplitude decreases to 1.75 p.u. for a 400 km line with closing resistor adopted, being less than 2.0 p.u. and meeting the requirements set forth in the standards; Moreover, the no-load line closing overvoltage can also be limited to 1.93 p.u. within the allowable range set forth in the standards by means of adding 2–3 groups of MOAs along the line. Considering the probability to close both ends of the line, respectively, several groups of MOAs should be distributed symmetrically. Therefore, the no-load line closing overvoltage can be limited to the range set forth in the standards for the 500 kV line with length between 200 and 400 km, with closing resistor or several groups of MOAs adopted.

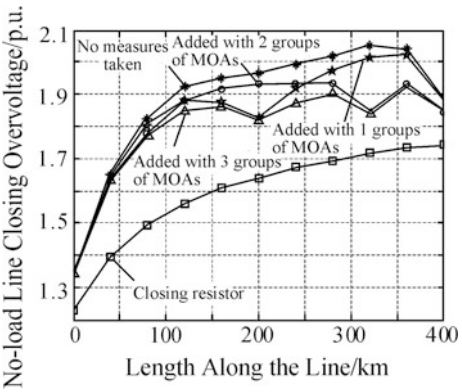

Fig. 6.43 No-load line closing overvoltage of a 400 km 500 kV transmission line equipped with closing resistors or multiple groups of MOAs. *Note* "No Measures Taken" means that a group of MOAs are provided at both ends of the line; in case of "Added with 1 Group of MOAs", one group of MOAs is added at the middle point of the line; in case of "Added with two Groups of MOAs", one group of MOAs is added at 1/5 and 4/5 of the line, respectively; in case of "Added with three Groups of MOAs", one group of MOAs is added at the middle point, 1/5, and 4/5 of the line, respectively

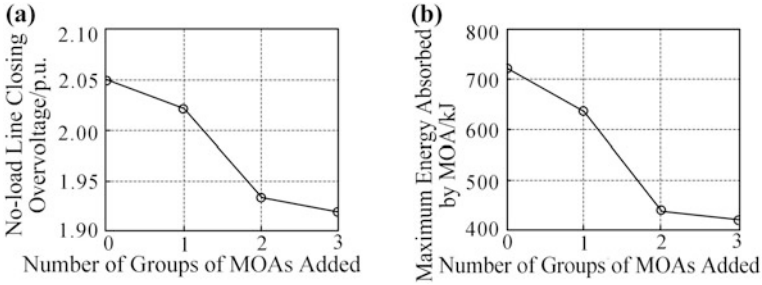

Fig. 6.44 Maximum no-load line closing overvoltage of a transmission line with multiple groups of MOAs and the maximum energy absorbed by MOAs

With several groups of MOAs adopted, it is possible to improve the overvoltage distribution and decrease the maximum overvoltage value, as shown in Fig. 6.44. The no-load line closing overvoltage decreases to 1.93 p.u. after being added with three groups of MOAs from 2.05 p.u. when "No Measure Taken" is taken; in view of the MOA's discharge current capacity, several groups of MOAs jointly absorb the impulse energy during closing; however, the energy absorbed by a single MOA decreases to 420 kJ absorbed in case of "Added with three groups of MOAs" from 720 kJ absorbed in case of "No Measure Taken", which is far less than the energy withstand limit 3–6 MJ of the MOAs for 500 kV AC line, so the MOA does not fail.

Table 6.42 Limitation effect of closing resistor on no-load line closing overvoltage of the 500 and 600 km 500 kV Lines

Closing resistor		No	1000 Ω	2000 Ω	3000 Ω
Line length	500 km	2.227	1.762	1.841	1.842
	600 km	2.410	1.782	1.966	1.967

For the 500 and 600 km 500 kV lines, due to the more apparent capacitance rise effect and with three groups of MOAs added along the line, the no-load line closing overvoltage still can reach 2.03–2.11 p.u., which are higher than the limit value set forth in the standards. At this moment, the overvoltage can be effectively limited only by adopting closing resistor, with limitation effect, as shown in Table 6.42.

As a consequence of the above, through the analysis carried out from the perspective of no-load line closing overvoltage limitation, it is feasible that the closing resistance measure can be canceled in a 500 kV line with length less than 100 km; it is required to carry out calculation verification for specific line to determine whether the closing resistor can be canceled in a line with length between 100 and 200 km; for a line with length between 200 and 400 km, the overvoltage is usually limited by means of closing resistor, or by installing 2–3 groups of MOAs along the line, but this method cannot be verified by specific practice; for a line with length between 400 and 600 km, the no-load line closing overvoltage should be limited by closing resistor.

6.3.5.2 Analysis on 1000 kV AC Line

1. Simulation Parameters

The no-load line three-phase closing overvoltage of the 1000 kV system still adopts the model, as shown in Fig. 6.39, with three-phase non-synchronism of 5 ms.

A reference is made to Southeast Shanxi–Nanyang–Jingmen UHV demonstration line in our country for the system parameters, and the high-voltage shunt reactor compensation degree is 80%, evenly distributed at both ends of the line; the tower is cat-head type; the conductor type is steel-cored aluminum strand 8× LGJ-500/35, with splitting spacing of 400 mm. The arrester is 1000 kV MOA recommended by the China Electric Power Research Institute, with parameters, as shown in Table 6.43.

2. Overvoltage Research

It can be known from the above research results that, for a 500 kV system, the closing resistor can be canceled in a short line; the closing resistor usually should be used in a long line, but several groups of MOAs can also be used to limit the no-load line closing overvoltage. Thus, it is required to determine whether the no-load line closing overvoltage limitation by the UHV system is consistent with

Table 6.43 Parameters of MOA in the UHVAC system in China

Rated voltage/kV	Continuous operating voltage/kV	Switching impulse residual voltage (Peak)/kV		Lightning impulse residual voltage (Peak)/kV	
828	636	1 kA 1430	2 kA 1460	10 kA 1553	20 kA 1620

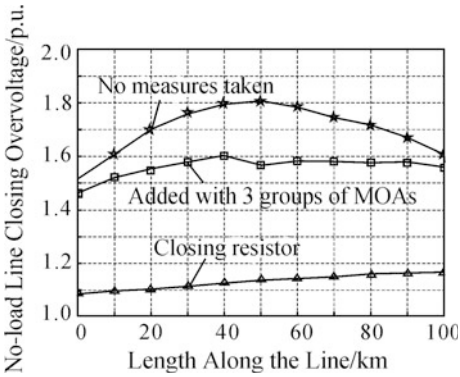

Fig. 6.45 Distribution of no-load line closing overvoltage along a 100 km 1000 kV line

that of the 500 kV system. The following gives an analysis explanation for calculation of the overvoltage for 1000 kV short line and long line.

(1) Analysis on short-line overvoltage

The no-load line closing overvoltage is calculated by taking the 100 km 1000 kV line as an example, with results, as shown in Fig. 6.45.

According to the calculation results, it can be known that:

① For a shorter line with no measures taken, the overvoltage can only be limited to approx. 1.8 p.u., which exceeds the allowable value of 1.7 p.u. set forth in the standards, unsatisfying the requirements specified in the UHV system standards.

② The overvoltage can be limited to meet the value of 1.6 p.u. specified in the specification only after three groups of MOAs added for joint protection along the line, but the margin is low, so it can be seen that it is very hard to limit the UHV overvoltage by only use of MOA measure; however, the overvoltage is limited apparently after the closing resistors are adopted. The amplitude is only 1.17 p.u., with a large margin and apparent effect.

(2) Analysis on long line overvoltage

Because the UHVAC line is usually long in China, such as Southeast Shanxi–Nanyang–Jingmen line, its two line sections are about 300 km. Therefore, the line

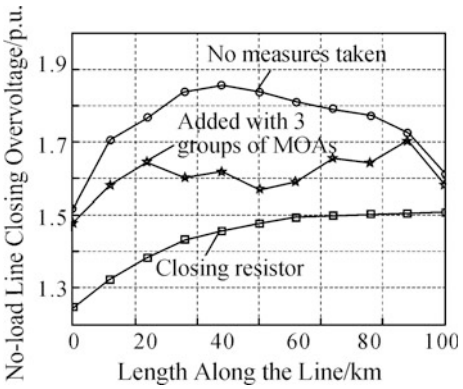

Fig. 6.46 Distribution of no-load line closing overvoltage along a 300 km 1000 kV line

with length of 300 km is taken as an example for analysis, with results, as shown in Fig. 6.46.

It can be known from Fig. 6.46 that, for a 300 km line, even with three groups of MOAs added along the line, the overvoltage is still more than 1.7 p.u., which is difficult to limit, so only adoption of MOAs along the line is not appropriate for the reason that the adding of more MOAs will lead to the increase in fault rate, unreasonable economy, and other problems; while with closing resistor adopted, the overvoltage amplitude is 1.5 p.u., which is limited effectively, and with a large margin.

As a consequence of the above, for a 1000 kV UHVAC transmission line, even it is only 100 km, without closing resistor adopted, the closing overvoltage still exceeds the limitation level of 1.7 p.u. Therefore, from the perspective of closing overvoltage control, the 1000 kV UHV circuit breaker usually requires to adopt the closing resistors.

(3) Research on relationship between closing resistor and line length

In fact, in all countries with the UHV lines around the world, such as former Soviet Union, Japan, America, etc., the lines adopt closing resistors. In addition, the practical operation experience shows that by use of closing resistors can effectively limit the closing overvoltage, with prominent effect.

As the line length differs in these countries, the resistance value of the closing resistor is also different. For the countries in which a shorter line is provided, such as Japan and Italy, the resistance value of the closing resistor used is higher, which is 700 and 500 Ω, respectively; for the countries in which a longer line is provided, such as former Soviet Union and America, the value of the closing resistor used is lower, which is 378 and 300 Ω, respectively.

The calculation results on the influence of the resistance value of the closing resistor on the no-load line closing overvoltage in lines with different length are as shown in Fig. 6.47.

It can be known from Fig. 6.47 that, with the increase in the resistance value of the closing resistor, the maximum overvoltage amplitude curve along the line

presents a V trend first decreasing and then increasing, and a most appropriate resistance value exists in a line with different length, leading to the lowest overvoltage; the minimum overvoltage obtained after the limitation of the closing resistor increases with the increase of the line length, but it is less than 1.25 p.u., obtaining apparent limitation effect, which is as shown in Fig. 6.48; when the longer lines adopt closing resistors with low resistance value and the shorter line adopt closing resistors with high resistance value, it is more beneficial to controlling the overvoltage, which is as shown in Fig. 6.49.

The causes for occurrence of such phenomenon are analyzed as follows: the use of closing resistor can be divided into two processes, as shown in Fig. 6.50. First, insert the resistor in the circuit (close Q_2), and open the closing resistor by means of short circuit (close Q_1) after a while, so as to mitigate the line impulse and reduce the overvoltage amplitude. In the process, switch-on/switch-off of the closing resistor may cause overvoltage, and it is advisable to maximize the resistance of the

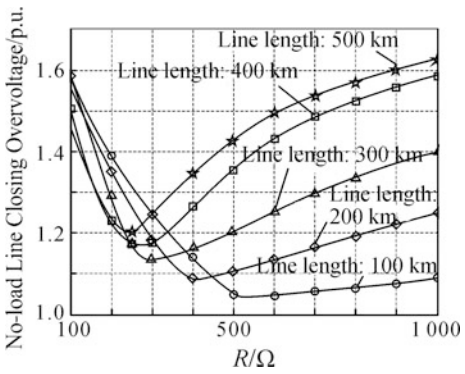

Fig. 6.47 No-load line closing overvoltage under different closing resistances

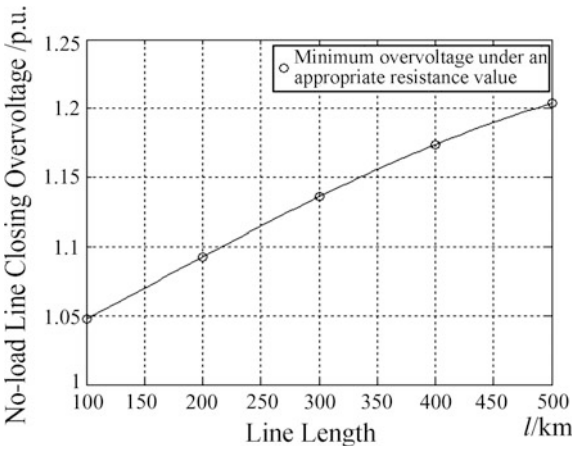

Fig. 6.48 Minimum no-load line closing overvoltage under an appropriate resistance value

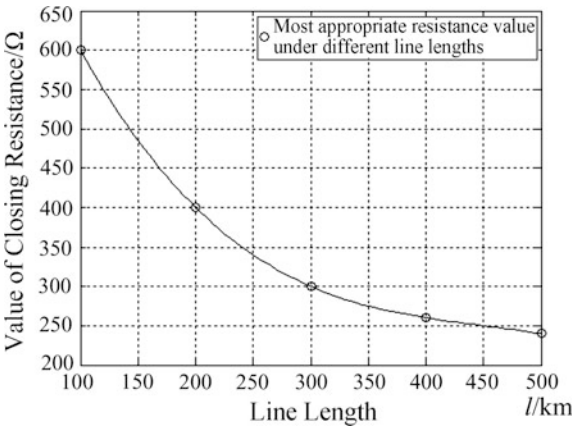

Fig. 6.49 Most appropriate resistance value of closing resistor in a line with different lengths

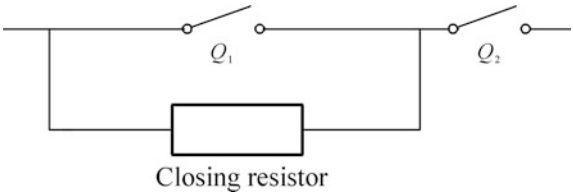

Fig. 6.50 Sketch for closing resistor

closing resistor during switch-on of the closing resistor, and minimize the resistance of the closing resistor during switch-off of the closing resistor.

Furthermore, as the capacitive reactance of the UHV no-load line is larger than the inductive reactance of the line, so the no-load line can be equal to capacitance. With closing resistor adopted, the voltage of the line is the voltage division result obtained by capacitor and closing resistor, as shown in Fig. 6.51a, b.

The switch-on process of the closing resistor is as shown in Fig. 6.51a. The equivalent capacitance C of the line increases, the capacitive reactance X_C decreases and the voltage $U_C = U_E/\sqrt{1+(R/X_C)^2}$ shared by the capacitor decreases in steady state if the line length increases under the condition where the resistance value keeps same. According to the estimation equation for the overvoltage amplitude:

$$U_{MAX} = 2U_{steadystate} - U_{initial} = 2U_C, \tag{6.11}$$

where

U_C the voltage shared by the capacitor in steady state;

$U_{steady\ state} = U_C$;

$U_{initial} = 0$.

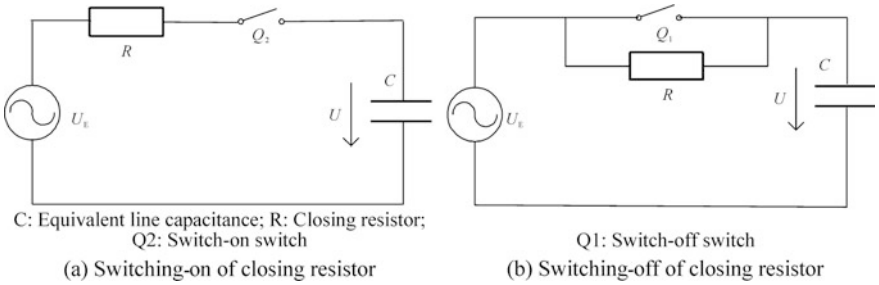

Fig. 6.51 Switch-on and switch-off processes of closing resistor

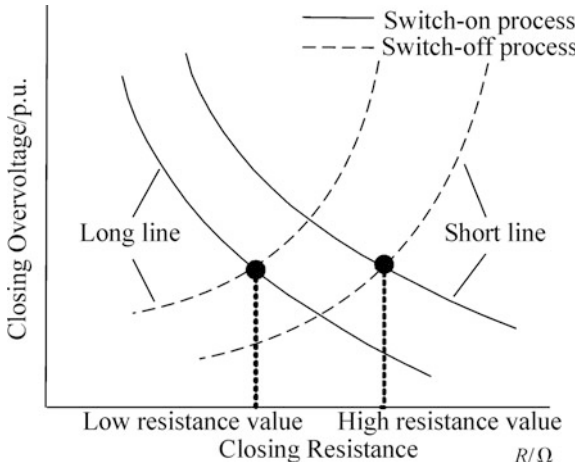

Fig. 6.52 Analysis diagram for the most appropriate resistance value of closing resistor in long and short lines. *Note* The horizontal coordinate of the intersection point in the figure is the most appropriate resistance value of the closing resistor for controlling the closing overvoltage under the line length circumstance

It can be known that the longer the line length is, the lower the overvoltage is. As shown in Fig. 6.52, the overvoltage of a longer line is lower than that of the shorter line in the switch-on process and under circumstance where the resistance value of the closing resistor remains unchanged.

The switch-off process of the closing resistor is as shown in Fig. 6.51b. Before switch-off, the steady-state voltage U_C borne by the line capacitor becomes the initial voltage, and after switch-off, the steady-state voltage is the power supply voltage U_E (a fixed value). Therefore, it can be known from the estimation equation:

$$U'_{MAX} = 2U_{steadystate} - U_{initial} = 2U_E - U_C, \tag{6.12}$$

where
$U_{steady\ state} = U_E$;
$U_{initial} = U_C$.

Therefore, with the increase of the line length, U_C becomes lower, so the overvoltage is higher. As shown in Fig. 6.52, the overvoltage of the longer line is higher than that of the shorter line in the switch-off process under circumstance where the resistance value of the closing resistor is the same.

It can be known from Fig. 6.52 that, with the increase of the value of closing resistor, the overvoltage decreases in the switch-on process, and with the increase of resistance, the overvoltage increases in the switch-off process. Therefore, an appropriate resistance value of the closing resistor exists, minimizing the overvoltage produced in the two processes as a whole, namely corresponding resistance value of the closing resistor at intersection point between the switch-on process curve and switch-off process curve for a line with same length, as shown in the figure. Moreover, the most appropriate resistance value of the closing resistor is low for a longer line, and high for a shorter line.

From the perspective of energy analysis, the above trend is also rational. With the increase of the line length, the no-load line closing overvoltage becomes more severe, the energy absorbed by the closing resistor also increases accordingly, while the energy absorbed by the closing resistor increases with the decrease of the resistance value, so the more energy can be absorbed by use of low resistance in the longer line to better reduce the overvoltage. According to calculation, the allowable maximum energy absorption required for different closing resistor is as shown in Table 6.44.

6.4 Opening Overvoltage

The opening overvoltage of the UHVAC system includes load shedding opening overvoltage and fault clearing overvoltage [1, 3]:

(1) The load shedding opening overvoltage of the UHVAC system mainly includes the single-phase grounding load shedding opening overvoltage and fault-free load shedding opening overvoltage. During the normal power transmission, the fault-free load shedding opening overvoltage occurs during sudden opening of the circuit breaker due to a certain cause; during live working, it is required to exit the reclosure device. At this moment, three phases of the circuit breaker will open if a single-phase ground fault occurs, so as to produce a single-phase grounding load shedding opening overvoltage whose characteristics are decisive factors to determine the minimum safe distance during live working in the UHVAC system.

Table 6.44 Allowable maximum energy absorption of closing resistors

Resistance value of closing resistor/Ω	200	300	400	500	600	700
Allowable maximum energy absorption/MJ	104.8	69.9	52.4	41.9	35.0	30.0

(2) The fault clearing overvoltage is a unique opening overvoltage, and after a fault occurs in a line and is cleared, a relatively high overvoltage appears in other neighboring lines, which is called fault clearing overvoltage.

This subsection mainly presents a research on these two kinds of opening overvoltage.

6.4.1 Load Shedding Overvoltage

The load shedding overvoltage is a typical opening overvoltage in the UHVAC system, mainly including fault-free load shedding overvoltage and single-phase grounding load shedding overvoltage, as shown in Fig. 6.53, of which the former one is caused by the load shedding due to sudden tripping with no fault of the circuit breaker when the line is in normal power transmission condition, and the latter one is caused by three-phase opening resulted from single-phase ground fault, because the single-phase reclosure device cannot be implemented during live working.

6.4.1.1 Mechanism for Generation

The process of the load shedding overvoltage of the system is very complicated, which comprehensively results in the increase in overvoltage resulted from the no-load capacitance effect of the line and the load shedding process of power supply, and especially the three-phase asymmetry resulted from the single-phase

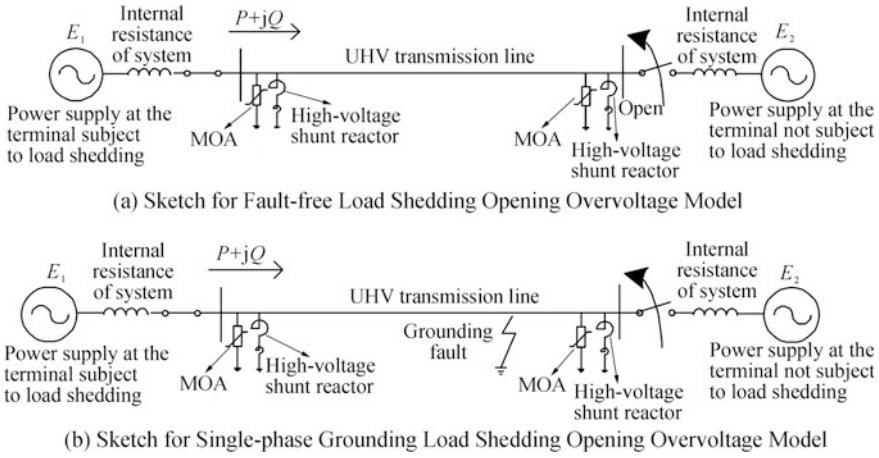

Fig. 6.53 Sketches for load shedding opening overvoltage models

ground fault can aggravate the severity of the overvoltage. Therefore, the fault-free load shedding overvoltage is usually lower than the single-phase grounding load shedding overvoltage in normal condition.

The following explains the mechanism of the overvoltage production through comparison of the change in steady-state voltage produced at individual point along the line before and after occurrence of load shedding, as shown in Fig. 6.54. The curve I in the figure shows the voltage distribution of the system before load shedding; the power supply voltage is U_s. As a certain voltage drop in the transmission power occurs under the influence of power supply impedance during normal operation of the line, so the voltage U_1 obtained after the power supply impedance is usually lower than the power supply voltage. After that, due to the capacitance rise effect of the line, and the limitation effect produced by the power supplies at both ends of the line and by voltage limitation measures, the voltage thereof is usually distributed in an arch form. The voltage at tail end of the line is U_2. In case of load shedding resulted from opening of the circuit breaker at terminal of the line, the voltage along the line varies apparently, which is as shown in curve II. At this moment, with the line terminal being opened, the current passing through the internal resistance of the system corresponds to a capacitive charging voltage, which is opposite to the current direction in normal operation condition, enabling the busbar voltage U_3 to be slightly higher than U_s. Then, the capacitance rise effect of the line gets the line voltage higher, obtaining a terminal voltage U_4 at the end of line.

As the voltage distribution of the line before and after the load shedding differs, an overvoltage occurs in the transient process in which the voltage at terminal of the line varies significantly from U_2 to U_4, so the overvoltage often becomes more severe, whose amplitude can be estimated by the following equation [4]:

$$U_{\max} = U_4 + (U_4 - U_2) = 2U_4 - U_2. \tag{6.13}$$

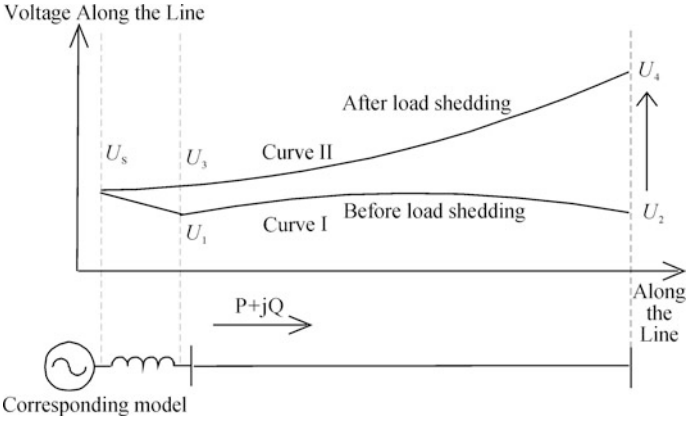

Fig. 6.54 Steady-state voltage variation before and after the occurrence of load shedding to the line

In case of a single-phase ground fault in operation of the line, the sound phase voltage rises under the influence of asymmetrical effect, so the subsequent load shedding process is completed on the basis of voltage rise, further aggravating the transition process. Hence, the superposition between the single-phase ground and load shedding process gets such overvoltage more severe.

6.4.1.2 Modeling and Simulation

The fault-free load shedding production process is simpler, for which the simulation model is as shown in Fig. 6.55. During normal operation of the system, three phases of the circuit breaker at one side of the line open suddenly, and the opening time of the circuit breaker should be subject to probability distribution within a power frequency cycle, and several times of statistical calculation should be carried out. The overvoltage waveform is as shown in Fig. 6.56. A reference is made to the Southeast Shanxi–Nanyang–Jingmen Demonstration Project established in China for parameters of the line and pole and tower.

The simulation model of the single-phase grounding load shedding overvoltage is as shown in Fig. 6.57. After the single-phase ground fault of the line occurs, three phases of circuit breaker at one terminal of the line open after a period (inherent time of relay protection and switch motion). The grounding time and opening time of the circuit breaker should be subject to the probability distribution within a power frequency cycle, and several times of statistical calculations should be carried out. The overvoltage waveform is shown Fig. 6.58. A reference is made to the Southeast Shanxi–Nanyang–Jingmen Demonstration Project established in China for parameters of the line and pole and tower.

6.4.1.3 Influence Factors

The factors that influence the load shedding overvoltage include line length, transmission power, system impedance, etc., and are related to whether the asymmetrical fault occurs.

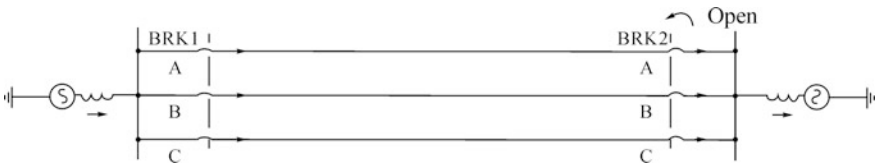

Fig. 6.55 Sketch for fault-free load shedding overvoltage model

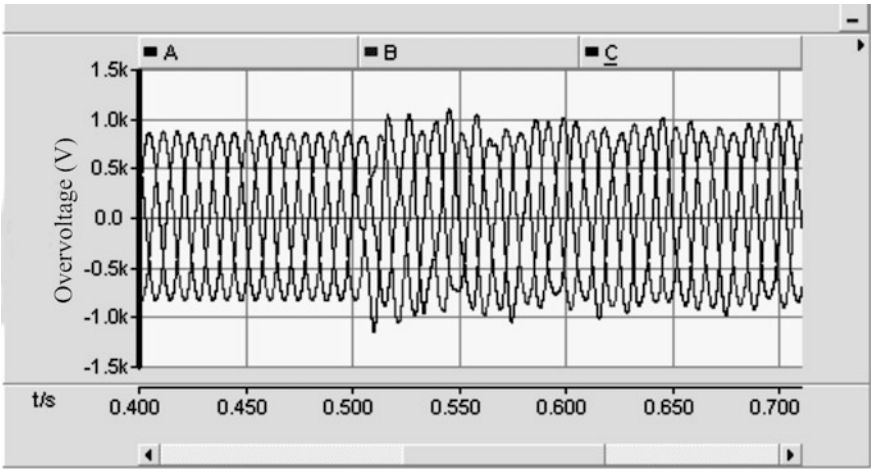

Fig. 6.56 Sketch for fault-free load shedding overvoltage waveform

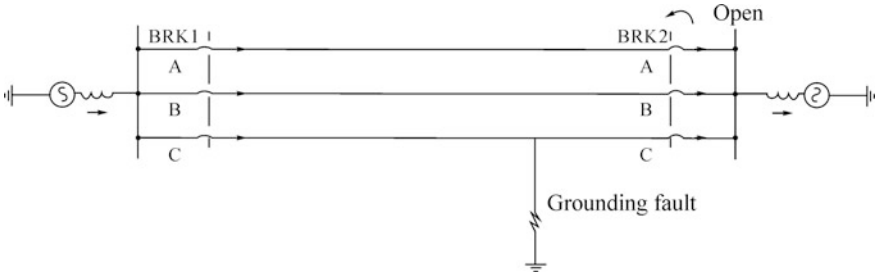

Fig. 6.57 Sketch for single-phase grounding load shedding overvoltage model

1. Line length

As mentioned above, the asymmetrical effect of the ground fault and the capacitance rise effect of the long line get the power frequency voltage higher, increasing the amplitude of the switching overvoltage to some extent.

The fault-free load shedding and single-phase grounding load shedding overvoltage are calculated for lines with different length, respectively, with results shown in Table 6.45. It can be seen that, with the increase of the line length, the overvoltage increases accordingly. In case of a single-phase ground fault, the overvoltage value gets higher, compared to that for lines with same length and without fault.

2. Transmission power

The line transmission power produces a voltage drop at the power supply impedance, and after the load is cleared, the voltage drop decreases abruptly. The larger the transmission power is, the higher the voltage drop is, and the oscillation

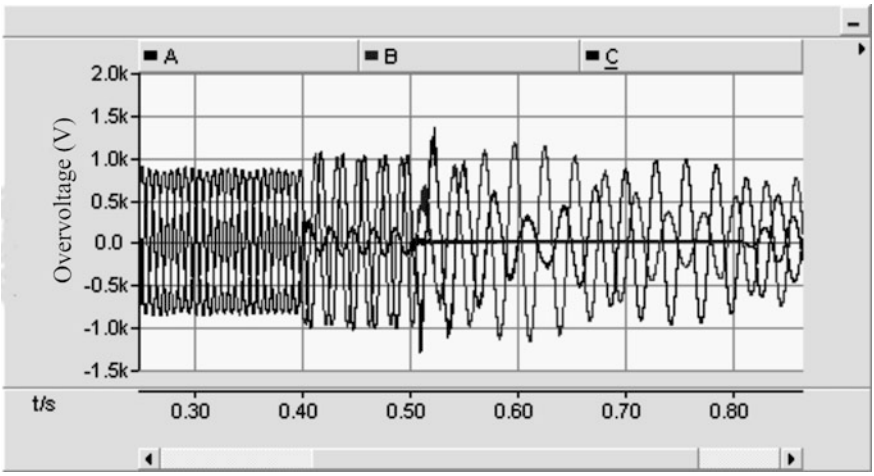

Fig. 6.58 Sketch for single-phase grounding three-phase load shedding overvoltage waveform

Table 6.45 Load shedding overvoltage in lines with different lengths

Load shedding overvoltage	Load shedding overvoltage in lines with different lengths (km)/p.u.				
	100	200	300	400	500
Fault-free	1.035	1.055	1.244	1.334	1.346
Single-phase ground fault	1.415	1.517	1.526	1.594	1.618

Table 6.46 Load shedding overvoltage under different powers

Load shedding overvoltage	Load shedding overvoltage under different powers (MW)/p.u.						
	0	500	1000	1500	2000	2500	3000
Fault-free	1.063	1.112	1.185	1.257	1.334	1.413	1.486
Single-phase ground fault	1.352	1.364	1.384	1.563	1.594	1.598	1.634

process gets violent. Therefore, the larger the transmission power is, the more severe the overvoltage is.

Table 6.46 shows the overvoltage amplitudes at different power levels of a 400 km line, and that the overvoltage increases as the transmission power increases.

3. Equivalent impedance of power supply

The equivalent impedance includes positive sequence impedance and zero-sequence impedance. The influence made by the ratio of positive sequence impedance to zero-sequence impedance on the load shedding overvoltage is as shown in Table 6.47. The results show that, with the increase of the positive sequence impedance, the fault-free load shedding overvoltage increases accordingly; however, the influence on the single-phase grounding load shedding overvoltage becomes less severe.

Table 6.47 Load shedding overvoltage under different system impedances

Ratio of positive sequence impedance to zero-sequence impedance	Load shedding overvoltage under different positive sequence impedance values (Ω)/p.u.							
	20		40		60		80	
	Fault-free	Grounding	Fault-free	Grounding	Fault-free	Grounding	Fault-free	Grounding
1:1	1.267	1.546	1.295	1.558	1.334	1.56	1.374	1.557
1:2	1.287	1.553	1.327	1.569	1.352	1.532	1.39	1.538
1:3	1.308	1.55	1.346	1.559	1.359	1.528	1.391	1.566

Note "Grounding" in the table denotes that the line is subject to a single-phase ground fault

In fact, the line transmission power is the most critical influence factor for the load shedding overvoltage.

6.4.1.4 Limitation Measures

As the single-phase load shedding overvoltage is more severe, this section discusses the main limitation measures for this overvoltage as the main discussion object.

1. Limitation effect of MOAs

The analysis is carried out through installing different groups of MOAs in the line to limit the load shedding overvoltage. Table 6.48 shows the limitation effect obtained by installing different groups of MOAs in a 600 km line.

It can be seen that the overvoltage limitation effect increases as the number of groups of the MOAs increases; with several groups of MOAs adopted, the overvoltage can be limited within required range.

2. Overvoltage limitation by opening resistors

By use of opening resistors to limit the load shedding, overvoltage has a certain effect. The following gives a simulation calculation for the single-phase grounding load shedding overvoltage for lines with different length, with results as shown in Table 6.49.

The results show that by use of opening resistors to limit the load shedding, overvoltage has a certain effect.

Table 6.48 Grounding load shedding overvoltage limitation effect of MOAs

Number of groups of MOA	Installation position of MOAs	Overvoltage (p.u.)
0	No	1.94
2	Both ends of the line	1.78
3	Head end, middle part and tail end	1.71
4	Head end, 1/3, 2/3, tail end	1.66
5	Head end, 1/4, 2/4, 3/4, tail end	1.62

Table 6.49 Limitation effect of opening resistors

		Single-phase grounding load shedding overvoltage/p.u.				
Line length/km		100	200	300	400	500
Opening resistor	No	1.415	1.517	1.526	1.594	1.618
	600 Ω	1.232	1.324	1.407	1.501	1.57

6.4.2 *Fault Clearing Overvoltage*

The fault clearing overvoltage is a unique opening overvoltage in the UHV system, which can be divided into single-phase grounding, two-phase grounding, three-phase grounding, and phase-to-phase short-circuit fault clearing overvoltage in terms of types. As the single-phase ground fault is the most common fault, and the occurrence probability of the latter three ones is extremely small, this section takes the single-phase ground fault clearing overvoltage as the main discussion object.

6.4.2.1 Mechanism for Generation

The single-phase grounding clearing overvoltage means, after one line is single-phase grounded and the fault is cleared, a higher overvoltage produced at the sound phase of the fault line and neighboring line due to the change of the voltage in the transition process.

The overvoltage can be divided into two processes: first, when the single-phase ground fault occurs, the voltage at the sound phase rises, and the voltage at each phase tends to be stable after several power frequency cycles; subsequently, the single-phase circuit breaker is activated to clear the fault, as shown in Fig. 6.59.

The overvoltage can be divided into the following two cases:

Case I: The single-phase grounding fault clearing overvoltage produced at fault line section is as shown in Fig. 6.60. For the fault line, the voltage at the fault phase 1 is low due to the existence of the fault, so no overvoltage occurs; the phase-to-phase voltage varies abruptly at sound phase 2 due to the clearance of the fault, so overvoltage occurs, but its transient process is not very violent and the overvoltage amplitude is usually not high.

Case II: The single-phase grounding fault clearing overvoltage produced in the neighboring line section, as shown in Fig. 6.61. As the sound phase 3 of the neighboring line section is still connected with the sound phase 2 of the fault section, its overvoltage resembles to that of the sound phase 2 of the fault section; however, the overvoltage at the fault phase of the neighboring line section is most serious. When the phase C of the circuit breaker BRK2 is disconnected from the fault current, the transient steady state after grounded is comprised, being

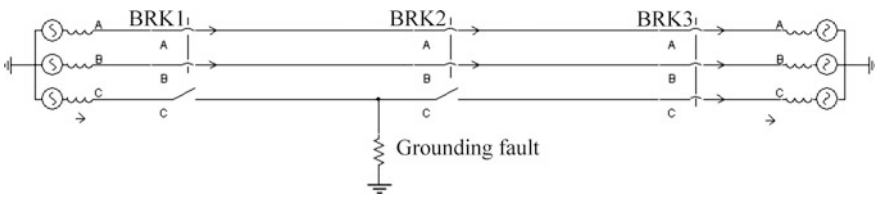

Fig. 6.59 Schematic diagram for single-phase grounding fault clearing overvoltage (I)

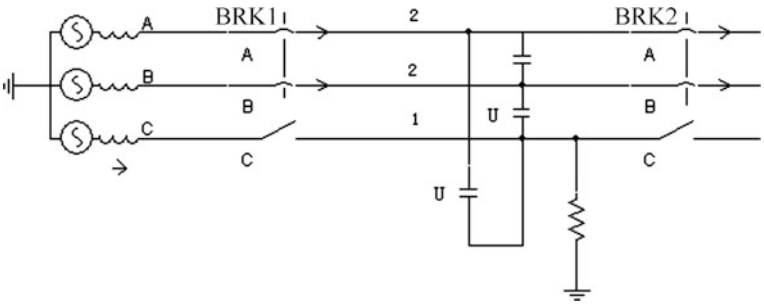

Fig. 6.60 Schematic diagram for single-phase grounding fault clearing overvoltage (II)

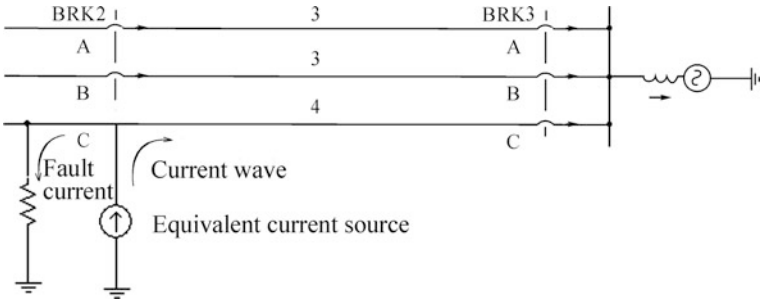

Fig. 6.61 Schematic diagram for single-phase grounding fault clearing overvoltage (III)

equivalent to installation of a current source with current direction opposite to the fault current in the vicinity of the circuit breaker at the phase C; the current amplitude from the current source is very high, which can flow and refract and reflect in the neighboring line, so as to produce a higher overvoltage. As such overvoltage develops toward to the neighboring sections at the same phase from the fault section; it is also called fault transfer overvoltage.

One characteristic of the fault clearing overvoltage is that it can inducts a higher transfer overvoltage in the next neighboring line section. When several line sections are connected at a switch station, disconnecting a line which subjects to single-phase ground fault can produce such overvoltage, whose amplitude is usually not more than 1.7 p.u. Such overvoltage also occurs in the EHV system, but such overvoltage has not a significant danger to the EHV system as a result of a high allowable overvoltage amplitude and large insulation margin of the EHV system (e.g., the limitation level of the switching overvoltage of 500 kV power grids is 2.0 p.u.). For a UHVAC system, the overvoltage limitation level is 1.7 p.u., so a great importance should be attached to such overvoltage in UHV systems.

In terms of types of faults cleared, the fault clearing overvoltage can be divided into single-phase grounding, two-phase grounding, three-phase grounding, and phase-to-phase short-circuit fault overvoltage, of which the single-phase grounding

fault overvoltage occurs frequently. For the reason that the probability of the latter three ones is very low, they are usually not considered in the practical project. The following mainly gives a discussion for the single-phase ground fault clearing overvoltage as an object.

6.4.2.2 Modeling and Simulation

In simulation, the single-phase grounding clearing overvoltage should consider the randomness of grounding position, grounding time, and fault clearing time. First, the occurrence time and clearing time of the line fault are taken as random variables, respectively, at fixed grounding position, which is made to be subject to normal distribution within a power frequency cycle, so that several times of simulation calculation are carried out to obtain a statistical overvoltage; then, the statistical overvoltage is calculated at different grounding positions where the fault occurs along the line, from which a maximum overvoltage can be taken.

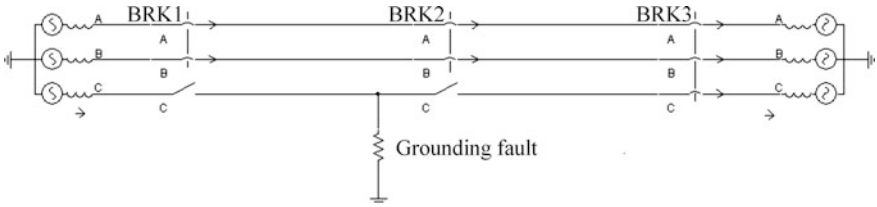

Fig. 6.62 Sketch for single-phase grounding overvoltage model

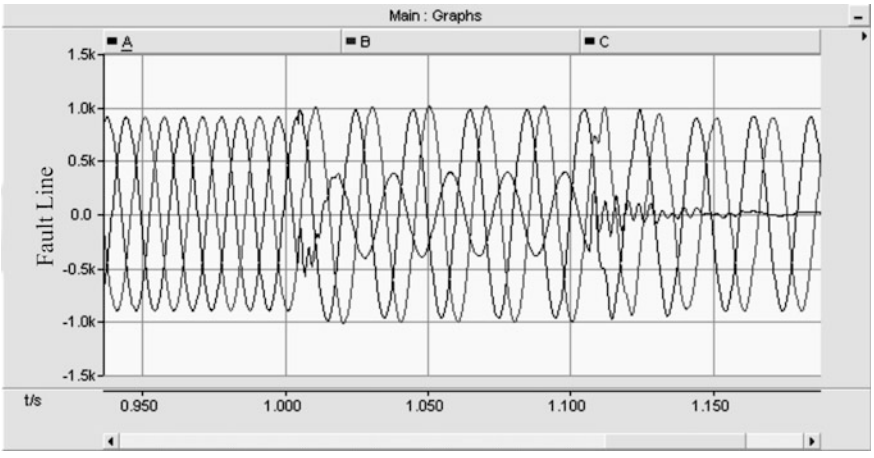

Fig. 6.63 Single-phase grounding fault clearing overvoltage waveform (fault line)

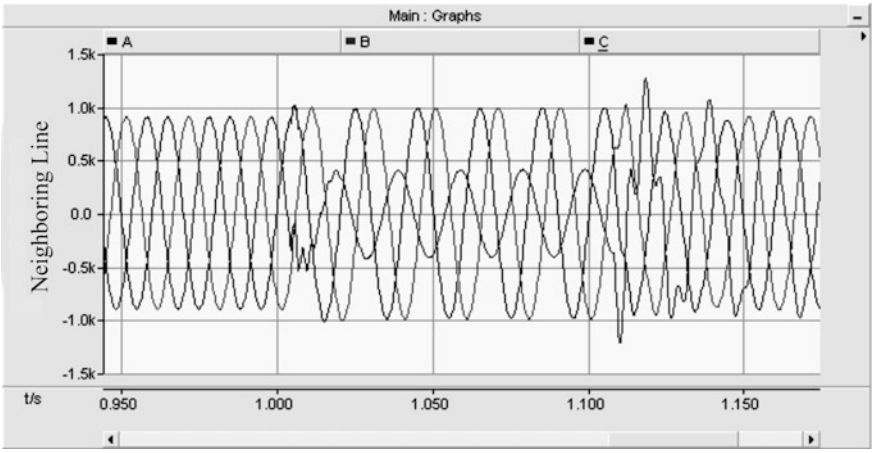

Fig. 6.64 Single-phase grounding clearing overvoltage waveform (neighboring line)

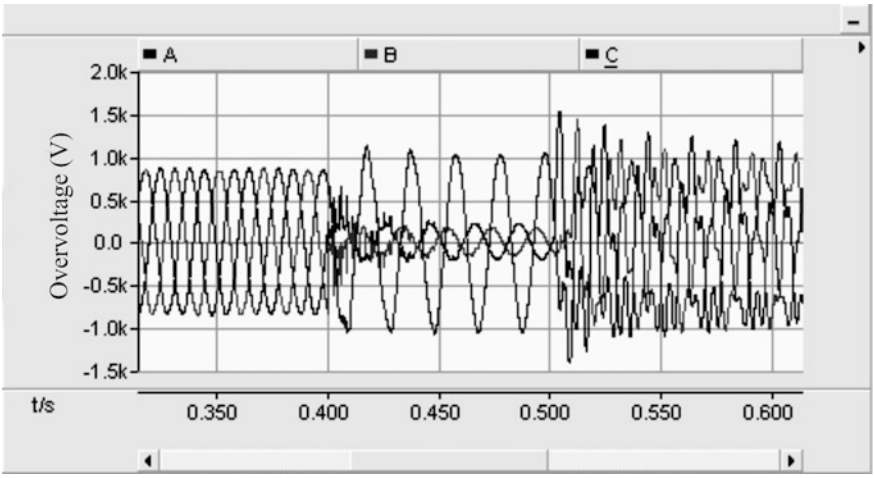

Fig. 6.65 Sketch for two-phase grounding clearing overvoltage waveform

The model of the single-phase grounding clearing overvoltage is as shown in Fig. 6.62. After a ground fault occurs in a line section, the circuit breakers of fault phase at both ends are actuated to disconnect the fault current, namely that it is possible to obtain overvoltage waveform and amplitude at sound phase of the fault line and the next neighboring line section, as shown in Figs. 6.63 and 6.64.

The two-phase grounding clearing overvoltage means the overvoltage produced in the line when the circuit breaker at fault phase in both sides clears the fault after the two-phase grounding fault occurs in the line, of which the waveform is as shown in Fig. 6.65. The three-phase grounding clearing overvoltage means the

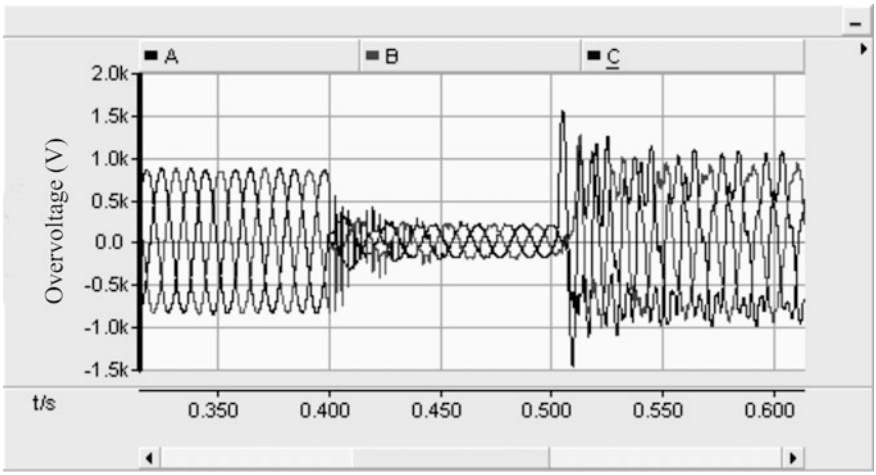

Fig. 6.66 Sketch for three-phase grounding clearing overvoltage waveform

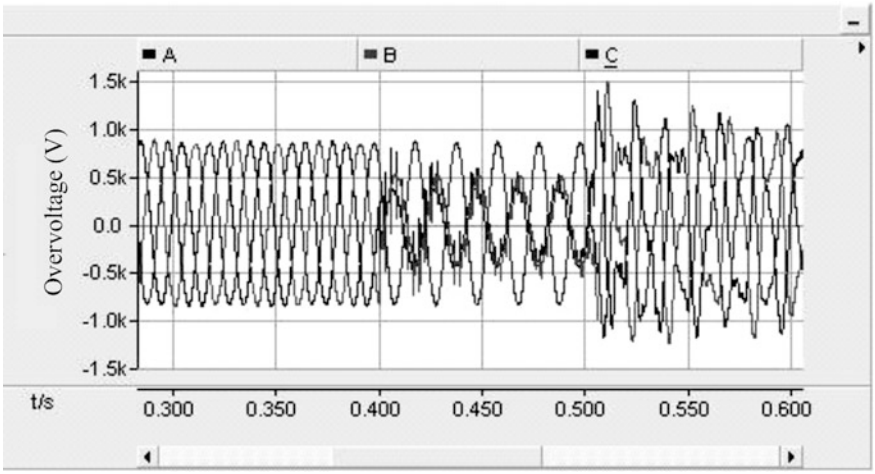

Fig. 6.67 Sketch for phase-to-phase short-circuit fault clearing overvoltage waveform

overvoltage produced after a three-phase ground fault occurs in the line and is cleared, of which the waveform is as shown in Fig. 6.66. The phase-to-phase short-circuit clearing overvoltage means the overvoltage produced after a phase-to-phase short-circuit fault occurs in the line and is cleared, of which the waveform is as shown in Fig. 6.67.

Table 6.50 Influence on single-phase grounding clearing overvoltage by grounding positions

Grounded line section		Overvoltage under different distances to switch station (B)					
A-B	Distance from grounding point to B/km	475	375	275	175	75	0
	Overvoltage/p.u.	1.434	1.486	1.533	1.545	1.575	1.652
B-C	Distance from grounding point to B/km	0	75	175	275	375	475
	Overvoltage/p.u.	1.670	1.650	1.586	1.550	1.535	1.486

Table 6.51 Influence on overvoltage by line transmission power

Transmission power/MW	0	500	1000	1500	2000
Overvoltage/p.u.	1.561	1.590	1.613	1.649	1.662

6.4.2.3 Influence Factors

The factors influencing the single-phase grounding clearing overvoltage mainly include grounding position, transmission power, etc. During the clearance of the single-phase ground fault, the transfer overvoltage produced in the next neighboring line section is more severe than that in the fault line section, so the following calculation takes the former as the discussion object.

1. Grounding position

The following adopts a line mode with total length of 500 + 500 km of a line comprising two sections A–B–C to research the influence of the grounding position on the overvoltage, in which point B is taken as a switch station. The research results are as shown in Table 6.50. It can be seen that the smaller the distance from the ground fault position to the switch station is, the larger the overvoltage produced in the neighboring line during clearance of the fault is.

1. Line transmission power

The following still adopts an A-B-C line mode to research the influence of the line transmission power on the overvoltage, with the calculation results, as shown in Table 6.51. It can be known from Table 6.51 that, with the increase of the transmission power, the single-phase grounding fault clearing overvoltage value increases.

6.4.2.4 Limitation Measures

1. Overvoltage limitation by multiple groups of MOAs

By use of MOAs can effectively limit the single-phase grounding clearing overvoltage. For a sectionalized UHV line, installation of MOAs at the sectionalizing point can limit the overvoltage within allowable range.

Table 6.52 Effect on single-phase grounding clearing overvoltage limitation by MOAs

Number of groups of MOAs	Installation position of MOA	Overvoltage (p.u.)
0	No	1.73
2	Both ends of line	1.71
3	Head end, middle part, and tail end	1.68
5	Head end, 1/4, 2/4, 3/4, and tail end	1.62

For the UHV transmission line with long distance that is divided into two 400 km sections, the overvoltage limitation effect of the MOAs is as shown in Table 6.52 when the transmission power is taken a larger value of 3000 MW. The grounding position is close to the sectionalizing point.

It can be known from Table 6.52 that, even for a long-distance UHV line subject to serious overvoltage, the overvoltage can be limited by installing MOAs at the sectionalizing points of the line. Therefore, installation of MOAs at sectionalizing points usually can effectively limit the single-phase grounding fault clearing overvoltage below the limitation level, without need to adopt other limitation measures.

2. Use of circuit breaker opening resistor

The opening resistor has an excellent overvoltage limitation effect, and can also reduce the recovery voltage of the circuit breaker and improve its operation condition, being beneficial to safe operation of the circuit breaker.

The following gives a study on the overvoltage limitation effect obtained by opening resistor in an A-B-C (300–300 km) line mode. The overvoltage in B–C line section, produced after a fault occurs in A-B line section, is cleared, as shown in Fig. 6.68.

Taking the Southeast Shanxi–Nanyang–Jingmen Line as an example, the maximum 2% overvoltage along the neighboring line is 1.66 p.u. during clearance of the single-phase ground fault, 1.76 p.u. during clearance of two-phase ground fault, and 1.79 p.u. during clearance of three-phase ground fault. In case of use of a 700 Ω opening resistor, the fault clearing overvoltage decreases to 1.37, 1.50, and 1.51 p.u., respectively.

3. Discussion on the use of opening resistors

It can be seen from the above contents that the fault clearing overvoltage amplitude under the phase-to-phase short-circuit, two-phase, and three-phase grounding fault is very high, and often cannot be limited within the standards only by use of MOAs at the head end and tail end of the line, but can be effectively limited by use of opening resistor.

However, the heat capacity required for the opening and closing resistors is far larger than the single-purpose opening resistor. The research conducted in Japan shows that the heat capacity required for the opening resistor can reach

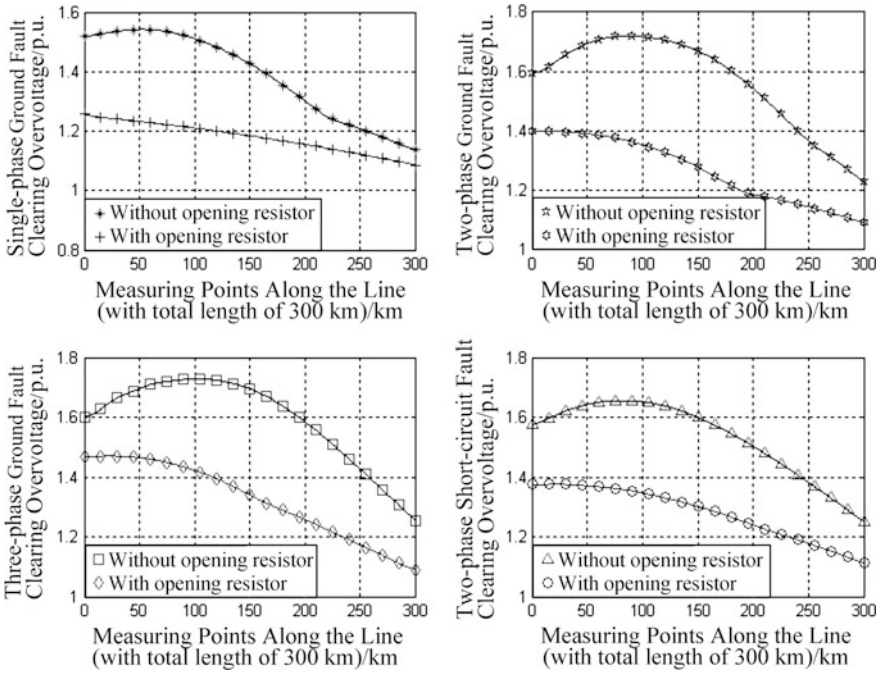

Fig. 6.68 Limitation of fault clearing overvoltage by opening resistor. *Note* The resistance of the opening resistor is 700 Ω

133 MJ. When the opening resistor is switched on, the line is still in operation state, and the normal power flow of the line even plus the fault current can pass through the opening resistor; and moreover, the switch-on time of the opening resistor is usually long, enabling the system to consume a huge energy at the opening resistor. Hence, higher requirement for its heat capacity will highly enhance the difficulty and cost of manufacturing of circuit breakers [16].

According to the analysis made in the previous two sections, it can be known that the opening resistor is mainly used to limit the phase-to-phase short-circuit, two-phase, and three-phase grounding fault clearing overvoltage, while the single-phase grounding fault clearing overvoltage usually can be limited by installing MOAs at the sectionalizing point.

In fact, the probability for occurrence of phase-to-phase short-circuit, two-phase, and three-phase grounding fault clearing overvoltage is very low, and it is usually deemed that such types of grounding fault clearing overvoltage hardly occur, meanwhile, considering the high cost and large failure rate of the opening resistor, so the opening resistor is hardly adopted in the UHV line, and single-phase grounding fault clearing overvoltage usually can be limited by installation of MOAs at sectionalizing point.

In addition, the studies in other countries outside of China show that such fault clearing transfer overvoltage also can appear in the 750 kV EHV system, but basically, no opening resistor is installed in the system at such voltage level around the world, and no problems occur as a result of the transfer overvoltage.

6.5 Influence on the Electromagnetic Transient Characteristics by Series Compensation Device

The UHV series compensation device is a capacitive reactive power compensation device that is connected in series in the UHVAC power transmission lines, which can be used to reduce the inductive impedance of the long-distance transmission line, simultaneously, enhance the utilization rate of the transmission line, and increase the stability limit and transmission ability of the electric power system. However, after the UHV line is installed with series compensation devices, it is probable to have some influence on such electromagnetic transient characteristics as secondary arc current during single-phase reclosure, power frequency overvoltage and switching overvoltage. This section gives a discussion on the change in electromagnetic transient characteristics of the system after the adoption of series compensation device.

6.5.1 Composition of Series Compensation Device

The UHV series compensation device is mainly composed of series capacitor, metal oxide varistor (MOV) for protection, damping circuit device, triggered spark gap, and bypass switch, as shown in Fig. 6.69 [17]. The MOV is the main protection to limit the capacitor voltage; the spark gap is the standby protection of the MOV and capacitor; the bypass switch is a necessary device for maintenance and dispatch of the system, and also offers some necessary conditions for spark gap and

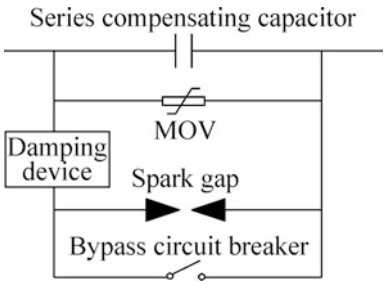

Fig. 6.69 Sketch for series compensation device, reprinted from Ref. [17], copyright 2014, with permission from China Electric Power Press

deionization; the damping circuit device is used to limit the discharge current of the capacitor, and prevent damage to the capacitor, gap, and bypass switch in the discharge process.

6.5.2 *Influence on the Closing Switching Overvoltage by Series Compensation Device*

The amplitude of the closing switching overvoltage is closely related to the position, arrangement method of series compensation device in the line, and the series compensation degree. For an ordinary UHV lines, the switching overvoltage can be reduced by installing series compensating capacitor in the line, and especially the no-load line closing overvoltage can be limited effectively. Meanwhile, when the series compensating capacitor is closer to the initial line section, the compensation degree gets higher, and the overvoltage limitation effect is better [18]. However, the closing operation may result in an impulse to the series compensating capacitor, influencing the service life of the series compensation device.

6.5.3 *Influence on Power Frequency Overvoltage by Series Compensation Device*

The UHV line is installed with series compensation device, resulting in the influence on the overvoltage with respect to the following aspects. On one hand, in case of the same tidal transmission current, the voltage at the power delivery side is at lower level, compared to that without series compensation device, being beneficial to reducing the power frequency voltage; on the other hand, after the series compensation device is subject to compensate positive sequence impedance of the line, the coefficient of grounding X_0/X_1 increases, and the power frequency overvoltage caused by the single-phase grounding load shedding rises [17].

Taking a 400 km 3000 MW UHV transmission line with power supplies at both ends and with compensation degree of 85% (as shown in Fig. 6.53) as an example, the line power frequency overvoltage is 1.277 p.u. when the line is not installed with series compensation device; after the line is installed with a 40% series compensation device, the power frequency overvoltage is 1.356 p.u. With series compensation device provided, the power frequency overvoltage is 0.079 p.u. higher than that produced in the line without series compensation device provided. The results show that the degree of the increase in power frequency overvoltage caused by the series compensation device in the line is more than the degree of the decrease in power frequency overvoltage caused by the series compensation device, resulting in the increase in the final power frequency overvoltage.

6.5.4 *Influence on Secondary Arc Current by Series Compensation Device*

When a single-phase ground fault occurs in the line, the circuit breaker at the fault phase at both sides of the line opens in succession. Due to the electrostatic coupling and electromagnetic coupling of the sound phase, a certain inductive current will flow in the arc channel, which is the secondary arc current. For the UHV transmission line with series compensation device, when a single-phase ground fault occurs at a place in the line and if the short-circuit flowing the series compensation device is small, the current and energy consumption of the MOV is small; at this moment, the spark gap of the series compensation device and bypass switch are not activated, so the series compensation device is not bypassed, and the residual charge at the series compensating capacitor is discharged by an oscillating circuit being composed of series compensation device, the HV reactor, and arc resistance at short-circuit point, as shown in Fig. 6.70 [17]. The oscillation frequency of the circuit is typically a few hertz, being far lower than the operating frequency. In addition, the secondary arc current amplitude at the fault point can reach dozens of or hundreds of ampere, featuring slow attenuation and less number of zero crossing points, thus extending the secondary arc extinguishing time, so it is very unbeneficial to the single-phase reclosure.

Similarly, a 400 km 3000 MW UHV transmission line with power supplies at both ends and with compensation degree of 85% (as shown in Fig. 6.53) is taken as an example. When the line is installed with series compensation device, the waveform of the secondary arc current is as shown in Fig. 6.71 below. The simulation results show that, when a single-phase ground fault occurs at one side of the line, the secondary arc current is a low-frequency and attenuated discharging current, whose frequency is approx. 7.3 Hz. And the existence of this low-frequency component reduces the number of zero crossing of the secondary arc current, being unbeneficial to the self-extinction of the secondary arc current. After the circuit breaker is open for 0.5 s, the current amplitude still remains very high, enabling the secondary arc current difficult to be extinguished. In case of a single-phase grounding fault, the bypass switch is activated to get the series capacitor shorted, so that the secondary arc current has no such low-frequency discharging component, and is self-extinguished in an easier manner.

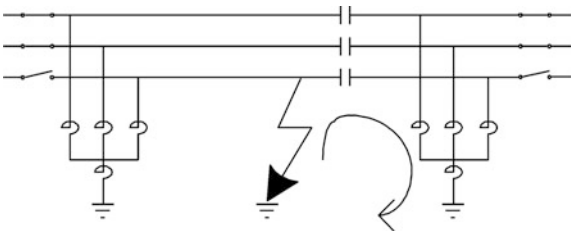

Fig. 6.70 Sketch for low-frequency oscillating circuit of series compensation system under the fault of single-phase grounded

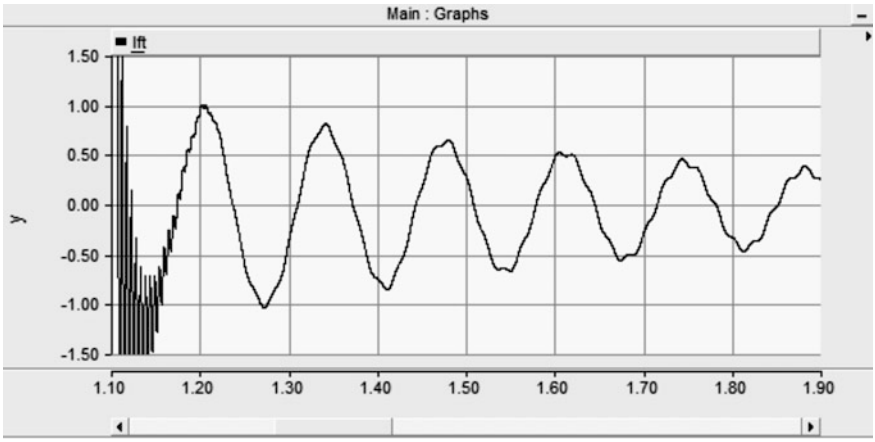

Fig. 6.71 Waveform of secondary arc current transient process during the single-phase reclosing process

6.5.5 Linkage Between Series Compensation Device and Circuit Breaker

In fact, before closing operation, it is usually required to close the bypass switch of the series compensation device to bypass the series compensation device for the purpose of reducing the impact on the series compensating capacitor due to no-load line closing operation during practical operation; to accelerate attenuation of the transient component of the secondary arc current in the reclosure process in which a single-phase ground fault occurs in the line, the series compensation device at fault phase is usually bypassed by means of a quick bypass linkage between the line circuit breaker and series compensation device [17]. Therefore, after use of a linkage operation between series compensation device and circuit breaker, the series compensation device installed in the UHV line has a little influence on the line closing and reclosing switching overvoltage, and also on the secondary arc current.

References

1. Liu Z. UHV power grid. Beijing: China Economic Press; 2005.
2. Wang X. Fundamentals of electric engineering. Xi'an: Xi'an Jiaotong University Press; 2009.
3. Liu Z. Overvoltage and insulation coordination of UHV AC transmission system. Beijing: China Electric Power Press; 2008.
4. Xie G. Overvoltage of electric power system. Beijing: Water Resources and Electric Power Press; 1985.
5. China Electric Power Research Institute. Research on overvoltage and insulation coordination of 1000 kV UHV AC double-circuit line on the same tower (part I). Beijing: China Electric Power Research Institute; 2009.

6. China Electric Power Research Institute. Research on overvoltage and insulation coordination of 1000 kV UHV AC double-circuit line on the same tower (part II). Beijing: China Electric Power Research Institute; 2009.
7. Chen S, Wu Z, Chen J, Wang F, Rong W. Research on limiting switching overvoltage by multistage closing resistors in 1000 kV transmission lines. Power Syst Technol. 2006;30 (20):10–13.
8. GB/T 50064-2014 Code for design of overvoltage protection and insulation coordination for AC electrical installations. 2014.
9. Zhu J. A discussion about overvoltage and insulation level of 1100 kV power grid of China [J]. Electr Equip. 2005;6(11):20–3.
10. Chen X, Chen W, Shen H, Li G, Zhang C, Che W, Sun J. Flexible measures to depress switching overvoltage in UHV transmission system. High Voltage Eng. 2007;33(11):1–5.
11. Zhang X, Zhou Z, Wang Y, Wang S, Zhou C, Cheng X, Ban L, Xiong M. Study on dynamic simulation of 1000 kV AC power transmission system. Power Syst Technol. 2006;30(7):1–4.
12. Yi Q, Zhou H, Ji R, Xu Q, Su F, Sun K, Chen J. Research on high-voltage reactor compensation of UHV AC transmission lines. Power Syst Prot Control. 2011;39(20):98–105.
13. Chen C. Fundamentals of electric engineering. Beijing: China Electric Power Press; 2003.
14. Jiang L, Wang Z, Zhang Q, Li Z. Impact of using 500 kV and 220 kV autotransformers to the single-phase short-circuit current. Power Syst Prot Control. 2008;36(18):108–16.
15. Ji R, Yi Q, Su Qiang F, Sun K, Chen J, Zhou H. Study on applicability of circuit breaker closing resistance in EHV and UHV AC system. Power Syst Technol. 2011;35(1):18–25.
16. Lin J, Chen W, Han B, et al. Failure rate calculation and necessity discussion on opening resistor of UHV circuit breakers. Proc CSEE. 2012;32(7):161–5.
17. Liu Z. Research result album of UHV AC transmission technologies (2011). Beijing: China Electric Power Press; 2012.
18. Zhou Y, Peng J, Wang G, Zhou C. Close-operation overvoltage of UHV AC transmission line with series compensation. Electr Power Autom Equip. 2008;28(1):23–6.

Chapter 7
Very Fast Transient Overvoltage of UHVAC System

Yang Li, Guoming Ma and Hao Zhou

Compared with 500 kV EHV GIS substation, 1000 kV UHV GIS/HGIS substation has different characteristics in terms of switchgear, system structure, insulation margin, requirements on safety and stability and importance. They are mainly reflected in the following aspects [1–7]:

1. The rated voltage of 1000 kV GIS substation is two times of that of 500 kV GIS substation, and the amplitude of very fast transient overvoltage (VFTO) overvoltage is also about two times of that of 500 kV GIS substation; however, the insulation level of 1000 kV GIS equipment is only 55% higher than that of 500 kV GIS equipment (not increased proportionally), so that the 1000 kV GIS equipment has smaller insulation margin and the hazardness of VFTO on UHV GIS is much heavier than that in 500 kV and below system.
2. The far-future system of 1000 kV UHV GIS substation is of large scale and complex layout, so that the VFTO conditions are more complex and difficult for prevention and analysis.
3. The winding turns of 1000 kV power transformer are more than that of 500 kV power transformer; therefore, under the effect of steep wave, the distribution of

Y. Li (✉)
State Grid Suzhou Power Supply Company, Suzhou, Jiangsu,
People's Republic of China
e-mail: 1041204573@qq.com

G. Ma
North China Electric Power University, Changping District,
Beijing, People's Republic of China
e-mail: ncepumgm@gmail.com

H. Zhou
College of Electrical Engineering, Zhejiang University,
Xihu District, Hangzhou, Zhejiang, People's Republic of China
e-mail: zhouhao_ee@zju.edu.cn

© Zhejiang University Press, Hangzhou and Springer-Verlag GmbH Germany 2018

H. Zhou et al. (eds.), *Ultra-high Voltage AC/DC Power Transmission*,
Advanced Topics in Science and Technology in China,
https://doi.org/10.1007/978-3-662-54575-1_7

inter-turn voltage is more uneven, and the head end winding of 1000 kV transformer is easier to be damaged due to VFTO.
4. In the power transmission system, the 1000 kV GIS substation has a higher importance, so that it requires higher safety and stability and not allows the hidden danger.

This chapter first discusses the generation mechanism, characteristics, harm, restriction, and prevention measures of VFTO, then studies the VFTO and the influence factors of 1000 kV GIS substation under different operation conditions, then compares the VFTO between 500 and 1000 kV GIS substations and between substation and power plant, then carries out research on restriction of VFTO wave front steepness invading port of the main transformer on the overhead line, and finally analyzes the GIS transient enclosure voltage (TEV) in GIS substation and power plant.

7.1 Generation Mechanism and Characteristics of VFTO

In the substation, the operations such as switching of no-load busbar with disconnector, and opening and closing of circuit breaker are all routine operations and the frequency and possibility of these operations are both large. These operations usually do not generate overvoltage with large harm in the general air insulated switchgear (AIS) substation. However, in the GIS substation or HGIS substation, these operations, especially operations of disconnector that without arc suppression ability, are possible to generate very fast transient overvoltage, namely VFTO. During the operation of 500 kV GIS in China, there have been many GIS internal breakdown and external connecting equipment accidents resulting from very fast transient phenomenon. For example, during the system commissioning of Guangdong Daya Bay Nuclear Power Project in 1992, the main insulation of one phase of the main transformer was broken down due to very fast transient overvoltage. In 2001, one 500 kV transformer of Zhejiang Beilun Power Plant was also damaged due to very fast transient overvoltage.

Usually, the arc suppression performance of circuit breaker in GIS substation or HGIS substation is very good, and it is rarely possible to generate arc restriking; therefore, the overvoltage generated during restriking can be neglected, and it is only required to consider the possible VFTO generated during operation of disconnector. The structure of UHV GIS disconnector is as shown in Fig. 7.1 [8].

Due to the slow opening and closing speed and poor arc suppression performance, during the opening and closing operations, the clearance between the fixed contact and the moving contact is easy to generate multiple arcing and arc quenching phenomena, as shown in Figs. 7.2 and 7.3. Here, one GIS branch not energized that is pulled open by operating the disconnector is taken as example. The branch not energized, as one electrically "isolated island" (also called as load side), can be approximately considered as one ground lumped capacitance. After the branch is disconnected by the disconnector, the residual charge is maintained on the branch that is not energized for a relatively long time; along with widening of

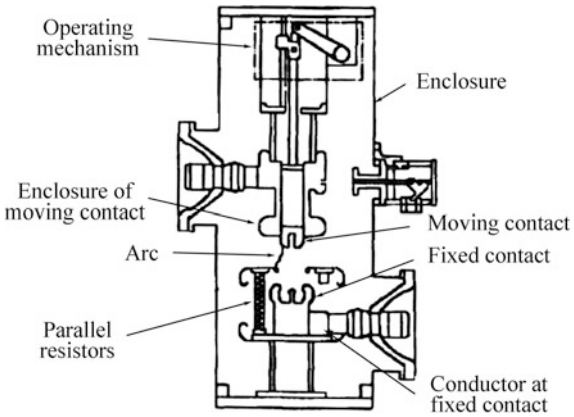

Fig. 7.1 Sketch of disconnector Reprinted from Ref. [8], Copyright 2014, with permission from Proceedings of the CSEE

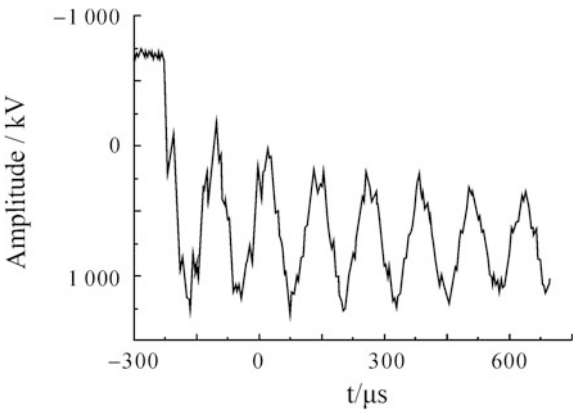

Fig. 7.2 Typical waveform of VFTO nearby the disconnector

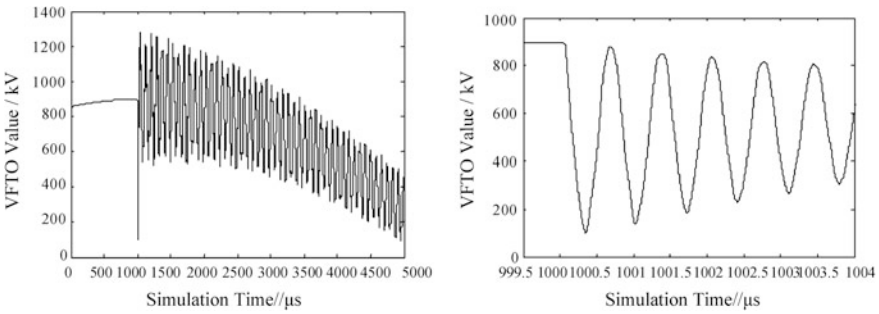

Fig. 7.3 Typical waveform of VFTO at the inlet of main transformer

the open contact of disconnector, the electrical potential of the contact at disconnector system side is varied together with the system; when the voltage difference between the two contacts obtains certain amplitude, the disconnector generates clearance breakdown and form the arc. This process is very similar to restriking phenomenon occurred when circuit breaker closes the no load line (or capacitor) in the power grid, and it is able to generate the overvoltage with large amplitude. As the GIS equipment is designed with electric field that is slightly uneven, and the open contact of GIS disconnector is smaller than that of AIS disconnector, the arcing time of the disconnector is very short (in nanosecond) and the overvoltage wave front time is very short and the wave front steepness is very great.

Due to the influence of many factors, such as movement of moving contact of disconnector and SF6 gas flow arc quenching in GIS, the high-frequency arc generated from breakdown between contacts in GIS is very easy to blow out and the arc duration is very short. Along with the variation of power voltage, the arc recovery voltage is increased for another time, so that, within short time, restriking is repeated for many times, thus to generate VFTO. As the opening and closing speed of the disconnector is too slow, during each operation of GIS disconnector, several hundred times of restriking occur. So, it generates a series of very fast transient overvoltage (namely VFTO) with very steep wave front steepness, very high frequency and both positive and negative polarity. During switching of no-load busbar with disconnector, the equivalent circuit is as shown in Fig. 7.4. In terms of the amplitude of overvoltage, the maximum value is:

$$U_{\max} = K \cdot U_s - U_{TC} \leq 3.0 \text{ p.u.} \tag{7.1}$$

where

K oscillation or overshoot factor, $0 \leq K \leq 2$;
U_{TC} voltage of residual charge, -1.0 p.u. $\leq U_{TC} \leq 1.0$ p.u.;
U_s the power voltage;
for 1000 kV UHV GIS: 1 p.u.$= 1000 \times 1.1/\sqrt{3} \times \sqrt{2} = 898$ kV.

Under the extreme conditions, during the closing of disconnector, $U_{TC} \rightarrow 1.0$ p.u., $U_s \rightarrow -1.0$ p.u., $K \rightarrow 2$, at this time, $\Delta U \rightarrow 2.0$ p.u. and $U_{\max} \rightarrow 3.0$ p.u.. The

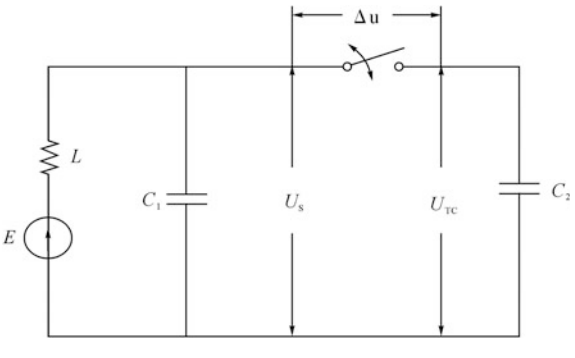

Fig. 7.4 Equivalent circuit for switching of no-load busbar with disconnector

oscillation frequency of very fast transient overvoltage (namely VFTO) depends on the substation parameters and GIS layout. The steep shock wave generated during opening and closing operation is spread to busbar at both sides along the open contact of disconnector, and the transmission speed is slightly lower than light speed; on the various electrical nodes connected on busbar, the refraction and reflection are emergent due to different characteristic impedance of the equipment, so that the transient waveform of very fast transient overvoltage tends to be complex.

Based on the generation mechanism of VFTO and characteristics of GIS equipment, VFTO has the following common characteristics:

(1) Steep wave front, for which the rise time is usually 2–20 ns: when restriking occurred to the contact clearance of disconnector, the arc striking process is very rapid; thus, the voltage waveform that injected into the network has very high ascending or descending steepness.
(2) Theoretically, the amplitude of VFTO can be up to 3.0 p.u. This extreme condition is generated when the polarities of voltage on both sides of the branch being open are reverse and both are the maximum values. Considering the actual reasons, such as residual voltage, damping and attenuation, the VFTO obtained in actual measurement or simulation test does not exceed 2.0 p.u. in most cases. Considering the worst case, the maximum overvoltage can be up to about 2.5–2.8 p.u. [9].
(3) The VFTO has a lot of high-frequency components, within the range of 30 kHz–100 MHz. This is because that GIS uses SF_6 gas as the medium, with insulation strength well above that of air. In addition, both spacing and busbar length between the adjacent electrical equipment are far less than that for similar type of AIS substation. The refraction and reflection time in traveling wave of VFTO in GIS is very short. After repeated superposing, it results in dramatic rise of overvoltage transient oscillation frequency.
(4) VFTO is closely related to the restriking and arc quenching moments of GIS disconnector and position of the disconnector nodes in GIS equipment. In addition, it is directly related to the operating wiring mode of GIS.

7.2 Harm of VFTO

From the perspective of harm of VFTO on electrical equipment, the VFTO can be divided into two types, namely internal VFTO and external VFTO. The internal VFTO refers to internal VFTO in the primary equipment of GIS, which exists in the primary electrical equipment, such as GIS pipe, circuit breaker, disconnector, etc., and poses a threat on main insulation of GIS body; the external VFTO refers to VFTO transmitted from primary equipment of GIS to external electrical equipment (such as power transformer, overhead line, instrument transformer and bushing), which poses a threat mainly on the main transformer and the secondary equipment within the substation.

7.2.1 Harm of VFTO to GIS Main Insulation

At present, the typical test waveform and withstand voltage standard for VFTO on the main insulation of UHV GIS equipment have not been determined in China. In general, it is considered that VFTO can be compared with LIWV (lightning impulse withstand voltage). The LIWV of UHV GIS is 2400 kV [10], some experts in China proposed that the withstand voltage standard for VFTO can be considered with 15% safety margin based on the LIWV; that is, VFTO shall not exceed 2087 kV (equivalent to 2.32 p.u.) [2]. Comparatively, the LIWV of 500 kV GIS is 1550 kV [11], and after considering 15% safety margin based on LIWV, the withstand voltage standard for VFTO is 1348 kV (equivalent to 3.0 p.u., where 1.0 p.u. $= 500 \times 1.1/\sqrt{3} \times \sqrt{2} = 449$ kV). Because the maximum amplitude of VFTO does not exceed 3.0 p.u., for main insulation of 500 kV GIS equipment, it does not cause harm in general; however, for UHV GIS equipment, the maximum amplitude of VFTO generated due to operation of disconnector can be up to 2.5 p.u., exceeding the withstand voltage ability of main insulation of the equipment, and possibly causing damage to the main insulation of the equipment.

7.2.2 Influence of VFTO on Power Transformer

7.2.2.1 Mechanism of Harm of VFTO to Main Transformer

In the all electrical equipment connected with GIS, the transformer is under the largest harm of VFTO, especially the inter-turn insulation at the inlet section of transformer directly connected with GIS.

When the VFTO steep wave is transmitted to the transformer, it is equal to add one steep wave front at the end of transformer. The rise time of VFTO steep wave is possibly only dozens of nanoseconds, far less than the wave front rise time during lightning impulse test (about 1.2 μs). For the transformer with short distance to GIS substation, under the effect of steep wave front voltage wave, the equivalent capacitive impedance of inter-winding and winding-to-ground is far less than the impedance value of its winding inductance, so that the simplified equivalent circuit of the transformer winding is as shown in the right figure of Fig. 7.5; where C_0 and K_0 are

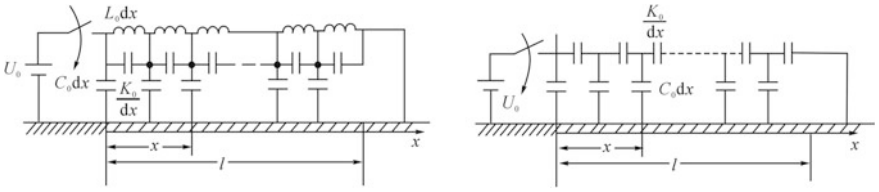

Fig. 7.5 Simplified equivalent circuit diagram when transient voltage is transmitted to single-phase winding

respectively the ground capacitance and inter-turn capacitance of unit length winding. In case of the equivalent model as shown in Fig. 7.5, the very uneven initial potential distribution is generated on the transformer winding, as shown in Fig. 7.6, where $\alpha = \sqrt{\frac{C_0}{K_0}}$, for ordinary transformer, αl = 5–15 , with an average of about 10. Thus, the inter-turn voltage at the head end of the transformer winding is very large, posing the threat on inter-turn insulation safety of the transformer, especially longitudinal insulation safety at the head end of transformer winding [12].

For the transformer with long distance to GIS substation, or the transformer that not directly connected, it passes through two bushings and one section of overhead line; therefore, the steep wave front wave tends to be gentle.

Actually, VFTO has certain harm on the main transformer, on the one hand, it generates uneven voltage distribution in the transformer coil due to the steep wave front and endanger the longitudinal insulation of the main transformer; on the other hand, the high-frequency component of VFTO may be corresponding to the oscillation frequency of the transformer, thus to cause electromagnetic oscillation in the transformer, generate relatively high overvoltage and result in damage to the inter-turn insulation and main insulation of the main transformer [13, 14]. When considering the influence on the inter-turn insulation of the main transformer due to internal resonance of main transformer coil resulting from high-frequency component of VFTO, the restriction standard and assessment method have not been clearly defined tentatively. Therefore, when introducing the threat of VFTO on the main transformer, major consideration shall be given to the influence on main insulation and the longitudinal insulation of the main transformer due to the amplitude and wave front steepness of VFTO arriving at port of the main transformer. When the amplitude of VFTO arriving at port of the main transformer and VFTO wave front steepness invading the port of the main transformer are, respectively, less than the corresponding VFTO restriction levels, it is considered that VFTO will not pose a threat to the main insulation and longitudinal insulation of the main transformer at this moment.

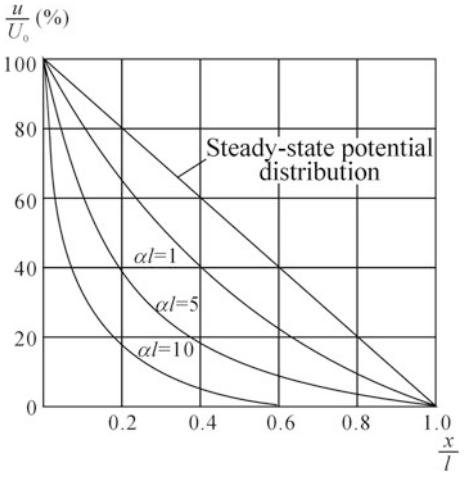

Fig. 7.6 Initial potential distribution of single-phase winding under the effect of steep wave front

7.2.2.2 Harm of VFTO on the Main Insulation of Main Transformer

When VFTO is transmitted to the transformer, it is necessary to consider the safety of main insulation of the transformer (insulation to ground and windings of other two phases).

The method similar to that mentioned in the above section can be used to determine the restriction level of the main insulation of the 1000 kV transformer on VFTO. The LIWV of main insulation of the 1000 kV transformer is 2250 kV [10], and its coordination factor is the same as that of main insulation of GIS. Therefore, the restriction level of main insulation of the transformer on VFTO is 1957 kV (2.18 p.u.). A lot of actual measurements and simulation results show that the maximum VFTO at the port of the transformer is usually far less than 2.18 p.u., and this is mainly because that when VFTO is transmitted to the port of the transformer through GIS equipment (such as disconnector, GIS pipe and bushing), the overvoltage amplitude will have large attenuation. In addition, the equivalent ground capacitance of both the transformer and the capacitor voltage transformer (CVT) connected with it is very large, and thus it will play a certain restriction role on the amplitude of the overvoltage at the port of the transformer. Therefore, VFTO usually do not cause harm to the main insulation of the transformer.

7.2.2.3 Harm of VFTO to the Longitudinal Insulation of Main Transformer

The VFTO transmitted to the main transformer has a large threat to the longitudinal insulation of the main transformer (insulation of inter-turn, inter-layer, inter-pie type coil, etc.). As the VFTO has steeper wave front steepness than that of lightning overvoltage, after being transmitted to the transformer, VFTO generates very uneven voltage distribution among the winding turns, especially at the head end of the winding, and it generates very large voltage difference, possibly causing breakdown of inter-turn insulation of the winding. Therefore, the maximum harm of VFTO on the transformer is the threat on longitudinal insulation resulting from wave front steepness.

The index to assess the harm of VFTO on longitudinal insulation of the transformer is mainly the VFTO wave front steepness. For standard lightning impulse wave overvoltage, the LIWV of the transformer is 2250 kV, the wave front time is 1.2 μs, and the wave front steepness is 1875 kV/μs. Usually, the transformer generated by the manufacturer can withstand such wave front steepness. At present, there is no unified assessment standard on the harm of VFTO on longitudinal insulation of the transformer, and considering that the VFTO wave front is steeper than that of lightning overvoltage and has larger harm on longitudinal insulation of the main transformer, the wave front steepness of 1875 kV/μs for standard lightning impulse wave overvoltage can be conservatively referred to assess the harm of VFTO wave front steepness on longitudinal insulation of the transformer. That is to say, usually, the longitudinal insulation of the main transformer can withstand the

wave front steepness of 1875 kV/μs; in case the VFTO wave front steepness at the port of the transformer is controlled below 1875 kV/μs, the longitudinal insulation of the main transformer is safe. Therefore, the restriction level of longitudinal insulation of the transformer on VFTO wave front steepness can be approximately taken as 1875 kV/μs.

7.2.3 *Influence of VFTO on the Secondary Equipment*

The amplitude of high-frequency component of VFTO is very high. In case of VFTO, the external transient electromagnetic field related to it is radiated to the periphery from GIS enclosure and overhead line, and any electronic equipment is under the influence of transient electromagnetic field. At the same time, the external VFTO is coupled with the enclosure and ground, causing dangerous transient ground potential rise (TGPR) and transient enclosure voltage (TEV) rise. TEV or TGPR causes interference in or even damage to the secondary equipment (such as control, protection, and signal) connected with GIS; therefore, secondary electrical equipment may also be damaged.

7.2.4 *Cumulative Effect of VFTO*

During the operation of primary equipment using the disconnector, it is possible to generate VFTO, thus to have a certain threat on the insulation safety of GIS equipment (such as the support insulator and bushing). Along with long-term operation of the disconnector, the damage effect of VFTO on the insulation of electrical equipment is continuously cumulated. The cumulative damage speeds up the insulation aging; at the same time, the insulation aging deteriorates the damage degree of cumulative effect. So, when the insulation at a certain point of electrical equipment is relatively weak, it is easy to be broken down.

7.3 VFTO in 1000 kV GIS Substation Under Different Operation Conditions

The amplitude and characteristics of VFTO are closely related to the main wiring and operation conditions of the substation. The wiring method in the manner of 3/2 circuit breakers has very high operation reliability and flexibility and it is convenient for dispatching and expansion; therefore, 1000 kV GIS substation is in general applied with the wiring method in the manner of 3/2 circuit breakers, as shown in Fig. 7.7. In this figure, the average distance between circuit breaker and disconnector (CB101 and DS1012) on each circuit breaker string is about 5 m, and the average

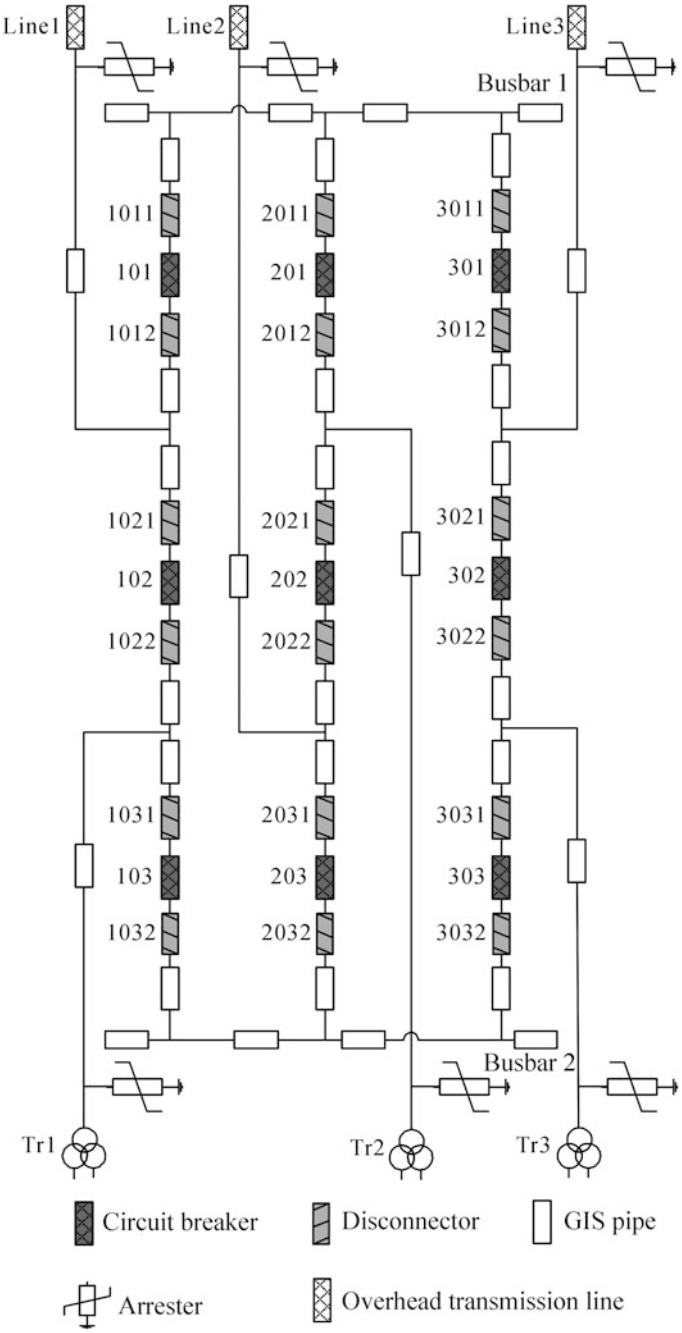

Fig. 7.7 System wiring diagram of GIS substation

distance between two adjacent disconnectors (DS1012 and DS1021) is about 14 m; the average length of GIS pipe busbar between GIS outlet bushing and circuit breaker string is 40 m; the length of overhead line between GIS outlet bushing and main transformer is 60 m. In terms of operating objects, the switching operations of 1000 kV GIS substation can be divided into three types, namely operation with main transformer, operation with outgoing line, and operation with busbar.

7.3.1 VFTO Generated Due to Operation with Main Transformer

Operation with main transformer can be divided into two types, namely switching off main transformer and switching on main transformer. Here, operation with main transformer Tr1 is taken as example. When switching off main transformer Tr1, it is necessary to open the circuit breakers 102 and 103 first, and then open the disconnectors 1021, 1032, 1022 and 1031; when switching on main transformer Tr1, it is necessary to close the disconnectors 1022, 1031, 1021 and 1032 first, and then close the circuit breakers 102 and 103. For switching of main transformer, when operating the disconnector, the circuit breaker had not been closed, at this time, it usually does not generate VFTO for opening and closing of disconnectors 1022 and 1031; however, when operating disconnectors 1021 and 1032, it may generate VFTO with large amplitude. The simulation and analysis show that the maximum value of VFTO generated on the GIS body due to operation with main transformer can be up to 2.38 p. u., possibly exceeding the insulation strength of GIS and having a certain threat on the main insulation of GIS body; however, while switching of main transformer and operation with disconnector, because the circuit breaker had not been closed, the maximum value of VFTO generated at the port of the main transformer is only 0.02 p. u., having no threat on the main insulation of the main transformer. During opening and closing of disconnectors 1021 and 1032, the circuit breakers 102 and 103 are both under open state to cut off the path from which VFTO invades into the main transformer; therefore, VFTO can only be transmitted to the open contact of the main transformer through the open contact capacitance of the circuit breaker. In addition, there is one overhead line with length of about 60 m from outlet of the main transformer to outlet of GIS bushing; therefore, VFTO wave front steepness transmitted to inlet of the main transformer due to such operation is small and about 412 kV/μs, having no harm on the inter-turn insulation of the main transformer.

7.3.2 VFTO Generated Due to Operation with Outgoing Line

The process for operation with outgoing line is similar to that for operation with main transformer. When switching off the outgoing line, it is necessary to open

corresponding circuit breaker first and then pull open the corresponding disconnector; when switching on the outgoing line, it is necessary to close the corresponding disconnector first and then close the corresponding circuit breaker. Here, switching off of outgoing line 1 is taken as example. When switching off the outgoing line, open the circuit breakers 102 and 101 first, and then open the disconnectors 1021, 1012, 1011 and 1022 in sequence; when switching on the outgoing line, the process is reverse to the above sequence. The opening and closing of above four disconnectors are all possible to generate VFTO. During operation with outgoing line, the maximum amplitude of VFTO on GIS body is about 2.37 p.u., exceeding the tolerance range of GIS insulation strength and possibly causing harm to the main insulation of GIS body. The maximum amplitude of VFTO at port of the main transformer is 1.09 p.u., far less than the restriction level of main insulation of the main transformer, and having no harm to the main insulation of the main transformer. When operating disconnector 1022, the VFTO wave generated can invade the port of the main transformer through GIS busbar; therefore, the VFTO wave front steepness transmitted to the inlet of the main transformer is higher than that during switching of main transformer. However, there is one overhead line with length of about 60 m from the port of the main transformer to the outlet of GIS bushing; therefore, the maximum wave front steepness arriving at the inlet of the main transformer is only 550 kV/μs, having no harm on the inter-turn insulation of the main transformer.

7.3.3 VFTO Generated Due to Operation with Busbar

When switching off the busbar, it is necessary to open all operating circuit breakers (such as circuit breakers 103, 203 and 303) connected to the busbar in turn first, and then open the disconnectors (such as disconnectors 1031, 1032, 2031, 2032, 3031 and 3032) on both sides of each busbar circuit breaker in turn. The disconnectors (1031, 2031 and 3031) are still connected with the system at one end, opening and closing of these switches may generate VFTO. However, at this time, the maximum amplitude of VFTO on GIS body is about 2.0 p.u., and the maximum amplitude of VFTO at the port of the main transformer is about 1.04 p.u., still having very large margin in comparison with the insulation strength. The maximum VFTO wave front steepness transmitted to the inlet of the main transformer is about 533 kV/μs, insufficient to pose a threat to the inter-turn insulation of the main transformer. When switching on the busbar, it is necessary to close the disconnectors on both sides of each busbar circuit breaker in turn first, and then close all (or partial) operating circuit breakers connected on the busbar in turn. During maintenance, the busbar discharges residual charge through ground switch and the voltage of residual charge on load side is zero potential, therefore, VFTO generated through closing disconnector at this time is much less than that generated when changed from operation to maintenance, having no threat to the main insulation of the substation and insulation of the main transformer.

Table 7.1 Calculation results of VFTO under different operating modes

Operating mode	Switching of main transformer	Switching of outgoing line	Switching of busbar
Maximum amplitude of VFTO in GIS substation/p.u.	2.38	2.37	2.0
Maximum amplitude of VFTO at port of the main transformer/p.u.	0.02	1.09	1.04
Wave front steepness at inlet of the main transformer/kV· μs^{-1}	412	550	533

According to the contents of the above three sections, the calculation results of VFTO can be obtained, as shown in Table 7.1.

It can be seen that the VFTO generated due to operation with busbar for the 1000 kV GIS substation does not pose a threat to the main insulation of GIS body. However, the VFTO generated due to operation with main transformer and operation with outgoing line poses a threat to the main insulation of GIS body. While there is one long overhead line between GIS bushing outlet and main transformer for the said 1000 kV GIS substation, under the above three operating modes, the VFTO wave front steepness invading the main transformer (as shown in Table 7.1) does not exceed the restriction level in all cases, not posing a threat to the longitudinal insulation of the main transformer.

However, for different substation, the length of overhead line mentioned above is different. Therefore, under different operating modes, whether VFTO poses threat to the longitudinal insulation of the main transformer is determined according to the actual conditions. Nevertheless, according to the research and discussion at the rear part of this chapter, for 1000 kV GIS substation, even if the length of overhead line is zero, the VFTO wave front steepness invading the main transformer under different operating modes with disconnectors does not exceed the restriction level of 1875 kV/μs, and has about 10% margin.

In conclusion, for 1000 kV GIS substation, VFTO does not pose a threat to both main insulation and longitudinal insulation of the main transformer within the substation. However, it poses a threat to the main insulation of GIS body. Therefore, main consideration shall be given to prevent the threat of VFTO on the main insulation of GIS body.

7.4 Influence Factors of VFTO

The amplitude and frequency of VFTO are dependent on multiple factors. It is not only related to the action characteristics, electric field distribution and dynamic insulation process of the switch, but also related to structure characteristics, dimensions and equipment parameters of GIS.

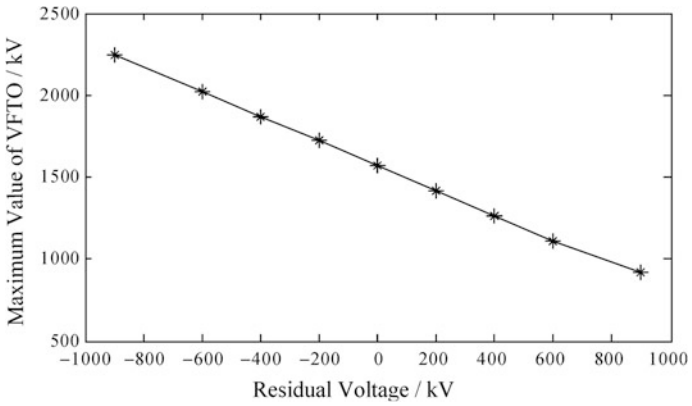

Fig. 7.8 Relationship between residual voltage and amplitude of VFTO

7.4.1 Influence of the Residual Voltage at Load Side on the Amplitude of VFTO

The magnitude of the residual voltage at load side has a direct influence on the amplitude of VFTO. The amplitude of VFTO and the value of residual voltage are basically in linear relation: the larger the residual voltage, the larger is the maximum value of VFTO. Figure 7.8 presents the maximum value of VFTO generated due to restriking under different residual voltage when system voltage is +1.0 p.u.

The residual charge voltage is closely related to the magnitude of capacitance current at load side, opening and closing speed of disconnector, restriking moment of switch, and charge leakage on busbar. In case the leakage resistance at load side is very large, it will maintain high residual voltage unchanged from several hours to several days, thus to generate large VFTO.

7.4.2 Influence of the Capacitance at Inlet of Transformer on VFTO

The capacitance at the inlet of the transformer is closely related to the amplitude of VFTO. As the voltage on the capacitance at the inlet of the transformer cannot be changed abruptly, the wave front transmitted to the inlet can only be increased gradually along with the gradual charging of capacitance. Therefore, along with the increase of capacitance value at the inlet of the transformer, the amplitude of VFTO at the inlet of the transformer is decreased gradually, and the wave front is leveled and the wave front steepness is decreased. Reversely, the amplitude of VFTO in GIS substation is increased along with the increase of capacitance value at the inlet

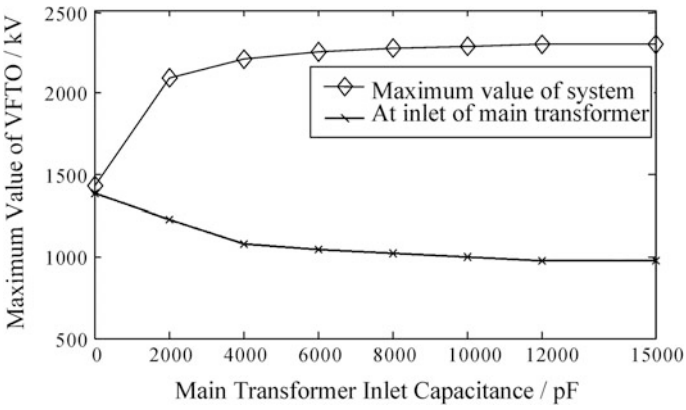

Fig. 7.9 Main transformer inlet capacitance and VFTO amplitude

of the transformer. However, the capacitance at inlet of the transformer is related to factors such as voltage level, capacity, and structure; the higher the voltage level and the larger the rated power of the transformer, the larger is the capacitance at the inlet (Fig. 7.9).

7.4.3 Influence of Arc Resistance on the Amplitude of VFTO

When restriking occurs in the disconnector of GIS, its arc resistance is one time varying parameter, consisting of one constant component and one time varying component, as shown in the following equation:

$$R(t) = R_S + R_0 e^{-t/T} \tag{7.2}$$

where $R_S = 0.5\ \Omega$, $R_0 = 10^{12}\ \Omega$, $T = 1$ ns.

During the arc start, the arc resistance is large. However, along with the increase of arc current, its attenuation component is attenuated rapidly, and the arc resistance is decreased gradually, and tends to be a stable value of constant component finally. In the process of analysis, it is usually simplified as one fixed resistance with very small value (about 2 Ω). The arc resistance has damping effect on VFTO and plays a certain restriction role, as shown in Fig. 7.10. However, the arc resistance is very small, whose restriction results are not obvious. The disconnector mounted with additional parallel resistance is equivalent to increase the arc resistance to reduce VFTO. Obviously, as long as the parallel resistance is within the range of dozens of ohms to hundreds of ohms, disconnector mounted with additional parallel resistance

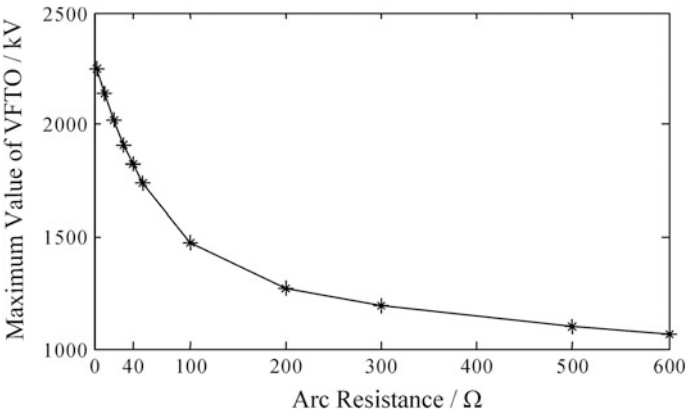

Fig. 7.10 Arc resistance and VFTO amplitude

can play a notable role to weaken VFTO and achieve obvious effect on control of VFTO.

7.4.4 Influence of Zinc Oxide Arrester on VFTO

The zinc oxide arrester nearly has no protection on VFTO; on the contrary, it causes the counter to generate frequent maloperation due to VFTO. Under the effect of VFTO, the zinc oxide arrester is equivalent to one nonlinear valve plate resistance and one ground stray capacitance about 20 pF that are paralleled. In general, the amplitude of VFTO on the arrester is not large; therefore, there cannot be excessive current in the valve plate resistance of the arrester to actuate the arrester. However, under the effect of VFTO for which the wave front time is in nanosecond, a series of high-frequency steep wave current ranging from several amperes up to dozens of amperes may flow through the ground stray capacitance of the arrester, thus to cause the maloperation on the counter of the arrester.

7.5 Comparison of VFTO in 500 and 1000 kV GIS Substations

This section gives main consideration to 500 and 1000 kV GIS substations, thus to discuss the influences of VFTO on main insulation of GIS body, main insulation of the main transformer and longitudinal insulation of the main transformer in the substation, and compare the VFTO characteristics for 500 and 1000 kV GIS substations.

7.5.1 Switch Operation Sequence in Substation Under Typical Disconnector Operating Mode

To analyze the influences of VFTO on main transformer and GIS equipment in both 500 kV GIS substation and 1000 kV GIS substation, it is necessary to determine the simulation calculation mode first.

Figures 7.11 and 7.12 are the main wiring diagrams for typical 1000 kV GIS substation and 500 kV GIS substation.

When studying the influences of VFTO on equipment in GIS substation, the amplitude of VFTO is closely related to the operating mode of the disconnector. The typical operating modes of the disconnector include switching of main transformer, switching of outgoing line, and switching of busbar. The structure of various circuit breaker strings between the two main busbars are similar; therefore, one circuit breaker string is here taken as an example to study the switching sequence of circuit breaker and disconnector under the above three typical operating modes, judge the disconnector that is possible to generate VFTO under different operating modes, and finally create the simulation model.

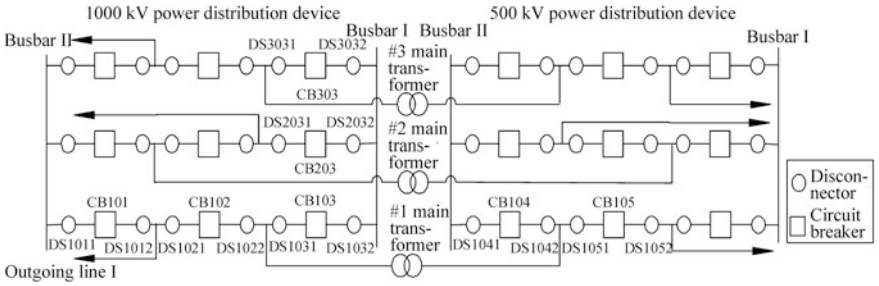

Fig. 7.11 Main wiring diagram for 1000 kV GIS substation

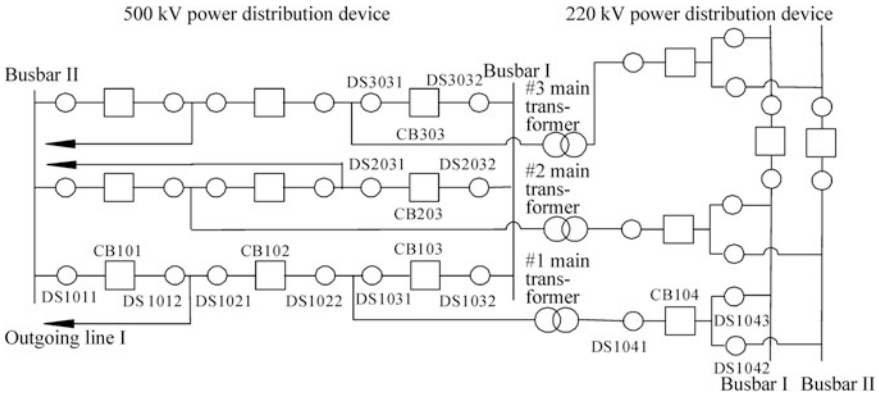

Fig. 7.12 Main wiring diagram for 500 kV GIS substation

7.5.1.1 Switch Operation Sequence in 500 kV GIS Substation Under Typical Disconnector Operating Mode

1. Switching of outgoing line.

Here, switching of outgoing line I is taken as an example. During switching-off outgoing line, it is necessary to open circuit breakers CB102 and CB101 first, and then open disconnectors DS1021, DS1012, DS1011, and DS1022 in turn. The switching on sequence is reverse of the above sequence. It is possible to generate VFTO by both opening and closing the above four disconnectors.

2. Switching of busbar.

While switching off the busbar, it is necessary to open all circuit breakers (such as CB103) connected with this busbar first, and then open the disconnectors (such as DS1032 and DS1031) at both sides of the circuit breaker. The disconnector at the power supply side (such as DS1031) is connected with power supply at one end. Therefore, switching off this disconnector may generate VFTO, while switching off disconnector DS1032 at busbar side will not generate VFTO, since the residual charge on the busbar is usually discharged completely. When switching on the busbar, the operating sequence is just reverse of the switching-off sequence of busbar. At this moment, considering that the busbar has been de-energized for a long time, closing of DS1032 does not generate VFTO usually; however, closing of DS1031 may generate VFTO.

3. Switching of main transformer.

Switch operation sequences for switching on the main transformer and switching off the main transformer are just reverse. Here, the switching off of #1 main transformer in the 500 kV substation is taken as example. During switching off of #1 main transformer, it is necessary to open circuit breakers CB104, CB102, and CB103 first, and then open the disconnectors at both load side and power supply side of the three circuit breakers in turn.

During shutdown operation of the main transformer, after opening of circuit breakers CB104, CB102, and CB103 in turn, the transformer is under de-energized state. Since the neutral point of the transformer is directly earthed, the GIS pipes and disconnectors (DS1022 and DS1031 as shown in Fig. 7.12) connected to the transformer discharge the electric charges through the transformer winding rapidly, thus to cause significant decrease of residual charge voltage on the disconnectors. Through simulation analysis, it can be seen that, after breaking of the transformer with power grid at both sides, the residual voltage on the disconnector connected with it is decreased to about 0.22 p.u. within only one power frequency cycle, as shown in Fig. 7.13. During actual operation, the disconnector can only be pulled open after confirming that the circuit breaker has been disconnected, the interval

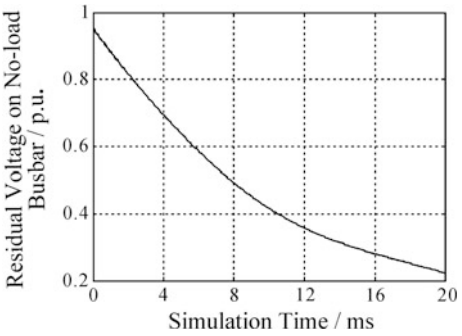

Fig. 7.13 Variation of residual voltage on no-load busbar connected with the main transformer with time after removal of the main transformer

from disconnection of circuit breaker to operation of disconnector can sufficiently reduce the residual charge voltage on the main transformer to very low level, and thus, the main transformer is basically not energized. Therefore, during opening of disconnectors DS1022 and DS1031, it is impossible to generate VFTO. During opening of disconnectors DS1021 and DS1032, it is possible to generate VFTO because the two disconnectors are connected with power supply at one end.

In conclusion, during the removal of main transformer, opening of disconnectors DS1022 and DS1031 does not generate VFTO, and opening of disconnectors DS1021 and DS1032 generates VFTO. In addition, during closing of main transformer, the main transformer has been de-energized for a long time; therefore, closing of disconnectors DS1022 and DS1031 does not generate VFTO usually, while closing of disconnectors DS1021 and DS1032 may generate VFTO.

7.5.1.2 Switch Operation Sequence in 1000 kV GIS Substation Under Typical Disconnector Operating Mode

For UHV GIS substation, the switch operation sequences for switching of outgoing line and switching of busbar are same as that for 500 kV GIS substation.

For switching of main transformer, here, switching off of 1# main transformer is taken as the example. During switching off of 1# main transformer, it is necessary to open circuit breakers CB102, CB103, CB104, and CB105 first, and then open the disconnectors at both load side and power supply side of the four circuit breakers in turn. Due to the discharge of residual charges on the main transformer, the operation of DS1022 and DS1031 does not generate VFTO. While during the operation of DS1021 and DS1032, it is possible to generate VFTO because the two disconnectors are connected with power supply at one end. During closing of the main transformer, as the main transformer is de-energized for a long time, the closing of DS1022 and DS1031 does not generate VFTO usually, while the closing of DS1021 and DS1032 may generate VFTO.

Table 7.2 Disconnectors in substation that may generate VFTO under different operating modes

Operating mode	Switching of outgoing line	Switching of busbar	Switching of main transformer
Disconnectors	DS1021, DS1012 DS1011, DS1022	DS1031 DS20131, DS3031	DS1021 DS1032

7.5.1.3 Conclusions

In conclusion, for both 500 kV GIS substation and 1000 kV GIS substation, the switch operation sequences for switching of outgoing line are same, and the switch operation sequences for switching of busbar are also same. However, for switching of main transformer, as the wiring manner of the two at LV side is different, during switching of main transformer, the quantities of switches requiring switching at LV side are different. During switching of main transformer for 1000 kV GIS substation, it is necessary to open two circuit breakers and four disconnectors at LV side, which is more complex than switch operation during switching of main transformer for 500 kV GIS substation.

In addition, it can be seen from the above analysis that, during operation of disconnector connected with the live system, it generates VFTO usually. Therefore, the disconnectors that can generate VFTO under the above three typical disconnector operating modes are as shown in Table 7.2. When opening of one disconnector can generate VFTO, closing of this disconnector can also generate VFTO; when opening of one disconnector does not generate VFTO, closing of this disconnector also does not generate VFTO.

According to the results shown in Table 7.2, when we calculate VFTO under corresponding disconnector operating modes, it is only necessary to consider VFTO generated when operating the disconnectors listed in this table.

7.5.2 VFTO Restriction Level by Equipment in 500/1000 kV GIS Substation

For EHVAC and UHVAC system, the typical waveform of test voltage representing VFTO and value of withstand voltage of equipment uniformly specified have not yet been proposed internationally. Usually, it is considered that VFTO can be compared with LIWV. After dividing LIWV of GIS equipment by a certain margin factor, the VFTO restriction level of GIS equipment can be obtained. In the UHV system, such margin factor is usually taken as 1.15. In the 1000 kV system, LIWV for GIS equipment and main transformer is 2400 and 2250 kV, respectively. After considering margin factor of 1.15, it can be obtained that, in the UHV system, the VFTO restriction level of main insulation of GIS body and main transformer is 2400/1.15 = 2087 kV and 2250/1.15 = 1956 kV, respectively. For 500 kV AC

Table 7.3 VFTO restriction level by EHV 500 kV equipment

Equipment name	Transformer		GIS body
	Main insulation	Longitudinal insulation	Main insulation
LIWV	1550 kV	–	1550 kV
Margin factor k	1.15	–	1.15
VFTO restriction level	1348 kV	1291 kV/μs	1348 kV

Table 7.4 VFTO restriction level by UHV 1000 kV equipment

Equipment name	Transformer		GIS Body
	Main insulation	Longitudinal insulation	Main insulation
LIWV	2250 kV	–	2400 kV
Margin factor k	1.15	–	1.15
VFTO restriction level	1956 kV	1875 kV/μs	2087 kV

system, the margin factor between LIWV of GIS equipment and VFTO tolerance level of equipment is also taken as 1.15. LIWV for both 500 kV GIS body and main transformer is 1550 kV, and the VFTO restriction level thereof is its LIWV of 1550 kV divided by coordination factor of 1.15, namely 1348 kV (3.0 p.u.).

The index to assess whether VFTO has harm on the longitudinal insulation of the transformer is mainly the VFTO wave front steepness. In the 500 kV AC system, for standard lightning impulse wave overvoltage, LIWV of the transformer is 1550 kV, the wave front time is 1.2 μs, and the wave front steepness which inlet of the transformer is able to undertake is 1291 kV/μs; in the UHV system, LIWV of the transformer is 2250 kV, and the wave front steepness which inlet of the transformer is able to undertake is 1875 kV/μs. Tables 7.3 and 7.4 present the VFTO restriction level of three types of insulation in the EHV 500 kV and UHV 1000 kV GIS systems, respectively.

7.5.3 Comparison of VFTO in Typical 500 and 1000 kV GIS Substations

Here, a certain 500 kV GIS substation and a certain far-future 1000 kV GIS substation are selected as the calculation model, thus to determine the influences of VFTO on GIS body and main transformer under typical disconnector operating modes through simulation calculation. As the disconnector mounted with parallel resistance has certain weakening effect on the VFTO, for the purpose of strictness, when discussing the VFTO characteristics in the substation in this section, the case that disconnector is not mounted with parallel resistance is considered.

Calculation example I: the 500 kV GIS substation is applied with wiring method in the manner of 3/2. The average distance between circuit breaker and disconnector

(CB101 and DS1012) on each circuit breaker string is about 2.5 m, and the average distance between two adjacent disconnectors (DS1012 and DS1021) is about 6.5 m; the average length of GIS pipe busbar between GIS outlet bushing and circuit breaker string is 15 m; the length of overhead line between GIS outlet bushing and main transformer is 107 m.

Calculation example II: the 1000 kV GIS substation is applied with wiring method in the manner of 3/2. The average distance between circuit breaker and disconnector (CB101 and DS1012) on each circuit breaker string is about 5 m, and the average distance between two adjacent disconnectors (DS1012 and DS1021) is about 14 m; the average length of GIS pipe busbar between GIS outlet bushing and circuit breaker string is 40 m; the length of overhead line between GIS outlet bushing and main transformer is 60 m.

7.5.3.1 Influence on Main Insulation of GIS Body and Main Transformer by VFTO

Under the three typical disconnector operating modes, the maximum VFTO at GIS body and port of main transformer in the substation shown in calculation example I and calculation example II is as shown in Table 7.5.

From Table 7.5, it can be seen that, during switching of main transformer, the amplitude of VFTO at the main transformer port is very small, basically approximating to zero; therefore, it can be considered that there is nearly no VFTO. This is because that, during opening and closing of DS1021 and DS1032, the two disconnectors are connected with the main transformer through the open circuit breaker. Therefore, VFTO is transmitted to the main transformer port through the fracture capacitance of circuit breaker and it has very small amplitude, basically approximating to zero.

For 500 kV GIS substation, under the above three typical disconnector operating modes, the maximum VFTO on GIS body in the substation is 2.13 p.u., and the maximum VFTO at port of the main transformer is 1.13 p.u.; both of them are far below the restriction level of 3.0 p.u. In addition, from the generation mechanism and characteristics of VFTO, it can be seen that the theoretical maximum VFTO can be up to 3.0 p.u. However, in the actual 500 kV GIS substation, VFTO in the GIS can be subject to large attenuation; therefore, the actual maximum VFTO is less

Table 7.5 Amplitudes of VFTO on GIS body and at main transformer port under typical disconnector operating modes

Operating mode (kV)		Switching of outgoing line	Switching of busbar	Switching of main transformer
GIS body (p.u.)	500	2.13	1.92	2.00
	1000	2.37	2.0	2.38
Main transformer port (p.u.)	500	1.13	1.12	0.04
	1000	1.09	1.04	0.02

than 3.0 p.u., and it does not pose a threat to the main insulation of GIS body and the main transformer usually.

For 1000 kV GIS substation, under the three typical disconnector operating modes, the maximum VFTO on GIS body in the substation is 2.38 p.u., and the maximum VFTO at port of the main transformer is 1.09 p.u. The VFTO on GIS body has exceeded the restriction level and, therefore, it shall be protected with special attention.

Upon above analysis, the following two conclusions can be obtained: ① In the 500 kV system, the restriction level of main insulation of GIS body and main insulation of the main transformer on VFTO are high and up to 3.0 p.u. Actually, the VFTO cannot achieve such value. Therefore, VFTO will not endanger the main insulation of GIS body and main insulation of the main transformer in the 500 kV GIS substation. ② In the 1000 kV system, the restriction level of main insulation of GIS body and main insulation of the main transformer on VFTO is, respectively, decreased to 2.32 and 2.18 p.u.; in addition, from the above simulation analysis, it can be seen that, under typical disconnector operating modes, the amplitude of VFTO on GIS body in the 1000 kV GIS substation may exceed the restriction level of 2.32 p.u. Therefore, VFTO may pose a threat to the main insulation of GIS body in the 1000 kV GIS substation. In addition, the port of the main transformer has a long distance to the disconnector generating VFTO, thus VFTO has large attenuation after being transmitted to the port of the main transformer, and usually does not exceed 2.18 p.u. Therefore, VFTO does not endanger the main insulation of the main transformer in 1000 kV GIS substation.

7.5.3.2 Influence on the Longitudinal Insulation of Main Transformer by VFTO

In this section, the harm of VFTO on longitudinal insulation of the main transformer in 500 and 1000 kV GIS substations is mainly studied. First, in terms of 500 kV GIS substation mentioned in calculation example I and 1000 kV GIS substation mentioned in calculation example II, the influence of VFTO on longitudinal insulation of the main transformer under typical disconnector operating modes is analyzed. Then, based on the above analysis, in terms of more common typical 500 and 1000 kV GIS substations, the influence of VFTO on longitudinal insulation of the main transformer is studied, thus to obtain the conclusion applicable to common EHV/UHV GIS substations.

1. Influence on the longitudinal insulation of main transformer in substation by VFTO.

In terms of 500 kV GIS substation mentioned in calculation example I and 1000 kV GIS substation mentioned in calculation example II, under the three typical disconnector operating modes, the VFTO wave front steepness invading the port of the main transformer is shown in Table 7.6.

Table 7.6 Wave front steepness of VFTO invading the main transformer under typical disconnector operating modes

Operating mode (kV)		Switching of outgoing line	Switching of busbar	Switching of main transformer
Wave front steepness of VFTO (kV/μs)	500	197.5	188.3	62.3
	1000	550	533	412

Table 7.7 Wave front steepness of VFTO invading the main transformer under typical disconnector operating modes when the overhead line length is 0 m

Operating mode		Switching of outgoing line	Switching of busbar	Switching of main transformer
Wave front steepness of VFTO (kV/μs)	500 kV	1041	1035	324
	1000 kV	1148	1129	736

From Table 7.6, it can be seen that, in terms of 500 and 1000 kV GIS substation, under the three operating modes, the VFTO wave front steepness invading the port of the main transformer is, respectively, smaller than restriction level (1291 and 1875 kV/μs) of longitudinal insulation of the main transformer on VFTO wave front steepness. Therefore, in the 500 and 1000 kV GIS substation, the threat of VFTO on longitudinal insulation of the main transformer is not large.

2. Influence on the longitudinal insulation of main transformer in substation by VFTO when the length of overhead line is 0 m.

The overhead line set up between the GIS outlet bushing and the main transformer has a certain weakening function on the VFTO wave front steepness. When carrying out design of the substation, the length of the overhead line is usually different for different substation. In terms of the above 500 kV GIS substation, the length of such overhead line is 107 and 60 m for the above 1000 kV GIS substation. For the purpose of strictness, the length of the overhead line is taken as 0 m. Under the three typical disconnector operating modes, the maximum VFTO wave front steepness invading the port of the main transformer in the substation is shown in Table 7.7.

By contrasting Tables 7.6 and 7.7, it can be seen that, in case overhead line is erected, the VFTO wave front steepness invading the main transformer is more serious than that in case overhead line is not erected. Therefore, by use of overhead line with appropriate length to restrict VFTO wave front steepness invading the main transformer has obvious results. In terms of above 500 and 1000 kV GIS substation, even if the overhead line length is 0 m, the maximum VFTO wave front steepness is 1041 and 1148 kV/μs, still not exceeding the restriction level of 1291 and 1875 kV/μs for, respective, voltage level. Therefore, it does not pose a threat to the longitudinal insulation of the main transformer.

In conclusion, even if the length of overhead line between the GIS bushing outlet and the main transformer is 0 m, VFTO will not pose a threat to the longitudinal insulation of the main transformer in the above 500 kV GIS substation and

1000 kV GIS substation, and it is usually not necessary for protection. According to the following analysis, it can be seen that, in fact, this conclusion also has significant guidance to the common substations.

3. Influence on the longitudinal insulation of main transformer in the above substations by VFTO under the most severe conditions.

Here, the influence of VFTO on the longitudinal insulation of the main transformer in the above substations under the most severe conditions is studied. Figure 7.14 presents the connections between circuit breaker string (in the manner of 3/2 wiring) and the main transformer in the typical 500 kV GIS substation and 1000 kV GIS substation. Through investigation on some famous GIS manufacturers in China, it can be seen that the spacing d_3 between circuit breaker and disconnector on each circuit breaker string (EF section as shown in Fig. 7.14) and the spacing d_4 between disconnector and adjacent GIS outgoing line port (FG section as shown in Fig. 7.14) have small variation, and can be considered unchanged basically. Therefore, for different substations, the two sections usually have little variation; however, the length d_2 of overhead line between GIS outlet bushing and the main transformer (CD section as shown in Fig. 7.14) and the average length d_1 of GIS pipe busbar between GIS outlet bushing and the circuit breaker string (AB section as shown in Fig. 7.14) are usually variable.

EF section, FG section, and AB section of GIS busbar and CD section of overhead line as shown in Fig. 7.14 also have an influence on the VFTO wave front steepness invading the main transformer. For different substations with same voltage level, usually the difference between EF section and FG section is not large. In addition, after simulation and calculation, it can be seen that, when EF section and FG section are varied within very small range, the variation of VFTO wave front steepness invading the main transformer also is very small. Therefore, AB section and CD section become the main factors influencing the VFTO wave front steepness invading the main transformer. GIS busbar of AB section and overhead line of CD section can weak VFTO wave front steepness invading the main transformer. We consider the most severe conditions, namely when the length of AB section and CD section is both 0 m. The simulation results are as shown in Table 7.8.

From Table 7.8, it can be seen that, even if it is under the most severe conditions, the wave front steepness of VFTO invading 500 and 1000 kV main

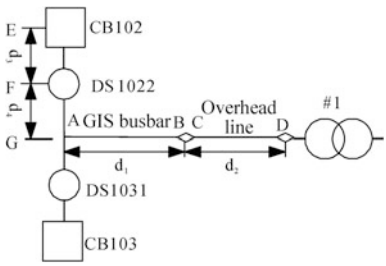

Fig. 7.14 Sketch for connection between circuit breaker string and main transformer

Table 7.8 Wave front steepness of VFTO invading the main transformer under the typical disconnector operating modes under the most severe conditions

Operating mode		Switching of outgoing line	Switching of busbar	Switching of main transformer
Wave front steepness of VFTO (kV/μs)	500 kV	1163	1150	463
	1000 kV	1531	1500	820

Table 7.9 Conclusions of harm on the three types of insulation by VFTO under different voltage levels

Voltage level (kV)	Whether there is any threat from VFTO		
	Main insulation of GIS body	Main insulation of main transformer	Longitudinal insulation of main transformer
500	No	No	No
1000	Yes	No	No

transformer are 1163 and 1531 kV/μs, respectively. By comparing with the restriction level of 1291 and 1875 kV/μs for respective voltage level, there still has the margin exceeding 10%. Therefore, it will not pose a threat to the longitudinal insulation of the main transformer. Therefore, the threat of VFTO on the longitudinal insulation of the main transformer in the typical 500 and 1000 kV GIS substations is not large.

In conclusion, in the typical 500 and 1000 kV GIS substations, even if it is under the most severe conditions, VFTO wave front steepness invading the main transformer still does not exceed restriction level, and there is still certain margin. Therefore, it is considered that VFTO does not endanger longitudinal insulation of the main transformer in the 500 and 1000 kV GIS substations in normal.

7.5.4 Conclusions on Influences on the 500 and 1000 kV GIS Substations by VFTO

According to analysis in the above two sections, in terms of common 500 and 1000 kV GIS substations, under typical disconnector operating modes, the threat of VFTO on the three types of insulation are shown in Table 7.9. For threat of VFTO on the longitudinal insulation of the main transformer, the influence of VFTO wave front steepness on longitudinal insulation of the main transformer is mainly considered.

From Table 7.9, it can be seen that, in terms of 500 and 1000 kV GIS substations, VFTO mainly poses a threat on the main insulation of 1000 kV GIS body. The harm on other types of insulation is not large usually. Therefore, special attention shall be given to prevent the threat of VFTO on the main insulation of GIS body in the 1000 kV GIS substation.

7.5.5 Discussion on Whether to Install Parallel Resistance of Disconnector in the 500 and 1000 kV GIS Substations

In comparison with disconnector in the 1000 kV GIS substation, the disconnector in the 500 kV GIS substation has smaller dimension, and usually it has no sufficient space to install parallel resistance of disconnector. The switching of parallel resistance needs to be completed through movement of operating mechanism, which causes complex structure of the disconnector, thus to reduce reliability, and be easy to generate fault and cause system accident. At the same time, the installation of parallel resistance of disconnector also increases the equipment investment and maintenance workload. In addition, the insulation margin of 500 kV GIS body is large and up to 3.0 p.u. The VFTO generated from operation of disconnector does not pose a threat to the main insulation of GIS body, and its wave front steepness does not pose a threat to the main transformer. After considering the above factors in comprehensive manner, usually, it is not considered to install parallel resistance of disconnector in the 500 kV GIS substation.

For the 1000 kV GIS substation, the 1000 kV GIS system has a larger scale, a larger equipment size in comparison with the 500 kV GIS system, and sufficient space to install parallel resistance of disconnector. In addition, from Table 7.9 it can be seen that for the 1000 kV GIS substation, VFTO usually endangers the main insulation of GIS body. Through disconnector additionally installed with parallel resistance, the amplitude of VFTO can be effectively restricted. In addition, as the backbone network of power grid at all levels, the UHV power grid plays a non-replaceable important role in securing national energy supply safety and optimizing energy resource distribution within larger range. Therefore, the 1000 kV GIS substation shall have strengthened structure to have higher safety.

Therefore, it is necessary to install parallel resistance of disconnector in the 1000 kV GIS substation.

7.6 Comparison of Characteristics of VFTO in Substation and Power Plant

7.6.1 Comparison of Wiring Diagrams for Substation and Power Plant

According to provisions of DL/T 500/2000 *Technical Code for Designing Fossil Fuel Power Plants*, when it is technically and economically reasonable, the generator outlet of a unit with capacity of 600 MW can be installed with circuit breaker GCB. According to relevant investigation results, some of the generator outlets in partial power plants in China have been installed with GCB [15]. Therefore, when

contrasting the VFTO characteristics between substation and power plant, it is necessary to consider two cases where the generator outlet in the power plant is with GCB and without GCB.

7.6.1.1 Comparison of Main Wiring Diagrams for Power Plant in Which the Generator Outlet Is not Equipped with GCB and Substation

Up to now, there is no UHV power plant in China which is mainly restricted by the UHV transformer manufacturing technology applied in the UHV power plant. In the northwestern regions of China, the 750 kV power plant has been emergent at present and the capacity of single generator unit is about 1000 MW, the rated voltage of LV side winding of transformer used for the 750 kV power plant is about 25–27 kV, and the rated voltage of HV side winding is 750 kV. It can be inferred that, the manufacturing of transformer used for the 1000 kV power plant is possible in the future. Actually, there are some colleges, universities and scientific research institutes in China who have started studies on the UHV transformer directly used for UHV power plants at present. Therefore, in the near future, the UHV power plant will be possible to appear. The main wiring diagram for the UHV power plant and GIS substation is as shown in Fig. 7.15, where the generator outlet is not equipped with GCB in the UHV power plant.

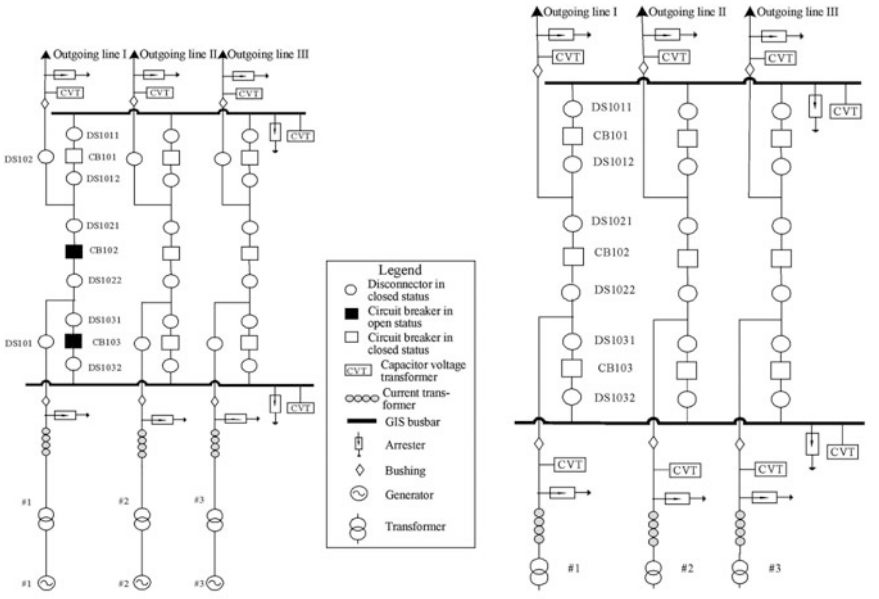

Fig. 7.15 Wiring diagrams for the UHV power plant in which the generator outlet is not equipped with GCB and the substation

It can be seen from Fig. 7.15a and b that the wiring method and equipment configuration of the UHV GIS substation and the UHV power plant at HV side are mainly different in two aspects: first, in comparison with the substation, the power plant is mounted with additional outgoing line outlet disconnector (DS102 in Fig. 7.15a) and transformer outlet disconnector (DS101 in Fig. 7.15a). The closer the distance from the operating disconnector to the main transformer, the larger is the VFTO wave front steepness transmitted to the port of the main transformer. Obviously, the one with the shortest distance to the main transformer is the transformer outlet disconnector of the power plant (DS101 in Fig. 7.15a); therefore, the VFTO wave front steepness generated when operating this disconnector has the largest harm on the main transformer. Second, in the power plant, the HV side outlet of the main transformer is not configured with CVT in general; however, it is necessary to configure CVT at the HV side outlet of the main transformer in the substation. The voltage at the capacitance cannot be changed abruptly, and the equivalent ground capacitance of CVT has a certain restriction effect on the VFTO wave front steepness. Therefore, in case the generator outlet is equipped without GCB, during switching of the main transformer, the VFTO wave front steepness has a larger threat on the main transformer in the power plant than the threat on the main transformer in the substation.

7.6.1.2 Comparison of Main Wiring Diagrams for Power Plant in Which the Generator Outlet Is Equipped with GCB and Substation

Figure 7.16a and b, respectively, present the main wiring diagram for the power plant for which the generator outlet is with GCB and the UHV GIS substation.

When the generator outlet is installed with GCB, the VFTO characteristics in this type of the power plant are different from the VFTO characteristics in the power plant for which the generator outlet is without GCB, and are similar to the VFTO characteristics in the UHV GIS substation. Here, the detailed discussion is not carried out.

7.6.2 Comparison of Characteristics of VFTO in the UHV GIS Substation and the Power Plant

Here, one far-future 1000 kV GIS substation (calculation example II) and the supposing 1000 kV power plant with the same GIS parameter as that of the said substation are taken as the calculation models (calculation example III), to study the influence of VFTO on GIS body and main transformer under typical disconnector operating modes through simulation and calculation. For the purpose of strictness, in this section, when discussing the VFTO characteristics in the substation and

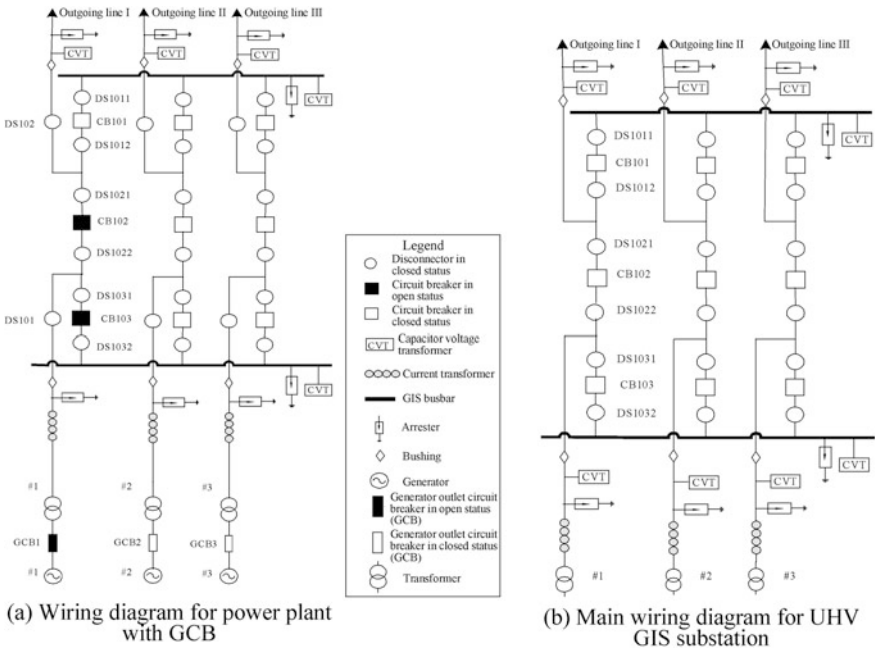

Fig. 7.16 Wiring diagrams for the UHV power plant in which the generator outlet is equipped with GCB and the substation

power plant, the case that the disconnector is not additionally installed with parallel resistance is discussed.

Calculation example III: referring to GIS parameters of the 1000 kV UHV GIS substation in the calculation example II, the power plant is also applied with wiring method in the manner of 3/2 circuit breakers. The average distance between circuit breaker and disconnector (CB101 and DS1012) on each circuit breaker string is about 5 m, and the average distance between two adjacent disconnectors (DS1012 and DS1021) is about 14 m; the average length of GIS pipe busbar between GIS outlet bushing and outgoing line disconnector of the main transformer is 40 m; the length of overhead line between GIS outlet bushing and main transformer is 60 m. It is also necessary to consider two cases, where the generator outlet in the power plant is with GCB and without GCB.

7.6.2.1 Contrast of the Influences on the Main Insulations of GIS Body and Main Transformer

Under the three typical disconnector operating modes, the maximum VFTO at GIS body and the port of the main transformer is as shown in Table 7.10.

Table 7.10 Comparison of the amplitudes of VFTO in substation and power plant under typical disconnector operating modes

Operating mode	Switching of outgoing line	Switching of busbar		Switching of main transformer
GIS body (p.u.)	Power plant (without GCB)	2.35	1.96	2.50
	Power plant (with GCB)	2.35	1.96	2.36
	Substation	2.37	2.00	2.38
Main transformer port (p.u.)	Power plant (without GCB)	1.13	1.15	1.43
	Power plant (with GCB)	1.13	1.15	0.03
	Substation	1.09	1.04	0.02

It can be seen from Table 7.10 that, for the 1000 kV GIS substation and power plant in the calculation example II and calculation example III, under the three typical disconnector operating modes, the maximum amplitude of VFTO on GIS body in the power plant and substation is both within 2.4–2.6 p.u., having exceeded the restriction level of 2.32 p.u., thus to pose a threat to the main insulation of GIS body. However, the maximum amplitude of VFTO on the port of the main transformer does not exceed 1.43 p.u., having not exceeded the restriction level of 2.18 p.u. Therefore, for such 1000 kV GIS substation and power plant, VFTO does not pose a threat to the main insulation of the main transformer.

1. Influence on the amplitude of VFTO in the power plant by GCB.

It can be seen from Table 7.10 that, for the UHV power plant, during switching of outgoing line, the amplitude of VFTO on the GIS body in the power plant for which the generator outlet is with GCB is 2.35 p.u., same as that in the power plant for which the generator outlet is without GCB; the amplitude of VFTO on the port of the main transformer in the power plant for which the generator outlet with GCB is 1.13 p.u., also same as that in the power plant for which the generator outlet is without GCB. In addition, during switching of busbar, the situation is also similar. Therefore, for the UHV power plant, under the two typical disconnector operating modes (namely switching of outgoing line and switching of busbar), whether the generator outlet is with GCB has no large influence on the amplitude of VFTO on GIS body and the port of the main transformer. However, for the operating mode of switching of main transformer, whether the generator outlet is with GCB has a large influence on the amplitude of VFTO. When the generator outlet is without GCB, the amplitude of VFTO on GIS body and the port of the main transformer is, respectively, 2.50 and 1.43 p.u., while when the generator outlet is with GCB, the amplitude of VFTO on two of them is, respectively, 2.36 and 0.03 p.u., both less than the value when the generator outlet is without GCB.

2. Comparison of the amplitude characteristics of VFTO in the power plant with GCB and the substation.

In addition, it can be seen from Table 7.10 that the characteristics of the amplitude of VFTO in the power plant for which the generator outlet is with GCB are similar to the characteristics of the amplitude of VFTO in the substation, namely when the generator outlet is with GCB, under the three typical disconnector operating modes, the amplitude of VFTO on GIS body and the amplitude of VFTO on the port of the main transformer in the power plant have no large difference from the amplitude of VFTO on GIS body and the amplitude of VFTO on the port of the main transformer in the substation. During switching of outgoing line, the difference between the amplitude of VFTO on GIS body in the power plant for which the generator outlet is with GCB and that in the substation is only 0.02 p.u., and the difference between the amplitude of VFTO on the port of the main transformers in the power plant and substation is only 0.04 p.u.; during switching of busbar, the difference on GIS body and the difference on the port of the main transformers in the power plant and substation are only 0.04 and 0.11 p.u. respectively; during switching of main transformer, the difference on GIS body and the difference on the port of the main transformers in the power plant and substation are only 0.02 and 0.01 p.u. Therefore, when the generator outlet is with GCB, the characteristics of the amplitude of VFTO in the power plant are similar to those in the substation.

In conclusion, for the UHV power plant, under the operating modes of switching of outgoing line and switching of busbar, whether the generator outlet is with GCB has no large influence on the amplitude of VFTO. However, under the operating mode of switching of main transformer, when the generator outlet is without GCB, the amplitude of VFTO on GIS body and the port of the main transformer both are higher than those when the generator outlet is with GCB. In addition, when the generator outlet is with GCB, under the three typical disconnector operating modes, the amplitude of VFTO in the power plant is similar to that in the substation.

7.6.2.2 Contrast of the Influences on the Longitudinal Insulation of Main Transformer

In this section, the harm of VFTO on longitudinal insulation of the main transformer in the 1000 kV GIS substation and power plant is mainly studied. According to the above analysis, both the overhead line between GIS bushing outlet and the main transformer and GIS pipe busbar between GIS bushing outlet and the circuit breaker string have weakening effect on the VFTO wave front steepness. For the purpose of strictness, suppose the length of such overhead line and GIS busbar is both 0 m. In terms of the 1000 kV GIS substation and power plant given in the calculation example II and calculation example III, under the three typical disconnector operating modes, the VFTO wave front steepness invading the port of the main transformer is as shown in Table 7.11. The results given in Table 7.11 are

Table 7.11 Comparison of the wave front steepness of VFTO invading the main transformers in substation and power plant under typical disconnector operating modes

Operating mode		Switching of outgoing line	Switching of busbar	Switching of main transformer
Wave front steepness of VFTO (kV/μs)	Power plant (without GCB)	2200	1678	5090
	Power plant (with GCB)	2200	1678	890
	Substation	1531	1500	820

obtained under strict conditions; therefore, these results also have reference value for common substation and power plant.

It can be seen from Table 7.11 that, for the UHV power plant, no matter the generator outlet is with GCB, under the three typical disconnector operating modes, the maximum VFTO wave front steepness invading the port of the main transformer all exceeds the restriction level of 1875 kV/μs, possibly posing a threat to the longitudinal insulation of the main transformer; for the UHV GIS substation, under the three typical disconnector operating modes, the maximum VFTO wave front steepness invading the main transformer is 1531 kV/μs, and usually does not exceed the restriction level of 1875 kV/μs, will not pose a threat to the longitudinal insulation of the main transformer.

1. Influence on the wave front steepness of VFTO in the power plant by GCB.

It can be seen from Table 7.11 that, for the UHV power plant, during switching of outgoing line, the VFTO wave front steepness invading the main transformer in the power plant for which the generator outlet is with GCB is 2200 kV/μs, same as that in the power plant for which the generator outlet is without GCB; during switching of busbar, the VFTO wave front steepness invading the main transformer in the power plant for which the generator outlet is with GCB is 1678 kV/μs, also same as that in the power plant for which the generator outlet is without GCB. Therefore, for the UHV power plant, under the above two operating modes (namely switching of outgoing line and switching of busbar), whether the generator outlet is with GCB has no large influence on the VFTO wave front steepness invading the port of the main transformer. However, under the operating mode of switching of main transformer, whether the generator outlet is with GCB has a large influence on the VFTO wave front steepness invading the port of the main transformer. Under the operating mode of switching of main transformer, when the generator outlet is without GCB, the VFTO wave front steepness invading the port of the main transformer is up to 5090 kV/μs, far above that (890 kV/μs) when the generator outlet is with GCB. Therefore, the main reason resulting in different VFTO wave front steepness invading the port of the main transformer in the two types of power plants during switching of main transformer is whether the generator outlet is with GCB. When the generator outlet is with GCB, the main transformer has been de-energized during operation of the relevant disconnector, thus causing great

weakening of VFTO wave front steepness invading the main transformer in the power plant. Therefore, in terms of the power plant, whether the generator outlet is with GCB has a large influence on VFTO wave front steepness invading the main transformer.

2. Comparison of the steepness characteristics of VFTO in the power plant with GCB and the substation.

In addition, it can be seen from Table 7.11 that, under the operating modes of both switching of busbar and switching of main transformer, the VFTO wave front steepness invading the main transformer in the power plant for which the generator outlet is with GCB is slightly lower than, however close to, the VFTO wave front steepness invading the main transformer in the substation. Under the operating mode of switching of outgoing line, the VFTO wave front steepness invading the main transformer in the power plant is up to 2200 kV/μs, higher than the restriction level, and the VFTO wave front steepness invading the main transformer in the substation is 1531 kV/μs. Therefore, under operating mode of switching of outgoing line, the VFTO wave front steepness invading the main transformer in the power plant for which the generator outlet is with GCB is larger than that in the substation, and this results from that CVT is installed at the HV side of the transformer in the substation.

7.6.3 Conclusions on Comparison of VFTO in UHV GIS Substation and Power Plant

In conclusion, for the 1000 kV GIS substation and power plant, under typical disconnector operating modes, the harm of VFTO on the three types of insulation are shown in Table 7.12. For the threat of VFTO on longitudinal insulation of the main transformer, the influence of VFTO wave front steepness on longitudinal insulation of the main transformer shall be mainly considered, where the power plant is considered in two cases, namely with GCB and without GCB.

It can be seen from Table 7.12 that VFTO has a threat on the main insulation of GIS body in both the UHV power plant and the substation, but has no threat on the main insulation of the main transformer. In addition, in terms of the UHV substation, VFTO usually does not pose a threat on the longitudinal insulation of the main transformer. However, in terms of the UHV power plant, no matter whether the generator outlet is with GCB, VFTO poses a threat on the longitudinal insulation of the main transformer in the power plant.

Therefore, in terms of 1000 kV GIS substation, main consideration shall be given to prevent the threat of VFTO on the main insulation of GIS body; in terms of 1000 kV power plant, main consideration shall be given to prevent the threat of VFTO on the main insulation of GIS body and longitudinal insulation of the main transformer.

Table 7.12 Conclusions of the harm on the three types of insulation in power plant and substation by VFTO

	Whether there is any threat from VFTO		
	Main insulation of GIS body	Main insulation of main transformer	Longitudinal insulation of main transformer
Power plant (with GCB)	Yes	No	Yes
Power plant (without GCB)	Yes	No	Yes
Substation	Yes	No	No

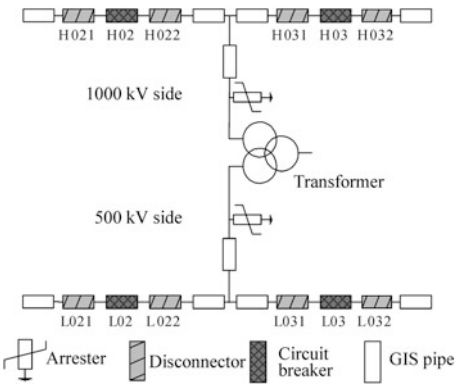

Fig. 7.17 GIS wiring at HV and LV sides of the 1000 kV main transformer

7.7 Restriction and Protection Measures

7.7.1 Rational Arrangement of Operation Sequence of Circuit Breakers and Disconnectors

During switching of main transformer, it is supposed to first disconnect the circuit breaker at 1000 kV side and the disconnectors at both sides of each circuit breaker, and then disconnect the circuit breaker at 500 kV side and the disconnectors at both sides of each circuit breaker. When disconnecting the disconnectors at both sides of circuit breaker at 1000 kV side, operation of each disconnector is possible to generate VFTO. According to the system structure of the UHV GIS substation, the operation sequence of circuit breakers and disconnectors can be rationally arranged, thus to eliminate the possibility of VFTO during operation of the main transformer. The GIS wiring at HV side and LV side of the 1000 kV main transformer is as shown in Fig. 7.17, during switching-off of the main transformer, first disconnect the circuit breakers H02, H03, L02 and L03, and thus the transformer is under de-energized state. Since the neutral point of the transformer is directly earthed, the GIS pipes and disconnectors (H022, H031, L022 and L031 in the figure) connected with the transformer discharge the charges through the transformer winding rapidly,

and thus it does not generate VFTO during the subsequent operation of the disconnectors. Through simulation analysis, it can be seen that after removal of system voltage from the transformer, the residual voltage on the disconnector connected with it is sufficient to be decreased to below 0.3 p.u. within 0.1 s. However, it normally requires several to over ten seconds to confirm that the circuit breaker is in the breaking position after breaking of the circuit breaker, and then it is allowed to pull open the disconnector. At this time, the residual voltage on the disconnector is very small and it is impossible to generate restriking and VFTO. The main transformer has been de-energized for a long time and the circuit breakers H02, H03, L02 and L03 have been under breaking state for a long time; therefore, when the main transformer is closed, large voltage difference is not generated at both sides after the disconnectors H022, H031, L022 and L031 are pulled open, and VFTO is also not generated after closing of these disconnectors.

It can be seen that, when it is applied with the above operation sequence for switching of main transformer, it is able to not only effectively eliminate VFTO generated in the GIS substation during operation of the main transformer and protect the main insulation of GIS body and main transformer against threat of VFTO, but also achieve higher safety reliability and perfect economic and technical efficiency without installation of excessive protection equipment.

7.7.2 Installation of Generator Outlet Circuit Breaker in the Power Plant

According to the investigation results, during early period, most power plants are applied with generator–transformer unit wiring and the generator outlet is not installed with generator outlet circuit breaker (GCB). Along with the development of manufacturing technology of international HV equipment, the GCBs applicable for generator units with capacity of 1000 MW or below have been developed and manufactured successfully by many manufacturers at present, and they have higher rated current, higher breaking capacity and perfect breaking performance, and can achieve stable, safe and reliable operation. For example, the famous companies, such as ABB, GEC-Alsthom, Siemens, Mitsubishi and Hitachi, are all able to manufacture such GCBs. Among them, ABB and GEC-Alsthom have a longest history and the strongest development and research capabilities and their products enjoy higher market share all over the world.

Installation of GCB and rational arrangement of the operation sequence of circuit breakers and disconnectors can eliminate the possibility of VFTO during operation of the main transformer in the power plant; the schematic diagram is as shown in Fig. 7.18. During switching-off of the transformer, first disconnect the circuit breakers 102, 103 and GCB, so that the transformer is under de-energized state; since the neutral point of the transformer is directly earthed, the GIS pipes and disconnectors (1022 and 1031 in the figure) connected with the transformer discharge the charges

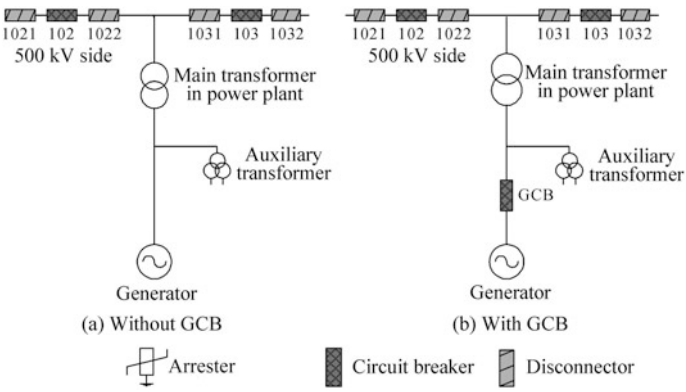

Fig. 7.18 Wiring at HV and LV sides of main transformer in the 500 kV power plant

through the transformer winding rapidly, thus not to generate VFTO during subsequent operation of the disconnectors. The main transformer has been de-energized for a long time and the circuit breakers 102 and 103 have been under breaking status for a long time; therefore, when the main transformer is closed, large voltage difference is not generated at both sides after the disconnectors 1022 and 1031 are pulled open, and VFTO is also not generated when closing of these disconnectors.

In addition, generator outlet circuit breaker also has the following advantages: protect the generator, the main transformer and the auxiliary transformer, and reduce fault loss; avoid the switchover between HV auxiliary operating power supply and standby power supply during normal startup, shutdown and emergency shutdown; simplify the relay protection wiring, shorten the fault recovery time and enhance unit utilization rate; facilitate test and commissioning.

Apart from technical advantages, the application of GCB also has economic advantages. For the scheme that generator outlet is installed with circuit breaker in the thermal power generator unit with capacity of 1000 MW or below in China, the annual operating costs can be reduced greatly though the Phase I investment of the power is increased. Based on the reduced annual operating costs, the power plant can recover the primary investment for installation of GCB within 2–3 years, and the overall economic benefit is obvious. In addition, in case of application of GCB, additional standby transformer is not required during phase II expansion and, therefore, the economic benefit during phase II construction will be more obvious.

At present, there are more than 50% nuclear power plants and more than 20% thermal power plants having adopted the GCB all over the world. According to the revision of China's *Technical Code for Designing Fossil Fuel Power Plants* of 2000 edition, when it is technically and economically reasonable, the generator outlet of unit with capacity of 600 MW can be installed with circuit breaker or load switch. At present, the power plants having adopted the GCB in China mainly include Tianjin Jixian, Liaoning Suizhong, Yimin Power Plant, Shajiao C Power Plant (3 × 600 MW), Shanghai Waigaoqiao Power Plant (2 × 900 MW), Tianjin

Panshan (2 × 600 MW), Gezhouba Hydropower Station, Ertan Hydropower Station, Lijiaxia, Tianshenqiao and other projects. In addition, among the current 600 MW and above generator units under design and construction, many of them have adopted the GCB scheme. Therefore, it can be seen that the opinions on setup of GCB in the large-sized generator units have been changed gradually in China, and the application of GCB in the large-sized generator units is more and more wide. Through breaking-off of GCB, it is able to make the main transformer in the substation under no load state, thus it is able to perfectly eliminate VFTO generated during operation of the main transformer for the purpose of maintenance.

In conclusion, after GCB is installed on the generator unit in the large-sized power plant, it is able to achieve isolation between main transformer in the power plant and power supply of the generator through breaking-off of GCB, thus to effectively eliminate VFTO generated during operation of the main transformer for the purpose of maintenance, and protect the main transformer in the power plant against harm of VFTO generated during switching of main transformer. In addition, it is not necessary to change the routine operation during maintenance of the main transformer in the substation, thus to enhance safety and reliability for equipment and system operation.

7.7.3 Additional Installation of Parallel Resistance on the Disconnector

At present, among various measures to inhibit the harm of VFTO, additional installation of parallel resistance on the disconnector has the most obvious effects, and is more technically mature, and has been widely used actually. The 1000 kV substation has very high requirements on safety and stability, and it does not allow fault of main insulation or secondary equipment due to VFTO. In addition, the margin of main insulation of GIS equipment is relatively small and the base value of system voltage is large, so that it is easy to generate problems in terms of main insulation and secondary equipment. Therefore, it is recommended to install parallel resistance on the disconnector in the UHV GIS substation, thus to prevent the harm of VFTO. At the same time, the 1000 kV GIS disconnector has large dimension, and it is more technically easy to additionally install the parallel resistance, in comparison with the 500 kV disconnector.

The disconnector installed with parallel resistance has the internal structure as shown in Fig. 7.19. Its movement process is similar to that of the ordinary circuit breaker installed with opening and closing resistance. When the disconnector is disconnected, the moving contact and fixed contact are first detached, the residual charges at load side are discharged to the system side through parallel resistance, arc electrode and arc; after the buffer action, the arc blows out to completely disconnect the disconnector; during closing, the system firstly charges the load side through arc, arc electrode and parallel resistance; after the buffer action, the moving

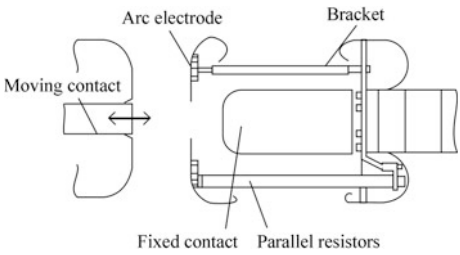

Fig. 7.19 Sketch for internal structure and action of disconnector installed with parallel resistance

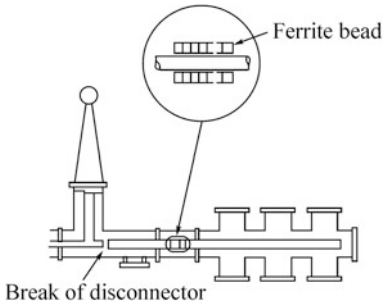

Fig. 7.20 Sketch for application of ferrite toroid, reprinted from Ref. [18], Copyright 2014, with permission from high-voltage engineering

contact and fixed contact are jointed, and the disconnector are closed. On one hand, the disconnector additionally installed with parallel resistance can discharge the residual charges at load side to be discharged to the power supply through parallel resistance, thus to reduce the possibility of restriking occurred to the disconnector; on the other hand, in case of restriking occurred to the disconnector, it can play the damping effect, thus to absorb the energy of VFTO and reduce the amplitude of overvoltage. When the resistance value is taken between 300 and 600 Ω, it is able to effectively inhibit the amplitude of VFTO at each node, reduce oscillation frequency, damp high-frequency component, reduce the steepness, and play a very obvious role in restriction of VFTO.

7.7.4 Ferrite Toroid

Ferrite is a kind of nonlinear high-frequency magnetic conductive material. When ferrite toroid as shown in Fig. 7.20 slips on GIS conductor rod or the port of the main transformer, it can absorb transient energy during restriking of the disconnector, thus to inhibit the VFTO.

The ferrite toroid slipping on the conductor rod can be simplified as a group of paralleled nonlinear inductance L_d and nonlinear resistance R_d that are connected on the conductor rod in series, as shown in Fig. 7.21. The ferrite toroid presents

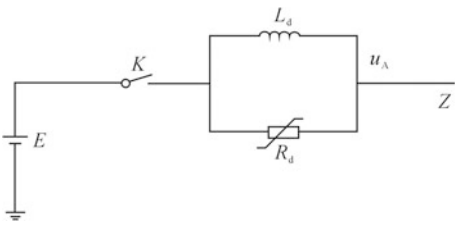

Fig. 7.21 Equivalent circuit of ferrite toroid slip on the conductor rod

different ferromagnetic characteristics under low-frequency and high-frequency operating conditions. Under low-frequency operating conditions, it mainly presents inductance characteristics, R_d is shorted and toroid loss is very small; under high-frequency operating conditions, it mainly presents resistance characteristics, majority of the current flows through R_d and high-frequency energy is converted into heat energy, thus to play the role of inhibiting overvoltage.

7.7.5 Overhead Line

The transformer is connected with GIS line by means of overhead line, and it is equivalent that one section of overhead line is inserted in the middle of GIS line before the transformer. The wave impedance of the overhead line is larger than that of GIS line, thus the VFTO traveling wave is subject to multiple refractions and reflections at the intersections between overhead line and GIS line. The voltage wave transmitted to the inlet of the transformer is superposed from refraction wave at each time, and presents successively increased waveform characteristics, thus to level the VFTO wave front steepness at the inlet of the main transformer. The longer the overhead line length is, the more favorable to reduce the VFTO wave front steepness at the inlet of the main transformer it is.

According to study results in the latter sections of this chapter, for the EHV power plant or substation, when the length of the overhead line between GIS outlet bushing and the main transformer is not less than 15 m, it can be guaranteed that the VFTO wave front steepness invading the main transformer can be reduced to below the restriction level and it has the margin of about 10%; for the UHV power plant or substation, as long as the length of the overhead line is not less than 25 m, it can achieve the same results. Therefore, the overhead line can be used to effectively restrict the VFTO wave front steepness invading the main transformer, and at the same time, it does not require large space. In terms of the thermal power plant and substation, erection of the overhead line is a very nice restriction measure. In terms of hydropower plant and pumped storage power plant, though the space is short of, the erection of 15 or 25 m overhead line does not occupy much space; therefore, for these two types of power plants, such measures can also be used to restrict VFTO.

7.7.6 *Other Measures*

Apart from the above methods for restriction of VFTO, some references proposed to install parallel capacitors and series wave trappers before inlet of the main transformer to restrict VFTO invading the main transformer [16].

Installation of parallel capacitors at inlet of the main transformer can effectively restrict VFTO wave front steepness invading the main transformer, and at the same time, filter out high-frequency components. However, the measures for which parallel capacitors are installed are also subject to the problems such as high fault rate and large capacity demand. When inlet of the main transformer is connected with series wave trappers, it may generate series resonance with the equivalent capacitance at inlet of the main transformer, thus to increase the amplitude of VFTO at HV side of the main transformer. At the same time, its effects of reducing wave front steepness invading the main transformer are not as good as those achieved through measures for which inlet of the main transformer is installed with parallel capacitors.

Therefore, the effectiveness of these two measures to restrict VFTO is worthy of further assessment, they have been rarely applied in the practices at present.

7.8 Quantitative Study on the Restriction of Wave Front Steepness of VFTO Invading the Main Transformer Port by the Overhead Line

VFTO is a kind of internal overvoltage with large amplitude, very steep wave front and very high frequency, which is generated in the GIS substation or power plant during operation of the disconnector. The VFTO with steep wave front poses a serious threat on insulation structure of electrical equipment (especially insulation structure of transformer) [17]. Therefore, it is of great importance to rationally, economically and effectively restrict the VFTO wave front steepness invading the main transformer.

At present, the main measures to restrict the VFTO wave front steepness invading the main transformer are installation of parallel resistance on the disconnector, installation of ferrite toroid on the GIS conductor rod or at the port of the main transformer, and erection of overhead line between GIS outlet bushing and the main transformer [6, 16, 18]. Among them, the overhead line is not expensive, and according to the studies given in this section, a very short overhead line can obviously reduce the VFTO wave front steepness invading the main transformer and achieve obvious restriction effects. Therefore, use of the overhead line is a very effective restriction method.

For the power plant for which the GIS bushing outlet is connected with the transformer by means of one overhead line, the overhead line can effectively weaken the VFTO wave front steepness arriving at the main transformer [2, 17],

and is not expensive. Among the current references, the issue of weakening the VFTO wave front steepness invading the main transformer by means of one overhead line is focused on qualitative analysis and the quantitative study is less. This section focuses on the quantitative study of the issue of the VFTO wave front steepness invading the transformer, thus to discuss the quantitative relation between the overhead line length (between GIS outlet bushing and the transformer) and the VFTO wave front steepness arriving at the transformer port from the perspective of protecting longitudinal insulation of the main transformer. According to above analysis, it can be seen that the harm of VFTO on longitudinal insulation of the main transformer in the power plant is larger than that on the main transformer in the substation, and the threat of VFTO on longitudinal insulation of the main transformer in the substation is not large. Therefore, in this section, discussion shall be mainly carried out from the perspective of power plant.

In this section, the experimental model is first created, and then the threat of VFTO on the main transformer in the 500 and 1000 kV power plants is discussed by simulation method, thus to propose the overhead line length ensuring that the VFTO wave front steepness invading the 500 and 1000 kV main transformer is restricted to below the restriction level [19].

7.8.1 Experimental Study of the Influence on the VFTO Wave Front Steepness by the Overhead Line Length

In this section, LV test is carried out to simulate the weakening effect of overhead line on the VFTO wave front steepness in the 500 kV system.

7.8.1.1 Experiment Platform

The 500 kV power plant or substation is usually applied with the wiring method in the manner of 3/2 circuit breakers at HV side, during the operation or shutdown process of the main transformer, according to the routine switching sequence, one section of no-load busbar (also called as "isolated island") is formed on a certain circuit breaker string in the manner of 3/2 wiring, and the part of "isolated island" can be equalized as a ground capacitance. When the disconnector closes the "isolated island" with residual charges and residual voltage, the VFTO wave generated transmits from the "isolated island" part to the side of the main transformer, thus to pose a threat to the longitudinal insulation of the main transformer, as shown in Fig. 7.22.

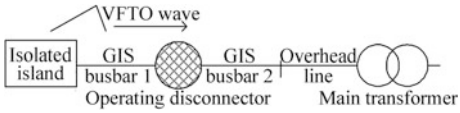

Fig. 7.22 Sketch for propagation path of VFTO wave invading the main transformer

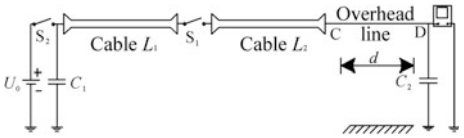

Fig. 7.23 Laboratory simulation circuit of VFTO

To study the influence of overhead line on the VFTO wave front steepness invading the main transformer in the actual 500 kV power plant or substation, refer to Fig. 7.22 and set up the corresponding LV test circuit as shown in Fig. 7.23. In the figure, U_0 is the 200 V LV DC power supply, used for pre-charging of the "isolated island"; C_1 represents the ground stray capacitance of the "isolated island" part, which has no significant change in the common 500 kV power plant and substation (here, taking the Zhejiang Liuheng Power Plant in Zhejiang Province of China as an example, this value is about 400 pF); C_2 represents the inlet stray capacitance of the transformer (for the 500 kV main transformer, this value is taken as 5000 pF in general); L_1 and L_2 (both of them are applied with LV coaxial cable) represent GIS busbar 1 and GIS busbar 2, respectively, for which the wave impedance is 70 Ω and the length is 2 m; S_1 and S_2 are LV switches; d is the overhead line length (according to radius of the overhead line, adjust the height of the overhead line, so that its wave impedance is 300 Ω). The parameters of this test model are basically corresponding to those of the actual 500 kV system, and the test is carried out under LV conditions.

The simulation test is carried out according to the test circuit as shown in Fig. 7.23. During test, first close the switch S_2, thus to pre-charge C_1 through DC power supply U_0; then disconnect S_2, and immediately close S_1, so that the capacitance C_1 charges the capacitance C_2, thus to generate the invading wave with very large steepness (as the simulated VFTO invading wave shown in Fig. 7.22); the invading wave with very large steepness arrives at point C along the cable line, and then arrives at point D through an overhead line, and takes effect on the transformer inlet capacitance represented as C_2, thus to simulate the process of VFTO wave invading the main transformer, as shown in Fig. 7.22. Therefore, such circuit can be used to study the overhead line length's influence on the VFTO wave front steepness and protection effect on the longitudinal insulation of the main transformer.

The value of overhead line length d is taken within the range of 0–20 m, once the value of d is changed, measure the voltage waveform that arrives at point D and taking effect on C_2, then obtain the steepness of transformer inlet wave, and finally obtain the variation relation between the wave front steepness at point D and overhead line length.

The test is carried out under LV conditions. When steep wave is transmitted on the overhead line, it does not generate impulsive corona, and the test results obtained are stricter than those obtained from actual EHV and UHV systems.

7.8.1.2 Experiment Results

When the value of overhead line length d is taken within the range of 0–20 m, the relation between VFTO wave front steepness at point D and overhead line length is shown in Fig. 7.24.

It can be seen from Fig. 7.24 that the overhead line can obviously weaken the VFTO wave front steepness. When the overhead line is short, the VFTO wave front steepness presents a notable decrease trend along with the increase of length; when the overhead line is long, the decrease speed of the VFTO wave front steepness tends to be smooth along with the further increase of length. In case the overhead line is short, the VFTO wave front steepness presents a notable decrease trend; therefore, it can be inferred that a short overhead line can restrict the VFTO wave front steepness invading the main transformer.

The principles of overhead line weakening the VFTO wave front steepness can be briefly analyzed as follows: when the traveling wave passes through series inductance or bypasses the parallel capacitance, the wave front steepness of the traveling wave is weakened [12]. When VFTO is transmitted on the overhead line, the overhead line itself has inductance (it behaves as the series inductance with large value is introduced on the path of VFTO invading the main transformer), thus the wave front of the traveling wave is leveled and the steepness is reduced.

In case LV test is used to verify the restriction performance of overhead line on the VFTO wave front steepness invading the main transformer in the 1000 kV system, the similar test circuit, as shown in Fig. 7.23 can be used. However, parameters of partial components in the test circuit are changed. At this moment, equivalent inlet capacitance of the main transformer is 6000 pF, the wave impedance of cable is 95.2 Ω, and the capacitance at "isolated island" side is 600 pF. Thus, it can be seen that in case LV test is used to verify the restriction results of overhead line on the VFTO wave front steepness invading the UHV main transformer, the test circuit is the same as that of the 500 kV system, just the parameters

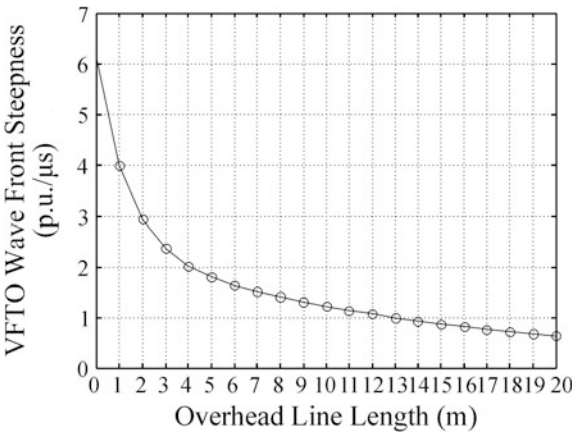

Fig. 7.24 Relationship between VFTO wave front steepness at point d and overhead line length

of partial components in the test circuit are changed slightly. Therefore, the test results shall be similar. That is to say, in terms of 1000 kV system, the overhead line can also achieve good restriction results on the VFTO wave front steepness invading the main transformer.

In terms of actual 500 kV line and 1000 kV UHV line, when VFTO is transmitted on them, it is possible to generate corona. Therefore, the performance of overhead line on weakening the VFTO wave front steepness shall be better than those obtained through this LV test [12].

7.8.2 *Simulation Analysis of the Influence on the VFTO Wave Front Steepness by Overhead Line Length*

7.8.2.1 Simplified Simulation Model

It can be seen from Sect. 7.6 that, during operation of DS101, the threat of VFTO generated on the main transformer is largest (because it is closest to the main transformer). The operations of DS101 are carried out in the shutdown or operation process of the main transformer in the power plant. According to operation procedures, the routine switching sequence for shutdown process of the main transformer is: first open the circuit breakers CB102 and CB103, and then open the disconnector DS101; the routine switching sequence for operation process of the main transformer is: first close the disconnector DS101, and then close the circuit breakers CB103 and CB102. From the above routine operation sequence, it can be seen that no matter it is shutdown or operation process of the main transformer, when the disconnector DS101 is operated, the circuit breakers CB102 and CB103 are both under open state, and other circuit breakers and disconnectors are under closing state. The influence of VFTO generated due to shutdown or operation process on the main transformer may be different; therefore, the following studies are all based on the most severe conditions of the two.

For different power plants, as long as VFTO is generated due to operation of the disconnector DS101, the simplified model, as shown in Fig. 7.25, can be used to

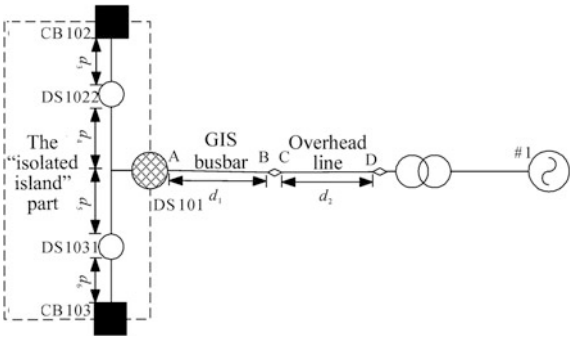

Fig. 7.25 Simplified model for VFTO simulation calculation

calculate the VFTO wave front steepness invading the main transformer through simulation calculation. To study the effect of overhead line to weaken the VFTO wave front steepness, in this section, the situation for which the transformer is connected with GIS by means of overhead line is mainly analyzed. The path of VFTO invading the transformer is GIS–bushing–overhead line–bushing–transformer coil. The dotted part, as shown in Fig. 7.25, is the "isolated island" generated on the circuit breaker string due to closing or opening of the main transformer. For different power plants, the compositions at the "isolated island" side are same, including the part of DS101, the part of two disconnectors DS1022 and DS1031 under closed state and two circuit breakers CB102 and CB103 under open state, and the GIS busbar section. d_3 and d_6 represent the length of the GIS busbar section between the disconnectors DS1022 and DS1031 and circuit breaker; d_4 and d_5 represent the length of the GIS busbar section between DS1022 and DS1031 and outgoing line disconnector DS101 of the transformer. The structure of the "isolated island" is symmetrical in general, that is to say, it can be considered that d_3 and d_6 are equal and d_4 and d_5 are equal.

7.8.2.2 Study on Quantitative Relationship Between VFTO Wave Front Steepness and Overhead Line Length

1. Calculation parameters.

Here, Liuheng Power Plant in Zhejiang Province is taken as an example. The wiring and equipment layout of Liuheng Power Plant at 500 kV side is similar to Fig. 7.15b; however, there are only two circuit breaker strings between the two main busbars, and the simplified simulation calculation equivalent circuit is as shown in Fig. 7.25. The average length d_3 of GIS busbar between the disconnector and the circuit breaker is 2.5 m, the three-phase average length d_4 of GIS busbar between the disconnector and outgoing line disconnector of the transformer is 3.3 m. At AB section, the three-phase average length of GIS busbar is 25 m, and the wave impedance is 70 Ω and wave speed is 3×10^8 m/s; at CD section, the model of overhead line is 2 × LGJQT-1440, the three-phase average overhead height is 15 m, and the three-phase average length is 54 m. (If not specifically indicated hereafter, the average length refers to the three-phase average length in all cases).

2. GIS directly connected with the main transformer through oil–gas bushing (i.e., the overhead line length is zero).

The overhead line can be used to level the VFTO wave front steepness; therefore, when GIS is directly connected with the main transformer through bushing (d_2 as shown in Fig. 7.25 is 0 m), the VFTO wave front steepness at port of #1 main transformer is largest. Suppose the transformer and GIS busbar of the Liuheng Power Plant are applied with hard wiring through oil–gas bushing, consider the

most severe conditions that arcing is generated when voltage difference at both sides of moving contact and fixed contact of the disconnector is largest (2 p.u.). Thus, the VFTO wave at port of the main transformer is as shown in Fig. 7.26. The wave front steepness is 2253 kV/μs, far above the restriction level of 1291 kV/μs allowed for the VFTO wave front steepness on the 500 kV main transformer, and posing a very large threat on the longitudinal insulation of the main transformer.

3. GIS connected with the main transformer through overhead line.

When variation range of overhead line length is within 0–15 m, the VFTO waveform invading the port of #1 main transformer in the Liuheng Power Plant is as shown in Fig. 7.27. Because the overhead line length is different, the time of VFTO wave transmitted to the transformer inlet is also different. Therefore, the four waveforms in the figure have certain translation. It can be seen from Fig. 7.27 that the longer the overhead line length is, the longer is the corresponding wave front time, and smaller the VFTO wave front steepness.

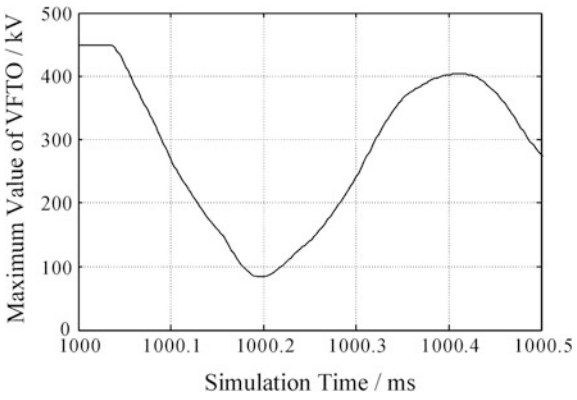

Fig. 7.26 VFTO waveform at the port of main transformer

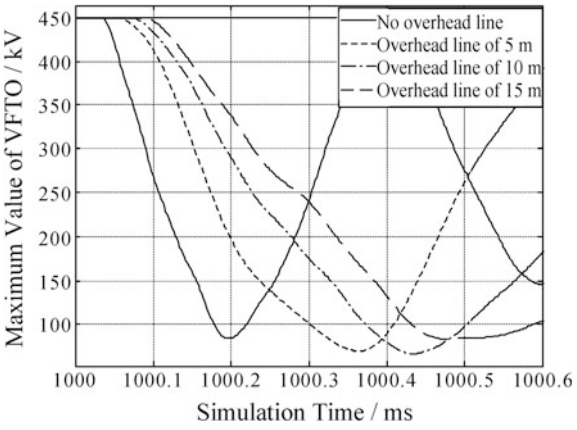

Fig. 7.27 VFTO waveform at the port of main transformer under different overhead line lengths

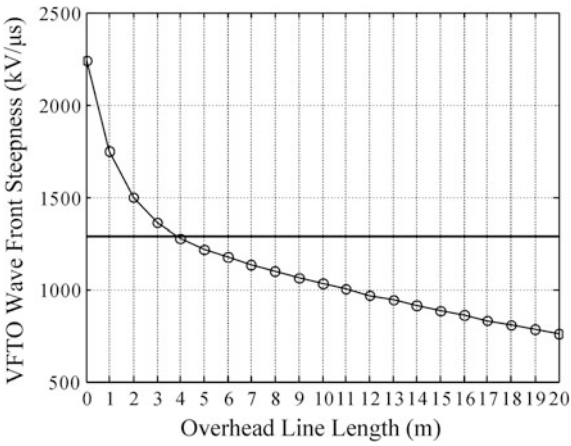

Fig. 7.28 Relationship between VFTO wave front steepness at the port of main transformer and overhead line length

Figure 7.28 presented the relation curve between overhead line length and VFTO wave front steepness at port of the main transformer. In the figure, the horizontal solid straight line means that the wave front steepness is 1291 kV/μs.

It can be seen from Fig. 7.28 that the effect of overhead line on restricting the VFTO wave front steepness is obvious, and this is similar to the results obtained in LV test. When the overhead line length is 3.8 m, the wave front steepness arriving at port of the main transformer is decreased to 1291 kV/μs. Meanwhile, along with the increase of the overhead line length, the decrease trend of wave front steepness becomes smooth. When the overhead line length is within the range of 0–5 m, along with the increase of the overhead line length, the decrease trend of wave front steepness at port of the main transformer is obvious. When the overhead line length is 5 m, the wave front steepness is decreased from previous 2253 kV/μs to about 1224.5 kV/μs, with a decreasing amplitude of up to 45.6%, and having 5% margin in comparison with 1291 kV/μs. When the overhead line length exceeds 5 m, along with the increase of the overhead line length, the decrease trend of wave front steepness at port of the main transformer becomes smooth. When the overhead line length is 10 m, the wave front steepness at port of the main transformer is about 1032 kV/μs, having 20% margin in comparison with the restriction level of 1291 kV/μs.

4. Influence on the VFTO wave front steepness by the GIS busbar between transformer's outgoing line disconnector and GIS outlet bushing.

As shown in Fig. 7.25, the ground stray capacitance of AB section GIS busbar is usually large, thus to weaken the VFTO wave front steepness. The longer this GIS busbar is, the more the VFTO wave front steepness is weakened. In the Liuheng Power Plant, there is one section of GIS busbar with average length of 25 m between the disconnector DS101 and GIS outlet bushing. For different power plants, the length of this GIS busbar is different and, therefore, the weakening effect on the VFTO wave front steepness is also different. According to the previous

description, the conclusion that the overhead line with length of 5 m between GIS and the transformer can be used to restrict the VFTO wave front steepness to below safe level is obtained based on the Liuheng Power Plant. In case the AB section GIS busbar in some power plants is short, the overhead line with length of 5 m may be unable to meet the requirements. Here the extreme conditions are considered, suppose the outgoing line disconnector of the transformer and the transformer are directly connected in the Liuheng Power Plant, that is to say, the length of GIS busbar between DS101 and GIS outlet bushing is 0 m. Thus, under such condition, the relation between overhead line length (between GIS outlet bushing and #1 transformer) and the VFTO wave front steepness arriving at the port of the main transformer is as shown in Fig. 7.29.

From Fig. 7.29, it can be seen that, when the overhead line length is same, the VFTO wave front steepness arriving at inlet of the transformer under extreme condition is larger than that under typical condition. Under extreme condition, when the overhead line length is 5 m, the VFTO wave front steepness is 1443.7 kV/μs, exceeding the restriction level.

After comparing the two curves as shown in Fig. 7.29, it can be seen that when the overhead line length is larger than 10 m, the VFTO wave front steepness has no large difference under the two above conditions. Both GIS busbar and the overhead line can be used to level the VFTO wave front; however, when the overhead line length is larger than 10 m, the effect of GIS busbar can be neglected basically and at the moment, the overhead line plays the main role.

In terms of the Liuheng Power Plant, under the most severe conditions, that is to say, the length of GIS busbar between the outgoing line disconnector of the main

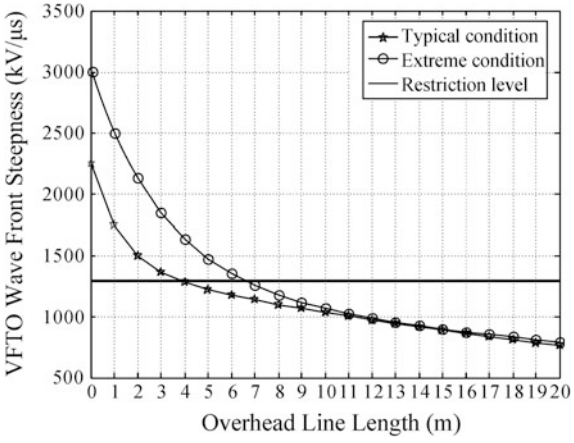

Fig. 7.29 Relationship between VFTO wave front steepness at the port of main transformer and overhead line length. *Note* for the Liuheng power plant, typical condition means that the outgoing line disconnector of the main transformer is connected with the transformer by means of GIS busbar with length of 26 m; extreme condition means that the outgoing line disconnector of the main transformer is directly connected with the transformer

transformer and GIS outlet bushing is 0 m and the length of overhead line between GIS outlet bushing and the main transformer is 10 m, the VFTO wave front steepness arriving at the port of the transformer is 1133 kV/μs, which is less than the restriction level of 1291 kV/μs and has been effectively controlled below the restriction level, and in addition, it has a margin of more than 10%. When EMTP simulation software is used to study the influence of overhead line on the VFTO wave front steepness, it does not consider the effect of impulsive corona on the overhead line, when corona effect is considered, the VFTO wave front steepness is further reduced [12].

In conclusion, in terms of the Liuheng Power Plant, when the length of overhead line between GIS and the transformer is 10 m, the VFTO wave front steepness arriving at the port of the main transformer can be controlled below the restriction level, and in addition, it has sufficient margin. Actually, in the Liuheng Power Plant, there is one overhead line with average length of 54 m between GIS busbar and the transformer (far above 10 m) and, therefore, it is sufficient to ensure that the VFTO wave front steepness invading the port of the transformer is below the restriction level. Therefore, such overhead line can perfectly protect the main transformer in the Liuheng Power Plant, and it is unnecessary to take other measures to restrict the VFTO wave front steepness invading the main transformer.

7.8.2.3 Analysis on the Most Severe Conditions

It can be seen from Sect. 7.8.2.1 that the compositions at "isolated island" side for different power plants are basically same. In the "isolated island" part of each power plant, the circuit breaker, the disconnector and the GIS busbar section length have no large difference [20–22]. For example, d_3–d_6 are as shown in Fig. 7.25, where d_3 is approximately equal to d_6 (in the common 500 kV power plant or substation, the length is about 3 m, and not exceed 5 m maximally); d_4 is approximately equal to d_5 (in the common 500 kV power plant or substation, such length is about 5 m, and not exceed 10 m maximally). Therefore, when d_3 is varied within the range of 1–5 m and d_4 is varied within the range of [1–10 m], it basically covers all parameters d_3 and d_4 of "isolated island" generated due to operation of DS101 in the 500 kV power plant. According to Sect. 7.8.2.2, it can be seen that the shorter the length of AB section GIS busbar, the larger is the VFTO wave front steepness invading the main transformer. Therefore, for the purpose of strictness, d_1 is taken as 0 m. When d_3 is varied within the range of 1–5 m and d_4 is varied within the range of 1–10 m (d_1 = 0 m), the variation of VFTO wave front steepness arriving at the port of the main transformer under different overhead line length are shown in Fig. 7.30.

It can be seen from Fig. 7.30 that, when the overhead line length is 0 m, the variation of the VFTO wave front steepness invading the main transformer is within the range of about 3000–3400 kV/μs; when the overhead line length is 5 m, the variation of the VFTO wave front steepness invading the main transformer is within the range of about 1400–1800 kV/μs; when the overhead line length is 10 m, the variation of the VFTO wave front steepness invading the main transformer is within

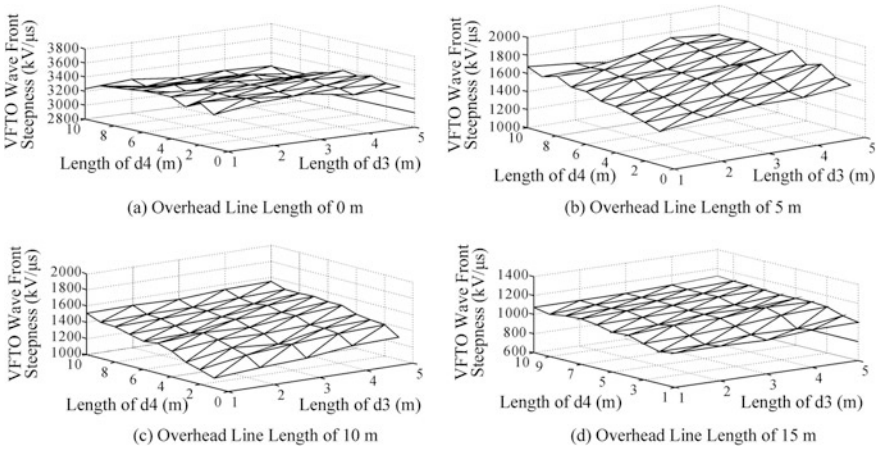

Fig. 7.30 Relationship between VFTO wave front steepness at the port of main transformer and overhead line length

the range of about 1100–1600 kV/μs; when the overhead line length is 15 m, the variation of the VFTO wave front steepness invading the main transformer is within the range of about 800–1200 kV/μs. Along with the increase of the overhead line length, the VFTO wave front steepness invading the main transformer is reduced. When the overhead line length is increased from 0 to 5 m, the VFTO wave front steepness at the port of the main transformer is subject to significant decrease. When the overhead line length is 15 m, under the combination of different d_3 and d_4, the maximum VFTO wave front steepness at the port of the main transformer is about 1120 kV/μs, still having a margin of 13% in comparison with the restriction level of 1291 kV/μs. This value is the calculation result of the VFTO wave front steepness invading the main transformer obtained under the most severe conditions.

In addition, it can be seen from Fig. 7.30 that, when d_1 and d_2 are both maintained unchanged and d_3 and d_4 are, respectively, changed from 1 to 5 m and from 1 to 10 m, the variation amplitude of VFTO wave front steepness invading the main transformer is relatively small. Therefore, in comparison with parameters d_1 and d_2, the influence of parameters d_3 and d_4 on the VFTO wave front steepness invading the main transformer is relatively small.

When the overhead line length is 15 m, in comparison with the restriction level, the VFTO wave front steepness invading the #1 main transformer still has a margin of more than 10% even if it is under the most severe conditions. After considering the influence of impulse corona, it can be considered that, in terms of 500 kV power plant, even if it is under the most severe calculation conditions, the VFTO wave front steepness arriving at the main transformer does not exceed the restriction level when the overhead line length between GIS bushing and transformer bushing is longer than 15 m. Therefore, to perfectly protect the longitudinal insulation of the

main transformer, the overhead line with length of 15 m is enough, and it is not necessary to take other protection measures.

In terms of 500 kV hydropower plants and pumped storage power plants for which the floor space is usually short, GIS and the main transformer are normally directly connected by means of oil–SF6 gas immersed bushing or directly connected by means of cable. The VFTO poses a larger threat on the longitudinal insulation of the main transformer in these power plants and, therefore, corresponding protection measures shall be taken to prevent it. Erection of one overhead line with length of 15 m between GIS and the main transformer does not require much space; therefore, in case design procedures and site conditions allow [15, 23], it can also be considered to erect one overhead line with length of above 15 m to inhibit the VFTO wave front steepness. In the power plants for which overhead line is not connected between the main transformer and GIS, such as China Tianhuangping Pumped Storage Power Plant and Sichuan Ertan Power Plant, the transformer insulation damage accident resulting from VFTO had been occurred [24, 25].

Considering that the situation of VFTO invading the main transformer in the power plant is usually more serious than that in the substation, installation of one overhead line with length of 15 m in the 500 kV substation can effectively protect the main transformer. However, according to the previous analysis, even if the overhead line is not installed, the VFTO wave front steepness invading the port of the main transformer in the 500 kV substation does not exceed the restriction level in fact.

In conclusion, in terms of 500 kV power plant, in case GIS and the transformer are connected by means of a very short overhead line, such overhead line can obviously weaken the VFTO wave front steepness invading the main transformer; in case GIS is connected with the main transformer by means of overhead line with the length larger than 15 m, the longitudinal insulation of the main transformer can be protected perfectly, these shall be considered during the design of power plant. For the established power plants or substations where the overhead line between GIS and the main transformer is very short, in case other conditions allow, line reconstruction can also be carried out, thus to make the overhead line longer than 15 m. Otherwise, other measures shall be taken to restrict the VFTO wave front steepness arriving at the port of the main transformer.

7.8.3 Further Discussion on Restriction of Wave Front Steepness of VFTO Invading the Main Transformer by Means of Overhead Line in the 1000 kV Power Plant

This section discusses how to restrict the VFTO wave front steepness invading the main transformer by means of overhead line in the 1000 kV system.

7.8.3.1 Study on Restriction of Wave Front Steepness of VFTO Invading the Main Transformer by Means of Overhead Line in the 1000 kV Power Plant

The main wiring diagram of the UHV power plant is as shown in Fig. 7.31.

At present, there are no UHV power plants; therefore, the existing UHV GIS substation (calculation example II) can be referred to obtain the parameters of each GIS busbar section and parameters of overhead line length as shown in Fig. 7.31, namely the parameters of the UHV power plant given in the calculation example III.

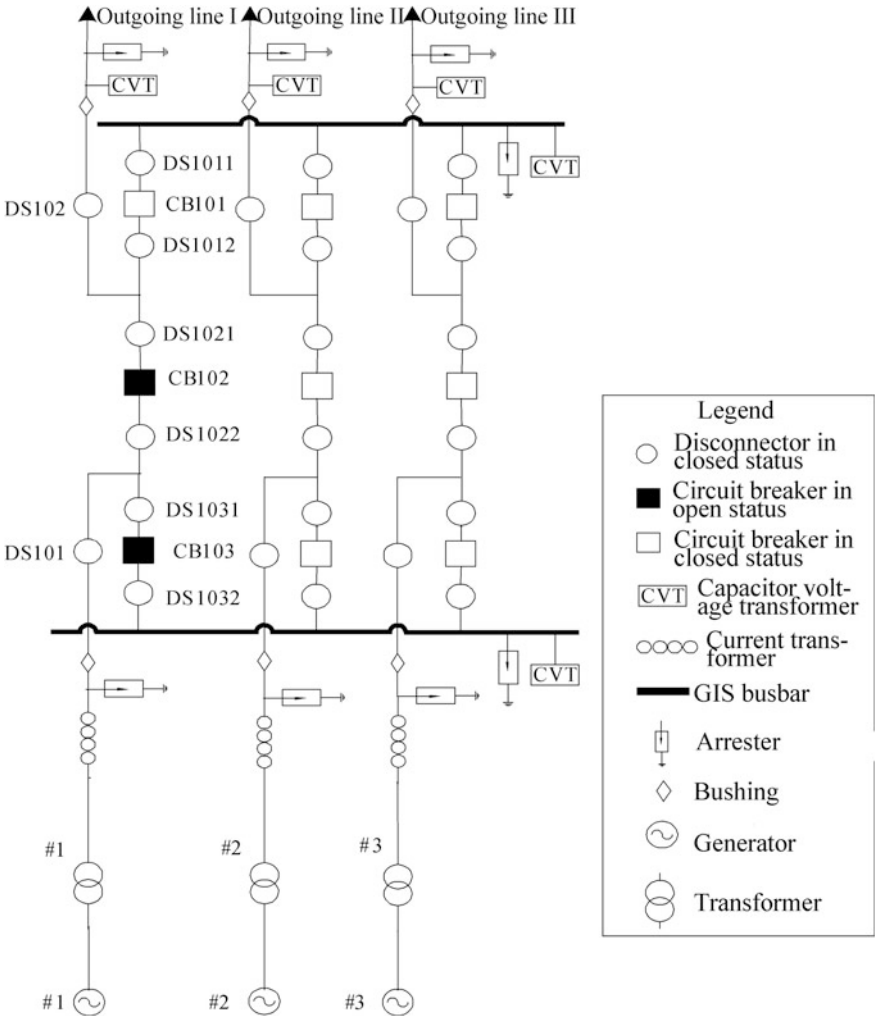

Fig. 7.31 Main wiring diagram for the UHV power plant

It can be seen from Sect. 7.8.2.1 that the simplified VFTO simulation calculation model is as shown in Fig. 7.32.

The two conditions, where AB section GIS busbar is 40 m long (typical condition) and 0 m long (extreme condition), respectively, are considered. Under the above two conditions, the variation relation between the VFTO wave front steepness invading the main transformer and the overhead line length is as shown in Fig. 7.33.

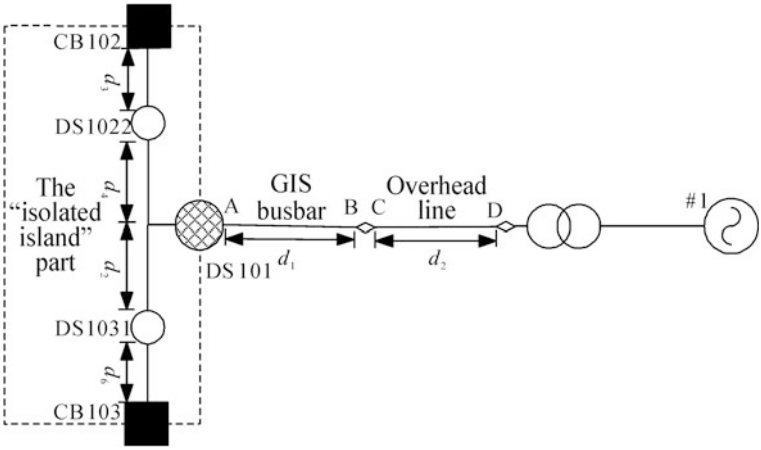

Fig. 7.32 Simplified model for VFTO simulation calculation

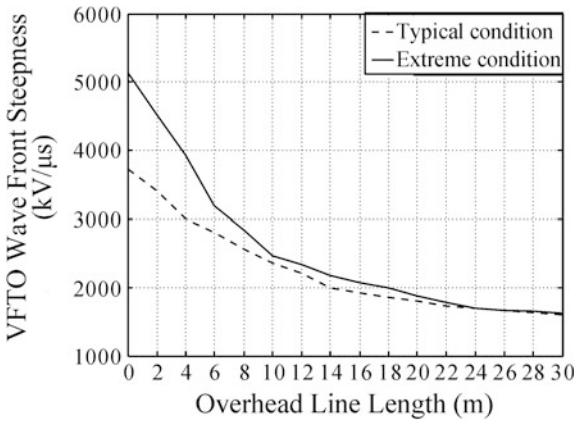

Fig. 7.33 Relationship between overhead line length and VFTO wave front steepness at the port of main transformer. *Note* the typical condition refers to that the outgoing line disconnector of main transformer is connected with the transformer through a 40m-long GIS busbar, while the extreme condition refers to that the outgoing line disconnector of main transformer is directly connected with the transformer

It can be seen from Fig. 7.33 that, in terms of the 1000 kV power plant, when the overhead line length between GIS outlet bushing and the main transformer is short, the VFTO wave front steepness invading the main transformer may exceed the restriction level of 1875 kV/μs. When the overhead line length is 0 m, the VFTO wave front steepness invading the main transformer under typical condition and extreme condition reaches 3721 and 5090 kV/μs, respectively; both of them are far above the restriction level of 1875 kV/μs and have large harm on the longitudinal insulation of the main transformer. Therefore, similar to the 500 kV power plant, main consideration shall be given to protect the longitudinal insulation of the main transformer in the 1000 kV power plant.

In addition, similar conclusion as that of the 500 kV system can be obtained from Fig. 7.33. That is to say, when the overhead line length is less than 10 m, along with the increase of the overhead line length, the VFTO wave front steepness is subject to obvious decrease; when the overhead line length is longer than 10 m, along with the increase of the overhead line length, the VFTO wave front steepness is subject to smooth decrease.

After comparing the two curves as shown in Fig. 7.33, it can be seen that, when the overhead line length is identical, the VFTO wave front steepness arriving at the inlet of the transformer under extreme condition is larger than that under typical condition. When the overhead line length is larger than 25 m, the VFTO wave front steepness under these two conditions has no large difference. Both GIS busbar and overhead line can be used to level the VFTO wave front. However, when the overhead line length is larger than 25 m, the effect of GIS busbar can be neglected basically, at this moment, the overhead line plays the main role. Under these two conditions, to ensure the VFTO wave front steepness invading the main transformer does not exceed the restriction level, the minimum overhead line length is 16 and 20 m, respectively.

Under the most severe conditions, namely when GIS busbar length is 0 m and overhead line length is 25 m, the VFTO wave front steepness arriving at the port of the transformer is 1680 kV/μs, lower than the restriction level of 1875 kV/μs, and having a margin of exceeding 10%. When EMTP simulation software is used to study the influence of overhead line on the VFTO wave front steepness, it does not consider the effect of impulsive corona on the overhead line. When corona effect is considered, the VFTO wave front steepness is further reduced. Therefore, it can be considered that, in terms of the UHV power plant, when the overhead line length between GIS outlet bushing and the main transformer is 25 m, the VFTO wave front steepness invading the main transformer does not exceed the restriction level, and VFTO does not endanger the longitudinal insulation of the main transformer.

Through investigation on some famous GIS manufacturers in China, it can be seen that, in terms of different UHV substation or power plant, d_3 and d_4 usually have no large difference, but d_1 and d_2 can be varied within a large range. Therefore, d_1 and d_2 are the main factors influencing the VFTO wave front steepness invading the main transformer. Through analysis of this chapter, it can be seen that, when d_1 is 0 m, as long as one overhead line with length of 25 m is set up between GIS busbar and the main transformer, the VFTO wave front steepness

invading the main transformer can be reduced to below 1875 kV/μs and has a margin of exceeding 10%. After considering the effect of impulsive corona, it can be seen that, in terms of the UHV power plant, as long as the overhead line length between GIS bushing and the transformer bushing is larger than 25 m, the VFTO wave front steepness arriving at the main transformer under the most severe conditions does not exceed the restriction level. Therefore, to perfectly protect the longitudinal insulation of the main transformer, the overhead line with length of 25 m is enough, and it is not necessary to take other protection measures.

7.8.3.2 Conclusions on Restriction of Wave Front Steepness of VFTO Invading the Main Transformer in the 1000 kV Power Plant by Means of Overhead Line

Based on the above analysis, in terms of the 1000 kV power plant, the following conclusions can be obtained:

1. According to the quantitative simulation calculation results, it can be seen that, in terms of the 1000 kV power plant, the overhead line with length of 10–25 m can obviously weaken the VFTO wave front steepness invading the main transformer.
2. Along with the increase of the overhead line length between GIS and the main transformer, the VFTO wave front steepness at the port of the main transformer presents a decrease trend; when the overhead line length is within 0–10 m, along with the increase of the overhead line length, the VFTO wave front steepness at the port of the main transformer presents an obvious decrease trend; when the overhead line length is more than 10 m, along with the increase of the overhead line length, the VFTO wave front steepness at the port of the main transformer presents a smooth decrease trend. Therefore, when the overhead line length between GIS and the transformer is 10 m, it can obviously reduce the VFTO wave front steepness invading the main transformer.
3. When the overhead line length is longer than 25 m, the VFTO wave front steepness invading the port of the main transformer can be controlled below 1875 kV/μs and has a margin of exceeding 10%. Therefore, when the overhead line length between GIS and the transformer is longer than 25 m, usually, it is able to restrict the VFTO wave front steepness invading the main transformer below the restriction level in the 1000 kV power plant.

7.9 Study on Transient Enclosure Voltage (TEV) of GIS in Substation and Power Plant

In the UHV power plant and substation, the VFTO generated due to operation of the disconnector is coupled between the enclosure and ground, thus to cause dangerous increase of transient enclosure voltage (TEV). The transient enclosure

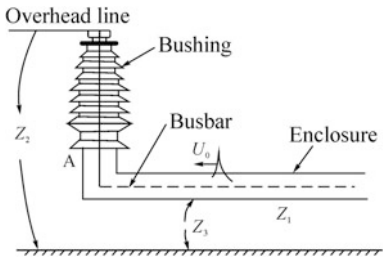

Fig. 7.34 GIS structure at the bushing Reprinted from Ref. [27], Copyright 2014, with permission from Journal of Shenyang University of Technology

voltage is one of key factors that has an influence on the insulation and safe operation of the substation, and is the important basis for electromagnetic compatibility design of the substation. Therefore, the insulation problems and secondary equipment interference problems resulting from the transient enclosure voltage have been attached with more and more importance [26, 27]. In this section, the causes, harms and restriction measures of the transient enclosure voltage in the GIS substation and power plant are discussed.

7.9.1 Principle for Its Generation

When the VFTO wave is transmitted on GIS pipe, the VFTO wave is subject to refraction and reflection at the node where the wave impedance is changed; at this time, the current will flow through the outer surface of GIS pipe enclosure, thus to cause the increase of GIS enclosure ground potential, namely forming transient enclosure voltage (TEV) [27]. The bushing connecting GIS pipe and overhead line is the node in the GIS structure where the impedance is the most discontinuous severely. Therefore, the transient enclosure voltage on the GIS pipe enclosure nearby the bushing is the most serious.

The GIS structure diagram at the bushing is as shown in Fig. 7.34. When the VFTO generated in the GIS pipe is transmitted to the bushing connecting GIS pipe and overhead line in manner of traveling wave, part of the VFTO is refracted to the overhead line, and transmitted along the overhead line; part of the VFTO is coupled between enclosure and ground by means of electromagnetic induction, thus to cause transient enclosure voltage (TEV) on the GIS pipe; part of the VFTO is reflected back into the GIS pipe [27].

7.9.2 TEV Calculation Method

7.9.2.1 Method for Modeling at Bushing Connecting Point

At the connection between GIS and bushing, three transmission line systems connected at one point are formed (as shown in Fig. 7.34), namely the circuit

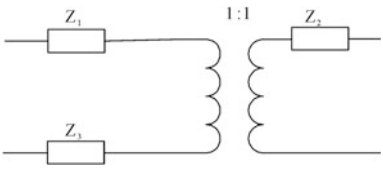

Fig. 7.35 Model of the connecting point between GIS and bushing

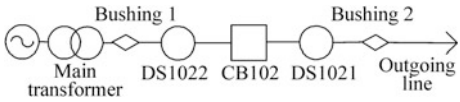

Fig. 7.36 Sketch for main electrical wiring of GIS

formed by wave impedance Z_1 between GIS conductor and enclosure inner surface, the circuit formed by wave impedance Z_2 between overhead line and ground and the circuit formed by wave impedance Z_3 between enclosure outer surface and ground. At point A, part of voltage wave is coupled between enclosure and ground, thus to cause the increase of transient enclosure voltage, and part of voltage wave is refracted to the overhead line. At this point of place, the ideal transformer model with transformation ratio of 1:1 is used to connect the three transmission lines, as shown in Fig. 7.35 [27]. Z_1 is the wave impedance between GIS conductor and enclosure, $Z_1 = 60\ln(R_1/R_2)$, where R_1 is the inner diameter of GIS enclosure and R_2 is the radius of GIS conductor; Z_2 is the wave impedance of overhead line at outer side of bushing, which is 300–400 Ω in general; Z_3 is the wave impedance between GIS pipe enclosure and ground, $Z_3 = 60\ln(2h/R)$, where h is the ground height of GIS pipe center and R is the outer diameter of GIS pipe enclosure.

7.9.2.2 Establishment of the Whole Model to Obtain Transient Enclosure Voltage (TEV)

When establishing the whole model to solve transient enclosure voltage, it is divided into two parts, namely internal circuit model and external circuit model, and both of them are connected by means of the ideal transformer model as shown in Fig. 7.35. First, establish the internal circuit according to the main electrical wiring diagram and various component parameters, then establish the external circuit consisting of wave impedance between the enclosure outer wall and ground and wave impedance between the overhead line and ground, and finally connect them by means of the ideal transformer model, thus to form the circuit describing the GIS transient process. Figure 7.36 shows one of the main electrical wiring manners of GIS. Figure 7.37 [27] shows the whole model established for solving the TEV during operate DS1022 when CB102 is open and DS1021 is closed.

In Fig. 7.37, $R(t)$ refers to the time-varying resistance of arc generated during operation of the disconnector, C_{CB102} refers to the open contact capacitance of

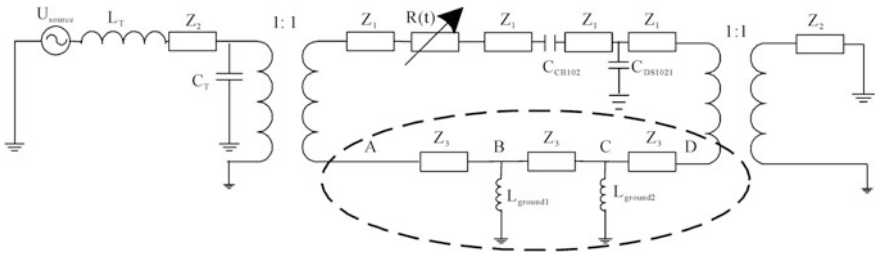

Fig. 7.37 Sketch for the whole circuit model to obtain TEV

circuit breaker CB102, C_{DS1021} and C_T refer to the equivalent ground capacitance during closing of the disconnector and the equivalent inlet capacitance of the transformer, respectively, $L_{ground1}$ and $L_{ground2}$ refer to the ground wire inductance of bushing 1 and bushing 2 at earthing bracket, respectively, and L_T refers to the equivalent inductance of the transformer. The dashed line box refers to GIS enclosure, and letters A–D refer to various TEV measuring points on the GIS enclosure where the TEV should be paid attention to during simulation.

7.9.3 Measures to Reduce the Transient Enclosure Voltage

The transient enclosure voltage may present harm to operation reliability of secondary equipment and even electric power system, and even endanger the safety of operation personnel. Therefore, certain restriction measures must be taken.

7.9.3.1 Addition of Parallel Resistance on the Disconnector

Through additional installation of parallel resistance on the disconnector, it is able to effectively reduce the amplitude of VFTO in the UHV substation or power plant, so that the TEV coupled to GIS enclosure is also reduced correspondingly. Therefore, additional installation of parallel resistance on the disconnector is also an effective measure to reduce TEV.

7.9.3.2 Reduction of Ground Wire Inductance at Bushing Outlet

The VFTO is transmitted to the GIS enclosure from the bushing; therefore, the smaller the ground wire inductance at bushing is, the smaller the voltage generated after VFTO wave flowing through the inductance is, that is to say, the smaller the enclosure voltage at bushing outlet is. Therefore, it shall be properly grounded at the point of bushing (grounding resistance shall be low, as shown in Fig. 7.38), and

(a) Sketch for earthing at bushing outlet of GIS substation

(b) Sketch for earthing at bushing outlet of HGIS substation

Fig. 7.38 Sketches for grounding at bushing outlet of GIS substation

to reduce the ground wire inductance at the bushing is the most effective means to inhibit TEV. According to the simulation test carried out by Zhejiang University, in the 500 and 1000 kV GIS, the copper grounding can achieve better effects.

Usually, the measures taken to reduce the ground wire inductance include increase of grounding down lead quantities at the bushing outlet, and use of materials with smaller magnetic permeability, such as copper and stainless steel. In comparison with ordinary steels, the inductance of unit length of copper and stainless steel is much smaller.

7.10 Experimental Investigation on VFTO Characteristics in the UHV GIS System in China

At present, the VFTO characteristics in the UHV GIS system are mainly studied through two methods, namely test and simulation. The previous section of this chapter mainly introduced the VFTO characteristics obtained through simulation; however, the actual experimental investigation is more able to reflect the true condition of VFTO. Therefore, this section mainly introduces some development in experimental investigation on the VFTO characteristics in the UHV GIS system in China.

7.10.1 VFTO Characteristic Test Circuit

In the GB 1985–2004 *High-voltage Alternating-current Disconnectors and Earthing Switches* and IEC standard 60129, the test circuit used to assess performance of the disconnector is presented, as shown in Fig. 7.39 [28].

In Fig. 7.39, AC power supply is the AC power supply at power supply side, and DC power supply is DC power supply at the load side, which is mainly used to charge the short busbar BS at load side, thus to generate residual voltage. *C* is the

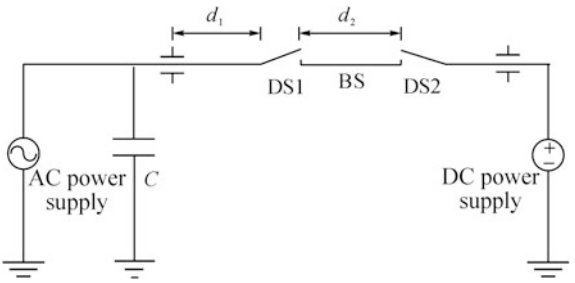

Fig. 7.39 Disconnector test circuit stipulated in GB 1985 and IEC standard

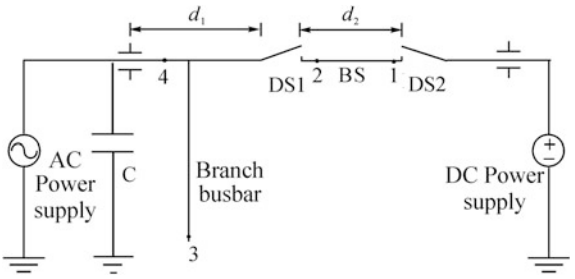

Fig. 7.40 UHV VFTO test circuit in China

lumped capacitance of circuit at power supply side; DS1 is the disconnector tested during test and DS2 is the auxiliary disconnector, mainly used to control the charging of the short busbar BS at load side; d_1 refers to the length between GIS bushing at power supply side and the disconnector DS1, and d_2 refers to the length between the disconnector tested and the auxiliary disconnector.

During the test, close DS2 first, thus to charge the short busbar BS through DC power supply. Then, the short busbar BS having been charged can be used to simulate the short busbar with residual voltage after opening of the disconnector, then the VFTO generated from closing and opening of DS1 is used for experimental investigation.

The VFTO test circuit shall be able to represent most wiring method as much as possible, and it shall be able to simulate the situation for which higher amplitude of VFTO is generated. According to the simulation research results in the UHV substation, and combined with Fig. 7.39, the test circuit with branch busbar is proposed in China, as shown in Fig. 7.40 [28].

In Fig. 7.40, figures 1–4 refer to VFTO measuring points.

The test circuit as shown in Fig. 7.40, in comparison with that as shown in Fig. 7.39, has an additional branch busbar at power supply side. When the disconnector DS1 is operated, the VFTO wave generated is subject to full reflection at the end of branch busbar, thus it is possible to generate serious VFTO. Therefore, in comparison with the test circuit as shown in Fig. 7.39, the test circuit as shown in Fig. 7.40 is possible to generate more serious VFTO.

Table 7.13 Technical parameters of the two types of disconnectors

Type of disconnector	Resistance value (Ω)	Opening speed (m/s)	Closing speed (m/s)
High speed, without parallel resistance	–	1.70	2.50
Low speed	–	0.54	0.54
High speed, with parallel resistance	500	1.70	2.50

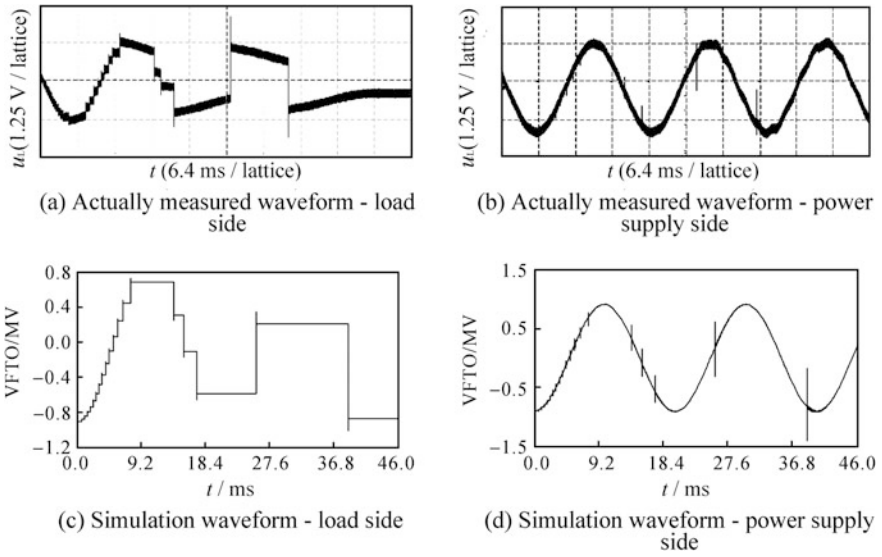

Fig. 7.41 Diagrams for tested VFTO waveform and simulated VFTO waveform during opening of disconnector

In addition, the disconnector can be divided into two types: one type is the high-speed disconnector, produced by Henan Pinggao Electric Co., Ltd. (called as Pinggao in short), for which the parallel resistance can be installed; the other type is the low-speed disconnector, produced by Xi'an XD Switchgear Electric Co., Ltd. (called as XD in short). These two disconnectors have the technical parameters as shown in Table 7.13 [29].

7.10.2 VFTO Generation Mechanism and Waveform Characteristics

According to the test circuit as shown in Fig. 7.40, the VFTO waveform at load side and power supply side during opening test and simulation calculation are, respectively, as shown in Fig. 7.41 [28].

It can be seen from Fig. 7.41 that the voltage waveform at load side presents approximate step-shaped change, each point on the waveform where the voltage is abruptly changed refers to one breakdown occurred between moving contact and fixed contact of the disconnector. At each point where the voltage is abruptly changed, it is usually accompanied with "burr", which is the VFTO. The voltage waveform at power supply side is the typical power frequency sine voltage waveform, superposed with "burr" voltage with different amplitude. In addition, it can be seen from Fig. 7.41 that, during opening process, the discharge phenomenon is relatively dense at the start, and then more and more sparse subsequently.

When the voltage waveform at both load side and power supply side (as shown in Fig. 7.41) is placed under one identical time coordinate axis, it is more favorable to understand the generation process of VFTO, as shown in Fig. 7.42 [8].

Figure 7.42 presents the schematic diagram of VFTO generation mechanism during opening process. In terms of opening process of the disconnector, during the operation process of the disconnector, when voltage between moving contact and fixed contact exceeds the breakdown voltage of contact clearance, the clearance between moving contact and fixed contact of the disconnector is broken down. During transmission process of breakdown voltage wave in the GIS, the voltage on the short busbar at load side generates high-frequency oscillation due to power frequency voltage at the breakdown moment, thus to generate the overvoltage [29]. Here, one clearance breakdown process as shown in Fig. 7.42 is taken as an example; U_1 is the value of the residual voltage at load side before breakdown, and U_S is the power frequency voltage at power supply side at the moment before breakdown; at this time, $|U_S| + |U_1|$ is just up to the breakdown voltage $U_{breakdown}$ of the clearance between moving contact and fixed contact of the disconnector, thus the clearance is broken down. And the voltage at the load side is under oscillation based on the power frequency voltage at power supply side, thus to generate VFTO.

When the high-frequency oscillation process is completed, the residual charges on the short busbar at load side generate residual voltage, due to less discharge of the charges, the value of residual voltage is maintained unchanged basically (in the actual measurement, the value of such residual voltage is reduced slightly before occurrence of next breakdown, as shown in Fig. 7.41a, till the value of residual voltage is changed to another power frequency voltage value after next breakdown

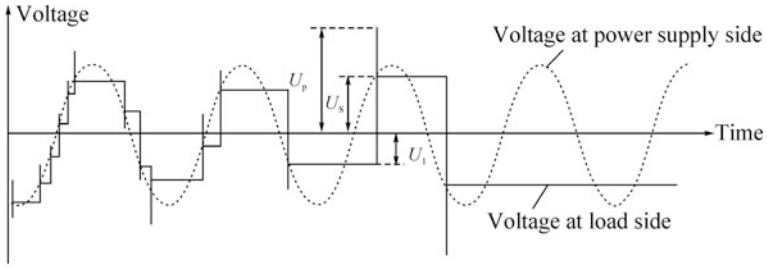

Fig. 7.42 Sketch for VFTO generation mechanism during opening process

is occurred. While the voltage at power supply side is changed continuously and regularly as per law of power frequency voltage. Therefore, the VFTO waveform has obvious step at load side, but no step at power supply side.

In addition, it can be seen from Figs. 7.41 and 7.42 that the VFTO generation process is actually the process of multiple breakdowns occurred between contacts. In terms of opening process, the breakdown phenomenon is more frequent at the beginning; then, along with time lapse, the interval between two adjacent breakdowns is larger and larger. This is because that when the change of the clearance voltage between moving contact and fixed contact is up to or exceeds the breakdown voltage, the clearance between the contacts can only be broken down. However, in terms of opening process, because the clearance between the contacts is larger and larger, the breakdown voltage of the clearance between moving contact and fixed contact is larger and larger, and thus, it is more and more difficult to generate breakdown; therefore, the interval between two breakdowns is longer and longer, and the breakdown process of final VFTO waveform is dense at the beginning and sparse subsequently. Only when the clearance between moving contact and fixed contact is very large during opening process, the clearance breakdown process is stopped, and then the VFTO generation process is ended.

Therefore, it can be inferred that, in terms of closing process of the disconnector, the clearance between moving contact and fixed contact is reduced gradually, so that the interval between clearance breakdowns is shortened, and the breakdown process of final VFTO waveform is sparse at the beginning and dense subsequently.

7.10.3 Tests on the Effect of Operating Speed of Disconnectors on VFTO

In this section, the opening operating speed of the disconnectors in the test circuit of Henan Pinggao Electric Co., Ltd. (hereinafter referred to as Pinggao) is reduced from about 1.7 to 0.7 m/s, and 450 operation tests have been conducted on the energized disconnectors under the condition that there is no direct current precharged, to study the effect of the operating speed of disconnectors on the VFTO characteristics.

7.10.3.1 Speed Adjustment of Disconnectors

The preliminary study shows that the operating speed of disconnectors has apparent effect on the distribution of residual voltage, and the residual voltage will directly affect the initial condition for subsequent breakdown and then affect the VFTO produced by the subsequent breakdown. In particular, the residual voltage of the final breakdown generated during the opening operation has greater impact on the VFTO to be generated by the first breakdown during the next closing operation.

Table 7.14 Technical parameters of Pinggao's disconnectors before and after the speed adjustment

Item		Closing speed (m/s)	Opening speed (m/s)
Measured results after speed adjustment	1	2.16	0.76
	2	2.01	0.66
	3	1.99	0.68
	4	2.19	0.78
	5	2.18	0.67
Mean value after speed adjustment		2.1	0.7
Typical value before speed adjustment		2.5	1.7

Generally, the first breakdown during the closing operation tends to produce serious VFTO, and thus the main emphasis shall be laid on the change of the opening speed for the speed adjustment of disconnectors, so as to evaluate the probability distribution of the residual voltage of the final breakdown generated during the opening operation and the resulting changes of the maximum VFTO amplitudes and probability distribution during the closing operation, and then identify the effect of the operating speed on the VFTO. As such, the speed adjustment of disconnectors focuses on the adjustment of opening speed.

The speed adjustment tests are conducted in the test circuit of Pinggao, with an aim to reduce the opening speed of disconnectors from original about 1.7–0.7 m/s, and no requirement is proposed for the closing speed of disconnectors. The electric spring operating mechanism is adopted for the test circuit of Pinggao. Through attempts and selection, the scheme for speed adjustment is finalized to change the original cylinder with oil hole in buffer to the one without oil hole, so as to reduce the operating speed through increasing the buffer. Due to the technical measures for reducing the opening speed, certain dispersion occurs to the closing speed. The measured operating speeds of the disconnectors after the speed adjustment and their comparison with the operating speeds before the speed adjustment are as shown in Table 7.14.

According to the results from the speed adjustment, the closing speed is reduced to about 80% of the original one, and the opening speed is reduced to about 40% of the original one. The reduction in the opening speed is obvious. The operation tests of the disconnectors can fully evaluate the effect of the speed on the VFTO characteristics.

7.10.3.2 Test Conditions

The test connection is as shown in Fig. 7.43. 450 tests have been conducted under the condition that the branch busbar in the test circuit is 9 m in length and the no-load short busbar is not precharged with direct-current voltage. The test points 1–4 have been marked in Fig. 7.43.

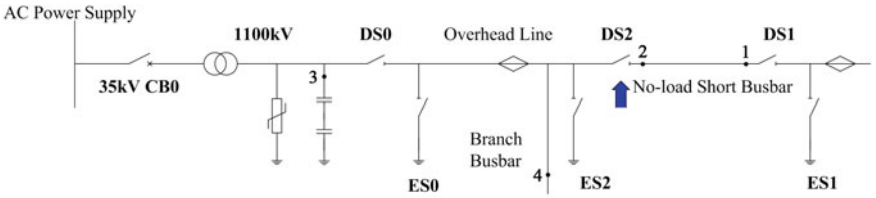

Fig. 7.43 Connection for tests on the impact of operating speed of disconnectors in Pinggao's test circuit

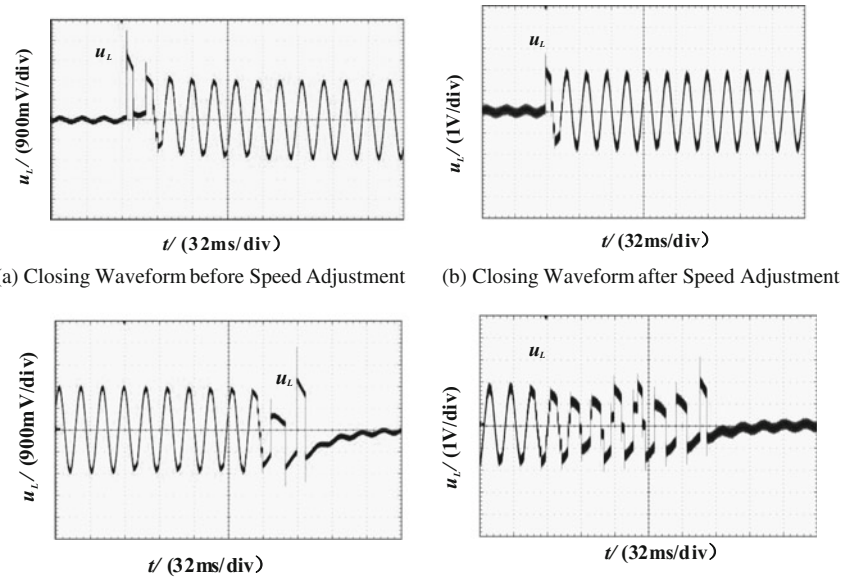

(a) Closing Waveform before Speed Adjustment (b) Closing Waveform after Speed Adjustment

(c) Opening Waveform before Speed Adjustment (d) Opening Waveform after Speed Adjustment

Fig. 7.44 Measured VFTO waveforms at measuring point #1 on the load side before and after speed adjustment

7.10.3.3 Comparison of VFTO Waveforms

1. VFTO whole-process waveforms.

The VFTO whole-process waveforms and the number of breakdowns are subject to great impact of the operating speed of disconnectors. The measured VFTO whole-process waveforms before and after the speed adjustment are as shown in Fig. 7.44.

When the operating speed of disconnectors reduces, both the pre-breakdown duration of the closing process and the arcing duration of the opening process

become longer, the number of breakdowns of the contact clearance increases accordingly, and the VFTO whole-process duration prolongs. During the speed adjustment tests, as the opening speed is greatly reduced, the aforesaid change is more obvious in the waveform of VFTO generated during the opening operation. As shown in Fig. 7.44c, d after the speed adjustment, the number of breakdowns in the waveform of VFTO generated during the opening operation increases largely and the duration prolongs significantly.

2. Number of breakdowns during the whole VFTO process.

A statistics is made on the number of breakdowns at which the breakdown voltage exceeds 0.3 p.u.in the VFTO whole-process waveforms during the closing and opening operations before and after the speed adjustment.

According to the statistical results, the average number of breakdowns during the closing process after the speed adjustment increases slightly, does not differ much from that before the speed adjustment; but the average number of breakdowns during the opening process after the speed adjustment increases significantly (about 15 breakdowns) and differs much from that before the speed adjustment.

7.10.3.4 Statistical Analysis on VFTO Characteristics

The change of the operating speed of disconnectors will mainly affect the VFTO characteristics in relation to the whole process of fracture gap breakdown, and have little impact on the waveform of single breakdown caused by the VFTO, frequency component at all measuring points, oscillation coefficient, etc. The following mainly analyzes the statistical characteristics of the VFTO before and after the speed adjustment of the disconnectors.

1. Maximum VFTO amplitudes.

The statistical results of the maximum VFTO amplitudes measured at the VFTO measuring points at all typical positions in Pinggao's test circuit are as shown in Table 7.15. The test units are Tsinghua University and North China Electric Power University which are referred to as Tsinghua and Huadian, respectively, in the table.

It can be known from the measured results that:

(1) Generally, the VFTO level of the test circuit is reduced to some extent after the reduction of the operating speed of disconnectors, and the maximum VFTO amplitude at each measuring point is generally reduced by more than 5%. The average maximum VFTO amplitude of the test circuit during the closing operation drops from 2.08 to 1.75 p.u., and the average maximum VFTO amplitude during the opening operation drops from 2.09 to 1.87 p.u., both dropping by more than 10%. This indicates that the reduction of the operating speed of disconnectors can lower the VFTO level of the test circuit.

Table 7.15 Statistical list of the measured maximum VFTO amplitudes before and after the speed adjustment of disconnectors

Measuring point no.	Test round	Maximum overvoltage value (p.u.)					
		Closing operation			Opening operation		
		Tsinghua	Huadian	Mean value	Tsinghua	Huadian	Mean value
1	After speed adjustment	1.60	1.69	1.65	1.65	1.75	1.70
	Before speed adjustment	**1.71**	**1.87**	**1.79**	**1.72**	**1.85**	**1.79**
2	After speed adjustment	1.62	1.71	1.67	1.65	1.77	1.71
	Before speed adjustment	**1.81**	**1.98**	**1.90**	**1.73**	**2.03**	**1.88**
3	After speed adjustment	1.20	1.20	1.20	1.22	1.23	1.23
	Before speed adjustment	**1.23**	**1.32**	**1.28**	**1.21**	**1.31**	**1.26**
4	After speed adjustment	1.78	1.72	1.75	1.90	1.83	1.87
	Before speed adjustment	**2.00**	**2.16**	**2.08**	**2.04**	**2.13**	**2.09**
Max. value	After speed adjustment	1.78	1.72	1.75	1.90	1.83	1.87
	Before speed adjustment	**2.00**	**2.16**	**2.08**	**2.04**	**2.13**	**2.09**

The figures in bold are the measured results obtained under the condition that the speed of the disconnector operating mechanism is normal (before speed adjustment), there is no direct-current voltage precharged and the branch busbar is 9 m in length

(2) After the speed adjustment of disconnectors, the maximum VFTO in the test circuit still occurs at the measuring point #5 at the end of the branch busbar, which is consistent with the results of the previous tests and studies.
(3) Because there is more reduction in the opening speed as compared with the opening operating speeds before the speed adjustment, a big difference exists between the closing and opening operating speeds, but the maximum VFTO amplitudes produced during the closing and opening operations are close.

2. Distribution of maximum VFTO amplitudes.

Taking the typical measuring points (measuring point #1 on the load side and measuring point #5 on the power supply side) in the test circuit as an example, a statistics is made on the probability distribution of the maximum VFTO amplitudes resulting from the operations during the tests to evaluate the effect of the speed adjustment of disconnectors on the VFTO amplitude probability distribution.

According to the statistical results of the maximum VFTO amplitude distribution at the measuring points #1 and #5, after the speed adjustment, the probability of

high-amplitude VFTO during the closing and opening operations is significantly reduced and, in terms of the overall distribution, the maximum VFTO amplitudes are centralized in the medium- and low-amplitude areas, and such change in the VFTO as produced during the closing operation is more obvious. Since the maximum VFTO during the closing operation is mainly decided by the first breakdown during the closing operation, while the said first breakdown is directly affected by the residual voltage produced by the final breakdown during the previous opening operation, it is foreseeable that the distribution of the residual voltage produced by the final breakdown during the opening operation after the speed adjustment has changed a lot.

3. Residual voltage distribution.

A statistics is made on the distribution of the measured residual voltage in Pinggao's test circuit as produced by the final breakdown during the opening operation before and after the speed adjustment.

According to the statistical results, the distribution of the residual voltage produced by the final breakdown during the opening operation after the speed adjustment is more concentrated with reduced distribution range and mainly concentrates in the negative and low-amplitude area, while the negative and high-amplitude residual voltage almost no longer appears (the maximum residual voltage drops to below 0.8 p.u.), neither does the positive residual voltage. It is hereby inferred that the reduction of the opening speed of disconnectors leads to the change of the residual voltage distribution and, as a result, the high-amplitude residual voltage is difficult to appear, and then the condition for the first breakdown during the closing operation changes and the occurrence probability of the high-amplitude VFTO reduces, eventually resulting in the change to the maximum VFTO amplitude distribution during the closing operation.

7.10.3.5 Conclusions

In this section, through the reduction of the opening operating speed of GIS disconnectors in Pinggao's test circuit, the effects of the operating speed on the waveforms and statistical characteristics of the VFTO are tested and studied. The study shows that the operating speed directly affects the opening arcing process of the fracture gap of disconnector, and then affects the number of breakdowns during the opening operation and the distribution of residual voltage on the short busbar and, subsequently, thus changing the condition for repeated breakdown of disconnector and the distribution of VFTO amplitudes. The test results show that the reduction of the operating speed of disconnectors can reduce the distribution of residual voltage, and then lower the overall VFTO level of the test circuit, but the relative magnitude of the maximum VFTO amplitudes at all measuring points in the test circuit does not change, and the maximum VFTO amplitudes produced during the closing and opening operations are close as well. The operating speed of disconnector affects the VFTO level. Therefore, through the optimization of the

operating speed, it is possible to reduce the VFTO produced by disconnector, so as to improve the safety and reliability in the disconnector operation.

7.10.4 Tests and Studies on the Effect of Branch Busbar Length on VFTO

In this section, the length of the branch busbar on the power supply side in Pinggao's test circuit is adjusted from 9 to 3 and 0 m, and 400 operation tests have been conducted on the energized disconnectors under the condition that there is no direct current precharged to study the effect of the branch busbar length on the VFTO.

7.10.4.1 Test Conditions

The tests on the impact of the branch busbar are conducted in Pinggao's test circuit under the condition that the no-load short busbar is not precharged with direct-current voltage and the speed of the disconnector operating mechanism is before speed adjustment. The test connection is as shown in Fig. 7.45. The test points 1–4 have been marked in Fig. 7.45. The power frequency voltage of 635 kV (the maximum phase-to-ground voltage, $1100/\sqrt{3} = 635$ kV) is applied on the AC power supply side, and the length of branch busbar is successively adjusted to 0, 3, and 9 m. During the tests, the auxiliary disconnector DS1 is kept open and the tested disconnector DS2 is operated. 400 effective tests have been carried out to study the effect of branch busbar length on the VFTO in the GIS under the natural open state under the condition that the no-load short busbar is not precharged with direct-current voltage.

7.10.4.2 Effect on VFTO Amplitudes

1. Maximum VFTO amplitudes

The statistical results of the maximum VFTO amplitudes measured at the VFTO measuring points at the typical positions of Pinggao's test circuit are referred to

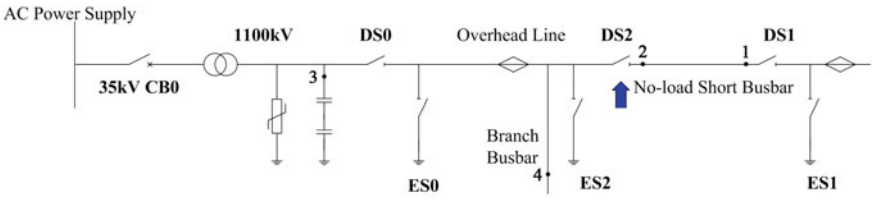

Fig. 7.45 Connection for tests on the impact of branch busbar in Pinggao's test circuit

Table 7.16 Statistical list of the maximum VFTO amplitudes measured during the tests on the impact of branch busbar

Measuring point no.	Length of branch busbar (m)	Maximum overvoltage (p.u.)					
		Closing operation			Opening operation		
		Tsinghua	Huadian	Mean value	Tsinghua	Huadian	Mean value
1	0	1.69	1.75	1.72	1.68	1.74	1.71
	3	1.68	1.90	1.79	1.65	1.86	1.76
	9	1.81	2.01	1.91	1.80	1.99	1.90
2	0	1.47	1.65	1.56	1.44	1.61	1.52
	3	1.47	**–**	**–**	1.44	**–**	**–**
	9	1.80	2.00	1.90	1.74	1.98	1.86
3	0	1.46	1.53	1.50	1.46	1.50	1.48
	3	1.30	**–**	**–**	1.29	**–**	**–**
	9	1.27	1.32	1.30	1.25	1.33	1.29
4	0[a]	–	–	–	–	–	–
	3	1.58	1.88	1.73	1.55	1.79	1.67
	9	2.00	2.23	2.12	1.94	2.19	2.07
Max. value	0	1.69	1.75	1.72	1.68	1.74	1.71
	3	1.68	1.90	1.79	1.65	1.86	1.76
	9	2.00	2.23	2.12	1.94	2.19	2.07

The bold refer to that the result cannot be obtained by normal measurement due to incidental factors during the field measurement

[a]When the length of branch busbar is adjusted to 0 m, the measuring point at the end of branch busbar no longer exists

Table 7.16. The test units are Tsinghua University and North China Electric Power University which are referred to as Tsinghua and Huadian, respectively, in the table.

It can be known from the measured results that:

(1) Generally, the maximum VFTO of the test circuit increases with the increase of the branch busbar length (the maximum VFTO amplitude of the test circuit corresponding to 0, 3, and 9 m branch busbar is, respectively, 1.75, 1.90, and 2.23 p.u.), consisting with the conclusion drawn from the simulation calculation, i.e., whether the branch busbar exists or not and whether its length changes or not have definite impact on the VFTO level of the test circuit, and the longer the branch busbar is, the higher the VFTO level of the test circuit will be.

(2) Although the maximum VFTO of the test circuit increases with the change of the branch busbar length, not all measuring points have monotonically increased VFTO (in the measured results, the maximum VFTO at the measuring points #1 and #2 on the no-load short busbar and at the measuring point #5 on the branch busbar is increased, while the maximum VFTO at the measuring point #4 under the bushing BG1 on the power supply side is slightly reduced) and, in addition, the position where the maximum VFTO occurs in the test circuit may change, but not always occurs at the end of branch busbar.

2. Distribution of maximum VFTO amplitudes.

Taking the typical measuring points (measuring point #1 on the load side and measuring point #5 on the power supply side) in the test circuit as an example, a statistics is made on the probability distribution of the maximum VFTO amplitudes resulting from the operations during the tests to evaluate the effect of the branch busbar length on the VFTO amplitude probability distribution.

According to the statistical results of the distribution of the maximum VFTO amplitudes at the measuring point #1 and measuring point #5, with the increase of the branch busbar length, the maximum VFTO amplitudes resulting from both the closing and opening operations that may occur at the measuring points are increased.

7.10.4.3 Impact on Residual Voltage

A statistics is made on the distribution of the measured residual voltage in Pinggao's test circuit as produced by the final breakdown during the opening operation under different lengths of branch busbar.

According to the statistical results, the distribution of the residual voltage caused by the final breakdown under different lengths of branch busbar is basically the same, the residual voltage is mainly distributed in the negative area, and the probability distribution shows certain normal distribution characteristics. This is because that the distribution of residual voltage is mainly decided by the mechanical characteristics of disconnectors and the moment they are opened, while the length of branch busbar can only change partial electrical characteristics of the test circuit, but cannot change the mechanical characteristics of disconnector.

7.10.4.4 Conclusions

The tests as described in this section study the effect of the length of branch busbar in the test circuit on the VFTO, and the results obtained show that, with the increase of the branch busbar length, the VFTO in the test circuit tends to increase, but the distribution of the maximum VFTO amplitudes and of the residual voltage at all measuring points is basically free from impact. This is because that the length of branch busbar has certain impact on the refraction, reflection, and superposition of the traveling wave of the disconnector's fracture breakdown voltage in the test circuit, which will lead to the change of the maximum VFTO amplitude in the test circuit, but the length of branch busbar has no impact on the characteristic of repeated breakdown voltage of the disconnector, and thus basically has no impact on the residual voltage distribution and the maximum VFTO amplitude distribution decided by it.

7.10.5 *Effect of Connection Direction of Disconnector Contacts on VFTO*

In this section, the connection direction of the contacts of disconnectors in the test circuit of Xi'an XD Switchgear Electric Co., Ltd. (hereinafter referred to as Xi'an Switchgear) is changed, and 400 operation tests have been conducted on the energized disconnectors under the condition that there is no direct current pre-charged to study the impact of the connection direction of disconnector contacts on the VFTO characteristics.

7.10.5.1 Test Conditions

The VFTO is produced by the continuous repeated breakdown, arcing and arc extinguishing of the fracture gap between the moving and stationary contacts during the movement of the disconnector contacts. The breakdown of gas clearance is related to the gas state (type, pressure, temperature, flow velocity, etc.), electric field condition (electric field intensity, electrode structure, degree of electric field unevenness, etc.) and others, and the structure of disconnector contacts has direct impact on the gas state and electric field condition of the fracture gap. Generally, the moving and stationary contacts are different in structure (refer to Fig. 7.46 for the internal structure of the tested disconnectors in Xi'an Switchgear's test circuit), and when different types of voltage are applied, the fracture gap will present a polarity effect in terms of its breakdown characteristic due to the asymmetric contact structures.

According to the engineering practice, at a substation site, it is a common practice to connect the moving contact of disconnector with the AC power supply side of the system, and connect the stationary contact with the load-side short

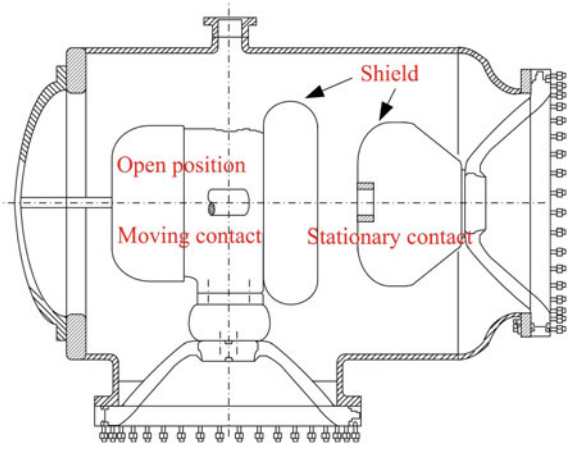

Fig. 7.46 Sketch for internal structure of disconnector in Xi'an Switchgear's test circuit

busbar (the short busbar between the disconnector and its adjacent circuit breaker) to be operated. During the VFTO characteristic tests described earlier, the connection between the equipment in the test circuit is made in this way. Considering the different structures of the moving and stationary contacts, the difference in contact polarity will affect the breakdown characteristics of contact clearance, and then affect the polarity and amplitude of the residual voltage on the load-side short busbar which is to be operated. Therefore, it is necessary to analyze the change of the contact clearance breakdown and of the polarity and distribution of the residual voltage following such breakdown after the connection direction of the disconnector is reversed.

The tests on the impact of the disconnector connection direction on the VFTO are conducted by changing the connection direction between the disconnector's moving and stationary contacts and the system, i.e., the moving contact end which is originally connected with the system's AC power supply side is changed to be connected with the load-side short busbar to be operated, and the stationary contact end which is originally connected with the load-side short busbar to be operated is changed to be connected with the system's AC power supply side, similarly to have the original contact clearance polarity "reversed".

The tests on the impact of the connection direction of disconnector contacts are conducted in Xi'an Switchgear's test circuit under the condition that the no-load short busbar is not precharged with direct-current voltage and the speed of the disconnector operating mechanism is before speed adjustment. The test connection is as shown in Fig. 7.47. The test points 1–4 have been marked in Fig. 7.47. The power frequency voltage of 635 kV (the maximum phase-to-ground voltage, $1100/\sqrt{3} = 635$ kV) is applied on the AC power supply side, and the length of branch busbar is 9 m. During the tests, the auxiliary disconnector DS1 and the original tested disconnector DS2 together with the short busbar between them are wholly reversed and then connected with other parts of the test circuit. After the reversal, DS2 serves as the auxiliary disconnector and is kept open; while DS1 serves as the disconnector tested. Since the disconnector DS1 is close to DS2 in terms of the mechanical characteristics, and 450 effective tests have been carried out, the effect of the connection direction of disconnector contacts on the characteristics of the VFTO in the GIS can be studied through a comparison between the current tests and the previous tests.

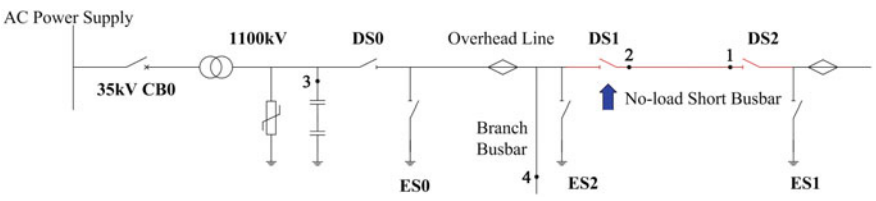

Fig. 7.47 Connection for tests on the impact of connection direction of disconnector contacts in Xi'an Switchgear's test circuit

7.10.5.2 Comparison of VFTO Waveforms

1. VFTO whole-process waveforms

The VFTO whole-process waveforms and the number of breakdowns are affected by the characteristics of breakdown of the disconnector contact clearance. The typical VFTO whole-process waveforms measured before and after the change of the connection direction of disconnector contacts are as shown in Fig. 7.48.

According to the VFTO whole-process waveforms, before and after the adjustment of the connection direction of disconnector contacts, a significant difference lies in the reversal of the polarity at the first breakdown during the closing operation and the final breakdown during the opening operation. Before the adjustment of connection direction, the polarity at the first breakdown during the closing operation and the final breakdown during the opening operation mainly appears as positive; after the adjustment of connection direction, the polarity at the first breakdown during the closing operation and the final breakdown during the

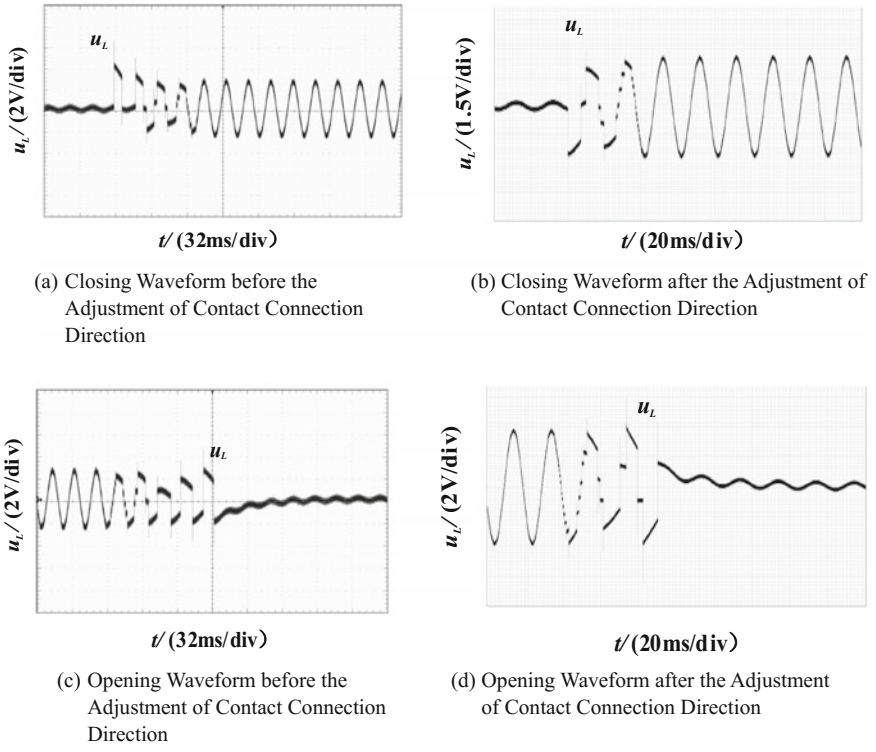

(a) Closing Waveform before the Adjustment of Contact Connection Direction

(b) Closing Waveform after the Adjustment of Contact Connection Direction

(c) Opening Waveform before the Adjustment of Contact Connection Direction

(d) Opening Waveform after the Adjustment of Contact Connection Direction

Fig. 7.48 Measured VFTO waveforms at measuring point #1 on the load side before and after the adjustment of connection direction of disconnector contacts

opening operation mainly appears as negative. Moreover, it can be directly seen from the VFTO whole-process waveforms that, no matter during the closing process or the opening process, the total number of breakdowns during the whole process is changed.

2. Number of whole-process breakdowns caused by VFTO.

To obtain the accurate information on the whole-process breakdowns caused by the VFTO, a statistics is made on the number of breakdowns at which the breakdown voltage exceeds 0.3 p.u.in the VFTO whole-process waveforms during the closing and opening operations before and after the adjustment of the connection direction of disconnector contacts.

According to the statistical results, after the adjustment of the connection direction of disconnector contacts, the average number of breakdowns during the closing and opening processes is about 8, lower than 11 which is the average number of breakdowns before the adjustment. This indicates that the change of the connection direction of disonnector affects the breakdown characteristics of the contact clearance and the polarity effect of contact clearance exists.

7.10.5.3 Statistical Analysis of VFTO Characteristics

The change of the connection direction of disconnector contacts will mainly affect the VFTO characteristics in relation to the whole process of the fracture gap breakdown, but have little impact on the waveform of single breakdown caused by the VFTO, frequency component at all measuring points, oscillation coefficient, etc. The following mainly analyzes the statistical characteristics of the VFTO before and after the adjustment of the connection direction of disconnector contacts.

1. Maximum VFTO amplitudes.

The statistical results of the maximum VFTO amplitudes at the VFTO measuring points at the typical positions of Xi'an Switchgear's test circuit as measured during the tests are referred to Table 7.17. The test units are Tsinghua University and North China Electric Power University which are referred to as Tsinghua and Huadian, respectively, in the table

It can be known from the measured results that:

(1) Generally, compared with the measured results obtained before the adjustment of the connection direction of contacts, the VFTO level of the test circuit has little change after the reversal of contact connection direction. The average maximum VFTO amplitude of the test circuit during the closing operation drops slightly from 1.98 to 1.97 p.u., and the average maximum VFTO amplitude during the opening operation increases slightly from 1. 96 to 1.97 p. u., both having extremely little change. This indicates that the connection direction of disconnector contacts has only limited impact on the maximum VFTO that may occur in the test circuit.

Table 7.17 Statistical list of the maximum VFTO amplitudes before and after the adjustment of connection direction of disconnector contacts measured during the tests

Measuring point no.	Test round	Maximum overvoltage (p.u.)					
		Closing operation			Opening operation		
		Tsinghua	Huadian	Mean value	Tsinghua	Huadian	Mean value
1	After adjustment	1.99	1.94	1.97	1.86	2.07	1.97
	Before adjustment	**1.89**	**2.04**	**1.97**	**1.82**	**2.10**	**1.96**
2	After adjustment	1.76	1.89	1.83	1.72	1.87	1.80
	Before adjustment	**1.78**	**2.06**	**1.92**	**1.73**	**2.10**	**1.92**
3	After adjustment	1.36	–	–	1.36	–	–
	Before adjustment	**1.29**	**1.4**	**1.35**	**1.31**	**1.41**	**1.36**
4	After adjustment	1.63	1.73	1.68	1.59	1.72	1.66
	Before adjustment	**1.69**	**1.74**	**1.72**	**1.71**	**1.76**	**1.74**
Max. value	After adjustment	1.99	1.94	1.97	1.86	2.07	1.97
	Before adjustment	**1.89**	**2.06**	**1.98**	**1.82**	**2.10**	**1.96**

The figures in bold are the measured results obtained before the adjustment of the connection direction of disconnector contacts under the condition that there is no direct-current voltage precharged and the branch busbar is 9 m

(2) After the adjustment of the connection direction of disconnector contacts, the maximum VFTO in the test circuit still roughly appears at the measuring point #1 at the end of the no-load short busbar, which is consistent with the results of the previous tests and studies.
(3) Although the maximum VFTO amplitudes measured at different measuring points before and after the adjustment of the connection direction of disconnector contacts have somewhat changed, they do not change much and do not increase or decrease simultaneously; meanwhile, the maximum VFTO amplitudes produced during the closing and opening operations are close.

2. Distribution of the maximum VFTO amplitudes.

Taking the typical measuring points (measuring point #1 on the load side and measuring point #5 on the power supply side) in the test circuit as an example, a statistics is made on the probability distribution of the maximum VFTO amplitudes resulting from the operations during the tests to evaluate the effect of the adjustment

of the connection direction of disconnector contacts on the VFTO amplitude probability distribution.

According to the statistical results of the maximum VFTO amplitude distribution at the measuring point #1 and measuring point #5, before and after the adjustment of the connection direction of disconnector contacts, the maximum VFTO amplitude distribution during the closing and opening operations generally tends to shift to the low-value area, especially at the measuring point #5 on the load side. This indicates that the change of the connection direction has impact on the characteristics of contact clearance breakdown, which leads to the change of the residual voltage polarity or distribution after the breakdown, and then affects the condition for breakdown and the VFTO amplitude distribution characteristics. However, such impact only has limited influence on the maximum VFTO which may appear in the test circuit, because so long as there is possibility of occurrence of high-amplitude residual voltage on the load side which results in a large fracture gap voltage difference, the possibility of high-amplitude VFTO to be produced by breakdown exists, merely that the probability of occurrence may be lower than before.

3. Residual voltage distribution.

A statistics is made on the distribution of the residual voltage caused by all breakdowns during the whole process as measured before and after the adjustment of the connection direction of disconnector contacts in Xi'an Switchgear's test circuit.

According to the statistical results:

(1) After the adjustment of the connection direction of disconnector contacts, the overall distribution of the residual voltage caused by all breakdowns during the closing and opening operations is consistent as compared with that before the adjustment, and the distribution of the positive and negative voltage before and after the adjustment is symmetric to a certain extent (i.e., the distribution of positive voltage before the adjustment of contact connection direction is approximate to the distribution of the negative voltage after the adjustment, and the distribution of the negative voltage before the adjustment of contact connection direction is approximate to the distribution of positive voltage after the adjustment).
(2) After the adjustment of the connection direction of disconnector contacts, the distribution of the residual voltage caused by the final breakdown during the opening operation is concentrated in the positive area, exactly opposite to the distribution of the residual voltage which is mainly negative voltage before the adjustment of contact connection direction, and is approximately symmetric.
(3) The statistical results show that the residual voltage distribution is directly related to the contact structure and the application method of AC power supply, while the difference in the residual voltage polarity will affect the VFTO amplitudes in test circuit and the probability distribution thereof.

7.10.5.4 Conclusions

In this section, through the change of the connection direction of the GIS disconnectors with the AC power supply and the no-load short busbar in Xi'an Switchgear's test circuit, tests have been conducted to study the effect of different connection directions of contacts on the VFTO characteristics. The test results show that the change of the connection direction of disconnector contacts has impacts on the characteristics of breakdown voltage of fracture gap, the number of breakdowns caused by the VFTO during the whole process, the residual voltage polarity and distribution as well as the probability distribution of the maximum VFTO amplitude, but has little impact on the maximum VFTO level of the test circuit.

7.11 Conclusions on VFTO Characteristics in the 500/1000 kV GIS Substation and Power Plant

After comprehensive analysis in this chapter, it can be seen that, in terms of 500 and 1000 kV GIS substation and power plant, the threat of VFTO on main insulation of GIS body, main insulation of the main transformer and longitudinal insulation of the main transformer are shown in Table 7.18, where, the threat of VFTO on longitudinal insulation of the main transformer is considered mainly as per influence of VFTO wave front steepness on longitudinal insulation of the main transformer.

After comprehensive analysis in this chapter and from Table 7.18, it can be seen that:

Table 7.18 Conclusions of harm on the three types of insulation by VFTO in the power plant and GIS substation under different voltage levels

		Whether There is Any Threat from VFTO		
		Main insulation of GIS body	Main insulation of main transformer	Longitudinal insulation of main transformer
GIS substation	500 kV	No	No	No
	1000 kV	Yes	No	No
Power plant (with GCB)	500 kV	No	No	Yes
	1000 kV	Yes	No	Yes
Power plant (without GCB)	500 kV	No	No	Yes
	1000 kV	Yes	No	Yes

1. In terms of 500 kV GIS substation, the VFTO in general has no threat on main insulation of GIS body, main insulation of the main transformer and longitudinal insulation of the main transformer. Usually, it does not need protection, and the disconnector is also not necessary to install parallel resistance.
2. In terms of 1000 kV GIS substation, the VFTO in general has no threat on main insulation and longitudinal insulation of the main transformer. However, it has a threat on main insulation of GIS body and, therefore, it shall be protected. According to the above analysis, after taking the measures to install parallel resistance on the disconnector, it is able to reduce the amplitude of VFTO. Therefore, it is recommended to install parallel resistance on the disconnector in the 1000 kV GIS substation.
3. In terms of 500 kV power plant, the VFTO does not endanger main insulation of GIS body and main insulation of the main transformer. However, it poses a threat on the longitudinal insulation of the main transformer. According to the previous analysis, to ensure the VFTO wave front steepness invading the main transformer in the 500 kV power plant is controlled below the restriction level, it is only required to set up one overhead line with length not less than 15 m between GIS bushing outlet and the main transformer outlet. Therefore, if case site conditions allow, it is recommended to set up one overhead line with length longer than 15 m between GIS bushing outlet and the main transformer outlet.
4. In terms of 1000 kV power plant, the VFTO does not endanger main insulation of the main transformer; however, it poses a threat on main insulation of GIS body and longitudinal insulation of the main transformer. According to the previous analysis, to ensure the VFTO wave front steepness invading the main transformer in the UHV power plant is controlled below the restriction level, it is only required to set up one overhead line with length not less than 25 m between GIS bushing outlet and the main transformer outlet. Therefore, in case site conditions allow, it is recommended to set up one overhead line with length longer than 25 m between GIS bushing outlet and the main transformer outlet. At the same time, to effectively reduce the amplitude of VFTO on GIS body, it is recommended to additionally install parallel resistance on the disconnector.
5. Whether the generator outlet installed with GCB in the power plant has a large influence on the VFTO characteristics, and it is mainly reflected in the following aspects: in terms of the two operating modes (namely switching of outgoing line and switching of busbar) in the UHV power plant, whether the generator outlet installed with GCB has no large influence on the amplitude of VFTO on GIS body, the amplitude of VFTO at the port of the main transformer, and the VFTO wave front steepness invading the port of the main transformer. However, in terms of switching of main transformer in the UHV power plant, when the generator outlet is not installed with GCB in the power plant, the amplitude of VFTO on GIS body is 2.50 p.u., the amplitude of VFTO at the port of the main transformer is 1.43 p.u., and the VFTO wave front steepness invading the port of the main transformer is 5090 kV/μs; when the generator outlet is installed with GCB in the power plant, the amplitude of VFTO on GIS body is 2.36 p.u., the amplitude of VFTO at the port of the main transformer is 0.03 p.u., and the

VFTO wave front steepness invading the port of the main transformer is 890 kV/μs (about 1/6 of the former). Therefore, whether the generator outlet is installed with GCB has a very large influence on the VFTO characteristics as a whole.

6. When the generator outlet is installed with GCB in the power plant, the VFTO characteristics under typical disconnector operating mode and the VFTO characteristics in the substation have no large difference, and it is mainly reflected in the following aspects: during switching of outgoing line, the difference between the amplitude of VFTO on GIS body in the power plant for which the generator outlet is installed with GCB and that in the substation is only 0.02 p.u., and the difference between the amplitude of VFTOs at the port of the main transformer in the two is only 0.04 p.u.; during switching of busbar, the difference between the amplitude of VFTOs on GIS body and the difference between the amplitude of VFTOs at the port of the main transformer in the two are only 0.04 and 0.11 p.u., respectively; during switching of main transformer, the difference between the amplitude of VFTOs on GIS body and the difference between the amplitude of VFTOs at the port of the main transformer in the two are only 0.02 and 0.01 p.u., respectively. In addition, in terms of the two operating modes (namely switching of busbar and switching of main transformer), the VFTO wave front steepness invading the port of the main transformer in the power plant is slightly higher than the VFTO wave front steepness invading the port of the main transformer in the substation; in terms of operating mode of switching of outgoing line, the VFTO wave front steepness of the former is larger than that of the latter. Therefore, when the generator outlet is installed with GCB, the VFTO characteristics in the power plant are relatively approximate to those in the substation.
7. Through installation of parallel resistance on the disconnector and improving the grounding conditions at bushing outlet (for example, increase of ground wire quantities, use of materials with smaller magnetic permeability, such as copper and stainless steel), it is able to effectively reduce the amplitude of TEV on GIS enclosure.
8. According to the test results, the largest VFTO generated during operation of high-speed disconnector is 2.27 p.u., and it is emerged at the end of branch busbar; the largest VFTO generated during operation of low-speed disconnector is 2.20 p.u., and it is emerged at the end of no-load busbar; the largest VFTO under the two operation conditions has no large difference.
9. According to the test results, when the disconnector is installed with parallel resistance, the amplitude of VFTO is greatly weakened. After the disconnector is installed with parallel resistance, the largest VFTO is reduced from 2.27 to 1.33 p.u., with the decrease amplitude up to 41%. In addition, after the disconnector is installed with parallel resistance, the VFTO wave front steepness and amplitude of high-frequency component can also be weakened perfectly.

References

1. Yan Z, Zhu D. HV insulation technology. Beijing: China Electric Power Press; 2007.
2. Gu D, Xiu M, Dai M, Zhou P. Study on VFTO of 1000 kV GIS Substation. High Volt Eng. 2007;33(11):27–32.
3. Shi B, Zhang W, Gu W, Qiu Y. Calculation and analysis of very fast transient overvoltage in GIS. High Volt Eng. 1997;23(4):19–21.
4. Shi B, Li Z, Zhang W, Qiu Y. Analysis of the reason why VFTO may endanger EHV GIS above 300 kV. Power Syst Technol. 1998;22(1):1–3.
5. Ruan Q, Shi W, Wang L. Study on suppression of switching overvoltage caused by operation of disconnector in GIS. High Volt Appar. 2006;42(1):18–20.
6. Xiang Z, Ding Y, Ban L, Lin J, Wang S, Wang X. Suppressing VFTO in UHV GISs with switching resistor. Electr Power. 2007;40(12):31–5.
7. China Electric Power Research Institute. UHV transmission technology—volume of AC transmission. Beijing: China Electric Power Press; 2012.
8. Chen W, Yan X, Wang S, Wang C, Li Z, Dai M, Li C, Liu W, Chen H, Zhang Q, Wei G, Zhang M. Recent progress in investigations on very fast transient overvoltage in gas insulated switchgear. Proc CSEE. 2011;31(31):1–11.
9. Yin Y, Liu S, Shi W, Wang S, Zhang L, Li L, Zhang Q, Zhao W, Wu K. Research and design of the 2.5 MV very fast transient overvoltage generator. Proc CSEE. 2011;31(31):48–55.
10. GB/Z 24842-2009. Overvoltage and insulation coordination of 1000 kV UHVAC transmission project. 2009.
11. GB 311.1-1997. Insulation co-ordination for high voltage transmission and distribution equipment. 1997.
12. Zhao Z. HV technology (the third edition). Beijing: China Electric Power Press; 2013. p. 141–50.
13. Zhang X. Time-domain Simulation calculation of and experimental research on the effect of VFTO on power transformers. China: University in Baoding; 2008.
14. Liang G. Study on modeling of power transformers and fast simulation algorithm under very fast overvoltages. China: University in Baoding; 2009.
15. GB 50229-2006. Code for design of fire protection for fossil fuel power plants and substations. 2006.
16. Hu W, Jin Z, Li S, Zhou H, Shen W. Selection of protection measure for very fast transient overvoltage of 500 kV GIS. High Volt Eng. 2005;31(1):35–7.
17. Chen S, Xu J, He J, Yang J. Very fast transient over-voltages and their effects on power transformers. J Tsinghua Univ (Sci Technol). 2005;45(4):573–6.
18. Guan Y, Zhang M, Yue G, Zhang X, Liu W. Simulation test on suppression VFTO in UHV GIS with magnetic-rings. High Volt Eng. 2011;37(3):651–7.
19. Zhou H, Li Y, Shen Y, Wan Y, Chen G, Sun K. Limiting the steepness of VFTO invaded wave to the EHV power transformers using overhead lines. High Volt Eng. 2013;39(4):943–50.
20. Yang Y, Wang Z, Shao C. Effect of GIS bus structure and parameters on VFTO waveform. High Volt Eng. 2009;35(9):2306–12.
21. Shao C, Yang Y, Liu W, Wang Z. Effect of breaker structural parameters on very fast-fronted transient overvoltage waveform in GIS. High Volt Eng. 2011;37(3):577–84.
22. Shao C, Yang Y, Wang Z. Modeling of GIS switching arc and its effect on VFTO waveforms. Power Syst Technol. 2010;34(7):200–5.
23. DL/T 5352-2006. Technical code for designing high voltage electrical switchgear. 2007.
24. Lu T, Li S, Feng Y, He T, Wang P. Calculation of very fast transient overvoltage in GIS. High Volt Eng. 2002;28(11):3–5.
25. Liu Y. Some key considerations of the design of the main electric connection of ertan hydro station. Water Power. 2000;5:33–5.
26. Xu J, Wang L, Li S. Simulation and analysis of enclosure voltage transient characteristic caused by disconnector operation in ultra high voltage gas insulated switch. High Volt Eng. 2012;38(2):288–94.

27. Lin X, Li S, Xu J. Enclosure over-voltage characteristics of UHV GIS. J Shenyang Univ Technol. 2009;31(6):606–10.
28. Dai M, Gu D, Sun G, Wang L, Zhou P, Yao T, Chen H, Wan L, Pang Q, Zou X, Chen J. Study on full-scale 1000 kV gas insulated switchgear test circuit for very fast transient overvoltage. Proc CSEE. 2011;31(31):28–37.
29. Chen W, Li Z, Sun G, Dai M, Liu W, Li C, Wang L, Wang H, Chen G, Yao T, Wang S, Lu J, Wu J, Zhang X, Li W, Li X. Experimental research on the characteristics of very fast transient overvoltage in ultra high voltage gas insulated switchgear. Proc CSEE. 2011;31(31):38–47.

Chapter 8
Lightning Protection of UHVAC System

Bincai Zhao, Hao Zhou, Yuchuan Han and Jingzhe Yu

The lightning protection of UHV system is always the subject of great concern. Its design and research are mainly based on the operating experience of similar projects and the corresponding calculation of lightning protection. Based on the design experience and lightning protection operation practice of the 750 and 500 kV EHVAC lines, the former Soviet Union and Japan meticulously designed the lightning protection for 1150 and 1000 kV UHVAC transmission lines. The designers initially thought that the UHVAC transmission lines should have good lightning withstand performance, but the trip accidents resulting from the direct lightning strike on the conductors still happened during the actual operation. Therefore, how to improve the lightning protection design level, lightning withstand performance, and operating reliability of the UHVAC transmission lines with such a large transmission capacity has become an important topic in the current research of UHVAC transmission.

This chapter first discusses the simulation models and calculation methods for the lightning shielding failure and back flashover of the UHVAC transmission lines, and then carries out simulation calculation for the overvoltage of lightning invasion

B. Zhao (✉)
State Grid Weifang Power Supply Company, Weifang, Shandong,
People's Republic of China
e-mail: zhaobincai@126.com

H. Zhou · J. Yu
College of Electrical Engineering, Zhejiang University,
Xihu District, Hangzhou, Zhejiang, People's Republic of China
e-mail: zhouhao_ee@zju.edu.cn

J. Yu
e-mail: 21510213@zju.edu.cn

Y. Han
College of Electrical Engineering, Zhejiang University,
Xihu District Hangzhou, People's Republic of China
e-mail: 1254452594@qq.com

© Zhejiang University Press, Hangzhou and Springer-Verlag GmbH Germany 2018

H. Zhou et al. (eds.), *Ultra-high Voltage AC/DC Power Transmission*,
Advanced Topics in Science and Technology in China,
https://doi.org/10.1007/978-3-662-54575-1_8

wave in UHV substations and analyzes the assessment methods for the lightning withstand performance in UHV substations, and finally discusses the protection measures for lightning invasion wave in UHV substations.

8.1 Lightning Protection of the UHVAC Lines

8.1.1 Overview

8.1.1.1 Summary of Operating Experience in Other Countries

Both the former Soviet Union and Japan carried out special lightning protection design for the lightning overvoltage protection of UHVAC lines, and deemed that the lightning withstand level of their UHV lines was quite high. However, the actual operating experience showed that the lightning trip-out rate of their UHV lines was still high, and the lightning was the main cause for line trips.

With different national conditions, the former Soviet Union and Japan have big differences in the landforms of the areas that the UHVAC lines go through and the designs of tower types, etc., so the measures taken for lightning protection are different. The followings are a brief analysis on the relevant operating conditions of the UHV lines in the both countries. The operating data are as shown in Table 8.1.

In the former Soviet Union, the 1150 kV UHV line mainly went through the terrain of plain, and the single-circuit horizontal guyed V-shape towers were used for the straight line towers, and the discrete type towers were used for angle towers. The typical tower types are as shown in Fig. 8.1. The former Soviet Union's UHV lines adopted the arrangement of double overhead ground wires, in which the 2-bundled 70/72 type aluminum stranded conductors steel reinforced was applied as the overhead ground wires (the experts of the former Soviet Union deemed that the 2-bundled configuration may increase the induced charge on the overhead ground wires, thereby enhancing their capability to lead lightning and reducing the

Table 8.1 Statistics of lightning trip-out rates for UHVAC lines in other countries [times/(100 km·a)]

Country	Tower height (m)	Protection angle (°)	Effective length of insulator string	Terrain	Lightning intensity	Lightning trip-out rate
Former Soviet Union	33–46	Tangent tower: 24–28 Angle tower: about 40	10–14 m	Plain	40–50 lightning hours	0.4[b]
Japan	88–148	−12	5.9–6.3[a]	Mountain areas, hills, plains	25 thunderstorm days	0.9

[a]In Japan, the insulator strings are installed with arcing horns, so the effective string length is shorter than the actual string length (7.68–7.8 m)

[b]Refers to the lightning trip-out rate during the operation at nominal voltage

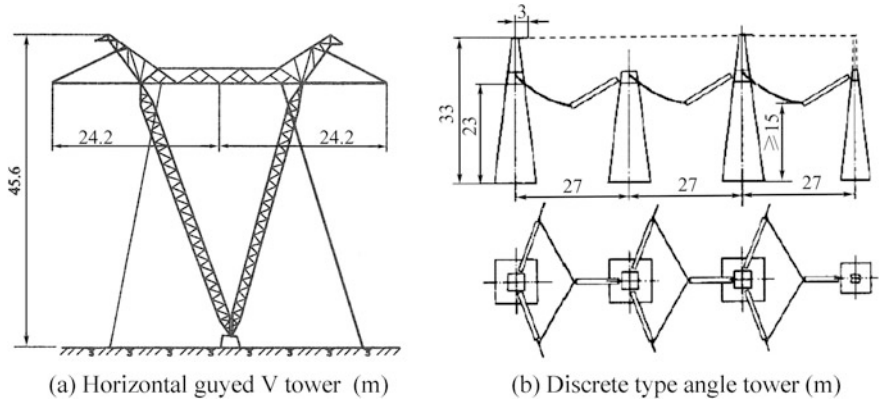

Fig. 8.1 Diagram of typical tower types of the UHV lines in the Former Soviet Union, reprinted from Ref. [1], copyright 2014, with permission from St. Petersburg Press

probability of shielding failure), and the overhead ground wire protection angle was generally around 22°. During the period of operation at nominal voltage of 1150 kV for the decade from 1986 to 1995 (3000 km·a), the statistic lightning trip-out rate was 0.4 times/(100 km·a), and the number of trips due to lightning strike over the whole period of operation (including operation at 500 and 1150 kV) was 21 times (16,700 km·a), which was equivalent to 0.13 times (100 km·a).

According to the actual measurement by the magnetic steel rod recorder, the root cause for the high lightning trip-out rate of the UHV lines in the former Soviet Union was the unreasonable structural design of the angle tower, because of which the lightning strikes the conductors after passing through the overhead ground wire of the angle tower. It can be known from Fig. 8.1 and Table 8.1 that the tangent tower's overhead ground wire protection angle is about 24° and the overhead ground wire spacing is about 35 m, while the angle tower's overhead ground wire protection angle to the jumper wire is up to about 40° and the overhead ground wire spacing is about 54 m. The angle tower's protection angle and overhead ground wire spacing are both greater than those of the tangent tower, which makes the angle tower more susceptible to shielding failure. Therefore, some experts of the former Soviet Union deemed that the main measure to improve the UHV lines' lightning withstand performance was to use a smaller overhead ground wire protection angle. It is also pointed out in *Russia's Lightning and Internal Overvoltage Protection Manual for 6–1150 kV Power Grids* in 1999 (hereinafter referred to as the Russia's 1999 *Manual*) that: "For the 1150 kV overhead lines, the urgent requirement is to improve the overhead ground wire protection; and the improvement in the lightning withstand performance of 1150 kV lines is guaranteed by using the tangent towers and tension angle towers with negative overhead ground wire protection angles" [1].

As the 1000 kV UHV lines often go through the mountainous regions, hills, and other areas with complex terrains, Japan adopts the double-circuit line on the same tower of self-supporting with the three-phase conductors arranged vertically, and

the tower height is 88–148 m (high tower is disadvantageous to the protection against shielding failure and back flashover). The typical tower type is as shown in Fig. 8.2. To improve the lightning withstand performance of the UHV lines, Japan adopts the double overhead ground wire arrangement, in which the protection angle is about −12°. Although, in Japan, there are only 25 annual thunderstorm days in the areas where the UHV lines are located, the effect of protection against shielding failure by the adoption of a negative protection angle is still not very satisfactory, and the lightning trip-out rate during the running period at the voltage reduced to 500 kV is up to 0.9 times/(100 km·a).

According to the analysis on the recorded data of Japan's lightning location system, the main cause for lightning trip-out of its UHV lines is still the shielding failure. It is deemed through theoretical analysis that the relevant factors include the relatively high tower height, too many mountainous regions and other areas with

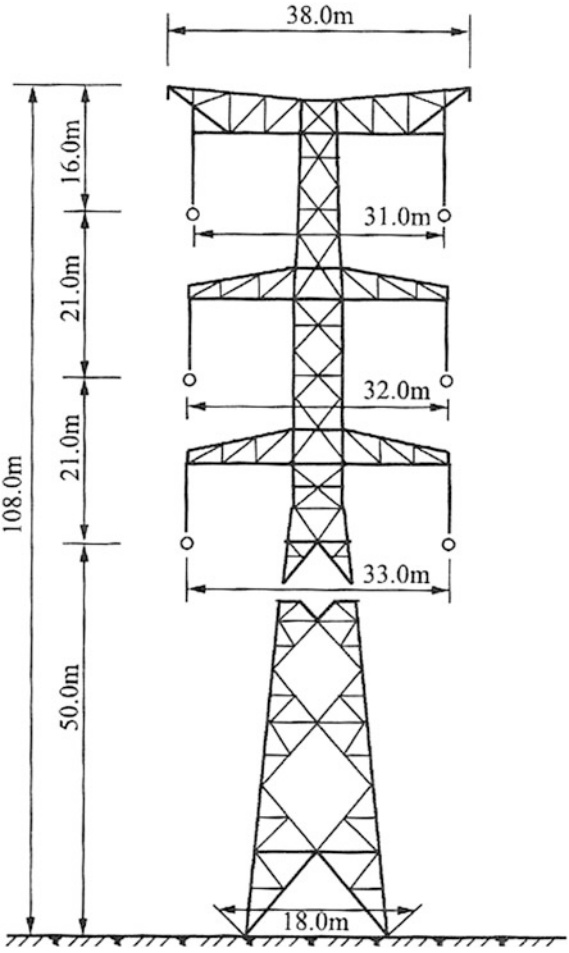

Fig. 8.2 Diagram of typical tower types of Japan's UHVAC line

complex terrains along the line, relatively low level of line insulation (due to the use of arcing horns), etc., causing conductors to be struck by lightning at sides and then lightning trips happen. The Japan's experience in operation shows that the lines in the mountainous regions shall preferably adopt a smaller negative protection angle.

It is shown by the operation experience of the UHV lines in the former Soviet Union and Japan that the main cause for the lightning trip-out is the lightning strike on conductors resulting from overhead ground wire's shielding failure. However, the main reasons for the high rates of lightning trip-out in these two countries are different—for the UHV lines in the former Soviet Union, it is because the structural design of the angle towers is not quite reasonable; while for the UHV lines in Japan, it is probably mainly related to the high tower height and the fact that many towers are located in the mountainous regions.

In addition, the operation experience of the UHV lines in the former Soviet Union and Japan also shows that, with the increase of the line voltage level, the lightning trip-out rate and the total trip rate both reduce to a certain extent, but the proportion of the lightning trips in the total trips increases. For example, during the decade from 1985 to 1994, the UHV lines in the former Soviet Union had a lightning trip-out which is up to 16 times (running for 12,124 km·a), accounting for 84.2% of its total number of trips; during the 15 years from 1993 to 2007, the Japan's UHV lines (at the voltage reduced to 500 kV) had a total of 68 line fault trips, including 67 lightning trips (and the rest one was caused by blizzard), accounting for 98.5% of the total number of trips.

It can be seen by integrating the operating experience of the former Soviet Union and Japan that the lightning is still the major hazard for the safe and reliable operation of the UHVAC lines, and the prevention shall mainly be made against the shielding failure in the actual projects. A good shielding design for the overhead ground wire is the fundamental measure to improve its lightning withstand performance. Particular attention shall be paid to the special shielding failure prevention design for the angle tower, providing it with a reasonable negative protection angle, and consideration may be given to the use of sideward lightning rods and the adoption of other shielding failure prevention measures. In addition, the lines in the mountainous regions shall also be equipped with a smaller negative protection angle.

8.1.1.2 Characteristics of Lightning Withstand Performance for UHVAC Lines

Compared with the HV and EHV lines, the UHVAC overhead transmission lines have the following characteristics of lightning withstand performance [2–5]:

(1) The UHV lines have high tower height, large overhead ground wire spacing, and increased line area subject to lightning strike, resulting in the increase of the probability of the line to be struck by lightning, which is disadvantageous to the prevention from the shielding failure and the back flashover;

(2) The UHV lines have a high insulation level, and their lightning withstand level of back flashover may be up to 200 kA and above, so the possibility of back flashover trip caused by the lightning strike on the overhead ground wire or the tower top is very low;
(3) With the increase of the height of the tower, the shielding effect of the overhead ground wire, and the ground weakens, so the lightning leader is more likely to strike the conductors. In addition, due to the high amplitude of the power frequency voltage on the conductors, the forward leader is more likely to be produced, which probably also leads to the increase of the lighting shielding rate. When the lightning strikes the conductors, a lightning current of more than 20 kA is capable of posing a threat of insulation flashover.
(4) In addition, it is shown by the operation of the HV and EHV transmission lines in China and abroad that, with the increase of the voltage level, the proportion of shielding failure in the lightning trips increases. For the HV lines of 110 and 220 kV, etc., both the shielding failure and the back flashover are the important causes for the lightning trip-out; for the EHV lines of 330 kV and above, the shielding failure presents a more serious hazard (the statistical data of the lightning location system also show that the shielding failure is the main cause for the lightning trip-out of China's 500 kV lines); for the UHV lines, the lightning trip-out is basically caused by the shielding failure and the probability of back flashover trip is very low.

In short, the lightning performance characteristics of the UHVAC lines are: high level of insulation, low possibility of the occurrence of the back flashover due to the lightning strike on the overhead ground wire or tower top, and high possibility of the lateral shielding failure due to the high height of tower.

8.1.1.3 Control Indexes for Lightning Withstand Performance

Currently, the major technical indexes for measuring the lightning withstand performance of the overhead transmission lines include the lightning withstand level and the lightning trip-out rate, which are respectively described as follows [6, 7].

1. Lightning withstand level

The lightning withstand level refers to the maximum lightning current amplitude that cannot cause insulation flashover or the minimum lightning current amplitude that can cause insulation flashover when the lightning strikes the line, in kA. For the 1000 kV UHVAC transmission lines, GB/Z 24842-2009 *Overvoltage and Insulation Coordination of 1000 kV UHV AC Transmission Project* stipulates that in the areas with normal soil resistivity (500 Ω·m and below), the line's lightning withstand level of back flashover shall not be lower than 200 kA.

2. Lightning trip-out rate

The lightning trip-out rate refers to the number of trips caused by lightning each year per 100 km-long transmission line based on the unified converted annual thunderstorm days T_d = 40, in time/(100 km·a). The reason for unified conversion is to facilitate the comparison of the advantages and disadvantages of the lightning withstand performances for transmission lines with different lengths and located in different regions.

The control indexes for the lightning trip-out rate are based primarily on the important degree of the line, the structure and safety margin of the grid, the criterion for the line circuit breaker operating resources, and other conditions, among which the criterion for the line circuit breaker operating resources refers to the allowable number of lightning trips for the overhead line circuit breaker during the maintenance period. For the UHVAC lines using SF_6 circuit breaker with high operating resources, the allowable number of lightning trips depends on the transformers, current transformers, and other equipment that are sensitive to the lightning overvoltage and short-circuit current. In consideration that the lightning trip-out rate is affected by the tower structure, overhead ground wire protection angle, insulation level and strength of lightning activity, soil resistivity, and landform along the line, as well as many other factors, the control indexes shall be determined properly based on the economic and technical comparison and according to the specific local conditions.

Another assessment index for evaluating the lightning withstand performance of the transmission lines is the "lightning strike accident rate", i.e., the unsuccessful reclosure after the lightning trip is regarded as a lightning strike accident, for which the core idea is to "allow the line to have a certain lightning trip-out rate." If the lightning strike accident rate is taken as the new lightning withstand index for the UHV lines, with high success rate of the single-phase reclosure of the transmission lines in China (>90%) in consideration, the calculated value of the actual allowable lightning trip-out rate will be relatively large. For the 110, 220, and 500 kV lines, the application of this index can be considered as relatively reasonable. However, there is still a large controversy on whether the lightning strike accident rate can be used as the lightning withstand index of the UHV lines. China's UHV power grid structure is weak, with small safety margin, and the UHV lines' transmission power capacity is large (may be up to 3000–5000 MW for single-circuit UHV lines); the lightning strike accident can, as a result, cause a great impact on the system, posing a serious threat to the safe and stable operation of the power grid. Therefore, the lightning strike accident rate shall not be used as a lightning withstand index for the UHVAC lines as the required control target value is too low.

In consideration that the statistical value of the actual lightning trip-out rate of China's 500 kV line is 0.14 times/(100 km·a), it is suggested that the expected design value of the lightning trip-out rate of the 1000 kV UHVAC line should not be higher than the value when in the plain areas, which can be taken as 0.1 times/(100 km·a), and the requirements may be easing for the lines in the mountainous areas, taken as 0.2 times/(100 km·a).

In addition, the control indexes for the lightning trip-out rate of the large span of the UHV lines are different from that for the conventional lines. It is described in Russia's 1999 *Manual* as below: ① the lightning-resistant indexes for the crossing span of the overhead line shall not be of much difference as compared to that for the ordinary line. For instance, the lightning trips of 1 km crossing span shall not exceed that of 10 km ordinary line; ② in consideration of the difficulty in the preventive test and the maintenance, the absolute times of the lightning flashover of the insulation of crossover towers shall guarantee that the interval of the maintenance for the insulator strings is not less than 25 years. It is specified in China's National Standard GB/Z 24842-2009 *Overvoltage and Insulation Coordination of 1000 kV UHV AC Transmission Project* that, for the 1000 kV UHVAC lines, the safe operation years of the large spans under the lightning overvoltage shall not be less than 50 years [8].

To sum up, the designed expected lightning trip-out rate of China's 1000 kV UHV lines shall be taken as 0.1 times/(100 km·a) in plains and 0.2 times/(100 km·a) in the mountainous regions. In addition, the anti-lightning safe operation of the large span of the UHV lines is taken as 50 years.

8.1.2 Calculation Methods for Assessment of Lightning Withstand Performance

8.1.2.1 Lightning Calculation Parameters

(1) Polarity and waveform of lightning current

It is shown by the actual measurement that 75–90% of the lightning current is negative pulse wave. Besides, in consideration of the lack of statistical data for the positive lightning strike parameters, therefore, only the negative lightning wave is generally taken for the lightning protection analysis.

In combination of the observations from different countries, the head length of lightning current wave T_1 is within the range of 1–5 μs in most cases, averaging at about 2.6 μs; and the lightning current wave length is within the range of 20–350 μs, averaging at about 50 μs. Therefore, the selection in engineering applications is made normally depending on the sensitivity; for example, the negative 2.6/50 μs is adopted for the lightning current waveform in the lightning protection design of the grids in China.

(2) Lightning channel wave impedance

In terms of the engineering applications, the channel of lightning leader can be approximated as a conductive channel with evenly distributed parameters such as inductance and capacitance, i.e., the main discharge can be considered to be transmitted along a infinitely long conductor with equivalent wave impedance Z_M, and its lightning channel wave impedance Z_M = 300–3000 Ω.

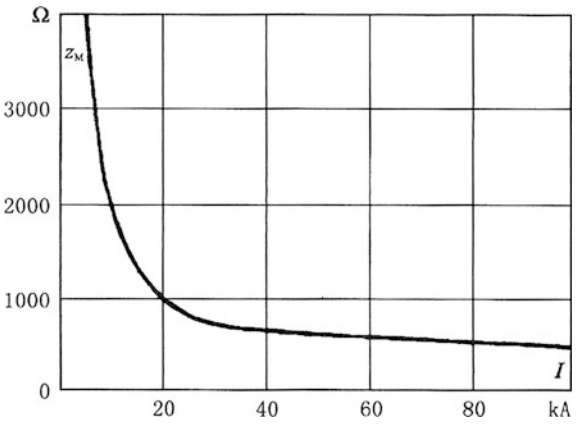

Fig. 8.3 Relationship between lightning channel wave impedance and lightning current amplitude

Research has shown that the lightning channel wave impedance is related to the lightning current of the main discharge channel and decreases as the lightning current amplitude increases, as shown in Fig. 8.3. In the figure, the UHVAC line's lightning withstand level of shielding failure is about 20–40 kA and its corresponding lightning channel wave impedance is about 1000–600 Ω, which, during the calculation of shielding failure, can be normally taken as 800 Ω or can also be estimated through Eq. (8.1). For the lightning withstand level of back flashover is above 200 kA, the corresponding Z_M is small, about 250–400 Ω, so the lightning channel wave impedance for the calculation of the lightning back striking can be approximately taken as 300 Ω.

$$Z_M = 1.6I^{1.345} + 21120/I - 148.4. \tag{8.1}$$

(3) Probability distribution of lightning current amplitude

As for the probability distribution of lightning current amplitude, the Code (DL/T 620-1997) uses the fitting equation for the actually measured data on lightning current of the Xin'anjiang Hydropower Station-Hangzhou Substation Line in Zhejiang Province with a total of 2824 km·a (during the period from 1962 to 1988, a total of 716 lightning strikes were measured by the magnetic steel rod in the 220 kV Xin'anjiang Hydropower Station-Hangzhou Substation Line Circuit *I*) [9]. It is specified in the Code that the probability of lightning current amplitude more than *I* can be calculated by the equation below in the common regions in China (where the average number of annual thunderstorm days is at least 20):

$$\log P(I) = -\frac{I}{88} \tag{8.2}$$

where

$P(I)$ is the probability for the lightning current amplitude greater than I;
I is the lightning current amplitude, in kA.

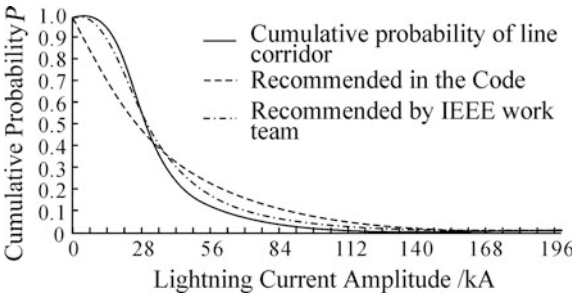

Fig. 8.4 Cumulative probability distribution of lightning current amplitude of the corridor of the UHV demonstration line

In addition, the State Grid Electric Power Research Institute has, using the lightning location system and its historical monitoring data, conducted the statistics on the probability distribution of lightning current amplitude of the line corridors of the Southeast Shanxi-Nanyang-Jingmen UHV Demonstration Project, as shown in Fig. 8.4. The fitting equation for the cumulative probability distribution curve of the corresponding lightning current amplitude is as shown in Eq. (8.3), and its rule of distribution is basically the same as Eq. (8.4) as recommended by CIGER and IEEE, but is to some extent different from the equation as recommended in the Code. As the operating life of the lightning monitoring system is still relatively short, the statistical results can be taken as reference temporarily:

$$P(I) = \frac{1}{1 + \left(\frac{I}{29.8}\right)^{3.1}} \tag{8.3}$$

$$P(I) = \frac{1}{1 + \left(\frac{I}{31}\right)^{2.6}}. \tag{8.4}$$

(4) Ground flash density

The ground flash density [N_g, times/(km^2·a)] refers to the number of ground lightning strikes per square kilometer and per year. The ground flash density has a linear proportional relationship with the lightning trip-out rate of the line, and its precision directly affects the calculation results of the lightning trip-out rate of the line.

There are two main methods to determine the values of ground flash density: ① calculated by the thunderstorm days T_d or thunderstorm hours T_h; ② directly obtained from the lightning location system.

The ground flash density used in China's engineering lightning protection calculation needs to be calculated by the thunderstorm days T_d, and it is recommended in the Code that, in the areas with 40 thunderstorm days, the ground lightning density γ (the number of ground lightning strikes per square kilometer and per thunderstorm day) should be taken as 0.07 times/(km^2·d), then $N_g = T_d \times \gamma$. Alternatively, the equation recommended by CIGRE can also be referred to:

$$N_g = 0.023 T_d^{1.3}. \tag{8.5}$$

However, it is shown by the actual measurement in East China that the thunderstorm days have a weak relation with the ground flash density, and that the ground flash density calculated by the thunderstorm days is lower than the measured value, indicating a large deviation. In addition, the IEEE also recommends that the ground lightning density which can be obtained directly shall be used priorly. Therefore, to guide the line lightning protection better, it is recommended to use the lightning location system to conduct statistics on the characteristics of lightning activities in the corridors along the line and plot the distribution diagram of the actually measured ground flash densities to replace the method of estimation based on the thunderstorm days.

8.1.2.2 Calculation Method for Shielding Failure

For the calculation of shielding failure of the UHV overhead transmission lines, it is recommended to use the electro-geometrical model (EGM) method recommended by IEC, IEEE, and other international organizations; while for the calculation of back flashover, the electro-magnetic transient program (EMTP) calculation program is recommended, which is mostly adopted around the world.

1. Overview of the calculation method for shielding failure

The methods used to calculate the shielding failure trip-out rate of the overhead transmission lines mainly include the regulation method, electro-geometrical model (EGM), and leader progression model (LPM), etc., among which, the regulation method is a statistical empirical method not considering the impact of the specific lightning strike process; the EGM only considers the final step of the lightning strike process, i.e., the breakdown process of the clearance between the lightning downward leader head and the struck object (or its upward leader head); and the LPM considers the impact of the whole lightning strike process.

To evaluate the lightning withstand performance of China's conventional HV and EHV overhead transmission lines, the calculation method recommended in *Overvoltage Protection and Insulation Coordination for AC Electrical Installations* DL/T 620-1997 is used (referred to as the "regulation method") [10]. This method deems that the probability of the lightning strike bypassing the overhead ground wire on the conductors is related to the protection angle of the overhead ground wire to the side-phase conductor, tower height and the topography, terrain, and geological conditions of the areas that the lines passing through. It puts forward the equations for the calculation of the shielding failure rate in the plains and mountainous regions, respectively. However, it is noteworthy that the regulation method is obtained by fitting the operating experience of the lines with voltage level of 220 kV and below, and it is only applicable to the cases in which the overhead ground wire protection angle is between 15° and 40° and the tower height is not

more than 50 m. Obviously, the corresponding parameters of the UHV lines are beyond the applicable scope of the regulation method. Therefore, the regulation method is not suitable to be used for the calculation of the lightning protection for the UHV lines.

The LPM is built on the basis of the study on the long-gap discharge and the physical process of the lightning strike, considering the progression of lightning downward leader, the generation of line upward leader, and the impacts of other factors, so it has a certain rationality and progressiveness. However, due to the limitation in the recognition of the physical process of lightning, there is a considerable dispute in some important criteria and calculation parameter values (For example, the upward leader inception criteria), resulting in a large difference in the LPM calculation results of various research institutions. Therefore, the LPM still needs further theoretical and experimental studies, and is generally not suitable to be directly used for the calculation of lightning protection of the UHV lines if not verified by the line operating experience.

The EGM, linking up the discharge characteristics of the lightning with the structure sizes of lines, is a geometric analysis and calculation model based on the field observed data. In addition, its accuracy has been verified by the operation data of the HV and EHV lines in the Western Europe, the United States, and other regions. The EGM, based on the striking distance theory, considers the impacts of the lightning current amplitude and the line structure on the shielding failure rate, and the calculation results obtained are basically consistent with the actual operating experience. The United States, Europe, and Japan as well as many other countries all use the EGM method to analyze the line shielding failure; IEC, IEEE, and other international organizations also recommend this method, so do China's latest national standards for UHV. Therefore, the EGM is recommended for calculating the shielding failure lightning-resistant performance of the UHV lines.

2. Brief introduction of EGM method

Currently, the EGM method used for the line shielding failure calculation mainly refers to the W'S EGM (i.e., the classical electro-geometrical model proposed by Whitehead et al.) and the IEEE EGM (recommended in the IEEE Std 1243-1997), among which, the W'S EGM considers the impacts of ground inclination angle and lightning leader incidence randomicity, and uses the equivalent lightning strike width (the exposed arc projection on the horizontal plane) to calculate the shielding failure flashover rate [11, 12]; while the IEEE EGM assumes that the lightning leader vertically strikes the ground and considers the impact of the subsequent lightning pulse during the calculation [13].

However, it is shown by the experience of Japan in the operation of EHV and UHV lines that the shielding failure trip-out rate of the lines using negative protection angle is still relatively high. Therefore, for the UHV lines with small or even negative protection angles, it is inadvisable to assume that the lightning leader always progresses vertically downward just to simplify the calculation. In addition, in consideration that the probability of shielding failure trip-out of the UHV lines caused by the

subsequent pulse is very small, it can be negligible. Therefore, it is recommended to use the W'S EGM for analysis on the shielding failure of the UHV lines.

The basic calculation principle of W'S EGM is based on the following concepts and assumptions:

(1) Before the leader channel head, which is progressing from the thundercloud to the ground, reaches the critical breakdown distance (striking distance) of the struck object, the striking point is uncertain. The object whose striking distance is first reached into by the leader channel head is to be discharged.
(2) The striking distance r_s is the function of the lightning current amplitude I.
(3) The impacts of the struck object's shape, proximity effect, and other factors on the striking distance are ignored, and the striking distances of the lightning leader to the tower, overhead ground wire, and conductor are made equal. In consideration of the difference in the breakdown field intensity of the conductor and the ground by the lightning leader, the ground striking distance r_{sg} shall be taken as: $r_{sg} = kr_s$ (k refers to the striking distance factor).
(4) The concept of leader incidence angle is introduced. The lightning leader does not always vertically strike the ground, and the side striking of lightning on the line also happens, namely, the case with a certain incidence angle ψ exists.

Figure 8.5a is the sketch of EGM corresponding to lightning current I (with corresponding striking distance r_s), where S is the overhead ground wire, W is the conductor, k is the striking distance factor, α is the overhead ground wire protection angle, and ψ is the leader incidence angle. When the lightning downward leader enters the shielded arc AB, the lightning will strike the overhead ground wire; when the leader enters the exposed arc BC, the lightning will strike the conductor; while the leader a little away from the line will strike the ground directly as it is closest to the ground.

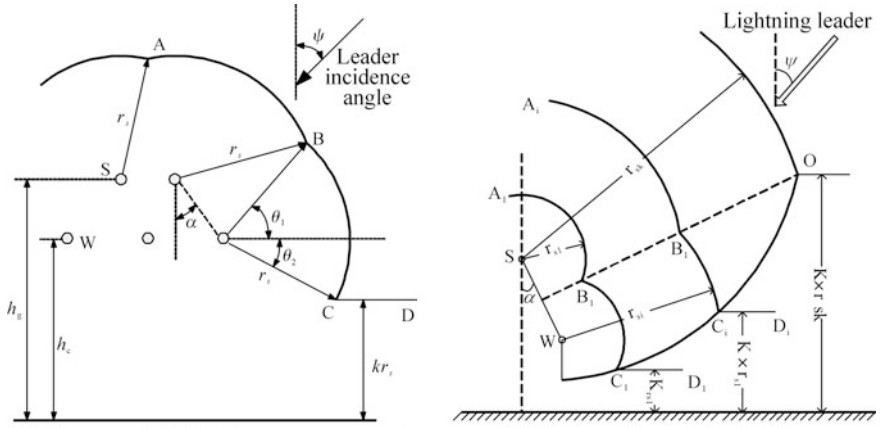

Fig. 8.5 Schematic diagram of W'S EGM

The W'S EGM calculates the corresponding equivalent lightning strike width of the conductor based on the projection of the exposed arc on the horizontal plane to obtain the shielding failure flashover rate of the line. It can be obtained from Fig. 8.5 that, with a given striking distance r_s, the corresponding lightning strike width X of the conductor on one side is as follows:

$$X = \int_{\theta_2}^{\theta_1} \int_{\psi_2(\theta)}^{\psi_1(\theta)} \frac{r_s \cdot \sin(\theta - \psi)}{\cos\psi} g(\psi) \mathrm{d}\psi \mathrm{d}\theta \tag{8.6}$$

where

$g(\psi)$ is the probability distribution function of the leader incidence angle.

The transmission lines have certain lightning withstand level, and the minimum shielding failure lightning current that can cause insulation flashover is called as the shielding failure lightning withstand level I_c (also known as "shielding failure flashover critical current"), and the corresponding striking distance is the critical minimum striking distance r_c. With the increase of lightning current amplitude, the striking distance increases, resulting in the reduction of the exposed arc of conductor. When the striking distance reaches a maximum value r_{max}, the exposed arc is reduced to zero (as shown in Fig. 8.5b). At this time, the corresponding lightning current is the maximum shielding failure lightning current I_{max} (the impact of ground inclination angle on the shielding failure rate is reflected as the impact on I_{max} in the W'S EGM). Therefore, the dangerous shielding failure lightning current range (I_c, I_{max}) of the lines can be obtained.

After the dangerous shielding failure lightning current range ($I_c < I < I_{max}$) is obtained, through the relational expression of the striking distance and the lightning current amplitude, the shielding failure flashover rate n_r of the conductor on one side [times/(100 km·a)] can be obtained as follows:

$$n_r = \frac{1}{10} N_g \int_{r_c}^{r_{max}} X f(r) \mathrm{d}r = \frac{1}{10} N_g \int_{I_c}^{I_{max}} \int_{\theta_2(I)}^{\theta_1(I)} \int_{\psi_2(\theta)}^{\psi_1(\theta)} \frac{r_s \cdot \sin(\theta - \psi)}{\cos\psi} g(\psi) f(I) \mathrm{d}\psi \mathrm{d}\theta \mathrm{d}I \tag{8.7}$$

where

N_g is the ground flash density, in time/(km^2 ·a);
I_c is the shielding failure lightning withstand level, in kA;
I_{max} is the maximum shielding failure lightning current, in kA;
$f(I)$ is the probability distribution function of the amplitude of lightning current.

It is noteworthy that the main purpose of EGM is being used to characterize that the protection angle of overhead ground wire shall change with the changes of tower height, i.e., the higher the tower is, the smaller the corresponding protection

angle shall be. Equation (8.7) shows that, when $I_c \geq I_{max}$, $n_r = 0$, no shielding failure trip-out accident will happen to the line, and such case is referred to as the "complete shielding". Therefore, for the design in the shielding failure prevention of the UHV lines, this principle can be used to properly determine the protection angle of overhead ground wire to achieve the complete shielding as far as possible.

3. Selection of EGM parameters

The EGM is based on experience and field data, as the specific conditions of the transmission lines studied by different scholars are different (such as the different line voltage levels, towers, and terrains); the W'S EGM and its various improved models may have certain differences in the parameter selection. The controversial parameters that affect the calculation results of the line's shielding failure trip-out rate mainly include the striking distance, the lightning withstand level of shielding failure, and the lightning leader incidence angle, etc., which are respectively described hereinafter.

(1) Striking distance and striking distance factor

The striking distance is the core of EGM theory. The general expression for the striking distance is $r_s = A \times I^B$, and the representative equations are as shown in Table 8.2 and Fig. 8.6.

It can be known from Fig. 8.6 that, under the lightning current with the same magnitude, what the equation recommended by the IEEE WG represents is the "minimum" striking distance, of which the calculated value is the minimum; what the Brown equation and Love equation represent is the "average" striking distance, of which the calculated value is relatively close, being at the middle; while the calculated value of the Armstrong equation is the maximum. Therefore, in case of

Table 8.2 Main EGM calculation equations of striking distance

Source	Parameters	
	A	B
Armstrong	6.7	0.80
Brown	7.1	0.75
IEEE WG	8	0.65
Love (IEEE Std)	10	0.65

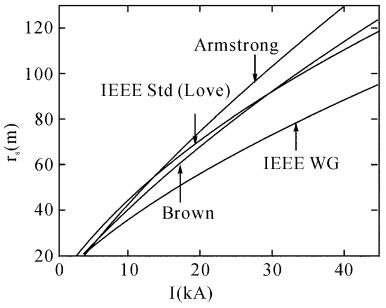

Fig. 8.6 Diagram for relationship between striking distance and lightning current

calculation of the line shielding failure trip-out rate, the Love equation representing the "average" striking distance is recommended, which is also recommended by the IEEE and IEC, etc.:

$$r_s = 10I^{0.65}. \tag{8.8}$$

In addition, it is easy to know from the EGM principle that the smaller the calculated value of the striking distance equation is, the greater the exposed arc curved surface of the conductor corresponding to the same shielding failure lightning current will be, then the smaller the overhead ground wire protection angle calculated for realization of complete shielding (i.e., make $I_{max} = I_c$) will be. Therefore, during the design of the protection angle of overhead ground wire for the lines, for the safety purpose, the IEEE WG recommended equation representing the "minimum" striking distance is recommended to be chosen, and the calculated protection angle at this time is more secure and more stringent.

For the striking distance factor k, the studies have shown that the striking distances of the lightning leader to the ground and to the conductor are not equal, which can be explained approximately by the different breakdown field intensities between the rod–rod gap and the rod–plane gap under the negative impulse switching voltage. The striking distance factor k is mainly affected by the line height and the nominal voltage level as well as other factors—for the LV lines (<110 kV) with low towers, k is normally taken as 1; for the HV lines below 330 kV, k is normally taken as 0.8 or 0.9; for the UHV lines with relatively high towers, k is in the range of 0.6–0.9.

Rizk proposed a linear Eq. (8.9), which can well characterize the variation trend of k with the line height. The equation is also recommended by the IEEE. In the shielding failure calculation of the UHV lines, the value of the striking distance factor k is recommended to be taken by referring to the equation:

$$k = \begin{cases} 0.36 + 0.17\ln(43 - h_c) & (h_c < 40\,\text{m}) \\ 0.55 & (h_c > 40\,\text{m}) \end{cases} \tag{8.9}$$

where

h_c is the conductor's average height to ground, in m

(2) Lightning withstand level of shielding failure

When the lightning strikes the conductor, the calculation principle of the overvoltage on the conductor is as shown in Fig. 8.7. It can be known from Fig. 8.7 that the calculation equation for the lightning withstand level of shielding failure is as follows:

$$I_c = 2\frac{U_{50\%}(Z_M + Z_{surge}/2)}{Z_M Z_{surge}} \tag{8.10}$$

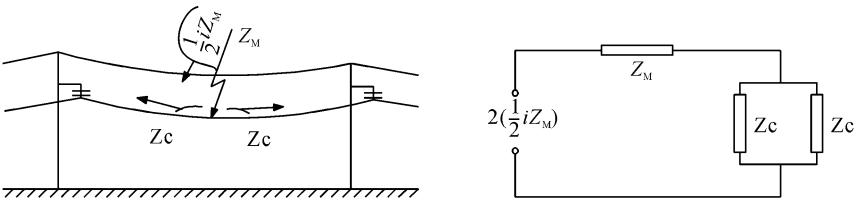

(a) Direct striking of lightning on conductor (b) Equivalent circuit for calculation of shielding failure

Fig. 8.7 Calculation diagram for shielding failure lightning withstand level

where

$U_{50\%}$ is the negative 50% flashover voltage of the insulator string under standard lightning wave, and can be approximated as 1.13 times the positive discharge voltage, in kV;

Z_M is the wave impedance of lightning channel, in Ω;

Z_{surge} is the conductor wave impedance with the corona effect considered, in Ω.

It is deemed in the Regulation (DL/T 620-1997) that $Z_M = Z_{surge}/2 = 400/2 = 200$ Ω, so the lightning withstand level of shielding failure is calculated as $I_c = U_{50\%}/100$. However, the lightning withstand level of shielding failure calculated by this equation is significantly larger, which is because the wave impedance value of lightning channel is too small in the case of shielding failure

For the AC overhead transmission lines at rated voltage of 500 kV and below, the wave impedance of lightning channel corresponding to the actual dangerous shielding failure lightning current (typically <15 kA) is usually much larger than the conductor wave impedance (i.e., considered as $Z_M \gg Z_{surge}/2$). Therefore, the IEEE recommended equation can be obtained approximately as shown in Eq. (8.11), and this simplified equation is usually recommended for calculation:

$$I_c = 2U_{50\%}/Z_{surge}. \tag{8.11}$$

For the 1000 kV UHVAC lines, the wave impedance of lightning channel corresponding to the dangerous shielding failure lightning current is normally 600–1000 Ω, and it is deemed to probably cause large error if $Z_M \gg Z_{surge}/2$. At this point, the lightning withstand level of shielding failure I_c for the UHV lines can be calculated in two steps: ① calculate the initial value of lightning withstand level I_c according to Eq. (8.11); ② refer to Fig. 8.5 to determine the wave impedance of lightning channel Z_M corresponding to I_c, and then use the following equation to calculate the exact value of lightning withstand level I'_c:

$$I'_c = I_c \frac{Z_M + Z_{surge}/2}{Z_M}. \tag{8.12}$$

(3) Incidence angle of lightning leader

Although the design of effective shielding of the line is independent of the distribution of incidence angles of lightning leader, to assess the lightning withstand performance of shielding failure on the line accurately, the probability distribution of leader angles is needed. Whitehead, Armstrong, and others believe that the leader incidence angle ψ follows a given probability distribution, and the universal calculation equation can be expressed as follows:

$$g(\psi) = k_{\mathrm{m}} \cos^{\mathrm{m}} \psi, \left(\int_{-\pi/2}^{\pi/2} k_{\mathrm{m}} \cos^{\mathrm{m}} \psi \mathrm{d}\psi = 1; -\frac{\pi}{2} < \psi < \frac{\pi}{2} \right). \tag{8.13}$$

Whitehead et al. have also found that, when the parameter $m = 2$, the number of shielding failures observed on the lines, which are partially shielded, well tallies with the estimated value (the value of m is taken as 3 in *Guidebook for Lightning Protection Design of Power Transmission Lines,* 1976, Japan). Therefore, in case of lack of other statistical data, the probability distribution equation of the leader incidence angle is recommended:

$$g(\psi) = \frac{2}{\pi} \cos^2 \psi \left(-\frac{\pi}{2} < \psi < \frac{\pi}{2}\right). \tag{8.14}$$

(4) Influence of power frequency voltage

In the procedures, the influence of power frequency voltage U_{n} on the transmission line is not taken into account in the lightning protection calculation. However, for the UHV system, the power frequency voltage can cover 15–20% or so of the discharge voltage of insulator string, so it is not appropriate if such voltage is not taken into account. The influence of amplitude of the power frequency voltage and the AC cycle on the shielding failure calculation is analyzed respectively below.

The relation between the negative discharge voltage and the striking distance under the long air clearance given by reference [2] is as follows:

$$r_{\mathrm{c0}} = 1.63 U_0^{1.125} \tag{8.15}$$

where

r_{c0} is the striking distance of conductor regardless of the influence of power frequency voltage (namely no voltage on the line), m;
U_0 is the head voltage of lightning leader, MV.

Considering the striking distance equation $r_{\mathrm{s}} = 10I^{0.65}$ in the IEEE Standard together with Eq. (8.15), the relation between the negative discharge voltage and the lightning current under the long air clearance can obtain:

$$U_0 = 5.015I^{0.578}. \tag{8.16}$$

After considering the power frequency voltage, the striking distance equation is as follows:

$$r_{c0} = 1.63(U_0 - U_{ph})^{1.125} = 1.63(5.015I^{0.578} - U_{ph})^{1.125} \tag{8.17}$$

where

r_c is the striking distance of conductor after the influence of power frequency voltage is imposed, m;
U_{ph} is the instantaneous value of power frequency voltage on the conductor, MV.

Considering the influence of amplitude of the power frequency voltage on the shielding failure lightning withstand level I_c, the following correction shall be made accordingly:

$$I_c = 2(U_{50\%} - U_{ph})/Z_{surge}. \tag{8.18}$$

Considering the influence of the power frequency voltage cycle, currently, there are two analytical methods mainly: First, only a certain fixed value or a typical value is considered, e.g., the peak value of phase voltage $\sqrt{2}U_n/\sqrt{3}$, or the average 0.52 U_n of phase voltage during half cycle, etc.; Second, use the statistical method to calculate the influence of power frequency voltage. When the lightning shielding failure occurs on the conductor, considering the randomness of occurrence of the AC voltage phase angle, the voltage phase angle can be considered as the discrete random variables of equal probability $Q = (Q_1, Q_2 \cdots Q_i \cdots Q_n)$. Therefore, the probability of line shielding failure trip is determined as:

$$P = \sum_{i=1}^{n} P_i/n \tag{8.19}$$

where

P is the statistical shielding failure trip rate of the line;
P_i is the shielding failure trip rate under the voltage phase angle Q_i;
n is the number of phase angles divided from one cycle of the alternating current.

8.1.2.3 Calculation Method for Back Flashover

1. Overview of calculation method for back flashover

Currently, the methods for the analysis on the back flashover lightning withstand performance of the overhead transmission lines mainly include: the regulation method, traveling wave method, and EMTP simulation method, etc.

The regulation method is a lumped parameter method (i.e., the towers and overhead ground wires, etc., are replaced by lumped inductance or resistance). In case of low tower height, it has been proven that the results obtained therefrom are close to those obtained by multiple reflection method. However, in case of high tower height, the calculated value of back flashover lightning withstand level obtained by the regulation method is significantly lower; besides, the method is difficult to calculate the problem of the simultaneous trip of both circuits. Therefore, the regulation method is not suitable to be applied to the back flashover calculation for the UHV lines.

The traveling wave method is a distributed parameter method, which equals the tower (or tower sections) to single-phase lossless transmission line and deems that different types of towers have specific wave impedances. The traveling wave method can reflect the transient propagation process of lightning on the tower and the impact of reflected wave on the node potentials of tower, and is much closer to the actual physical process of lightning strike. However, the programming calculation by the traveling wave method is quite complicated and cumbersome, not suitable in engineering.

The EMTP is the most widely used simulation software in the research field of transient process of power system. In the calculation of lightning overvoltage, the traveling wave method is taken as the calculating principle for EMTP, by which not only the impacts of such factors as power frequency voltage, induced voltage, and the variation process of potential difference at both ends of insulator string with the time can be considered, but also the complex and cumbersome programming process of the traveling wave method can be avoided. Because of this, the EMTP is widely applied in the lightning protection design [14].

In summary, the EMTP is recommended for the calculation of the lightning withstand level of back flashover for the UHV lines, and then supplemented by the regulation method for the calculation of back flashover trip-out rate.

2. Selection of EMTP model and calculation parameters

During the back flashover calculation by EMTP, to determine the simulation model, it is necessary to consider the reasonable selection of the equivalent models for lightning current, towers, lines, and tower impulse grounding resistance, etc., and the criteria for lightning flashover, as well as the treatment of calculation components such as induced voltage and power frequency voltage.

(1) Lightning current model

The lightning current is equivalent as a current source in parallel with lightning channel wave impedance. The current source adopts a 2.6/50 μs negative oblique wave, and the lightning channel wave impedance is taken as 300 Ω.

(2) Tower model

Currently, the simulation of tower is usually carried out by the three models for lumped inductance, single-wave impedance and multi-wave impedance (the

equivalent inductance and the wave impedance for tower given in China's regulations are, respectively, 0.50 μH/m and 150 Ω). Among these three models, the inductance model is normally applicable to the single-circuit lines with relatively low towers ($h_t \leq 40$ m); the single-wave impedance model is often applicable to the single-circuit lines with relatively high towers (40 m < $h_t \leq 100$ m); and the multi-wave impedance model is mainly used for multi-circuit lines on the same tower and the large-span lines with ultra-high towers [15].

With the wave impedance model, the delayed effect of electro-magnetic wave propagation can be considered, so that the lightning transient characteristics of a high tower can be reflected correctly. In this case, using wave impedance model to calculate the lightning withstand level of back flashover for the UHV line is generally recognized as reasonable. It is noteworthy that, as there are many factors affecting the equivalent treatment of wave impedance model of tower, its value is still difficult to accurately evaluate, resulting in a large dispute on the calculating value of wave impedance.

At present, the tower wave impedance models that are more widely used in China are the Sargent single-wave impedance model and the Hara segmented lossless transmission line model, among which, the Sargent model is a single-wave impedance model from theoretical derivation, and the calculated value thereof is slightly larger than the measured value of the small tower model test and the result of the back flashover calculation obtained therefrom is a little strict, while the Hara model is a multi-wave impedance model established on the basis of the actual measurement and is basically consistent with the measured results of other scholars. However, because the calculation of some parameters of the model is rather complicated and has not been verified by the line operating experience, thus this method has not yet been widely adopted. The following gives a brief introduction to these two wave impedance models [16, 17].

Sargent, et al. took a conventional double-circuit tower (as shown in Fig. 8.8a) as the conical model and obtained the following equation for wave impedance of the tower through the analysis on electro-magnetic field theory:

$$Z = 60 \ln(\sqrt{2}/\sin\theta) = 60 \ln(\sqrt{2}\sqrt{r^2 + h^2}/r) \tag{8.20}$$

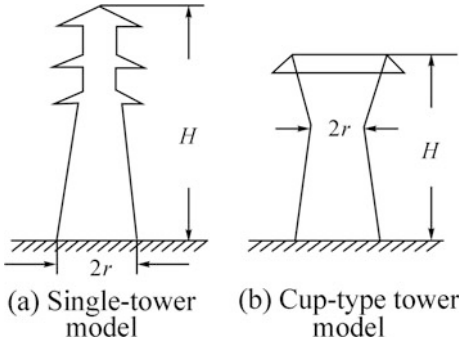

Fig. 8.8 Diagram for the towers of different structures

where

θ is the cone half angle, in °;
h is the height of conical tower model, in m;
r is the equivalent radius of the conical tower model, in m.

The IEEE recommends using the Sargent calculation equation, which is also used to design the double-circuit line on the same tower in the United States. Sargent et al. also pointed out that, if the cylinder is used for equivalence (as shown in Fig. 8.8b), the expression of tower wave impedance under the oblique waveform and double exponential waveform shall be converted as follows:

$$Z = 60 \ln \sqrt{2}(2h/r) - 60. \tag{8.21}$$

As described above, the Sargent wave impedance model simplifies the tower with complex shapes and rods to an equivalent cone or cylinder, without considering the impacts of cross arms and supports, etc., on the tower wave impedance. In contrast, the segmented wave impedance model for tower proposed by Hara deems that the tower consists of three parts which are the tower body (main pillar), the support (sway rod), and the cross arm, and the wave impedance of each part is represented by the equation expressing its size and geometry, and thus, this model is more broadly representative.

The wave response characteristics calculated based on the Hara model approximate to the actual measurements of tower, and, in addition, the wave response characteristics obtained from the tower model considering the cross arm are much closer to the real tower than those obtained from the model not considering the cross arm, thus indicating that the lossless line model has a certain rationality. The Hara model is specifically shown in Fig. 8.9, in which Z_h, Z_z, and Z_x represent the wave impedance of the cross arm, the main pillar, and the diagonal member, respectively. Among them, the cross arm is considered as the transmission line wave impedance parallel to the ground, and the calculation equation for the wave impedance of main pillar is as follows:

$$Z = 60\left(\ln \frac{2\sqrt{2}h}{r} - 2\right) \tag{8.22}$$

where

h is the height of the corresponding tower section, in m;
r is the equivalent radius of the corresponding tower section, in m.

For the wave propagation velocity in the tower body and the cross arm, it can be taken as around 0.8 times the speed of light in the Sargent model, i.e., 2.5×10^8 m/s. While in the Hara model, the impacts of the diagonal member and the cross arm have been considered, so the wave velocity may be taken as the speed of light.

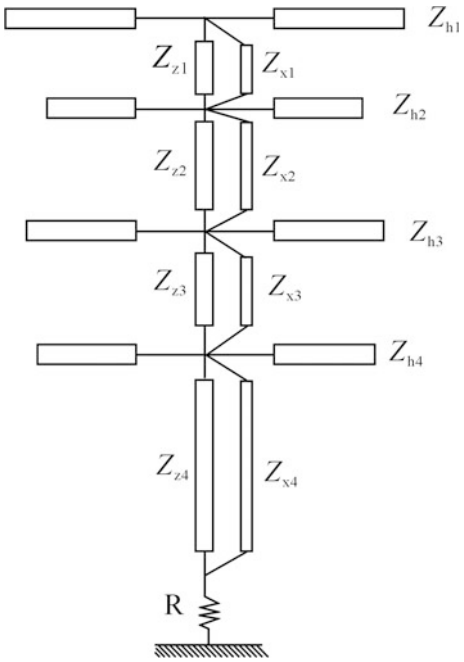

Fig. 8.9 Hara segmented wave impedance model for tower

(3) Line model

The common overhead transmission line models provided by EMTP include the π model, the Bergeron model, and the J-Marti model, among which the π model is a lumped parameter model and cannot reflect the characteristics of the actual line impedance parameters associated with the frequency (such as the skin effect), only applicable to the cases in which the line is short and the wave process is not considered; the Bergeron model is a distributed parameter model primarily characterizing a certain reference frequency and applies to the cases in which the power flow dominates under such reference frequency, such as the steady-state power flow calculation; the J-Marti model is a distributed parameter model associated with the frequency and can simulate the cases with great changes in frequency (such as the line overvoltage calculation), being relatively the most comprehensive line model with the most powerful function.

In the calculation of lightning overvoltage, the J-Marti model associated with the frequency is used for the equivalent calculation of the transmission lines.

(4) Tower impulse grounding resistance model

In general, the measured value of the tower grounding resistance shall be adopted for the purpose of strictness.

Alternatively, the method recommended by IEC may also be used [18, 19]. Due to the high amplitude of the current into the ground when the lightning strikes the tower, the ionization effect shall be taken into consideration, and the grounding connection of tower can be expressed as a nonlinear resistance $R(I)$, which is specifically calculated as follows:

$$R(I) = \begin{cases} R_0 & (I < I_g) \\ \frac{R_0}{\sqrt{1 + I/I_g}} & (I > I_g) \end{cases} \tag{8.23}$$

$$I_g = \frac{E_0 \rho}{2\pi R_0^2} \tag{8.24}$$

where

R_0 is the resistance under small current and low frequency, in Ω;
I is the lightning current flowing through the impedance at the root of tower, in A;
I_g is the current limiting threshold, in A;
ρ is the soil resistivity, in Ω·m;
E_0 is the soil ionization gradient, the recommended value is 400 kV· m^{-1}.

It should be noteworthy that, according to IEC 60071-2, this model is valid only when the extension radius of the tower foundation and its grounding body is less than 30 m.

(5) Lightning flashover criteria

The common lightning flashover criteria are the voltage threshold method and the intersection method.

The method used in the Regulation is the voltage threshold method, i.e., in case the lightning overvoltage peak on both ends of the insulator string is greater than the critical discharge voltage, and the flashover and breakdown will occur to the insulation. It is noteworthy that the critical discharge voltage taken in the Regulation refers to the standard lightning impulse wave $U_{50\%}$. However, in fact, due to the impact of the reflected wave from the tower grounding resistance, the voltage on both ends of the insulator string when the lightning strikes the tower is not a standard lightning impulse full wave, but a short-tail wave with the wavelength is less than 10 μs. In addition, 50% of the disruptive discharge voltage of the short-tail wave is about 1.2–1.3 times the standard wave. Therefore, the lightning withstand level of back flashover calculated by this method is a little small, not recommended for use.

In the back flashover calculation of the UHV lines, it is recommended to take the intersection method recommended in IEC 60071-4 as the criteria for the insulator string flashover. That is to say, if the wave of overvoltage $U_{in}(t)$ stressed on the insulator string intersects with the curve of voltage–time characteristics $V(t)$ of insulation impulse discharge, it will be judged as flashover [18], as shown in Fig. 8.10.

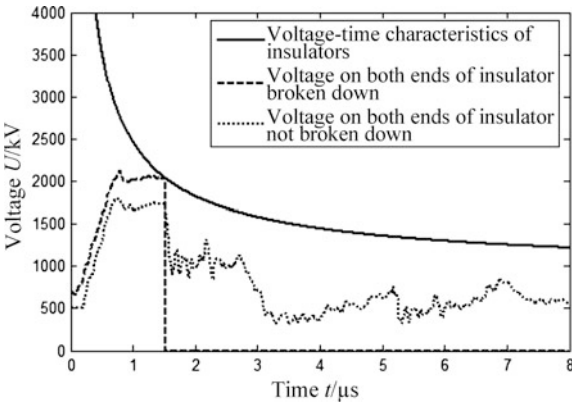

Fig. 8.10 Voltage–time characteristic curve and overvoltage waveforms on both ends of insulator string, reprinted from Ref. [18], copyright 2014, with permission from the International Electrotechnical Commission

The use of intersection method requires the voltage–time characteristic curve for the short-tail wave of insulator strings, but so far, no voltage–time characteristic curve for the short-tail wave above 3 m is available in the world yet. Therefore, the voltage–time characteristic curve for the standard lightning wave is normally used for substitution (which may cause the calculating result of back flashover lightning withstand level to be a little small). In addition, according to the principle of the voltage–time characteristic curve, at the time of wavefront discharge, $U_{\text{in}}(t)$ and $V(t)$ are intersect; while at the time of wavetail discharge, they do not intersect. Hence, the case of wavetail discharge may be missed using the intersection method (leading to a little larger calculating result).

Nevertheless, it is shown by the high tower operating experience of the former Soviet Union that the discharge flashover of insulator string mostly occurs at the wave head, which shows that using the voltage-time characteristics of the standard wave instead of the short-tail wave is reasonable; the gap discharge voltage of the short-tail wave is higher than that of the standard lightning wave, and the use of the voltage-time characteristic curve of the standard wave is a little lower and strict in the calculating result, which offsets the impact caused by the loss of the wavetail discharge to some extent; in addition, the results obtained from the adoption of intersection method in many countries are basically in line with the operational experience. Therefore, it is relatively appropriate to take the intersection method as the criterion for the insulator flashover.

For the voltage–time characteristic curve of the insulator string, in case of absence of measured data, the equation proposed by IEEE may be referred to [20]:

$$V_{\text{if}}(t) = \left(400 + \frac{710}{t^{0.75}}\right) L_{\text{in}} \tag{8.25}$$

where

t is the flashover time (the applicable scope thereof is 0.5–16 μs, and the corresponding value of 16 μs is the positive $U_{50\%}$), in μs;
L_{in} is the effective length of the insulator string, in m.

(6) Impact of induced voltage

When the lightning strikes the tower, the induced overvoltage on the conductor consists of two components which are electrostatic and electro-magnetic components. The electrostatic field, which is generated by the charges in the lightning leader channel, induces large number of heterocharges on the conductor close to the leader channel. The electrostatic component is generated by the sudden disappearance of the electrostatic field after the start of the main discharge. The electro-magnetic component is caused by the magnetic field change resulting from the strong lightning current in the lightning channel. Since the leader channel is approximately perpendicular to the line direction, it is normally deemed that the electrostatic component of the induced overvoltage on the conductor is much greater than the electro-magnetic component thereof, and hence the former can be the only to be considered.

At present, there is still a certain dispute on whether the induced voltage should be considered in the lightning protection calculation, and, in addition, in consideration of the induced voltage, there is also a big difference in the calculation equations for the lightning induced voltage as proposed by different scholars or institutions. It is specified in the Regulation that, for the lines with a normal height and having overhead ground wires, the maximum value of induced overvoltage can be calculated according to Eq. (8.23). However, this equation is the research result of the former Soviet Union half a century ago, so the calculation result is significantly higher for the high and ultra-high towers:

$$U_i = \alpha h_c \left(1 - k_0 \frac{h_g}{h_c}\right) \tag{8.26}$$

where

α is the lightning current steepness, in kA/μs;
h_g is the overhead ground wire's average height to ground, in m;
k_0 is the geometric coupling coefficient of overhead ground wire and conductor.

China Electric Power Research Institute and State Grid Electric Power Research Institute put forward their own equations, which are specifically as follows:

$$U_i = 2.2I^{0.4}h_c\left(1 - k_0\frac{h_g}{h_c}\right) \tag{8.27}$$

$$U_i = 60\frac{\alpha h_c}{\beta c}\ln\frac{h_T + d_R + \beta ct}{(1+\beta)(h_T + d_R)} \tag{8.28}$$

where

I is the amplitude of the lightning current, in kA;
β is the ratio of back discharge speed to light velocity, taken as 0.3;
c is the light velocity, in m/μs;
h_T is the tower height, in m;
d_R is taken as 1/2 of the striking distance r_s, in m.

The other countries' institutions (such as in Europe, America and Japan) have also ever proposed the corresponding calculation equations for induced voltage, but they deem that the induced overvoltage on the conductor when the lightning strikes the tower top is relatively small, so it is not considered in the lightning protection calculation, which is different from the practices in the former Soviet Union and in China.

(7) Impact of power frequency voltage

In the UHV back flashover calculation, it is also recommended to consider the impact of the power frequency voltage by the statistical method, which is the same as the method for the shielding failure calculation.

In addition, the impact of the corona is ignored for the purpose of strictness.

8.1.2.4 Calculation Method for Lightning Protection of Large-Span Lines

The large-span overhead transmission lines are characterized by high towers and large spans, being more susceptible to lightning damage than the conventional route lines. At present, the standard used to assess the lightning withstand performance of the normal crossing lines in China is only the *Overvoltage Protection Regulation* issued in 1959 by the Ministry of Water Resources and Electric Power (the lightning protection calculation methods provided in the current regulations are only applicable to the conventional route lines, not to the large-span lines). However, this standard only proposed a calculation graph for the lightning withstand level of the "high towers" at that time, which has a specific applicable scope ($h_c/R \leq 8$, R is the grounding resistance of tower). With the Hanjiang River large-span tower taken as an example, even if h_c is taken as 90 m and R taken as 10 Ω, it is still beyond the

applicable scope of this standard. Therefore, this standard does not applicable to the lightning protection calculation for the UHV large-span lines.

Due to the lack of theoretical analysis and model test data, no other mature and authoritative calculation methods for the lightning protection of the large-span and high tower engineering are available for reference yet. Under the premise that there is no other mature calculation method, for the lightning protection calculation of the UHV large-span sections, the use of EGM and EMTP methods is also recommended. However, it is noteworthy that the lightning protection calculation for the large-crossing spans is different from that for the conventional route lines to some extent. The characteristics of large span and large sag of the large-crossing lines determine that the shielding failure calculation shall be done in sections, and the impact of wind deflection shall be taken into account. The characteristic of high height of towers results in that the calculation methods for the tower model, the lightning strike width and the lightning striking rate against poles, etc. vary greatly from the conventional route lines and, besides, the strike of lightning on the mid-span shall also be verified.

1. Sectional calculation

Because of the high towers and large sag of the large-span lines and the big difference in the height of conductors within the same span (for instance, the height of conductors at the suspension point and at the largest sag point may have significant difference), if the average height of conductors (Eq. (8.29)) is still used to calculate the shielding failure trip-out rate, it may cause certain error.

In such case, it is recommended to use the catenary equation (i.e., the hyperbolic cosine function, as shown in Eq. (8.31) to conduct the sectional calculation for lines. The calculation principle is as shown in Fig. 8.11:

$$h_{\mathrm{c}} = h_{\mathrm{ct}} - \frac{2}{3} s_{\mathrm{ag}} \tag{8.29}$$

$$y = a \cosh\left(\frac{x}{a}\right) + c \tag{8.30}$$

where

h_{ct} is the height of conductor suspension point, in m;
s_{ag} is the conductor sag, in m;
a and c is undetermined constants depending on span and sag, etc. jointly.

2. Analysis on impact of wind deflection

The increased height of the large-span tower makes the absolute speed of the wind acting on the line increase. Besides, in consideration that the wind deflection angles of the conductor and the overhead ground wire under the same wind speed are somewhat different, the overhead ground wire protection angle may be increased,

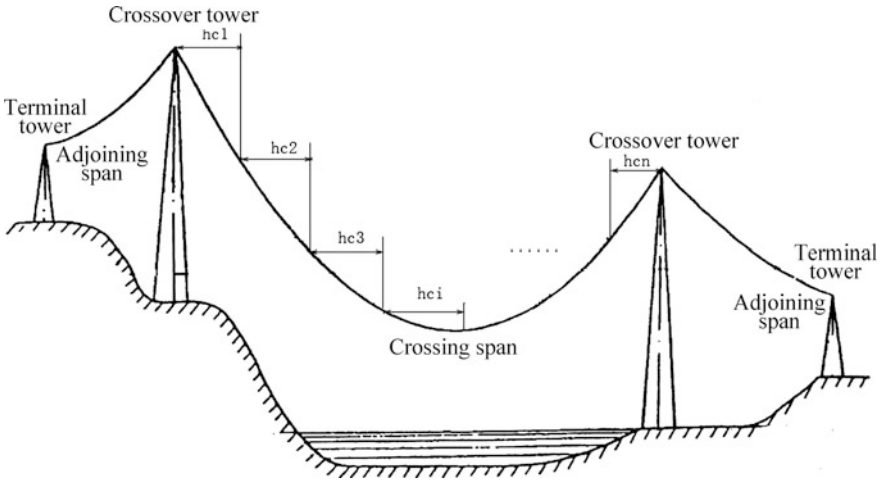

Fig. 8.11 Diagram for sectional calculation of the large-span line

resulting in the increase of the shielding failure rate of the line. Therefore, the impact of wind deflection shall be taken into account in the shielding failure calculation for the large-span line.

Under the certain wind speed v, the suspension insulator string and the wind deflection angle of the conductor are as shown in Fig. 8.12. Where, φ is the wind deflection angle of the suspension insulator string; ξ is the wind deflection angle of the conductor. The calculation method for the wind deflection angle of overhead ground wire is the same with that of the conductor. The detailed calculation method for wind deflection angle is shown as follows:

Wind deflection angle of suspension insulator string:

$$\varphi = \arctan\left[\left(\frac{m_{\mathrm{i}}}{2S} + L_{\mathrm{s}}g_2\right) / \left(\frac{m_{\mathrm{j}}}{2S} + L_{\mathrm{c}}g_1\right)\right]. \tag{8.31}$$

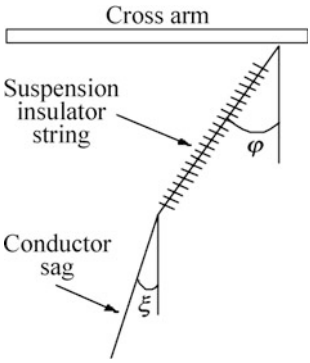

Fig. 8.12 Diagram for wind deflection of the line

Wind deflection angle of conductor:

$$\xi = \arctan(g_2/g_1) \tag{8.32}$$

where

L_s and L_c is the horizontal and vertical spans, respectively, in m;
g_1 and g_2 respectively, refers to the conductor's deadweight specific load and wind load specific load, in kg/(m·mm^2);
m_i and m_j is the mass of insulator string and the wind load, respectively, in kg;
S is the conductor sectional area, in mm^2.

With the impact of the bundled conductor spacing considered, the wind deflection angle of the suspension insulator string is corrected as follows:

$$\varphi = \arctan\left[\left(\frac{m_i}{2S} + L_s g_2\right)/\left(\frac{m_j}{2S} + L_c g_1\right)\right] + \arctan\left(\frac{d}{2L_i}\right) \tag{8.33}$$

where

L_i is the length of insulator string, in m;
d is the bundled conductor spacing, in m.

After the wind deflection angles of the conductor and the overhead ground wire are obtained, with the conductor on the leeward side taken as an example, assuming that the co-ordinates of the conductor and the overhead ground wire at the lowest span point under no wind are (x_c, y_c) and (x_g, y_g), respectively, after the wind deflection is considered, the co-ordinates may be corrected as follows:

$$x'_c = x_c + L_i \sin\varphi + f_c \sin\xi_c \tag{8.34}$$

$$y'_c = y_c + L_i(1 - \cos\varphi) + f_c(1 - \cos\xi_c) \tag{8.35}$$

$$x'_g = x_g + f_g \sin\xi_g \tag{8.36}$$

$$y'_g = y_g + f_g(1 - \cos\xi_g) \tag{8.37}$$

where

f_c and f_g respectively, the conductor sag and the overhead ground wire sag, in m;
ξ_c and ξ_g respectively, the wind deflection angles of conductor and overhead ground wire.

For the wind speed v used for the shielding failure calculation, due to the extremely short time of lightning strike, it may usually be taken as 1/3 of the maximum wind speed. In addition, during the analysis on the impact of wind deflection on the shielding failure rate, the windward side and the leeward side of the line shall be analyzed separately.

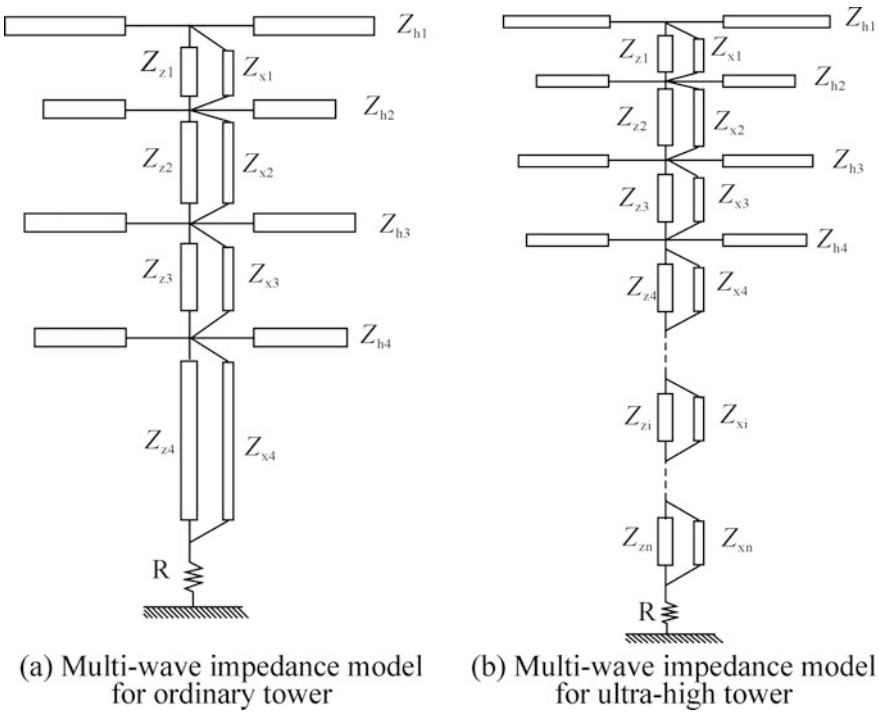

Fig. 8.13 Comparison of multi-wave impedance models for towers

3. Correction of tower wave impedance model

In the conventional wave impedance model, the tower body below the undermost cross arm of tower is treated as wave impedance for simplification, which can meet the calculation accuracy of the tower with normal height. However, for the large-span ultra-high tower, the tower body below the undermost cross arm varies greatly in the structures and dimensions of all parts, causing that the wave impedances at the top and the bottom vary greatly; besides, this section of the tower body is relatively long, and hence, large error may be caused if it is still treated as an average wave impedance. Therefore, the ultra-high tower's tower body below the cross arm shall be segmented appropriately, as specifically shown in Fig. 8.13.

4. Analysis on the strike of lightning on the midspan

According to the theoretical analysis and the operating experience, it is specified in China's regulations that the distance between the conductor and the overhead ground wire at the midspan of the overhead transmission line shall meet Eq. (8.38). The long-term operating experience shows that, for the conventional route lines, as long as the air distance s between the conductor and the overhead ground wire at the

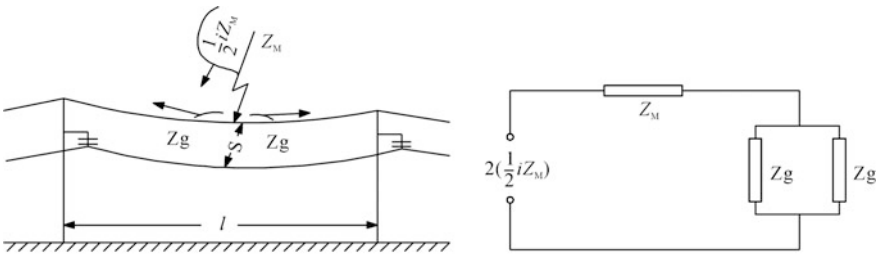

(a) Sketch for the lines (b) Equivalent circuit diagram

Fig. 8.14 Lightning striking at the midspan of overhead ground wire and its equivalent circuit diagram

midspan is determined as per the equation, when the lightning strikes the midspan, the clearance between the conductor and the overhead ground wire will normally not be broken down.

$$s = 0.012l + 1 \tag{8.38}$$

where

s is the distance between the conductor and the overhead ground wire at the midspan, in m;
l is the span length, in m.

However, for the large-crossing section with large span, when the lightning strikes the overhead ground wire at the midspan, the reflected waves of opposite polarities from the crossover towers on both sides have not yet reached the point of strike before the lightning current reaches its peak, so the overvoltage at the point of strike may be a little high, leading to the clearance flashover. Figure 8.14a represents the case in which the midspan of the overhead ground wire is struck by lightning. Under the premise that the impacts of the transmitted wave from the neighboring towers are ignored, its equivalent circuit diagram can be drawn according to the Peterson principle, as shown in Fig. 8.14b. The lightning withstand level of back flashover at the middle of large span can be calculated as per the following equation:

$$I_{\mathrm{mc}} = \frac{SE}{Z_{\mathrm{g}}(1 - k_0)} \times \frac{2Z_{\mathrm{M}} + Z_{\mathrm{g}}}{Z_{\mathrm{M}}} \tag{8.39}$$

where

E is the discharge voltage gradient of clearance, taken as 700–750 kV/m for estimation;
Z_{g} is the wave impedance of the overhead ground wire with the impact of the corona considered, in Ω;

k_0 is the coupling coefficient of the conductor and the overhead ground wire after the impact of the corona is considered;
Z_M is the lightning channel wave impedance, in Ω.

In fact, due to the large spacing between the conductor and the overhead ground wire at the midspan of large-crossing line, the arcing rate for the conversion of impulse flashover to the power frequency current is very low. Moreover, during the operation of the 500 kV large-span lines in China, the lightning flashover accident has never occurred at the middle of the large-crossing span. Therefore, for the large-span lines meeting the requirements on the spacing between the conductor and the overhead ground wire as specified in the regulation, the overvoltage may not be calculated any more.

5. Other differences in the calculation

In the calculation of the back flashover trip-out rate of the large-span lines, it shall be noted that the results obtained from the calculation equation for the lightning strike width provided in the regulation may be a little large. With the Hanjiang River large-span line section taken as an example, the spacing between the two overhead ground wires b is 56 m, the overhead ground wires' average height to ground h_g is around 90 m, and hence, the lightning strike width calculated by the regulation method is $w = b + 4h_g = 416$ m. However, according to the theory of striking distance, even if the shielding effect of the ground is ignored, the calculated lightning strike width is $w' = b + 4\bar{r}_s = 246$ m, which is far less than the value calculated by the regulation method. Therefore, for the UHV lines, it is recommended to refer to Russia's 1999 *Manual* for the calculation equation of lightning strike width of the large-span lines:

$$w = \begin{cases} 2(b/2 + 5h_g - 2h_g^2/30) & (h_g \le 30\,\text{m}) \\ 1.5(b/2 + h_g + 90) & (h_g > 30\,\text{m}). \end{cases} \tag{8.40}$$

For the calculation equation of the lightning striking rate against the pole, it is considered in the Regulation that it is related to the number of overhead ground wires and the terrain, but this only applies to the conventional lines. In fact, the lightning distribution between the tower and the overhead ground wire is related to the tower height and the span length, i.e., the longer the span, the smaller the lightning striking rate against pole. Similarly, by referring to Russia's 1999 *Manual*, the number of lightning strikes on the tower is recommended to be taken as the sum of 1/2 of the number of lightning strikes on the adjacent span plus 1/4 of the number of lightning strikes on the crossing span [1].

In addition, due to the lack of relevant statistical lightning data of the high tower lines, reference can be made temporarily to the Regulation for the lightning current polarity, amplitude probability distribution, and other parameters.

8.1.3 *Assessment for Lightning Withstand Performance of 1000 kV UHV Lines in China*

With reference to China's 1000 kV Southeast Shanxi-Nanyang-Jingmen UHVAC Demonstration Project and Huainan-South Anhui-North Zhejiang-West Shanghai 1000 kV UHVAC Power Transmission Project with double-circuit line on the same tower, the lightning withstand performance of 1000 kV UHVAC lines is calculated, and the affecting factors such as the tower type, the ground inclination angle, and the tower grounding resistance are analyzed [21].

8.1.3.1 Analysis on Lightning Withstand Performance of UHVAC Lines

For the 1000 kV Southeast Shanxi-Nanyang-Jingmen UHV Line, the cat-head-type towers are used in the plain areas, with M-type triangular arrangement (i.e., "I"-type and "V"-type insulator strings are, respectively, used for the side-phase and middle-phase conductors); the cup-type towers are used in the mountainous areas, with M-type horizontal arrangement. In addition, the type of 8 × LGJ-500/35 aluminum conductor steel reinforced is used as the conductors, with bundled spacing of 400 mm; a JLB20A-170 aluminum-clad steel stranded conductor is used for one of the overhead ground wires, and an OPGW-175 is used for the other. In addition, 54 porcelain insulators with structural height of 195 mm are used for the line insulation (Grade 2 pollution area), and the horizontal span of the towers is taken as 500 m.

For the Huainan-South Anhui-North Zhejiang-West Shanghai 1000 kV Power Transmission Project with double-circuit line on the same tower, the drum-shaped towers are adopted, with type "I" insulator string arrangement. The specific typical tower types are as shown in Fig. 8.15. In addition, 8 × LGJ-630/45 aluminum conductors steel reinforced is used as the conductors, with bundled spacing of 400 mm; an LBGJ-240-20AC aluminum-clad steel stranded conductor is used for one of the overhead ground wires, and an OPGW-240 is used for the other. In addition, 50 porcelain insulators with structural height of 195 mm are used for the line insulation (Grade 2 pollution area), and the horizontal span of towers is taken as 500 m.

(1) Calculation of shielding failure trip-out rate

Based on the tower types as shown in Fig. 8.15, the shielding failure trip-out rate N_r of China's 1000 kV UHV lines is calculated. The results therefrom are as shown in Table 8.3 [the ground flash density N_g is taken as 2.8 times/(100 km^2·a)].

It can be known from Table 8.3 that, under the existing conditions, for the 1000 kV lines, the cup-type tower has the optimal lightning withstand performance of shielding failure followed by the drum-type tower, and the cat-head type tower has relatively the highest shielding failure trip-out rate, but the shielding failure

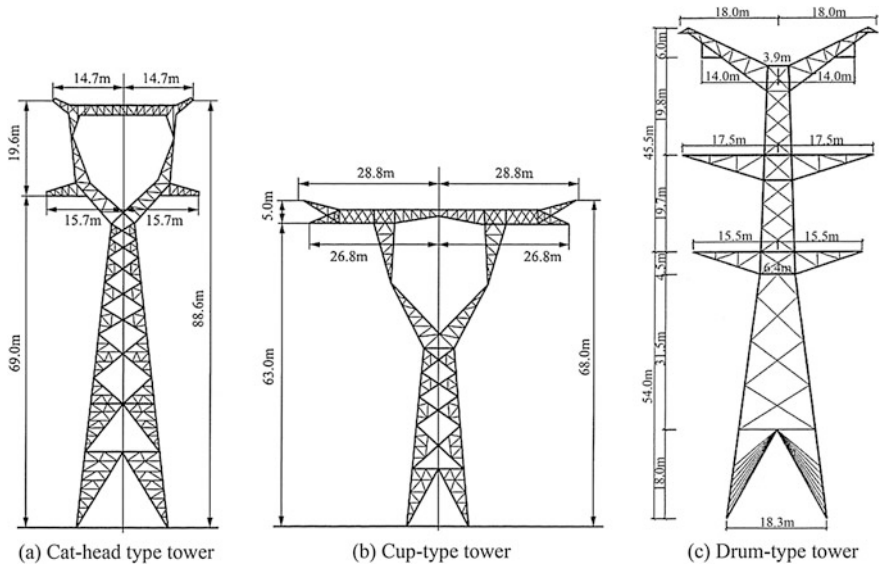

Fig. 8.15 Typical tower types of 1000 kV UHVAC lines

Table 8.3 Shielding failure trip-out rate of single-circuit for China's 1000 kV UHV lines

Tower type	Tower height (m)	Protection angle (°)	Ground inclination angle (°)	Shielding failure trip-out rate [times/(100 km·a)]
Cat-head type tower	88.6	1.8	0	0.0464
Cup-type tower	68	−6.7	0	0
Drum-type tower	99.5	−0.8	0	0.0002

Note The protection angle of drum-type tower is the protection angle of the overhead ground wire to the middle-phase conductor, similarly hereinafter

trip-out rates corresponding to the lines with such three towers all meet the expected lightning trip-out rates, which are in the acceptable range.

It can be known from the operating experience in the HV and EHV transmission lines that the shielding failure trip-out rate of a line is directly related to the overhead ground wire protection angle and the ground inclination angle. The following gives an analysis on the impacts of the protection angle and the ground inclination angle on the shielding failure trip-out rate of the UHV lines, and the calculation results are as shown in Tables 8.4, 8.5 and Fig. 8.16.

It can be known from Table 8.4 that the overhead ground wire protection angle has a large impact on the shielding failure trip-out rate of the line, and hence, the reduction of the protection angle is the most effective measure to improve the line's

Table 8.4 Impact of overhead ground wire protection angle on the shielding failure trip-out rate of single circuit for the 1000 kV UHV lines

Tower type	Overhead ground wire protection angle (°)						
	10	5	2.5	0	−2.5	−5	−10
Cat-head type tower	0.4982	0.1570	0.0639	0.0144	0.0002	0	0
Cup-type tower	0.1173	0.0147	0.0013	0	0	0	0
Drum-type tower	0.4004	0.0657	0.0136	0.0009	0	0	0

Table 8.5 Impact of ground inclination angle on the shielding failure trip-out rate of single circuit for the 1000 kV UHV lines

Tower type	Ground inclination angle (°)					
	0	5	10	15	20	30
Cat-head type tower	0.0464	0.2800	0.6948	1.2340	1.8016	2.7522
Cup-type tower	0	0	0.0264	0.1750	0.4760	1.2590
Drum-type tower	0.0002	0.039	0.1532	0.3307	0.5746	1.1179

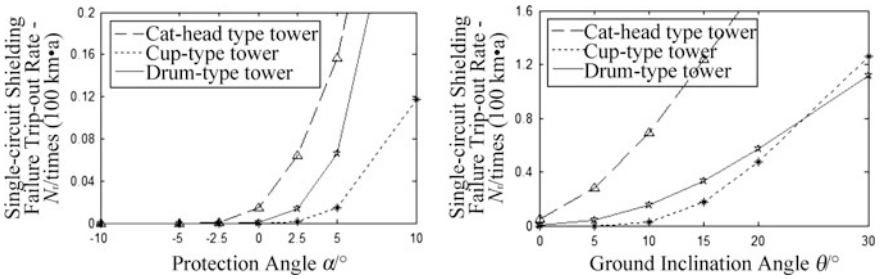

Fig. 8.16 Impacts of overhead ground wire protection angle and ground inclination angle on the shielding failure trip-out rate of the UHV lines

performance against shielding failure. For example, when other related conditions are kept unchanged, if the overhead ground wire protection angle is increased from 0° to 5°, the shielding failure trip-out rate of the 1000 kV line with cat-head type tower will be significantly increased. Therefore, to ensure the lightning protection performance of the UHV lines, the overhead ground wire protection angle for the line sections in the plains shall be less than 0°.

It can be known from Table 8.5 that the shielding failure trip-out rate increases with the increase of the ground inclination angle, which is consistent with the experience that the lines on the hillsides are prone to shielding failure during the actual operation. In addition, it can be known from the operating experience of Japan in the UHV lines that the shielding failure trips mostly occur in the mountainous areas with large ground inclination angle (corresponding to about 20°–30°). With the typical towers shown in Fig. 8.2 taken as an example, in case of 30° ground inclination angle and 25 thunderstorm days, the shielding failure trip-out

rate of single-circuit calculated using the EGM method is 0.74 times/(100 km·a), which is close to the actual statistical value of 0.9 times/(100 km·a). This shows, on one hand, that a smaller ground wire protection angle shall be used in the mountainous areas, and, on the other hand, the use of the EGM method for calculating the shielding failure trip-out rate of the UHV line is relatively reasonable.

Therefore, special attention shall be paid to the shielding failure protection for the lines in the mountainous areas with large ground inclination angles, and all efforts shall be made to avoid erecting transmission lines at the locations with large ground inclination angles, but if it is, indeed, necessary to do so, it is recommended to adopt a smaller negative protection angle or install the line-mounted sideward lightning rod or take other measures to improve the shielding failure protection performance of the lines.

In summary, the ground inclination angle is one of the main reasons for the high shielding failure trip-out rate, while the reduction of the overhead ground wire protection angle can significantly reduce the shielding failure trip-out rate of the line and is the most effective measure to improve the shielding failure protection performance of the line. Therefore, during the selection of the overhead ground wire protection angle of the UHV lines, special attention shall be paid to the impacts of the topographical factors (i.e., the ground inclination angle θ).

For the 1000 kV UHVAC lines, the overhead ground wire spacing is large, and there is also a possibility that the lightning may strike the conductors from between the two overhead ground wires. Now, with the ZBS2 cup-type tower with the largest overhead ground wire spacing taken as an example, based on the analysis through electro-geometrical model, the results indicate that the possibility that the lightning strikes the conductor from between the overhead ground wires exists, but the current of lightning that can strike the conductor is very small and is only 8 kA at maximum even when the overhead ground wire protection angle is −2.5°, which is far less than the lightning withstand level of shielding failure for the 1000 kV line and will not cause the line insulation flashover. For the other tower types, the overhead ground wire spacing is smaller, so it is unnecessary to consider the possibility of line insulation flashover resulting from the lighting strike on the conductors from between the overhead ground wires. Nevertheless, in the incoming line sections of substation and other special occasions, to further improve the reliability in lightning protection of the UHV substation, three overhead ground wires may be considered to be installed.

(2) Calculation of back flashover trip-out rate

The 1000 kV lines have a high insulation level, so the lines' lightning withstand level of back flashover is normally at 250 kA and above. Besides, no records on the back flashover trip exist for the UHV lines in other countries (the former Soviet Union and Japan). Therefore, for the purpose of strictness, if the tower impulse grounding resistance is taken as 15 Ω, the back flashover lightning withstand levels and the trip-out rates corresponding to the typical tower types are as shown in Table 8.6.

Table 8.6 Back flashover trip-out rate of single circuit for the 1000 kV UHV lines

Tower type	Tower height (m)	Grounding resistance (Ω)	Back flashover lightning withstand level (kA)	Back flashover trip-out rate [times/(100 km·a)]
Cat-head type tower	88.6	15	310	0.0038
Cup-type tower	68	15	318	0.0027
Drum-type tower	99.5	15	252(383)	0.0110(0)

Note For the drum-type tower, the lightning withstand levels of back flashover inside and outside the parenthesis are for the single-circuit and double-circuit lines, respectively

It can be known from Table 8.6 that, for the 1000 kV Southeast Shanxi-Nanyang-Jingmen Single-circuit Line, its back flashover trip-out rate of single-circuit is very low, not exceeding 0.0038 times/(100 km·a) at maximum; for the 1000 kV Huainan-South Anhui-North Zhejiang-West Shanghai Power Transmission Project with double-circuit line on the same tower, its lightning withstand level of back flashover is lower than that of the single-circuit line, but is still above 250 kA. Therefore, the lightning withstand level of back flashover for the UHV lines is quite high, and the probability of back flashover trip-out rate caused by lightning striking on towers or nearby overhead ground wires is very small.

In addition, because the theoretical calculation value of the simultaneous back flashover trip rate of both circuits for the UHV double-circuit line on the same tower is very low, and in consideration that no simultaneous trip of both circuits has ever occurred in China's 500 kV and Japan's 1000 kV double-circuit line on the same tower, the probability thereof can be considered as zero. As a result, it is unnecessary to consider the unbalanced insulation in the UHV double-circuit line on the same tower.

It can be known from the experience in the operation of the HV and EHV transmission lines that the back flashover trip-out rate of the line is directly related to the value of the tower grounding resistance. The following gives an analysis on the impact of tower grounding resistance on the UHV line's lightning withstand performance of back flashover. The calculation results are as shown in Fig. 8.17. It can be known from the calculation results that, to ensure the back flashover protection performance of the UHV lines, especially the double-circuit line on the same tower, the tower grounding resistance shall not be more than 15 Ω.

In summary, for the 1000 kV UHVAC lines, the back flashover is not the main cause for lightning trip of the lines, and hence, the lightning protection of the UHV lines shall be realized mainly by strengthening the research on the protection against the shielding failure.

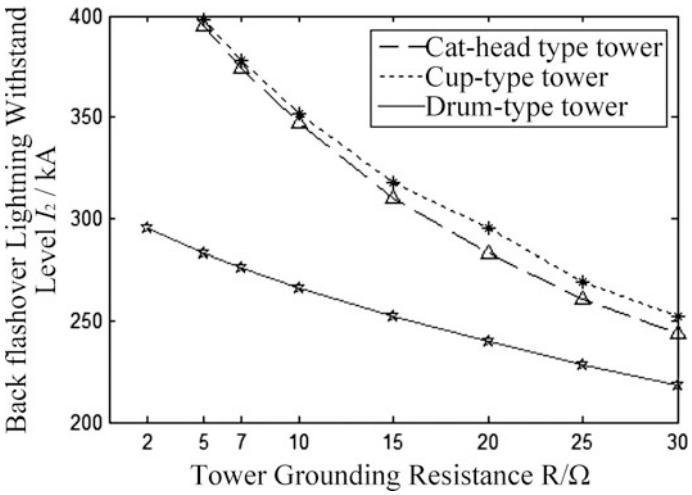

Fig. 8.17 Impact of tower grounding resistance on the single-circuit back flashover lightning withstand level of the UHV lines

8.1.3.2 Study on Lightning Protection for Large Span of the UHVAC Demonstration Project

There are totally two large-crossing sections in the 1000 kV Southeast Shanxi-Nanyang-Jingmen UHVAC Demonstration Project, i.e., the Hanjiang River large-crossing and the Yellow River large-crossing. Now, take the Hanjiang River crossing section with high tower and large span as an example, the lightning withstand performance of the UHV large-span lines is studied.

The Hanjiang River large-crossing section is built in the strain-tangent-tangent-strain form, with the maximum crossing span up to 1650 m. The section is as shown in Fig. 8.18. In addition, the cup-type towers with the nominal height of 170 m and the total height of 181.8 m are used as the tangent towers; the single-circuit "干"-shaped towers with the nominal height of 40 m and the total

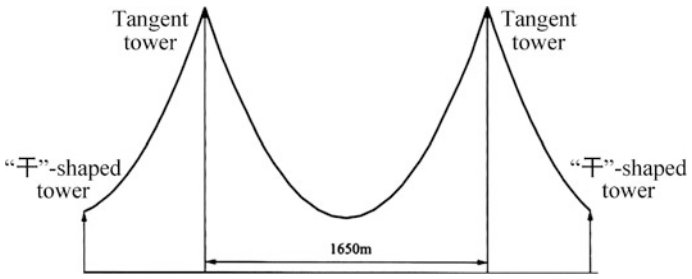

Fig. 8.18 Section of Hanjiang River large-crossing

height of 72 m are used as the strain towers. 8 × AACSR/EST-410/153 type aluminum alloy stranded conductors steel reinforced with the ultra-high strength are used as the conductors; a JLB14-240 aluminum-clad steel stranded conductor is used for one of the overhead ground wires, and a OPGW-24B1-246 optical cable is used for the other; the line insulation adopts 48 420 kN porcelain insulators connected in series; and the tower grounding resistance is taken as 15 Ω.

For the Hanjiang River UHV large-crossing line, as shown in Fig. 8.19, the method described in Sect. 8.1.2 is used to assess the lightning withstand performance of the large-crossing line section, and the results are as shown in Tables 8.7 and 8.8.

The shielding failure trip-out rate of Hanjiang River large-crossing is 1.22 times/(100 km·a), and the equivalent annual number of shielding failure trips is 0.02 times/a, corresponding to one shielding failure trip in 50 years. To further reduce the rate of lightning trip of the large-crossing line section, according to Fig. 8.20, the overhead ground wire protection angle can be reduced to $\leq -5°$ and the line-mounted arresters may also be considered to install on the side-phase conductor.

The back flashover lightning withstand level of Hanjiang River large-crossing is 206 kA, the back flashover trip-out rate thereof is 0.08 times/(100 km·a), and the equivalent annual number of back flashover trips is 0.0013 times/a, corresponding to one back flashover trip in 769 years. Therefore, the back flashover lightning withstand performance is excellent.

It is noteworthy that, for the large-crossing ultra-high towers, the reduction of the grounding resistance of tower cannot effectively improve the back flashover protection performance (as shown in Fig. 8.20).

To sum up, the total lightning trip-out rate of Hanjiang River large-crossing is 1.3 times/(100 km·a) and the safety life for the lightning protection is 46 years, which is close to the required index (50 years) for the lightning protection of the large-crossing.

8.1.4 Lightning Protection Measures for the UHVAC Lines

To ensure the safe operation of the UHV lines, by considering the actual situations of the lines and starting with the causes for lightning trip, appropriate lightning protection measures shall be taken according to the local conditions and in a targeted manner.

Both the operating experience and the simulation calculation show that the lightning hazard is the main cause for the trips of the UHVAC transmission lines, while the shielding failure is the main cause for the lightning trips of the UHV lines. Therefore, the improvement of the shielding failure protection performance is the key to improve the lightning protection performance of the UHV transmission lines.

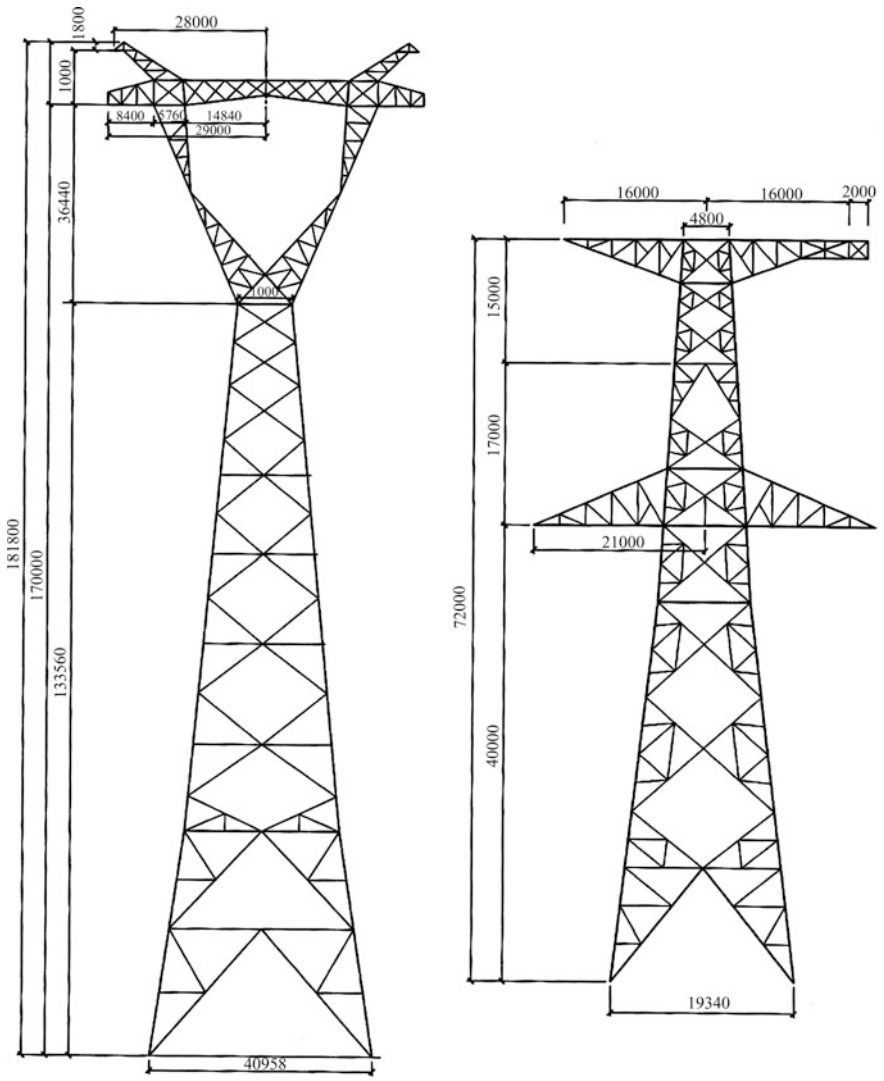

Fig. 8.19 Structural diagrams for crossover tower and anchor tower of Hanjiang River large-crossing (mm)

8.1.4.1 Reduction of the Overhead Ground Wire Protection Angle

The most effective measure to reduce the shielding failure trip-out rate of the UHV line is to decrease the overhead ground wire protection angle, especially for the lines in the mountainous areas.

The overhead ground wire protection angle shall not be selected in a "one fits all" manner; instead, it shall be decided based on the terrain along the line, tower

Table 8.7 Calculation results of shielding failure trip-out rate of Hanjiang River large-crossing section

Tower height (m)	Protection angle (°)	Shielding failure trip-out rate [times/(100 km·a)]		Equivalent to single-circuit
		Windward side	Leeward side	
181.8	2.9	0.5081	0.7079	1.2160

Note During the shielding failure calculation, the crossing span is equally divided into 100 sections; when the wind deflection is considered, the reference wind speed at 10 m above the ground is taken as 10 m/s

Table 8.8 Calculation results of back flashover lightning withstand level of Hanjiang River large-crossing section

Tower height (m)	Grounding resistance (Ω)	Back flashover lightning withstand level (kA)
181.8	15	206

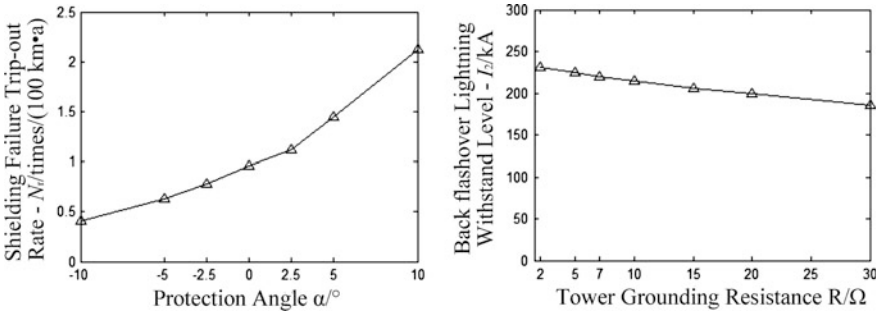

Fig. 8.20 Impacts of overhead ground wire protection angle and tower grounding resistance on the lightning trip-out rate of Hanjiang River large-crossing Section

types, and intensity of lightning activity, as well as other factors. For the typical tower types of China's UHVAC lines (as shown in Fig. 8.15), the curves of the line shielding failure trip-out rate with the change in the overhead ground wire protection angle are, respectively, plotted as shown in Fig. 8.21.

The Regulation GB/Z 24842-2009 gives a rough required value for the overhead ground wire protection angle of the UHVAC lines, without making quantitative requirements on the topographical conditions. In consideration of the actual projects, the ground inclination angles of the plain, hilly, and mountainous regions are normally taken as 0°–10°, 10°–20°, and 20°–30° respectively. Under the condition that the shielding failure trip-out rate of single-circuit is not higher than the limit of 0.1 times/ (100 km·a), the overhead ground wire protection angle α is put forward through calculation as follows:

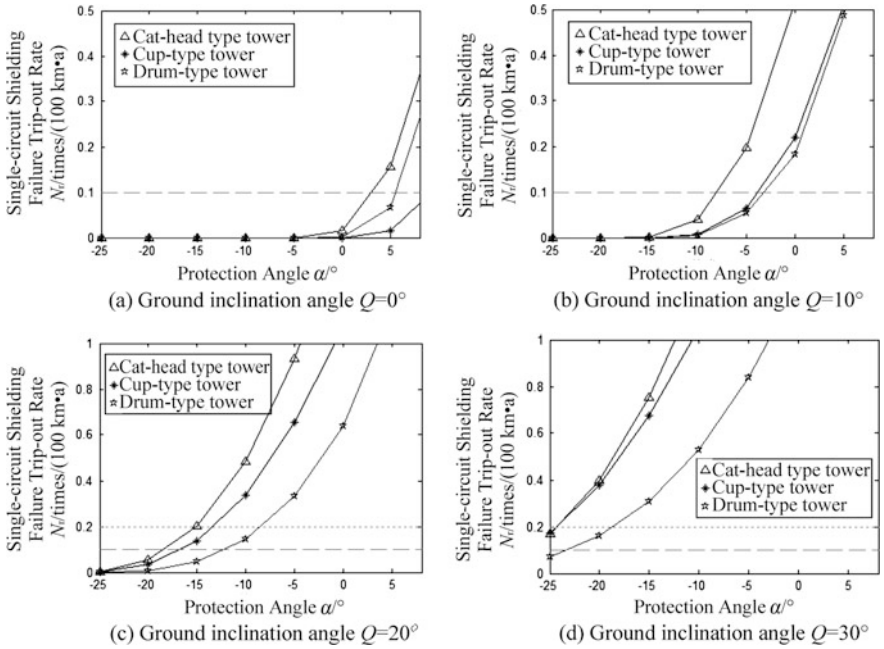

Fig. 8.21 Shielding failure trip-out rates of the UHV lines with typical tower types under different terrains and protection angles

(1) For the cat-head type tower, $\alpha \leq 0°$ when in the plain regions, $\alpha \leq -10°$ when in the hilly regions, and $\alpha \leq -20°$ when in the mountainous regions.
(2) For the cup-type tower, $\alpha \leq 5°$ when in the plain regions, $\alpha \leq -5°$ when in the hilly regions, and $\alpha \leq -20°$ when in the mountainous regions;
(3) For drum-type tower, $\alpha \leq 5°$ when in the plain regions, $\alpha \leq -5°$ when in the hilly regions, and $\alpha \leq -15°$ when in the mountainous regions.
(4) In the mountainous regions with greater ground inclination angles and in the regions with intense lightning activity, according to the actual project conditions, the measures such as the further reduction of the protection angle and the addition of overhead ground wires and coupling wires can be taken to reduce the lines' lightning trip-out rate.

8.1.4.2 Optimization of Tower Design and Application of Sideward Lightning Rod

The operating experience of the former Soviet Union in the UHV lines shows that the shielding failure trips mostly occur at the angle and strain towers. Therefore, special attention shall be paid on improving the lightning protection design of the

angle and strain towers to provide them with a reasonable negative protection angle. In the tower design, the tower height shall also be minimized, which is beneficial for the protection against the shielding failure and the back flashover.

For the UHV angle towers, to further enhance the protection performance against the shielding failure, it is recommended to install multiple line-mounted sideward lightning rods on the cross arms of towers. The literature [22] shows the obvious protection effect of the sideward lightning rods against the shielding failure of the high tower lines. The sideward rod may guide the lightning leader to progress towards the tip of lightning rod to convert the shielding failure into the back flashover, thereby reducing the rate of the shielding failure on the lines. Especially for the UHV lines, due to the high lightning withstand level of back flashover, the installation of sideward rods does not increase the trip-out rate.

It is shown by the experience in the operation of the lines in Zhejiang, Jiangxi, and other places that the installation of sideward rods can, to some extent, effectively reduce the shielding failure trip-out rate of the lines and improve the lightning protection performance of the lines. The scope of protection by the sideward rod for the conductors at both sides of the tower is about 25–30 m (the sideward rod is 3 m long). Besides, the shielding failure for the angle tower mostly occurs to the lines in the vicinity of the tower (about 30 m away from both sides of the tower). Therefore, the sideward rod has a good effect in the protection against the shielding failure.

The sideward rod not only can effectively reduce the shielding failure trip-out rate of the line near the tower, but is also economic, durable, and easy to install and maintain, etc., and its effect on the lightning protection of UHVAC lines will be analyzed in detail in Sect. 8.1.5.

8.1.4.3 Lightning Protection Measures for the Large-Crossing Sections

To optimize the lightning protection performance of the large-crossing sections of the UHV lines, the crossing sections shall be arranged in a multi-span and low-tower pattern, while the specific lightning protection scheme shall be conducted for each span separately.

To reduce the lightning trip-out rate of the large-crossing sections, the specific recommendations are as follows: to reduce the shielding failure trip-out rate, the overhead ground wire protection angle is recommended to be less than −5°; to ensure the lightning withstand performance of back flashover, the tower grounding resistance is recommended to be no more than 15 Ω; to further improve the reliability in the lightning protection, the installation of the line-mounted arresters may also be considered for the large-crossing sections when necessary.

For the insulation level of the large-crossing sections (number of insulators), it is not appropriate to follow the requirements in the procedure saying “one insulator with structural height of 146 mm shall be added for each increment of 10 m for the towers with height more than 40 m”; instead, it shall be determined by the calculation of simulation for the lightning overvoltage.

8.1.4.4 Other Measures

(1) Reasonable selection of the line routes

The ground slope (i.e., the ground inclination angle) has a great impact on the shielding failure trip-out rate of the overhead transmission lines. Therefore, lines shall be avoided to be erected at the places with large slope [23]. In addition, it can also be known from the experience of Japan in operation of the UHV lines that China's UHV lines shall be avoided to be erected in the mountainous regions with large ground inclination angle.

(2) Reduction of the tower grounding resistance

The UHV lines have a high lightning withstand level of back flashover, so it is normally unnecessary to take special protection measures against the back flashover. However, for the purpose of safety, the impact of the tower grounding resistance cannot be ignored completely. The legs and the foundations of the UHV overhead transmission line towers buried underground are of large size, with the good performance in the current diffusion, so the grounding resistance is easy to be controlled within the target range. It can be known from the calculation results in Sect. 8.1.3 that the tower grounding resistance shall be less than 15 Ω as far as possible. For the mountainous areas with high soil resistivity, if the tower grounding resistance cannot meet the required value, the following measures can be taken: the use of external grounding device, the deep burial of ground electrode, the filling of materials with low resistivity (such as soil and resistance reducing agent), and the explosion grounding, etc.

In addition, with reference to the China's experience in operating the HV and EHV lines, at the points or in the sections where susceptible to the lightning strike in the UHV lines, the installation of the line-mounted arresters, the bypassing of overhead ground wires (the erection position and height thereof shall be determined reasonably), and other measures may also be used for preventing from the shielding failures.

8.1.5 Analysis of Sideward Lightning Rod in Lightning Protection of UHVAC Line

8.1.5.1 Structure of Sideward Lightning Rod and its Application Status

The sideward lightning rod is a fine metallic rod with a tip which is usually fixed on the outside of the tower's cross arm by angle steel. It can guide the lightning leader to develop towards the tip of lightning rod, and convert the shielding failure into the back flashover. As the transmission line's lightning withstand level of back flashover is far higher than the lightning withstand level of shielding failure, when the

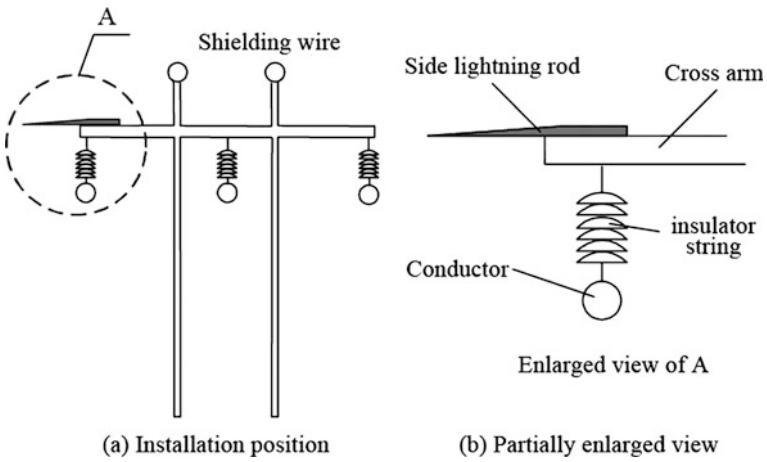

Fig. 8.22 Sketch for installation position of sideward lightning rod

shielding failure is converted into the back flashover by the sideward lightning rod, so long as the line has high enough lightning withstand level of back flashover, the line will normally not trip. Therefore, the sideward lightning rod can protect the key dangerous zones subject to shielding failure around the towers along the transmission line. Reference [22] shows that the sideward lightning rod has an obvious protection effect against shielding failure for the line with high towers (Fig. 8.22).

The shielding failure protection effect of the sideward lightning rod has been proven effective through its application in some HV projects, for example, its application on the 110 kV Jiande-Jiangjia Line by Jinhua Electric Power Bureau. The 110 kV Jiande-Jiangjia Line 1679 is located in the mountainous area of Qiandao Lake. The main line has 189 base towers in total, among which most are of 220 kV towers and only a few are of 330 kV towers. Up to 1993, since the 110 kV Jiande-Jiangjia Line was put into operation in 1970, the average lightning trip-out rate of the whole line during the 23 years reached up to 4.11 times/(100 km·a) (the annual average thunderstorm days were 47.17 days), being a "long-standing" problem among the transmission lines suffering from lightning in Zhejiang Province. The electric power department had successively taken some comprehensive lightning protection measures since 1993, and, however, the operation thereof during the 7 years thereafter showed that the lightning trip-out rate was still up to 3.87 times/(100 km·a). In 2003, the electric power department carried out; once again, the lightning protection work on the section of the Jiande-Jiangjia Line from towers Nos. 1–91, but the lightning trip occurred many times after the reconstruction work and the expected effect was not achieved.

In the early of 2006, the local electric power department proposed to carry out lightning protection reconstruction on the Nos. 92–189 towers along the line through the co-operation with Zhejiang University. During the reconstruction, besides some conventional comprehensive lightning protection measures (for

example, the application of line arrestors or increase of number of insulators on a few lines), Zhejiang University used especially the 3 m-long sideward lightning rods on all of the towers within this section for protection. During the six thunderstorm seasons (from March 2006 to August 2011) after the reconstruction, only one lightning trip accident occurred on this section of the line which is about 40 km long, and the lightning trip-out rate was 0.42 times/(100 km·a), which is far below 3.87 times/(100 km·a) prior to the reconstruction. In addition, the sideward lightning rods also achieved satisfactory shielding failure protection effect in the HV projects in Zhejiang Province and Jiangxi Province, etc.

Relevant studies show that the conductors nearby the tower will attract the lightning due to electric field distortion caused by the tower, so the conductors cannot obtain the effective shielding protection of tower, which causes the great increase in the rate of line shielding failure in this area. Meanwhile, due to the sag effect, the protection angle of overhead ground wire nearby the tower is normally larger than the midspan, which also causes the shielding failure accidents to concentrate nearby the tower. Reference [24] concluded through the relevant model tests that the shielding failure probability in the area nearby the tower is far higher than that in the midspan, and that the shielding failure of the HV transmission line mostly occurred on the line about 30 m to both sides of the tower.

For the UHV transmission line, since its back flashover lightning withstand level is very high, the probability of back flashover to be occurred on it is extremely small, and the lightning trips are mostly caused by shielding failure. Meanwhile, since such line has very high towers and large sag, the shielding failure happened in the area nearby the tower, especially the strain and angle towers, is the most serious. The experience in the operation of the UHV lines obtained by the former Soviet Union shows that the shielding failure trip-out mostly occurs nearby the angle tower and strain tower. In addition, the 1000 kV North Zhejiang-Fuzhou AC Line operating in Zhejiang Province had one lightning trip accident due to shielding failure within the territory of Lishui, and the position of such trip was exactly on the jumper of the single-circuit strain tower.

In the below, analysis will be made on the lightning protection effect of sideward lightning rod applied on the UHVAC line. First of all, a brief introduction will be given to the shielding system model of sideward lightning rod and the calculation of protection distance, and then, analysis will be made on the protection effect of sideward lightning rod applied on three typical types of the UHV towers.

8.1.5.2 Analysis on Protection Effect of Sideward Lightning Rod Applied on the UHVAC Line

A model of the single-circuit transmission line is as shown in Fig. 8.23a. The sectional view of the two-dimensional plane in a distance of d to the tower is as shown in Fig. 8.23b.

Arc AB, arc BC, and arc CD shown in Fig. 8.23a are located on the two-dimensional plane in a distance of d to the tower, among which arcs AB and

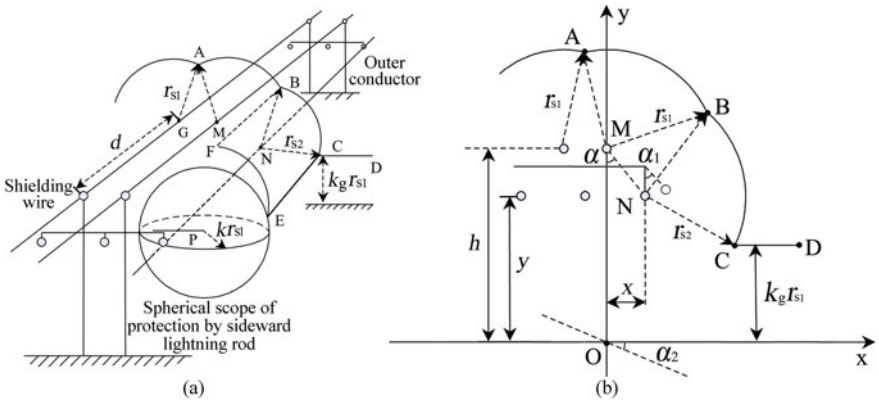

Fig. 8.23 Model of the shielding system of sideward lightning rod, reprinted from Ref. [16], copyright 2014, with permission from power system technology

CD are the overhead ground wire and ground shielded arc, respectively, and arc BC is the exposed arc of conductor. Along the span length direction, the exposed arcs of conductors on the two-dimensional plane at each position are connected as a curved surface BCEF, as shown in Fig. 8.23a, that is, the three-dimensional exposed curved surface of shielding failure for outer conductor under the overhead ground wire and ground shielding system. The ground striking distance shall be taken as k_g times the striking distance of overhead ground wire under the same lightning current amplitude, while the striking distance of sideward lightning rod shall be taken as k times the striking distance of overhead ground wire under the same lightning current amplitude. k_g and k are the striking distance factors. The discharge of sideward lightning rod occurs at the tip thereof, and its curved surface of striking distance can be expressed by a spherical surface with the tip being taken as the center of the sphere and the striking distance kr_{s1} being taken as the radius, i.e., sphere P, as shown in Fig. 8.23a. When the spherical surface of shielded sphere P of the sideward lightning rod is intersected with the exposed curved surface of conductor BCEF, the sideward lightning rod can shield the exposed curved surface of conductor located inside sphere P according to the striking distance theory.

Figure 8.23b is the sectional view of the two-dimensional plane in a distance of d to the tower, where M, N, and P are the respective points of overhead ground wire, outer conductor, and tip of sideward lightning rod on such plane. A co-ordinate system as shown in the figure is established with point O being taken as the origin. The co-ordinate of overhead ground wire is (o, h) and that of conductor is (x, y). During the calculation of the co-ordinates of overhead ground wire and conductor, the influence of sag shall be taken into consideration. Under the effect of wind, the offset angle of conductor insulator is α_1, and the ground inclination angle thereof is α_2.

For certain lightning current amplitude I, when the whole exposed arc of a point on the conductor is within the protection scope of sphere P, it indicates that such point is shielded completely by the sideward lightning rod. Increase gradually the

distance of such point to the tower until sphere P cannot shield completely the exposed arc of conductor at such point. In such case, its distance to the tower is the maximum protection distance l of sideward lightning rod. Within such distance l, shielding failure will not occur on the line, because the line is shielded completely by the sideward lightning rod. First of all, calculate the maximum protection distance l of sideward lightning rod corresponding to lightning current with different amplitudes I when the critical current of shielding failure flashover reaches to be within the range of maximum shielding failure lightning current; then, carry out weighted average calculation on the calculation results according to the distribution probability of lightning current amplitudes to obtain the distance of protection of sideward lightning rod against shielding failure.

Through the use of three-dimensional EGM method, analysis shall be carried out on the shielding failure protection effect of the sideward lightning rods applied on the three typical types of the UHV towers as shown in Fig. 8.15. During the analysis, the influence of the three factors, i.e., sideward lightning rod length, wind deflection angle, and ground inclination angle, on the shielding failure protection effect of the sideward lightning rod shall be taken into account.

(1) Analysis on shielding failure protection effect of sideward lightning rod applied on the cat-head-type tower along the single-circuit UHV transmission line in plain areas

The model ZMP2 cat-head-type tower is of M-type triangular configuration, and the tower structure is as shown in Fig. 8.15a, which is mainly applied in plain areas. When the wind deflection angle α_1 and the ground inclination angle α_2 are 0°, the variation in the protection distance of sideward lightning rod when the length of sideward lightning rod is changed is as shown in Fig. 8.24. As seen from the figure, the 3 m-long sideward lightning rod is able to protect the conductors within the scope of about 30 m to both sides of the tower.

Since the occurrence of lightning disaster is normally accompanied with strong wind, it is necessary to take into account the influence of wind deflection angle on the protection effect of sideward lightning rod. Considering that the wind velocity is 15 m/s [25] at the time of lightning strike, the wind deflection angle of the conductor can reach up to 25° [26]. The variation in the protection distances of sideward lightning rods with different lengths is as shown in Fig. 8.25 when the wind

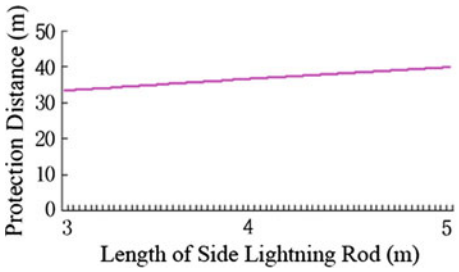

Fig. 8.24 Length of sideward lightning rod versus protection distance

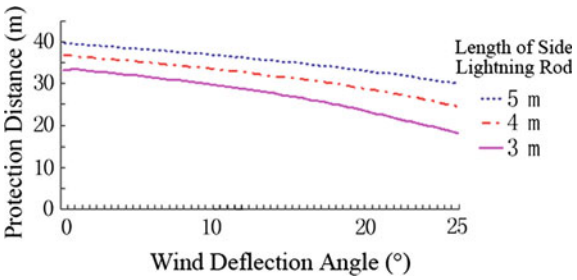

Fig. 8.25 Wind deflection angle versus protection distance of sideward lightning rod

deflection angle α_1 is changed under the condition that the ground inclination angle α_2 is 0. Since the shielding failure of the HV transmission line mostly occurs at about 30 m to both sides of the tower, as known from Fig. 8.25, we may consider using the sideward lightning rods with a length of 4–5 m for the cat-head-type tower.

(2) Analysis on shielding failure protection effect of sideward lightning rod applied on the cup-type tower along the single-circuit UHV transmission line in mountainous areas

The cup-type tower is of M-type horizontal configuration, and its tower structure is as shown in Fig. 8.15b, which is mainly applied in the mountainous areas. Even though negative protection angle is adopted for the model ZBS2 cup-type tower, when the wind deflection angle α_1 or the ground inclination angle α_2 is not zero, the overhead ground wire may not be able to provide complete shielding for the transmission line. In such case, it is necessary to protect the line using the sideward lightning rods.

It is found through calculation that when α_2 is less than 18°, the overhead ground wire is able to shield completely the transmission line; when the ground inclination angle α_2 is no less than 18°, the risk of shielding failure on the conductor exists. Therefore, the variation in the protection distances of sideward lightning rods with different lengths is as shown in Fig. 8.26 when α_2 is increased from 18° under the condition that α_1 is 0°. As known from the figure, when α_2 is 18° and 30°, the protection distances of the 6 m-long sideward lightning rod are about 37–28 m, respectively, and the protection effect is good. Based on this, the curve of the protection distance of 6 m-long sideward lightning rod varying with the ground inclination angle α_2 under different wind deflection angles α_1 is calculated with the

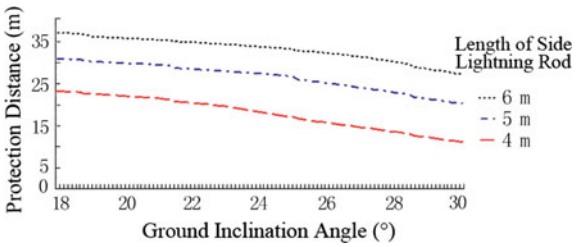

Fig. 8.26 Ground inclination angle versus protection distance

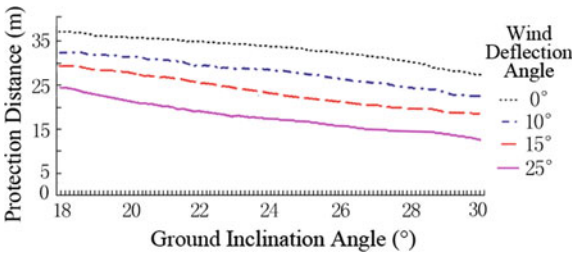

Fig. 8.27 Wind deflection angle versus ground inclination angle and protection distance

results as shown in Fig. 8.27. The calculation results show that when the wind deflection angle is less than 15° and the ground inclination angle is in the range of 18°–30°, the 6 m-long sideward lightning rod has a minimum protection distance of about 20 m and still has certain protection effect for the transmission line. Therefore, the sideward lightning rods with a length of 6 m or above can be considered to be installed on the cup-type tower.

(3) Analysis on shielding failure protection effect of sideward lightning rod applied on the drum-type tower along the double-circuit UHV transmission line on the same tower

The drum-type tower is of I-type insulator string configuration, and its tower structure is as shown in Fig. 8.15c, which is mainly applied in the plain and hilly areas. Because the overhead ground wire has a very small shielding angle for the lower phase conductor and the conductor sits at a very low position, within the reasonable variation range of the wind deflection angle, the shielding wire can always provide complete shielding for the lower phase conductor, and hence, it is not necessary to take into account the protection effect of sideward lightning rod on the lower phase conductor. When the ground inclination angle and the wind deflection angle are 0°, the protection distances of 3 m-long sideward lightning rod installed at three different cross arm positions on the drum-type tower for the upper and intermediate-phase conductors are calculated with the results, as shown in Table 8.9. As known from the table, the sideward lightning rod when installed on the middle cross arm has the maximum protection distance for the upper and intermediate-phase conductors and, in such case, can provide protection for the conductors within about 30 m to both sides of the tower, and hence, it is considered

Table 8.9 Influence of sideward lightning rod at different installation positions on the protection distance for conductor of drum-type tower

Position of sideward lightning rod	Protection distance	
	Upper phase conductor (m)	Intermediate-phase conductor (m)
Upper phase cross arm	14.2	7.2
Intermediate-phase cross arm	38.0	34.8
Lower phase cross arm	22.1	17.3

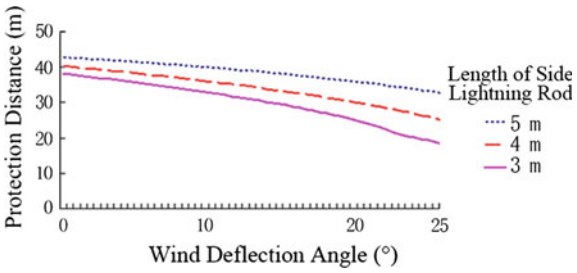

Fig. 8.28 Wind deflection angle and length of sideward lightning rod versus protection distance for upper phase conductor

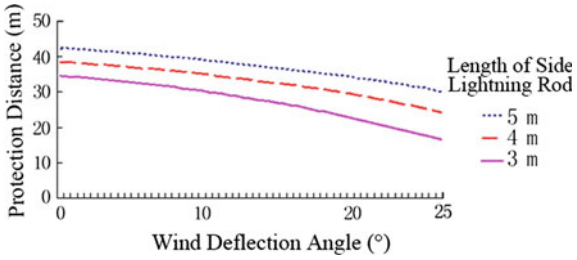

Fig. 8.29 Wind deflection angle and length of sideward lightning rod versus protection distance for intermediate-phase conductor

to install the sideward lightning rod on the intermediate-phase cross arm of the drum-type tower.

Under the condition that the sideward lightning rod is installed on the intermediate-phase cross arm and the ground inclination angle is 0°, the protection distances of sideward lightning rods with different lengths are, respectively, calculated based on varying wind deflection angle. In such case, the protection distance provided by the sideward lightning rod for the upper phase conductor is as shown in Fig. 8.28, and that for the intermediate-phase conductor is as shown in Fig. 8.29. Because the shielding failures of the HV transmission line mostly occur at about 30 m to both sides of the tower, as known from the figures, for the drum-type tower, the sideward lightning rod with a length of 4–5 m can be considered to be installed on the intermediate-phase cross arm of the tower.

In conclusion, the calculation of simulation for the UHV transmission line shows that the sideward lightning rod can improve the lightning protection performance of the line. The experience in operation of the 110 kV Jiande-Jiangjia Line and 220 kV Xuefeng Line and the experience in operation of the transmission lines in Zhejiang Province and Jiangxi Province, etc., show that the installation of the sideward lightning rod can reduce effectively the shielding failure trip-out rate of the transmission line. Moreover, as the sideward lightning rod also has the advantages of economy, durability and convenience in installation and maintenance, etc., its application in the lightning protection of the UHV strain tower and angle tower can be especially considered.

8.2 Lightning Protection of the UHV Substations (Switch Stations)

8.2.1 Overview

The importance of the UHV substations (switch stations) as the hub of the UHV power grid is self-evident. If a lightning strike accident occurs to the UHV substation, it may cause large-area and long-time power outage, seriously affecting the national economy and the peoples' lives.

The lightning hazard on the primary side of the UHV substation may come from two aspects: one is the direct lightning striking overvoltage, i.e., the lightning directly strikes the facilities in the substation; and the other is the lightning intruding overvoltage, i.e., the lightning overvoltage generated by the striking of lightning on the overhead transmission line invades the substation along the line.

The main measure to prevent from the direct lightning strike in the UHV substation is also the use of lightning rod or overhead ground wire. Both these two measures are used in the UHV substations in the former Soviet Union and China; while mostly, only the overhead ground wire is used in Japan. With reference to China's experience in operating the 110–500 kV substations for many years, so long as the lightning rods, overhead ground wires and grounding devices are properly installed in the substations as required by the Standards, the effect on preventing from the direct lightning strike is reliable. Therefore, the prevention from direct lightning strike in the UHV substations is not a big problem.

In consideration that the probability of striking of lightning on the transmission line is much larger than that directly on the substation, and the HV and EHV substations' reliability in protection from the direct lightning strike is higher than that from the lightning invasion wave; therefore, the lightning invasion wave may be the main cause for the lightning accidents of the UHV substations and needs to be specially protected.

Compared to the HV and EHV substations, the UHV substation's lightning invasion wave protection has some unique features:

(1) The UHV substation has higher requirements on lightning withstand level

The UHV substation, due to its high-voltage level and more important position in the power grid, has higher requirements on protection. The safe operation life of the 1150 kV substation as recommended in Russia's 1999 *Manual* is 1200–1500 years [1]. In consideration that the safe operation life of China's 500 kV substation is 800–1000 years, it is specified in China's National Standard GB/Z 24842-2009 *Overvoltage and Insulation Coordination of 1000 kV UHV AC Transmission Project* that the safe operation life of the UHV substation shall not be less than 1500 years [8].

(2) The UHV substation's capability to withstand against lightning intruding overvoltage is improved significantly

The UHV substation's capability to withstand against the lightning intruding overvoltage is improved mainly because of the following reasons: ① the insulation level of the devices within the substation has greatly improved compared to that of the EHV system; ② for the purpose of limiting the switching overvoltage of the line, MOAs are installed at the substation's incoming lines and transformers, and, in addition, MOAs are also normally installed at the busbars for the sake of safety, which also greatly improves the lightning withstand performance of the UHV substation; ③ the back flashover lightning withstand level of the incoming line section is very high (>250 kA), so it can be deemed that the back flashover lightning intruding overvoltage normally does not appear.

(3) The shielding failure lightning intruding overvoltage has become the key point of protection for the UHV substation

There are two types of lightning invasion waves in the substation: one is the back flashover lightning intruding overvoltage generated by the insulation back flashover resulting from the striking of lightning on the tower or the overhead ground wire; the other is the shielding failure lightning intruding overvoltage generated by the striking of lightning on the conductor. However, for the UHV substation, due to the high back flashover lightning withstand level of the incoming line section, the back flashover normally does not happen, so the probability of the generation of the back flashover lightning invasion wave is very low. For the shielding failure lightning intruding overvoltage, although the protection angle of the incoming line section of the UHV line is normally very small, but because of the high height of the UHV tower and the large clearance between the overhead ground wire and the conductor, the maximum shielding failure lightning current of the incoming line section may still be large, so the shielding failure lightning intruding overvoltage shall be taken as the key point of protection for the UHV substation.

8.2.2 Assessment Methods for the Lightning Withstand Performance of the UHV Substation

The first part of this subsection will describe the modeling methods for the simulation calculation of the lightning intruding overvoltage; the second part will describe the assessment methods for the substation lightning withstand performance used in the actual project (i.e., the routine method and the statistical method); finally, as a reference and for comparison purpose, Japan's calculation method for the lightning intruding overvoltage of the UHV substation will be given.

8.2.2.1 Models for Simulation Calculation of Lightning Intruding Overvoltage

Currently, the substation lightning intruding overvoltage is normally studied by the numerical simulation methods. Russia uses its self-developed special numerical simulation calculation program to calculate the lightning intruding overvoltage of the UHV substation, while China and Japan use the electro-magnetic transient software EMTP for calculation [22, 27].

I. Models for simulation calculation

The lightning intruding overvoltage of the substation depends on the amplitude and the waveform of the overvoltage invading the substation from the overhead line, and the traveling wave characteristics of the substation itself. Therefore, to accurately simulate the actual situation of the lightning intruding overvoltage of the UHV substation, the lightning source, the substation, and the incoming line section shall be combined together and regarded as a unified system for analysis.

The simulation model for the "lightning source-incoming line section-substation" unified system is established as follows:

1. Lightning source model

There are two methods for the simulation of the lightning source, which are the voltage source method and the current source method. To simulate the waveform of the actual lightning invasion wave more accurately, the ideal current source is normally adopted and also recommended by IEC.

For the lightning protection calculation of China's UHV substations, the use of current source method is recommended. Similar to the lightning protection design of the transmission line, the lightning current source can be equivalent to an ideal current source and wave impedance in parallel—the ideal current source adopts negative 2.6/50 μs double oblique wave; during the back flashover calculation, the lightning channel wave impedance is about 250–400 Ω, usually taken as 300 Ω; during the shielding failure calculation, the lightning channel wave impedance is about 600–1000 Ω, usually taken as 800 Ω.

2. Incoming line section model

In China's power system, the incoming line section is the line of about 2 km starting from the substation. If the gantry tower in the UHV substation is numbered as #0 tower, the towers outside are successively numbered as #1 tower, #2 tower, etc., and the spans between the towers except that between #0 and #1 towers are mostly within the range of 400–500 m, then the incoming line section normally includes five towers (#1–#5), and the striking of lightning on #6 tower can be regarded as the far-field lightning strike.

In the lightning protection calculation of China's UHV substations, the near-field lightning strike is normally taken into consideration, that is, the simulation model shall accurately simulate #1–#5 towers and the spans between the towers, while the

far-field line beyond #6 tower can be replaced by the equivalent impedance. If the far-field lightning strike needs to be verified, then #6 tower and several towers after it shall be accurately simulated, and similarly the line beyond shall be replaced by the equivalent impedance.

The specific simulation model for the incoming line section involves the establishment of equivalent models for conductor and overhead ground wire, tower and tower impulse grounding resistance, and the reasonable selection of lightning flashover criteria. The method for establishing the incoming line section model is the same as the lightning protection design of the transmission line, that is, J-Marti model is used for the conductor and the overhead ground wire, the segmented wave impedance model is used for the tower, and the intersection method is used for the line insulation flashover criteria.

3. Substation model

During the calculation of the lightning intruding overvoltage, the following devices inside the substation shall be considered: transformers, arresters, busbars, reactors, circuit breakers, disconnectors, current transformers, voltage transformers, and in-substation conductors (or GIS cables). The establishment of substation model shall follow the following principles:

① The conductors and busbars in the substation shall use the distributed parameter line model, in which the GIS busbar can be simulated by the single-phase Clarke model (there is no coupling among the busbars of three phases and each single-phase enclosed busbar can be treated as a single-phase conductor.);
② The in-substation equipment such as transformers, reactors, voltage transformers, current transformers, disconnectors, circuit breakers, and GIS outgoing line bushings shall be simulated by the equivalent inlet capacitance;
③ The relative positions and distances of equipment in the substation shall be treated according to the actual mounting positions and the measured distances;
④ The insulation margins of all electrical equipment within the substation must be considered. Usually, with reference to IEC standards, the internal insulation margin is taken as 1.15 and the external insulation margin is taken as 1.05–1.0 (the smaller external insulation margin is mainly due to no cumulative effect).

The transformers, the GIS wave impedance and arresters can be treated as follows:

(1) Transformer is inlet capacitance

The transformer is equivalent inlet capacitance which normally adopts the data provided by the manufacturer. In case of lacking this data, it may be taken as 5000 pF.

(2) GIS wave impedance

The UHV GIS is of the single-phase single-sleeve structure, and the wave impedance can be used in the lightning protection calculation during simulation. The GIS wave impedance is normally between 60 and 100 Ω, about 1/5 of that for the overhead lines. The specific GIS wave impedance may be estimated by the following equation:

$$Z_{\mathrm{GIS}} \approx \frac{1}{\sqrt{\varepsilon_{\mathrm{r}}}} 60 \ln \frac{R_1}{r_1} \tag{8.41}$$

where

ε_{r} is the relative dielectric constant of SF_6 gas, being about 1;
R_1 is the inner radius of the busbar sleeve, in m;
r_1 is the outer radius of the busbar conducting rod, in m.

As for the wave propagation speed in GIS, because of the relative dielectric constant of SF_6 gas $\varepsilon_{\mathrm{r}} \approx 1$, it is normally deemed that its wave speed is equal to the speed of light.

(3) Arrester

In the simulation calculation with EMTP software, the volt–ampere characteristics of arresters shall be treated with the method of piecewise linearization. The electrical characteristics of the metal oxide arresters in a 1000 kV AIS substation in China are shown in Table 8.10.

To simulate the lightning intruding overvoltage accurately, the total simulation time shall not be less than 10 μs, and the value of the step length shall not be less than the transmission time of the lightning wave in the shortest wave impedance of the simulation model. During the calculation of the lightning intruding overvoltage, if one of the following two conditions is met, failure can be judged to have occurred to the substation insulation: ① the overvoltage on the equipment within the substation is greater than the allowable overvoltage value of the equipment (i.e., the equipment lightning impulse withstand voltage divided by the margin coefficient); ② the discharge current in the arrester is greater than the nominal discharge current 20 kA thereof. Furthermore, the impact of the corona is usually not considered, so the calculation results are a bit strict.

Table 8.10 Electrical characteristics of the metal oxide arresters in a 1000 kV AIS substation in China

Installation location	Rated voltage (kV)	Residual voltage value under different discharge currents (kV)			
		8 mA	2 kA	10 kA	20 kA
In the substation/on the line side	828	1114	1460	1553	1620

II. Analysis on affecting factors

The lightning intruding overvoltage of the substation may be affected by many factors, including the point of strike, the lightning current amplitude and steepness, the invasion wave type (the shielding failure or the back flashover), the substation operating mode, the electrical distance between the in-substation equipment and arresters, the overhead ground wire protection angle of the incoming line section, the tower grounding resistance, the tower type, and the tower height. In addition, the phase angle of conductors' power frequency voltage and the incoming line section's insulation level, etc., also have a certain impact on the lightning intruding overvoltage.

Among these factors, the substation operating mode, the point of strike, and the lightning current amplitude and steepness have a relatively large impact on the lightning intruding overvoltage of the substation, and is specially analyzed as below.

1. Operating modes of substation

When the substation is under different operating modes, the overvoltage amplitudes on the in-substation equipment caused by the lightning invasion wave may vary widely. This is because, under various operating modes, the substation may subject to, the more the in-substation equipment (including the incoming line and the transformer) are put into operation, the greater degree the lightning current is shunted and the lower the lightning intruding overvoltage amplitude is.

It is specified in China's National Standard GB/Z 24842 ~ 2009 *OverVoltage and Insulation Coordination of 1000 kV UHV AC Transmission Project* that both the normal and the special operating modes shall be considered in forecasting the UHV substation's lightning overvoltage [8].

(1) Normal operating mode

The selection of the normal operating mode shall follow the same method of the HV and EHV substations. The selection methods of various research institutions may vary. The common selection methods for the normal operating mode are as follows:

① Selection of the most severe single-line and single-transformer mode, including the mode of single-line, single-transformer, and single-busbar or the mode of single-line, single-transformer, and double-busbar;
② "$N-m$" method, that is, the substation operating mode is selected as per the "$N-1$" or "$N-2$" principle;
③ Selection of the most severe operating mode that may arise in the storm season;
④ Statistical method, that is, the safe operation life of the substation under all possible operating modes in the lightning season is calculated first and then weighted and averaged according to the probability of occurrence thereof.

Since the probabilities of occurrence of various operating modes of the substation are difficult to accurately predict, for the purpose of safety, the single-line and single-transformer operating mode is recommended for the UHV substation lightning protection calculation. In addition, as the double busbars of the substation normally operate simultaneously, and the terminals of the busbar are often the furthest part away from the arrester, and the lightning intruding overvoltage with the maximum amplitude also often appears at this place, during the simulation calculation, the double busbars shall be simultaneously put into operation, that is, the single-line, single-transformer, and double-busbar mode shall be used. During the selection of the specific single-line, single-transformer, and double-busbar mode, the two affecting factors, i.e., the relative distance between the equipment and the arrester and the number of the equipment put into operation, shall all be considered.

(2) Special operating mode

During the calculation of the lightning invasion wave of the 1000 kV substation, the special operating mode, i.e., single line—the circuit breaker of the outgoing line is on–off state (also known as "single-line mode") which shall also be taken into consideration. This operating mode refers to the state in which the circuit breaker on the line-side opens and the disconnectors on both sides have been closed, and mainly appears in the following two situations: one is that the circuit breaker is in hot standby state, and the other is that the circuit breaker trips due to the line failure and fails to reclose.

This operating mode is the most severe operating mode for the analysis of the lightning invasion wave of the UHV substation, and is not considered at the time of the arrester configuration in China's 500 and 750 kV substations. However, under the single-line operating mode, many accidents in which the circuit breakers are destroyed by the invasion wave have occurred in China's 220 and 500 kV substations. Besides, in consideration of the importance of the UHV substation, it is recommended to consider the single-line operating mode. It shall be noted that the overvoltage under the single-line operating mode is more serious than that under the normal operating mode, but the probability of occurrence of the lightning invasion wave under the single-line operating mode is relatively low.

In summary, during the calculation of the lightning intruding overvoltage of the UHV substation, both the normal operating mode and the special operating mode (the single-line mode) shall be considered. Among the normal operating modes, the single-line, single-transformer, and double-busbar operating mode is the most typical mode and shall be specially considered.

2. Location of point of strike

According to the provisions of China's current procedure DL/T 620-1997, it shall be ensured that the lightning intruding overvoltage generated by the far-field lightning strike more than 2 km away from the substation does not cause damage to the insulation of the in-substation equipment, while the near-field lightning strike is

not considered [10]. This follows the practice for low-voltage-level substations, but is unreasonable in the EHV and UHV systems. In the past, due to the low transmission voltage levels, the overhead ground wires might not be provided along the whole line or its protection angle was large. To prevent from the damage by the lightning intruding overvoltage, it is specified in the procedure that the overhead ground wires must be provided in the incoming line section, and, at the same time, more stringent requirements are proposed for the protection angle and the grounding resistance. Therefore, the lightning withstand performance of the incoming line section is much better than that of the nonincoming line sections, and the probability of lightning invading substation of the incoming line section is rather smaller compared with that of the nonincoming line sections. Therefore, it is deemed in the procedure that the lightning overvoltage invading the substation is mostly from the far-field lightning strike.

Nevertheless, in the study of the protection from the lightning invasion wave of the UHV substation (switch station), the focus shall be placed on the near-field lightning strike. This is because that, for the EHV and UHV systems provided with double overhead ground wires along the whole line, the strict lightning protection measures have already been taken, so there is no essential difference between the lightning withstand performances of the incoming line section and the nonincoming line sections. For the far-field lightning strike 2 km away, because of the corona attenuation and the line damping effect, the steepness and the amplitude of the lightning invasion wave are both significantly reduced, and the overvoltage formed on the equipment inside the UHV substation normally will not damage the equipment insulation. In such case, the hazard of near-field lightning strike becomes prominent. In fact, the United States, Western Europe, Japan, and CIGRE Working Group all take the near-field lightning strike as the main object of study for the substation invasion wave [28–30].

For the near-field lightning strike, the strike of lightning on which tower or which span causes the most serious lightning intruding overvoltage is discussed in detail as follows:

(1) Back flashover invasion wave

The farther the point of strike is away from the substation, the lower the amplitude and steepness of the back flashover invasion wave caused by the same lightning current will be. In China, the distance between #1 tower and #0 gantry type tower is very close (with actual distance normally less than 100 m), plus that the grounding resistance of 0# tower is normally very small, due to the limitation of the reflected wave of opposite polarity from #0 tower, the insulation flashover is not easy to happen on #1 tower to form a back flashover invasion wave. And even when the flashover happens, the caused overvoltage on the equipment inside the substation is low. Therefore, the lightning invasion wave caused by the strike of lightning on #2 tower may be the most serious. Because of this, the research on the back flashover lightning invasion wave of China's UHV substations focuses on the direct strike of lightning on #2 tower.

However, the above conclusion applies only to the case in which the span between #0 tower and #1 tower is very small. For the cases in which the span between #0 tower and #1 tower is large, the point of strike shall be selected on #1 tower or #0 tower, and confirmed by simulation calculation.

In addition, when the statistical method is used to assess the substation's performance against the back flashover lightning invasion wave, the back flashover lightning intruding overvoltage caused by the strike of the lightning on other towers shall also be considered.

It is noteworthy that, in the UHV system, the back flashover lightning withstand level of the line is very high, and the probability of the insulation back flashover is extremely small. For China's UHV demonstration project lines, even the lightning current up to 300 kA does not cause line insulation flashover. Therefore, the lightning intruding overvoltage of the UHV substation mainly results from the near-filed shielding failure.

(2) Shielding failure invasion wave

For the shielding failure invasion wave, the research is focused on the strike of lightning on the conductors near #1 tower, which is also recommended by IEC. For the #0 tower located inside the substation, as it is under the protection of the direct lightning protection device in the substation, it is normally deemed that the conductors near it do not be stricken by the lightning. In addition, as the conductors near the towers are high in position, their probability of being stricken by the lightning is the largest. Therefore, in the invasion wave calculation, the point of the strike can normally be selected on the conductors near #1 tower.

Similarly, when the statistical method is used to assess the substation's performance against the shielding failure lightning invasion wave, the lightning intruding overvoltage generated by the shielding failure at the incoming (outgoing) line and other positions shall also be studied.

In summary, based on China's specific conditions, the calculation of the lightning invasion wave of the UHV substation shall focus on the near-field lightning strike. For the amplitude of the overvoltage caused by the lightning invasion wave on the device in the substation, it is normally deemed that the back flashover lightning intruding overvoltage caused by the strike of the lightning on #2 tower is relatively severe, and the shielding failure lightning intruding overvoltage caused by the strike of lightning on the conductors near #1 tower is relatively serious.

(3) Amplitude and steepness of lightning current

(1) Lightning current amplitude

In the lightning protection calculation of the UHV substation, the different assessment methods for lightning withstand reliability indexes may take different lightning current amplitude values. The following shows the range of the lightning current amplitude, while the specific values need to be determined based on the assessment methods.

In the calculation of the back flashover invasion wave overvoltage, the back flashover lightning current amplitude is ranged in [I_2, I_∞], in which, I_2 is the back flashover lightning withstand level of the incoming line section, in kA; I_∞ is the maximum lightning current in nature obtained by statistics and may be taken as 300 kA.

In the calculation of the shielding failure invasion wave overvoltage, the shielding failure lightning current amplitude is ranged in [$I_{\min}$, $I_{\max}$], in which, $I_{\min}$ is the minimum lightning current in nature obtained by statistics, in kA. $I_{\max}$ is the maximum shielding failure lightning current and can be determined by the EGM method.

In the calculation of the maximum shielding failure lightning current $I_{\max}$, the maximum strike distance r_{s_max} that the lightning can strike the conductor can be calculated first, and then, the strike distance equation can be used to obtain $I_{\max}$ through reverse deduction. In consideration of the impact of the ground inclination angle, the general calculation equation for the maximum strike distance r_{s_max} is as follows:

$$\begin{cases} r_{s_max} = \dfrac{k(h+y)+\sqrt{(h+y)^2-G}\sin(\theta_s-\theta_g)}{2F}\cos\theta_g \\ F = k^2-\sin^2(\theta_s-\theta_g) \\ G = F\left[\dfrac{h-y}{\cos(\theta_s-\theta_g)}\right]^2 \end{cases} \tag{8.42}$$

where

h is the overhead ground wire's average height to ground, in m;
y is the conductor's average height to ground, in m;
k is the striking distance factor;
θ_s is the overhead ground wire protection angle, in °;
θ_g is the ground inclination angle, in °. It should be noted that the sign of θ_g is "−" when the ground inclination angle slopes downward at the tower, and "+" otherwise.

(2) Lightning current steepness

It can be known from the protection principle of the arrester (as shown in Fig. 8.30) that, for the lightning invasion wave, the voltage difference between the arrester and the protected equipment is as follows:

$$\Delta U = 2\alpha\Delta t = 2\alpha\frac{\Delta l}{v} \tag{8.43}$$

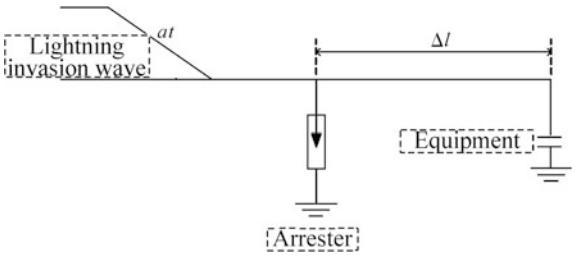

Fig. 8.30 Sketch for locations of the arrester and the protected equipment in the substation

where

α is the lightning current steepness, in kA/μs;
Δt is the shortest propagation time of the lightning invasion wave between the arrester and the protected equipment, in μs;
Δl is the shortest electrical distance between the arrester and the protected equipment, in m;
v is the propagation velocity of the lightning invasion wave, in m/μs.

It can be known from Eq. (8.43) that the lightning intruding overvoltage on the equipment in the substation is directly related to the lightning invasion wave steepness, which is a more important parameter compared to the magnitude.

Studies have shown that the time to wavefront of lightning current is associated with the amplitude (about 20 kA/μs), that is, the lightning current steepness is considered to be related to the amplitude. However, currently, in the calculation of the lightning invasion wave of the UHV substations, Russia, Japan, and China do not consider the correlativity between the time to wavefront of lightning current and the amplitude. For instance, Russia considers the lightning current amplitude and steepness as mutually independent normal distribution; Japan has the lightning current waveform taken as 1/70 μs; while China, in the lightning protection calculation of the power system, defines the lightning current waveform as 2.6/50 μs, that is, the lightning current steepness is stipulated to be proportional to the amplitude.

Normally, it is believed that the minimum time to wavefront of lightning current is about 0.5–1 μs, while, in consideration of the distortion effect of the corona on the lightning current waveform, the actual time to wavefront of the lightning wave invading the substation shall not be less than 1 μs. Therefore, for the calculation of substation lightning invasion wave, Japan's lightning current steepness value is stringent.

8.2.2.2 Assessment Methods for Lightning Withstand Reliability Indexes

The assessment methods for the lightning withstand reliability indexes of the substation include the routine method (also known as "certainty method") and the

statistical method. The difference between the two methods is that different treatment methods are used for the affecting factors of lightning intruding overvoltage, including the substation operating mode, the point of strike, the lightning current amplitude and steepness, and the instantaneous value of power frequency voltage on conductors at the moment of lightning strike. In the two assessment methods, the routine method only considers the typical cases of various affecting factors, with advantages of intuition and simpleness, and is mainly used to determine the layout scheme for the arresters in the substation and the insulation level of the in-substation equipment; while the statistical method has the probability of occurrence of each factor considered and can be used for the quantitative calculation of the safe operation life of the substation under lightning protection.

1. Routine method

The calculation principle of the routine method is to first determine the representative (or the most dangerous) overvoltage acting on the insulation, and then, based on the operating experience, select a large enough margin coefficient, which can offset the error resulting from the impacts of various factors during the estimation of the maximum overvoltage, and finally multiply the maximum overvoltage by the margin coefficient to obtain the insulation level.

In the simulation calculation of the substation lightning invasion wave, the general practice of the routine method is to select the representative or the most serious case of each factor to figure out the value of the lightning overvoltage of the in-substation equipment under such case, and thus to verify if the lightning protection scheme for the substation meets the requirements. When the routine method is used to calculate the lightning intruding overvoltage of China's UHV substations, the relevant parameters may be taken as follows:

For the lightning current:

① The lightning current waveform adopts 2.6/50 μs double oblique wave.
② For the lightning channel wave impedance, during the calculation of the back flashover lightning invasion wave, it is taken as 300 Ω; during the calculation of the shielding failure lightning invasion wave, it is taken as 800 Ω;
③ For the lightning current amplitude, it is taken as 250 kA for the back flashover calculation, and taken as the maximum shielding failure lightning current I_{max} for the shielding failure calculation;
④ For the point of strike, during the calculation of the back flashover invasion wave, in case #0 tower and #1 tower are close to each other, #2 tower shall be selected, and in case the distance is long, #1 tower shall be selected; during the calculation of shielding failure lightning invasion wave, the conductors near #1 tower shall be selected.

For the incoming line section:

① The incoming line section (i.e., #1–#5 towers and the spans among them) shall be accurately simulated, the conductors and overhead ground wires adopt J-Marti model, the towers adopt the segmented wave impedance model, and the tower grounding resistance adopts the measured value;
② The far-field lines beyond #6 tower can be replaced by the equivalent impedance Z_{eq};
③ The intersection method shall be used as the line insulation flashover criteria;
④ For the power frequency voltage, an AC voltage source can be connected at the equivalent impedance for equivalence, and the value of the line voltage can be taken as 1100 kV.

The selection methods for the substation operating modes can be referred to Sect. 8.2.2.1. Among them, the single-line, single-transformer, and double-busbar mode and the single-line mode are the most typical modes and shall be specially considered.

In summary, the advantages of the routine method are intuition and simpleness. Besides, the insulation level of the substation determined by this method has a large margin. This method can be mainly used to determine the layout scheme for the arresters in the substation and the insulation level of in-substation equipment.

However, the probabilities of occurrence of the substation's various operating modes, points of strike, and lightning current amplitudes and steepnesses, etc., are not considered in the routine method, so the probability of the insulation failure cannot be quantitatively estimated. Because of this, the insulation requirements are a little strict and the investment costs are a little high. To overcome this drawback, some people in China and abroad use the statistical method to analyze the lightning protection reliability of the substation.

2. Statistical method

With the statistical method, the probabilities of occurrence of all affecting factors can be considered, and the probability of discharge in the insulation of the in-substation equipment can be quantitatively estimated, so that the safe operation life of the substation under the lightning invasion wave can be calculated.

However, the occurrence probabilities of partial affecting factors of the lightning intruding overvoltage (e.g. substation operating mode) are difficult to accurately predict, so a simplified interval combination statistical method can be used—for the affecting factors whose occurrence probabilities are difficult to predict, e.g., the substation operating mode (including the single-line, single-transformer, and double-busbar mode and the single-line mode), the typical values thereof shall be taken. For the factors whose occurrence probabilities can be estimated, such as the point of strike, the lightning current amplitude and the power frequency voltage phase angle, treatment can be carried out through the statistical method.

The basic idea of the interval combined statistical method is that the frequency of the occurrence of the dangerous lightning invasion wave is dependent on the lightning withstand performance of the overhead lines connected to the substation. The specific calculation steps are as follows:

(1) Segmented treatment of lightning current

All the lightning current that may form the lightning invasion wave shall be treated in segments, and the average value of the lightning current amplitude of each segment shall be taken as the lightning current of this segment. Among them, the back flashover lightning current is ranged in [I_2, 300 kA], and the shielding failure lightning current is ranged in [$I_{\min}$, $I_{\max}$].

(2) Calculation of the dangerous length of incoming line section

The dangerous length of the incoming line section of the substation corresponding to each small segment of the lightning current shall be calculated. Due to the corona attenuation and the line damping effect, only when the lightning current with certain amplitude strikes the dangerous section of the incoming line corresponding to it, the overvoltage that is dangerous to the substation insulation will be produced.

(3) Calculation of the frequency of dangerous overvoltage for substation

The sum of the total frequencies of the dangerous overvoltage resulting from the strike of lightning on the incoming line of substation within 1 year is the annual probability of the substation suffering from the lightning hazards. Since the probabilities of the occurrence of the back flashover lightning invasion wave and the shielding failure lightning invasion wave have their own statistical methods, they shall be calculated separately.

The annual average frequency of the dangerous overvoltage caused by the back flashover lightning invasion wave shall be determined by the following equation:

$$N_{\text{backflashover}} = \sum_{j=1}^{n} \left[(1 - k_{\text{j}}) N_{\text{g}} W g \eta \sum_{i=1}^{m} (p_{\Delta \text{i}} l_{\Delta \text{i}}) \right] \tag{8.44}$$

where

n is the number of the substation incoming (or outgoing) lines taken for the calculation of the lightning intruding overvoltage;
k_{j} is the shielding factor of the other lines of the substation to the jth line;
N_{g} is the annual ground lightning density in the substation area, in time/(km^2 ·a);
W is the lightning strike width of the line, in km;
g is the lightning striking rate against the pole;
η is the arcing rate;
$p_{\Delta \text{i}}$ is the probability of the lightning current in the interval $I_{\text{i}} \leq I \leq I_{\text{i+1}}$;
$l_{\Delta \text{i}}$ is the dangerous length of the incoming line corresponding to the lightning current amplitude $I_{\text{i}} \leq I \leq I_{\text{i+1}}$, in km.

The annual frequency of the dangerous overvoltage caused by the shielding failure lightning invasion waves shall be calculated as follows:

$$N_{\text{shielding}} = \sum_{j=1}^{n} \left[(1 - k_{\text{j}}) N_{\text{g}} W \sum_{i=1}^{m'} (p_{\Delta \text{i}} p_{a\Delta \text{i}} l_{\Delta \text{i}}) \right] \tag{8.45}$$

where

$p_{\alpha\Delta \text{i}}$ is the shielding failure rate corresponding to the lightning current amplitude $I_{\text{i}} \leq I \leq I_{\text{i+1}}$, which can be obtained by the EGM method.

The annual frequency of the dangerous overvoltage invading the substation caused by the strike of lightning on the lines shall be as follows:

$$N = N_{\text{back}} + N_{\text{shielding}}. \tag{8.46}$$

(4) Calculation of the safe operation life for substation

The reciprocal of the dangerous overvoltage frequency N is the average safe operation life of the substation (the recurrence interval of the dangerous overvoltage), namely:

$$T = \frac{1}{N}. \tag{8.47}$$

In summary, the statistical method may be used to calculate the lightning withstand indexes of the substation quantitatively, and, in particular, can be used for the comparison of the lightning protection reliability of the substations with different voltage levels and different insulation types. However, the statistical method also has the defect of the cumbersome and complex calculation. Therefore, the specific assessment method for lightning withstand reliability shall be determined according to the specific project needs.

8.2.2.3 Japan's Calculation Method for Lightning Invasion Wave of the UHV Substations

For reference and comparison purpose, Japan's calculation method for the lightning intruding overvoltage of the UHV substations is described as below.

Japan adopts the routine method to analyze the lightning intruding overvoltage of the UHV substations. In addition, through the comparison of the routine methods used in China and Japan, it is found that the main difference between the calculation methods exists in the selection of lightning current sources, incoming line section parameters and the treatment of some affecting factors, as shown in Table 8.11.

Table 8.11 Main differences between the routine methods used by China and Japan to calculate the lightning invasion wave of the UHV substations

Simulation model		Country	
		China	Japan
Lightning current source	Invasion wave type	Shielding failure and back flashover	Back flashover
	Point of strike	Shielding failure: conductors near #1 tower Back flashover: #2 tower	Back flashover: #1 tower
	Lightning current waveform	2.6/50 μs	1/70 μs
	Lightning current amplitude	Shielding failure: maximum shielding failure lightning current I_{max} Back flashover: 250 kA	Back flashover: 200 kA
	Lightning channel wave impedance	Shielding failure: 800 Ω Back flashover: 300 Ω	Back flashover: 400 Ω
Incoming line section	Tower model	Segmented wave impedance model	Segmented transmission line model with damping branches
	Tower grounding resistance	In plain regions: 7 Ω In mountainous regions: 15 Ω	10 Ω
	Flashover criterion	Intersection method (voltage-time characteristic curve)	Leader progression model method
Substation	Operating mode	Single-line, single-transformer and double-busbar mode; single-line mode	Single-line mode; single-line and single-busbar mode; single-line, single-transformer and single-busbar mode
	Insulation margin	Outer insulation: 5% Inner insulation: 15%	0%

It can be known from Table 8.11 that, compared with China, the main differences of the calculation method used by Japan are as follows: ① Japan only calculates and verifies the back flashover lightning intruding overvoltage of the UHV substation, without considering the shielding failure lightning invasion wave; ② the first tower (i.e., #1 tower) of the incoming line section is taken as the point of strike, and the segmented transmission line model with damping branches is adopted as the tower model; (3) the lightning current waveform adopts the 1/70 μs double oblique wave, and the lightning current amplitude is taken as 200 kA (150 kA corresponding to 500 kV substation in Japan); (4) Japan deems that the calculation conditions are very strict, and hence, the insulation margin is taken as 0.

It can be known from Eq. (8.40) that, under the premise of the same layout scheme for the in-substation arresters, the factor mostly affecting the invasion wave overvoltage on the in-substation equipment is the invasion wave steepness. It can be

known from Table 8.11 that the lightning current steepness is taken as 200 kA/μs in Japan, while in China, both the shielding failure and the back flashover lightning current steepnesses are taken as I_{max} kA/2.6 μs and 250 kA/2.6 μs, respectively, which shows that the calculation conditions in Japan are stricter.

It is noteworthy that, in the determination of the maximum lightning overvoltage that can be withstood by the in-substation equipment, Japan's principle of insulation coordination of the UHV substation has a great difference from IEC standards, without safety margin reserved between the maximum lightning overvoltage and the rated lightning impulse withstand voltage.

8.2.3 Lightning Intruding Overvoltage Protection of the UHV Substations

8.2.3.1 Japan's Research on Lightning Invasion Wave Protection of the UHV Substations

During the design of the lightning invasion wave protection scheme for the UHV substation, the actual insulation level of the in-substation equipment and the overvoltage protection measures adopted shall be considered comprehensively. On the basis of safety and reliability, the economic requirements shall also be met as far as possible. Hereunder, with a typical substation in Japan's UHVAC system taken as an example, the selection method for its lightning invasion wave protection scheme is described.

Japan once adopted EMTP to analyze the lightning invasion wave protection scheme for a typically structured UHV substation of Tokyo Electric Power Company. The main connection of the substation is as shown in Fig. 8.31 [14, 31]. The substation under study is of the GIS structure, and adopts the double-busbar segmentation for the main electrical wiring, with a total of six circuits of UHV transmission lines and four banks of transformers.

It is known from the foregoing that, to limit the switching overvoltage of the UHV lines, a bank of MOAs needs to be installed at the substation's incoming (outgoing) line circuit breaker's line-side CVT and in the transformer circuit respectively, while, to limit the lightning intruding overvoltage, the digital simulation calculation is required to determine if MOAs need to be installed at the busbar and at the incoming line high-voltage shunt reactors, and the required number of MOAs as well as the distance from MOAs to the protected equipment.

In the practical engineering, the possible schemes for the installation of arresters in each busbar include three cases: not to install, to install one bank, and to install one bank at both ends, namely 0, 1, and 2 banks. The possible schemes for the installation of arresters at the shunt reactors include two cases, namely 0 and 1 banks. Under several operating wiring conditions, Japan carried out calculation and

comparison of the lightning impulse withstand voltage on the in-substation equipment and the costs incurred under the above six (3 × 2) arrester arrangement schemes. The results are as shown in Table 8.12.

It can be known from Table 8.12 that, under the condition that the extremely strict lightning invasion wave is selected, scheme F is the most economic, under which the lightning impulse withstand voltage of the transformer and the GIS is taken as 1950 and 2250 kV, respectively, and the corresponding arrester arrangement scheme is that: a bank of arresters is installed in each transformer circuit; a bank of arresters is installed at both ends of each busbar segment (i.e., two banks for each busbar segment), and a bank of arresters is installed at each line entry and at each shunt reactor (i.e., two banks for each outgoing line).

It can be known from Table 8.12 that, for the UHV substation, if the space inside the substation allows, the number of protective arresters can be considered to be appropriately increased. In terms of the overall economy, it is cost-effective, because it effectively controls the overvoltage throughout the substation, allowing all major electrical equipment to be adequately and effectively protected. And such design method and idea of the lightning protection scheme for the UHV substations in Japan is worthy of reference by China. China can refer to Japan's method, and comprehensively balance the selection of in-substation equipment insulation level

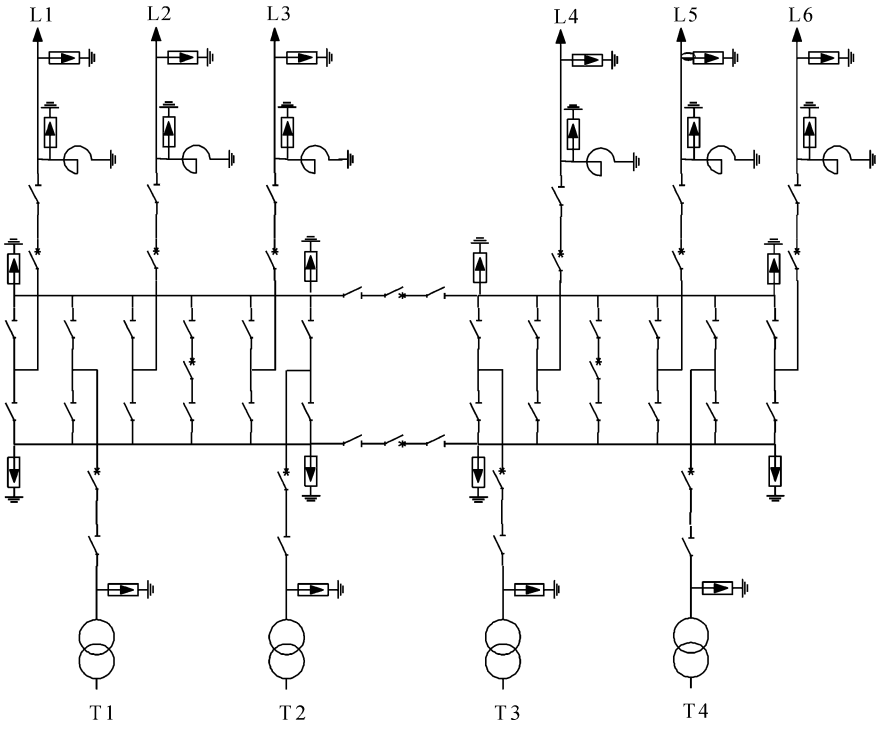

Fig. 8.31 Main wiring diagram for Japan's 1000 kV UHV GIS substation

Table 8.12 Relationship among MOAs arrangement schemes, equipment insulation levels and costs of Japan's UHV substations

		Scheme A	Scheme B	Scheme C	Scheme D	Scheme E	Scheme F
Number of arresters	At incoming line	1	1	1	2	2	2
	Busbar	0	1	2	0	1	2
	Transformer	1	1	1	1	1	1
Transformer	Required withstand voltage (kV)	1950	1943	1895	1943	1938	1896
	Adopted withstand voltage (kV)	1950	1950	1950	1950	1950	1950
GIS	Required withstand voltage (kV)	2898	2854	2703	2628	2506	2208
	Adopted withstand voltage (kV)	2900	2900	2900	2700	2550	2250
	Costs (assuming 100 for Scheme F)	102	105	109	103	103	100

and the application of overvoltage limiting measures (mainly the number of MOAs), considering both the safety and economy in the lightning protection of substation, to determine a reasonable insulation coordination scheme for the UHV substation.

8.2.3.2 China's Research on Lightning Invasion Wave Protection of the UHV Substations

Hereunder, with the 1000 kV Huainan GIS substation of the UHV power transmission project with double-circuit line on the same tower taken as an example, the maximum lightning overvoltage on the in-substation equipment under different operating modes is calculated, and the routine method is used to assess its lightning withstand reliability.

The main electrical wiring of Huainan 1000 kV substation (the initial design scheme) is as shown in Fig. 8.32. According to the specific conditions of the incoming line section, in case of the ground inclination angle of 0°, the maximum shielding failure lightning current on the conductors near #1 tower in the incoming line section calculated by EGM is 21 kA.

The insulation level of the UHV lines is very high, and the back flashover lightning withstand level is not less than 250 kA. The overvoltage transmitted into the substation is mainly the induced overvoltage, with low amplitude, so it is no longer considered. Here, only the shielding failure lightning intruding overvoltage under different operating modes and different arrester arrangement schemes is calculated, and the results therefrom are as shown in Tables 8.13 and 8.14, in which, T, REA, CVT, OGS, and BG represent the transformer, the high-voltage reactor, the capacitor voltage transformer, the open grounding switch, and the bushing, respectively.

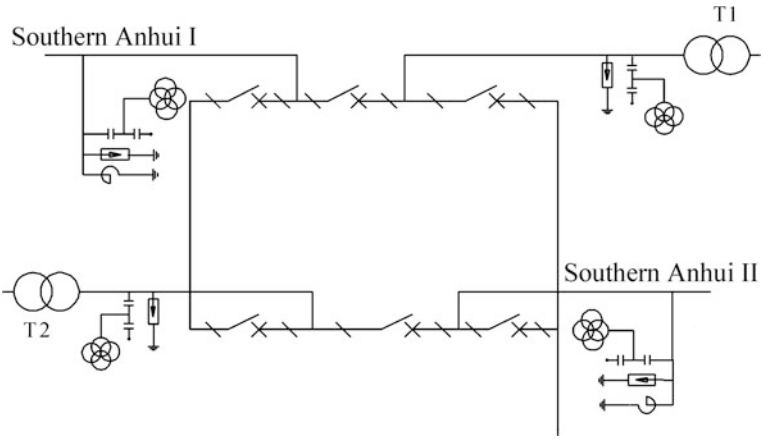

Fig. 8.32 Main electrical wiring diagram of Huainan 1000 kV substation

Table 8.13 Lightning intruding overvoltage of Huainan substation under single-line, single-transformer and double-busbar operating mode

MOA arrangement scheme	Value of lightning intruding overvoltage on the equipment within the substation (kV)						MOA current (kA)	
	T	ERA	CVT	OGS	GIS	BG	T	Others
Scheme 1	1610	1582	1677	1710	1924	1769	11	13
Scheme 2	1595	1536	1543	1549	1806	1681	9	<9
Scheme 3	1573	1514	1555	1506	1570	1545	7	<7
Allowable value	1957	1957	2087	2087	2087	2087	20	20

Note Under Scheme 1, a bank of MOAs is installed respectively near T and REA; under Scheme 2, a bank of MOAs is installed respectively near T, REA, and CVT; under Scheme 3, a bank of MOAs is installed respectively near T, REA, CVT, and each group of busbar. In addition, 15% of safety margin has been considered for the "allowable value" of overvoltage

Table 8.14 Lightning intruding overvoltage of Huainan substation under single-line operating mode

MOA arrangement scheme	Value of lightning intruding overvoltage on the devices within the substation (kV)					MOA current (kA)
	REA	CVT	OGS	GIS	BG	
Scheme 1	5329	5298	5306	5332	5319	0
Scheme 2	1728	1830	1915	2077	2034	21.99
Scheme 3	1638	1575	1564	1681	1646	9/11.2
Allowable value	1957	2087	2087	2087	2087	20

Note Under Scheme 1, no MOA is installed; under Scheme 2, a bank of MOAs is installed near REA; under Scheme 3, a bank of MOAs is respectively installed near REA and CVT

It can be known from Table 8.13 that, under the premise of the maximum shielding failure lightning current of 21 kA, for the single-line and single-transformer operating mode, even the use of Scheme 1 (that is, a bank of MOAs is respectively installed at REA and T only) can meet the insulation requirements of the in-substation equipment. In addition, for the GIS, if a bank of MOAs is added for each busbar segment, the overvoltage level thereof can be significantly reduced, so the addition of MOAs is recommended.

It can be known from Table 8.14 that, under the premise of the maximum shielding failure lightning current of 21 kA, for the single-line operating mode, the lightning intruding overvoltage level under Scheme 1 is significantly high; under Scheme 2 (only a bank of MOAs is installed at the incoming line), MOAs' discharge current can be a little bit large; both the in-substation equipment overvoltage level and the MOAs' discharge current under Scheme 3 reach the standard.

For the 1000 kV Huainan substation, based on the comprehensive consideration of the requirements on limiting the switching overvoltage, the following MOA arrangement scheme is recommended:

(1) Two banks of MOAs shall be installed at the incoming line end, in which, one bank shall be installed close to REA and the other bank shall be installed between CVT and GIS bushing and close to GIS as far as possible;
(2) One bank of MOAs shall be installed at the side of each transformer;
(3) One bank of MOAs shall be installed at each busbar side.

For the arrester arrangement scheme of the UHV substation, to limit the switching overvoltage, normally, it is required to install a bank of arresters at each incoming line end and near each transformer of the substation; to prevent the insulation breakdown accident between the open contacts of circuit breakers under the single-line operating mode, usually a bank of arresters shall be added at each incoming line end near GIS. It can also be known from the above analysis that, to reduce the lightning intruding overvoltage level on GIS, it is recommended to install a bank of arresters on each busbar segment. Based on the comprehensive consideration, the typical MOA arrangement of the UHV substation recommended in this book is as follows (the practical application of the scheme shall be subject to verification by numerical calculation):

(1) Two banks of MOAs shall be installed at the entry of each circuit of line, in which one bank shall be installed close to the high-voltage shunt reactor and the other bank shall be installed between CVT and GIS bushing and close to GIS as far as possible;
(2) One bank of MOAs shall be installed at the side of each transformer;
(3) One bank of MOAs shall be installed at each busbar segment.

8.2.4 Lightning Invasion Wave Protection Measures for the UHV Substations

Similar to the HV and EHV substations, the basic ideal of the lightning invasion wave protection for the UHV substation is also that: the installation of metal oxide arresters (MOAs) is the main measure to limit the substation lightning intruding overvoltage; moreover, to avoid the overburdening for MOAs (too high impulse current flowing through), it also needs the coordination of the "incoming line section protection".

1. MOA protection

The MOA protection of the substation includes the selection of the lightning impulse protection level of arresters and the determination of installation location and the number of arresters, in which the lightning impulse protection level of arresters is mainly determined by the manufacturing level of the arresters. Under the premise that the lightning impulse protection level of arresters has been determined, it is particular important to determine properly the installation location and the number of arresters.

It is specified in China's UHV standards that one bank of arresters shall normally be installed on each main transformer and each busbar segment of the substation. 1–2 bank(s) of arresters shall be installed at the entry of each circuit of line, and the location and the number of arresters shall be determined through the calculation of lightning intruding overvoltage.

Through the calculation and analysis, the typical MOA arrangement of the UHV substation recommended in this book (the practical application of the scheme shall be subject to verification by numerical calculation) is as follows:

(1) Two banks of MOAs shall be installed at the entry of each circuit of line, in which one bank shall be installed close to the high-voltage shunt reactor, and the other bank shall be installed between CVT and GIS bushing and close to GIS as far as possible (to prevent the insulation breakdown accident between the open contacts of circuit breakers under the single-line operating mode);
(2) One bank of MOAs shall be installed at the side of each transformer;
(3) One bank of MOAs shall be installed at each busbar segment.

2. Incoming line section protection

The incoming line section protection refers to strengthening the lightning protection measures on the incoming (outgoing) line section of the substation, e.g., reducing the tower grounding resistance in the incoming line section, reducing the overhead ground wire protection angle, and installing the line-mounted lightning arresters. Since the lightning invasion wave posing a threat to the safe operation of the UHV substation is usually caused by the near-field lightning strike and the lightning withstand performance of the incoming line section is directly related to the hazard extent of the lightning invasion wave to the substation, and thus, it is necessary to strengthen the incoming line section protection.

The incoming line section protection has two effects: ① to reduce the number of occurrences of shielding failures or back flashover, thus to minimize the number of dangerous lightning invasion waves generated on the incoming line section; ② to reduce the amplitude of the maximum shielding failure lightning current I_{max} of the incoming line section and improve the back flashover lightning withstand level, thus to limit the amplitude of the impulse current flowing through the MOA.

It is specified in China's UHV Standard GB/Z 24842 ~ 2009 *Overvoltage and Insulation Coordination of 1000 kV UHV AC Transmission Project* that measures shall be taken to reduce the probabilities of occurrence of the shielding failure and the back flashover to the conductors within the range of 2 km overhead incoming line section, and the back flashover lightning withstand level shall not be less than 250 kA. The protection angle of overhead ground wire shall be less than −4° in the plain regions and shall be further reduced in the mountainous regions if the conditions permit. The protection angle of the overhead ground wire to the jumper for the line strained angle towers shall be less than −4°, and other measures may also be taken for protection. In addition, when the distance between the two overhead

Fig. 8.33 Diagram of tower head of the tower in the incoming line section of China's UHVAC demonstration line

ground wires of the tower in the incoming line section of single-circuit line is more than four times the vertical distance between the conductor and the overhead ground wire, the third overhead ground wire shall be added to prevent the intermediate-phase conductor from being struck by lightning.

For China's UHVAC demonstration line projects, the lightning intruding overvoltage of substations is caused by the shielding failure of the incoming line section. To reduce the hazard of the shielding failure lightning invasion wave, the cup-type towers with negative protection angle (<−4°) are adopted in the incoming line section, and, to prevent the strike of lightning on the conductor between the two overhead ground wires, the third overhead ground wire is erected as shown in Fig. 8.33.

Through the calculation and analysis, the erection of three overhead ground wires in the incoming line section of the UHV lines is recommended in this book. The erection of three overhead ground wires can not only reduce the probability of the intermediate-phase conductor being subject to shielding failure, but also completely prevent the intermediate-phase conductor from being subject to the shielding failure. This measure also allows the outward expansion of the overhead ground wires at both sides to reduce the protection angle, thereby reducing the maximum shielding failure lightning current amplitude of the outside conductors, which is helpful to reduce the amplitude of the shielding failure lightning invasion wave. In addition, the erection of three overhead ground wires can further improve the back flashover lightning withstand level of the lines, and is also helpful to prevent from the back flashover lightning invasion wave. In short, the erection of three overhead ground wires is not only helpful to prevent from the shielding failure and back flashover lightning invasion waves, but also involves small investment. Therefore, it shall be a novel design idea for line lightning protection worthy of recommendation, being especially suitable for the large tower head lines' incoming line sections or the EHV/UHV large tower head and high tower lines.

References

1. Russian Electric Power and Electrification Joint Stock Company "Unified Energy System of Russia". Lightning and internal overvoltage protection guides for 6–1150 kV Networks. St. Petersburg: St. Petersburg Press; 1999.
2. Zhenya L. UHV power grid. Beijing: China Economic Press; 2005.
3. Ying X, Shiheng X. Overvoltage protection and insulation co-ordination of AC power system. Beijing: China Electric Power Press; 2006.
4. Xidong L, Changyu C, Yuanxiang Z. High voltage engineering. Beijing: Tsinghua University Press; 2004.
5. Zhenya L. Overvoltage and Insulation co-ordination of UHV AC system. Beijing: China Electric Power Press; 2008.
6. Hao Z. Self-learning guidance on high voltage technology. Zhejiang: Zhejiang University Press; 2001.
7. National Power Dispatching and Communication Center. Practical technology Q&A on power system relay protection. Beijing: China Electric Power Press; 2000.
8. GB/Z 24842-2009. Overvoltage and insulation coordination of 1000 kV UHV AC Transmission Project; 2009.
9. Ping S. Statistical analysis on lightning current amplitude measurement on 220 kV Xin-Hang line. Electr Power. 2000;33(3):72–5.
10. DL/T 620-1997. Overvoltage protection and insulation coordination for AC electrical installations; 1997.
11. Armstrong HR, Whitehead ER. Field and analytical studies of transmission line shielding. IEEE Trans Power Appar Syst. 1968;87(1):270–81.
12. Brown GW, Whitehead ER. Field and analytical studies of transmission line shielding: part II. IEEE Trans Power Appar Syst. 1969;88(5):671–626.
13. IEEE Std 1243-1997. IEEE guide for improving the lightning performance of transmission lines; 1997.
14. Ametani A, Kawamura T. A method of a lightning surge analysis recommended in Japan using EMTP. IEEE Trans Power Deliv. 2005;20(2):867–75.
15. Zhaoxiang Y, Li H, Ling X. Influence of different tower models on the lightning back-strike intruding wave overvoltage for UHV substation. High Volt Eng. 2008;34(5):867–72.
16. Sargent MA, Darveniza M. Tower surge impedance. IEEE Trans. 1969;PAS-88(5):193–204.
17. Hara T, Yamamoto O. Modeling of a transmission tower for lightning surge analysis. IEE PGTD. 1996;143(3):283–9.
18. IEC 60071-4. Insulation co-ordination-part 4: computational guide to insulation co-ordination and modeling of electrical networks; 2004.
19. IEC 60071-2. Insulation coordination-part 2: application guide; 1996.
20. Imece AF, Durbak DW, Elahi H, Kolluri S, Lux A, Mader D, McDemott TE, Morched A, Mousa AM, Natarajan R, Rugeles L, Tarasiewicz E. Modeling guidelines for fast front transients. IEEE Trans Power Deliv. 1996;11(1):493–506.
21. Jiahong C, Shanqiang G, Xiaolan L, Xuefang T. Analysis of lightning distribution characteristics for 1000 kV UHV AC transmission line corridor. Electr Power. 2007;40 (12):27–30.
22. Zhiheng S, Bincai Z, Hao Z, Deng X, Zhigang G, Wendong J, Cancan W, Wujun W, Ke S, Dongju W. Analysis on effect of protecting transmission lines from shielding failure by sideward rods installed onto crossarm of towers. Power Syst Technol. 2011;35(11):169–77.
23. GB 50665-2011. Code for design of 1000 kV overhead transmission line; 2011.
24. Guanjun Q, Xiaoyu W, Xianzhi X, Yan W, Yizheng D, Zhaolin L. The variation of shielding failure probability along transmission line. High Volt Eng. 1999;25(1):23–5.
25. Maocheng W, Zhiqu Z, Jie T, Xueqi C, Qiang L, Shanhao J, Haifeng D. Lightning shielding failure protection for 1000 kV single circuit UHVAC transmission line. Power Syst Technol. 2008;32(1):1–4.

26. Shengxue W, Guangning W, Jianbin F, Jun Zhou, Wei Jiang. Study on flashover of suspension insulator string caused by windage yaw in 500 kV transmission lines. Power Syst Technol. 2008;32(9):65–9.
27. Fei G, Weijiang C, Zhifang L, Xianglian Y. Protection of series compensation station against lightning intruded wave in 1000 kV AC transmission system. High Volt Eng. 2010;36 (9):2199–205.
28. Anderson JG, Clayton R, Elahi H, Eriksson AJ, Grzybowski S, Hileman AR, Janischewskyj W, Longo VJ, Moser CH, Mousa AM, Orville RE, Parrish DE, Rizk FAM, Renowden JR. Estimating lightning performance of transmission lines. II: Updates to analytical models. IEEE Trans Power Deliv. 1993;8(3):1254–67.
29. Anonymous. A simplified method for estimating lightning performance of transmission lines. IEEE Trans Power Appar Syst. 1985;104(4):918–32.
30. CIGRE SC33-WG01. CIGRE guide to procedure for estimating the lightning performances of transmission line. Parie: CIGRE SC33-WG01; 1991.
31. Insulation design of 1100 kV substation of Tokyo electric power company. In: Proceedings of international symposium of UHV transmission technology; 2005.

Chapter 9
Insulation Coordination of UHV Substations

Fei Su, Hao Zhou and Yang Li

With the high-voltage level and large transmission capacity, the UHV power grid has a very important position in the system. Therefore, compared to the power grid of low-voltage levels, the insulation coordination of the UHV power grid has its particularity. First, because of the important position of the UHV power grid in the power system, the insulation coordination of equipment must ensure a high stability of the system; second, due to the high requirements on the insulation of the UHV power grid, the investment on the insulation of the power transmission and transformation equipment accounts for a large proportion in the total investment of equipment, so the reasonable determination of the insulation level has a huge economic benefit; finally, due to the increase of voltage level, the overvoltage having a dominant role in the insulation coordination will differ from the low-voltage level systems, and the principles of insulation coordination will change accordingly.

In this chapter, the main method for insulation coordination of the UHV substation is discussed first, and then, the determination of the air clearance of substation and the selection of equipment insulation are discussed in detail.

F. Su (✉)
State Grid Jinan Power Supply Company, Jinan, Shandong
People's Republic of China
e-mail: 285701397@qq.com

H. Zhou
College of Electrical Engineering, Zhejiang University, Xihu District,
Hangzhou, Zhejiang, People's Republic of China
e-mail: zhouhao_ee@zju.edu.cn

Y. Li
State Grid Suzhou Power Supply Company, Suzhou, Jiangsu
People's Republic of China
e-mail: 1041204573@qq.com

© Zhejiang University Press, Hangzhou and Springer-Verlag GmbH Germany 2018

H. Zhou et al. (eds.), *Ultra-high Voltage AC/DC Power Transmission*,
Advanced Topics in Science and Technology in China,
https://doi.org/10.1007/978-3-662-54575-1_9

9.1 Basic Concept and Principles of Insulation Coordination

The insulation coordination refers to the reasonable determination of the insulation level of equipment based on a comprehensive consideration of the various voltage that the electrical equipment in the power system may be subject to (working voltage and overvoltage) the characteristics of the protection devices and the characteristics of the equipment insulation to withstand the various voltages applied, to minimize the equipment costs, maintenance costs, and the accident losses caused by insulation failure of the equipment, and to achieve the highest collectivity benefit in the economy and the safe operation.

For insulation coordination, it is necessary not only to well deal with the coordination relationship among various applied voltages, voltage-limiting measures, and equipment insulation withstand voltage technically, but also to well co-ordinate the relationship among the investment costs, maintenance costs, and accident losses economically. In this way, neither the unnecessary waste be caused due to the large equipment dimensions and too expensive manufacturing costs resulting from the too high insulation level being taken, nor is large increase in the losses incurred by power failures and maintenance costs caused by the increased accident rate of the equipment during operation resulting from the too low insulation level being taken. To achieve the purpose of optimal comprehensive economic benefit in the three aspects of equipment manufacturing costs, operation and maintenance costs, and accident losses, the impacts of many factors such as voltage level and system structure must be taken into account for insulation coordination.

The overvoltage to be considered for the insulation coordination mainly includes lightning overvoltage, switching overvoltage, and power frequency overvoltage. In the power grids of 220 kV and below, because of the low-voltage level, it is difficult to limit the lightning overvoltage to the internal overvoltage level. Therefore, the insulation level of the electrical equipment in these grids is mainly affected by the lightning overvoltage. For the EHV and UHV power grids above 220 kV, with the increase of voltage level, the amplitudes of switching overvoltage and power frequency overvoltage increase accordingly, while the hazards of lightning overvoltage have been greatly weakened due to the limitation by various lightning protection measures, so the internal overvoltage gradually plays a decisive role in the insulation coordination gradually. In the EHV insulation coordination, the switching overvoltage plays a dominant role. In the UHV power grid, the internal overvoltage is limited to 1.6–1.8 p.u., so the equipment insulation level in such case is mainly decided by power frequency overvoltage, long-duration working voltage, or switching overvoltage.

The insulation coordination involves line insulation coordination and substation insulation coordination, mainly covering the selection of type and number of insulators, the determination of distance from line to tower, the determination of air clearance of substation, and the determination of insulation level of equipment in substation.

For the above insulation coordination content, the three kinds of overvoltage have different effects, which need to be considered separately.

Line insulator: the selection of insulator type is determined mainly with reference to the pollution and altitude of the area in which the operation is carried out, and the string length is mainly determined by the maximum operating voltage of the system.

Line's air clearances: the impacts of tower type and wind deflection shall be considered for the determination of the clearances from the conductor to the tower. For the cat-head-type tower and the cup-type tower, the side-phase insulators usually use I-type strings, which need to be verified under the power frequency overvoltage, switching overvoltage, and lightning overvoltage to ensure that no clearance breakdown happens under the three overvoltages; the intermediate-phase insulators usually use V-type strings, and, as the clearance distance from the conductors to the tower window has been determined and is far beyond the requirements in the power frequency discharge voltage, normally, it only needs to verify if the clearance meets the required value of the discharge voltage of the switching overvoltage and lightning overvoltage; for the double-circuit tower's I-type insulators, the three-phase air clearances also need to be verified under the three types of overvoltage to ensure that the clearance breakdown does not occur.

Substation's air clearances: the air clearances not affected by wind deflection are mainly determined by the switching overvoltage; the air clearances affected by wind deflection need to be verified for compliance with the requirements in discharge distance under the three types of overvoltages.

Substation equipment insulation: the electric equipment shall be subject to the long-duration power frequency live-line test at factory to ensure its reliability under the continuous operating power frequency voltage. The impulse voltage withstand level of equipment shall be determined primarily through the selection of a certain coordination factor by reference to the protection level of arresters and the insulation characteristics of equipment.

9.2 Insulation Coordination Methods for UHV Power Grid

The insulation coordination methods can be divided into two categories: one is to use a series of coordination factors to determine the insulation level based on the operating experience and in consideration of the impacts of various factors, referred to as the conventional procedure. The other is to design the equipment insulation through the probabilistic method based on the condition that the flashover voltage under which insulation can be self-restored is a random variable, while the overvoltage applied to the insulation is also a random variable, referred to as the statistical procedure.

The conventional procedure is applicable to both the insulation with self-restoring capability (gas insulation) and the insulation without self-restoring capability (liquid or solid insulation). The statistical procedure requires a lot of insulation breakdown data which are difficult to obtain in the practical application, so it only applies to the self-restoring insulation.

1. Conventional procedure

The conventional procedure realizes the insulation coordination in accordance with the concepts of the maximum overvoltage acting on the insulation and the minimum insulating strength of equipment. With this method, the most dangerous overvoltage that may appear on the insulation of the electrical equipment shall be first determined and then multiplied by a margin coefficient in consideration of the impacts of various factors based on the experience, so as to determine the voltage level that the insulation shall withstand, namely:

$$U_{\mathrm{j}} = kU_{\mathrm{gmax}} \tag{9.1}$$

where

U_{j} the insulation level of equipment;
U_{gmax} the maximum overvoltage amplitude in the system;
k the coordination factor which is usually greater than 1.

The conventional procedure has the advantages of simplicity and intuition, but also has very obvious shortcomings. When this method is used for the determination of insulation level, it is normally required to provide a large margin, which often makes the determined insulation level a little high. For the UHV power grid, though the conventional procedure can ensure that the system has a high security, it can substantially increase the manufacturing costs of equipment. In addition, the use of conventional procedure cannot quantitatively estimate the probability of accidents that may occur to the equipment. Because of these shortcomings of the conventional procedure, the statistical procedure and the simplified statistical procedure have been gradually promoted and applied in the design of external insulation of the UHV power grid.

2. Statistical procedure

The statistical procedure is, based on the condition that the overvoltage amplitude and the insulation withstand strength are both random variables, to calculate the probability of insulation discharge and the line trip-out rate with the known probability distribution of overvoltage amplitude and insulation discharge voltage, and finally reasonably determine the insulation level based on the technical and economic comparisons.

Assuming that the overvoltage probability density function is $f(U)$, the insulation breakdown probability distribution function is $P(U)$, and $f(U)$ is unrelated to $P(U)$. As shown in Fig. 9.1, $f(U_0)\mathrm{d}U$ is the probability of occurrence of overvoltage within the range of $\mathrm{d}U$ in the vicinity of U_0, and $P(U_0)$ is the probability of

insulation breakdown under the action of overvoltage U_0. The probability of occurrence of such high overvoltage leading to the insulation breakdown can be obtained as follows:

$$\mathrm{d}R = P(U_0)f(U_0)\mathrm{d}U \tag{9.2}$$

where

$\mathrm{d}R$ the differential of failure rate, which corresponds to the small diagonally shaded area in Fig. 9.1.

Conventionally, during the overvoltage statistics, normally, the statistics is made only on the absolute values of the overvoltage, and the polarity is not distinguished (the positive and negative polarities can be considered as fifty–fifty), so that it can be obtained that the distribution range of overvoltage amplitude shall be $U_{\mathrm{xg}} \sim \infty$ (U_{xg} refers to the maximum working phase voltage amplitude of the system). The following equation can be obtained through the integral calculation of the discharge probability:

$$R = \text{Total shaded area} = \int_{U_{\mathrm{xg}}}^{\infty} P(U)f(U)\mathrm{d}U \tag{9.3}$$

where

R the accident probability of the insulation being broken down under the applied overvoltage, namely the failure rate.

It can be known from Eq. (9.3) that the failure rate R is the total shaded area in Fig. 9.1. If the insulating strength is increased, that is, the curve $P(U)$ moves to the

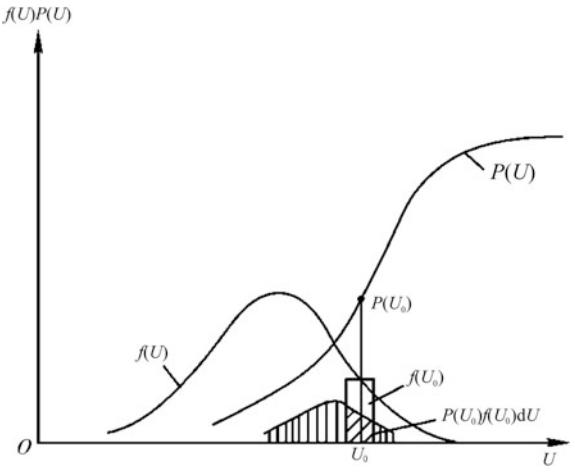

Fig. 9.1 Estimation of insulation failure rate, reprinted from Ref. [2], copyright 2014, with permission from China Electric Power Press

right, the shaded area will be reduced, the insulation failure rate will be reduced, but, at the same time, the cost of equipment investment will be increased. Therefore, the adoption of statistical procedure can have some key factors adjusted according to the needs, coordinate between the insulation cost and the failure rate through the technical and economic comparisons, and select the reasonable insulation level on the premise that the predetermined failure rate index is satisfied. Nevertheless, during the application, it shall be noted that the use of statistical procedure for the insulation coordination must have clear the probability distribution of the discharge voltage of the equipment insulation, which, however, is difficult to obtain in practice. Currently, the statistical procedure (including the simplified statistical procedure) is normally used only in the design of the external insulation of the UHV power grid.

3. Simplified statistical procedure

When the statistical procedure is used in the practical engineering for the insulation coordination, the process is relatively cumbersome. For this reason, the International Electrotechnical Commission (IEC) recommended a "simplified statistical procedure" to facilitate the practical application. Simply speaking, the simplified statistical procedure is the simplified calculation method combining the thoughts of both the statistical procedure and the conventional procedure.

In the simplified statistical procedure, it is assumed that the overvoltage and insulation discharge probabilities are both subject to the normal distribution, and that the mathematical expectation and standard deviation of their overvoltage (or overvoltage multiples) are known. Based on these assumptions, the overall probability distribution of the overvoltage and the electric insulation strength can be represented by a point corresponding to a certain reference probability. According to the IEC insulation coordination standards, the overvoltage value with 2% probability of occurrence is recommended as the "statistical overvoltage U_s", and the withstand voltage value with 10% probability of discharge, namely 90% probability of withstand, is recommended as the "statistical withstand voltage U_w" of the insulation.

The above "statistical overvoltage U_s" and "statistical withstand voltage U_w" are used to replace the maximum overvoltage U_{gmax} and the minimum insulation withstand voltage U_j in the conventional procedure, respectively, and the ratio of the "statistical withstand voltage U_w" to the "statistical overvoltage U_s" is defined as the "statistical safety factor K_s", so that the conventional procedure is improved on the original basis, as shown in the following equation:

$$K_S = \frac{U_W}{U_S}. \tag{9.4}$$

Obviously, in case that the overvoltage remains constant, if the insulation level is raised, the statistical withstand voltage and the statistical safety factor will both increase accordingly, and the insulation failure rate will reduce.

The expression form in Eq. (9.4) is very similar to the conventional procedure. It can be considered that: the simplified statistical procedure is essentially a combined insulation coordination method adopting the probabilistic statistical characteristics of the overvoltage and the electric insulation strength while following the calculation equation of the conventional procedure.

In summary, in the insulation coordination of the UHV power grid, the external insulation levels of the overhead transmission lines and the substation equipment shall be determined primarily by the statistical procedure to reduce the cost of equipment insulation as far as possible under the premise of the stability guaranteed. For the internal insulation of substation equipment, because of the importance of the UHV equipment, the conventional procedure shall be used to obtain high operating stability of the substation as far as possible.

9.3 Insulation Coordination of the UHV Substation

The insulation coordination of substation covers the verification of air clearance distance of substation and the determination of equipment insulation level. For the former, because the air clearance is of self-restoring insulation, the statistical procedure can be used for the insulation coordination. For the substation equipment, the insulating media thereof are mostly solid or liquid, belonging to non-self-restoring insulation, and because of the importance of the UHV substation equipment, the conventional procedure is usually used for the insulation coordination in the practical application to ensure that the equipment has a high enough safety.

This section will discuss the main design philosophy in insulation coordination of the UHV substation based on the national standard GB/Z 24842-2009 *Overvoltage and Insulation Coordination of* 1000 kV *Transmission Project*.

9.3.1 Determination of Air Clearance of the UHV Substation

The air clearance of substation consists of the minimum electrical distance from conductor to framework, the minimum electrical distance from substation equipment to framework, and the minimum phase-to-phase electrical distance of substation. The air clearance shall be able to withstand the actions by the power frequency overvoltage, switching overvoltage, and lightning overvoltage.

9.3.1.1 Determination of Air Clearance Under Power Frequency Overvoltage

1. Phase-to-ground air clearances

Most of the phase-to-ground air clearances of substation are not affected by wind deflection. In the determination of the air clearance distance, the substation's maximum phase-to-ground power frequency temporary overvoltage U_p (1.4 p.u.) shall be considered as the representative power frequency overvoltage to be verified.

The required value of the 50% power frequency discharge voltage of the substation phase-to-ground air clearance shall meet the requirement in the following equation:

$$U_{50.1.r} = k_s k_c U_p = 1.05 \times 1.06 \times 1.4 \text{ p.u.} = 1399 \text{ (kV)}$$

where

k_s the safety factor, taken as 1.05;
k_c the coordination factor, taken as 1.06.

Hereunder, the air clearance power frequency discharge curve is the power frequency peak voltage discharge curve, and the 50% discharge voltage is the power frequency peak voltage.

The atmospheric correction factor k_a at the altitude of 1000 m is 1.131. It can be obtained that the required withstand voltage of the air clearance at the altitude of 1000 m under the reference atmosphere is 1582 kV.

After the required value of the power frequency discharge voltage of the equipment air clearance is obtained, the air clearance distance can be obtained by reference to the power frequency discharge voltage curve of the equipment's phase-to-ground air clearance.

The phase-to-ground air clearance's power frequency discharge voltage curve [1] is as shown in Fig. 9.2:

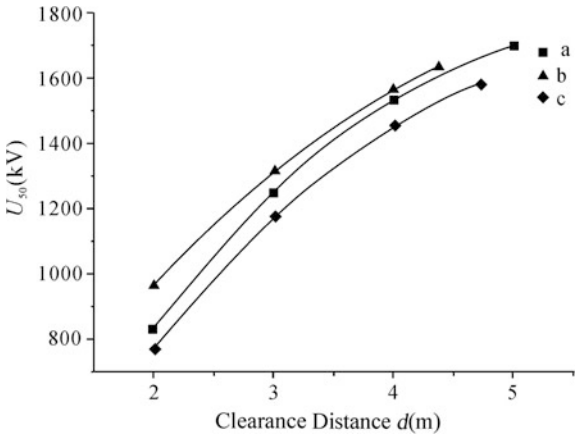

Fig. 9.2 Power frequency discharge voltage curve of the phase-to-ground air clearance of substation. *Note* **a** Power frequency discharge curve of the flexible conductor to the framework column, **b** power frequency discharge curve of the tubular busbar to the framework column, and **c** power frequency discharge curve of the grading ring to the framework column

According to the requirements on power frequency discharge voltage, by refer to the related discharge voltage curve mentioned above, the power frequency discharge clearance distance of the phase-to-ground clearance of substation can be obtained, as shown in Table 9.1.

It is specified in the Standard that, for the substations at the altitude not more than 1000 m, the phase-to-ground clearance distances under the power frequency voltage are recommended, as shown in Table 9.2.

The equipment to framework clearance distance obtained according to the discharge voltage curve is 4.6 m, while the equipment to framework clearance distance recommended in the literature [1] is 4.2 m. There is a certain deviation between these two values, but it does not affect the final selection of the air clearance distance, because the switching impulse and lightning impulse also need to be comprehensively considered for the equipment to framework clearance distance. According to the analysis in Sect. 9.3.1.2, the equipment to framework air clearance under the switching impulse is recommended as 7.5 m, which is significantly higher than the clearance distance required under the power frequency voltage. Therefore, the certain deviation between the equipment to framework clearance distances obtained according to the discharge voltage curve in this section and the recommended values does not affect the final results.

2. Phase-to-phase clearance

When the maximum phase-to-phase voltage occurs at the time of the trouble-free opening of the double-circuit line, the phase-to-phase voltage U_p may be up to 1.3 $\sqrt{3}$ p.u. In this case, the 50% discharge voltage of the clearance is as follows:

$$U_{50.1.r} = k_s k_c U_{pp} \tag{9.5}$$

where

k_s the safety margin, taken as 1.05;

Table 9.1 Phase-to-ground clearance distances of substation under power frequency voltage

Required value of power frequency discharge voltage (kV)		1582
Clearance distance (m)	Conductor to framework column	4.21
	Tubular busbar to framework column	4.08
	Grading ring to framework column	4.62

Table 9.2 Minimum air clearance distances of substation's phase-to-ground clearances under power frequency voltage

Clearance type	Conductor to framework	Equipment to framework
Clearance distance (m)	4.2	4.2

Note The conductor to framework includes the flexible conductor to framework column and the tubular busbar to framework column; the equipment to framework includes the grading ring to framework column

k_c the coordination factor, taken as 1.06 [1];
U_{pp} the maximum phase-to-phase power frequency overvoltage, taken as 1.3 $\sqrt{3}$ p.u.

The required value of the power frequency discharge voltage of the phase-to-phase clearance is as follows:

$$U_{50.1.r} = 1.05 \times 1.06 \times 1.3\sqrt{3}\text{p.u.} = 2250\ (\text{kV}).$$

In consideration of the correction factor of 1.131 at the altitude of 1000 m, the corrected value is 2545 kV.

9.3.1.2 Determination of Air Clearance Under Switching Impulse

1. Phase-to-ground clearance

With the substation's statistical phase-to-ground switching overvoltage U_{rp} (1.7 p.u.) taken as the typical overvoltage, the phase-to-ground clearance switching impulse 90% withstand voltage U_{rw} is as follows:

$$U_{rw} = k_s k_{cs} U_{rp} \tag{9.6}$$

where

U_{rp} the phase-to-ground typical switching overvoltage of substation;
k_s the safety factor, taken as 1.05;
k_{cs} the statistical coordination factor, taken as 1.15.

It is converted to the required value of 50% discharge voltage as follows:

$$U_{50.1.r} = \frac{U_{rw}}{1 - 1.28\sigma_1^*} = \frac{k_s k_{cs} U_{rp}}{1 - 1.28\sigma_1^*} \tag{9.7}$$

where

σ_1^* the variation coefficient of switching impulse discharge voltage distribution, taken as 0.06. $U_{50.1.r}$ is calculated to be 1997 kV.

Since the front time of the test wave of the switching impulse discharge curve of the substation in this chapter is 250 μs, while the front time of the switching overvoltage of the UHV systems is mostly beyond 1000 μs, it is necessary to conduct a waveform correction, with the correction factor taken as 1.13, and the required value of 50% discharge voltage after the correction is 1767 kV.

The substations at high altitudes shall be subject to the altitude correction. The altitude correction factor of the switching discharge voltage at the altitude of 1000 m is 1.056, and the value after the correction is 1866 kV.

The standard phase-to-ground clearance switching impulse discharge voltage curve [1] is as shown in Fig. 9.3.

Based on the requirements on switching impulse 50% discharge voltage, by refer to the above-related discharge voltage curve, the clearance distance required under the switching impulse voltage can be obtained, as shown in Table 9.3.

It is specified in the standard that, for the substations at the altitude not more than 1000 m, the phase-to-ground clearance distances under the switching impulse voltage are recommended, as shown in Table 9.4.

2. Phase-to-phase clearance

With the substation's statistical phase-to-phase switching overvoltage U_{rp} (not more than 2.9 p.u.) taken as the typical overvoltage, the phase-to-ground clearance switching impulse 90% withstand voltage U_{rw} is calculated as follows:

$$U_{rw} = k_s k_{cs} U_{rp} \tag{9.8}$$

where

U_{rp} the typical phase-to-phase switching overvoltage of substation;
k_s the safety factor, taken as 1.05;
k_{cs} the statistical coordination factor, taken as 1.15.

It is converted to the required value of 50% discharge voltage as follows:

$$U_{50.1.r} = \frac{U_{rw}}{1 - 1.28\sigma_1^*} = \frac{k_s k_{cs} U_{rp}}{1 - 1.28\sigma_1^*} \tag{9.9}$$

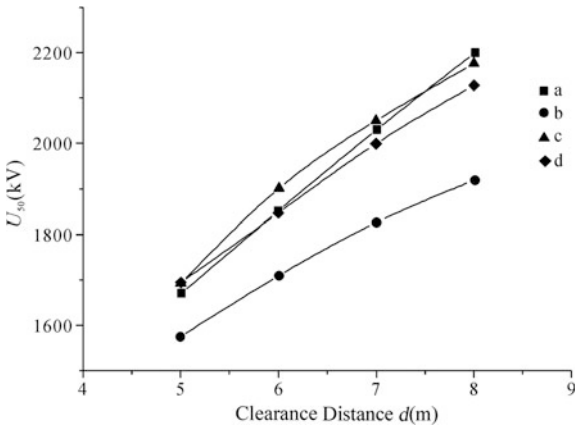

Fig. 9.3 Switching overvoltage discharge voltage curve of the phase-to-ground clearance of substation. *Note* **a** Discharge curve of the tubular busbar to the framework column, **b** discharge curve of the grading ring to the framework column, **c** discharge curve of the flexible conductor to the framework beam, and **d** discharge curve of flexible conductor to the framework column

Table 9.3 Phase-to-ground clearance distance of substation under the switching impulse voltage at the altitude of 1000 m

Required value of switching impulse discharge voltage (kV)		1866
Clearance distance (m)	Flexible conductor to framework beam	5.82
	Flexible conductor to framework column	6.13
	Tubular busbar to framework column	6.08
	Grading ring to framework column	7.41

Table 9.4 Minimum air clearance distances of the phase-to-ground clearances of the substations under switching impulse voltage

Clearance type	Conductor to framework	Equipment to framework
Clearance distance (m)	6.8	7.5

Note The conductor to framework includes the flexible conductor to framework column and the tubular busbar to framework column; the equipment to framework includes the grading ring to framework column

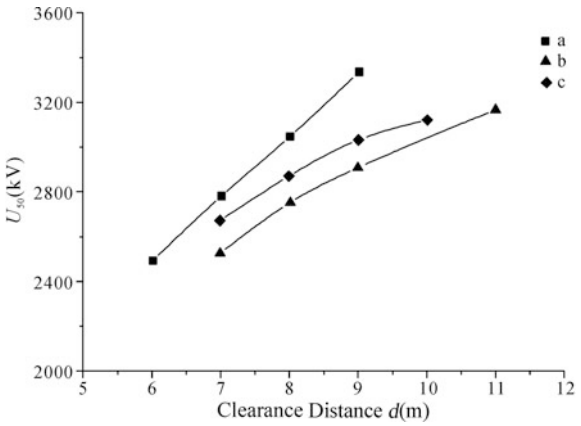

Fig. 9.4 Phase-to-phase clearance switching overvoltage discharge voltage curve. *Note* **a** Phase-to-phase discharge voltage of flexible conductor, **b** phase-to-phase discharge voltage of tubular busbar, and **c** phase-to-phase discharge voltage of grading ring

where

σ_1^* the variation coefficient of switching impulse discharge voltage distribution, taken as 0.06. $U_{50.1.r}$ is calculated to be 3270 kV.

The waveform correction factor is 1.131, and the required value of discharge voltage after the correction is 2894 kV.

The substations at high altitudes shall be subject to the altitude correction. The altitude correction factor of the switching discharge voltage at the altitude of 1000 m is 1.065, and the required value of the discharge voltage after the correction is 3082 kV.

The substation phase-to-phase clearance switching impulse discharge voltage curve [1] is as shown in Fig. 9.4.

Based on the requirements on substation phase-to-phase switching discharge voltage, by refer to the above-related discharge voltage curve, the required phase-to-phase clearance distance of the switching overvoltage can be obtained, as shown in Table 9.5.

It is specified in the Standard that, for the substations in the areas at altitude not more than 1000 m, the substation's minimum phase-to-phase air clearances under the switching impulse are recommended as shown in Table 9.6.

9.3.1.3 Determination of Air Clearance Under Lightning Impulse

1. Phase-to-ground clearance

The 50% discharge voltage U_{50} of the positive lightning impulse voltage wave of the substation's phase-to-ground air clearance shall meet the requirement in the following equation:

$$U_{50} \geq k_a k_4 U_{pl} \tag{9.10}$$

where

U_{pl} the rated residual voltage value of arresters at the nominal lightning current of 20 kA, taken as 1620 kV;

k_4 the lightning overvoltage coordination factor of the phase-to-ground air clearance of substation, taken as 1.45;

Table 9.5 Phase-to-phase air clearance distance corresponding to the required value of switching impulse discharge voltage of substation

Clearance type	Flexible conductor to flexible conductor	Tubular busbar to tubular busbar	Grading ring to grading ring
Clearance distance corresponding to the required value of discharge voltage (m)	8.12	10.32	9.49

Table 9.6 Recommended values of substation's minimum phase-to-phase air clearances under switching impulse

Clearance type	Flexible conductor to flexible conductor	Tubular busbar to tubular busbar	Grading ring to grading ring
Recommended value of the minimum air clearance distance (m)	9.2	11.3	10.1

k_a the altitude correction factor, taken as 1.131 at the altitude of 1000 m.

It is obtained through calculation that the required value of the positive (the positive lightning breakdown voltage is slightly lower than the negative one; based on a strict consideration, the positive lightning discharge voltage value is selected for the calculation in this chapter) lightning impulse discharge voltage at the altitude of 1000 m is 2657 kV.

The substation phase-to-ground clearance lightning impulse discharge curve [1] is as shown in Fig. 9.5.

Based on the requirements on substation phase-to-ground clearance lightning impulse discharge voltage, by refer to the above-related discharge voltage curve, the clearance distances corresponding to the required value of lightning impulse discharge voltage are as shown in Table 9.7.

It is specified in the standard that, for the substations in the areas at altitude not more than 1000 m, the lightning impulse phase-to-ground clearance distances are recommended as shown in Table 9.8.

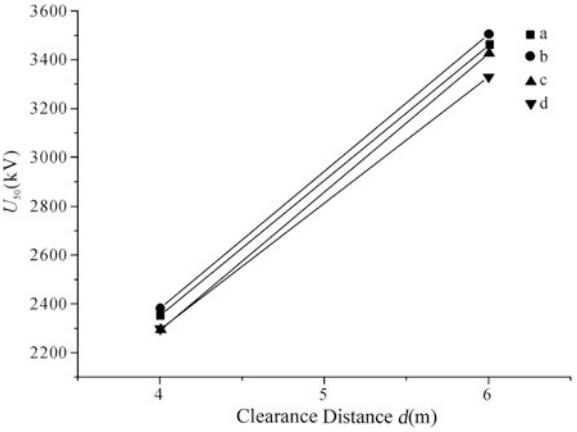

Fig. 9.5 Substation phase-to-ground clearance lightning impulse 50% discharge voltage curve. *Note* **a** Discharge voltage curve of the conductor to framework column clearance, **b** discharge voltage curve of the conductor to framework column clearance, **c** discharge voltage curve of the tubular busbar to framework column clearance, and **d** discharge voltage curve of the grading ring to framework column clearance

Table 9.7 Substation phase-to-ground clearance distances under lightning impulse voltage

Required value of lightning impulse discharge voltage (kV)		2657
Clearance distance (m)	Conductor to framework beam	4.51
	Conductor to framework column	4.57
	Tubular busbar to framework column	4.66
	Grading ring to framework column	4.72

Table 9.8 Minimum air distance of substation phase-to-ground clearance under lightning impulse voltage

Clearance type	Conductor to framework	Equipment to framework
Clearance distance (m)	5	5

2. Phase-to-phase clearance

For the phase-to-phase air clearance under the lightning impulse, due to the impact of power frequency voltage, the clearance breakdown voltage may be decreased, so it is recommended in the literature [1] that the phase-to-phase clearance distance can be taken as 1.1 times the phase-to-ground clearance.

9.3.1.4 Recommended Values of Substation Minimum Air Clearance Distance

It is specified in the standard that, for the 1000 kV substations in the areas at altitude not more than 1000 m, the recommended values of the minimum air clearance distances are as shown in Table 9.9.

9.3.2 Selection of Insulation for the UHV Equipment

The principle of insulation coordination for the UHV equipment is to determine the insulation level of other equipment on the basis of the insulation coordination of the transformer. Under the power frequency voltage, to ensure the operation reliability of the electrical equipment, the equipment insulation shall be able to withstand the maximum power frequency operating voltage for a long time (5 min). Under the switching overvoltage and lightning impulse overvoltage, the protection of equipment in the substation is achieved mainly through the arrangement of arresters to reduce the steepness and amplitude of the overvoltage impulse wave; therefore, the levels of switching impulse withstand voltage and lightning impulse withstand voltage of the electrical equipment are mainly determined based on the protection level of the arresters. The following gives a discussion on the equipment insulation coordination under the three types of overvoltages, respectively.

Table 9.9 Minimum air clearances of the UHV substation (m)

Type of applied voltage	Conductor to framework	Equipment to framework	Phase to phase
Power frequency	4.2	4.2	6.8
Switching impulse	6.8	7.5	Conductor to conductor: 9.2
			Ring to ring: 10.1
			Tubular busbar to tubular busbar: 11.3
Lightning impulse	5.0	5.0	5.5

9.3.2.1 Insulation Coordination of Electrical Equipment Under Power Frequency Voltage

The principles of insulation coordination of the equipment under power frequency voltage are as follows: ① the local pollution conditions shall be considered for the equipment external insulation; ② the electric equipment shall be subject to the power frequency withstand voltage test for a long time at factory to ensure the reliability of equipment insulation under the long-term operating voltage; ③ the equipment shall be able to withstand the continuous operating voltage and the transient overvoltage with certain amplitude and duration.

The power frequency voltage withstand value of the electrical equipment is as follows:

$$U_{\mathrm{w}} \geq k_{\mathrm{c}} k_{\mathrm{s}} U_{\mathrm{rp}} \tag{9.11}$$

where

U_{rp} the representative power frequency overvoltage, taken as the maximum power frequency overvoltage which is 1.3 p.u. at the substation side;
k_{c} the coordination factor, taken as 1;
k_{s} the safety factor, $k_{\mathrm{s}} = 1.15$ for the equipment internal insulation, $k_{\mathrm{s}} = 1.05$ for the equipment external insulation.

It is obtained through calculation that the withstand voltage (effective value) of the internal insulation is 949 kV and that of the external insulation is 867 kV.

For the external insulation of equipment, it is also necessary to consider the atmospheric correction factor corresponding to the altitude, so as to conduct the altitude correction for the external insulation withstand voltage of the equipment in the substations at high altitude.

For the external insulations of electric porcelain material, such as the transformer bushing, in addition to the verification of the withstand voltage, it shall also ensure that they can satisfy the specific creepage distance corresponding to the pollution degree of the local areas.

For the power frequency withstand voltage U_{w} of the longitudinal insulation of switchgear (the internal insulation between the open contacts of circuit breakers and the external insulation between the open contacts of circuit breaker and disconnector), the impact of the reverse-polarity continuous operating voltage shall be considered and shall satisfy the following equation:

$$U_{\mathrm{wg}} \geq U_{\mathrm{w}} + U_{\mathrm{m}}/\sqrt{3} \tag{9.12}$$

where

U_{w} the rated power frequency withstand voltage of phase-to-ground insulation of circuit breaker and disconnector, taken as 1100 kV;
U_{m} the maximum operating voltage of system, taken as 1100 kV.

Table 9.10 Withstand voltages of factory withstand voltage test on 1000 kV equipment

Equipment	Withstand voltage values of voltage withstand test (kV)
Transformer, reactor	1100 (5 min)
GIS	1100 (1 min)
Post-insulator, disconnector	1100 (1 min)
Voltage transformer	1200 (5 min)
Bushing (transformer, reactor)	1200 (5 min)
Bushing (GIS)	1100 (1 min)
Switchgear longitudinal insulation	1100 + 635 (1 min)

To ensure the reliability of equipment insulation under the long-term operating voltage, the electric equipment shall be subject to the power frequency withstand voltage test at factory. Compared to the factory withstand voltage test of the EHV transformer, the duration of the withstand voltage test of the UHV transformer at factory is extended from 1 to 5 min. This is because that, according to the partial discharge test of the transformer insulation model, the 5 min withstand voltage test can better test the strength of the internal insulation of transformer and whether the partial discharge phenomenon exists. In addition, the operating experience has shown that the transformer damages mostly occur under the power frequency voltage, so the test on the transformer insulation withstand capability under the power frequency voltage is more important. Therefore, to improve the operation stability of the system in the UHV power grid, it is reasonable to extend the time duration of the transformer factory withstand voltage test from 1 to 5 min.

The withstand voltage values of the factory withstand voltage test on various 1000 kV equipment recommended in the Standard are as shown in Table 9.10.

9.3.2.2 Insulation Coordination of Electrical Equipment Under Switching Overvoltage

The calculation methods for the insulation level are given in the national standard GB/Z 24842-2009 *Overvoltage and Insulation Coordination of* 1000 kV *UHV AC Transmission Project*.

1. Determination of the insulation level of equipment based on the switching impulse protection level of arresters.

The values of the phase-to-ground switching impulse withstand voltage of the electrical equipment internal and external insulations shall meet:

$$U_{\mathrm{rw.1}} \geq 1.15 U_{\mathrm{ps}} \tag{9.13}$$

where

U_{ps} the switching overvoltage protection level of arresters, taken as 1460 kV. $U_{\mathrm{rw.1}}$ is calculated to be 1679 kV.

The switching impulse withstand voltage of the longitudinal insulation of switchgear shall meet:

$$U_{\mathrm{w}} \geq U_{\mathrm{w(p-g)}} + U_{\mathrm{m}}\sqrt{\frac{2}{3}} \tag{9.14}$$

where

$U_{\mathrm{w(p\text{-}g)}}$ the rated switching impulse withstand voltage of switchgear, taken as 1675 kV;

$U_{\mathrm{m}}\sqrt{\frac{2}{3}}$ the power frequency voltage with polarity opposite to that of $U_{\mathrm{w(p\text{-}g)}}$;

U_{m} the maximum operating voltage of the system, taken as 1100 kV.

The switching impulse withstand voltage U_{w} of the longitudinal insulation of the switchgear is 1675 + 900 kV.

2. Determination of the insulation level of equipment based on the maximum switching overvoltage.

(1) Internal insulation of equipment

The required value of the switching impulse withstand voltage shall be as follows:

$$U_{\mathrm{w}} \geq k_{\mathrm{cd}} k_{\mathrm{s}} U_{\mathrm{rp}} \tag{9.15}$$

where

U_{rp} the maximum switching overvoltage obtained through statistical calculation, in kV;

k_{cd} the deterministic coordination factor, taken as 1.05;

k_{s} the safety factor of internal insulation, taken as 1.15.

The maximum phase-to-ground statistical switching overvoltage of substation shall not be more than 1.6 p.u., with U_{rp} taken as 1.6 p.u. In addition, the rated phase-to-ground switching impulse withstand voltage of the equipment internal insulation is calculated to be 1735 kV.

(2) External insulation of equipment

The rated phase-to-ground switching impulse withstand voltage of the equipment insulation shall be as follows:

$$U_{\mathrm{w}} \geq k_{\mathrm{s}} k_{\mathrm{cs}} U_{\mathrm{rp}} \tag{9.16}$$

where

U_{rp} the maximum switching overvoltage obtained through statistical calculation, in kV;
k_{cs} the statistical coordination factor, taken as 1.15;
k_s the safety factor of external insulation, taken as 1.05.

With U_{rp} taken as 1.6 p.u., the rated phase-to-ground switching impulse withstand voltage of the equipment external insulation is calculated to be 1735 kV.

(3) Phase-to-phase insulation of equipment

The rated phase-to-phase switching impulse withstand voltage of the equipment insulation shall be as follows:

$$U_w \geq k_s k_{cs} U_{rp} \tag{9.17}$$

where

U_{rp} maximum phase-to-phase overvoltage obtained through statistical calculation;
k_{cs} the statistical coordination factor, taken as 1.15;
k_s the safety factor of internal insulation, taken as 1.15.

The values of the rated switching impulse withstand voltage of various 1000 kV equipment insulations recommended in the Standard are as shown in Table 9.11.

To sum up, there is a little difference between the values of phase-to-ground switching impulse withstand voltage of internal and external insulations of equipment calculated with the two methods, and the required value of the equipment phase-to-ground switching impulse withstand voltage calculated based on the statistical switching overvoltage of substation is slightly larger than that calculated based on the protection level of arresters, but both are lower than the rated switching impulse withstand voltage value of equipment insulation.

Table 9.11 Rated switching impulse withstand voltage of 1000 kV equipment

Equipment	Switching impulse withstand voltage value (kV)
Transformer, reactor	1800
GIS	1800
Post-insulator, disconnector	1800
Voltage transformer	1800
Bushing (transformer, reactor)	1950
Bushing (GIS)	1800
Switchgear longitudinal insulation	1675 + 900

9.3.2.3 Insulation Coordination of Electrical Equipment Under Lightning Overvoltage

The arrangement of the arresters in the substation has a great impact on the lightning overvoltage on equipment. Because of the important position of the transformer among the substation equipment, the arresters are normally arranged closely to the transformer, while a certain distance is maintained between the bushings, current transformers, etc., and the arresters, and hence, the protection effect of the arresters is impacted to some extent. Therefore, when the insulation coordination is carried out based on the lightning impulse protection level of arresters, the impact of the distance factor needs to be considered.

The required value of the full-wave lightning impulse withstand voltage of the internal and external insulations of transformers and shunt reactors shall meet the requirement in the following equation:

$$U_{\mathrm{rw.1}} \geq 1.33 U_{\mathrm{pl}} \tag{9.18}$$

where

U_{pl} the lightning impulse protection level of arresters, taken as 1620 kV.

The coordination factor is 1.33, which is obtained based on the consideration of the margin coefficient of 1.15 and equipment aging coefficient of 1.15. $U_{\mathrm{rw.1}}$ is calculated to be 2155 kV. The rated withstand voltage recommended in the Standard is 2250 kV.

The rated lightning impulse withstand voltage of the chopped wave is taken as 1.1 times that of the full wave of the corresponding equipment. The chopped-wave lightning impulse withstand voltage is calculated to be 2371 kV. The rated chopped-wave withstand voltage recommended in the Standard is 2400 kV.

The required value of the full-wave lightning impulse withstand voltage of the high-voltage electrical appliances and current transformers as well as the bushings, busbar post-insulators and cables and their accessories, etc. to be tested separately shall be as follows:

$$U_{\mathrm{rw.1}} \geq 1.45 U_{\mathrm{pl}} \tag{9.19}$$

where the coordination factor of 1.45 is obtained based on the consideration of the margin coefficient of 1.15, equipment aging coefficient of 1.15, and distance coefficient of 1.1. $U_{\mathrm{rw.1}}$ is calculated to be 2349 kV. The rated full-wave withstand voltage recommended in the Standard is 2400 kV.

The lightning impulse withstand voltage of the longitudinal insulation of switchgear shall meet:

$$U_{\mathrm{w}} \geq U_{\mathrm{w(p-g)}} + U_{\mathrm{m}} \sqrt{\frac{2}{3}} \tag{9.20}$$

where

$U_{w(p\text{-}g)}$ the rated lightning impulse withstand voltage of the phase-to-ground insulation of switchgear, taken as 2400 kV;

$U_m\sqrt{\frac{2}{3}}$ the power frequency voltage with polarity opposite to that of $U_{w(p\text{-}g)}$;

U_m the maximum operating voltage of the system. The rated full-wave withstand voltage of the longitudinal insulation of switchgear is 2400 + 900 kV.

The values of the rated lightning impulse withstand voltage of various 1000 kV equipment insulations recommended in the Standard are as shown in Table 9.12.

9.3.2.4 Insulation Levels Recommended for 1000 kV UHV Equipment

Based on China's current manufacturing capability and overvoltage level, the insulation levels recommended for 1000 kV equipment are as shown in Table 9.13.

Table 9.12 Rated lightning impulse withstand voltage of 1000 kV equipment

Equipment	Lightning impulse withstand voltage value (kV)
Transformer, reactor	2250 (2475 for chopped wave)
GIS	2400
Post-insulator, disconnector	2550
Voltage transformer	2400
Bushing (transformer, reactor)	2400
Bushing (GIS)	2400
Switchgear longitudinal insulation	2400 + 900

Table 9.13 Selection of insulation levels for 1000 kV UHV equipment

Equipment	Withstand voltage (kV)		
	Lightning impulse	Switching impulse	Short-duration power frequency
Transformer, reactor	2250 (2475 for chopped wave)	1800	1100 (5 min)
GIS (circuit breakers, disconnectors)	2400	1800	1100 (1 min)
Post-insulators, disconnectors (open type)	2400	1800	1100 (1 min)
Voltage transformer	2400	1800	1200 (5 min)
Bushing (transformer, reactor)	2400	1950	1200 (5 min)
Bushing (GIS)	2400	1800	1100 (1 min)
Switchgear longitudinal insulation	2400 + 900	1675 + 900	1100 + 635 (1 min)

9.3.2.5 Comparison of Main UHV Electrical Equipment in Different Countries

The insulation levels of the UHV transformers in different countries are as shown in Table 9.14 [2–4].

It can be found through the comparison of the transformer insulation levels in different countries that the former Soviet Union has the highest transformer insulation levels. This is first because that the former Soviet Union has the maximum operating voltage of 1200 kV, which is higher than that of other countries; it is then because that the former Soviet Union reserves a large margin for the transformer insulation to ensure the stable operation of the lines due to its low-manufacturing level of arresters and the poor protection effect thereof.

Japan has significantly lower UHV transformer insulation levels than other countries. This is first because that the maximum operating voltage in Japan is 1100 kV, which is lower than that in the former Soviet Union; it is then because that the MOAs used in Japan have excellent performance and low residual voltage, and, besides, Japan tends to use many MOAs in the arrangement mode, making the overall overvoltage level throughout the substation lower. For example: Japan once carried out research on the impacts of the adoption of different arrangement schemes for the arresters of the 1100 kV UHV substation on the lightning withstand levels and costs of the electrical equipment [2], as shown in Table 9.15.

It can be seen from Table 9.15 that, under the condition that the extremely strict lightning invasion wave is selected, Scheme F is the most economic. When many arresters are adopted, the requirement on the withstand voltage of the in-substation equipment is lowered, so a great economic efficiency can be achieved [5]. Such design method and idea of the lightning protection scheme for the UHV substations of Japan are worthy of reference by China. China can refer to Japan's treatments, and comprehensively balances the selection of in-substation equipment insulation level and the application of overvoltage limiting measures (mainly the number of MOAs), considering both the safety and economy in lightning protection of substation, to determine a reasonable insulation coordination scheme for the UHV substation.

Table 9.14 Selection of insulation levels of the UHV transformers in different countries (kV)

Country	Lightning impulse withstand voltage (ULWP)	Switching impulse withstand voltage (USWP)	Short-duration power frequency withstand voltage (UW)[a]
Japan	1950	1425	1100 (5 min)
Former Soviet Union	2400	1950	1100 (1 min)
China (recommended)	2250	1800	1100 (5 min)

[a]Phase-to-ground power frequency voltage

Table 9.15 Relationship among MOA arrangement schemes, equipment insulation levels, and costs of Japan's UHV substation

		Scheme A	Scheme B	Scheme C	Scheme D	Scheme E	Scheme F
Number of arresters	At incoming line	1	1	1	2	2	2
	Busbar	0	1	2	0	1	2
	Transformer	1	1	1	1	1	1
Transformer	Required withstand voltage (kV)	1950	1943	1895	1943	1938	1896
	Adopted withstand voltage (kV)	1950	1950	1950	1950	1950	1950
GIS	Required withstand voltage (kV)	2898	2854	2703	2628	2506	2208
	Adopted withstand voltage (kV)	2900	2900	2900	2700	2550	2250
Costs (assuming 100 for Scheme F)		102	105	109	103	103	100

Table 9.16 Selection of insulation levels of the UHV reactors in different countries (kV)

Country	Lightning impulse withstand voltage	Switching impulse withstand voltage
Japan (early)	2100	1425 (or 1550)
Former Soviet Union	2550	2100
China (recommended)	2250	1800

Through the comparison with the former Soviet Union and Japan, China adopts the MOAs with excellent performance. And considering its current manufacturing level, China reserves an appropriate insulation margin, so its selected insulation levels are between those of Japan and the former Soviet Union.

The selection of the insulation levels of reactors [2] is as shown in Table 9.16. Due to the limitation by the manufacturing process, plus the poor performance of arresters, the former Soviet Union adopts high withstand voltage values, while China, because of the improved manufacturing performance of MOAs, has reactor insulation levels lower than those of the former Soviet Union, but higher than those of Japan.

References

1. GB/Z 24842-2009. Overvoltage and insulation coordination of 1000 kV UHV AC transmission project; 2009.
2. Liu Z. Overvoltage and insulation coordination of UHV AC system. Beijing: China Electric Power Press; 2008. p. 106.
3. Guangfan L, Xiaoning W, Peng L, Lin S, Bo L, Jinzhong L. Insulation level and test technology of 1000 kV power transformers. Power Syst Technol. 2008;32(3):1–6.
4. Guangfan L, Cuixia Z, Jinzhong L, Bo L, Wang Xiaoning D, Shuchun GD. Discussion on insulation level of 1000 kV transformer. Power Syst Technol. 2009;33(18):1–4.
5. Dingxie G, Peihong Z, Min D, Muhong X, Huiwen H. Comparison and analyses on over-voltage and insulation coordination of UHV AC transmission system between China and Japan. High Volt Eng. 2009;35(6):1248–53.

Chapter 10
Insulation Coordination of UHVAC Transmission Lines

Hao Zhou, Fei Su and Jingzhe Yu

The rational selection of the insulation level of the UHV overhead lines is of great significance to the safe operation of the UHV lines. The insulation coordination of the lines mainly covers the selection of the number of insulators in an insulator string and the selection of the line's air clearance. Both the insulator string and the line's air clearance belong to the self-restoring insulation, for which the statistical method can be used to achieve the insulation coordination, thus to obtain high economic benefit.

This chapter first analyzes the selection of the type and form of insulator strings in the UHVAC transmission line, and then discusses the calculation methods of the number of insulators and the UHV line's air clearance.

10.1 Selection of Type and Form of UHV Insulator Strings

The UHV line has a high-voltage level, and the length of the insulator strings is more than one time of the insulator strings in the 500 kV line; the eight-bundled conductors are adopted on the line and the load borne of the insulators is far better than that of the ordinary line. Therefore, the diameter (disk diameter), structural

H. Zhou (✉) · J. Yu
College of Electrical Engineering, Zhejiang University, Xihu District, Hangzhou, Zhejiang, People's Republic of China
e-mail: zhouhao_ee@zju.edu.cn

J. Yu
e-mail: 21510213@zju.edu.cn

F. Su
State Grid Jinan Power Supply Company, Jinan, Shandong People's Republic of China
e-mail: 285701397@qq.com

© Zhejiang University Press, Hangzhou and Springer-Verlag GmbH Germany 2018

H. Zhou et al. (eds.), *Ultra-high Voltage AC/DC Power Transmission*, Advanced Topics in Science and Technology in China,
https://doi.org/10.1007/978-3-662-54575-1_10

height, and rated mechanical load of the insulators used are much higher than those of the 500 kV EHV power grid, and, in most cases, the insulator arrangement in which the V-type string and 2–4 I-type strings are paralleled is adopted; the steel tower spacing is large and the height thereof is over twice that of the EHV line steel tower. Because of these operating conditions which are different from the EHV system, the selection of the UHV insulator types has its own particularity [1].

10.1.1 Comparison Among Three Different UHV Transmission Line Insulators

10.1.1.1 Electrical Characteristics of the UHV Transmission Line Insulators

The UHV line insulators mainly include glass insulator, composite insulator, and porcelain insulator, all of which have been actually applied in China's UHV transmission line. Presently, the insulators that are widely used in China's lines mainly include: the double-umbrella-type insulator XWP-300, three-umbrella-type porcelain insulator CA-876, standard porcelain insulator CA-590, and glass insulator FC300 are mainly used in the regions subject to light or medium pollution; the composite insulator is mainly used in the heavily polluted regions and high-altitude regions.

In Ref. [2], the common insulators in several lines are selected for research, and the particular structures thereof are shown in Fig. 10.1.

The geometric parameters of the common insulators are shown in Table 10.1.

Through the artificial pollution test carried out on the insulators above, Ref. [2] obtained, under the standard atmospheric pressure, the 50% flashover voltage (kV/m) curves per unit length of the insulators of three different materials under different equivalent salt deposit densities, as shown in Fig. 10.2a, and the 50% flashover voltage (kV/m) curves per unit length of the porcelain insulators of three different umbrella types under different equivalent salt deposit densities are shown in Fig. 10.2b.

From Fig. 10.2a, it can be seen that the composite insulator has the largest flashover voltage per unit length under different equivalent salt deposit densities and, in addition, with the increase of the equivalent salt deposit density (ESDD), the flashover voltage decreases slowly, and the pollution flashover withstand performance thereof is excellent. It is followed by the three-umbrella-type porcelain insulator, which has a high flashover voltage per unit length under small equivalent salt deposit density; however, with the increase of equivalent salt deposit density, the flashover voltage decreases quickly. In comparison with the three types of insulators above, the standard-type glass insulator has the worst pollution flashover withstand performance.

In Fig. 10.2b, the pollution flashover withstand performances of the three-umbrella-type porcelain insulators are compared. It can be seen that the shed shape has a large influence on the pollution flashover withstand performance of the

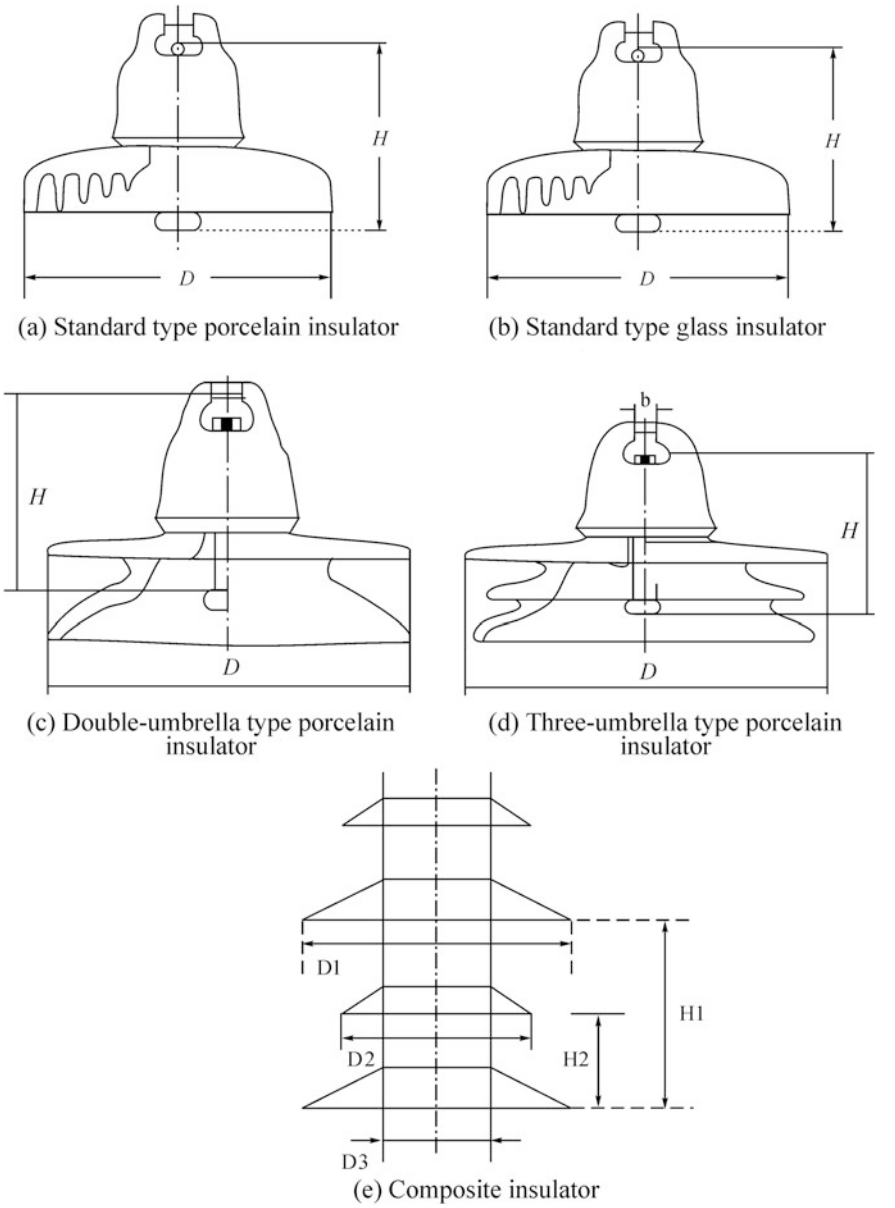

Fig. 10.1 Sketch of types and structures of insulators

insulators of the same material: the pollution flashover withstand performance of the umbrella-type insulator is obviously better than that of the standard-type insulator, and the pollution flashover withstand performance of the three-umbrella-type insulator is better than that of the double-umbrella-type insulator.

Table 10.1 Geometric parameters of insulators

Material of insulator	Umbrella type	Structural height (mm)	Creepage distance (mm)	Disk diameter (mm)
Porcelain	Standard	195	505	320
	Double umbrella	195	495	330
	Three umbrella	195	675	400
Glass	Standard	195	485	330
Silicon rubber	Rod	2890	10640	215/167/50

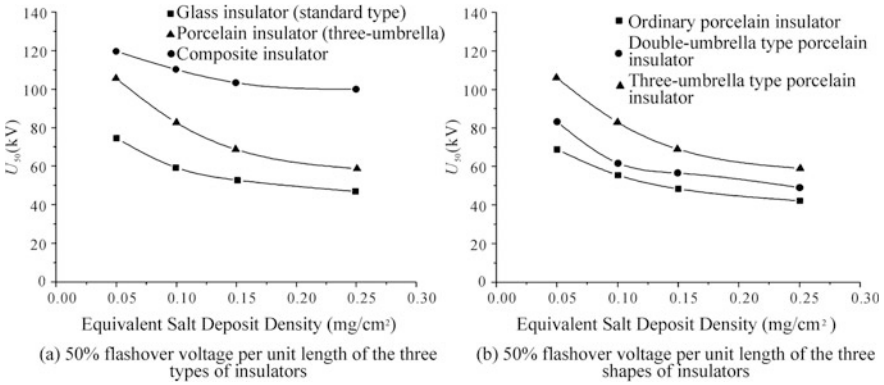

(a) 50% flashover voltage per unit length of the three types of insulators

(b) 50% flashover voltage per unit length of the three shapes of insulators

Fig. 10.2 Curve of relationship between the flashover voltage along unit length of insulator and equivalent salt deposit density under different equivalent salt deposit densities

10.1.1.2 Characteristics of UHV Transmission Line Insulators Under High Altitude

The UHV line may pass through the high-altitude regions. With the increase of the altitude, the atmospheric pressure decreases, and the flashover voltage of the polluted insulator also decreases. Reference [3] proposed the linear expression between the altitude of the transmission line insulator and the flashover voltage, as shown below:

$$\frac{U}{U_0} = 1 - kH \tag{10.1}$$

where

U_0 the flashover voltage of insulator under standard atmospheric pressure;
U the flashover voltage at the altitude of H (km);
k the descending slope (km^{-1}), namely the descending percentage of flashover voltage of insulator for every 1 km increase of the altitude, which reflects the influence of the altitude of the transmission line insulator on the flashover voltage.

Table 10.2 Descending slope k of insulators with different types (km^{-1})

ESDD mg/cm^2	Umbrella type				
	Standard porcelain insulator, CA-590	Double-umbrella-type porcelain insulator, XWP-300	Three-umbrella-type porcelain insulator, CA-876	Glass insulator, FC300	Composite insulator
0.05	0.079	0.075	0.065	0.054	–
0.10	–	0.048	–	0.052	0.029

– means that there are no related data

Reference [2] carried out the research on the flashover voltage of the insulator under low atmospheric pressure, and obtained the result that flashover voltage of the insulators of different types under different altitudes, and thus obtained the descending slope of the insulator, as shown in Table 10.2. With the suspension insulator CA-590 given in the table taken as an example, its descending slope k is 0.079, indicating that under the pollution condition under which the equivalent salt deposit density is 0.05 mg/cm^2, the flashover voltage of CA-590 decreases by 7.9% for every 1 km increase of the altitude.

From Table 10.2, it can be seen that the descending slope of composite insulator is small, that is to say its insulation performance under high altitude is good; in the regions subject to light pollution, the glass insulator has better high-altitude withstand performance than the three types of porcelain insulators; with the increase of the altitude, the insulation performance of double-umbrella-type porcelain insulator and three-umbrella-type porcelain insulator is subject to drop significantly.

10.1.1.3 Consideration on Other Particularities of the UHV Transmission Line Insulators: Grading Performance and Arc Resistance Performance

In the actual application, it is not only necessary to investigate the insulators' pollution flashover withstand performance and characteristics under high altitude, but also to consider the particularities of the UHV power grid and investigate the grading performance, arc resistance performance of the insulators, etc.

1. Grading performance

The length of the UHV line insulator string is around twice over that of the EHV line insulator string. In such case, the voltage distribution on the insulator string is quite uneven, and the voltage drop is mainly concentrated on the both ends of the insulator string, resulting in significant decrease in the utilization rate of the overall insulator string. Therefore, during the type selection, the grading design of the insulator shall be fully considered.

The dielectric constant of the glass insulator is slightly larger than that of the porcelain insulator, because of which the main capacitance of the glass insulator is larger than that of the porcelain insulator. When the insulators are used in strings, each insulator will be under a relatively small influence of the bypass stray capacitances to ground and to conductor. Therefore, in comparison with the porcelain insulator, the voltage distribution on the entire string of the glass insulator is more even. This is favorable to reduce the radio interference, lower the corona loss, and prolong the service life of insulator; in addition, it can also enhance the flashover voltage of the glass insulator string. The State Grid Electric Power Research Institute measured the voltage distribution on the porcelain insulator string and the glass insulator string provided with identical grading rings, respectively, and the results show that the overall voltage distribution trend on the glass insulator string is similar to that of the porcelain insulator string, but the voltage undertaken by several glass insulators on the conductor side is about 8% lower than that undertaken by the porcelain insulators.

Under the power frequency voltage, the surface electric field intensity and the voltage distribution on the composite insulator are extremely uneven, the connection between the core rod and the fittings, the electric field intensity is up to 6.5 kV/cm, while the voltage distributed on the first shed on the conductor side is far above the average distributed voltage on the entire insulator string in general, and this shed may, under the effect of long-duration working voltage, be subject to premature aging, losing insulating capacity and finally resulting in scrapping of the entire insulator. In the actual application, the grading rings may be installed to improve the issue that the electric field intensity is concentrated on the ends of the composite insulator. In addition, the composite insulator and several glass insulators can also be mixed in series to solve the problem; that is, several glass insulators are connected in series at the head of the composite insulator, so that the maximum distributed voltage will be undertaken by the glass insulator adjacent to line side, thus to prevent the premature aging of the composite insulator under strong electric field intensity.

2. Arc resistance capability

When the flashover has occurred to the insulator, there will be arc with extremely high temperature flowing through, leaving burns on the surface and damaging the insulation performance of the insulator. Different insulators have diffident arc resistance capabilities, which shall be concerned especially for the insulators in the UHV line. The test results have shown that the arc burn resistance capability of the glass insulator is obviously better than that of the porcelain insulator; after the glass insulator is subject to lightning arc burn, one layer of glass will be flaked off from the surface, but the new surface will still be smooth glass, the insulating strength thereof will not be reduced and it can still be subject to long-term operation; however, after the porcelain insulator is subject to arc burn, the enamel layer will be flaked off from the surface, and the exposed porcelain body will be easy to be polluted, resulting in decrease in the insulation performance. Therefore, the porcelain insulators subject to lightning burn must be replaced; the composite

insulators subject to lightning strike, generally, only have white arc trace left which does not affect their use and thus need not be replaced, but attention must be paid to the ablation of the fittings on both ends.

In conclusion, the three-umbrella-type and double-umbrella-type porcelain insulators have good pollution flashover withstand performance and have been widely used in the practical engineering in China; the glass insulator has excellent mechanical and electrical performances, high strength, good arc resistance performance and more even voltage distribution; however, at present, the pollution flashover withstand capability of the standard-type glass insulator is not as good as that of the three-umbrella-type and double-umbrella-type porcelain insulators; the composite insulator, being light in mass, good in hydrophobicity, perfect in pollution flashover withstand performance and high-altitude insulation performance, and having excellent mechanical impact resistance capability, can shorten the reconstruction period of the transmission line and reduce the engineering cost.

10.1.2 Selection of Type and Form of the UHV Transmission Line Insulator Strings

Combined with the discussion in the previous section, as to the selection of the type and form of the UHVAC insulator strings, the following recommendations are provided as reference:

(1) For the regions subject to light pollution, the suspension string, the V-type string, and the tension string generally adopt the double-umbrella porcelain insulators or standard glass insulators.
(2) For the regions subject to medium and above pollution, the suspension string generally adopts the composite insulators, the V-type string generally adopts the composite insulators, as well, while the tension string shall adopt the double-umbrella porcelain insulators or standard glass insulators.
(3) For the regions with heavy ice, the composite insulator will, after covering with ice, lose its hydrophobicity; in addition, as the shed of the composite insulator is small, two adjacent sheds are prone to be bridged by icicle, resulting in significant decrease in the insulation performance. Therefore, in the regions with heavy ice, the double-umbrella porcelain insulators or standard glass insulators are more apt to be adopted. In such case, the suspension string generally adopts the double-umbrella porcelain insulators or standard glass insulators; the V-type string generally adopts the double-umbrella porcelain insulators or standard glass insulators; the tension string generally consists of the double-umbrella porcelain insulators or standard glass insulators.
(4) For the regions at high altitude, the suspension string generally consists of the composite insulators; the V-type string also generally consists of the composite insulators; while the tension string consists of the double-umbrella porcelain insulators or standard glass insulators.

(5) The three-umbrella porcelain insulator is complex in structure and high in cost. Therefore, its application in the practical engineering is not yet as much as that of the double-umbrella porcelain insulator, but at present is a developing trend.

10.2 Methods to Determine the Number of the UHV Transmission Line Insulators

The study and the engineering experience in the UHV transmission lines show that, with the increase of the voltage level, the lightning withstand level of the UHV power grid is enhanced, the switching overvoltage amplitude is decreased, thus, the working voltage gradually plays the dominant role in the determination of the number of insulators. In the HV and EHV power grids, the switching overvoltage and lightning overvoltage play the dominant role in the selection of insulator string length. However, in the UHV power grid, in the clean regions and the regions subject to light pollution, the switching overvoltage determines the insulator string length, in the regions subject to medium and heavy pollution, the working voltage determines the insulator string length.

The selection of the number of insulators in a suspension insulator string on the tangent tower of the 1000 kV line generally needs to meet the requirements to withstand the effects of the long-duration working voltage and switching overvoltage, and the lightning overvoltage is generally not regarded as a decisive condition for the selection of the number of insulators, but only as a condition to verify whether the lightning withstand level meets the corresponding requirements.

10.2.1 Selection of the Number of Insulators Based on Power Frequency Voltage

There are two methods to determine the number of insulators based on power frequency voltage, namely the specific creepage distance method and the pollution withstand voltage method. The former is simple and easy to implement and is widely used in the power grids with low voltage level, but the disadvantage is that it does not consider the influence of the insulator's different umbrella shapes; the latter is directly related to the pollution withstand capability of the insulator and makes up the disadvantage of the former, with the test results being closer to the actual operating conditions; however, due to the complex test method, it is mainly used in the EHV and UHV systems.

10.2.1.1 Specific Creepage Distance Method

1. Porcelain and glass insulators

The specific creepage distance (namely specific leakage distance) λ refers to the surface creepage distance required for per kV voltage, namely

$$\lambda = K_e \frac{nL_0}{U_m} (\text{cm/kV}) \tag{10.2}$$

where

n the number of insulators in each string;
L_0 the geometric creepage distance of each insulator, in cm;
U_m the effective value of the maximum working voltage of the system (in this case, λ is the specific creepage distance of the insulator under the maximum voltage) or the nominal voltage (in this case, λ is the specific creepage distance of the insulator under the nominal voltage), in kV;
K_e the efficiency coefficient of the creepage distance of the insulator (according to the electric power industry standard DL/T 620-1997: with the XP-160 insulator with geometric creepage distance of 290 mm taken as the reference standard, K_e is tentatively taken as 1; when the insulators of other types are used, K_e shall be determined by the following equation).

$$K_e = \frac{L_{01} U_{50.2}}{L_{02} U_{50.1}} \tag{10.3}$$

where

L_{01} and L_{02} the geometric creepage distances of the XP-160 insulator and the insulator of other types;
$U_{50.1}$ and $U_{50.2}$ the 50% flashover voltages of the XP-160 insulator and the insulator of other types.

The operating experience shows that, for the 1000 kV UHV transmission line, in the regions subject to light pollution, it is recommended to take the efficiency coefficient K_e of the standard-type, double-umbrella-type and three-umbrella-type porcelain insulators as 1.0, and the efficiency coefficient K_e of the bell-type insulator as 0.9; in the regions subject to medium and above pollution, it is recommended to take the efficiency coefficient K_e of the standard disk-type, double-umbrella-type and three-umbrella-type insulators as 0.95, and the efficiency coefficient K_e of the bell-type insulator as 0.85 [4].

To not make the flashover happen to the insulator, the geometric creepage distance of the corresponding insulator string shall be larger than the value of the creepage distance required for the polluted regions; thus, the number of insulators in each string can be obtained:

$$n \geq \frac{\lambda_0 U_{\mathrm{m}}}{K_{\mathrm{e}} L_0} \tag{10.4}$$

For the regions subject to different pollution classes, different specific creepage distances λ_0 are required. The pollution classification standards [4] for the HV overhead line are as shown in Table 10.3.

For the purpose of strictness, the maximum value shall usually be taken as the specific creepage distance.

For the insulators in a tension string, on one hand, due to their good self-cleaning performance, their specific creepage distance is less than that of the insulators in a suspension string in the same polluted region; however, on the other hand, in consideration that the insulators in a tension string bear large pull, it is easy to generate zero-value insulator. Therefore, based on the comprehensive consideration, the number of insulators in a tension string is usually more than the number of insulators in a suspension string.

When the altitude of the region where the insulators are located is above 1000 m, with the decrease of the atmospheric pressure, the DC and AC discharge voltages of the polluted insulators will both decrease. Therefore, the number of insulators in each string in the high-altitude regions needs to be corrected. The correction equation [4] is shown below:

$$n_{\mathrm{H}} = n e^{0.1215 m_1 (H-1)} \tag{10.5}$$

where

n the required number of insulators in each string in the plain regions;
n_{H} the required number of insulators in each insulator string in the high-altitude regions;
H the altitude (km), $H \leq 3.5$ km (when the altitude is larger than 1000 m, it shall be subject to correction);
m_1 the characteristic index, indicating the influence of the atmospheric pressure on the pollution flashover voltage.

The values of m_1 for various types of insulators shall be determined according to the actual test data. The values of m_1 for the insulators with different shapes are as shown in Table 10.4 [4].

With the UHV line in the regions subject to medium pollution provided with double-umbrella-type insulators for coordination taken as an example, the steps to determine the number of insulators in each string through the specific creepage distance method are as follows:

U_{m} takes the nominal voltage of the system, i.e., 1000 kV.

Table 10.3 Pollution classification standards for HV overhead line

Pollution class	Pollution and moisture characteristics	Equivalent salt deposit density (mg/cm^2)	Specific creepage distance of the line (cm/kV)
0	The atmospherically clean regions, and the regions which are more than 50 km away from the coastal salt field and not subject to obvious pollution	Less than 0.03	1.50 (1.60)
I	The regions subject to light atmospheric pollution, industrial regions and low population concentration regions, and the regions which are 10–50 km from the coastal salt field. The regions subject to dryness and less fog (including drizzle) or more rainfall in the pollution flashover season	0.03–0.06	1.50–1.87 (1.60–2.00)
II	The regions subject to medium atmospheric pollution, the regions subject to slight salinity and furnace smoke pollution, and the regions which are 3–10 km from the coastal salt field. The regions subject to moisture, more fog (including drizzle) and less rainfall in the pollution flashover season	0.06–0.10	1.87–2.34 (2.00–2.50)
III	The regions subject to heavy atmospheric pollution, the regions subject to heavy fog and heavy salinity pollution, the regions which are 1–3 km from the coastal salt field, industrial regions and high population concentration regions, and the regions subject to heavy pollution which are 300–1500 m from the chemical pollution and furnace smoke pollution	0.10–0.25	2.34–3.00 (2.50–3.20)
IV	The regions subject to especially heavy atmospheric pollution, the regions which are within 1 km from the coastal salt field, the regions which are within 300 m from the chemical pollution and furnace smoke pollution	0.25–0.35	3.00–3.56 (3.20–3.80)

The specific creepage distance λ is the value calculated based on the system's maximum working voltage of 1100 kV; the figures in brackets are the values calculated based on the nominal voltage

The pollution class is II, the specific creepage distance λ takes the calculated value under the nominal voltage and, for the purpose of strictness, it takes the maximum value of 2.50.

The insulator is the double-umbrella insulator and the geometric creepage distance L_0 = 485 mm.

The efficiency coefficient K_e = 1.

Then, the number of insulators n shall meet:

$$n \geq \frac{\lambda_0 U_m}{K_e L_0} \Rightarrow n \geq \frac{2.5 \times 1000}{1.0 \times 48.5} \tag{10.6}$$

Through calculation, $n \geq 51.5$, after rounding, n = 52. Therefore, in the Class II polluted regions, when the double-umbrella insulators with creepage distance of 485 mm are used, the number of insulators n in the UHV line shall be 52.

For the Classes 0 and I regions where lightly polluted, the number of insulators in each string obtained by the specific creepage distance method is shown in Table 10.5.

From the above table, it can be known that, in the Classes 0 and I polluted regions, when only the power frequency voltage is considered and the number of insulators in each string is determined by the specific creepage distance method, the insulator string length is usually shorter than that required by the overvoltage; in such case, though the flashover along the insulator string does not happen under the power frequency voltage, the short insulator string makes the conductor-to-tower air clearance unable to meet the requirements on switching impulse discharge voltage, hence the conductor-to-tower air clearance discharge is apt to occur. In addition, the impulse flashover is apt to occur along the short insulator string.

Table 10.4 Reference values of characteristic index m_1 for insulators with different shapes

Insulator type	Standard type	Double-umbrella type	Three-umbrella type
m_1	0.65	0.38	0.31

Table 10.5 Number of insulators in each string in classes 0 and I regions under different altitudes obtained by the specific creepage distance method

Polluted region (equivalent salt deposit density)	Insulator type	Creepage distance (mm)		Number of insulators		Insulator string length (mm)	
		1000 m	1500 m	1000 m	1500 m	1000 m	1500 m
Class 0 regions (less than 0.03 mg/cm^2)	Standard type 450 mm	16,000	16,474	36	37	7020	7215
	Double-umbrella type 485 mm			33	34	6435	6630
Class I regions (0.03–0.06 mg/cm^2)	Standard type 450 mm	20,000	20,592	45	46	8775	8970
	Double-umbrella type 485 mm			42	43	8190	8385

Table 10.6 The minimum number of standard-type insulators on UHV line in clean regions and regions subject to light pollution

Altitude (m)	500	1000	1500
Number of insulators (XWP-300)	48	52	53
String length (mm)	9360	10,140	10,335

Taking the V-type string of the double-circuit tower as an example, for the double-umbrella insulators in the Class I polluted regions, the number of insulators determined by the specific creepage distance method is 42. In consideration of the length of the fittings, the distance of the lower phase conductor to the lower cross arm is about 7.30 m (as shown in Fig. 10.22), and the corresponding switching impulse discharge voltage is only 2013 kV, while the required value of the switching impulse discharge voltage is 2032 kV; in such case, the line-to-tower air clearance may be broken down due to the switching impulse. In addition, when the number of the standard insulators is 45, the corresponding line-to-tower switching impulse discharge voltage is 2052 kV, just meeting the required value of the switching discharge voltage. To secure certain margin, Ref. [4] recommended the number of standard insulators in each string in the clean regions and the regions subject to light pollution, as shown in Table 10.6.

Actually, the number of insulators in the Classes 0 and I polluted regions are selected mainly to ensure that the overall length of the insulator string reaches up to a certain length so as to make the impulse discharge voltage of the conductor-to-tower clearance meet the required value. With the 485 mm double-umbrella insulators in the Class I polluted region taken as an example, at the altitude of 1000 m, the number of insulators determined by the specific creepage distance method is 42 and the insulator string length is 8.19 m; however, such insulator string length cannot meet the required value of the impulse discharge voltage in the Class I region, and hence the number of insulators shall be corrected to 52.

The selection of the number of insulators in a string shall meet the requirements in two aspects. First, the creepage distance of the insulator string shall meet the required value of creepage distance in the polluted regions, so as to ensure the stable operation of the line under the power frequency voltage; second, the insulator string shall achieve certain length, so that there is sufficient conductor-to-tower clearance distance, thus to ensure that the impulse discharge voltage of the conductor-to-tower clearance meets the required value. For the Classes 0 and I regions, the pollution degree is low and the required value of creepage distance is small, in such case, only a few number of insulators are needed to meet the required value of the creepage distance in the polluted regions. However, since the insulator string length is small, the switching impulse flashover is apt to occur to the insulator string, and hence the total length of the insulator string needs to be verified. For the regions subject to medium (Class II regions) and above pollution, the pollution is serious, the required value of creepage distance is high and the insulator string length meeting the requirements on creepage distance is larger than the required

value of the switching impulse discharge voltage of the conductor-to-tower clearance; therefore, it is only required to ensure that the creepage distance of insulator meets the required value, and not required to verify the insulator string length.

2. Composite insulator

For the composite insulator, the creepage distance is selected mainly by reference to the pollution degree of the polluted regions in which the porcelain insulators are located. Usually, the creepage distance of the porcelain insulator is multiplied by certain factor to determine the creepage distance of the composite insulator. The US Electric Power Research Institute (EPRI) recommended taking 0.8 times of the creepage distance of the porcelain insulator as the creepage distance of the composite insulator, while Ref. [5] simplified the specific creepage distance of the composite insulator to 20 and 25 mm/kV. The former corresponds to the specific creepage distance of 25 mm/kV of the porcelain insulator, equivalent to 0.8 times of the creepage distance; while the latter corresponds to the specific creepage distance of 32 mm/kV of the porcelain insulator, equivalent to 0.78 times of the creepage distance. In the case of the creepage distance taken as 80% of the porcelain insulator, the structural length H of the composite insulator can be calculated by referring to the following equation:

$$H = \left(\frac{0.8 \cdot \lambda \cdot U}{L_0}\right) h \tag{10.7}$$

where

λ the specific creepage distance, in cm/kV;
U the nominal voltage of system, in kV;
L_0 the geometric creepage distance of insulator, in cm;
h the structural height of insulator, in m.

With a 500 kV insulator in China taken as an example, L_0 is 1375 cm, h is 4.45 m, and λ in the Class III polluted region is 3.2 cm/kV. Therefore, the structural height H of the composite insulator is

$$H = \left(\frac{0.8 \cdot \lambda \cdot U}{L_0}\right) \quad h = \left(\frac{0.8 \times 3.2 \times 1000}{1375}\right) \times 4.45 = 8.28 \text{ m}$$

3. Comparison between the calculation results of porcelain insulator and the results recommended in the code

The number of porcelain insulators obtained by the above specific creepage distance method is as shown in Table 10.7.

Through the analysis shown in Tables 10.7 and 10.8, it can be known that the quantities of insulators in Class II polluted regions as recommended in the two tables are different, which mainly results from the selection of different efficiency coefficients of insulators. In Table 10.7, Class II polluted regions are considered as

Table 10.7 Number of porcelain insulators and length of insulator strings in different polluted regions and under different altitudes obtained by specific creepage distance method

Polluted region and equivalent salt deposit density	Insulator type	Creepage distance (mm)		Number of insulators		Length of insulator string (mm)	
		1000 m	1500 m	1000 m	1500 m	1000 m	1500 m
Class 0 regions less than 0.03 mg/cm^2	Standard type 450 mm	16,000	16,474	52	53	10,140	10,335
	Double-umbrella type 485 mm						
Class I regions 0.03–0.06 mg/cm^2	Standard type 450 mm	20,000	20,592	52	53	10,140	10,335
	Double-umbrella type 485 mm						
Class II regions 0.06–0.10 mg/cm^2 2.5 cm/kV	Standard type 485 mm	25,000	25,740	55	56	10,725	10,920
	Bell type 690 mm			43	44	10,320	10,560
	Double-umbrella and three-umbrella types 485 mm			55	56	10,725	10,920
	Three-umbrella type 635 mm			42	43	8190	8385
	Composite type			–	–	–	–
Class III regions 0.10–0.25 mg/cm^2 3.2 cm/kV	Standard type 485 mm	32,000	32,950	70	72	13,650	14,040
	Bell type 690 mm			55	57	13,200	13,680
	Double-umbrella and three-umbrella types 485 mm			70	72	13,650	14,040
	Three-umbrella type 635 mm			54	55	10,530	10,725
	Composite type			–	–	–	–
Class IV regions >0.25 mg/cm^2 3.8 cm/kV	Standard type 485 mm	38,000	39,130	83	85	16,185	16,575
	Bell type 690 mm			65	67	15,600	16,080
	Double-umbrella and three-umbrella types 485 mm			83	85	16,185	16,575
	Three-umbrella type 635 mm			63	65	12,285	12,675
	Composite type			–	–	–	–

GB 50665-2011 *Code for design of 1000 kV overhead transmission line* has specified the number of porcelain insulators in different polluted regions, as shown in Table 10.8

Table 10.8 Number of porcelain insulators and length of insulator strings in different polluted regions and under different altitudes recommended by the code

Polluted region and equivalent salt deposit density	Insulator type	Creepage distance (mm)		Number of insulators		Length of insulator string (mm)	
		1000 m	1500 m	1000 m	1500 m	1000 m	1500 m
Class II regions 0.06–0.10 mg/cm^2, 2.5 cm/kV	Standard type 485 mm	25,000	25,740	52	54	10,140	10,530
	Bell type 690 mm			41	42	9840	10,080
	Double-umbrella and three-umbrella types 485 mm			52	54	10,140	10,530
	Three-umbrella type 635 mm			40	41	7800	7995
	Composite type			–	–	–	–
Class III regions 0.10–0.25 mg/cm^2, 3.2 cm/kV	Standard type 485 mm	32,000	32,950	70	72	13,650	14,040
	Bell type 690 mm			55	57	13,200	13,680
	Double-umbrella and three-umbrella types 485 mm			66	72	12,870	14,040
	Three-umbrella type 635 mm			54	55	10,530	10,725
	Composite type			–	–	–	–
Class IV regions >0.25 mg/cm^2, 3.8 cm/kV	Standard type 485 mm	38,000	39,130	83	85	16,185	16,575
	Bell type 690 mm			65	67	15,600	16,080
	Double-umbrella and three-umbrella types 485 mm			83	85	16,185	16,575
	Three-umbrella type 635 mm			63	65	12,285	12,675
	Composite type			–	–	–	–

the regions subject to medium pollution, and for the standard disk-type, double-umbrella-type and three-umbrella-type insulators, the value of efficiency coefficient K_e is taken as 0.95, and for the bell-type insulators, the value of efficiency coefficient K_e is taken as 0.85 [4]; while in the table recommended in GB 50665-2011 Code for Design of 1000 kV Overhead Transmission *Line*, Class II polluted regions may be considered as the regions subject to light pollution, and the value of efficiency coefficient K_e for calculation is taken as 1.0 for the standard-type, double-umbrella-type and three-umbrella-type insulators, and as 0.9 for the bell-type insulators.

10.2.1.2 Pollution Withstand Voltage Method

In case of the application of the pollution withstand voltage method, it is required to first carry out a large number of artificial pollution flashover tests on each type of insulator under different degrees of pollution and different pollution distribution in the test of environment simulating the actual pollution conditions, and then calculate the flashover voltage or withstand voltage of each type of the insulator under different degrees of pollution according to the test results of the flashover voltage, and finally calculate the number of insulators according to the withstand voltage U_s required for the system operation.

The specific steps for insulation coordination of the pollution withstand voltage method are as follows:

(1) Determine the site pollution degree of the target region and convert the equivalent salt deposit density (ESDD) to the salt deposit density (SDD)

The ESDD in the polluted regions is mainly determined by the equivalent replacement of the conducting ion in the natural pollutant with sodium ion to make the electric conductivity of artificial pollutant equal to the electric conductivity of natural pollutant. The conducting ions in the natural pollutant are mainly the sodium ion and calcium ion. The calcium ion is mainly from $CaSO_4$; when the equivalent salt deposit density of $CaSO_4$ is higher than 0.01 mg/cm^2, it cannot be fully dissolved, and hence the part of $CaSO_4$ of which the equivalent salt deposit density is higher than 0.01 mg/cm^2 is ineffective in electric conduction, resulting in the reduction of the actual electric conductivity of the natural pollutant and the increase of the pollution flashover voltage. Therefore, the part of $CaSO_4$ of which the equivalent salt deposit density is higher than 0.01 mg/cm^2 needs to be deducted from ESDD, and hence it is necessary to correct ESDD. In case $CaSO_4$ is the main insoluble component, ESDD can usually be corrected by the following equation:

$$\mathrm{SDD} = \mathrm{ESDD}\,(1 - \mathrm{CaSO_4}\%) + 0.01 \tag{10.8}$$

Table 10.9 SDD for HV overhead line in polluted regions under $CaSO_4$ content of 20 and 40%

Pollution class	ESDD (mg/cm^2)	SDD (mg/cm^2) (under $CaSO_4$ content of 20%)	SDD (mg/cm^2) (under $CaSO_4$ content of 40%)
0	Less than 0.03	Less than 0.034	Less than 0.028
I	0.03–0.06	0.034–0.058	0.028–0.046
II	0.06–0.10	0.058–0.09	0.046–0.07
III	0.10–0.25	0.09–0.21	0.07–0.16
IV	0.25–0.35	0.21–0.29	0.16–0.22

where

SDD the salt deposit density, in mg/cm^2;
ESDD the equivalent salt deposit density, in mg/cm^2;
$CaSO_{4\%}$ the percentage of $CaSO_4$ in ESDD;

the maximum soluble equivalent salt deposit density of $CaSO_4$ is taken as 0.01 mg/cm^2.

Through the research on the samples taken from different types of pollutants along the UHV line in China, it is found that the content of $CaSO_4$ in the pollutant ranges from 10 to 49% (30–49% in most regions). With the content of $CaSO_4$, respectively, taken as 20 and 40%, the SDD after correction of ESDD in the polluted regions is as shown in Table 10.9.

(2) Determine the withstand voltage of single insulator as per the value of SDD

According to the method specified in Ref. [6], the artificial pollution withstand voltage test shall be carried out on single insulator to obtain the test data and the relevant curve of the artificial pollution 50% flashover voltage of the corresponding insulator along with the variation of the equivalent salt deposit density.

The relationship between the 50% flashover voltage of single insulator and the equivalent salt deposit density on the line can be expressed as:

$$U_{50} = a \cdot \mathrm{SDD}^b \tag{10.9}$$

where

SDD the salt deposit density;
a and b constants obtained by fitting of the artificial pollution flashover test data.

In the artificial pollution flashover test, during the fitting of the relationship curve between insulator's pollution flashover voltage and salt deposit density, according to the different pollution classes, the non-soluble deposit density is ranging from 0.1 to 2.0 mg/cm^2 in general, and, in case of serious case, usually taken as 1.0 mg/cm^2 [7].

The withstand voltage of single insulator can be expressed as:

$$U_{\max 1} = U_{50}(1 - k\sigma_s) \tag{10.10}$$

where

σ_s the variation coefficient of pollution flashover voltage of insulator, recommended as 7%.

The correction factor k for design pollution withstand voltage of the 1000 kV line is taken as 1.04 [4] (corresponding to the single string flashover probability of 15%, obtained through the checking of the normal distribution table).

(3) Correction of non-soluble deposit density

The non-soluble deposit density (NSDD) refers to the value obtained through dividing the non-soluble substances on the insulator surface by the surface area, and it is used to quantitatively indicate the content of non-soluble residue on the insulator surface. The pollution layer on the insulator surface consists of soluble and non-soluble components, in which, the content of soluble component is indicated by the equivalent salt deposit density (ESDD), and the content of non-soluble component is indicated by the non-soluble deposit density (NSDD).

In the natural pollution, the non-soluble substance has an influence on the pollution flashover voltage of the insulator. Therefore, it is necessary to correct the non-soluble deposit density based on the artificial pollution test results.

At present, it is popularly considered that the pollution flashover voltage of the insulator is negatively exponentially correlated with the non-soluble deposit density.

According to the pollution flashover test, the correction factor of non-soluble deposit density proposed by Wuhan High-Voltage Research Institute [8] is:

$$K_n = (\mathrm{NSDD}/1.0)^{-0.1341} \tag{10.11}$$

The withstand voltage of single insulator is corrected as follows:

$$U_{\max 2} = K_n U_{\max 1} \tag{10.12}$$

(4) Correction of uneven contamination on the upper and lower surfaces

The uneven contamination on the upper and lower surfaces of the insulator has an influence on the pollution flashover voltage and, therefore, it needs to be corrected. The correction factor is

$$K_d = 1 - N \ln(T/B) \tag{10.13}$$

where

K_d the correction factor for uneven pollution distribution on upper and lower surfaces;
N the constant related to the insulator shape, taken as 0.054 for standard-type insulator and 0.17 for umbrella-type insulator [8];
T/B the contamination uniformity ratio.

In consideration of the uneven contamination, the withstand voltage of the insulator is corrected as follows:

$$U_{max3} = K_d U_{max2} \tag{10.14}$$

(5) Determination of the pollution withstand voltage U_s.

The determination of pollution withstand voltage U_s needs to consider two factors. One is that the pollution flashover of the insulator usually occurs in the early morning when fogging and dewing is apt to occur, while the system voltage is usually the highest in the early morning and, therefore, the maximum system operating voltage (namely 1100 kV) shall be adopted in design; the other is that a suitable allowance needs to be reserved for other unexpected conditions, usually taken as 10%. Therefore, the withstand voltage is:

$$U_s = 1100 \times 1.1/\sqrt{3} = 698\,(\text{kV}) \tag{10.15}$$

(6) Determination of the number of insulators

By simply substituting the corrected parameters into the following equation, the number of line insulators N can be obtained:

$$N = U_s/U_{max3} \tag{10.16}$$

(7) Correction of the number of insulators in different string types

For the insulator strings of different string types with insulators of different umbrella types, the pollution flashover voltage is also different, and it is necessary to correct the number of insulators as follows:

$$N_f = N/K \tag{10.17}$$

where

K the correction coefficient;
N_f the corrected number of insulators.

With the standard-type insulators in the single I-type string taken as the benchmark, the ratio between the flashover voltage of another insulator string and

Table 10.10 Correction factors of the number of insulators of different string types with insulators of different umbrella types

Item	Standard porcelain insulators in single I-type string	Standard porcelain insulators in double I-type string	Standard porcelain insulators in single V-type string		Double-umbrella porcelain insulators in single I-type string
Contrasting salt deposit density (mg/cm^2)	–	0.06	0.1	0.15	0.1
Correction factor K	1	0.94	1.04	1.06	1.06

Note Contrasting salt deposit density is the value of SDD

the single I-type string under certain equivalent salt deposit density is taken as the correction coefficient K of the said string type. For example, when SDD/NSDD is 0.06/0.5 mg/cm^2, the pollution flashover voltage of the standard-type insulators in the double I-type string is reduced by 6% compared with that of the standard-type insulators in the single I-type string, and hence the string-type correction coefficient of the double I-type string is 0.94.

For the correction factors of the insulator strings of different string types with insulators of different umbrella types, the following table can be referred [9] (Table 10.10).

Now, with the insulation coordination of single I-type string of standard porcelain insulators in the regions subject to light pollution taken as an example, the pollution withstand voltage method is adopted in the following steps:

Step 1: correction of SDD

Correction is carried out based on the $CaSO_4$ content of 20% as follows:

$$\begin{aligned} \mathrm{SDD} &= \mathrm{ESDD} \cdot (1 - \mathrm{CaSO_4}\%) + 0.01 = 0.06 \times (1 - 0.2) + 0.01 \\ &= 0.058\,(\mathrm{mg/cm^2}) \end{aligned} \tag{10.18}$$

Step 2: calculation of the withstand voltage of insulator

For the CA590 300 kN standard porcelain insulator, the regression equation of artificial pollution withstand voltage curve of the insulator in the long string based on SDD is as shown in the following equation [8]

$$U_{50} = 7.021 \cdot \mathrm{SDD}^{-0.202} \tag{10.19}$$

When the salt deposit density of 0.058 mg/cm^2 obtained through calculation is substituted into Eq. (10.19), U_{50} obtained is 12.48 kV, which is then substituted into Eq. (10.10) to get the withstand voltage of single insulator as follows:

$$U_{\max 1} = U_{50}(1 - k \cdot \sigma_s) = 12.48 \times (1 - 1.04 \times 0.07) = 11.57(\text{kV}) \quad (10.20)$$

Step 3: correction of non-soluble deposit density

The non-soluble deposit density is of standard value, being 1.0 mg/cm^2; therefore, the correction factor K_n = 1 and $U_{\max 2}$ is 11.57 kV.

Step 4: unevenness correction

For the corridor along the 1000 kV line, the measured range of uneven contamination ratio of the standard-type insulator is 1:2.2–1:12.9. The average value of 1:8.9 is recommended [10].

$$U_{\max 3} = K_d U_{\max 2} = (1 - 0.054 \times \ln 1/8.9) \times 11.57 = 12.94(\text{kV}) \quad (10.21)$$

Step 5: calculation of the number of insulators

$$N = U_s / U_{\max 3} = 698 \div 12.94 = 54 \quad (10.22)$$

The required number of CA590 300 kN standard porcelain insulators and CA887 300 kN double-umbrella porcelain insulators under different pollution degrees is, respectively, calculated by the pollution withstand voltage method. The calculation results are as shown in Table 10.11.

Table 10.11 Number of insulators required under different pollution degrees obtained by the pollution withstand voltage method (pcs)

Degree of pollution	ESDD (mg/cm^2)	CA590		CA887	
		N_1	N_2	N_1	N_2
0	0.03	48	48	48	48
I	0.06	52	54	49	51
II	0.10	56	59	53	56
III	0.25	67	70	63	67
IV	0.35	71	75	67	71

N_1 is the number of insulators obtained after ESDD is corrected as per $CaSO_4$ content of 41%; N_2 is the number of insulators obtained after ESDD is corrected as per $CaSO_4$ content of 20%; the number of double-umbrella insulators is obtained by correction based on calculation results of the number of standard insulators (correction factor is 1.06); the number of insulators of 48 in the Class 0 polluted regions is the number of insulators meeting the minimum insulator string length

Reference [4] presented the recommended number of CA590 standard porcelain insulators and CA887 300 kN double-umbrella porcelain insulators, as shown in Table 10.12.

It can be seen that the calculation results and the recommended number in the standard have very small difference. The number corrected based on the umbrella-type correction factor is basically as same as that in the actual calculation results.

In addition, for the determination of the number of the large-tonnage insulators on the UHV line, the utilization rate of specific creepage distance on the surface shall also be considered.

During the design of the 1000 kV line, Japan carried out a large number of artificial pollution tests on the fog-type insulators of various tonnages, and obtained the withstand voltage of the single fog-type insulators in the suspension string and, meanwhile, worked out the number of insulators required in different polluted regions, as shown in Table 10.13 [10].

Table 10.12 Number of insulators required under different pollution degrees recommended in the standard (pcs)

Degree of pollution	ESDD (mg/cm^2)	CA590		CA887
		N_1	N_2	
0	0.03	48	48	45
I	0.06	52	54	49
II	0.10	56	59	53
III	0.25	66	71	63
IV	0.35	71	75	67

N_1 is the number of insulators obtained after ESDD is corrected as per $CaSO_4$ content of 41%; N_2 is the number of insulators obtained after ESDD is corrected as per $CaSO_4$ content of 20%; the number of double-umbrella insulators is obtained after ESDD is corrected as per $CaSO_4$ content of 41%

Table 10.13 The design withstand voltage and withstand gradient along surface of single fog-type insulator in Japan

Item		Maximum salt deposit density in polluted regions (mg/cm^2)				
		0.01	0.03	0.06	0.12	0.25
210 kN	Withstand voltage (kV/pc)	17.0	13.0	11.2*	9.5	8.3*
	Withstand gradient along surface (kV/m)	45.9	35.1	30.3	25.7	22.4
300 kN	Withstand voltage (kV/pc)	19.5	15.0	12.9*	11.0	9.6*
	Withstand gradient along surface (kV/m)	42.4	32.6	28.0	23.9	20.9
400 kN	Withstand voltage (kV/pc)	20.5	15.8	13.6	11.6	10.1
	Withstand gradient along surface (kV/m)	39.0	30.1	25.9	22.1	19.2
530 kN	Withstand voltage (kV/pc)	24.0	18.5	15.7	13.4	11.6
	Withstand gradient along surface (kV/m)	35.8	27.6	23.4	20.0	17.3

The data marked with * are the values obtained by fitting according to other data

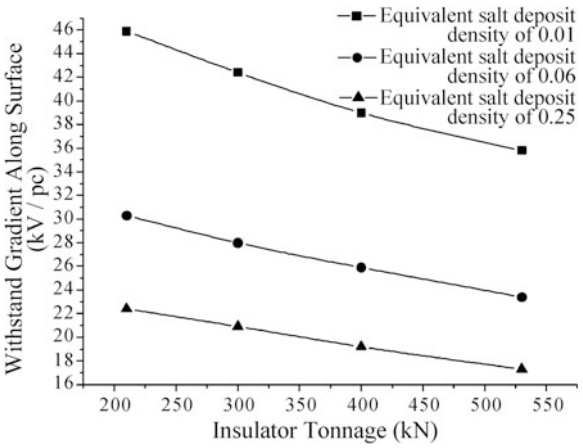

Fig. 10.3 Descending curve of withstand gradient along surface of insulator under three equivalent salt deposit densities

When the equivalent salt deposit density is, respectively, 0.01, 0.06 and 0.25 mg/cm^2, the curve of withstand gradient along surface of insulator descends with tonnage as shown in Fig. 10.3 [10].

It can be seen that, under identical degree of pollution, with the increase of insulator tonnage, the withstand gradient along surface of insulator decreases gradually, and the utilization of specific creepage distance on the surface of insulator is more and more insufficient. In addition, it can also be seen that, under different equivalent salt deposit densities, with the increase of insulator tonnage, the descending speed of withstand gradient along surface is basically the same. Therefore, during the selection of the large-tonnage insulators, the utilization rate of specific creepage distance shall be considered, and the number of insulators shall be properly increased.

10.2.2 Selection of the Number of Insulators as Per Switching Overvoltage

The 50% discharge voltage $U_{50\%}$ of positive switching impulse voltage wave of the line insulator string required by switching overvoltage shall comply with the following equation:

$$U_{50\%} \geq K_1 \cdot U_s \tag{10.23}$$

where

U_s the line's statistical phase-to-ground switching overvoltage, in kV;

K_1 the statistical coordination coefficient of switching overvoltage for the line insulator string, which is recommended to be 1.27 in Ref. [11] and recommended to be 1.25 in Ref. [12].

In the actual engineering, when the pollution degree is larger than or equal to II, the switching overvoltage often has no effect on the selection of the number of insulators in the insulator string, and the number of insulators in the insulator string is determined by power frequency voltage.

10.2.3 Checking of the Number of Insulators as per Lightning Overvoltage Requirements

The external insulation level of the UHV transmission line determined by power frequency voltage and switching overvoltage is very high and usually can meet the requirements on the line's lightning withstand level and lightning trip-out rate. Therefore, in the UHVAC transmission line, the lightning overvoltage does not play a decisive role in the selection of the number of insulators in insulator string, and is only taken as a condition to check whether the lightning withstand level meets the requirements.

10.3 Determination of Air Clearances of the UHV Line

The air clearances to be considered for the transmission lines mainly include conductor-to-ground, conductor-to-conductor, conductor-to-overhead ground wire as well as conductor-to-tower and conductor-to-cross arm ones. The conductor-to-ground clearance mainly considers the safe distance between the highest object under the conductor and the conductor; the conductor-to-conductor distance is mainly determined by the minimum clearance between the lowest sag points of the conductors being able to withstand the working voltage in case of asynchronous swing under the effect of wind; the conductor-to-ground wire clearance is determined based on the condition that the lightning strikes on the midspan of shielding wire do not cause the breakdown of air clearance between conductors. For the determination of air clearance of the UHV line, the determination of the conductor-to-tower and conductor-to-cross arm clearances is the most important.

For the UHV transmission line, the determination of the air clearance shall consider the following points:

1. Overvoltage waveform

The voltage waveform mainly refers to the wave front length and the wave tail length. The front time generates a large influence on the clearance breakdown voltage under switching impulse. In the EHV system, the wave front length of switching overvoltage during the test is 250 μs. While in the UHV system, the wave front length of 95% switching overvoltage is above 1000 μs. Therefore,

during the UHV switching impulse test, it is necessary to specify the wave front length of switching overvoltage, thus to ensure that the test results comply with the requirements of the UHV power grid.

2. Lateral width of the tower

The lateral width of the tower at the air clearance has an obvious influence on the discharge voltage of the air clearance of the UHV towers. With the increase of lateral width of the tower, the switching impulse discharge voltage of the air clearance of the tower reduces correspondingly. According to the laboratory test results, the scholars of the former Soviet Union considered that the influence of the tower body width on the discharge voltage of the air clearance can be expressed as the following relation [13, 14]:

$$U_{50}(\omega) = U_{50}(1)(1.03 - 0.03\omega) \tag{10.24}$$

where

$U_{50}(\omega)$ the discharge voltage when the tower body width is ω m;
$U_{50}(1)$ is the discharge voltage when the tower body width is 1 m;
ω tower body width, in m.

3. Influence of wind deflection angle

For the breakdown voltage of the air clearance of the line, the amplitude of lightning overvoltage is the highest, followed by the switching overvoltage and then the working voltage. However, in terms of the voltage action time, the sequence is reverse. During the determination of the conductor-to-tower clearance distance, the wind deflection angle for swing of insulator string under the effect of wind must be considered. As the working voltage acts on the conductor for a long time, the wind deflection angle θ_p corresponding to the maximum wind speed in a 100-year return period is taken for calculation, as the switching overvoltage has a short duration, the wind deflection angle θ_s under 50% of the maximum wind speed is taken for calculation; as the lightning overvoltage has an extremely short duration, the wind deflection angle θ_1 under 10 m/s wind speed is taken for calculation. During the test, the wind deflection angles used to simulate the discharge of insulator to tower under working voltage, switching overvoltage, and lightning overvoltage are, respectively, set at 50°, 20°, and 12°.

4. Tower structure

During the determination of the air clearance of the line, it is necessary to consider not only the influence of the wind deflection, but also the factor of tower structure. For the UHV lines, the towers mainly include the cat-head-type tower, the cup-type tower and the double-circuit tower. The structures are as shown in Fig. 10.4.

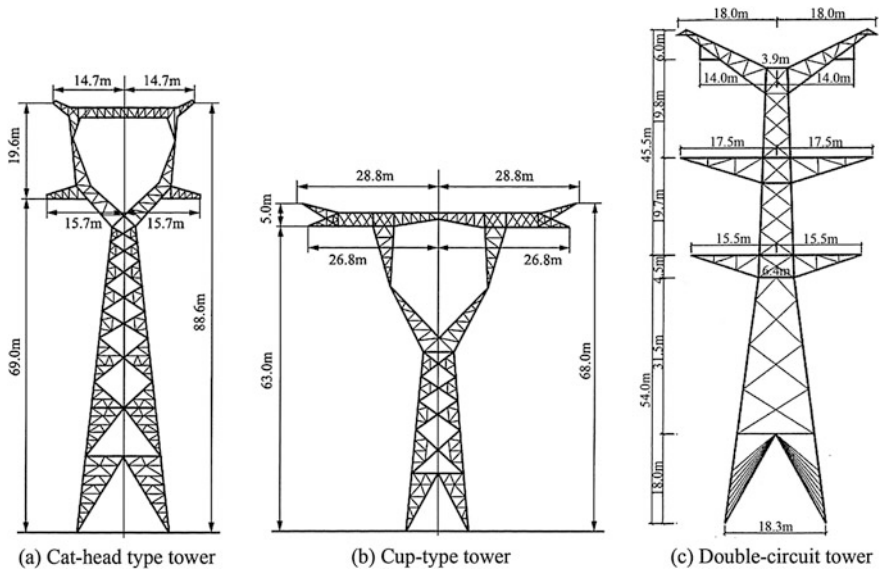

Fig. 10.4 Diagram of UHV tower structures

It can be seen that the side-phase conductor-to-tower air clearances of the cat-head-type tower and cup-type tower are subject to the influence of wind deflection and, therefore, it is necessary to check whether the clearance distance can meet the requirements under the three types of overvoltage, respectively. While due to the pull of the V-type insulator string, the intermediate-phase conductor is not subject to the influence of wind deflection and, therefore, it is only necessary to check whether the air clearance of the line can meet the discharge distance requirements of the switching overvoltage and lightning overvoltage.

For the double-circuit tower, due to the long insulator string length, the conductor is actually difficult to discharge the upper cross arm and, therefore, the conductor-to-adjacent lower cross arm clearance and the conductor-to-tower body clearance shall mainly be considered. When the insulators in I-type string are used, all the clearances among the three phases shall consider the influence of wind deflection. During the checking of the air clearance distance between the upper phase conductor and the intermediate-phase conductor, no matter whether the I-type or V-type insulator string is adopted, the influence of the adjacent lower cross arm shall be considered. For the air clearance of the conductor to the adjacent lower cross arm, as the air clearance between the upper phase conductor and the adjacent lower cross arm and that between the intermediate-phase conductor and the adjacent lower cross arm are basically the same, the clearance distance between the upper phase conductor and the adjacent lower cross arm can normally be referred to the test results of that between the intermediate-phase conductor and the adjacent lower cross arm. In addition, for the conductor-to-tower body air clearance, as the tower body width adjacent to the intermediate-phase conductor is larger than that adjacent

to the upper phase conductor; the breakdown voltage of the intermediate-phase conductor is slightly lower than that of the upper phase conductor under the same clearance. Therefore, the determination of the air clearance of the upper phase conductor can be referred to the test results of that of the intermediate-phase conductor; in this way, certain allowance can be ensured, as well.

Considering that the adjacent conductors are spaced out by cross arm or tower window, the phase-to-phase spacing of the conductor is usually not defined.

5. Influence of multi-gap parallel connection on discharge voltage and variation coefficient thereof

The so-called multi-gap parallel discharge voltage refers to the air clearance discharge voltage of a line section in which there are multiple towers and each tower has corresponding conductor-to-tower air clearance, i.e., the discharge voltage after the multiple clearances are parallel connected.

The breakdown voltage under multi-gap parallel connection is smaller than the discharge voltage under single clearance. The relationship is as shown in the following equation [4]:

$$U_{50.\mathrm{m}} = U_{50.1}(1 - Z\sigma_1^*) \tag{10.25}$$

where

$U_{50.\mathrm{m}}$ and $U_{50.1}$ respectively, are the 50% discharge voltages under the parallel connection of m clearances and under single clearance;
Z dependent on the number of the paralleled clearances m;
σ_1* the variation coefficient of single-clearance discharge voltage.

The relationship between the variation coefficient of multi-gap discharge voltage σ_m* and that of single-clearance discharge voltage σ_1* is as shown in the following equation [4].

$$\beta = \sigma_m^*/\sigma_1^* \tag{10.26}$$

Under different voltage, the number of clearances m shall be determined according to different principles. Under the power frequency voltage, the determination of the number of paralleled clearances m shall mainly consider the number of towers of which the conductors have the maximum wind deflection angle at the same time; under the switching overvoltage (usually, the maximum statistical 2% switching overvoltage along the line is taken as the typical switching overvoltage), the line length subject to typical switching overvoltage shall be mainly considered. Through reference to the experience in design and operation of the UHV lines of the former Soviet Union, for the purpose of strictness, it can be taken as m = 100. Therefore, through reference to the experience in China and abroad, it is usually taken as m = 100. The influence of different number of paralleled clearances m on Z and β is as shown in Table 10.14 [4].

Table 10.14 Influence of number of paralleled clearances m on Z and β

m	1	100	500
$\beta = \sigma_m^*/\sigma_1^*$	1	0.4	0.36
Z	0	2.45	3

As the clearance discharge voltage of the line is disperse, the flashover probability of the line insulation shall be not larger than 0.13%. Therefore, the multi-gap parallel discharge voltage $U_{50.\mathrm{m}}$ under power frequency voltage shall meet the following equation:

$$U_{50.\mathrm{m}} \geq \frac{U_{\mathrm{n.m}}}{(1 - 3\sigma_m^*)} \tag{10.27}$$

where

$U_{\mathrm{n.m}}$ the maximum system operating voltage.

$$U_{\mathrm{n.m}} = \frac{\sqrt{2}}{\sqrt{3}} \times 1.1 U_{\mathrm{n}} = \frac{\sqrt{2}}{\sqrt{3}} \times 1.1 \times 1000 = 898(\mathrm{kV}) \tag{10.28}$$

Substitute Eq. (10.25) into Eq. (10.27) to obtain:

$$U_{50.1} \times (1 - Z\sigma_1^*) \geq \frac{U_{\mathrm{n.m}}}{(1 - 3\sigma_m^*)} \tag{10.29}$$

Thus, it can be obtained that, when the influence of multi-gap parallel connection is considered, the single-clearance 50% discharge voltage $U_{50.1}$ shall meet the following equation:

$$U_{50.1} \geq \frac{U_{\mathrm{n.m}}}{(1 - Z\sigma_1^*)(1 - 3\sigma_m^*)} \tag{10.30}$$

The required single-clearance 50% discharge voltage $U_{50.1.\mathrm{r.pf}}$ when power frequency voltage is considered shall be:

$$U_{50.1.\mathrm{r.pf}} = \frac{U_{\mathrm{n.m}}}{(1 - Z\sigma_1^*)(1 - 3\sigma_m^*)} \tag{10.31}$$

Similarly, the required single-clearance 50% discharge voltage $U_{50.1.\mathrm{r.s}}$ when switching overvoltage is considered shall be:

$$U_{50.1.\mathrm{r.s}} = \frac{U_{\mathrm{S}}}{(1 - Z\sigma_1^*)(1 - 3\sigma_m^*)} \tag{10.32}$$

In Eq. (10.32), U_S is the maximum statistical (2%) switching overvoltage along the UHVAC transmission line, taken as 1.7 p.u., namely

$$U_S = 1.7U_{n.m} = 1.7 \times \frac{\sqrt{2}}{\sqrt{3}} \times 1.1U_n = 1.7 \times \frac{\sqrt{2}}{\sqrt{3}} \times 1.1 \times 1000 = 1526.8(\text{kV}) \tag{10.33}$$

Under the power frequency voltage, the variation coefficient of the single-clearance discharge voltage is usually taken as $\sigma_1^* = 0.3$; while, under the switching overvoltage, the variation coefficient of single-clearance discharge voltage is higher than that under the power frequency voltage and is usually taken as $\sigma_1^* = 0.6$ [4].

6. Influence of altitude on the air clearance discharge voltage

When needed to be converted to the discharge voltage (U_{P_H}) in the region with altitude of $H(m)$, the air clearance discharge voltage (U_{P_0}) can be corrected by the following equation:

$$U_{P_H} = k_a \cdot U_{P_0} \tag{10.34}$$

where

U_{P_0} the required value of the air clearance discharge voltage or withstand voltage under standard weather conditions, in kV;
k_a is the altitude correction coefficient.

The calculation of correction coefficient k_a can be referred to as Ref. [15], namely

$$k_a = e^{m(H/8150)} \tag{10.35}$$

where the value of m is as shown below: for the short-duration withstand voltage of air clearance and clean insulator, $m = 1.0$; for the lightning impulse voltage, $m = 1.0$; for the switching impulse voltage, the value of m is selected as per Fig. 10.5.

The checking of the air clearance under switching impulse of the UHV line at the altitude of 1000 m is taken as an example to illustrate the steps of altitude correction.

Calculate the required value of 50% switching impulse discharge voltage of air clearance under the standard atmospheric conditions as follows:

$$U_{50.1r} = k_s k_c U_s = 1 \times 1.26 \times 1.7 \times 898 = 1924\,\text{kV}$$

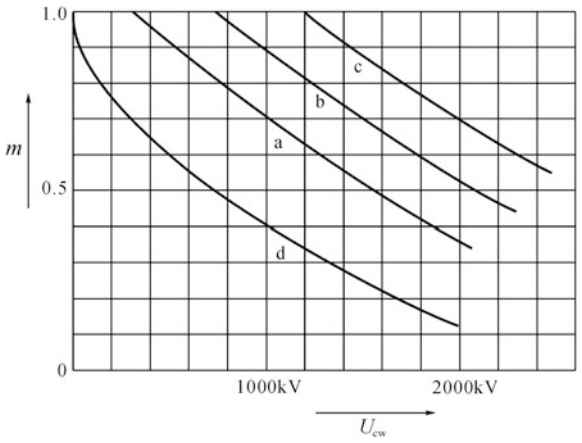

Fig. 10.5 Dependence of exponent m on the coordination switching impulse withstand voltage, reprinted from Ref. [15], copyright 2014, with permission from Water Resources and Electric Power Press (China). *Note a* Phase-to-earth insulation; *b* longitudinal insulation; *c* phase-to-phase insulation; *d* rod–plane clearance (reference clearance)

Then determine the value of m. The air clearance of the line is the conductor-to-tower clearance, and it belongs to the phase-to-earth insulation. Therefore, the curve *a* is selected. As the discharge voltage is above 1900 kV, it can be seen that the value of m ranges from 0.35 to 0.4. To reserve certain allowance, it is taken as $m = 0.39$.

Calculate the correction factor of altitude as follows:

$$k_a = e^{m(H/8150)} = e^{0.39\times 1000/8150} = 1.049$$

The corrected discharge voltage is

$$U_{P_H} = k_a \cdot U_{P_0} = 1.049 \times 1924 = 2018\ (\text{kV})$$

10.3.1 Determination of Air Clearance Under Power Frequency Voltage

10.3.1.1 Long-Clearance Discharge Characteristic Curve Under Power Frequency Voltage

The conductor-to-tower discharge breakdown model under power frequency voltage can be referred to the rod–plane and rod–rod breakdown models under long air clearance. The scholars of the former Soviet Union, such as Александров, proposed the curves of long-clearance breakdown voltage and insulator AC flashover voltage, as shown in Fig. 10.6 [14, 15].

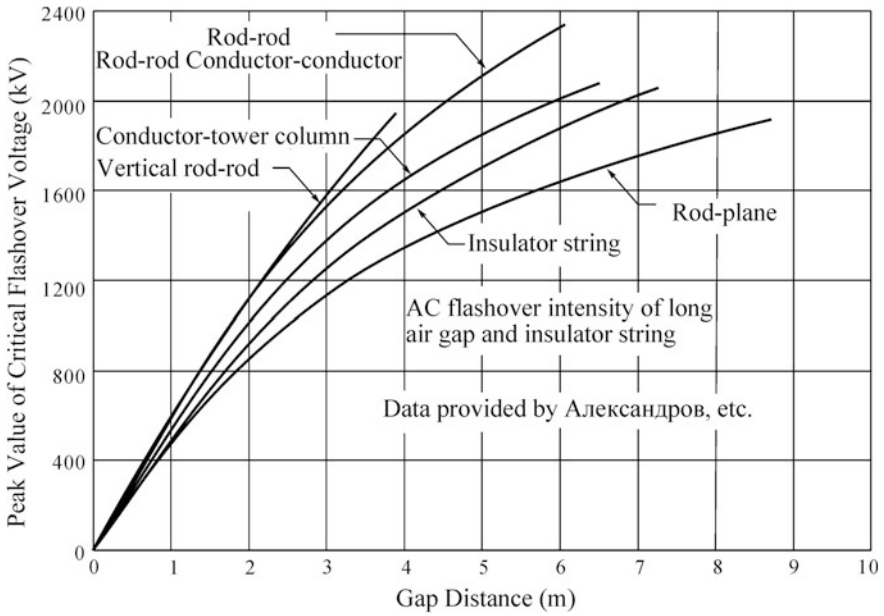

Fig. 10.6 Curves of long-clearance breakdown voltage and insulator AC flashover voltage, reprinted from Ref. [14], copyright 2014, with permission from International Electrotechnical Commission

From Fig. 10.6, it can be seen that, when the clearance distance is short, the critical breakdown voltage presents approximate linear increase with the increase of the distance, but, after the distance increases to a certain extent, the linearity of the curve becomes poor and the breakdown voltage does not increase much as the clearance distance increases. It shall be noted that during the design that, as the voltage level of the UHV line is high, the conductor-to-tower clearance breakdown voltage is apt to enter the non-linear zone and, therefore, the increase of clearance distance does not have an obvious effect on the enhancement of the breakdown voltage.

10.3.1.2 Required Value of the Power Frequency Discharge Voltage of the Air Clearance

The calculation method of the clearance insulation coordination under power frequency voltage is shown as follows [7].

The 50% power frequency discharge voltage of air clearance shall consider the following factors: the influences of the maximum wind speed in a 100-year return period, the maximum system operating voltage and the multi-gap parallel connection on the discharge voltage.

Based on the comprehensive consideration of the above factors, the required value of 50% power frequency discharge voltage of single clearance is

$$U_{50.1.r} = k_a \cdot k_s \cdot k_c \cdot U_m \cdot \sqrt{2}/\sqrt{3} \tag{10.36}$$

where

k_s is the safety margin, taken as 1.05;
k_c is the coordination coefficient, mainly considering the influence of the multi-gap parallel connection on discharge voltage;
U_m is the maximum system operating voltage, taken as 1100 kV;
k_a is the altitude correction coefficient: under power frequency voltage, when H = 500 m, k_a = 1.063; when H = 1000 m, k_a = 1.131; when H = 1500 m, k_a = 1.202.

The coordination coefficient k_c is calculated as shown in Eq. (10.37), where the number of paralleled clearances m = 100, Z = 2.45 and σ_1*is taken as 0.03 [4].

$$k_c = \frac{1}{(1 - Z\sigma_1^*)(1 - 3\sigma_m^*)} = \frac{1}{(1 - 2.45 \times 0.03)(1 - 3 \times 0.012)} = 1.12 \tag{10.37}$$

In the national standard GB/Z 24842-2009 *Overvoltage and Insulation Coordination of 1000 kV UHV AC Transmission Project*, it is recommended that the coordination coefficient k_c should be taken as 1.1 [16]. Actually, the calculation result of Eq. (10.37) is very close to the value recommended in the national standard. For the calculation in this section, the coordination coefficient k_c is the value recommended in the national standard, taken as 1.1.

Considering the influence of the altitude, the required value of air clearance power frequency discharge voltage $U_{50.1.r.pf}$ is

when H = 500 m, $U_{50.1.r.pf} = 1.063 \times 1.05 \times 1.1 \times 1100 \times \sqrt{2}/\sqrt{3} = 1103(\text{kV})$;
when H = 1000 m, $U_{50.1.r.pf} = 1.131 \times 1.05 \times 1.1 \times 1100 \times \sqrt{2}/\sqrt{3} = 1173(\text{kV})$;
when H = 1500 m, $U_{50.1.r.pf} = 1.202 \times 1.05 \times 1.1 \times 1100 \times \sqrt{2}/\sqrt{3} = 1247(\text{kV})$.

10.3.1.3 UHV Full-Scale Tower Test Arrangement and Discharge Curve

(1) Single-circuit tower

The UHV single-circuit tower mainly consists of the cup-type tower and the cat-head-type tower, both of which, the intermediate phase is applied with V-type insulator string and the side phase is applied with I-type insulator string. Since the

V-type string is not subject to the influence of wind deflection, the conductor-to-tower window clearance distance usually meets the required value of power frequency discharge voltage. Therefore, for the UHV single-circuit tower, it is only necessary to check whether the clearance distance of I-type string on the side phase of the two types of towers meets the requirements for power frequency discharge voltage.

For the UHV cup-type tower and cat-head-type tower, the full-scale tower test is arranged as shown in Fig. 10.7.

For the two types of towers, what mainly occurs is the conductor-to-tower leg discharge. In the test, the simulated wind deflection angle is around 50°, the conductor-to-tower leg distance is 2–4 m, and the curve between clearance distance d and discharge voltage is as shown in Fig. 10.8 [16]. Thus, according to the required value of power frequency discharge voltage, the relevant discharge voltage curve can be checked to obtain the clearance distance required under power frequency discharge voltage for the single-circuit tower.

(2) Double-circuit tower

For the insulator string of double-circuit tower, since the V-type string is not subject to the influence of wind deflection, the conductor-to-tower window clearance distance usually meets the required value of power frequency discharge voltage, and the air clearance between the insulators in I-type string is still mainly to be checked.

The clearance distance of the conductor to the adjacent lower cross arm of the double-circuit tower is mainly determined by the switching overvoltage and can usually reach up to 5–8 m, while the required value of the clearance distance under the power frequency voltage is only around 3 m. In such case, the clearance

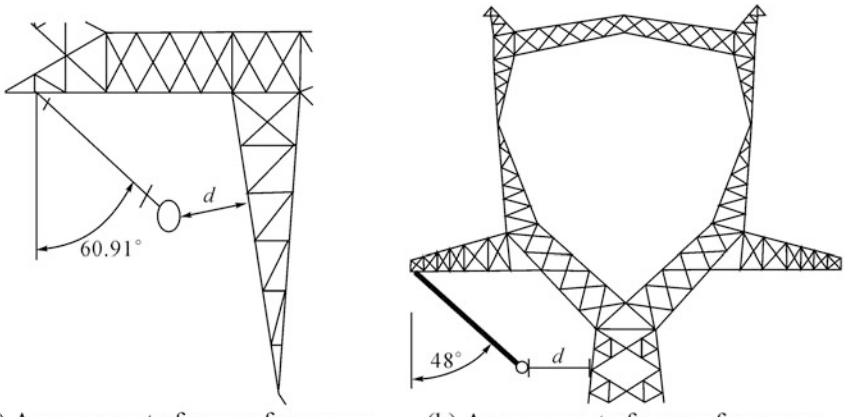

(a) Arrangement of power frequency discharge test of side phase of cup type tower

(b) Arrangement of power frequency discharge test of side phase of cat-head type tower

Fig. 10.7 Power frequency discharge test arrangement of single-circuit tower

distance of the conductor to the adjacent lower cross arm can fully meet the requirements of power frequency discharge voltage. Therefore, for the power frequency discharge clearance of the double-circuit tower, main consideration shall be given to the conductor-to-tower body clearance distance under wind deflection.

The test arrangement of the UHV double-circuit full-scale drum-type steel tower is as shown in Fig. 10.9. For the upper phase and the intermediate phase, it is mainly the conductor-to-tower body discharge, while for the lower phase, it is mainly the conductor-to-tower leg discharge and, therefore, these two cases shall be tested, respectively. As it is conductor-to-tower body discharge on both the upper

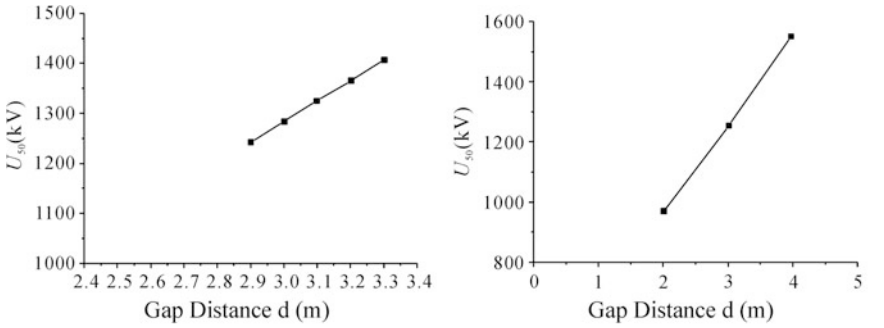

Fig. 10.8 Power frequency discharge voltage curve of single-circuit tower

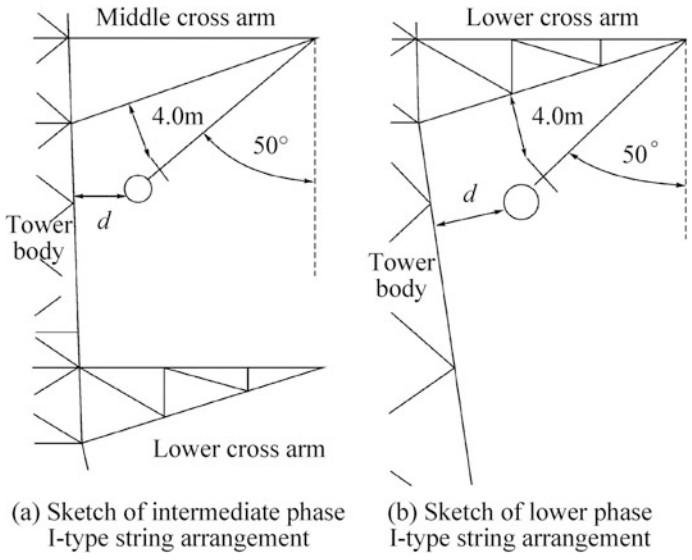

Fig. 10.9 Arrangement of power frequency discharge test of double-circuit tower

phase and the intermediate phase, and the discharge modes of the two are basically the same, considering that the breakdown voltage of the intermediate-phase conductor is slightly lower than that of the upper phase conductor under the same clearance, for the purpose of strictness, the determination of the air clearance for the upper phase conductor can be referred to the test results of the intermediate-phase conductor. Therefore, the test is mainly carried out for the intermediate phase and lower phase. The requirements for the air clearance distance of the upper phase can be referred to those for the intermediate phase and are, in general, same as those for the intermediate-phase conductor.

For the power frequency discharge voltage of the conductor-to-tower body clearance of the double-circuit steel tower, the simulated wind deflection angle used in the test is around 50°, and the curve between clearance distance d and power frequency discharge voltage is as shown in Fig. 10.10 [16]. Thus, according to the required value of power frequency discharge voltage, the relevant discharge voltage curve can be checked to obtain the clearance distance required for the double-circuit tower under power frequency discharge voltage.

10.3.1.4 Recommended Value of Clearance Distance

According to the requirements on power frequency discharge voltage, the relevant discharge voltage curve can be checked to obtain the clearance distance required under power frequency discharge voltage, as shown in Table 10.15.

During the determination of the air clearance under power frequency voltage, it shall be ensured that the clearance distance under the wind deflection angle of 50° is not less than the values given in Table 10.15. In the national standard GB/Z 24842-2009 *Overvoltage and Insulation Coordination of 1000 kV UHV AC Transmission Project,* the recommended required values of clearance distance under power frequency voltage are as shown in Table 10.16, in accordance with the results obtained in Table 10.15.

10.3.2 Determination of Air Clearance Under Switching Impulse Voltage

10.3.2.1 Wave Front Time

During the determination of the air clearance distance under switching impulse, it is first necessary to determine the waveform of switching impulse wave. Under the switching overvoltage, the discharge voltage of air clearance is related to the wave front length of switching overvoltage. For the 1000 kV UHV power grid, Ref. [16] recommended that the front time of the standard switching impulse wave be taken as 1000 μs; Russia's UHV standard also recommended that the front time of

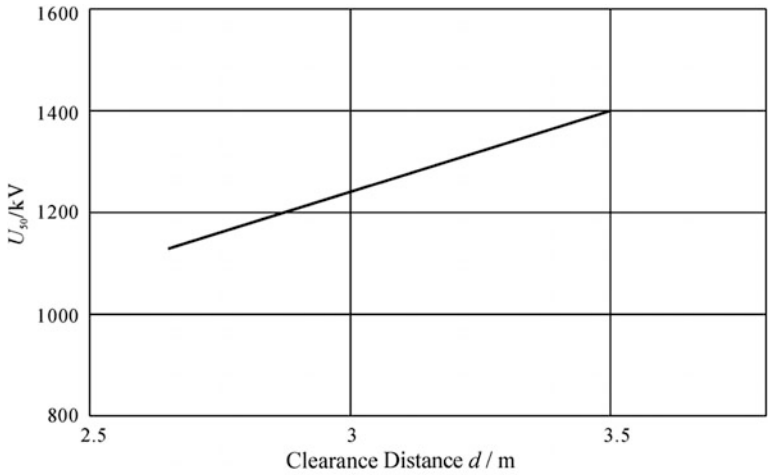

(a) Intermediate-phase conductor-to-tower body discharge voltage curve

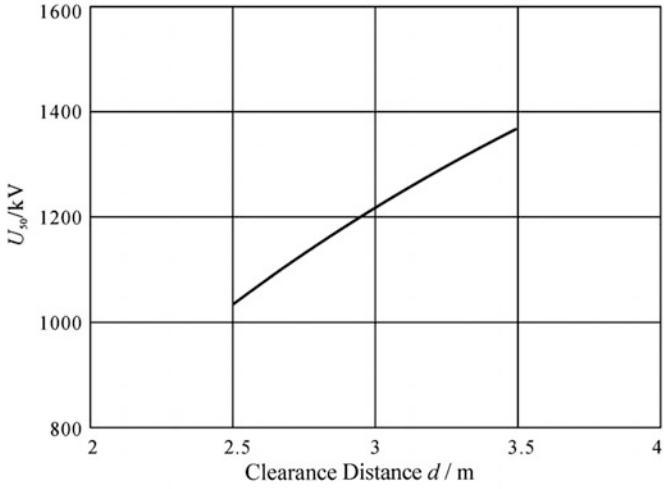

(b) Lower-phase conductor-to-tower leg discharge voltage curve

Fig. 10.10 Intermediate-phase and lower phase power frequency discharge voltage curves of double-circuit tower

switching impulse wave be taken as 1000 μs. Through the simulation calculation of the UHV line, Zhejiang University obtained that the wave front length of various switching overvoltage ranges between 800 and 4500 μs, in which more than 95% of the wave front length of switching overvoltage is larger than 1000 μs. Reference [17] presented the curve of relationship between the front time and discharge voltage as shown in Fig. 10.11, from which we can see that, within 1000–5000 μs, with the increase of the front time, the clearance discharge voltage increases

Table 10.15 Side-phase clearance distances of tower corresponding to the required values of power frequency discharge voltage

Altitude (m)		H = 500	H = 1000	H = 1500
Required value of power frequency discharge voltage (kV)		1103	1173	1247
Clearance distance (m)	Side phase of cup type tower	2.56	2.74	2.91
	Side phase of cat-head type tower	2.48	2.72	2.97
	Intermediate phase of double-circuit tower	2.59	2.79	3.02
	Lower phase of double-circuit tower	2.67	2.87	3.08

The test results of the upper phase of the double-circuit tower can be referred to those of the intermediate phase, and the type of insulator strings on all towers are I-type strings

Table 10.16 Required values of minimum air clearance under power frequency voltage

Altitude (m)		H = 500	H = 1000	H = 1500
Required value of clearance distance (m)	Single-circuit tower	2.7	2.9	3.1
	Double-circuit tower	2.7	2.9	3.1

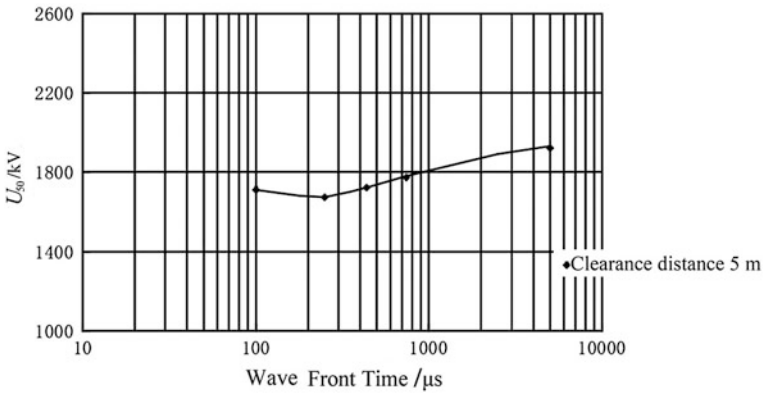

Fig. 10.11 Impact of wave front time on clearance discharge voltage

slightly. Therefore, the adoption of the switching voltage wave whose front time is 1000 μs in the test can ensure certain allowance of the test results. Therefore, the switching overvoltage wave whose front time is 1000 μs is usually applied as the impulse overvoltage wave during the test.

10.3.2.2 Required Value of Switching Overvoltage

The clearance discharge voltage under switching impulse voltage shall comply with the requirements of the following equation:

$$U_{50.1.\mathrm{r}} = k_{\mathrm{s}} k_{\mathrm{c}} k_{\mathrm{a}} U_{\mathrm{s}} \tag{10.38}$$

where

U_{s} the maximum statistical 2% switching overvoltage along the line, taken as 1.7 p.u.;
k_{s} the safety margin, taken as 1;
k_{a} the altitude correction coefficient: under switching impulse, the altitude correction factor m = 0.39; when H = 500 m, k_{a} = 1.024; when H = 1000 m, k_{a} = 1.048; when H = 1500 m, k_{a} = 1.072.

The coordination coefficient k_{c} is calculated as per Eq. (10.39), where the number of paralleled clearances m = 100, Z = 2.45, σ_1* is taken as 0.06 [4].

$$k_{\mathrm{c}} = \frac{1}{(1 - Z\sigma_1^*)(1 - 3\sigma_m^*)} = \frac{1}{(1 - 2.45 \times 0.06)(1 - 3 \times 0.024)} = 1.263 \tag{10.39}$$

In the national standard GB/Z 24842-2009 *Overvoltage and Insulation Coordination of 1000 kV UHV AC Transmission Project*, it is recommended that the coordination coefficient k_{c} be taken as 1.26 for insulators in I-type string and taken as 1.27 for insulators in V-type string. Actually, the calculation result of Eq. (10.39) is very close to the value recommended in the national standard. For the calculation in this section, the coordination coefficient k_{c} is taken as the value recommended in the national standard.

The required values of single-clearance switching impulse discharge voltage of I-type string are as follows:

when H = 500 m, $U_{50.1.\mathrm{r.s}} = k_{\mathrm{s}} k_{\mathrm{c}} k_{\mathrm{a}} U_{\mathrm{s}} = 1 \times 1.26 \times 1.024 U_{\mathrm{s}} = 1970(\mathrm{kV})$;
when H = 1000 m, $U_{50.1.\mathrm{r.s}} = 1 \times 1.26 \times 1.048 U_{\mathrm{s}} = 2016(\mathrm{kV})$;
when H = 1500 m, $U_{50.1.\mathrm{r.s}} = 1 \times 1.26 \times 1.072 U_{\mathrm{s}} = 2062(\mathrm{kV})$.

The required values of single-clearance switching impulse discharge voltage of V-type string are as follows:

when H = 500 m, $U_{50.1.\mathrm{r}} = k_{\mathrm{s}} k_{\mathrm{c}} k_{\mathrm{a}} U_{\mathrm{s}} = 1 \times 1.27 \times 1.024 U_{\mathrm{s}} = 1986(\mathrm{kV})$;
when H = 1000 m, $U_{50.1.\mathrm{r}} = 1 \times 1.27 \times 1.048 U_{\mathrm{s}} = 2032(\mathrm{kV})$;
when H = 1500 m, $U_{50.1.\mathrm{r}} = 1 \times 1.27 \times 1.072 U_{\mathrm{s}} = 2079(\mathrm{kV})$.

10.3.2.3 UHV Single-Circuit Full-Scale Tower Test Arrangements and Discharge Curves

For the single-circuit tower, the insulator string of the side-phase conductor is of I-type string, and hence it is necessary to consider the influence of the wind deflection and mainly check the clearance distance between the conductor and the tower body; as the insulator string of the intermediate-phase conductor is of V-type string, it is not necessary to consider the influence of the wind deflection, but necessary to check the clearance distance of conductor to the tower window. Therefore, the side-phase conductor and the intermediate-phase conductor shall be discussed, respectively.

(1) Side-phase conductor

For the side-phase conductor, the wind deflection angle under switching overvoltage is considered to be 20°. The side-phase conductor switching impulse discharge voltage test arrangements for the two typical single-circuit towers are as shown in Fig. 10.12, and the discharge voltage curves with the front time of 250 μs are as shown in Fig. 10.13.

For the UHV single-circuit full-scale tower, the switching impulse discharge voltage curve with front time T_f = 1000 μs shall be used. Therefore, it is necessary to carry out equivalent conversion of the switching impulse discharge voltage curve with front time T_f = 250 μs.

Reference [18] points out that the side-phase switching impulse discharge voltage with front time T_f = 1000 μs is about 7% higher than that with front time T_f = 250 μs. The required value of single-clearance switching impulse discharge voltage of I-type string obtained through calculation in the previous subsection

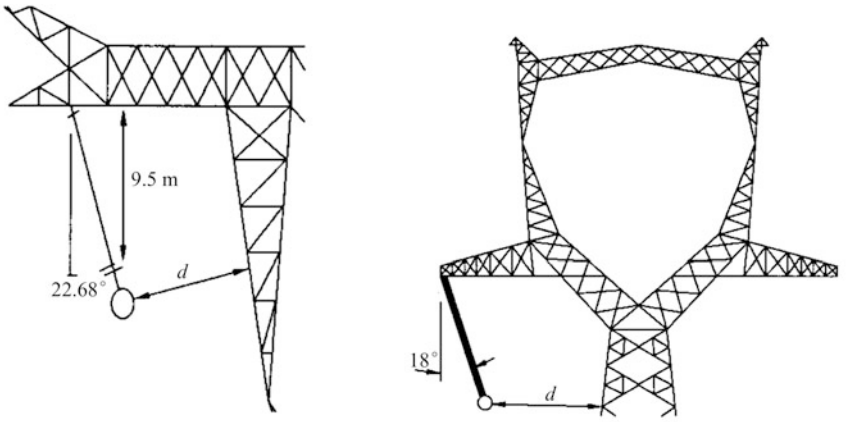

(a) Side phase switching overvoltage discharge test arrangement for cup type tower

(b) Side phase switching overvoltage discharge test arrangement for cat-head type tower

Fig. 10.12 Switching overvoltage discharge test arrangements for single-circuit towers

(with the front time of 1000 μs) can be multiplied by 0.93 to obtain the required value of discharge voltage with the front time of 250 μs, which then can be used to obtain the clearance distance required for the side phase of the single-circuit tower under the switching impulse voltage based on Fig. 10.13, as shown in Table 10.17.

During the determination of the air clearance under switching impulse voltage, it shall be ensured that, under the wind deflection angle of 20°, the clearance distance shall not be less than the values given in Table 10.17. In the national standard GB/Z 24842-2009 *Overvoltage and Insulation Coordination of 1000 kV UHV AC Transmission Project*, it is recommended that the required values of clearance distance under power frequency voltage be as shown in Table 10.18, which correspond to the results obtained in Table 10.17.

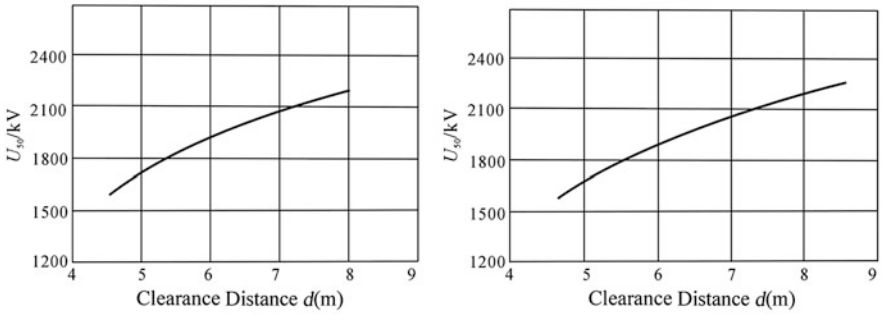

Fig. 10.13 Side-phase discharge voltage curves of cup-type tower and cat-head-type tower

Table 10.17 Clearance distance of side phases of single-circuit towers under switching impulse voltage

Altitude (m)		H = 500	H = 1000	H = 1500
Required value of switching overvoltage discharge voltage (kV)		1970	2016	2062
Calculated value of discharge voltage under 250 μs (kV)		1839	1884	1928
Clearance distance (m)	Cup-type tower	5.75	5.96	6.20
	Cat-head-type tower	5.86	6.09	6.34

All the required values of switching overvoltage discharge voltage are the withstand voltage of I-type string insulator clearance

Table 10.18 Required value of the minimum air clearance of side phase for single-circuit tower under switching overvoltage

Altitude (m)	H = 500	H = 1000	H = 1500
Required value of clearance distance of side phase for single-circuit tower (m)	5.9	6.2	6.4

(2) Intermediate-phase conductor

For the intermediate-phase conductor, the insulator string is V-type string. When the string length is determined, the conductor-to-tower window distance is also determined accordingly, and it does not be subject to the influence of the wind deflection. The test arrangement is as shown in Fig. 10.14.

The 1000 μs switching impulse discharge voltage under the two arrangements is as shown in Table 10.19 [9].

According to the calculation results in the previous section, in case of the altitude of 500 m, the required value of the switching impulse discharge voltage of the insulators in V-type string is 1986 kV. In such case, the two arrangements for both the cup-type tower and the cat-head-type tower can meet the switching impulse discharge clearance, and hence both towers can be used in the UHV power grid at an altitude of 500 m. In case of the altitude of 1000 m, the discharge voltage of the cat-head-type tower is lower than the required value 2032 kV, and the breakdown may occur, while the discharge voltage of the cup-type tower meets the required value, and hence it is recommended that, in case of the altitude of 1000 m, the cup-type tower be adopted for the lines. In case of the altitude of 1500 m, the

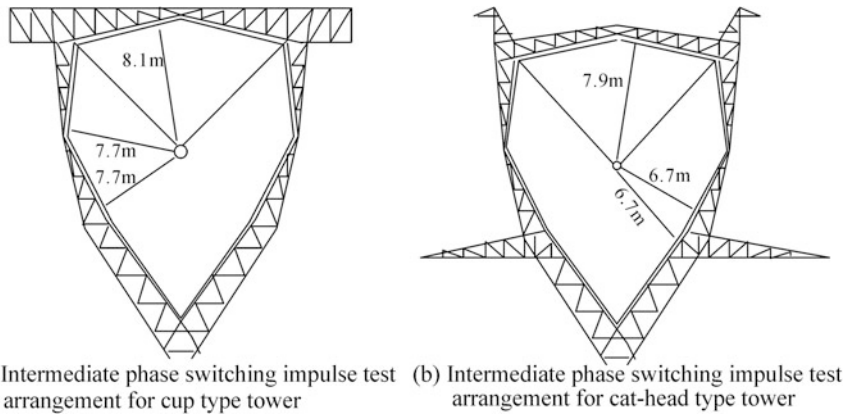

Fig. 10.14 Intermediate-phase switching impulse test arrangements for cup-type tower and cat-head-type tower

Table 10.19 Intermediate-phase conductor-to-tower switching impulse discharge voltage of cup-type tower and cat-head-type tower

Conductor arrangement	Intermediate-phase arrangement for cup-type tower	Intermediate-phase arrangement for cat-head-type tower
Switching impulse 50% discharge voltage of 1000 μs (kV)	2083	2015

Table 10.20 Recommended values of clearance distance for intermediate-phase under switching overvoltage

Altitude (m)	H = 500	H = 1000	H = 1500
Required value of clearance distance of intermediate phase of single-circuit tower (m)	6.7/6.9	7.2/8.0	7.7/8.1

Note The values above and below the oblique line, respectively, represent the distance of intermediate-phase live conductor to wedge and to upper cross beam

discharge voltage of the cat-head-type tower is lower than the required value 2079 kV, and the breakdown may occur, while the discharge voltage of the cup-type tower meets the required value, and hence it is recommended that, in case of the altitude of 1500 m, the cup-type tower be adopted for the lines.

The required values of clearance distance for intermediate-phase under the switching overvoltage are as shown in Table 10.20 [16].

Comprehensively, the cat-head-type tower has small tower window and small intermediate-phase air clearance, and hence is mainly used in the low-altitude regions; while the cup-type tower has large tower window, large intermediate-phase air clearance, and large distance among conductors, it is mainly used in the high-altitude regions.

10.3.2.4 UHV Double-Circuit Full-Scale Tower Test Arrangements and Discharge Curves

Under the switching overvoltage, the clearance distances between the insulators in both V-type string and I-type string of the double-circuit tower need to be checked. The switching overvoltage test arrangement and discharge curve for the insulators in both I-type string and V-type string will be discussed hereinafter, respectively. As it is conductor-to-tower body discharge on both the upper phase and the intermediate phase, and the discharge modes of the two are basically the same, considering that the breakdown voltage of the intermediate-phase conductor is slightly lower than that of the upper phase conductor under the same clearance, for the purpose of strictness, the determination of the air clearance of the upper phase conductor can be referred to the test results of the intermediate-phase conductor. Therefore, the test is mainly carried out for the intermediate phase and lower phase. The requirements for the air clearance distance of the upper phase are same as those for the intermediate-phase conductor.

Actually, under the switching overvoltage, for the clearance distances between the suspension conductors on the insulators in the V-type string and I-type string of the double-circuit tower and the tower, the focus is to check the air clearance distance between the conductor and the adjacent lower cross arm. As for the upper phase conductor and intermediate-phase conductor, the distances between them and their adjacent upper cross arm and tower body can, in general, meet the requirements; for the lower phase conductor, the distances between it and the adjacent

upper cross arm and tower leg can also meet the requirements. Therefore, actually, the clearance distance of conductor to adjacent upper cross arm, tower body and tower leg need not to be checked any more.

1. Insulators in I-type string

The test arrangement for the insulators in I-type string is as shown in Fig. 10.15. For the actual tower, when the simulated wind deflection angle is around 20°, the distances between the intermediate-phase conductor and the tower's intermediate-phase cross arm and tower body is usually above 9 m, which usually meets the requirements for switching impulse discharge voltage, and hence the discharge generally occurs at the clearance d_1 between the conductor and the lower cross arm. For the lower phase conductor, however, the distance between it and the tower's lower phase cross arm is usually above 8 m, and hence the discharge generally occurs at the clearance d_2 between the conductor and the tower body.

The conductor-to-tower discharge voltage curve is as shown in Fig. 10.16 [16].

According to the requirements for the switching impulse discharge voltage, the clearance distances corresponding to the required values of the switching impulse discharge voltage of the insulators in the I-type string of the double-circuit tower can be obtained through the checking of the above relevant discharge voltage curves, as shown in Table 10.21.

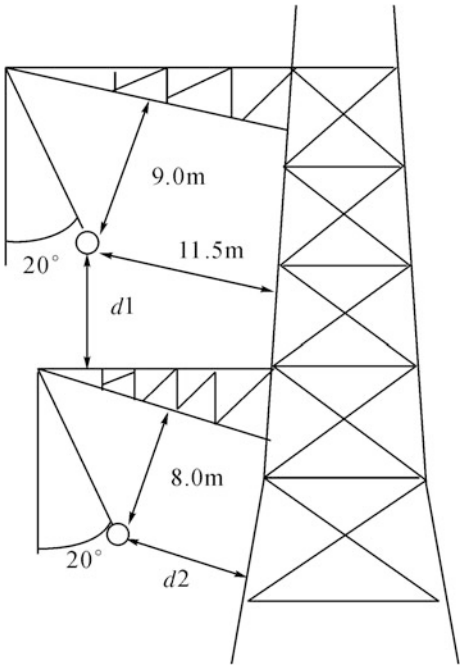

Fig. 10.15 Switching impulse test arrangement for clearances of intermediate-phase and lower phase conductors on I-type string of double-circuit tower to tower

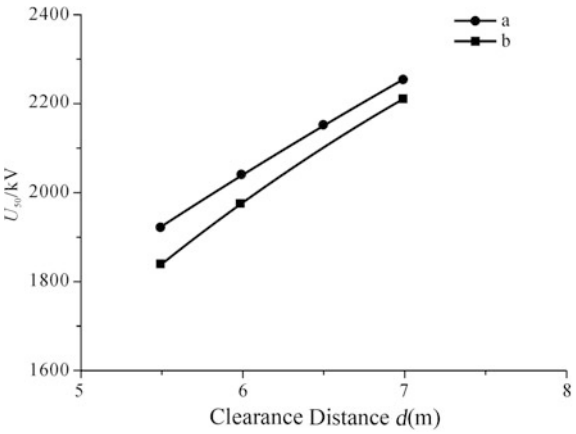

Fig. 10.16 Discharge voltage curve for clearance of insulators in *I*-type string of double-circuit tower under switching impulse. *Note a* is the intermediate-phase conductor to lower cross arm discharge voltage curve, and *b* is the lower phase conductor to tower body discharge voltage curve

Table 10.21 Side-phase clearance distances of double-circuit tower corresponding to the required values of switching impulse discharge voltage

Altitude (m)		H = 500	H = 1000	H = 1500
Required value of the switching impulse discharge voltage (kV)		1968	2016	2063
Clearance distance (m)	Intermediate phase of double-circuit tower	5.68	5.89	6.09
	Lower phase of double-circuit tower	5.96	6.16	6.35

Table 10.22 Required values of minimum air clearance of side phase for double-circuit tower under switching impulse voltage

Altitude (m)	H = 500	H = 1000	H = 1500
Required value of clearance distance of insulators in double-circuit tower (m)	6.0	6.2	6.4

In the national standard GB/Z 24842-2009 *Overvoltage and Insulation Coordination of 1000 kV UHV AC Transmission Project*, the recommended required values of the clearance distance of the side phase of the double-circuit tower under switching impulse voltage are as shown in Table 10.22, in accordance with the results obtained in Table 10.21.

2. Insulators in V-type string

Under the switching overvoltage, the conductors of V-type insulator string are not subject to the influence of the wind deflection and, however, it is necessary to check whether the conductor-to-cross arm air clearance and the conductor-to-tower

body air clearance meet the requirements for switching impulse discharge voltage. This can be divided into two cases, namely the intermediate-phase conductor and the lower phase conductor.

(1) Intermediate-phase conductor

The arrangement of the intermediate-phase conductor of the V-type string insulators during operation is as shown in Fig. 10.17.

For the determination of the conductor to tower body distance d_2 and the conductor to intermediate-phase cross arm distance d_3, the most severe case in which the insulator string length is the shortest (the number of insulators is the least) is considered. In case of the altitude H = 500 m, the insulator string length shall be 11.5 m at least. With the included angle of the V-type string insulators considered at 90°, the calculated distance of the conductor to the intermediate-phase cross arm shall be 8.13 m at least and that of the conductor to the tower body shall be at least 7.13 m (the estimated value with the inclination of tower body considered). In such case, the minimum air clearance distances of the conductor to the tower's intermediate-phase cross arm and to the tower body are as shown in Table 10.23.

The switching impulse test arrangements for the clearances of the intermediate-phase conductor on the V-type string of the double-circuit tower to the tower body and to the cross arm are as shown in Fig. 10.18, and the discharge voltage curves are as shown in Fig. 10.19.

According to the required discharge values of switching overvoltage under different altitudes and in combination with the discharge voltage curves as shown in Fig. 10.19, the required distances of the intermediate-phase conductor on the V-type string of the double-circuit tower to the intermediate-phase cross arm and to the tower body can be obtained as shown in Table 10.24.

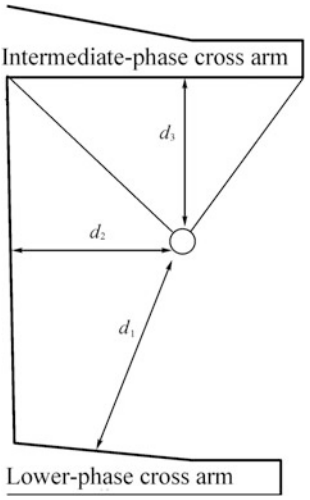

Fig. 10.17 Arrangement of intermediate-phase conductor of V-type string insulators during operation

Table 10.23 Air clearance distances of intermediate-phase conductor to the tower on V-type insulators of double circuit

Altitude (m)	H = 500	H = 1000	H = 1500
Number of insulators (XWP-300)	48	52	53
Distance of conductor to intermediate-phase cross arm (m)	8.13	8.68	8.82
Distance of conductor to tower body (m)	7.13	7.68	7.82

The included angle of V-type insulators is 90°, and all the conductor-to-tower distances are obtained through calculation based on the insulator length, with certain margin considered

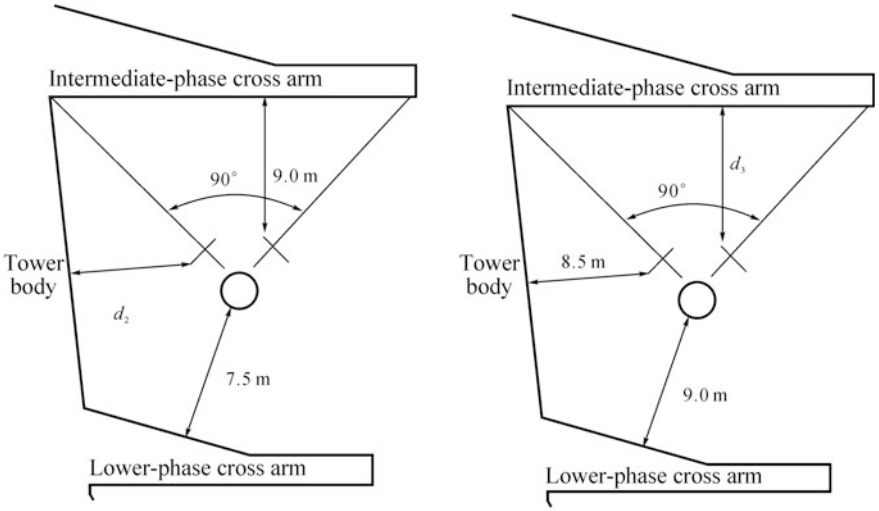

(a) Test arrangement for gap of the intermediate-phase conductor on the V-type string to the tower body

(b) Test arrangement for gap of the intermediate-phase conductor on the V-type string to the intermediate cross arm

Fig. 10.18 Switching impulse test arrangement for clearances of the intermediate-phase conductor on V-type string of double-circuit tower to tower body and to cross arm

Through the contrast of Tables 10.23 and 10.24, it can be seen that, under different altitudes, even if the most severe case in which the number of insulators is the least in the clean regions (the clearance distances of the conductor to the tower's lower cross arm and to the tower body are both the shortest) is considered, the discharge voltage of the clearances of the conductor to the intermediate cross arm and to the tower body can both meet the required value of switching impulse discharge voltage, and proper margin is reserved. Therefore, during the checking of the air clearance of the V-type string of the double-circuit tower, the clearances of the conductor to the tower body and to the intermediate cross arm need not be considered, and it is only necessary to check the clearance d_1 of the conductor to the lower phase cross arm.

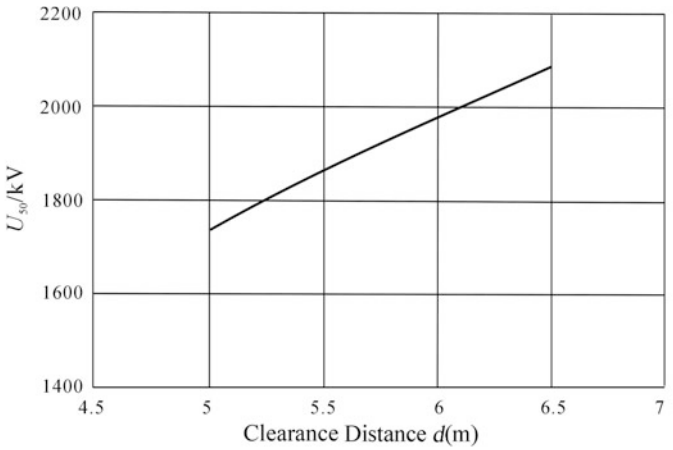

(a) Discharge Voltage Curve of Gap of the Intermediate-phase Conductor on the V-type String of the Double-circuit Tower to the Intermediate Cross Arm

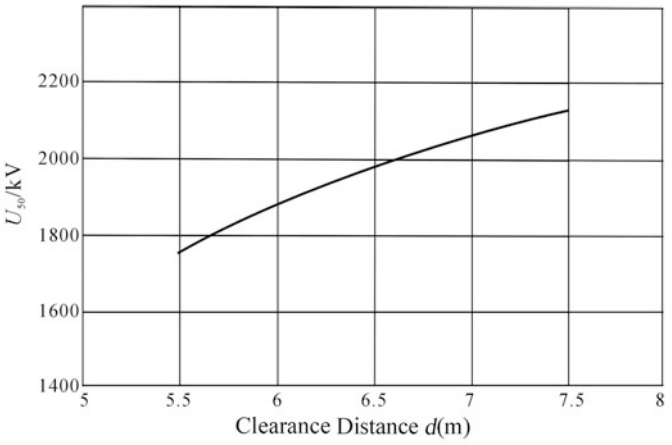

(b) Discharge Voltage Curve of Gap of the Intermediate-phase Conductor on the V-type String of the Double-circuit Tower to the Tower Body

Fig. 10.19 Switching impulse (1000 μs) 50% discharge voltage curves of clearances of intermediate-phase conductor on V-type string of double-circuit tower to the intermediate cross arm and to the tower body

Table 10.24 Required air clearance distances of intermediate-phase conductor on insulators in V-type string of double-circuit tower to tower

Altitude (m)	H = 500	H = 1000	H = 1500
Number of insulators (XWP-300)	48	52	53
Required discharge value under switching overvoltage	1986	2032	2079
Required distance of conductor to intermediate-phase cross arm (m)	6.6	6.8	7.2
Required distance of conductor to tower body (m)	6.1	6.25	6.5

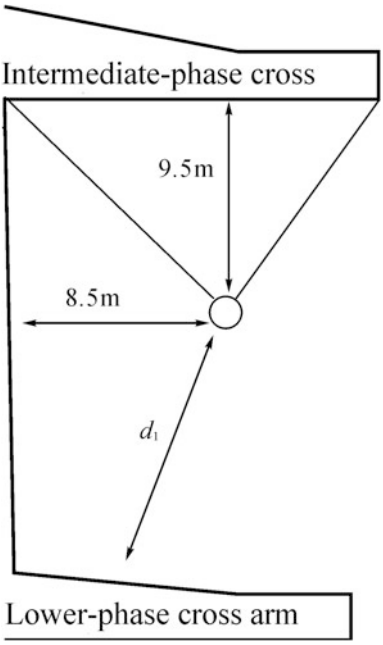

Fig. 10.20 Switching overvoltage test arrangement for air clearance of intermediate-phase conductor on V-type string

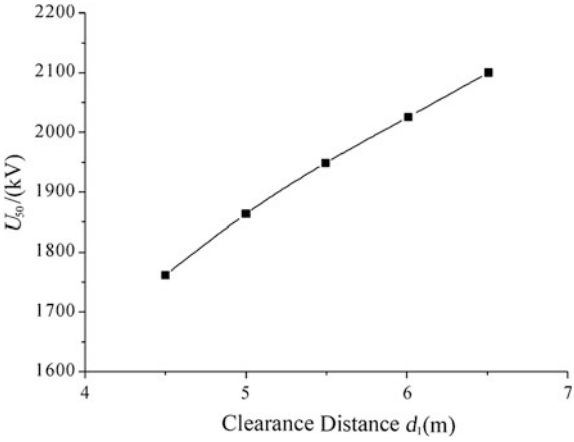

Fig. 10.21 Switching impulse (1000 μs) 50% discharge voltage curve of clearance of intermediate-phase conductor on V-type string to the lower cross arm

The test arrangement for the air clearance of the intermediate-phase conductor is as shown in Fig. 10.20, and the discharge voltage curve of the conductor to the lower cross arm is as shown in Fig. 10.21 [16].

According to the required values of the switching impulse discharge voltage, the clearance distances corresponding to the required values of switching impulse discharge voltage can be obtained through the checking of the discharge voltage curves in Fig. 10.21, as shown in Table 10.25.

Table 10.25 Required clearance distance of the intermediate-phase conductor on the V-type string to the lower cross arm under switching impulse discharge voltage

Altitude (m)	H = 500	H = 1000	H = 1500
Required value of switching impulse discharge voltage (kV)	1985	2032	2079
Required value of clearance distance (m)	5.73	6.04	6.35

Table 10.26 Required values of the minimum air clearance of side-phase conductor of the double-circuit tower under switching impulse voltage

Altitude (m)	H = 500	H = 1000	H = 1500
Required value of clearance distance of insulators in double-circuit tower (m)	6.0	6.2	6.4

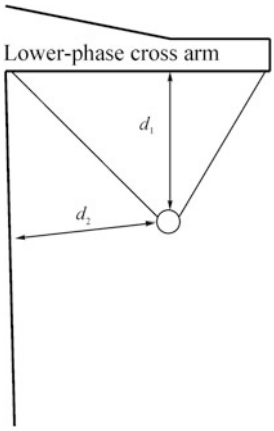

Fig. 10.22 Arrangement of lower phase conductor during operation

The clearance distance of the intermediate-phase conductor to the lower cross arm shall be larger than the values listed in Table 10.25.

In the national standard GB/Z 24842-2009 *Overvoltage and Insulation Coordination of 1000 kV UHV AC Transmission Project*, the recommended required values of the clearance distance of the side-phase conductor of the double-circuit tower under switching impulse voltage are as shown in Table 10.26, in accordance with the results obtained in Table 10.25.

(2) Lower phase conductor

For the lower phase conductor, the clearance distance between the conductor and the tower body and the clearance distance between conductor and lower cross arm as shown in Fig. 10.22 are required to be checked. In case of the altitude H = 500 m (considering that the number of insulators is the least in clean regions, and, in such case, the clearance distances of the conductor to the tower's lower cross arm and to the tower body are both the shortest), the insulator string length

Table 10.27 Minimum clearance distances of lower phase conductor on insulators in V-type string of double-circuit tower to lower phase cross arm and to tower leg

Altitude (m)	H = 500	H = 1000	H = 1500
Number of insulators (XWP-300)	48	52	53
Distance of conductor to lower phase cross arm (m)	8.13	8.68	8.82
Distance of conductor to tower leg (m)	7.13	7.68	7.82

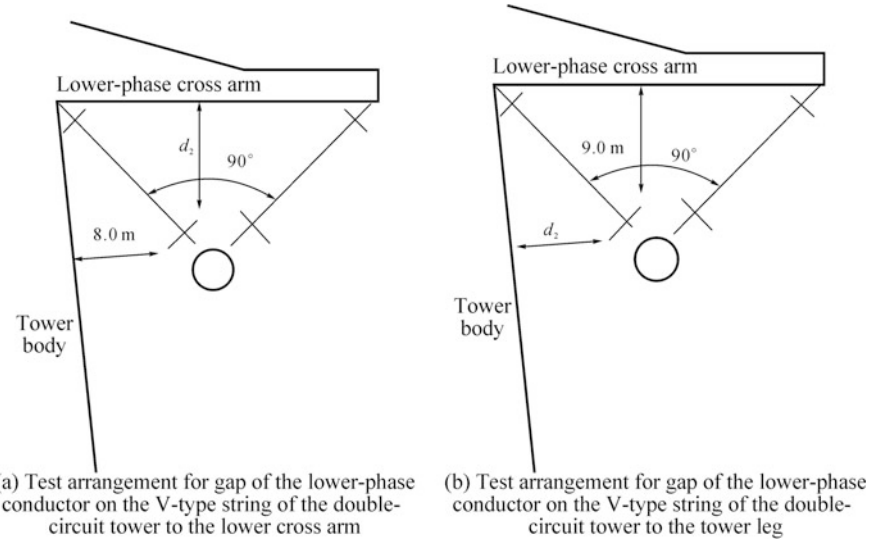

(a) Test arrangement for gap of the lower-phase conductor on the V-type string of the double-circuit tower to the lower cross arm

(b) Test arrangement for gap of the lower-phase conductor on the V-type string of the double-circuit tower to the tower leg

Fig. 10.23 Switching impulse test arrangement for clearance of lower phase conductor on V-type string of double-circuit tower to tower

shall be 11.5 m at least. With the included angle of the V-type string insulators considered at 90°, the calculated distance of the conductor to the lower phase cross arm shall be 8.13 m at least and that of the conductor to the tower body shall also be at least 7.13 m (the estimated value with inclination of tower body considered). In such case, the minimum clearance distances of the conductor to the tower's lower phase cross arm and to the tower leg are as shown in Table 10.27.

The test arrangements are as shown in Fig. 10.23. First, maintain d_2 at 8.0 m and change the clearance distance d_1 of the lower phase conductor to the lower cross arm to obtain the curve relationship between the discharge voltage U_{50} of the lower phase conductor and the lower cross arm and the clearance distance d_1 as shown in Fig. 10.24a. Then maintain d_1 at 9.0 m and change the clearance distance d_2 between the lower phase conductor and the tower leg to obtain the curve relationship between the discharge voltage U_{50} of conductor and the tower leg and the clearance distance d_2 as shown in Fig. 10.24b [16].

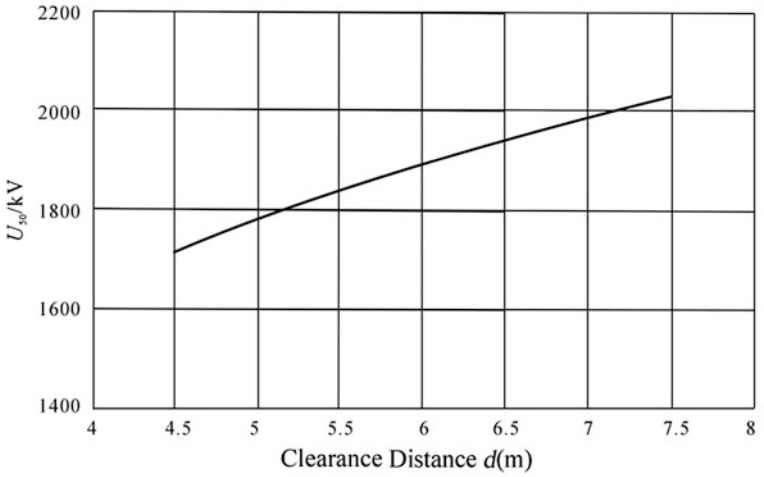

(a) Discharge Voltage Curve of Gap of the Lower-phase Conductor on the V-type String of the Double-circuit Tower to the Lower Cross Arm

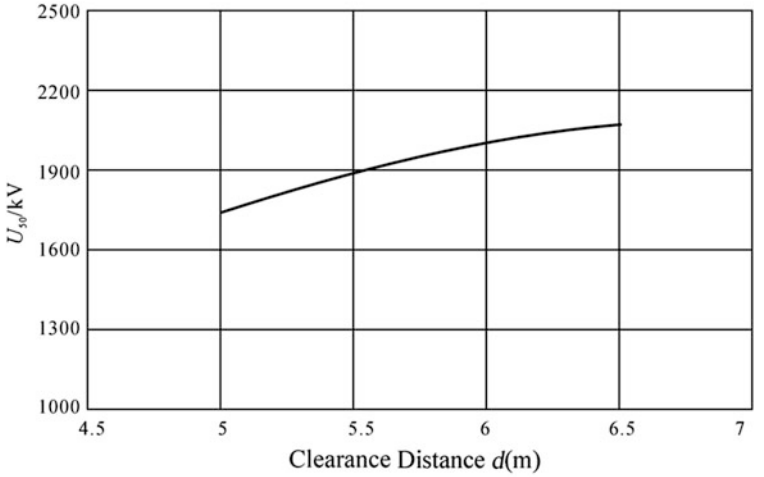

(b) Discharge Voltage Curve of Gap of the Lower-phase Conductor on the V-type String of the Double-circuit Tower to the Tower Leg

Fig. 10.24 Switching impulse (1000 μs) 50% discharge voltage curve of clearances of lower phase conductor on V-type string of double-circuit tower to lower cross arm and to tower leg

According to the required discharge values of switching overvoltage under different altitudes and in combination with the discharge voltage curves as shown in Fig. 10.19, the required distances of the lower phase conductor on the V-type string of the double-circuit tower to the lower cross arm and to the tower leg can be obtained from Table 10.28.

Table 10.28 Required air clearance distances of lower phase conductor on V-type insulators of double-circuit tower to lower cross arm and to tower leg

Altitude (m)	H = 500	H = 1000	H = 1500
Number of insulators (XWP-300)	48	52	53
Required discharge value under switching overvoltage	1986	2032	2079
Required distance of conductor to the lower cross arm (m)	7.1	7.6	8.2
Required distance of conductor to tower leg (m)	6.1	6.3	6.7

Through the contrast of Tables 10.27 and 10.28, it can be seen that, under different altitudes, even if the most severe case in which the number of insulators is the least in the clean regions (the clearance distances of the conductor to the tower's lower cross arm and to the tower body are both the shortest) is considered, the discharge voltage of the clearances of the conductor to the lower cross arm and to the tower leg can both meet the required value of the switching impulse discharge voltage, and proper margin is reserved. Therefore, in practice, the clearance of the lower phase conductor to the tower need not to be checked, and is considered to meet the requirements of the switching impulse discharge voltage.

For the double-circuit tower, under the switching overvoltage, the air clearance distance of the conductor to the adjacent upper cross arm is mainly determined by the insulator string length, and can generally meet the requirements for clearance distance; the distances of the conductor to the tower body and to the tower leg are mainly determined by the electromagnetic environment of the conductor (to meet the requirements for audible noise and radio interference, sufficient clearance distance must be maintained between conductors), and can also generally meet the requirements for clearance distance of discharge voltage under switching impulse; the clearance distance of the conductor to the adjacent lower cross arm is to be mainly checked.

10.3.3 Determination of Air Clearance Under Lightning Impulse Voltage

Under the lightning overvoltage, the positive lightning impulse discharge voltage of the air clearance shall match the 50% lightning impulse discharge voltage of the insulator string. In the 500 kV and below transmission lines, the 50% discharge voltage of the positive lightning impulse voltage wave for the air clearance of the line conductor to the tower with the wind deflection being considered is usually selected at 0.85 times the corresponding voltage of the insulator string [12]. In the design of the EHV 750 kV line, this value is taken as 0.8 times the corresponding voltage of the insulator string [17]. In the design of the UHV 1000 kV line, this value is taken as 0.8 times the corresponding voltage of the insulator string [4].

In the 1000 kV transmission line, the 50% lightning breakdown voltage of the air clearance and the lightning flashover voltage of the insulator string shall have the coordination relationship shown as follows:

$$U'_{50\%} = 0.8U_{50\%} \tag{10.40}$$

where

$U_{50\%}$ the lightning flashover voltage of insulator string, in kV, and the insulator string length shall be the length under conditions in Class 0 polluted regions (under such conditions, the insulator string length is the shortest);
$U'_{50\%}$ the 50% lightning breakdown voltage of air clearance, in kV.

Reference [11] presented the minimum number of insulators in each string of the overhead line in the regions with altitude not exceeding 1000 m and the equivalent salt deposit density not exceeding 0.06 mg/cm^2, as shown in Table 10.29.

The lightning flashover voltage equation for the insulator string recommended by IEEE is as follows [19]:

$$U_{\mathrm{p}} = \left(400 + \frac{710}{t^{0.75}}\right) \times L \tag{10.41}$$

where

U_{p} the flashover voltage of insulator string, in kV;
t the time after lightning strike, in μs, and when t is 16 μs, it corresponds to the 50% discharge voltage of insulator string;
L the insulator length, in m.

The structural height of XWP-300 insulator is 0.195 m. Through the calculation, the 50% flashover voltage of the insulator under different altitudes can be obtained: when H = 500 m, $U_{50\%}$ = 4575 kV; when H = 1000 m, $U_{50\%}$ = 4956 kV; when H = 1500 m, $U_{50\%}$ = 5051 kV. The 50% lightning breakdown voltage $U'_{50\%}$ of air clearance is as shown in Table 10.30.

Table 10.29 Minimum number of insulators in the UHV line

Altitude (m)	H = 500	H = 1000	H = 1500
Number of insulators (XWP-300)	48	52	53

Table 10.30 Required values of lightning discharge voltage

Altitude (m)	H = 500	H = 1000	H = 1500
$U_{50\%}$ (kV)	4575	4956	5051
$U'_{50\%}$ (kV)	3660	3965	4041

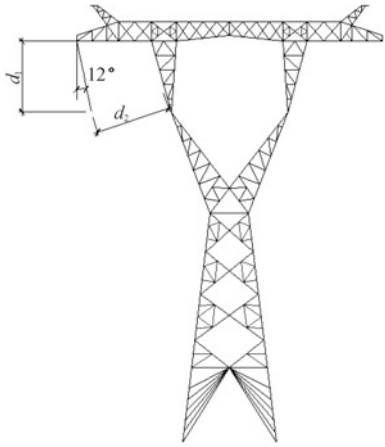

Fig. 10.25 Distance of side-phase conductor to the tower for cup-type tower

Under the lightning overvoltage, the simulated wind deflection angle is 12° when the wind speed used for calculation is 10 m/s. For the single-circuit tower, as to the cup-type tower shown in Fig. 10.25, the distances of the side-phase conductor to the cross arm and to the tower body are usually above 9 m, being relatively large, and, in case of the lightning strike on the conductor, the flashover along the insulator string will be mainly generated, while the air clearance of the conductor to the tower body will normally not be broken down; in addition, the distance between the intermediate-phase conductor and the tower window can also meet the requirements of the lightning discharge voltage. As for the cat-head-type tower, the case is basically similar. Therefore, the air clearance distance under lightning overvoltage does not govern the super structure dimension of the single-circuit tower, and in the national standard, the clearance distance of conductor to the tower for the single-circuit line is not specified.

For the double-circuit tower, to reduce the shielding failure rate, the tower height usually is reduced, resulting in the reduction of the distances of both the upper phase conductor and the intermediate-phase conductor to their adjacent lower cross arms, which are usually less than the distance of the conductor to the tower body (with the wind deflection angle considered). In such case, the clearance between the conductor and the lower cross arm is the most major lightning discharge path. Therefore, for the double-circuit tower, it is important to check the lightning overvoltage of the air clearance distance between the conductor and the adjacent lower cross arm.

For the insulators in the I-type string of the double-circuit tower, under the lightning overvoltage, when the distances of the conductor to the tower body and to the upper cross arm are being considered, the simulated wind deflection angle is 12° and can usually meet the requirements of discharge voltage, and hence it is generally not necessary to have it checked. When the distance of the conductor to the lower cross arm is being considered, the test shall be carried out as per the severe

case in which the wind deflection angle of the conductor is zero (in such case, the distance of the conductor to the adjacent lower cross arm is the minimum).

The lightning overvoltage test arrangement for the clearance of the intermediate-phase conductor on the I-type string of the double-circuit tower to the lower cross arm is as shown in Fig. 10.26, and the lightning impulse discharge voltage curve for the clearance of the intermediate-phase conductor of the double-circuit tower to the lower cross arm is as shown in Fig. 10.27 [16].

The lightning overvoltage test arrangement for the insulators in the V-type string of the double-circuit tower is as shown in Fig. 10.28, and the lightning impulse discharge voltage curve of the air clearance of the intermediate-phase conductor on the V-type string of the double-circuit tower to the lower cross arm is as shown in Fig. 10.29 [16].

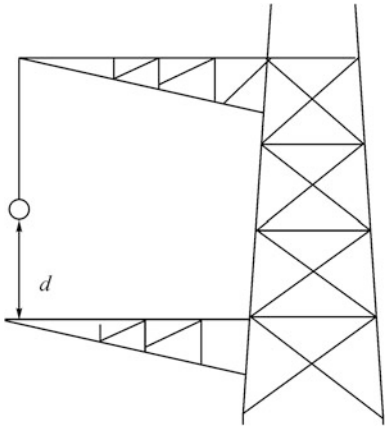

Fig. 10.26 Lightning overvoltage test arrangement for air clearance of intermediate-phase conductor on I-type string of double-circuit tower to the lower cross arm

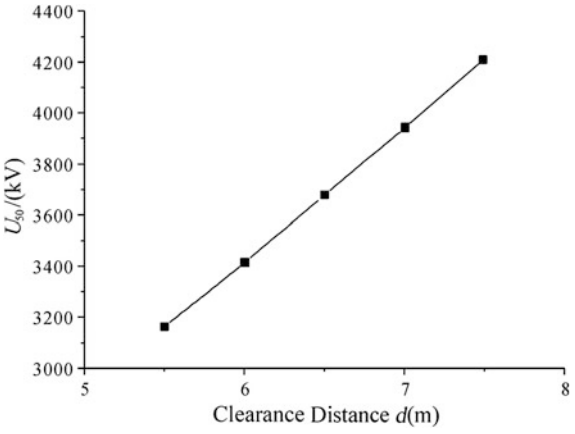

Fig. 10.27 Lightning overvoltage discharge voltage curve of air clearance of intermediate-phase conductor on I-type string of double-circuit tower to the lower cross arm

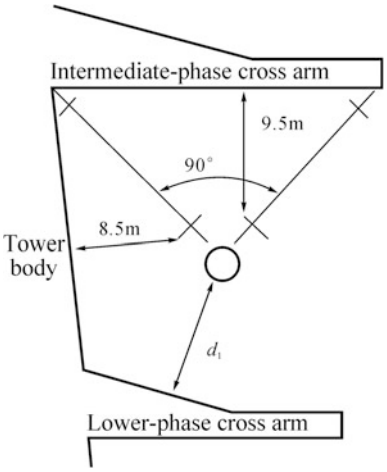

Fig. 10.28 Lightning overvoltage test arrangement for air clearance of intermediate-phase conductor on V-type String of double-circuit tower to the lower cross arm

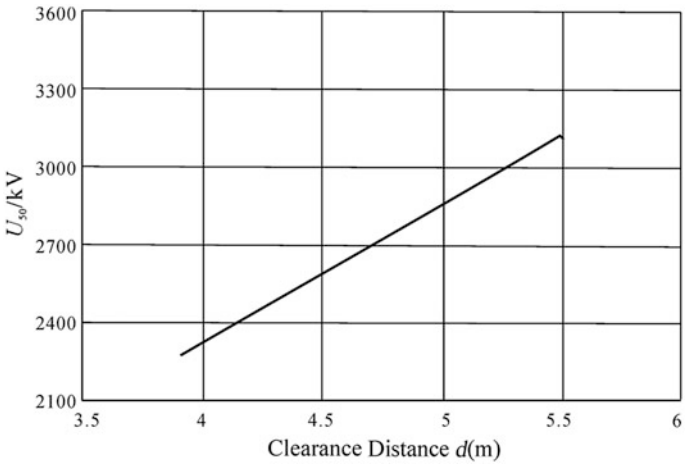

Fig. 10.29 Lightning overvoltage discharge voltage curve of air clearance of intermediate-phase conductor on V-type string of double-circuit tower to the lower cross arm

According to the requirements for lightning discharge voltage, the clearance distances required under the lightning discharge voltage of the air clearance of the line can be obtained through the checking of the above relevant discharge voltage curves, as shown in Table 10.31.

Table 10.31 Air clearance distances corresponding to the required values of lightning discharge voltage

Altitude (m)		H = 500	H = 1000	H = 1500
Lightning discharge voltage (kV)		3660	3965	4041
Clearance distance (m)	I-type string	6.47	7.04	7.20
	V-type string	6.45	6.99	7.14

Table 10.32 Recommended air clearances for double-circuit tower under lightning impulse voltage

Altitude (m)		H = 500	H = 1000	H = 1500
Clearance distance (m)	Same tower and double circuit	6.7	7.1	7.6
	Single circuit	–	–	–

In the national standard GB/Z 24842-2009 *Overvoltage and Insulation Coordination of 1000 kV UHVAC Transmission Project*, the recommended air clearance distances of the line under the lightning overvoltage are as shown in Table 10.32.

In Table 10.32, the clearance distances recommended in the national standard GB/Z 24842-2009 basically tally with the clearance distances obtained from the required values of discharge voltage as shown in Table 10.31.

10.3.4 Selection of Line's Air Clearance of the UHV System Under Three Types of Overvoltage

The selection of the line's air clearance of the UHV system under three types of overvoltage is as shown in Table 10.33 [16].

In the "lightning" column in Table 10.33, the recommended distances for plains and mountains are given, respectively, based on the consideration of the actual situation that the lines in the mountains need larger clearance distances due to the large inclination angle of the ground which makes the line more apt to suffer from the lightning strike. However, this also brings some problems: on the one hand, the tower shapes need to be designed, respectively, for plains and mountains, bringing inconvenience to the tower design; on the other hand, the increase in the tower dimension also results in the increase in cost.

Actually, the air clearance of the UHV transmission line is mainly determined by the switching overvoltage.

Table 10.33 Required values of the minimum air clearance of 1000 kV line (m)

Type of applied voltage	Line type	Minimum air clearance distance		
		Altitude of 500 m	Altitude of 1000 m	Altitude of 1500 m
Power frequency	Single circuit	2.7	2.9	3.1
	Double circuit on the same tower	2.7	2.9	3.1
Switching	Single circuit	Side phase: 5.9; intermediate phase: 6.7/7.9	Side phase: 6.2; intermediate phase: 7.2/8.0	Side phase: 6.4; intermediate phase: 7.7/8.1
	Double circuit on the same tower	6.0	6.2	6.4
Lightning	Single circuit	–	–	–
	Double circuit on the same tower	Plains: 6.7; mountains: 7.0	Plains: 7.1; mountains: 7.4	Plains: 7.6; mountains: 7.9

Note The values above and below the oblique line in the "switching" column, respectively, represent the distance of intermediate-phase live conductor to the wedge and to the upper cross beam

10.3.5 Selection of Air Clearance of the UHV Lines in Various Countries

The comparison of the selection of air clearance of the UHV lines in various countries is as shown in Table 10.34 [20].

From Table 10.34, it can be seen that the rated voltage of the UHV in both China and Japan is 1000 kV, and for the selection of air clearance distances under working voltage and switching overvoltage in both countries the recommended values are relatively close.

The selected clearance distance of the UHV line under switching overvoltage in the former Soviet Union is larger than that in China. This is because, in the former Soviet Union, the operating voltage is 1200 kV and the switching overvoltage is 1.8 p.u., and, in addition, at that time, the performance of arresters is poor and the residual voltage is high, resulting in the relatively high absolute value of switching overvoltage and the relatively large air clearance selected.

Table 10.34 Conductor-to-tower air clearance of UHV overhead transmission line (m)

Country	Working voltage	Switching overvoltage	Lightning overvoltage
China	2.9	Single circuit: side phase: 6.2; intermediate phase: 7.2/8.0	Single circuit: unspecified
		Double circuit on the same tower: 6.2	Double circuit on the same tower: plains: 7.1; mountains: 7.4
Japan	3.09	I-type string: 6.0/6.55	I-type string: 6.62
		Tension string: 5.69/6.75	Tension string: 6.2
Former Soviet Union	2.5	I-type string: 6.0–7.0	–
		V-type string: 8.0–9.0	

Note

The altitude at which the air clearance distances are specified is: 1000 m in China and less than 1800 m in Japan. For Japan, only the data for double-circuit line are available

In the column of "switching overvoltage" for China, the data for intermediate phase, respectively, correspond to the distances of intermediate-phase live conductor in the tower window to the wedge and to the upper cross beam; in the column of "switching overvoltage" for Japan, the data, respectively, correspond to the conductor to lower cross arm and conductor to tower body clearances

In the column of "Switching Overvoltage" for former Soviet Union, the smaller value and the large value, respectively, correspond to the clearances of conductor to tower body and to tower window

References

1. Wu G, Liu J. Problems that should be studied and considered for operation property of 1000 kV UHV insulator. Electr Equip. 2008;9(12):16–8.
2. Su Z, Zhou J, Li W, Xu Y. Study on the selection of UHV AC 1000 kV insulator type. Electr Power. 2006;39(10):15–20.
3. Zhou J. Research on discharge characteristics and type selection of polluted insulators in high-altitude regions. Beijing: Tsinghua University; 2004.
4. GB 50665-2011. Code for design of 1000 kV overhead transmission line; 2011.
5. GB/T 20876.2-2007. Composite string insulator units for overhead lines with a nominal voltage greater than 1000 V; 2007.
6. GB/T 4585-2004. Artificial pollution tests on high-voltage insulators to be used on A.C. systems; 2004.
7. Q/GWD 152-2006. Pollution classification and external insulation selection for electric power system; 2006.
8. Xinyuan J. Selection of the number of insulators in 1000 kV UHV AC transmission line. High Tech Ind. 2009;3:82–6.
9. Zhenya L. External insulation of UHV AC transmission system. Beijing: China Electric Power Press; 2008.
10. Liang X. Selection of insulations for UHV transmission line. Int Sem of UHV Trans Technol, 2005.
11. Q/GDW. Overvoltage and insulation coordination of 1000 kV UHV Transmission project (draft for comments); 2008.
12. DL/T 620-1997. Overvoltage protection and insulation coordination for AC electrical installations; 1997.

13. Du S. Discussion on selection of air gap of EHV/UHV transmission line under switching overvoltage. In: Proceedings of the 2006 academic annual meeting of overvoltage and insulation co-ordination research team of CSEE High-Voltage Commission; 2006.
14. Александров ГА, et al. Design of EHV transmission line. Beijing: Water Resources and Electric Power Press (China); 1987.
15. IEC 60071-2. Insulation coordination—part II: application guide; 1996.
16. GB/Z 24842-2009. Overvoltage and insulation coordination of 1000 kV UHV AC transmission project; 2009.
17. Q/GDW 179-2008. Code for design of 110–750 kV overhead transmission line; 2008.
18. Q/GDW 178-2008. Tentative technical regulations on design for 1000 kV AC overhead transmission lines; 2008.
19. IEEE std 1243-1997. IEEE guiding for improving the lightning performance of transmission lines; 1997.
20. Zhenya L. UHV power grid. Beijing: China Economic Press; 2005.

Chapter 11
UHVAC Electrical Equipment

Xiande Hu, Yang Li and Xiujuan Chen

The UHVAC electrical equipment, which is the base of the UHVAC project and whose performance directly affects the stability of the UHV line, is the important research content of the UHVAC technology. This chapter will introduce the status quo of the main UHVAC electrical equipment in China and other countries (including the UHV transformer, UHV shunt reactor, UHV instrument transformer, UHV arrester, UHV switchgear, UHV bushing, and UHV series compensation device) and analyze the characteristics thereof, so that the reader can have a comprehensive understanding on the UHVAC electrical equipment.

11.1 UHV Transformer

The UHV transformer is one of the key equipments of the UHVAC transmission project, and its quality condition will directly affect whether the UHVAC line can operate in a safe and reliable manner. In consideration that the UHV transformer has the characteristics of high-voltage level, large capacity, large volume and large

X. Hu (✉)
State Grid Wenzhou Power Supply Company, Wenzhou, Zhejiang,
People's Republic of China
e-mail: 462100391@qq.com

Y. Li
State Grid Suzhou Power Supply Company, Suzhou, Jiangsu,
People's Republic of China
e-mail: 1041204573@qq.com

X. Chen
China Electric Power Research Institute, Haidian District, Beijing,
People's Republic of China
e-mail: xjchen@epri.sgcc.com.cn

© Zhejiang University Press, Hangzhou and Springer-Verlag GmbH Germany 2018

H. Zhou et al. (eds.), *Ultra-high Voltage AC/DC Power Transmission*,
Advanced Topics in Science and Technology in China,
https://doi.org/10.1007/978-3-662-54575-1_11

weight, its design, and manufacturing are different from those of the former 750 or 500 kV transformer, and its research and manufacturing technology is also an important constituent of the UHVAC transmission technology.

11.1.1 Status Quo of the UHV Transformers in China and Other Countries

The existing UHVAC transmission lines all over the world are not quite many, and there are few countries being able to manufacture the UHV transformers. Italy, Japan, the former Soviet Union (Russia and Ukraine), and the USA are the countries which earlier started the research and development of the UHV transmission technology. Italy's 1000 kV AC Transmission Project, which was initiated by the Italian Electric Power Company (ENEL) in 1971 and later participated in by the companies from Brazil, Argentina, and Canada, etc., is a UHV power transmission and transformation project under international cooperative research and development, and its 1000 kV UHV transformers are all manufactured by the Milan Transformer Factory of Ansaldo Company. Deciding to construct the 1000 kV system in 1978, Japan completed the trial manufacturing of the main equipment in the early 1990s and carried out test in New Haruna Substation (140 km to the north of Tokyo) in 1996. This substation has three sets of 1000 kV/1000 MVA single-phase transformers, among which the phase A, phase B, and phase C transformers were, respectively, the products of Toshiba, Hitachi, and Mitsubishi. Ukraine's Zaporozhye Transformer Factory had ever manufactured the 1150 kV-class power transformer for the former Soviet Union, and the latter also manufactured the 1150 kV/667 MVA single-phase transformer in the 1980s.

In China, the research and manufacturing of the UHV transformers were started late. The technical research on the UHV transformer and the development of the equipment thereof were not started until the 1990s. Nevertheless, the successful passing of all the tests by the 1000 kV/1000 MVA UHVAC transformer designed and manufactured independently by Baoding Tianwei Baobian Electric Co., Ltd., in Jul. 2008 signaled that China has already been equipped with the capability to independently research and manufacture the UHV transformers. At present, TBEA Shenyang Transformer Co., Ltd. (hereinafter referred to as Shenyang Transformer), Xi'an XD Transformer Co., Ltd. (hereinafter referred to as Xi'an Transformer), and Baoding Tianwei Baobian Electric Co., Ltd. (hereinafter referred to as Baobian) are all equipped with the capability to design and manufacture the UHV transformers. The UHV transformers manufactured by the three companies have their own characteristics in design and structure. The UHV transformer manufactured by Shenyang Transformer is of single-phase four-limb core structure, in which the series connection of HV windings on two limbs can effectively reduce the working voltage between disks. The cores of the UHV transformers manufactured by both Xi'an Transformer and Baobian are of single-phase three-limb core, and the overall

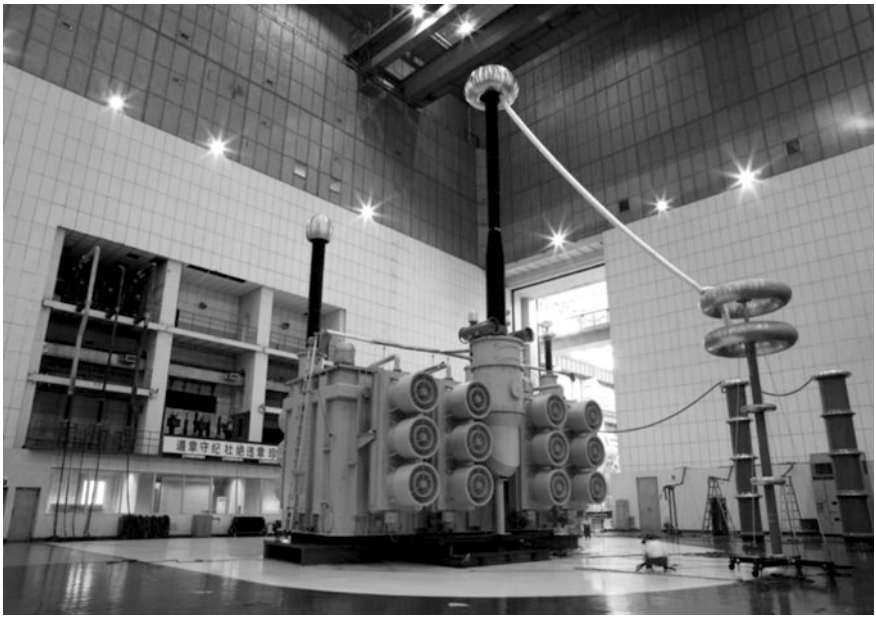

Fig. 11.1 First UHV transformer manufactured by Baobian

transformer structures are similar but not completely the same; the voltage-regulating coil manufactured by Xi'an Transformer is placed outside the HV coil, and the extreme tapping deviation is large; however, the voltage-regulating coil manufactured by Baobian is placed inside the LV coil, and the no-load loss and cost are increased to some extent. The UHV transformers used in the "Southeast Shanxi-Nanyang-Jingmen UHVAC Demonstration Project", the first UHVAC project in China, are, respectively, designed and manufactured by Shenyang Transformer and Baobian. The first UHV transformer manufactured by Baobian is as shown in Fig. 11.1.

11.1.2 Characteristics and Type Selection of the UHV Transformer

The main characteristics of the UHV transformer are:

1. Huge capacity: the capacity of the three phases is usually at 1000 MVA and above, even reaching up to thousands MVA;
2. High insulation level: the basic insulation level (lightning impulse insulation level) is high, generally between 1950 and 2250 kV or even higher;

3. The huge capacity and high insulation level make the corresponding weight and volume of the transformer become large and may cause difficulty in transportation.

During the type selection and design of the UHV transformer, these characteristics shall be fully considered to ensure that the developed UHV transformer can operate safely and reliably.

11.1.2.1 Type Selection

The huge capacity and high insulation level make the weight and volume of the UHV transformer which become large, resulting in the increasing difficulty in transformer manufacturing, transportation, and installation. The application of autotransformer can effectively reduce the volume and weight of the transformer, and the selection of the single-phase transformer to replace the three-phase transformer can also reduce the restrictions in transportation. Furthermore, the autotransformer also has the advantages such as low manufacturing cost, low loss, high operating efficiency, and ability to improve the system stability. In addition, when the transformer is damaged, the replacement of the single-phase transformer is quicker than that of the three-phase transformer, and thus, it is able to restore the power supply as soon as possible, as well as increase the system stability. Therefore, the UHV transformer shall preferably adopt the single-phase autotransformer, which is adopted for the existing mainstream 1000 kV transformers all over the world.

11.1.2.2 Voltage Regulation Mode

The analysis of the voltage regulation mode is mainly focused on whether the transformer adopts the on-load voltage regulation or the non-field excitation voltage regulation, and the selection of the voltage regulation position, namely the connection mode between the voltage-regulating transformer and the main transformer.

Compared with the non-field excitation voltage regulation, the on-load voltage regulation allows regulating the voltage under load, but it increases the structural complexity and equipment manufacturing cost of the transformer and reduces the reliability of the equipment operation. In the EHV system, Germany and Japan adopt the transformers fitted with on-load tap changer, America, and French, etc., adopt the transformers with non-field excitation tap changer, while England and Italy, etc., adopt the transformers without tap changer [1]. In the EHV system in China, both the on-load voltage regulation and the non-field excitation voltage regulation co-exist in the 500 kV transformer, while the autotransformers with non-field excitation tap changer are used in the Northwest China 750 kV Power Transmission Demonstration Project. In the 1000 kV UHV system, normally, the voltage fluctuation range of the main grid is very small. The quality of the regional

power supply voltage can rely on the reactive power regulation and the inferior power grid's transformers fitted with on-load tap changer, and the non-field excitation voltage regulation can fully meet the regulation demand for seasonal operation. Therefore, from the perspective of reliability, economy, and system operation mode, the UHV transformer shall be applied with the non-field excitation voltage regulation.

For the selection of the voltage regulation position, the 500 kV-class and 750 kV-class single-phase autotransformers are usually applied with the mode of voltage regulation at the medium-voltage line end, and the schematic diagram thereof is as shown in Fig. 11.2. Under the mode of voltage regulation at the medium-voltage line end, the voltage of each turn of the winding during voltage regulation on the medium-voltage side is not changed, and thus, it does not cause change to the magnetic flux of the core, and hence, the voltage on the LV side is not influenced or influenced to a small extent [2]. However, the mode of voltage regulation at the medium-voltage line end requires high insulation level of the voltage regulator. For example, for the 500 kV transformer, the insulation level of the voltage regulator under such mode shall be 220 kV; however, for the 1000 kV transformer, the corresponding required insulation level of the voltage regulator shall be enhanced to 500 kV, leading to the increase in the design difficulty and manufacturing costs of the voltage regulator. Therefore, in consideration of the insulation, the 1000 kV UHV transformer shall not be applied with the mode of voltage regulation at the medium-voltage line end.

In the UHV transformer, the neutral point voltage regulation mode, i.e., the voltage-regulating winding of the voltage-regulating transformer is connected in series at the neutral point of the original transformer and the excitation winding of the voltage regulator is paralleled with the third winding of the main transformer, shall be selected, as shown in Fig. 11.3. The neutral point voltage regulation mode can effectively reduce the insulation level of the voltage-regulating transformer, solving the most important insulation problem.

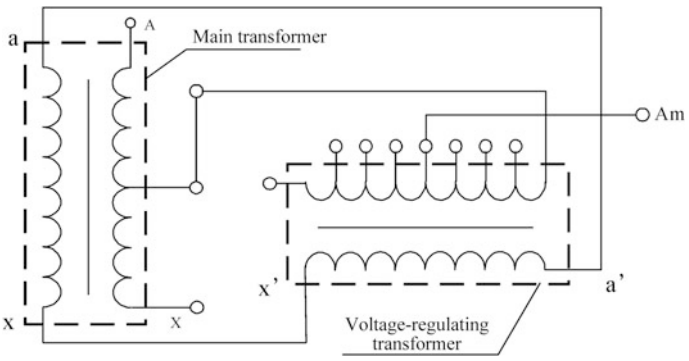

Fig. 11.2 Voltage regulation at the medium-voltage line end

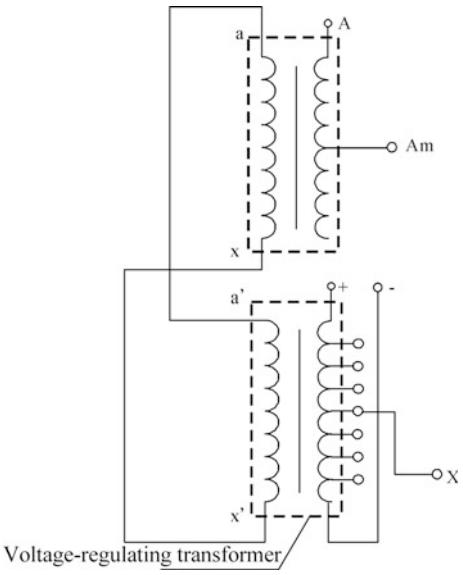

Fig. 11.3 Neutral point voltage regulation

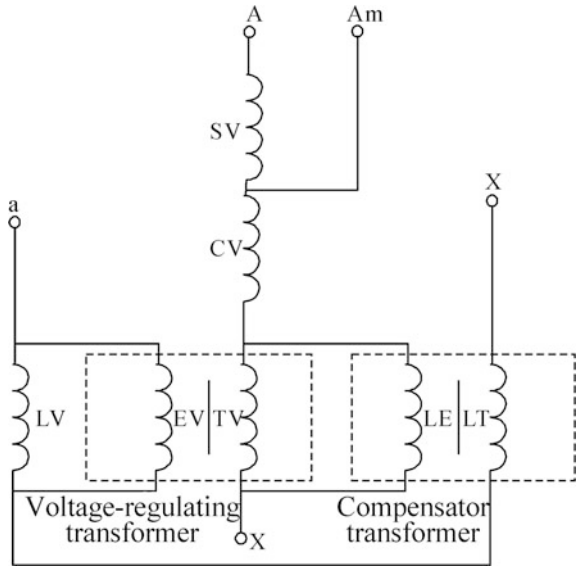

Fig. 11.4 Wiring of compensation windings

However, after the application of the neutral point voltage regulation mode, the HV and MV of the autotransformer will be common neutral point, and, during the voltage regulation, the potential of turn at each tap position and the magnetic flux density of the core will be changed. To prevent the change of LV output voltage along with the change at the tap positions, the LV compensation winding shall be designed to compensate the LV voltage fluctuation. Therefore, the UHV

transformer shall be applied with the neutral point non-field excitation voltage regulation and designed with the LV compensation winding. The wiring of the corresponding compensation windings is as shown in Fig. 11.4, where SV, CV, LV, TV, EV, LE, and LT are, respectively, the series winding, common winding, LV winding, voltage-regulating winding, voltage-regulating excitation winding, LV excitation winding, and LV compensation winding.

11.1.2.3 Structures of Transformer's Core and Body

The core of the conventional 500 kV single-phase autotransformer is usually applied with the single-phase three-limb structure (the structure with single core limb and two side limbs). However, for the 1000 kV transformer, as it has huge capacity, if the three-limb structure is still adopted, the problem in temperature rise will be difficult to solve, and hence, the four-limb structure (the structure with two core limbs and two side limbs) or the five-limb structure (the structure with three core limbs and two side limbs) can be considered. For the core of five-limb structure, as the capacity of each limb is small, it can reduce the height of the core limbs effectively and reduce the difficulty in transportation. Therefore, in the UHVAC demonstration projects, the 1000 kV main transformer is applied with the single-phase five-limb core, in which three core limbs are mounted with coil winding.

The UHV transformer is featured by high-voltage, large-capacity, multiple windings and complex internal structure. To simplify the structure of main transformer and enhance the insulation reliability, the main transformer of the UHV transformer can be separated from the voltage-regulating compensator transformer, and the both can be connected by tubular busbar. The voltage-regulating compensator transformer consists of voltage regulator and LV voltage compensator sharing one oil tank. Usually, the UHV transformers used for the UHVAC demonstration projects are of split structure [3].

11.1.3 Main Parameters of the UHV Transformers Used for the UHVAC Demonstration Project

The transformers used in the Southeast Shanxi Substation of the UHVAC Demonstration Project are manufactured by Baobian, and the main parameters thereof are:

(1) Product type: single-phase, oil-immersed, and autotransformer with non-field excitation tap changer at neutral point, provided with external voltage-regulating compensator transformer, the product model is ODFPS-10000000/1000.
(2) Rated capacity: 1000 MVA/1000 MVA/334 MVA.

Table 11.1 Internal insulation level of 1000 kV transformer

Winding	Power frequency withstand voltage (kV)	Lightning impulse withstand voltage (peak value) (kV)		Switching impulse withstand voltage (peak value) (kV)
		Full wave	Chopped wave	
HV (1000 kV end)	1100	2250	2400	1800
MV (500 kV end)	630	1150	1675	1175
LV (110 kV end)	275	650	750	–
Neutral point	140	325	–	–

(3) Rated voltage: $1050/\sqrt{3}/(525/\sqrt{3} \pm 4 \times 2.25\%)/110$ kV.
(4) Connection symbol: Ia0i0.
(5) Nominal short-circuit impedance: HV–MV: 18%; HV–LV: 62%; MV–LV: 40%.
(6) Cooling mode: forced-oil and forced-air cooling (OFAF) for the main transformer, and oil natural air natural cooling (ONAN) for the voltage-regulating compensator transformer.
(7) Internal insulation level: as shown in Table 11.1.

On Jan 6, 2009, the 1000 kV Southeast Shanxi-Nanyang-Jingmen UHVAC Demonstration Project was formally put into commercial operation. Up to now, the UHV transformers selected and designed according to the characteristics of the UHV transformer have been being under stable operation. The accumulated experience in the operation thereof will help us have a clearer and deeper understanding on the UHV transformer.

11.2 UHV Shunt Reactor

The UHV shunt reactor is an important constituent of the UHVAC equipment and is usually installed in the substations and switchyards along the UHVAC line. The UHV shunt reactor can effectively improve the operation condition of the UHVAC line, including mitigating the capacitance effect of the UHV line to reduce the power frequency transient overvoltage; improve the voltage distribution on the long-distance transmission line; balance the reactive power of the line, reduce the line loss, and enhance the transmission efficiency; reduce the power frequency steady-state voltage on the HV busbar when large unit and system are paralleled so as to facilitate the synchronous parallel operation of the generator; prevent the self-excitation resonance phenomenon that may occur to the synchronous generator with no-load long line; effectively reduce the secondary arc current amplitude; and

speed up the arc blowout when the neutral point of the shunt reactor is earthed by small reactor, so as to enhance the success ratio of single-phase automatic reclosure.

In comparison with the foreign countries, China's research on the UHV shunt reactor started late. Nevertheless, along with the deepening of the UHV transmission project, China's reactor manufacturers have also gradually mastered the design and manufacturing technology of the UHV shunt reactor. On Feb 13, 2008, the first main equipment, the 1000 kV/240 Mvar UHV single-phase shunt reactor, used for China's 1000 kV UHV demonstration project was successfully manufactured by Xi'an XD Transformer Co., Ltd.; in March of the same year, the 1000 kV/320 Mvar HV shunt reactor with the highest voltage level and the largest capacity in the world, independently designed and manufactured by the company, passed all the type tests. In May 2009, the 1100 kV/200 Mvar UHVAC shunt reactor independently manufactured by TBEA Hengyang Transformer Co., Ltd. (hereinafter referred to as TBEA Hengyang) also successfully passed the type tests. Up to then, the UHV shunt reactors with the above three different capacities required for the UHVAC demonstration project had all completed the type tests and entered into the supply stage.

The high-voltage level and long transmission distance of the UHVAC line cause the single-phase capacity of the UHV shunt reactor to be apparently higher than that of the EHV shunt reactor, which determines that the UHV reactor is different from the EHV shunt reactor in the structural design, insulation design, cooling mode, and noise control, etc. The 320 Mvar UHV shunt reactor manufactured by Xi'an XD Transformer Co., Ltd. is as shown in Fig. 11.5.

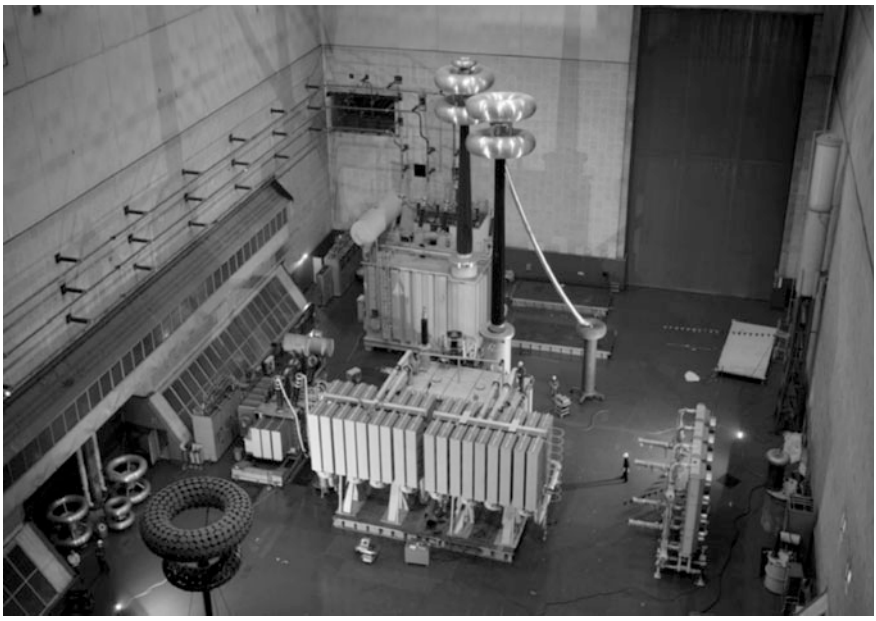

Fig. 11.5 320 Mvar UHV shunt reactor manufactured by Xi'an XD transformer Co., Ltd

11.2.1 Structural Design

The capacity of the UHV shunt reactor is several times that of the EHV shunt reactor. If the common three-limb (single core limb and two side limbs) structure in which only one core limb is mounted with winding is still used, the technical problems such as too large core diameter, difficult control of leakage flux, and increased axial electric field intensity will occur.

In combination with the manufacturing experience of the EHV shunt reactor and according to the characteristics of the UHV shunt reactor, China's manufacturers design and manufacture the core of the UHV shunt reactor in two structures, namely the double-body structure or four-limb structure (two cores plus two side yokes), to prevent the technical problems resulting from the too large diameter and height of single core.

The double-body structure consists of two body windings connected in series which are placed in one tank. Besides, the single body has the same structure with single core limb and two side limbs as that of the EHV shunt reactor, as shown in Fig. 11.6. Such double-body structure is of independent structure, with each body having only one core disk, and, as the compaction of the core disk of single body is relatively easy, the vibration and noise are apparently reduced. Of course, the double-body structure also increases the consumables and weight of the shunt reactor. The UHV shunt reactor used in Jingmen Substation of the Southeast Shanxi-Nanyang-Jingmen UHVAC Demonstration Project is manufactured by TBEA Hengyang and is of the double-body structure.

The four-limb structure consists of two core limbs plus two side limbs, as shown in Fig. 11.7. The four-limb structure can rationally allocate the main leakage flux and effectively control the distribution of leakage flux, thus to reduce the stray loss resulting from leakage flux and prevent local overheating. In addition, it can also save materials and reduce the overall weight of reactor. However, this structure also has shortcoming which is reflected in the increased manufacturing difficulty as it requires compacting the two core limbs with air clearance at the same time to reduce the vibration and noise. The UHV shunt reactors used in Southeast Shanxi

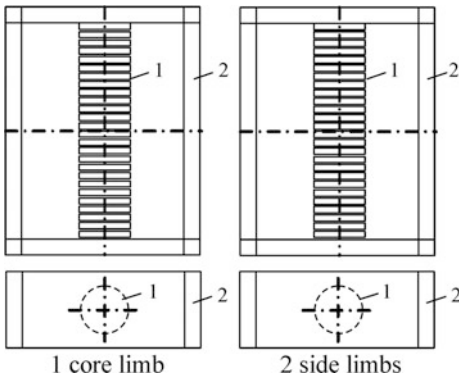

Fig. 11.6 Sketch for UHV shunt reactor of double-body core structure

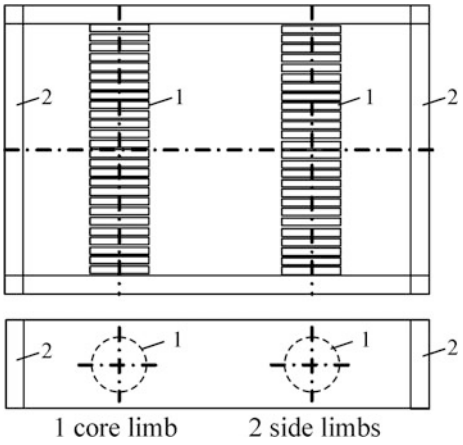

Fig. 11.7 Sketch for UHV Shunt reactor of four-limb core structure

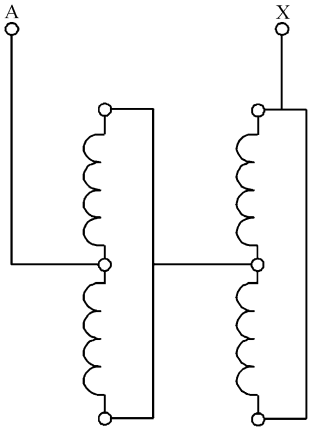

Fig. 11.8 Sketch for connection method of parallel connection before series connection for shunt reactor windings

Substation and Nanyang Switchyard are manufactured by Xi'an Transformer, and the cores thereof are of the four-limb structure.

The UHV shunt reactors of both double-body structure and four-limb structure consist of two cores, and each core winding consists of upper and lower coils. The four coils of the two cores can be considered to be connected in two ways: parallel connected before series connected (as shown in Fig. 11.8), namely both the upper and the lower coils of single core winding are connected in parallel and then connected in series; series connected before parallel connected (as shown in Fig. 11.9), namely the upper and the lower half windings of the two cores are, respectively, connected in series and then connected in parallel. In the winding connection method of series connection before parallel connection, as the upper and the lower half windings of the two cores are required to be, respectively, connected in series, the symmetry of the upper half magnetic circuit and the lower half magnetic circuit is difficult to guarantee, and therefore, it is not applied in the

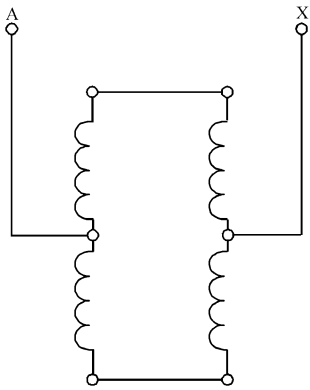

Fig. 11.9 Sketch for connection method of series connection before parallel connection for shunt reactor windings

Table 11.2 Insulation levels of UHV shunt reactor

Winding	Short-duration power frequency withstand voltage (kV)	Lightning impulse withstand voltage (peak value) (kV)		Switching impulse withstand voltage (peak value) (kV)
		Full wave	Chopped wave	
HV end	1100 (5 min)	2250	2400	1800
Neutral point end	230 (1 min)	550	650	–

practical design. Both the UHV shunt reactor of double-body structure manufactured by TBEA Hengyang and the UHV shunt reactor of four-limb structure manufactured by Xi'an Transformer are applied with the winding connection method of parallel connection before series connection.

11.2.2 Insulation Design

The axial central insulation structure between the UHV shunt reactor's core limb outer diameter and winding inner diameter and the axial central insulation structure between the reactor's core side yoke and winding outer diameter are the key of the main insulation design. During the design, it is necessary to eliminate the weak parts of the entire insulation system through the optimization of insulation structure. The insulation levels of the UHV shunt reactor are as shown in Table 11.2.

11.2.3 Cooling Mode

Due to the characteristic of huge capacity, the UHV shunt reactor is different from the EHV shunt reactor to some extent in terms of the cooling mode. The difference

is reflected in two aspects, namely the cooling mode and the radiator installation method.

The EHV shunt reactors, such as the 330, 500, and 750 kV shunt reactors, are all basically applied with the ONAN mode, and the cooling equipment is the plate radiator. However, the cooling mode of the UHV shunt reactors includes the ONAN mode and the oil natural air forced cooling (ONAF) mode, and the latter is better in the cooling effect. Due to the increase of the single-phase capacity, the loss of single UHV shunt reactor is apparently higher than that of the EHV shunt reactor, but the temperature rise limit is not increased. As a result, when the temperature rise of the UHV shunt reactor under the ONAN mode cannot meet the requirements, the ONAF mode with better cooling effect is considered. In the UHVAC demonstration project, the UHV shunt reactor manufactured by TBEA Hengyang is applied with the ONAN mode, while the UHV shunt reactor manufactured by Xi'an Transformer is applied with the ONAF mode.

In addition, the plate radiator used in the EHV shunt reactor is applied with the wall-mounted structure. However, for the UHV shunt reactor, due to the increased cooling capacity, the dead weight of the plate radiator of corresponding reactor and the weight of the insulating oil therein are also increased. As a result, if it is still applied with the wall-mounted structure, the mechanical strength of tank wall will be difficult to meet the requirements. Therefore, the plate radiator used in the UHV shunt reactor is required to be independently mounted on the supporting base.

11.2.4 Noise Control

As the UHV project equipment has large capacity and high noise energy, the effective noise control is one of the important technologies to be researched in the construction of the UHV project. The operation noise of the UHV shunt reactor is one of the main noise sources in the UHV substations, and such noise is mainly generated from three sources, namely the magnetic core (noise resulting from magnetostriction and generated at the connection), noise resulting from electromagnetic force in the coil (slot wall and magnetic field) and fans of the cooling system [4].

The noise can be regarded as pollution only when the sound source, propagation path, and receptor co-exist [4]. The noise control of the UHV shunt reactor is also carried out in such three aspects.

The sound sources are reduced through the manufacturing and selection of low-noise equipment and the application of equipment subject to silent design to reduce the sound power of the noise source. For example, the particular measures include the selection of high-magnetic conductivity sheet steel and multi-stage stepping core structure to reduce the magnetostriction, the application of advanced process to strength the fixing of winding coils, thus to reduce the noise resulting from electromagnetic vibration and the selection of high-quality and highly efficient fans to reduce the fan noise.

The control of the propagation path is to arrange the sound insulation facilities outside the UHV shunt reactor, thus to inhibit the propagation of noise. The particular measures include the application of fully enclosed or non-fully enclosed noise reduction enclosure to enclose the shunt reactor and the arrangement of noise barrier. Among such measures, the application of fully enclosed enclosure can achieve prominent noise reduction effect, but is unfavorable to the heat dissipation of the equipment. Therefore, the non-fully enclosed sound insulation equipment or noise barriers are usually adopted in practice and the heat dissipation effect of the shunt reactor is guaranteed, while the requirements for noise control are met. In the UHVAC demonstration project, the 320 Mvar shunt reactor proper used in Southeast Shanxi Substation is mounted with sound insulation enclosure, while in both Jingmen and Nanyang Substations, and the embedded sound barrier foundation is used to reduce the noise.

The control of the reception of noise by the receptors is to provide hearing protection to the receptors, so that the strong noise cannot be transmitted into their ears. The corresponding measure, for example, is to install the sound insulation doors and windows in the buildings. Such measure, however, applies to the receptors, and has nothing to do with the design and construction of the substations. Therefore, the noise control in the UHV project mainly refers to the reduction of the noise sources and the control of the propagation path.

11.2.5 UHV Controllable Shunt Reactor

The shunt reactor in the UHV line plays the role to compensate the capacitive reactive power of the line and inhibit the power frequency overvoltage [5]. During the initial stage of the UHV project, the line is applied with the fixed shunt reactor, but in case of the occurrence of power frequency overvoltage, the controllable shunt reactor can rapidly increase the compensation degree and reduce the amplitude of overvoltage. Meanwhile, it can regulate the reactive capacity according to the operation mode of the system, thus to meet the reactive power balance under different operation modes. On the premise of limiting the power frequency overvoltage, it has two major advantages of giving full play to the transmission capacity of the UHV line and waiving the cost of the LV reactive power equipment, which ensures the safe and reliable operation of the UHV line and better adapts to the development of the UHV power grid. It is the development trend of the UHV shunt reactor.

At present, the controllable shunt reactors that can be used in the EHV and UHV systems mainly consist of the magnetic valve type controllable shunt reactor (MCSR) and the transformer type controllable shunt reactor (TCSR), both of which can rapidly regulate the reactor capacity in a continuous or stepped manner. Their emergence makes it possible to solve the contradiction between the reactive power balance and the power frequency overvoltage restriction and achieve the controllable reactive power of the UHV system.

The smooth operation of the EHV controllable shunt reactor demonstration project provides reference to the design and manufacturing of the UHV controllable shunt reactor. It is believed that, along with the development of the UHV project, the UHV controllable shunt reactor will gradually emerge and play the role of reactive power compensation and overvoltage control in the UHV line.

In Chap. 4 of this book, the necessity, development history, and status quo of the UHV shunt reactor are studied in detail.

11.3 UHV Instrument Transformer

The UHV instrument transformer includes the UHV voltage transformer and the UHV current transformer, which refers to the equipment converting voltage or current as per certain proportion. Through converting the high voltage to low voltage and large current to small current, it is used to measure or protect the system.

11.3.1 Status Quo of the UHV Voltage Transformers and Current Transformers in China and Other Countries

The types of the voltage transformer selected for the UHV project in different countries are different to some extent. In the former Soviet Union, the UHVAC substation is of open structure, and the selected type of the voltage transformer is the post-type capacitor voltage transformer (CVT). In 1000 kV New Haruna Substation in Japan, due to the application of the gas insulated metal enclosed switchgear (GIS), the selected voltage transformer thereof is the capacitor divider electronic voltage transformer (EVT). Based on the experience in the design of the EHV voltage transformer, China's manufacturers, such as Guilin Power Capacitor Co., Ltd., Nissin Electric Wuxi Co., Ltd., and so on, have also equipped with the capability to design and manufacture the UHV voltage transformers, and the China's UHV demonstration projects adopt the post-type CVTs.

For the UHV current transformers, different structure types are used on the UHV lines in different foreign countries. In the former Soviet Union, the conventional cascade current transformer is used; while in New Haruna Substation in Japan, the 1000 kV GIS is applied with the packaged current transformer winding consisting of cored winding and hollow-cored winding, in which the former is used for electric energy metering and measurement, and the latter is used for system protection. In the 1000 kV UHVAC demonstration projects in China, the packaged ring-type TA windings are selected and mounted on the GIS bushing, circuit breaker terminals, and transformer bushing.

11.3.2 UHV Voltage Transformer

The voltage transformer can be divided into the post-type CVT, tank-type voltage transformer (including tank-type CVT and tank-type inductive voltage transformer), and electronic voltage transformer.

1. Post-type CVT

The UHV post-type CVT has the same principle as that of the post-type CVT at other voltage levels, and the schematic diagram thereof is as shown in Fig. 11.10. The capacitor divider consisting of multiple capacitors connected in series is used to divide the primary voltage, and then obtain, through the electromagnetic unit consisting of MV transformer, compensation reactor ,and damper, the secondary voltage which is used for measurement or relay protection. The part bearing the main insulation is the coupling capacitor divider, for which the voltage distribution is relatively even. From the perspective of engineering safety and reliability, the post-type CVTs are suitable for the open-type substation.

With the increase of the voltage level, higher requirements are presented on the insulation level of the UHV CVT. The insulation levels of the 1000 kV post-type CVT specified by State Grid are as shown in Table 11.3.

The 1000 kV CVT researched and manufactured by Xi'an XD Power Capacitor Co., Ltd. (hereinafter referred to as Xi'an Capacitor Company) is applied in Nanyang Switchyard of the 1000 kV "Southeast Shanxi-Nanyang-Jingmen UHVAC Demonstration Project" in China, and its main parameters are as shown in Table 11.4 [6].

2. Tank-type voltage transformer

The tank-type voltage transformer is divided into tank-type CVT and tank-type inductive voltage transformer.

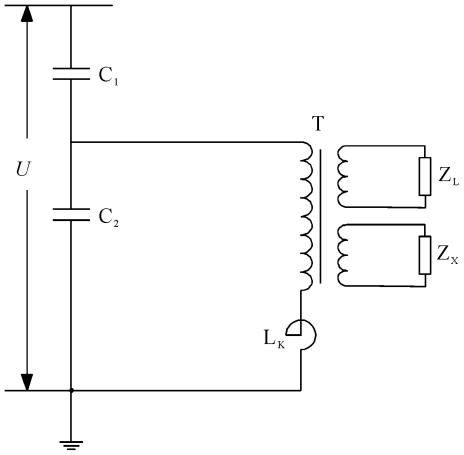

Fig. 11.10 Schematic diagram of post-type CVT. C_1 and C_2 capacitor dividers, L_k compensation reactor, T MV transformer, Z_L secondary load, Z_x damper

Table 11.3 Insulation levels of 1000 kV post-type CVT specified by state grid

Maximum operating voltage of equipment (kV)	Short-duration power frequency withstand voltage (kV)	Lightning impulse withstand voltage (kV)	Switching impulse withstand voltage (kV)
1100	1300	2400	1960

Table 11.4 Main parameters and performance of 1000 kV CVT researched and manufactured by Xi'an Capacitor Company

Maximum working voltage (kV)	1100
Rated capacitance (pF)	5000
Rated transformation ratio (kV)	$1000/\sqrt{3} : 0.1/\sqrt{3} : 0.1/\sqrt{3} : 0.1/\sqrt{3} : 0.1$
Rated secondary voltage (kV)	
Main secondary winding	$0.1\sqrt{3}$
Residual voltage winding	0.1
Insulation level (kV)	
Lightning impulse withstand voltage (1.2/50 μs) (peak value)	2600
Switching impulse withstand voltage (peak value) (250/2500 μs peak value)	1860
5 min power frequency withstand voltage (root-mean-square value)	1300

The 1000 kV tank-type CVT has the same principle as that of the post-tank CVT, i.e., utilizing the voltage division effect of capacitor. The main difference of the two lies in the main insulation materials: the tank-type CVT's voltage-dividing capacitor is located in the coaxial cylindrical tank filled with SF_6 gas whose insulation performance can be restored, while the post-type CVT's capacitor divider consists of multiple capacitor elements connected in series, and the insulation medium thereof is the organic insulation material whose insulation performance cannot be restored. Figure 11.11 shows the schematic diagram of the tank-type CVT of independent cabin type structure.

The tank-type inductive voltage transformer has the same principle as that of the ordinary inductive voltage transformer, i.e., utilizing the electromagnetic principle to achieve voltage conversion. The difference lies in that the tank-type inductive voltage transformer is applied with SF_6 gas as the main insulation medium, and that it is mainly used in the GIS substation.

In addition, in comparison with the tank-type CVT, the tank-type inductive voltage transformer has better error performance in case of high-voltage level. Because the tank-type CVT has many internal energy storage elements, and thus, the factors influencing the error are more than that of the tank-type inductive voltage transformer. However, the tank-type CVT has better insulation performance. Because it can reduce the lightning wave front steepness and thus enhance the lightning impulse withstand performance; meanwhile, the inductive voltage

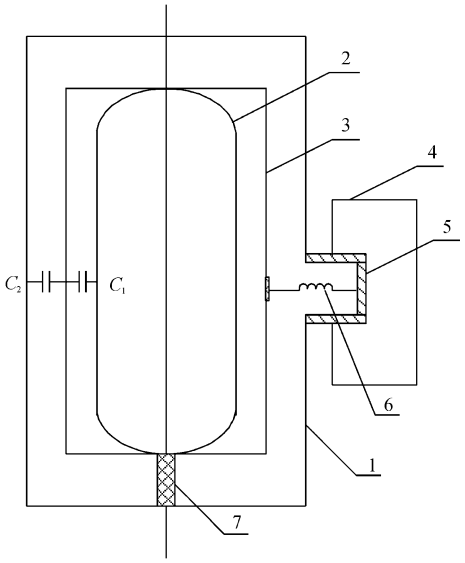

Fig. 11.11 Schematic diagram of tank-type CVT of independent cabin type structure. *1* The sealed tank body, *2* the HV electrode, *3* the MV electrode, *4* the electromagnetic unit, *5* the outgoing line bushing, *6* the inductive reactance with small resistance, *7* the insulation support member

transformer is of coil equipment and is apt to generate series ferroresonance with the capacitor between open contacts of the circuit breaker.

3. Electronic voltage transformer

The 1000 kV electronic voltage transformer is under the development stage. Based on the present research, its sensor part still applies the voltage divider principle, and the resistance divider, inductance divider, capacitance divider or resistance-capacitance divider can be selected. Although, at present, the reliability of the electronic voltage transformer is not as good as that of the traditional voltage transformer, the electronic voltage transformer is featured by small volume, good transient performance and convenience for the implementation of relay protection and control. Therefore, the electronic voltage transformer is the development direction of the digital substation technology in future.

11.3.3 UHV Current Transformer

In the 1000 kV UHVAC projects, the current transformers are mainly installed at the transformer and reactor bushings and on both sides of GIS circuit breakers, and are all the bushing current transformer [7], which has no primary winding and is of simple structure with the live conductor directly passing through the middle.

In terms of the function, the current transformer (TA) can be divided into the metering TA and protective TA; in terms of the structure, it can be divided into the cored current transformer and hollow-cored current transformer. In the UHV

system, the hollow-cored current transformer shall be selected for busbar protection, because the system busbar is applied with the differential current protection, in case the non-hollow-cored current transformer is adopted, the current transformer will be unable to properly transmit the current information due to the core saturation phenomenon in case of short circuit outside the busbar area, resulting in the misoperation of the busbar protection [8]. The core saturation degree of the current transformer is related to the time constant of the system. For the UHV system, in case of fault, the attenuation time constant of the DC component of the fault current is very large, and thus, the problem of core saturation of the current transformer is more serious. Therefore, in the UHV system, the hollow-cored current transformer shall be selected for busbar protection. The hollow-cored current transformer is of coreless structure, and thus, it does not encounter the problem of magnetic saturation and is able to enhance the measurement accuracy and the busbar protection stability in case of fault.

11.3.4 Photoelectric UHV Instrument Transformer

In addition to the conventional electromagnetic instrument transformer and capacitor instrument transformer, the photoelectric instrument transformer made by the optical sensing technology also comes out with the rapid development of the optical technology.

The photoelectric instrument transformer can be divided into the passive and active types. The passive photoelectric instrument transformer directly converts the current or voltage into the optical signal by the magneto-optical effect and electro-optic effect, while the active photoelectric instrument transformer needs to first convert the current signal or voltage signal into the small voltage signal by the electromagnetic induction or voltage division principle, and then convert the small voltage signal into the optical signal which is finally transmitted to the secondary equipment.

The photoelectric instrument transformer has many advantages. First, the photoelectric instrument transformer transmits the signal through optical fiber, having stable insulating property, and meanwhile, isolates electrically the high-voltage and low-voltage circuits, greatly improving the safety and reliability. Second not using oil as the insulating medium, the photoelectric instrument transformer can avoid the dangers like oil leakage and explosion, and meanwhile, because of the coreless structure, it is not subject to the magnetic saturation or ferroresonance phenomenon, having good stability. Finally, the photoelectric instrument transformer also has advantages like large dynamic range, light weight, small volume, and adaptive to the requirements of the modern electric power system on digital signal processing. In conclusion, the photoelectric instrument transformer will have a wide application prospect in the UHV power grid.

11.4 UHV Arrester

The arrester is an important electrical device used to restrict the lightning overvoltage transmitted from the line or the internal overvoltage resulting from switching operations. In the UHV system, the application of the arrester with high performance and rational insulation coordination with the equipment can enhance the reliability of the transmission system, reduce the insulation level of the system, and reduce the volume and weight of the power transmission and transformation equipment. Therefore, the design and manufacturing of the UHV arrester is the important research content of the UHV technology.

11.4.1 Status Quo of the UHV Arresters in China and Other Countries

There are several countries having the capability to manufacture the UHV arresters, such as the former Soviet Union, Japan, and Sweden. Early in the 1980s, the former Soviet Union had developed the 1150 kV arrester and put into operation in the power grid; in 1995, Japan developed the SF_6 tank-type arrester used for 1000 kV GIS substation; Sweden has already developed the SF_6 tank-type arrester used for 1050 kV GIS substation [9].

For the most common no clearance metal oxide arrester (MOA), the EHV and UHV arrester technologies in those countries are relatively mature, and the MOAs of 500 kV voltage level above have widely been used in the system, with many years of operation and assessment experience having been accumulated. The operating voltage of the MOA products manufactured by GE and OB in the USA, ABB in Sweden and Switzerland, Electric Porcelain Industry Joint Company in Russia, and EMP in the UK, etc., has all reached up to 1150 kV [10].

The UHV arrester technology in China is also more and more mature. Xi'an XD High Voltage Porcelain Insulator Co., Ltd., Fushun Electric Porcelain Manufacturing Co., Ltd., Langfang EPRI Toshiba Arrester Co., Ltd., and Nanyang Jinguan Electric Co., Ltd. have already had the capability and experience to manufacture the UHV arresters, and have jointly supplied the UHV arresters for the Southeast Shanxi-Nanyang-Jingmen UHVAC Demonstration Project [11, 12].

11.4.2 Characteristics of the UHV Arrester

The UHVAC arrester has similar structure as that of the EHV arrester; however, due to the enhanced rated voltage, raised discharge current capacity and increased volume and weight, the UHV arrester also has its unique structure characteristics and key technologies compared with the EHV arrester.

11.4.2.1 Structure Characteristics

The varistor of the UHV arrester is of four-column parallel structure, and in addition, the UHV arrester needs to be installed with support.

To reduce the insulation level of the protected equipment and enhance the discharge current capacity of the arrester [13], the interior of the elements of the UHV arrester is applied with the four-column parallel structure, instead of the single-limb core structure used for the arresters with voltage level of 750 kV and below.

In addition, in comparison with the EHV arrester, the UHV arrester is featured by high height, large diameter, and heavy weight, and is usually installed with support. The characteristic of heavy dead weight of the UHV arrester makes its mechanical performance and seismic resistance performance quite important, and in the UHV project, the seismic fortification intensity required for the arrester shall be not less than 8°. Corresponding measures, such as the application of high-strength aluminum porcelain to replace the silicon porcelain, the increase in the cross section of the root of porcelain shell to reduce the stress thereon, and the increase in the cementing depth at the end can be taken to guarantee the seismic resistance performance of the arrester.

11.4.2.2 High-Performance Varistor

The UHV arrester has higher requirements on its varistor in the aspects such as discharge capacity, voltage–current characteristic and voltage ratio performance. Through the application of the new formula for the varistor by the arrester manufacturer, the adverse compositions that affecting the discharge capacity are reduced, and the addition of various elements is rationally optimized. Meanwhile, the rational manufacturing process is developed, so that the performance of the varistor is enhanced obviously, specifically including:

(1) Reduced voltage ratio of the zinc oxide varistor;
(2) Obviously improved discharge capacity of the varistor;
(3) Improved aging behavior of the varistor.

11.4.2.3 Even Potential Distribution of Arrester

The voltage distribution of the arrester directly affects the service life thereof. While the height of the UHV arrester makes the distribution of its stray current to ground more uneven, the parallel voltage-sharing capacitor can be additionally installed by the side of the internal varistor of the UHV arrester to improve the longitudinal voltage distribution of the arrester.

In addition, due to the application of varistor with high potential gradient, the number of varistors required to be connected in series in the UHV arrester is obviously reduced. Meanwhile, the adoption of the four-column varistor parallel structure for the internal components greatly increases the capacitance of the arrester body and reduces the influence of the stray current on the arrester body, being advantageous to the even potential distribution of the arrester. Therefore, the unevenness coefficient of the 1000 kV UHV arrester is smaller than that of the EHV 500 and 750 kV arresters [13].

11.4.3 Main Parameters of the UHV Arresters Used in the UHVAC Demonstration Projects

The main parameters of the 1000 kV UHV arresters used in the UHVAC demonstration projects are as shown in Table 11.5.

11.4.4 UHVAC Controllable Arrester

With respect to the controllable arrester technology [14], on the basis of the preliminary study, the two schemes of switch controllable arrester [15] and thyristor valve controllable arrester [16, 17] are preliminarily selected.

Table 11.5 Main parameters of UHV arrester

Parameters	Value
Nominal system voltage (kV)	1000
Rated voltage (kV)	828
Continuous operating voltage (kV)	638
Nominal discharge current (kA)	20
Residual voltage (kV, not larger than)	
Under 1/10 μs and 20 kA, steep wave impulse	1782
Under 8/20 μs and 20 kA, lightning impulse	1620
Under 30/60 μs and 2 kA, switching impulse	1460
DC 8 mA reference voltage (kV, not less than)	1114
Power frequency reference voltage (peak value/2, kV, not less than)	828
2 ms square wave withstand current (kA)	8000
Number of paralleled columns	4
Unevenness coefficient of current distribution (not larger than)	1.10
Unevenness coefficient of voltage distribution (not larger than)	1.15

11.4.4.1 Switch Controllable Arrester

The sketch of the structure of the switch controllable arrester is as shown in Fig. 11.12. The body of such arrester consists of the fixed element MOA1 and the controlled element MOA2, while the control unit CU consists of the switch K and the controller. The MOA2 and the CU are connected in parallel.

In case of closure and single-phase reclosure, the CU will be closed in advance before the circuit breakers in the substation close to limit the switching overvoltage resulting from the closure and single-phase reclosure; after the switching overvoltage ends, the CU will open and the MOA1 and MOA2 will act jointly to guarantee the operating reliability of the arrester.

Under the system's continuous operating voltage, temporary overvoltage, and lightning overvoltage, the CU will break and the MOA1 and MOA2 will jointly undertake the system's continuous operating voltage, temporary overvoltage, and lightning overvoltage.

The switch controllable arrester is mainly used to limit the switching overvoltage resulting from closure and reclosure, allowing to eliminate the closing resistor of the circuit breaker. Currently, the samples of the UHVAC switch controllable arrester with controllable ratio of 15% have been developed by China Electric Power Research Institute and have been tested and researched at Wuhan UHVAC Test Base as shown in Fig. 11.13. Its technical feasibility has basically been verified.

11.4.4.2 Thyristor Valve Controllable Arrester

The sketch of the structure of the thyristor valve controllable arrester is as shown in Fig. 11.14. The body of such arrester consists of the fixed element MOA1 and the controlled element MOA2, while the control unit CU consists of the thyristor valve

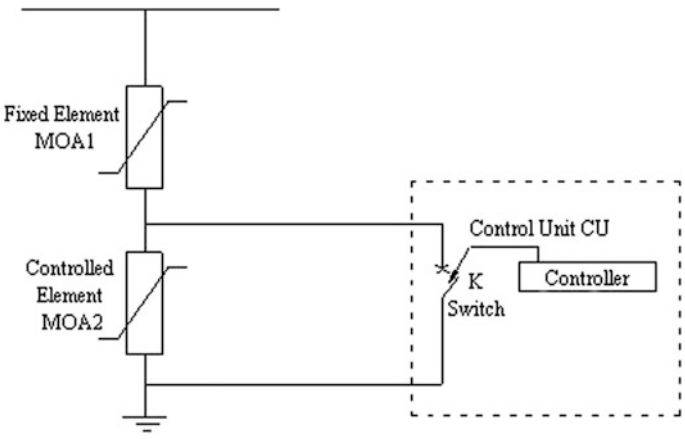

Fig. 11.12 Structure sketch of switch controllable arrester

Fig. 11.13 Samples of UHVAC switch controllable arrester with controllable ratio of 15%

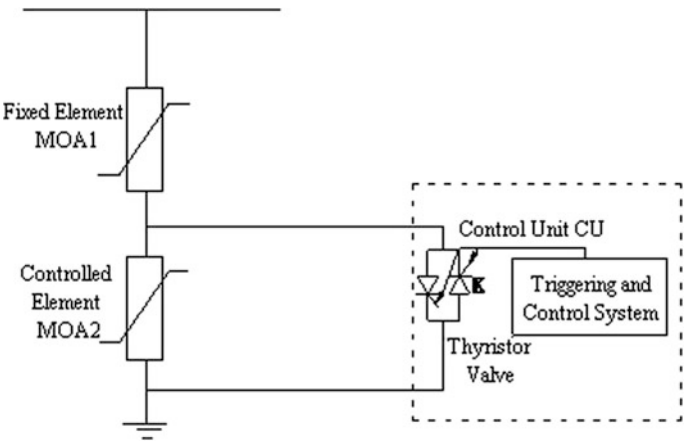

Fig. 11.14 Structure sketch of thyristor valve controllable arrester

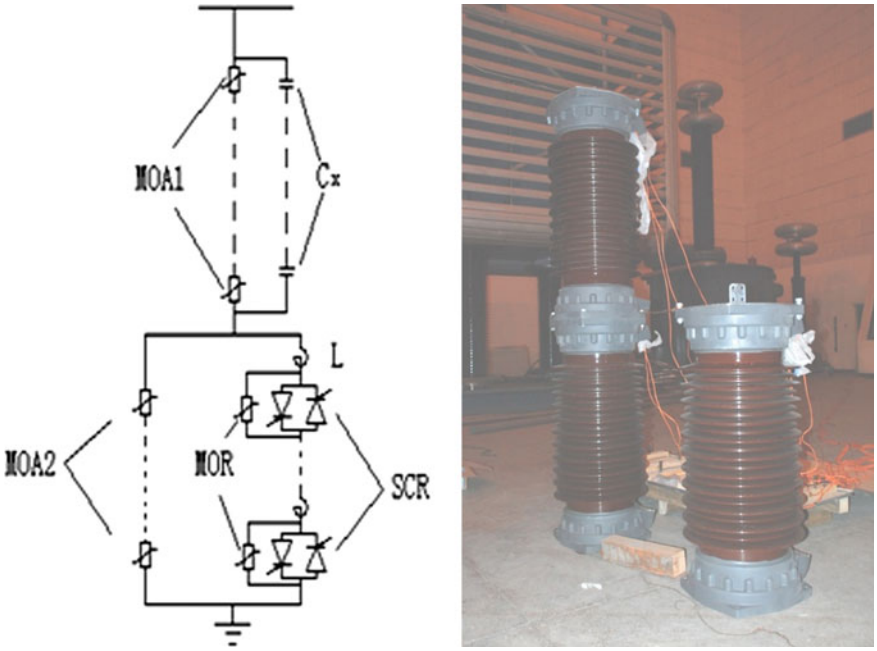

(a) Structure (b) Appearance

Fig. 11.15 Sketch of the 110 kV thyristor valve controllable arrester's structure and appearance

and the triggering and control system. The MOA2 and the CU are connected in parallel.

Under the switching overvoltage, the K will trigger, the CU will close, the MOA2 will be short circuited, and the MOA1 will have low residual voltage which may deeply reduce the system's switching overvoltage.

Under the system's continuous operating voltage, temporary overvoltage, and lightning overvoltage, the CU will break and the MOA1 and MOA2 will jointly undertake the system's continuous operating voltage, temporary overvoltage, and lightning overvoltage.

Currently, the model of the thyristor valve controllable arrester at voltage level of 110 kV has been developed, as shown in Fig. 11.15, and has passed the operating characteristic test, potential distribution test, and other tests carried out under the switching overvoltage, temporary overvoltage, and lightning overvoltage. Its technical feasibility has been verified as well. The thyristor valve controllable arrester at voltage level of 1000 kV is still researching.

11.5 UHV Switchgear

The UHV switchgear mainly includes the circuit breaker, disconnector, grounding switch, and combination of the above equipment and other electrical equipment. In the UHV power transmission and transformation equipment, the manufacturing of the UHV circuit breaker and the UHV GIS is one of the most critical and difficult tasks.

11.5.1 Status Quo of the UHV Switchgear in China and Other Countries

Some countries, such as America, Italy, and Japan, have already completed the research and manufacturing of the UHV SF_6 circuit breaker, whose breaking current capacity is up to the level of 63 kA and total breaking time lasts for two cycles in general. In China, Shenyang High Voltage Switchgear Factory, Pingdingshan High Voltage Switchgear Factory, and Xi'an High Voltage Switchgear Factory have also successfully researched and manufactured the UHVAC circuit breaker one after another.

For the 1000 kV UHV disconnector, many manufacturers already have equipped with the manufacturing capability, such as Siemens in Germany, SSL in the USA, and ABB in Switzerland [18].

For the high-speed grounding switch (HSGS), Mitsubishi, Toshiba, and Hitachi, three companies in Japan, have already manufactured the UHV HSGS, which is used in New Haruna UHV Test Station in Japan [19].

The 1100 kV high-performance GIS is an important component part of the UHVAC transmission system. Mitsubishi, Toshiba, and Hitachi, three companies in Japan, respectively, developed the 1100 kV GIS of the SF_6 circuit breaker with double breaks in 1995 and carried out the long-time energized test to it in New Haruna UHV Test Station of Tokyo Electric Power Company in 1996 [20]. China's GIS manufacturing was started late but has witnessed rapid development. Through introducing and digesting the 1100 kV GIS manufacturing technology of Japan's AE-POWER Company and conducting cooperative development together with AE Company, Shenyang High Voltage Switchgear Factory has gradually mastered the core manufacturing technology and gradually realized the localization of the 1100 kV GIS equipment [20]. At present, China's manufacturers have already completed the research and manufacturing of the 1100 kV GIS switchgear with short circuit breaking current capacity of 63 kA, and had it applied in the UHVAC demonstration and expansion project [21], being the first in the world. The UHV GIS equipment is as shown in Fig. 11.16.

Fig. 11.16 UHV GIS equipment

11.5.2 Characteristics of UHV Switchgear

Due to the increased voltage level, higher requirements are presented to the UHV switchgear in the aspects such as breaking capacity and arc extinction performance. Therefore, in comparison with the EHV switchgear, the UHV switchgear has different structure characteristics.

11.5.2.1 Characteristics of UHV Circuit Breaker

There are many types of UHV circuit breakers. In terms of the arc-extinguishing medium, it can be divided into oil circuit breaker, air (vacuum) circuit breaker, and sulfur hexafluoride (SF_6) circuit breaker, etc., among which the SF6 circuit breaker, due to the advantages such as high break voltage, strong breaking capacity and large continuous short-circuit current breaking times, is widely used in the EHV and UHV project, but, in comparison with the EHV circuit breaker, the UHV circuit breaker is different in terms of the structure.

1. Paralleled closing and opening resistors of the UHV circuit breaker

The paralleled closing resistors of the circuit breaker can effectively restrict the closing overvoltage in the EHVAC and UHVAC systems. However, due to the complex structure of the closing resistor, its intrinsic defects can increase the system failure rate. Meanwhile, the circuit breaker applied with the closing resistor is expensive in price. For the EHVAC transmission line, such as the 500 kV line, when the line length is less than 100 km, the closing resistor may usually be canceled. As the UHV line has high requirements on insulation level and is long in the line length, the 1000 kV UHV circuit breaker is usually applied with the closing resistor to reduce the closing overvoltage. This is the main difference between the UHV circuit breaker and the EHV circuit breaker at present.

The main role of the opening resistor of the UHV circuit breaker is to restrict the fault clearing and transfer overvoltage. Besides, it also has a certain effect on the restriction of the transient recovery voltage (TRV) of the circuit breaker. However, in the UHVAC transmission system in China, even if the circuit breaker is not installed with the opening resistor, the TRV on the circuit breaker is already lower than that specified in the relevant standard. In addition, although the opening resistor of the circuit breaker can reduce the fault clearing and transfer overvoltage to some extent, it will require large energy and is expensive in manufacturing, as well as reducing the reliability of the circuit breaker. Therefore, generally, the UHV circuit breaker is not necessary to be installed with the opening resistor [22].

2. Multiple-break arcing chamber structure

The arcing chamber of the EHV circuit breaker usually consists of single break or double breaks. Due to the increased system voltage level, the voltage difference at both ends of the UHV circuit breaker before and after the opening is apparently higher than that of the EHV circuit breaker, causing that single break can hardly undertake it, and therefore, the arcing chamber of the UHV circuit breaker is mostly of multi-break structure. At present, there are two types of structure for the 1000 kV circuit breaker, namely the double-break and four-break structures. In the 1000 kV Southeast Shanxi-Nanyang-Jingmen UHV AC Demonstration Project, the 1000 kV switchgear used in Southeast Shanxi Substation is the GIS equipment, the 1000 kV switchgear used in Nanyang Switchyard is the HGIS equipment, and the circuit breakers used for the switchgear in both substations are all of double-break structure, while the circuit breakers used for the 1000 kV HGIS switchgear in Jingmen Substation are of circuit breaker with four breaks [23].

11.5.2.2 Characteristics of the UHV Disconnector and High-Speed Grounding Switch

The UHV disconnector and high-speed grounding switch are similar to the EHV disconnector and high-speed grounding switch in the structures and functions.

At the closed position, the disconnector is able to undertake the normal working current. However, since it is not provided with the arc-extinguishing device, it is unable to cut off the short-circuit current and the excessive working current. In comparison with the UHV circuit breaker, the UHV disconnector is simple in structure, and the same as the EHV disconnector in terms of structure and function [24]. In terms of structure, the disconnector can be, in general, divided into four types, namely the single-column vertical retractable type, double-column horizontal rotary type, double-column horizontal retractable type, and three-column horizontal rotary type. Inside the EHV and UHV open-type substations, to save area, the single-column vertical retractable type disconnector is usually used [25].

The high-speed grounding switch is the grounding switch having the capability to close the short-circuit current and cut off and close the electrostatic induced current and electromagnetic induced current. It can be used to suppress the secondary arc current and enhance the success ratio of the automatic reclosure after single-phase grounding. Its structure is basically the same as that of the normal grounding switch and the only difference is that its moving and static contacts are attached with the copper-tungsten alloy material able to resist arc burning.

11.5.2.3 Characteristics of the UHV GIS

The GIS is the packaged distribution equipment consisting of the electrical components in the substation other than the transformer, including busbar, circuit breaker, disconnector, voltage transformer, current transformer, etc., all of which are installed in the enclosed metal container filled with the high-pressure SF_6 insulating gas. Therefore, the characteristics of the UHV GIS include the characteristics of the above-mentioned equipment such as the UHV circuit breaker, UHV disconnector, and UHV voltage transformer. In addition, due to the high operating voltage, the very fast transient overvoltage (VFTO for short) in the UHV GIS substation is more prominent, and the corresponding VFTO protection measures shall be taken in the UHV GIS.

For the UHV substation, the steep front VFTO can endanger the GIS equipment, main transformer, and secondary equipment in the substation. The addition of shunt resistance to the disconnector not only can effectively restrict the maximum amplitude of VFTO in the substation and protect the main insulation of GIS equipment, main insulation of the transformer, and secondary equipment in the substation, but also can reduce the wave front steepness value of VFTO invading the main transformer, thus to well protect the longitudinal insulation of the main transformer. The other effective method to inhibit the wave front steepness of VFTO invading the main transformer and thus to protect the longitudinal insulation of the main transformer is to connect the main transformer with one overhead line before connecting it with GIS. Such method can obviously weaken the wave front steepness of VFTO and reduce the wave front steepness to a safe range with only a

short length of overhead line, thus to well protect the longitudinal insulation of the main transformer. In addition, the occupied area required for laying of the overhead line is not large, and therefore, it can be considered in the actual construction.

Apart from the measure of the addition of shunt resistance to the disconnector, the secondary equipment can also be protected through the increase of the number of grounding points on the GIS enclosure, replacement of the material of GIS outlet bushing steel frame with stainless steel material, and copper material, etc.

In addition, the installation of ferrite toroid on the GIS conductor rod or before the port of the main transformer can also well restrict the VFTO value and protect the primary equipment and secondary equipment in the substation. However, the ferrite material is mainly applied to the high-frequency attenuator in the radio-frequency circuit, and its application in the restriction of VFTO is still at the research, test, and verification stage in China and other countries.

11.6 UHV Bushing

The bushing is used for the high-voltage conductor to pass through the wall or the metal enclosure of power equipment with potential different from the conductor potential, and plays the role of insulation and support. The bushing has the features of both internal and external insulation, complex electric field, and strict requirements on structure and dimension, etc.

11.6.1 Status Quo of UHV Bushing in China and Other Countries

In the UHV system, due to the high electric field intensity, the requirements on the height and diameter of the UHV bushing are very strict, usually restricting the manufacturing of the UHV equipment. At present, all over the world, there are only a few companies having the capability to manufacture the UHV bushing, such as ABB in Switzerland, P&V in Italy and Trench in England, etc. In China, the 1100 kV UHV transformer bushing developed by Nanjing Electric (Group) Co., Ltd. passed the national technical appraisal on Nov. 24, 2007. This 1100 kV UHV transformer bushing was of the international advanced level and broke the monopoly by the foreign companies [26]. In addition, China's Xi'an XD High Voltage Porcelain Insulator Co., Ltd. and Trench Fushun Bushing Co., Ltd. also have equipped with the capability to manufacture the UHV bushings.

The main transformer bushings used in the UHVAC demonstration project are manufactured by P&V in Italy, and the shunt reactor bushings are manufactured by ABB.

11.6.2 Characteristics of the UHV Bushing

In terms of application, the UHV bushing can be divided into the UHV transformer bushing, UHV reactor bushing and UHV GIS bushing, among which the former two have similar structures, and the characteristics thereof are hereinafter analyzed in a unified manner.

11.6.2.1 Characteristics of the UHV Transformer Bushing and Reactor Bushing

The UHV transformer bushing and reactor bushing not only have the structure characteristics of "long in length, wide in diameter and heavy in weight", but also need to meet the strict requirements of the UHV project on high reliability and performance such as electrical property, bending resistance, seismic resistance, sealing and temperature rise, etc., and key design and manufacturing technologies shall be established accordingly.

For the main insulation of the UHV transformer and reactor bushings, namely the capacitor core, it can be designed according to the capacitor voltage division principle of equal sectioned thickness, unequal capacitance, and maximally even interlayer insulation margin to ensure the insulation margin.

In addition, to ensure the good sealing performance of the bushing, the overall sealing structure assembled by high-strength spring compression, bolt and nut tightening, elastic plate fitting, local radial positioning, and rubber sealing gasket with good elasticity and toughness can be adopted. Meanwhile, to ensure that the entire HV bushing has good "rigid" structure and bending, seismic and vibration resistance, the porcelain shell can be manufactured by the high-strength electric porcelain formula; the central conductive tube can be drawn with rigid brass and tightened and assembled with the zero-layer copper tube to form the overall conductive tube structure; the mounting flange components of the body can be welded with thick steel plate; and auxiliary machinery can be used to strengthen the structure.

11.6.2.2 Characteristics of the UHV GIS Bushing

Both the dimension and weight of the 1000 kV GIS bushing are far above those of the 500 kV GIS bushing, and therefore, the base dimension thereof is also increased obviously. For example, the selected base height of the 1000 kV bushing in Japan is up to 4.5 m.

The working voltage of the UHV GIS is very high. To balance the electric field intensity inside and outside the bushing, the voltage-sharing measures can be taken inside the bushing. The corresponding voltage-sharing structure can be divided into

three types: (1) voltage sharing by the combination of several metal shields; (2) voltage sharing by pure end shielding structure; (3) voltage sharing by multiple layers wound with tin foil and polyester film.

In addition, similar to the EHV GIS bushing, the 1000 kV UHV SF_6 gas insulated bushing is also applied with the multi-pole metal shielding cylinder structure. Such structure not only can meet the requirements of the UHV project on insulation level, but also is relatively simple in manufacturing process, light in weight, the lowest in cost, easy in installation and use, and the highest in operation reliability.

11.7 UHV Series Compensation Device

Both the UHV and EHV transmission lines are applied with the series capacitor compensation device, which can reduce the reactance of the line and reduce the phase angle difference at both sides of the line, thus to effectively enhance the transmission capacity of the line and the stability of the system. In addition, it also has a certain regulation effect on the tidal current distribution of the transmission line [23, 24]. For the UHV series compensation device, the capacity and rated current thereof are obviously above those of the EHV series compensation device. For example, in the expansion project of the UHVAC demonstration project, the capacity of single capacitor of the UHV series compensation device is up to 1500 Mvar, about 3–4 times that of the 500 kV series compensation device, and the rated current thereof is up to 5080 A, nearly twice over that of the 500 kV series compensation device.

11.7.1 Status Quo of the UHV Series Compensation Device in China and Other Countries

Since the 1960s, the USA, the former Soviet Union, Italy, Japan, and some other countries have carried out a lot of tests and studies on the UHV transmission technology. However, all these studies do not cover the application of the UHV series compensation device [27].

With the deepening of the UHV research and the development of the UHV project, China has gradually mastered the core technology for the manufacturing of the UHV series compensation device. On Nov 20, 2011, in the expansion project of Southeast Shanxi-Nanyang-Jingmen UHVAC Demonstration Project, the artificial single-phase short-circuit grounding test of the series compensation line was successfully passed at the first time, and this marked that the development of the world's first UHV series compensation device undertaken by China EPRI Science & Technology Co., Ltd. was succeeded.

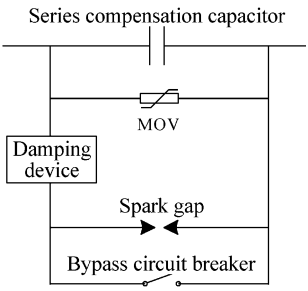

Fig. 11.17 Sketch for structure of series compensation device adopting the mode of protection by MOV with parallel gaps

11.7.2 Protection Mode of the UHV Series Compensation Device

The metal oxide voltage limiter (MOV) with parallel gaps can be selected as the protection mode for the UHV series compensation device. Such protection mode has the advantages such as rapid reconnection of the series compensation device, reduction in the MOV capacity, and provision of the backup protection. It can enhance the transient stability of the system. The sketch for its structure is as shown in Fig. 11.17, in which the MOV is the main protection of series compensation capacitor. The spark gap is the backup protection of MOV and series compensation capacitor, the bypass circuit breaker is used for system overhaul and debugging, and the damping device can restrict the discharge current of the capacitor to prevent the series compensation capacitor, gap, and bypass circuit breaker against damage during the process of discharge [28].

References

1. Cao Z. Inquire into configuration principles for on-load regulation transformers. Electr Power Constr. 1999;9:27–9.
2. Yuan M, Li Z, Tian Q. Analysis on problems of voltage regulation for UHV transformer. Water Resour Power. 2008;26(4):172–4.
3. Liu Z. AC electrical equipment for UHV. Beijing: China Electric Power Press; 2008. p. 8.
4. Ding Y, Wang S, Qiu N, Ou Y, Gao J, Mi C, Wang D. Development and Application of noise pollution control technology and equipment for 320 Mvar/1100 kV shunt reactor. In: Proceedings of 2009 international conference on UHV transmission technology; 2009, p. 1–4.
5. Xie Y, Li M. Application research on controlled shunt reactor in ultra-high voltage power grid. J Electr Power. 2009;24(4):266–9.
6. Ren C, Xue D. R&D of 1000 kV capacitive voltage transformer. Electr Equip. 2007;8(5): 35–7.
7. Zhao Y, Yu X. Research on testing scheme of 1000 kV GIS pipe current transformer. Mech Eng Autom. 2008;5:152–153, 156.
8. He B, Ma Y. The influence of current transformer saturation on bus protection. Relay. 1998;26(2):16–20.

9. Chen S. The research on switching overvoltage in 1000 kV transmission lines. Changsha: Hunan University; 2007.
10. Zhao H. Development situations of EHV (UHV) transmission and insulator surge arrester. Electrotech J. 2002;08:73–5.
11. Li M, Song J, Han S, Fang Y. Development and application of tank type surge arrester for 1000 kV system in China. High Volt Eng. 2009;35(11):2618–23.
12. Yang Y, Wang B, Xiong Y, Tang L, Zuo Z. Long-term live test and the engineering operation of the UHV MOA. High Volt Appar. 2011;47(7):1–8.
13. Liu F. Break through the key technology to ensure reliable operation of 1000 kV UHV surge arrester. China High Tech Enterp. 2011;1:64–5.
14. Chen X. Study on the UHVAC controllable metal oxide arresters. Beijing: China Electric Power Research Institute; 2009.
15. Chen X, Chen W, Shen H, He Z, Chen L, Che W, Song J. Calculation method for voltage distribution of controlled metal oxide arresters. Proc CSEE. 2010;30(25):130–4.
16. Chen X, Chen W, Shen H, Li G, He Z. Voltage sharing method for series-connected thyristor valves of controllable metal oxide arrester. Power Syst Technol. 2012;36(6):32–6.
17. Chen X, Chen W, Shen H, He Z, Li G, Ge D. Simulation analysis, testing and limitation measurements on voltage rise rate and current rise rate of thyristor valve in the controllable metal oxide surge arrester. High Volt Eng. 2012;38(2):322–7.
18. Lan Z. Type selection and technical conditions for 1000 kV UHV outdoor AC switch-disconnecto. Electr Equip. 2005;6(5):17–20.
19. Wan Q, Wu W, Wu X. Summary of manufacturing capability of UHV AC power transmission and transformation equipment abroad. Electr Equip. 2005;6(9):33–5.
20. Sun Y, Zhang D, Meng W, Wei J. Research and development of 1100 kV GIS. Electr Power Constr. 2007;28(4):1–6.
21. Guo Y, Cui B, Wang C, Sun G. Development and implementation of gas-insulated metal-enclosed switchgear with breaking capability of 63 kA for 1100 kV AC power transmission project. Power Syst Technol. 2011;35(12):20–5.
22. Lin J, Chen W, Han B, Ban L, Xiang Z. Failure rate calculation and necessity discussion on opening-resistor of ultra high voltage circuit breakers. Proc CSEE. 2012;32(7):161–6.
23. Xia W, Wang C, Xu S. Two technical solutions for UHV 1100 kV GIS. High Volt Appar. 2011;47(9):44–9.
24. Zeng Q. UHV power grid. Beijing: China Electric Power Press; 2010. p. 144.
25. Liu Z. UHV power grid. Beijing: China Economic Press; 2005. p. 402.
26. Zhao X. UHV transformer bushing of nanjing electric passed the appraisal. China Electr Equip Ind. 2007;12:1.
27. Gao F, Chen W, Liu Z, Yan X. Protection of series compensation station against lightning intruded wave in 1000 kV AC transmission system. High Volt Eng. 2010;36(9):2199–205.
28. Zhong S. Problems caused by adding series compensation devices to EHV transmission system and their solution. Power Syst Technol. 2004;28(6):26–30.

Chapter 12
UHV Power Frequency Electromagnetic Induction

Baoju Li, Jidong Shi and Yijing Su

Due to the high operating voltage and large working current, the 1000 kV UHVAC transmission line often generates the relatively serious electromagnetic induction problem to the adjacent AC and DC transmission lines, which includes mainly the following two aspects.

First of all, it is the influence on the other AC transmission lines and overhead ground wires. For example, the 1000 kV UHVAC transmission line will have an influence on the 1000, 500, and 220 kV AC transmission lines erected on the same tower. Since the electrostatic and electromagnetic coupling exists between the circuits, the UHVAC circuit will generate relatively serious induced voltage and current in other adjacent circuits subject to interruption maintenance. The analysis on the induced voltage and current generated by the operating circuit on the circuit subject to interruption maintenance and ground wire is quite important to the repair and maintenance of the 1000 kV double-circuit line on the same tower, and directly concerns the proper selection of the parameters of such line equipment as the earth isolator and the proper establishment of the safety measures for the maintenance of the line subject to power interruption. In addition, the UHV transmission line generates high induced voltage and induced current on the ground wire through the electromagnetic and electrostatic coupling, and hence, it is necessary to conduct

B. Li (✉)
Jilin Power Dispatching Center, Changchun, Jilin, People's Republic of China
e-mail: 385569768@qq.com

J. Shi
State Grid Jiangsu Maintenance Branch Company, Nanjing,
Jiangsu, People's Republic of China
e-mail: 838380475@qq.com

Y. Su
College of Electrical Engineering, Zhejiang University,
Xihu District, Hangzhou, Zhejiang, People's Republic of China
e-mail: 1164582214@qq.com

© Zhejiang University Press, Hangzhou and Springer-Verlag GmbH Germany 2018

H. Zhou et al. (eds.), *Ultra-high Voltage AC/DC Power Transmission*,
Advanced Topics in Science and Technology in China,
https://doi.org/10.1007/978-3-662-54575-1_12

analysis on the influences of the different grounding methods for the overhead insulated ground wire and optical fiber composite overhead ground wire (OPGW) on the induced voltage, induced current, and ground wire energy consumption.

Second, the UHVAC transmission line also generates electromagnetic induction to the adjacent UHVDC transmission line erected in parallel with it, and generates the power frequency induced voltage and current in the DC transmission line. The power frequency current enters the converter stations at both ends through the DC transmission line, and generates DC biasing current at the valve side of the converter transformer under the effect of the converter. After the DC biasing current enters the converter transformer, it will influence the magnetization curve of the transformer core and make the transformer operate under the DC biasing condition, leading to the increase in the loss, temperature rise, and noise of the transformer, or even affecting the service life thereof.

This chapter first calculates the induced voltage and current in the out-of-operation circuit of the 1000 kV double-circuit line on the same tower under the condition that one circuit is in operation and the other is out of operation for maintenance, then analyzes the influences of the different grounding methods for the overhead insulated ground wire and optical fiber composite overhead ground wire (OPGW) adopted for the 1000 kV AC transmission line on the induced voltage, induced current, and energy consumption in the ground wires, and finally discusses the power frequency electromagnetic influences (especially the influences of DC bias on main converter transformer) of the UHVAC transmission line on the UHVDC line erected in parallel with it.

12.1 Induced Voltage and Current of the 1000 kV Double-Circuit Line on the Same Tower

12.1.1 Generation Mechanism and Four Different Induction Parameters

For the double-circuit line on the same tower, when one circuit is in operation, while the other is out of operation, since the electrostatic and electromagnetic coupling exists between the circuits, the induced voltage and current will be generated on the out-of-operation line. For the double-circuit line on the same tower with voltage level of 1000 kV, the induced voltage can reach up to tens of kV or even nearly a 100 kV. Furthermore, the operating transmission line can also generate high induced voltage and current on the ground wires through the electrostatic coupling and electromagnetic induction.

Due to the existence of the capacitance between the double-circuit lines and the maintenance circuit-to-ground capacitance, the operating line will generate electrostatic induction parameters on the out-of-operation line through the electrostatic induction: electrostatic induced voltage and electrostatic induced current. Since the mutual inductance exists between the double-circuit lines, the operating line will also

generate electromagnetic induction parameters on the out-of-operation line through electromagnetic induction: electromagnetic induced voltage and electromagnetic induced current.

There are totally four different induction parameters on the out-of-operation line: electromagnetic induced voltage, electromagnetic induced current, electrostatic induced voltage, and electrostatic induced current, which, respectively, represent the quantities of induction on the out-of-operation line under different conditions, specifically as shown below [1]:

1. Electromagnetic induced current is the circulating current caused by the potential induced by the live operating line on the out-of-operation line when the grounding switches at both ends of the out-of-operation line are grounded.
2. Electromagnetic induced voltage is the voltage induced by the live operating line on the out-of-operation line when the grounding switch at one end of the out-of-operation line is grounded and the grounding switch at the other end thereof is not grounded.
3. Electrostatic induced current is the grounding capacitive current generated by the live operating line on the out-of-operation line through the capacitive coupling when the grounding switch at one end of the out-of-operation line is grounded and the grounding switch at the other end thereof is not grounded.
4. Electrostatic induced voltage is the capacitive voltage generated by the live operating line on the out-of-operation line through the capacitive coupling when the grounding switches at both ends of the out-of-operation line are not grounded.

Based on the above four quantities of state of the out-of-operation line and grounding switches, the induced voltage and induced current generated on the out-of-operation line can be calculated using the following equations:

1. Condition under which the grounding switches at both head and tail ends of the line are not grounded

The electrostatic induced voltage U_1 and U_2 at the head and tail ends are as follows:

$$U_1 = U_2 = \frac{C_{\mathrm{AA}'} + \left(-\frac{1}{2} j \frac{\sqrt{3}}{2}\right) C_{\mathrm{BA}'} + \left(-\frac{1}{2} + j \frac{\sqrt{3}}{2}\right) C_{\mathrm{CA}'}}{C + C_{\mathrm{AA}'} + C_{\mathrm{BA}'} + C_{\mathrm{CA}'}} \times U_{\mathrm{A}} \tag{12.1}$$

where

$C_{\mathrm{AA}'}$, $C_{\mathrm{BA}'}$, and $C_{\mathrm{CA}'}$ respectively, the capacitances between phases A, B, and C of the operating line and phase A′ of the maintenance line;
C_0 the capacitance of phase A′ of the maintenance line to ground;
U_{A} the voltage of phase A of the operating line.

When both ends of the maintenance line are not grounded, the electrostatic induction component of the induced voltage plays a dominant role, and its magnitude is proportional to the voltage level of the transmission line, but is not quite related to the line length and transmission power.

2. Condition under which only one end of the line is grounded

The condition under which the head end of the line is not grounded and the grounding switch at the tail end thereof is grounded is hereby taken as an example. The electromagnetic induced voltage U_1 at the head end and the electrostatic induced current I_2 at the tail end are, respectively, as follows:

$$U_1 = \omega \times l \times \left[M_{AA'} + \left(-\frac{1}{2} - j\frac{\sqrt{3}}{2}\right)M_{BA'} + \left(-\frac{1}{2} + j\frac{\sqrt{3}}{2}\right)M_{CA'}\right] \times I_A \tag{12.2}$$

$$I_2 = \omega \times l \times \left[C_{AA'} + \left(-\frac{1}{2} - j\frac{\sqrt{3}}{2}\right)C_{BA'} + \left(-\frac{1}{2} + j\frac{\sqrt{3}}{2}\right)C_{CA'}\right] \times U_A \tag{12.3}$$

where

I_2	the electrostatic induced current of the grounding switch at the tail end of the maintenance line;
$M_{AA'}$, $M_{BA'}$, and $M_{CA'}$	respectively, the mutual inductance between phases A, B, and C of the operating line and phase A′ of the maintenance line;
l	is the length of the double-circuit line on the same tower;
I_A	the current of phase A of the operating line.

When the head end of the line is not grounded and the tail end thereof is grounded, the electromagnetic induction component of the induced voltage at the head end plays a dominant role, and its magnitude is proportional to the line length and transmission power; the electrostatic induction component of the induced current at the tail end plays a leading role, and its magnitude is proportional to the line length, but has nothing to do with the transmission power.

3. Condition under which the grounding switches at both head and tail ends of the line are grounded

The electromagnetic induced currents I_1 and I_2 at the head and tail ends are, respectively, as follows:

$$I_1 = I_2 = \left[M_{AA'} + \left(\frac{1}{2} - j\frac{\sqrt{3}}{2}\right)M_{BA'} + \left(-\frac{1}{2} + j\frac{\sqrt{3}}{2}\right)M_{CA'}\right] \times I_A/L \tag{12.4}$$

where

I_1 and I_2	respectively, the induced current of the grounding switches at the head and tail ends of the maintenance line;
L	the self-inductance of phase A′ of the maintenance line.

When both ends of the maintenance line are grounded, the electromagnetic induction component of the induced current plays a dominant role, and its magnitude is proportional to the transmission power of the line, but has nothing to do with the line length.

In this section, the transmission line section from Huainan to South Anhui of the Huainan–South Anhui–North Zhejiang–West Shanghai 1000 kV UHVAC same-tower double-circuit line transmission project is taken as an example to carry out the simulation analysis on the induced voltage and current. Under the operating condition that the line operates stably and is not subject to any type of overvoltage, the induced voltage and induced current generated by the operating circuit on the maintenance circuit and overhead ground wire when one circuit of the line is out of operation for maintenance are calculated through the simulation by the EMTP software, and the discussion and analysis are conducted on the influence factors such as the length of transmission line, magnitude of transmission power, and transposition or not.

12.1.2 Simulation Calculation of Induced Voltage and Current

To save the line corridor and improve the transmission capacity of unit corridor width, it is planned by State Grid Corporation to construct the Huainan–South Anhui–North Zhejiang–West Shanghai 1000 kV AC Same-tower Double-circuit Line Transmission Project in the east China grid in 2010. It is the second 1000 kV UHVAC transmission project in China, and also the first 1000 kV AC same-tower double-circuit line transmission project in China.

1. System overview and line parameters

The total length of the Huainan–South Anhui–North Zhejiang–West Shanghai 1000 kV AC Same-tower Double-circuit Line Transmission Project is 642.5 km, of which the length of line from Huainan to South Anhui is 326.5 km, and the maximum transmission capacity is 10,000 MW for the long-term planning. 4 × 720 MVA high-voltage shunt reactors are configured at both sides of the double lines from Huainan to South Anhui totally, the reactance value of the neutral point is taken as 700 Ω, the system parameters are as shown in Table 12.1, and the system sketch is as shown in Fig. 12.1.

Table 12.1 System parameters of Huainan to South Anhui power transmission line

Length of line (km)	Transmission capacity (MW)	Capacity of high-voltage shunt reactor (MVA)		Small reactance at neutral point of high-voltage shunt reactor (Ω)
		Huainan	South Anhui	
326.5	10,000 (long-term planning)	2 × 720	2 × 720	700

Fig. 12.1 Configuration of HV shunt reactors in Huainan to South Anhui power transmission line

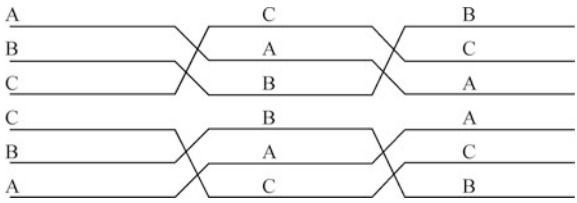

Fig. 12.2 Full transposition in reverse direction

The 8× LGJ-630/45 aluminum conductors steel reinforced (ACSR) is adopted for the Huainan–South Anhui–North Zhejiang–West Shanghai UHV Same-tower Double-circuit Line Transmission Project. One ground wire is the LBGJ-240-20AC concentric-lay-stranded aluminum-clad steel conductors, which is sectionalized and grounded at one point; the other ground wire is the OPGW-24B1-254 optical fiber composite overhead ground wire, which is grounded continuously at multiple points. The conductors used in Huainan–South Anhui Line are arranged in reverse phase sequence and transposed fully twice, as shown in Fig. 12.2. The model of the double-circuit line on the same tower is shown as in Fig. 12.3.

2. Simulation calculation results of induced voltage and current

For the Huainan–South Anhui Line Section (twice full transposition along the whole line), the same-tower double-circuit line, when one circuit is out of operation and the other is in normal operation, due to the different grounding statuses, different induced voltage, and current will be generated. When both sides of the out-of-operation line are grounded, the induced current (electromagnetic induced current) at the grounding points is as shown in Table 12.2; when one end of the out-of-operation line is grounded (grounded at the Huainan side), the induced voltage (electromagnetic induced voltage) at the South Anhui and the induced current (electrostatic coupled current) at the grounding point are as shown in Table 12.3; when both ends of the out-of-operation line are not grounded, the induced voltage (electrostatic coupled voltage) is as shown in Table 12.4 [2].

It is noteworthy that, in the simulation, the grounding resistances at both ends of the out-of-operation line have large influence on the simulation results. The grounding resistance of 10 and 1 Ω can lead to the results with large difference. In consideration that the grounding resistance in the UHV substation is normally very small (0.1–1 Ω), the grounding resistance is taken as 0.5 Ω in the simulation in this section.

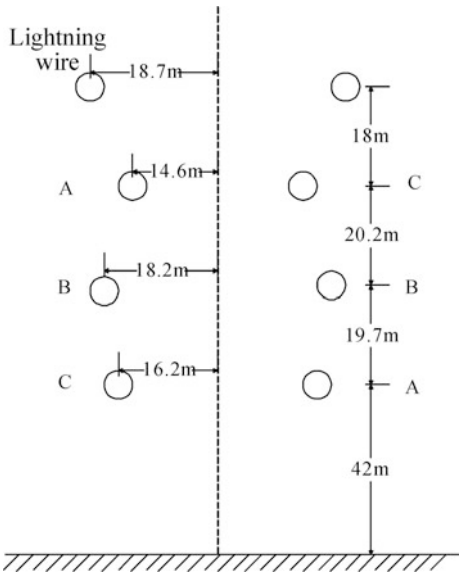

Fig. 12.3 Model of double-circuit line on the same tower

Table 12.2 Electromagnetic induced current on the out-of-operation line of Huainan–South Anhui Transmission Line when one circuit is out of operation and the other is in normal operation

Transmission capacity (MW)	Induced current (A)
5000	197
10,000	383

Table 12.3 Electromagnetic induced voltage and electrostatic coupled current on the out-of-operation line of Huainan–South Anhui transmission line

Transmission capacity (MW)	Electromagnetic induced voltage (kV)	Electrostatic coupled current (A)
5000	17.2	42.9
10,000	34.1	49.5

Table 12.4 Electrostatic coupled voltage on the out-of-operation line of Huainan–South Anhui transmission line

Transmission capacity (MW)	Electrostatic coupled voltage (kV)
5000	27.9
10,000	32.9

In addition, the transposition mode of the line will also have large influence on the results, and will cause serious asymmetry among the three phases. For example, under the condition that the transmission power of the Huainan–South Anhui Line Section is 5000 MW and no transposition is conducted along the whole line, the electrostatic coupled voltage is 90 kV, electromagnetic induced current is 530 A, electrostatic coupled current is 103 A, and electromagnetic induced voltage is 59 kV, all of which are far above the corresponding values given in Tables 12.2, 12.3 and 12.4 for the condition that the transmission power of the Huainan–South Anhui Line Section is 5000 MW and full transposition is conducted twice along the whole line.

12.1.3 Analysis on Influence Factors of Induced Voltage and Induced Current

The main factors that influence the induced current and voltage include the voltage of live line, load current, line length, phase-to-phase distance and circuit-to-circuit distance, compensation degree of HV shunt reactor of the out-of-operation line, height of conductor, transposition of line, and overhead ground wire, etc. [5, 6]. The main characteristics of the four induced electricity quantity are as follows:

1. Electromagnetic induced current: its magnitude is related to the magnitude of current of the live circuit, which is essentially in a proportional relation, but almost has nothing to do with the line length.
2. Electromagnetic induced voltage: its magnitude is related to the magnitude of current of the live operating circuit and the length of the line erected on the same tower, which is essentially in a proportional relation.
3. Electrostatic induced current: its magnitude is related to the voltage of the live circuit and the length of the line erected on the same tower, which is essentially in a proportional relation, but is not quite related to the power transmitted by the live operating circuit.
4. Electrostatic induced voltage: its magnitude is related to the voltage of the live circuit and the ratio of the phase-to-phase capacitance to the capacitance of out-of-operation circuit to ground, and is not quite related to the power transmitted by the live operating circuit and the line length.
5. HV shunt reactor: the HV reactor has very large influence on the electrostatic coupled voltage and very small influence on the electrostatic coupled current and electromagnetic induced voltage and current. When the double-circuit line on the same pole is installed with HV reactor, due to the compensation by the shunt reactor, the capacitance to ground will be reduced, the electrostatic induction generated by the operating line on the maintenance line will increase significantly, leading to the significant increase in the electrostatic coupled voltage.

12.2 Induced Voltage and Induced Current on Overhead Ground Wires of 1000 kV AC Transmission Line

For the UHV transmission line (no matter for single-circuit line or double-circuit line), since the overhead ground wires are not symmetrical to the conductors of the transmission circuit in the aspect of the spatial location, the transmission circuit will generate induced voltage and induced current on the overhead ground wires through electromagnetic and electrostatic coupling.

Normally, one of the overhead ground wires of the 1000 kV UHV transmission line is of the overhead insulated ground wire, and the other is of the optical fiber composite overhead ground wire (OPGW). The induced voltage and current on the ground wires are related to the grounding modes of the overhead ground wire. The mode of grounding at each tower is adopted for the optical fiber composite overhead ground wire, which generates high induced current on the composite ground wire; the graded insulation mode is adopted for the overhead insulated ground wire, that is, the overhead insulated ground wire is normally single-point grounded at a tower in the middle of the strain section while insulated with other towers, and this can generate high induced voltage at both ends of the overhead insulated ground wire in this section. The calculation of the induced current on OPGW is the key to evaluate the loss of electric energy in the ground wire, while the calculation of the induced voltage on the overhead insulated ground wire under the normal condition and failure condition is the basis to determine the insulation gap, being of vital importance to the implementation of the insulation technology for ground wires.

According to the theory of electromagnetic field, in the space, mutual inductance and distributed capacitance between the conductors exist between the parallel conductors, and the phase conductors and insulated ground wires of the line are such a parallel conductor system. Due to the existence of the mutual inductance, the phase conductor with current flowing through it can generate electromagnetic induced voltage on the insulated ground wire in parallel with it; meanwhile, due to the existence of the distributed capacitance between the conductors, the phase conductor can also generate electrostatic induced voltage on the insulated ground wires through the capacitance. However, since the insulated ground wire is grounded at one point, the electrostatic induced voltage can be neglected, and what needs to be considered mainly is the electromagnetic induced voltage.

For a section of insulated ground wire, three-phase conductors and ground wire itself are arranged with no transposition in a short range, so the coupled inductance between ground wire and each phase conductor for the single-circuit line is as shown in the following equation:

$$Z_{\mathrm{mn}} = 0.05 + j0.145 \lg \frac{D_0}{d_{\mathrm{mn}}} \tag{12.5}$$

where

d_{mn} the distance between ground wire and each phase conductor, m;

D_0 equivalent depth of current in the earth, m, whose value is determined by current frequency and soil resistivity.

The electromagnetic induced voltage on the ground wire is determined by load current and coupled inductance together. Therefore, the length of the insulated section of the ground, arrangement location of the conductor and ground wire, load current, and soil resistivity, etc., all have influence on the induced voltage on the insulated ground wire, and these factors shall be taken into consideration during the simulation calculation [7].

According to the electromagnetic field theory, in the space, the conductor with current flowing through it can generate the induced current in the conductor circuit close to it which forms a closed loop. As for the OPGW for which the mode of grounding at each tower is adopted, it forms a closed loop of ground wire-tower-ground-tower-ground wire together with the tower and ground in the vicinity of the phase conductor; when current flows through the phase conductor, the induced current will be generated in the said loop. If the tower resistance and grounding resistance are neglected, the circulating current I_g on the ground wire will be as shown in the following equation:

$$I_g = -\frac{Z_{gA}I_A + Z_{gB}I_B + Z_{gC}I_C}{Z_{gg}} \tag{12.6}$$

where

I_A, I_B, and I_C respectively, the phase current of phases A, B, and C;
Z_{gA}, Z_{gB}, and Z_{gC} respectively, the mutual impedance of conductors of phases A, B, and C to the ground wire;
Z_{gg} the self-impedance of the ground wire.

Since the distance between each phase conductor and the ground wire is different, the mutual impedance of each phase conductor to the ground wire is not completely equal. Even if the current of the three phases in the phase conductor is symmetrical, I_g will not be zero, and the circulating current is thus formed among the ground wire, tower, and ground.

The mode of grounding at each tower is adopted for OPGW, and this can generate circulating current in the loop of ground wire-tower-ground. It is assumed that, under the ideal conditions, all the tower resistances and tower grounding resistances are equal and the mutual impedance values between phase conductors and ground wires along the whole line are constant; when the line is in normal operation, it can be regarded that the phase current in each span keeps unchanged, and since the OPGW is grounded at each tower, the adjacent circulating current in the line will be mutually offset on the common tower, which is equivalent to that the current flowing through the tower resistance and tower grounding resistance approximates to zero, that is, except for the first and last spans of the line section, the circulating current in other spans can be calculated by Eq. (12.6).

The electric energy loss of the UHV transmission line on the ground wire can be estimated approximately as follows (the electric energy loss is mainly concentrated on OPGW, and the energy consumption on the tower and grounding resistance is small):

$$W_g = I_g^2 R_g \tag{12.7}$$

where

R_g the resistance of unit length of OPGW, in Ω/km.

By combining the parameters sourced from China's first UHV single-circuit transmission line-Southeast Shanxi–Nanyang–Jingmen UHVAC Transmission Project and the first UHV Double-circuit Transmission Line on the same tower-Huainan–South Anhui–North Zhejiang–West Shanghai UHVAC Same-Tower Double-Circuit Line Transmission Project, this section carries out simulation calculation of the induced voltage and induced current on the overhead ground wire under different operating conditions, and conducts calculation, and analysis on the influence factors thereof. The software used for simulation calculation is the electromagnetic transient program (EMTP).

12.2.1 Induced Voltage and Induced Current on Overhead Ground Wires of the UHV Single-Circuit Line

The transmission capacity of the 1000 kV Southeast Shanxi–Nanyang–Jingmen single-circuit transmission line is 5000 MW, and the type of tower adopted is as shown in Fig. 12.4. One of the overhead ground wires is the overhead insulated ground wire, and the other is the optical fiber composite ground wire. Under the condition of normal power of 5000 MW being transmitted, the EMTP simulation is conducted on the induced voltage and induced current on the overhead ground wires of the said line in terms of different sectional lengths of different overhead insulated ground wires. There are two modes for the single-point grounding of the overhead insulated ground wire: mode of grounding at the middle of the strain section or mode of grounding at either end of the strain section.

In the simulation, the overhead insulated ground wire of the strain section is sectioned as 3, 5 and 7 km. The overhead insulated ground wire can be grounded in two modes, i.e., grounded at the middle of the strain section and grounded at either end of the strain section. The calculation results thereof are as shown in Tables 12.5 and 12.6.

As can be seen from the simulation results, during the normal operation, the induced voltage on the insulated ground wire of the 1000 kV UHVAC single-circuit transmission line can reach hundreds of volts, and the induced voltage increases as the sectional length of the insulated ground wire increases. The induced current on the composite ground wire can reach over a hundred of ampere.

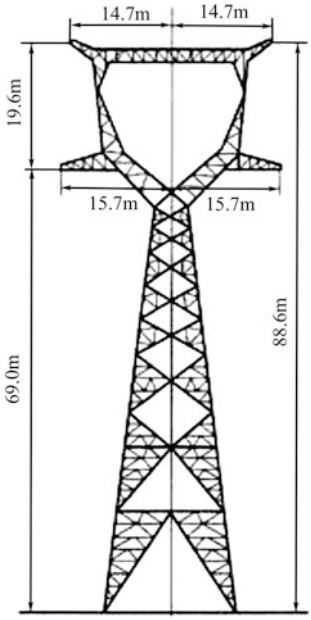

Fig. 12.4 Tower type of 1000 kV UHVAC single-circuit transmission line

Table 12.5 Induced voltage on insulated ground wire of UHV single-circuit line (during normal operation)/V

Sectional length (km)	Transmission load of line 5000 MW	
	Grounded at the middle	Grounded at either end
3	194	367
5	290	586
7	396	798

Table 12.6 Induced current on composite ground wire of UHV single-circuit line (during normal operation)

Transmission load of line (MW)	5000
Induced current (A)	127

In case of the occurrence of the single-phase grounding short-circuit fault, the EMTP simulation is conducted to the induced voltage on the line's overhead insulated ground wire with different short-circuit currents and different sectional lengths. The results therefrom are as shown in Table 12.7.

As can be seen from the simulation results, in case of the short-circuit fault, the induced voltage on the insulated ground wire of the 1000 kV UHVAC

Table 12.7 Induced voltage on insulated ground wire of UHV single-circuit line (in case of short-circuit failure)/kV

Sectional length (km)	Short-circuit current					
	10 kA		30 kA		50 kA	
	Grounded at the middle	Grounded at either end	Grounded at the middle	Grounded at either end	Grounded at the middle	Grounded at either end
3	5.0	10.0	15.6	31.1	25.8	52.7
5	7.6	15.3	23.6	47.3	40.2	80.6
7	9.8	19.5	30.7	61.5	50.2	100.0

single-circuit transmission line can reach tens of kilovolts, and the induced voltage increases as the sectional length of the insulated ground wire increases.

In addition, the induced voltage generated on the overhead insulated ground wire which is grounded at either end of the strain section is exactly twice over that generated on the overhead insulated ground wire which is grounded at the middle of the strain section. The former is much higher than the latter, because the distance of the grounding end to the insulated end of the former is exactly twice over that of the latter. In the actual projects, in case of the short strain section (for example, the length of the strain section is 3–5 km), the mode of directly grounding at either end of the strain section may be considered; in case of the long strain section (for example, the length of the strain section is 5–7 km or longer), the mode of grounding at the middle of the strain section may be considered.

12.2.2 Induced Voltage and Induced Current on Overhead Ground Wires of the UHV Double-Circuit Line on the Same Tower

For the system overview and line parameters of the UHV double-circuit line on the same tower, please refer to Sect. 12.1.2. The tower model of the double-circuit line on the same tower is as shown in Fig. 12.5.

When the double-circuit conductors are arranged in the same phase sequence or reverse phase sequence, the calculation results of the induced current on the composite ground wire and the induced voltage on the insulated ground wire are as shown in Tables 12.8 and 12.9 [3].

It is obvious that, in case of the arrangement in reverse phase sequence, the induced voltage and induced current on the overhead ground wires of the UHV double-circuit line are significantly lower than those in case of the arrangement in the same phase sequence.

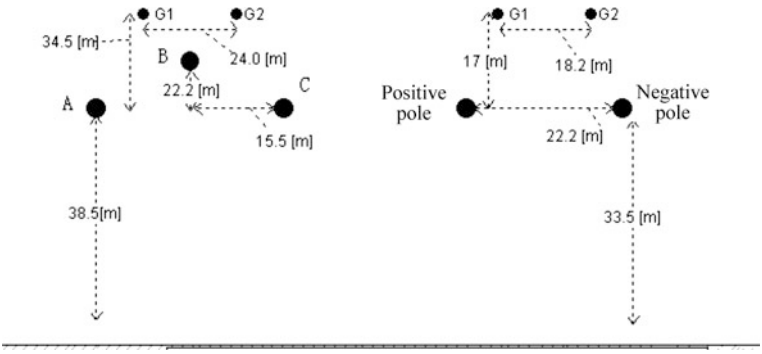

Fig. 12.5 Tower arrangement for UHVAC/DC lines erected in parallel

Table 12.8 Induced voltage on insulated ground wire of 1000 kV UHVAC double-circuit line (effective value)/V

Sectional length (km)	Transmission load of line 2 × 5000 MW	
	Reverse phase sequence	Same phase sequence
3	157	237
5	262	387
7	366	537

Table 12.9 Induced current on composite ground wire of 1000 kV UHVAC double-circuit line (effective value)

Transmission capacity of line (MW)	2 × 5000	
	Reverse phase sequence	Same phase sequence
Induced current (A)	67	205

12.2.3 Selection of Insulation Gap and Withstand Voltage of the UHV Overhead Insulated Conductors

The induced voltage on the overhead insulated ground wire is the main basis for selecting the insulation gap and withstand voltage of the overhead insulated conductors. In general, it needs to meet the two requirements: during the normal operation, the insulation to the towers shall be kept to reduce the electric energy loss; in case of the short circuit, the insulation gap needs to be broken down to release the short-circuit current as soon as possible. During the normal operation, the induced voltage on the overhead insulated conductors is normally hundreds of volts, and hence, the withstand voltage of the insulation gap shall usually exceed 1 kV at least; in case of the short circuit, the induced voltage on the overhead

insulated conductors is normally tens of kilovolts, and hence, the withstand voltage of the insulation gap generally does not exceed 20 kV. At present, for the 330 and 500 kV EHV transmission lines in China, the mode of the graded insulation of the ordinary ground wires and the OPGW grounding at each tower is adopted, the insulation gap is taken as 10–20 mm, and the power frequency discharge voltage of the ground wire insulators corresponding to the gap distance of 20 mm is 8–30 kV. The insulation gap of the ground wires adopted for the 1000 kV UHV transmission lines in China is normally about 18 mm.

12.3 Power Frequency Electromagnetic Induction Influence of the AC Line on the UHVDC Line Erected in Parallel with It

As the scale of the power transmission network is expanded unceasingly, the power transmission line corridor resource is becoming increasingly short. The erection of the AC transmission line in parallel with the UHVDC transmission line can improve the utilization rate of the corridors.

The AC transmission line, through the electromagnetic coupling, generates the power frequency induced voltage and current on the UHVDC transmission line erected in parallel with it. When the power frequency current enters the converter stations at both ends through the DC transmission line, it will generate the DC biasing current at the valve side of the converter transformer under the effect of the converter. After the DC biasing current enters the converter transformer, it will influence the magnetization curve of the transformer core, making the magnetization curve offset from the zero coordinate axis. If the transformer is operating in the DC biasing condition, it will cause the increase in the loss, temperature rise, and noise of the transformer, or even cause influence to the service life.

Based on the parameters of the ±800 kV UHVDC line from Yunnan to Guangdong, the simulation model for the AC/DC transmission system is established [8]. In case the single-phase grounding failure occurs to the AC line, in terms of the various cases, such as different parallel erection lengths of AC and DC lines, different spacings between AC and DC lines (the spacing refers to the distance between the centerlines of the AC and DC transmission line towers), different soil resistivity, and different modes of transposition of AC and DC lines, the simulation calculation is carried out to the induced voltage and current on the UHVDC line and the DC biasing current at the valve side of the converter transformer. Moreover, the comparative analysis is also conducted on the electromagnetic influences of the single-circuit and the same-tower double-circuit EHV/UHVAC lines on the UHVDC line erected in parallel.

12.3.1 Power Frequency Electromagnetic Induction by the UHVAC Line to the UHVDC Line Erected in Parallel with It

1. System overview and line parameters

With the parallel erection of the 1000 kV UHVAC transmission line and the ±800 kV Yunnan–Guangdong UHVDC transmission line taken as an example, the analysis is conducted on the power frequency electromagnetic induction influence of the UHVAC line on the UHVDC line erected in parallel with it. The total length of the Yunnan–Guangdong UHVDC line is 1446 km, and the bipolar transmission power is 5000 MW. The parameters of the AC/DC lines and the arrangement of the towers are as shown in Tables 12.10 and 12.11 and Fig. 12.5.

2. Simulation calculation of the UHVAC/DC lines erected in parallel

The DC voltage and current waveforms at the rectifier side and the inverter side of the UHVDC line erected separately are as shown in Fig. 12.6. The DC voltage and current waveforms at the rectifier side and the inverter side of the UHVDC line erected in parallel with the UHVAC line (the parallel erection length is 100 km and the spacing between each other is 50 m) are as shown in Fig. 12.7. The DC biasing current waveforms when the UHVAC/DC lines are erected in parallel are as shown in Fig. 12.8.

Through the comparison of Figs. 12.6, 12.7 and 12.8, it can be seen that, when the AC/DC lines are erected in parallel, the power frequency components of voltage and current on the UHVDC line are increased significantly. The UHVAC line induces stable power frequency voltage and current on the UHVDC line erected in parallel with it. A significant DC biasing current is generated at the valve side of the converter transformer of the UHVDC line [4].

Table 12.10 Parameters of conductors and ground wires of ±800 kV DC line

Name	Line	Ground wire
Model of conductor	6× LGJ-630/45	LBGJ-180-20AC
Outer diameter of conductor (cm)	3.36	1.75
DC resistance/(Ω/km)	0.04633	0.7098
Bundled conductor spacing (cm)	45.0	–

Table 12.11 Parameters of conductors and ground wires of 1000 kV AC Line

Name	Line	Ground wire
Model of conductor	8× LGJ-500/45	LBGJ-150/20
Outer diameter of conductor (cm)	3.00	1.58
DC resistance/(Ω/km)	0.059	0.582
Bundled conductor spacing (cm)	40.0	–

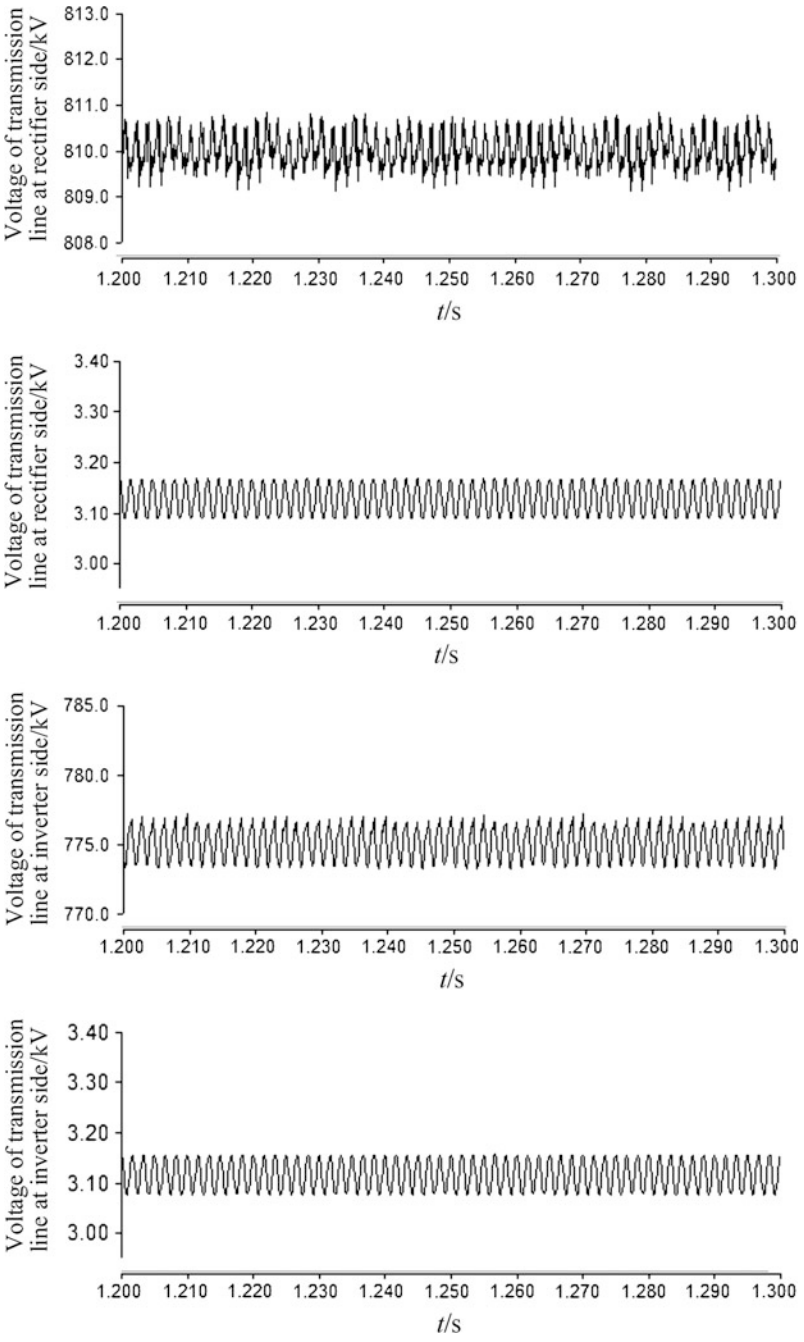

Fig. 12.6 Operating voltage and current of UHVDC line erected separately

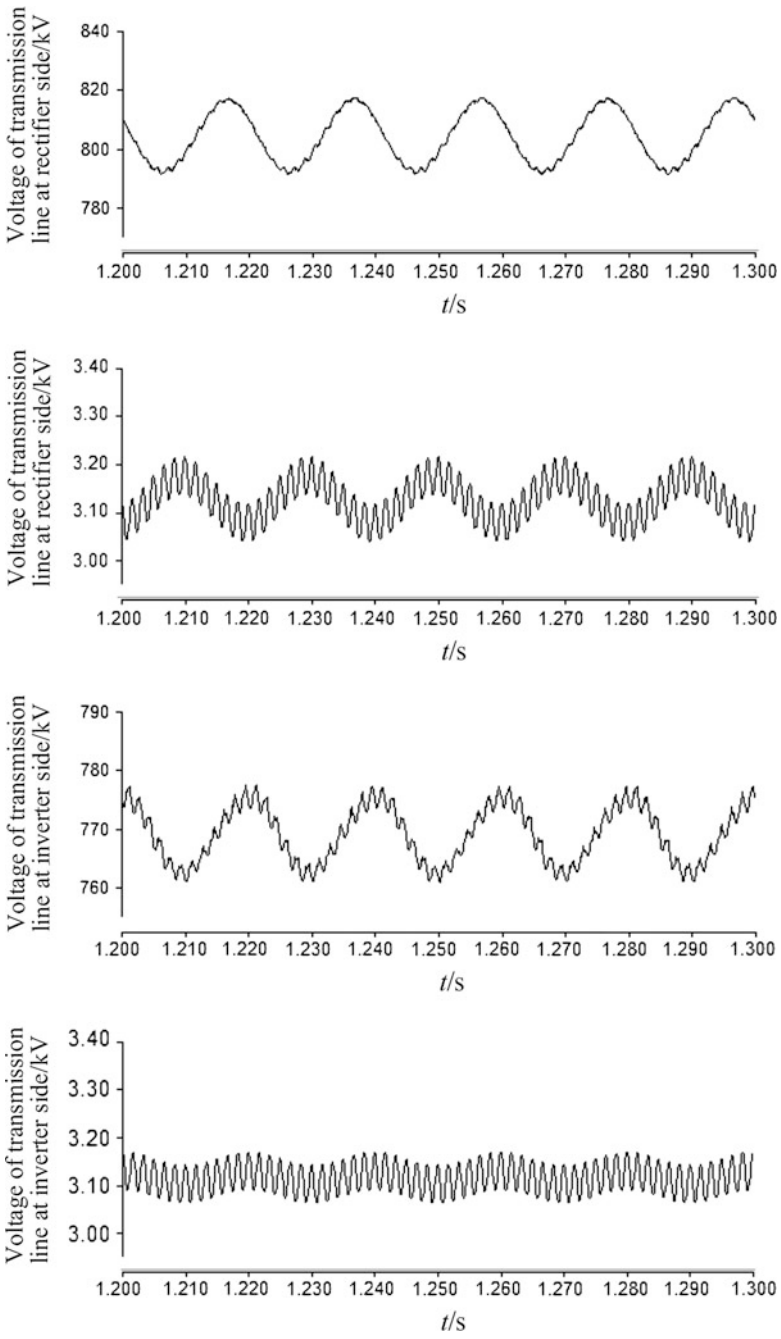

Fig. 12.7 Voltage and current of UHVDC line erected in parallel with UHVAC line

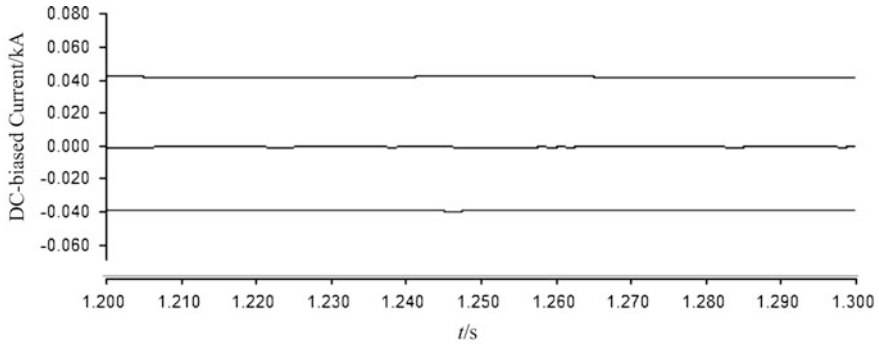

(a) Waveform at rectifier side

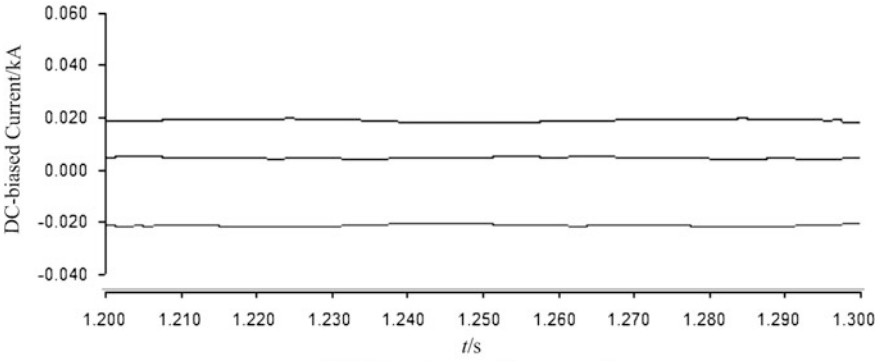

(b) Waveform at inverter side

Fig. 12.8 DC biasing current waveform when UHVAC/DC lines are erected in parallel

12.3.2 Influence Factors of the Electromagnetic Induction by the AC Line to the DC Line Erected in Parallel with It

1. Parallel erection length of and spacing between AC/DC lines

Under the different parallel erection lengths and different spacings, the induced power frequency voltage and current on the UHVDC line are as shown in Figs. 12.9 and 12.10.

As can be seen from Figs. 12.9 and 12.10, the power frequency induced voltage and current are in an approximately linear incremental relationship with the parallel erection length of the AC/DC lines, while in a very obvious non-linear relationship with the spacing between the AC/DC lines. When the spacing between AC/DC lines is small (less than 80 m), the power frequency induced voltage and current increase rapidly in a non-linear manner as the spacing between the AC/DC lines reduces; when the spacing between the AC/DC lines is large (greater than 80 m),

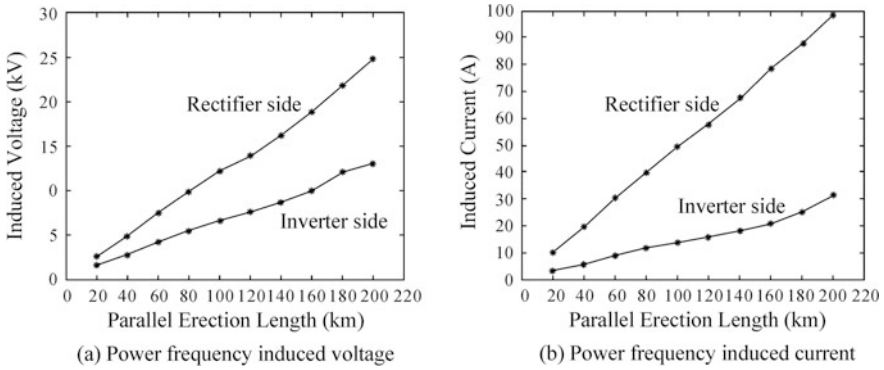

Fig. 12.9 Electromagnetic coupling influence under different parallel erection lengths

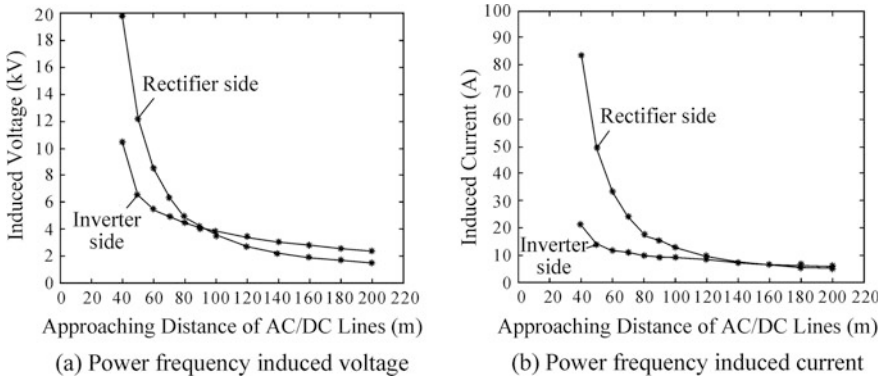

Fig. 12.10 Electromagnetic coupling influence under different spacings

the attenuation amplitude of the power frequency induced component slows down obviously and tends to be stable gradually as the spacing increases.

The change of the DC biasing current at the valve side of the converter transformers in the rectifier station and inverter station with the parallel erection length of and spacing between the AC/DC lines are as shown in Figs. 12.11 and 12.12. As can be known from Figs. 12.11 and 12.12, the DC biasing current at the valve side of the converter transformers in the rectifier station and inverter station is in an approximately linear incremental relationship with the parallel erection length of the AC/DC lines, while in a very obvious non-linear relationship with the spacing between the AC/DC lines. When the spacing between the AC/DC lines is small (less than 80 m), the DC biasing current increases rapidly in a non-linear manner as the spacing between the AC/DC lines reduces; when the spacing between the AC/DC lines is large (greater than 80 m), the attenuation amplitude of the DC biasing current slows down obviously and tends to be stable gradually as the spacing increases.

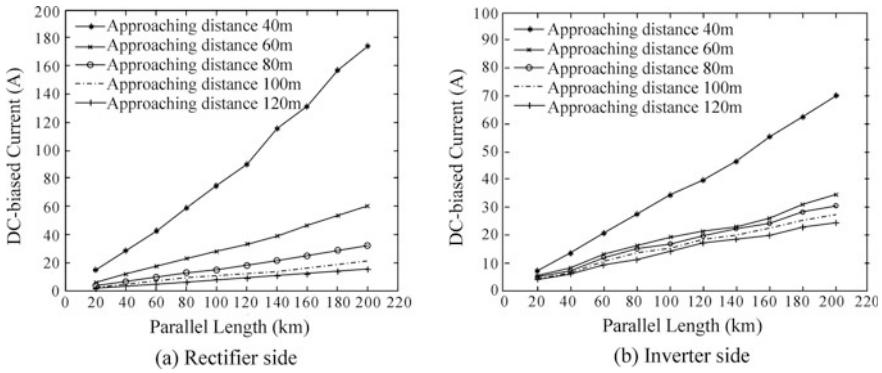

Fig. 12.11 DC biasing current under different parallel erection lengths

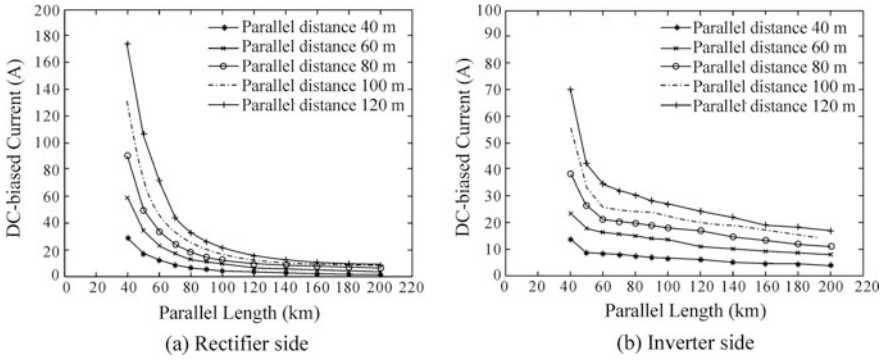

Fig. 12.12 DC biasing current under different spacings

According to the requirements in the standards, the DC biasing current withstood for a long time at the valve side of the converter transformer shall not be higher than 30 A. To maintain the safe operation of the converter transformer, the DC biasing current at the valve side shall be controlled within 30 A as far as possible. Therefore, the parallel erection length of the AC/DC lines and the spacing between them will be restricted by the maximum DC biasing current withstood by the converter transformer.

2. Soil resistivity and tower grounding resistance

Figures 12.13 and 12.14 give the changes to the power frequency induced voltage and current as well as DC biasing current on the DC line under the different soil resistivity and tower grounding resistance.

As can be known from Figs. 12.13 to 12.14, the soil resistivity and tower grounding resistance of the parallel erection section of the AC and DC lines have very small influence on the power frequency induced voltage and current as well as DC biasing current of the DC line.

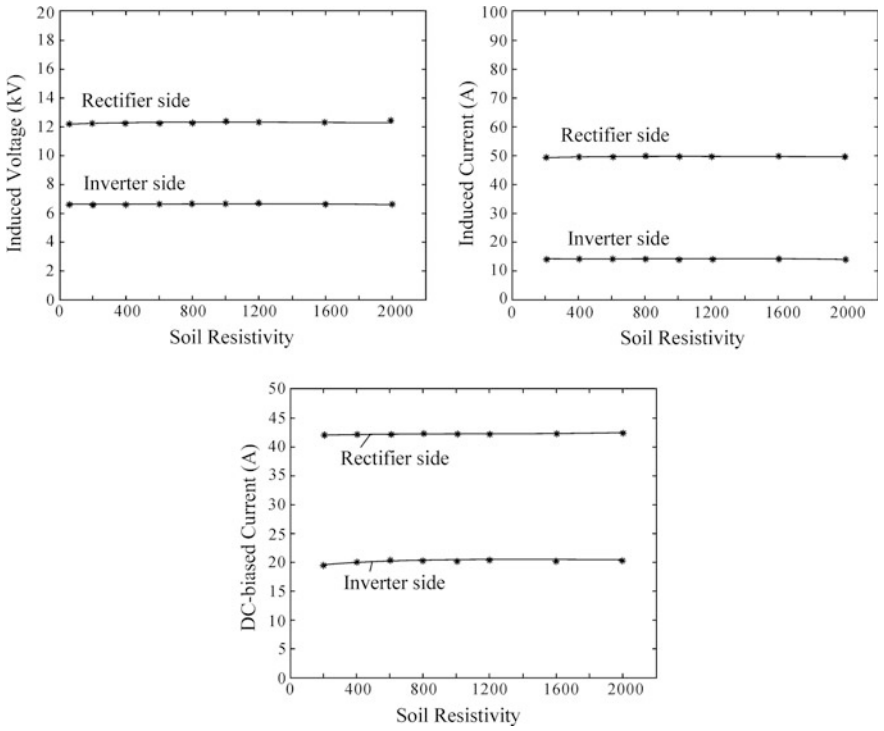

Fig. 12.13 Variation trend of power frequency induced voltage and current and DC biasing current on the DC line with the change of soil resistivity

3. Mode of transposition

Based on the three different modes of transposition for the parallel section of the UHVAC line, namely, without transposition, equal-interval transposition once, and equal-interval transposition twice, as shown in Fig. 12.15, the induced voltage and current on the UHVDC line erected in parallel with it and the DC biasing current at the valve side of the converter transformer are calculated and analyzed with the results, as shown in Table 12.12.

As can be seen from Table 12.12, when the AC line is transposed, the power frequency induced voltage and current on the DC line and the DC biasing current at the valve side of the converter transformer thereon are reduced significantly. When the AC line within the parallel section is fully transposed once (equal-distance transposed once), the induced voltage and current of the DC line and the DC biasing current at the valve side of the converter transformers at the rectifier side and inverter side of the DC line are reduced to about 50% of those under the case without transposition. When the AC line within the parallel section is fully transposed twice (equal-distance transposed twice), the induced voltage and current at

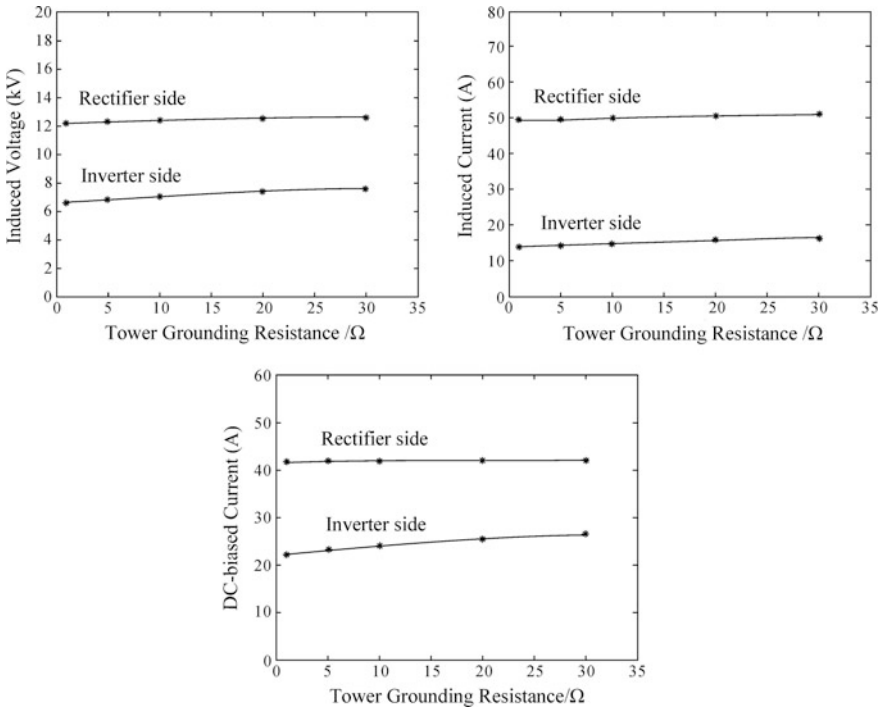

Fig. 12.14 Variation trend of power frequency induced voltage and current and DC biasing current on the DC line with the change of tower grounding resistance

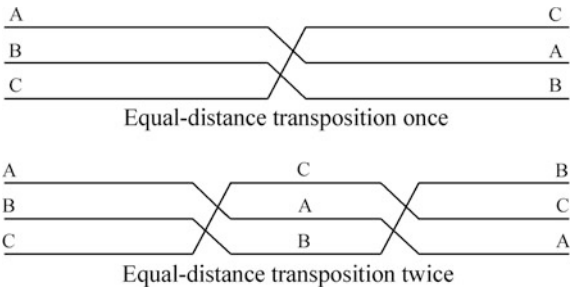

Fig. 12.15 Mode of transposition

the rectifier side of the DC line and the DC biasing current at the valve side of the converter transformer at the rectifier side are reduced to about 5% of those under the case without transposition, and the induced voltage and current at the inverter side and the DC biasing current at the valve side of the converter transformer at the inverter side are reduced to about 7% of those under the case without transposition. When the AC line within the parallel section is fully transposed twice, the induced voltage and current on the DC line and the DC biasing current of the converter transformer thereon are reduced significantly to a low level.

Table 12.12 Influence of transposition of the UHVAC line

Mode of transposition (length of transposed line/km)	Rectifier side			Inverter side		
	Induced voltage (kV)	Induced current (A)	DC biasing current (A)	Induced voltage (kV)	Induced current (A)	DC biasing current (A)
No transposition (100)	12.2	49.57	41.69	6.59	13.84	22.16
Equal-distance transposition once (50 + 50)	6.8	27.48	21.21	3.7	7.89	13.35
Equal-distance transposition twice (33.3 + 33.3 + 33.3)	0.64	2.57	1.97	0.44	0.97	1.92
No transposition (200)	25.29	95.75	82.48	14.89	27.79	48.31
Equal-distance transposition once (100 + 100)	14.4	59.55	45.83	7.21	16.78	26.86
Equal-distance transposition twice (66.7 + 66.7 + 66.7)	1.41	5.64	4.76	1.03	2.04	4.53

The transposition of the AC line can effectively balance the three-phase electromagnetic coupling effect of the AC line. Therefore, the transposition of the conductors on the AC line within the parallel section can effectively reduce the electromagnetic coupling influence of the AC line on the DC line erected in parallel with it, and the more the transposition is made, the more the significant effect on reduction will be.

In addition, Table 12.13 also analyzes through calculation the influence of the DC line transposition on the reduction of the electromagnetic coupling by the AC line to the DC line.

As can be known from Table 12.13, when the DC line within the parallel section is transposed, the electromagnetic induction parameters (power frequency induced voltage and current and DC biasing current at valve side of converter transformer) on the positive pole of the DC line are reduced significantly, while the electromagnetic induction parameters on the negative pole are increased significantly, and the differences between the electromagnetic induction parameters on the positive and negative poles of the DC line are reduced significantly compared with those prior to transposition. This is because that the transposition of the DC line section erected in parallel has changed the approaching distances between the positive and negative poles of the DC line and the AC line, making them equalized and hence causing the electromagnetic influences of the AC line on the positive and negative poles of the DC line to be basically the same.

4. Influences of the UHVAC line on the UHVDC line erected in parallel with it in case of single-phase grounding failure

Table 12.13 Influence of transposition of the UHVDC line on the electromagnetic coupling by the AC line to the DC line

Mode of transposition (length of transposed line/km)	Rectifier side					
	Induced voltage (kV)		Induced current (A)		DC biasing current (A)	
	Positive pole	Negative pole	Positive pole	Negative pole	Positive pole	Negative pole
No transposition (100)	12.2	6.61	49.57	18.24	41.69	15.74
Equal-distance transposition once (50 + 50)	9.18	9.37	31.19	31.24	28.27	28.47
No transposition (200)	24.13	12.94	107.4	44.98	80.31	30.48
Equal-distance transposition once (100 + 100)	19.47	19.36	66.71	64.66	62.18	55.89
Mode of transposition (length of transposed line/km)	Inverter side					
	Induced voltage (kV)		Induced current (A)		DC biasing current (A)	
	Positive pole	Negative pole	Positive pole	Negative pole	Positive pole	Negative pole
No transposition (100)	6.59	3.54	13.84	10.83	22.16	17.32
Equal-distance transposition once (50 + 50)	5.04	4.92	12.39	12.76	19.84	19.72
No transposition (200)	14.75	7.64	27.45	20.23	45.01	40.55
Equal-distance transposition once (100 + 100)	11.76	11.58	24.16	23.27	43.49	42.35

When the AC line erected in parallel is subject to the single-phase grounding failure, the waveform of the electromagnetic induction parameters of the DC line fluctuates violently for a very short duration and then reaches another steady state. As for the three conditions under which the single-phase grounding failure occurs at the beginning end, the middle, or the terminal end of the AC line erected in parallel, Table 12.14 presents the electromagnetic influence of the AC line on the DC line under such conditions.

From Table 12.14, it can be seen that, among phase A, B, and C, the electromagnetic environment influence on the DC system is the most serious when the grounding failure occurs at phase C. Because the line of phase C is closer to the DC line, the short-circuit current of phase C increases rapidly when the single-phase ground fault occurs, thus to increase the electromagnetic induction influence on the DC line. As shown in Fig. 12.16, when the failure occurs at the beginning end or the terminal end of the line erected in parallel, the short-circuit current is in one direction and cannot be offset; however, when the failure occurs at the middle of the line erected in parallel, the electromagnetic coupling influence of the short-circuit

Table 12.14 Electromagnetic influence under single-phase ground fault

Mode of operation		Rectifier side			Inverter side		
		Induced voltage (kV)	Induced current (A)	DC biasing current (A)	Induced voltage (kV)	Induced current (A)	DC biasing current (A)
Normal operation		12.2	49.57	41.69	6.59	13.84	22.16
The beginning end	Phase A	41.67	138.54	137.67	50.76	144.31	173.32
	Phase B	24.98	65.26	87.69	49.19	128.12	155.72
	Phase C	56.67	194.74	183.94	79.76	240.58	227.55
The middle	Phase A	11.31	45.95	38.45	7.07	14.81	22.48
	Phase B	13.23	53.99	45.4	6.4	13.13	22.21
	Phase C	13.4	58.17	54.09	15.57	40.56	46.49
The terminal end	Phase A	42.49	164.85	149.74	63.19	189.21	190.72
	Phase B	56.56	203.11	175.09	60.26	191.14	196.83
	Phase C	64.49	217.12	212.19	89.14	257.16	248.43

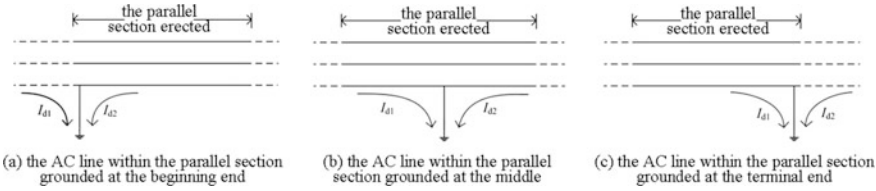

Fig. 12.16 Schematic diagram of single-phase ground fault

current at both sides on the DC line can be weakened. Therefore, the electromagnetic influence on the DC line caused when the single-phase grounding failure occurs at the both ends of the AC line within the parallel section is much bigger than that caused when the single-phase grounding failure occurs at the middle of the line.

12.3.3 Comparative Analysis on Parallel Erection of the UHV Single-Circuit and Double-Circuit on the Same Tower of AC Line and the UHVDC Line

This section focuses on studying the influences of the UHV single-circuit AC line and same-tower double-circuit AC line on the UHVDC line. To make such two conditions intercomparable, the transmission power of the 1000 kV AC single-circuit and double-circuit lines on the same tower are both taken as 5000 MW. Table 12.15 shows the conductor and ground wire parameters of the 1000 kV AC double-circuit line on the same tower, and Fig. 12.17 shows the

Table 12.15 Conductor and ground wire parameters of the 1000 kV double-circuit AC line on the same tower

Description	Line	Ground wire
Model of conductor	8× LGJ-630/45	LBGJ-150/20
Outer diameter of conductor/cm	3.36	1.58
DC resistance/(Ω/km)	0.046	0.582
Bundled conductor spacing/cm	40.0	–

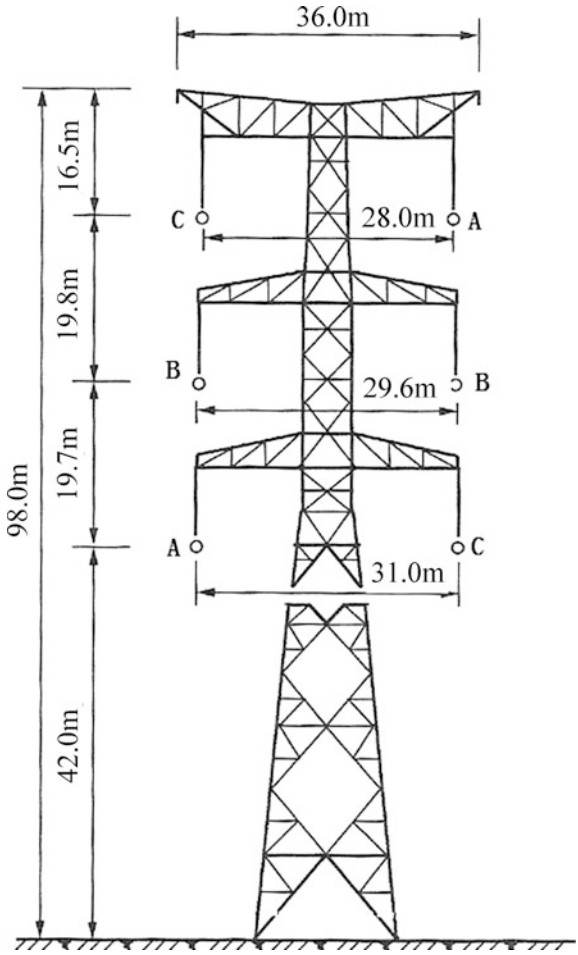

Fig. 12.17 Model of double-circuit line on the same tower

conductor arrangement for the towers of the double-circuit line on the same tower. When the parallel length is 100 km and the approaching distance is 50 m, the electromagnetic coupling influences of the UHV single-circuit AC transmission line and the UHV double-circuit AC transmission line on the same tower on the UHVDC line and the comparison results thereof are as shown in Table 12.16.

Table 12.16 Electromagnetic coupling influences of UHV single-circuit and double-circuit lines on the UHVDC line

Line	Rectifier side			Inverter side		
	Induced voltage (kV)	Induced current (A)	DC biasing current (A)	Induced voltage (kV)	Induced current (A)	DC biasing current (A)
①	12.2	49.57	41.69	6.59	13.84	22.16
②	8.65	37.26	34.98	6.41	13.72	20.79
③	5.83	26.24	24.28	4.59	10.38	16.88
④	10.33	43.29	41.29	8.06	17.85	30.02
⑤	3.17	12.10	11.09	4.62	10.88	18.28

① Triangularly arranged single-circuit line; ② double-circuit line arranged in the same phase sequence; ③ double-circuit line arranged in reverse phase sequence; ④ I circuit of double-circuit line arranged in reverse phase sequence out of operation; ⑤ II circuit of double-circuit line arranged in reverse phase sequence out of operation

As can be seen from Table 12.16, under the same transmission power, the electromagnetic influence of the double-circuit transmission line on the same tower (vertically arranged) on the DC system is smaller than that of the single-circuit line (triangularly arranged), the electromagnetic influence of the double-circuit line on the same tower arranged in reverse phase sequence on the DC system is smaller than that of the line arranged in the same phase sequence, and the electromagnetic influence of the double-circuit line on the same tower arranged in reverse phase sequence when I circuit thereof is out of operation is much more serious than that of the double-circuit line arranged in reverse phase sequence. The influence caused when circuit II of the double-circuit line on the same tower is out of operation is much smaller than that caused when circuit I is out of operation, because the line of circuit II is closer to the UHVDC line.

12.3.4 Comparative Analysis on Parallel Erection of the EHV/UHVAC Transmission Line and UHVDC Line

The conductor arrangements for the EHV compact-type line and EHV conventional line are as shown in Fig. 12.18, and the conductor parameters thereof are as shown in Tables 12.17 and 12.18 [9, 10].

To compare the erection of the UHVDC line in parallel, respectively, with the UHVAC line, EHV compact-type line, and EHV conventional line, 1 kA is specially taken as the operating current of the AC line, and, under such particular condition, the electromagnetic induction parameters of the DC line are calculated with the results, as shown in Table 12.19.

In consideration of the actual difference in the transmission power of the UHV transmission line, EHV compact-type transmission line, and EHV conventional

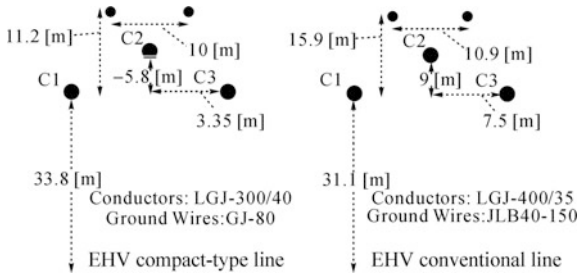

Fig. 12.18 Conductor arrangements for the EHV compact-type line and EHV conventional line

Table 12.17 Conductor and ground wire parameters of the EHV compact-type line

Description	Line	Ground wire
Model of conductor	6× LGJ-300/40	GJ-80
Outer diameter of conductor/cm	2.394	1.105
DC resistance/(Ω/km)	0.07389	2.8645
Bundled conductor spacing/cm	37.5	–

Table 12.18 Conductor and ground wire parameters of the EHV conventional line

Description	Line	Ground wire
Model of conductor	4× LGJ-400/35	LBGJ-180-20AC
Outer diameter of conductor/cm	2.682	1.575
DC resistance/(Ω/km)	0.07389	0.2952
Bundled conductor spacing/cm	45.0	–

Table 12.19 Electromagnetic influences of EHV/UHV lines on the UHVDC line erected in parallel (I)

Line	Rectifier side			Inverter side		
	Induced voltage (kV)	Induced current (A)	DC biasing current (A)	Induced voltage (kV)	Induced current (A)	DC biasing current (A)
UHV	10.64	44.03	37.75	4.88	9.73	16.85
EHV compact-type	1.28	5.31	5.36	1.06	2.35	4.39
EHV conventional	3.5	13.3	11.89	3.18	7.3	12.89

transmission line, the calculation is conducted based on three different conditions under which the transmission power of the UHV single-circuit line, the EHV compact-type line, and the EHV conventional line is, respectively, 3000, 1500 and 1000 MW. The calculation results of the electromagnetic induction parameters of the DC line under such conditions are as shown in Table 12.20.

Table 12.20 Electromagnetic influences of EHV/UHV lines on the UHVDC line erected in parallel (II)

Line	Rectifier side			Inverter side		
	Induced voltage (kV)	Induced current (A)	DC biasing current (A)	Induced voltage (kV)	Induced current (A)	DC biasing current (A)
UHV (3000 MW)	9.54	39.76	34.57	4.35	8.73	13.74
EHV compact-type (1500 MW)	1.19	5.13	5.14	0.98	2.26	4.17
EHV conventional (1000 MW)	2.38	9.44	7.93	1.34	2.61	5.17

As can be seen from Tables 12.19 and 12.20, the electromagnetic coupling influence of the EHVAC line on the UHVDC line is much smaller than that of the UHVAC line; the electromagnetic influence of the EHV compact-type AC line on the UHVDC line is reduced significantly as compared to that of the conventional AC line, and this is mainly because that the geometric dimension of the compact-type line is small, which, as a result, reduces the unbalance of the electromagnetic coupling influence caused by the three-phase AC line on the DC line.

References

1. Han Y, Qi W, Zhang P, Xue J, Xie X. Selection of neutral reactor and earthing switches in 750 kV transmission lines. Shaanxi Electr Power. 2008;36(9):10–3.
2. Li B, Zhou H. Calculation and analysis on induced voltage and current of 1000 kV transmission line adopting structure of double circuit on the same tower. Power Syst Technol. 2011;35(3):14–9.
3. Li B, Zhou H. Simulation and analysis of induced voltage and current on overhead ground Wire of Huainan–Wanna–Zhebei–Huxi 1000 kV UHVAC double-circuit transmission line. Power Syst Prot Control. 2011;39(10):86–89, 96.
4. Li B, Zhou H, Gou L. Electromagnetic Influence of AC transmission lines on parallelly erected UHVDC transmission lines [J]. Power Syst Prot Control. 2013;41(10):20–6.
5. Han Y, Huang X, Du Q. Induced voltage and current on double circuits with same tower [J]. High Voltage Eng. 2007;33(1):140–3.
6. Zhao H, Ruan J, Huang D. Calculation of the induction voltage on double circuit transmission lines [J]. Relay. 2005;33(22):37–40.
7. Zeng L, Zhang P, Feng Y, Hu P. Simulation calculation of induced voltage and induced current on 750 kV overhead ground wires [J]. Power Syst Clean Energy. 2008;24(6):21–3.
8. Wang Q, Zeng R, Tang J. Study on electromagnetic interference of Luo-Bai AC transmission line on Yun-Guang ± 800 kV DC transmission line [J]. South Power Syst Technol. 2007;3(1):27–31.
9. Yao J, Guo Z, Zhu Z, Liu Z. Reseach on inductive voltage and inductive current of 500 kV double-circuit transmission line [J]. North China Electric Power. 2006;1:23–5.
10. Guo Z, Yao J, Cheng X, Zhu Z. Study and measurement of induced voltage and current for 500 kV double-circuit line on same tower [J]. High Voltage Eng. 2006;32(5):11–4.

Chapter 13
Electromagnetic Environment of UHVAC System

Xiao Zhang, Haiqing Lu, Yang Shen and Chuan He

The impacts of the UHVAC transmission project on the electromagnetic environment are mainly manifested in the land utilization, communication interference caused by the corona and audible noise as well as the impacts of the power frequency electromagnetic field on the ecology, etc. The high voltage of the UHV power transmission can definitely result in the increase of the intensity of electric fields on the conductor surface and in the space around the transmission equipment. Therefore, whether the corona phenomenon and strong electric field effect brought about by the UHV transmission lines and substations will endanger the human body and the ecologic environment is always the issue of great concern.

After the voltage level has developed to the UHV stage, the electromagnetic environment requirements determine the selection of cross section of the conductor of transmission line, determination of air clearance for conductor to ground and the delimitation of the line corridor, etc. and affect the construction cost of the line directly, have become a critical issue in the construction of the UHV power transmission project.

X. Zhang (✉)
State Grid Weifang Power Supply Company, Weifang, Shandong,
People's Republic of China
e-mail: 154476875@qq.com

H. Lu
State Grid Zhejiang Electric Power Research Institute,
Hangzhou, Zhejiang, People's Republic of China
e-mail: 410640469@qq.com

Y. Shen
China Energy Engineering Group, Zhejiang Electric Power Design Institute Co., Ltd.,
Hangzhou, Zhejiang, People's Republic of China
e-mail: shenyangzju@21cn.com

C. He
Anhui Electric Power Corporation, Hefei, Anhui, People's Republic of China
e-mail: zjuhechuan@gmail.com

© Zhejiang University Press, Hangzhou and Springer-Verlag GmbH Germany 2018

H. Zhou et al. (eds.), *Ultra-high Voltage AC/DC Power Transmission*,
Advanced Topics in Science and Technology in China,
https://doi.org/10.1007/978-3-662-54575-1_13

This Chapter first compares the electromagnetic environment of the EHV/UHV power transmission lines, and then analyzes the electromagnetic environment of the UHVAC power transmission line, including the power frequency electric field, the power frequency magnetic field, the corona loss, the radio interference and the audible noise, and discusses the optimization of the phase sequence of the UHV double-circuit transmission line, and sequentially analyzes and calculates the safe distance of the UHV transmission line over the buildings, and finally make a preliminary discussion on the electromagnetic environment of the UHVAC substation.

13.1 Comparison Between Electromagnetic Environment of UHV and EHV Transmission Lines

The outstanding problems of the electromagnetic environment of the UHV transmission line include the impact of power frequency electric field on physiology and ecology and the audible noise derived from the corona effect. In terms of the design, construction and operating experience, the controlling conditions of the electromagnetic environment of the UHV transmission line have changed as compared with those of the EHV transmission line, as shown in Fig. 13.1. For the transmission lines with voltage level of 500 kV and below, the power frequency electric field is generally considered as the main influence factor of the electromagnetic environment. In such case, because of the low voltage level of the line, the corona is very difficult to be incepted on the conductors, and the values of the radio interference and the audible noise are both fairly low, so the transmission line is easy to meet the standard. For the 750 kV transmission line, the radio interference is the main controlling condition of the line design. The requirements on the audible noise can be met naturally so long as the line is designed in such a way that the limits of the radio interference are met. For the UHV line, however, the audible noise, instead of the radio interference, becomes the controlling condition of the line design and determines the conductor selection, configuration and arrangement of the UHV transmission line.

Compared with the general environmental noise of the same sound pressure level, the audible noise generated by the corona discharge of the transmission line is usually more wearing. Several 500 and 765 kV AC lines built up early in the USA had high electric field intensity on the conductor surface, and the noise caused thereby aroused a large number of complaints by the residents nearby, and even lawsuits filed by the

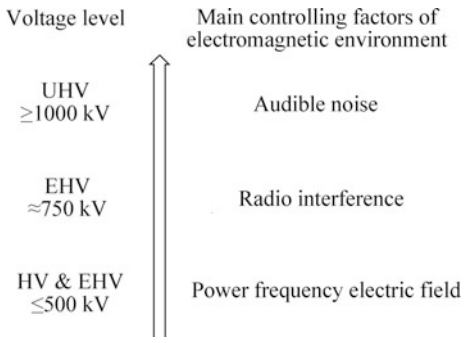

Fig. 13.1 Change of main controlling factor of electromagnetic environment of transmission line with voltage level

residents due to the audible noise. Thereafter, there was no alternative but to have these EHV transmission lines stepped down for operation or replaced with conductors with a large diameter. It is shown by some studies that, for the UHV lines, the audible noise, especially the audible noise generated in bad weather conditions, is the major factor to select the conductor configuration and determine the transmission voltage. Meanwhile, it is also the major factor influencing the costs.

In addition, the audible noise of the UHV lines in China is exacerbated by the high altitude. The audible noise increases by about 1 dB for each 300 m increase in altitude. For example, for the cup-type tower line of the Southeast Shanxi-Nanyang-Jingmen UHV Demonstration Project, when the altitude is higher than 1500 m, the audible noise measured at 20 m away from the side-phase conductor of the line exceeds 55 dB which is the specified limit. Therefore, the outstanding problem in the electromagnetic environment of the UHV transmission line is the audible noise generated by the corona.

The USA's Bonneville Power Administration (BPA) compared the UHV line through test with BPA's typical 500 kV transmission line in terms of the electric field level at the 1200 kV UHV test field in Lyons. The test results showed that the power frequency electric field level of the UHVAC transmission line could be made basically comparable to that of the EHVAC 500 kV transmission line having been accepted generally by the public, so long as the conductors of the UHVAC line were designed reasonably and the ground height of the line was selected appropriately.

China Electric Power Research Institute, Wuhan High Voltage Research Institute and other institutes carried out research on the power frequency magnetic field of the UHVAC line. The research results showed that the power frequency magnetic field level of the UHV line under the rated current was comparable to that of the EHV line under the maximum transmission power. No matter the EHV or the UHV transmission lines, the power frequency magnetic field levels thereof will not exceed the limit of 0.1 mT specified by the International Commission on Non-Ionizing Radiation Protection (ICNIRP) in *Guidelines for Limiting Exposure to Time-varying Electric, Magnetic and Electromagnetic Fields (up to 300 GHz).*

The USA, Japan, and other counties have ever implemented research on the radio interference caused by the UHVAC transmission line. It is shown by the research results that the radio interference level of the UHVAC transmission line can be made comparable to that of the EHV line if the number and diameter of the sub-conductors are selected appropriately.

The USA's Bonneville Power Administration (BPA) has carried out a large number of tests on the audible noise of the conductors of various configurations. It is demonstrated by the test results that the audible noise level of the UHVAC line can be made comparable to that of the EHV line so long as the conductors are designed reasonably.

As mentioned above, the experience in research on the electric field, the magnetic field, the audible noise, and the radio interference of the EHV and UHV lines both in China and abroad shows that the electromagnetic environment level of the UHV line can be reduced to be comparable to that of the EHV line so long as the conductors are reasonably designed and the ground height of the line is appropriately selected.

13.2 Electromagnetic Environment of the UHVAC Transmission Line

13.2.1 Power Frequency Electric Field

13.2.1.1 Characteristics of Power Frequency Electric Field

When the AC transmission line is under live operation, the charges on the conductor will generate the power frequency electric field in the space around the conductor. Assuming that the soil on the ground is a good conductor and the impacts of the tower and surrounding objects are neglected, the horizontal component of the electric field intensity near the ground approximates to zero, and the resultant electric field intensity approximates to the vertical component. Therefore, within the area about 2 m above the ground, the direction of the electric field is basically vertical, while the horizontal component thereof is negligible.

The electric field intensity of the power transmission line is determined mainly by the voltage of the line, and does not change with the transmission capacity and the line current. No matter the line is under no load or full load, so long as the voltage on the line is relatively stable, the intensity of power frequency electric field will basically keep unchanged.

The electric field will result in the movement of the charges on the conductor surface when encountering the conductor, and the charges on the conductor will also generate a field, which is superposed on the original electric field to change the whole electric field around the conductor, thus resulting in the increase of the electric field around the conductor due to distortion. Similarly, trees and buildings themselves have certain conductivity, and the electric field around them will increase due to distortion, while the internal electric field thereof will be impaired greatly due to the shielding effect. Therefore, the internal electric field of the buildings may not be taken into consideration in the actual engineering.

13.2.1.2 Limits of Power Frequency Electric Field

At present, the limits for the electric field intensity of the transmission line are mainly determined by reference to the relevant stipulations as specified by the State Environmental Protection Administration and electric power industry. From the perspective of environmental protection, the limits for the power frequency electric field of the UHV transmission lines in China are identical to those for the 500 kV AC transmission lines, as shown in Table 13.1 [1], that is, with respect to the power frequency electric field intensity under the line and at 1.5 m above the ground, the limit of the field intensity is taken as 7 kV/m in the general areas, such as the area accessible by the public and the place where the line crosses over the highway, and as 10 kV/m in the area where the line crosses over the farmland. When the line is

Table 13.1 Limits for power frequency electric field intensity of UHV transmission line in China

	Near civil buildings	Crossing over farmlands	Crossing over highways
Limit for electric field intensity (kV/m)	4	10	7

adjacent to the civil building, the maximum field intensity without distortion at 1.5 m above ground at the place where the building locates is taken as 4 kV/m.

For the purpose of reference and comparison, the requirements related to the electric field intensity limits for the transmission line in other countries are given as below:

(1) America

For the power frequency electric field under the transmission line, the field intensity at the edge of the line corridor is generally controlled at 2 kV/m. For the maximum electric field intensity under the line inside the line corridor, the electric power companies in the USA have different limits, among which, the design requirement for the electric field intensity specified by BPA is 9 kV/m inside the line corridor and 5 kV/m at the edge of the line corridor and at the place where the line crosses over the highway.

(2) Japan

In Japan, the limit for the electric field intensity is determined by the degree of discomfort caused by the spark discharge from umbrella to human body when a person holding up an umbrella walks under the line. The limit is taken as 3 kV/m in the area in which there are frequently human activities, while the maximum value of ground electric field intensity is taken as 10 kV/m in the mountainous regions and forests, etc.

(3) Other standards

It is specified in *Guidelines for Limiting Exposure to Time-varying Electric, Magnetic and Electromagnetic Fields (up to 300 GHz)* by the International Commission on Non-Ionizing Radiation Protection (ICNIRP) that the limit for 50 Hz electric field is 5 kV/m (for the common public). It is specified in IEEE standard C95.6TM-2002 that the limit for 50 Hz electric field is 5 kV/m for the common public while 20 kV/m for the controlled area.

As mentioned above, the limits for the power frequency electric field are specified differently because of the different environmental protection policies in different countries. In addition, CIGRE has ever summarized the limits for the electric field intensity in the space under the transmission lines as specified by some countries and found something in common among the limit requirements of various

Table 13.2 Limits for electric field intensity in the space under transmission lines specified by some countries (CIGRE)

Country	Limits for electric field intensity/kV m^{-1}	Place	Criterion
Czech	10	Places where line crosses over Class I and II highways	
	1	At the edge of line corridor	
Japan	3	Places where a person holding up an umbrella passes by	A
Poland	10		A, C
	1	Places where hospitals, housings and schools are located	A, C
Former Soviet Union	20	Places inaccessible	A, C
	15	Places not open to the public	A, C
	10	Places where line crosses over highways	A, C
	5	Areas for public activities	A, C
	1	Areas where there are buildings	A, C
	0.5	Residential areas	C
The USA			
Minnesota	8		
Montana	7	Places where line crosses over highway	B
	1	Residential areas at the edge of line	C
New York	11.8		B
	11	Places where line crosses over private paths	
	7	Places where line crosses over highway	
	1.6	At the edge of line corridor	
New Jersey	3	At the edge of line corridor	
North Dakota	8		
Oregon	9	Accessible areas	
Florida	2	At the edge of line corridor	

A to prevent from the discomfort caused by transient electric shock, *B* to prevent the steady-state electric shock current from being greater than let-go current, *C* to restrict the ecological effect caused by long-term electric field effect

countries, as specifically shown in Table 13.2. It can be seen from Table 13.2 that the electric field intensity required by various countries is lower than 5 kV/m in the public activity area or near the civil building, 7–10 kV/m at the place where transmission line crosses over the highway and 10–15 kV/m at most under the line.

13.2.1.3 Calculation Method of Power Frequency Electric Field

The intensity of the power frequency electric field in the space under the HV transmission line shall be calculated by the method recommended by "CIGRE Working Group 36.01", i.e., the intensity of the power frequency electric field under the single-phase or three-phase transmission line is calculated by the equivalent charge method (charge simulation method).

The overhead ground wire has little influence on the electric field intensity near the ground. It is shown by the calculation of the EHV and UHV transmission lines with single circuit horizontally arranged that the electric field intensity without the overhead ground wire is about 1–2% higher than that with the overhead ground wire. Therefore, the influence of the overhead ground wire is usually ignored to simplify the calculation process.

13.2.1.4 Simulation Calculation of Power Frequency Electric Field

To understand the distribution of the power frequency electric field of the UHV line, this section uses the typical tower types of the 1000 kV Southeast Shanxi-Nanyang-Jingmen UHV Demonstration Project for the simulation of the power frequency electric field of the transmission line. The typical tower types are as shown in Fig. 13.2. The Cat-head type tower with M-type triangular configuration is used in the plains, while the cup-type tower with M-type horizontal configuration is used in the mountainous regions.

The 8 × LGJ-500/35 aluminum conductors steel reinforced with bundled conductor spacing of 400 mm are used for the 1000 kV line, and the JLB20A-170 concentric-lay-stranded aluminum-clad steel conductors are used for the shielding wire.

Figure 13.3 shows the transverse distribution of the power frequency electric field under the line erected on the cat-head type tower and cup-type tower and at 1.5 m above the ground. Compared with the EHV line, the UHV line is featured by high voltage level, high steel tower, and wide line corridor, etc. For the cat-head type tower, with the maximum sag taken into consideration, the minimum height above the ground of the bottom-phase conductor is over 40 m, and the power frequency electric field intensity under the line is 3.18 kV/m at most, meeting the limits specified and reaching the standard. Compared with the cat-head type tower, the cup-type tower is lower, and the maximum power frequency electric field intensity under the line is 4.71 kV/m, and the width of the line corridor meeting the electric field intensity of 4 kV/m is about 91 m.

13.2.1.5 Influence Factors of Power Frequency Electric Field

The value of the power frequency electric field intensity at a certain point in the space is related to the voltage applied on the conductor, i.e., related to the charge

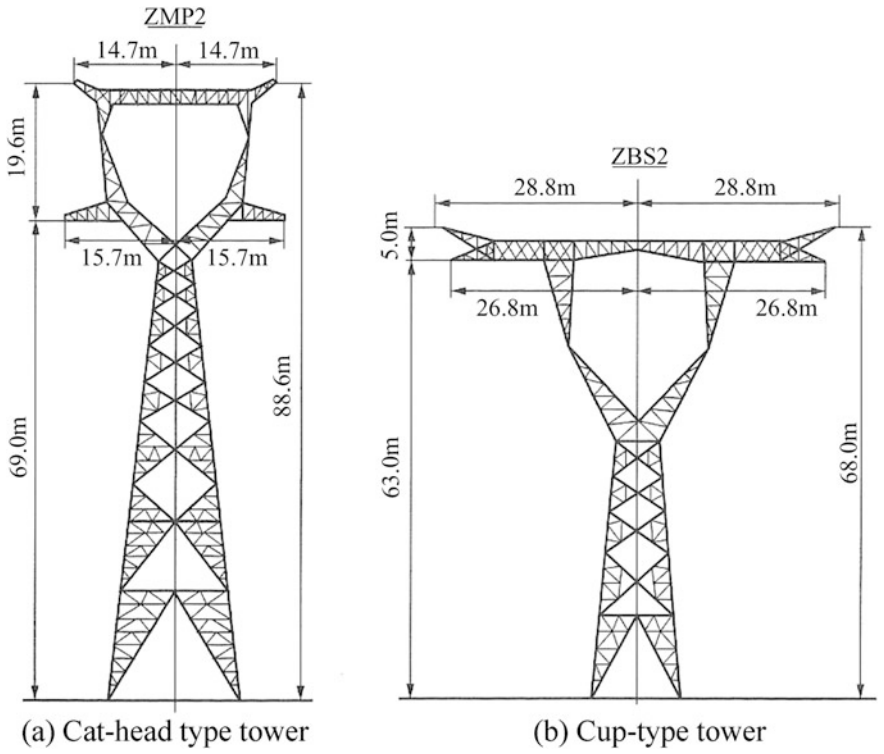

Fig. 13.2 Typical towers along 1000 kV Southeast Shanxi-Nanyang-Jingmen transmission line

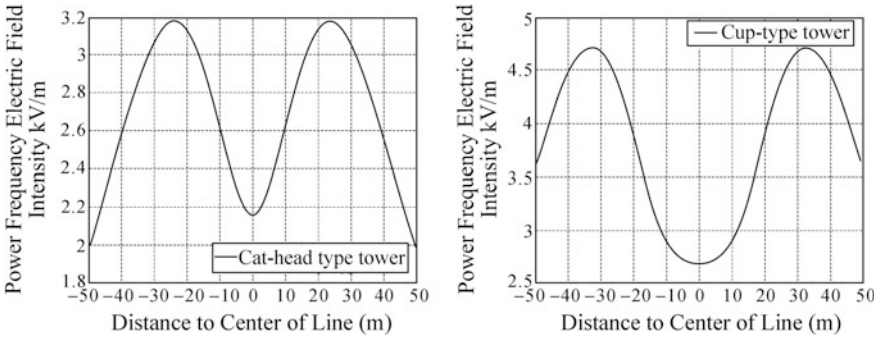

Fig. 13.3 Transverse distribution of power frequency electric field under UHV line

quantity on the conductor, the distance from the point to the conductor, the geometric location and the dimension of the conductor. Therefore, the conductor configuration, the height above the ground, the phase-to-phase distance, the number of sub-conductors, the bundled conductor spacing and the cross section of

conductor as well as the phase sequence arrangement of multi-circuit line conductor are all the factors influencing the distribution and the amplitude of the power frequency electric field intensity under the line.

Taking the case of the cup-type tower along the 1000 kV Southeast Shanxi-Nanyang-Jingmen UHV Demonstration Project, this section analyzes to what extent the factors such as the height above the ground, the phase-to-phase distance and the conductor parameters affect the power frequency electric field of the line. The simulation results are as shown in Fig. 13.4.

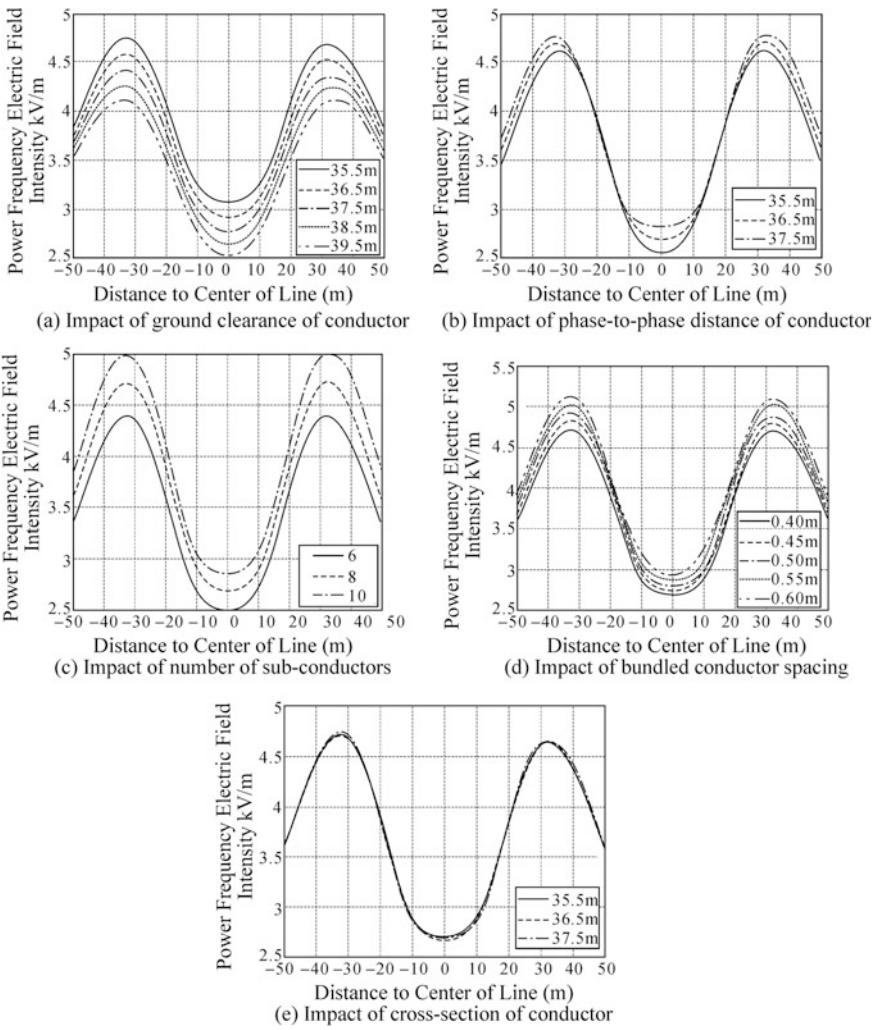

Fig. 13.4 Impacts of various influence factors on power frequency electric field of line

It can be seen from Fig. 13.4 that the conductor's height above the ground and number of sub-conductors affect the power frequency electric field of the line significantly, and the increase in the height above the ground of the conductor is an effective measure to reduce the power frequency electric field intensity, but attention shall be paid that the decrease rate of the electric field intensity slows down gradually with the increase in the height above the ground of the conductor. The reduction of the number of sub-conductors can also attenuate the power frequency electric field intensity under the line, but it will increase the radio interference and the audible noise, so comprehensive consideration shall be given to the method during line design. Other factors, such as the phase-to-phase distance of conductor, the bundled conductor spacing and the cross-section area of conductor, slightly affect the power frequency electric field.

The conductor configuration of the transmission line is also a major factor influencing the power frequency electric field of the line. There are three different conductor configurations available for the 1000 kV single-circuit line, i.e., horizontal, regular triangular, and inverted triangular configurations. The calculation models for the power frequency electrical fields under such three conductor configurations, in which the minimum height between the phase conductor and the ground is 18 m, are established, respectively, as shown in Fig. 13.5. The transverse distributions of the power frequency electric fields at 1.5 m above the ground in the three calculation models are as shown in Fig. 13.6. Compared with the regular

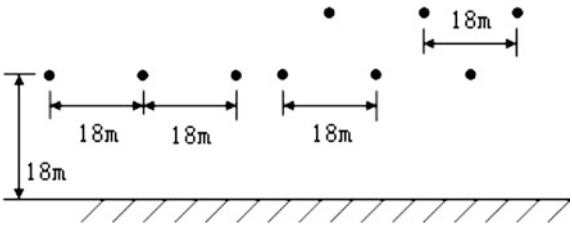

Fig. 13.5 Simplified simulation models for the three conductor configurations

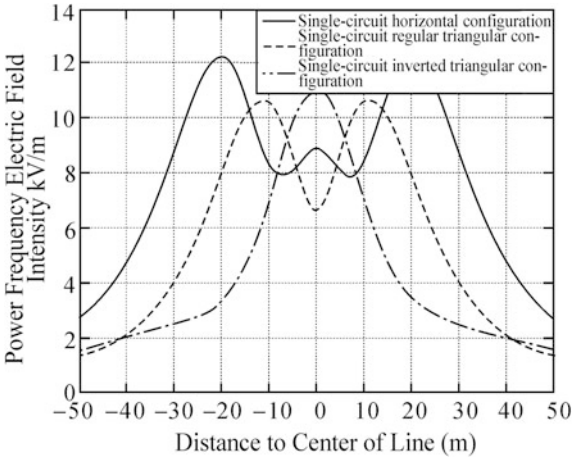

Fig. 13.6 Distribution of electric field intensity under the three conductor configurations

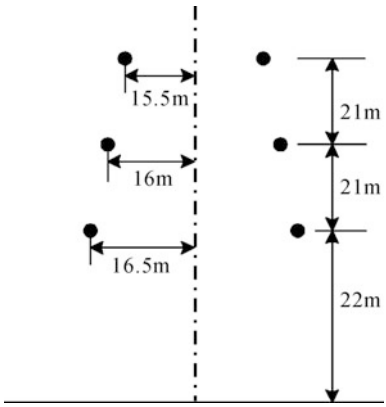

Fig. 13.7 Simplified model for double-circuit line on the same tower

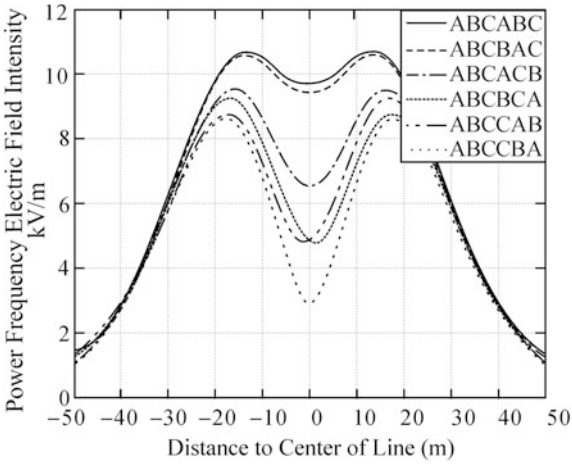

Fig. 13.8 Transverse distribution of electric field intensity under different conductor configurations

triangular configuration and the horizontal configuration, the inverted triangular configuration is centralized in the electric field intensity and narrow in the distribution range of the high electric field intensity area. The coverage of the high electric field intensity area is the largest when the conductors are in horizontal configuration. The limit and coverage of the high electric field intensity area are both the smallest when the conductors are in the inverted triangular configuration.

The UHV double-circuit transmission line on the same tower has six phase sequence arrangements: ABCABC, ABCBAC, ABCACB, ABCBCA, ABCCAB and ABCCBA. Figure 13.8 shows the transverse distribution of the power frequency electric field at 1.5 m above the ground under different phase sequence arrangements (taking the case of the model of Japan's UHV transmission line shown in Fig. 13.7). It is evident that, under the reverse phase sequence arrangement of ABCCBA, the maximum value of the power frequency electric field

intensity under the line and the range of the high electric field intensity are both the smallest.

The adoption of the inverted triangular configuration for the UHV single-circuit line and the adoption of the reverse phase sequence arrangement for the UHV double-circuit line on the same tower can effectively reduce the maximum value of the power frequency electric field intensity under the line and save the line corridor. It is noteworthy that the corona loss will be increased if the reverse phase sequence arrangement is adopted for the UHV double-circuit transmission line on the same tower, resulting in the increase of the radio interference and the audible noise of the line. This shall be taken into comprehensive consideration in the line design.

13.2.1.6 Measures for Improvement of Power Frequency Electric Field

The power frequency electric fields of the transmission lines of various voltage levels are generated in the same mechanism and so can be analyzed by the same method. The measures to improve the power frequency electric field of the transmission line on the basis of the above research are summarized as below:

The increase in the height above the ground of the conductor is the most effective measure to reduce the power frequency electric field. For the double-circuit line on the same tower, the change of the phase sequence arrangement of the conductor can also reduce significantly the power frequency electric field intensity under the line. The adoption of the inverted triangular configuration for the UHV single-circuit line and the adoption of the reverse phase sequence arrangement for the UHV double-circuit line on the same tower can both effectively reduce the maximum value of the power frequency electric field intensity under the line and save the line corridor. It is noteworthy that the corona loss will be increased if the reverse phase sequence arrangement is adopted for the double-circuit line, resulting in the increase of the radio interference and the audible noise of the line. So this shall be taken into comprehensive consideration in the line design. If it is necessary to control the power frequency electric filed intensity under the transmission line to a fairly low level because of frequent activities of persons or special needs, several shielding wires can be installed between the phase conductor and the ground to reduce the electric field intensity under the transmission line.

13.2.2 Power Frequency Magnetic Field

The power frequency magnetic field of the transmission line is generated by the current flowing through the line. Generally, only the magnetic material can change the distribution of the magnetic field in the space. Therefore, the power frequency magnetic field around the line is not so easy to distort as the electric field. The trees and houses hardly have any shielding effect on the power frequency magnetic field,

Table 13.3 Limits for power frequency magnetic field radiation by IRPA/INIRC

Exposed object	Exposure duration	Magnetic flux density/mT
Occupation	Whole working day Short duration Only on limbs	0.5 5 25
Public	No more than 24 h Several hours/day	0.1 1

but the power frequency magnetic field attenuates with the increase of distance more quickly than the power frequency electric field does.

As for the limits of the power frequency magnetic field, the EU recommends its member states to apply the guidelines specified by the International Commission on Non-Ionizing Radiation Protection (IRPA/INIRC) as the compulsory standards. The limits for the 50 Hz magnetic field as recommended by INIRC are shown in Table 13.3. INIRC categorizes the exposure limits into occupational exposure limits and public exposure limits. For the public, the magnetic flux density under continuous exposure to magnetic field shall not be higher than 0.1 mT [2]. In China, HJ/T 24-1998 *Technical Regulations on Environmental Impact Assessment of Electromagnetic Radiation Produced by 500* kV *Ultrahigh Voltage Transmission and Transfer Power Engineering* is generally taken as reference. In consideration of the criteria recommended for the 500 kV line, the limit of 0.1 mT under all-day public exposure recommended by INIRC can be taken as the limit for the magnetic flux density for the 1000 kV transmission line [1].

The power frequency magnetic field intensity in the space under the transmission line can be calculated by the method recommended by "CIGRE Working Group 36.01" [2]. Since the current and its electromagnetic performance under the power frequency have quasi-static characteristics, the magnetic field intensity around the conductors can be obtained by applying Ampere's Law and superposing the calculation results of various conductors in the vector manner.

As for the calculation of the power frequency magnetic field of the transmission line, what differs from the calculation of the power frequency electric field intensity is the consideration on the mirror image conductors. Compared with the height h of the conductor above the ground, these mirror image conductors are buried in a great depth d underground, i.e., $d \gg h$. In consideration that the refined calculation of the magnetic field generated by the current-carrying conductors above the ground needs to use Carlson's equation to estimate the poor conductive effect of the ground, the distance d of the mirror image conductor to the ground surface is specifically calculated as below [2].

$$d = 660\sqrt{\frac{\rho}{f}} \tag{13.1}$$

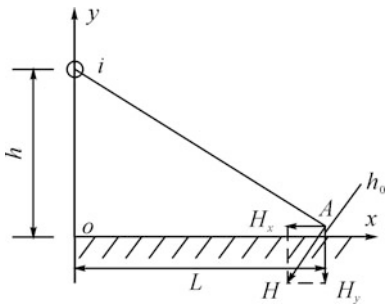

Fig. 13.9 Schematic diagram for calculation of power frequency magnetic field

where

ρ Ground resistivity (Ω·m);
f Frequency (Hz).

In consideration that the ground resistivity is generally 30–2000 Ω·m, the minimum mirror image distance under the 50 Hz power frequency (with the minimum resistivity taken as 30) is $d = 511$ m. Therefore, in case the power frequency magnetic field is available, $d \gg h$, so the impact of the mirror image conductors on the ground magnetic field is insignificant. In general, during the calculation, only the actual conductors in the space are taken into consideration and the mirror image conductors thereof are ignored. The calculation results under such case are sufficiently comparable to the actual condition. As shown in Fig. 13.9, in case the mirror image conductor of conductor i is not considered, the magnetic field intensity generated by it at point A is calculated as below:

$$H = \frac{I}{2\pi\sqrt{(h - h_0)^2 + L^2}} \tag{13.2}$$

where

I Current in conductor i;
h_0 Height of point A to be calculated;
h Height of conductor i;
L Horizontal distance from the conductor to the calculated point.

For the three-phase line, the horizontal and the vertical components of the magnetic field intensity generated by the different phases must have the phase angles between the current taken into consideration and shall be subject to the phase vector composition.

Figure 13.10 shows the transverse distribution of the power frequency magnetic field of the line erected on the cat-head type tower and the cup-type tower of the 1000 kV Southeast Shanxi-Nanyang-Jingmen UHV Demonstration Project at 1.5 m above the ground under the maximum transmission power (corresponding to the line current of 6400 A). The maximum value of the power frequency magnetic field

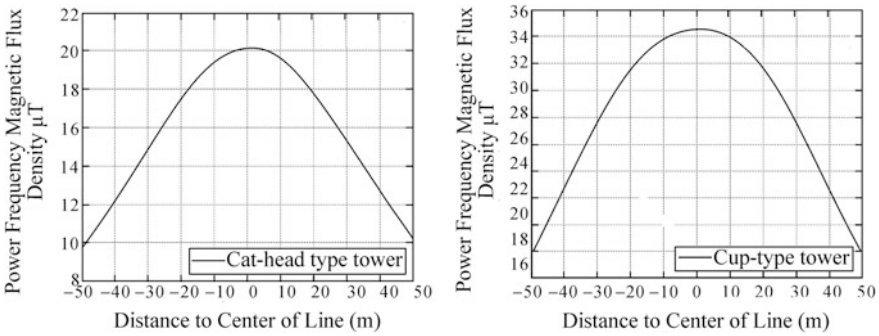

Fig. 13.10 Transverse distribution of power frequency magnetic field under UHV line

intensity under the line erected on such two types of towers is lower than 35 μT, much lower than the limit specified for the power frequency magnetic field. Therefore, the power frequency magnetic field of the UHV line reaches the standard.

In addition, China Electric Power Research Institute, Wuhan High Voltage Research Institute and other research institutes also researched and calculated the power frequency magnetic field of the 1000 kV UHVAC transmission line. The conductors thereof are 15–23 m above the ground, and the maximum magnetic flux density under the UHV single-circuit and the double-circuit lines is lower than 35 μT; besides, the maximum magnetic flux density under the lines with the maximum operating current is also lower than the specified limit of 0.1 mT. Therefore, the power frequency magnetic field is not a key factor limiting the electromagnetic environment of the UHVAC line.

The amplitude of the magnetic field intensity in the space under the transmission line is not only related to the amplitude of the line load current, but also to the configuration and the geometric position of the conductor, etc. The power frequency magnetic field intensity decreases with the increase of the height above the ground of the conductor, and hence the increase in the height above the ground of the conductor is a relatively effective way to reduce the magnetic field intensity under the transmission line. Besides, the change of the phase sequence can also reduce the magnetic field intensity. The magnetic field intensity under the line can also be decreased effectively if the inverted triangular configuration is adopted for the single-circuit line and the reverse phase sequence arrangement is adopted for the double-circuit line. However, the bundled conductor spacing and the number and the diameter of sub-conductors have little impact on the power frequency magnetic field under the line.

13.2.3 Corona Loss

The potential gradient on the conductor surface of the transmission line increases under the effect of the high voltage. When the electric field intensity on the surface

of the conductor exceeds the breakdown field intensity of air, ionization discharge will occur to the air around the conductor. The charged ions produced by the discharge will move to and fro around the conductor under the effect of alternating electric field, and generate, at the same time, blue-purple glow and hiss mildly. The energy consumed in these phenomena is collectively called as the corona loss.

The corona loss of the AC transmission line is mainly concerned with the electric field intensity on the conductor surface and the voltage level of the line, etc. Among them, the electric field intensity on the conductor surface is affected mainly by the weather conditions. Therefore, this section discusses the corona loss under different weather conditions (fine, rainy, and snowy days).

The corona loss of the line on a fine day lies mainly in the leakage loss of insulators, being about several kilowatts per km and accounting for only a small portion of the resistance loss of the line, and is over a hundred times lower than that on a rainy day or a snowy day. In consideration of the whole operation duration, however, the fine days account for the largest proportion of the time, and hence, from the perspective of the total energy consumption, the loss on the fine days is still of a certain economic significance. On a rainy day, water drops will form on the underneath of the conductor, seriously distorting the electric field intensity on the conductor surface and sharply increasing the corona loss. On a snowy day, especially on a wet snowy day, the corona loss is the highest. The wet snow adheres to the surface of the conductor, causing the surface of the conductor to become rougher and the distribution of electric field around the conductor to be extremely uneven, and, as a result, leading to the great increase of the corona loss. After the wet snow turns into dry snow, it is difficult to adhere to the conductor, and the corona loss decreases consequently.

The corona loss is a technical and economic indicator in the electric power industry. Its estimation is a basic work in the optimal line design, which must be first verified in the design of power grid, especially in the design of the long-distance transmission line at a high altitude and with the high corona loss. However, it is demonstrated by the relative research results of other countries that the corona loss has increasingly smaller influence on the determination of the conductor configuration with the rise of the voltage level, while the audible noise and the radio interference produced by the corona play a decisive role in the design of the UHV line. Therefore, this section will no longer explicitly calculate and analyze the corona loss of the UHV line, but only describe its calculation method.

As the corona loss of the transmission line varies greatly under different weather conditions and the weather conditions vary greatly in different countries, though the corona loss of the transmission line has been studied for many years, there is no corona loss estimation method acknowledged internationally yet. The below will briefly introduce the corona loss estimation method in the design manual for the high-voltage transmission line of the electric power engineering.

1. Electric Field Intensity on Conductor Surface

The Markt-Mengele method can meet the engineering requirements in terms of the calculation accuracy and is relatively simple. This book utilizes it to calculate the electric field intensity on the surface of the transmission line.

(1) The equivalent radius r_{eq} of bundled conductor is calculated as follows:

$$r_{eq} = R\sqrt[n]{\frac{nr}{R}} \tag{13.3}$$

where

R Radius of the bundled conductor, in m;
n Number of sub-conductors;
r Radius of sub-conductors, in m.

(2) The charges Q of each equivalent conductor determined by the Maxwell's potential coefficient method are as follows:

$$[Q] = [P]^{-1}[U] \tag{13.4}$$

where

$[Q]$ Column matrix of charges on the conductor;
$[U]$ Column matrix of the voltage on the conductor;
$[P]$ Matrix composed of self-potential coefficient and mutual-potential coefficient of the conductor.

(3) Maximum average electric field intensity on the bundled conductor surface.

$$E_{av} = \frac{Q}{2\pi\varepsilon}\frac{1}{nr} \tag{13.5}$$

$$E_{max} = E_{av}\left[1 + \frac{r}{R}(n-1)\right] \tag{13.6}$$

where

E_{av} Average electric field intensity on the sub-conductor surface, in kV/cm;
E_{max} Maximum electric field intensity on the conductor surface, in kV/cm.

2. Corona Inception Electric-Field Intensity

According to the Peek's equation, the maximum value of the parallel conductors' critical potential gradient (corona inception electric-field intensity) E_0 is as follows:

$$E_0 = 3.03m\delta^{2/3}\left(1+\frac{0.3}{\sqrt{r}}\right) \tag{13.7}$$

where

m Surface coefficient of the conductor, generally taken as 0.82 for the stranded conductor;
δ Relative air density;
r radius of the conductor, in cm.

3. Corona Loss

The annual average corona loss of the transmission line is the sum of the corona power loss of the three-phase conductors under various weather conditions (fine day, snowy day, rainy day and rime day).

$$P_{\mathrm{k}} = \frac{n^2r^2}{8760}\times\left\{\left[\sum_{i=1}^{3}F_1\left(\frac{E_{\mathrm{mi}}}{\delta^{2/3}E_0}\right)\right]T_1+\left[\sum_{i=1}^{3}F_2\left(\frac{E_{\mathrm{mi}}}{\delta^{2/3}E_0}\right)\right]T_2 + \left[\sum_{i=1}^{3}F_3\left(\frac{E_{\mathrm{mi}}}{\delta^{2/3}E_0}\right)\right]T_3+\left[\sum_{i=1}^{3}F_4\left(\frac{E_{\mathrm{mi}}}{\delta^{2/3}E_0}\right)\right]T_4\right\} \tag{13.8}$$

where

P_{k} the total average power loss of three phases, in W/m;
E_{m1}, E_{m2} and E_{m3} respectively, the surface potential gradient of the three-phase conductors, taken as E_{m} for the single conductor and as the maximum value of average potential gradient for the bundled conductor, in MV/m;
F_1, F_2, F_3 and F_4 respectively, the corona loss function for fine days, snowy days, rainy days and rime days and can be obtained from the curve; T_1, T_2, T_3 and T_4 are, respectively, the hours of fine days, snowy days, rainy days and rime days in a year.

In Ref. [3], the annual average corona loss of UHVAC single-circuit and double-circuit transmission lines is studied. It is shown by the results that the annual average corona loss of the Southeast Shanxi-Nanyang-Jingmen transmission line of the 1000 kV UHVAC Single-circuit Line Demonstration Project is about 18.87 kW/km. As for Xilin Gol League-Nanjing transmission line of the 1000 kV same-tower double-circuit transmission line project, the calculation results of the corona loss and the annual average loss of various conductors under different

Table 13.4 Corona Loss of 1000 kV same-tower double-circuit line under different weather conditions (kW/km)

Weather condition	Conductor model		
	8 × JL/GIA-500/35	8 × JL/GIA-630/45	8 × JL/GIA-710/50
Fine day	3.0	2.6	2.5
Rainy day	150.4	130.3	125.2
Snowy day	108.7	96.9	90.3
Rime day	1828.0	1612.0	1520.0
Annual average	52.8	46.6	43.9

weather conditions are as shown in Table 13.4 [3]. Obviously, the corona loss of the line is mainly dependent on the bad weather.

It is shown by the relevant research that the corona loss of the UHV transmission line is generally 10–20% of the resistance loss of the line.

13.2.4 Radio Interference

13.2.4.1 Characteristics of Radio Interference

The corona discharge of the transmission line is the main source of the radio interference. When the current pulse produced by the corona is injected into the conductor and flows towards both ends of the injection point along the conductor, the pulsed magnetic field, i.e., the radio interference field, is formed around the conductor.

In the low-frequency range, the radio interference level is high. When the frequency is higher than 10 MHz, the radio interference is quite low and the effect thereof can be neglected. Generally, it is sufficient to have the frequency of the radio interference considered up to 30 MHz. The International Special Committee on Radio Interference (CISPR) recommends 0.5 MHz as the measuring frequency of the radio interference.

For the radio interference limit of the HV transmission line, the International Special Committee on Radio Interference (CISPR) recommends the 80%/80% principle, i.e., within one year, the radio interference field intensity produced by the transmission line shall be no more than the said limit value during 80% of the time and shall have a degree of confidence of 80%.

The radio interference of the transmission line decreases gradually with the increase of the distance to the line. Figure 13.11 shows the transverse attenuation characteristics of the radio interference produced by the line erected on the cat-head type and cup-type towers of the 1000 kV Southeast Shanxi-Nanyang-Jingmen UHV Demonstration Project at 1.5 m above the ground. It can be seen from Fig. 13.11 that the radio interference attenuates quickly with the increase of the distance to the line, and nearly approximates to the background noise (30 dB) when it is over 200 m to the line.

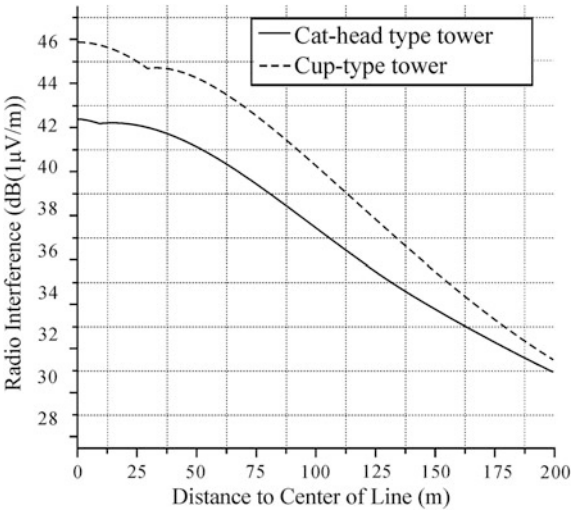

Fig. 13.11 Transverse attenuation characteristics of radio interference of UHV line

The radio interference is random in itself. During the measurement of the radio interference of the line, the measured results vary with the time due to the changes of climate conditions along the line and surface conditions of conductors even if the measuring position and the frequency are maintained unchanged. The measured results of the radio interference are usually presented by means of statistics analysis. It is generally analyzed on the basis of the cumulative distribution function, and represented by 95% value (heavy rainy days), sunny day 50% value (average of fine days[1]) and double 80%//80% value (all-weather 80% value):

−80% value (measurement: under all-weather condition, its result represents the limit of the radio interference), i.e., double 80%//80% value. It means the interference level which is not exceeded in 80% of the time within one year and has the degree of confidence of 80%. For the samples measured continuously at an equal time interval, "the interference level which is not exceeded in 80% of the time" and "the interference level which has the degree of confidence of 80%" have the same meaning.

−95% value (measurement: under all weather conditions, while its result represents the radio interference value on heavy rainy days), i.e., after a long-term measurement (e.g., after 1 year, generally including all weather conditions), the interference level which is not exceeded in 95% of the time (or has degree of confidence of 95%—for the samples measured continuously at an equal time interval). It can normally represent the radio interference level on heavy rainy days. The rain can generally be considered as heavy rain if the rainfall is over 0.6 mm/h. The radio interference level in heavy rain is the most stable and can be recurred.

[1]"Average" refers to the mathematical expectation of probability in the strict sense, instead of the mean value.

Therefore, the average level of the radio interference in heavy rain is often chosen by the researchers as the reference level to calculate the radio interference.

−50% value (measurement: on sunny days, its result represents the average of the radio interference under the good weather condition), i.e., the average under good weather condition. It means the radio interference value which is not exceeded in 50% of the time (or has the degree of confidence of 50%—for the samples measured continuously at an equal time interval) after the radio interference is measured under good weather condition (e.g., a long-term measurement, but including only the fine days). It represents the average radio interference of dry conductors under fine weather condition. Although the measurement of the radio interference under fine weather condition is highly dispersed, the measurement is easy to implement, and the reliable result can be obtained after multiple measurements.

The double 80%//80% value is often between the 50% value (average on fine days) and the 95% value (on heavy rainy days), and is affected less by instability compared with the average on fine days.

13.2.4.2 Limits of Radio Interference

For the limits of radio interference of the transmission line, there is not yet any international standard, because the situations are different in different countries and the parameters and corridors of the transmission lines are defined diversely. The CISPR-18 publication of the International Special Committee on Radio Interference (CISPR) only recommends the definition of the limits and the principle for setting the limits. Table 13.5 lists the stipulations on the radio interference limits in various countries.

It is specified in China's national standard GB 15707-1995 *Limits of Radio Interference from AC High Voltage Overhead Power Transmission Lines* that, at the point that is 20 m away from the projection of the side-phase conductor of the three-phase line, when the measuring frequency on fine day is 0.5 MHz, the limits of the radio inference generated (the limit which is not exceeded in 80% of the time and has the degree of confidence of 80%) are as shown in Table 13.6.

The limits under other frequencies can be corrected by the following equation:

$$E = E_0 + 5(1 - 2\lg(10f)^2) \tag{13.9}$$

where

E_0 the limit listed in Table 13.6, in dB;
f the frequency, in MHz.

China has ever studied the impact of the UHV transmission line on the environment in 1990s, and recommended that the limits of the radio interference of the UHV transmission line under 0.5 MHz be between 55 and 60 dB. This recommendation is brought forth after the calculation and the analysis on various

Table 13.5 Limits of radio interference in various countries

Country	Line voltage (kV)	Frequency (MHz)	Distance (m)	Limit (dB)	Type of instrument	Remarks
Japan	275–500	1	10	60 (rainy day)	As per Japan's standard	
Switzerland	<100 >150	0.5	20	34 48	STMG-3800 (comply with CISPR standard)	Based on the average value on fine days, 10% is permitted to exceed the standard in the time
Former Soviet Union	<220 >220	1	50 100	40	As per CISPR	Subject to 80% of the time Not exceeding the limit
DDR (Deutsche Demokratische Republik)	All voltages	0.5	20	57.5	As per CISPR	Subject to 99.5% of the level Not exceeding the limit
BRD (Bundes Republik Deutschland)	All voltages	1	100	20	STMG-3800	Signal-to-noise ratio: 40 dB
Canada	70–200 200–300 300–400 400–600	1	15	46 50 53 57	As per CSA standards	
Italy	420	0.5	30 70	35 35	As per CISPR	Densely populated area Sparsely populated area

Table 13.6 Limits of Radio Interference Specified in GB 15707-1995

Voltage level/kV	110	220–330	550
Limit of radio interference/dB	46	53	55

conductor parameters that may be adopted for the UHV line. Viewed from the change of China's standard, the limits of radio interference of the UHV transmission line is slightly higher than that of the 500 kV line.

It is specified in China's national standard GB 50665-2011 *Code for Design of 1000* kV *Overhead Transmission Line* that, in the area at altitude of 500 m or below, at the point that is 20 m away from the outside edge of the horizontal projection of the line's side-phase conductor on the ground and 2 m above the ground, the design control value of the radio interference shall not be higher than 58 dB (μV/m) under the frequency of 0.5 MHz.

13.2.4.3 Calculation Methods for Radio Interference

For the calculation methods for the radio interference of the transmission line, when the number of sub-conductors changes, the calculation methods also vary to some extent. When the number of sub-conductors is not more than 4, the radio interference is generally calculated by the empirical method; when the number of sub-conductors is more than 4, the radio interference is usually calculated by the excitation function method. The calculation methods are introduced as below.

1. In Case of the Number of Sub-conductors ≤ 4

When the number of sub-conductors is ≤ 4, the radio interference can be calculated by applying the equation provided in China's national standard GB 15707-1995 *Limits of Radio Interference from AC High Voltage Overhead Power Transmission Lines*. The equation is described as below:

$$E = 3.5g_{\max} + 12r - 30 + 33 \lg \frac{20}{D} \tag{13.10}$$

where

E the radio interference field intensity, in dB (μV/m);
r the radius of the conductor, in cm;
D the distance from the observation point to a phase conductor of the transmission line, in m;
$g_{\max}$ the maximum potential gradient on conductor surface, kV/cm.

The result obtained from Eq. (13.10) is the radio interference value in 50% of the time under fine weather condition. The double 80%//80% value can be obtained by adding 6–10 dB (μV/m) to the result.

2. In Case of the Number of Sub-conductors > 4

It can be known from DLT 691-1999 *Methods of Calculation of Interference from High Voltage Overhead Power Transmission Lines* that, when the number of sub-conductors is >4, the calculation method for the radio interference shall be based on the excitation function obtained by the test line or the corona cage measurement, which is used mainly for the calculation of the radio interference of the UHV transmission line under the heavy rain condition. The calculation process is described as below [2]:

(1) The heavy rain excitation function put forward by America's Electric Power Research Institute (EPRI) is the relatively appropriate excitation function, shown specifically as follows:

$$\Gamma_{\text{heavyrain}} = 70 - 585/g_{\max} + 35\lg d - 10\ \lg(n) \tag{13.11}$$

where

$g_{\max}$ the effective value of the maximum potential gradient on the sub-conductor surface, in kV/cm;
d the diameter of sub-conductors, in cm;
n the number of sub-conductors.

(2) Calculate the corona current matrix on the three-phase transmission line by applying the following expression:

$$[i_0] = \frac{[C]}{2\pi\varepsilon_0}[\Gamma] \tag{13.12}$$

where

matrix $[C]$ the capacitance matrix of the three-phase transmission line. When phase 1 conductor produces the corona, matrix $[\Gamma] = [\Gamma, 0, 0]\text{T}$.

(3) Convert the corona circuit on the three-phase transmission line into the mode current by means of the mode conversion as below:

$$[i_{0\text{m}}] = [S]^{-1}[i_0], \quad m = 1, 2, 3 \tag{13.13}$$

where

$[S]$ the mode conversion matrix, and $S^{-1}S = 1$.

(4) Calculate the mode current after it propagates by distance x:

$$[i_{\mathrm{m}}(x)] = 0.5\mathrm{e}^{(L_{\mathrm{m}}x)}[i_{0\mathrm{m}}] \tag{13.14}$$

where

$L_{\mathrm{m}} = \alpha_{\mathrm{m}} + j\beta_{\mathrm{m}}$ the propagation constant of the transmission line, which can be obtained by calculating the characteristic value of matrix $[B] = [Y][Z]$, where matrix $[Y]$, $[Z]$, respectively, represent the shunt admittance matrix and the series impedance matrix of the transmission line.

(5) Convert the mode current calculated reversely into the phase current as below

$$[i(x)] = [S][i_{\mathrm{m}}(x)] \tag{13.15}$$

(6) Assuming that phase k conductor of the three-phase transmission line is h_{k} above the ground and y_{k} away from the observation point horizontally, when phase 1 conductor produces the corona, the field intensity $E_1(x)$ at the observation point produced by the differential element of the current is:

$$E_1(x) = 60\sum_{k=1}^{3} i_{\mathrm{k}}(x)\left[\frac{h_{\mathrm{k}} - h_1}{(h_{\mathrm{k}} - h_1)^2 + y_{\mathrm{k}}^2} + \frac{h_{\mathrm{k}} + h_1 + 2p}{(h_{\mathrm{k}} + h_1 + 2p^2) + y_{\mathrm{k}}^2}\right] \tag{13.16}$$

where

$i_{\mathrm{k}}(x)$ the element in Row k of $[i(x)]$;
h_{k} is the height of phase k conductor;
y_{k} is the projection distance of phase k conductor to the observation point;
h_1 is the height of the observation point above the ground, usually taken as 2 m;
p is the penetration depth of magnetic field, expressed as below:

$$p = \sqrt{\frac{\rho}{\mu_0 \pi f}}$$

where

ρ the soil resistivity, in Ω·m;
f the frequency, in Hz;

$$\mu_0 = 4\pi \times 10^{-7}.$$

(7) Assuming that the corona current distributes uniformly on the whole conductor, when phase 1 conductor produces the corona, the field intensity at the observation point is calculated according to the average sum rule as follows:

$$E_1 = \sqrt{2\int_0^{\infty} |E_1(x)|^2 \mathrm{d}x} \tag{13.17}$$

Similarly, when phase 2 and phase 3 conductors produce the corona, respectively, the radio interference field intensity E_2 and E_3 at the observation point can be calculated. For the three-phase conductor, the value of the radio interference of one phase conductor to the observation point, which is at least 3 dB (V/m) higher than that of any other phase conductors to the same observation point, shall be the value of the radio interference of the HVAC overhead transmission line; otherwise, it shall be calculated by the following equation:

$$E = \frac{E_1 + E_2}{2} + 1.5 \tag{13.18}$$

where

E the radio interference field intensity of HVAC transmission line, in dB (V/m);

E_1, E_2 the two highest field intensities of the radio interference of two phase conductors in three-phase line to the observation point, in dB (V/m).

It shall be noted that the result from the above method is the radio interference value in heavy rain. The double 80%//80% value can be obtained by deducting 10–15 dB (μV/m) from the value under heavy rain condition (95% value) [2]. In the actual engineering, a value within this range is usually taken. The radio interference value under the condition that 50% of the time is of fine weather can be obtained by deducting 6–10 dB (μV/m) from the double 80%//80% value [4]. In the actual engineering, a value within this range is usually taken.

13.2.4.4 Radio Interference Level of UHV Transmission Line

To understand the distribution of the radio interference of the UHVAC transmission line, the values of the radio interference of the single-circuit and double-circuit UHV lines (with 8 × LGJ-500/35 aluminum conductors steel reinforced) at 20 m away from the outside of the projection of the side-phase conductor under different minimum heights above the ground of the conductor are calculated with the results as shown in Table 13.7.

Table 13.7 Values of radio interference at 20 m away from the outside of projection of side-phase conductor of UHV transmission line (dB)

Height of conductor (m)	18	19	20	21	22
Single-circuit					
Cat-head type tower	50.6	50.3	49.7	49.2	48.7
Cup-type tower	48.8	48.2	47.6	47.1	46.5
Double-circuit	52.6	52.1	51.6	51.0	50.4

It can be seen from Table 13.7 that, for the UHVAC single-circuit and double-circuit transmission lines, the values of the radio interference at 20 m away from the outside of the projection of the side-phase conductor under the minimum height of the conductor of 18.0 m as specified by the code are all lower than the specified limit of 58.0 dB. Therefore, the radio interference is not a key factor limiting the design of the UHV transmission line.

13.2.4.5 Influence Factors of and Improvement Measures for Radio Interference

The corona discharge and the spark discharge generated by the high electric field intensity on the conductor surface are the major root causes for the generation of the radio interference of the power line. The generation of the corona is usually hard to avoid on the EHV transmission line due to its high voltage level; after the voltage level develops to the UHV, the generation of the corona is even more unavoidable. Therefore, the only way to limit the generation of the corona is to increase the critical voltage that generating the corona. When the transmission voltage and the conductor configuration are kept unchanged, the radio interference of the line is concerned with the number of sub-conductors, conductors' average height, the phase-to-phase distance and the radius of sub-conductors, etc. Among these factors, the number and radius of sub-conductors affect the radio interference greatly. In addition, the high altitude will also intensify the radio interference.

This section still takes the case of the cup-type tower of the 1000 kV Southeast Shanxi-Nanyang-Jingmen UHV Demonstration Project to analyze to what extent the height of the conductor, the phase-to-phase distance, conductor parameters and altitude, etc. affect the radio interference of the transmission line, and summarize the effective measures to improve the radio interference of the line. Please refer to Fig. 13.12 for the simulation results.

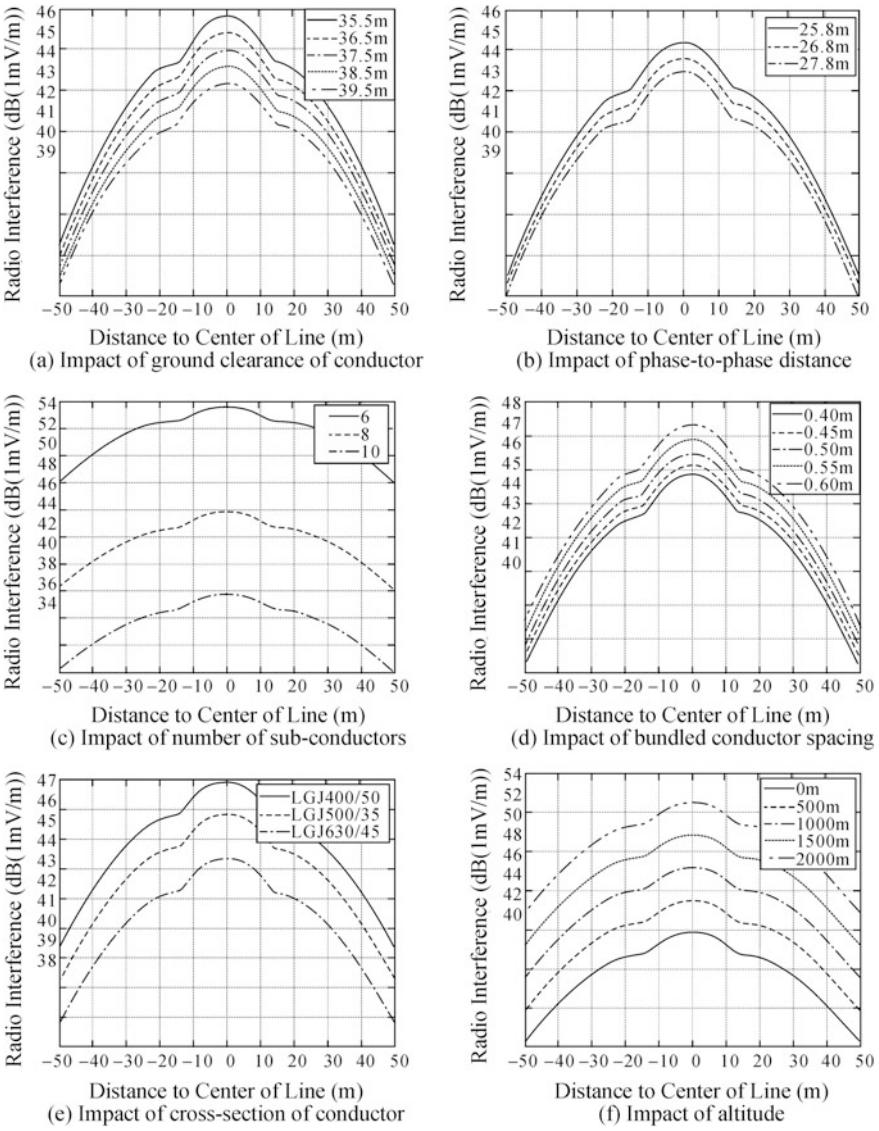

Fig. 13.12 Impacts of various influence factors on radio interference of line

It can be seen from Fig. 13.12 that the increase of height above the ground of the conductor, the phase-to-phase distance, numbers of sub-conductors and the cross-section area of the conductor and the decrease of the bundled conductor spacing can all reduce the radio interference under the transmission line, which are the effective measures to reduce the radio interference under the transmission line.

13.2.5 Audible Noise

13.2.5.1 Characteristics of Audible Noise

The audible noise of the transmission line is a kind of noise which is generated by the corona and the spark discharge around the conductor and can be heard directly. It is of audio frequency interference. The audible noise of AC transmission line has two characteristic components: one is the wideband noise (crack, cheep or hiss), and the other is the AC pure sound with frequency of 100 Hz (or 120 Hz) and its integer multiple (hem and hum). The wideband noise is generated by the haphazard pulse caused by the corona discharge of the conductor surface in the air, while the AC pure sound is generated by the direction change of the air pressure because of the charges in the space around the conductor moving back and fro.

The audible noise due to the corona of the transmission line is only a problem for lines with the voltage level of 500 kV and above. The problem was ignored before because the voltage level of the transmission line is not high and the audible noise is usually small. But now, UHV transmission lines have been set up in China. It is demonstrated by research of other countries that, with respect to UHV lines with voltage level of 1000 kV and above, the audible noise will become an outstanding problem. The minimum cross-section area of the conductor is generally determined according to the audible noise. This audible noise will disturb residents near the UHV line and people working nearby. It is unbearable if it is serious. If the problem is not treated well, the normal life and work of people near the transmission line may be affected.

On the dry or fine days, the corona source points caused by dust, insects and burrs on the conductor itself mainly exist on the conductor, and the noise caused thereby is relatively low. On rainy days, the collision and gathering of rain drops on the conductor increase the corona discharge intensity, and thus increase the audible noise. The audible noise on rainy days is 15–20 dB (A) higher than that on fine days. Therefore, for the AC transmission line, the restriction of the audible noise shall give primary consideration to the rain condition.

13.2.5.2 Limits for Audible Noise

Up to now, all countries have not yet established officially the standards for limiting the audible noise of the UHVAC transmission line, but just brought forth some limits in the code of design of the UHVAC line according to each national situation thereof. Table 13.8 exhibits the limits for audible noise in some countries. It can be seen from the table that the limit range of audible noise of the UHV transmission line is 50–60 dB.

China's current noise-related standard GB 3096-2008 *Environmental Quality Standard for Noise* is shown in Table 13.9 [5]. This standard defines the audible noise at different places during different periods of time.

Table 13.8 Limits for audible noise of UHVAC line in some countries

Country		Rated voltage (kV)	Maximum operating voltage (kV)	Mode of bundled conductors	Measuring position	Design value of audible noise dB (A) (rainy days L_{50})
USA	BPA	1100	1200	8 × 41 mm/410 mm	At edge of line corridor	55/50 (noise sensitive area)
	AEP	1500	1600	10 × 46.3 mm/380 mm	15 m away from the outside of projection of side-phase conductor	58
Former Soviet Union		1150	1200	8 × 26.2 mm/360 mm	45 m away from the outside of projection of side-phase conductor	55
Japan		1000	1100	8 × 38.4 mm/810 mm	Under the conductor	50
Italy		1000	1050	8 × 31.5 mm/560 mm	15 m away from the outside of projection of side-phase conductor	56–58 (wet conductor after rain) 58–60 (rainy days)

Table 13.9 Noise standard in China (equivalent sound level L_{eq}: dB (A))

Category	Day-time	Night-time
0	50	40
1	55	45
2	60	50
3	65	55
4		
4a	70	55
4b	70	60

Category 0 applies to sanitariums, senior villas, exclusive hotels, etc. where quietness is needed (inapplicable to the noise at the boundary of industrial enterprises)
Category 1 applies to the area in which there are mainly residences and cultural and educational institutions. This category can be the reference to decide the standard implemented in the rural residential environment
Category 2 applies to the areas where residence, commercial activities and industrial activities are mixed up
Category 3 applies to the industrial areas
Category 4a applies to both sides of main roads in urban areas and both banks of courses of inland rivers passing through urban areas
Category 4b applies to the areas at both sides of main lines of railways newly built (including the extended railways with new corridors) whose environmental impact assessment document is approved as of January 1, 2011

The limits for the audible noise of the UHVAC transmission line are specified in GB 50665-2011 Code for Design of 1000 kV Overhead Transmission Line: for the areas at altitude of 500 m and below, the designed controlling value of the audible noise of wet conductor at 20 m away from the outside of the horizontal projection of the side-phase conductor of the line on the ground shall not be higher than 55 dB (A), and shall comply with the sound environment indicator approved by the competent environmental protection authority.

13.2.5.3 Calculation Method for Audible Noise

In accordance with the code *Provisional Technical Code for Design of 1000* kV *AC Overhead Transmission Line*, the audible noise of the UHV line can be calculated by applying the USA's BPA equation.

The estimation equation [6] of the audible noise recommended by the USA's BPA is:

$$\mathrm{SLA} = 10 \times \lg \sum_{i=1}^{z} \lg^{-1}\left(\frac{\mathrm{PWL}(i) - 11.4 \times \lg(R_\mathrm{i}) - 5.8}{10}\right) \tag{13.19}$$

where

SLA A-weighted sound pressure level;
PWL(i) sound power level of phase i conductor;
R_i distance from the measuring point to phase i conductor measured (m);
z number of phases.

PWL in Eq. (13.19) is calculated by the following equation:

$$\mathrm{PWL} = -164.4 + 120 \lg E + 55 \lg d_{\mathrm{eq}} \tag{13.20}$$

E in Eq. (13.20) represents the conductor surface gradient (kV/cm), and d_{eq} is the equivalent diameter. d_{eq} can be calculated by the following equation:

$$d_{\mathrm{eq}} = 0.58 \times n^{0.48} \times d \tag{13.21}$$

where

n number of sub-conductors;
d diameter of sub-conductors (mm).

This equation applies to all conventional symmetrically bundled conductors with the bundled conductor spacing of 30–50 cm and the conductor surface gradient of 10–25 kV/cm.

13.2.5.4 Audible Noise Level of UHV Transmission Line

To understand the distribution of the audible noise of the UHVAC transmission line, the values of the audible noise of the single-circuit and double-circuit UHV lines (with 8 × LGJ-500/35 aluminum conductors steel reinforced) at 20 m away from the outside of the projection of the side-phase conductor under different minimum heights of conductors are calculated with the results as shown in Table 13.10.

It can be known from Table 13.10 that, when the UHV single-circuit transmission line adopts 8 × LGJ-500/35 conductors and the minimum height above the ground of conductors is 18.0 m as specified by the code, audible noise values at 20 m away from the outside of the projection of the side-phase conductor satisfy the

Table 13.10 Values of audible noise at 20 m away from the outside of projection of side-phase conductor of UHV transmission line (dB (1A))

Height above the ground of conductor (m)	18	19	20	21	22
Single-circuit					
Cat-head type tower	54.4	54.2	54.0	53.8	53.7
Cup-type tower	53.1	52.9	52.7	52.5	52.3
Double-circuit	57.3	57.1	57.0	56.8	56.7

specified limit value of 55.0 dB, and, therefore, the audible noise is up to the standard.

The audible noise of the UHV double-circuit line under the same condition does not reach the standard. Therefore, the measures such as the increase in the height above the ground of conductor and the cross-section area of the conductor shall be taken to reduce the audible noise under the line. If 8 × LGJ-500/35 conductors are adopted, the audible noise of the double-circuit line will reach the standard only when the height above the ground of conductors is raised to 39 m; if 8 × LGJ-630/45 conductors are adopted, the audible noise of the double-circuit line will reach the standard when the height above the ground of conductors is raised to 25 m.

It is concluded that the audible noise of the UHV transmission line determines the confirmation of the ground clearance and the selection of the conductors and is the factor controlling the electromagnetic environment of the UHV transmission line.

13.2.5.5 Influence Factors of Audible Noise

Similar to the radio interference, the audible noise caused by the corona discharge is concerned with the number of sub-conductors, conductors' average height, the phase-to-phase distance and the radius of sub-conductors, among which, the number and the radius of sub-conductors affect the audible noise significantly, and hence the increases in the number and the diameter of sub-conductors are effective measures to reduce the audible noise of the line. In addition, the altitude will also increase the audible noise. Figure 13.13 shows to what extent these factors affect the audible noise.

13.2.5.6 Improvement Measures for Audible Noise

The increases in the number of sub-conductors and in the cross-section area of conductors are effective measures to reduce the audible noise of the UHV transmission line. In addition, some relative measures to reduce the audible noise level of the transmission line are also put forward internationally.

(1) If the sub-conductors are distributed symmetrically, increase the number of sub-conductors and control the bundled conductor spacing to reduce the field intensity on the conductor surface.
(2) If the sub-conductors bundled asymmetrically are adopted, make great effort to uniformly distribute the charges on the sub-conductors as far as possible to improve the electric field distribution on the conductor surface. Figure 13.14 gives the Russia's depressed eight-bundled conductor model used to reduce the corona loss of the line on rainy days. Figure 13.15 provides the USA's unequally spaced bundled conductor model ($\Delta 5/\Delta 1 = 2$).

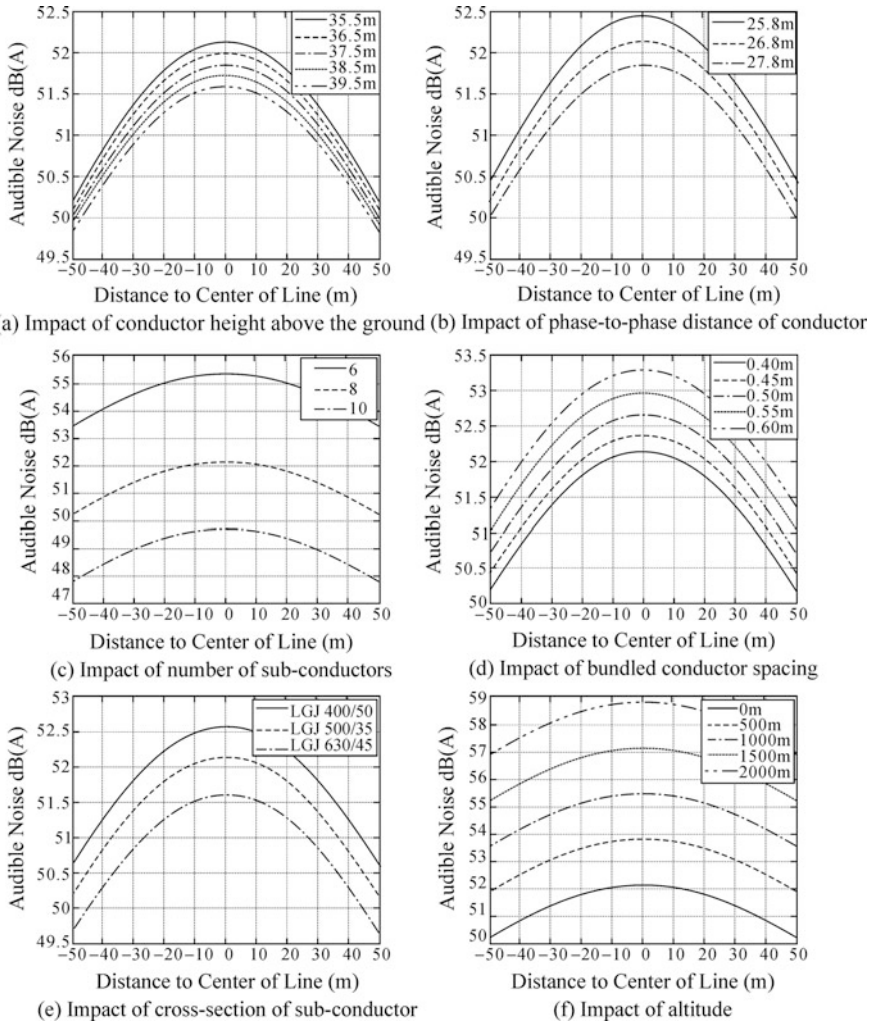

Fig. 13.13 Impacts of different influence factors on audible noise of the line

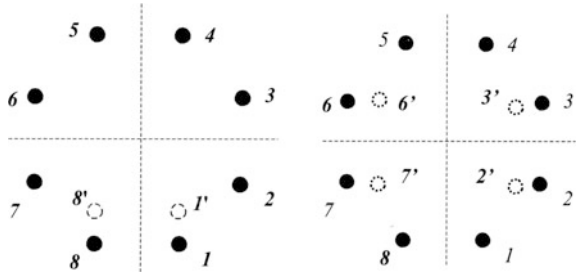

Fig. 13.14 Depressed eight-bundled conductor (Russia)

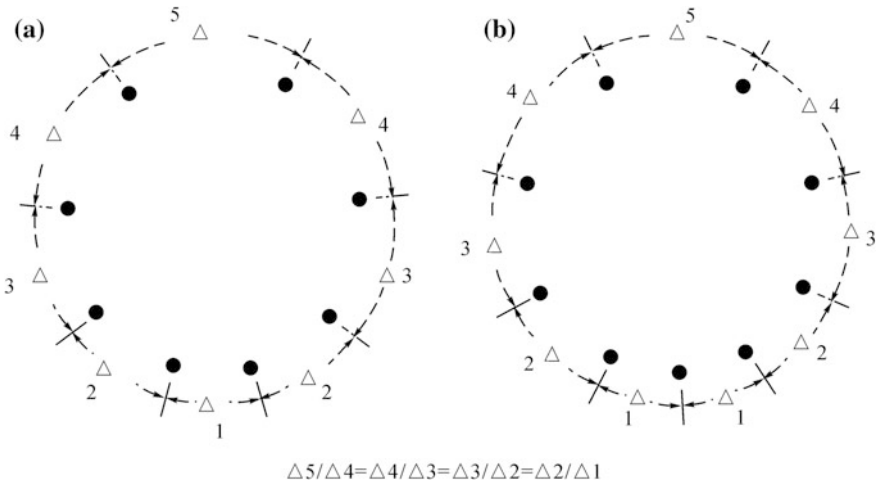

Fig. 13.15 Unequally spaced bundled conductors (USA)

(3) Install additional sub-conductors in the symmetrically bundled conductor to improve the charge distribution on the surface of each sub-conductor and reduce the field intensity on the conductor surface.
(4) Apply water-repellent coating on the conductor to reduce the water drops adhering to the conductor on rainy days, and thus reduce the corona discharge intensity to reduce the audible noise.

13.3 Optimized Phase Sequence Arrangement of the UHV Double-Circuit Transmission Line

The UHV power transmission, which can alleviate effectively the shortage in electric power supply, optimize the configuration of power resources, improve the structure of the power grid and increase the utilization rate of line corridors, has become the strategic planning of China to construct the strong power grid. Compared with the single-circuit line, the double-circuit line on the same tower has the advantages such as saving the line corridors and enhancing the reliability of power supply, and is the most important way for China to construct the UHVAC transmission lines. In the future, the majority of the UHVAC transmission projects to be constructed in China will adopt the same-tower double-circuit transmission mode.

For the double-circuit transmission line on the same tower, its phase sequence arrangement includes 6 forms, namely, ABC/ABC, ABC/ACB, ABC/BAC, ABC/BCA, ABC/CAB and ABC/CBA. The conductor configuration implements some effects on the electromagnetic environment, the line corridor, the transmission

power, unbalance degree, the lightning protection performance and the ground wire's induced voltage and induced current as well as other electrical characteristics. Therefore, the reasonable selection of the optimal phase sequence arrangement for the conductors on the double-circuit line on the same tower is of great significance to the improvement of the line's electromagnetic environment, the increase of the line's transmission power and the optimization of the line design, etc.

With the 1000 kV Huainan-West Shanghai UHVAC Demonstration transmission Project to Transmit Electricity from Anhui to Eastern China taken as an example, CDEGS software package, MATLAB and EMTP programs are utilized to simulate and calculate the electric field, the magnetic field, the radio interference, the audible noise, the natural power, the unbalance degree of the line, the back flashover striking trip-out rate, the ground wire's induced current and induced voltage of the double-circuit line on the same tower under various conductor configurations, and then the optimal phase sequence arrangement for the line is obtained based on the comprehensive consideration of the impacts of all electrical

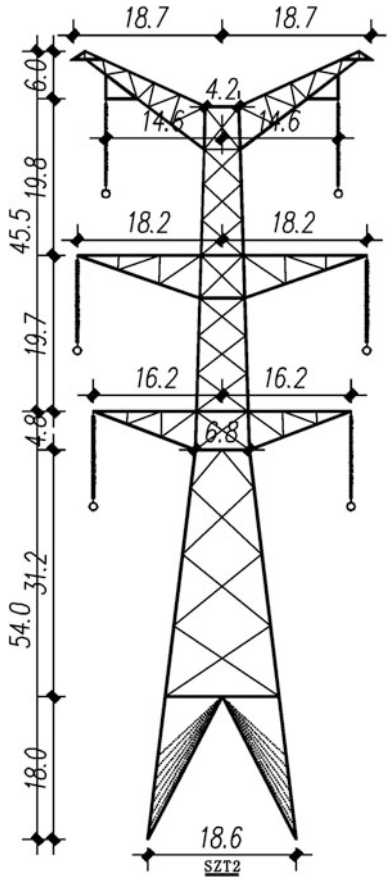

Fig. 13.16 Diagram of tower type of 1000 kV double-circuit line on the same tower (m)

characteristics. The calculation method and result can be referred to in the actual engineering.

The typical tower type used for the 1000 kV Huainan-West Shanghai UHV double-circuit transmission line to Transmit Electricity from Anhui to Eastern China is as shown in Fig. 13.16. For the tower shown in Fig. 13.16, its total height is 99.5 m and its nominal height is 54.0 m. The other parameters of the system: the conductors are 8 × LGJ-630/45 aluminum conductors steel reinforced, one ground wire is LBGJ-240-20A concentric-lay-stranded aluminum-clad steel conductor and the other is OPGW-24B1-254 optical fiber composite overhead ground wire.

For the UHV Huainan-South Anhui-North Zhejiang-West Shanghai Same-tower Double-circuit Transmission Project, the Huainan-South Anhui line is 326.5 km long, the South Anhui-North Zhejiang line is 151 km long, and the North Zhejiang-West Shanghai line is 165 km long. The total length is 642.5 km. The land along the whole line is flat with the altitude lower than 1000 m. The highest altitude is 480 m, located at the mountainous region in North Zhejiang. The weather condition along the line is as shown in Table 13.11.

13.3.1 Impact on Electromagnetic Environment

The phase sequence arrangement of the line affects the electromagnetic environment of its directly, and the latter determines the selection of the cross-section area of the conductor, the confirmation of the ground clearance of conductor and the determination of the width of the line corridor, and influences the construction cost of the line directly. Therefore, it is necessary to study the impact of the phase sequence arrangement on the electromagnetic environment of the line to seek for the optimal arrangement.

As for the 1000 kV transmission line in the residential area, the power frequency electric field intensity shall not exceed 4 kV/m, the power frequency magnetic field intensity shall not exceed 0.1 mT, and the radio interference and the audible noise at 20 m away from the outside of the projection of the side-phase conductor shall not exceed 58 and 55 dB, respectively [7].

Table 13.12 shows the power frequency electric field intensity, the line corridor width, the power frequency magnetic field intensity, the radio interference and the audible noise at 20 m away from the outside of the projection of the side-phase conductor under the 1000 kV double-circuit line on the same tower under six phase sequence arrangements when the bottom-phase conductor thereof is at least 25 m above the ground (with the maximum sag considered).

It can be seen from Table 13.12 that the phase sequence arrangement affects the electromagnetic environment of the double-circuit line on the same tower. The

Table 13.11 Weather condition along the line

Weather condition	Fine days	Snowy days	Rainy days	Rime days
Time (hours per year)	7372	182	1042	164

Table 13.12 Impact of phase sequence arrangements on electromagnetic environment

Phase sequence arrangement	ABC/ABC	ABC/ACB	ABC/BAC	ABC/BCA	ABC/CAB	ABC/CBA
E_{max} (kV/m)	9.79	8.12	9.67	7.71	7.72	7.15
W (m)	71.8	70.6	71.7	69.8	69.8	69.2
B_{max} (μT)	27.22	26.65	27.13	26.55	26.55	26.26
RI (dB)	53.01	54.49	52.97	55.12	55.12	54.43
AN (dB)	49.04	50.42	49.64	51.16	51.16	51.14

selection of the appropriate phase sequence arrangement can improve the electromagnetic environment under the line effectively. Among the six phase sequence arrangements, the maximum power frequency magnetic induction intensity is 27.22 μT, far below the specified limit of 0.1 mT for the power frequency magnetic field intensity; the maximum radio interference at 20 m away from the side-phase conductor is 55.12 dB, lower than the specified limit of 58 dB; the maximum audible noise at 20 m away from the side-phase conductor is 51.16 dB, lower than the specified limit of 55 dB. Therefore, the magnetic field, the radio interference and the audible noise are not the key factors determining the optimal phase sequence arrangement of the line.

Among the parameters of this double-circuit line on the same tower, the power frequency electric field of the line, which determines the confirmation of the ground clearance of the conductor and the delimitation of the line corridor width, is one of the key factors determining the optimal phase sequence arrangement of the line. The power frequency electric field intensity and the line corridor width under the positive phase sequence arrangement ABC/ABC are the highest and those under the negative phase sequence arrangement ABC/CBA are the lowest. Therefore, considered from the angle of the optimal electromagnetic environment, the optimal phase sequence arrangement for the 1000 kV double-circuit line is ABC/CBA.

13.3.2 Impact on Natural Power

The higher the natural power of the line is, the higher the energy that can be transmitted by it will be. The natural power is inversely proportional to the wave impedance of the line. The wave impedance of a transmission line varies with different phase sequence arrangements of the line, so the natural power transmitted by the line varies.

Table 13.13 lists the natural power of the 1000 kV double-circuit line on the same tower under six phase sequence arrangements.

It can be seen from Table 13.13 that the phase sequence arrangement affects the natural power of the line, which is relatively low under the positive phase sequence arrangement while the highest under the negative phase sequence arrangement. The

Table 13.13 Impacts of phase sequence arrangements on natural power

Phase sequence arrangement	ABC/ABC	ABC/ACB	ABC/BAC	ABC/BCA	ABC/CAB	ABC/CBA
P (MW)	8504	8700	8401	9135	9135	9233

natural power under the negative phase sequence arrangement is 729 MW (8.57%) higher than that under the positive phase sequence arrangement, which means that the selection of the appropriate phase sequence arrangement can raise the transmission power of the line. Therefore, considered from the angle of the optimal transmission capacity of the line, the optimal phase sequence arrangement for the 1000 kV double-circuit line is ABC/CBA.

13.3.3 Impact on Unbalance Degree of Line

The unbalance degree of the transmission line is an important indicator to measure the performance of the line and the power quality. The reasonable control of the indicator is of great significance to both the transmission line and the whole electric power system. Since the parameters of various phase conductors are unbalanced, the impedance and the admittance of each phase conductor under the normal operation of the line are made unequal, which, as a result, causes the asymmetrical current and voltage to be generated in the system. When the unbalance degree of the voltage and the current of the system exceed the permissible level, they may affect negatively the equipment of the electric power system in many aspects. Therefore, the selection of the optimal phase sequence to reduce the unbalance degree of the line is of great significance to the design and the operation analysis of the transmission line and to the configuration and the setting of the relay protection devices, etc.

It is specified in the relevant code that, during the normal operation of the power grid, the unbalance degree of the negative sequence voltage shall not exceed 2%, and the short-term unbalance degree shall not exceed 4%. The short-term asymmetrical operation mainly refers to the operating status resulting from the asymmetrical failure occurred in the system. Herein, 2% is provisionally taken as the limit of the unbalance degree of the transmission line (with the unbalance degree of voltage taken as an example).

The asymmetry of the parameters of the transmission line will result in the unbalance of electric quantities of the system during operation. The unbalance degrees of the current and voltage of the system can be measured by the negative sequence and the zero sequence unbalance degrees, respectively.

$$\varepsilon_{U2} = U_2/U_1 \times 100\% \tag{13.22}$$

$$\varepsilon_{U0} = U_0/U_1 \times 100\% \tag{13.23}$$

$$\varepsilon_{I2} = I_2/I_1 \times 100\% \tag{13.24}$$

$$\varepsilon_{I0} = I_0/I_1 \times 100\% \tag{13.25}$$

where

ε_{U2} and ε_{U0} the negative sequence and the zero sequence unbalance degrees of the voltage;
ε_{I2} and ε_{I0} the negative sequence and the zero sequence unbalance degrees of the current;
U_2 and I_2 refer to the negative sequence voltage and current;
U_1 and I_1 refer to the positive sequence voltage and current;
U_0 and I_0 refer to the zero sequence voltage and current.

In the three-phase system, if the amplitude and the phase of the three-phase voltage and current are known, the positive, negative and zero sequence components can be calculated, respectively, by the method of symmetrical components, and the unbalance factor degree of the line can be obtained by Eqs. (13.22)–(13.25).

Taking the case of the North Zhejiang-West Shanghai line Sect. (165 km) to study the impact on the unbalance degree of the line, Table 13.14 lists the negative sequence and the zero sequence unbalance factors of the voltage before the transposition of the line.

It can be known from Table 13.14 that the phase sequence arrangement has great impact on the unbalance degree of the line. The line with the reverse phase sequence arrangement has the lowest unbalance factor, with the unbalance degrees of the negative sequence and the zero sequence voltage being lower than 1%, and no line transposition is required; the line with positive phase sequence arrangement has the highest unbalance factor, beyond the specified limit of 2%, and so the line transposition is required. Please refer to Table 13.15 for the length of the line required to be transposed under six phase sequence arrangements.

It can be known from Table 13.15 that, when the length of the line with the positive phase sequence arrangement is up to 105 km, the unbalance degree of the

Table 13.14 Impacts of phase sequence arrangements on unbalance degrees of negative sequence and zero sequence voltage of UHV double-circuit line

Phase sequence arrangement		ABC/ABC	ABC/ACB	ABC/BAC	ABC/BCA	ABC/CAB	ABC/CBA
ε(%)	ε_{U2}	3.09	2.99	2.93	1.84	1.84	0.94
	ε_{U0}	2.49	2.11	2.44	1.75	1.75	0.82

Table 13.15 Length of Line to be transposed of 1000 kV double-circuit line under various phase sequence arrangements

Phase sequence arrangement	ABC/ABC	ABC/ACB	ABC/BAC	ABC/BCA	ABC/CAB	ABC/CBA
Length of line to be transposed (km)	105	110	115	180	180	350

line exceeds the specified limit and the transposition need to be considered; however, for the line with the reverse phase sequence arrangement, the transposition need to be considered only when the line is up to 350 km long. Therefore, considered from the angle of the optimal unbalance degree of the line, the optimal phase sequence arrangement for the 1000 kV double-circuit line is ABC/CBA.

13.3.4 Impact on Lightning Withstand Performance

The phase sequence arrangement has certain influence on the simultaneous trip-out rate of the double or multiple circuits of the multi-circuit line on the same tower. With the double-circuit line on the same tower with conductors vertically configured taken as an example, for the conductors of two phases at the same layer of the cross arm, if the voltage phases are the same, the over voltages at both ends of the insulator string when the tower top is stricken by the lightning are approximately the same, and the probability of the simultaneous flashover of these two phases is relatively high; if the voltage phases are different, there is a certain phase difference between the conductors of these two phases, equivalent to the formation of a certain differential insulation, which decreases the probability of the simultaneous trip of two circuits. Therefore, in general, the simultaneous lightning trip-out probability under the positive phase sequence arrangement is high and that under the negative phase sequence arrangement is low.

The EMTP is used herein to calculate the back flashover lightning withstand level of the UHV line under six different phase sequence arrangements. In the calculation model, the lightning current adopts the 2.6/50 μs negative ramp wave and the lightning channel wave impedance is taken as 300 Ω; the intersection method as recommended by IEC is used as the flashover criterion for the insulator string; the line adopts the J-Marti model for equivalence; the tower adopts the Hara sectionalized transmission line model for equivalence, the cross arm of the tower is considered as the transmission line wave impedance parallel with the ground, and the propagation velocity rate of the wave on the tower body and the cross arm is light velocity. In addition, the impact of the power frequency voltage of the line is considered by the statistical method and the impact of the corona is neglected temporarily (for the purpose of strictness).

The 1000 kV UHV line has a high insulation level. Even though the impulse grounding resistance of tower is taken as 15 Ω, the back flashover lightning withstand level corresponding to the simultaneous trip of the double-circuit line is still higher than 300 kA under various phase sequence arrangements. It can be deemed that the simultaneous trip of the two circuits will not occur to the 1000 kV UHV double-circuit line on the same tower. Therefore, the impact of the phase sequence arrangement on the lightning protection of the UHV line is negligible. Nevertheless, for the sake of safety, the positive phase sequence arrangement is still not recommended.

13.3.5 Impact on Induced Voltage and Current of Ground Wire

When the transmission line is under normal operation, the spatial positions of the overhead ground wire and the conductors in the transmission circuit are asymmetrical. The transmission circuit generates the induced voltage on the ground wire through the electromagnetic and electrostatic coupling. If there is a current path between the ground wire and the ground, current will be produced, thus resulting in unnecessary energy loss. The loss on the ground wire of the UHV transmission line is relatively prominent, which shall not be neglected. Moreover, if the induced current frequently flows through the ground wire, the ground wire and some transmission equipment will heat and, consequently, age, and their service life will be affected negatively.

For the double-circuit transmission line on the same tower, since the two circuits of lines are set up on the same tower, the conductors are spaced closely, so the electromagnetic coupling and the electrostatic coupling between the conductors and between the conductor and the ground are enhanced, which results in higher induced voltage and induced current on the ground wire. The phase sequence arrangement of the double-circuit line has certain impact on the induced voltage and current. Therefore, the selection of the optimal phase sequence is of great significance to the reduction of the loss on the ground wire in the UHV transmission line and to the optimization of the design.

With the Huainan-South Anhui line section in UHVAC Demonstration Project to Transmit Electricity from Anhui to Eastern China (326.5 km long, and full transposition once for the line) taken as an example, one overhead ground wire is the overhead insulated ground wire, and the other is the optical fiber composite overhead ground wire. EMTP simulation is implemented for the induced voltage and current on the overhead ground wires of the line under the maximum transmission power of the line, and the results are as shown in Table 13.16.

It can be seen from Table 13.16 that the induced voltage and current on the overhead ground wire is the highest under positive phase sequence arrangement, and is the lowest under negative phase sequence arrangement. Therefore,

Table 13.16 Impacts of phase sequence arrangements on induced voltage and current on ground wire

Phase sequence arrangement	ABC/ABC	ABC/ACB	ABC/BAC	ABC/BCA	ABC/CAB	ABC/CBA
Induced voltage (V)	605.74	605.35	484.46	295.43	427.35	258.59
Induced current (A)	37.82	34.41	26.04	17.27	22.19	11.79

considered from the angle of the optimal induced voltage and current on the ground wire, the optimal phase sequence arrangement for the 1000 kV double-circuit line is ABC/CBA.

13.3.6 Recommended Optimal Phase Sequence for UHV Double-Circuit Line on the Same Tower

For the 1000 kV double-circuit line on the same tower, on the basis of the comparison and the analysis of the electromagnetic environment, the natural power, the unbalance degree of the line, the lightning withstand performance and the ground wire's induced voltage and current under six phase sequence arrangements, it can be known that the power frequency electromagnetic field, the radio interference, the audible noise and the back flashover lightning withstand level, etc. are not the key degrees determining the optimal phase sequence arrangement of the line.

The power frequency electric field intensity of the line determines the confirmation of ground clearance of conductor and the delimitation of line corridor width. The natural power embodies the transmission capacity of the line, and the unbalance degree measures the line performance and power quality. The three factors shall be taken into comprehensive consideration during the selection of the optimal phase sequence of the double-circuit line on the same tower, so as to choose an arrangement with the relatively low cost, the low electromagnetic pollution, the high transmission power and the low unbalance degree of the line. The simulation results in this section shows that the line with ABC/CBA reverse phase sequence arrangement has the lowest power frequency electric field, the highest natural power, the lowest unbalance degree of the line and the smallest induced current and voltage of the ground wire. Therefore, it is recommended that the reverse phase sequence ABC/CBA be adopted for the 1000 kV double-circuit line on the same tower.

It is noteworthy that, when the line passes the areas at a high altitude, the radio interference, the audible noise and the corona loss of the line will increase. When the altitude is higher than 1000 m, the audible noise of the line under the reverse phase sequence arrangement will exceed 55 dB, beyond the limit, becoming an important factor restricting the erection of the line. In this case, it is recommended to raise the ground clearance of conductor, increase the cross-section area of the

conductor and the number of sub-conductors and apply the water-repellent material on the surface of the conductor as well as take other measures to reduce the audible noise of the line.

13.4 Safe Distance of UHV Transmission Line Over Buildings

13.4.1 Necessity of Research on Safe Distance

As the corridor resource of the transmission line is running shorter and shorter, the cost in the requisition of the land for corridor use and in the compensation for demolition is accounting for higher and higher percentage in the construction investment of the transmission line, it is inevitable that the transmission line spans over or is erected adjacent to the buildings.

When the transmission line is spanning over or adjacent to the building, the necessary safe distance between the line and the building is mainly determined by two factors: one is the clearance required for the electrical insulation, and the other is the electromagnetic environment. For the non-residential buildings, the safe distance depends on the clearance between the building and the line. The relevant code recommends the vertical safe distance (D_c) and horizontal safe distance (D_s) required between the transmission lines of different voltage levels and the buildings when the lines span over the buildings, as shown in Table 13.17 [8]. These recommendations can be adopted in the actual engineering. For the residential (civil) buildings, the safe distance depends mainly on the electromagnetic environment. This section mainly studies the distortion degree of the electromagnetic environment of the transmission line spanning over or being adjacent to the residential buildings and the safe distance between the building and the line.

The field distorts because of the intervention of objects. When the transmission line spans over the buildings, the power frequency electric field of the line is easy to be affected by the buildings, so the electric field intensity around the buildings will distort more seriously. The magnetic field, however, does not distort as obviously as the electric field does because the distribution of the magnetic field will not be

Table 13.17 Vertical and horizontal safe distances required for transmission line over non-residential buildings

Voltage level of line	110 kV	220 kV	330 kV	500 kV	750 kV	1000 kV
D_c(m)	5.0	6.0	7.0	9.0	11.5	15.5
D_s(m)						
Without wind deflection	2.0	2.5	3.0	5.0	6.0	7.0
Maximum wind deflection	4.0	5.0	6.0	8.5	11.0	15.0

changed unless the magnetic material is introduced into the power frequency magnetic field. Meanwhile, the existence of the buildings changes the distribution of the space charges and the electric field intensity on the conductor surface, and consequently affects the radio interference and the audible noise of the line.

When the transmission line spans over the building, the electromagnetic field intensity, the radio interference and the audible noise inside the building are attenuated to varying extents because of the shielding effect of the building, while the indicators of the electromagnetic environment on the roof platform of the building and on the balcony close to the line are prone to increase beyond the limit due to the influence of distortion, becoming the main subject to be studied.

It is shown by the study that, when the line spans over or is adjacent to the building, the power frequency magnetic induction intensities inside and outside the building are both lower than the specified limit of 0.1 mT provided that the safe distance recommended by the code is kept, and so may not be considered in the actual engineering.

The building affects the field intensity on the conductor surface to some extent. However, the distortion degree of the field intensity on the conductor surface decreases with the increase of the distance between the building and the conductor. When the distance between the building and the conductor exceeds 20 m, the distortion degree of the field intensity on the conductor surface approximates to zero; in such case, it can be deemed that there is no distortion in the radio interference and the audible noise of the line.

The power frequency electric field distorts to a great extent due to the existence of the buildings, and attenuates at a slow rate with the increase of the safe distance between the conductor and the building. Therefore, the distorted electric field is the key factor restricting the safe distance between the conductor and the building.

With the Huainan-West Shanghai 1000 kV UHV Double-circuit Transmission Line to Transmit Electricity from Anhui to Eastern China taken as an example, the distortion of the power frequency electric field on the roof and the balcony of the building when the line spans over or is adjacent to the building is simulated, and the minimum vertical and horizontal safe distances required for the line over the building are obtained.

13.4.2 Calculation Methods and Simulation Models

13.4.2.1 Calculation Methods

(1) Power Frequency Electromagnetic Field

There are a variety of numerical calculation methods for the space power frequency electromagnetic field of the transmission line. In the past, the charge simulation method and the analytic method were generally used when the space medium was uniformly distributed, without consideration of the existence of buildings near the

line; the space power frequency magnetic field intensity of the line was generally calculated by the two-dimensional method derived from Ampere's Circuital Law (recommended by the International Council on Large Electric Systems) and the three-dimensional calculation method derived from Biot-Savart Law. However, when the line spans over the buildings, the space medium becomes non-uniform and the change of the attribute of medium results in the change of the space electric field intensity and the magnetic induction intensity, especially severe distortion of the field intensity at the boundary between the building and the air. The 3D finite element method can usually be used to analyze the space electromagnetic field with the non-uniform medium. In this section, the HIFREQ module (3D finite element method) in the CDEGS software is used to stimulate the distortion degree of the electric field and the magnetic field when the UHV transmission line spans over or is adjacent to the buildings.

(2) Radio Interference and Audible Noise

Due to the complicated impacts of the weather conditions on the radio interference and the audible noise of the transmission line, with multiple random factors and the high dispersity, the forecasting of the radio interference and the audible noise in various countries are generally derived from the simulation in the corona cage or from the statistics and the analysis of the values measured from the test line section in a long duration. In China, it is suggested to utilize the excitation function method to calculate the radio interference field intensity of the UHVAC transmission line and the method recommended by Bonneville Power Administration (BPA) to forecast the audible noise.

The key factor affecting the radio interference and the audible noise of the line is the electric field intensity on the conductor surface. When the transmission line spans over or is adjacent to a building, the change in the distribution of the space charges due to the existence of the metallic objects inside the building affects the electric field intensity on the conductor surface, and the radio interference and the audible noise of the line, as well. In this section, the CDEGS software is used to simulate the distortion degree of the field intensity on the conductor surface of the transmission line when there are buildings near the transmission line, and then the calculated field intensity on the conductor surface is substituted into the calculation equation for the radio interference and the audible noise to obtain the distortion degree of the radio interference and the audible noise caused by the buildings.

13.4.2.2 Simulation Models

The building is simulated with the simplified structure and the impact of building walls and other media is ignored. According to the overall structure of the building and in consideration of the simplest outline of the building, it is equivalent to the reinforcement bracket structure, as shown in Fig. 13.17a, b. In the figure, the reinforcement bar is 0.015 m in radius, and 21 (pcs/100 m^2) in density; the building area is 10 × 10 m^2, the first storey is 4 m high and other storeys are 3 m high.

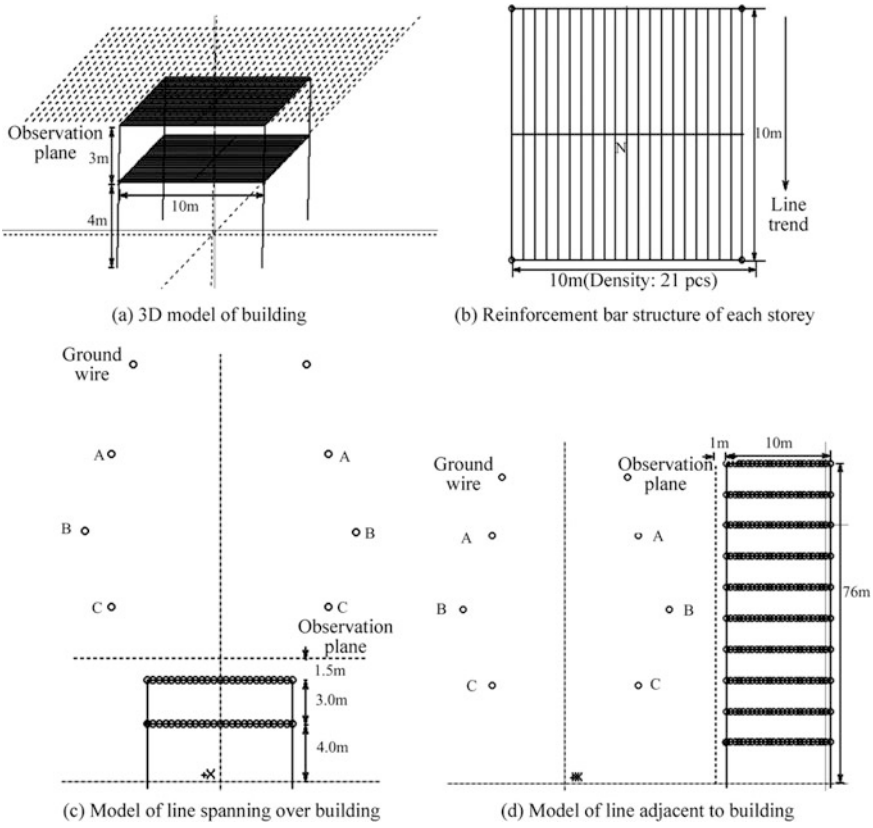

Fig. 13.17 Simulation of transmission line spanning over and adjacent to building

When the transmission line spans over a building (the building is located under the line), the electric field intensity inside the building decreases greatly due to the shielding effect of the building, while the electric field intensity on the roof of the building increases due to the impact of the distortion. Therefore, when the line spans over the building, the building's roof platform shall be taken as the major object to be observed. The observation plane shall be the horizontal plane 1.5 m above the building's roof platform, as shown in Fig. 13.17c.

When the transmission line is adjacent to the building (the building is located beside the line), similarly, the impact of the distorted electric field inside the building is neglected, but the electric field at the balcony and the window that close to the line is apt to exceed the specified limit due to the impact of distortion. In such case, the observation plane shall be positioned at the building balcony close to the line, as shown in Fig. 13.17d.

13.4.3 Discussion on Influence Factors of Distorted Electric Field

The distorted electric field is a key factor determining the safe distance between the line and the building. The reinforced bar structure of the building affects the distribution of space charges and changes the space electric field intensity. The differences in the structure of building, such as the area, the height, the density and the diameter of the reinforcement, result in the varied distortion degrees of the power frequency electric field adjacent to the building. In addition, the height of the tower (the ground clearance of conductor) and the phase sequence arrangement have obvious impact on the power frequency electric field of the line, and are also the key factors influencing the distorted electric field.

4 kV/m is taken as the criterion to assess the power frequency electric field to which the public are exposed in a whole day in the relevant code, which is also taken as a basis of the design and the construction of the transmission line in China. With respect to the distorted electric field, because of the lack of relevant study both in China and other countries, no limit is specified clearly, so 4 kV/m is used as the limit provisionally in this section to estimate the safe distance required for the UHV line over the building.

To calculate the safe distance for the UHV line over the building accurately, this section takes the case of the 1000 kV double-circuit line on the same tower to calculate to what extent the distorted electric field and the safe distance at the roof and the balcony of the building change with the change of the building structure, the tower height and the phase sequence arrangement, etc., and establish the effective measures to reduce the distorted electric field intensity adjacent to the building and save the line corridor.

In the calculation hereinafter, it is assumed that the bottom-phase circuit of the double-circuit line is 25 m above the ground, which is the minimum value as specified in the relevant code. With the increase of the height of the bottom-phase circuit above the ground, the vertical and horizontal safe distances required for the line will decrease to some extent.

13.4.3.1 Impact of Building Structure

1. Impact of Building Height

The building height has certain impact on the vertical and horizontal safe distances required for the line over the building. This section first analyzes the impact of the building height on the distorted electric field intensity and the vertical safe distance when the building being spanned over is 4–22 m high. During the analysis, the vertical safe distance between building and transmission line is taken as the recommended practice value 15.5 m (as shown in Table 13.17), then the distorted electric field intensity on the top of buildings can be obtained. Then the vertical safe distance

needed by the building can be calculated by taking 4 kV/m as the limit value standard. In addition, this section analyzes the impact of the building height on the distorted electric field intensity and the horizontal safe distance when the building adjacent to the line is 4–91 m high. During the analysis, the horizontal safe distance between building and transmission line is taken as the recommended practice value 7.0 m (as shown in Table 13.17), then the distorted electric field intensity near the balcony of buildings can be obtained. Then the horizontal safe distance needed by the building can be calculated by taking 4 kV/m as the limit value standard. The calculated results are as shown in Table 13.18, Figs. 13.18 and 13.19.

It can be seen from Table 13.18 that, under the vertical and horizontal safe distances recommended by the code, the distorted electric field intensity at the building's roof and balcony (close to the line) is much higher than the limit of 4 kV/m. Moreover, when the distance between the line and the building is kept constant, the higher the building is, the higher the distorted electric field intensity will be. The maximum distorted electric field intensity on the building's roof increases from 10.18 to 14.21 kV/m when the building height is raised from 4 to 22 m; the maximum distorted electric field intensity on the building's balcony increases from 6.42 to 56.33 kV/m when the building height is raised from 4 to 91 m.

It can be known from Fig. 13.18 that the higher the building is, the larger the vertical safe distance required between the building and the conductor will be. It is noteworthy that the safe distance increases at an increasingly slower rate with the increase of the building height.

It can be know from Fig. 13.19 that the higher the building is, the larger the horizontal safe distance required between the building and the conductor will be. It is noteworthy that the safe distance increases at an increasingly slower rate with the increase of the building height. When the building is higher than 37 m, the required horizontal safe distance keeps constant, i.e., 33.6 m.

2. Impact of Building Area

Table 13.19 shows the impact of the building area on the distorted electric field intensity and the vertical and horizontal safe distances required between the building and the conductor.

It can be seen from Table 13.19 that, when the line spans over the building, the larger the building area is, the higher the distorted electric field intensity will be, and the larger the required vertical safe distance will be. The vertical safe distance increases by 9.9 m when the building area increases from 36 to 196 m^2; when the line is adjacent to the building, the larger the building area is, the lower the distorted electric field intensity will be and the smaller the required horizontal safe distance will be. The horizontal safe distance decreases by 0.6 m when the building area increases from 36 to 196 m^2. It can be concluded that the building area has little impact on the horizontal safe distance of the line.

3. Impact of Density of Reinforcement Bars in Building

When the density of reinforcement bars in building increases from 11 to 31 pcs per 100 m^2, the changes of the distorted electric field intensity and the vertical and the

Table 13.18 Impact of building height on distorted electric field intensity and safe distance

Building height	Building spanned over			
	The vertical safe distance recommended by code D_s (m)	The calculated distorted electric field intensity E_{max} (kV/m)	The limit of distorted electric field intensity E_{max} (kV/m)	The vertical safe distance needed by calculation D_s (m)
1-storey (4 m)	15.5	10.18	4	33.2
2-storey (7 m)		11.63		35.7
3-storey (10 m)		12.58		39.2
4-storey (13 m)		13.21		41.1
5-storey (16 m)		13.65		42.7
6-storey (19 m)		13.97		44.0
7-storey (22 m)		14.21		45.1
Building height	Building adjacent			
	The horizontal safe distance recommended by code D_s (m)	The calculated distorted electric field intensity E_{max} (kV/m)	The limit of distorted electric field intensity E_{max} (kV/m)	The horizontal safe distance needed by calculation D_s (m)
1-storey (4 m)	7.0	6.42	4	15.4
5-storey (16 m)		18.14		27.4
10-storey (31 m)		31.40		32.9
15-storey (46 m)		55.22		33.6
20-storey (61 m)		55.64		33.6
25-storey (76 m)		56.32		33.6
30-storey (91 m)		56.33		33.6

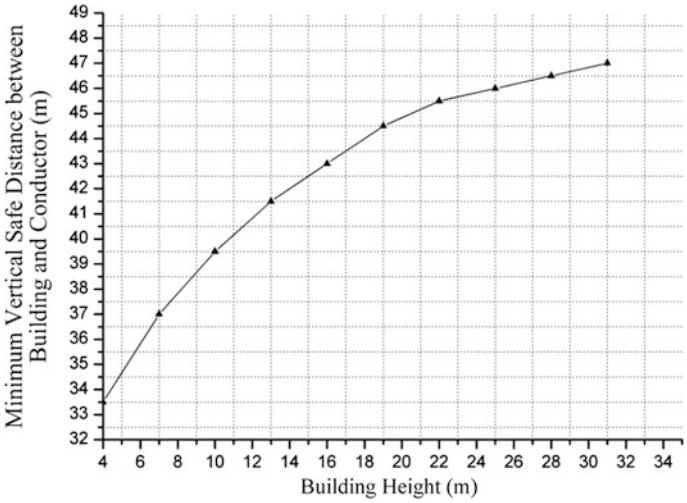

Fig. 13.18 Diagram of impact of building height on vertical safe distance

horizontal safe distances required between the building and the conductor are as shown in Table 13.20.

It can be seen from Table 13.20 that, with the increase of the density of reinforcement bars on each storey of the building, the distorted electric field intensity on the building's roof increases and the vertical safe distance required increases, while the distorted electric field intensity on the building's balcony and the horizontal safe distance required basically keeps unchanged. When the density of reinforcement bars on each 100 m^2 increases from 11 to 31 pcs, the vertical safe distance only increases by 1.5 m, while the horizontal safe distance basically keeps unchanged. Therefore, the density of reinforcement bars on each storey affects little the safe distance required between the building and the line.

4. Impact of Radius of Reinforcement Bars in Building

When the radius of the reinforcement bars in building increases from 0.005 to 0.025 m, the changes of the distorted electric field intensity and the vertical and horizontal safe distances between the building and the conductor are as shown in Table 13.21.

It can be seen from Table 13.21 that, with the increase of the radius of reinforcement bars used in the building, the distorted electric field intensity on the roof and the balcony of the building increases and the vertical and horizontal safe distances required slightly increase. When the radius of the reinforcement bars increases from 0.005 to 0.025 m, the vertical safe distance only increases by 0.5 m and the horizontal safe distance only increases by 0.9 m. Therefore, the radius of reinforcement bars in the building has little impact on the safe distance required between the building and the line.

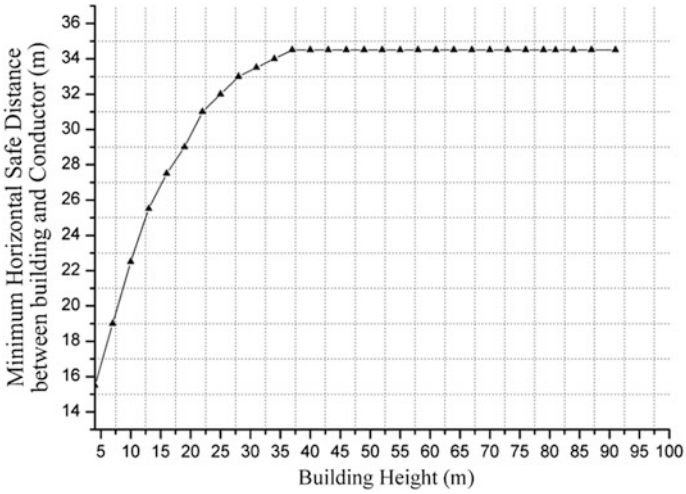

Fig. 13.19 Diagram of impact of building height on horizontal safe distance

Table 13.19 Impact of building area on distorted electric field intensity and safe distance

Building area (m^2)	Building spanned over (2-storey)			
	The vertical safe distance recommended by code D_s (m)	The calculated distorted electric field intensity E_{max} (kV/m)	The limit of distorted electric field intensity E_{max} (kV/m)	The vertical safe distance needed by calculation D_s (m)
6 × 6	15.5	8.31	4	27.3
8 × 8		9.27		28.7
10 × 10		11.63		36.7
12 × 12		12.60		36.8
14 × 14		13.64		37.2
Building area (m^2)	Building adjacent (15-storey)			
	The horizontal safe distance recommended by code D_s (m)	The calculated distorted electric field intensity E_{max} (kV/m)	The limit of distorted electric field intensity E_{max} (kV/m)	The horizontal safe distance needed by calculation D_s (m)
6 × 6	7.0	55.81	4	34.1
8 × 8		55.45		33.9
10 × 10		55.22		33.6
12 × 12		55.19		33.5
14 × 14		55.15		33.5

Based on study of the impacts of the building height, the building area, the density and the radius of reinforcement bars on the distorted electric field intensity and the safe distance, it is concluded that:

1. The building height has obvious impact on the distorted electric field intensity and the safe distance. The higher the building is, the larger the distorted electric field intensity will be, and the larger the required safe distance between the building and the conductor will be. However, with the increase of building height, the safe distance increases at an increasingly slower rate.
2. The building area, the density and the radius of reinforcement bars have little impact on the distorted electric field intensity and the safe distance required between the building and the line.

13.4.3.2 Impact of Tower Height

When the line spans over the building, the increase of the tower height increases the vertical safe distance between the line and the building, and can reduce the distorted electric field intensity on the roof of the building. However, the change of the tower

Table 13.20 Impact of density of reinforcement bars in building on distorted electric field intensity and safe distance

Density of reinforcement bars (pcs/100 m^2)	Building spanned over (2-storey)			
	The vertical safe distance recommended by code D_s (m)	The calculated distorted electric field intensity E_{max} (kV/m)	The limit of distorted electric field intensity E_{max} (kV/m)	The vertical safe distance needed by calculation D_s (m)
11	15.5	11.35	4	35.5
16		11.54		35.9
21		11.63		36.7
26		11.71		36.9
31		11.76		37.0
Density of reinforcement bars (pcs/100 m^2)	Building adjacent (15-storey)			
	The horizontal safe distance recommended by code D_s (m)	The calculated distorted electric field intensity E_{max} (kV/m)	The limit of distorted electric field intensity E_{max} (kV/m)	The horizontal safe distance needed by calculation D_s (m)
11	7.0	55.40	4	33.7
16		55.28		33.6
21		55.22		33.6
26		55.19		33.6
31		55.17		33.6

height can also affect the horizontal safe distance. This section studies mainly the relationship between the tower height and the distorted electric field intensity and the horizontal safe distance when the line is adjacent to the building. Two typical conditions are chosen for simulation: one-storey building of 4 m high (low building) and 15-storey building of 46 m high (high building).

Table 13.22 shows the change in the distorted electric field intensity and the horizontal safe distance when the bottom-phase conductor is raised from 25.0 to 33.0 m above the ground.

Table 13.22 shows that, for the line adjacent to the one-storey building of 4 m high, when the height of the bottom-phase conductor is raised from 25.0 to 33.0 m, the horizontal safe distance decreases by 2.0 m; for the line adjacent to 15-storey building of 46 m high, when the height of the bottom-phase conductor is raised from 25.0 to 33.0 m, the horizontal safe distance basically keeps unchanged.

For the UHV transmission line, the increase of the ground clearance of the conductor does not affect greatly the distorted electric field intensity and horizontal safe distance at balcony. Meanwhile, the increase of the height above the ground of conductor can increase the construction cost and cut down the lightning withstand performance of the line. Therefore, the increase of the tower height and the line corridor width shall be weighed and compared from the perspective of cost efficiency in the actual engineering to determine the reasonable height of the conductor.

Table 13.21 Impact of radius of reinforcement bars in building on distorted electric field intensity and safe distance

Radius of reinforcement bar (m)	Building spanned over (2-storey)			
	The vertical safe distance recommended by code D_s (m)	The calculated distorted electric field intensity E_{max} (kV/m)	The limit of distorted electric field intensity E_{max} (kV/m)	The vertical safe distance needed by calculation D_s (m)
0.005	15.5	11.41	4	36.3
0.010		11.56		36.5
0.015		11.63		36.7
0.020		11.71		36.8
0.025		11.76		36.8
Radius of reinforcement bar (m)	Building adjacent (15-storey)			
	The horizontal safe distance recommended by code D_s (m)	The calculated distorted electric field intensity E_{max} (kV/m)	The limit of distorted electric field intensity E_{max} (kV/m)	The horizontal safe distance needed by calculation D_s (m)
0.005	7.0	53.00	4	33.0
0.010		54.33		33.3
0.015		55.22		33.6
0.020		55.90		33.8
0.025		56.47		33.9

13.4.3.3 Impact of Phase Sequence Arrangement

The phase sequence arrangement has obvious impact on the electromagnetic environment of the double-circuit line on the same tower. The selection of the reasonable phase sequence arrangement can economically and effectively reduce the power frequency electric field intensity under the line. This section calculates the changes in the distorted electric field intensity and the horizontal safe distance under two phase sequence arrangements of the 1000 kV same-tower double-circuit transmission line spanning over or being adjacent to the building. The results are shown in Table 13.23.

It can be seen from Table 13.23 that the selection of the appropriate phase sequence arrangement can reduce effectively the distorted electric field intensity and the safe distance between the line and the building when the line spans over the building. When the line spans over or is adjacent to the building, the positive phase sequence arrangement (ABC/ABC) results in the highest distorted electric field intensity at the roof and the balcony of the building and the largest vertical and horizontal safe distance, while the reverse phase sequence arrangement (ABC/CBA) is contrary thereto. Compared with the positive phase sequence

Table 13.22 Impact of tower height on distorted electric field intensity and horizontal safe distance

Height of the bottom-phase conductor (m)	1-storey building of 4 m High			
	The horizontal safe distance recommended by code D_s (m)	The calculated distorted electric field intensity E_{max} (kV/m)	The limit of distorted electric field intensity E_{max} (kV/m)	The horizontal safe distance needed by calculation D_s (m)
25.0	7.0	6.42	4	15.4
27.0		6.19		14.7
29.0		5.97		14.3
31.0		5.75		13.9
33.0		5.54		13.4
Height of the bottom-phase conductor (m)	15-storey building of 46 m High			
	The horizontal safe distance recommended by code D_s (m)	The calculated distorted electric field intensity E_{max} (kV/m)	The limit of distorted electric field intensity E_{max} (kV/m)	The horizontal safe distance needed by calculation D_s (m)
25.0	7.0	55.22	4	33.6
27.0		55.19		33.6
29.0		55.17		33.5
31.0		55.16		33.5
33.0		56.15		33.5

Table 13.23 Impact of phase sequence arrangement on distorted electric field intensity and safe distance

Phase sequence arrangement	Building spanned over (2-storey)			
	The vertical safe distance recommended by code D_s (m)	The calculated distorted electric field intensity E_{max} (kV/m)	The limit of distorted electric field intensity E_{max} (kV/m)	The vertical safe distance needed by calculation D_s (m)
ABC/ABC	15.5	20.48	4	78.0
ABC/CBA		11.63		36.7
Phase sequence arrangement	Building adjacent(15-storey)			
	The horizontal safe distance recommended by code D_s (m)	The calculated distorted electric field intensity E_{max} (kV/m)	The limit of distorted electric field intensity E_{max} (kV/m)	The horizontal safe distance needed by calculation D_s (m)
ABC/ABC	7.0	59.23	4	66.0
ABC/CBA		55.22		33.6

arrangement, the reverse phase sequence arrangement reduces the vertical safe distance by 41.3 m and the horizontal one by 32.4 m. In conclusion, the reasonable selection of the phase sequence arrangement of the double-circuit line is the most cost-effective measure to reduce the distorted electric field intensity and save the line corridor.

13.4.4 Calculation of Safe Distance for UHV Transmission Line Over Building

To enable the study results to better guide the actual engineering, this section calculates the vertical and horizontal safe distances required for the UHV single-circuit and double-circuit transmission lines spanning over and being adjacent to the buildings of various heights, as shown in Table 13.24. In the simulation of transmission line adjacent to the building, the height of the bottom-phase conductor of the line is determined at the minimum height of the conductor in the residential area as specified in the relevant code, i.e., 27 m for the sing-circuit line and 25 m for the double-circuit line.

Table 13.24 Safe distance for UHVAC line spanning over or being adjacent to building

Vertical safe distance D_c (m)			Horizontal safe distance D_s (m)		
Building height	Single-circuit line	Double-circuit line	Building height	Single-circuit line	Double-circuit line
1-storey (4 m)	36.0	33.2	1-storey (4 m)	32.0	15.4
2-storey (7 m)	40.5	36.7	5-storey (16 m)	47.8	27.4
3-storey (10 m)	43.8	39.2	10-storey (31 m)	56.5	32.9
4-storey (13 m)	46.4	41.1	15-storey (46 m)	60.0	33.6
5-storey (16 m)	48.6	42.7	20-storey (61 m)	61.7	33.6
6-storey (19 m)	50.6	44.0	25-storey (76 m)	61.7	33.6
7-storey (22 m)	52.2	45.1	30-storey (91 m)	61.7	33.6

13.5 Electromagnetic Environment of UHVAC Substation

The impact of the UHVAC substation on the surrounding electromagnetic environment is usually manifested by the 4 indicators, namely, the power frequency electric field, the power frequency magnetic field, the radio interference and the audible noise. When the electromagnetic environment of the substation deteriorates, it may interfere with the normal receipt of the radio and may affect negatively the daily working and living of the workers in the substation and the surrounding residents. Therefore, the electromagnetic environment of the UHVAC substation must be studied and supervised, and controlled within the safety limits through certain measures.

13.5.1 Power Frequency Electric Field

Certain power frequency electric field must inevitably exist around the live conductors and HV equipment in the outdoor substation. The electric field intensity depends on the voltage level and the distance to the electrified object. The electric field intensity attenuates gradually with the increase of distance. In general, in the substation, the electric field intensity near the switches, instrument transformers and other equipment as well as near the conductor intersection points is relatively high, and shall be specially paid attention to. In the substation installed with GIS, however, the electric field intensity is relatively low because of the shielding effect of the GIS metal bushing.

It is specified in Q/GDW 305-2009 *Limits for Electromagnetic Environment of 1000* kV *Overhead Transmission Line* of State Grid that the electric field intensity shall not exceed 4 kV/m at the electromagnetic environment-sensitive object 1.5 m above the ground; not exceed 7 kV/m where the line spans over the highways; not exceed 10 kV/m at the object that is not sensitive to the electromagnetic environment or where the line spans over the farmland [9].

The power frequency electric field with too high intensity may impair the human health and the normal operation of the secondary sensitive equipment. The following measures can be taken to mitigate the damage caused by the electric field with too high intensity:

1. Use the metal pipes to shield the radiation of the electric field generated by equipment and conductors by introducing the GIS technology.
2. Optimize the design of the substation, raise the height of line equipment appropriately and prevent the path for patrol inspection passing though the high-intensity area.
3. Utilize the buildings and facilities in the substation to form a metallic shielding network to realize the passive shielding.
4. Require the working personnel in the substation to wear shielding clothing, shoes and helmet to protect safety when necessary.

13.5.2 Power Frequency Magnetic Field

The power frequency magnetic field in the substation is determined by the power frequency current flowing through the live object and the distance to the live object. Compared with the electric field, the actual distribution of the magnetic field attenuates at a much faster rate with the increase of the distance. Unlike the power frequency electric field, there is little difference between the power frequency magnetic field radiation in the GIS substation and the outdoor substation, because the metallic material of the GIS bushing is relatively low in the magnetic conductivity and has minor effect on the shielding of magnetic field. In addition, the air-cored reactor adopted in some substations can generate intense magnetic field to the surroundings because it has no closed magnetic loop.

By reference to Q/GDW 305-2009 *Limits for Electromagnetic Environment Generated by 1000* kV *Overhead Power Transmission Lines*, the power frequency magnetic flux density at the object sensitive to the electromagnetic environment and at 1.5 m above the ground shall not exceed the limit of 0.1 mT [9].

The following measures can be taken to mitigate the negative impact on the equipment and the human body due to the power frequency magnetic field with too high intensity:

(1) Similar to the measures to control the power frequency electric field, optimize the design of the substation and arrange the main control room, the patrol

inspection paths and other major areas far away from the magnetic field sources.

(2) If the air-cored reactor is adopted in substation, there will be high power frequency magnetic field intensity around it. To solve the problem, use current-limiting reactor with the iron core to replace the air-cored reactor or set up special shields.

13.5.3 Radio Interference

The radio interference of substation is generated by the corona discharge, the gap spark discharge and other high-frequency pulse current, among which the corona discharge is the most important factor. Compared with the outdoor substation, the GIS substation can eliminate the impact from the corona discharge of the conductor (busbar) and fittings, and hence its radio interference level will be reduced dramatically.

By reference to Q/GDW 305-2009 *Limits for Electromagnetic Environment Generated by 1000* kV *Overhead Power Transmission Lines*, the radio interference shall be lower than 58 dB at 20 m away from the outside of the projection of the side-phase conductor on the ground and 2 m above the ground when the frequency is 0.5 MHz, so that the radio interference measurement value under good weather condition is not higher than 55 dB. The altitude correction is based on the height of 500 m. The radio interference is increased by 1 dB for every 300 m rise in altitude [9].

In the UHVAC substation, the radio interference generated by the main equipment is impossible to be eliminated completely, but it can be reduced by enhancing the corona discharge voltage through the rational planning of the design of the conductor (busbar) and fittings and the enlargement of annular and tubular diameters of fittings, or by alleviating the impact of the corona discharge through the utilization of GIS equipment.

13.5.4 Noise

The noise resources in the UHVAC substation includes mainly the corona noise caused by corona discharge of the live object, electromagnetic and mechanical noises generated by transformers, reactors and other main equipment in operation.

By reference to Q/GDW 305-2009 *Limits for Electromagnetic Environment Generated by 1000* kV *Overhead Power Transmission Lines*, the audible noise of a wet conductor shall not exceed 55 dB (A) at 20 m away from the outside of the projection of the side-phase conductor of the transmission line and shall satisfy the acoustic environment standard approved by the environmental protection authority [9].

According to the law of sound propagation, the control of the noise impact can be realized by controlling the noise source, the propagation path and the receiver. The corresponding measures to reduce the noise pollution of the substation include:

(1) Reduce the electromagnetic and mechanical noises of transformers and reactors, the corona noise of conductors and fittings by means of design optimization.
(2) Utilize the sound-absorbing and sound-insulating barriers to interrupt the propagation of noise.
(3) Require the working personnel in the substation to wear ear plugs and earmuffs to guard against the occupational injury.

References

1. DL/T 1187-2012. Control levels for electromagnetic environment produced by 1000 kV overhead transmission line. 2012.
2. HJ/T 24-1998. Technical Regulations on environmental impact assessment of electromagnetic radiation produced by 500 kV ultrahigh voltage transmission and transfer power engineering. 1998.
3. Liu W, Zhao Q, Hu Z, Li X, Kang L, Zhao Y. Study on the corona loss estimate under the 1000 kV UHVAC transmission line. Electr Power Constr. 2011;32(10):27–9.
4. GB 15707-1995. Limits of radio interference from AC high voltage overhead power transmission lines. 1996.
5. GB 3096-2008. Environmental quality standard for noise. 2008.
6. Q/GDW 550-2010. Design and construction guide for reducing audible noise of transmission line. 2010.
7. Q/GDW 304-2009. Technical regulations for impact assessment of electromagnetic environment produced by 1000 kV transmission and transfer power engineering. 2009.
8. Q/GDW 178-2008. Provisional technical code for design of 1000 kV AC overhead transmission line. 2008.
9. Q/GDW 305-2009. Limits for electromagnetic environment generated by 1000 kV overhead power transmission lines. 2009.

Chapter 14
Principles and Configurations of UHVAC Protection

Laqin Ni, Jiyuan Li and Zhiyong Qiu

14.1 Basic Overview of UHVAC Protection

14.1.1 Basic Requirements of UHVAC Protection

The operating experience of UHVAC transmission project shows that the insulation flashover or breakdown on the power transmission line and electrical equipment in the substation is the main reason leading to the electric power system failure. The UHV power grid has high requirements on insulation, and the electrical equipment such as line insulators, arrestors, transformers and switches has lower withstand margin for overvoltage. Occurrence of failure will cause considerable loss, and therefore, overvoltage limitation is the primary factor to be considered in the relay protection configurations of UHVAC system. The basic requirements of protection configuration schemes are as follows [1, 2]:

(1) The four requirements of rapid action, sensitivity, selectivity, and reliability for relay protection shall be met, and the whole system shall meet, as a whole, the higher level of such four requirements.

L. Ni (✉) · Z. Qiu
East Branch of State Grid Corporation of China, No. 882, South of Pudong Road, Shanghai, People's Republic of China
e-mail: ni_lq@ec.sgcc.com

Z. Qiu
e-mail: qiu_zy@ec.sgcc.com

J. Li
College of Electrical Engineering, Zhejiang University, Xihu District, Hangzhou, Zhejiang, People's Republic of China
e-mail: lijiyuan_ee@zju.edu.cn

© Zhejiang University Press, Hangzhou and Springer-Verlag GmbH Germany 2018

H. Zhou et al. (eds.), *Ultra-high Voltage AC/DC Power Transmission*, Advanced Topics in Science and Technology in China,
https://doi.org/10.1007/978-3-662-54575-1_14

(2) When making up the protection configuration scheme, it is allowable can be guaranteed that only the failures are cleared in case of occurrence of multiple failures at the same time.
(3) For each of the protected objects in the UHV power grid (main equipment or power transmission lines), two sets of protection devices, with the main protection integrated with the backup protection, shall be configured. The secondary input/output (including tripping and closing) circuit, information transmission channel, and power input circuit for each set of protection devices shall be independent of another protection device.
(4) The current transformer (CT) for protection shall be configured, so that the dead zone of the main protection can be avoided. When the secondary winding of CT that is connected to the protection is distributed, the dead zone of protection action shall be avoided in case of occurrence of any failures in the protected zone when a protection is out of service, and meanwhile, the impact of CT shall be mitigated as far as possible in case of failure by itself.
(5) To improve the reliability of transmitting the tripping order, an independent remote tripping device and an independent order transmission channel shall be established.
(6) Reasonable overvoltage limiting devices shall be configured according to various overvoltage cases that might exist in the UHV power grid.
(7) The protection device shall be provided with independent starting elements. Only when any disturbance occurs on the electric power system, the opening of the outlet tripping circuit can be allowed.
(8) When the line has any unexpected abnormal power frequency overvoltage that endangers the insulation, the overvoltage protection shall be able to disconnect the relevant circuit breakers. When the system is running properly or under the interference by the transient process of the system, there should not be any mis-operations.

14.1.2 Setting Principles of the UHVAC Protection

The setting of UHVAC protection is almost similar to the setting of extra high-voltage (EHV) protection as a whole. However, since the UHVAC system has different equipments and strengths of grid framework structure with EHVAC system, there is some differences in protection setting [3–5].

(1) The common operating modes on which the setting calculation of the UHV system is based are similar to those of the EHV system. For transmission lines with the level above 220 kV, the normal operation mode of a primary circuit or one element's maintenance adjacent to the protected equipment is normally taken into consideration. Considering the homochronous tripping of the

double-circuit lines on the same tower in UHV power grid, it is necessary to consider disconnecting two elements in sequence. However, for the EHV power grid with sufficient strength of grid framework structure, it is necessary to consider disconnecting 2–3 elements in sequence, since there are many elements and circuits on its busbar.

The actual operation shows that, for 500 kV transmission lines, the accident of the homochronous tripping of the double-circuit lines on the same tower is difficult to happen, which is almost impossible to occur for 1000 kV transmission lines. Therefore, the setting calculation mode of disconnecting two elements in sequence considering the accident of the homochronous tripping of the double-circuit lines on the same tower in UHV power grid deserves further discussion.

(2) The UHV system has similar setting coordination of the protections with different principles to the EHV system. In principle, the step-by-step coordination of the action time shall be met, in case the requirements of rapid action, selectivity, or sensitivity cannot be taken into account at the same time, and the incomplete coordination mode, which the time is coordinated, but the scope of protection is not coordinated, can be adopted.

(3) The general principles for relay protection setting of the UHV system are similar to those of the EHV system. For the setting of the relay protection, the main protection and backup protection of the lines and the elements shall be configured in a reasonable manner with the principle of enhancing the main protection and simplifying the backup protection, and the protection setting can be simplified appropriately. However, when the two sets of the main protections refuse to act, the backup protection of the UHV system shall be able to clear off the faults reliably and selectively, and in such case, the EHV system shall allow for losing selectivity partially.

(4) The UHV protection setting and the EHV protection setting lay respective emphasis on the "four requirements" coordination. The relay protection setting of power grid shall meet the requirements of rapid action, selectivity, and sensitivity. In case the requirements of rapid action, selectivity or sensitivity cannot be taken into account at the same time due to the operating mode of power grid, device performance, etc., reasonable choice shall be made at the time of performing the setting. For the UHV power grid, in particular, for the UHV power grid at the initial stage of construction, since the current grid framework is weaker, it is of great importance to reduce the scope of faults to be cleared off, prevent the protection being overridden, and clear off the faults selectively. Therefore, priority shall be given to the selectivity at the time of setting. However, for the EHV power grid with sufficient strength of grid framework, the probability of having the protection mis-operation is generally small, so priority shall be given to the sensitivity at the time of setting.

14.1.3 Characteristics of UHVAC Protection

The UHVAC system has some electrical features different from those of the EHV power grid, which are mainly reflected in the parameter characteristics of bundled conductors, overvoltage, electromagnetic environment, etc. of the UHV system, which will bring forth the relevant different impacts on the primary and secondary equipments of the system. The main characteristics of the relay protection of UHVAC system are expounded concretely according to different types of relay protection devices.

14.1.3.1 Characteristics of Line Protection

As compared with the 500 kV EHVAC line, the UHV transmission line has the characteristics of small resistance per unit length, small leaking conductance, and big distributed capacitance, which will have bigger impacts on the protection of UHV transmission line. The protection of 1000 kV UHVAC line mainly has the following characteristics.

(1) The attenuation time of harmonic component and DC component is long. For 1000 kV UHVAC transmission line, the ratio of resistance to inductance per unit length is reduced obviously, the positive-sequence impedance angle is about 89°, and the attenuation time constant of short-circuit fault current is about three times that of 500 kV transmission line. Therefore, in the short-circuit fault current of 1000 kV system, the attenuation of non-periodic component is much slower than that of 500 kV system. Even if the filtering algorithm is normally adopted to effectively reduce the impact of non-periodic component in the digital-type relay protection device, in such a way, the increase in the attenuation constant of non-periodic component after occurrence of UHV system failure will not have a too big direct impact on the digital-type protection. However, in case the UHV transmits the power in a long distance, the increase in the attenuation constant of non-periodic component will lead to the transient saturation phenomena of CT and have a critical impact on the differential protection of line current. Therefore, the CT saturation-resistant property of the differential protection for UHV system needs to be improved accordingly. In addition, when there are any faults on the UHV line, the DC component and other HF (high frequency) component harmonics that attenuate slowly may also have large impacts on the conventional protection algorithms applied in the EHV line originally, and will have direct impacts on the performance of relevant protection principles, for example, the distance protection can cause the transient override more easily. For all of these, it is necessary to adopt specific algorithms to reduce the impacts caused by the above unfavorable factors.
(2) The current of distributed capacitance is big. The UHV line is normally longer, and the distributed capacitance of long line will generate bigger capacitive current, as shown in Table 14.1. It is necessary to take into account sufficiently

Table 14.1 Typical parameters of 100 km capacitive reactance and capacitive current on AC transmission line with different voltage classes

Line voltage/kV	Positive-sequence capacitive reactance/Ω	Zero-sequence capacitive reactance/Ω	Effective value of capacitive current/A
500	2590	3790	111
750	2330	3424	186
1000	2269	3525	255

the impacts of distributed capacitance on the longitudinal differential protection and the relevant direction protections. Therefore, in the UHV system, it is needed to study the precise compensation capacitive current, or the differential protection principles that have nothing to do with the capacitive current (namely, not affected by the capacitive current). The conventional compensation method for the capacitive current of EHV line protection is normally to compensate the steady-state capacitive current. In the transient process of no-load closing, fault clearing off outside the zone and etc. on the UHV transmission line, the transient capacitive current in the line is pretty big, which may probably cause mis-operation of the differential protection at this time.

(3) The transmitting power is big. The UHVAC line is normally the main trunk link line for the system, which has big transmitting power and can cause the system oscillation easily. Therefore, the impact of system oscillation must be taken into account sufficiently in the configured line protection, that is, the 1000 kV UHVAC line protection shall not mis-operate due to system oscillation. Moreover, in case of any occurrences of faults during oscillation, such fault must be able to be cleared off selectively in a reliable manner. In addition, for the UHV line protection, the impacts of heavy load on differential protection and distance protection also need to be taken into account.

(4) The impact on the protection by the zero-sequence mutual inductance of the double-circuit lines on the same tower is big. For the double-circuit UHV lines on the same tower, the impact on the protection by the zero-sequence mutual inductance of the line, in particular, the impact on the Distance Section I, shall not be neglected. In addition, the UHV line protection shall be self-adaptive and gone through a special treatment to achieve its action reliably by phase selection when such faults as jumper wire failure occur.

14.1.3.2 Characteristics of CB Protection

As the most complicated and important device in the HV switchgear, the CB can close, carry, and break the normal current and specified overload current (for example, short-circuit current) in the operating circuit. Therefore, it is widely applied in the power generation plants, substations, and switchyards, undertaking the double tasks of control and protection. The UHV CB has the functions of ordinary HV CB, and meanwhile, it needs to reduce the operating overvoltage during breaking and closing as far as possible to reduce the insulation level of the

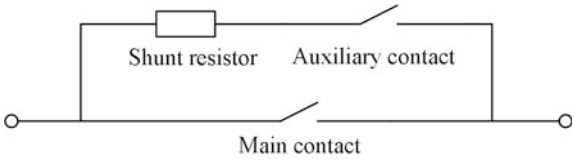

Fig. 14.1 Action principle of opening and closing resistors

power transmission line and substation equipment, and reduce the construction cost. It is normal to install an opening resistor and closing resistor to achieve the above goal and its working principle is shown in Fig. 14.1.

At the time of opening, the main contact of CB is disconnected first; when an opening resistor is connected to the circuit, after about 30 ms, the auxiliary contact connected in series at the opening resistor side is disconnected. At the time of closing, the action sequence is reverse. First, the auxiliary contact connected in series with the closing resistor is closed, and after about 10 ms, the main contact of CB is closed, that is, an impedance circuit is connected in parallel and closed in the circuit in such a way to limit the value of amplitude for closing overvoltage. Analysis on the parameters of opening and closing resistors as well as the time for the auxiliary contact to turn off in lagging way and to close in advance needs to be conducted according to the system and line situation to calculate and determine the specific values. In general, selecting closing resistor with smaller resistance value and opening resistor with higher resistance value can reduce the operating overvoltage. By taking into account the simplification of structure, as well as the level of overvoltage to be restricted, normally, only the closing resistor is adopted, and the operating overvoltage of opening is restricted by making use of arrestor. The characteristics of the relay protection for UHV CB are as follows:

(1) Impact of the overvoltage characteristics on the CB protection

Being different from the ordinary HV and EHV systems, the primary task of UHV relay protection is to eradicate any overvoltage that could cause damage to the equipment and insulators completely and the second task is to ensure the system in a stable state. The relevant documents show that the allowable multiple of overvoltage for the 1000 kV transmission line is 1.6–1.8 fold, which is obviously lower than the allowable twofold of overvoltage for the 500 kV system. Therefore, within a short period, the overvoltage margin allowed by the insulators of UHV transmission line is smaller. When the overvoltage reduces its insulating property or even when it breaks through the insulators, the economic loss caused by power cutoff for the reason of replacing the insulators may be far more than the loss caused by destruction of the system stability. Therefore, as compared with the requirement for rapid action of relay protection, it is of more importance to reduce the level of overvoltage. To make the overvoltage not over the limit, the clearing time difference at both ends allowed by the line is extremely short, which is far below the time for removing the fault by the protections at both ends through actions successively. Therefore, the protections at both ends of UHV transmission line must act at the same time within the shortest period to remove the fault occurred on it, and it is forbidden for the protections at both ends to act successively.

(2) Impact of capacitive current on the CB protection

Bundled conductors are adopted in the UHV transmission line, which has big transmission capacity, long transmission distance, and bigger arc sag. Under the impacts of such objective factors as geology, landform, and man-made conditions, the three-phase parameters of the line are not consistent completely. The characteristics of the system with long line can generate larger distributed capacitive current, and the distributed-parameter characteristics present more obvious transient wave process of fault. The distributed capacitive current makes a great change to the amplitude values and phase angles of currents at both sides of the line, and, meanwhile, has some protections with differential principles interfered greatly. When the load current is smaller, the sensitivity and reliability of the differential protection are more affected. In particular, at the time of being grounded through big transition resistance, it is more often to have such phenomena that the protection refuses to act. Therefore, there is stricter requirement on the small current breaking property of circuit breakers.

(3) Impact of secondary arc current on CB protection

When a single-phase arcing ground fault occurs on the line, the CBs at both sides of the ground phase will break, and other sound phases will almost maintain its original phase voltage and load current. At this time, the sound phases or adjacent lines will make certain current still flow through the fault point by electrostatic coupling and electromagnetic coupling. This is called secondary arc current. The longer the line, the higher the voltage class, and the bigger the load current, the bigger the secondary arc current value will be.

When the UHV system is grounded with heavy current, occurrence of single-phase grounding fault covers more than 80% of the total faults. When the single phase of fault trips, the secondary arc current is larger and the arc phenomenon is more intensified than that of the EHV system. Especially, when the CB breaks the short-circuit current, the extinguishing, reigniting, and extinguishing process of the arc will become more obvious. The arc extinguishing time of secondary arc may reach 0.7 s, or even longer. Moreover, the existence of arc can also affect the breaking capacity of CBs directly. Therefore, measures should be taken to reduce the secondary arc current. At the same time of clearing off the fault by the relay protection, the corresponding measures for reducing the secondary arc current shall be incorporated. For example, in case the self-adaptive reclosing based on the arc characteristics is adopted, when a single-phase fault occurs on the UHV line, the fault phase CBs at both sides will also trip, and a repeated process will experience to distinguish if the arc at fault point has extinguished so as to judge if the reclosing can be opened. If the judgment result shows that the arc has extinguished, reclosing shall be done immediately; if the arc is not extinguished, continue to distinguish until the longest time limit of operation under non-full-phase condition allowed by the system is reached; and if the arc is still not extinguished, disconnect the CB at the non-fault phase.

The CB breaker-failure protection for the UHV project has no big difference with that for the EHV project, and the line reclosing function is configured in the CB protection. The single-phase one shot recloser is adopted for the reclosing of UHV transmission project.

14.1.3.3 Characteristics of Busbar Protection

Busbar is an important part of power generation plants and substations, responsible for executing the important tasks like collecting and distributing the electric energy. For the busbar of 1000 kV UHVAC system, the connection mode with one and a half circuit breaker is mostly adopted, as shown in Fig. 14.2, in which F1 and F2 represent the fault inside the zone and the fault outside the zone, respectively. When the busbar of UHVAC transmission system has a fault outside the zone at short range, such circumstances unfavorable for correct action of the protection as the saturation of CT can easily happen, and therefore, the configuration requirement for its relay protection setting is much higher. It is required that the protection acts in fast speed and have strong capability of resisting the CT saturation and good electromagnetic compatibility (EMC).

Due to long distance and big distributed capacitance of the UHVAC transmission line, when the busbar has a fault inside the zone, the HF component in the short-circuit current of the line will be bigger than that of the conventional EHV transmission line, which will cause some impacts on the ratio-differential of power frequency variation. The impact of the HF component in the short-circuit current on the break-variable differential protection is shown in Fig. 14.3, where Fig. 14.3a is the waveform of the current in branch circuit, and Fig. 14.3b is the waveform of ratio-differential of power frequency variation. The dotted lines in the two figures represent the power supply branches, while the solid lines represent the long lines.

It can be seen from Fig. 14.3 that, in case of occurrence of a fault, the long line is affected by the distributed capacitance obviously. Since the distributed capacitance is relatively big, HF component is generated in the short-circuit current of the line, causing the current to reverse in some periods of time, leading to the decrease in the sensitivity of ratio-differential. Therefore, within 3 ~ 5 ms after occurrence of fault, the ratio-differential of power frequency will come back, having the weighted

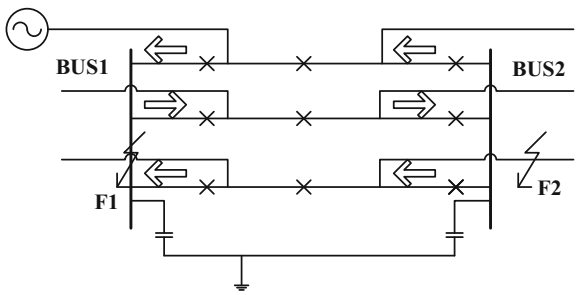

Fig. 14.2 Schematic diagram of busbar connection with one and half CB

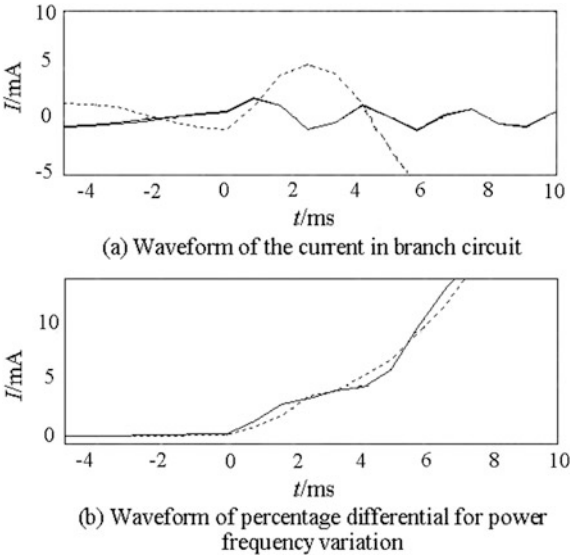

Fig. 14.3 Impact of HF component on break-variable differential protection

criteria for self-adaption affected in case of occurrence of a fault inside the zone. Meanwhile, it also can be seen from the figure that, within 3 ms at the initial stage of fault, its impact on the line is relatively small.

14.1.3.4 Characteristics of Transformer Protection (Including Main Transformer, Voltage-Regulating Transformer, and Compensating Transformer)

The UHV transformer is divided into on-load voltage-regulating transformer and no-load voltage-regulating transformer. Currently, the UHV voltage-regulating transformer and compensating transformer have two modes of connections, namely, complete compensation and incomplete compensation. Although the two modes have different structures, their principles and impacts on the protection are similar. Due to the restriction of volume and capacity, for the UHV transformer, the three-phase transformer bank consisting of three single-phase autotransformers is normally adopted. Meanwhile, to resolve the problem of temperature rise due to the increase in the capacity of transformer, the iron core of UHV transformer is of single-phase four-post type (two-core column and two-bypass column structure). The elementary wiring diagram of UHV three-winding autotransformer is shown in Fig. 14.4.

It can be seen from Fig. 14.4 that the voltage-regulating winding is connected in series with the HV winding of the main transformer for the purpose of stabilizing the voltage at the MV side. The LV compensation winding is connected in series with the LV winding of the main transformer for the purpose of compensating the

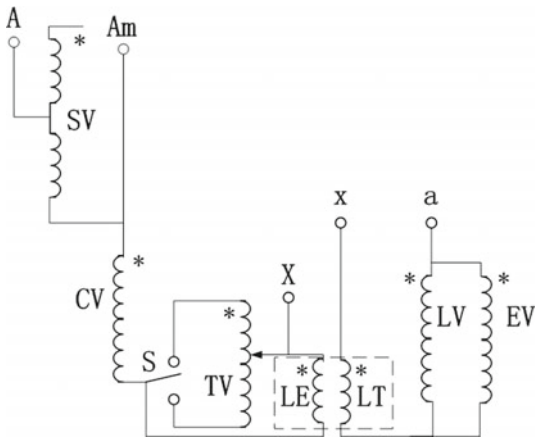

CV- common winding; SV- series winding; LV- LV winding; LT- LV compensation winding; LE- LV excitation winding; EV- voltage regulation excitation winding; TV- voltage regulation winding

Fig. 14.4 Elementary wiring diagram of UHV 3-winding autotransformer

impact on the LV side at the time of regulating the voltage at the MV side of the main transformer, and stabilizing the voltage at the LV side. The voltage-regulating and compensating transformers are independent of the main transformer, and they are connected through hard busbar.

For the UHV transformer in voltage-regulating mode, the voltage regulating on neutral point is normally adopted at present. In such connection mode, the number of turns attributable to the voltage-regulating transformer and compensating transformer is relatively less compared to the turns of the whole transformer, and the turn-to-turn voltage of both is also very small relative to the main transformer. When the voltage-regulating transformer or compensating transformer has a slight turn-to-turn fault, such fault would be slighter if it is viewed from the point of the whole transformer. It is very difficult for the transformer differential protection to act in such a case when the scope of the protection is the whole transformer. Figure 14.5 shows the waveform of a fault when the voltage-regulating transformer is at 25% turn-to-turn fault in a dynamic simulation test carried out by China Electric Power Research Institute on the protection of 1000 kV transformer.

It can be seen from the waveform shown in Fig. 14.5 that, even if the voltage-regulating transformer has 25% turn-to-turn faults (the turn-to-turn fault at this ratio has already been a very serious internal fault for the voltage-regulating transformer), the amplitude value of differential current sensed by the differential protection of the main transformer is 0.47 I_e only, which just exceeds the start setting 0.4 I_e of differential protection. When the short-circuit turn-to-turn ratio of voltage-regulating transformer continues decreasing, the differential protection of the main transformer cannot even be started.

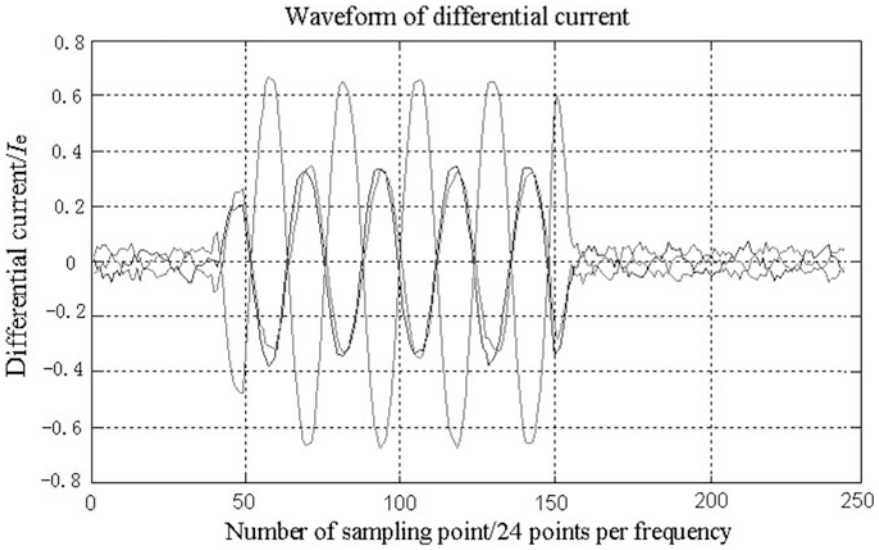

Fig. 14.5 Waveform of 3-phase differential current when voltage-regulating transformer is at 25% turn-to-turn fault

The excitation surge generated by putting the no-load UHV transformer in service causes the protection of the main transformer to mis-operate. The UHV transformer has low iron core saturation point and big remanence. When the UHV no-load transformer is closed, the excitation surge with small current and long attenuation time can be generated easily. The size and attenuation time of excitation surge are related to such factors as phase angle of system voltage, remanence of iron core, system equivalent impedance, winding wiring mode, etc. of the no-load transformer. As for the conventional method for identifying the excitation surge, such as second harmonic restraint, etc., too small secondary harmonic wave in the excitation surge can lead to the mis-operation of differential protection. The key to ensure the correct action of differential protection is to distinguish the excitation surge and internal fault current correctly.

14.1.3.5 Characteristics of HV Shunt Reactor

The capacity of UHV shunt reactor is several times than that of the EHV shunt reactor. By taking into account the increase in the difficulties of controlling the leakage flux due to the increase in the capacity, the increase in the risk of partial overheating, and etc., the UHV shunt reactor is of four-column type (double-core column provided with two bypass yokes) structure and double-body structure. For the winding, the connection mode of parallel connection followed by series connection is adopted, which is shown in Fig. 14.6.

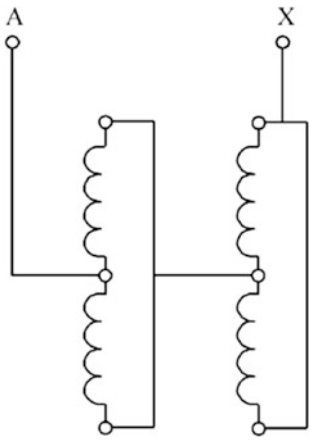

Fig. 14.6 Schematic diagram of connection mode with parallel connection followed by series connection

As compared with the 500 kV EHVAC system, the UHVAC system influences the protection of HV shunt reactor in various aspects, which are mainly reflected in the following: large attenuation time constant of non-periodic component in the short-circuit fault current, big reactor capacity, high EMC (electro magnetic compatibility) requirement, large impact on the reactor interturn protection of zero-sequence power directional principle, low sensitivity of protection action, etc.

The turn-to-turn short circuit is a common internal fault in the HV shunt reactor. Moreover, the fault current has through characteristics over the longitudinal differential protection, making the longitudinal differential protection has no way to reflect the turn-to-turn short-circuit fault. In the EHV system, zero-sequence impedance elements are normally used as the protection criteria. However, in the UHV system, due to the impacts of transformer and long line, the zero-sequence impedance of the system is big, which may cause the interturn protection to refuse action. The protection scheme needs to be improved so as to ensure the sensitivity and reliability of interturn protection.

To resolve the contradiction between the reactive power balance and the limitation of power frequency overvoltage in the UHV power grid, it has a broad prospect to develop the controllable HV shunt reactor. The controllable HV shunt reactor has many types, for example, magnetically controlled type, and hierarchical and thyristor-controlled type. In practice, the controllable HV shunt reactor applied to the UHV system is mainly divided into two categories, namely, magnetically controlled type (DC excited type and magnetic-valve type) and transformer type (hierarchical and thyristor-controlled transformer type). The structure comparison of controllable HV shunt reactor is shown in Table 14.2.

As compared with the HV shunt reactors in the UHV projects put into operation, it is obvious that the structure of controllable HV shunt reactor is more complicated, and it is more difficult to protect the non-electrical quantity. Moreover, there is not any good means to improve the sensitivity of small turn-to-turn short-circuit

Table 14.2 Structure comparison of controllable HV shunt reactor

	DC excited type	Magnetic-valve type	Hierarchical	Thyristor-controlled transformer type
Control winding	Yes	Yes	No	No
Compensation winding	No	Yes	No	No
Thyristor	No	No	Yes	Yes

protection of the controllable HV shunt reactor up to now. To some extent, this has restricted the application of controllable HV shunt reactors in the UHV projects.

14.1.3.6 Characteristics of LV Shunt Reactor and LV Capacitor Protection

In the UHV transmission project, the capacitor and reactor at 110 kV side of UHV main transformer are installed with CB and load switch. Due to the restriction of the interrupting capacity of load switch, when the internal fault current is relatively big, the load switch is unable to interrupt the faulty equipment. However, if any of the faults trips the main CB of the main transformer branch directly, the capacitive current of switching by the CBs has a big impact on the service life of CB; especially, the capacitive current of switching over two capacitors has more serious damage to the CB. Therefore, the protection devices for the capacitor and reactor at 110 kV side are installed with the switching function for outlet tripping, that is, such device can choose to trip the CB at the LV side of the main transformer, or trip the load switch in this bay according to the amplitude of fault current.

14.2 Principles and Configurations of UHVAC Protection

The UHVAC protection consists of six parts, namely, line protection, CB protection, busbar protection, transformer protection, HV shunt reactor protection as well as LV shunt reactor and LV capacitor protection, where the CB protection, busbar protection, HV shunt reactor protection as well as LV shunt reactor and LV capacitor protection are similar to those for the EHVAC system. However, the line protection has some differences, and the transformer protection is quite different.

14.2.1 Principles and Configurations of Line Protection

14.2.1.1 Principles of Line Protection

The conventional method for compensating the capacitive current of EHV line protection is normally to compensate the steady-state capacitive current only. For the long-distance UHV transmission line, it is necessary to take the impact of distributed capacitive current of the line into account. As known from Table 14.1, when the 1000 kV transmission line, on which eight-bundled conductors are adopted, transmits the natural power, the capacitive current per phase is 255 A for each 100 km line. Furthermore, the ratio of capacitive current to voltage class is becoming bigger and bigger. This indicates that with the increasing voltage class and the length of transmission line, the amplitude value of capacitive current increases faster and faster. Except for the operation under steady state, in the process of no-load closing, clearing of the fault outside the zone on the UHV transmission line, the transient capacitive current is very big on the line. Especially, under the transient state, there are many HF components in the voltage, the capacitive current is proportional to the frequency, and consequently, the capacitive current with bigger amplitude value is generated. At this time, it may probably cause mis-operation of the differential protection. Therefore, according to such characteristics of the UHV line, each protection device manufacturer has taken different measures. Some of the manufacturers of relay protection devices adopt the compensating method for travelling wave capacitive current based on Bergeron Model. This method can compensate the capacitive current under transient state accurately and the capacitive current under steady state. Moreover, the principle of split-phase current differential protection based on Bergeron Model has also been applied in the engineering practice, and the developed protection devices have been applied in several 1000 kV UHVAC transmission projects already put into operation in China. For line protection, some of the manufacturers adopt the time-domain compensating differential method, which can also compensate the capacitive current under transient state and the capacitive current under steady state very well.

The Bergeron Model raised by Bergeron is a relatively precise model for power transmission line. According to the principle of wave process, analyzing of multiple refractions and reflections of the wave is performed by applying the pattern of mixed wave, and the typical Bergeron Model of power transmission line is thus derived by the differential equation of distributed-parameter transmission line. The core of Bergeron method is to make the distributed-parameter elements equivalent to the lumped-parameter elements, and the wave process on the line is calculated by the commonly used numerical solution method for lumped parameters.

During normal operation, that is, before the protection device is started, perform calculation of $|I_M + I_N| = I_C$, where I_M and I_N, respectively, represent the currents on the lines at the M and N ends, and I_C is the actually measured capacitive current of the line. After the protection is started, with I_C being used as the floating

threshold, make precise compensation for the capacitive current utilizing the actually measured voltages at both sides of the line after occurrence of a fault. This is called a half-compensation scheme, which means making compensations for the capacitive currents at both sides of the line by half each.

Figures 14.7, 14.8, 14.9, respectively, represent the π-type equivalent circuit diagrams of positive sequence, negative sequence, and zero-sequence on the lines at the M and N ends. The calculation equations for their capacitive currents are derived as follows.

On basis of phase A, the positive-sequence, negative-sequence, and zero-sequence capacitive currents at the M side are shown in Eqs. (14.1), (14.2), and (14.3).

$$I_{MC1} = U_{M1}/(-j2X_{C1}) \tag{14.1}$$

$$I_{MC2} = U_{M2}/(-j2X_{C2}) \tag{14.2}$$

$$I_{MC0} = U_{M0}/(-j2X_{C0}) \tag{14.3}$$

where

I_{MC1}, I_{MC2}, and I_{MC0} the positive-sequence, negative-sequence and zero-sequence capacitive currents, respectively;

U_{M1}, U_{M2}, and U_{M0} the positive-sequence, negative-sequence and zero-sequence voltages, respectively;

X_{C1}, X_{C2}, and X_{C0} the positive-sequence, negative-sequence and zero-sequence reactances, respectively.

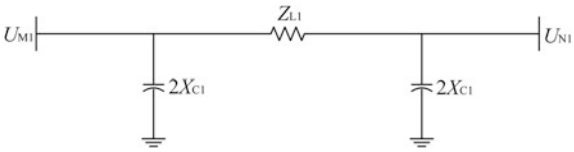

Fig. 14.7 Positive-sequence π type equivalent circuit of transmission line

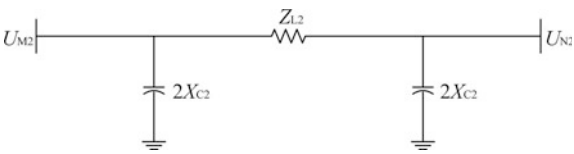

Fig. 14.8 Negative-sequence π type equivalent circuit of transmission line

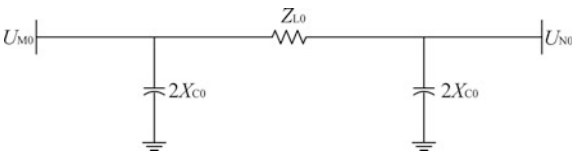

Fig. 14.9 Zero-sequence π type equivalent circuit of transmission line

The capacitive current of each phase at the M side is as follows (assume $X_{C1} = X_{C2}$):

$$\begin{aligned} I_{MAC} &= I_{MC1} + I_{MC2} + I_{MC0} \\ &= (U_{M1} + U_{M2} + U_{M0} - U_{M0})/(-j2X_{C1}) + U_{M0}/(-j2X_{C0}) \\ &= (U_{MA} - U_{M0})/(-j2X_{C1}) + U_{M0}/(-j2X_{C0}) \end{aligned} \tag{14.4}$$

$$\begin{aligned} I_{MBC} &= \alpha^2 I_{MC1} + \alpha I_{MC2} + I_{MC0} \\ &= (\alpha^2 U_{M1} + \alpha U_{M2} + U_{M0} - U_{M0})/(-j2X_{C1}) + U_{M0}/(-2jX_{C0}) \\ &= (U_{MB} - U_{M0})/(-j2X_{C1}) + U_{M0}/(-2jX_{C0}) \end{aligned} \tag{14.5}$$

$$\begin{aligned} I_{MCC} &= \alpha I_{MC1} + \alpha^2 I_{MC2} + I_{MC0} \\ &= (\alpha U_{M1} + \alpha^2 U_{M2} + U_{M0} - U_{M0})/(-j2X_{C1}) + U_{M0}/(-2jX_{C0}) \\ &= (U_{MC} - U_{M0})/(-j2X_{C1}) + U_{M0}/(-2jX_{C0}) \end{aligned} \tag{14.6}$$

Similarly, we can obtain the capacitive current of each phase at the N side as follows:

$$I_{NAC} = (U_{NA} - U_{N0})/(-j2X_{C1}) + U_{N0}/(-j2X_{C0}) \tag{14.7}$$

$$I_{NBC} = (U_{NB} - U_{N0})/(-j2X_{C1}) + U_{N0}/(-j2X_{C0}) \tag{14.8}$$

$$I_{NCC} = (U_{NC} - U_{N0})/(-j2X_{C1}) + U_{N0}/(-j2X_{C0}) \tag{14.9}$$

Theoretically, the principle of line differential protection based on Bergeron Model has automatically taken the impact of capacitive current into account, which is the most precise algorithm up to now for achieving the compensation for distributed capacitive current using the software. However, in the differential protection based on Bergeron Model method, there is a problem that the sampling frequency is hard to coordinate with the length of transmission line. Therefore, some manufacturers have put forward the differential protection using the time-domain capacitive current compensation based on π-type equivalent circuit. This differential protection mentioned above makes compensation for the instantaneous value using the differential equation model, which can effectively eliminate the impacts of capacitive currents under transient state and under power frequency steady state. This has resolved the defect of the conventional compensation method by power frequency phasor quantity that can only compensate the capacitive current under steady state and the calculating data window is too long.

The conventional compensation method for capacitive current only can compensate the capacitive current under steady state. In the transient process of no-load closing, clearing of a fault outside the zone, etc., the transient capacitive current of the line is very large. In this case, the steady compensation cannot compensate the capacitive current at this time. For the time-domain compensation differential

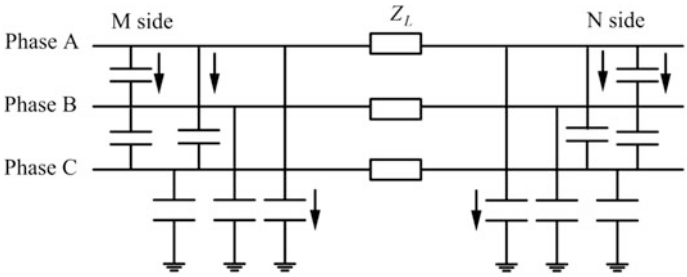

Fig. 14.10 π Type equivalent circuit of the line without shunt reactor

current, the compensation method for capacitive current under transient state is adopted, and the transient component of capacitive current is compensated.

For the transmission line without shunt reactor, its π-type equivalent circuit is shown in Fig. 14.10.

The current of each capacitor in Fig. 14.10 can be obtained through calculation using Eq. (14.10).

$$i_{\mathrm{C}} = C\frac{\mathrm{d}u_{\mathrm{c}}}{\mathrm{d}t} \tag{14.10}$$

where

i_{C} the current passing through each capacitor;
C the capacitance value;
u_{C} the voltage drop across the capacitor.

When the current of each capacitor is obtained, the capacitive current of each phase can be obtained. Now that the capacitor voltage and current with different frequencies have such relation, as shown in Eq. (14.10), for the steady-state component and transient-state component of the capacitive current in the cases of normal operation, no-load closing, clearing of a fault outside the zone and the like, and the capacitive current obtained through calculation using Eq. (14.10) can provide better compensation, which has improved the sensitivity of differential protection.

For the transmission line installed with shunt reactors, part of the capacitive current is compensated by the shunt reactors. When setting up the differential protection, the capacitive current needing to be compensated is the capacitive current calculated using Eq. (14.10) minus the current of shunt reactors.

The equivalent circuit, and its relevant currents and voltages of the connection of the neutral point of shunt reactor mounted with small-reactance are shown in Fig. 14.11.

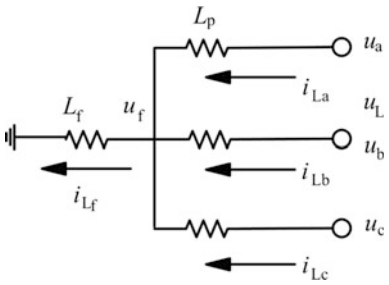

Fig. 14.11 Equivalent circuit of connection of the neutral point of shunt reactor mounted with small-reactance

The relation between current and voltage on the reactor is shown in Eq. (14.11):

$$u_L(t) - u_f(t) = L_p \frac{di_L(t)}{dt}. \tag{14.11}$$

Have Eq. (14.11) integrated within the time from the moment $(t - \Delta t)$ to the moment t, and the integration procedure is shown as follows:

$$i_L(t) = i_L(t - \Delta t) + \frac{1}{L_P} \int_{t-\Delta t}^{t} [U_L(t) - U_f(t)]dt \tag{14.12}$$

$$i_C = C \frac{du_C}{dt} - i_L(t). \tag{14.13}$$

Besides, for the distance protection of conventional lumped-parameter model for 1000 kV long line, in particular, the Distance Section I protection, its measured impedance will be affected by the capacitive current seriously, so that the requirement of the Distance Section I transient overreach being below 5% cannot be satisfied.

14.2.1.2 Configurations of Line Protection

The UHV line protection is slightly different from the EHV line protection. Double configurations are adopted for the main protection of EHV line, for which normally, three types of protection configurations are adopted according to the channel conditions, namely, two sets of HF (high frequency) protection, one set of HF protection + one set of split-phase current differential protection, or two sets of split-phase current differential protection. Double configurations are also adopted for the main protection of UHV line, for which two sets of split-phase current differential protection are normally adopted. In addition, considering the fact that the requirements of the optical fiber channel conditions for the UHV line are higher than those for the EHV line, double channels are adopted for each set of split-phase current differential protection [6]. For example, the first set is the split-phase current differential protection PCS-931GMM-U+PCS-925G for overvoltage and local discrimination for remote trip manufactured by Nanjing Nanrui Relay Protection

Electrical Co., Ltd; the second set is the split-phase current differential protection CSC-103B+CSC-125A for overvoltage and local discrimination for remote trip manufactured by Beijing Sifang Relay Protection Automation Co., Ltd. Each set of split-phase current differential protection has two optical fiber channel interfaces, and the two channels work at the same time. Among them, Channel A carries out transmission through the OPGW of 1000 kV line by multiplexing 2 M; Channel B carries out transmission through the circuitous OPGW of 500 kV line by multiplexing 2 M. If there is only one fault in either of the two channels, the operation of split-phase current differential protection for the line will not be affected.

Each set of line protection is configured with one set of local discrimination device for remote trip, and the local discrimination device is used in conjunction with the overvoltage protection. The local discrimination device at each side of each circuit of line is configured according to the tripping logic of double configuration, and "one-to-one", that is, one set of local discrimination device corresponds to the channel of a set of line protection. The local discrimination for remote trip adopts the criteria of split-phase low active power, and it will be OK if any of the phases can meet the criteria of low active power.

Each circuit of line is configured with overvoltage protection, and split-phase voltage measuring elements are adopted for the overvoltage protection. The action conditions for the overvoltage protection configured for the line are such that when the line CB at this side has detected overvoltages in all three phases in the disconnected position of three phases. After the overvoltage protection acts, it trips the CB at the opposite side of the line through the remote tripping circuit with a time delay. The sending and receiving of the remote tripping signals of overvoltage protection are shared with the remote tripping of breaker-failure protection and the HV shunt reactor protection. The protection configurations of the first set of line protective panel are shown in Table 14.3, and the protection configurations of the second set of line protective panel are shown in Table 14.4.

The connection mode for multiplexing both channels in double channel 2048 kbit/s is shown in Fig. 14.12.

14.2.1.3 Setting of Line Protection

Due to the characteristics of UHV line protection, the setting of line protection shall observe the following principles [7–9].

(1) Turn-off-in-sequence principle: when carrying out the solution of branch coefficients and the verification of settings under various preset operating modes, turning off in sequence will be carried out for the lines and transformers of the plants or substations at both sides of the line. The recommended principle for the number to be turned off in sequence is as follows: 1 element to be turned off in sequence in case of 1–4 elements; 2 elements to be turned off in sequence in case of 5–8 elements; and 3 elements to be turned off in sequence in case of 9 or above elements. Special consideration shall be given in case of special mode. For the

Table 14.3 Protection configurations of the first set of line protective panel

Model		Name of protection		Remarks
The first set of line protection for 1000 kV line	Line microprocessor-based protection PCS-931GMM-U	Main protection	Split-phase current differential protection for steady-state Section I	
			Split-phase current differential protection for steady-state Section II	Act with a time delay of 25 ms
			Zero-sequence current differential protection	Act with a time delay of 40 ms; selective tripping
			Differential protection for power frequency variation	
		Backup protection	Distance protection for power frequency variation	Distance protection for power frequency variation
			Distance protection for grounding of three sections	
			Distance protection for phase to phase of three sections	
			Closing of distance protection upon occurrence of fault	At the time of single-phase reclosing, the Distance Section II trips 3 phases with a time delay of 25 ms due to the oscillation blocking control. At the time of 3-phase reclosing, choose to accelerate the Distance Sections II and III not subjected to oscillation blocking through the setting control word,

(continued)

Table 14.3 (continued)

Model		Name of protection		Remarks
				otherwise the Distance Section II subjected to oscillation blocking is always accelerated Distance Section III is always accelerated at the time of manual closing
			Closing of zero-sequence protection upon occurrence of fault	In case of manual closing, when the zero-sequence current is greater than the acceleration setting, 3 phases will trip with a time delay of 100 ms.
			Overcurrent protection of zero-sequence inverse time limit	The minimum action time is 0.5 s
	PCS-925G local discrimination for remote trip and overvoltage	Local discrimination		When receiving the remote trip signal from the opposite side, this side carries out the discrimination of the low power of single phase
		Overvoltage protection		Discriminate the opening position of the corresponding CB at this side; detect the overvoltage in 3 phases; do not trip the CB at this side, and send out the remote trip signal

lines erected in parallel on the same tower, it is necessary to turn off the two circuits of lines at the same time.

(2) For the split-phase current differential protection, the main provisions are as follows: when the current at fault point is greater than 800 A, the protection shall be able to clear the fault through phase-selection action; the compensation function of capacitive current shall be put into service; in case the CT for split-phase current differential protection is disconnected, the differential protection shall not be blocked, but the setting for starting threshold of the differential protection shall be increased accordingly. At the initial stage of the UHV construction, the system is weak. To avoid the mis-operation of the

Table 14.4 Protection configurations of second set of line protective panel

Model		Name of protection		Remarks
The second set of line protection for 1000 kV line	CSC-103Bl line protection device	Main protection	Split-phase current differential protection	
			Zero-sequence current differential protection	Act with a time delay of 100 ms; selective tripping
		Backup protection	Fast distance protection	
			Distance protection for grounding of three sections	
			Distance protection for phase to phase of three sections	
			Closing of distance protection upon occurrence of fault	Manual closing upon occurrence of fault; the distance protection will accelerate the Distance Sections I, II and III After reclosing, the functional elements will be accelerated: (1) Acceleration due to closer reactance (after reclosing, when the measured impedance of original fault phase is in Section II, and when the reactive component is closer to the reactive component before tripping, the protection will accelerate to act.). The fixed time for putting in service of such function is 100 ms (2) Instantaneous acceleration section II. If the control word is in "oscillation blocking element" mode, the mode by oscillation blocking is entered

(continued)

Table 14.4 (continued)

Model		Name of protection		Remarks
				(3) Section III is accelerated by evading the time delay for oscillation within 1.5 s
			Closing of zero-sequence protection upon occurrence of fault	The acceleration section protection is closed manually, with a time delay of 60 ms
			Overcurrent protection of zero-sequence inverse time limit	The minimum action time is 0.5 s
	CSC-125A local discrimination for remote trip and overvoltage	Local discrimination		When receiving the remote trip signal from the opposite side, this side carries out discriminating the low power of single-phase
		Overvoltage protection		Discriminate the opening position of the corresponding CB at this side, detect the overvoltage in three phases, do not trip the CB at this side, and send out the remote trip signal

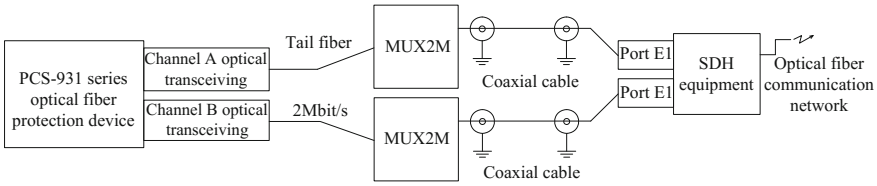

Fig. 14.12 Connection mode for multiplexing double channel 2048 kbit/s

protection in case of CT disconnection, the differential protection can be blocked directly when the CT is judged as line broken by the line protection.

(3) The line protection setting adopts the local backup principle. If permitted by the conditions, a mode of combining the remote backup and local backup shall be adopted, and there are no requirements on the sensitivity coefficient of remote backup.

(4) The sensitivity of distance protection for grounding and phase-to-phase shall be calibrated according to metallic faults. The Distance Section I shall be set as not stretching out the busbar at the opposite side so as to evade the busbar fault at this side reliably.

(5) In normal cases, the grounding Distance Section II of the line protection shall be set according to the requirement of sufficient sensitivity being available when a metallic fault occurs at the end of such line, and coordinated with the grounding Distance Section I or Section II of adjacent lines. It can also be coordinated with the pilot protection of adjacent lines, and the time is coordinated with the action time of breaker-failure protection of the CB at the opposite side. The phase-to-phase Distance Section II shall be set according to the requirement of sufficient sensitivity being available when a metallic phase-to-phase short-circuit fault occurs at the end of such line, and coordinated with the phase-to-phase Distance Section I or the pilot protection of adjacent lines. In case of being unable to coordinate, it can be set by coordinating with the phase-to-phase Distance Section II of adjacent lines. The action time of the Distance Section II for phase-to-phase and grounding shall not be greater than 1.7 s.

(6) If the setting of the Distance Section II of the upper level of line protection stretches out the busbar with lower level of voltage class of the main transformer at the opposite side, the setting limits of corresponding elements with lower level of voltage class shall be decreased. If the setting of the Distance Section II of the lower level of line protection stretches out the busbar with upper level of voltage class of the main transformer at opposite side, the Distance Section II can be coordinated with the pilot protection of line with upper level of voltage class.

(7) In normal mode, the Distance Section III shall be coordinated with the Distance Section II of the adjacent line, and if it is difficult to coordinate with the Distance Section II of the adjacent line, it can be coordinated with the Distance Section III of the adjacent line. If it is impossible to coordinate with the Distance Section III of the adjacent line, the incomplete coordination shall be adopted. The Distance Section III shall also evade the minimum load impedance and system-oscillating period corresponding to the maximum overload when an accident occurs on this line. Such time is normally 1.7 s or above.

(8) There is large zero-sequence mutual inductance between the double-circuit UHV lines on the same tower. Due to the uncertainty of the impact of the zero-sequence mutual inductance between the double-circuit lines under different operating conditions, the measuring error of grounding distance protection is larger. In case the protection device can only provide one setting for zero-sequence compensation coefficient, such coefficient cannot meet the requirements of the Distance Section I and Section II at the same time. To ensure the reliability, the coordination K value of the software for setting calculation shall be consistent with the setting K value, for which $K_{\max}$ shall be taken unitedly. The reliability coefficient of the Distance Section I shall be

reduced accordingly. The most fundamental method is that the protection device manufacturer shall be able to provide these two coefficients of K_{max} and K_{min} (the calculation of K_{max} and K_{min} is shown in Standards Q/GDW 422-2010 6.2.8).

(9) The zero-sequence current protection shall ensure that the lines with relevant voltage classes can be switched off in case of occurrence of high-resistance grounding fault reliably. The inverse time limit zero-sequence current protection shall be set according to the inverse time limit curve. The inverse time zero-sequence current of all the lines shall adopt the standard inverse time limit curve family. The time constant shall be 0.4, and the starting value shall not be greater than 400 A. If the minimum action time is in "series connection" logic with the intrinsic time of inverse time limit zero-sequence current, it shall be set at not below 0.5 s; if it is in "parallel connection" logic, it shall be set at not below 1.0 s.

(10) Since the protection devices with different principles cannot coordinate with each other in the setting of upper and lower levels, if two sets of the pilot protection refuse to act at the same time, the backup protection shall be able to clear the fault reliably and selectively.

(11) The currents under static state and steady state shall be set according to the requirement of evading the maximum normal load of the line reliably.

(12) The impedance line for load limitation shall reliably evade the steady-state operating current of the single-circuit line after occurrence of $N-1$ fault.

14.2.2 Principles and Configurations of CB Protection

14.2.2.1 Principles of CB Protection

As an important element for relay protection, CB constitutes an important relay protection for the AC system by coordinating with other elements. According to the experiences obtained in the UHV projects in China and abroad, the common main electrical connection modes include double-busbar double-sectional connection, double-circuit breaker connection, and 3/2-circuit breaker connection. These three connection modes are compared comprehensively, as shown in Table 14.5. By analyzing in view of reliability, in the double-circuit breaker connection mode, the fault occurrence on the busbar or any of the elements will not cause the line power off. In the 3/2- circuit breaker connection mode, the CB in the string has high rate of failure and high maintenance cost, which causes the slight decrease in the reliability of such mode. In the double-busbar double-sectional connection mode, the CB maintenance on any of the circuits will cause the circuit power off. Therefore, if considering the reliability only, the double-circuit breaker connection mode has the max advantages. However, if analyzed in view of economic efficiency, the maximum number of CBs is used in the double-circuit breaker connection mode, which

Table 14.5 Comprehensive comparison of three connection modes

Type of main connection	Number of CB	Level of reliability	Complexity of operation	Fault of CB
Double CB	24	High	Simple	A fault on any of the CBs will not affect the power supply
3/2 CB	18	Moderate	Moderate	In case of a fault on the middle CB in the complete string, two elements will be out of service; in case of a fault on other CBs, one element will be out of service
Double-busbar double-section	16	General	Complicated	When a fault occurs on the busbar or the line CB, the whole plant is powered off. When a fault occurs on other CBs, one of the units will be shut down. Power supply can be restored quickly if a fault occurs on the CB of busbar, the operation can be achieved only after such CB is repaired in case a fault occurs on any of other CBs

leads to higher cost. In the 3/2-circuit breaker connection mode, the number of the equipment used is less, so it has better economic efficiency. By taking the technology and economy into comprehensive consideration, it is more appropriate to adopt the 3/2-circuit breaker connection mode in the UHVAC system, whose connection mode is shown in Fig. 14.13.

In the 3/2-circuit breaker connection mode, the breaker-failure protection, auto reclosing, and three-phase inconsistent protection, etc. are incorporated in the same device. The UHV system has high-voltage class and more complicated main connection, and its protection configurations are more difficult. The circuit breaker protection in 3/2 connection mode is configured on basis of CB unit, and each CB is configured with one CB protective panel.

14.2.2.2 Configurations of CB Protection

The 1000 kV CB protection is configured with an independent CB protection device. The CB protection includes the functions of reclosing, breaker-failure protection and charging overcurrent protection [10]. The charging overcurrent protection includes the two-section phase overcurrent protection, which is put into service or removed out of service by a hard pressing plate; such protection has the functions of instantaneous trip and time-delay trip.

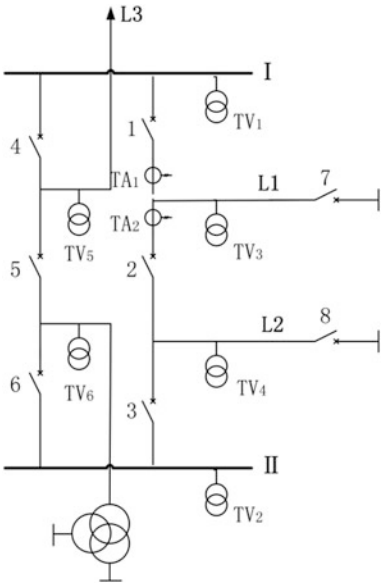

Fig. 14.13 Schematic diagram of typical 3/2 CB connection

Table 14.6 Configurations of CB protection

CB No.	Name of Protection		Remarks
T0XX	PCS-921G CB failure and auto reclosing device	Auto reclosing	The CB at side recloses in 1.0 s; the CB in the middle recloses in 1.3 s
		Charge overcurrent protection	Normal shutdown
		Breaker-failure protection	Re-trip the fault phase of this CB instantaneously, and trip the adjacent CBs with a time delay of 200 ms, and send out the remote trip signals
		3-Phase inconsistency	Out of service, and the three phases of the CB mechanism which is in operation are not consistent

The three-phase inconsistent protection of CB adopts the three-phase inconsistent protection of CB body, and the three-phase inconsistent protection inside the CB protection device is removed out of service. The configurations of CB protection are shown in Table 14.6 [11].

14.2.2.3 Setting of CB Protection

1. Breaker-failure protection of CB

For the breaker-failure protection of CB, in normal cases, it is considered that only one CB at both sides of the line refuses to act in single phase. However, for the main transformer, it is considered that only one CB at the HV, MV, and LV sides refuses to act in single phase (for the CB of three-phase link gear at the LV side of the main transformer, the case that three phases will refuse to act shall be taken into account) [7].

(1) The criteria for breaker-failure protection current of line CB

The criteria for breaker-failure protection current of line CB include the negative-sequence or zero-sequence current and phase current. The time for the breaker-failure protection to trip the adjacent CBs with time delay shall be set to evade the sum of the reliable trip time of CB and protection return time, with some time margin taken into consideration, for which 0.2 s is selected. They are explained specifically as follows:

The phase current shall be set by ensuring the sensitivity available when a short circuit occurs at the end of the line under the system minimum operation mode, and shall evade the load current as far as possible. The sensitivity coefficient shall be greater than 1.3. The zero-sequence current shall be set to evade the max zero-sequence unbalanced current, and by ensuring sufficient sensitivity when a fault occurs at the end of the protection scope. The negative-sequence current of breaker-failure protection shall be set by avoiding the max unbalanced negative-sequence current, and by ensuring the sufficient sensitivity when a fault occurs at the end of the protection scope.

(2) Current criteria for CB breaker-failure protection of the main transformer

The current criteria for CB breaker-failure protection of the main transformer include the negative-sequence current or zero-sequence current. The negative-sequence starting current shall be normally set by ensuring sufficient sensitivity when a fault occurs at the LV side of such transformer, and the sensitivity coefficient shall be greater than 1.3. The time for the breaker-failure protection to trip the adjacent CBs with a time delay shall be set to evade the sum of the reliable CB tripping time and the return time of the protection, with some time margin taken into consideration, for which 0.2 s is selected.

2. Overcurrent protection of CB

For the overcurrent protection of line CB, normally, only Section I is put into service. Its current setting shall ensure a sufficient sensitivity when a fault occurs at the end of the protection scope, and evade the charge current of the line reliably. The specified time is 0 s.

For the overcurrent protection of the main transformer CB, normally, Section I and Section II are put into service. The overcurrent Section I shall be set by ensuring sufficient sensitivity when any faults occur on the main transformer bushing and lead wire at the installation side of CB. The sensitivity coefficient shall not be less than 2, and the time shall be 0.01–0.2 s. The overcurrent Section II shall ensure a sufficient sensitivity when a fault occurs at the LV side of such transformer. The sensitivity coefficient shall be greater than 1.5, and the time shall be 0.3–1.5 s.

3. Reclosing protection of CB

The time setting for line reclosing shall meet the requirements of safety and stability of relevant power grid, and take into full consideration of the impacts of CB itself and the secondary arc current. Time coordination shall be adopted for reclosing of two adjacent CBs to meet the requirements of closing sequence for reclosing.

4. Three-phase inconsistent protection of CB

For the three-phase inconsistent protection of CB, the three-phase inconsistency of the body, 3/2 connection, and the CBs related to the line shall be adopted. The action time shall be set in principle by evading the single-phase reclosing time reliably. The three-phase inconsistent time of CB is normally considered as 2.5 s unitedly. The time for three-phase inconsistent protection of the CB, of which the generator–transformer unit etc. do not need to coordinate with the reclosing time, can be set as 0.5 s.

14.2.3 Principles and Configurations of Busbar Protection

14.2.3.1 Principles of Busbar Protection

1. Variable characteristics differential algorithm based on the transient saturation and full-course measuring
   The busbar differential protection device can mis-operate when the CT is seriously saturated and differential current occurs in case a fault outside the zone close to the busbar happens. Therefore, the protection device is installed with the detecting elements for CT saturation according to the generation mechanism of CT saturation as well as the waveform characteristics of secondary current after occurrence of CT saturation. These detecting elements are used to discriminate if the differential current is caused by the saturation of the faulty CT outside the zone. Such algorithm is called as the variable characteristics differential algorithm based on the transient saturation and full-course measuring. In case of a fault inside the busbar zone as well as fault CT saturation outside the busbar

zone, the action time sequence of ΔI_d element is totally different with that of ΔI_r element. Moreover, when the CT saturates, each frequency has a linear transfer section though the waveform of differential current distorts, and there are rich harmonic components existing in the waveform of transient saturation. The time at which the CT saturation occurs can be detected precisely, and the relevant algorithms of differential shall be adjusted on real time, providing it with extremely strong CT saturation-resistant capability.

2. Fast-speed and high-sensitivity duplex ratio-differential protection
   The protection device with fast-speed and high-sensitivity duplex ratio-differential protection is adopted, whose action equation is shown in Eq. (14.14):

$$\begin{cases} I_d > I_{dset} \\ I_d > K_r \times (I_d - I_r) \end{cases} \tag{14.14}$$

where

I_{dset} the starting current setting of differential protection;
K_r the setting of duplex ratio factor (braking factor).

Compared to the conventional criteria for ratio braking, the criteria for the duplex ratio-differential presents extremely strong braking characteristics in case of a fault occurrence outside the busbar zone due to introduction of the differential current into the calculation of braking quantity. In case of a fault inside the busbar zone, there is no braking and the scope of braking coefficient selection is wider. Therefore, it can distinguish the faults outside the zone and the faults inside the zone precisely, and the action will be more accurate.

3. Impacts of HF and non-periodic component
   By combing the various algorithms, the protection device can eliminate the DC component and the impact of HF harmonic wave on the protection effectively. In case of a fault inside the zone, the protection acts rapidly and reliably, and in case of a fault outside the zone, the protection is blocked reliably.

4. Characteristics of busbar differential protection at the 110 kV side of UHV main transformer
   In view of improving the reliability and sensitivity of power grid operation, it is more suitable for each branch at the 110 kV side of UHV main transformer to be installed with two sets of busbar differential protection.

As there are two types of configurations in the LV shunt reactor bay and capacitor bay, namely, the CBs and load switches, the 110 kV busbar differential protection has the following characteristics.

(1) The blocking protection function for large current, which is designed on basis of bay, is newly added. In case of any action of the protection, it will automatically choose to trip the outlet of this bay, or directly trip the CBs at the LV side of the main transformer according to the size of fault current.
(2) The unique double breaker-failure protection functions for CB. In case of a fault occurrence on any of the reactive power compensating equipment, such as the capacitors, reactors, etc., at the LV side of the main transformer, if the CB in this bay fails, the busbar breaker-failure protection will trip the CBs at the LV side of the main transformer directly. Considering the failure of CBs at the LV side of the main transformer at the same time, the busbar breaker-failure protection is required to intertrip the CBs at the other sides of the main transformer to clear the fault.

14.2.3.2 Configurations of Busbar Protection

Each of 1000 kV busbar in the UHV station is configured with two sets of 1000 kV busbar protections [12]. For example, the first set of busbar protection is the WMH-800A microprocessor-based busbar protection device manufactured by Xuji Electrical Co., Ltd; the second set of busbar protection is the BP-2CS-H microprocessor-based busbar protection device manufactured by Changyuan Shenrui Relay Protection Automation Co., Ltd. Each set of busbar differential protection devices has an independent main panel, and the 1000 kV busbar differential protection in a station has four protective panels in total.

WMH-800A series microprocessor-based busbar protection devices are installed with the special detecting elements for CT saturation, in which the method for monitoring the harmonic content is utilized. The specific configurations of the whole set of devices are shown in Table 14.7. The second set of BP-2CS-H microprocessor-based busbar protection devices is suitable for the busbars with various voltage classes of 1000 kV or below in various main connection modes, specifically used in the connection mode with one and half circuit breaker for UHV and EHV voltage classes. It can achieve the functions of busbar differential protection, tripping the CBs through the busbar differential protection in case of CB failure, blocking the CTs in case of CT disconnection, and giving warning in case of CT disconnection, of which tripping by the differential protection and CB failure through the protection busbar can be put into service or removed out of service through selection, respectively. The specific configurations are the same as those in Table 14.7.

Two sets of the busbar protection devices for one busbar have the busbar differential protection function and breaker-failure protection function, and act on different tripping coils of CBs. Intertripping the outlets of other CBs by the CB

Table 14.7 Configurations of the first set of protection device for the 1000 kV UHV system busbar

Model	Name of protection		Remarks
WMH-800A	Busbar protection setting	Starting current setting of differential protection	
		Alarming setting of CT disconnection	Low setting gives alarming only
		Blocking setting of CT disconnection	High setting blocks the busbar differential protection
	Control word	Differential protection	Put the differential protection function into service
		Failure trips through busbar differential protection	CB breaker-failure protection trips the relevant CBs of busbar through the outlet of busbar differential protection

failure shall share the outlets with the busbar protection. The busbar protection is installed with the sensitive, failure open current elements that do not require setting, and provided with a fixed time delay of 50 ms to prevent the mis-operation of intertripping by breaker-failure protection due to such reasons as abnormal input to breaker-failure protection.

14.2.3.3 Setting of Busbar Protection

(1) The differential current starting elements of busbar protection shall ensure sufficient sensitivity in case of a fault on the busbar under the minimum mode, and the sensitivity coefficient shall not be less than 1.5 [13].
(2) Setting shall be done by evading the maximum unbalanced current in case of a fault outside the zone reliably, and by evading the differential current due to the maximum load current as far as possible in case of disconnection of the current circuit of any elements.
(3) The busbar differential protection shall be blocked reliably in case of CT disconnection. The low setting of CT disconnection is normally set once, with the setting not greater than 300 A, which is used for giving alarming signal only; the high setting is normally set as 1.5 times of the low setting, which is used for giving alarming and blocking the busbar differential protection.

14.2.4 Principles and Configurations of Transformer Protection

14.2.4.1 Principles of Transformer Protection

The UHV voltage-regulating transformer and compensating transformer are three-phase split-phase transformers. During operation, due to different CT transformation ratios and tap positions, the amplitude of current at each side is different. Such current needs to be compensated using such methods as balance coefficient, polarity conversion, etc. to eliminate the difference in current amplitude. The differential protection for voltage-regulating transformer and compensating transformer is specifically installed for preventing insufficient sensitivity by the main transformer protection against the turn-to-turn fault of voltage-regulating transformer and compensating transformer. The conventional protection for voltage-regulating transformer and compensating transformer is only suitable for no-load voltage regulation mode. To adapt to the on-load voltage regulation mode, the existing protection for voltage-regulating transformer and compensating transformer must be modified.

1. Impacts of on-load voltage regulation on the main transformer and compensating transformer
   (1) During on-load tap position shifting, the scope of voltage regulation for the voltage at the MV side of the main transformer is 5%. As the setting i done according to the principle for setting the main transformer differential setting, the impact of voltage regulation error on the main transformer protection is small, that is, the impact of on-load tap position shifting on the main transformer can be neglected.
   (2) During on-load tap position shifting, the transformation ratio of compensating transformer will not change, so no differential current of the compensating transformer will occur during tap position shifting. If the protection setting area is not switched over, only the sensitivity of differential protection will be affected. When a low tap position is shifted to a high tap position, the sensitivity increases; when a high tap position is shifted to a low tap position, the sensitivity decreases. However, the rated current of compensating transformer does not change too much under various tap positions, of which the maximum difference between them is 130 A, about 0.2 I_e. This has a small impact on the sensitivity, that is, the impact of on-load tap position shifting on the compensating transformer can be neglected.

2. Impact of on-load voltage regulation on the protection of voltage-regulating transformers

(1) Since the voltage-regulating transformer has several tap positions (for example, tap positions 1–9, or tap positions 1–21, etc.), under different tap positions, each tap position corresponds to a group of system parameter settings. The group number of settings is same as that of the tap positions. When the tap position is smaller than the middle tap position, it is a positive tap position; when the tap position is greater than the middle tap position, it is a negative tap position. For a voltage-regulating transformer with 21 tap positions, the 11th tap position is the middle one. Correspondingly, tap positions 1–10 are positive tap positions, and 12–21 tap positions are negative ones. When the voltage-regulating transformer is in the middle tap position and the differential protection of voltage-regulating transformer calculates the differential current, the current at the LV side is set as 0 fixedly. When in the negative tap positions, since the dotted terminal on the primary circuit of voltage-regulating transformer changes under the negative tap positions, the current polarity at the angle side of voltage-regulating transformer will not change, while the polarity at the star side of voltage-regulating transformer will change at the time of calculating the differential current. The changing of the polarity is adjusted automatically by the protection software internally.

(2) The on-load voltage-regulating transformer can regulate the tap position under load to control the change in the transformation ratio of transformer to adapt to the change in the system voltage. The differential current occurs with the change in the tap of transformer. Since the change in ΔU of the voltage-regulating transformer is in a range of $\pm 100\%$, the differential current of voltage-regulating transformer cannot be calculated using the fixed transformation ratio. Therefore, in the setting, it is necessary to increase the rated current setting at the original and secondary side (angle side/star side) of the voltage-regulating transformer to adapt to the switching over of tap positions, and further to adjust the balance coefficient of differential protection and improve the calculation of differential current.

(3) Each tap position of the voltage-regulating transformer corresponds to a group of system parameter settings. In each tap position, the rated current ratio of transformer is different, and the corresponding balance coefficient K_n is different. During on-load voltage regulation, in the transient process of switching the tap positions, a process of short circuit exists in the two adjacent tap positions during on-load tap position shifting. However, since the transition resistance exists on the on-load switch between the short circuits, the short circuit of two adjacent tap positions will not cause the voltage-regulating transformer to generate differential current, that is, the impact of the short circuit of two adjacent tap positions on the differential current can be neglected. The main factor of generating the differential current is that the definite settings

may be different with the actual tap positions, causing the differential current of differential protection beyond the limit. Assuming that the currently definite tap position is n, and the operating tap position is $n + 1$, the calculated differential current and ratio braking coefficient at the HV side are shown in Eq. (14.15):

$$\begin{cases} I_{\mathrm{d}} = I_{\mathrm{l}}K_{\mathrm{n}} - I_{\mathrm{l}}K_{\mathrm{n}+1} = \frac{(K_{\mathrm{n}}-K_{\mathrm{n}+1})}{K_{\mathrm{n}}} I_{\mathrm{ne}} \\ k_{\mathrm{r}} = 2\frac{I_{\mathrm{l}}K_{\mathrm{n}}-I_{\mathrm{l}}K_{\mathrm{n}+1}}{I_{\mathrm{l}}K_{\mathrm{n}}+I_{\mathrm{l}}K_{\mathrm{n}+1}} = 2\frac{(K_{\mathrm{n}}-K_{\mathrm{n}+1})}{(K_{\mathrm{n}}+K_{\mathrm{n}+1})} \end{cases}. \tag{14.15}$$

In positions nearby the maximum positive and negative tap, since the transformation ratio of adjacent tap positions has small change, after shifting the tap position, smaller differential current will occur. For example, tap positions 1↔2 and tap positions 20↔21, such differential current will normally not be greater than 0.2 I_{e}, which will not cause the mis-operation of differential protection, but will make the differential current to exceed the limit and to alarm.

However, in the middle tap positions nearby the tap position 11, when the tap position is shifted to other tap positions, since the transformation ratio changes much, larger differential current will occur after shifting the tap position, which may cause the mis-operation of differential protection. By taking tap positions 9–10, for instance, the differential current is estimated using Eq. (14.16):

$$\begin{cases} I_{\mathrm{d}} = I_{\mathrm{l}}K_9 - I_{\mathrm{l}}K_{10} \approx 0.5I_{\mathrm{e}} \\ k_{\mathrm{r}} = 2\frac{I_{\mathrm{l}}K_9-I_{\mathrm{l}}K_{10}}{I_{\mathrm{l}}K_9+I_{\mathrm{l}}K_{10}} \approx 0.67 \end{cases} \tag{14.16}$$

where $K_9 = 1/18.5$ and $K_{10} = 1/18.5$, which means that the setting needs to set as 0.5 I_{e} at least, and the slope is at least greater than 0.67 to evade the fault outside the zone reliably.

Theoretically, by adjusting the differential settings and slopes, it is possible to evade any faults outside the zone except for shifting tap position 0 of the middle tap positions; because in the tap position 0 of the middle tap positions, the differential calculation of voltage-regulating transformer shall not be included in the current at the LV side of voltage-regulating transformer. However, during tap position shifting, as it is impossible for the protection to know the current tap position, if the operation setting group is different from the actual tap position, the mis-operation cannot be avoided in case of a fault outside the zone.

As for the tap position shifting related to adjusting the polarity (for example, the positive polarity is adjusted to the negative polarity), according to the above calculation equation for braking coefficient, the calculation equation shown in Eq. (14.17) shall be used to avoid the faults outside the zone:

$$k_{\mathrm{r}} = 2\frac{I_{\mathrm{l}}K_{\mathrm{n}} + I_{\mathrm{l}}K_{\mathrm{m}}}{I_{\mathrm{l}}K_{\mathrm{n}} + I_{\mathrm{l}}K_{\mathrm{m}}} = 2. \tag{14.17}$$

As we can see, since the polarity changes, the braking coefficient shall be greater than 2. However, in case of a fault occurrence inside the zone, the maximum braking coefficient will not exceed 2, and the protection will not act in case of a fault occurrence inside the zone if the setting is made by following the requirement of braking coefficient being greater than 2. Therefore, the setting for tap position shifting related to polarity conversion is contradictory when we need to achieve such goal as the fault outside the zone is evaded, while the fault inside the zone is reflected. Namely, prevention of the mis-operation will for sure lead to action refusal, and prevention of the action refusal will for sure lead to the mis-operation.

14.2.4.2 Configurations of Transformer Protection

There is great difference between the UHV transformer protection and the EHV transformer protection. The UHV transformer consists of the main transformer, voltage-regulating transformer, and compensating transformer, of which the differential protections for the voltage-regulating transformer and the compensating transformer require a separate device to achieve its goal. However, the EHV transformer is not provided with voltage-regulating transformer and compensating transformer. The EHV transformer protection is normally installed with two sets of electrical quantity protections and one set of non-electrical quantity protection. Each transformer protection has three panels, which consist of the first set of differential protection for the main transformer, the second set of differential protection for the main transformer as well as the non-electrical quantity protection for the main transformer. The UHV transformer protection includes the main transformer protection, and the protections for voltage-regulating transformer and compensating transformer. The electrical quantity protections for the main transformer, voltage-regulating transformer, and compensating transformer are double configured, while only one set of protection is configured for the non-electrical quantity protection, and the protections for the main transformer, voltage-regulating transformer, and compensating transformer shall be distributed in different protection devices, for which separate panels shall be provided. Each UHV transformer protection has five panels, which, respectively, consist of the first set of differential protection for the main transformer, the second set of differential protection for the main transformer, the non-electrical quantity protection for the main transformer, the first set of differential protection for voltage-regulating transformer and compensating transformer + the non-electrical quantity protection for voltage-regulating transformer and compensating transformer, as well as the second set of differential protection for voltage-regulating transformer and compensating transformer [14, 15].

1. Configurations of the main transformer protection
   The configurations of the main transformer protection are detailed as follows:

   (1) The main transformer protection is configured with a differential quick-break, a differential that can reflect the fault component without being set (for example, break-variable differential), longitudinal differential protection, and side differential protection.
   (2) Each side of the main transformer is configured with backup trip protection and overload alarming protection. At each side, a set of overcurrent protection or zero-sequence current protection without any blocking is installed for serving as the general backup protection for transformer. At the HV side and the MV side is the zero-sequence current protection, and at the LV side is the overcurrent protection.
   (3) For the overcurrent of the main transformer due to the external phase-to-phase short circuit, the phase-to-phase impedance protection is adopted.
   (4) For the overcurrent of the main transformer due to the external single-phase grounding short circuit, the grounding impedance protection is adopted.
   (5) The main transformer is installed with overexcitation protection. The overexcitation protection has the functions of definite time-delay signaling under low setting, and inverse time-limit tripping. The inverse time-limit characteristics shall coordinate with the excitation characteristics of the protected transformer. The overexcitation protection is installed at the 1000 kV side of the main transformer.
   (6) The LV side of transformer is configured with a voltage offset protection, which acts after sending the signal.

2. Protection configurations of voltage-regulating transformer and compensating transformer

   (1) Only differential protection is configured, and no backup protection is configured.

   The number of turns attributable to the voltage-regulating transformer and compensating transformer is relatively less compared to that of the whole transformer. When a slight turn-to-turn fault occurs, it looks slighter from the view of the main transformer, and it is very difficult for the longitudinal differential protection of the main transformer to act. Therefore, differential protections shall be configured separately for the voltage-regulating transformer and the compensating transformer, and incorporated in a separate electrical quantity protection device. In addition, separate non-electrical quantity protection devices shall also be installed. The purpose of configuring the protections for the voltage-regulating transformer and compensating transformer is to improve the sensitivity of the internal turn-to-turn fault of voltage-regulating transformer and

compensating transformer. Therefore, the voltage-regulating transformer and compensating transformer are configured with the differential protections only, and no backup protection is configured.

(2) Only longitudinal differential protection is configured, and no differential quick-break protection and break-variable differential protection are configured.
Since the voltage-regulating transformer and the compensating transformer has much smaller capacity than the main transformer, during no-load closing of the main transformer, very large excitation surge current will occur in the voltage-regulating transformer and the compensating transformer. The action current setting of differential quick-break protection is normally set according to 6–8 times the rated current of transformer. During no-load closing, the differential quick-break protections for the voltage-regulating transformer and the compensating transformer may mis-operate. Therefore, the voltage-regulating transformer and the compensating transformer are configured with the longitudinal differential protections only, and no differential quick-break protection and break-variable differential protection are configured.

3. Protection function and protection scope of each differential protection
The protection scope of each differential protection for the main transformer is shown in Fig. 14.14.

(1) Longitudinal differential protection (in service): such protection consists of the Current transformer CTH1/CTH2 at the HV side, the Current transformer CTM1/CTM2 at the MV side and the Current transformer CTL1/CTL2 at the LV side, which can reflect the various faults at each side of transformer. Since the magnetic coupling relation exists in the differential circuit, the criteria for blocking the excitation surge current are installed.
(2) Split-phase differential protection (out of service): such protection consists of the Current transformer CTH1/CTH2 at the HV side, the Current transformer CTM1/CTM2 at the MV side and the bushing CT4 at the LV side. Its protection scope includes all the faults on the internal winding of transformer, and the faults on the lead wires at the HV side and the MV side. Since magnetic coupling relation exists in the differential circuit, the criteria for blocking the excitation surge current are provided. As compared with the longitudinal differential protection, there is no Y/Δ winding relation, the differential current has realized the real split-phase calculation, the zero-sequence component is also introduced into the differential circuit, and the characteristics of differential current are more real, which makes the discrimination of the blocking logic for excitation surge current become more clear and simple.
(3) Side differential protection (in service): such protection consists of the Current transformer CTH1/CTH2 at the HV side, the Current transformer

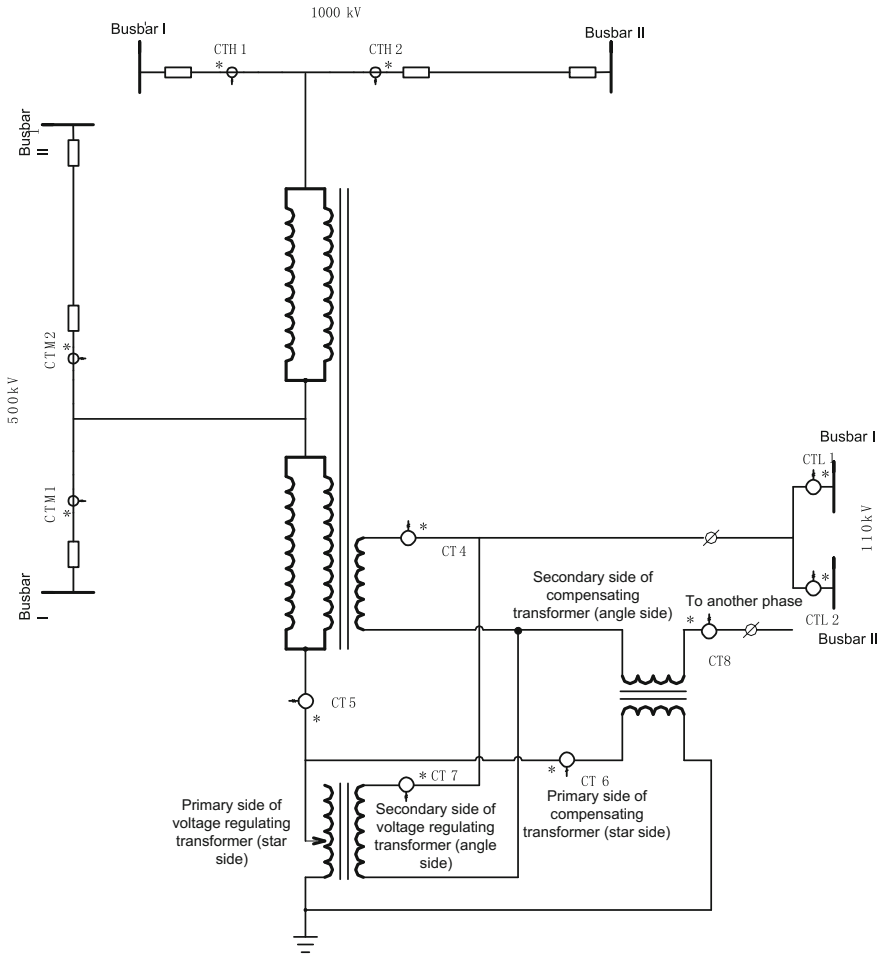

Fig. 14.14 CT configurations of UHV transformer

CTM1/CTM2 at the MV side and the common winding bushing CT5. Its protection scope includes the grounding and phase-to-phase faults on the winding and lead wires at the HV side and the MV side, excluding the turn-to-turn faults of winding. Since no magnetic coupling relation exists in the differential circuit, such protection will not be affected by the excitation surge current.

(4) Differential protection for LV side (out of service): such protection consists of the bushing CT4 at the LV side, the Current transformer CTL1/CTL2 at the LV side, and the bushing at the secondary side of the voltage-regulating transformer. Its protection scope includes the grounding and phase-to-phase faults on the lead wires at the LV side, excluding the turn-to-turn faults of

winding. Since no magnetic coupling relation exists in the differential circuit, such protection will not be affected by the excitation surge current.

(5) Differential protection of compensating transformer (in service): such protection consists of CT8 and CT6. Its protection scope includes all of the faults on the internal winding of compensating transformer and the faults on the lead wires. Since the magnetic coupling relation exists in the differential circuit, the criteria for blocking the excitation surge current are installed.

(6) Differential protection of voltage-regulating transformer (in service): such protection consists of CT5, CT6, and CT7. Its protection scope includes all of the faults on the internal winding of voltage-regulating transformer and the faults on the lead wires. Since the magnetic coupling relation exists in the differential circuit, the criteria for blocking the excitation surge current are installed.

The typical configurations for the electrical quantity protection and non-electrical quantity protection of #1 main transformer, and for the first set of protective panels of the voltage-regulating transformer and compensating transformer in a 1000 kV substation are shown in Tables 14.8, 14.9 and 14.10, respectively [16].

14.2.4.3 Setting of Transformer Protection

Each protection setting shall be determined according to the rated parameters of transformer. The parameters of 1000 kV UHV transformer are shown in Table 14.11.

According to the parameters of the UHV transformer, the primary rated current at each side can be calculated as follows:

HV side: 1649.6 A; MV side: 3299.2 A; LV side: 15746.4 A (tap position shifted to full capacity), 5248.8 A (tap position shifted to minimum capacity).

1. Setting of the main transformer protection

   The differential protection of transformer shall be set by following the principle that the internal faults of transformer can be cleared rapidly and mis-operation due to any fault outside the zone will not happen. The starting current of differential protection is normally (0.2–0.6) I_e (I_e is the rated current at the HV side of the UHV main transformer) [7, 13].

   The distance protection is the backup protection for part of the winding of transformer, and it does not serve as the backup protection for the faults at the LV side of the transformer. For the impedance protection with the offset characteristics, the impedance directing to the transformer shall not go beyond the busbar at the opposite side, and the reliable factor should be 70%. The settings for the busbar side shall be set by ensuring sufficient sensitivity in case of a metallic fault on the busbar. The HV side shall be set by 10% of the impedance directing to the transformer side, and the MV side shall be set by 20% of the

Table 14.8 Configurations for electrical quantity protection of #1 main transformer in a 1000 kV substation

Model	Name of protection		Remarks
For example: SGT756	Main protection	Ratio-differential	
		Differential quick-break	
		Ratio-differential for power frequency variation	
		Zero-sequence ratio-differential	
	Backup protection	Phase-to-phase impedance at the HV side	
		Grounding impedance at the HV side	
		Overcurrent in compound voltage direction at the HV side	Out of service
		Overcurrent in zero-sequence direction at the HV side	
		Overexcitation	Definite time-limit alarm under low setting; inverse time-limit tripping
		Phase-to-phase impedance at the MV side	
		Grounding impedance at the MV side	
		Overcurrent in compound voltage direction at the MV side	Out of service
		Overcurrent in zero-sequence direction at the MV side	
		Overcurrent in zero-sequence at common winding	Out of service
		Overcurrent protection at the LV side	Trip the CBs on the LV branches of the main transformer by the action in the first time limit; trip the CBs at three sides by the action in the second time limit
		Overload	Alarm

(continued)

Table 14.8 (continued)

Model	Name of protection		Remarks
		Overcurrent of LV bushing	Trip all the CBs on the LV branches of the main transformer by the action in the first time limit; trip the CBs at three sides by the action in the second time limit
		Differential for the LV side	Out of service
		Zero-sequence overvoltage at the LV side	Alarm
		PT disconnection	Alarm

Table 14.9 Configurations for non-electrical quantity protection of #1 main transformer in a 1000 kV substation

Model		Name of protection	Remarks
Non-electrical quantity protection of main transformer	For example: PST-1210UA	Heavy gas protection of main transformer	Trip
		Light gas protection of main transformer	Alarm (there are different requirements by the Life Movement Department of every province and city for putting in service the Pressure release or having it tripped)
		Cooler of main transformer completely shut down	
		Pressure release of main transformer	
		Cooler oil flow fault of main transformer	
		Oil temperature HIGH of main transformer	
		Winding temperature HIGH of main transformer	
		Oil level HIGH of main transformer	
		Oil level LOW of main transformer	

Table 14.10 Protection configurations for the first set of protective panel of voltage-regulating transformer and compensating transformer of #1 main transformer in a 1000 kV substation

Model		Name of protection	Remarks
Protection 1 of voltage-regulating transformer and compensating transformer of #1 main transformer	For example: SGT756	Heavy gas protection of main transformer	Trip the ratio-differential protection of voltage-regulating transformer
		Ratio-differential protection of power frequency variation for voltage-regulating transformer	Out of service
		Ratio-differential protection of compensating transformer	
		Ratio-differential protection of power frequency variation for compensating transformer	Out of service
Non-electrical quantity protection of voltage-regulating transformer & compensating transformer of #1 main transformer	For example: PST1210UA	Heavy gas protection of voltage-regulating transformer and compensating transformer	Trip
		Light gas protection of voltage-regulating transformer and compensating transformer	Alarm
		Pressure release of voltage-regulating transformer and compensating transformer	
		Oil temperature HIGH of voltage-regulating transformer and compensating transformer	
		Winding temperature HIGH of voltage-regulating transformer and compensating transformer	

(continued)

Table 14.10 (continued)

Model		Name of protection	Remarks
		Oil level HIGH of voltage-regulating transformer and compensating transformer	
		Oil level LOW of voltage-regulating transformer and compensating transformer	
		Oil level ABNORMAL of voltage-regulating switch	
		Heavy gas protection of voltage-regulating switch	

Table 14.11 Parameters of 1000 kV UHV transformer

Main transformer	Rated capacity of single phase	1000/1000/334MVA
	Rated voltage of single phase	606/303(1 ± 5%)/110 kV
	Short-circuit impedance/%	High-middle: 18; High-low: 62; Middle-low: 40
Voltage-regulating transformer	Rated capacity of single phase	59MVA
Compensating transformer	Rated capacity of single phase	18MVA

impedance directing to the transformer side. The time setting shall evade the system oscillation period and meet the requirement of the thermal overload of the main transformer, which is normally 2 s.

The zero-sequence section II current protection at the HV side and the MV side of the transformer shall be set by ensuring the sensitivity of the busbar at this side in case of 100 Ω high-resistance grounding fault. The time setting shall coordinate with the zero-sequence current protection in the inverse time-limit direction at the outgoing line of this side. The action time of the zero-sequence Section II current protection for two or above transformers in the same substation, which are in operation in parallel shall be set according to different time limits, for which the time difference shall be 0.3 s.

The setting of the three-phase overcurrent protection for the bushing at the LV side of transformer shall be set to evade the rated current at the LV side reliably, and calibrated by ensuring the sensitivity in case of phase-to-phase fault at the LV side of the transformer. The setting of three-phase overcurrent protection for the branches at the LV side of the transformer shall be set to evade the rated current of the LV branches reliably, and calibrated by ensuring the sensitivity in case of phase-to-phase fault at the LV side of the transformer. The alarm setting of overexcitation protection shall be 1.06 times the multiples of overexcitation. In case of 1.1 times the multiples of overexcitation, the inverse time-limit trip curve shall start, and the trip time shall coordinate with the overexcitation capability curve provided by the main transformer manufacturer.

2. Setting of voltage-regulating transformer and compensating transformer
The sensitivity differential of voltage-regulating transformer and the differential of compensating transformer shall be set by following the principle that the internal faults of each transformer can be cleared rapidly and mis-operation will not happen due to any fault outside the zone. The starting current of differential protections for the voltage-regulating transformer and the compensating transformer shall be normally 0.5 I_e (I_e is the rated current at 110 kV side determined by the rated current of the main transformer and the rated current of common winding.). The settings of all the tap positions for the differential protection of compensating transformer shall be set based on the highest tap position. The setting of each tap position of the differential protection for the voltage-regulating transformer shall be set based on the rated current of each tap position. Each tap position in operation has a corresponding group of setting groups, of which, the neutral tap position (rated tap position, middle tap position) shall be set based on the highest tap position.
For the non-sensitivity differential of on-load voltage-regulating transformer, only the rated current and voltage of the tap position corresponding to the middle tap position of voltage-regulating winding shall be selected. For example, for the voltage-regulating transformer with 21 tap positions, tap position #5 or #17 shall be selected, and shall be set based on 1.2 times the rated current. The CT disconnection will block the differential protections for the main transformer, the voltage-regulating transformer and the compensating transformer, but when it is detected that the differential current has reached a certain value, the differential protections for the main transformer, the voltage-regulating transformer and compensating transformer will restart.

14.2.5 Principles and Configurations of HV Shunt Reactor Protection

14.2.5.1 Protection Principles of HV Shunt Reactor

The turn-to-turn short circuit of HV shunt reactor is a common internal fault. When the number of short-circuit turns is small, the unbalance of three-phase current caused by a turn-to-turn short circuit in one phase is small. It is very difficult for the relay protection device to detect such current. In spite of how much the number of short-circuit turns is, the longitudinal differential protection always cannot reflect the turn-to-turn short-circuit faults. Therefore, the sensitive and reliable interturn protection must be adopted for the HV shunt reactor.

Zero-sequence power directional elements, self-adaptive, and compensating type: in case of an internal turn-to-turn short-circuit fault in the reactor, the phase-lead zero-sequence voltage of the zero-sequence current will approach to 90°. In case of an internal single-phase grounding short-circuit fault in the reactor, the phase of zero-sequence current will go ahead of the zero-sequence voltage. In case of an external single-phase grounding short-circuit fault in the reactor, the phase of zero-sequence current will lag behind the zero-sequence voltage. Therefore, utilizing the phase relation between zero-sequence current and zero-sequence voltage at the head end of the reactor, it is possible to distinguish the turn-to-turn short circuits and internal grounding short circuits of the reactor, as well as the external grounding short circuits of the reactor. Compared with the zero-sequence impedance of reactor, the zero-sequence impedance of the system is very small. When a turn-to-turn short circuit occurs, its zero-sequence source is within the reactor, and the zero-sequence current has a very small voltage drop (zero-sequence voltage) across the system zero-sequence impedance. To improve the sensitivity of turn-to-turn short-circuit protection, the zero-sequence voltage needs to be compensated.

Zero-sequence impedance elements: the primary zero-sequence impedance of reactor is normally several thousands of ohms while that of the system is normally dozens of ohms. By measuring the zero-sequence impedance at the port of reactor, the protection device can judge whether a turn-to-turn fault has occurred. When a turn-to-turn short circuit and an internal single-phase grounding fault occurs on the reactor, the zero-sequence impedance measured at the port of reactor is the zero-sequence impedance of the system; when an external single-phase grounding fault occurs on the reactor, the zero-sequence impedance measured at the port of reactor is the zero-sequence impedance of the reactor. Utilizing the big difference in these two measured values, the turn-to-turn short circuit and internal grounding short circuit of the reactor as well as the external grounding short circuit of the reactor can be distinguished.

Starting elements of interturn protection: the interturn protection device is installed with the starting elements with floating thresholds to ensure that the interturn protection will not mis-operate in the transient process, e.g.,

non-full-phase operation of the line (or series compensated line), reclosing of the reclosing device after a grounding fault occurrence on the line (or series compensated line), non-synchronism of the switch, reactor with energization unloaded line (or series compensated line), LC oscillation after tripping of the switches at both ends of the line, faults outside the zone, and non-full-phase accompanying the system oscillation.

The self-adaptive and compensating type zero-sequence power directional elements, the zero-sequence impedance elements as well as the starting elements of the turn-to-turn short-circuit protection with floating thresholds for power frequency variation constitute jointly the turn-to-turn short-circuit protection. Such configuration can not only improve the action sensitivity of the interturn protection, but also ensure that no mis-operation will occur in case of external short circuit or any abnormal operating conditions. The logic of the interturn protection is shown in Fig. 14.15.

14.2.5.2 Configurations of HV Shunt Reactor Protection

The 1000 kV HV shunt reactor is normally configured with the double main and backup electrical quantity protections, and one set of non-electrical quantity protection. The main protection for the HV shunt reactor includes differential protection, zero-sequence differential protection and interturn protection. The backup protection for the HV shunt reactor includes overcurrent protection, zero-sequence overcurrent protection and overload protection. The neutral point reactor of the HV shunt reactor is configured with overcurrent protection and overload protection. The non-electrical quantity protection for HV shunt reactor includes the main reactor

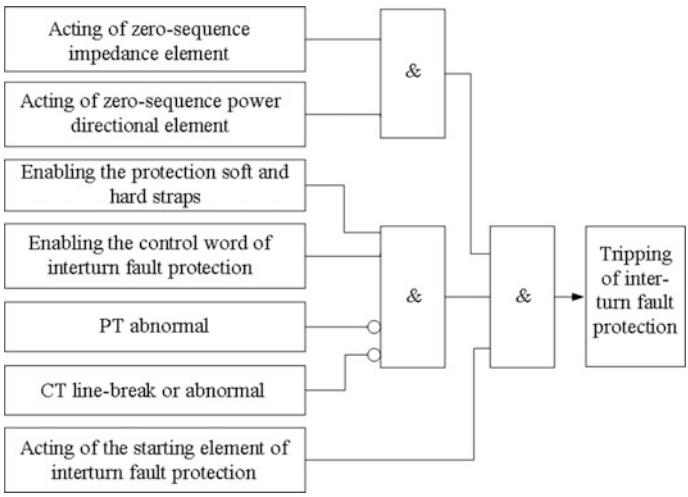

Fig. 14.15 Logic block diagram of interturn protection

and the neutral point reactor. In addition, in case no special CBs are provided for the HV shunt reactor of the line, the acting of the electrical quantity protection for HV shunt reactor shall be able to trip the CBs at the opposite side of the line through the remote tripping circuit besides tripping the line CBs at this side [17]. The typical configurations of the HV shunt reactor protection are shown in Fig. 14.16.

The protections shown in Fig. 14.16 are completed in one device, and all the electrical quantities are connected to the device once. The second group of CTs and the second device are utilized to furnish the second set of protection functions (the same as the first set) in such a way to constitute the double main protections and double backup protections.

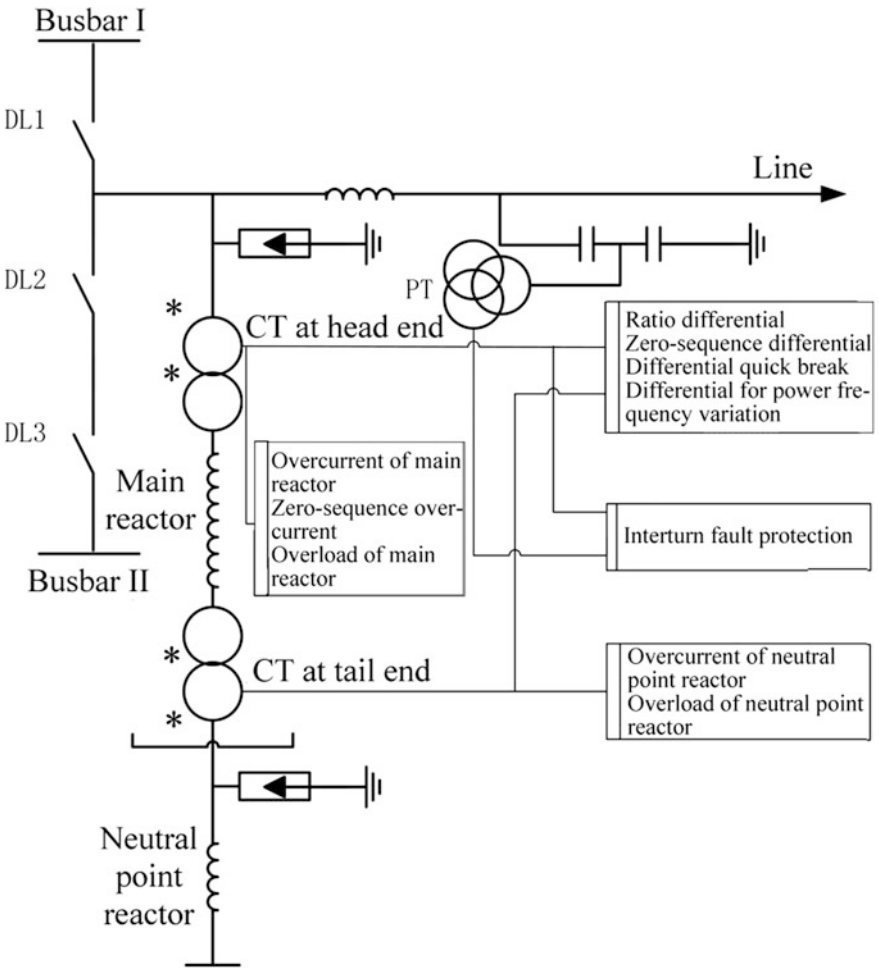

Fig. 14.16 Typical configurations of HV shunt reactor protection

The configurations of shunt HV reactor protection for a UHV line are as follows: the first set of protection is the model CSC-330A digital-type reactor protection device and the model CSC-336C1 digital-type non-electrical quantity protection device, manufactured by Beijing Sifang Automation Co., LTD. The second set of protection is the HV shunt reactor package protection device, model PCS-917G, manufactured by Nanrui Electric Co., LTD. The configurations are detailed in Table 14.12.

14.2.5.3 Setting of HV Shunt Reactor Protection

The rated parameters of HV shunt reactor in a UHV project are shown in Table 14.13.

The minimum current setting of differential protection shall be set to evade the maximum unbalanced current under the rated load of reactor reliably. In the practical setting calculation, $I_{\text{op.min}} = 0.2 \sim 0.5 I_{\text{e}}$ may be selected, and the unbalanced current in the differential circuit shall be measured, and enlarged if necessary [13].

The setting of differential quick-break protection shall evade the maximum unbalanced current generated out of the non-synchronization closing of the line reliably, for which 3–6 times the rated current of reactor can be generally selected.

The zero-sequence differential protection shall be set by avoiding the maximum zero-sequence differential current that may occur during the normal operation and the unbalanced current in case of an external single-phase grounding, for which 0.2–0.5 times the rated current of reactor can be generally selected.

The overcurrent protection of the main reactor shall evade the overcurrent of reactor that may occur in the transient process. Its current setting shall be set based on 1.4 times the rated current of reactor, with a time delay of 1.5–3 s.

The zero-sequence overcurrent of the main reactor shall be set to evade the zero-sequence excitation surge current when putting into service under no load, and the zero-sequence current during non-full-phase operation. Its current setting can be set based on 1.35 times the rated current of reactor, and its time limit shall normally coordinate with the backup section of the line grounding protection, for which 2 s is generally selected.

The overload protection of the main reactor shall evade the rated current of the main reactor. Its current setting can be set based on 1.1 times the rated current of the main reactor, with a time delay of 5 s.

The setting of the overcurrent protection of small neutral point reactor shall be normally set based on five times the rated current of small neutral point reactor. The time delay shall reliably evade the non-full-phase operation time of the line and the attenuation time of excitation surge current when the reactor is put into service under no load, for which 5 s is generally selected.

Table 14.12 Configurations of shunt reactor protection for UHV line

Name of Protections	Models		Configurations	Remarks
The first set of reactor protection	Digital-type reactor protection device CSC-330A	Main protection	Differential protection of main reactor	
			Zero-sequence differential protection of main reactor	
			Interturn protection of main reactor	
		Backup protection	Overcurrent protection of main reactor	
			Zero-sequence overcurrent protection of main reactor	
			Overcurrent protection of neutral point reactor	
			Overload alarming of main reactor protection	
			Overload alarming of neutral point reactor protection	
	Digital-type non-electrical quantity protection device CSC-336C1	Heavy gas protection of main reactor		
		Heavy gas protection of small reactor		
		Light gas protection of small reactor		
		Oil temperature HIGH I of small reactor		
		Oil temperature HIGH II of small reactor		
		Oil level ABNORMAL of small reactor		
		Light gas protection of bushing ascending flange (HV shunt reactor in Hu-An Line I)		
		Heavy gas protection of bushing ascending flange (HV shunt reactor in Hu-An Line I)		
		Pressure release of main reactor		

(continued)

Table 14.12 (continued)

Name of Protections	Models	Configurations		Remarks
		Oil temperature HIGH I of main reactor		
		Oil temperature HIGH II of main reactor		
		Winding temperature HIGH I of main reactor		
		Winding temperature HIGH II of main reactor		
		Oil level ABNORMAL of main reactor		
		Pressure release of small reactor		
		Light gas protection of main reactor		
The second set of reactor protection	HV shunt reactor package protection device PCS-917G	Main protection	Differential quick break	
			Ratio-differential	
			Zero-sequence differential	
			Ratio-differential for power frequency variation	
			Interturn protection	
		Backup protection	Overcurrent protection	
			Zero-sequence overcurrent	
			Overcurrent of neutral point reactor	
			Overload alarming of main reactor	
			Overload alarming of neutral point reactor	

Table 14.13 Rated Parameters of 1000 kV UHV Shunt Reactor

Parameter	Phase A	Phase B	Phase C	Neutral Point Reactor
Rated capacity (kvar)	240000	240000	240000	630
Rated voltage (kV)	$1100/\sqrt{3}$	$1100/\sqrt{3}$	$1100/\sqrt{3}$	–
Rated current (A)	377.9	377.9	377.9	30

The setting of the overload protection of small neutral point reactor shall be generally set based on 1.2 times the rated current of small neutral point reactor. The time delay shall reliably evade the non-full-phase operation time of the line and the attenuation time of excitation surge current when the reactor is put into service under no load, for which 10 s is generally selected.

The CT disconnection shall block the differential protection of the HV shunt reactor. However, after the CT line is broken, when the differential current reaches 1.2 I_e, the differential protection is automatically unblocked, and opens the tripping outlet.

14.2.6 Principles and Configurations of LV Shunt Reactor and LV Capacitor Protection

14.2.6.1 Protection Principles of LV Shunt Reactor and LV Capacitor

Utilizing the setting of control word "enable or disable the heavy current blocking", the protection device controls the enable/disable of the switching function of outlet tripping. The specific logics are as follows:

(1) When enabling the control word of "enable or disable heavy current blocking", different outlets will be selected by the protection of the device according to the current amplitude at that time when it acts on the outlet tripping. When the current is greater than the setting for heavy current blocking, the outlet tripping shall be that as set according to the outlet matrix of heavy current (that is, tripping the CBs at the LV branches of the main transformer). When the current is smaller than the setting for heavy current blocking, the outlet tripping shall be that as set according to the outlet matrix of small current (that is, tripping the load switch in this bay). Such logic is adopted for the LV shunt reactor and the LV capacitor installed with the load switches.
(2) When disabling the control word of "enable or disable heavy current blocking", the outlet tripping shall be that as set according to the outlet matrix of heavy current when the protection of the device acts on the outlet tripping. The LV shunt reactor and the LV capacitor installed with CBs shall operate on such logic.

14.2.6.2 Configurations of LV Shunt Reactor and LV Capacitor Protection

In the UHV projects in China, the LV shunt reactors at the LV side of the main transformer are all dry type. The configurations for LV shunt reactor protection are very simple, including overcurrent quick-break protection, overcurrent time-delay protection and overload protection (signaling).

Table 14.14 Configurations of LV capacitor protection in UHV project

Name of Protection	Model	Configuration	Action result
110 kV capacitor bank protection	For example: WDR-851/P	Current quick-break protection with a short time of delay	Tripping the relevant CBs
		Overcurrent protection	
		Overvoltage protection	
		Bridge differential unbalanced current protection	
		Loss of voltage protection	
		Overload protection	Alarm

The configurations of capacitor protection consist of current quick-break protection with a short time of delay, overcurrent protection, overload protection, overvoltage protection, loss of voltage protection and bridge differential unbalanced current protection [17].

The configurations of LV capacitor protection in the UHV project are shown in Table 14.14.

14.2.6.3 Setting of LV Shunt Reactor and LV Capacitor Protection

1. The equipment parameters of the LV shunt reactor in a UHV project are shown in Table 14.15.
2. Setting of reactor protection

   (1) At the LV side of the UHV main transformer, CBs are installed. The backup protection for the LV side of the main transformer normally trips the LV side in 1.4 s, and the overcurrent protection for the LV shunt reactor shall coordinate with the overcurrent protection for the LV side of the main transformer.
   (2) The CBs for LV shunt reactors are located at the head end. The LV shunt reactor protection is provided with the functions of two-section overcurrent protection and overload alarming.
   (3) The setting of overcurrent Section I (current quick break) shall be set to evade the excitation surge current at the time when the reactor is put into service, and such setting can be normally set as 5–7 times the rated current I_e, for which time of 0.1–0.2 s is selected.
   (4) The setting of overcurrent Section II shall be set to evade the rated current of reactor. Such setting can be normally set as 1.5–2.0 times the rated current I_e, for which time of 0.5–1 s is selected.
   (5) The alarming setting of overload can be 1.05 times the rated current I_e, meanwhile, a return coefficient of 0.85 shall be taken into account, and an alarm shall be given after a time delay of 5 s.

Table 14.15 Rated Parameters of LV Shunt Reactor Equipment in UHV Project

No.	Name of Item	Parameter
1	Model	BKK-80000/110 (to be set according to the actual equipment name)
2	Rated capacity	80 Mvar (single phase)
3	Rated phase voltage	105/kV
4	Rated current	1320/A
5	TA transformation ratio	1600/1

Table 14.16 Equipment parameter settings of capacitor WDR-851 in UHV project

No.	Name of item	Parameter	
1	Equipment (C)	1122, 1142	1121, 1141
2	Model (AQW)	TBB110-240000	TBB110-240000
3	Reactance rate (%)	5	12
4	Rated phase voltage (kV)	126.32	136.4
5	Rated current (A)	1097.1	1015.9
6	Wiring mode	Double-bridge differential wiring, single star type (12 in parallel, 12 in series)	
7	TA transformation ratio	1600/1	

3. Taking a UHV project as an example, the reactance rate of capacitors 1122C and 1142C at the LV sides of two main transformers is 5%, and the reactance rate of capacitors 1121C and 1141C is 12%. The equipment parameters of reactor protection WDR-851/R1 are set according to the actual conditions, which are detailed in Table 14.16.
4. Setting of capacitor protection

   (1) At the LV side of the UHV main transformer, CBs are installed. The backup protection for the LV side of the main transformer normally trips the LV side in 1.4 s, and the overcurrent protection for the capacitor shall coordinate with the overcurrent protection for the LV side of the main transformer.
   (2) The overcurrent Section I (current quick break) protection shall be set based on five times the rated current I_e. There is slight difference in the rated currents with a reactance rate of 5 and 12%. The primary values corresponding to the reactance rate shall be $5 \times 1097.1 = 5485.5$ A and $5 \times 1015.9 = 5057.5$ A, respectively, and the time delay is 0.2 s.
   (3) The overcurrent Section II protection shall be set based on two times the rated current I_e. Similarly, there is slight difference in the rated currents with a reactance rate of 5 and 12%, and the time delay is 0.5 s.
   (4) The setting of overvoltage protection shall be set by not exceeding 1.1 times the rated voltage of capacitor. The time shall normally not be greater than 10 s, and the trip shall occur with a time delay of 3 s after the protection acts.

(5) The loss of voltage protection shall be set in such a manner that it can act reliably when the busbar connected with the capacitor loses its voltage, for which 0.3–0.6 times the rated voltage is selected. In terms of time, such protection shall coordinate with the sensitivity of the outgoing line protection for the same level of busbar properly, for which 0.5–0.8 s is normally selected. To prevent TV disconnection protection from mis-operation, the loss of voltage protection can be set based on 0.5–0.8 times the rated current I_e through the current blocking. A fixed value of 50 V is selected, namely 0.5 times the rated line voltage 100 V, with a time delay of 0.8 s. The setting of current blocking is 0.5 times the rated current I_e.

(6) The double-bridge differential unbalanced current protection shall be set based on 1.29 times the rated voltage of capacitor and by ensuring reliable action with a certain unbalance factor taken into account. The time delay is 0.2 s for such setting.

References

1. Liu Z. UHV power system. Beijing: China Economic Press; 2005.
2. He J. UHV AC & DC transmission protection and control technologies. Beijing: China Electric Power Press; 2014.
3. GB/Z25841-2010. Guide of relaying protection for 1000 kV power system; 2010.
4. GB/T14285-2006. Technical code for relaying protection and security automatic equipment; 2006.
5. DL/T559-2007. Setting guide for 220 kV*750 kV power system protection equipment; 2007.
6. Q/GDW327-2009. Technical specification for 1000 kV transmission line protection equipment; 2009.
7. Q/GDW422-2010. Technical specification for protection setting of state grid; 2010.
8. Q/GDW1161-2014. Standardization design specification for transmission line protection and auxiliary equipment; 2014.
9. Dong X, Su B, Bo Z, He J. Study of special problems on protective relaying of UHV transmission line [J]. Autom Electr Power Syst. 2004;28(22):19–22.
10. Q/GDW329-2009. Technical specification for 1000 kV circuit breaker protection equipment; 2009.
11. Li S, Ni L, Qiu Y, Li J, Zhou H. Relay protection configuration and setting of circuit breaker in UHV AC system. Electr Power Constr. 2015;36(11):103–7.
12. Q/GDW328-2009. Technical specification for 1000 kV busbar protection equipment; 2009.
13. Q/GDW1175-2013. Standardization design specification for power transformer, high voltage shunt reactor, busbar protection and auxiliary equipment; 2013.
14. DL/T684-1999 Guide of calculating settings of relay protection for large generator and transformer; 1999.
15. Q/GDW325-2009. Technical specification for 1000 kV transformer protection equipment; 2009.
16. Li J, Ni L, Li S, Qiu Y, Zhou H. Disposition and settings of transformer relay protection in UHVAC system [J]. Electr Power Constr. 2015;36(8):22–8.
17. Q/GDW326-2009 Technical specification for 1000 kV reactor protection equipment; 2009.

Part III
Direct Current

Compared to the conventional HVDC transmission system, the system structure and operating mode of the UHVDC transmission system are more complicated, and there are also more overvoltage conditions and types for the UHVDC power transmission system, so it is required to study the overvoltage mechanism and control methods specifically. For the UHVDC insulation coordination, it is required to consider more equipment. The insulation coordination among equipment, configuration of arresters, and design of the external insulation are also more complicated; moreover, the UHV equipment manufacturing difficulty has reached the limit of the current manufacturing technology, but the rational insulation coordination design can help to solve the problem. Additionally, the UHV transmission system faces the adverse influences imposed by long air clearance insulation saturation, high altitude, etc., resulting in reduction of relative insulation margin in the UHVDC transmission system, so the UHV transmission system imposes higher requirements for the overvoltage limit and insulation coordination. Furthermore, the electromagnetic environment issue for the UHV transmission projects has become one of important factors having influence on the power grid construction and development. What is more, there are also some differences between the EHV protection and the UHV protection. With respect to the aforementioned problems in aspects, it is worthwhile to carry out an in-depth research.This section will focus on a discussion of such issues in the process of UHVDC transmission as overvoltage mechanism and its control method, insulation coordination of converter stations and transmission lines in UHVDC system, electromagnetic environment, the UHVDC system protection, etc.

Chapter 15
Basic Information and Calculation of Main Parameters for UHVDC Transmission System

Yang Shen, Xilei Chen and Yuting Qiu

The DC transmission system is composed of two converter stations and the DC line between them. In the converter station, the main equipment includes AC switch, AC filter, converter transformer, smoothing reactor, electrode line in the DC field, neutral busbar and transfer breaker, DC filter, and arresters distributed in various positions. Compared to the ±500 kV DC transmission system, the UHVDC system characteristics a more complicated operating principle, more flexible operating modes, and higher requirements for reliability. This chapter mainly discusses the operating principles and operating modes of the UHVDC system, and calculation of parameters for its main circuits.

15.1 Operating Principle of Converter

The converter is a core equipment to implement AC/DC conversion in the DC transmission system, and the operation of the DC transmission system is mainly achieved under control of the converter. The converter is known as rectifier when it is used to convert the alternating current to direct current, and vice versa, known as inverter. The converter that is operated as a rectifier or inverter depends on the

Y. Shen (✉)
China Energy Engineering Group, Zhejiang Electric Power Design Institute Co., Ltd., Hangzhou, Zhejiang, People's Republic of China
e-mail: shenyangzju@21cn.com

X. Chen
State Grid Ningbo Power Supply Company, Ningbo, Zhejiang, People's Republic of China
e-mail: 285487205@qq.com

Y. Qiu
State Grid Shanghai Power Supply Company, Shanghai, People's Republic of China
e-mail: ytqiu0927@163.com

© Zhejiang University Press, Hangzhou and Springer-Verlag GmbH Germany 2018

H. Zhou et al. (eds.), *Ultra-high Voltage AC/DC Power Transmission*,
Advanced Topics in Science and Technology in China,
https://doi.org/10.1007/978-3-662-54575-1_15

control mode. Usually, the basic unit of the converter is a three-phase bridge circuit, which is shown in Fig. 15.1. The converter has 6 bridge arms being composed of thyristors, on which the thyristor is also called converter valve or valve, so the converter is also called 6-pulse converter; if two AC power supplies with phase angle difference up to 30° are formed by a different connection method of the transformer, which input current to two 6-pulse converter, respectively, and then the two converters are connected in series to obtain a 12-pulse converter. Due to the limited voltage withstand level of a single thyristor, the converter valve in the high-voltage transmission system is normally structured by multiple thyristors being connected in series. In the UHVDC transmission system, it is required to connect 12-pulse converters in series (e.g., connecting two 12-pulse connectors in series) to obtain the rated voltage on the basis of the connecting multiple thyristors in series, due to limitation by voltage withstand level of the converter valve and grading requirements and in view of such factors as capacity and volume of the UHV converter transformer; what is more, the UHVDC transmission system adopts a 6-in. thyristor converter valve technology to meet the requirements for transmission capacity. Up to now, the rated discharge capacity of the thyristor valve developed is able to reach 5000 A, being bigger than 3000 A discharge capacity in a ±500 kV DC system.

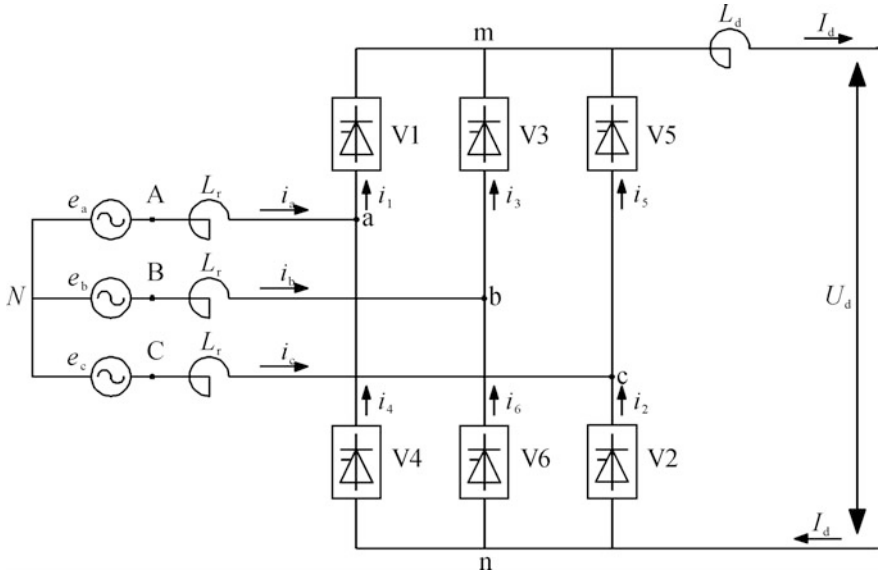

Fig. 15.1 Circuit diagram of 6-pulse converter

15.1.1 6-Pulse Converter

15.1.1.1 Rectifier

Figure 15.1 shows a three-phase bridge circuit, in which e_a, e_b, and e_c represent a three-phase voltage source, L_r represents the equivalent reactance between AC power supply and converters, referred to as commutation reactance; V1–V6 represent the 6 thyristors on the bridge arm, i_a, i_b, i_c represent the current of the three phases on AC side, i_1–i_6 represent the current flowing through 6 converter valves, L_d represents the smoothing reactor in the DC circuit, I_d represents the DC current, and U_d represents the DC voltage.

1. Ideal uncontrolled rectifier

The rectifier is connected by two valves which are on conduction simultaneously at any time, which are placed in the anode half-bridge and cathode half-bridge, respectively. As shown in Fig. 15.1, the V1, V3, and V5 are the cathode half-bridges, and V2, V4, and V6 are the anode half-bridges. Under the action of AC voltage, the six valves are turned on and off alternately in sequence. The voltage waveform output from the rectifier in a cycle is formed by six segments of line voltage, which is close to the DC voltage, namely that the rectifier rectifies the three-phase voltage to a DC voltage formed by six pulses in a cycle, so the rectifier is called a 6-pulse rectifier.

It is assumed that the DC current is smooth where the DC smoothing reactor is big enough. Within a power frequency cycle, the current flowing time for each valve is 1/3 cycle. For an AC three-phase source, each phase is connected with two converter valves at its upstream and downstream, which corresponds to the input phase current and output phase current, respectively, namely that, within a cycle, the current input time, and output time for each phase of the AC system last 1/3 cycle, so the current flows through each phase for 2/3 time in the cycle, and the input or output current equals the DC current I_d.

The output voltage of the rectifier will become a smooth DC voltage after going through a smoothing reactor which is big enough. It is possible to calculate the average value U_d of the DC voltage by the output voltage curve as shown in Fig. 15.2. Because the waveform of U_d includes 6 pulse cycles within one AC power frequency cycle, it is possible to calculate the average value of the DC voltage only by use of any pulse cycle, as shown in Eq. (15.1).

$$U_d = \frac{\int_{-\pi/6}^{\pi/6} \sqrt{2}E \cos \omega t}{\pi/3} = \frac{3\sqrt{2}}{\pi} E = 1.35E, \tag{15.1}$$

where

E effective value of the line voltage for the three-phase source on the valve side.

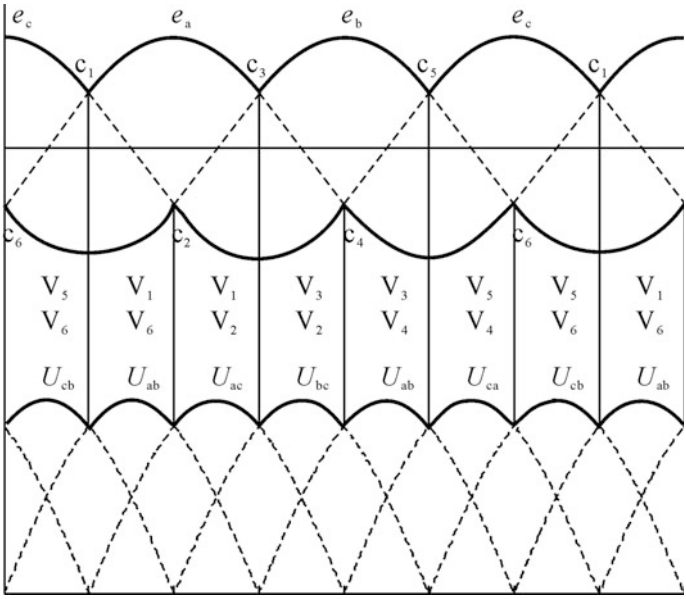

Fig. 15.2 Voltage of ideal uncontrolled rectifier

2. Ideal controlled rectifier

After the voltage stressed on the converter valve becomes positive, the control system will send a trigger pulse to the valve to conduct it. In view of the change in the AC voltage waveform of the real system and in order to ensure that the converter valve is triggered stably, it is triggered by the control system a short while after the voltage stressed on the converter valve becomes positive. As shown in Fig. 15.3, the valve V1 is triggered to be turned on a period after c_1, and the delay time is represented by the angle α, which is called trigger angle of the valve. Before the trigger pulse comes to the valve, the valve that has been turned on previously remains on as its current does not crosses the zero, and until the trigger pulse conduct the next valve to change the direction of the voltage endures at the previously closed valve, then the current flowing through the valve will cross the zero, and the valve is turned off. Compared to the uncontrolled rectifier, all valves of the controlled rectifier are triggered to be turned on by means of lagging a α angle. From Fig. 15.3, it can be known that the output voltage waveform of the ideal controlled rectifier is also formed by six same segments of line voltage, so it is possible to calculate the average DC voltage output from the ideal controlled rectifier by the equation as shown in Eq. (15.2).

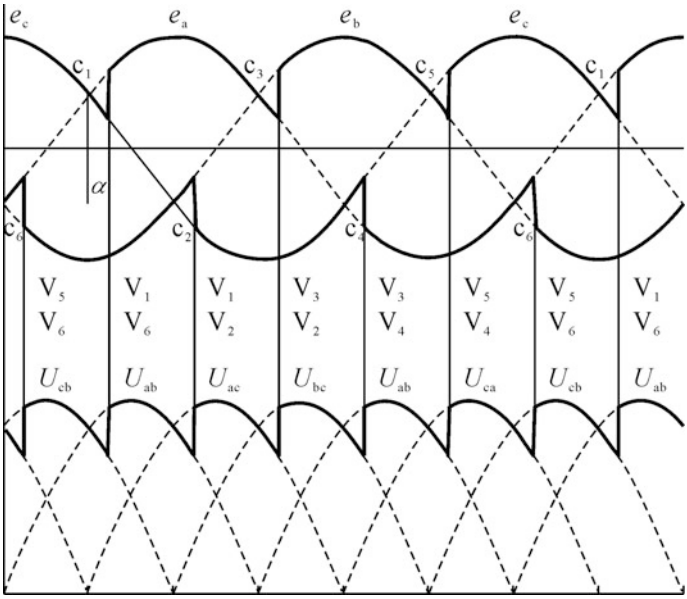

Fig. 15.3 Voltage waveform of ideal controlled rectifier

$$U_{d1} = U_d \cos \alpha, \tag{15.2}$$

where

U_d average DC output voltage of the ideal uncontrolled rectifier.

It can be known from the Eq. (15.2) that, in case of $\alpha = 0$, the rectifier is an ideal uncontrolled rectifier, whose output DC voltage also reaches the maximum value; in case of $\alpha < 90°$, the average output voltage of the rectifier is a positive value; in case of $\alpha = 90°$, the average output voltage is zero; in case of $90° < \alpha < 180°$, the average output voltage of the rectifier is a negative value, but the rectifier cannot be used as a power supply for energy supply at this moment because the current can flow through the valve in only one direction. To sum up, the trigger angle range of the rectifier in an ideal condition is 0°–90° to deliver energy to the DC side. The DC voltage output from the rectifier is directly related to the trigger angle, and for actual DC transmission projects, the DC voltage is regulated within an extremely small range, or cannot be regulated, so the trigger angle of the rectifier also can be regulated within a very small range. In view of fluctuation of the voltage waveform of the AC system, the minimum α angle is usually 5°, ensuring that valves in the rectifier can be triggered to turned on; on the other hand, when α is big the output voltage of the converter is fluctuated significantly, even after undergoing the smoothing reactor, the output DC voltage quality is very low, so the angle α should not be too big; meanwhile, the angle α can be adjusted within a certain range in case

that the system is interfered or varied. In a word, the trigger angle is normally varied within 5°–20°, and during normal operation, the trigger angle is often varied within 15° ± 2.5°.

3. Considering a controlled rectifier with commutation reactance

In the DC transmission system, the AC side of the converter is directly connected with the three-phase winding of the converter transformer. The converter transformer is same to the ordinary AC transformer with respect their principle, converting the voltage on AC side to a voltage level required for DC output. The coil at the converter valve is a part of the commutation circuit of the converter, so the inductance necessarily exists in the commutation circuit, namely $L_r > 0$. This is different from the ideal controlled rectifier described above. Still, it is assumed that the DC current I_d remains unchanged, and when the trigger pulse comes to one valve, the valve is turned on; however, the current in the valve cannot increase immediately to I_d due to the existence of inductance in the commutation circuit; similarly, the current in the previous conducted valve also cannot decrease to zero immediately; the current transfer and conversion between these two valves last a period, and the angle μ corresponding to this time is called commutation angle, and the whole process is called commutation process.

The average DC voltage of the 6-pulse rectifier during normal operation is calculated as follows:

$$\begin{cases} U_{d1} = U_d \cos\alpha - \frac{3}{\pi} X_{r1} I_d = U_d \cos\alpha - d_{r1} I_d \\ X_{r1} = \omega L_r \\ d_{r1} = 3X_{r1}/\pi \end{cases}, \tag{15.3}$$

where

X_{r1} the equivalent commutation reactance;

d_{r1} called commutation voltage drop, representing the average value of the DC voltage drop resulting from commutation during the normal operation when the DC output current value of the converter is one unit.

The calculation equation is only applicable for the circumstance when the next commutation begins and the previous commutation has been completed, namely $\mu < 60°$.

The calculation equation for commutation angle μ is as follows:

$$\mu = \arccos\left(\cos\alpha - \frac{\omega X_r I_d}{\sqrt{2}E}\right) - \alpha \tag{15.4}$$

For a rectifier, the bigger the trigger angle is, the smaller the overlap angle is, vice versa.

When the valve is turned on, the voltage stressed on the valve is zero, and when the valve is turned off, the valve will endure an AC line voltage. Taking the valve V1 as an example, the commutation process of V2–V4, V3–V5, V4–V6 has an

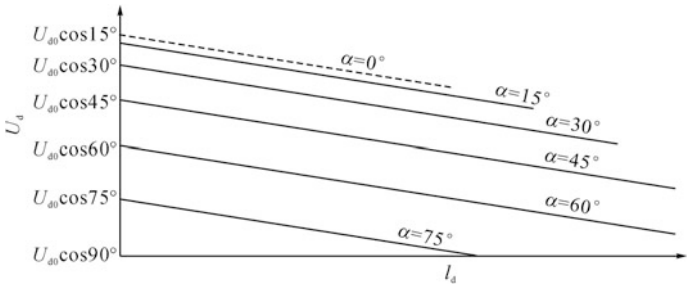

Fig. 15.4 Output external characteristic of the rectifier

influence on the three-phase voltage during closure of the V1, resulting in saw tooth on the voltage waveform of the V1. In addition, due to the existence of stray capacitance and commutation reactance in the system, transient voltage oscillation occurs during turn-off of the V1 converter valve, which is called reverse overshoot. The reverse overshoot will get the voltage stressed on the valve increased, having risk to lead to reverse breakthrough of the valve; hence, an inductance–resistance circuit is connected in parallel onto the valve for a real project, so as to equalize the distribution of the electric potential in the valve and limit the reverse overshoot magnitude.

The relationship between the average DC output voltage and direct current of the rectifier is called the external characteristic of the rectifier [1]. According to the aforementioned analysis, the external characteristic function of the rectifier can be represented as follows:

$$U_{\mathrm{d}} = U_{\mathrm{d0}} \cos \alpha - \frac{3\omega L_{\mathrm{r}}}{\pi} I_{\mathrm{d}} \tag{15.5}$$

In case of commutation angle $\mu < 60°$, a family of straight lines at a slope of -du for same trigger angle α can be mapped for the external characteristic of the rectifier by baking the direct current as the x-axis and DC voltage as the y-axis, in which the intercept of the lines on the y-axis equals the ideal controlled no-load DC voltage $U_{\mathrm{d0}} \cos \alpha$. As the trigger angle increases, the $U_{\mathrm{d0}} \cos \alpha$ decreases, and the external characteristic curve moves downward in a parallel manner, as shown in Fig. 15.4.

15.1.1.2 Inverter

The process converting direct current to alternating current is called inversion. At present, most DC transmission projects adopt the active inversion method, by which the receiving end must be provided with an AC power supply.

The inverter has a same hardware structure as the rectifier. In the previous description of the rectifier, it is mentioned that, when the trigger angle α exceeds

90°, the rectifier will become an inverter. Similar to the rectifier, the average DC voltage of the inverter is calculated as follows:

$$U_{d2} = -(U_{d02}\cos\alpha + d_{r2}I_d), \tag{15.6}$$

where

U_{d02} the ideal DC no-load voltage of inverter, and $U_{d02} = 1.35E_2$, E_2 is the effective value of the no-load line voltage on winding at the valve side of the converter transformer for the inverter;

B the advance trigger angle, meeting the condition of $\beta = 180 - \alpha$;

d_{r2} the specific commutation voltage drop of inverter, calculated by equation: $d_{r2} = 3X_{r2}/\pi$, where X_{r2} is the equivalent commutation reactance of inverter.

The similarity to the rectifier is that the voltage waveform of the V1 valve is also influenced by the V2–V4, V3–V5, and V4–V6 commutation process, and commutation tooth appears, which is shown in Fig. 15.5.

If the commutation process of the inverter fails to be completed before c4, the commutation process will be inverted, V1 begins to be turned off, and V5 will be turned on continuously because u_a is smaller than u_c after c4. This results in commutation failure. If the V5/V1 commutation is completed successfully, the voltage stressed on the valve V5 will become forward in a short time after the commutation is completed, and it is also required to consider the margin for forward blocking recovery time of the thyristor. Hence, here gives a definition of the extinction angle, namely, the time from extinction of the valve to the recovery of the voltage which is represented by an electric degree, which is called extinction

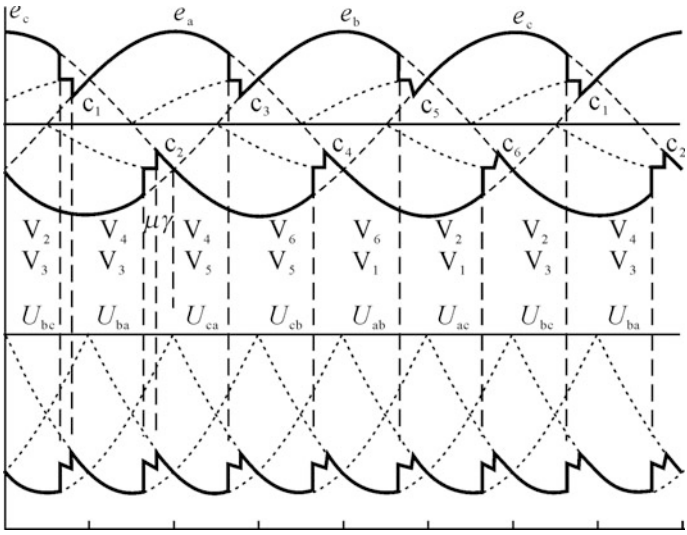

Fig. 15.5 Voltage waveform of inverter

angle γ. The relationship among the extinction angle γ, advance trigger angle β and commutation angle μ_2 is as follows:

$$\gamma = \beta - \mu_2 \tag{15.7}$$

The commutation angle μ_2 of the inverter is calculated as follows:

$$\mu_2 = \arccos\left(\cos\gamma - \frac{2X_{r2}I_d}{\sqrt{2}E_2}\right) - \gamma \tag{15.8}$$

The commutation angle of the inverter is relative to the commutation reactance X_{r2}, direct current I_d and voltage E_2 on the valve side of the converter transformer. When the direct current rises or the voltage on the valve side of the converter transformer declines, the commutation angle μ_2 will increase. If the advance trigger angle on the inverter side is too small, it is probable to lead to the commutation failure resulting from the decrease in extinction angle when the commutation angle increases. Considering the influence imposed by asymmetry of voltage at the three phases on the AC side, the extinction angle should have an abundant margin, which is typically limited to a rating being not less than 15°–18°, called γ_0. If the extinction angle is set too big, the inverter will undergo a significant fluctuation of DC voltage and poor operating characteristic, so the extinction angle taken for practical DC transmission project is usually not less than a fixed value of γ_0, and then, it is possible to obtain a corresponding commutation angle μ_2 through calculation, and adjust the advance trigger angle β.

Typically, the commutation failure issue existed in the inverter does not occur in the rectifier. This is because the time to keep a positive voltage stressed on the conducted valve after commutation of the rectifier is long enough, and the time to keep a negative voltage stressed on the shutoff valve is also long enough, while the trigger time of the inverter is relatively lagged, so that less time is left for actuation of the conducted and shutoff valve; Then, for the rectifier, even the AC voltage waveform distortion makes the valve triggered when the voltage stressed on it has not become positive, the time held by the trigger pulse still can ensure that there is trigger pulse applied to when the voltage stressed on the valve is positive in most conditions, while the voltage of the triggered valve becomes negative upon commutation of the inverter, it is probable to lead to commutation failure. As a result, the inverter is liable to result in commutation failure. The commutation failure of the inverter can result in voltage turnover on the inverter side and the abrupt increase in direct current which will lead to overcurrent of the converter valve, causing a shock to the equipment and AC system on the inverter side and influencing the safe and stable operation of the system.

The aforementioned discussion for extinction angle γ, advance trigger angle β, and commutation angle μ_2 of the inverter is based on the condition of $\beta < 60°$. In case of $\beta > 60°$, the commutation tooth triggered at this time will impose an influence on the forward voltage waveform of the previously triggered valve,

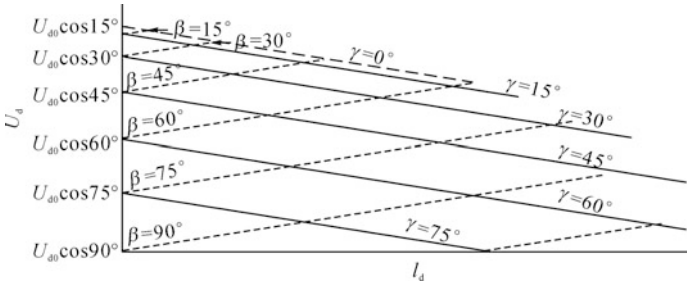

Fig. 15.6 External characteristic of inverter output

enabling the real extinction angle triggered previously to be less than the calculated value in case of $\beta < 60°$. If the commutation angle is bigger, it is probable to lead to commutation failure.

The external characteristic lines of the inverter are as shown in Fig. 15.6 [1], which are also a family of straight lines with an equivalent slope. The intercept of the equivalent β external characteristic curve at the y-axis equals the ideal controlled DC no-load voltage $U_{d0} \cos \beta$ at a slope of d_{r2}, and when the advance trigger angle β increases, the external characteristic curve moves downward in a parallel manner; the intercept of equivalent γ external characteristic curve at the y-axis equals the ideal controlled DC no-load voltage $U_{d0} \cos \gamma$ at a slope of $-d_{r2}$, and when the extinction angle γ increases, the external characteristic curve moves downward in a parallel manner.

In case of a constant advance trigger angle β, the external characteristic function is as follows:

$$U_d = U_{d0} \cos \beta + \frac{3\omega L_r}{\pi} I_d \tag{15.9}$$

In case of a constant extinction angle γ, the external characteristic function is as follows:

$$U_d = U_{d0} \cos \gamma - \frac{3\omega L_r}{\pi} I_d. \tag{15.10}$$

15.1.2 12-Pulse Converter

The DC output voltage of the 6-pulse converter fluctuates significantly. In practical DC transmission projects, two groups of AC power supplies with phase difference of 30° are derived by connecting the converter transformer in Y-connection and delta-connection, and then by connecting the 6-pulse converter units for the two groups of AC power supplies in series, a group of 12-pulse converter is formed,

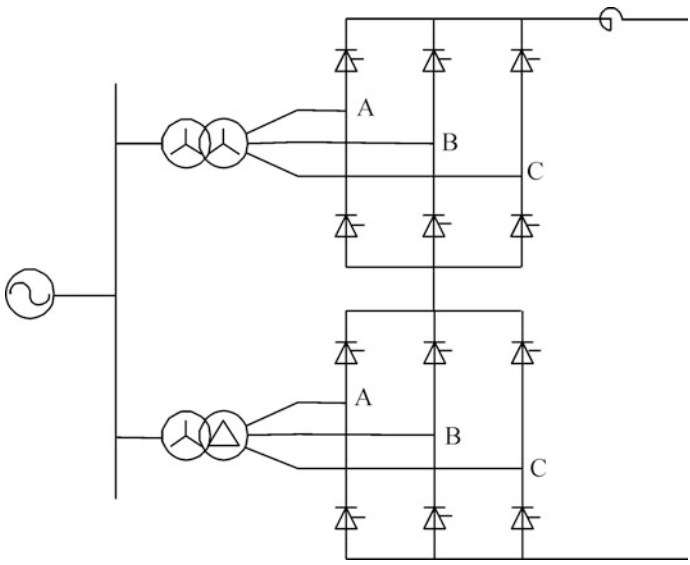

Fig. 15.7 12-pulse converter

which is shown in Fig. 15.7. The DC output voltage wave of the 12-pulse converter is smoother, and the harmonic component contained is smaller.

The DC voltage and current for the two 6-pulse converters forming a 12-pulse converter is equal, and the DC voltage of the formed 12-pulse converter is superimposed by the voltage of the two 6-pulse converters with phase difference of 30°. The 12 valves are turned on in sequence, and the difference in the trigger pulse time is 1/12 power frequency cycle. In a power frequency cycle, the DC voltage waveform has 12 pulses, so it is called 12-pulse converter.

15.1.3 Double 12-Pulse Converter Connected in Series

The "Electricity Transmission from West to East China" requires a large capacity and long distance power transmission method. The DC transmission power can be enhanced by way of increasing the current and voltage. In case that the power is increased by means of increasing the current and the transmission voltage still adopts ±500 kV DC voltage, the current is doubled, the sectional area of the line is also doubled, and the line loss is two times that resulting from the use of UHV, as well as the line cost will increase. Moreover, up to 2016, the maximum transmission current of 6-in. thyristors with maximum capacity that can be used in projects is about 5000 A. If required to further enlarge the transmission current, it is possible to use two groups of converters in parallel, but the control system of the converter systems in parallel is also complicated. To sum up, this solution is not economic.

The other solution is to increase the DC voltage, namely UHVDC transmission. If the DC voltage is increased by means of directly increasing the DC rated voltage of the converters, it is possible to increase the size of the converter transformer and converter valve equipment, exceeding the actual transportation limitation; furthermore, the increase in voltage level also imposes higher requirements for insulation level of equipment and voltage sharing design, so that the equipment manufacturing cost is multiplied, and shutdown of a single large volume equipment due to fault will lead to a big shock to the system, being unbeneficial to stable operation of the system. The other thought to increase the voltage level is to connect several converters in series. Although this solution has higher requirements for insulation level of high-end converter transformers, but it overcomes other shortcomings of the solutions mentioned above. To sum up, it is the most cost-efficiency solution. Therefore, two groups of 12-pulse converters with equal voltage are connected in series in UHVDC transmission projects.

Compare to the single 12-pulse converter for HVDC system, the double 12-pulse converter connected in series for UHVDC transmission has higher requirements for the control system, and the two groups of 12-pulse converters should be controlled separately; meanwhile, the stable operation of the system can be guaranteed only when the two control systems being operated simultaneously and coordinated closely. The voltage level of the equipment in the ±800 kV UHVDC system is complex, including ±800, ±600, ±400, ±200 kV, and neutral busbar for main equipment. Corresponding insulation coordination is provided for and between each voltage levels. In case that the converter is shorted, the fault part is related to the faulty converter and the normal converter. In fault state, the transient characteristics are more complicated than the ±500 kV DC system. Furthermore, in case the system is failed, the high-voltage equipment may be connected to the LV equipment, and the difference between the high and LV level is bigger than the conventional DC system, and the fault consequence is more severe than the conventional DC system, either.

15.2 Operating Modes of the UHVDC Transmission System

The conventional DC system with the bipolar neutral grounding at two terminals is shown in Fig. 15.8. It is composed of three parts, namely, rectifier station, DC transmission line, and inverter station, and adopts the connection method in which two monopolar ground return systems are capable of operating separately. This connection method, featuring flexible operation and high reliability, is widely used by most DC transmission projects.

In the DC transmission system, the rectifier station and inverter station are known as converter station collectively, and the rectifier and inverter in the converter station are also known as converter collectively. The operating principle of

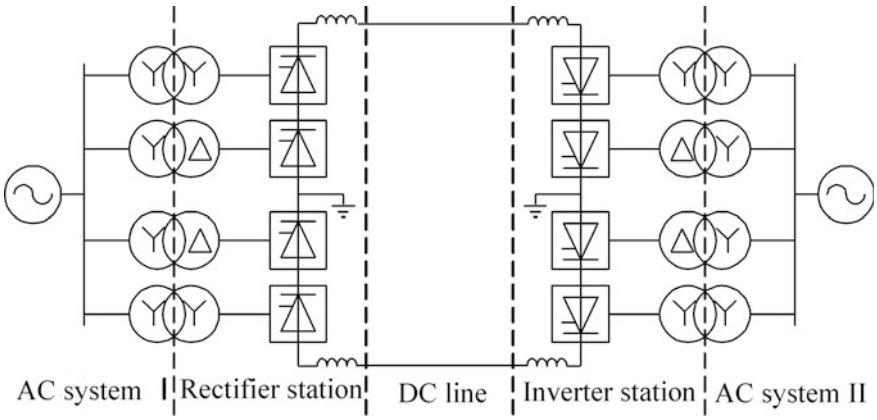

Fig. 15.8 Conventional DC system with bipolar neutral grounding at two terminals

the DC transmission systems at two terminals is as follows: the AC power is converted to a DC power via the converter station; and then the DC power is transmitted by the DC transmission line to the inverter station at the receiving end; finally, the DC power is converted to an AC power in the inverter station, and then the AC power is delivered to the AC system at the receiving end. For the two-terminal DC transmission system in which the power can be delivered back, its converter at the sending end adopts a same structure as the one at the receiving end, the converter on any side cannot only be operated as a rectifier, but also as an inverter. So, during reverse transmission of power, the rectifier station corresponds to the inverter station used during forward power transmission, and the inverter station corresponds to the rectifier station used during forward power transmission.

15.2.1 Selection of Voltage Level of UHVDC Converters

With respect to the method by which a 12-pulse converter is connected in the conventional EHVDC transmission system as shown in Fig. 15.8, in view of such factors as equipment manufacturing ability, transportation limitation, and shock influence on the AC system,the UHVDC transmission system is connected with two 12-pulse converter in series at each pole and the two 12-pulse converter are at equal voltage level (400 + 400 kV). Compared to the use of two 12-pulse converters in series with different voltage level, e.g., the typical 500 + 300 kV combination, the connection of two 12-pulse converters in series with equal voltage level boasts following benefits:

(1) The tap switches for high-voltage (HV) converter transformer and low-voltage (LV) converter transformer can be designed in a unified manner, and the HV converter valve and LV converter valve adopt a same water cooling system, and

the standby equipment also is kept the same, so as to reduce the equipment manufacturing cost and investment in the standby equipment.

(2) The maximum operating voltage of the DC bypass circuit breaker at both ends of the 12-pulse converter in parallel is 400 kV, and compared to the maximum operating voltage of 500 kV for the two converters in series with different voltage level, the manufacturing difficulty is smaller.

(3) In the 400 + 400 kV mode, the operating voltage of the four 6-pulse converters is 200, 400, 600, and 800 kV, respectively; in the 500 + 300 kV mode, the corresponding operating voltage of the four 6-pulse converters is 250, 500, 650, and 800 kV, respectively. By comparing the two modes, except that the operating voltage of the valve at uppermost layer is identical, other three operating voltages for the four 6-pulse converters in the 400 + 400 kV mode are lower than that for the latter mode. This is more beneficial to the design of insulation structure on the converter transformer valve side, bushing selection, and configuration of surge arresters.

(4) Due to the adoption of 400 + 400 kV series connection mode at two terminals, the converters at two terminals can be operated in a cross and flexible manner, and the transmission power loss is small in case of different faults.

15.2.2 Operating Modes of UHVDC System

The operating mode of the DC transmission projects means the steady-state operation conditions available for selection by the operator during operation, including: connection mode on DC side, DC power transmission direction, full voltage or reduced voltage operating mode, and control methods of the DC system, etc. The UHVDC transmission system adopts the bipolar neutral grounding at two terminals, and the two 12-pulse converters are connected in series (400 + 400 kV) at each pole. For the reason that a bypass circuit breaker and a disconnector are connected in parallel onto each 12-pulse converter, as shown in Fig. 15.9, the 12-pulse converter can be put into operation or shorted, so that it is possible to select double-12-pulse 800 kV operating mode at each pole, and also select single-12-pulse 400 kV operating mode by short-circuiting a 12-pulse converter. Therefore, compared to the connection method for the traditional 500 kV DC transmission system, the ±800 kV UHVDC transmission system can be operated by such special "semi-polar" connection modes as 1/2 bipolar operating mode, 3/4 bipolar operating mode and 1/2 monopolar operating mode, etc., and its operating mode are more flexible and diverse, and can be selected based on the actual condition.

There are many operating modes available for the ±800 kV UHVDC transmission project, and based on different connection methods, they are can be generally divided into bipolar and monopolar operating modes.

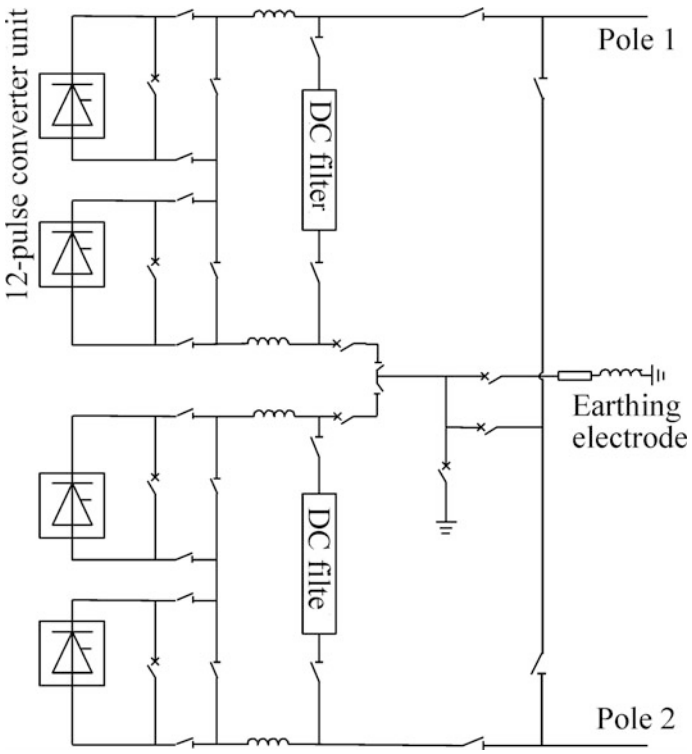

Fig. 15.9 Bipolar neutral grounding at two terminals

15.2.2.1 Bipolar Operating Mode

1. Complete bipolar operating mode

The complete bipolar operating mode is the most fundamental operating mode for bipolar DC transmission projects; all poles of the two 12-pulse converters at each pole of the bipolar are put into service during operation, which is shown in Fig. 15.10.

The complete bipolar operating circuit can be viewed as two independent monopolar ground return circuits, and the current direction of the positive pole in the ground return is opposite to the negative pole, and the current on the ground electrode is the difference between the current of two poles. During the symmetrical operation of the two poles, the ground electrode has only a little imbalance current, thus the ground electrode is corroded at the slowest speed, being beneficial to extend its service life.

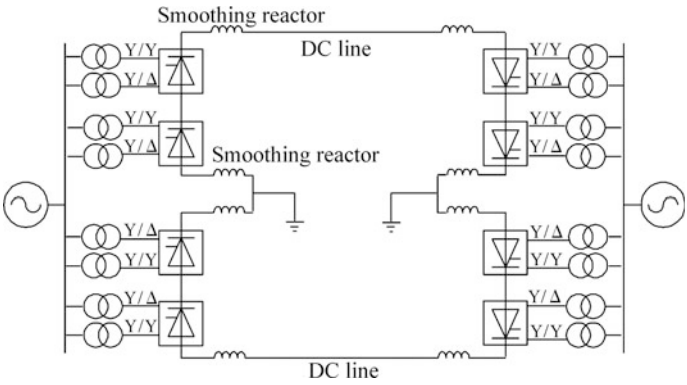

Fig. 15.10 Complete bipolar operating mode

2. 1/2 bipolar operating mode

The 1/2 bipolar operating mode means that each pole is put into operation at a voltage level of 400 kV, and only one 12-pulse converter is put into operation for each pole. The rectifier station and inverter station can select the converter to be put into operation and shorted at each pole by carrying out corresponding operation of the bypass circuit breaker and disconnector that are connected in parallel onto each 12-pulse converter. When the two converter stations at the same pole are operate in the mode of the HV converters are in operation and the low-voltage converters are shorted, or the low-voltage converters are in operation while the HV converters are shorted, this mode is called symmetrical operating mode; relatively, the mode in which the converters at different ends of both substations are put into operation is called cross operating mode. Therefore, it is possible to select symmetrical operating mode and cross operating mode for the two poles of the two substations, and there are 16 operating modes in total.

3. 3/4 bipolar operating mode

In the 3/4 bipolar operating mode, one pole is put into operation at voltage level of 800 kV, and the other pole of these two converter stations is put into operation in symmetrical or cross operating mode at a voltage level of 400 kV. During complete bipolar operation, when one 12-pulse converter in the converter station or inverter station is failed, it is possible to switch to 3/4 bipolar operating mode in a in-line manner by operating the bypass circuit breaker and disconnector, without need to stop the whole DC system, so as to improve the utilization rate of the energy. When the system is operated in a 3/4 bipolar mode, it is possible to set a same operating current for the two poles, so as to reduce the current flowing through the ground electrode, and extend service life of the ground electrode.

15.2.2.2 Monopolar Operating Mode

1. Complete monopolar operating mode

During complete monopolar operation, the operating mode in which the ground is taken as a return and only one conductor is used as the power transmission line is called monopolar ground return operating mode, as shown in Fig. 15.11. Because a big direct current flows through the ground electrode for a long period in this operating mode, it will cause electrochemical corrosion of the underground metallic facilities in the vicinity of the ground electrode, and result in such problems as magnetic saturation of the transformer, due to the increase in DC bias of the earthing transformer at a neutral point of the neighboring power station. Hence, the monopolar ground return operating mode is mainly applied at the beginning of the DC system construction, and mainly used as a transition when two poles are under construction and power transmission is required. After two poles are fully completed, this operating mode is hardly adopted.

During complete monopolar operation, the operating mode in which the transmission line for the other pole is used as a metallic return is called monopolar metallic return operating mode, as shown in Fig. 15.12. Because of preventing a great current from flowing through the ground wire, and solving the electrochemical corrosion problem of underground metallic facilities in the vicinity of the ground electrode, and magnetic saturation of the transformer resulting from DC bias of the

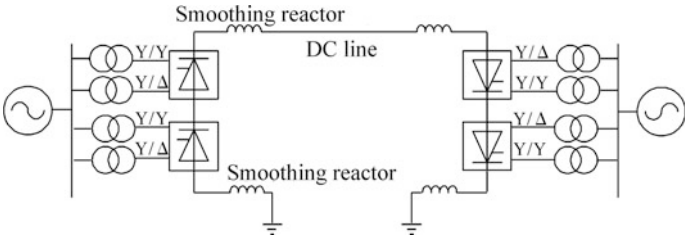

Fig. 15.11 Monopolar ground return operating mode

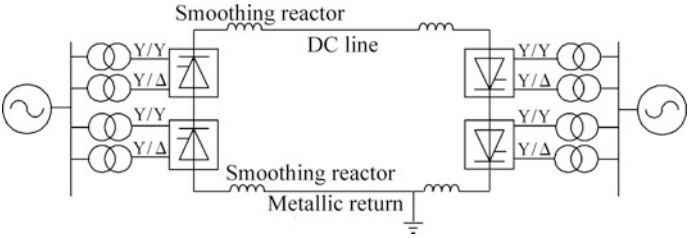

Fig. 15.12 Monopolar metallic return operating mode

earthing transformer at the neutral point, this operating mode is usually used in case of monopolar fault.

2. 1/2 monopolar operating mode

During operation in 1/2 monopolar operating mode, only one 12-pulse converter is put into operation at a single pole, and the converter can be operated by selecting a symmetrical or cross operating mode. The operating mode is divided into monopolar ground return operating mode and monopolar metallic return operating mode in terms of different turn, and the characteristics of different circuit mode are same to that of the complete monopolar operating mode.

15.2.2.3 UHVDC Ice Melting Operating Mode

China is one of the countries which are most vulnerable to icing of power transmission lines in the world, so the ice melting of the power transmission lines becomes a problem that we have to face. The most simple and effective method to carry out ice melting of iced transmission lines is to improve the current density of the iced conductors, so as to melt the ice by heat produced by the conductor. This section gives an introduction to the typical UHVDC ice melting and connection method by combining connection characteristics of the UHVDC converter stations.

Taking the Xiangjiaba–Shanghai ±800 kV UHVDC Transmission Project and Jinping-South Jiangsu ±800 kV UHVDC Transmission Project as examples, the bipolar power rating of the projects is 6400 or 7200 MW, the rated DC voltage is ±800 kV, the rated direct current is 4000 or 4500 A, the valve module at each pole adopts two 12-pulse converter units for connection in series, and each 12-pulse converter unit is provided with a bypass switch circuit. The main connection of the UHVDC converter station is shown in Fig. 15.10.

For the purpose of meeting the requirement for ice melting of DC conductor, the current that is transmitted on the DC line reaches 6000–8000 A. In ordinary connection and normal operating mode, however, due to the restriction by the rated current and discharge capacity of the converter valve, it is difficult to meet the requirement for ice melting of the iced DC lines only by making use of overload capacity of the converter valve module. A bypass circuit breaker and a disconnector are connected in parallel onto each 12-pulse converter in the UHVDC system, so it is able to consider connection of two 12-pulse converter valve modules in parallel to increase the transmission current of the DC line to 8000 or 9000 A in rated condition to meet the requirement for ice melting of the lines.

One typical ice melting connection solution is to enable the 12-pulse converter valves at LV ends of the pole 1 and 2 to be out of service by operating the bypass switch, and then connect the 12-pulse converter valves at HV ends of both poles in parallel, so that a 8000 or 9000 A ice melting current can flow through the line at this moment, and the current of the two converter valves operated in parallel is rated to 4000 or 4500 A, meeting the design requirement for the valve modules. In case of use of this connection method, the DC system is equivalent to a monopolar

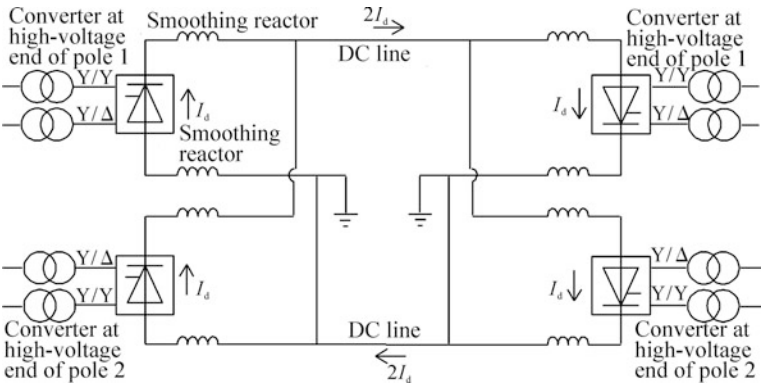

Fig. 15.13 UHVDC ice melting operating mode

400 kV metallic return, but, unlike the operating mode of the ordinary metallic return, two 12-pulse valve modules are put into operation in parallel at each pole in this condition, and the simplified operation diagram is shown in Fig. 15.13.

The ice melting method that 12-pulse valve modules at HV ends of both poles are put into operation in parallel can meet the requirement for increasing the transmission current of the iced DC lines (rated current of the line can be up to 8000 or 9000 A), without need to change the technical parameters of main equipment including converters. By this ice melting method, the current of each valve module operating in parallel is still rated to 4000 or 4500 A, meeting the original design conditions for the converter valves: The operating current of the smoothing reactors connected in the pole and neutral busbar is still rated to 4000 or 4500 A, without raising the requirement for ice melting operation of the smoothing reactors; furthermore, the operating current of pole lines, neutral line and metallic lines and all equipment in the DC field are identical to that during normal operation.

15.2.2.4 Characteristics of UHVDC Operating Modes

1. Diversity of operating modes

Many operating modes can be selected for the UHVDC transmission systems. Even considering the most unfavorable conditions, the system, due to the connection of double 12-pulse connectors in series with equal voltage level, is still able to maintain transmission power by an appropriate operation method as long as one intact 12-pulse converter is provided in the same pole. All in all, the UHVDC transmission system can be operated in monopolar or bipolar operating mode; with respect to a pole being put into operation, there are two operating modes available for selection, namely double 12-pulse and single 12-pulse modes; with respect to

single 12-pulse operating mode, it can be operated in selecting symmetrical or cross operating mode. So, the operating modes of the UHVDC transmission system available for selection are far more than the EHVDC transmission system. There are 45 operating modes at maximum by use of different connection combinations, and during practical operation, it is possible to flexibly select an operating mode to achieve the most economic operation effect.

2. 12-pulse converter can be put into service and put out of service in an online manner

For the connection method by which two 12-pulse converters are connected in series for the UHVDC transmission systems, a bypass circuit breaker and a disconnector are connected in parallel ONTO each 12-pulse converter, and by operating the DC bypass circuit breaker and disconnector, it is possible to put the 12-pulse converters into operation or out of service in an in-line manner; so when some faults happen like one converter or converter transformer is failed in complete bipolar operating mode, it is only required to get the fault 12-pulse converter out of service, and switch the operating mode to 3/4 bipolar operating mode to ensure that the DC system still can transmit most power, so as to reduce loss of the DC transmission power resulting from the fault, and lessen the shock to and influence on the AC systems at two terminals.

15.3 Calculation of Main Circuit Parameters of UHVDC System

This section, by taking the Xiangjiaba–Shanghai ±800 kV UHVDC transmission project as an example, gives a detailed introduction for calculation of main circuit parameters for the UHVDC systems in connection with calculation of the switching overvoltage. The main circuit parameters of the UHVDC system include two categories: The first one include original parameters provided in the engineering data, such as rated voltage of the DC system, rated transmission power, and DC line length; the second one include parameters derived from calculation based on the original parameters, e.g., rated voltage of the inverter station for the DC system, rated voltage, and current and capacity of the converter transformer, maximum DC voltage, minimum DC current, and maximum operating current, etc. The main circuit parameters for the project are detailed in Table 15.1.

The following gives analysis and calculation of the main circuit parameters for the UHVDC system from 6 aspects.

Table 15.1 Main system parameters of Xiangjiaba-Shanghai ±800 kV UHVDC transmission project and their sources

Category of parameter	Description	Sources of data
Rated operating parameters of DC system	DC rated voltage, rated current and rated transmission power, rated trigger angle, rated extinction angle	Provided in the engineering data (initial setting by the engineering)
Rated operating parameters of AC system	Rated voltage of AC side	Provided in the engineering data
DC line parameters	DC line length, conductor types, arrangement of towers	Provided in the engineering data
Rated operating parameters at inverter side	DC voltage in rated operating mode of inverter side	Calculated by rated parameters at the rectifier side and DC resistance of the line
Equipment parameters	Rated voltage, current and capacity of converter transformer	Calculated by rated operating voltage and current parameters of the converter station
	Short-circuit impedance of converter transformer, tap positions	Provided in the engineering data
	Smoothing reactor	Provided in the engineering data
	Blocking filter	Provided in the engineering data
	PLC/RI filter	Provided in the engineering data
	Neutral busbar capacitor	Provided in the engineering data
	Forward drop of converter	Provided in the engineering data
	Equipment manufacturing and measurement errors	Provided in the engineering data
	Rated no-load DC voltage of converter	Calculated per rated voltage and current of converter station, and rated capacity and short-circuit impedance parameter of converter transformer
Equipment parameters	Commutation angle of converter	Calculated per rated no-load DC voltage, rated trigger angle, and extinction angle of converter
	Reactive power consumed by the converter station	Calculated per rated no-load DC voltage, rated trigger angle, extinction angle, and commutation of converter
	Parameters of AC/DC filter	Calculated per reactive power consumed by the converter station
Operating parameters of DC system	Max. DC voltage, min. DC current, max. operating current	Calculated per DC rated parameters, converter rated parameters, and equipment measurement errors
Overvoltage operating condition	DC voltage and DC current	Select rated, max. or min value per overvoltage types

(continued)

Table 15.1 (continued)

Category of parameter	Description	Sources of data
Surge arrester	Arrangement scheme for and parameters of surge arrester	First determine the preliminary basic parameters of the arresters per the continuous operating voltage at the place where the surge arrester is installed, and then determine the final parameters by adjustment and verification based on overvoltage calculation and insulation coordination result

15.3.1 Main Connection and Operation Modes of UHVDC Transmission Project

According to current UHVDC transmission technologies and equipment manufacturing level, the converters for existing ±800 kV UHVDC transmission projects and the ones under construction in China adopts the structure in which two 12-pulse converters are connected in series at each pole, and voltage of each 12-pulse converter is 400 kV. The smoothing reactor is a split type, which is arranged in the DC pole and neutral busbar. The connection of the converter is shown in Fig. 15.14. It mainly includes six operating modes: complete bipolar operating mode, 3/4 bipolar operating mode, 1/2 bipolar operating mode, complete monopolar operating mode, 1/2 monopolar operating mode, and ice melting operating mode.

During the design of main circuit parameters, it is required to consider all of the operating modes above, and calculate rated system parameters in forward power transmission method and complete bipolar operating mode.

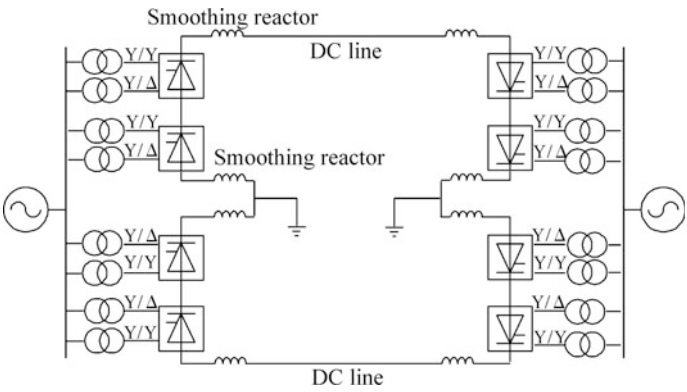

Fig. 15.14 Connection method for Xiangjiaba-Shanghai ±800 kV UHVDC transmission project

15.3.2 Rated Operating Parameters of DC System

The Xiangjiaba–Shanghai ±800 kV UHVDC transmission demonstration project starts at Sichuan Fulong Converter Station, and ends at Shanghai Fengxian Converter Station, with total line length up to 1907 km and the main DC steady-state control parameters as shown in Table 15.2.

Unlike the AC system, the energy transmission direction of the DC system depends on the voltage level on both sides, and the voltage on the rectifier side is certainly higher than the inverter side. The voltage level of the DC system usually means the DC voltage at the rectifier side, and the voltage at the inverter side equals the voltage of the rectifier side minus the voltage drop in the DC line, so the voltage in the inverter station of the DC system fully depends on the resistance of the DC line. For different DC transmission projects with same voltage level, the rated voltage and rated capacity of the inverter side are also different due to the difference in their transmission distance, transmission capacity, and conductor types. The rated voltage at the inverter side for the project is calculated as Eq. (15.11):

$$U_{\mathrm{dNI}} = U_{\mathrm{dNR}} - I_{\mathrm{dN}} \times R_{\mathrm{b}}, \tag{15.11}$$

where

U_{dNI} rated DC voltage at the inverter side;
U_{dNR} rated DC voltage at the rectifier side;
R_{b} DC resistance of the DC line.

For specific values, refer to Sect. 15.3.4, DC line parameters.

So,

$$U_{\mathrm{dNI}} = 800 - 4 \times 13.75 = 745\,\mathrm{kV}.$$

Table 15.2 Steady-state control parameters of DC system

Parameters	Definitions	Value
U_{dN}	Rated DC voltage at rectifier side	800 kV
P_{dN}	Rated power	6400 MW
I_{dN}	Rated DC current	4000 A
α_{N}	Rated trigger angle	15°
$\Delta\alpha_{\mathrm{N}}$	Steady-control range of trigger angle	±2.5°
α_{min}	Min. trigger angle	5°
α_{N}	Rated extinction angle	17°
U_{dN1}	DC voltage at inverter side in rated operating mode	745 kV
$\Delta U_{\mathrm{dOLTC}}$	DC voltage change corresponding to change of the tap by 1 position	0.625% U_{dN}
$\Delta I_{\mathrm{dOLTC}}$	DC voltage change corresponding to change of the tap by 1 position	0.625%I_{dN}

15.3.3 Rated Operating Parameters of AC System

The steady-state voltage and frequency of the AC systems at two terminals for the Xiangjiaba–Shanghai ±800 kV UHVDC transmission project are as shown in Table 15.3.

During simulation of the DC switching overvoltage, it is required to consider maximum and minimum voltage operating modes of the AC systems at two terminals. Taking the Xiangjiaba–Shanghai ±800 kV UHVDC transmission system as an example, the Fulong Station at the rectifier side is operated at a three-phase short-circuit current of 63 kA in maximum operating mode, and 18.1 kA in minimum operating mode; the Fengxian Station at the inverter side is operated at a three-phase short-circuit current of 63 kA in maximum operating mode, and 26 kA in minimum operating mode.

15.3.4 Parameters of DC Line

The DC line of the Xiangjiaba–Shanghai ±800 kV UHVDC transmission project spans about 1907 km. The DC conductor uses 6× ACSR-720/50 and 6× AACSR-720/50 aluminum alloy steel-reinforced conductor. Two ground wires are installed along the whole line, of which one wire is LBGJ-180-20AC or LBGJ-240-20AC aluminum clad steel stranded wire, and the other one is OPGW fiber cable that has similar characteristics. For Fulong Converter Station as the sending end of the project, the ground electrode line is about 79 km long, the conductor are 2× NRLH60GJ-500/45 thermal resistant aluminum alloy steel-reinforced conductors, and a ground wire is installed along the whole line, adopting GJ-80 stranded galvanized steel wire. For Fengxian Converter Station as the receiving end of the project, the ground electrode line is about 97 km long, the conductor are 2× NRLH60GJ-500/45 thermal resistant aluminum alloy steel-reinforced conductors, and a ground wire is installed along the whole line, adopting GJ-80 stranded galvanized steel wire. Among them, the rated resistance of the DC line is 13.75 Ω, the maximum resistance is 17.22 Ω, and the minimum resistance is 11.00 Ω [2].

Table 15.3 Steady-state parameters of AC system

Converter station	AC busbar voltage (kV)					System frequency (Hz)
	Rated	Max.	Min.	Max. at pole end	Min. at pole end	
Fulong	530	550	500	550	475	50 ± 0.2
Fengxian	515	525	490	550	475	50 ± 0.1

15.3.5 Equipment Parameters

15.3.5.1 Manufacturing Tolerances and Measurement Errors of DC Equipment

In view of the inevitable errors existed in the actual manufacturing process of high-voltage DC equipment, it is required to consider equipment manufacturing tolerances and measurement errors during the design of main circuit parameters. The manufacturing tolerances and measurement errors of equipment for the Xiangjiaba–Shanghai ±800 kV UHVDC transmission project is shown in Table 15.4.

15.3.5.2 Calculation of Main Parameters of Converter Transformer

The converter transformer is one of the most important equipments for the UHVDC transmission projects. Its capacity is huge, and is restricted by manufacturing the ability of single three-phase large capacity transformer and transportation conditions. At present, the UHVDC transmission projects often adopt single-phase double-winding transformer solution.

1. Rated voltage, current, and capacity of converter transformer

The relationship between the line voltage of the converter transformer at the valve side and the ideal no-load voltage of the converter is as follows:

$$U_{\mathrm{v}} = \frac{U_{\mathrm{dio}}}{\sqrt{2}} \frac{\pi}{3} \tag{15.12}$$

So, the rated voltage of the converter transformer at the valve side of the converter station and inverter station is calculated as follows, respectively:

Table 15.4 Equipment manufacturing tolerances and measurement errors

Parameter	Definition	Error
d_{x}	Max. manufacturing error δd_{x} of converter transformer on the inductive voltage drop within normal DC voltage operation range	+5%/ −7%d_{xN}
U_{d}	DC voltage measurement error $\delta U_{\mathrm{dmeas}}$	±0.5% U_{dNR}
I_{d}	DC voltage measurement error $\delta I_{\mathrm{dmeas}}$	±0.3% I_{dN}
γ	Extinction angle measurement error	±1.0°
α	Trigger angle measurement error	±0.5°
U_{dio}	Capacitive potential transformer measurement error δU_{dioN}	±1.0% U_{dioN}

$$U_{\mathrm{vNR}} = 170.3(\mathrm{kV}), \quad U_{\mathrm{vNI}} = 157.6(\mathrm{kV})$$

The relationship between the effective value of the AC line current on the valve side and DC current is as follows:

$$I_{\mathrm{v}} = \sqrt{\frac{2}{3}} I_{\mathrm{d}} \tag{15.13}$$

The rated current of winding Y and Δ on the converter transformer at the valve side is calculated as follows, respectively:

$$I_{\mathrm{vYN}} = I_{\mathrm{vN}}, \quad I_{\mathrm{v}\Delta\mathrm{N}} = \frac{I_{\mathrm{vN}}}{\sqrt{3}} \tag{15.14}$$

The rated current of the winding Y and Δ on the converter transformer at the valve side is as follows, respectively:

$$I_{\mathrm{vYN}} = 3266\,\mathrm{A}, \quad I_{\mathrm{v}\Delta\mathrm{N}} = 1886\,\mathrm{A}$$

Thus, it is possible to obtain the total three-phase rated capacity of the converter transformer for the 6-pulse converter by the following equation:

$$S_{\mathrm{n}} = \sqrt{3} U_{\mathrm{vN}} I_{\mathrm{vN}} = \frac{\pi}{3} U_{\mathrm{dioN}} I_{\mathrm{dN}} \tag{15.15}$$

A single-phase double-winding transformer is adopted in the UHVDC transmission project, whose rated capacity is 1/3 of the (15.15), i.e.,

$$S_{\mathrm{n}2\omega} = \frac{\pi}{9} U_{\mathrm{dioN}} I_{\mathrm{dN}} \tag{15.16}$$

To sum up, the rated capacity of the single-phase double-winding transformer for the converter station and inverter station is calculated as follows, respectively:

$$S_{\mathrm{n}2\omega\mathrm{R}} = 321.1\,\mathrm{MVA}, \quad S_{\mathrm{n}2\omega\mathrm{I}} = 297.1\,\mathrm{MVA}.$$

2. Short-circuit impedance of the converter transformer, and tap position

The converter transformer is one of the most important equipments for the UHVDC transmission projects. Being similar to the AC transformer, the short-circuit impedance is one of the main parameters for the converter transformer. The bigger the short-circuit impedance is, the bigger the commutation angle of the converter is, and the bigger the inductive reactive power produced by the converter transformer is. In the Xiangjiaba–Shanghai ±800 kV UHVDC transmission project, the design value for the short-circuit impedance of the converter transformer for Fulong

Table 15.5 Design parameters for converter transformer in Fulong converter station

Parameter	Windings at AC side	Windings at valve side	
		Y winding	Δ winding
Rate phase voltage (kV)	$530/\sqrt{3}$	$170.3/\sqrt{3}$	170.3
Max. steady-state phase voltage (kV)	$550/\sqrt{3}$	$175.9/\sqrt{3}$	175.9
Rated power capacity (MVA)	321.1	321.1	321.1
Rated current (A)	1049	3266	1886
Number of tap positions		+23/−5	
Step size of tap (%)		1.25	
Short-circuit impedance (%)		18.0 ± 0.6	

Table 15.6 Design parameters for converter transformer in Fengxian Converter Station

Parameters	Windings at AC side	Windings at valve side	
		Y winding	Δ winding
Rated phase voltage (kV)	$515/\sqrt{3}$	$157.6/\sqrt{3}$	157.6
Max. steady-state phase voltage (kV)	$550/\sqrt{3}$	$164.7/\sqrt{3}$	164.7
Rated power capacity (MVA)	297.1	297.1	297.1
Rated current (A)	999	3266	1886
Number of tap positions		+22/−6	
Step size of tap (%)		1.25	
Short-circuit impedance (%)		16.7 ± 0.6	

Converter Station on the rectifier side is 18%, and the design value for the short-circuit impedance of the converter transformer for Fengxian Converter Station on the inverter side is 16.7%.

The step size of the converter transformer tap is 1.25%. The number of tap positions of the converter transformer in the Fulong Station is designed to +23/−5, and the number of tap positions of the converter transformer in the Fengxian Station is designed to +22/−6.

To sum up, the parameters for the converter transformer at two terminals of the Xiangjiaba–Shanghai UHVDC transmission project are shown in Tables 15.5 and 15.6.

15.3.5.3 Calculation of Main Parameters of Converter

1. DC voltage drop of converter

When the direct current flows through the thyristor, a voltage drop occurs, which is called as the forward drop U_T of the thyristor. The forward drop of the thyristor is relevant to the material and manufacturing technology of the thyristor, and is slightly related to the change in current flowing through the thyrsitor. In practical

projects, the voltage drop can be considered a constant value. In the Xiangjiaba–Shanghai ±800 kV UHVDC transmission project, the forward drop of each 6-pulse converter thyristor is 0.3 kV.

Except the forward drop of the thyristor, it is required to consider the resistive voltage drop of the thyristor and copper loss of the converter transformer at the valve side. The copper loss is called the relative resistive voltage drop of the converter d_r, and d_r of 6-pulse converter is calculated as follows [3]:

$$d_r = \frac{P_{cu}}{U_{dioN} I_{dN}} + \frac{2R_{th} I_{dN}}{U_{dioN}}, \tag{15.17}$$

where

P_{cu} Resistive loss of the converter transformer and smoothing reactor in rated operation condition of the 6-pulse converter;

R_{th} Resistive loss of the converter valve, before which a factor 2, is multiplied for the reason that two converter valves are always turned on during normal operating of the 6-pulse converter;

U_{dioN} Rated no-load DC voltage of the converter valve side.

According to engineering experience, d_r of the 6-pulse converter is normally taken as 0.3%.

2. Rated no-load DC voltage of converter

The 6-pulse converter voltage calculation equation is as follows [3]:

$$\frac{U_{dR}}{n} = U_{dioR}\left[\cos\alpha - (d_{xR} + d_{rR})\frac{I_d}{I_{dN}}\frac{U_{dioNR}}{U_{dioR}}\right] - U_T \tag{15.18}$$

$$\frac{U_{dI}}{n} = U_{dioI}\left[\cos\gamma - (d_{xI} - d_{rI})\frac{I_d}{I_{dN}}\frac{U_{dioNI}}{U_{dioI}}\right] + U_T, \tag{15.19}$$

where

U_{dR} DC voltage on the rectifier side;

U_{dI} DC voltage on the inverter side;

n number of 6-pulse converters contained at each pole of the converter station, 4 for the UHVDC transmission project;

U_{dioR} no-load DC voltage at the rectifier side;

U_{dioI} no-load DC voltage at the inverter side;

d_{xR} relative inductive voltage drop of the converter on the rectifier side;

d_{xI} relative inductive voltage drop of the converter on the inverter side;

U_{dioNR} rated no-load DC voltage at the rectifier side;

U_{dioNI} rated no-load DC voltage at the inverter side.

In the DC system, the relationship between the DC voltage on the rectifier side and inverter side is as follows:

$$U_{\mathrm{dI}} = U_{\mathrm{dR}} - I_{\mathrm{d}} \times R_{\mathrm{d}} \tag{15.20}$$

According to the Eq. (15.20), it is possible to obtain the following results by transformation of the Eqs. (15.18) and (15.19):

$$U_{\mathrm{dioNR}} = \frac{\frac{U_{\mathrm{dNR}}}{n} + U_{\mathrm{T}}}{\cos\alpha_{\mathrm{N}} - (d_{\mathrm{xNR}} + d_{\mathrm{rNR}})} = 230\,\mathrm{kV}$$

$$U_{\mathrm{dioNI}} = \frac{\frac{U_{\mathrm{dNR}} - I_{\mathrm{dN}} \times R_{\mathrm{dN}}}{n} - U_{\mathrm{T}}}{\cos\gamma_{\mathrm{N}} - (d_{\mathrm{xNI}} - d_{\mathrm{rNI}})} = 212.8\,\mathrm{kV}$$

3. Rated relative inductive voltage drop of converter

According to the definition of the relative resistive voltage drop d_{r} of the 6-pulse converter given in the previous sections, the relative inductive voltage drop d_{x} of the converter is defined as follows [3]:

$$d_{\mathrm{xN}} = \frac{3}{\pi}\frac{X_{\mathrm{t}} I_{\mathrm{dN}}}{U_{\mathrm{dioN}}}, \tag{15.21}$$

where

X_{t} the commutation reactance, which is provided only by the short-circuit resistance of the converter transformer when no PLC filter is adopted.

The relation between the rated relative inductive voltage drop d_{xN} of the converter and the short-circuit resistance u_{k} of the converter transformer is as follows:

$$d_{\mathrm{xN}} = \frac{3}{\pi}\frac{X_{\mathrm{t}} I_{\mathrm{dN}}}{U_{\mathrm{dioN}}} = \frac{3}{\pi}\frac{I_{\mathrm{dN}}}{U_{\mathrm{dioN}}} u_k \frac{U_{\mathrm{vN}}^2}{S_{\mathrm{n}}}, \tag{15.22}$$

where

U_{vN} the rated line voltage of the converter transformer at the valve side;
S_{n} the rated total three-phase capacity of the converter transformer.

According to the Eqs. (15.12) and (15.15), the Eq. (15.22) can be simplified as follows:

$$d_{\mathrm{xN}} = \frac{1}{2} u_{\mathrm{k}} \tag{15.23}$$

Although no PLC filter is provided in this UHVDC transmission project any more, but the PLC filter will be considered in some design because a standby space is reserved for the PLC equipment. Its relative inductive voltage drop is small, normally between 0.2 and 0.3%. It is possible to obtain the following equation when considering the inductive voltage drop of PLCs:

$$d_{xN} \approx \frac{1}{2} u_k + u_{PLC} \tag{15.24}$$

So, it is possible to calculate the rated relative inductive voltage drop of the converter stations at two terminals by the Eq. (15.24) in case of use of PLC filters, respectively:

$$d_{xNR} = 0.092, \quad d_{xNI} = 0.0855$$

Without PLC filters provided, the rated relative inductive voltage drop of the converter stations at two terminals is as follows, respectively.

$$d_{xNR} = 0.09, \quad d_{xNI} = 0.0835$$

The PLC filters has little influence on the calculation of the switching overvoltage of the system. This section does not consider the parameters of the PLC filters during calculation of main parameters.

4. Commutation angle of converter

The commutation angle means that the time for commutation of the converter is represented by a corresponding phase angle, which is one of the important parameters of the converter, and calculated by following equations [3]:

$$\cos(\alpha + \mu_R) = \cos\alpha - 2d_{xNR} \frac{I_d}{I_{dN}} \frac{U_{dioNR}}{U_{dioR}} \tag{15.25}$$

$$\cos(\gamma + \mu_I) = \cos\gamma - 2d_{xNI} \frac{I_d}{I_{dN}} \frac{U_{dioNI}}{U_{dioI}} \tag{15.26}$$

According to the Eqs. (15.25) and (15.26), it is possible to obtain the commutation angle of the rectifier station and inverter station in rated operating condition, which is as follows, respectively:

$$\mu_R = 23.6^\circ, \quad \mu_I = 21.3^\circ$$

(5) Reactive power consumed by converter

The converter will consume a great deal of reactive power during operation, which needs to be compensated by reactive power compensation equipment. In rated operating condition, the reactive power consumed by the 12-pulse converters is calculated by the following calculation equation [3]:

$$Q_{dN} = 2\chi I_{dN} U_{dioN} \tag{15.27}$$

$$\chi = \frac{1}{4} \times \frac{2\mu + \sin 2\alpha - \sin 2(\alpha + \mu)}{\cos\alpha - \cos(\alpha + \mu)}. \tag{15.28}$$

For the inverter side, the α in the Eq. (15.28) can be replaced by the γ. Each converter has two poles and 4-pulse converters in total, so it is possible to obtain reactive power consumed in the rated operating condition of the converters at two terminals, with calculation results listed as follows:

$$Q_{\mathrm{dNR}} = 3476\,\mathrm{Mvar}, \quad Q_{\mathrm{dNI}} = 3272\,\mathrm{Mvar}.$$

15.3.5.4 Smoothing Reactor

The smoothing reactor is one of the important equipments in the UHVDC transmission project. Together with the DC filter, it is used to form the DC filter circuit of the converter to reduce the DC harmonic component, and restrict the steep front impulse of the voltage on the DC line side to enter the valve hall and suppress the DC impulse. The Xiangjiaba–Shanghai ±800 kV UHVDC transmission project adopts such an arrangement method that two 75 mH dry type air core high-voltage reactors in the pole line of each pole, and two 75 mH dry type air core high-voltage reactors in the neutral line. The total inductance of the smoothing reactor at each pole is 300 mH.

15.3.5.5 Neutral Bus Capacitor

Because the converter transformer winding and wall bushing produce stray capacitance, which forms a harmonic current circuit together with the neutral bus and ground, so that a 3rd harmonic current flows between the neutral bus and ground. If no measures are taken, the harmonic current component flowing through the ground electrode line and ground electrode will increase, so it is required to install a capacitor in the neutral line to provide a harmonic circuit to eliminate the harmonic current. When determining the capacitance value of the capacitor, it is also required to avoid the production of a resonance together with sensitive frequency of the ground electrode wire. In the Xiangjiaba–Shanghai ±800 kV UHVDC transmission project, the capacitance value of the neutral bus capacitor for Fulong Converter Station as the sending end is 16, and 15 μF for Fengxian Converter Station as the receiving end.

15.3.5.6 AC Filter

Fulong Converter Station is configured with 4 AC filter banks, including 14 AC filter sub-banks in total, of which there are 4 BP11/13 filter sub-banks, 4 HP24/36 filter sub-banks, 1 HP3 filter sub-bank, and 5 SC parallel filter sub-banks. Fengxian Converter Station is configured with 4 AC filter banks, including 15 AC filter sub-banks in total, of which there are 8 HP12/HP24 filter sub-banks, 7 SC parallel

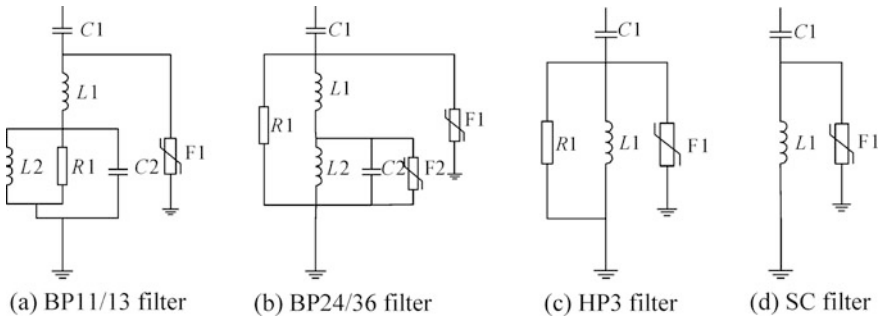

Fig. 15.15 Diagram for AC filters in Fulong Converter Station

Fig. 15.16 Diagram for AC filters in Fengxian converter station

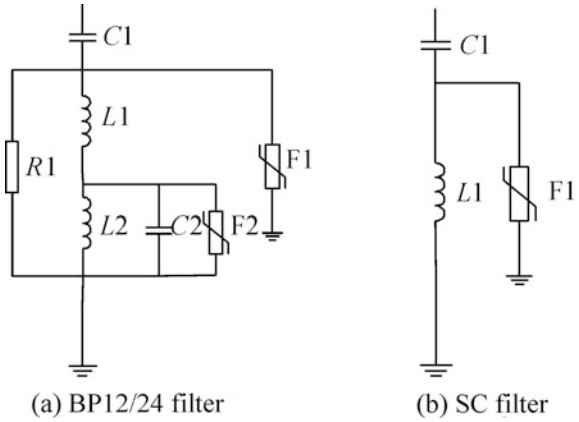

filter sub-banks. Each filter circuit and specific parameters are as shown in Figs. 15.15 and 15.16, and in Tables 15.7 and 15.8, and the parameters of arresters in the AC filters are shown in Table 15.9 [4].

15.3.5.7 DC Filter

Fulong Converter Station and Fengxian Converter station are configured with one group of 2/12/39 DC tuned filters, whose specific circuit and parameters are as shown in Fig. 15.17 and in Table 15.10 [5].

The parameters for arresters in the DC filters are shown in Table 15.11.

Table 15.7 Parameters for AC filters in Fulong Converter Station

Component	Type of filters			
	BP11/13	HP24/36	HP3	SC
$C1$ (μF)	2.523	2.537	2.541	2.541
$L1$ (mH)	27.91	4.285	498.5	2.0
$C2$ (μF)	92.34	13.48	20.33	–
$L2$ (mH)	0.784	0.917	–	–
$R1$ (Ω)	165	425	1253	–
Three-phase rated capacity (MVA)	220	220	220	220
Number	4	4	1	5

Table 15.8 Parameters for AC filters in Fengxian converter station

Component	Type of filters	
	HP12/24	SC
$C1$ (μF)	3.107	2.855
$L1$ (mH)	8.705	2.0
$C2$ (μF)	7.475	–
$L2$ (mH)	5.738	–
$R1$ (Ω)	200	–
Three-phase rated capacity (MVA)	260	238
Number	8	7

Table 15.9 Parameters for arresters in AC filters

Converter station	Arrester	CCOV (kV)	SIPL/current (kV/kA)	LIPL/current (kV/kA)
Fulong converter station	BP11/13 (F1)	159	365/7.7	447/62
	HP24/36 (F1)	48	267/7.7	337/80
	HP24/36 (F2)	21.5	90/12	97/12
	HP3(F1)	141	268/7.8	338/81
	SC(Fl)	10	278/7.8	337/79
Fuxian converter station	HP12/24 (F1)	44	271/9.5	342/88
	HP12/24 (F2)	24.8	86/7	94/8
	SC(F1)	13.8	269/8.7	339/83

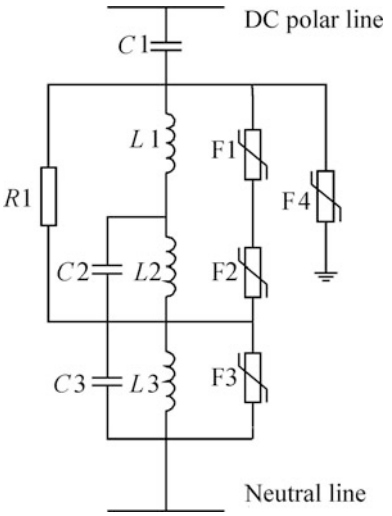

Fig. 15.17 Circuit diagram for DC filters

Table 15.10 Parameters of DC filters

Component	Converter station	
	Fulong station	Fengxian station
*C*1 (μF)	1.05	1.05
*L*1 (mH)	9.847	9.847
*C*2 (μF)	3.286	3.286
*L*2 (mH)	582.95	582.95
*C*3 (μF)	5.105	5.105
*L*3 (mH)	11.745	11.745
*R*1 (Ω)	3095	3095

Table 15.11 Parameters for arresters in DC filters

Converter station	Arrester	CCOV (kV)	SIPL/current (kV/kA)	LIPL/current (kV/kA)
Fulong converter station	F1	24	623/3.1	687/10.4
	F2	261	536/2.7	–
	F3	48	138/8.6	–
	F4	289	553/6.7	688/80.0
Fengxian converter station	F1	24	623/3.1	687/10.4
	F2	261	536/2.7	–
	F3	48	138/8.6	–
	F4	289	553/6.7	688/80.0

15.3.5.8 Blocking Filter

The neutral bus in Fulong Converter Station for the Xiangjiaba–Shanghai ±800 kV UHVDC transmission project is provided with a blocking filter to prevent the production of resonance by DC system in the vicinity of 50 Hz frequency. The blocking filter is formed by a 75 mH dry type air core high-voltage reactor and a 135 μF capacitor in parallel.

15.3.5.9 PLC/RI Filter

A great deal of harmonic component produced in the AC system during operation of the DC system imposes an influence on the carrier communication of the AC line, so in the past PLC filters (Power Line Carrier Noise Filter) were adopted in ±500 kV DC transmission projects to reduce its influence on the AC power line carrier communication by the DC system. However, with technical development, the optical fiber and microwave communication method has been adopted in power systems, and no line and substation adopting AC line carrier communication have been used for the AC system in the vicinity of the converter station on both sides of the Xiangjiaba–Shanghai ±800 kV UHVDC transmission project, so the UHVDC projects will not be provided with PLC filters any longer.

Being similar to the AC line, the DC line also imposes an interference with the radio communication in the area along the line, due to existence of the harmonic component. To solve this problem, a radio interference filter (RI filter) is introduced to the DC system. The RI filter is formed by an earth capacitor at the AC side of the converter transformer and series inductor for the outgoing cable of the valve hall. The inductance value of the RI filter for the Xiangjiaba–Shanghai ±800 kV UHVDC transmission project is 0.5 mH and its capacitance value is 2.8 nF.

15.3.6 Operating Parameters of DC System

15.3.6.1 DC Voltage

According to the 1.25% change in tap position of the converter transformer, it can be known that, if the tap for one of two converter transformers at each pole is changed by one position, the corresponding voltage is changed by 1.25%/2 = 0.625%, namely $\Delta U_{\mathrm{dOLTC}} = 0.625\%$, and considering the error $\delta U_{\mathrm{dmeas}} = 0.5\%$ of the DC voltage measurement system, it is possible to obtain the practical maximum DC voltage of the UHVDC system by the following equation:

$$U_{\mathrm{dmax}} = U_{\mathrm{dN}} \times (1 + \Delta U_{\mathrm{dOLTC}} + \delta U_{\mathrm{dmeas}}) \tag{15.29}$$

Namely: U_{dmax} = 800 × (1 + 0.625% + 0.5%) = 809 kV.

15.3.6.2 DC Current

Without overload operation of the DC system being considered, and being similar to the DC voltage calculation, it is also required to consider the change quantity $\Delta I_{\mathrm{dOLTC}}$ = 0.625% with change by one position of the transformer tap, and current measurement error of $\delta I_{\mathrm{dmeas}}$ = 0.3%. The practical maximum and minimum current of the DC system are calculated by following equations, respectively:

$$I_{\mathrm{dmax}} = I_{\mathrm{dN}} \times (1 + \Delta I_{\mathrm{dOLTC}} + \delta I_{\mathrm{dmeas}}) \tag{15.30}$$

Namely: I_{dmax} = 4000 × (1 + 0.625% + 0.3%) = 4037 A.

$$I_{\mathrm{dmin}} = I_{\mathrm{dN}} \times (0.1 - \Delta I_{\mathrm{dOLTC}} - \delta I_{\mathrm{dmeas}}) \tag{15.31}$$

Namely: I_{dmin} = 4000 × (0.1 − 0.625% − 0.3%) = 363 A.

In case that the overload condition of the DC system is considered, the allowable maximum operating power of the Xiangjiaba–Shanghai ±800 kV UHVDC transmission project is 1.2 p.u., namely 1.2 × 6400 MW = 7680 MW. At this transmission power level, the DC no-load voltage on the rectifier side is kept at the rated no-load voltage level, and according to the Eq. (15.18), the DC voltage on the rectifier side calculated is 779.8 kV. Thus, the direct current in condition of 1.2 p.u. transmission power is calculated by the following equations:

$$I_{\mathrm{dN1.2}} = 1.2 \times 6400 \div 2 \div 779.8 = 4924\,\mathrm{A}$$

Similarly, considering the error of the measurement system, the maximum direct current is calculated as follows:

$$I_{\mathrm{dmax}} = 4924 \times (1 + 0.625\% + 0.3\%) = 4970\,\mathrm{A}$$

15.3.6.3 Overvoltage Operating Condition

According to the calculation results above, it is possible to take a maximum value of 809 kV and rated value of 800 kV for the DC voltage at the rectifier side, and to take a maximum value of 4037 or 4970 A, rated value of 4000 A, and minimum value of 363 A for the direct current, based on different overvoltage requirements during overvoltage simulation calculation.

References

1. Xijie D. DC transmission base. Beijing: China Water & Power Press; 1990.
2. Zhenya L. Album of research achievements on UHVDC. Beijing: China Electric Power Press; 2008.
3. DL/T 5426-2009. System design standard for ±800 kV HVDC system; 2009.
4. ABB Power Systems. Xiangjiaba-Shanghai ±800 kV UHVDC transmission project AC filter arresters. London: ABB Power Systems; 2007.
5. ABB Power Systems. Xiangjiaba-Shanghai +800 kV UHVDC transmission project DC filter performance. London: ABB Power Systems; 2008.

Chapter 16
Switching Overvoltage of UHVDC System

Dongju Wang, Hao Zhou and Jiyuan Li

The UHVDC transmission system, used for large-capacity, cross-region, and extra-long-distance electric energy transmission, is a backbone framework of China's power grid and plays an extremely important role in the power grid. The operating voltage of the UHVDC system is higher than that of the ±500 kV DC system, and the UHVDC converter is composed of two 12-pulse converters connected in series, the structure, connection method, and control and protection system of which are more complicated than those of the ±500 kV DC system. Therefore, regardless of the fault types and magnitude of the overvoltage, the ±800 kV DC system is more complicated and severe than the ±500 kV DC system. Moreover, at the UHV level, as the requirement for air insulation distance gets higher, long air clearance insulation saturation begins to appear, resulting in a tremendous increase in size of equipment and manufacturing cost with an increase in voltage. In order to lower the manufacturing cost of UHV equipment and guarantee equipment operation reliability, a stricter requirement is put forward for overvoltage protection of the UHVDC system. In addition, as the West China's landform characteristics, mountain land and plateau, and the DC converter stations and lines may be situated in or pass through the high-altitude region, the high-altitude condition also imposes more stringent requirements for overvoltage protection and insulation coordination of the UHVDC transmission system. Thus, it is very urgent and necessary to carry out research on overvoltage of the UHVDC transmission system and appropriate control and protection measures.

D. Wang (✉) · H. Zhou · J. Li
College of Electrical Engineering, Zhejiang University,
Xihu District, Hangzhou, Zhejiang, People's Republic of China
e-mail: wangdongju@zju.edu.cn

H. Zhou
e-mail: zhouhao_ee@zju.edu.cn

J. Li
e-mail: lijiyuan_ee@zju.edu.cn

© Zhejiang University Press, Hangzhou and Springer-Verlag GmbH Germany 2018

H. Zhou et al. (eds.), *Ultra-high Voltage AC/DC Power Transmission*,
Advanced Topics in Science and Technology in China,
https://doi.org/10.1007/978-3-662-54575-1_16

This chapter primarily focuses on the investigating switching overvoltage of the UHVDC system. First, this chapter provides a discussion on the classification and characteristics of switching overvoltage in the UHVDC systems. Then, by taking the Xiangjiaba–Shanghai ±800 kV UHVDC transmission project as an example, this chapter provides a detailed introduction for calculation of typical kinds of switching overvoltage and its simulation model based on the main circuit parameters introduced in Chap. 15. Finally, this chapter provides an analysis and discussion for main switching overvoltage mechanisms and control and protection strategies.

16.1 Classification and Characteristics of Switching Overvoltage in UHVDC System

16.1.1 Classification of Switching Overvoltage

With respect to varieties of the switching overvoltage, the UHVDC system is more complicated than the UHVAC system. In terms of different areas in which the switching overvoltage is applied in the converter station, the overvoltage can be divided into switching overvoltage at the AC side, overvoltage in the valve hall, and overvoltage in the DC field.

1. Switching overvoltage at the AC side

The switching overvoltage at the AC side represents the switching overvoltage appeared in the AC busbars of the converter station and equipment connected on the busbars. The equipment connected on the AC busbars are protected mainly by AC busbar arresters A which are installed on the busbars being close to the converter transformer and the busbars of each AC filter bank. Each fault that occurred in the AC system or operation implemented, such as single-phase ground fault and clearing, three-phase ground fault and clearing, and loss of AC power supply at the inverter side, switch-on and switch-off of AC filter, etc., will result in high overvoltage in the relevant equipment at the AC side. This chapter lays an emphasis on the introduction of three typical conditions in which this kind of switching overvoltage occurs:

1. three-phase ground fault and clearing;
2. fault resulting from the loss of AC power supply at the inverter side; and
3. internal overvoltage of AC filters;

2. Switching overvoltage in valve hall.

The switching overvoltage in the valve hall is mainly referred to as the switching overvoltage applied to the converter valve and converter busbar. According to different overvoltage positions, and production mechanisms, the switching overvoltage in the valve hall can be classified into the following categories (classified in terms of the arresters used to limit it):

1. switching overvoltage on the valve arrester V11/V1;
2. switching overvoltage on the valve arrester V12/V2;
3. switching overvoltage on the valve arrester V3; and
4. switching overvoltage on the converter busbar;

(3) Switching overvoltage in DC field.

The DC field includes DC pole line, neutral busbar, DC filter and changeover switch, and other equipment, and the switching overvoltage in the DC field can be classified into three categories in terms of application areas:

1. DC pole line overvoltage;
2. neutral busbar overvoltage; and
3. internal overvoltage of DC filters.

This chapter provides a simulation modeling and calculation analysis for three major categories of overvoltage (including ten minor categories of overvoltage) and discusses the overvoltage mechanisms and appropriate protection measures in detail.

16.1.2 Characteristics of UHVDC Switching Overvoltage

Compared to the conventional ±500 kV HVDC system, the UHVDC system has two primary differences with respect to the structure of the main connection: two 12-pulse converters are used; the smoothing reactors are arranged on the DC pole line and neutral busbar in a split manner. This enables switching overvoltage of the UHVDC system to have the following different characteristics, compared to the conventional EHVDC system.

1. Overvoltage of valve

The overvoltage of converter valve in the conventional ±500 kV HVDC system is divided into two categories: overvoltage stressed on the valves at the uppermost layer and other layers. The UHVDC system, compared to the conventional ±500 kV HVDC system, has one more category of valve overvoltage which is divided into overvoltage stressed on the valve at the uppermost layer of the upper 12-pulse converter and the lower 12-pulse converter, and overvoltage stressed on the valves at the other layers.

In case of a ground fault of the outgoing line at the valve side of the uppermost converter transformer at the rectifier side in the DC system, the DC pole line voltage is applied to the converter valve at the uppermost layer of the converter directly connected with the DC pole line, so that a serious overvoltage occurs on the both terminals of valve at the uppermost layer. The overvoltage in the UHVDC system is more serious than that in the conventional EHVDC system, the causes of which are analyzed as follows:

(1) During normal operation, the design value of withstand voltage stressed on the valves in the UHVDC system is lower than that in the conventional EHVDC system.

In the conventional ±500 kV HVDC system, the normal operating withstand voltage of the converter valve is about half the rated voltage of the system, being approx. 250 kV plus the impulse and overshoot; in the UHVDC system, the normal operating withstand voltage of the converter valve for the upper 12-pulse converter is about one-forth of the rated voltage of the system, being approx. 200 kV plus the impulse and overshoot. So the design value of withstand voltage stressed on the converter valve in the UHVDC system is lower than that in the conventional EHVDC system.

(2) In case of a ground fault of the outgoing line at the valve side of the uppermost converter transformer at the rectifier side in the DC system, the overvoltage stressed on the converter valve at the uppermost layer in the UHVDC system is much higher than that in the conventional EHVDC system.

When the above-mentioned fault occurred, the overvoltage endured by the converter valve at the uppermost layer is the difference between the voltage of pole line and the outgoing line at the valve side of the converter transformer. For the conventional EHVDC system, the voltage difference can reach approx. 500 + 300 kV in extreme cases (without considering the arrester protection, the overvoltage is caused jointly under the action of the DC pole line voltage and the voltage of the outgoing line at the valve side of the converter transformer, and 300 kV is the peak voltage of the outgoing line at the valve side of the converter transformer); for the UHVDC system, it is considered that the overvoltage can reach approx. 800 + 250 kV in extreme case (similarly, no arrester protection is considered, and 250 kV is the peak voltage of the outgoing line at the valve side of the converter transformer).

(3) The length of the transmission line for the UHVDC transmission system is usually far longer than that for the conventional ±500 kV HVDC system, so the energy stored on the UHVDC transmission line is much more than that on the conventional EHVDC line.

To sum up, the overvoltage endured by the converter valve at the uppermost layer in the UHVDC system is far more severe than that in the conventional EHVDC system.

In addition, when the UHVDC system is put into operation only by use of the lower 12-pulse converter (namely 1/2 polar operating mode), the valves at the uppermost layer of the lower 12-pulse converter unit are also endangered by the overvoltage mentioned above.

2. Overvoltage on neutral busbar

To reduce the harmonic component of the voltage on the converter busbar, the UHVDC system adopts the split smoothing reactor arrangement solution; namely, smoothing reactors are installed on the DC pole line and neutral busbar at the same time, so the overvoltage on the neutral busbar is also different from the conventional EHVDC system. In the UHVDC system, it is required to calculate the overvoltage on both sides of the smoothing reactor in the neutral busbar, respectively, namely the overvoltage at the valve side of the smoothing reactor and at the line side of the

smoothing reactor, while there is only one kind overvoltage of neutral busbar in the conventional EHVDC system.

For the UHVDC system, the neutral busbar is divided by the smoothing reactor into two sections which have different overvoltage protection levels and be equipped with arresters having different protection levels. The protection level of the arrester at the valve side of the smoothing reactor of the neutral busbar is higher than that at the line side. But the neutral busbar of the conventional EHVDC system is not sectionalized.

16.1.3 Type of Faults Resulting in Switching Overvoltage

The switching overvoltage in the UHVDC system is caused mainly by various categories of faults in the system, which are mainly divided into the following categories:

1. Short-circuit fault in the converter station

In the converter station, the short-circuit fault causing switching overvoltage, in terms of its occurrence position, can be categorized into the following categories:

- Ground fault of the outgoing line on the valve side of the converter transformer

  This kind of fault mainly causes a severe overvoltage stressed on the valve or a severe neutral busbar overvoltage and also causes overvoltage of pole line which is less severe.

- Ground fault of the uppermost layer of valves for the converter

  This kind of fault mainly causes severe overvoltage on neutral busbar.

- Ground fault at the neutral point of the 12-pulse converter and between the upper and lower 12-pulse converters

  This kind of fault mainly causes an overvoltage on the neutral busbar.

- Ground fault of the DC polar busbar

  This kind of fault mainly causes severe overvoltage on neutral busbar.

- Short-circuit fault between the outgoing lines at the valve side of the converter transformer

  This kind of fault mainly causes an unobvious overvoltage in the system, but it is able to cause overcurrent of the converter transformer, endangering the converter transformer.

- Short-circuit fault between the uppermost layer of valves and neutral line

  This kind of fault directly leads to an overvoltage on neutral line, which is not severe but will endanger the converter.

- Short-circuit fault between both terminals of the 6-pulse converter

This kind of fault of the lowest 6-pulse converter will directly lead to an overvoltage on the neutral line, which is not severe but will endanger the converter.

- Short-circuit fault between both terminals of the 12-pulse converter

Being similar to the short-circuit fault between both terminals of the 6-pulse converter, this kind of fault stressed on the lower 12-pulse converter will cause an overvoltage on the neutral line, which is not severe but will endanger the converter.

2. Fault of DC control system

There are two kinds of faults in the DC control system resulting in the overvoltage: full voltage start of DC transmission with open inverter, and the bypass pair is unblocking while the inverter is blocking.

3. Switching impulse on the AC side

The voltage wave of switching impulse, which results from operation, fault, or other causes at the AC side, will apply an overvoltage to some converter valves being not turned on at the appropriate time through the converter transformer and the closed valve in the converter.

4. Load shedding of AC system

In case of this kind of fault, the inverter side will impose an overvoltage at the AC side due to the electromagnetic oscillation between converter transformer and AC filter.

The mechanism of overvoltage resulting from these faults will be analyzed in detail in this chapter.

16.2 Simulation Model of DC System

The control system of the DC transmission system is complicated, the control and protection characteristics of which are the most important factors to determine the operating characteristics of the DC transmission system and impose an influence on the response to the DC system faults. Hence, compared to the simulation model of the AC system, the model of the DC control system, except the main circuit model, is another important part of the whole simulation model. This section will introduce the simulation modeling for the UHVDC transmission system.

16.2.1 Model for Main Circuit of DC System

The main circuit of the DC system includes AC system at both terminals, AC filter, converter transformer, converter, smoothing reactor, DC filter, DC line, ground electrode line, and ground electrode at both terminals. For the parameters of these

main circuit equipment models, refer to the calculation results for parameters of the main circuit given in Chap. 15.

16.2.2 Model of DC Control System

Compared to the AC system, a significant characteristic of the HVDC system is that it can change direction and magnitude of the transmission power rapidly by quick adjustment and control of the converters at both terminals. The HVDC control system is a core of the DC transmission system, and the performance of the DC transmission system is highly dependent on the control system. The model of the DC control system directly determines the accuracy of the switching overvoltage simulation.

16.2.2.1 Main Control Functions to be Realized

With respect to the simulation analysis of the switching overvoltage for the DC system, the main functions of the HVDC control system to be realized include the following:

1. startup and shutdown control of the DC system,
2. transmission power control of the DC system,
3. monitoring the operating parameters of the DC system, and
4. fault protection and control.

16.2.2.2 Layered Structure of DC Control System

The system status parameters involved in the DC control system are complicated. Its control functions are divided into several layers. Usually, six levels are set for the DC transmission control system.

1. This control level is a macro-control level in the whole system, the main functions of which include contact with the dispatch system, receiving dispatch order, emergency power support, tidal current transfer, and AC system frequency adjustment. This control level does not work in the switching overvoltage control, so it is not reflected in the switching overvoltage simulation model.
2. Bipolar control level

This control level coordinates the operation of both poles of the DC system, determines the respective transmission power of both poles in terms of the power value given by the system control level, balances current of both terminals according to the setting, and controls switch-on and switch-off of the reactive power compensation equipment based on voltage of the AC busbar. The control level

works during the normal operation of DC system, which is necessary to be realized in the switching overvoltage simulation model.

3. Monopolar control level

This control level controls the operation of a single pole of the DC system, including delivery of DC voltage and current settings to the converter control level based on the power order given by the bipolar control level or manually set power order, coordination of the remote communication for the same pole of the substation, and fault handling, such as phase shift stop, automatic re-starting, and low-voltage current limiting control. The control level is important in switching overvoltage simulation, which must be realized in the simulation model.

4. Converter control level

This control level completes the operation control of a single converter and controls trigger angle of the converter valve based on the voltage and current setting value delivered from the pole control level, so as to realize the control of the constant current, constant extinction angle, constant voltage, and lock and unlock converter units. This control level is an important control segment in the switching overvoltage simulation, which must be realized in the simulation model.

5. Independent control level

In the DC converter station, except direct control over the converter, it is required to control other equipment surrounding the converter to coordinate the operation of the converter, such as control of converter transformer tap, switch on/off control of filter unit, control of circuit breaker and disconnector in the AC/DC switch yard, and control and monitoring of cooling system for the converter valve module. This part of control is completed by the independent control level. The equipment controlled by this control level play an important role in switching overvoltage protection, such as control of circuit breaker and disconnector in the AC/DC switch yard, and control of filters, which are necessary to be realized in the simulation model.

6. Converter valve control level

This control level magnifies the valve trigger signal from the controller, delivers the magnified signal to the trigger electrode of the thyristor, and monitors operation of the thyristor, including valve temperature, current, and other parameters. This control level mainly controls the hardware operation and is not required in the switching overvoltage simulation model.

16.2.2.3 Key Control Segments Required to Be Realized for Modeling

According to the instructions for layering the control of the UHVDC system, it is required to realize the following key control segments in the process of switching overvoltage simulation modeling for the UHVDC system.

1. Constant extinction angle control segment

This link is a main link for the inverter side control, and also one of the core links of the DC control system, at which it is possible to constantly compare the actual measurement value of the extinction angle on the inverter side with the reference value, so as to give a corresponding trigger angle by coordinating with the voltage control segment to control operation of the converter at the inverter side. In the DC transmission project utilizing constant extinction angle control method at the inverter side, it often has two such links, of which one is controlled based on the given extinction angle and the other one is used to limit the minimum extinction angle.

2. Voltage control segment

This link is one of the core links of the DC control system, which constantly compares the output voltage of the converter with the given reference voltage, gives a corresponding trigger angle by coordinating with the current control segment on the rectifier side, and gives a trigger angle by coordinating with the constant extinction angle control segment on the inverter side. In the DC transmission project utilizing constant voltage control method on the inverter side, this link directly controls the voltage of the DC system.

3. Current control segment

This link is one of the core links of the DC control system, which compares the output current value on the rectifier side with the given reference current constantly and gives a corresponding trigger angle on the rectifier side. On the inverter side, when the current is reduced to a certain value, the DC control over the valve module is transferred to this link.

4. Valve firing pulse generation segment

The valve firing pulse generation segment is one of the key control segments of the switching overvoltage simulation model for the UHVDC system, the accuracy of which is related to stability of the control of the DC control system. Its task is to, based on the trigger angle order and by making a reference to the phase angle of the AC three-phase voltage, give a trigger impulse at an accurate time and deliver it to the valve trigger gate. For the control segment, the most direct solution is to carry out a real-time comparison with the phase angle of the three-phase voltage, so as to generate a trigger impulse in time after reaching the phase angle required. When the system is operated normally and the harmonic component is very small, this solution has a high accuracy. But, when the system is subject to a fault or waveform distortion of the reference AC voltage due to a large harmonic component, the impulse generated by this solution will be inaccurate completely, resulting in the failure of the system control, and aggregating the disorder of system operation. In real systems, the constant phase interval control method is used to generate impulse. For a 12-pulse converter, 12 trigger impulses are produced in one alternating cycle, so that 12 trigger impulses are produced in each alternating cycle for the impulse

trigger link, and the time interval between two impulses is a time period with about 30° phase angle. For the triggering time of the next impulse, a reference is made to the time interval between the previous two impulses. This prevents an inaccurate trigger angle resulting from abrupt change in the reference phase due to distortion of the AC waveform.

5. Measurement segment for extinction angle of valve

The measurement segment for extinction angle of valve is also one of key links for simulation model of switching overvoltage for the UHVDC system, the actual accurateness of which directly determines the stability of voltage control on the inverter side, and stable startup of the DC system. Its task is to accurately measure the extinction angle of the valve, and deliver it back to the control system, and then the control system, based on the measured extinction angle, limits the maximum value of the trigger angle on the inverter side, so as to prevent the voltage from being overturned due to occurrence of commutation failure in the transient state of the fault, resulting in a DC voltage oscillation of the system.

6. Low-voltage current limiting segment

This link is one of key links in the DC control system, and when the output voltage of the converter is reduced to a certain level, an appropriate reference value of the current controller is also reduced as per a rule to maintain the control system's ability to control the DC system, so as to prevent a big oscillation of the voltage for that the system gets out of control.

16.2.2.4 Coordination Among Control Segments in Simulation Model

As described in previous section, the converter station control system has three main core control segments: constant extinction angle control segment, voltage control segment and current control segment. These three control segments are operating simultaneously when the DC system is operating, but only one control segment works at any time, and the other two control segments are acted as standby control segments. In case of occurrence of a fault or system adjustment, the control of the system is changed over among the links according to a preset rule. The basic changeover rule is specified as follows.

When the rectifier converter station is operated normally, the current control segment achieves its control purpose directly. When the system voltage rises to a presetting value, the control over the trigger angle at the rectifier side is changed over to the voltage control segment, so as to limit the DC system voltage; when the system voltage is declined to a preset value, the current presetting value in the current control segment is adjusted to a lower level by the low-voltage current limiting segment. The constant extinction angle control segment does not work when the converter is in rectification state.

When the inverter converter station controlled by constant extinction angle control method is operating normally, the constant extinction angle control segment

achieves its control purpose directly. When the system voltage rises to a presetting value, the control over the trigger angle at the inverter side is changed over to the voltage control segment, so as to limit the DC system voltage; when the extinction angle is too small, the control of trigger angle at the inverter side is changed over to another constant extinction angle link, so as to limit the trigger angle of the system; when the DC current of the system is declined to below a fixed value, usually 0.9 times of the current presetting value, the control of trigger angle at the inverter side is changed over to current control segment.

16.2.3 Scheme for Arrangement of Arresters in Converter Station

The safe operation of the UHVDC transmission system cannot be achieved unless an overvoltage protection device is provided. The modern DC transmissions adopt gapless zinc oxide arrester as a key equipment for overvoltage protection, which is used to limit overvoltage, and protect equipment, having a decisive effect in determining insulation level of the whole project.

The UHVDC converter station arresters are configured based on the following basic rules: the AC side overvoltage in the converter station is limited by the AC side arresters; the DC side overvoltage is limited by the DC side arresters; the important equipment in the converter station are protected by the arrester being close to it; and some equipment can be protected by 2 or more arresters in series, for example, the bushing to earth insulation at the valve side of the converter transformer is protected by several arresters in series.

Furthermore, it is required to consider volt–ampere characteristic deviation of the arrester in the simulation calculation. During the calculation of the maximum protection level of the arrester, it is required to use the maximum deviation characteristic of the arrester; however, when determining the maximum energy requirement for the arrester at a specific position, the arrester adopts the minimum deviation characteristic.

With the Xiangjiaba–Shanghai ±800 kV UHVDC project taken as an example, the scheme for arrangement of the arresters is shown in Fig. 16.1, and the parameters of the arrester are shown in Table 16.1.

According to the operating parameters for the Xiangjiaba–Shanghai ±800 kV UHVDC transmission project mentioned above, a switching overvoltage simulation model is built for the UHVDC transmission system to carry out simulation calculation of the typical switching overvoltage in the system, and analyze the overvoltage production mechanism and give some appropriate suppression measures.

It can be known from the analysis given above that, the switching overvoltage of the UHVDC transmission system, based on the occurrence position, is usually fallen into overvoltage at AC side, overvoltage in valve hall and overvoltage in DC field, which are introduced in the following contents.

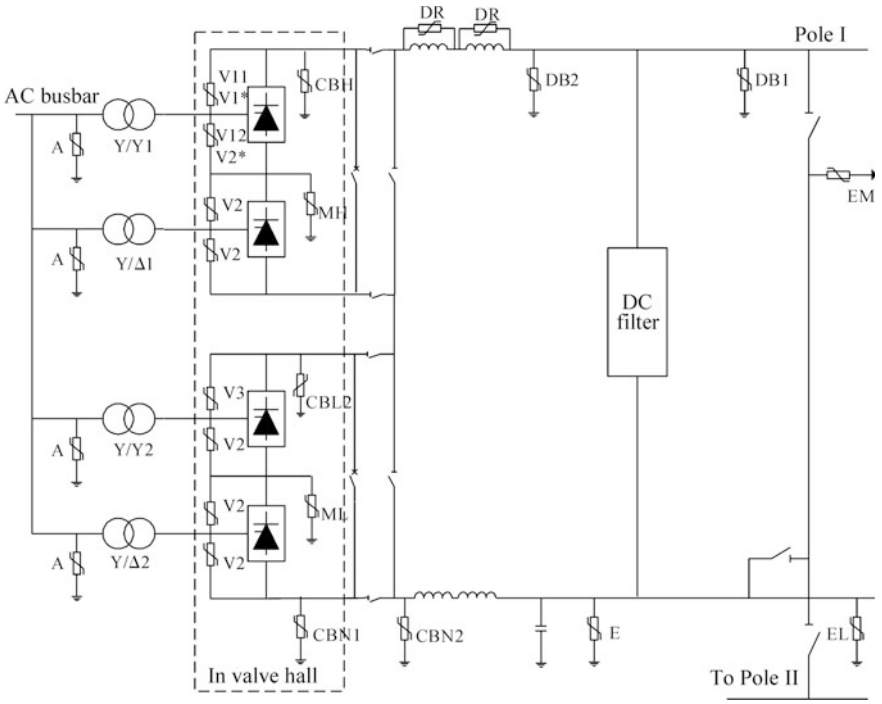

Fig. 16.1 Scheme for the arrangement of arresters in the converter station of Xiangjiaba–Shanghai ±800 kV UHVDC transmission project. *Note* V1 and V2 marked with * in the figure are valve arresters in the inverter station; V11 and V12 are valve arresters in the rectifier station

16.3 Switching Overvoltage at AC Side

The switching overvoltage at AC side means the switching overvoltage appeared in the AC busbar and in the equipment connected onto the busbar in the converter station. The equipment connected on the AC busbar are mainly protected by the arrester A of the AC busbar, which is installed close to the converter transformer and on the busbar of each AC filter bank. Various faults occurred in the AC system or operation implemented, e.g., single-phase and three-phase ground fault and fault clearing of AC system, switch-on and switch-off of AC filter, etc., will cause high overvoltage on relevant equipment at AC side. The following gives an analysis and discussion of three kinds of typical overvoltage, including overvoltage resulting from three-phase ground fault and fault clearing, overvoltage resulting from loss of AC power supply at the inverter side, and overvoltage occurred in the AC filter.

Table 16.1 Parameters of arresters in converter station of Xiangjiaba–Shanghai UHV transmission project

Arrester	CCOV (kV)	PCOV (kV)	U_{ref} (kV)	Energy capacity (MJ)
	(Xiangjiaba/Shanghai)	(Xiangjiaba/Shanghai)	(Xiangjiaba/Shanghai)	(Xiangjiaba/Shanghai)
V11/V1	249/233	288/278	288/278	10.1/7.5
V12	248/–	288/–	288/–	5.1/–
V2	249/233	296/278	296/278	5.3/3.7
V3	249/233	296/278	296/278	5.3/3.7
DB1	824/824	–/–	969/969	13.5/13.3
DB2	824/824	–/–	969/969	13.5/13.3
CBH	878/859	916/895	1070/1048	19.0.19.0
MH	649/638	704/672	794/779	14.6/14.2
CBL2	443/434	496/469	553/529	9.9/9.7
ML	293/250	–/–	358/358	3.3/3.3
CBN1	137/77	175/112	333/333	3.1/3.1
CBN2	137/77	175/112	304/304	13.1/8.5
E	83/20	–/–	304/219	2.85/2.0
EL	20/20	–/–	202/202	5.6/5.6
EM	83/20	–/–	278/219	27.0/2.0
DR	44/44	–/–	483/483 (rms)	3.3/3.3
A	318/318	–/–	396/396 (rms)	3.42/3.42

16.3.1 Three-Phase Ground Fault and Clearing

16.3.1.1 Simulation Calculation Conditions

When a AC filter branch in the converter station, or the AC line connected with the busbar of the converter station is subject to a three-phase ground fault occurs in the vicinity of the converter station, and the faulty line is disconnected by the relay protection device of the AC system from the system, a load shedding overvoltage will occur on the AC busbar of the converter station, the simplified diagram of which is shown in Fig. 16.2. This overvoltage condition is one of the most severe conditions that the arrester A of the AC busbar underwent.

This overvoltage condition is relevant to fault occurrence and clearing time. By selecting different fault clearing time in simulation, and in view of the volt–ampere characteristic deviation of the arrester A, the maximum protection characteristic and minimum protection characteristic are used for calculation, respectively, so as to find out the most severe overvoltage condition on the arrester of the AC busbar.

16.3.1.2 Simulation Calculation Results

With the overvoltage calculation in case of occurrence of three-phase ground fault in Fulong Converter Station as the sending end of the Xiangjiaba–Shanghai ±800 kV UHVDC project taken as an example, the corresponding calculation results are shown in Table 16.2. The calculation results show that the voltage of the AC busbar in Fulong Converter Station is rated to 530 kV, and after occurrence of this fault, the overvoltage on the AC busbar rises to 766 kV, and the maximum

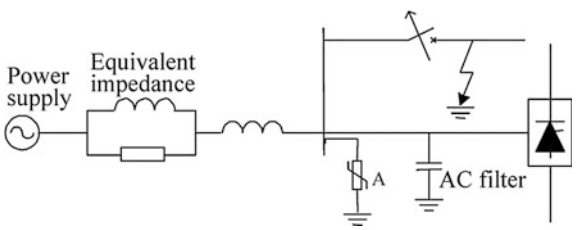

Fig. 16.2 Simplified sketch of AC three-phase ground fault clearing overvoltage

Table 16.2 Simulation results of overvoltage on AC busbar arrester A in Fulong Converter Station at the time of occurrence of three-phase ground fault and clearing

Characteristics of arrester	Max. voltage (kV)	Max. current (kA)	Max. energy (MJ)
Max. protection characteristic	766	1.35	0.55
Min. protection characteristic	743	1.50	0.69

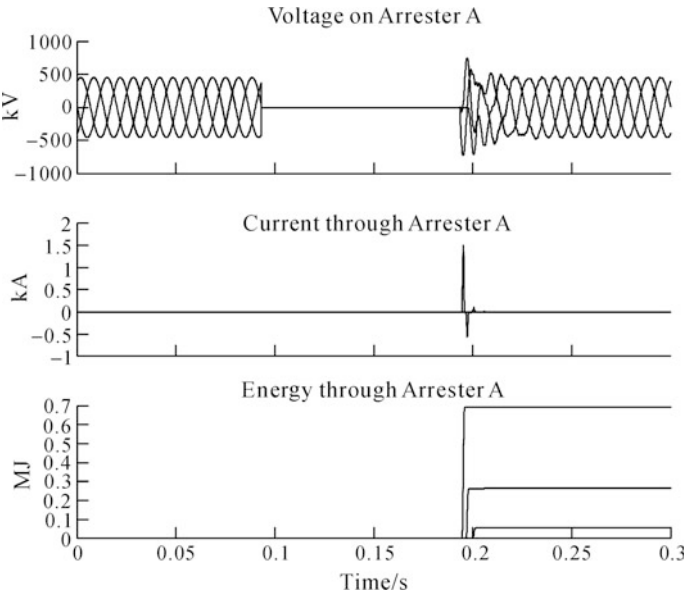

Fig. 16.3 Waveforms of overvoltage, current, and energy on AC busbar arrester A in Fulong Converter Station at the time of the occurrence of three-phase ground fault and clearing

energy flowing through the arrester A is 0.69 MJ. Because this fault is a symmetrical fault, the energy flowing through the arrester A at one phase may reach the maximum value when this fault occurs at different time within one power frequency cycle. Figure 16.3 shows the waveforms of the overvoltage, current and energy when the maximum energy flows through the arrester A at phase a.

16.3.1.3 Analysis of Overvoltage Mechanism

The overvoltage mechanism is analyzed as follows: in case of occurrence of a three-phase ground fault, the energy stored in the AC filter bank (including capacitor bank) is released by the fault point, and in the subsequent fault clearing process, the system power supply charges the AC filter bank through the system impedance (usually inductive) to cause transient electromagnetic oscillation, so that an overvoltage occurs on the busbar of the AC side.

16.3.1.4 Control and Protection Measures of Overvoltage

From the aforementioned overvoltage calculation results, it can be known that the overvoltage magnitude and energy are less severe. If the equipment is designed in accordance with the conventional AC system design procedure and configures the

arresters in the vicinity of the converter transformer, AC filter banks and other equipment, the overvoltage normally does not endanger the AC equipment in the converter station.

16.3.2 Loss of AC Power Supply at the Inverter Side

16.3.2.1 Simulation Calculation Conditions

The HVDC transmission system adopts an active inversion method at the inverter side. If the inverter station is subject to a loss of AC power supply, the inversion process cannot be carried out. If the DC line continues to transmit the active power to the inverter station at this moment, the converter transformer and filter bank in the inverter station will be subject to oscillation, resulting in a significant overvoltage on the AC busbar in the inverter station, so that bigger current and energy will flow through the arrester A of the AC busbar. This is a critical challenge for the converter in the DC transmission system and AC field equipment. The simplified diagram for the fault is shown in Fig. 16.4.

During simulation, the DC system is set to be operated at rated power of both poles, and the AC power supply at the inverter side should be disconnected, but the filter bank on the busbar should be maintained. Based on the experience in debugging of the DC transmission projects and actual control and projection configuration conditions, the DC system can get the bypass pair locked from the inverter side immediately when the last circuit breaker at the inverter side is tripped off to prevent the energy from flowing to the AC side. Such overvoltage condition is one of the most severe conditions for the arrester A of the AC busbar.

In addition, the allowable maximum transmission power for the DC transmission projects is considered in some research. For example, the allowable maximum transmission power for the Xiangjiaba–Shanghai ±800 kV UHVDC project is 1.2 times that of the rated power; however, when the system is operated at a high power

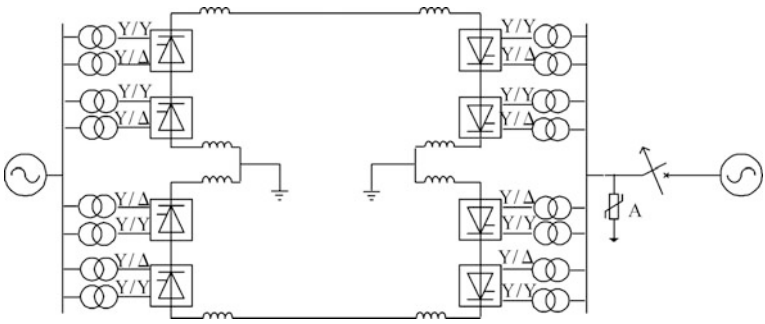

Fig. 16.4 Diagram for loss of AC power supply fault at the inverter side

level during the actual operation, the fault resulting from the loss of AC power supply occurs hardly ever, so this section takes the rated power operating condition as the condition for calculation of the most severe overvoltage.

The control and protection method adopted in this section is that the bypass pair at the inverter side is locked after being put into operation. According to different actuation times of control and protection systems, the following conditions are considered:

1. When the last AC circuit breaker is tripped off, the bypass pair at the inverter side is put into operation and locked.
2. After the last AC circuit breaker is tripped off for 10 ms, the bypass pair at the inverter side is put into operation and locked.
3. After the last AC circuit breaker is tripped off for 20 ms, the bypass pair at the inverter side is put into operation and locked.
4. After the last AC circuit breaker is tripped off for 30 ms, the bypass pair at the inverter side is put into operation and locked.

Such overvoltage severity is related to the trip time of the AC switch, so the calculation and analysis are carried out during simulation, based on four kinds of actuation time for the control and protection mentioned above, respectively.

During simulation, find out the most severe overvoltage condition on the arrester of the AC busbar, through selecting different fault occurrence times within one power frequency cycle and in view of volt–ampere characteristic deviation of the arrester A (the calculation is carried out by use of the maximum protection characteristic and minimum protection characteristic, respectively). So as to find out the most severe overvoltage condition on the arrester of the AC busbar.

16.3.2.2 Simulation Calculation Results

With the overvoltage calculation in case of such fault in Fengxian Converter Station as the receiving end of the Xiangjiaba–Shanghai ±800 kV UHVDC project taken as an example, the corresponding calculation results are shown in Table 16.3. The calculation results show that the voltage of AC busbar in Fengxian Converter Station is 515 kV, the maximum overvoltage on the AC busbar is 763 kV in case of the fault, as well as the maximum energy flowing through the arrester A is 2.4 MJ. For the reason that the fault is a symmetrical fault, when the fault occurs at different times within one power frequency cycle, the energy flowing through the arrester A at a certain phase may reach the maximum level. Figure 16.5 shows the waveforms of overvoltage, current, and energy of the arrester when the maximum energy flows through the arrester A by such method that the bypass pair at the inverter side is put into operation and locked after the last AC circuit breaker is tripped off for 10 ms.

Table 16.3 Simulation results for overvoltage on AC busbar arrester A in Fengxian Converter Station at the time of loss of AC power supply at the inverter side

Time of placement of bypass pair into operation at the inverter side (ms)	Characteristics of arrester	Max. voltage (kV)	Max. current (kA)	Max. energy (MJ)
0	Max. protection characteristic	728	0.282	0.264
	Min. protection characteristic	707	0.462	0.421
10	Max. protection characteristic	758	0.903	1.33
	Min. protection characteristic	712	1.01	1.39
20	Max. protection characteristic	762	1.10	1.74
	Min. protection characteristic	717	1.20	2.03
30	Max. protection characteristic	763	1.17	2.20
	Min. protection characteristic	717	1.20	2.41

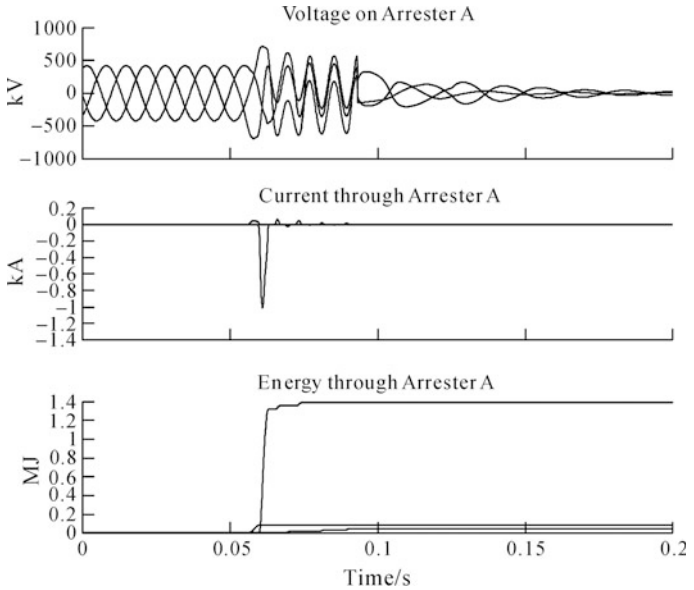

Fig. 16.5 Diagram for waveforms of overvoltage and energy on AC busbar arrester A in Fengxian Converter Station at the time of the loss of AC power supply at the inverter side

16.3.2.3 Analysis of Overvoltage Mechanism

According to the calculation results and overvoltage waveform described above, the overvoltage mechanism is analyzed as follows:

1. After the loss of AC power supply at the inverter side, the DC line continues to deliver energy to the converter transformer and AC filter bank to make the voltage on the AC busbar risen, resulting in an electromagnetic oscillation between the AC filter and converter transformer winding, so that a higher overvoltage appears. Therefore, the energy resulting in such overvoltage is supplied by the DC line via the converter, and the main cause leading to such oscillating overvoltage is the oscillation between the coil at the AC side of the converter transformer and AC filter bank.
2. After such fault occured, the control and protection system of the DC system is actuated, and after the bypass pair of the converter in the inverter station is put into operation, the energy on the DC line cannot be transmitted to the converter transformer and AC filter bank via the converter anymore, and the oscillating overvoltage existing on the AC busbar gets attenuated and disappears immediately.

It can be seen that the overvoltage energy is directly related to the transmission capacity of the DC system and time of getting the bypass pair into operation when the fault occurs. Upon the occurrence of such fault, the bigger the transmission capacity of the DC system is, the more severe the overvoltage is; in addition, the faster the actuating speed of the control and protection system is, the less the energy delivered to the AC busbar side is, and the lower the overvoltage energy flowing through the arrester A of the AC busbar.

Additionally, if the UHVDC transmission system is operated at the operating mode of reverse power transmission, the loss of AC power supply in Fulong Converter Station will also result in overvoltage at the AC side in Fulong Converter Station; however, the overvoltage resulting from the occurrence of such fault in Fulong Converter Station is lower than that in Fengxian Converter Station because the maximum reverse transmission power for the Xiangjiaba–Shanghai ±800 kV UHVDC project is only 62.5% of the rated forward transmission power.

During practical operation, the inverter station is usually connected with several AC lines in the condition of DC system transmitting a large transmission power, and it is nearly impossible that several lines are tripped simultaneously to cause loss of AC power supply of the inverter station at this moment.

However, for the DC system transmitting a small transmission power, and under the circumstance where the inverter station is connected with only one or two AC lines, it is probable that a fault resulting from the loss of AC power supply occurs in the inverter station, but the overvoltage is often not severe at this moment, because the transmission power of the DC system is small and less AC filters are put into operation. So such overvoltage is not primarily considered in some studies on UHVDC switching overvoltage.

16.3.2.4 Overvoltage Control and Protection Measures

According to the analysis of the overvoltage mechanism given above, the protection measures are mainly considered for such overvoltage with respect to the following two aspects:

1. Quick disconnection of the overvoltage energy source, namely the protection system, should judge the fault as soon as possible and send a signal in time to get the bypass pair into operation and lock it.
2. Quick disconnection of the AC filter. The AC filter is one of the main oscillating sources causing such overvoltage, so disconnecting the AC filter can reduce the overvoltage as quick as possible.

Considering that disconnection of the AC filter is restricted by the mechanical response speed of the switch, such overvoltage should be limited mainly by means of quickly putting the bypass pair into operation.

16.3.3 Internal Overvoltage of AC Filters

An internal electromagnetic transient process may be caused by AC busbar fault, voltage fluctuation, and other reasons during the operation of the AC filter, which results in internal overvoltage of the filter. The internal overvoltage of the AC filter mainly includes AC busbar ground fault and switching overvoltage impulse. The following will provide a discussion on the calculation method for two typical kinds of internal overvoltage of the filter.

16.3.3.1 Simulation Calculation Conditions

The internal switching overvoltage of the AC filter is mainly caused by the following two conditions: earthing of the filter busbar and switching overvoltage impulse. For simulation research of these two kinds of overvoltage, it is possible to carry out a separate research on the filter. The following provides an analysis of the conditions by taking the HP24/36 filter used in Fulong Converter Station as an example:

1. Ground fault of filter busbar

The ground fault that occurred at the top of the AC filter HP24/36 is shown in Fig. 16.6. The left part in the figure presents a filter mode, in which L_{C1} is the parasitic inductance of high-voltage capacitor, and R_{L1} and R_{L2} are the DC resistors of the reactor, the resistance values of which can be calculated by the quality factor of the reactor; the right part presents an earth branch model of the ground fault inductor L_x. When the filter is charged to a high electric potential, a ground fault

occurs on the filter busbar, and at this moment the arrester F1, capacitor C1, and fault point constitute a fault circuit, so that F1 will endure a high fault overvoltage. Meanwhile, L1, L2, and R1 circuits will also release energy stored in the C1 to cause an oscillation process inside the filter, and an overvoltage on the arrester F2.

For BP11/13, HP3, and SC filter in the Fulong Substation and SC filter in the Fengxian Station equipped with only one arrester F1 (see AC Filter in the Sect. 15.3.5.6 hereof), it is only required to consider the maximum overvoltage on the arrester F1; however, for HP24/36 in the Fulong Converter Station and HP12/24 in the Fengxian Station equipped with arresters F1 and F2, it is required to consider the respective maximum overvoltage of these two arresters, due to different positions of the two arresters and different conditions for calculation of their respective maximum overvoltage. The following provides a discussion on the respective overvoltage of the two arresters.

(1) Arrester F1

With respect to the arrester F1, its overvoltage results from the discharge of $C1$ through F1 when the AC busbar has a ground fault. If the precharging voltage on the capacitor at the HV end of the filter gets higher, the energy stored by the filter gets higher and the overvoltage occurred on the arrester F1 gets more severe. Additionally, the overvoltage magnitude on the arrester F1 gets higher if L_x is smaller.

The wave front of the maximum overvoltage on the arrester F1 is very steep, which is more close to the lightning impulse, so the result calculated here should correspond to the lightning impulse protection level.

The most severe conditions for overvoltage calculation are as follows:

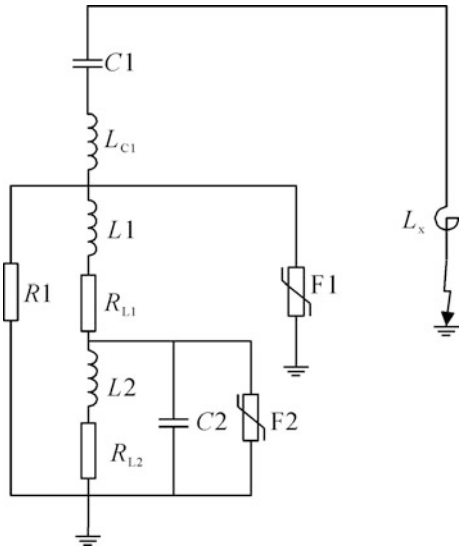

Fig. 16.6 Simulation circuit diagram for ground fault at the top of HP24/36 filter in Fulong Converter Station

① AC filter precharging voltage

Considering that the maximum voltage on the AC filter cannot exceed the protection level of the arrester for the AC busbar, it is required that, pursuing the principle of strictness, the precharging voltage can be selected as the switching impulse protection level (SIPL) of the arrester of the AC busbar, namely 761 kV.

② Parasitic inductance L_{C1} of the HV capacitor

According to the equipment manufacturing experience, the ABB company believes that the parasitic inductance of capacitor $C1$ at the HV end of the AC filter can be 50 μH.

③ L_x taken as the minimum value

The fault inductance value is mainly referred to as the AC busbar parasitic inductance. The AC filter terminal is usually placed at a higher position, where the air clearance is large, so it is usually not liable to ground fault. The position at which it is liable to ground fault is usually at about 10–20 m distance from the AC filter. So L_x is typically the parasitic inductance of the AC busbar between the ground fault point and capacitor $C1$ at the HV end of the DC filter. The ABB company believes that this value should not be less than 10 μH and usually take an inductance value of 20 μH.

④ Maximum and minimum protection characteristics of the arrester

When calculating the maximum load of an arrester, it is required to use the minimum protection characteristic of the arrester based on the principle of strictness. If there are other arresters in the filter, it is required to use the maximum protection characteristic for these arresters based on the principle of strictness, so as to reduce the shunt.

(2) Arrester F2

Unlike the arrester F1, the overvoltage on the arrester results from the transient oscillation of L_2 and C_2 circuits, so the condition for calculating the maximum overvoltage on the arrester F2 is that L_x is not the minimum value, but a value between the minimum value and the maximum value (usually, the minimum value is not less than 10 μH and the maximum value can reach 100 mH), which is usually determined by gradual test in the simulation calculation.

The steepness of maximum overvoltage wave front on the F2 is more close to the switching impulse (the waveform of the maximum overvoltage on the arrester F1 is more close to lightning impulse), so the results calculated here should correspond to the switching impulse protection level.

Except the value of L_x, other conditions for calculation model of the maximum overvoltage are the same as those for the arrester F1.

2. Switching overvoltage impulse

The analysis of the internal overvoltage of the AC filter should also take account of the intruding switching impulse, the simulation diagram of which is shown in Fig. 16.7. During calculation, a 250/2500 μs switching impulse is applied to the AC busbar, and pursuing the principle of strictness, the switching impulse magnitude is the switching impulse withstand level of the AC busbar, namely 761 kV.

16.3.3.2 Simulation Calculation Results

1. Ground fault of filter busbar

Taking the Xiangjiaba–Shanghai ±800 kV UHVDC project as an example, the calculation results for the internal overvoltage of the AC filter are shown in Table 16.4. Figure 16.8 shows the waveforms of overvoltage, current, and energy when the maximum overvoltage flows through the arrester F1 in the filter HP24/36.

2. Switching overvoltage impulse

With respect to such overvoltage condition, a switching impulse of 250/2500 μs is usually used for simulation. The simulation circuit diagram is shown in Fig. 16.7, and the simulation calculation results are shown in Table 16.5, in which it can be seen that the energy flowing through arrester F1 and arrester F2 in case of such overvoltage is very small.

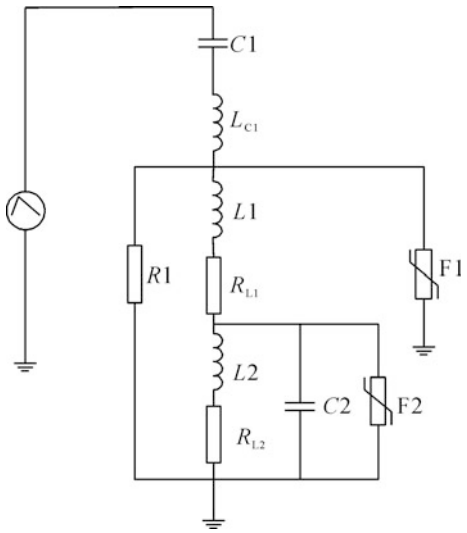

Fig. 16.7 Simulation circuit diagram for switching overvoltage impulse of HP24/36 filter in Fulong Converter Station

Table 16.4 Calculation results for overvoltage on arrester in AC filter in case of a ground fault at the top of AC filter

Converter station	Arrester	Protection characteristics of arrester	Max. voltage (kV)	Max. current (kA)	Max. energy (MJ)
Fulong	Arrester F1 in BP11/13	Max. protection characteristic	447	62	0.72
		Min. protection characteristic	413	68	0.73
	Arrester F1 in HP24/36	Max. protection characteristic	337	80	0.68
		Min. protection characteristic	312	85	0.68
	Arrester F2 in HP24/36	Max. protection characteristic	97	12	0.23
		Min. protection characteristic	91	12	0.24
	Arrester F1 in HP3	Max. protection characteristic	338	81	0.71
		Min. protection characteristic	313	86	0.71
	Arrester F1 in SHC	Max. protection characteristic	337	79	0.67
		Min. protection characteristic	311	84	0.67
Fengxian	Arrester F1 in HP12/24	Max. protection characteristic	342	88	0.84
		Min. protection characteristic	317	94	0.84
	Arrester F2 in HP12/24	Max. protection characteristic	94	8	0.40
		Min. protection characteristic	88	8	0.40
	Arrester F1 in SHC	Max. protection characteristic	339	83	0.76
		Min. protection characteristic	314	88	0.76

Apart from the simulation calculation, the operating current for the arrester F1 in the AC filter (as shown in Figs. 15.15 and 15.16) can be estimated by the following equation [1, 2]:

$$I \approx C\frac{\mathrm{d}u}{\mathrm{d}t} = C\frac{\mathrm{SIPL}}{250}, \tag{16.1}$$

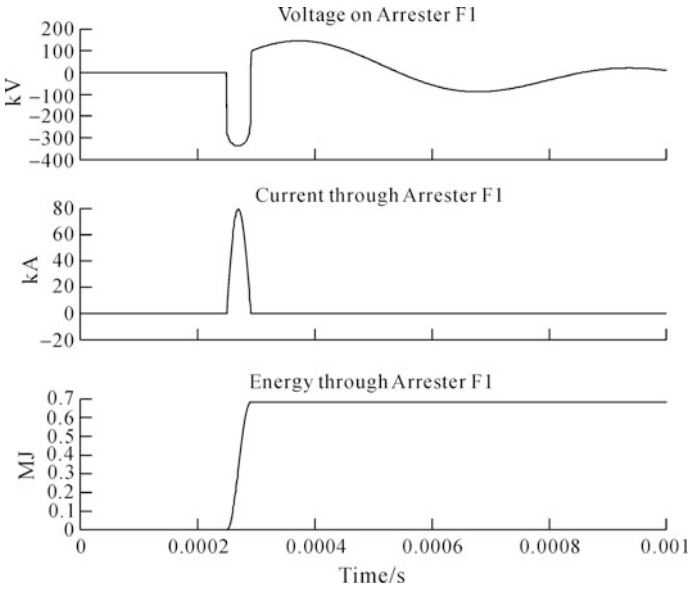

Fig. 16.8 Diagram for waveforms of overvoltage, current, and energy on arrester F1 in case of ground fault at the top of HP24/36 filter in Fulong Converter Station

where

C is the capacitance $C1$ of the HV filter (the capacitance value for each filter is shown in Tables 15.7 and 15.8)
$\mathrm{d}u/\mathrm{d}t$ is the voltage change rate, and
SIPL is the switching impulse protection level of the AC busbar

Taking the arrester F1 in BP11/13 filter in Fulong Converter Station as an example, if the SIPL of the F1 is 761 kV, the calculation is as follows:

$$I \approx C\frac{\mathrm{SIPL}}{250} = 2.523\ \mu\mathrm{F} \times \frac{761\ \mathrm{kV}}{250\ \mu\mathrm{s}} = 7.7\ (\mathrm{kA}).$$

In practice, due to the shunting effect of the filter inductance $L1$ and parallel resistance $R1$, the operating current calculated by the formula above would have an appropriate margin.

The operating current under the influence of the overvoltage is calculated by this simplified method, and then the voltage value under the influence of the operating current of the corresponding arrester can be obtained according to the maximum volt–ampere characteristic curve of the arrester, which is the calculation result of the overvoltage magnitude.

It can be seen from the calculation results obtained by the simulation method in Table 16.5 that, under the influence of the switching impulse, the overvoltage

Table 16.5 Calculation results for overvoltage on arresters in AC filter under switching impulse wave

Converter station	Arrester	Protection characteristics of arrester	Max. voltage (kV)	Max. current (kA)	Max. energy (MJ)
Fulong	Arrester F1 in BP11/13	Max. protection characteristic	366	7.2	0.45
		Min. protection characteristic	350	8.1	0.41
	Arrester F1 in HP24/36	Max. protection characteristic	267	6.7	0.16
		Min. protection characteristic	254	6.9	0.16
	Arrester F2 in HP24/36	Max. protection characteristic	90	12.2	0.13
		Min. protection characteristic	85	12.8	0.14
	Arrester F1 in HP3	Max. protection characteristic	274	9.0	0.46
		Min. protection characteristic	261	10.0	0.35
	Arrester F1 in SHC	Max. protection characteristic	283	13.3	0.20
		Min. protection characteristic	267	16.2	0.20
Fengxian	Arrester F1 in HP12/24	Max. protection characteristic	268	6.9	0.21
		Min. protection characteristic	256	8.0	0.21
	Arrester F2 in HP12/24	Max. protection characteristic	86	6.8	0.18
		Min. protection characteristic	82	6.8	0.18
	Arrester F1 in SHC	Max. protection characteristic	287	17	0.27
		Min. protection characteristic	271	18	0.27

energy of each arrester is very small. So the energy does not need to be verified by use of this simplified method for calculating the overvoltage inside the filters, and it is only required to calculate the overvoltage magnitude, namely the overvoltage calculation results in the condition of the maximum volt–ampere characteristic of the arrester.

Accordingly, by use of the simplified method, the switching overvoltage results of the arrester F1 in the other kinds of filters can be calculated, as shown in Table 16.6.

Table 16.6 Calculation results for overvoltage on arresters in AC filter under standard switching impulse voltage wave

Converter station	Arrester	Max. voltage (kV)	Max. current (kA)
Fulong	Arrester F1 in BP11/13	365	7.7
	Arrester F1 in HP24/36	267	7.8
	Arrester F1 in HP3	268	7.8
	Arrester F1 in SHC	268	7.8
Fengxian	Arrester F1 in HP12/24	271	9.5
	Arrester F1 in SHC	269	8.7

16.3.3.3 Analysis of Overvoltage Mechanism

With respect to the arrester F1 in these AC filters, the overvoltage occurs because $C1$ discharges directly through F1 when the AC busbar is grounded.

With respect to the low-voltage arrester F2 in HP24/36 and HP12/24 filter, the overvoltage is mainly attributed to the electromagnetic oscillation of $C2$ and $L2$ in case of the occurrence of a ground fault of the filter busbar, and the maximum of overvoltage is different from F1.

16.3.3.4 Overvoltage Control and Protection Measures

For the internal overvoltage of the AC filter, the existing UHVDC systems usually adopt arresters (F1, F2) in the filters for direct protection. From the calculation results obtained above, it can be known that the overvoltage is not severe and can be protected perfectly by use of arresters F1 and F2.

16.4 Switching Overvoltage in Valve Hall

According to Fig. 16.1, a diagram for the arrangement of arresters in converter station, the valve hall is mainly equipped with valve arresters V11 (Fulong Converter Station), V1 (Fengxian Station), V12, V2, and V3 connected in parallel stressed on the valve, converter busbar arresters CBH, MH, CBL2, and ML, and neutral line arrester CBN1. The CBN1 is mainly used to protect against the lightning impulse overvoltage intruded along the neutral busbar, but this chapter focuses on the discussion of switching overvoltage, so no discussion is made for the CBN1 arrester here. The following provides a discussion and analysis with respect to the arresters based on the respective decisive overvoltage conditions of the arresters.

Among these arresters, their decisive overvoltage condition is different from each other because the different valve arresters are placed at different positions. Accordingly, the valve arresters can be divided into three groups:

1. valve arrester V11/V1, placed at the uppermost layer of the 12-pulse converter;
2. valve arrester V12/V2, placed at the other layers of the upper 12-pulse converter except the uppermost layer, and
3. valve arrester V3, placed at the uppermost layer of the lower 12-pulse converter.

The operating conditions for these three groups of valve overvoltage are analyzed as follows:

1. When the valve is turned on, the voltage stressed on the valve arrester is zero, so an overvoltage occurs stressed on the valve arrester only when the valve is turned off.
2. When the DC system is operating normally, the voltage stressed on the converter valve typically does not exceed the line voltage at the valve side of the converter transformer. However, when the electric potential undergoes an abrupt change at one side or both sides of the converter valve due to operation or fault, it is possible to lead to overvoltage stressed on the converter valve.
3. Based on structure and operating principle of the DC system, one end of three converter valves at each layer is connected with the three-phase outgoing line at the valve side of the converter transformer, respectively, and the other end is connected with the same DC busbar, respectively. In this structure, if one valve among the three valves is conducted, the voltage stressed on the other two valves does not exceed the line voltage at the valve side of the converter transformer; if the three valves are not conducted at all, the voltage stressed on the valve is determined by the electric potential of the DC busbar and of the corresponding outgoing line at the valve side of the converter transformer. Therefore, the valve overvoltage is produced by the following two conditions:

   (1) If at least one valve is conducted among the three valves at the same layer, the overvoltage stressed on the valves at this layer is caused by the overvoltage impulse transmitted by the line voltage at the valve side of the converter transformer.
   (2) If three valves at the same layer are turned off, the overvoltage stressed on the valves at the layer is caused by an abrupt change in the electric potential stressed on the valves (namely the electric potential of the DC busbar and outgoing line at the converter transformer valve side).

According to the analysis above, the overvoltage condition and decisive overvoltage condition that may be endured by the three groups of valves are described as follows:

1. With respect to the valve arrester V11/V1 placed at the uppermost layer of the upper 12-pulse converter, both overvoltage conditions set forth above may occur, of which the second one is the decisive overvoltage condition.
2. With respect to the valve arrester V12/V2 placed at the other layers of the upper and lower 12-pulse converters except the uppermost layer, the first overvoltage condition may occur, which is the decisive overvoltage condition.

3. With respect to the valve arrester V3 placed at the uppermost layer of the lower 12-pulse converter, being similar to V11/V1, these two overvoltage conditions may occur, of which the second one is the decisive overvoltage condition.

In addition, the converter busbar arresters CBH, MH, CBL2, and ML are classified into one group, the decisive overvoltage conditions of which are the same.

To sum up, the arresters in the valve hall will be divided into the following four groups for discussion:

1. valve arrester V11/V1,
2. valve arrester V12/V2,
3. valve arrester V3, and
4. converter busbar arrester CBH, MH, CBL2, and ML.

16.4.1 Switching Overvoltage on Valve Arrester V11/V1

16.4.1.1 Simulation Calculation Conditions

The arresters V11/V1 are the valve arresters at the uppermost layer of the upper 12-pulse converter. In case a ground fault occurs on the outgoing line at the valve side of the converter transformer at the HV Y/Y of the converter station, the energy on the DC line and DC filter is released through the valve arrester V11/V1 at the uppermost layer of the upper 12-pulse converter, resulting in a high overvoltage and energy stressed on the arrester V11/V1. The fault circuit is shown in Fig. 16.9.

The most severe overvoltage condition is as follows: the DC system is operated in bipolar balance operating mode; the DC voltage is set to the maximum value, e.g., the DC voltage for the Xiangjiaba–Shanghai ±800 kV UHVDC project is 809 kV; the DC current is set to the minimum value, e.g., the DC current for the Xiangjiaba–Shanghai ±800 kV UHVDC project is 363A; and the fault occurs in the phase A outgoing line in design condition. After the occurrence of the fault, the DC control and protection system operates and the fault pole is stopped. The overvoltage condition is related to the fault occurrence time, and through selecting different fault clearing times during simulation and considering volt–ampere characteristic deviation of the valve arrester V11/V1, it is required to use the maximum protection characteristic and minimum protection characteristic for calculation, respectively, and find out the most severe overvoltage condition on the valve arrester V11/V1.

In addition, some studies proposed a more severe condition based on the condition, like double-fault condition, which means that an opposite pole has a ground fault when the fault mentioned above occurs, so that the pole DC voltage gets higher and the energy flowing through the valve arrester V11/V1 gets higher when the fault occurs. However, the probability of the double fault in practical projects is very small, so the double-fault condition will be ignored in the study.

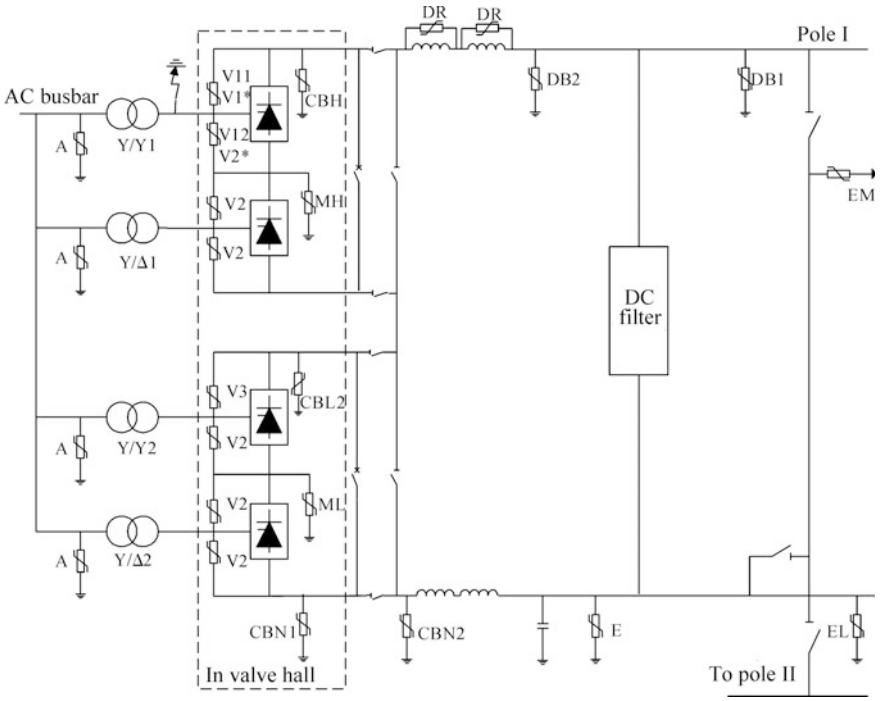

Fig. 16.9 Sketch for ground fault of the outgoing line at the valve side of the converter transformer at HV Y/Y of converter station

In order to discuss the most severe overvoltage condition during simulation calculation in this section, the most severe double-fault condition is taken as a case for the simulation calculation, still.

16.4.1.2 Simulation Calculation Results

With the calculation of overvoltage in Fulong Converter Station as the sending end of the Xiangjiaba–Shanghai ±800 kV UHVDC project under such fault taken as an example, the corresponding calculation results are shown in Table 16.7. The calculation results show that the maximum overvoltage stressed on the valve arrester V11 in Fulong Converter Station under this fault is 377 kV, and the maximum energy flowing through the arrester V11 is 7.12 MJ. Such fault is the asymmetrical fault. The energy flowing through the valve arrester V11 at phase C resulting from the ground fault of the outgoing line at phase A reaches the maximum level, and the energy at the other two phases resulting from such fault is smaller. Figure 16.10 shows the waveforms of overvoltage, current, and energy of three-phase valve arrester V11 when the maximum energy flows through the valve arrester V11 at phase C.

Table 16.7 Calculation results for maximum overvoltage of valve arrester V11/V1

Arrester	Characteristics of arrester	Max. voltage (kV)	Max. current (kA)	Max. energy (MJ)
V11 in Fulong Converter Station	Max. protection characteristic	377	2.49	6.82
	Min. protection characteristic	365	2.54	7.12
V1 in Fengxian Station	Max. protection characteristic	368	2.16	5.61
	Min. protection characteristic	357	2.26	5.86

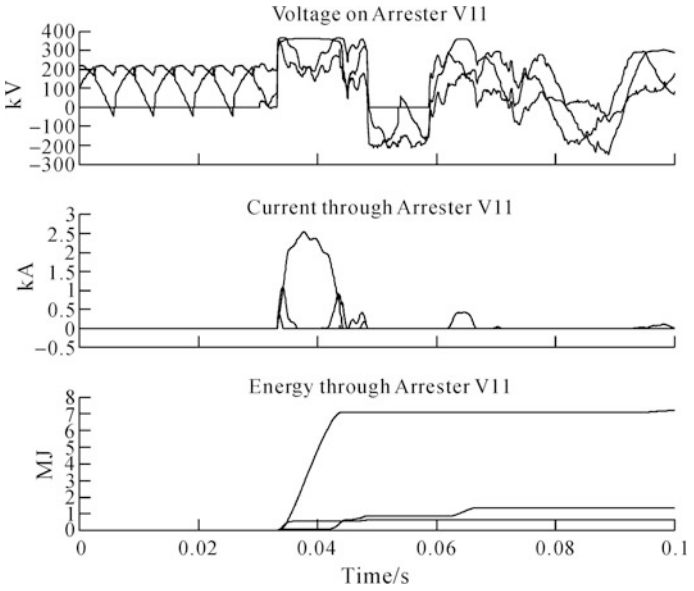

Fig. 16.10 Diagram for waveforms of maximum overvoltage, current, and energy of valve arrester V11 in Fulong Converter Station

When the DC system is operated in reverse power transmission mode, i.e., namely Fengxian Converter Station is operated as the rectifier side, and Fulong Converter Station is operated as the inverter side, the maximum overvoltage stressed on valve arrester V1 in Fengxian Converter Station is calculated as shown in Table 16.7. Under the influence of such fault, the maximum overvoltage stressed on the lower valve arrester V1 in Fengxian Converter Station is 368 kV, and the maximum energy flowing through the arrester V1 is 5.86 MJ.

16.4.1.3 Analysis of Overvoltage Mechanism

Such overvoltage condition is the most severe condition of the valve arrester V11/V1. According to the calculation results and overvoltage waveform listed above, the overvoltage mechanism is analyzed as follows [3, 4]:

1. The valve overvoltage is the one resulting from an abrupt change in the electric potential stressed on the valves after the three valves at the same layer are turned off. The specific process is as follows:
   It is assumed that the VT1 is in ON state when the fault takes place, as shown in Fig. 16.11. The point a at the cathode of the valve bank is connected to DC pole line. The voltage at point a is DC pole-to-earth operating voltage. Occurrence of ground fault at anode point b will cause the reduction of potential at point b, so that the valve VT1 is turned off under the influence of reverse voltage at both terminals. In addition, because DC pole-to-earth operating voltage is higher than the phase B and C-to-earth voltage (because phase A has been grounded, the phase B and C-to-earth voltages at this moment are only equal to the line voltage at the valve side of the converter transformer which is lower than the DC line operating voltage), so that the other two valves in this layer, VT3 and VT5, are unable to be turned on because the voltage at both terminals is always in reverse state, eventually making the three valves turn off.
   At this moment, all the three valves, VT1, VT3, and VT5, are already OFF. The voltage endured by shunt-wound valve arresters is the difference between DC pole-to-earth voltage and the three-phase outgoing line-to-earth voltage at the valve side of the converter transformer, where the valve arrester having the highest voltage difference on both terminals absorbs most of the energy of the overvoltage and the other two valve arresters absorb the rest of the energy. Because the three-phase outgoing line-to-earth voltage at the valve side of the converter transformer is different at different fault moments, this will affect the energy flowing through the three valve arresters directly. Therefore, simulation calculation is required for different fault moments to determine the most severe

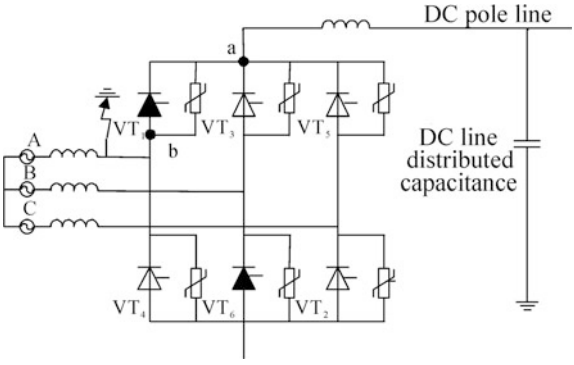

Fig. 16.11 The 6-pulse converter at the rectifier side that is connected with DC pole line

overvoltage operating condition. The valve overvoltage produced by the fault is directly related to the moment when the fault takes place.

2. Such overvoltage is impossible to occur on the inverter side, and the analysis thereof is as follows:
   Firstly, assume that the valve VT_4 is in ON state when the fault takes place, as shown in Fig. 16.12. The point a at anode of the valve bank is connected to DC pole line. The voltage at point a is DC pole-to-earth operating voltage. Occurrence of ground fault with phase A (point b of cathode of VT_4) will make the reduction of potential at point b. At this moment, the point a at anode of VT_4 has a higher potential than that of point b at cathode and the voltage across both terminals is still in positive direction. Therefore, VT_4 will not become OFF and will still remain in ON state. When phase B or phase C has a ground fault, because DC pole-to-earth operating voltage is higher than any of the three phase-to-earth voltage, the potential at point a is always higher than the cathode potential at point b. That is, at least one of the three top layer valves VT_2, VT_4, and VT_6 will remain in ON state. In this way, it is not possible that the voltage on valve arrester shunt-wound across valves VT_2, VT_4, and VT_6 is higher than the line voltage on the converter transformer valve side, i.e., no overvoltage will occur.

It can be known from the above discussion of overvoltage mechanism that the amplitude and energy of the overvoltage are determined by two factors: voltage and energy on DC pole line, and the moment the fault occurs.

It can be seen from the previously described operating parameters of DC system that, to obtain the most severe operating conditions of valve arrester V11, the requirements on the following four aspects have to be met.

(1) The maximum value for the pole voltage of DC system shall be taken.
(2) The energy stored on the distributed capacitances of DC line must be the highest after the converter valve on the inverter side has been turned off.

As shown in Figs. 16.13 and 16.14, the residual energy that can be released is determined by two factors: energy stored on distributed capacitance of DC line (the

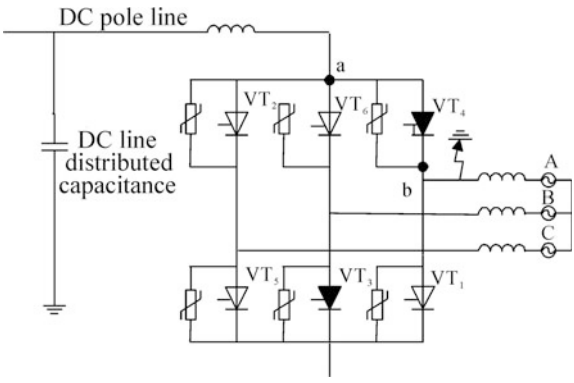

Fig. 16.12 The 6-pulse converter at the inverter side that is connected with DC pole line

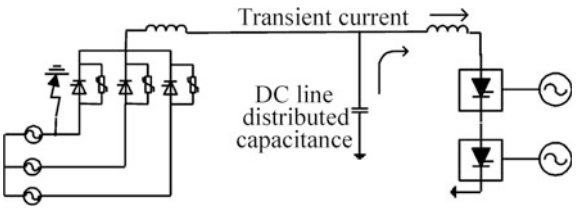

Fig. 16.13 Sketch for the release of energy on DC pole line before shut-off of the inverter side

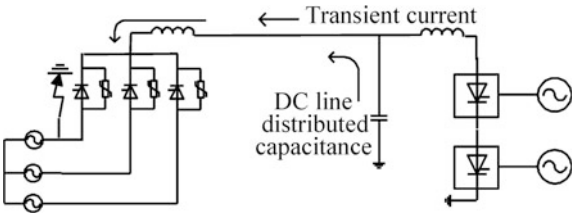

Fig. 16.14 Sketch for the release of energy on DC pole line after shut-off of the inverter side

energy is determined by the length of DC line and the operating voltage, which is usually constant); when fault occurs, DC line will release energy via the inverter before the converter valve on the inverter side is turned off. The higher the direct current is, the more the energy the DC line will release via the inverter side. Therefore, in order to have the highest releasable residual energy on DC line distributed capacitances, the minimal direct current shall be taken.

(3) AC phase voltage causing overvoltage of the valve has the longest duration.

The overvoltage of the valve is formed by the joint action of DC pole line voltage and the lowest phase voltage in the AC three-phase voltage output by the converter transformer.

As the three-phase voltage in the AC system is alternating constantly, the AC phase voltage causing overvoltage of the valve shall have the longest duration. Taking the occurrence of phase A ground fault as an example, the moment point should be close to the cross-point between phases B and C (being contrary to the polarity of the pole voltage, when the fault pole is the anode, take the negative cross-point; when the fault pole is the cathode, take the positive cross-point).

(4) Three-phase short-circuit capacity output by the converter transformer reaches the maximum level.

The short-circuit capacity is mainly determined by two factors: the first one is that the short-circuit capacity of the AC system reaches the maximum level; the other one is that the equivalent impedance of the converter transformer reaches the minimum level, that is to say, the transformation ratio of the converter transformer should be as small as possible. Hence, such fault's extreme condition is that the AC system connected to the converter station is at the maximum operating mode, and the AC busbar voltage in the converter station is the minimum operating voltage.

To sum up, calculation conditions for the most severe overvoltage that occurred on the valve arrester V11 are as follows [3]:

(1) The DC system is operated at bipolar operating mode in balance.
(2) The converter station is operated in rectification state.
(3) The DC operating voltage takes the maximum DC voltage, 809 kV for the Xiangjiaba–Shanghai ±800 kV UHVDC project.
(4) The DC current takes the minimum operating current, 363A for the Xiangjiaba–Shanghai ±800 kV UHVDC project.
(5) The AC system of the converter station takes the minimum voltage, 475 kV for the Fulong Converter Station of the Xiangjiaba–Shanghai ±800 kV UHVDC project.

16.4.1.4 Overvoltage Control and Protection Measures

Such overvoltage is the most severe overvoltage endured by the valve arrester of the UHVDC system, so the number of parallel columns for such valve arrester in the system reaches the maximum number, and the discharge capacity also reaches the maximum level.

The development process of such overvoltage has little relation to protection strategy of the DC system, and its harm can be limited only by decreasing the protection level of the valve arrester V11/V1 as far as possible. However, reducing the protection level of the arrester will lead to an increase in discharge capacity of the arresters under such fault. Typically, the energy requirement can be met by connecting multi-column arresters in parallel.

16.4.2 Switching Overvoltage on Valve Arrester V12/V2

16.4.2.1 Simulation Calculation Conditions

The valve arresters V12/V2 are the ones at the other layers of valves except the uppermost layer of valves in the upper and lower 12-pulse converters (as shown in Fig. 16.1). Unlike the valve arrester V11/V1, the valve arrester V12/V2 is not directly connected to the DC pole line. In this case, such overvoltage described above will not occur for the arrester V11/V1. However, a phase-to-phase switching overvoltage impulse takes place in the AC system of the converter station due to fault, switching operation, and other causes, which is transmitted to the valve hall through the converter transformer winding and applied to both terminals of the converter valve, so that the a bigger overvoltage occurs stressed on the valve arrester V12/V2. In practical, the valve arresters V11 and V1 are also subject to such switching impulse overvoltage; however, the overvoltage described in the previous section applied to both terminals of the arresters V11 and V1 is far more

severe than such overvoltage. Thus, the application of such overvoltage to both terminals of the valve arrester V11/V1 is not discussed.

Such overvoltage condition is the most severe overvoltage condition for the valve arrester V12/V2, the severity of which is related to the ON/OFF state of each valve at the moment of the occurrence of a fault. Based on alternating On/Off operating condition of the 6-pulse converter valve and by combining polarity analysis of the switching overvoltage impulse transmitted to the converter, it is possible to determine the impulse occurrence moment of the switching overvoltage occurred stressed on the specified valve. For example, the switching overvoltage impulse, resulting from the switching impulse from phases A and C when VT1 and VT6 are turned on, is applied to both terminals of the valve VT5, the equivalent circuit of which is shown in Fig. 16.15.

The switching impulse magnitude from the AC side is generally dependent on the protection level of AC busbar arrester A. Considering the most severe condition, the phase-to-phase switching overvoltage peak amplitude can be taken as 1.7 times the phase-to-earth overvoltage. If the protection level taken for the AC busbar arrester A in the Xiangjiaba–Shanghai ±800 kV UHVDC transmission project is 761 kV, and then the magnitude of phase-to-phase switching overvoltage impulse on the AC side busbar should be $1.7 \times 761 = 1293$ (kV).

16.4.2.2 Simulation Calculation Results

According to the simulation condition described above and by taking overvoltage in Fulong Converter Station as the sending end of the Xiangjiaba–Shanghai ±800 kV UHVDC project under such fault, it is possible to find out the most severe overvoltage condition on the valve arrester V12/V2. The corresponding calculation results are shown in Table 16.8. The calculation results show that the maximum overvoltage stressed on the valve arrester V12 in Fulong Converter Station under the influence of such fault is 374 kV, and the maximum energy flowing through the arrester is 0.46 MJ; the valve arrester V1 in Fengxian Converter Station under such

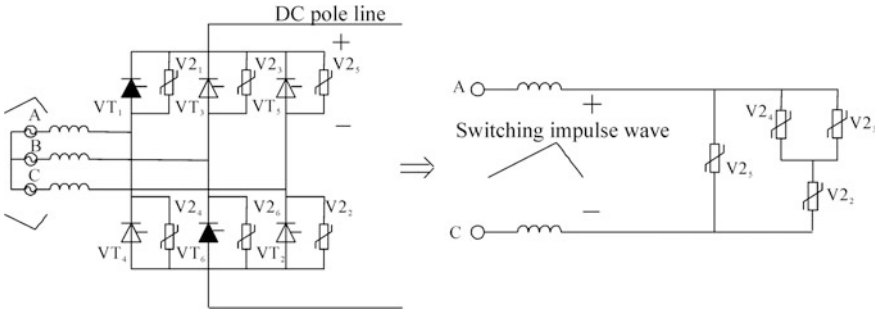

Fig. 16.15 Diagram for transmission of switching overvoltage of AC system into valve hall and equivalent circuit diagram

Table 16.8 Calculation results for overvoltage and energy stressed on valve arrester V12/V2

Arrester	Max. voltage (kV)	Max. current (kA)	Max. energy (MJ)
V12 in Fulong Converter Station	374	1.0	0.46
V2 in Fulong Converter Station	383	0.84	0.38
V2 in Fengxian Station	365	0.89	0.30

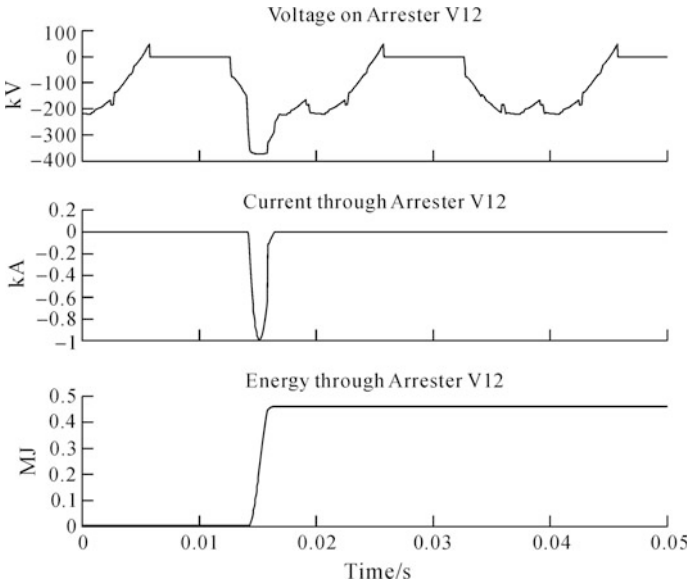

Fig. 16.16 Waveforms of maximum voltage, current, and energy on valve arrester V12 in Fulong Converter Station under AC phase-to-phase switching overvoltage impulse

fault is 383 kV, and the maximum energy flowing through the arrester is 0.38 MJ; the maximum overvoltage stressed on the valve arrester V2 in Fengxian Converter Station under such fault is 365 kV, and the maximum energy flowing through the arrester is 0.30 MJ; Fig. 16.16 shows the waveforms of overvoltage, current, and energy of the valve arrester V12 in the Fulong Converter Station.

16.4.2.3 Analysis of Overvoltage Mechanism

The fault condition is the decisive condition for the valve arrester V12/V2, the overvoltage mechanism analysis of which is as follows: its simplified fault diagram is shown in Fig. 16.15. With valves VT_1 and VT_6 turned on, the switching impulse from phases A and C is transmitted to the valve hall, of which the impulse at phase

A is of positive polarity, and the impulse at phase C is of negative polarity; at this moment, the valve arrester $V2_5$ parallelled with the valve VT_5 will endure switching impulse overvoltage from phases A and C [3, 4].

16.4.2.4 Overvoltage Control and Protection Measures

According to the overvoltage mechanism and calculation results mentioned above, it can be known that such overvoltage mainly results in an overvoltage stress stressed on the valve, respectively, and its overvoltage energy depends on the energy of the switching impulse leading to such overvoltage. This part of energy is much smaller than that stored in the DC line-to-earth capacitor, so the overvoltage magnitude stressed on the valve arrester V12/V2 is higher, but the energy flowing through the valve arresters is not high.

The production and development of such overvoltage have little relation to the protection strategy of the DC system, and such overvoltage can be limited only by means of reducing the protection level of the valve arrester V12/V2.

In addition, although the energy flowing through the arrester V12/V2 is not high when they are subject to this overvoltage, these arresters adopt the multi-column parallel design in existing UHVDC project, and as shown in Table 16.1, the design energy capacity is much larger than the actual energy. This design is mainly used to reduce the overvoltage level effectively. The voltage level of the UHVDC transmission system remains very high, and the converter overvoltage withstand level is reduced appropriately, which can not only reduce the equipment manufacturing cost, but also improve the operating reliability of the converter valve. So these arresters adopt a multi-column configuration to reduce manufacturing cost of the converter valve and improve the operating reliability of the converter valve.

16.4.3 Switching Overvoltage on Valve Arrester V3

16.4.3.1 Simulation Calculation Conditions

Arrester V3 is the valve arrester at the uppermost layer of the lower 12-pulse converter. When the 1/2 pole of the lower 12-pulse converter in the rectifier station is put into operation and the outgoing line at the valve side of the Y/Y converter transformer at the LV end is subject to a ground fault, the energy on the DC line and DC filter is released by the valve arrester V3 at the uppermost layer of the lower 12-pulse converter, so that a high overvoltage is applied to both terminals of the arrester V3 and high energy flows through the arrester. The fault circuit is shown in Fig. 16.17.

The most severe overvoltage condition is as follows: the DC system is operated in 3/4 bipolar imbalance operating mode, and the lower 12-pulse converter is put into operation for pole I, and the upper 12-pulse converter quit operation from the

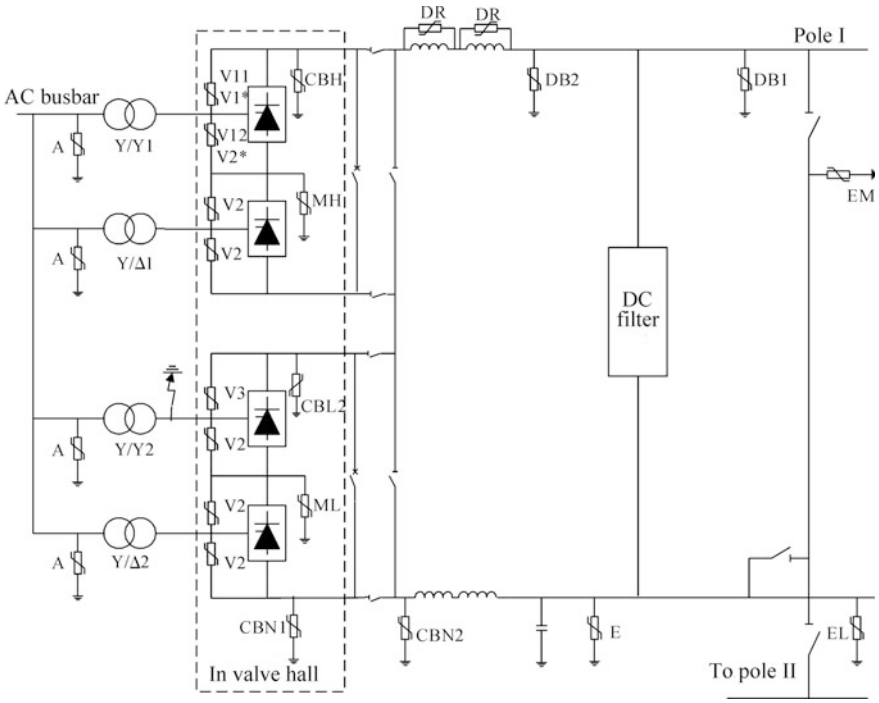

Fig. 16.17 Diagram for ground fault of the outgoing line at the valve side of low-voltage Y/Y converter transformer of converter station

DC system by disconnecting the corresponding disconnector; and the double 12-pulse converter is put into operation for pole II. The pole I DC voltage is set to the maximum value, e.g., 405 kV for the Xiangjiaba–Shanghai ±800 kV UHVDC project, and the DC current is set to the minimum value, e.g., 363 A for the Xiangjiaba–Shanghai ±800 kV UHVDC project, as well as the fault takes place in the outgoing line at phase A. After the occurrence of the fault, the control and protection system of the DC system is put into operation, stopping the fault pole. The severity of such overvoltage is related to the fault moment. By selecting different fault clearing moments during simulation and considering volt–ampere characteristic deviation of the arrester V3, the maximum protection characteristic and minimum protection characteristic are used for calculation, respectively, so as to find out the most severe overvoltage condition on the valve arrester V3.

Being similar to the valve arrester V11/V1, it is also required to consider the fault on the opposite pole for the valve arrester V3, that is to say, take the double fault (a ground fault occurs at pole II at the same time) for simulation calculation.

16.4.3.2 Simulation Calculation Results

With the calculation of overvoltage in Fulong Converter Station as the sending end of the Xiangjiaba–Shanghai ±800 kV UHVDC project under the fault taken as an example, the corresponding calculation results are shown in Table 16.9. The calculation results show that the maximum overvoltage stressed on the valve arrester V3 in Fulong Converter Station under such fault is 388 kV, and the maximum energy flowing through the arrester V3 is 3.22 MJ. Such fault is an asymmetrical fault. The energy flowing through the valve arrester V3 at phase C resulting from ground fault of the outgoing line at phase A reaches the maximum level, and the energy flowing through the arrester at other phases resulting from the fault remains small. Figure 16.18 shows the waveforms of overvoltage, current, and energy of the three-phase valve arrester V3 when the energy flowing through the valve arrester V3 at phase C reaches the maximum.

When the DC system is operated in reverse power transmission mode, namely, when Fengxian Converter Station is operated as the rectifier side and Fulong Converter Station is operated as the inverter side, the calculation of the maximum overvoltage stressed on the valve arrester V3 of the Fengxian Converter station is shown in Table 16.9. The maximum overvoltage stressed on the valve arrester V3 in Fengxian Converter Station in case of such fault is 368 kV, and the maximum energy flowing through the arrester V3 is 2.50 MJ.

16.4.3.3 Analysis of Overvoltage Mechanism

Being similar to the overvoltage mechanism of valve arrester V11/V1, such overvoltage cannot take place at the inverter side. The calculation conditions for the most severe overvoltage are as follows:

1. Both poles of DC system are operated in an imbalance manner, of which one pole is operated in the lower 12-pulse converter, and the other one is operated in the double 12-pulse converter.

Table 16.9 Calculation results for maximum overvoltage on valve arrester V3

Arrester	Characteristics of arrester	Max. voltage (kV)	Max. current (kA)	Max. energy (MJ)
V3 in Fulong Converter Station	Max. protection characteristic	388	1.33	2.47
	Min. protection characteristic	375	1.21	3.22
V3 in Fengxian Station	Max. protection characteristic	368	1.16	2.03
	Min. protection characteristic	354	1.04	2.50

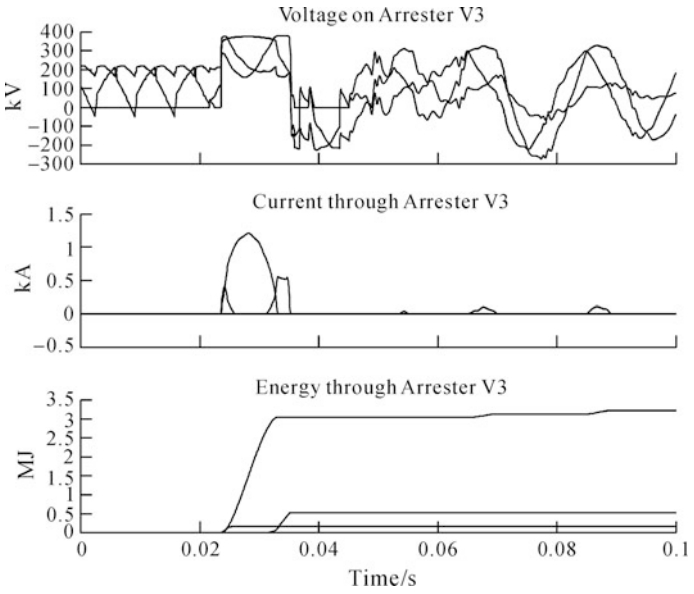

Fig. 16.18 Diagram for waveforms of maximum overvoltage, current, and energy on valve arrester V3 in Fulong Converter Station

2. The converter station is operated in rectification state.
3. For the pole that is operated in the single 12-pulse converter, its DC voltage is the maximum DC voltage, 405 kV for the Xiangjiaba–Shanghai ±800 kV UHVDC project.
4. The direct current is the minimum operating current, i.e., 363 A for the Xiangjiaba–Shanghai ±800 kV UHVDC project.
5. The voltage of the AC system in the converter station is the minimum voltage, i.e., 475 kV for the Xiangjiaba–Shanghai ±800 kV UHVDC project.

16.4.3.4 Overvoltage Control and Protection Measures

Development of such overvoltage has little relation to protection strategy of the DC system, and its harm can be limited only by reducing the protection level of the valve arrester V3 as far as possible. However, reducing the protection level of the arrester will result in an increase in energy discharge capacity of the arrester under this fault, so the energy requirement is met by connecting multi-column arresters in parallel, typically.

16.4.4 Switching Overvoltage on DC Converter Busbar Arrester

16.4.4.1 Simulation Calculation Conditions

As shown in Fig. 16.1, the busbars between two 6-pulse bridges in the upper and lower 12-pulse converters is protected directly by the arresters MH and ML, respectively. The DC busbar between the upper and lower 12-pulse converters is protected directly by the arrester CBL2, and the HVDC busbar of 12-pulse converter on the converter, wall bushing, and other equipment are protected directly by the arrester CBH. The main causes resulting in the occurrence of the switching overvoltage at these positions include reflection superposition of the fault voltage impulse in the DC line, and system operating voltage rise. Due to existence of the voltage control segments, the DC system cannot be subject to excessively high operating voltage, so DC busbar overvoltage for the converter is mainly caused by the reflection superposition of voltage impulse in the DC line caused by the fault. The most severe overvoltage condition is the full voltage starting.

During the normal startup of the DC system, the inverter station is deblocked before the rectifier station is deblocked, and the DC voltage and current are controlled by the regulating system and rise to a rated value at a smooth slope, respectively, without a high overvoltage in normal condition. However, if the control system is failed, the rectifier station is deblocked at the minimum trigger angle when the inverter station is still blocked, and then the DC system will start up at a full voltage. At this moment, the blocked inverter station is in open-circuit state, and the full voltage impulse makes a reflection at the open end of the line, producing a high overvoltage on the arresters DB, CBH, MH, CBL2, ML, etc.

During simulation, it is required to first disconnect the inverter station from the DC line, then adjust the trigger angle on the rectifier side to the minimum value, and lastly clear the impulse blocking signal on the rectifier side, so that a rated DC voltage appears abruptly on the rectifier side, resulting in an overvoltage on the converter busbar.

Table 16.10 Calculation results for overvoltage, current, and energy on converter busbar arrester in case of full voltage starting fault

Converter station	Arrester	Max. voltage (kV)	Max. current (kA)	Max. energy (MJ)
Fulong	CBH	1354	0.11	0.53
	MH	958	≈0	≈0
	CBL2	672	≈0	≈0
	ML	438	≈0	≈0
Fengxian	CBH	1338	0.15	0.91
	MH	943	≈0	≈0
	CBL2	611	≈0	≈0
	ML	364	≈0	≈0

16.4.4.2 Simulation Calculation Results

Taking the calculation of overvoltage in Fulong Converter Station as the sending end of the Xiangjiaba–Shanghai ±800 kV UHVDC project under such fault as an example, the overvoltage of DC converter busbars in the valve hall obtained by the simulation calculation are shown in Table 16.10, and the waveforms of overvoltage, current, and energy on the arrester CBH in the Fulong Converter Station are shown in Fig. 16.19.

16.4.4.3 Analysis of Overvoltage Mechanism

Such overvoltage mechanism is analyzed as follows: as shown in Fig. 16.20, when the DC system is in open-circuit state at the inverter side and the rectifier side is started up in full voltage, the DC voltage impulse reaches the end of the line on the inverter side and makes a reflection at the open end of DC line, enabling voltage magnitude of the DC line to be 2 times the original input voltage magnitude. This voltage impulse reflected back to the rectifier side along the DC line, so that a corresponding overvoltage takes place on the busbars of DC converter at the rectifier side. Such overvoltage impulse first gets to the arresters DB1 and DB2 and smoothing reactor on the DC pole line in the rectifier station. Due to overvoltage suppression of the DC pole line arresters DB1 and DB2 and overvoltage impulse

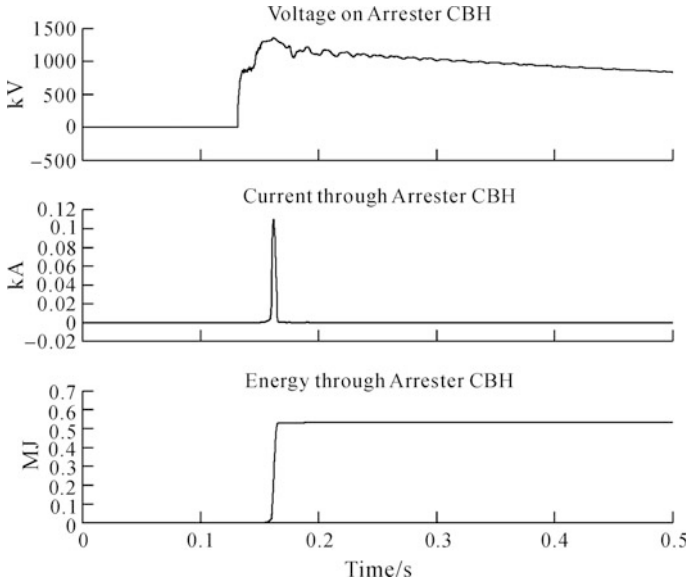

Fig. 16.19 Diagram for waveforms of overvoltage, current, and energy on arrester CBH in Fulong Converter Station in case of starting of DC system with full voltage fault

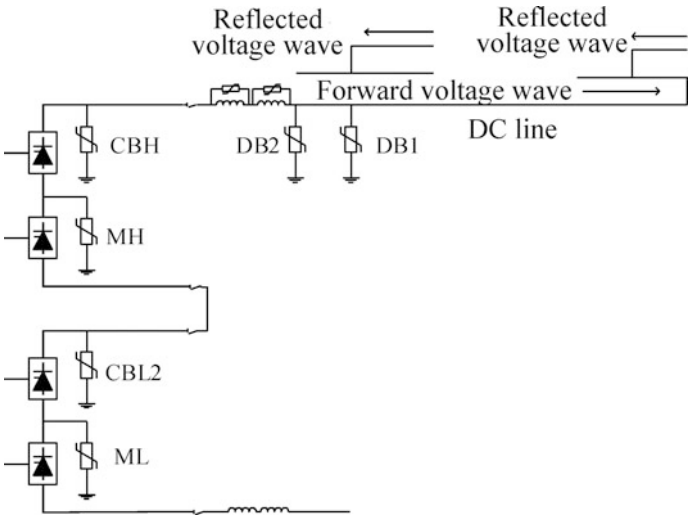

Fig. 16.20 Sketch for overvoltage mechanism in case of startup of DC system with full voltage starting fault

blocking action of the smoothing reactor, such overvoltage applied to the DC busbar in the valve hall is less severe than that applied to the DC pole line. So the practical overvoltage energy flowing through the arresters CBH, MH, CBL2, and ML arranged on the busbar of DC converter in the valve hall is not high.

Such overvoltage is influenced by the DC line length, so the DC line is longer and the energy stored in the line gets higher and the overvoltage gets more severe.

16.4.4.4 Control and Protection Measures of Overvoltage

The overvoltage has little relation to control and protection strategy of the DC system and is protected mainly by the arresters. From the calculation results, the overvoltage on the busbars of DC converter in the valve hall is less severe, and the energy is also small. So configuration of arresters can achieve effective protection for the DC busbar in the valve hall.

In addition, although in case of a full voltage starting fault, the overvoltage energy flowing through the arresters CBH, MH, CBL2, and ML is small, but these arresters adopt multi-column design. As shown in Table 16.1, the design energy discharge capacity is much higher than that of the actual energy. This design is mainly used to effectively reduce the overvoltage level. Therefore, adoption of multi-column configuration for these arresters is mainly to reduce the equipment manufacturing cost and improve the system operating reliability.

16.5 Switching Overvoltage in DC Field

The switching overvoltage in the DC field can be classified into the overvoltage on DC pole line, the overvoltage on neutral busbar, and the overvoltage on DC filter in terms of application areas. The following provides a discussion for calculation of these three kinds of overvoltage.

16.5.1 Overvoltage on DC Pole Line

The switchgears at the line side of the smoothing reactor on the DC pole line of converter station are protected mainly by arrester DB1 on DC pole line and arrester DB2 on DC busbar which are used to limit the overvoltage on the DC pole line resulting from lightning and switching impulse (the arresters DB1 and DB2 on DC pole line with the same parameters are separated by a distance on the DC pole line to limit lightning overvoltage; for the switching overvoltage, however, such a distance between two arresters on pole line is very short. The switching overvoltage, current, and energy are still distributed equally between DB1 and DB2, so these two arresters are designated by DB in the following switching overvoltage analysis). Two conditions resulting in the most severe switching overvoltage in the DC pole line, including full voltage starting, and inverter station blocked without bypass pair deblocking fault. The following provides an introduction to these two conditions.

16.5.1.1 Simulation Calculation Conditions

1. Full voltage starting

Being similar to the conditions causing the busbar overvoltage in the valve hall, one of the most severe conditions causing switching overvoltage on the DC pole line is full voltage starting. As discussed in the previous section, the overvoltage resulting from full voltage starting fault is one of the decisive conditions for the arrester DB1/DB2.

During simulation, it is required to first disconnect the inverter station from the DC line, then adjust the trigger angle on the rectifier to the minimum value, and lastly clear the impulse blocking signal on the rectifier side, so that a rated DC voltage appears abruptly on the rectifier side, resulting in an overvoltage on the DC pole line.

2. Inverter station blocked without bypass pair deblocking

Inverter station blocked without bypass pair deblocking causes a switching overvoltage on the DC pole line, which is more severe than the overvoltage resulting from full voltage starting and is attributable to the fault of pulse trigger control system in the converter station. In practical operation, however, the pulse trigger system in the converter station usually adopts three control systems being operated simultaneously, so it is possible to avoid the occurrence of such mistake during operation of the control system by use of two-in-three system redundancy strategy. Hence, such control system fault of the inverter station blocks suddenly under this kind of configuration of the protection system, resulting in a very low probability of overvoltage. In some studies on UHVDC switching overvoltage, such overvoltage will not be considered as a main aspect. In order to comprehensively explain the switching overvoltage in the DC system, this book provides an analysis and a discussion of such overvoltage.

When the DC system sends a shutdown order through the inverter side due to a fault at the inverter side or other conditions, the normal operating sequence is that the bypass pair on the inverter side is first put into operation and then a notification is given to the rectifier to complete phase shift to reduce the direct current at the same time. After the direct current is reduced to approximately zero, the rectifier and inverter all blocked the trigger impulse to stop the DC system. If the inverter is directly blocked without bypass pair deblocking, or the inverter is abruptly blocked due to a fault when the DC transmission system is operating normally, the inverter station will be out of control, and the converter valve cannot complete a normal commutation, resulting in a commutation failure; then, the AC voltage will transmit into the DC system to cause a turnover of the DC voltage polarity and transient process featuring a significant oscillation of the voltage on the DC line, so that a higher overvoltage will take place on the DC pole line.

During simulation, it is required to enable the DC system to be operated at rated condition for both poles and then block the inverter impulse suddenly; after that, the control and protection system of the DC system is actuated to block commutation of the rectifier. Finally, it is required to record the overvoltage on the DC pole arresters DB1 and DB2 in the converter stations on both sides.

16.5.1.2 Simulation Calculation Results

1. Full voltage starting

Taking the calculation for overvoltage in Fulong Converter Station as the sending end in the Xiangjiaba–Shanghai ±800 kV UHVDC project under such voltage as an example, the overvoltage results on the DC pole line obtained by simulation calculation are shown in Table 16.11. The calculation results show that the maximum overvoltage of arresters DB1 and DB2 on the DC pole line in Fulong Converter Station under such fault is 1358 kV, and the maximum energy flowing

Table 16.11 Calculation results for overvoltage, current, and energy on DC pole line arresters DB1 and DB2 in case of full voltage starting fault

Arrester	Max. voltage (kV)	Max. current (kA)	Max. energy (MJ)
Fulong Converter Station DB1/DB2	1358	0.72	5.60
Fengxian Station DB1/DB2	1341	0.52	3.31

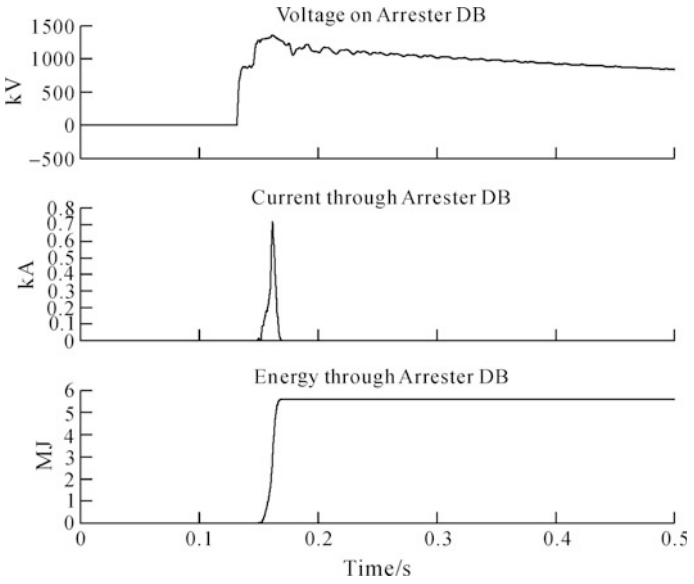

Fig. 16.21 Diagram for waveforms of overvoltage, current, and energy on arresters DB1 and DB2 in Fulong Converter Station in case of full voltage starting fault

through them is 5.60 MJ; that the maximum overvoltage of arresters DB1 and DB2 on the DC pole line in Fengxian Converter Station under the influence of such fault is 1341 kV, and the maximum energy flowing through them is 3.31 MJ. Figure 16.21 shows the waveforms of overvoltage, current, and energy of arresters DB1 and DB2 on the DC pole line in Fulong Converter Station.

2. Inverter station blocked without bypass pair deblocking

With the calculation for overvoltage in Fengxian Converter Station as the receiving end in case of such fault during forward transmission of the DC power for the Xiangjiaba–Shanghai ±800 kV UHVDC project taken as an example, the overvoltage on the DC pole line by the simulation calculation is shown in Table 16.12. The calculation results show that the maximum overvoltage of arresters DB1 and DB2 on the DC pole line in Fulong Converter Station under such fault is 1307 kV,

and the maximum energy flowing through them is 1.56 MJ; that the maximum overvoltage of arresters DB1 and DB2 on the DC pole line in Fengxian Converter Station under such fault is 1395 kV, and the maximum energy flowing through them is 8.69 MJ; Fig. 16.22 shows the waveforms of overvoltage, current, and energy of arresters DB1 and DB2 on the DC pole line in the Fengxian Converter Station. When the DC power of the UHVDC transmission system is transmitted in a reverse manner, the transmission power and current are small, and the overvoltage is far less severe than during forward transmission of the power, so the situation of reverse transmission is not discussed any longer.

Table 16.12 Calculation results for overvoltage, current, and energy on DC pole arresters DB1 and DB2 in case of inverter station blocked without bypass pair deblocking

Arrester	Max. voltage (kV)	Max. current (kA)	Max. energy (MJ)
DB in Fulong Converter Station	1307	0.29	1.56
DB in Fengxian Station	1395	1.69	8.69

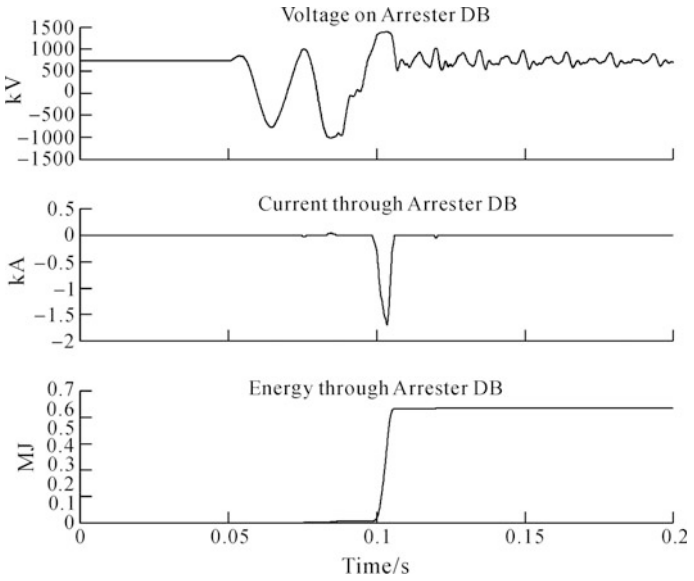

Fig. 16.22 Diagram for waveforms of overvoltage, current, and energy on arresters DB1 and DB2 in Fengxian Station in case of inverter station blocked without bypass pair deblocking

16.5.1.3 Analysis of Overvoltage Mechanism

1. Full voltage starting

The mechanism of such overvoltage has been discussed in the Converter Busbar Overvoltage in the previous section hereof, which is not detailed here. Similarly, such overvoltage is influenced by the DC line length. If the DC line is longer, the energy stored in the line is higher and the overvoltage will get more severe.

2. Inverter station blocked without bypass pair deblocking

In order to discuss this overvoltage mechanism, two current measuring points, at the valve top and the DC pole line outlet, are set up on the rectifier and inverter sides in the DC system simulation model, respectively, which are shown in Fig. 16.23. The current measurement waveforms for these four measuring points will be used for the explanation of such overvoltage in the following mechanism discussion. During the occurrence of such overvoltage, the waveform of DC pole line voltage on the rectifier and inverter sides, and current at the valve top and the DC pole line outlet and trigger angle on the rectifier side are shown in Fig. 16.24.

According to the aforementioned figures, the overvoltage mechanism is analyzed as follows:

(1) Be out of control due to the occurrence of fault and commutation failure on the inverter side

At moment as shown in the figure, the inverter side is blocked suddenly due to a fault of the control system, the inverter station is out of control, and the converter valve is subject to a commutation failure, so that the AC voltage enters the DC system to cause turnover of the DC voltage polarity and oscillation and the direct current starts oscillating with the AC waveform under the influence of the alternating current component. This oscillating process is shown in Fig. 16.24, and an overvoltage occurs in the DC pole line on the rectifier side.

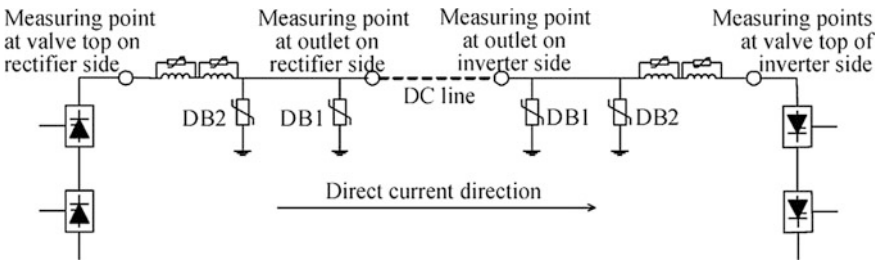

Fig. 16.23 Sketch for the position of current measuring points at valve top and pole line outlet on the rectifier and inverter sides of DC system

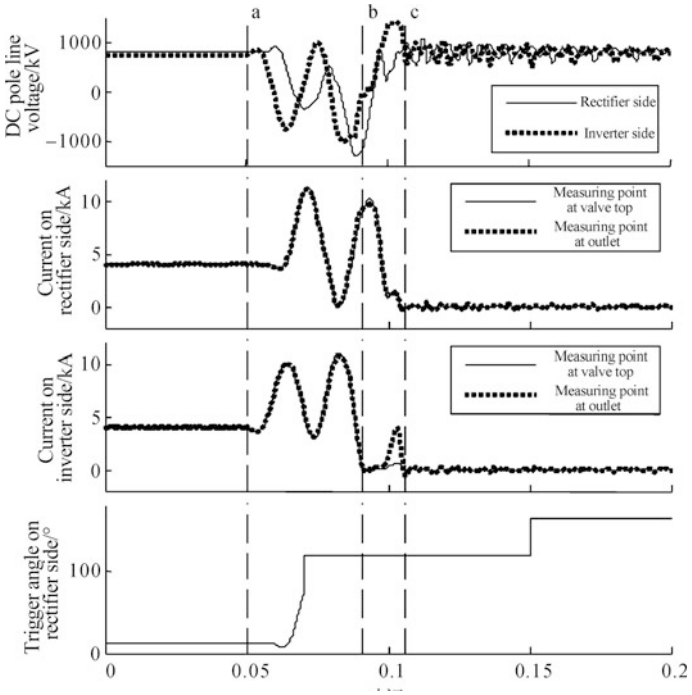

Fig. 16.24 Diagram for waveforms of DC voltage, current, and trigger angle of system with blocking of inverter side without bypass pair deblocking

(2) The converter valve goes off after the protection of the rectifier side is actuated and the current of the inverter side is declined to zero.

Due to the rapid increase of direct current at the rectifier side in the previous oscillation process, the protection of rectifier starts actuation, so that the trigger angle moves to 120° rapidly, the current at the inverter side at moment b is decreased to zero, and the converter valve on the inverter side is turned off.

(3) The DC line continues to charge the inverter side that has been turned off, resulting in a severe overvoltage at the inverter side

Although, after the moment b, the converter valve on the inverter side has been turned off, and the current at the outlet of rectifier-side remains large. In other words, the distributed inductor of the DC line has stored energy and charges the inverter capacitor, resulting in constant increase of voltage in the pole line on inverter side until a severe overvoltage occurs.

(4) The rectifier-side current is turned off after zero crossing and the completion of overvoltage process.

Up to moment c, after the current on the rectifier side is declined to zero and because the trigger angle on the rectifier side has moved to 120° to enable the

converter to be operated in an inversion mode, it is unable to deliver energy to the DC line, having the converter valve turned off; after that, the converter valve on the rectifier side is blocked.

From the current waveform as shown in Fig. 16.24, it can also be seen that the current at the valve top on the rectifier side is basically consistent with that at the outlet; however, the waveform of current at the outlet on the inverter side during the period from moment b to c is slightly different from that at the valve top. Practically, the difference between these two measuring points on the rectifier side or the inverter side is the current flowing through the pole arrester DB. It can be seen from Fig. 16.24 that the pole line overvoltage at the rectifier side is not very severe, and the difference between the valve top current and the outlet current is very small; however, the overvoltage at the inverter side is more severe, and thus two arresters DB are actuated, on which a current of 4 kA flows through altogether, so that the difference between the outlet current and the valve top current is very high.

From the analysis above, it can be seen that the overvoltage resulting from the inverter station blocked without bypass pair deblocking fault is totally different from that resulting from the full voltage starting. Practically, the overvoltage caused by such fault is a large electromagnetic oscillation occurred in the DC line after the voltage of the AC system enters the DC system, the wave front time of which is much longer than the full voltage starting fault, and the overvoltage energy is much higher than that under a full voltage starting fault.

16.5.1.4 Overvoltage Control and Protection Measures

1. Full voltage starting

The overvoltage resulting from a full voltage starting cannot be suppressed by the DC control and protection system, so it is protected mainly by the configuration of arresters, and the corresponding arrester should have enough capacity.

2. Inverter station blocked without bypass pair deblocking

After the occurrence of the inverter station blocked without bypass pair deblocking, the inverter station is out of control due to the loss of trigger pulse on the inverter side. So the DC system that is operating can be stopped only by actuating the control and protection system on the rectifier side, namely the emergency shutdown protection.

In the practical operation, the pulse trigger system in the converter station typically adopts three control systems being operated simultaneously and use a two-in-three system redundancy strategy to avoid mistake occurred in the control system. In this configuration of protection system, such control system fault of the

inverter station abruptly blocks, resulting in a very low probability of overvoltage. Hence, in some research on UHVDC switching overvoltage, such overvoltage is not considered as a main aspect.

16.5.2 Overvoltage on Neutral Busbar

The neutral busbar is the part with the lowest operating voltage in the DC system, and in case of the occurrence of a fault in the DC system, it is liable to be influenced by other parts of the system, resulting in an overvoltage. The possible condition for the occurrence of an overvoltage on the neutral busbar includes the following [5–7]:

1. Overvoltage of ground fault

In case of the occurrence of a ground fault in the outgoing line at the valve side of HV Y/Y converter transformer of the rectifier station, ground fault of valve top, DC pole line, DC busbar, etc., an overvoltage will occur on the neutral busbar, as shown in Fig. 16.25. Such overvoltage mainly results in the actuation of arresters CBN2, EL, or EM, but the arrester E does not work under such switching overvoltage (its actuating voltage is higher than those of EL and EM, and it is mainly used to protect against the lightning overvoltage), so it is not discussed here.

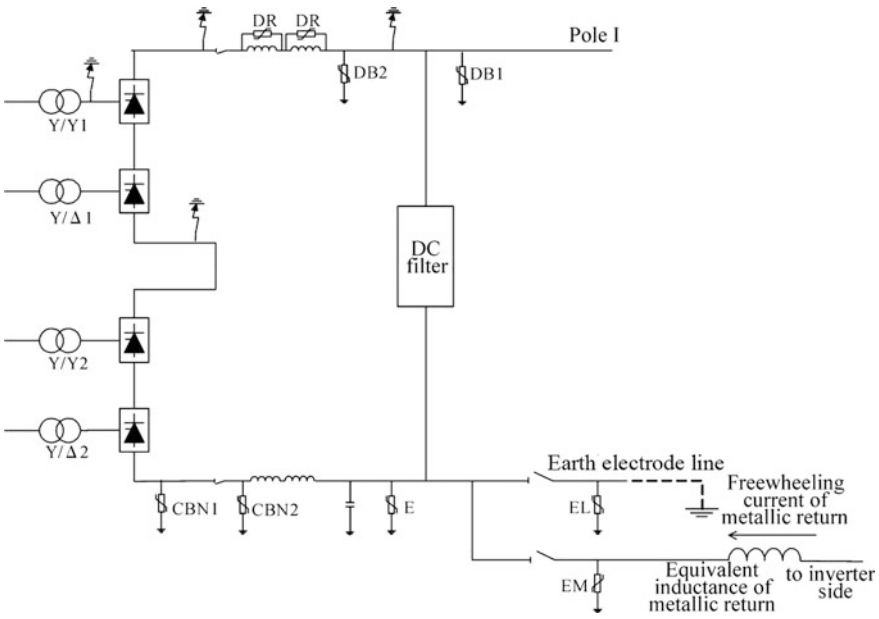

Fig. 16.25 Sketch for overvoltage fault of neutral line

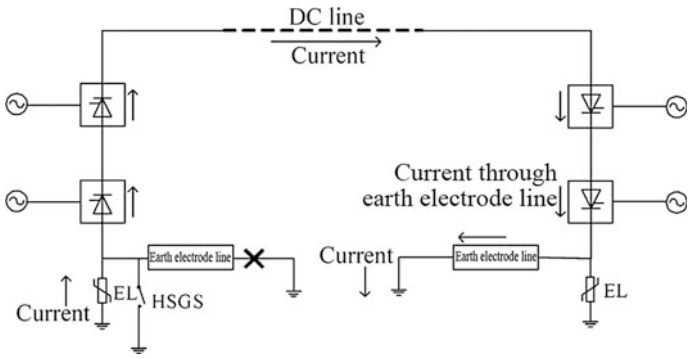

Fig. 16.26 Sketch for disconnection fault under monopolar operation with ground return of DC system

It is worthwhile to pay attention that, for the arresters EL and EM, they are not connected to the DC system simultaneously, and when the DC system is operated as a metallic return, the EM is connected to the DC system, but the EL is not; when it is operated by other methods, the EL is connected to the DC system, but the EM is not.

In addition, when the inverter station is subject to the fault above, such faults will not cause an overvoltage on the neutral busbar because the converter operated in inversion state does not output energy.

2. Overvoltage of disconnection fault

When the DC system is operated as a monopolar ground return, the direct current will form a circuit through the arrester EL on the break side if the ground electrode line on one side is subject to a disconnection fault, resulting in an overvoltage on the neutral busbar of the converter station being disconnected, as shown in Fig. 16.26.

When the DC system is operated as a monopolar metallic return, the direct current will form a circuit through the arrester EM for the metallic return on the ungrounded side if the metallic return is subject to a disconnection fault, resulting in an overvoltage on the neutral busbar of the converter station, as shown in Fig. 16.27. By combining with Fig. 16.26, it can be seen that the main fault circuits for these two kinds of overvoltage are similar after the occurrence of a fault, and the direct current flows back to the converter through the arrester (EL or EM) on the neutral busbar of the converter station on the ungrounded side.

The aforementioned overvoltage mainly results in the actuation of the arrester EL or EM, but the arresters CBN1, CBN2, and E do not work basically. The reason is that the actuation voltage of CBN1, CBN2, and E is higher than that of EM and EL.

To sum up, it is required to focus on the arresters CBN2, EL, and EM under the influence of the neutral busbar overvoltage. According to the different installation

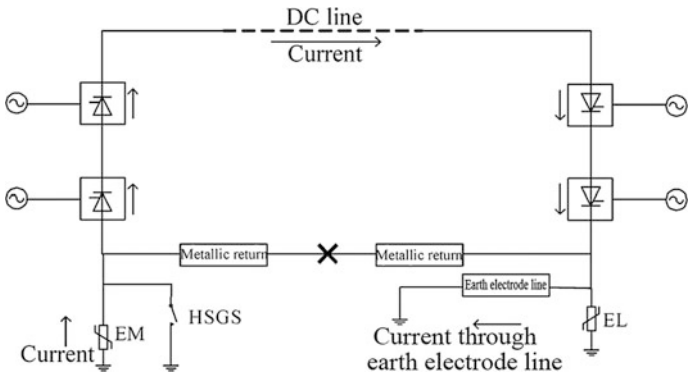

Fig. 16.27 Sketch for disconnection fault under metallic return operation mode of DC system

positions of these three arresters on the neutral busbar, they can be divided into two categories of arresters, including arrester CBN2 at the valve side of the smoothing reactor and arrester EL/EM at the line side. The following provides a specific discussion of them.

16.5.2.1 Simulation Calculation Conditions

1. Overvoltage of ground fault

According to the introductions about DC system in the previous chapter, the UHVDC transmission system is operated mainly in three operating modes: bipolar operation, monopolar ground circuit, and monopolar metallic return operating modes, of which the converter stations at both terminals are directly grounded through the ground electrode line in the bipolar operation and monopolar ground circuit operating modes, but in the monopolar metallic return operating mode, the converter station at one end is not grounded. Generally, the converter station being not grounded in a project is kept unchanged; for example, Fulong Converter Station in the Xiangjiaba–Shanghai ±800 kV UHVDC project is not grounded in monopolar metallic return operating mode, while Fengxian Converter Station is grounded in any operating mode.

Therefore, the overvoltage condition for the Fulong Converter Station should be monopolar metallic return operating mode during simulation of busbar overvoltage, because Fulong Converter Station is not grounded directly in such mode, resulting in more severe overvoltage on the neutral busbar. However, during the calculation of overvoltage on the neutral busbar for Fengxian Converter Station, overvoltage on the neutral busbar that occurred in all operating modes differs slightly because the converter station is always grounded.

The most severe overvoltage condition on the neutral busbar in Fulong Converter Station is as follows: the DC system is operated in monopolar metallic return mode, the direct current is the maximum current, the power is transmitted in a forward manner, and a single-phase ground fault occurs to the outgoing line at the valve side of the uppermost Y/Y converter transformer, or a ground fault occurs at the valve top, DC pole line, DC busbar, etc. After the occurrence of the fault, the control and protection system of the DC system is actuated to stop the fault pole. For Fulong Converter Station, the overvoltages on the arresters CBN2 and EM are mainly considered.

The most severe overvoltage condition on the neutral busbar in Fengxian Converter Station is as follows: the power is transmitted in a reverse manner with the maximum transmission power, and a single-phase ground fault occurs to the outgoing line of the uppermost Y/Y converter transformer valve side. After the occurrence of the fault, the control and protection system of DC system is actuated to stop the fault pole. For Fengxian Converter Station, the overvoltage on the arresters CBN2 and EL are mainly considered.

Such overvoltage condition is related to the fault occurrence moment, and by selecting different fault clearing moments during simulation and considering the volt–ampere characteristic deviation of the neutral busbar arresters CBN2, EL, and EM, it is required to adopt the maximum protection characteristic and minimum protection characteristic for calculation and find out the most severe overvoltage condition on the neutral busbar arrester.

2. Overvoltage of disconnection fault

According to the discussion given in the previous context, the neutral busbar overvoltage of the DC system resulting from the disconnection fault of the ground electrode line in monopolar operation with ground return is similar to the disconnection fault of the metallic return in monopolar operation with metallic return, so it is possible to select one operating mode as the most severe typical condition for simulation calculation and discussion. During simulation, the DC system is set to monopolar operation with ground return, the direct current is the maximum current, the power is transmitted in a forward manner, and the ground electrode line is disconnected to the rectifier side; Some time after the occurrence of this fault of the DC system, the direct current control and protection system is actuated to close the HSGS switch, and the rectifier side sends a shutdown signal at the same time.

Such overvoltage condition is irrelevant to the fault occurrence moment, but is directly relevant to the action time of the protection system of the DC system after the occurrence of the fault. During simulation, it is required to use different protection action times for calculation and comparison, such as 10, 20, and 30 ms, consider volt–ampere characteristic deviation of the arrester EL, and adopt the maximum protection characteristic and minimum protection characteristic for calculation, respectively.

16.5.2.2 Simulation Calculation Results

1. Overvoltage of ground fault

The calculation of overvoltage in Fulong Converter Station as the sending end of the Xiangjiaba–Shanghai ±800 kV UHVDC project is taken as an example, and the neutral busbar overvoltage is calculated under ground fault of the outgoing line at the Y/Y valve side of the converter transformer at the HV end, valve top ground fault, and DC pole line ground fault.

The calculation results for arrester CBN2 are shown in Table 16.13. It can be seen from the calculation results that the overvoltages on the arrester CBN2 under the influence of the valve top ground fault and DC pole line ground fault are less severe than the ground fault of the outgoing line on the Y/Y valve side of the converter transformer at the high-voltage end, so the most severe overvoltage condition on the arrester CBN2 is the occurrence of ground fault of the outgoing line on the Y/Y valve side of the converter transformer at the high-voltage end; at this moment, the maximum overvoltage at both terminals is 425 kV and the maximum energy flowing through the arrester CBN2 is 11.1 MJ. Figure 16.28 shows the waveforms of overvoltage, current, and energy when the maximum energy flows through the arrester CBN2 of the Fulong Converter Station.

The calculation results for the arrester EM are shown in Table 16.14. It can be seen from the calculation results that the overvoltage on the arrester under the influence of the valve top ground fault and DC pole line ground fault is less severe than the ground fault of the outgoing line at the valve side of the HV Y/Y converter transformer, so the most severe overvoltage condition on the arrester EM is the ground fault of the outgoing line at the valve side of the HV Y/Y converter transformer. At this moment, the maximum overvoltage at both terminals is 379 kV, and the maximum energy flowing through the arrester EM is 11.8 MJ. Figure 16.29 shows the waveform of overvoltage at both terminals when the maximum energy flows through the arrester EM of the Fulong Converter Station, and also the waveforms of current and energy flowing through the arrester.

Table 16.13 Calculation results for overvoltage, current, and energy stressed on arrester CBN2

Arrester	Type of fault	Max. voltage (kV)	Max. current (kA)	Max. energy (MJ)
CBN2 in Fulong Converter Station	Ground fault of outgoing line at the valve side of Y/Y converter transformer (HV end)	425	4.19	11.1
	Ground fault at the valve top	408	2.48	7.73
	Ground fault at the pole line	400	1.70	5.62
CBN2 in Fengxian Station	Ground fault of outgoing line at the valve side of Y/Y converter transformer (HV end)	419	1.31	0.99

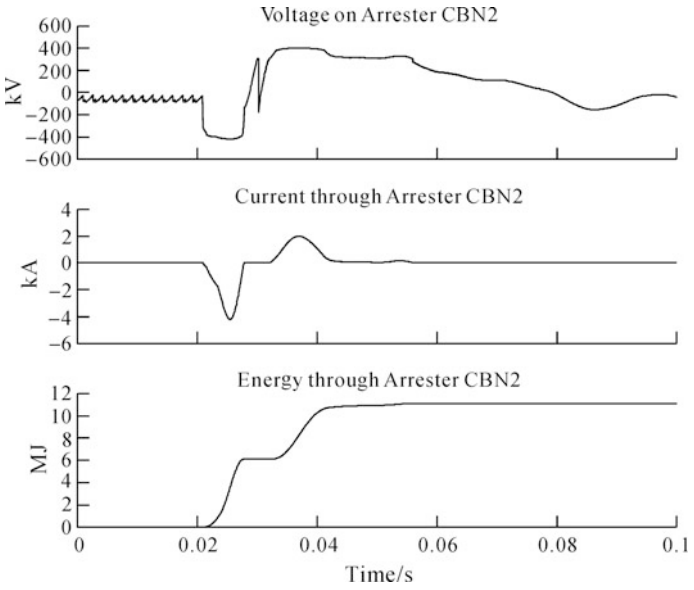

Fig. 16.28 Diagram for waveforms of overvoltage, current, and energy on arrester CBN2 in Fulong Converter Station under ground fault of the outgoing line at the valve side of HV Y/Y converter transformer

Table 16.14 Calculation results for overvoltage, current, and energy on neutral busbar arrester EM/EL

Arrester	Type of fault	Max. voltage (kV)	Max. current (kA)	Max. energy (MJ)
EM in Fulong Converter Station	Ground fault of outgoing line at the valve side of Y/Y converter transformer (HV end)	379	3.25	11.8
	Ground fault at the valve top	366	2.82	10.3
	Ground fault at the pole line	366	2.71	11.1
EL in Fengxian Station	Ground fault of outgoing line at the valve side of Y/Y converter transformer (HV end)	291	4.13	2.63

In addition, it should be noted that, for the neutral busbar overvoltage resulting from the DC pole line ground fault, the DC system usually adopts such a protection strategy that it is restarted after deionization of the line upon commutation for a while and is stopped if the same fault exists still after re-starting, so this means that the neutral busbar is subject to overvoltage impulse twice continuously under the influence of a permanent fault, and the discharge capacity of the neutral busbar arrester under the influence of the same fault is two times the single overvoltage

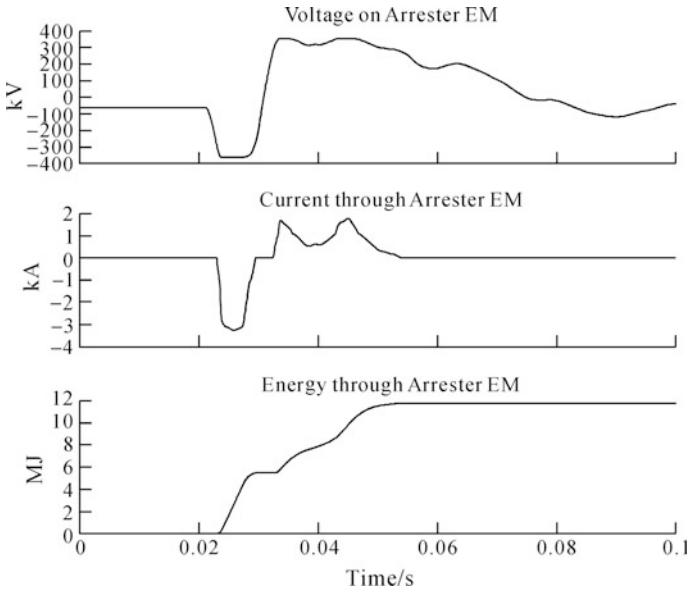

Fig. 16.29 Diagram for waveforms of overvoltage, current, and energy on arrester EM in Fulong Converter Station under ground fault of the outgoing line at the valve side of HV Y/Y converter transformer

energy. Taking the arrester EM in the Fulong Converter Station as an example, the maximum overvoltage energy flowing through the arrester when a DC pole line ground fault occurs, as shown in Table 16.14, is 11.1 MJ, so the discharge capacity of the arrester should be at least above two times the value of 11.1 MJ, i.e., 22.2 MJ.

For Fengxian Converter Station, when it is operated in rectification state (the DC system is operated in reverse power transmission mode), the most severe overvoltage condition on its arrester CBN2 is also the ground fault of the outgoing line at the valve side of HV Y/Y converter transformer; and at this moment, the maximum overvoltage at both terminals is 419 kV, and the energy is 0.99 MJ. The most severe overvoltage condition on the arrester EL is also the ground fault of the outgoing line at the valve side of HV Y/Y converter transformer, and at this moment, the maximum overvoltage at both terminals is 291 kV and the energy is 2.63 MJ. These two calculation results are far less than those for the Fulong Converter Station because the neutral busbar is always grounded via the ground electrode line regardless of which operating mode is adopted in Fengxian Station.

2. Overvoltage of disconnection fault

Taking the calculation for overvoltage in Fulong Converter Station as the sending end in the Xiangjiaba–Shanghai ±800 kV UHVDC project under the influence of such fault as an example, the corresponding calculation results are shown in

Table 16.15 Calculation results for overvoltage, current, and energy on Fulong Converter Station EL under different protection action times in case of disconnection fault of DC system

Protection action time (ms)	Characteristics of arrester	Max. voltage (kV)	Max. current (kA)	Max. energy (MJ)
10	Max. characteristic	288	3.68	8.64
	Min. characteristic	280	3.69	8.48
20	Max. characteristic	288	3.68	18.4
	Min. characteristic	280	3.69	18.0
30	Max. characteristic	288	3.68	26.6
	Min. characteristic	280	3.69	26.1

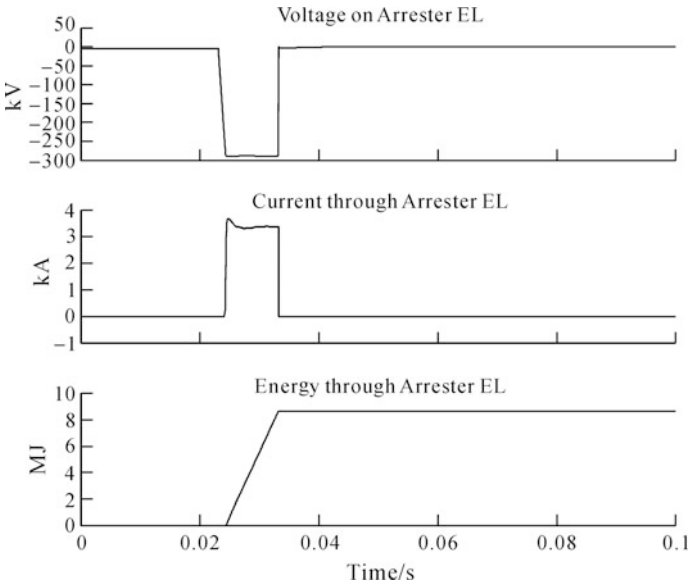

Fig. 16.30 Calculation results for overvoltage on Fulong Converter Station EL under the protection action time of 10 ms in case of disconnection fault of DC system

Table 16.15. The calculation results show that the maximum overvoltage stressed on arrester EL in Fulong Converter Station is 288 kV under the influence of the fault, and the maximum energy flowing through the arrester EL is 26.6 MJ. Figure 16.30 shows the waveforms of overvoltage, current, and energy when the maximum energy flows through arrester EL in the Fulong Converter Station.

It can be seen from Table 16.15 that, when a disconnection fault occurs in the DC system, the shorter the DC system protection action time is, the less the

overvoltage energy accumulated on the arrester EL is. Such fault energy is directly related to the protection action time, so the high-speed ground switch (HSGS) should be put into operation as soon as possible to meet the overvoltage protection requirement.

16.5.2.3 Analysis of Overvoltage Mechanism

The following provides an analysis and discussion on the mechanism of the ground fault overvoltage and disconnection fault overvoltage. For the convenience of discussion, the following provides a specific analysis of a single-phase ground fault occurred in the outgoing line bushing on the Y/Y valve side of the converter transformer at the uppermost end and the disconnection fault of DC ground electrode line.

1. Single-phase ground fault of the outgoing line at the valve side of converter transformer Y/Y at the uppermost end

The neutral busbar overvoltage resulting from such fault can be divided into two stages in terms of development mechanism: ① the energy is supplied by the rectifier-side converter; ② the energy is supplied by the metallic return freewheeling current. The overvoltage mechanism at two stages is different, the

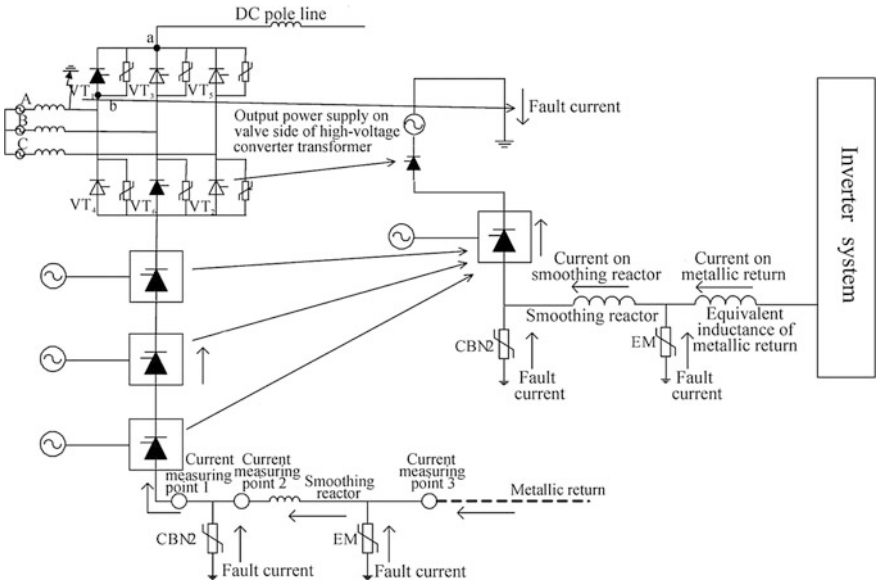

Fig. 16.31 Schematic diagram for the 1st stage of neutral busbar overvoltage in case of single-phase ground fault of the outgoing line on the valve side of converter transformer Y/Y at the uppermost end

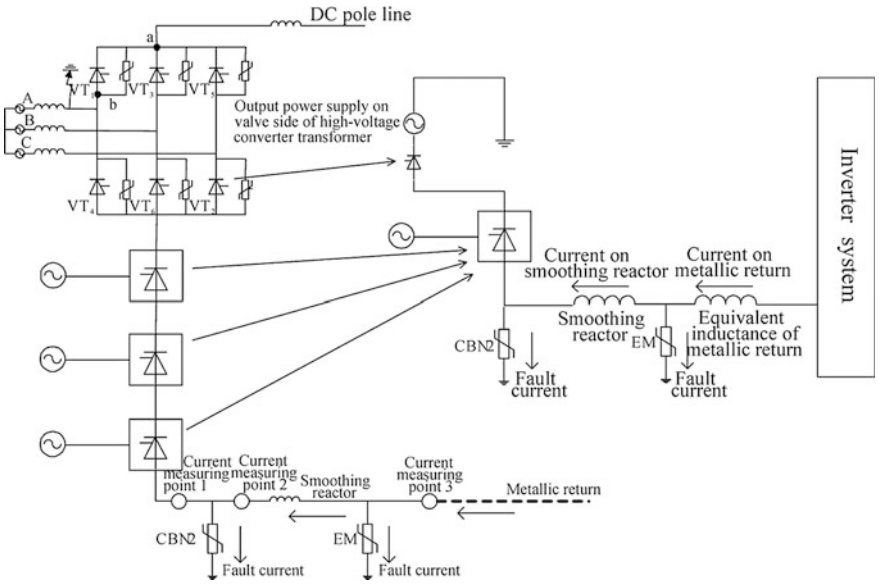

Fig. 16.32 Schematic diagram for the 2nd stage of neutral busbar overvoltage in case of single-phase ground fault of the outgoing line on the valve side of converter transformer Y/Y at the uppermost end

diagram of which is shown in Figs. 16.31 and 16.32, respectively, in which the left part is a circuit diagram and the right part is an equivalent schematic diagram. In addition to the 6-pulse converter at the uppermost end shown in the circuit diagram on the left side of the figure, the lower three 6-pulse converters are equivalent to a DC power supply in the schematic diagram at the right side, as shown by the arrow in the figure. The following provides an analysis of each stage, specifically.

(1) 1st stage at which the energy is supplied by the rectifier-side converter

The waveform at the time of the occurrence of a single-phase ground fault occurs in the outgoing line on the Y/Y valve side of the converter transformer at the uppermost end is shown in Fig. 16.33, and the fault occurs at moment a (0.021 s). The equivalent circuit of the system is shown in the right part of Fig. 16.31 after the occurrence of the fault. The fault point is earth point, the converter transformer at the uppermost end is equivalent to an AC power supply, and the lowest layer of valves at the highest-voltage end are equivalent to the thyristor at the right side of the figure. Except the 6-pulse converters at the uppermost end, the other three 6-pulse converters are equivalent to a DC power supply. At this moment, the equivalent AC and DC power supplies mentioned above are superposed with the DC power supply to form an overvoltage power supply with one end grounded via the fault point and the other end connected to the neutral busbar, which forms a circuit via the ground, and is stressed on the neutral busbar arrester CBN2 and EM, resulting in overvoltage on these two arresters. It can be seen from Fig. 16.33 that

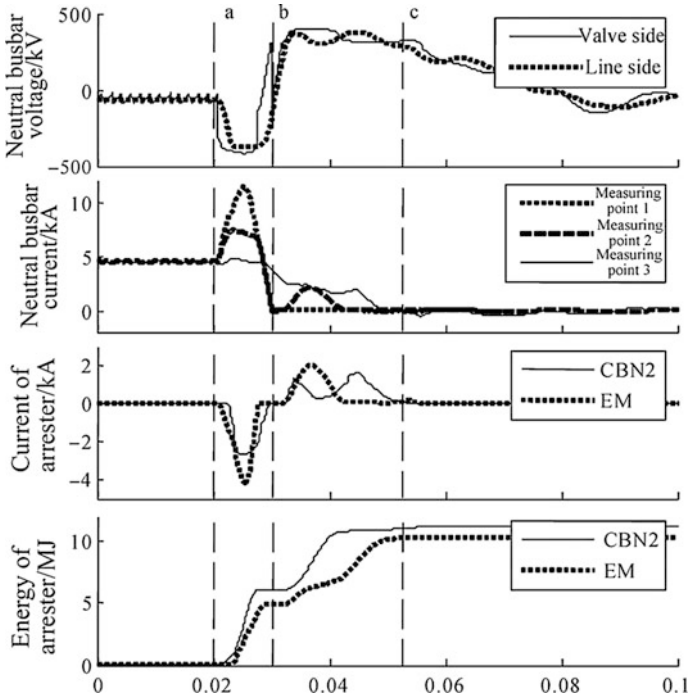

Fig. 16.33 Diagram for waveforms of neutral busbar overvoltage resulting from single-phase ground fault of the outgoing line on the valve side of converter transformer Y/Y at the uppermost end

the HV end of the power supply is grounded and the low-voltage end is connected to the neutral busbar because the polarity of such overvoltage power supply is positive, so that the overvoltage polarity on the arresters CBN2 and EM at this stage is negative.

Up to moment b (0.03 s), the direct current is declined to zero due to actuation of the protection system, that is to say, the current at the bottom of converter valve of the neutral busbar that is measured at measuring point 1 in the waveform chart declined to zero. The DC converter valve is turned off at this moment, and the overvoltage power supply mentioned in the 1st stage does not form a circuit together with the neutral busbar anymore, and the overvoltage at the 1st stage disappears. The overvoltage energy at this stage is directly related to the capacity transmitted when the DC system is failed. The larger the transmission capacity is, the larger the overvoltage energy in this stage is.

(2) 2nd stage at which the energy is supplied by the freewheeling current of the metallic return.

As shown in Fig. 16.33, the current in the metallic return is not reduced to zero at moment b, that is to say, the current measured at measuring point 3 is not zero at

moment b, so the residual current in the metallic return causes the 2nd stage of overvoltage on the neutral busbar. At this stage, for the reason that the converter valve has been turned off, the residual current of the metallic return can flow continuously only through the circuit formed by the arrester connected to the neutral busbar and the ground, so that the neutral busbar voltage is gradually changed from negative polarity at the 1st stage to positive polarity because the residual current in the metallic return flows from the line to the neutral busbar. This positive overvoltage results in the 2nd stage of overvoltage on the arresters CBN2 and EM, being contrary to the 1st stage of overvoltage with respect to its polarity. Such overvoltage energy is directly related to the residual energy in the distributed inductor of the metallic return. The longer the metallic return (namely the DC line) is, the larger the direct current is at the time of occurrence of the fault, and the larger the overvoltage energy at the 2nd stage is.

To sum up, the overvoltage is formed by two stages. The energy of first stage overvoltage is directly related to the transmission capacity when the DC system is failed, that is to say, the larger the transmission capacity is, the larger the overvoltage energy at this stage is; the energy of the second stage overvoltage is directly related to the residual energy in the metallic return, that is to say, the longer the metallic return (namely the DC line) is, and the larger the direct current is at the time of the occurrence of the fault, the larger the overvoltage energy at the 2nd stage is.

Additionally, in case of the occurrence of such fault on the inverter side, the overvoltage power supply mentioned at the first stage cannot be formed because the inverter side cannot output energy to the DC line side; moreover, because the neutral busbar is always connected to the ground electrode line on the inverter side and the ground electrode line length is far shorter than that of the DC line, the residual current is insufficient to form the second stage overvoltage on the neutral busbar. Hence, the occurrence of such fault on the inverter side will not result in a neutral busbar overvoltage.

The neutral busbar overvoltage mechanism of valve top ground fault and pole ground fault is similar to the neutral overvoltage mechanism of the ground fault on the outgoing line at the valve side of Y/Y converter at the HV end; however, the energy of overvoltage resulting from these two kinds of faults that flows through CBN2 is smaller than the former one and is not discussed here.

2. Disconnection fault of DC line

The diagram of the DC disconnection fault is shown in Figs. 16.26 and 16.27. If the ground electrode line or metallic return line on one side is subject to a disconnection fault when the DC system is operated in monopolar ground return or monopolar metallic return mode, the direct current circuit will be formed by the arrester EL of the ground electrode line for the neutral line or the arrester EM of the metallic return on the disconnection side, that is to say, the arrester is connected to the current circuit of rectifier side–inverter side. For the reason that the rectifier side of the DC system is controlled by the constant current control strategy, the overvoltage resulting from such fault is equivalent to that resulting from the connection of one

current source and neutral busbar arrester EM/EL in series. Thus, the energy flowing through the arrester is proportional to the duration of the overvoltage.

16.5.2.4 Overvoltage Control and Protection Measures

With respect to the neutral busbar overvoltage resulting from the single-phase ground fault of the outgoing line on the Y/Y valve side of converter transformer at the uppermost end and the valve top ground fault in the converter station, the corresponding DC protection action is emergency shutdown of the DC system. Under the emergency shutdown protection condition, the harm of such overvoltage can be limited only by lowering the protection level of the neutral busbar arresters CBN2, EM, and EL; however, lowering the protection level of the arrester will lead to an increase in discharge capacity of the arrester under the fault, which is usually met by connecting multi-column arresters in parallel.

With respect to the neutral busbar overvoltage resulting from the ground fault of DC pole line, the DC system is usually protected by such strategy that it is restarted after deionization of the line upon commutation for a while and is stopped if the same fault still exists after re-starting. When using the commutation restart protection strategy, the harm of such overvoltage can be limited only by lowering the protection level of the neutral busbar arresters CBN2, EM, and EL; however, the energy flowing through the arrester under the influence of such overvoltage is high in general, and it is required that the energy requirement be met by connecting multi-column arresters in parallel.

With respect to the disconnection fault in the DC system, the shorter the protection action time is, the smaller the overvoltage energy resulting from such fault is. So after a disconnection fault is confirmed, the protection should be actuated as soon as possible to close the high-speed ground switch (HSGS) in the substation to limit the harm of the overvoltage.

16.5.3 Internal Overvoltage of DC Filter

Being similar to the AC filter, the DC filter can cause an electromagnetic transient process in the filter due to DC pole line fault, voltage fluctuation, and other reasons, resulting in an internal overvoltage of the filter. This section presents a discussion on the calculation method for internal overvoltage of the DC filter resulting from two typical faults, namely DC pole line ground fault and switching overvoltage impulse.

The circuit diagram of the DC filter and the arresters' installation position of the DC filter can be seen in Sect. 15.3.5, which introduces the DC filter.

16.5.3.1 Simulation Conditions

The switching overvoltage in the DC filter is caused mainly by two conditions: ground fault of filter busbar and switching overvoltage impulse. The simulation research on these two kinds of overvoltage can be carried out by separating the filter system from the system. This book presents an analysis of these two conditions by taking Fulong Converter Station in the Xiangjiaba–Shanghai ±800 kV UHVDC transmission project as an example:

1. Ground fault of DC pole line

Figure 16.34 shows the diagram for ground fault at the top of the DC filter. The left part represents a filter model, in which L_{C1} represents the high-voltage parasitic inductance and R_{L1}, R_{L2}, and R_{L3} represent the DC resistance values of the reactor,

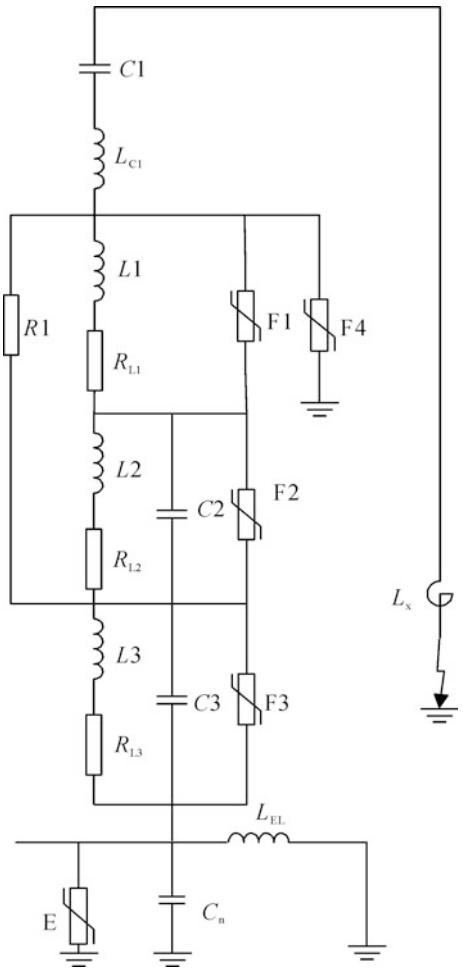

Fig. 16.34 Simulated circuit diagram for DC pole line earth fault

which can be calculated by the quality factor of the reactor; the right part represents an earth branch model for the ground fault inductance L_x. When the filter is charged to a high potential, the filter busbar will be subject to a ground fault, and at this moment, a fault circuit is formed by arresters F4, HV-end capacitor $C1$, neutral busbar capacitor C_n, neutral busbar arrester E, equivalent inductor of the ground electrode line L_{EL}, and fault point, and the arrester F4 endures a higher fault overvoltage. At the instant of the occurrence of a ground fault, the HV-end capacitor $C1$ and inductor L_1 mainly endure the steep front overvoltage, and the arresters F1 and F4 connected in parallel consume higher energy. Because of the damping action of $C1$ and $L1$, the low-voltage end equipment $L2$, $L3$, $C2$, and $C3$ do not endure the steep front overvoltage basically, but do endure the switching overvoltage resulting from the electromagnetic oscillation of the filter inductor and capacitor.

In the DC filter, because arresters F1, F2, F3, and F4 are placed at different positions, the calculation conditions for their respective maximum overvoltage differ, and it is required to consider the maximum overvoltage condition of these four kinds of arresters for simulation calculation. The following will provide a discussion on the maximum overvoltage condition of these four kinds of arresters [8, 9].

Arresters F1 and F4

The calculation condition for the maximum overvoltage of arresters F1 and F4 is identical. Their overvoltages all result from the discharge of $C1$ through F1 and F4 when the DC pole line is grounded. If the precharging voltage on the capacitor at the HV end of the filter gets higher, the energy stored in the filter also gets higher, and the overvoltage on the arresters F1 and F4 gets more severe. In addition, the overvoltage magnitude gets higher when L_x is smaller.

For the reason that the wave front of the maximum overvoltage on arresters F1 and F4 is very steep and closer to the lightning impulse, the results calculated here should correspond to the lightning impulse protection level.

The most severe calculation conditions for such overvoltage are as follows:

(1) Precharging voltage of DC filter

Considering that the maximum voltage on the DC filter does not exceed the protection level of the DC pole line arrester, the precharging voltage should be the switching impulse protection level (SIPL) of the DC pole line arrester based on the principle of strictness, e.g., 1391 kV for the Xiangjiaba–Shanghai ±800 kV UHVDC transmission project.

(2) Parasitic inductance L_{c1} of HV capacitor C1

According to the equipment manufacturing experience, ABB company believes that the parasitic inductance of the HV capacitor C1 can be 50 μH [10].

(3) Minimum L_x

The inductance value in such fault mainly represents the DC parasitic inductance. The terminal of the DC filter is usually at a higher position, with a big air clearance, being not liable to a ground fault. The distance between capacitor $C1$ and earth point is usually between about 10–20 m, so L_x is normally the parasitic inductance of the DC pole between the earth point and capacitor $C1$ at the HV end of the DC filter. ABB Company believes that this value should not be less than 20 μH, so the value is usually set to 30 μH [9].

(4) Equivalent inductance L_{EL} of ground electrode line

Based on the ground electrode line length of 60 km, such equivalent inductance is set to 60 mH, which has no influence on the overvoltage calculation results, basically.

(5) Maximum and minimum protection characteristics of arrester

During the calculation of the maximum load of an arrester, the arrester should adopt the minimum protection characteristic based on the principle of strictness. If other arresters are provided in the filter, these arresters should adopt the maximum protection characteristic based on the principle of strictness to reduce their shunt.

Arresters F2 and F3

Unlike the arrester F1, the overvoltages on arresters F2 and F3 are caused by the oscillation at the transient state of $L2$ and $C2$, and $L3$ and $C3$. Thus, the value of L_x for the calculation of the maximum overvoltage on arresters F2 and F3 is not set to the minimum value, but is set to a value between the minimum value and the maximum value (the minimum value is usually not less than 20 μH, and the maximum value is up to 100 mH), which is usually determined by gradual test and calculation during simulation.

The wave front steepness values of the maximum overvoltage that occurred on F2 and F3 are closer to the switching impulse (unlike the maximum overvoltage on arrester F1 that is closer to the lightning impulse), so the result calculated here should correspond to the switching impulse protection level.

In addition to L_x, other conditions of calculation model for the maximum overvoltage are identical to arrester F1.

2. Switching overvoltage impulse

During the analysis of the internal overvoltage of the DC filter, it is also required to consider the switching impulse of the DC pole line. The simulation diagram is shown in Fig. 16.35.

During calculation, a switching impulse of 250/2500 μs is applied to the DC line, and based on the principle of strictness, the switching impulse magnitude should be the switching impulse protection level (SIPL) of the DC pole line arrester, namely 1391 kV. Also, the switching impulse withstand level up to 1600 kV for the DC pole line is considered in some researches.

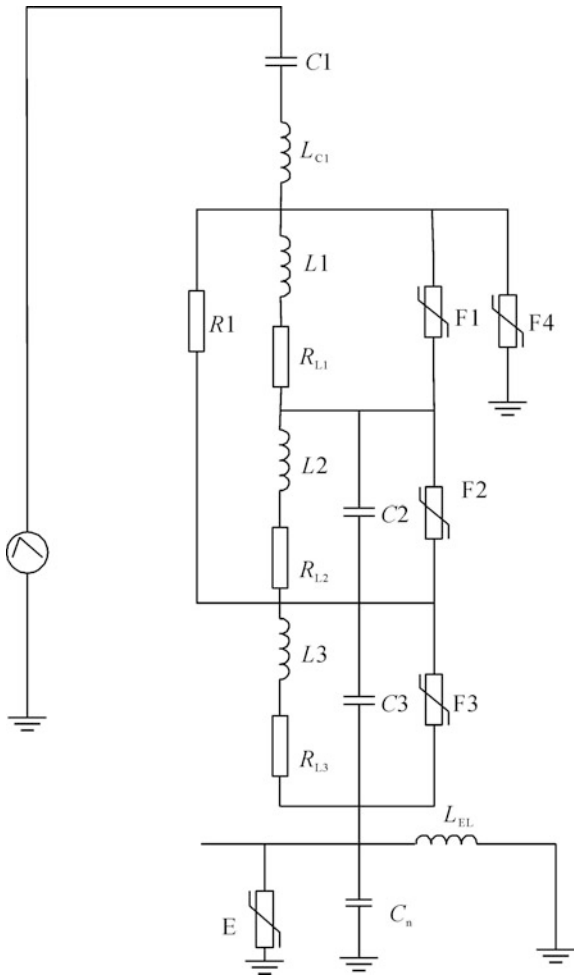

Fig. 16.35 Simulated circuit diagram for operation overvoltage of DC filter

16.5.3.2 Simulation Calculation Results

1. DC pole line ground fault

Taking Fulong Converter Station in the Xiangjiaba–Shanghai ±800 kV UHVDC project as an example, the calculation results of internal overvoltage of the DC filter are shown in Table 16.16. Figure 16.36 shows the waveforms of overvoltage, current, and energy when the arrester F4 withstands the maximum overvoltage.

2. Switching overvoltage impulse

In this case, a switching impulse of 250/2500 μs is usually applied for simulation. During simulation, two kinds of switching impulse overvoltage magnitude values

Table 16.16 Calculation results for overvoltage on DC filter arresters under DC pole line ground fault

Arrester	Max. voltage (kV)	Max. current (kA)	Max. energy (MJ)
F1	687	10.4	0.23
F2	500	2.9	0.31
F3	138	8.6	0.60
F4	688	80	0.92

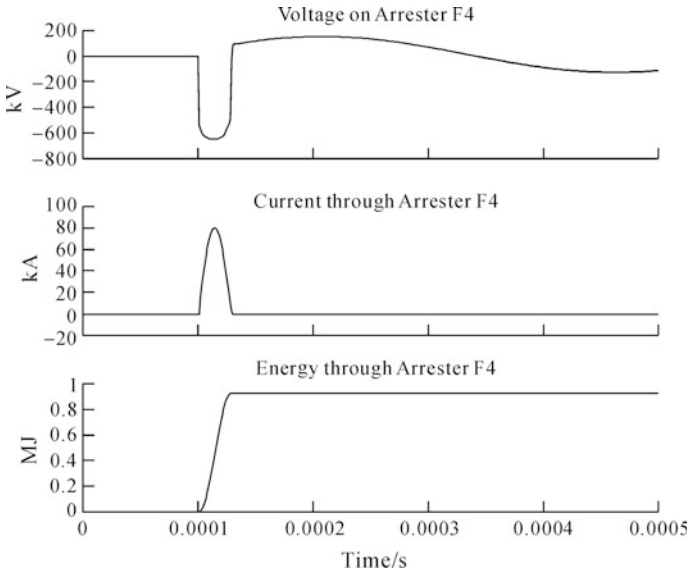

Fig. 16.36 Diagram for waveforms of overvoltage, current, and energy on arrester F4 under DC pole line ground fault

Table 16.17 Overvoltage calculation results on DC filter arresters under switching impulse wave

Arrester	Max. voltage (kV)	Max. current (kA)	Max. energy (MJ)
F1	622/630	2.94/3.36	0.10/0.12
F2	418/444	0.09/0.12	≈0/≈0
F3	134/135	5.85/6.19	0.14/0.15
F4	522/535	1.32/2.76	0.14/0.18

Note The value at the left side of the slash is the result calculated by taking SIPL (1391) as the impulse voltage magnitude, and the value at the right side of the slash is the result calculated by taking SIWL (1600 kV) as the impulse voltage magnitude

(SIPL: 1391 kV and SIWL: 1600 kV) are taken for calculation, respectively, with the calculation results shown in Table 16.17. The energy flowing through the arresters F1, F2, F3, and F4 under the influence of such overvoltage is low.

In addition to direct simulation calculation, ABB company believes that the operating current under the influence of such switching impulse can be estimated by the following equation with respect to arrester F4 in the DC filter [11]:

$$I \approx C\frac{\mathrm{d}u}{\mathrm{d}t} = C\frac{\mathrm{SIWL}}{250} = 1.05\ \mu\mathrm{F} \times \frac{1600\ \mathrm{kV}}{250\ \mu\mathrm{s}} = 6.72\ (\mathrm{kA}),$$

where

C is the capacitance of the high-voltage filter,
$\mathrm{d}u/\mathrm{d}t$ the voltage change ratio, and
SIWL the switching impulse protection level of the DC pole line (also can adopt SIPL of the DC pole line arrester, namely 1391 kV).

The SIPL of arrester F4 corresponding to such current is 553 kV.

In practice, the operating current value obtained above would have an appropriate margin because the filter inductor $L1$ and arrester F1 in parallel have shunting action.

16.5.3.3 Analysis of Overvoltage Mechanism

With respect to arresters F1 and F4 in these DC filters, when the filter busbar is subject to a ground fault, the overvoltage results from the discharge of $C1$ directly through F1 and F4 where the DC pole is grounded.

With respect to arresters F2 and F3, the maximum overvoltage is totally different from F1 and F4 when the DC pole line is subject to a ground fault. The overvoltage mainly results from the electromagnetic oscillation between $L2$ and $C2$, and $L3$ and $C3$.

16.5.3.4 Overvoltage Control and Protection Measures

It is required to adopt arresters (F1, F2, F3, and F4) to protect against these two categories of overvoltage. From the calculation results, it can be known that these overvoltages are not severe, and safe protection of the DC filters can be achieved only by use of arresters.

16.6 Monopolar Ground Fault Overvoltage of DC Line

Although different kinds of operations may cause overvoltage on the DC line, the monopolar ground fault overvoltage of the DC line is often the focus of study [12–15]. For example, the closing of no-load line at the AC side, closing of no-load converter transformer and switching of AC filter, failure of DC control and

protection system (for example, full voltage starting), continuous loss of valve pulse, blocking of inverter station but failure to deblock bypass pair, faulty conduction of valve, AC power loss of inverter station, and operation of the switches at the DC side (for example, closing and opening of the bypass switches of the upper and lower 12-pulse converter units or switching of DC filter by disconnector, etc.) can all cause overvoltage on the DC line, but the overvoltage resulting from these operations is restrained by the D-type lightning arrester on the DC busbars and the DC line entry of both converter stations at the faulty pole and is usually lower than the per-unit value 1.66 [16]; moreover, when the overvoltage is transmitted to the line, due to the damping of the capacitance and resistance of the line, its amplitude is usually lower than the maximum overvoltage generated by the monopolar ground fault on the sound pole line. Therefore, this section focuses on the study of the overvoltage generated by the monopolar ground fault on the DC line.

The monopolar ground fault overvoltage is the overvoltage generated due to the occurrence of monopolar ground fault when the DC system is operating in bipolar mode. The occurrence probability of such overvoltage is higher on the UHVDC transmission line. The monopolar ground fault will not generate overvoltage on the faulty pole line, but will generate relatively serious overvoltage on the sound pole line. In this section, simulation of such overvoltage is carried out in combination with the Xiangjiaba–Shanghai UHVDC transmission project, and the mechanism of such overvoltage is analyzed in detail.

16.6.1 Conditions for Simulation

1. Conditions of simulation system

When the DC system is operating in bipolar mode, a group of DC filters will be provided between the DC pole line and the neutral line on the rectifier station and the inverter station, respectively. Figure 16.37 shows the monopolar ground fault occurred on the DC line.

In the simulation analysis, the DC system is set to be operating completely in bipolar mode, the monopolar ground fault is made to occur at the midpoint of the DC line positive pole, and the overvoltage on the sound pole line is calculated through EMTDC. The overvoltage is mainly related to the main capacitor parameters of DC filters, position of monopolar ground fault, structure and parameters of the DC transmission line as well as various other factors. In this section, by means of the calculation software EMTDC and traveling wave theory, study is carried out on the impacts of various factors on such overvoltage through simulation, the most severe conditions of such overvoltage are determined, and its generating mechanism and restrictive measures are analyzed.

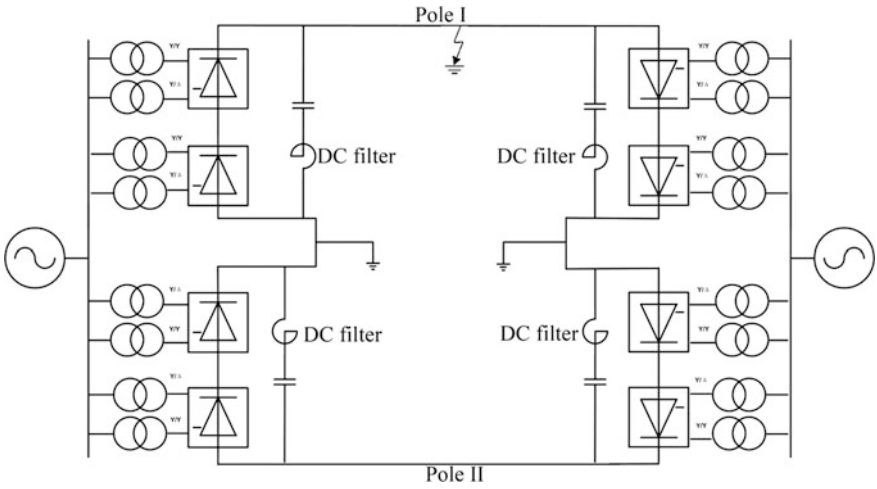

Fig. 16.37 Sketch for monopolar ground fault on the DC line when the DC system is operating in bipolar mode

2. Discussion on influencing factors

When the monopolar ground fault occurs on the DC line, the overvoltage generated on the sound pole line may be affected by various factors. The overvoltage mainly depends upon the electromagnetic coupling between the faulty pole line and the sound pole line, and is linked directly with the mutual inductance coupling coefficient between the polar lines. The influencing factors can be classified into the following two categories according to their degrees of influence:

(1) Key influencing factors

There are two key influencing factors, that is, the position of monopolar ground fault and the parameter of main capacitor of DC filter.

The position of monopolar ground fault has a great influence on the overvoltage resulting from monopolar ground fault. The maximum value of such overvoltage usually occurs at the fault position to which the sound pole line corresponds; moreover, when the fault occurs at the midpoint position of the line, the overvoltage is the most serious. Therefore, the occurrence of grounding fault at the midpoint of the faulty pole line is one of the most severe conditions for calculating such overvoltage.

The parameter of the main capacitor of DC filter will also have a great influence on the overvoltage resulting from monopolar ground fault. The parameters of DC filter affect the amplitude of such overvoltage mainly through the main capacitance value. The higher the main capacitance is, the higher the discharge current generated by the faulty pole DC filter will be and, in such case, the higher the current induced on the sound pole line through the electromagnetic coupling between the faulty pole and the sound pole will also be, which will charge the capacitor to

ground of the sound pole line and, as a result, generate higher overvoltage on the sound pole line. The main capacitance value, which will affect directly the amplitude of such overvoltage, is the most important factor to be taken into consideration for calculating such overvoltage.

(2) General influencing factors

The general influencing factors mainly include the parameters of DC transmission line, length and transmission power of transmission line, grounding resistance of tower, and lightning arrester installed or not on the tower at the midpoint of the line and DC control systems. These influencing factors are separately analyzed as follows:

The parameters of DC transmission line include mainly the ground clearance of polar conductor, interpolar clearance, bundle spacing of polar conductors, number of bundled polar conductors, and cross-sectional area of sub-conductors. In the actual operation, the electromagnetic environment requirements for the UHVDC transmission line determine directly the structure and parameters of the UHVDC transmission line. Normally, the parameters do not change much, and the coefficient of mutual inductance coupling between the polar lines does not change much, either. Therefore, they have little influence on such overvoltage.

The length of the UHVDC transmission line is usually reasonably long with a large variation range. However, since the line structure and parameters are usually irrelevant to the length of the line, and the coefficient of mutual inductance coupling between the polar lines has little to do with the length of the line, the variation in the length of the UHVDC line normally has little influence on such overvoltage value, which has also been proven by the simulation calculation.

As the transmission power increases, the current of the DC line increases, causing the voltage along the DC line to drop and leading to the decrease of such overvoltage; however, as the DC resistance of the DC line is small and the range of variation of the voltage along the line is not large, the transmission power has a small influence on such overvoltage, which has also been verified in the simulation calculation.

The increase of the grounding resistance of the tower will generate appropriate damping effect. This can decrease the transient component of flashover to ground of the line, consequently decreasing the overvoltage level of the sound pole line. However, since the grounding resistance of the towers along the UHVDC transmission line has a small range of variation (normally 0–15 Ω), as a matter of fact, the grounding resistance of the towers has little influence on such overvoltage, either. For strict calculation, the grounding resistance of the tower is taken as 0 Ω.

The line lightning arrester installed on the tower at the midpoint of the line will restrict, to a certain extent, such overvoltage when the amplitude of the overvoltage on the sound pole line is large, but the restriction effect is not very obvious, which has been proven by the simulation calculation.

In the end, whether the DC control system will have influence an on such overvoltage will be discussed. Since the time for the overvoltage of the sound pole

line to reach its peak is only several milliseconds (the required time for the wave to propagate forth and back between the fault point and the converter station), and during such short time the control systems at both sides cannot make any response to such fault at all, the DC control system will generally not have any influence on the amplitude of such overvoltage.

In conclusion, the parameters of the DC transmission line, length of the line, grounding resistance of the tower, lightning arresters installed or not, etc. will have a certain influence on such overvoltage, but the influence is usually small. The DC control system will generally not have any influence on such overvoltage.

3. Parameters for simulation calculation

In this section, the simulation calculation is carried out based on the ±800 kV Xiangjiaba–Shanghai DC Power transmission project. The transmission line parameters of such project are shown in Table 16.18.

A group of DC 2/12/39 triple-tuned DC filters are provided for Fulong Converter Station and Fengxian Converter Station, respectively. The specific circuits and parameters are shown in Fig. 16.38 and Table 16.19.

16.6.2 Simulation Calculation Results

1. Influence of the position of monopolar ground fault

When the monopolar ground fault occurs along the positive pole line from 0 to 100% thereof, the calculation results of the overvoltage distribution along the corresponding sound negative pole line (0–100%) are shown in Fig. 16.39. In addition, when the monopolar ground fault occurs on the positive pole line within ±30 km to the midpoint, the calculation results of the overvoltage distribution

Table 16.18 Parameters of ±800 kV DC transmission line

DC transmission line	Overhead ground wire	Conductor
Model	LBGJ-180-20AC	6× ACSR-720/50 aluminum conductor steel reinforced
Outer diameter (mm)	17.5	36.2
DC resistance (Ω/km)	0.4696	0.0398
Horizontal distance (m)	27.8	22
Suspension height (m)	63	48
Sag (m)	13	18
Bundle spacing (mm)	–	450
Ground wire grounded in sections or not	Yes	–

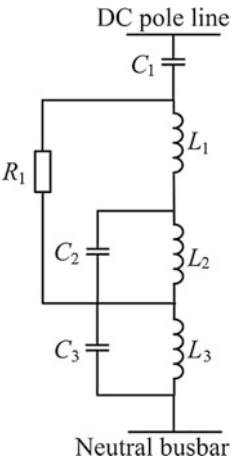

Fig. 16.38 Circuit diagram of DC filters adopted in Xiangjiaba–Shanghai DC power transmission project

Table 16.19 Parameters of DC filters adopted in Xiangjiaba–Shanghai DC power transmission project

Element	Converter station	
	Fulong Converter Station	Fengxian Station
C_1 (μF)	1.05	1.05
L_1 (mH)	9.847	9.847
C_2 (μF)	3.286	3.286
L_2 (mH)	582.95	582.95
C_3 (μF)	5.05	5.105
L_3 (mH)	11.745	11.745
R_1 (Ω)	3095	3095

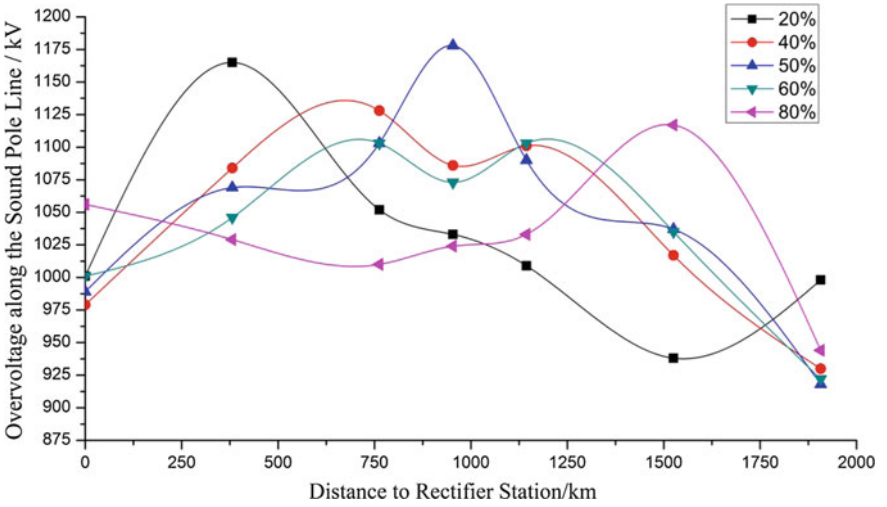

Fig. 16.39 Overvoltage distribution along the sound pole line when grounding fault occurs along the faulty pole line

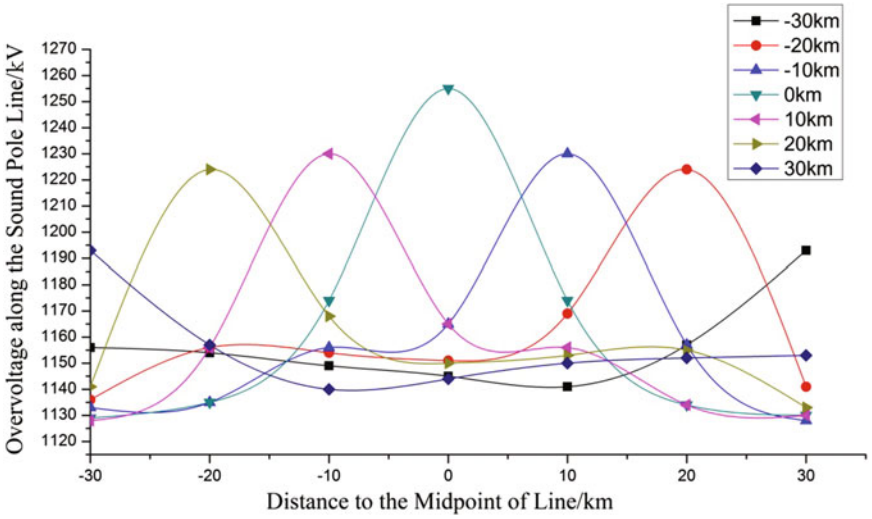

Fig. 16.40 Overvoltage distribution along the sound pole line when grounding fault occurs on the faulty pole line within ±30 km to the midpoint

along the corresponding sound negative pole line within ±30 km to the midpoint are shown in Fig. 16.40.

As shown in Figs. 16.39 and 16.40, the position of monopolar ground fault has a great influence on the overvoltage resulting from monopolar ground fault; when the DC system is running under complete bipolar mode, such overvoltage will be the maximum when the monopolar ground fault occurs at the midpoint of the line; when the fault point is far away from the midpoint of the line, the overvoltage along the sound pole line normally reaches the maximal value at the position of the corresponding grounding fault, while when the fault point is close to the midpoint of the line, the overvoltage along the sound pole line normally reaches the maximal value at the symmetrical position of the corresponding grounding fault relative to the midpoint of the line (that is, the position where the discharge current waves of the DC filters of the converter stations at both terminals encounter with each other on the line).

2. Influence of the main capacitance of DC filter

As for the DC filters of the Xiangjiaba–Shanghai DC Power transmission project as shown in Fig. 16.38, when the main capacitance of the DC filters is 1, 2, 3, and 4 μF, respectively [16], the simulation calculation results of the overvoltage at the midpoint of the corresponding sound pole line in case of the occurrence of monopolar ground fault at the midpoint of the faulty pole line (the most severe condition) are shown in Table 16.20.

As shown in Table 16.20, the main capacitance of the DC filter is a key factor that affects the overvoltage resulting from monopolar ground fault. The higher the

main capacitance, the higher the overvoltage amplitude. When the main capacitance is 2 μF, such overvoltage amplitude is 1357 kV, which reaches 1.7 p.u.

3. Influence of the configuration of DC filter

Among the UHVDC power transmission projects, the Xiangjiaba–Shanghai DC Power transmission project adopted one group of DC 2/12/39 triple-tuned DC filters at each pole of each station, the specific circuits and parameters of which are shown in Fig. 16.38 and Table 16.19; the Jinping–South Jiangsu DC Power transmission project adopted the DC filters consisting of one group of 2/39 double-tuned filters and one group of 12/24 double-tuned filters connected in parallel at each pole of each station, the specific circuits and parameters of which are shown in Fig. 16.41 and Table 16.21; the Yunnan–Guangzhou DC Power transmission project adopted one group of 12/24/45 triple-tuned DC filters at each pole of each station, the specific circuits and parameters of which are shown in Fig. 16.42 and Table 16.22.

Table 16.20 Influence of different main capacitance values of DC filters on the overvoltage resulting from monopolar ground fault

Main capacitance of DC filter (μF)	1	2	3	4
Overvoltage (kV)	1243 (1.55 p.u.)	1357 (1.70 p.u.)	1400 (1.75 p.u.)	1422 (1.78 p.u.)

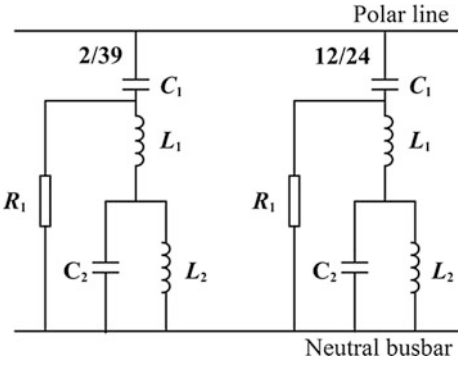

Fig. 16.41 Circuit diagram of DC filters adopted in Jinping–South Jiangsu DC power transmission project

Table 16.21 Parameters of DC filters adopted in Jinping–South Jiangsu DC power transmission project

Group name	Group 1	Group 2
Configuration	2/39	12/24
Number of groups/pole	1	1
C_1 (μF)	0.80	0.35
L_1 (mH)	11.99	89.35
C_2 (μF)	1.825	0.810
L_2 (mH)	964.0	48.86
R_1 (Ω)	5700	10,000

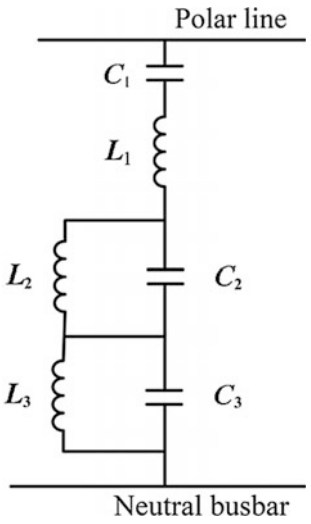

Fig. 16.42 Circuit diagram of DC filters adopted in Yunnan–Guangzhou DC power transmission project

Table 16.22 Parameters of DC filters adopted in Yunnan–Guangzhou DC power transmission project

Element	Converter station	
	Chuxiong Station	Huidong Station
C_1 (μF)	1.2	1.2
L_1 (mH)	9.345	9.345
C_2 (μF)	2.824	2.824
L_2 (mH)	15.919	15.919
C_3 (μF)	2.647	2.647
L_3 (mH)	4.656	4.56

In this section, the configuration of DC filters adopted in the Xiangjiaba–Shanghai UHVDC Power transmission project is replaced with the configurations of DC filters adopted in the Jinping–South Jiangsu and Yunnan–Guangzhou DC Power transmission projects, respectively, to carry out the simulation calculation of the overvoltage at the midpoint of the sound pole line. The calculation results of the overvoltage in such three cases are shown in Table 16.23.

As shown in Table 16.23, the three configurations of the DC filters almost have no influence on the amplitude of such overvoltage. In addition, a characteristic can also be found during the inspection of three different configurations of DC filters, that is, the total main capacitance values thereof are 1.05, 1.15, and 1.2 μF, respectively, which are reasonably close to each other. Therefore, under the condition that the main capacitance parameter values of DC filters are close to each other, even if different configurations of DC filters are adopted, they will generally

Table 16.23 Influence of different configurations of DC filters on the overvoltage resulting from monopolar ground fault

Configuration of DC filters	DC filters adopted in the Xiangjiaba–Shanghai DC power transmission project	DC filters adopted in the Jinping–South Jiangsu DC power transmission project	DC filters adopted in the Yunnan–Guangzhou DC power transmission project
Main capacitance (μF)	1.05	1.15	1.2
Overvoltage (kV)	1254	1263	1258

Table 16.24 Influence of different tower grounding resistances on the overvoltage resulting from monopolar ground fault

Tower grounding resistance (Ω)	0	1	5	10	15
Overvoltage (kV)	1254	1251	1240	1227	1214

not cause too much influence on the overall level of such overvoltage, and the main capacitance value of DC filters is the most critical factor that affects the overvoltage resulting from monopolar ground fault.

4. Influence of DC control system

Considering that, when a fault occurs on the line, the time required for the DC protection device to send out protection order is generally longer than the time the overvoltage resulting from monopolar ground fault needs to reach its maximal value, the control systems at both sides have no way to make response to such fault in a timely manner. Therefore, the DC control system usually does not cause any influence on the amplitude of such overvoltage.

5. Influence of tower grounding resistance

The tower grounding resistance can reduce the transient component of flashover to ground of the line, consequently causing the amplitude of the overvoltage on the sound pole line to decrease to a certain extent; however, it almost has no influence on the overall waveform of such overvoltage and the occurrence time of amplitude thereof. The simulation calculation results of the overvoltage at the midpoint of the sound pole line under different tower grounding resistances are shown in Table 16.24.

As shown in Table 16.24, as the tower grounding resistance increases, the amplitude of the overvoltage at the midpoint of the sound pole line decreases slightly, but the influence is small.

6. Influence of lightning arresters installed on the tower at the midpoint of the line

Under the four conditions that the main capacitance of the DC filter is taken as 1, 2, 3, and 4 μF, respectively, with the tower grounding resistance being taken as 0 Ω,

Table 16.25 Influence of lightning arrester installed on the tower at the midpoint of line on the overvoltage resulting from monopolar ground fault

Lightning arrester installed on the tower at the midpoint of line or not	Overvoltage value of line (kV)			
	C_1 = 1 μF	C_1 = 2 μF	C_1 = 3 μF	C_1 = 4 μF
Lightning arrester not installed	1243	1357	1400	1422
Lightning arrester installed	1211	1312	1331	1340

Table 16.26 Influence of different lengths of the line on the overvoltage resulting from monopolar ground fault

Length of line (km)	1500	1700	1900	2100	2300
Overvoltage (kV)	1249	1254	1253	1255	1279

the influence of the lightning arrester (with the same characteristics as those on the polar line of the converter station) installed on the tower at the midpoint of the line on such overvoltage is analyzed. When the monopolar ground fault occurs at the midpoint of faulty pole line, the influence of such lightning arrester on the amplitude of the overvoltage at the midpoint of the sound pole line is shown in Table 16.25.

As shown in Table 16.25, the lightning arrester installed at the midpoint of the line has a certain restrictive effect on such overvoltage, but the effect is not quite obvious. Under the condition that the main capacitance is taken as 4 μF, the installation of a lightning arrester on the tower at the midpoint of the line can cause the overvoltage to drop to 1340 kV from 1422 kV, with the overvoltage level being decreased by 5.8% only. Therefore, the restriction of such overvoltage by installing a line lightning arrester on the tower at the midpoint of the line is normally not recommended.

7. Influence of line length

The line length of the ±800 kV Xiangjiaba–Shanghai DC Power transmission project is 1907 km. Under different lengths of the line, when the grounding fault occurs at the midpoint of the faulty pole line, the relation between the overvoltage at the midpoint of the sound pole line and the length of the line is shown in Table 16.26.

As shown in Table 16.26, as the length of the DC power transmission line increases gradually, the overvoltage level goes up and down slightly, but the law of variation is not obvious. This is mainly because the change in the length of line will not cause much influence on the coefficient of mutual inductance coupling. Therefore, the change in the length of the UHVDC line normally has little influence on the amplitude of such overvoltage.

8. Influence of transmission power

When the DC system is running in bipolar balance mode, the influence of several typical transmission powers on the overvoltage resulting from monopolar ground

Table 16.27 Influence of different transmission powers on the overvoltage resulting from monopolar ground fault

Transmission power (p.u.)	0.1	0.25	0.5	0.75	1.0	1.05
Overvoltage (kV)	1264	1256	1252	1245	1239	1229

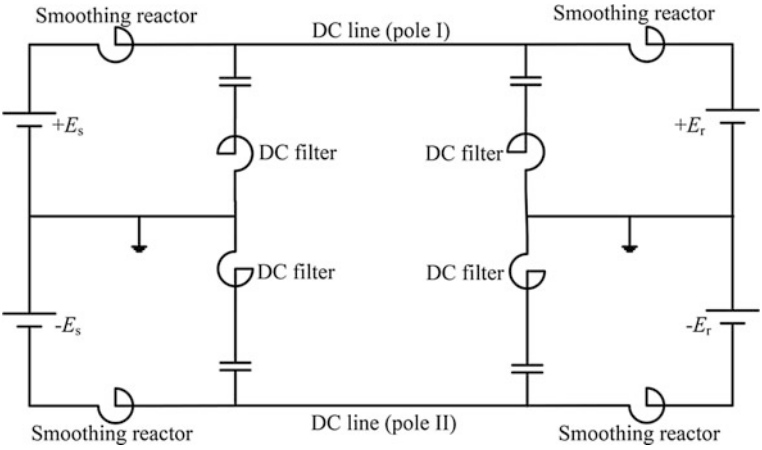

Fig. 16.43 Schematic diagram of DC power transmission system under bipolar operation mode

fault is shown in Table 16.27, where the transmission power is expressed in per-unit value.

As shown in Table 16.27, as the transmission power increases, the overvoltage level tends to decrease. When the transmission power increases to 1.05 p.u. from 0.1 p.u., the overvoltage level decreases by 2.8% only. It can be seen that the transmission power has a small influence on the overvoltage resulting from monopolar ground fault.

16.6.3 Analysis of Overvoltage Mechanism

The DC power transmission system mainly consists of the converter stations at both terminals, DC filters, smoothing reactors, DC line, ground electrode, etc. The schematic diagram of the DC transmission line in bipolar operation mode is shown in Fig. 16.43, where the converters at both terminals of the line are represented by voltage source. In the analysis below, it is assumed that a monopolar ground fault occurs on the positive pole.

Through the simulation calculation of the Xiangjiaba–Shanghai DC Power transmission project, the waveform curve of the overvoltage at the midpoint of the sound pole (negative pole) line when the midpoint of the faulty pole (positive pole) line is grounded is obtained as shown in Fig. 16.43, and represented, respectively,

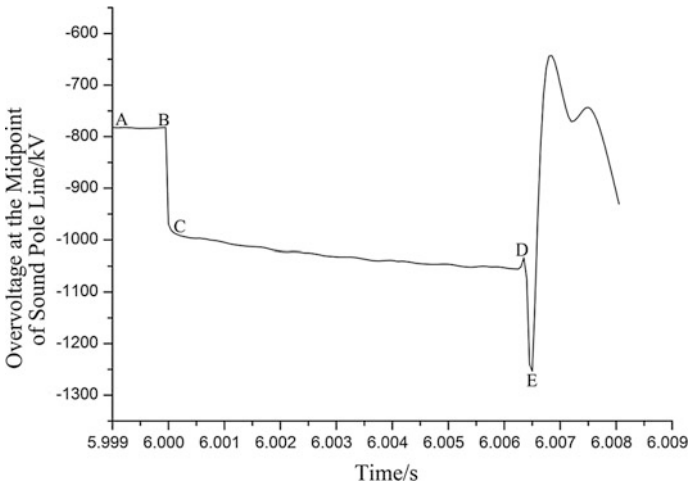

Fig. 16.44 Waveforms of overvoltage at the midpoint of sound pole line when the grounding fault occurs at the midpoint of faulty pole line

by points A, B, C, D, and E. As shown in Fig. 16.44, under the normal working voltage, the voltage at the midpoint of the sound pole line reached its peak after two jumps. At the beginning, the system was under stable operation, and the voltage at the midpoint of the sound pole line was about −783 kV as shown in curve section AB; at the moment of 6 s, a monopolar ground fault occurred at the midpoint of the faulty pole line, and the voltage at the midpoint of the sound pole line jumped instantly up to −981 kV from −783 kV as shown in curve section BC; within curve section CD, the voltage at the midpoint of the sound pole line rose up gradually to −1055 kV from −981 kV and such process lasted for about 6.5 ms (it is exactly the required time for the fault current wave to propagate from the fault point to the end of the converter station and then return back to the fault point); at the moment when the fault current wave returned back to the fault point, the voltage at the midpoint of the sound pole line jumped for the second time, with the voltage amplitude rising up to 1254 kV as shown in curve section DE.

When the monopolar ground fault occurs on the DC line, two processes will mainly occur on the faulty pole: firstly, at the moment of being grounded, a voltage wave (which has the same amplitude as, but with polarity opposite to, the voltage on the faulty pole) propagates from the fault point to the converter stations at both sides, causing the voltage on the faulty pole line to drop to zero and generating the corresponding current wave; then, when the wave propagates to both sides of the converter stations, the main capacitor of the DC filter on the faulty pole line will begin to send back a discharge wave to the fault point and generate a relatively large pulse discharge current along the faulty pole line.

Assuming that the faulty pole is the positive pole and the capacitor to ground of the whole line is charged to U_0 = +800 kV under stable operation, if a metallic

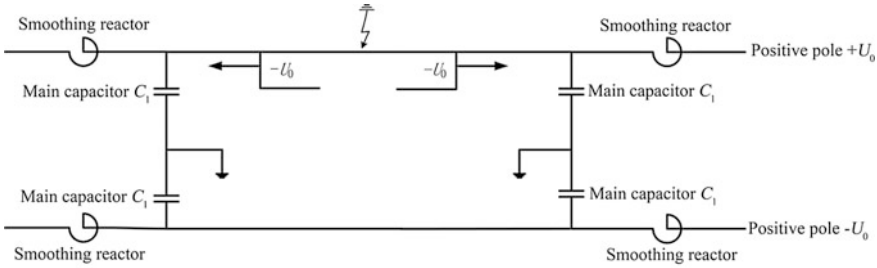

Fig. 16.45 Propagation process of the voltage traveling wave along faulty pole line when the monopolar ground fault occurs at the midpoint of positive pole line

monopolar ground fault occurs at the midpoint of the line, the voltage at the grounding fault point of the faulty pole line will drop instantly to zero from U_0 = +800 kV. This means that a voltage traveling wave with an amplitude of $-U_0$ propagates at the same time from the fault point along the faulty pole line to the converter stations at both sides, and the propagation process of such traveling wave along the faulty pole line is shown in Fig. 16.45.

With regard to the propagation process of the voltage wave $-U_0$ from the fault point to the left side, normally, the propagation of the current and voltage traveling waves to the right is regarded as the forward direction; therefore, the voltage wave $-U_0$ that propagates to the converter station on the left side from the fault point is a opposite voltage traveling wave, and the corresponding opposite current traveling wave generated on the line is as follows:

$$i_0 = -(-U_0)/Z, \tag{16.2}$$

where

Z is the wave impedance; and
i_0 is the current generated by the opposite traveling wave on the faulty pole line

The waveform of the current at the midpoint of the faulty pole line obtained through the simulation calculations is shown in Fig. 16.46. As shown in the figure, at the beginning, the system was under stable operation, and the operating current of the line was the rated current of 4 kA as shown in curve section AB; then the current at the midpoint of the faulty pole line jumped twice: at the moment when the fault occurred, the current jumped from the rated working current 4–6.38 kA as shown in curve section BC, and at 6.5 ms later after the fault occurred, the current at the faulty pole jumped once again to 6.50 kA from 6.03 kA as shown in curve section DE. In fact, the first current jump was caused by the opposite voltage traveling wave $-U_0$ that propagated to the converter stations. According to References [16, 17], it can be estimated that the wave impedance of the DC line of the Xiangjiaba–Shanghai DC Power transmission project is about 380 Ω; when it is substituted into Eq. (16.2), it can be estimated that the first current jump on the

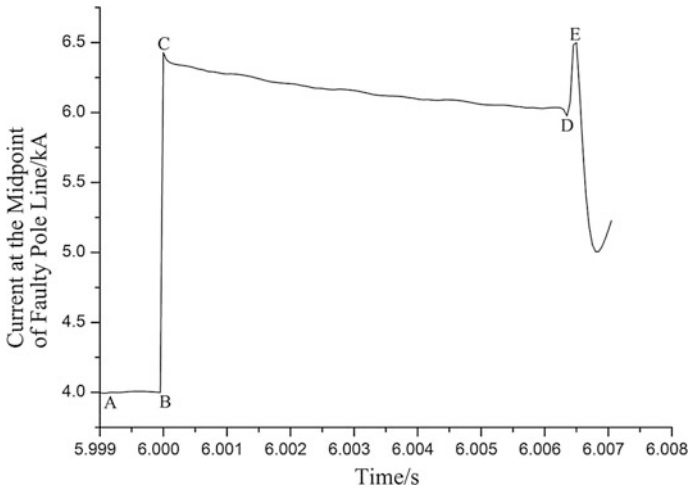

Fig. 16.46 Waveform of the current at the midpoint of faulty pole line

faulty pole line made the line current rise up to 6.13 kA, close to 6.38 kA obtained through simulation calculation, which proved that, at the moment the fault occurred, the voltage wave $-U_0$ exactly began to propagate from the fault point to the converter stations at both terminals, while the second current jump was caused by the discharge wave sent back by the main capacitor of the DC filter on the faulty pole line, and its value is directly related to the magnitude of main capacitance (see the subsequent analysis).

Near the left side of the fault point, the corresponding relation between the current on the faulty pole line and the current on the sound pole line is shown in Fig. 16.47. It can be seen that, due to the electromagnetic coupling between the polar lines, corresponding to the two current jumps of the faulty pole line (the positive abrupt change on the basis of the rated current of +4 kA), the current on the sound pole line also jumped twice reversely (negative abrupt change on the basis of the rated current of −4 kA).

While the DC system is working in bipolar operation mode, when the grounding fault occurs on a pole, the fault voltage wave propagating simultaneously to the converter stations at both terminals (with the same amplitude as, but opposite polarity to, the voltage on the faulty pole) will be generated at the fault point of the faulty pole line, and the corresponding fault current wave will be generated. Due to the electromagnetic coupling between the polar lines, section BC where the current of the fault current wave changes abruptly will generate the corresponding reverse abruptly changing pulse current B′C′ on the sound pole line through induction and will charge the capacitance to ground of the sound pole line near the fault point, consequently leading to the first voltage jump of the sound pole line; afterwards, when the wave propagates to the converter stations at both terminals, the main capacitor of the DC filter on the faulty pole line will discharge to the fault point and

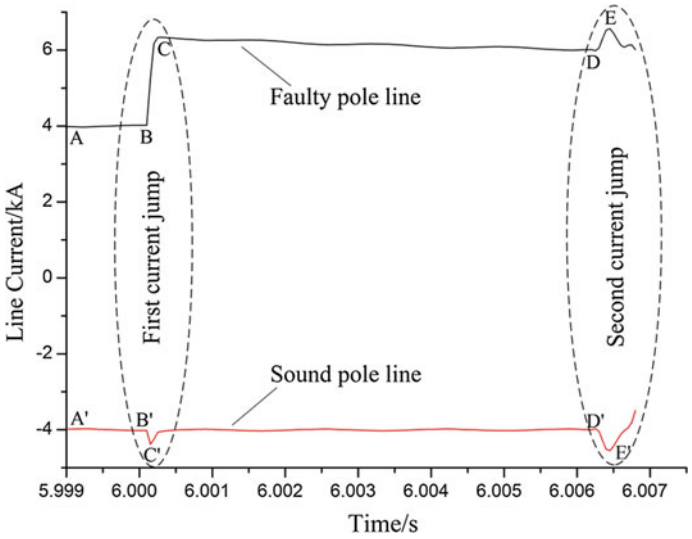

Fig. 16.47 Waveforms of current on faulty pole line and sound pole line near the left side of fault point

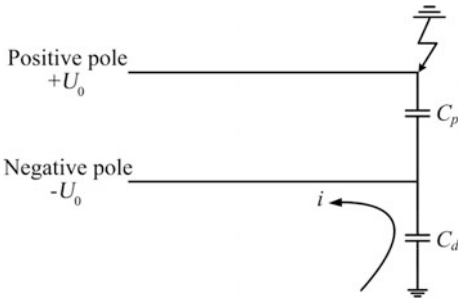

Fig. 16.48 Charging of capacitor to ground at the midpoint of line by negative current pulse of sound pole line on the left side of fault point

generate a relatively large abruptly changing pulse fault current section DE, and, similarly, due to the electromagnetic coupling between the polar lines, such abruptly changing fault current will also induce a reverse abruptly changing pulse current wave D′E′ on the sound pole line (its magnitude is mainly determined jointly by the discharge pulse current of the main capacitor of DC filter on faulty pole line and the coefficient of mutual inductance coupling between polar lines). Such reverse pulse current wave will also charge the capacitance to ground of the sound pole line near the fault point, resulting in the second voltage jump of the sound pole line. The above two voltage jumps are superposed on the normal working voltage (to ground) of such pole, consequently causing a relatively serious overvoltage on the sound pole line. In addition, if the monopolar ground fault occurs at the midpoint of the faulty pole line, the second voltage jump caused by the discharge of the main capacitor of the filters at both terminals will cause the

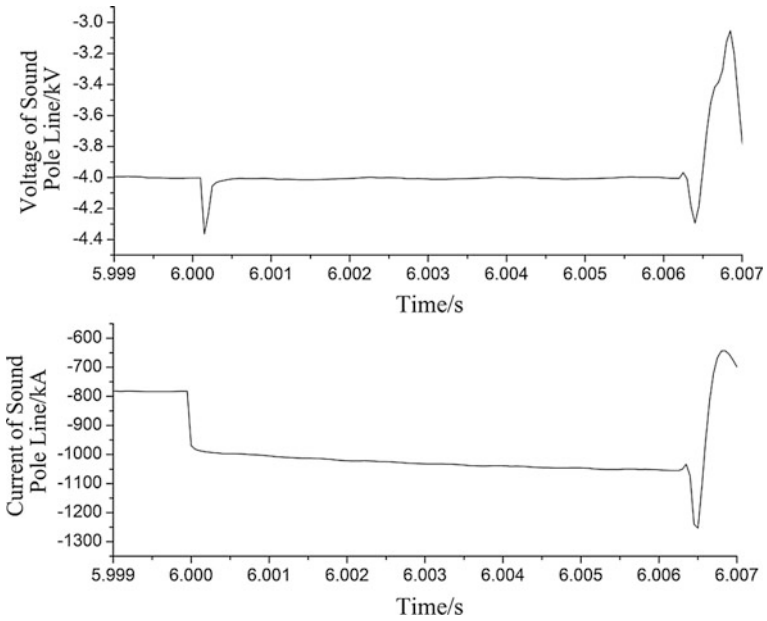

Fig. 16.49 Waveforms of current and voltage of sound pole line

simultaneous superposition at the midpoint of the sound pole and lead to the most serious overvoltage resulting from monopolar ground fault; if the monopolar ground fault occurs at other positions (rather than the midpoint) of the faulty pole line, the second voltage jump will not cause the simultaneous superposition on the sound pole line, and, in such case, the generated overvoltage resulting from monopolar ground fault is not as serious as the former one. Therefore, when the monopolar ground fault occurs at the midpoint of the faulty pole line, the overvoltage on the sound pole line is the most serious.

As shown in Fig. 16.47, on the sound pole line, the negative current pulse jump (negative abrupt change) will occur twice on the left side of the fault point, which will charge reversely the capacitance to ground of the sound pole line (negative pole), with the charging process as shown in Fig. 16.48, causing the two jumps of the voltage of the sound pole line on the basis of the rated voltage (−800 kV). The corresponding relation between the current and the voltage is shown in Fig. 16.49. Similarly, on the right side of the fault point, the positive current pulse jump (positive abrupt change) will occur twice on the sound pole line, which will also charge reversely the capacitance to ground of the sound pole line (negative pole), causing twice jumps of the voltage of the sound pole line on the basis of the rated voltage (−800 kV) as well.

In fact, the first voltage jump is generated by the first process during which −800 kV fault voltage wave propagates to the converter stations at both terminals at the moment the faulty pole line is grounded and is generally uncontrollable, while the second voltage jump is caused by the second process during which the main capacitor of the DC filter on the faulty pole line discharges to the fault point and can be controlled through the main capacitance of the DC filter.

The simulation calculation shows that the increase of the main capacitance of the DC filter will directly lead to the obvious increase in the second jump effect of the overvoltage resulting from monopolar ground fault. Under the four conditions in which the main capacitance value of the DC filter is taken as 1, 2, 3, and 4 μF, the current of the faulty pole line and the current of the sound pole line are shown in Figs. 16.50 and 16.51, respectively. It can be seen that as the main capacitance of the DC filter increases, the discharge current generated on the faulty pole line increases, and hence, through the electromagnetic coupling between the polar lines, the induced current generated on the sound pole line increases, consequently causing such overvoltage to rise. This has further proven that the main capacitance value of the DC filter is a critical influencing factor for the overvoltage resulting from monopolar ground fault.

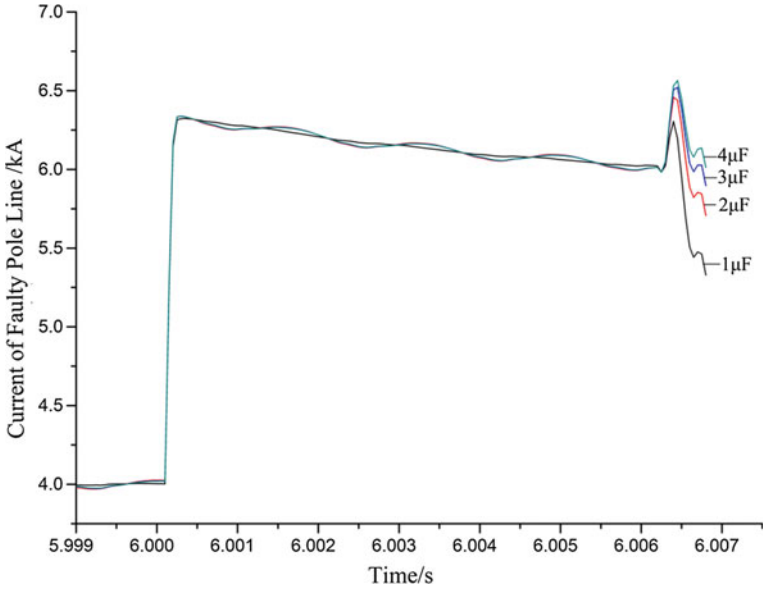

Fig. 16.50 Relation between current of faulty pole line and main capacitance

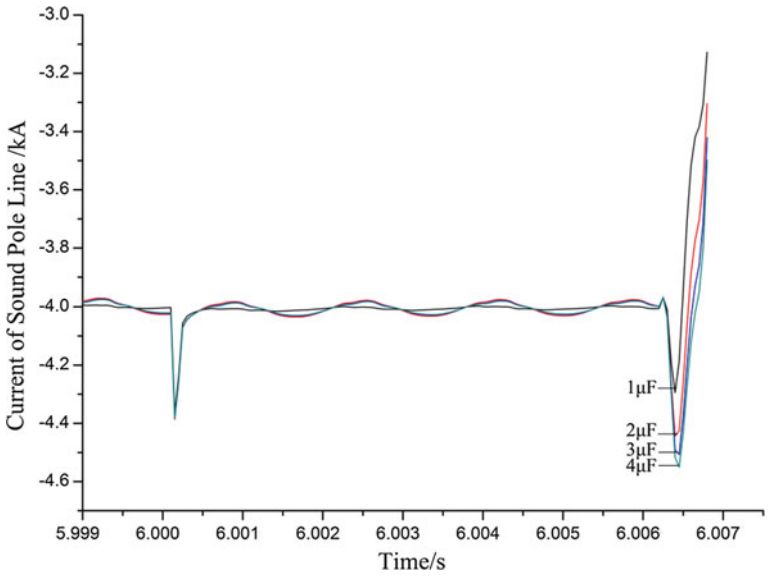

Fig. 16.51 Relation between current of sound pole line and main capacitance

16.6.4 Overvoltage Control and Protection Measures

(1) The main capacitance of the DC filter is the most critical factor that affects the overvoltage resulting from monopolar ground fault. It affects directly the amplitude of such overvoltage. Through the appropriate control of the main capacitance value, the overvoltage resulting from monopolar ground fault can be controlled effectively. In addition, when the total main capacitance is close, the configuration of the DC filter (double-tuned, triple-tuned, etc.) has little influence on the overvoltage resulting from monopolar ground fault. The study shows that, in order to make the overvoltage level resulting from monopolar ground fault not exceed 1.7 p.u., the main capacitance of the DC filters on the ±800 kV UHV line has to be better controlled between 1 and 2 μF.

(2) When the monopolar ground fault occurs at the midpoint of the faulty pole line, the maximum overvoltage will be generated at the midpoint of the sound pole line, and hence this is usually taken as the basic condition for calculating such overvoltage.

(3) The structure and parameters of the DC transmission line include mainly the ground clearance of polar conductor, interpolar clearance, bundle spacing of polar conductors, number of bundled polar conductors, and cross-sectional area of sub-conductors. They will cause a certain influence on the overvoltage resulting from monopolar ground fault, but usually do not have large influence; considering the limitation of the electromagnetic environment of the DC line,

the structure and parameters of the DC transmission line usually do not change much, and hence, as a matter of fact, the structure and parameters of the DC transmission line usually have little influence on the overvoltage resulting from monopolar ground fault. The tower grounding resistance normally has very small influence on the overvoltage resulting from monopolar ground fault; when the tower grounding resistance increases from 0 to 15 Ω, the overvoltage decreases by 3.2% only. Moreover, the DC control system does not have any influence on such overvoltage, and the length and transmission power of the transmission line have little influence on such overvoltage.

(4) The installation of the line lightning arrester on the tower at the midpoint of the line can reduce such overvoltage appropriately; however, the effect is not obvious. Under the condition that such overvoltage is 1.78 p.u., if a lightning arrester with the same characteristics as those on the polar line of the converter station is installed on the tower at the midpoint of the line, such overvoltage will drop by 5.8% only. Therefore, the installation of a line lightning arrester at the midpoint of the line is usually not adopted to limit the overvoltage resulting from monopolar ground fault.

References

1. Xiangjiaba-Shanghai ±800 kV UHVDC transmission project AC filter transient rating. ABB Power Systems; 2007.
2. Xiangjiaba–Shanghai ±800 kV UHVDC transmission project AC filter arresters [R]. ABB Power Systems; 2007.
3. Dongju W, Deng X, Hao Z, Xilei C, Anwen X, Yang S. Research on converter valve overvoltage mechanism and calculation conditions of ±800 kV converter station (English). High Voltage Eng. 2012;38(12):3189–97.
4. Chen X, Zhou H, Yuan S, Wang D, Tian J, Huang Z, Lu Y. Overvoltage mechanism of converter valves for HVDC power transmission project from Tianshengqiao to Guangzhou. Power Syst Technol. 2012;36(3):88–94.
5. Wang D, Deng X, Zhou H, Shen Y, Sun K. On the DC transient overvoltage in the converter stations of ±800 kV Xiluodu-Zhexi HVDC project. South Power Syst Technol. 2012;6(2):6–13.
6. Yuan S, Wang D, Chen X, Huang Z, Lu Y, Tian J, Chen W, Sun K, Zhou H. Study on neutral-bus overvoltage mechanism of ±500 kV DC power transmission project from Tianshengqiao to Guangdong. Power Syst Technol. 2011;35(5):216–22.
7. Chen X, Tian J, Wang D, Yuan S, Zhou H. Analysis on overvoltage in renovated control and protection system for HVDC power transmission project from Tianshengqiao to Guangzhou. Power Syst Technol. 2011;35(6):101–6.
8. Xiangjiaba–Shanghai ±800 kV UHVDC transmission project DC filter steady state rating. ABB Power Systems; 2008.
9. Xiangjiaba–Shanghai ±800 kV UHVDC transmission project DC filter transient rating; 2008.
10. Xiangjiaba–Shanghai ±800 kV UHVDC transmission project insulation coordination. ABB power systems; 2007.
11. Xiangjiaba–Shanghai ±800 kV UHVDC transmission project DC transient overvoltage; 2008.
12. Hingorani NG. Transient overvoltage on a bipolar HVDC overhead line caused by DC line Faults. IEEE Trans Power Appar Syst. 1970;PAS-89(4):592–610.

13. Melvold DJ, Odam PC, Vithayathil JJ. Transient overvoltage on an HVDC bipolar line during monopolar line faults. IEEE Trans Power Appar Syst. 1977;96(2):591–601.
14. Shi L. Study on the overvoltage on ±500 kV DC transmission line. Power Syst Technol. 1987;01:33–6.
15. Wu Y, Jiang W, Zhu Y, et al. Research on inner overvoltage in UHVDC transmission line caused by flashover to ground fault. Power Syst Technol. 2009;33(4):6–10.
16. Zhou P, Lv J, Dai M, et al. Slow front overvoltage and insulation coordination of ±800 kV UHVDC transmission line. High Volt Eng. 2009;35(7):1509–17.
17. Deng J, Xiao Y, Fan Y, et al. Calculation method of distributed parameters and application of DC projects in HVDC transmission lines based on two phase power. Resource. 2015;41 (7):2451–6.

Chapter 17
Lightning Overvoltage of UHVDC Transmission System

Pan Dai, Hao Zhou and Bincai Zhao

Compared to HV and EHVDC transmission lines, the UHVDC transmission line has characteristics of longer line, higher tower, and higher operating voltage of the conductors, being unbeneficial to the lightning protection. The experience in operation of several DC lines in China shows that lightning issue for the ±500 kV DC lines is serious, because its lightning flashover rate is higher than 500 kV AC lines with approximate voltage level. Thus, it is required to attach importance to carry out research on the lightning protection during construction of UHVDC projects. This chapter presents a discussion on lightning protection of UHVDC transmission line and DC converter station.

P. Dai (✉)
State Grid Zhejiang Economic Research Institute,
Hangzhou, Zhejiang, People's Republic of China
e-mail: 21429095@qq.com

H. Zhou
College of Electrical Engineering, Zhejiang University,
Xihu District, Hangzhou, Zhejiang, People's Republic of China
e-mail: zhouhao_ee@zju.edu.cn

B. Zhao
State Grid Weifang Power Supply Company,
Weifang, Shandong, People's Republic of China
e-mail: zhaobincai@126.com

© Zhejiang University Press, Hangzhou and Springer-Verlag GmbH Germany 2018

H. Zhou et al. (eds.), *Ultra-high Voltage AC/DC Power Transmission*,
Advanced Topics in Science and Technology in China,
https://doi.org/10.1007/978-3-662-54575-1_17

17.1 Lightning Protection of UHVDC Transmission Line

17.1.1 Main Differences in Lightning Protection of AC and DC Lines

Compared to the AC lines, the DC line is unique in line structure and arrangement, the development process of lightning accidents and other aspects, so lightning protection characteristics of AC and DC lines are different. The following gives a brief introduction for main difference in protection action mode, lightning protection indexes, lightning protection calculation method, etc. [1, 2].

1. Protection action method after lightning flashover

For the AC transmission line, after insulation flashover caused by the line being subjected to lightning strike and arcing, the relay protection is actuated and the circuit breaker is tripped immediately to shut off the fault current. If an automatic reclosing device is provided, the reclosure operation will be completed within specified time to recover power supply of the line.

The protection of DC line is actuated by a method different from the AC line. After the DC line is subjected to lightning strike, which causes an insulation flashover, the control and regulating system is actuated to complete the voltage drop, de-energization, restart, and other processes quickly and automatically by regulating the trigger angle on the rectifier side, and lastly recover power supply. Being similar to automatic reclosure measures of the AC system, the DC system can also be protected by means of "voltage drop before restart" or "automatic restart for several times" to improve restart success rate.

2. Lightning protection index

First, the definition of lightning protection indexes is different for the AC line and the DC line. For the AC transmission line, the "lightning trip rate" is taken as a main technical index for measuring the lightning withstand performance; however, the DC line is free from the tripping problem of circuit breaker, so no "lightning trip rate" concept exists. Moreover, unlike the cyclic zero crossing of conductor voltage in the AC line, the voltage on the DC conductor is kept constant. Typically, it can be deemed that the DC line is arced stably following insulation flashover. Therefore, the "lightning flashover rate" is taken as a technical index for lightning protection of the DC line.

Secondly, the basis for determining lightning protection indexes of AC and DC lines is not totally the same. The determination of lightning protection indexes for the AC line is mainly limited by the principle of operating resources for the circuit breaker (namely allowable actuation times within one overhaul period for the circuit breaker) and workload for line maintenance; however, the control and regulating system of the DC line is not limited by operating times, and the lightning protection indexes are determined mainly by workload for line maintenance. The "workload for the line maintenance" is the economic and time cost required for investigation of

Table 17.1 Statistics of lightning damage for ±500 kV DC lines by state grid corporation (2004–2007)

Description of line	Line length (km)	Times of lightning flashover					Lightning flashover rate (times/(100 km·a))
		2004	2005	2006	2007	Total	
Gezhouba–Nanqiao	1045	4	0	3	4	11	0.26
The three Gorges–Changzhou	895	1	2	1	4	8	0.22
The three Gorges–Guangzhou	940	1	2	4	4	11	0.29
The three Gorges–Shanghai	1070	/	/	/	5	5	0.47
Total: 12,590 km·a				Total: 35 times/4a			0.28

the fault point along the line by the operator and replacement of the burned insulator in accordance with the requirements specified by the China's DC operation department.

Lastly, according to the lightning statistic data between 2004 and 2007 for the ±500 kV DC lines owned by the State Grid Corporation (as shown in Table 17.1), it can be known that the lightning flashover rate for the ±500 kV DC lines reaches 0.28 times/(100 km·a), being far higher than the operating statistic value 0.14 times/(100 km·a) that of the lightning trip rate for the 500 kV AC lines. By making a reference to the data above, the lightning shielding of the UHVDC line may be severe, and the lightning flashover rate may be difficultly decreased to the control level of the UHVAC line; however, considering that the control and regulating system of the DC line is not limited by operating times, the control index for the lightning flashover rate of the UHVDC line can be relaxed appropriately.

3. Damage resulting from lightning fault

The difference in hazard resulting from a lightning fault is mainly due to the operation independence of both poles for the DC line. After the DC line is subjected to a lightning strike, the non-fault pole of the DC line can still be operated normally even if the fault pole cannot be restarted successfully, half or more power capacity can be transmitted continuously; however, in the event that the AC single-circuit line is subjected to a lightning fault and the reclosure cannot be completed successfully, the conductors at three phases will be tripped off.

The difference in hazard resulting from lightning flashover includes the difference in short-circuit current of AC and DC lines after lightning flashover, so as to result in different damages to the insulators and fittings. Generally, the short-circuit current of the AC line is larger than that of the DC line. The calculation shows that the short-circuit current of single-phase ground on the AC line ranges from several thousands of amperes to 30 kA, while the short-circuit current of single-pole grounding on the DC line is often not more than 20 kA.

4. Calculation method of lightning protection

Similar to the UHVAC line, the calculation method of lightning protection for the UHVDC line is also fallen into shielding failure and back flashover methods. Among them, it is recommended to use the electro-geometric model (EGM) method recommended by the IEC, IEEE, and other international organizations for shielding failure calculation of the UHVDC line; it is also recommended to use the EMTP software used by most of the countries worldwide to calculate back striking.

However, it is worthwhile to note that partial calculation parameters of lightning protection, such as operating voltage, 50% flashover voltage of insulator string, and arcing rate, should be considered particularly because the DC pole line is operated at a constant voltage.

The pole operating voltage of the UHVDC line is kept constant and its magnitude remains very high and has reached about 15–20% of 50% flashover voltage of the line insulators, which should be taken account of. Especially when calculating the probability of simultaneous flashover at both poles, the calculation result will get higher if the pole line operating voltage is not taken into account. During specific lightning protection calculation, the conductor voltage of the AC system is usually analyzed by use of peak value, effective value, or adopting statistic method, while a real value can be taken for the DC line.

With respect to the influence of the DC voltage on 50% flashover of the insulator string, the test results obtained from other countries' research institutes show that, regardless of dry or rainy condition, the heteropolarity DC voltage gets 50% flashover voltage of the insulator string reduced by slightly less than such DC voltage. When the pole line operating voltage U_n is within 300–600 kV, it is able to calculate the actual 50% flashover voltage of the insulator string by Eq. (17.1). The lightning protection of the UHVDC line can be calculated by making a reference to Eq. (17.1):

$$U'_{50\%} = U_{50\%} - U_n + 100, \tag{17.1}$$

where

$U_{50\%}$ is the 50% flashover voltage without influence by U_n, represented in kV.
$U'_{50\%}$ is the 50% flashover voltage with considering the influence of U_n, represented in kV.

Besides, the pole line operating voltage is very high for the UHVDC line. Generally, it can be deemed that the lightning flashover can lead to arcing, so the arcing rate η can be set to 1.

5. Other lightning withstand characteristics

With respect to the bipolar DC line, its operating voltage at positive and negative poles is contrary, and most lightning electricity in the nature is negative, making the positive pole of the DC line more liable to lightning strike. The lightning shielding failure and back flashover characteristics of the DC line are highly different from the AC line.

For the lightning shielding of the line, because more than 90% lightning strikes present negative polarity, the positive pole will be more liable to lightning shielding failure. For the AC line, however, the operating voltage of the conductors being symmetrical at both sides is alternated regularly, so the lightning shielding probability is usually identical.

For back flashover of the line, because the lightning strikes usually present negative polarity, the insulator of the positive pole line is more liable to flashover; however, the back flashover probability of the conductors being symmetrical at both sides of the AC line is identical. In addition, the unbalance factor resulting from the pole line voltage is bigger (e.g., the UHVDC can reach approx. 1600 kV), the probability of back flashover occurred in negative and positive pole lines simultaneously is low, and the power supply reliability is usually superior to the AC double-circuit line with a same tower and adopting unbalanced insulation.

17.1.2 Characteristics of Lightning Withstand Performance for UHVDC Line

Compared to HV and EHVDC lines, the lightning withstand performance characteristics of the UHVDC line are as follows [3, 4]:

(1) Small back flashover probability

Due to very high insulation level of the UHVDC line, the back flashover lightning protection level usually can reach above 250 kA. However, the probability of a cloud-to-ground lightning current amplitude more than 300 kA is very thin, so the probability of a back flashover resulting from a lightning strike to the overhead ground wire or tower top is very low.

(2) The lightning flashover of the line is dominated by shielding failure

The causes mainly include the following two aspects: ① the tower of UHV line is higher, making the lightning shielding probability increased; ② the operating voltage on the UHV lines and conductors is so high that the lightning strike is caused for the reason that the leader is developed upward in advance on the conductor with polarity opposite to the thundercloud, making the lightning shielding probability increased.

More than 90% cloud-to-ground lightning strikes in the nature present negative polarity, so the positive conductor of the UHVDC line has an obvious lightning effect. Thus, the probability of lightning shielding occurred in the positive conductor is far higher than the negative conductor. Additionally, the experience in practical operation of China's ±500 kV DC transmission lines also shows that the positive conductor is more liable to lightning shielding.

To sum up, the lightning protection characteristics of the UHVDC line are as follows: the UHV line, in spite of its high insulation level, is still immune from the

lightning disturbances; the lightning disturbances are primarily caused by shielding failure, and the probability of back flashover is very small. Moreover, most lightning shielding flashovers occur on the side of the positive conductor.

17.1.3 Analysis of Lightning Protection for the ±800 kV UHVDC Transmission Line

Now, the Yunnan–Guangdong ±800 kV UHVDC transmission project undertaken by the China South Power Grid Corporation is taken as an example for calculating and analyzing the lightning withstand performance of the UHVDC line, and carrying out a research on the lightning protection effect of such lightning protection measures as reducing protection angle of overhead ground wires, decreasing the ground resistance of towers, increasing insulation level of lines, etc.

The Yunnan–Guangdong ±800 kV UHVDC line adopts a bipolar symmetrical arrangement, with a typical ZV2 tower, as shown in Fig. 17.1. In the transmission line, the conductor adopts the type of 6× LGJ-630/45 steel-cored aluminum strand, with a split spacing of 450 mm; the overhead ground wire adopts LBGJ-180-20AC

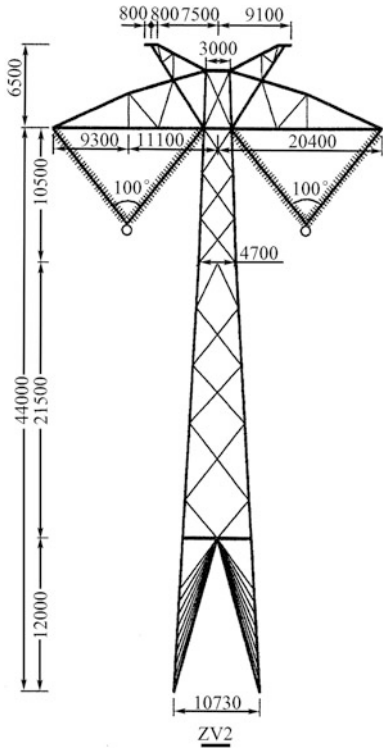

Fig. 17.1 Diagram for type ZV2 towers of Yunnan–Guangdong ±800 kV UHVDC transmission project (the values in the figure are in mm)

aluminum clad steel strand; the sag of the conductor and overhead ground wire is 16 and 11 m, respectively. Additionally, the line insulation adopts 64 pieces of porcelain insulators with a height of 170 mm, and the horizontal span between towers is 510 m.

17.1.3.1 Analysis for Lightning Withstand Performance of Shielding Failure

With respect to the tower type shown in Fig. 17.1, the shielding flashover probability N_{Dr} is calculated for the Yunnan–Guangdong ±800 kV UHVDC line, with the results shown in Table 17.2 [the cloud-to-ground lightning flash N_g is 2.8 times/(100 km^2·a)].

From Table 17.2, it can be known that, in existing conditions, the shielding failure rate of the line is 0 time/(100 km·a), meeting the expected limiting index of the lightning flashover rate. The type ZV2 tower has excellent lightning withstand performance of shielding failure, which is mainly because the tower height is lower (compared to that for the UHVAC system) and the insulation level is higher.

A part of line corridor for the Yunnan–Guangdong ±800 kV DC transmission line goes through Southwest China featuring complex landform, strong lightning, and high soil resistivity, so the various lines' lightning withstand performance of shielding failure may be different. Here gives a calculation for the line's flashover rate of shielding failure in such conditions as different ground inclination angles, nominal height of towers, insulation levels, and protection angle of overhead ground wire, with calculation results shown in Figs. 17.2 and 17.3.

From the calculation results, it can be known that, under the premise that other conditions are kept unchanged, the line's shielding failure flashover rate increases as the ground inclination angle or nominal height of tower increases, so decreasing the protection angle of the overhead ground wire and increasing the insulation level of the line can reduce the shielding failure flashover rate effectively. It is noted that the insulation level of the UHVDC line is mainly determined by the anti-pollution flash, and considering such adverse influences as increase in tower head size and tower height resulting from longer insulator string, the increase in insulation level is usually not taken as a main measure for improving the line lightning protection of shielding failure flashover. Therefore, being similar to the AC line, decreasing the protection angle of the overhead ground wire is the most effective measure to reduce the line's shielding failure flashover rate.

Table 17.2 Shielding failure flashover rate of Yunnan–Guangdong ±800 kV UHVDC line

Type of tower	Tower height (m)	Protection angle (°)	Ground inclination angle (°)	Shielding failure flashover rate (time/(100 km·a))
ZV2 tower	50.5	6.7	0	0

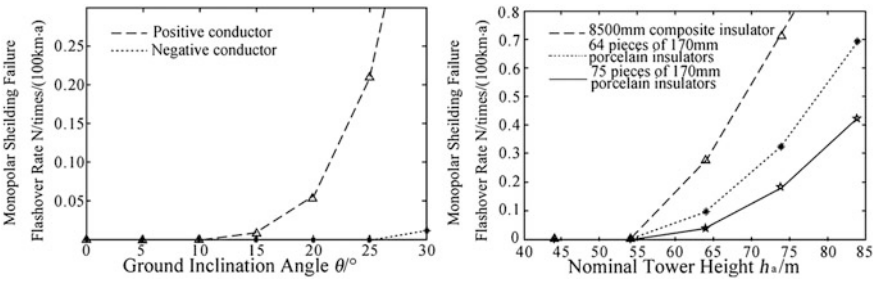

Fig. 17.2 Flashover rate of shielding failure for transmission line under different ground inclination angles, insulation levels, and tower heights

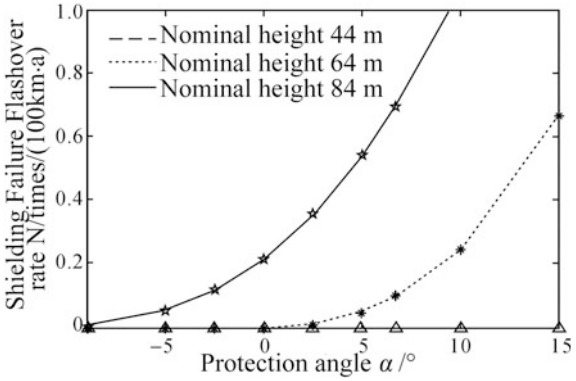

Fig. 17.3 Influence of overhead ground wire protection angle on shielding failure flashover rate of UHVDC line

In addition, it can be known from Fig. 17.2 that the shielding failure flashover rate of the positive conductor is much higher than the negative conductor, which is aligned with the experience in operation of ±500 kV DC lines.

Therefore, it is required to pay particular attention to lightning protection of shielding failure for the lines in mountain areas with a large ground inclination angle, a higher tower height, and a high intensity of lightning activities. Continuous line stringing in mountain areas should be avoided as far as possible, especially for the line with a large ground inclination angle or high tower. It is suggested to improve the anti-shielding failure performance of the line by adopting a smaller negative protection angle or installing side lightning rod of line type and other means.

17.1.3.2 Analysis for Lightning Withstand Performance of Back Flashover

Being similar to the UHVAC line, the UHVDC line has a higher insulation level, so that the lightning withstand level of back flashover is 250 kA and more, and the probability of back flashover is very small. For the Yunnan–Guangdong ±800 kV UHVDC line, where the tower grounding resistance is 15 Ω based on the principle of strictness, the lightning withstand level of back flashover and the flashover rate of the corresponding typical tower type are shown in Table 17.3.

It can be known from the calculation results that, even if the tower grounding resistance is 15 Ω, the lightning withstand level of back flashover for the Yunnan–Guangdong ±800 kV UHVDC line is still up to 401 kA, and the back flashover rate is only 0.0003 time/(100 km·a). Therefore, the lightning withstand level of back flashover is very high, and the probability of back flashover is very small, which is caused by lightning strike on tower or its neighboring overhead ground wire.

In addition, the calculation results show that the magnitude of the lightning current resulting in back flashover at both poles simultaneously in the UHVDC line is very high, and considering that the ±500 kV bipolar DC lines in China have not been subjected to flashover disturbance at both poles simultaneously, it can therefore be thought that the probability is zero.

In order to comprehensively evaluate the lightning withstand level of back flashover on the UHVDC line, it is calculated under conditions of different tower grounding resistance, nominal tower height, and insulation level, respectively, with the results shown in Fig. 17.4. It can be known from the calculation results that, for the purpose of ensuring that the UHVDC line's lightning withstand level of back flashover is not less than 300 kA, the grounding resistance of the type ZV2 tower should not be more than 30 Ω; the line's lightning withstand level of back flashover is decreased obviously as the tower height increases; considering that the ordinary composite insulator's structural height is lower, and the high and ultra-high towers provided in the whole line, it is suggested for lightning protection of the line to use porcelain insulators with a higher withstand voltage of lightning impulse, or consider lengthening the composite insulators properly.

Table 17.3 Back flashover rate of Yunnan–Guangdong ±800 kV UHVDC line

Type of tower	Tower height (m)	Grounding resistance (Ω)	Back flashover lightning withstand level (kA)	Back flashover rate (time/(100 km·a))
ZV2 tower	50.5	15	401(645)	0.0003

Note The lightning withstand level of back flashover in the parentheses is the lightning withstand level when the both poles are subjected to back flashover

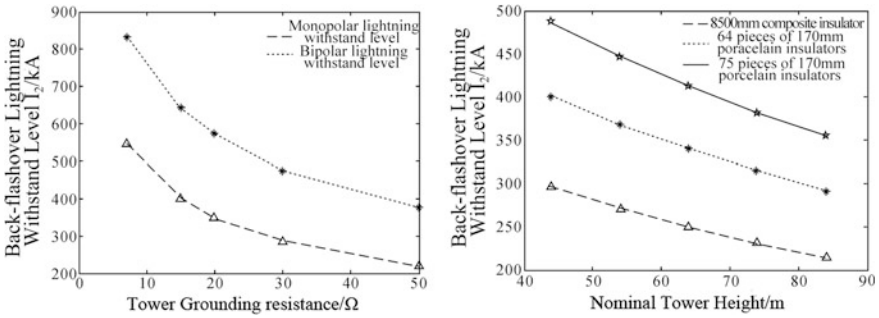

Fig. 17.4 Influence of tower grounding resistance, insulation level, and other factors on line's lightning withstand level of flashover

17.2 Lightning Protection of UHVDC Converter Station

Being identical to the ordinary AC substation, the lightning overvoltage of the DC converter station comes from a direct lightning strike to the facilities in the substation and a lightning impulse from the overhead line. The protective measures for direct lightning of the converter station is also to install lightning rods or overhead ground wires, and it is required to pay close attention to take measures against the back flashover lightning. China's UHVDC converter station and UHVAC substation are often provided with lightning rods and overhead ground wires. By making a reference to China's years of experience in ±500 kV DC converter stations, where the converter station is designed and installed with lightning rods, overhead ground wires, and grounding devices properly in accordance with the corresponding procedures, its direct lightning protection effect is reliable.

The lightning damages of the UHVDC converter station are mainly derived from the lightning invasion wave of the overhead line [5].

17.2.1 Protection Characteristics of Lightning Invasion Wave for DC Converter Station

The lightning invasion wave protection of the DC converter station has not substantial difference from that of the AC substation. However, due to co-existence of AC and DC in the DC converter station, the substation structure is more complicated, and the voltage level and insulation level of equipment in the substation differ significantly, so the design of lightning protection is more complicated than the AC substation.

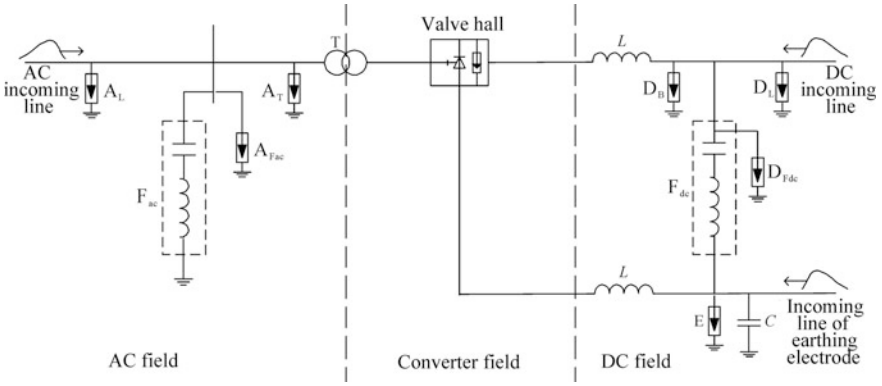

Fig. 17.5 Sketch for overvoltage protection of lightning invasion wave in UHVDC converter station

According to AC/DC areas and severity of the lightning invasion wave, the DC converter station is divided into AC field, DC field, and converter field, as shown in Fig. 17.5.

1. AC field

The AC field represents the area from the AC transmission line inlet to the line terminal of the converter transformer. The lightning invasion wave of the AC field comes from the AC transmission line.

Compared to the 500 kV AC substation, the AC field of UHVDC converter station has more outgoing lines and is connected with several capacitor banks, AC filter banks F_{AC}, PLC, etc., as well as is provided with arresters A_L, A_{Fac}, A_T, etc. at incoming line inlet and on the filter busbar and converter transformer, so the lightning overvoltage in the AC field of the converter station is less serious than that in the AC substation [6].

2. DC field

The DC field area represents the area from the DC transmission line inlet to the terminal at the valve side of the smoothing reactor. The lightning invasion wave of the DC field comes from the DC transmission line and ground electrode line (or metallic return).

With respect to the pole line in the DC field, because the DC line, busbar, DC filter, and other equipment are installed with arresters D_L, D_B, D_{Fdc}, etc. and the pole busbar is connected with DC filter F_{dc}, PLC, etc., the lightning overvoltage on the pole line is usually less serious; however, it is probable that a higher overvoltage occurs on the smoothing reactor due to lightning invasion wave.

With respect to the ground electrode line in the DC field, because the neutral busbar is installed with several banks of arresters E and the neutral busbar is connected with an impulse absorption capacitor C, the lightning overvoltage on the ground electrode line is usually less serious, either.

3. Converter field

The converter field represents the area from the terminal at the valve side of the converter transformer to the terminal at the valve side of the smoothing reactor.

The converter field is protected by the converter transformer in the AC field and smoothing reactor in the DC field, and the magnitude value of the actual lightning overvoltage is lower, which is transmitted to the valve hall through the capacitor between coils and turns, and its waveform is more similar to a switching impulse, so the lightning intruding overvoltage in the converter field is usually not taken into account.

It can be known from the above discussion that, during research on lightning intruding overvoltage in the UHVDC converter station, the emphasis should be placed on the analysis of the DC field and AC field, and that the converter field (valve hall) is typically neglected.

17.2.2 Calculation Method for Lightning Intruding Overvoltage in DC Converter Station

The lightning intruding overvoltage of the UHVDC converter station is calculated usually by use of the international electromagnetic transient program EMTP. The calculation method is basically identical to that for the AC substation.

However, having regard to such characteristics as co-existence of AC field and DC field, complex operation, and big difference in insulation level of equipment in the DC converter station, the operating mode, lightning current amplitude, and other aspects should be selected to reflect their uniqueness during calculation of lightning invasion wave for the converter station, which are instructed as follows:

17.2.2.1 Selection of Operating Mode

The UHVDC converter station can be operated by many operating modes, including bipolar operating mode in full voltage, bipolar operating mode in half voltage, bipolar operating mode with one pole in full voltage and the other in half voltage, monopolar operating mode in full voltage with metallic return, monopolar operating mode in full voltage with ground return, monopolar operation in half voltage with metallic return, and monopolar operating mode in half voltage with ground return, and the selection of the operating mode of the AC field is directly related to selection of the operating mode of the DC field. Therefore, selection of a rational operating mode of the converter station is critical to the calculation of lightning invasion wave by use of a conventional method.

1. Selection of operating mode for the AC field

By making a reference to experience in operation of the AC substations, the more the number of outgoing lines and equipment (such as transformers and AC

filters) put into operation in the AC field of the DC converter station are, the lower the overvoltage of lightning invasion wave applied on the AC field equipment is. Corresponding to typical operation condition of the DC field in the UHVDC converter station—DC monopolar operation in full voltage, the lightning protection level of the AC field is calculated by selecting an operating mode that the monopolar double 12-pulse converter transformer and a minimum number of filter banks are put into operation (the minimum number of filter banks should meet normal operation requirement).

In addition, where the DC converter station is operated in bipolar or monopolar operating mode in half voltage, the AC field should be operated in such a mode that the monopolar single 12-pulse converter transformer and a minimum number of filter banks are put into operation, based on the principle of strictness.

2. Selection of operating mode for the DC field

First, it should be noted that, for the DC field in the converter station, the maximum overvoltage of lightning invasion wave applied to the equipment in the station will not appear necessarily in case of a homopolarity lightning strike. Unlike calculation for overvoltage of lightning invasion wave in the AC field, because the smoothing reactor, PLC and DC filters, and other equipment in the DC field of the converter station are connected with inductive components in series, the lightning strike may lead to a high overvoltage magnitude stressed on the inductive equipment; thus, the research on lightning invasion wave of the DC field requires calculating not only the equipment voltage to ground, but also the overvoltage stressed on the equipment to confirm whether the requirement is met. It should be noted that the maximum equipment voltage to ground usually occurs in the condition where polarity of the lightning invasion wave is identical to that of operating voltage of the equipment (namely polarity of the DC voltage is identical to the lightning current, and the overvoltage value reaches the maximum level by adding the two voltages); however, the maximum overvoltage stressed on the equipment usually occurs in the condition where the polarity of the lightning invasion wave is contrary to the operating voltage polarity (namely the DC voltage is opposite to the lightning current with respect to their polarity). Meanwhile, for the reason that the probability of the negative lightning current in the nature usually remains above 90%, and the negative lightning should be selected for calculation of lightning protection level for the converter station. Therefore, when calculating the maximum equipment voltage to ground, the DC operating voltage of the pole busbar should be of negative polarity; when calculating the maximum voltage stressed on the equipment, the DC voltage should be of positive polarity.

In view of different insulation levels and invasion wave sources of the pole busbar and neutral busbar in the DC field, the calculation for lightning invasion wave of the DC field is divided into two parts, including pole busbar overvoltage and neutral busbar overvoltage.

(1) Selection of operating mode for calculating lightning overvoltage of the pole busbar

For the lightning overvoltage of the UHVDC pole busbar, it is required to select the monopolar negative operating mode with ground return for calculating the equipment overvoltage to ground caused by lightning invasion wave based on the principle of strictness, and monopolar positive operating mode with ground return for calculating the overvoltage of lightning invasion wave stressed on the equipment. In practical, however, the lightning damages for UHVDC mainly means the lightning shielding failure on the positive conductor, and the probability of the lightning shielding failure on the negative conductor is very small.

For the DC filter banks, based on the principle of strictness, only one bank is put into operation and the other one gets out of service for maintenance.

(2) Selection of operating mode for calculating lightning overvoltage of the neutral busbar

For the lightning overvoltage of the UHVDC neutral busbar, the lightning invasion wave source mainly includes ground electrode line or metallic return line. In order to prevent insulator string breakage accidents, arcing horns are provided at both ends of the insulator string for the ground electrode line. Taking Suidong Converter Station of the Yunnan–Guangdong UHVDC Transmission Project as an example, the air gap between arcing horns of the ground electrode line is about 0.5 m, and even 90% breakdown voltage is only 320 kV, so the overvoltage magnitude is very low, which is caused by the lighting intruding in the neutral busbar through the ground electrode line.

However, the tower where the metallic return is placed is far higher than the ground electrode tower, being more liable to lightning strike. And the insulation level of the metallic return is far higher than the ground electrode, and the magnitude of lightning overvoltage intruding into the converter station from the metallic return gets higher; thus, the lightning invasion wave on the neutral busbar is calculated by selecting the monopolar operating mode with metallic return. Furthermore, because the operating voltage on the metallic return is very low, which is only several thousand volts, its polarity can be neglected.

To sum up, the operating modes selected to calculate the overvoltage of lightning invasion wave in the UHVDC converter station can be summed up as follows:

AC field: Single line or monopolar converter transformer or minimum number of filter banks put into operation

DC field
- The pole busbar
  - The voltage of equipment to the ground: monopolar positive operating mode with ground return
  - The voltage at both terminals of equipment: monopolar negative operating mode with ground return
- The neutral busbar: monopolar operating mode with metallic return

When calculating overvoltage of the pole busbar, it is required to pay attention to differentiate the equipment voltage to ground and voltage at both terminals of the equipment.

17.2.2.2 Selection of Lightning Current Amplitude

The lightning overvoltage on the equipment of the substation or converter station is proportional to the steepness α of invasion wave front, while the standard wave front time of the lightning invasion wave specified in China's procedures is 2.6 μs, and the steepness α of the invasion wave front can be approximated to I/2.6 μs, so that the overvoltage of the equipment inside the station is proportional to the lightning current amplitude selected. Thus, selection of the lightning current amplitude is very important.

At present, however, China's relevant electric power standards are silent on specific requirements for the lightning current amplitude; when evaluating lightning invasion wave protection level of the DC converter station by a conventional method or carrying out design of insulation coordination of the equipment inside the station, scientific research institutions or design units still have discrepancies on the selection of the lightning current amplitude I. Due to the existence of this problem during calculation of lightning invasion wave for the AC and DC system, it is worthwhile to take further thinking and discussion.

1. Amplitude of back flashover lightning current

The amplitude of back flashover lightning current is selected usually according to the principle of "the higher the voltage level of the substation or converter station is, the smaller the probability of the back flashover lightning current is." First, an cumulative probability is selected according to the requirements for lightning protection reliability of the substation or converter station; then it is possible to calculate the amplitude value of back flashover lightning current using the probability distribution function of lightning current amplitude, and the function is specified in the procedures. However, this method has a certain randomness and blindness because the value taken by research institutions is different for the reason of being lack of relevant standards and references when selecting a cumulative probability of the lightning current amplitude. So the method for determining a value of the cumulative probability is to be further discussed.

Taking the Japan's experience as an example, the lightning current amplitude of back flashover for 500 and 1000 kV AC substation is 150 and 200 kA, respectively, and according to the probability distribution curve of lightning current amplitude as shown in Eq. (17.2), which is used by Japan, it can be known that the corresponding occurrence probability is $P(I > 150\ \text{kA}) = 0.3\%$ and $P(I > 200\ \text{kA}) = 0.1\%$ by inverse calculation.

$$f(I) = 0.0475\mathrm{e}^{(-I/120)} + 0.001\mathrm{e}^{(-I/150)} \tag{17.2}$$

According to Chinese overvoltage protection procedure DL/T 620-1997, *Overvoltage Protection and Insulation Coordination for AC Electrical Installations*, it can be inferred by the cumulative probability distribution (given by Eq. 17.3) of the lightning current amplitude that the lightning current amplitude of back flashover in China's 500 and 1000 kV AC substation should be I

($P = 0.3\%$) = 222 kA and $I(P = 0.1\%)$ = 267 kA, respectively. From the above, it can be known that compared to Japan's reliability requirements for lightning protection, the lightning current amplitude of back flashover in the 500 kV AC field in China's UHVDC converter stations is 250 kA, which is strict enough to ensure the system safety.

$$\log P = -\frac{I}{88}, \tag{17.3}$$

where

I is the lightning current amplitude, kA.
P is the occurrence probability of a lightning current amplitude more than I.

Additionally, the maximum lightning current of flashover is 250 kA (the lightning withstand level of back flashover required for the incoming line section should not be less than 250 kA) when calculating the overvoltage of lightning invasion wave in the UHV substation according to the GB/Z 2484-2009, *Overvoltage and Insulation Coordination of 1000 kV UHVAC Transmission Projects*. Under the premise of no relevant standards, the lightning current amplitude of back flashover in DC field of China's UHV converter station can be selected by making a reference to this value.

To sum up, the lightning current amplitude selected for calculating the lightning invasion wave of the AC and DC field in the UHV converter station is determined by making a reference to the GB standard for UHVAC projects, temporarily taken as 250 kA.

2. Amplitude of shielding failure lightning current

For the amplitude of the shielding failure lightning current, most research institutions usually consider the conductor's maximum lightning current I_{max} that causes shielding failure in the vicinity of towers, which are in the incoming line section.

It should be noted that, with respect to lightning protection design of shielding failure for the incoming line section of the substation or converter station, the procedure only gives the requirements for protection angle of the overhead ground wires in the incoming line section and does not present specific requirements for the allowable maximum lightning current that causes shielding failure. Due to different landform, tower design, and line insulation level in incoming line sections of the substation or converter station, the lightning current amplitude of shielding failure I_{max} may have a huge difference, which is considered during research on lightning protection. This will lead to a significant difference in the calculation results of lightning overvoltage or design scheme of insulation coordination for the same substation or converter station. Especially in case that the incoming line goes through a mountain area, and considering that the ground inclination angle may be bigger even though the protection angle meets the requirements specified in the procedure, the maximum current of shielding failure calculated by use of EGM still

can reach 30 kA or more. In this case, the design for the protection of lightning invasion wave in the substation or converter station is more difficult, that is to say, an excellent insulation coordination cannot be obtained between the substation and incoming line section. In addition, during the design of lightning protection for the substation or converter station, the lightning protection design of line and substation is usually completed by different designers, so the insulation coordination between the transmission line section and substation is often neglected. In order to obtain a better lightning protection of the substation or converter station, it is suggested that the industry standards provide specific requirements for the maximum lightning current of shielding failure in the incoming line section, so that the design for protection of shielding failure in the incoming line section can be standardized.

The experience shows that the shielding failure lightning current of the 500 kV AC line is usually less than 20 kA, but according to the requirements specified in the procedure the protection angle of the overhead ground wire in the incoming line section is usually less than the ordinary path line, so the lightning current of shielding failure in the incoming line section is smaller. Based on the principle of strictness, a reference can be made to such value with respect to the design of lightning protection in the incoming line section of the EHV and UHV substation or converter station, namely the design value is up to 20 kA, which is for the lightning current of shielding failure in the incoming line section. For the DC line, the lightning withstand level of shielding failure for the DC tower is usually not more than 20 kA.

Thus, it is possible to directly adopt a lightning current amplitude of 20 kA for shielding failure, if a conventional method is used to carry out an initial design of lightning protection for the EHV or UHV substation or converter station when the substation or converter station is at the initial design stage (the design of incoming line section is not completed).

In a word, the overvoltage of lightning invasion wave for the UHVDC converter station is calculated by use of the following lightning current amplitude:

For the AC field, the lightning current amplitude of the back flashover is 250 kA, and the maximum shielding failure lightning current in the vicinity of towers for the incoming line section is taken as the lightning current of shielding failure (it can be taken as 20 kA during the initial design of lightning protection for the converter station).

For the DC field, the lightning current amplitude of back flashover is 250 kA, I_{max} is the lightning current of shielding failure (it can be 20 kA during the initial design of lightning protection for the converter station).

17.2.3 Analysis for Overvoltage Protection of Lightning Invasion Wave in ±800 kV DC Converter Station

This section takes Suidong Converter Station on the inverter side of the Yunnan–Guangdong ±800 kV UHVDC Transmission Project as an example, a conventional method is used to carry out a research on the overvoltage of lightning invasion wave [7].

17.2.3.1 Calculation Parameters of Suidong Converter Station

During compilation of this book, the design of Suidong Converter Station is in the progress of feasibility study, and the type of equipment, which is in the incoming line section and inside the station, and specific arrangement scheme are not determined. Some calculation parameters given below may be slightly different from the actual condition.

1. Calculation parameters for the AC field of Suidong Converter Station

(1) Main electrical connection of the AC field

Based on the principle of strictness, Suidong Converter Station is operated in DC monopolar mode, and the corresponding 500 kV AC system is operated in such mode that the single AC incoming line/single busbar/two AC filter sub-banks are put into operation. The diagram for main electrical connection of the AC system is shown in Fig. 17.6. The AC side of Suidong Converter Station has 6 circuits of AC incoming lines, of which only one line, Zengcheng B, is put into operation for delivering power to the converter transformer of pole 1, based on the principle of strictness; the busbar II gets out of service for maintenance, and among the two busbars, only the busbar I is put into operation; for the purpose of meeting the requirement of using the minimum amount of filter banks, two filter sub-banks selected from the #4 AC filter bank are put into operation; the substation transformers get out of service.

With respect to the AC side equipment, the AC filter FL and AC noise filter PLC can use an equivalent physical model directly, and other AC side equipment, such as converter transformer, voltage transformer, and circuit breaker, can be equivalent to the capacitance of impulse inlet, as well as components are connected to each other with lines of distributed parameter. The values of equivalent inlet capacitance for equipment in lightning condition are shown in Table 17.4.

The AC noise filter PLC is installed at the valve side of the converter transformer, with electrical connection diagram as shown in Fig. 17.7. The parallel arresters of AC PLCs are operated at a continuous operating voltage of 36 kV, with volt–ampere characteristics shown in Table 17.5.

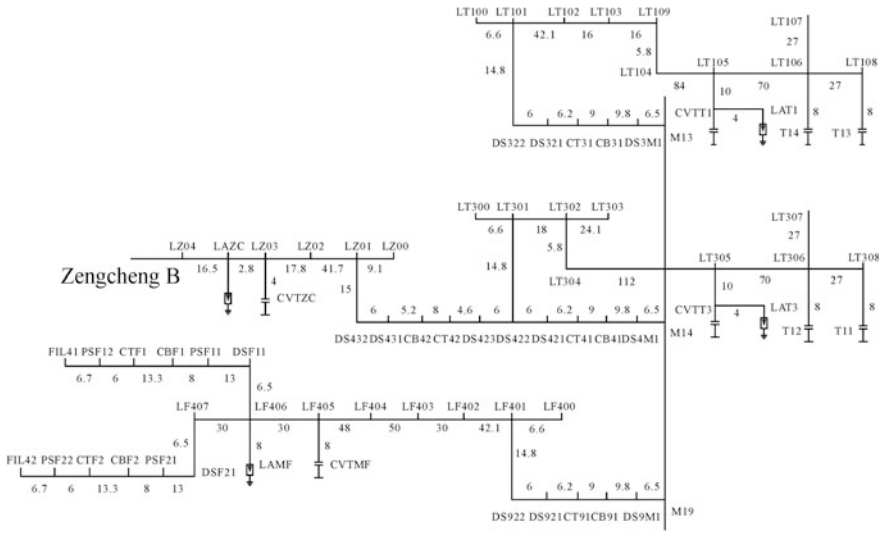

Fig. 17.6 Diagram for main electrical connection corresponding to lightning protection calculation of AC field in Suidong Converter Station

Table 17.4 Equivalent inlet capacitance of AC equipment (*unit* pF)

Description	Converter transformer T	Voltage transformer CVT	Current transformer CT	Circuit breaker CB
Inlet capacitance	5000	5000	80	300

Description	Disconnector DS	Support insulator PS	Filter FL
Inlet capacitance	150	150	500

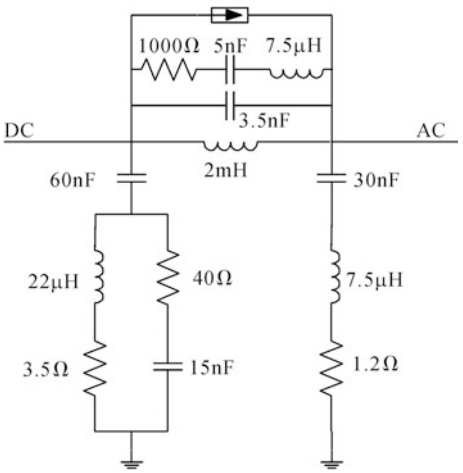

Fig. 17.7 Diagram for electrical connection of AC PLC

Table 17.5 Volt–ampere characteristics of AC PLC arrester

Current (8/20 μs) (kA)	5	10	15	20
Voltage (kV)	105	115	121	126

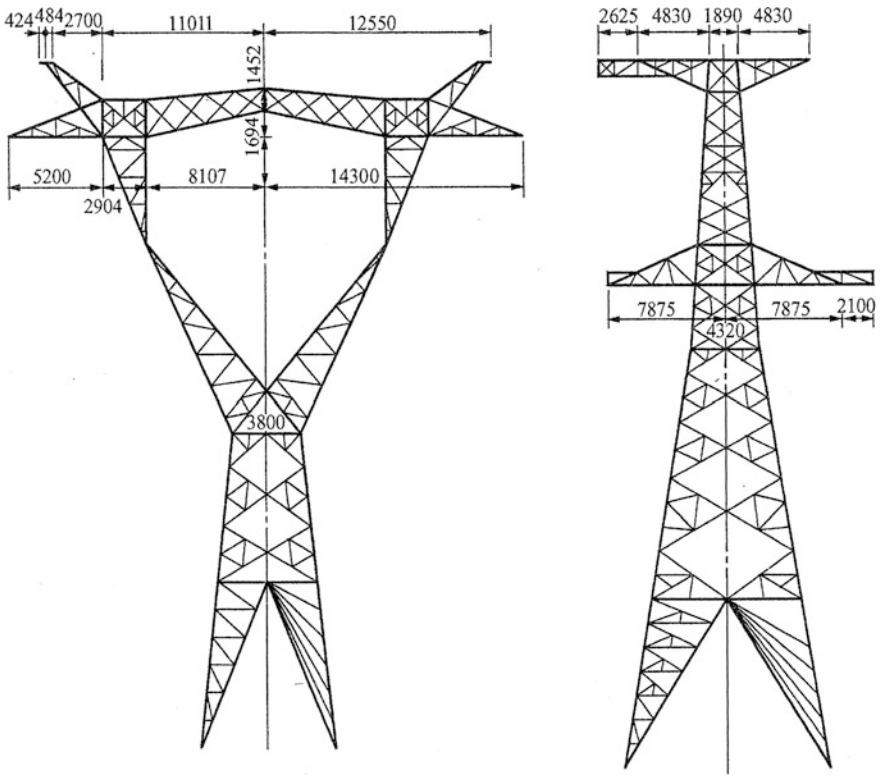

Fig. 17.8 Diagram for towers of AC line section in Suidong Converter Station (the values in the figure are in mm)

(2) Parameters of AC incoming line section

For the 500 kV AC incoming line section of Suidong Converter Station, #1 tower is a strain tower, and the towers from #2 are straight line towers, with typical tower type as shown in Fig. 17.8. The conductor is a 4× LGJ-720/50 steel-cored aluminum strand, with a split distance of 450 mm; the overhead ground wire adopts LBGJ-120-40AC aluminum clad steel strand and OPGW; the insulation of the #1 strain tower is 27 piece of insulators with a structural height up to 170 mm; the sag of the conductor and overhead ground wire is 2 and 1 m, respectively, and the span between #1 tower and portal tower is 70 m; the straight line tower adopts composite insulators with a structural height up to 4500 mm, and the sag of the conductor and overhead ground wire is 14 and 10 m, respectively, with a span of 450 m.

Table 17.6 Volt–ampere characteristics of MOAs in the AC field of Suidong Converter Station

Mounting position	Voltage rating (kV)	Residual voltage value under different discharge currents (kV)				
		0.001 kA	1 kA	3 kA	10 kA	20 kA
Line side	444	662	848	868	976	1063
Converter transformer side	420	629	778	825	936	1015

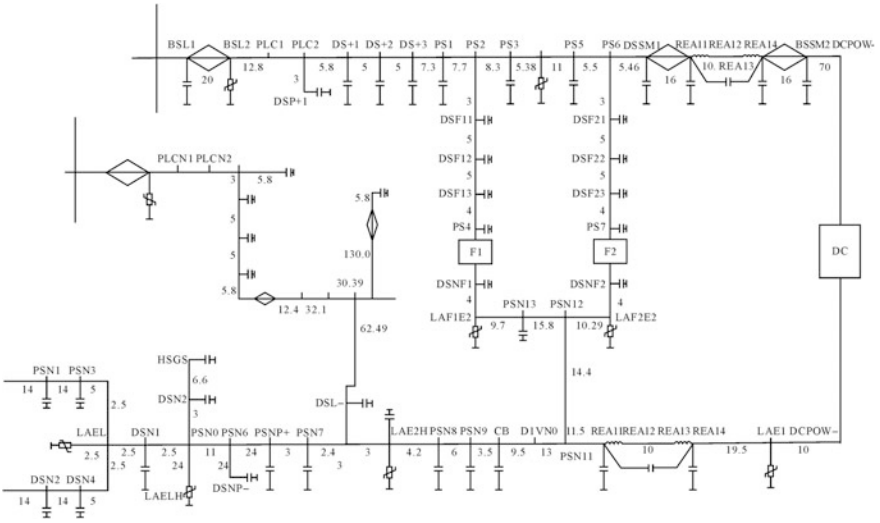

Fig. 17.9 Diagram for main electrical connection corresponding to lightning protection calculation of DC field in Suidong Converter Station

Additionally, the soil resistivity in the incoming line section is 100 Ω·m, and the tower ground resistance considered is 10 Ω.

(3) Arresters in AC field

According to the initial design scheme for Suidong Converter Station, MOAs are provided at the inlet of each 500 kV outgoing line beside each converter transformer, and the busbar is not installed with MOAs. The volt–ampere characteristics of the MOAs are shown in Table 17.6.

2. Calculation parameters for DC field of Suidong Converter Station

(1) Main electrical connection of DC field

Based on the principle of strictness, the lightning invasion wave of pole line is calculated by selecting the monopolar operating mode with ground return, and the lightning invasion wave of neutral busbar is calculated by selecting the circuit operating mode with metallic return. The main electrical connection of the DC field is shown in Fig. 17.9.

Table 17.7 Equivalent inlet capacitances of DC equipment (*unit* pF)

Description of equipment	Neutral busbar capacitor C	Voltage divider DIV	DC circuit breaker CB	Disconnector DS	Wall bushing BS	Support insulator PS
Inlet capacitance	1.5 × 107	300	300	300/150 (closed/open)	300	150

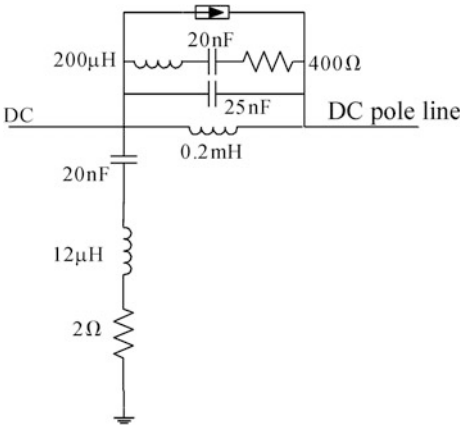

Fig. 17.10 Diagram for electrical connection of DC PLC

Table 17.8 Volt–ampere characteristics of DC PLC arrester

Current (kA)	0.5	5	10
Residual voltage (max.) (kV)	31	36	40

Similarly, with respect to the DC equipment, such as smoothing reactor REA, DC filter FL, and DC PLC, equivalent physical models can be used directly, and other DC side equipment are equivalent to impulse inlet capacitances, as shown in Table 17.7.

The DC PLC is installed at the DC line inlet, with electrical connection diagram as shown in Fig. 17.10. For the reason that no parameters of volt–ampere characteristic are available for the ±800 kV DC PLC arresters in parallel, the calculation is carried out temporarily based on the parameters for the 500 kV DC PLC arresters (lightening protection level is 40 kV/10 kA) obtained from the ABB company, with specific volt–ampere characteristics as shown in Table 17.8.

The tuned frequency of the DC filter is 12/24/36 times, and two banks of triple-tuned filters for each pole are arranged, with specific connection as shown in Fig. 17.11.

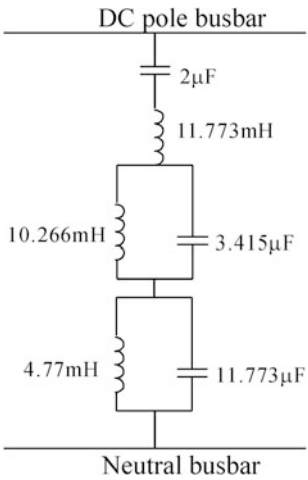

Fig. 17.11 Diagram for electrical connection of single-bank DC filter

(2) Parameters for incoming line section of DC pole and ground electrode line

With respect to Yunnan–Guangdong ±800 kV UHVDC line and ground electrode line, the #1 tower is a strain tower and other towers are straight line towers. The towers in the incoming line section are shown in Figs. 17.12 and 17.13, respectively.

The conductor for the DC line is a 6× LGJ-630/45 steel-cored aluminum strand, with a split distance of 450 mm; the overhead ground wire is an LBGJ-180-20AC aluminum clad steel strand; the sag of the conductor and overhead ground wire is 16 and 11 m, respectively. In addition, for the line insulation, the straight line tower adopts 62 pieces of porcelain insulators with a structural height of 170 mm, and the strain tower adopts four insulator strings in parallel, each composed of 60 pieces of insulators with a structural height up to 195 mm; the horizontal span between towers is 450 m.

The conductor type for ground electrode line is 2 × 2 × ACSR-720/50, with a split distance of 500 mm; the overhead ground wire is GJ-80; and the sag of the conductor and overhead ground wire is 10 and 8 m, respectively.

(3) Arrester in DC field

According to the initial design scheme for Suidong Converter Station, the arresters DL and DB for DC pole line are installed at the line side of the smoothing reactor and at the valve side close to the DC filter, which are used for lightning protection of DC busbar equipment, and whose volt–ampere characteristic parameters are shown in Table 17.9, type D. The arresters E1, E2, E2H, EL, and EM are arresters for neutral busbar, of which E1 is used to protect the equipment at valve bottom; E2 is used to protect equipment at the bottom of the neutral busbar capacitor and DC filter; E2H is made up of 5 type E arresters in parallel (other neutral busbar arresters

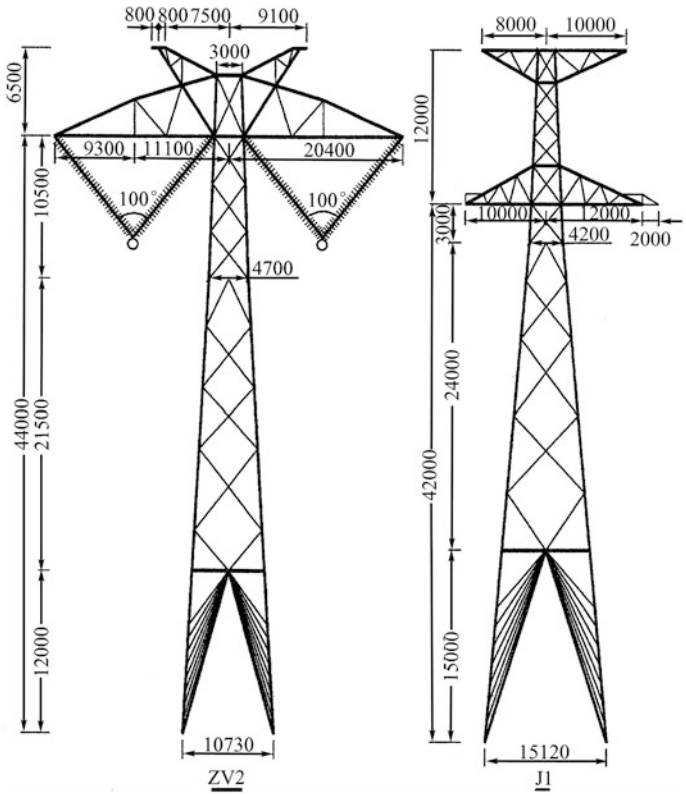

Fig. 17.12 Diagram for towers in incoming line section of Suidong Converter Station's DC line (the values in the figure are in mm)

are type E) and used to absorb overvoltage energy caused by switching; EL is installed at the inlet of ground electrode line; EM is installed in the metallic return line. Arresters SR are connected in parallel at both ends of the smoothing reactor on the DC busbar and used for lightning protection of the smoothing reactor. Arresters F_{dc1}, F_{dc21}, F_{dc22}, and F_{dc23} are installed in the branch of DC filter. The parameters for DC arresters are shown in Table 17.9.

17.2.3.2 Analysis for Overvoltage of Lightning Invasion Wave in the AC Field

For the purpose of analyzing the lightning withstand performance in the AC field of the UHVDC converter station, the typical operating mode "Single incoming line/monopolar converter transformer/minimum number of filters put into operation" is selected to calculate the overvoltage of lightning invasion wave caused by shielding failure and back flashover in the AC field, respectively.

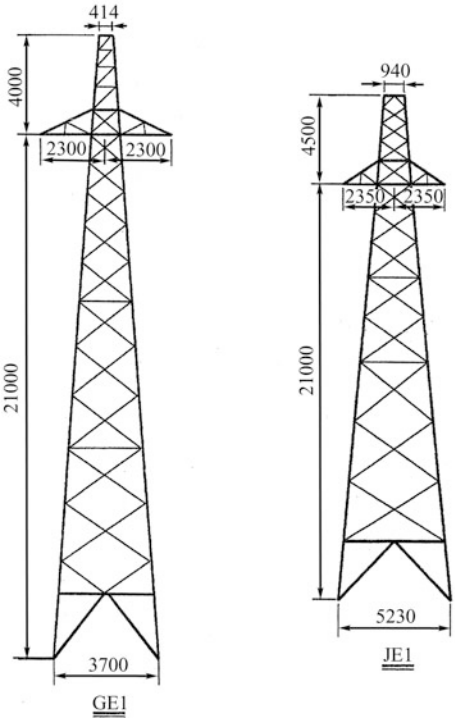

Fig. 17.13 Diagram for towers in incoming line section of Suidong Converter Station's ground electrode line (the values in the figure are in mm)

Table 17.9 Volt–ampere characteristics of DC arrester in Suidong Converter Station

Installation position of arresters	Type of arresters	Residual voltage under different discharge currents (kV)							
		1 kA	3 kA	10 kA	20 kA	80 kA	93 kA	99 kA	113 kA
DC pole	D	1365	1448	1580	1683	–	–	–	–
Neutral busbar	E	241	254	273	290	–	–	–	–
Smoothing reactor	SR	608	655	719	779	–	–	–	–
DC filter	F_{dc1}	–	–	–	–	544	–	–	–
DC filter	F_{dc21}	–	–	–	–	–	160	–	–
DC filter	F_{dc22}	–	–	–	–	–	–	143	–
DC filter	F_{dc23}	–	–	–	–	–	–	–	165

During calculation, having regard to the randomness of the magnitude of operating voltage and phase of the equipment in AC field, at the moment of lightning strike, the calculation results for overvoltage magnitude of equipment and discharge

current of the arresters listed below are the peak values obtained in the harshest condition of power frequency voltage [8, 9].

For the nominal lightning impulse withstand voltage of the equipment in AC field, a reference is made to the requirements for an ordinary 500 kV substation. For the converter transformer T, circuit breaker CB, and current transformer CT, the nominal lightning impulse withstand voltage is 1550 and 1675 kV for the busbar M, capacitive voltage transformer CVT, and disconnector DS.

1. Overvoltage of lightning invasion wave caused by shielding failure

It can be known from Sect. 17.2.2 that the amplitude of lightning current caused by shielding failure is usually considered as the maximum lightning current I_{max} that causes shielding failure of the conductors in the vicinity of the towers. According to the W'SEGM model proposed by Whitehead et al., I_{max} is directly related to the conductor arrangement (i.e., tower type) and ground inclination angle (i.e., landform). At present, however, for the reason that no data on landform of the incoming line section or accurate tower design is available, based on the principle of strictness, a lightning current amplitude of 20 kA is considered to calculate lightning invasion wave of shielding failure by a conventional method, and the lightning point is in the conductor close to the #1 tower.

For the purpose of comparing the lightning withstand performance of the AC field in the ordinary AC substation and DC converter station, the lightning intruding overvoltage is calculated in such conditions as DC monopolar operating mode in half voltage, with a minimum number of filter banks putting into operation but FL not being operated and PLC not being operated, etc., respectively. The calculation results are shown in Table 17.10.

Table 17.10 Overvoltage of lightning invasion wave caused by shielding failure in the AC field of converter station

Operation condition of equipment			Equipment overvoltage to ground (kV)						MOA current (kA)		
Operating voltage	FL	PLC	T	CVT	M	CB	PS	FL	T	L	MFL
Full voltage	Put into operation	Put into operation	840	998	957	959	883	884	3.4	10.9	5
Half voltage	Put into operation	Put into operation	858	1010	1013	1013	925	927	4.2	12	6.1
Full voltage	Out of service	Put into operation	852	1038	1028	1028	–	–	3.9	12	–
Full voltage	Put into operation	Out of service	835	998	951	952	898	901	3.1	10.9	4
Full voltage	Out of service	Out of service	846	1010	959	960	–	–	3.7	12	–

Note In the table, "M" denotes the busbar, "PS" denotes the support insulator, and "M_{FL}" denotes the filter busbar

From Table 17.10, it can be known that the overvoltage of invasion wave on equipment in the AC field is far less than the lightning impulse withstand voltage even though the AC busbar is not provided with arresters in the typical operating mode of "Single incoming line/monopolar converter transformer/minimum number of filters put into operation" and under the premise that the lightning current amplitude of shielding failure is taken as 20 kA, so the protection performance of lightning invasion wave in the AC field of the DC converter station is superior to the AC substation.

Besides, it can also be known that, compared to typical operating mode, the lightning overvoltage is higher in the DC monopolar operating mode in half voltage; putting the branch of the AC filter FL into operation helps improve the lightning performance of the AC field; although putting the PLC into operation gets some equipment's lightning overvoltage increased, it can reduce overvoltage on the FL branch to some extent. FL, PLC, and other equipment help improve the protection performance of lightning invasion wave in the AC field.

2. Invasion wave overvoltage of back striking

Being similar to the incoming line section of the AC substation, a back striking accident to #1 tower takes place less readily, because the distance between the #1 tower and the portal tower is usually less than 100 m. So the top of #2 tower is taken as the lightning point and the lightning current amplitude of the back striking is taken as 250 kA when using a conventional method to calculate the lightning invasion wave caused by back striking.

The calculation results for the equipment's overvoltage of lightning invasion wave caused by back striking in the AC field are shown in Table 17.11.

From Table 17.11, it can be known that, under the premise that the AC busbar is not provided with arresters, the overvoltage peak on the CVT equipment is the most serious, but is still within an allowable range (in view of 15% of safety margin coefficient, the allowable overvoltage of the CVT is 1675/1.15 = 1457 kV). The overvoltage on other equipment is far less than their rated lightning impulse withstand voltage, having an enough insulation margin.

From Tables 17.10 and 17.11, it can be known that, even though the calculation condition for calculation of the lightning invasion wave taken in this book is very harsh, the equipment's overvoltage of lightning invasion wave caused by back striking in the AC field of the UHVDC converter station is still much lower than that in an ordinary 500 kV AC substation, and the protection performance of lightning invasion wave is more excellent. In addition, a great amount of calculation results show that the 500 kV busbar of the AC field has no need to be provided with

Table 17.11 Equipment's overvoltage of lightning invasion wave caused by back striking in the AC side of converter station

Equipment voltage to ground (kV)						MOA current (kA)		
T	CVT	Bus	CB	PS	FL	T	L	MFL
877	1324	1128	1143	1078	1077	5.2	7.2	4.8

arresters. The recommended typical method for the arrangement of MOA in UHVDC converter station's AC field is as follows (this scheme should be checked by numerical calculation during practical application):

(1) One group of MOAs is provided at the inlet of each 500 kV line, being as close as possible to the high-voltage reactor and CVT.
(2) One group of MOAs is provided beside each converter transformer.
(3) One group of MOAs is provided on each AC filter busbar.

17.2.3.3 Analysis for Overvoltage of Lightning Invasion Wave in DC Field

It can be known from Sect. 17.1.3 that, even though the tower ground resistance is 30 Ω, the Yunnan–Guangdong ±800 kV UHVDC line's lightning withstand level of back flashover can be up to about 300 kA, so the probability of a lightning invasion wave caused by back flashover in the DC field is extremely low. Here we focus on researching overvoltage of lightning invasion wave caused by shielding failure in the DC field.

For the reason that no relevant standards are available for rated lightning impulse withstand voltage of the equipment in the DC field, the rated lightning impulse withstand voltage is set to 1950 kV for the equipment of DC pole line, such as pole line smoothing reactor REA, PLC, voltage divider DIV, disconnector DS, and pole line wall bushing BG, 650 kV for the neutral busbar bushing, and 450 kV for other equipment.

1. Overvoltage of lightning invasion wave for DC pole busbar

For the reason of being lack of topographical data in the incoming line section and based on the principle of strictness, a lightning current amplitude of −20 kA is taken for a conventional method to calculate the overvoltage of lightning invasion wave caused by shielding failure, and the lightning point is the conductor in the vicinity of #1 tower. Table 17.12 shows the overvoltage of lightning invasion wave on the pole busbar in various conditions, and the corresponding operating mode is monopolar operating mode with ground return.

It can be known from Table 17.12 that the maximum overvoltage of equipment to the ground in the DC field is only 1543 kV, the maximum overvoltage at both terminals of the equipment is only 1566 kV, and a safety margin of 20% (1950/1.2 = 1675 kV) is considered by making a reference to the IEC 60071-5, all equipment can meet the insulation requirements, in the harshest condition that all DC filter banks FL are not put into operation. In addition, the number of FLs has a significant influence on overvoltage of the DC field, and considering normal operation requirements, it is recommended to select the typical operating mode of putting a single filter bank into operation for calculating the lightning protection level in the DC field.

Table 17.12 Overvoltage of lightning invasion wave caused by shielding failure on pole busbar in converter station

Polarity of operating voltage	Negative polarity			Positive polarity		
Number of FLs	2	1	0	2	1	0
Voltage of equipment to the ground (kV)						
PLC	1508	1508	1538	1020	1173	1378
FL	1282	1368	–	1003	1126	–
DIV	1471	1471	1506	1013	1143	1369
DS	1293	1364	1491	1002	1133	1370
PS	1286	1364	1482	1001	1137	1370
BS	1513	1513	1543	1023	1176	1381
Voltage at the both terminals of equipment (kV)						
REA	363	493	917	360	584	1566
PLC	40	40	39	40	40	40
MOA current (kA)						
DL	6	6	7	0	0	5
DB	<1	1	4	0	0	1
PLC	15	15	10	19	18	15

Additionally, it can be known from Table 17.12 that the operation voltage polarity of the pole busbar has a significant influence on the calculation of equipment's overvoltage of lightning invasion wave in the DC field, which cannot be neglected. The maximum voltage of equipment to the ground occurs in the monopolar negative operating mode with ground return; the maximum voltage at both terminals of the equipment appears in monopolar positive operating mode with ground return. So, when calculating lightning invasion wave of the DC field, the monopolar negative operating mode with ground return should be selected for calculating the voltage of equipment to the ground, and the monopolar positive operating mode with ground return should be selected for calculating the voltage at both terminals of the equipment.

2. Overvoltage of lightning invasion wave on neutral busbar

Based on the principle of strictness, the lightning current amplitude of shielding failure is taken as 20 kA at the time of a lightning strike to the conductor in the vicinity of the #1 tower. The monopolar operating mode with metallic return is selected for calculating the lightning invasion wave on the neutral busbar, with the calculation results shown in Table 17.13.

It can be known from Table 17.13 that the maximum lightning overvoltage on the metallic return bushing BS_M is 902 kV, which is bigger than the rated lightning impulse withstand voltage (650 kV), and the overvoltage of other equipment meets requirements. This is because the low-voltage bushing BS_M on the metallic return has a lower lightning impulse withstand voltage; moreover, BS_M is far from the E_M arrester (approx. 100 m), which cannot be protected effectively, so it is suggested to install an arrester E_M beside the bushing of each metallic return.

Table 17.13 Equipment's overvoltage of lightning invasion wave caused by shielding failure on neutral busbar in converter station

Voltage of equipment to the ground (kV)						Voltage at both terminals of equipment (kV)		MOA current (kA)		
CB	C	PS	BS_M	BS	DS	PLC	REA	DL	EM	PLC
62	62	71	902	1075	1026	40	21	<1	8	19

Note In the table, BS_M denotes the bushing on the metallic return, BS denotes the pole busbar bushing, and DS denotes the disconnector switch on the pole busbar

To sum up, the lightning withstand voltage of the equipment in the DC field is acceptable under the premise that the nominal lightning withstand voltage of the equipment on the DC pole busbar and the neutral busbar is 1950 and 450 kV, respectively, obtaining a better lightning withstand performance.

References

1. Ying X, Shiheng X. Overvoltage protection and insulation coordination of AC power systems. Beijing: China Electric Power Press; 2006.
2. Xidong L, Changyu C, Yuanxiang Z. High voltage engineering. Beijing: Tsinghua University Press; 2004.
3. Zhida Z. Some considerations on lightning protection and insulation coordination of EHVDC overhead lines]. J Zhejiang Univ. 1984;2:1–7.
4. Zhida Z. Lightning performance analysis and lightning protection of HVDC overhead lines. J Zhejiang Univ. 1984;4:17–25.
5. Cuixia Z, Dong G, Yin Yu. Lightning protection of HVDC transmission system. High Volt Eng. 2008;34(10):2070–4.
6. DL/T 620-1997. Overvoltage protection and insulation coordination for AC electrical installations; 1997.
7. SIEMENS. Insulation coordination, Part 2 study report Tianshengqiao & Guangzhou Station.
8. GB/Z 24842-2009. Overvoltage and insulation coordination of 1000 kV UHV AC transmission and transformation project; 2009.
9. China Southern Power Grid Co., Ltd. Study on ±800 kV UHVDC transmission technology. Beijing: China Electric Power Press; 2006.

Chapter 18
Insulation Coordination of UHVDC Converter Station

Xilei Chen, Hao Zhou and Xu Deng

The purpose of UHVDC converter station's insulation coordination is to determine a suitable layout of arrester and a selection scheme of its parameter, in order to ensure the insulation level and cost of equipment in DC system are within a reasonable range, under the condition that the project's operation is safe and reliable. The ±800 kV UHVDC transmission system characteristics with high-voltage level and high insulation level of equipment highly increase the manufacturing difficulty and cost of the UHVDC equipment. Therefore, enhancing overvoltage limitation and more sophisticated insulation coordination are important in reducing insulation level of equipment and controlling the cost of the whole project. Meanwhile, the UHVDC transmission system adopts two 12-pulse converters connected in series with identical structure at each pole, getting the structure of the converter station more complicated. From perspective of overvoltage, a complicated system structure will lead to much more varieties of overvoltage due to operation, fault, lightning or other reasons, and gets the overvoltage mechanism and development process more complicated. From the perspective of the arrester, it is required to use more varieties and number of DC arresters due to complexity of the system structure and overvoltage. Even for the same equipment placed at different positions in the converter

X. Chen (✉)
State Grid Ningbo Power Supply Company, Ningbo, Zhejiang,
People's Republic of China
e-mail: 285487205@qq.com

H. Zhou
College of Electrical Engineering, Zhejiang University, Xihu District,
Hangzhou, Zhejiang, People's Republic of China
e-mail: zhouhao_ee@zju.edu.cn

X. Deng
Guangzhou Municipal Commission of Commerce,
Guangzhou, Guangdong, People's Republic of China
e-mail: dengxu926@163.com

© Zhejiang University Press, Hangzhou and Springer-Verlag GmbH Germany 2018

H. Zhou et al. (eds.), *Ultra-high Voltage AC/DC Power Transmission*,
Advanced Topics in Science and Technology in China,
https://doi.org/10.1007/978-3-662-54575-1_18

station, the protection requirement is different. The factors above make the configuration scheme and parameters of arresters for the UHVDC converter station more complicated. Therefore, compared to the conventional DC transmission system, the UHVDC system requires more accurate, rational, and complicated insulation coordination due to its more complicated system structure.

The insulation coordination of the UHVDC converter station mainly includes the determination of insulation level of converter station equipment and external insulation design. Determination of insulation level of converter station equipment mainly includes arrester configuration and parameter selection, and insulation level selection of equipment; and the external insulation design of the converter station mainly includes the selection of minimum air clearance and external insulation design of pollution. This chapter gives a detailed discussion on these contents.

18.1 Basic Procedures for Determining the Insulation Level of Equipment

In HVDC system, the basic principle for insulation coordination of converter station's DC equipment is to determine the equipment's insulation level from aspects of safety, technology, and economy, according to the overvoltage level that may appear on the equipment, considering the protection level of the corresponding arrester at the same time, and finally realizing an overall optimal scheme for equipment's cost of manufacture, maintenance, and accident.

Specifically, the process of insulation coordination is determining the connection mode and basic parameters of converter system first, and then determining the arrester layout for converter stations according to the basic principle of arrester configuration, and calculating the basic parameters of the arrester, next, establishing the detailed simulation model according to the AC/DC project's parameters of system, characteristics of arrester, control strategy of converter, and using the model to calculate the equipment's representative overvoltage, arrester's current and energy flowing through it, after that, selecting arrester's coordinating current and protection level, and determining equipment's withstand voltage by using the conventional method, and ultimately, determining equipment's insulation level.

The basic steps determining insulation level of equipment in UHVDC converter station are as follows:

(1) determine the connection mode and basic parameters of converter system, and related content has been introduced detailedly in Chap. 15 of this book;
(2) determine the arrester layout for converter stations;
(3) calculate the basic parameters of the arrester;
(4) establish the overvoltage simulation model, and related content has been introduced detailedly in the sixteenth chapter of this book;

(5) calculate the equipment's representative overvoltage, arrester's current and energy, and related content has been introduced detailedly in the sixteenth chapter of this book;
(6) select arrester's parameters such as rated voltage, coordinating current, energy that flows through the arrester and other parameters;
(7) determine equipment's withstand voltage; and
(8) determine equipment's insulation level.

It is important to note that when using the above steps to determine the equipment's insulation level, comprehensive consideration between arrester's performance requirements and equipment's insulation level should be made to realize optimization, and then determine relevant equipment's parameters.

18.2 Overview of UHVDC Arrester

The UHVDC transmission system cannot be operated safely unless overvoltage protection devices are installed, and modern DC transmission systems adopt gapless metal oxide arresters (MOA) as the key overvoltage protection equipment to limit overvoltage and protect equipment, playing a decisive role in determination of insulation level of the whole project. A rational arrester configuration can not only effectively improve system reliability but also reduce equipment cost, achieving the best technical and economic benefit.

18.2.1 Characteristics of UHVDC Arrester

The UHVDC system has these characteristics with high-voltage level, complex structure, varieties of overvoltage in fault condition, and harsh operating condition of the arrester, so the varieties and number of arresters used in the UHVDC system are more than that in conventional DC system. Compared to the arresters in the AC system and conventional DC system, the UHVDC arresters have many differences, including:

(1) Many varieties and large difference in performance parameters

According to different installation positions, the UHVDC arresters can be divided into valve arrester, DC busbar arrester, DC line arrester, and neutral busbar arrester, and some arresters are unique for the UHV systems, such as busbar arrester at midpoint between upper and lower 12-pulse converters. Different arresters can withstand different operating conditions, whose reference voltage, protection level, and energy withstand capability (also called discharge capacity in some references) are different significantly.

(2) Complicated continuous operating voltage

The UHVDC system characteristics have a more complicated system structure. The continuous operating voltage on the DC arrester includes DC component, fundamental component, and harmonic component. The waveform of withstand voltage is complex, for example, a commutation overshoot will occur to the valve arrester during switch-off of converter valve, resulting in irregular waveform.

(3) Strong energy withstand ability and high requirement for current sharing due to connection of the multi-column arresters in parallel.

The arresters at some positions such as arrester at the valve side of the neutral busbar smoothing reactor discharge much energy when the UHVDC system is subject to some faults such as grounding at the valve side of the highest-voltage converter transformer, so the actual requirements can be met usually by connecting multi-column arresters in parallel. In case of using multi-column parallel structure, even distribution of energy on each column imposes an important influence on safe and stable operation of the arrester; thus, strict requirements are put forward to current sharing of the arrester.

(4) Some arrester ungrounded

For example, both ends of valve arresters and pole line smoothing reactor arrester are ungrounded.

(5) Heavily polluted

For DC arresters installed outdoor, it is required to increase its specific creepage distance to enhance the anti-pollution ability because the DC pollution accumulation is severe than that in the AC system.

18.2.2 Definition of Basic Parameters of UHVDC Arrester

In order to make it easier for the type selection and parameter determination of arresters for the UHVDC converter station, it is required to know the following basic parameters of the arrester.

Reference voltage (U_{ref}) means the initial actuating voltage of the arrester, i.e., the voltage at the turning point where the volt–ampere characteristic curve enters the flat part of the large current area from the rise part of the small current area and when the arrester starts working to limit overvoltage. The current flowing through the arrester at reference voltage level is usually 1–20 mA.

Reference current (I_{ref}) means the peak of current flowing through the arrester corresponding to the reference voltage.

The allowable maximum continuous operation voltage (MCOV) means the effective voltage allowed to continuously stress on the arrester; at this moment, the thermal stability of the metal oxide arrester is not be destroyed.

The continuous operating voltage of the DC arrester is superposed by DC voltage and harmonic voltage, and the continuous operating voltage has the following three different values:

(1) Peak value of continuous operating voltage (PCOV) means the maximum peak value of continuous operating voltage. In case of commutation overshoot for the continuous operating voltage, the PCOV is the maximum voltage considered for commutation overshoot.
(2) Crest value of continuous operating voltage (CCOV) means the maximum crest value of continuous operating voltage, excluding the commutation overshoot.
(3) Equivalent continuous operating voltage (ECOV): be equivalent to the voltage producing the same power consumption at the actual operating voltage level.

Residual voltage of arrester means the peak value of the maximum voltage appeared on the arrester when a discharging current flows through it.

Coordinating current means the current corresponding to protection level of the arrester during insulation coordination.

Protection level means the residual voltage on the arrester when the coordinating current flows through it.

Chargeability means the ratio of peak value of continuous operating voltage (PCOV) to reference voltage U_{ref}, characterizing the voltage load on the unit varistors of the arrester.

18.3 Configuration of Arresters in Converter Station

18.3.1 Basic Principles for Configuration of Arresters

The basic principles for configuration of arresters in the UHVDC converter station are as follows:

(1) The overvoltage produced at AC side of the converter station is limited by the arresters at AC side, and the AC busbar arresters should play active role in limiting the overvoltage.
(2) The overvoltage produced at the DC side of the converter station is limited by the arresters at DC side, that is to say, it is limited by the arresters at the incoming point of the DC line, and on the DC busbar and neutral busbar in the converter station.
(3) The important equipment in the converter station is directly protected by arresters connected in parallel, e.g., the converter valves are directly protected by the valve arresters; the winding at the grid side of the converter transformer is directly protected by the AC busbar arresters.

(4) Some equipment can be protected by two or more arresters in series, for example, the insulation protection of bushings at the valve side to the ground of the lower converter transformer is achieved by several arresters connected in series.

18.3.2 Configuration Scheme of Arresters in Converter Station

At present, the configuration of arresters in the converter station of the Xiangjiaba–Shanghai and Yunnan–Guangdong ±800 kV UHVDC transmission projects that have been put into operation represents two typical technical solutions, so it is necessary to conduct a detailed introduction, respectively. Figures 18.1 and 18.2 show the scheme for configuration of arresters in the converter station of the Xiangjiaba–Shanghai and Yunnan–Guangdong transmission projects, respectively, and simple descriptions for arresters are given in Tables 18.1 and 18.2.

The following gives an introduction to the arresters configured in these two schematics and their respective main protection effects.

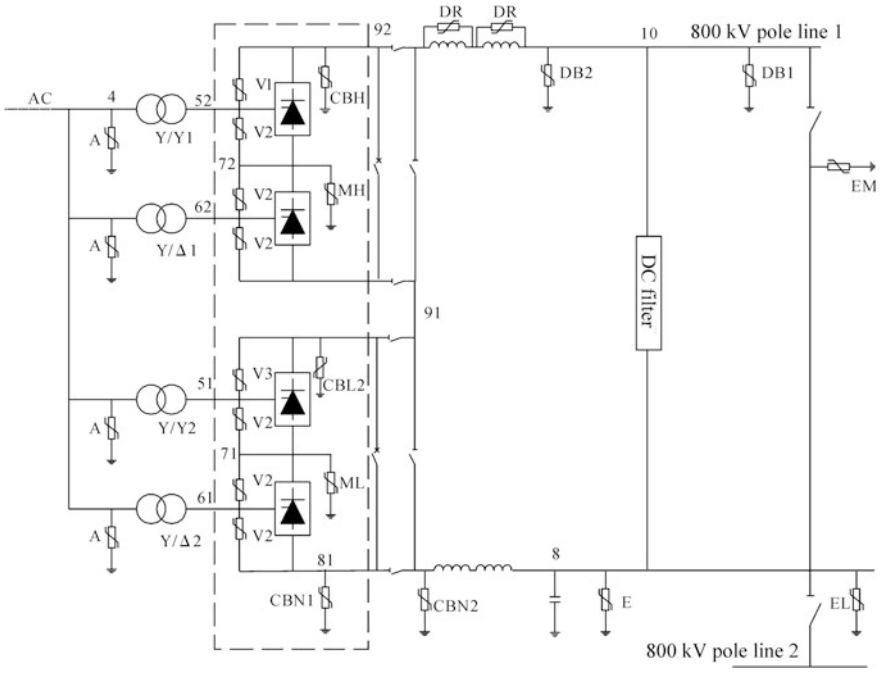

Fig. 18.1 Schematic for arrangement of arresters in converter station of Xiangjiaba–Shanghai ±800 kV UHVDC transmission project

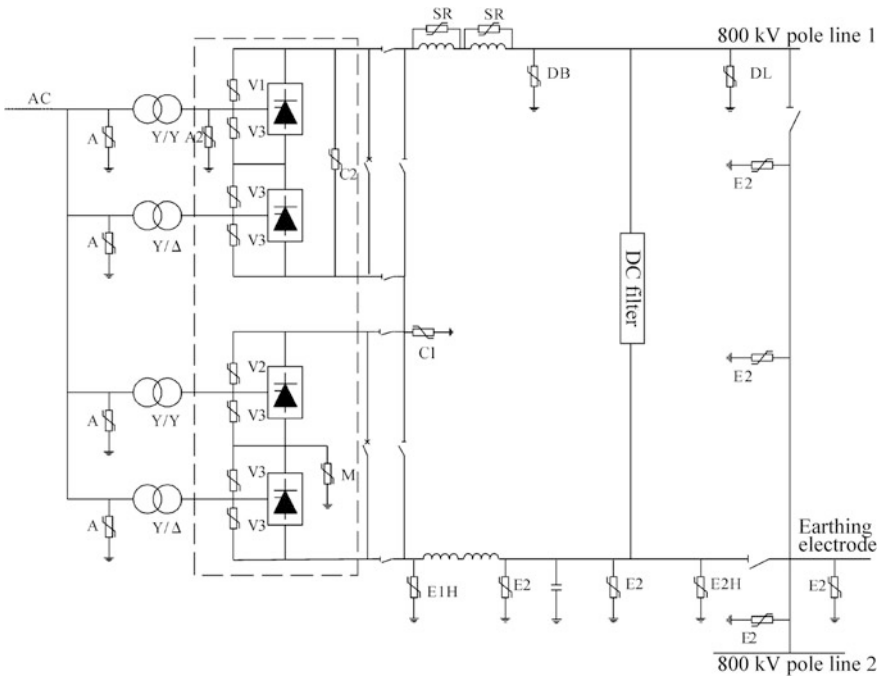

Fig. 18.2 Schematic for arrangement of arresters in converter station of Yunnan–Guangdong ±800 kV UHVDC transmission project

Table 18.1 Description of arresters for Xiangjiaba–Shanghai ±800 kV UHVDC transmission project

Arrester	Description
A	AC busbar arrester
V1/V2/V3	Valve arrester
MH/ML	6-pulse bridge arrester for upper/lower 12-pulse converter unit
CBH	DC busbar arrester of upper 12-pulse converter unit
CBL2	DC busbar arrester between 12-pulse converter units
CBN1/CBN2	Arrester at LV end of converter
DB1/DB2	DC busbar/line arrester
DR	Parallel arrester for smoothing reactor
E	Neutral busbar arrester
EM, EL	Metal return and electrode line arrester

1. Arresters for the Xiangjiaba–Shanghai UHVDC transmission project

(1) AC busbar arrester A: Be installed at AC side of AC busbar and converter transformer, which is mainly used to limit temporary overvoltage and switching overvoltage produced at AC side due to various reasons. In addition,

Table 18.2 Description of arresters for Yunnan–Guangdong ±800 kV UHVDC transmission project

Arresters	Description
A	AC busbar arrester
A2	Arrester at the valve side of converter transformer at the highest-voltage end
V1/V2/V3	Valve arrester
M	Neutral point arrester for lower 12-pulse converter unit
C2	Arrester for upper 12-pulse converter unit
Cl	Arrester for lower 12-pulse converter unit
DB/DL	DC busbar/line arrester
SR	Parallel arrester for smoothing reactor
E1H	High-energy arrester at the valve side of smoothing reactor of neutral busbar
E2	Neutral busbar arrester
E2H	High-energy arrester for neutral busbar

such arrester can also be used to limit overvoltage produced at AC side and transmitted to the DC side through the converter transformer.

(2) Valve arrester V: Be directly connected in parallel on the converter valve to protect it against switching overvoltage transmitted from AC side through the converter transformer or overvoltage at DC side produced due to various causes. The valve arresters at different positions have different requirements for energy absorption. Usually, the high-energy absorption ability can be achieved by connecting multi-column arresters in parallel, so the V-type arrester can be divided into several varieties of arresters, such as V1, V2, and V3.

(3) MH, ML: 6-pulse bridge arresters for upper and lower 12-pulse converter, respectively, which are used to directly protect DC busbar between 6-pulse bridges. Additionally, MH is connected with V2 arrester in series to protect the winding at the valve side of Y/Y1 converter transformer at HV end of the upper converter, and ML is connected with V2 arrester in series to protect the winding at the valve side of Y/Y2 converter transformer at HV end of the lower converter.

(4) CBH: Be installed on the DC busbar at the valve side of smoothing reactor. Due to superposition of harmonic voltage, the normal operating voltage at DC valve top is very high, so installing the CBH can directly protect the DC busbar, wall bushing, and relevant equipment.

(5) CBL2: In an actual design layout for the converter station, the upper and lower 12-pulse converter units with identical structure are usually arranged in the upper and lower valve halls, and the CBL2 is installed on the busbar at midpoint between the upper and lower 12-pulse converters to protect the middle DC busbar, the wall bushing, and disconnector which are used to connect the upper and lower 12-pulse converter units. During the operation of both two converters, CBL2 is connected with V2 in series to protect the

winding at the valve side of Y/Δ1 converter transformer at LV end of the upper converter.

(6) CBN1, CBN2: Arrester at LV end of the lower 12-pulse converter, of which CBN1 is installed in the valve hall, and CBN2 is installed outside the valve hall. CBN2 is a high-energy arrester, being made up of several arrester columns in parallel, which is used to protect relevant equipment at the valve side of the smoothing reactor on the neutral busbar. For the reason that the UHVDC system adopts separate arrangement of smoothing reactors, the smoothing reactor on the neutral busbar can suppress the bleeder current flowing to other neutral busbar arresters. Most energy can be released only by CBN2, so CBN2 will endure a high-energy stress; thus, CBN2 is often a high-energy arrester composed of multiple columns in parallel. Meanwhile, CBN2 should be installed outside the valve hall to prevent rupture endangering other valve hall equipment due to an excessive energy released by CBN2. Arrester CBN1 is superior to CBN2 with respect to protection characteristic, which is mainly used to limit the lightning overvoltage transmitting into the valve hall, without high-energy requirement. Additionally, the winding at the valve side of Y/Δ2 converter transformer at LV end of the lower converter is protected by CBN2+V2 (for switching impulse) and CBN1 +V2 (for lightning impulse) in series.

(7) DB1, DB2 mean the DC pole line arrester and DC busbar arrester, respectively, which are identical in electric parameters and different in installation position. DB2 is positioned at line side of DC pole line smoothing reactor and close to the smoothing reactor, and DB1 is positioned at the outlet of DC line. Both of them are used to limit lightning overvoltage and switching overvoltage of the DC switchyard. It is necessary to install DB2 because, with respect to lightning overvoltage, DB1 is used for the first protection and DB2 for the second protection. For the lightning impulse is a high frequency component, the smoothing reactor has a huge impedance, and the overvoltage impulse reflected back increases significantly, be possible to impose a serious damage to the insulation of the smoothing reactor. Through the installation of arrester DB2, it is possible to limit overvoltage of the reflection impulse, and reduce end-to-end overvoltage of the smoothing reactor.

(8) DR: Be directly bridged on the DC busbar smoothing reactor, which is mainly used for lightning impulse protection. When the outlet of pole line is subject to a reverse polarity lightning strike, it is assumed that the voltage at the valve side of the smoothing reactor still remains unchanged, the end-to-end voltage of the smoothing reactor will be very high at this moment, being equal to the protection level of DB2 plus the pole line voltage, which is almost applied to the smoothing reactor close to the DB2 (two smoothing reactors are provided on the high-voltage pole line for the UHVDC project), so that a very high requirement is put forward to the insulation of the smoothing reactor. Installation of parallel arresters DR on the smoothing reactor of pole line can limit this kind of lightning impulse and reduce the insulation level. For the reason that most lightning strike is negative, arresters DR have more

significant protection effect for smoothing reactors on the positive DC busbar of the converter station.

(9) E: Be positioned at the neutral busbar side of the smoothing reactor, whose volt–ampere characteristic curve is higher than the arrester EM and EL, and which is used to limit lightning impulse transmitted to the neutral busbar.

(10) EM, EL: Be installed on the metallic return and ground electrode line, respectively. When the rectifier side is operated in metallic return mode, the switching impulse is absorbed jointly by the arrester CBN2 and EM; when the rectifier side is operated in bipolar or monopolar ground return mode, the switching impulse is absorbed jointly by the arrester CBN2 and EL. Because the inverter side is always grounded, the switching impulse on the neutral busbar of inverter side is absorbed jointly by the arrester CBN2 and EL, regardless of the operating mode. Meanwhile, EM and EL can limit lightning impulse from the metallic return and ground electrode line.

2. Arresters for the Yunnan–Guangdong UHVDC transmission project

The arresters in the lower 12-pulse converter unit and on the neutral busbar for the converter station of the Yunnan–Guangdong UHVDC project are arranged basically same to the Xiangjiaba–Shanghai project, having difference in arrangement of arresters in the upper 12-pulse converter unit. In the Yunnan–Guangdong project, arrester A2 is configured at the valve side of the converter transformer at the highest-voltage end and arrester C2 is configured for the whole upper 12-pulse converter unit. Meanwhile, the arresters MH and CBH adopted in the Xiangjiaba–Shanghai project are not used.

(1) A2: Due to the rise of operating voltage in UHVDC system, the maximum operating voltage of the converter transformer for the upper 12-pulse converter unit, especially the valve side of the Y/Y converter transformer at the highest-voltage end, is very high, being approximated to 900 kV, and in some fault condition, this overvoltage is very large, so it is needed to install arrester A2 at Y/Y valve side of the high-voltage converter transformer at the highest-voltage end, to directly protect winding and equipment at the valve side of the converter transformer being at maximum electric potential level. In fact, the protection function described above can be realized by arresters MH and V2 in the Xiangjiaba–Shanghai project as well.

It should be noted that these two protection methods have their respective advantages and disadvantages. Use of arrester A2 for the Yunnan–Guangdong project is advantageous to realize direct protection of equipment. Separate arrangement of the smoothing reactors can reduce PCOV of arrester A2, and a higher chargeability can be selected to obtain a lower protection level for the reason that the arrester A2 withstands the high-voltage only in half cycle. However, three arresters are required for each pole in each substation; because the arresters' characteristic with high rated voltage, the arresters will occupy a larger space, and there is difficulty in installation and the large air clearance is required. The

Xiangjiaba–Shanghai project adopts the protection means of MH+V2, having such advantages as only one arrester MH required for each pole of each substation, low rated voltage, small height of the arrester, simpler arrangement in the valve hall, and small occupation space, but having such disadvantages as higher protection level obtained by means of MH+V2 than that a single arrester A2, and higher requirements for insulation level of bushing and winding at the valve side of converter transformer.

(2) C2: Be used to directly protect the whole upper 12-pulse converter unit, especially when the upper 12-pulse converter unit is operated separately, it can effectively protect the converter unit and its internal equipment. In addition, after being connected with C1 arrester in series, it can protect DC busbar at the valve side of the smoothing reactor, which is identical to arrester CBH for the Xiangjiaba–Shanghai project with respect to its function. From this point, the protection effect obtained by both protection means is equivalent basically.

18.3.3 Characteristics for Configuration of Arresters in UHVDC Converter Station

It can be seen from specific arrangement of arresters in the converter station of the Xiangjiaba–Shanghai and Yunnan–Guangdong UHVDC projects that, compared to the conventional DC transmission projects, the UHVDC converter station is configured with more varieties and quantities of arresters, the protection is more sophisticated, and almost all equipment are provided with special arresters for protection. Among them, the end-to-end protection of DC pole line smoothing reactor and protection of winding at the valve side of the converter transformer at the highest-voltage end are the distinctive characteristics of the protection scheme for the UHVDC projects.

For the UHVDC projects, the dry-type smoothing reactors are arranged separately on the DC pole line and neutral busbar. When the DC pole line is subject to a back flashover lightning strike, a very high overvoltage will be produced on the pole line smoothing reactor, so a strict requirement is put forward to the insulation level of the smoothing reactor, resulting in a high manufacturing difficulty and cost. The arresters DR/SR are installed in parallel on the pole line smoothing reactor for end-to-end protection of the Xiangjiaba–Shanghai and Yunnan–Guangdong UHVDC projects, effectively reducing the insulation level of the pole line smoothing reactor.

The UHVDC system adopts a structure for double 12-pulse converter units connected in series. As superposition of DC voltage for each 6-pulse converter unit, the voltage at the valve side of corresponding converter transformer increases significantly; so, the insulation requirement is very high if the voltage on Y/Y converter transformer valve side at the highest-voltage end is very high. The

excessively high insulation requirement will lead to increase in transformer volume, resulting in more difficult equipment manufacturing and transportation; thus, it is required to take protection measures to reduce the overvoltage level and equipment insulation level. However, different projects are designed on different ideas and will adopt different protection means. For example, the winding at the valve side of the converter transformer at the highest-voltage end can be protected by means of MH +V2 or A2. Both protection means have their respective advantages and disadvantages.

18.4 Selection of Parameters for UHVDC Arresters

This section gives a detailed instruction for basic principles and specific methods for selection of parameters for arresters of the UHVDC converter station based on the Xiangjiaba–Shanghai ±800 kV UHVDC transmission project.

18.4.1 Basic Principles for Selection of Parameters for Arresters

According to the preceding chapters, parameters of UHVDC arrester mainly include the continuous operating voltage, chargeability, reference voltage, coordinating current, the protection level, etc., and the following briefly introduces basic principles for the selection of the parameters.

The arresters withstand operating voltage for a long period in the practical operating process, and the leakage current flowing through the arrester will lead to heat generation of the zinc oxide varistors, and as the time flows, the arrester will be aged, so as to influence the reliability and stability of the arrester, shorten its service life, and endanger the safe operation of the system. Thus, when determining the performance parameters of the arrester, it is first required to make sure that the continuous operating voltage MCOV, CCOV, PCOV of the arrester are higher than the maximum operating voltage at the place where it is installed, to avoid accelerated aging due to absorption of excessive energy by the arrester.

The chargeability of the DC arrester is the ratio of CCOV/PCOV to the reference voltage, which characterizes the voltage load on the varistor of arrester unit. The continuous operating voltage CCOV/PCOV depends on the DC system, so, with respect to most arresters in the converter station, the chargeability directly determines the reference voltage of the arresters. A low chargeability will lead to a higher reference voltage of the arrester, so the arrester has a low leakage current under the long-term operating voltage, and is not liable to aging; a higher chargeability will lead to a low reference voltage of the arrester, which can reduce the protection level of the arrester and is important to reduce the insulation level of

the equipment. After the DC arrester's chargeability is determined, the arrester's reference voltage can be determined.

The arrester's protection level is the residual voltage when the coordinating current flows through the arrester, and the selection of the arrester's protection level is mainly considered as follows: Firstly, from the perspective of insulation coordination, a lower protection level of the arrester helps reduce the insulation level of the equipment, so as to lower the equipment manufacturing difficulty and cost. However, an excessively low protection level will get the arrester absorb much energy under influence of overvoltage stress, so that much more arresters or large-volume arresters are required to satisfy high-energy requirements. This enhances the manufacturing difficulty and cost of the arresters, and much more arresters or large-volume arresters will occupy a larger space, increasing the difficulty in arrangement of arresters and other equipment in the converter station. Therefore, when determining the DC arrester's coordinating current and protection level, it is necessary to achieve optimization combining with the overvoltage calculation results of actual DC project.

The energy absorbed by the UHVDC arresters under influence of overvoltage stress can be determined by sophisticated electromagnetic transient calculation, whose value is far larger than the arrester for the conventional DC system. Thus, the energy requirement should be met by connecting multi-column arresters in parallel with identical characteristics. For the parallel connection of the arresters, it is possible to connect multi-column varistors in parallel in a porcelain bushing, or connect multiple arresters in parallel outside the porcelain bushing. Usually, the manufacturer should control unevenness coefficient of current distribution between multi-column arresters within the specified range.

Therefore, when selecting parameters of arresters, it is required to comprehensively consider the maximum continuous operating voltage, chargeability, lightning and switching impulse protection level and energy requirement and other factors, so that the overvoltage level on the equipment is declined as far as possible, without too many arresters and excessively high cost.

18.4.2 Arresters at AC Side

The voltage of the AC system at both sides of the UHV converter station is rated to 500 kV. 500 kV AC arresters are configured at the grid side of each converter transformer and on the busbar of AC filter. The main electrical parameters of the arrester at AC side are the continuous operation voltage U_c and the arrester's rated voltage U_r.

1. Continuous operation voltage U_c of the AC arrester

The continuous operating voltage U_c of the AC arrester is an effective value of the power frequency voltage that is allowed to be applied continuously on the arrester,

which is a very important parameter. For the gapless metal oxide arrester, the operating voltage directly applied to the varistors of the arrester will cause aging of the varistors. In order to ensure a long service life, the voltage applied to the arrester for a long period should not exceed the continuous operating voltage of the arrester, so as to avoid over-temperature and thermal breakdown of the varistors [1]. Therefore, selection of this parameter mainly depends on the maximum continuous operating voltage MCOV of the system.

The voltage of the AC system with the neural point grounded effectively in the converter station at both terminals of the UHVDC system is rated to 500 kV, and the maximum operating voltage is usually 550 kV, and the effective value of the phase-to-ground maximum continuous operating voltage is MCOV = 550/$\sqrt{3} = 318$ kV, so the continuous operating voltage of the AC arrester finally selected should not be less than 318 kV.

2. Rated voltage U_r of the AC arrester

The rated voltage of the AC arrester means the effective value of the allowable maximum power frequency voltage applied on the arrester, and the arrester designed based on this voltage level can be operated normally under the temporary overvoltage in the specified operating duty test. So, the rated voltage is an important parameter showing operating characteristic of the arrester, and it is selected by mainly considering temporary overvoltage of the system.

For the temporary overvoltage, it mainly means the power frequency overvoltage or overvoltage with frequency close to the power frequency. Chinese electric power industry standard [2] provides that the power frequency overvoltage at busbar side of the system with 500 kV voltage level usually does not exceed 1.3 p.u. Generally, duration of the power frequency overvoltage depends on the system voltage regulating measures, disturbance pattern, actuating time of relay protection, and actuating time of circuit breaker. Although the duration of 1.3 p.u. power frequency overvoltage is not specified in the same standard, but the neutral point of 500 kV system is grounded effectively, and the power frequency overvoltage lasts for not more than 1 s.

If the arrester's characteristic curve of power frequency voltage withstand time supplied by the manufacturer is available, it is possible to carry out verification directly based on the characteristic curve, enabling the selected arrester to have enough temporary overvoltage withstand ability, that is to say, it is possible to keep thermal stability within the duration when it is subject to overvoltage; when the arrester's characteristic curve of power frequency voltage withstand time is not available, it is possible to carry out estimation by the following method.

In principle, the system requirement is met as long as the arrester selected can keep thermal stability within duration when it is subject to temporary overvoltage, but different power system and different variety of temporary overvoltage have different durations, so the arrester must withstand the temporary overvoltage equivalent to the value of rated voltage for 10 s after absorption of specified energy at temperature of 60 °C in the operating duty test according to the IEC standard [3]

and equivalent Chinese GB standard [1]. Therefore, through the conversion equation recommended by the IEC standard [4], as shown in Eq. (18.1), it is possible to convert the 1.3 p.u. power frequency overvoltage for 1 s duration in the 500 kV system to an equivalent temporary overvoltage U_{eq} for 10 s duration, and the rated voltage of the arrester selected eventually should not be less than the temporary overvoltage equivalent to such value.

$$U_{eq} = U_t \left(\frac{T_t}{10}\right)^m, \tag{18.1}$$

where

U_t is the temporary overvoltage,
T_t is the temporary overvoltage duration,
U_{eq} is the equivalent temporary overvoltage for 10 s duration,
m is the factor describing the arrester's characteristic curve of power frequency voltage withstand time, which is varied within 0.018–0.022 for different varieties of arresters, and an average value of 0.02 is taken during calculation.

A result is obtained by the following calculation:

$$U_{eq} = 1.3 \times 550/\sqrt{3} \times \left(\frac{1}{10}\right)^{0.02} = 394.2\,(\text{kV})$$

It is required to select a rated voltage U_r of the arrester, being equal to or more than 394.2 kV.

In addition, considering that the AC arrester with rated voltage of 396 kV is available for selection for the 500 kV systems as in Ref. [5], an AC arrester with rated voltage of 396 kV or above is appropriate for the project.

18.4.3 Arresters at DC Side

18.4.3.1 Continuous Operating Voltage CCOV/PCOV

The continuous operating voltage of the HVDC arrester is different from the AC system, which is not a single power frequency voltage, but a voltage that is composed of DC voltage, fundamental frequency voltage, harmonic voltage, and high frequency transient voltage. The continuous operating voltage CCOV and PCOV of the arrester should be higher than the maximum operating voltage at the place where it is installed, and the harmonic voltage and high frequency transient operation voltage superposed in the harsh condition should be taken account of, so as to avoid accelerated aging due to absorption of excessive energy by the arrester, and reduction in reliability. The following takes the Fulong Station at the rectifier side

of the Xiangjiaba–Shanghai ±800 kV UHVDC transmission project as an example to explain the calculation of continuous operating voltage of the arrester at the DC side of the converter station. The arrangement of arresters is shown in Fig. 18.1.

1. Valve arrester V

The transient voltage produced when the valve is turned on or off is superposed onto the commutation voltage, especially at the time of turning off the valve, the commutation overshoot is added with voltage of the winding at the valve side of converter transformer, and is applied to the valves and arresters. Figure 18.3 shows the continuous operating voltage waveform of the valve arrester, whose magnitude is proportional to the maximum ideal no-load DC voltage U_{dim}, and decided by the following equation [6]:

$$\mathrm{CCOV} = \pi/3 \times U_{\mathrm{dim}} \tag{18.2}$$

In the Xiangjiaba–Shanghai UHVDC project, the continuous operating voltage of the valve arrester is CCOV = $\pi/3 \times 237.6 = 248.8$ kV due to $U_{\mathrm{dim}} = 237.6$ kV for the rectifier station.

The continuous operating voltage PCOV is equal to CCOV plus the commutation overshoot when commutation overshoot is taken into account. The PCOV is related to the inherent characteristic of the thyristor valve, damping resistance and capacitance, capacitance and inductance of valves and commutation circuit, trigger angle and overlap angle and other factors, and it is possible to build a detailed model including the factors above to estimate it, and it can also be determined by the ratio of PCOV to CCOV based on project experience. At present, the commutation overshoot coefficient is about 15–19% for HVDC projects, i.e., the ratio of PCOV to CCOV is about 1.15–1.19. In the Xiangjiaba–Shanghai UHVDC project, the commutation overshoot of the rectifier station is 16%, i.e., the commutation overshoot coefficient is 1.16.

2. DC pole line arresters DB

The maximum operating voltage of the DC pole line arresters DB1 and DB2 are almost a pure DC voltage, and CCOV of the arrester is the maximum operating

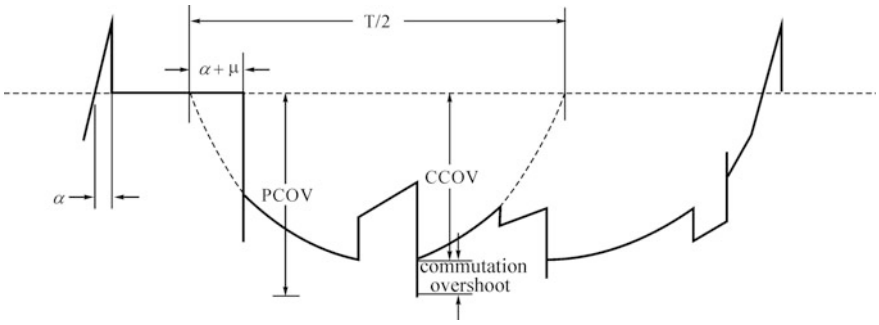

Fig. 18.3 Continuous operating voltage waveform of valve arrester

voltage of the DC pole line, e.g., 824 kV is taken for the Xiangjiaba–Shanghai UHV project. In other projects, this value is taken as 816 kV sometimes.

3. Arrester CBH at HV end of the converter

The operating voltage of the arrester CBH at HV end of the converter is equal to continuous operating voltage of the 12-pulse converter unit, plus the voltage of the busbar between the upper and lower 12-pulse converter units, in which the continuous operating voltage CCOV being represented by the following equation for commutation overshoot is neglected:

$$\mathrm{CCOV} = 2 \times \cos^2(15^\circ) \times \frac{\pi}{3} \times U_{\mathrm{dim}} + U_{\mathrm{offset}} \tag{18.3}$$

where

U_{offset} is the maximum operating voltage of the busbar between the upper and lower 12-pulse converter units, which is approximated to a pure DC voltage for the reason that the UHV converter station adopts separate arrangement of the smoothing reactors, e.g., 412 kV is taken for the Xiangjiaba–Shanghai UHV project.

The continuous operating voltage PCOV considering commutation overshoot is equal to CCOV of the arrester plus commutation overshoot. The commutation overshoot is selected by the following two methods, at present:

(1) Each 12-pulse converter unit is composed of two 6-pulse converter in series in the UHVDC system, and the difference between phases of the converter is 30°, as well as commutation time of the upper and lower 6-pulse converter is different, so that the commutation overshoot of two 6-pulse converters occurs at different time, and the commutation overshoot amplitude of the 12-pulse converter unit superposed by two 6-pulse converters is actually equal to that of a single 6-pulse converter; therefore, the PCOV of the arrester CBH is calculated as follows:

$$\mathrm{PCOV} = \mathrm{CCOV1} + \text{Commutation overshoot} = \mathrm{CCOV1} + k_1 \times \mathrm{CCOV2} \tag{18.4}$$

where

CCOV1 is the continuous operating voltage of the arrester CBH with commutation overshoot being not considered, which is calculated by Eq. (18.3),

k_1 is the commutation overshoot of the 6-pulse converter, e.g., 16% taken for the rectifier station of the Xiangjiaba–Shanghai UHVDC project, and

CCOV2 is the continuous operating voltage of the 6-pulse converter, which is calculated by Eq. (18.2), i.e., $\mathrm{CCOV2} = \pi/3 \times U_{\mathrm{dim}}$.

(2) The commutation overshoot of the voltage of the 12-pulse converter unit is taken account of, which is usually taken as 10%, i.e., the commutation overshoot coefficient is 1.1, so PCOV of the arrester CBH is calculated as follows:

$$\mathrm{PCOV} = k \times 2 \times \cos^2(15^\circ) \times \frac{\pi}{3} \times U_{\mathrm{dim}} + U_{\mathrm{offset}} \tag{18.5}$$

where

U_{offset} is the maximum operating voltage of the busbar between the upper and lower 12-pulse converter units, which is approximated to a pure DC voltage for the reason that the UHV converter station adopts separate arrangement of the smoothing reactors, and

k is the commutation overshoot coefficient of the voltage of the 12-pulse converter unit, which is taken as 1.1.

In the Xiangjiaba–Shanghai UHVDC project, the following result is calculated by substituting relevant parameters into Eq. (18.5):

$$\mathrm{CCOV} = 2 \times \cos^2(15^\circ) \times \frac{\pi}{3} \times 237.6 + 412 = 876\ (\mathrm{kV})$$

The PCOV results obtained by the above two methods are as follows:

$$\mathrm{PCOV}_1 = 876 + 0.16 \times \frac{\pi}{3} \times 237.6 = 916\ (\mathrm{kV})$$

$$\mathrm{PCOV}_2 = 1.1 \times 2 \times \cos^2(15^\circ) \times \frac{\pi}{3} \times 237.6 + 412 = 923\ (\mathrm{kV})$$

4. 6-Pulse bridge arrester MH for the upper 12-pulse converter unit

The operating voltage of the 6-pulse bridge arrester MH for the upper 12-pulse converter unit is equal to the continuous operating voltage on the valve, plus the voltage of the busbar between the upper and lower 12-pulse converter unit, which is represented as follows:

$$\mathrm{CCOV} = \pi/3 \times U_{\mathrm{dim}} + U_{\mathrm{offset}} \tag{18.6}$$

$$\mathrm{PCOV} = k \times \pi/3 \times U_{\mathrm{dim}} + U_{\mathrm{offset}} \tag{18.7}$$

where

U_{offset} is the maximum operating voltage of the busbar between the upper and lower 12-pulse converter units, and 412 kV is taken for the Xiangjiaba–Shanghai UHV project, and

k is the commutation overshoot coefficient of the voltage of the 6-pulse converter units.

In the Xiangjiaba–Shanghai UHVDC project, the following result is calculated by substituting relevant parameters into Eqs. (18.6) and (18.7):

$$\mathrm{CCOV} = \pi/3 \times 237.6 + 412 = 661\ (\mathrm{kV})$$

$$\mathrm{PCOV} = 1.16 \times \pi/3 \times 237.6 + 412 = 701\ (\mathrm{kV})$$

5. Arrester CBL2 on the busbar between the 12-pulse converter units

The operating voltage of the arrester on the busbar between the 12-pulse converter units is equal to the continuous operating voltage of the 12-pulse converter unit, plus the voltage to ground at the valve side of the smoothing reactor on the neutral busbar. The CCOV and PCOV are calculated by a principle similar to that of the arrester CBH, which are represented as follows:

$$\mathrm{CCOV} = 2 \times \cos^2(15^\circ) \times \frac{\pi}{3} \times U_{\mathrm{dim}} + U_{\mathrm{offset}} \tag{18.8}$$

$$\mathrm{PCOV}_1 = \mathrm{CCOV1} + \mathrm{Commutation\ overshoot} = \mathrm{CCOV1} + k_1 \times \mathrm{CCOV2} \tag{18.9}$$

$$\mathrm{PCOV}_2 = k_2 \times 2 \times \pi/3 \cos^2(15^\circ) \times U_{\mathrm{dim}} + U_{\mathrm{offset}} \tag{18.10}$$

where

U_{offset} is the voltage to ground at the valve side of the smoothing reactor on the neutral busbar,

CCOV1 is the continuous operating voltage of the arrester CBL2 without commutation overshoot considered,

k_1 is the commutation overshoot of the 6-pulse converter, e.g., 16% taken for the rectifier station of the Xiangjiaba–Shanghai UHVDC project,

CCOV2 is the continuous operating voltage of the 6-pulse converter, which is calculated by Eq. (18.2), i.e., CCOV2 = $\pi/3 \times U_{\mathrm{dim}}$, and

k_2 is the commutation overshoot coefficient of the voltage of the 12-pulse converter unit, which is usually taken as 1.1.

With respect to the determination for the voltage to ground at the valve side of the smoothing reactor on the neutral busbar U_{offset}, it is required to take account of DC voltage and harmonic voltage. During actual operation of the system, the voltage includes the DC voltage drop of the ground electrode line and harmonic voltage drop of the smoothing reactor. The voltage to ground during normal operation of the system is low, and the voltage polarity is opposite to the voltage polarity of the busbar between the upper and lower 12-pulse converters, so when determining the maximum continuous operating voltage of arresters CBL2 and ML, the voltage can be neglected, i.e., U_{offset} is zero.

In the Xiangjiaba–Shanghai UHVDC project, it is possible to obtain the following results by substituting relevant parameters into Eqs. (18.8), (18.9), and (18.10), respectively:

$$\mathrm{CCOV} = 2 \times \cos^2(15^\circ) \times \pi/3 \times 237.6 = 464\ (\mathrm{kV})$$

$$\mathrm{PCOV}_1 = 464 + 0.16 \times \frac{\pi}{3} \times 237.6 = 504\ (\mathrm{kV})$$

$$\mathrm{PCOV}_2 = 1.1 \times 2 \times \cos^2(15^\circ) \times \frac{\pi}{3} \times 237.6 + 0 = 511\ (\mathrm{kV})$$

where

$\mathrm{PCOV}_1/\mathrm{PCOV}_2$ is the calculation results obtained by two different methods.

6. 6-Pulse bridge arrester ML for the lower 12-pulse converter unit

Be similar to the 6-pulse bridge arrester MH for the upper 12-pulse converter unit, the continuous operating voltage of the 6-pulse bridge arrester ML for the lower 12-pulse converter unit is equal to the continuous operating voltage on the valve plus the voltage to ground at the valve side of the smoothing reactor on the neutral busbar, which is calculated as follows:

$$\mathrm{CCOV} = U_{\mathrm{dim}} \times \pi/3 + U_{\mathrm{offset}} \tag{18.11}$$

$$\mathrm{PCOV} = k \times \pi/3 \times U_{\mathrm{dim}} + U_{\mathrm{offset}} \tag{18.12}$$

where

U_{offset} is the voltage to ground at the valve side of the smoothing reactor on neutral busbar, which is taken as zero when determining the maximum continuous operating voltage of the arrester ML.

In the Xiangjiaba–Shanghai UHVDC project, it is possible to obtain the following results by substituting relevant parameters into Eqs. (18.11) and (18.12), respectively:

$$\mathrm{CCOV} = \pi/3 \times 237.6 = 248.8\ (\mathrm{kV})$$

$$\mathrm{PCOV} = 1.16 \times \pi/3 \times 237.6 = 289\ (\mathrm{kV})$$

7. Neutral busbar arresters

The neutral busbar arresters include the arrester CBN1 and CBN2 at the valve side of the neutral busbar smoothing reactor, neutral busbar arrester E, ground electrode

line arrester EL, and metallic return arrester EM. For these arresters, the commutation overshoot is neglected, and the continuous operating voltage of the arresters is described as follows:

The arresters CBN1 and CBN2 are installed at the valve side of the neutral busbar smoothing reactor, of which CBN1 is positioned inside the valve hall and CBN2 is positioned outside the valve hall. For the maximum continuous operating voltage CCOV of the arrester, it is required to take account of DC voltage and harmonic voltage simultaneously, and during calculation, it is equal to the DC voltage drop occurred on the ground electrode line plus the harmonic voltage produced by the harmonic current flowing through the smoothing reactor of the neutral busbar in metallic return (rectifier station) or ground return (inverter station) operating mode of the DC system.

Arrester E of the neutral busbar is installed on the neutral busbar at the valve side of the smoothing reactor. For the rectifier station, the maximum operating voltage of the arrester is the DC voltage drop resulting from the direct current in the ground electrode line in monopolar operating mode with metallic return of the DC system; for the inverter station, the maximum operating voltage of the arrester E is the voltage drop produced by the direct current in the ground electrode line of the inverter station as the inverter station is always grounded in various operating modes.

The metallic return arrester EM is installed on the metallic return of the converter station. For the rectifier station, the maximum operating voltage of the arrester is the DC voltage drop produced by the direct current in the ground electrode line in monopolar operating mode with metallic return of the DC system; for the inverter station, the maximum operating voltage of the arrester is the voltage drop produced by the direct current in the ground electrode line of the inverter station.

Arrester EL for the ground electrode line is installed at the ground electrode line inlet of the converter station, and the maximum continuous operating voltage CCOV of the arrester is the maximum voltage drop produced by the direct current on the ground electrode line.

18.4.3.2 Chargeability

For most arresters at DC side of the UHVDC converter station, the chargeability will determine its reference voltage directly. Selecting a rational chargeability should comprehensively take account of the influences of continuous operating voltage CCOV/PCOV of the system, DC voltage component, environmental pollution on the electric potential distribution of the arrester bushing, influence of the temperature on the volt–ampere characteristic, as well as the installation position (indoor and outdoor) of the arrester, and other factors. As described above, the chargeability has a significant influence on aging of the arresters. Reducing the chargeability can result in a decrease in leakage current of the arresters under long-term operating voltage and enable the arresters to be not liable to aging; increasing the chargeability can lower reference voltage and protection level of the

arresters, and is important in finally reducing the insulation level of the equipment. The chargeability of arresters in UHVDC converter station is determined as follows:

1. V-type arrester is connected in parallel with the converter valve, and when the valve is turned on, the voltage on the valve arrester becomes zero; when the valve is turned off, the valve voltage is applied to the valve arrester. In each AC cycle, turn-on time of the converter is about 2/3 cycle, and turn-off time is about 1/3 cycle, so the heat produced by leakage current caused by the valve voltage in a cycle is very small. In addition, the valve arrester is positioned inside the valve hall, so the environmental pollution can be neglected; moreover, the valve hall is installed with an air conditioner, so the indoor temperature and heat dissipation can be controlled well; therefore, a higher chargeability of the valve arrester can be taken, being close to 1.
2. D type arresters (DB1, DB2) withstand a very high pure DC voltage during operation, having a very high rated voltage. And they are installed at a higher place due to the external insulation requirements. Considering that they are placed at line side of DC pole line smoothing reactor and at the DC line outlet, they are usually installed outdoor. Thus, the outdoor environmental pollution will impose an influence on the uniformity of electric potential distribution of the arrester bushing, and partial heat generated by the bushing is transmitted to the internal part of the arrester leading to over-temperature of some varistors; the outdoor temperature has a significant influence on volt–ampere characteristic and heat dissipation of the arresters. When the outdoor temperature is very high in summer, leakage current of the arrester under normal operating voltage will get increased, and the high temperature also compromises heat dissipation of the arrester. So, the chargeability of type D arresters is usually at a rational level, which can be selected between 0.8 and 0.9, for example, the chargeability is taken as 0.85 for the arrester of the Xiangjiaba–Shanghai project.
3. Arresters CBH, MH, CBL2, and ML endure a DC voltage superposed by a 12-pulse harmonic voltage during operation. The heat produced by the harmonic voltage on varistors of the arresters is less than that produced by the DC component, and these arresters are installed in the valve hall, so the environmental pollution can be neglected, and the indoor temperature and heat dissipation can be controlled well, so a higher chargeability can be taken, approx. 0.9.
4. The continuous operating voltage of the arrester CBN2 at valve side of neutral busbar smoothing reactor, and neutral busbar arresters E, EL, and EM is very low, without influence on selection of reference voltage of the arresters; thus, the chargeability is usually neglected.

18.4.3.3 Reference Voltage

For most arresters at DC side, it is possible to determine the reference voltage after determining the continuous operating voltage and chargeability; however, for the

parallel arresters (DR/SR) for the smoothing reactor, arresters at the valve side of the neutral busbar smoothing reactor(CBN2), and neutral busbar arresters (E, EL, and EM), their respective operating voltage is very low, but the energy flowing through them is very huge in case of some faults, so their respective continuous operating voltage has no effect on the selection of reference voltage. During determination of reference voltage, it is required to comprehensively consider the following factors, and carry out optimization and selection of the reference voltage by combining overvoltage simulation results and according to the quantity of arresters and insulation level of the equipment.

(1) If the arresters with a lower reference voltage are selected and the energy flowing through the arrester is larger in case of an AC or DC ground fault, it is required to connect relatively many arresters in parallel, so that a bad current sharing effect may exist between arresters resulting in damage to certain arrester due to overload, and it is highly difficult to replace the damaged arrester with a new one with consistent characteristic; however, a lower reference voltage also can reduce the insulation level of relevant equipment, having certain economic benefits.
(2) If the arresters with a higher reference voltage are selected, less number of arresters are required, but, due to a higher protection level and after taking account of an insulation margin, the insulation level of the neutral busbar equipment, component on LV side of DC filter, converter valve close to the neutral busbar, and winding at the valve side of the converter transformer at LV end is increased accordingly, resulting in an increase of cost.

In fact, based on current practical engineering experiences, arresters with a higher reference voltage are selected in these positions.

In addition, it should be noted that, among the arresters for DC systems, the DR/SR arresters are unique, whose reference voltage is far higher than its continuous operating voltage, and parameters of this arrester for different projects differ significantly for the reason that arresters DR/SR are mainly used to prevent an excessive high-voltage difference between both ends of the smoothing reactor under the influence of lightning overvoltage. Because the lightning overvoltage is far higher than the continuous operating voltage on the smoothing reactor, it is required to mainly take account of the lightning overvoltage withstand value on the smoothing reactor when determining a protection level of the arresters.

18.4.3.4 Arresters Connected with Multiple Columns in Parallel

Many arresters are connected with multiple columns in parallel in the UHVDC system. This is decided by two aspects, i.e., meeting energy requirement in case of an overvoltage and reducing protection level of the arresters. When connecting the arresters with multiple columns in parallel, it is required to pay close attention to current sharing of each column.

It is mentioned in the introductions for characteristics of UHVDC arresters given in the Sect. 18.2 of this chapter that the arresters usually absorb much energy in overvoltage condition of the UHVDC system, e.g., the maximum energy absorption of the valve arrester in some faults can be up to several MJ, so it is often required to adopt arresters connected with multiple columns in parallel in this case. Additionally, connecting arresters with multiple columns in parallel is to reduce the insulation level of the equipment under protection. The voltage level of the UHVDC system is very high and the insulation level of the equipment is also very high. The principle for reducing insulation level by connecting arresters with multiply columns in parallel is that: after being connected in parallel, it is possible to reduce the coordination current of each column, so as to reduce the protection level of the arrester, finally reducing the insulation level of the equipment. The arresters for the UHVDC pole busbar are often designed with multiple columns based on such consideration.

When connecting the arrester with multiple columns in parallel, it is required to ensure that uniform distribution of current on each column, which is a problem in need of special attention. This is because, when the arrester is actuated, the voltage on each column is identical; the distribution of energy on each column is equivalent to distribution of the current. A deviation always exists in the practical manufacturing process of the arrester, so, if the volt–ampere characteristic of one of the columns is too low, an excessively large current will flow through the arrester and an excessively large energy will be absorbed; once the energy absorbed exceeds the maximum energy absorption capacity, it will influence the safe and stable operation of the whole arrester under the overvoltage.

Normally, in order to reach even distribution of energy on each column, the manufacturers should do their best to adopt varistor units with identical characteristics to form the arrester, so as to control the current unevenness coefficient β of the multi-column arrester within a certain range, which is defined as follows:

$$\beta = nI_{\max}/I_{\text{arr}} \tag{18.13}$$

where

n is the number of columns connected in parallel,
$I_{\max}$ is the maximum current peak of any column, and
I_{arr} is the current peak of the whole arrester.

The aforementioned β can be obtained through carrying out current distribution test for the whole arrester when leaving the factory. The State Grid Corporation's company standard provides that such current unevenness coefficient β should be not more than 1.1.

18.4.3.5 Coordinating Current and Protection Level of Arresters

According to the selection principle of arrester's parameters, it is more conducive to lowering the equipment's insulation level, when the arrester's protection level is lower. But low protection level would make the arrester absorb too much energy when overvoltage occurs, which requires very large quantity or volume of the arrester to meet the requirements of high energy, thus being bound to increase the difficulty of arrester's manufacture and cost. And the arresters whose quantity and volume is too large will occupy a larger space, increasing the layout difficulty of arresters and other equipment in converter station. Therefore, when determining the DC arrester's coordinating current and protection level, it is necessary to achieve optimization combining with the overvoltage calculation results of actual DC project. The detailed optimization method is as follows: firstly, make simulation and calculation for representative overvoltage of converter station's equipment, according to the arrester's parameters which are determined initially; secondly, determine the maximum current and energy flow through arresters under the typical fault; next, adjust the arrester's column number according to the calculation results, and then make overvoltage calculation again until suitable coordinating current and protection level of the arrester are selected.

In Xiangjiaba–Shanghai UHVDC project, the arresters' finalized protection level is shown in Table 18.3.

18.4.4 Difference in Parameters of Arresters for Converter Stations at Both Terminals

Since the direct current will cause a voltage drop on DC lines during operation of the DC transmission system, the operating voltage of the inverter station is lower than the rectifier station. When the DC line is shorter and the direct current is small, this voltage drop is usually small. In order to lower the equipment manufacturing difficulty, simplify the varieties of equipment and complexity of the test, it is possible to select arresters with identical parameters such as reference voltage for the converter stations at both terminals. At present, the conventional HVDC transmission projects put into operation worldwide are configured with the same arresters in the converter stations at both terminals. When the line of the DC system is longer and the transmission current is large, the operating voltage of the inverter station is far lower than the rectifier station, so that it is possible to select a reference voltage for the arresters based on the actual operating voltage of the inverter station to reduce the protection level of the arrester in the inverter station and insulation level of the equipment, achieving a significant economic benefits in UHVDC projects.

Table 18.3 Protection levels of arresters in Xiangjiaba–Shanghai UHVDC project

Arrester	LIPL (kV)	Coordination current (kA)	SIPL (kV)	Coordination current (kA)
V1	369	1	397	8
V2	387	1	409	4
V3	387	1	409	4
DB1	1625	20	1391	1
DB2	1625	20	1391	1
CBH	1426	0.5	1385	0.2
MH	1078	1	1027	0.2
CBL2	752	1	717	0.2
ML	495	1	485	0.5
CBN1	458	1	–	–
CBN2	419	1	437	4
E	478	5	–	–
EL	311	10	303	8
EM	431	20	393	5
DR	900	0.5	–	–
A	961	20	761	14
A′	–	–	261	–

Note A′ refers to the voltage on secondary side of the converter transformer obtained by converting the protection level of the arrester A by transformation ratio of the converter transformer

Up to 2015, six ±800 kV UHVDC transmission projects had been put into operation in China, including Yunnan–Guangdong, Xiangjiaba–Shanghai, Jinping–South Jiangsu, Nuozhadu–Guangdong, South Hami–Zhengzhou, and Xiluodu–Zhexi projects. The DC line of the Yunnan–Guangdong UHVDC project is about 1418 km long, and its current is rated to 3.125 kA, as well as the DC voltage of the inverter station is about 35 kV lower than the rectifier station. The DC lines of the Xiangjiaba–Shanghai and Jinping–South Jiangsu UHV projects are longer, being up to 1907 and 2075 km, respectively; their current are large, being up to 4 and 4.5 kA, and the voltage difference between converter stations at both terminals is above 50 kV.

Among the current projects, the Yunnan–Guangdong and Nuozhadu–Guangdong project adopts identical arresters in converter stations at both terminals; however, the Xiangjiaba–Shanghai, Jinping–South Jiangsu, and other projects adopt arresters with different reference voltage in converter stations at both terminals.

18.5 Determination for Insulation Level of Converter Station's Equipment

18.5.1 Method for Insulation Coordination of Converter Station's Equipment

The final destination of insulation coordination for converter station's equipment is to determine a rational insulation withstand voltage of electrical equipment. At present, the insulation coordination method for the DC converter station is identical to the AC system, namely the insulation coordination is carried out by the conventional method. The basic thought for the conventional method is that leave a certain margin between the maximum overvoltage that may appear on the electrical equipment and withstand voltage required for the equipment, and the final equipment insulation withstand voltage is equal to or higher than the required withstand voltage set forth above, which is shown in Eq. (18.14).

$$U_{\mathrm{rw}} = K \times U_{\mathrm{rp}} \tag{18.14}$$

where

U_{rw} is the required withstand voltage,
U_{rp} is the representative overvoltage, which is equal to the protection level of the arresters for the equipment directly protected by arresters,
K is the insulation margin coefficient, whose determination will be discussed in the following chapter.

For the AC systems, it is possible to obtain an equipment insulation withstand voltage, based on the required withstand voltage calculated above and by making a reference to the standard withstand voltage. For the DC systems, especially the UHVDC systems, however, no standard withstand voltage level is available and it is considered that slight increase in insulation level of the UHVDC system will lead to sharp increase in equipment size and manufacturing cost, so an appropriate approximate integral value is usually taken as the equipment insulation withstand voltage, and it is determined by neglecting the custom that the ratio of switching impulse withstand level to the lightning impulse insulation level is less than 0.83.

18.5.2 Insulation Margin

The insulation withstand level of the electrical equipment should be higher than the protection level of the arresters, ensuring safety of the equipment when it is subject to overvoltage stress. In view of time-dependent aging (e.g., aging of insulation material) of equipment insulation, decrease in insulation level of the equipment under influence of weather factors (rain and fog, etc.), aging of arresters,

environmental pollution, and high altitude influence and other factors, the required insulation withstand voltage is obtained by multiplying the protection level of the arrester by a coefficient which is called insulation margin coefficient *K*. The equipment at different positions and adopting different insulation methods have different requirements for insulation margin.

As mentioned above, the insulation coordination of the UHVDC system does not only consider economy but also safe and stable operation of the system. An excessively large insulation margin will cause unnecessary economic waste, and a small insulation margin cannot ensure safety and stability of the system, so an appropriate insulation margin is very important.

Table 18.4 specifies the requirements for insulation margin of the equipment in the HVDC transmission projects below altitude of 1000 m given in the GB/T 311.3-2007 [6].

For the UHVDC system, the influence of switching overvoltage is more serious, and the insulation level of each equipment should correspond to certain specific overvoltage stresses when carrying out insulation design, so the insulation margin is often selected by a means being different from the conventional ones. For example, the recommended values given by the Siemens and ABB company for switching impulse insulation margin and lightning impulse insulation margin of the oil insulation and air insulation equipment for the ±800 kV UHVDC system is 15% and 20%, respectively, and the recommended value given the Siemens for the steep front impulse margin is 20%, but ABB company recommends that it is maintained at 25%.

For the converter valve in converter station, the selection of its insulation margin should be corrected. The converter valve is core equipment of the DC transmission

Table 18.4 Insulation margins of equipment in HVDC transmission projects recommended by GB/T 311.3-2007

Type of equipment	RSIWV/SIPL	RLIWV/LIPL	RSFIWV/STIPL
Busbar, outdoor insulator and other conventional equipment in AC switchyard	1.20	1.25	1.25
AC filter component	1.15	1.25	1.25
Converter transformer (oil-immersed)	–	–	–
Grid side	1.20	1.25	1.25
Valve side	1.15	1.20	1.20
Converter valve	1.15	1.15	1.20
Equipment in DC valve hall	1.15	1.15	1.25
Equipment in DC switchyard (outdoor equipment include DC filters and smoothing reactors)	1.15	1.20	1.25

Note: *RSIWV* refers to required switching impulse withstand voltage; *SIPL* refers to switching impulse protection level; *RLIWV* refers to required lightning impulse withstand voltage; *LIPL* refers to lightning impulse protection level; *RSFIWV* refers to required steep front impulse withstand voltage; *STIPL* refers to steep front impulse protection level

system. Most converter valves used in the modern DC transmission systems adopts the air insulation and water-cooled indoor suspension multi-valve structure. Due to high manufacturing cost, rationality of the insulation margin selected has a great influence on cost of the whole project. The insulation of the converter valve has following characteristics:

(1) The converter valve is installed in the valve hall, and the indoor environmental conditions can be controlled well, and are not affected by the external environmental factors (e.g., humidity, temperature, and dust) basically. That is the most important cause why the converter valve insulation is different from insulation of other equipment.
(2) The converter valve unit is provided with monitoring devices to easily find the malfunctioning thyristors and other valve components (including valve reactors and voltage equalizing damping capacitors, etc.). After maintenance or replacement of the malfunctioning components every time, it can be believed that the insulation capacity of the valve is reset to the initial value.
(3) With technical progress, an excellent volt–ampere characteristic can still be maintained after the zinc oxide arresters are operated for several years, that is to say, the arresters used to directly protect the converter valves still can have an excellent protection action under influence of overvoltage stress.
(4) For the reason that the valve cost and loss are approximately proportional to the valve insulation level, lowering the valve insulation level can also reduce the height of the valves and valve hall.

In view of the characteristics above, it can be believed that appropriate reduction in insulation margin of the UHVDC system is feasible technically, and brings in significant economic benefits. Several research institutes including ABB and Siemens suggest that the valve insulation margin be reduced to 10 and 15%.

Finally, the insulation margins adopted in the Yunnan–Guangdong and Xiangjiaba–Shanghai UHVDC projects are shown in Tables 18.5 and 18.6. In addition, GB/T 28541-2012 *Insulation coordination for equipments of* ±800 kV *high-voltage direct current converter stations* gives recommended insulation margin for equipment in HVDC converter station, which is the same as GB/T 311.3-2007 *Insulation Coordination-Part 3: Procedures for High-voltage Direct Current* (*HVDC*) *Converter Stations*, and the insulation margin is shown in Table 18.4. But the standard also points out that the given insulation margin is for general design, the final ratio can be adjusted according to the selected performance index (increase or decrease).

18.5.3 Protection Level and Insulation Level

The equipment's insulation level can be determined according to Eq. (18.14), when the equipment's insulation margin and arrester's protection level have been

Table 18.5 Insulation margins adopted in Yunnan–Guangdong UHVDC project (%)

Equipment	Switching impulse	Lightning impulse	Steep front impulse
Converter valve	15	15	25
Converter transformer	15	20	25
Smoothing reactor	15	20	25
Equipment in DC valve hall	15	15	25
DC field	15	20	25

Table 18.6 Insulation margins adopted in Xiangjiaba–Shanghai UHVDC project (%)

Equipment	Switching impulse	Lightning impulse	Steep front impulse
Converter valve	10	10	15
Other DC equipment	15	20	25
DC field	15	20	25

determined. When determining the insulation level of equipment in converter station, the converter valve, converter transformer, busbar, and other equipment in the converter station can be directly protected by an arrester or by two or more arresters connected in series. When the equipment are protected by several arresters connected in series, the protection level of the arresters connected in series is determined by adding the protection level of all arresters directly, and the corresponding coordination current is determined by the coordination current in individual arresters connected in series [7]. In fact, the maximum coordination discharging current cannot appear on all arresters connected in series in case of a fault, so this method gives an additional margin for the insulation coordination. In the aforementioned calculation for arrester's parameters, Table 18.3 shows the arresters' protection level of Xiangjiaba–Shanghai UHVDC project. The insulation level of equipment at DC side of converter station (rectifier station) can be determined according to Table 18.3 and Eq. (18.14), and the results are shown in Table 18.7.

18.6 Scheme for Separate Arrangement of Smoothing Reactors

The smoothing reactor, as one of the key equipments in the UHVDC converter station, is mainly used to prevent current interruption in light load condition, and is connected with the DC filter to jointly form a DC filter circuit of the converter station to lower the DC harmonic component, and smooth the fluctuation of the DC voltage, as well as limit the steep front impulse from the DC line to enter the valve hall under some fault conditions and suppress quick increase in the DC fault

Table 18.7 Insulation levels of equipment in DC field of Xiangjiaba–Shanghai UHVDC project

Position	Arrester	LIPL (kV)	LIWL (kV)	Insulation margin (%)	SIPL (kV)	SIWL (kV)	Insulation margin (%)
Between valves	Max(Vl, V2, V3)	387	426	10	409	450	10
AC busbar	A	961	1550	61	761	1175	54
DC busbar to ground at the valve side	CBH	1426	1800	26	1385	1600	15
DC busbar to ground at line side	Max(DB1, DB2)	1625	1950	20	1391	1600	15
600 kV busbar to ground	MH	1078	1294	20	1027	1182	15
400 kV busbar to ground	CBL2	752	903	20	717	825	15
200 kV busbar to ground	ML	495	594	20	485	558	15
HV Yy converter transformer phase-to-ground, valve side	V2 + MH	1454	1745	20	1386	1584	15
HV Yd converter transformer phase-to-ground, valve side	V2 + CBL2	1139	1367	20	1126	1295	15
LV Yy converter transformer phase-to-ground, valve side	V2 + ML	882	1059	20	894	1029	15
LV Yd converter transformer phase-to-ground, valve side	Max (V2 + CBN1, V2 + CBN2)	845	1019	20	846	973	15
YY converter transformer phase-to-phase, valve side	$2 \times A'$	–	–	–	522	601	15
YD converter transformer phase-to-phase, valve side	$\sqrt{3} \times A'$	–	–	–	452	520	15
Neutral point on HV Yy converter transformer, valve side	A′ + MH	–	–	–	1288	1482	15
Neutral point on LV Yy converter transformer, valve side	A′ + ML	–	–	–	746	858	15

(continued)

Table 18.7 (continued)

Position	Arrester	LIPL (kV)	LIWL (kV)	Insulation margin (%)	SIPL (kV)	SIWL (kV)	Insulation margin (%)
Between 12-pulse converter bridges	Max(Vl, V2) + V2	763	916	20	806	927	15
Between smoothing reactors	DR	900	1080	20	–	–	–
Neutral busbar, valve side	Max(CBN1, CBN2)	458	550	20	437	503	15
Neutral busbar, line side	Max(E, EL, EM)	478	574	20	393	452	15
Ground electrode busbar	EL	311	374	20	303	349	15
Metallic return busbar	EM	431	518	20	393	452	15

current, so as to protect the converter valve from being damaged due to overvoltage and overcurrent to some extent.

At present, all smoothing reactors are arranged on the DC pole line in the conventional HVDC transmission projects, while smoothing reactors for the Xiangjiaba–Shanghai and Yunnan–Guangdong ±800 kV UHVDC transmission project are arranged by means of separating it into two parts, of which one part is arranged on the DC pole line, and the other one is arranged on the neutral busbar. This arrangement method is called separate arrangement of smoothing reactor on the DC pole line and neutral busbar, or separate arrangement of smoothing reactor for short. For example, the inductance value is 300 mH for the smoothing reactor provided in each substation at each pole of the Yunnan–Guangdong UHVDC project which is made up of four sets of 75 mH dry-type smoothing reactors, of which two sets are arranged on the DC pole line, and the other two sets are arranged on the neutral busbar.

18.6.1 Economic and Technical Advantages of Separate Arrangement of Smoothing Reactors

Due to restriction by manufacturing technology and craft, the reactance of a single dry-type smoothing reactor used for the UHVDC projects cannot be too large, so it is required to configure several smoothing reactors. For example, four sets of smoothing reactors are required at each pole of the above-mentioned Yunnan–Guangdong project, and if these four smoothing reactors are all arranged on the DC

pole line, it will significantly increase the difficulty in arrangement of converter station equipment. Obviously, separate arrangement of smoothing reactors helps reduce the difficulty in arrangement of electrical equipment for the converter station, and it is more important that the separate arrangement of smoothing reactors has obvious economic and technical advantages in the UHVDC transmission projects.

On one hand, due to high-voltage level of the UHVDC system, a high requirement is put forward to insulation level of the smoothing reactors on the DC pole line, and the manufacturing difficulty and cost are very high. In case of using separate arrangement, the insulation level is much lower due to the voltage of the neutral busbar is very low, significantly reducing the manufacturing difficulty and cost of the smoothing reactors in the neutral busbar. On the other hand, separate arrangement of the smoothing reactors can significantly reduce the maximum continuous operating voltage at several positions of the converter station, especially each point of the upper 12-pulse converter unit, so reference voltage and protection level of relevant arresters, and insulation level of relevant equipment can be reduced. These two factors are beneficial to lower manufacturing difficulty and cost of equipment at the converter stations (including arresters), reducing investment and achieving very high economic and technical benefits.

The following takes one pole of the UHVDC transmission system as an example to carry out a detailed discussion on benefits of separate arrangement of smoothing reactors.

The simplified equivalent diagram for the UHVDC monopolar system is shown in Fig. 18.4. In the figure, the rectifier adopt a structure of the double 12-pulse converter units connected in series; half of the smoothing reactors are arranged on the DC pole line, and the other half ones are arranged on the neutral busbar. The smoothing reactor at the rectifier side, the DC line out of the DC filter outlet, and the inverter side are taken as a whole to be equivalent to an impedance.

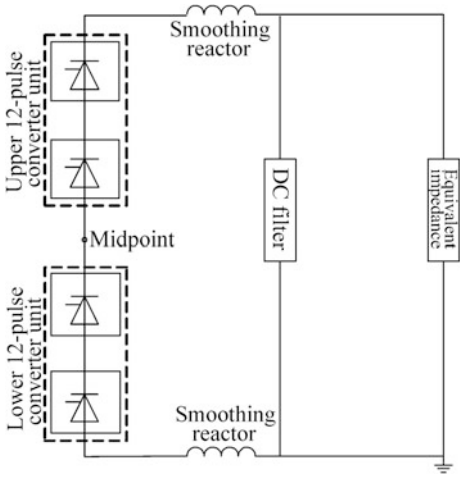

Fig. 18.4 Simplified equivalent diagram for UHVDC monopolar system

Considering that each 12-pulse converter unit also can be equivalent to a power supply, such power supply does not only contain the direct current component but also contains the harmonic component. Thus, it is possible to carry out further equivalence for the monopolar system, as shown in Fig. 18.5, that is to say, each 12-pulse converter unit is replaced by connecting one pure DC power supply U_d and one harmonic voltage source U_h in series.

Then the above-mentioned equivalent circuit is further handled, according to the superposition principle in the electric circuit principle, to obtain an equivalent circuit as shown in Fig. 18.6.

As shown in Fig. 18.6, the electric circuit (a) can be obtained by superposing the pure DC voltage source circuit (b) and harmonic voltage source circuit (c). In the pure DC voltage source circuit (b), the direct current does not flow through the DC filter, and the branch is equivalent to be open, so only the circuit for equivalent impedance is given. For the reason that the pure direct current does not produce a voltage drop on the smoothing reactor, the voltage of the busbar between the upper and lower converter units (i.e., the "midpoint" in the figure) is a pure DC voltage U_d. In the harmonic voltage source circuit (c), the harmonic current only flows through the DC filter, and only a DC filter circuit is given. For the reason that the DC filter reflects a low resistance property under the influence of harmonic current, it can be deemed that it is short circuit to the harmonic source. Thus, the harmonic voltage of $2U_h$ for the upper and lower 12-pulse converters is fully applied to the two smoothing reactors, so the electric potential at the "midpoint" in (c) is zero.

Thus, the electric potential at "midpoint" in the electric circuit (a) is equal to the electric potential at "midpoint" in the electric circuit (b) plus the electric potential at "midpoint" in the electric circuit (c), namely U_d, so that the voltage at the valve side of the smoothing reactor on the DC pole line is $2U_d + U_h$. The voltage of DC line

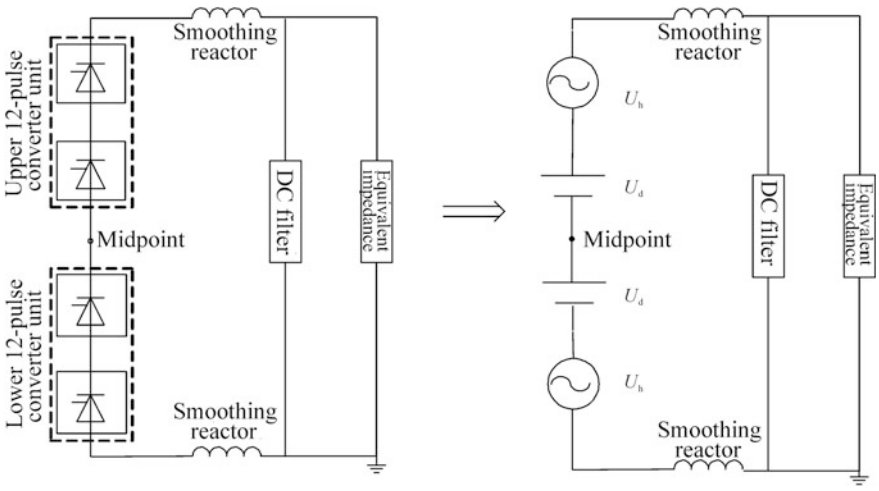

Fig. 18.5 Equivalent diagram for UHVDC monopolar system

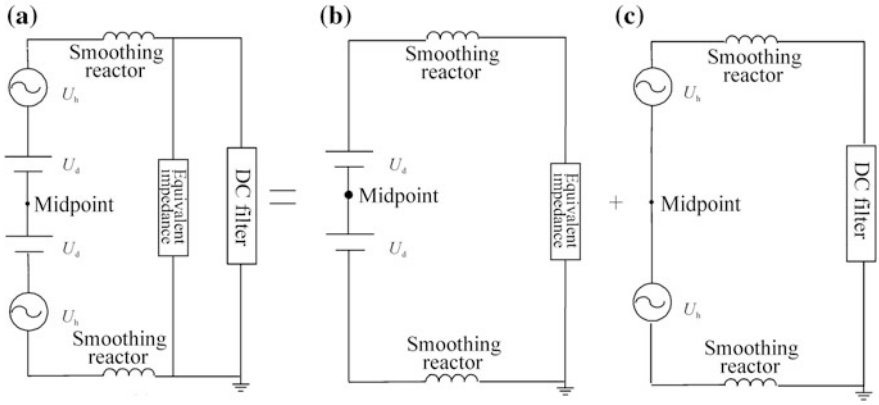

Fig. 18.6 Equivalent diagram for monopolar system adopting superposition theorem

outlet is $2U_d$, i.e., 800 kV for the ±800 kV UHVDC systems. Therefore, in case of separate arrangement of smoothing reactors, the voltage on the busbar between the upper and lower 12-pulse converter units is approximated to a pure DC voltage U_d = 400 kV, and the voltage at the valve top is superposed by a voltage of a converter unit, i.e., $2U_d + U_h$ = 800 kV + U_h.

The smoothing reactors are arranged by the means other than separate arrangement means, as shown in Fig. 18.7, that is to say, all smoothing reactors are arranged on the DC pole line. The following content briefly explains the magnitude of voltage on the busbar between the upper and lower 12-pulse converter units and voltage at the valve top when the smoothing reactors are not arranged in separate arrangement manner. Obviously, the "midpoint" voltage is a voltage of one 12-pulse converter unit, namely $U_d + U_h$ = 400 kV + U_h; the voltage at valve top is the sum of voltage of the two 12-pulse converter units, namely 2 ($U_d + U_h$) = 800 kV + $2U_h$.

From the analysis given above, it can be seen that, when all smoothing reactors are arranged on the pole line, the voltage on the busbar between 12-pulse converter units and at the valve top is 400 kV + U_h and 800 kV + $2U_h$, respectively; and when the smoothing reactors are arranged separately, the voltage on the busbar between 12-pulse converter units and at the valve top is 400 kV and 800 kV + U_h, respectively. Obviously, after the smoothing reactors are arranged separately, the operating voltage on the busbar between 12-pulse converter units and at the valve top decreases. Because these two positions are at both ends of the upper 12-pulse converter unit, the maximum continuous operating voltage at each point in the whole upper 12-pulse converter unit (including each point on converter valve side) will decrease.

Figure 18.8 gives a comparison between waveforms obtained at relevant positions when the smoothing reactors are separately arranged and not separately arranged. The numbers in the figures represent positions of waveform measuring points in the converter station, and the corresponding position number is shown in

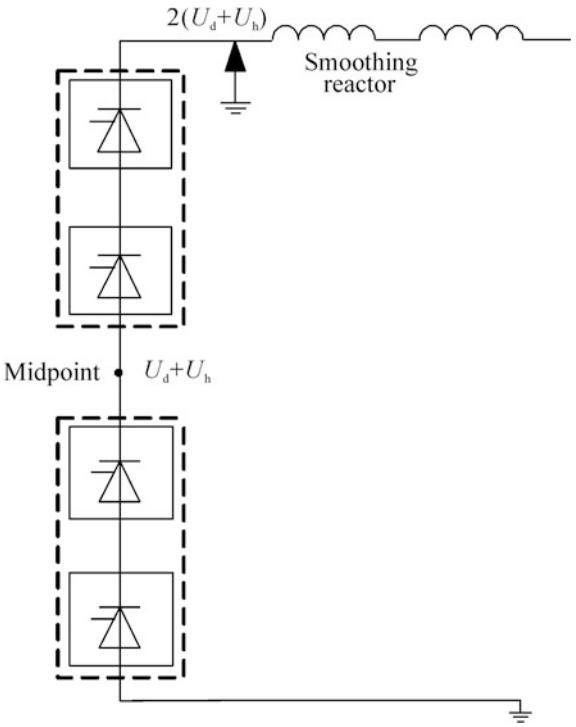

Fig. 18.7 Diagram for smoothing reactors not separately arranged

Fig. 18.1 for arrangement of arresters in the Xiangjiaba–Shanghai UHVDC Project. Of course, the voltage on the busbar between 12-pulse converter units always contains a harmonic voltage during actual operation of the system, and is not a pure DC voltage of 400 kV. This mainly depends on the symmetry of the upper and lower 12-pulse converter units, including symmetry of leakage reactance, trigger angle, damping parameter, reactance value of smoothing reactor and other parameters of upper and lower converter transformers.

Of course, use of separate arrangement also has some disadvantages, which are as follows:

(1) Due to the use of separate arrangement of the smoothing reactors, its influence to the upper 12-pulse converter unit is opposite to its influence to the lower 12-pulse converter units, and the harmonic wave produced by the smoothing reactors on the neutral busbar rises the operating voltage at bottom of the lower converter unit, including the operating voltage at the valve side of the converter transformer that is at the minimum electric potential level. This improves the protection level of relevant arresters and insulation level of relevant equipment, so that the insulation level will be higher than the line side of the neutral busbar smoothing reactor. Certainly, as the voltage of the lower converter unit is low, improvement in insulation level of relevant positions does not cause a technical challenge.

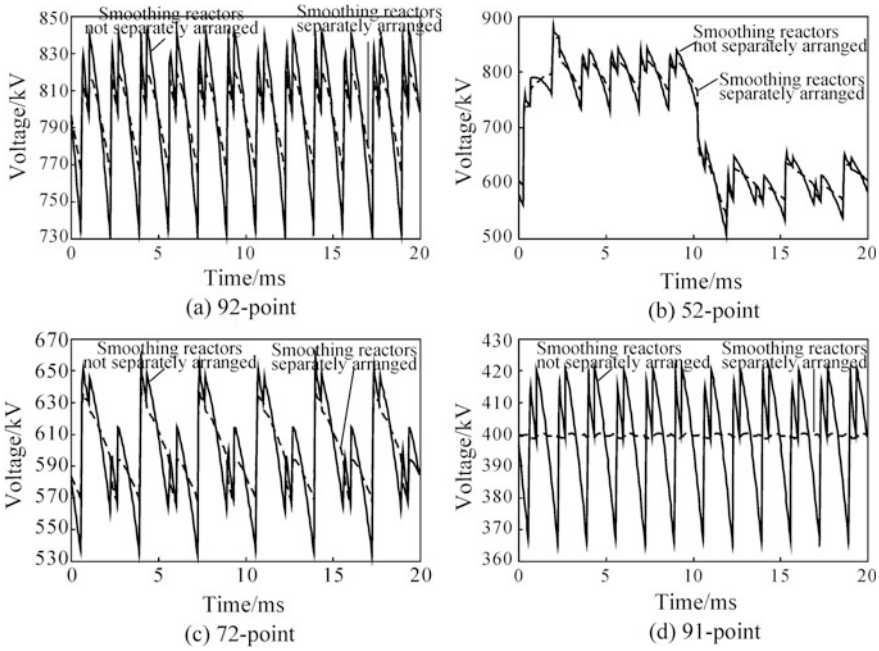

Fig. 18.8 Comparison of waveforms at various positions of DC system

(2) In some fault conditions, the smoothing reactor of the neutral busbar will limit the leakage current flowing to the neutral busbar arresters, and most energy can be released only by the arrester at the valve side of the smoothing reactor, so a very high requirement is imposed for the energy absorption capacity of the arrester, and it is required to connect the arrester with multiple columns in parallel. Meanwhile, the arresters should be placed outside the valve hall to prevent the arrester at the valve side of the smoothing reactor from explosion endangering safety of other equipment in the valve hall due to excessive energy absorption.

Therefore, the shortcomings of separate arrangement of the smoothing reactors are easily overcome, without adverse influence on the DC system.

18.6.2 Necessity for Adoption of Separate Arrangement of Smoothing Reactors in UHVDC System

It should be noted that, when the voltage level is within UHV range, the insulation becomes a major problem, especially in the high-altitude area, the insulation

problem will be more serious. The experiences show that, when the voltage level is not high, the equipment cost is approximately proportional to the third power of the equipment size, and the size of equipment is approximately proportional to the equipment insulation level, so the equipment cost is approximately the third power of insulation level of the equipment. Firstly, after the voltage level rises to the UHV range, the specific creepage distance, air clearance, and other factors will present a non-linear characteristic relationship with the operating voltage. For example, if the operating voltage increases by 60% (from 500 to 800 kV), the air clearance should be increased by about 100%, and increase in operating voltage and intensification of non-linear factors will make the size of the equipment increased rapidly; secondly, a very high insulation level imposes higher requirements for electrical and mechanical characteristics of the equipment, including uniformity of material, high-voltage withstand level, anti-pollution property, corrosion resistance and voltage equalization measures; in addition, an excessively high insulation level also has higher requirements for such tests as type tests which is necessary to the UHVDC equipment and enhance the test difficulty and cost. Therefore, the aforementioned three points get the final equipment cost be more than the third power of the insulation level, presenting a stronger non-linear characteristic. Thus, slight decrease in insulation level of the UHVDC equipment can result in a significant decrease in equipment volume, manufacturing cost, test cost, and transportation difficulty, and obtain excellent economic benefits.

With respect to the conventional ±500 kV DC transmission projects, their costs have been controlled within a rational range due to rich experiences in actual operation, and mature and stable equipment manufacturing and test technologies; moreover, for the reason that the voltage level is lower than that of the UHVDC projects, if the insulation level of equipment is decreased slightly, it cannot bring in significant benefits like the UHVDC project. Additionally, in case that the smoothing reactors are arranged separately, it is equivalent that the whole DC system is provided with neutral busbar smoothing reactors as additional equipment, reducing the reliability of the whole system. Therefore, it is not required that the smoothing reactors be arranged separately for ±500 kV DC transmission projects.

In a word, the separate arrangement method of smoothing reactors is a good technical means adopted in the UHVDC transmission projects, which has obvious economic benefits. It can be predicted that the separate arrangement method will be the preferred method for arrangement of smoothing reactors in the newly built UHVDC projects in future.

18.7 Minimum Air Clearance in Converter Station

The external insulation design of the UHV converter station is one of the key technologies for the UHVDC projects, and safe and stable external insulation design is one of the conditions for normal and stable operation of the whole DC system. The external insulation of the converter station mainly includes air

clearance insulation and solid medium insulation in terms of physical mediums. This section focuses on discussion of air clearance insulation.

After determining the protection level of arresters and insulation level of the equipment in the converter station, it is required that the equipment have an air clearance distance away from the surrounding ground bodies. Because the HV end of the DC equipment in the converter station is at a very high-voltage, large-size grading rings or shielding rings are installed at the top and corners of each equipment (i.e., converter valve bank and smoothing reactors) to improve the distribution of electric field. Therefore, the air clearance distance of equipment away from the surrounding ground bodies is actually the minimum air clearance of the grading ring or shielding ring from the surrounding wall or other ground bodies. Compared to the ±500 kV HVDC transmission system, the UHVDC transmission is at a higher voltage level, and the maximum DC operating voltage can be up to 816 kV, and the discharging voltage of the air clearance under a higher overvoltage will present a saturation characteristic. Moreover, the altitude of the Chuxiong Converter station as the sending end of the Yunnan–Guangdong UHVDC project that has been completed is close to 2000 m, and the altitude the Jinping Converter station as the sending end of the Jinping–South Jiangsu UHVDC project is 1530 m. A high altitude has an obvious influence on the discharging voltage of the air clearance. As the altitude increase, the air gets thinner gradually and the atmospheric pressure and air density decrease, so that the discharging voltage is decreased accordingly as the electric strength of the air clearance is decreased, and the converter station in high-altitude areas should consider the altitude correction; for the UHVDC converter station provided with more equipment in the valve hall and DC field and more busbars connected to the equipment, it is required to determine more air clearance distances, mainly including 800 kV busbar to ground clearance, 800 kV busbar to 400 kV busbar clearance, and clearance of converter transformer winding at the highest end to ground. Details are shown in Table 18.8.

During determination of the air clearance at DC side of the converter station, it is required to mainly take into account of the voltage formed by the DC, AC, lightning and switching impulses. For the reason that most live conductors in the converter station are fixed electrodes, the air clearances are mainly decided by the lightning and switching impulses. The discharging voltage characteristics of lightning impulse and switching impulse for varieties of converter stations are required for design of air clearance. In order to accurately calculate the air clearance at DC side, some curves of discharge characteristic are required, including the curve between the flexible overhead conductors and frameworks, the curve between the hard tubular busbar and frameworks, the curve between the electrical equipment (grading ring) and frameworks, and the curve between the tubular busbar and steel columns of the valve hall. When determining air clearances in the valve hall, it is also required to consider the atmospheric density correction and humidity correction.

Many test data obtained from sources worldwide show that, for the lightning impulse, the flashover voltage presents a linear relationship with the clearance length, and non-linear with the clearance length for the switching impulse. From the

Table 18.8 Typical air clearances in UHVDC converter station

Busbar to busbar	800 kV busbar to 400 kV busbar 400 kV busbar to DC neutral busbar
Midpoint of busbar/valve bank to ground	800 kV busbar at the valve side of smoothing reactor to ground 400 kV busbar to ground DC neutral busbar at the valve side of the smoothing reactor to ground Midpoint of HV 6-pulse converter unit to ground Midpoint of LV 6-pulse converter unit to ground
Busbar to neutral point of valve bank	800 kV busbar to midpoint of HV 6-pulse converter unit 400 kV busbar to midpoint of HV 6-pulse converter unit 400 kV busbar to midpoint of LV 6-pulse converter unit DC neutral busbar to midpoint of LV 6-pulse converter unit
Point related to converter transformer	Neutral point of Y winding converter transformer to ground Δ winding of converter transformer, phase-to-ground Between phases of converter transformer, valve side Neutral point of Y winding HV converter transformer to 800 kV busbar Y winding phase of converter transformer to neutral point Between lines on Y winding valve side and Δ winding valve side of converter transformer Y winding of HV converter transformer to 800 kV busbar Δ winding of LV converter transformer to midpoint of LV 6-pulse converter unit Y winding of HV converter transformer to 400 kV busbar Δ winding of LV converter transformer to DC neutral busbar

data on relation of rod-plane clearance critical flashover voltage and the clearance length obtained after a great amount of impulse voltage tests carried out in America, Japan, and Italy and other countries, it can be seen that the discharging voltage presents a non-linear saturation trend as the voltage level increases, and the voltage of about 1600 kV is a very obvious inflection point. Usually, due to the existence of saturation characteristic of the air clearance under the influence of switching impulse, the required air clearance distance is far larger than the clearance distance decided by the lightning impulse, and according to the State Grid Corporation's company standard [8] and experience in other DC projects worldwide, the switching impulse calculation value is taken as the minimum air clearance distance.

The voltage level of ±800 kV UHVDC transmission system is new, in the design of air clearance in converter station, there is no actual operation or design experience in this voltage level can be referred. Therefore, the determination of minimum air clearance in converter station should accord to the ±800 kV converter station's discharge test curves in real air clearance. But when there are no discharge curves, it can be determined by related formulas recommended by various research institutions. In this section, the first part introduces the air clearance discharge characteristics test between UHVDC converter station's pole bus and its surrounding grounding body, which is conducted by China Electric Power Research Institute; the second part introduces the formulas for minimum air clearance design;

and the third part introduces the correction method for the minimum air clearance design under non-standard atmospheric conditions.

18.7.1 Air Clearance Discharge Characteristic Test of Pole Busbar in Converter Station

When the electrode shape of DC field equipment in the converter station is different, the switching impulse discharge characteristic of air clearance differs significantly. For example, with respect to the equipment including converter valve bank and smoothing reactors that are installed with a large-size grading ring, a better air clearance shape is formed by the surrounding ground bodies, so the discharging voltage is higher, and the required clearance distance is smaller; a worse air clearance shape is formed because the size of pole busbar and its grading ring is smaller, so the required clearance distance is larger, relatively. Therefore, China Electric Power Research Institute (hereafter referred to as CEPRI) mainly carries out an experimental study on discharge characteristic of air clearance formed between the pole busbar and surrounding ground bodies [9].

During the test, the switching impulse discharge characteristic test is carried out in the following two typical electrode modes with pole busbar to ground: the first one is the pole busbar to the grounded protection fence; the second one is the pole busbar to the bottom support of post insulator.

1. Discharge characteristic in mode of pole busbar to the grounded protection fence

Considering that there are often two types of pole busbars connected to each high-voltage equipment in the valve hall and DC field in the converter station, namely rigid busbar (tubular, also called tubular busbar) and flexible busbar (multi-bundle flexible conductor). The CEPRI carries out tests for these two types of busbars. During the tests, the rigid busbar selected is an aluminum tube with length of 11.5 m and diameter of 250 mm, and a sphere electrode is provided at both ends of the busbar to improve the electric field distribution at the ends; the flexible busbar is a 4-bundle conductor with length of 12 m and spacing of 500 mm (the subconductor diameter is 33 mm), and grading rings are provided at both ends of the busbar, and the busbar is risen by about 8–9° to simulate the sag of the flexible conductor. The stainless steel tube with ground height of 1.88 m is used to simulate the grounded fence, with diameter of about 75 mm.

Considering that the positive switching impulse discharging voltage produced when the pole busbars and fences are arranged vertically is lower than that when they are arranged horizontally, the pole busbars and fences are arranged vertically during the test, and the clearance distance between the pole busbar and fence is within 3–10 m. The test samples are arranged as shown in Figs. 18.9 and 18.10.

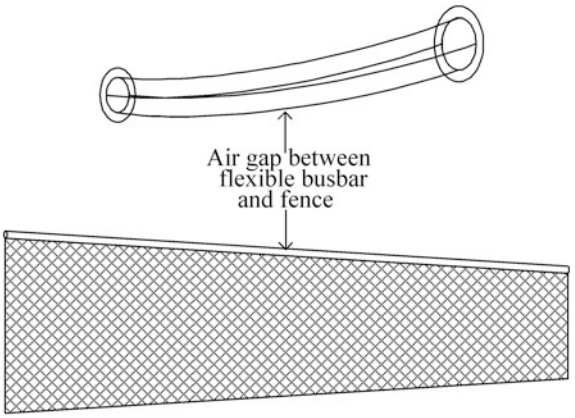

Fig. 18.9 Sketch for arrangement of flexible Busbar-Fence clearance test

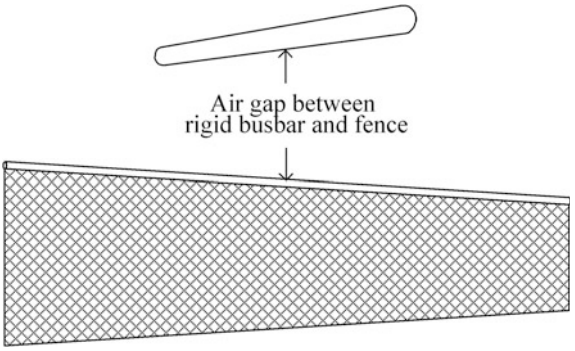

Fig. 18.10 Sketch for arrangement of rigid Busbar-Fence clearance test

The test results show that:

(1) There is a little discharging voltage difference between rigid busbar and flexible busbar

It can be seen from the test results [9] that 50% switching impulse discharging voltage of the rigid busbar and flexible busbar to the air clearance mainly depends on the air clearance distance, but is slightly related to the busbar type. The discharging voltage of two busbars with identical air clearance differs within 3%.

(2) The switching impulse discharging voltage of the pole busbar is approximately linear with the air clearance distance

When the air clearance is within 3–10 m in such test condition, 50% switching impulse discharging voltage is basically linear with the air clearance distance [9].

2. Discharging characteristic of pole busbar to the bottom support of post insulators

The rigid busbar selected for the test is still an aluminum tube with diameter of 250 mm, whose bottom support of post insulator is a steel structure with height of about 8 m. During the test, the rigid busbar and post insulator are arranged as shown in Fig. 18.11. The height of the post insulator structure is between 4 and 10 m [10].

The test results show that

(1) The switching impulse discharging voltage of the pole busbar is approximately linear with the height of the post insulators

In such test condition, 50% switching impulse discharging voltage is basically linear with the height of the post insulator structures, which is shown in Fig. 18.12 [10].

(2) The discharging voltage is higher and the air clearance distance required is smaller

Plot the test results of the pole busbar to the grounded fence in a same coordinate system together with results of the present test, which is shown in Fig. 18.12 [10]. It can be seen from the figure that the discharging voltage of the pole busbar to the bottom support of the post insulator is higher, so that a smaller air clearance is required at the same switching overvoltage level. This is mainly because the electrode shape of the pole busbar to the bottom support of the post insulators is similar to the rod–rod clearance, and the discharging voltage remains high, as well as the electrode shape of the pole busbar to grounded fence is slightly less similar to the typical rod–rod clearance, so the discharging voltage is lower than the discharging voltage of the pole busbar to the bottom support of the post insulators.

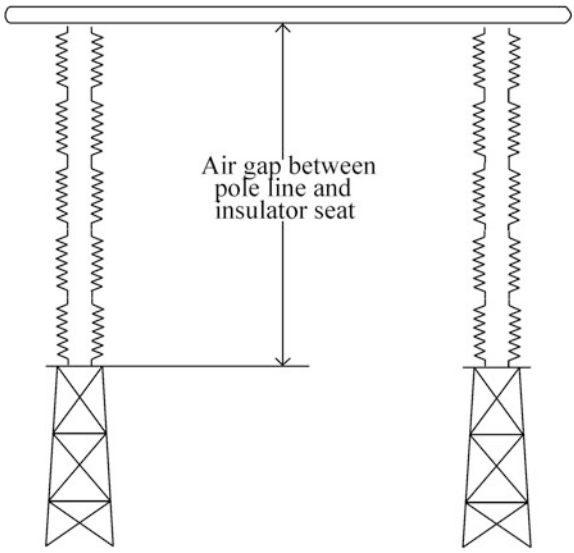

Fig. 18.11 Sketch for arrangement of ±800 kV post insulator test

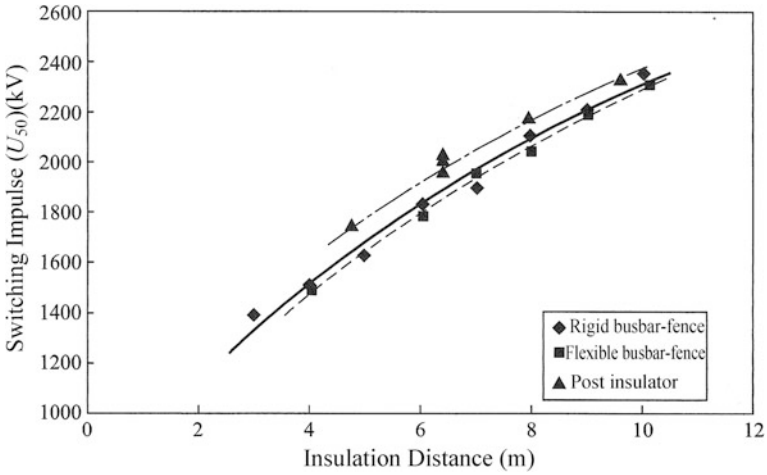

Fig. 18.12 Comparison between switching impulse discharge characteristics of busbar and post insulators

18.7.2 Equation Method for Design of Minimum Air Clearance

At present, there are three formulas recommended by research institutions to calculate minimum air clearance in converter station, including the International Council on Large Electric Systems (CIGRE), Electric Power Research Institute (EPRI), and Chinese DC Transmission Projects. The three calculation formulas will be discussed in the following.

1. Calculation method recommended by International Council on Large Electric Systems (CIGRE)

The 50% impulse discharge voltage of the air clearance is calculated by the following equation recommended in the report [11] published in 1984 by the CIGRE:

$$U_{50} = \frac{K_1 U_{\mathrm{p}}}{(1 - 2\sigma)K_2} \tag{18.15}$$

where

K_1 is the margin coefficient, which is taken as 1.2 and 1.25 for switching impulse and lightning impulse, respectively;
U_{P} is the protection level of corresponding arrester;
σ is the coefficient of variation for the impulse discharge voltage of the air clearance, whose recommended values are 6 and 3% for the switching impulse and lightning impulse, respectively;

K_2 is the meteorological correction factor for the impulse discharge voltage of the air clearance, which is taken as $K_2 = 1$ in the area with altitude below 1000 m.

After determining 50% switching and lightning impulse discharge voltage of the air clearance, it is possible to calculate the minimum air clearance distance by the following equations.

$$\text{Switching impulse: } U_{50} = k \times 500 \times d^{0.6} \tag{18.16}$$

$$\text{Lightning impulse : } U_{50} = k \times 540 \times d \tag{18.17}$$

where

d is the air clearance distance,
k is the clearance coefficient of the electrode shape characteristic, which is selected as follows: configuration of conductor to plane, $k = 1.15$; configuration of conductor to conductor, $k = 1.3$; configuration of rod to rod, $k = 1.4$.

2. Calculation method recommended by Electric Power Research Institute (EPRI)

The 50% impulse discharge voltage of the air clearance is calculated by the following equation given in the report [12] published in 1985 by the EPRI:

$$U_{50} = \frac{\text{SIWL}}{1 - 3\sigma} \tag{18.18}$$

where

SIWL is the switching impulse withstand level of the equipment,
σ is the coefficient of variation for the impulse discharge voltage of the air clearance, which is taken as about 4–6%.

Based on the 50% switching impulse discharge voltage of the air clearance, the minimum air clearance distance required for the switching impulse can be calculated by the following equations:

$$\begin{cases} U_{50} = k \times 500 \times d^{0.6} & d < 5\text{m} \\ U_{50} = k\frac{3400}{1+\frac{8}{d}} & 5\text{m} < d < 15\text{m} \end{cases} \tag{18.19}$$

where

k is the clearance coefficient of the electrode shape characteristic, which is selected by the same method as the one recommended by the CIGRE.

3. Method adopted by Chinese DC transmission projects

The following equation is recommended in the electric power industry standard of the People's Republic of China to calculate the 50% impulse discharge voltage of the minimum air clearance:

$$U_{50} = \frac{U_{\mathrm{W}}}{1 - 2\sigma} \tag{18.20}$$

where

U_{50} is the 50% impulse discharge voltage of the air clearance,
U_{w} is the impulse withstand level of the equipment (SIWL and LIWL),
σ is the coefficient of variation for the impulse discharge voltage of the air clearance, which is normally taken as 3 and 6% for the lightning and switching impulse, respectively.

The minimum air clearance distance is determined by the same equations as Eqs. (18.16) and (18.17) recommended by the CIGRE. It is required to point out that the influence imposed by the electrode shape usually can be neglected in engineering applications, and a conservative value is taken as the electrode shape coefficient, namely $k = 1$. Thus, a larger air clearance distance value will be obtained to maintain a larger safety margin.

Table 18.9 gives the minimum air clearance distance for the DC pole busbar of the converter station. The CEPRI's tests are carried out for the rigid busbar, flexible busbar, and post insulator, respectively, and other three equation calculation methods are for both rigid busbar and flexible busbar.

According to the practical test curve for real air clearance of the simulation model obtained by CEPRI, the minimum air clearance of the switching impulse to the pole busbar of the converter station is approximately 6 m, while it is approximately 7–8 m calculated by equations recommended by International Council on Large Electric Systems (CIGRE) and Electric Power Research Institute (EPRI), being 15% larger than the former one, and it is up to 8.6 m by the method used in DC engineering design in China. The aforementioned results show that the methods have their respective advantages and disadvantages.

Because the former method is to carry out discharge test for real air clearance of the converter station, and then conduct design based on the actual discharge test

Table 18.9 Minimum air clearance distance between pole busbar and post insulator in DC field of ±800 kV converter station

Methods used	U_{50} (kV)	Rigid Busbar-Fence (m)	Flexible Busbar-Fence (m)	Post insulator (m)
Test by CEPRI	1818.2	5.97	6.18	5.33
CIGRE	1896.8	7.31		–
EPRI	1951.2	7.97		–
Method used by projects in China	1818.2	8.60		–

results, so that more accurate and reliable design results are obtained; however, in respect that there are many equipment in the valve hall and DC field of the UHVDC converter station and many busbars connected to the equipment, it is required to determine many air clearance distances, and the electrode shape of individual air clearances differs significantly; therefore, using this method requires conducting discharge tests for all air clearances with different shapes, having a high test difficulty and significant work intensity. With respect to the latter method, it is still required to verify whether relevant empirical equations used are applicable for the air clearance design of the ±800 kV UHVDC converter station, and the calculated results are larger than the test results; however, the minimum air clearance requirement can be obtained only by a simple equation calculation, and it is possible to obtain the minimum value of different air clearances at individual positions of the converter station simultaneously, being easier than the former method.

The equations recommended by the CIGRE and EPRI are still different in some aspects. The former one is to calculate 50% discharge voltage U_{50} of the air clearance according to the corresponding arrester's protection level U_p, the margin coefficient K_1 for the switching impulse is taken as 1.2 and then the calculated result is divided by $(1–2\sigma)$; the latter one is to directly calculate U_{50} based on the switching impulse withstand level of the equipment. As discussed in the previous section, the margin coefficient between the switching impulse withstand level (SIWL) and protection level of corresponding arrester in the current UHVDC transmission systems is taken as 15%, that is to say, the result obtained is smaller than the method recommended by the CIGRE; moreover, the SIWL will be divided by $(1–3\sigma)$, obtaining a result smaller than by $(1–2\sigma)$ used in the method recommended by the CIGRE, so the difference between the results obtained by two methods is small.

The result obtained by the method recommended in Chinese DC engineering design or standard [13] is the largest. The main cause is that the influence of the electrode shape is usually not taken into consideration in engineering applications. Taking the electrode shape coefficient as $k = 1$ can obtain a larger air clearance value to reserve a larger safety margin.

Currently, in the design of UHVDC transmission projects in China, the minimum air clearance of equipment in converter station is mainly calculated by Eq. (18.20), and the results are conservative.

18.7.3 Non-standard Atmospheric Correction Method

The analysis and discussion above does not involve high-altitude correction of the air clearance, but the altitude of the Chuxiong converter station for Yunnan–Guangdong UHVDC project is approximated to 2000 m, and the altitude of the Jinping converter station for the Jinping–South Jiangsu UHVDC project is 1530 m. With the increase of altitude, the air gets thinner gradually and the atmospheric pressure and relative air density decrease, so the electric strength of the air clearance is reduced, and the discharge voltage is declined accordingly; additionally, it is

often required to take the influence of humidity, temperature, and other factors into consideration when carrying out correction of the atmosphere in the valve hall of the converter station whose internal atmosphere is regulated by the air conditioning system; therefore, the altitude correction for external insulation in non-standard meteorological conditions is still one of important issues to be concerned in the UHVDC transmission projects.

At present, there are several existing standards and methods for altitude correction, but the correction results differ in some degree. For some methods, an altitude correction factor can be obtained only by use of corresponding altitude or typical meteorological conditions, and these methods are easy to use, and in case of lack of relevant data, the calculation results have a certain referential value, but still rough; for some other methods, many influential factors are taken into account and detailed meteorological data are required at the place where the project is situated, but obtaining these data is difficult and these methods are complicated. Here we introduce several main altitude correction methods and conclusions obtained after the high-altitude corrections are tested by the China Electric Power Research Institute.

1. Method applied in the IEC 60071-2:1996 *Insulation Coordination-Part 2: Application Guide*

Reference [14] gives the altitude correction equation when the air clearance withstand voltage is corrected from the standard atmospheric condition to the atmospheric condition at altitude of 2000 m:

$$K_{\mathrm{a}} = e^{m\left(\frac{H}{8150}\right)} \tag{18.21}$$

where

H is the altitude above sea level,

m is the factor associated with voltage type and air clearance structure and is taken as 1 for correcting lightning impulse and power frequency withstand voltage; when correcting switching impulse, m is the function of switching impulse withstand voltage U_{cw}, as shown in Fig. 18.13, in which a is the phase-to-ground insulation curve, b is the longitudinal insulation curve, c is the phase-to-phase insulation curve, and d is the rod-plane insulation curve.

The switching impulse withstand level for the pole busbar of the converter station is 1600 kV, whose air clearance belongs to phase-to-ground insulation, so taking the altitude of 2000 m as an example, the altitude correction factor is calculated by selecting curve a and taking a factor of 0.49:

$$K_a = \mathrm{e}^{m\left(\frac{H}{8150}\right)} = \mathrm{e}^{0.49\left(\frac{2000}{8150}\right)} = 1.12$$

The calculation results of correction factors for other altitudes are listed in Table 18.10.

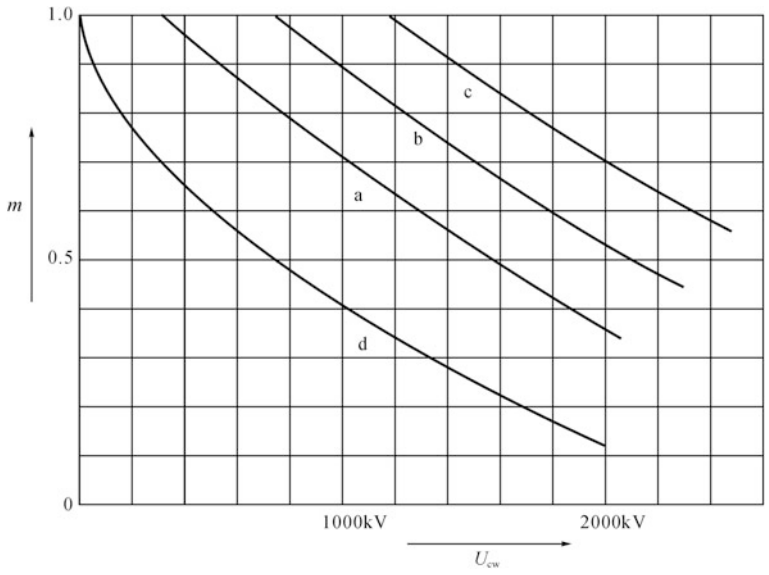

Fig. 18.13 Correction factor *m*

Table 18.10 Comparison of correction factors in different correction methods

Altitude (m)	Correction method		
	IEC 60071-2:1996	DL/T 620-1997	Method recommended by EPRI
1000	1.06	1.05	–
1500	1.09	1.08	–
2000	1.12	1.10	1.12

2. Method used in the DL/T 620-1997 *Overvoltage Protection and Insulation Coordination for AC Electrical Installations*

Reference [4] gives the following altitude correction method in Appendix D, and when atmospheric conditions in the area where the external insulation is placed are different from the standard atmospheric conditions, the discharge voltage is calculated from

$$u = \frac{\delta^n u_0}{H^n} \tag{18.22}$$

where

u is the actual discharge voltage,
u_o is the discharge voltage in the standard atmospheric conditions,

δ is the relative air density,

H is the air humidity correction coefficient, for switching impulse, $H = 1 + 0.009 \times (11 - h)$, h is air humidity, whose value corresponding to different altitude can be obtained by referring the standard (or adopt the real measurement value),

n is the characteristic factor, e.g., $n = 1.12 - 0.12\, l_i$, for the positive switching impulse, in which the applicable range of air clearance distance l_i is 1–6 m, and when l_i exceeds 6 m, it is recommended that the factor n is determined based on air clearance up to 6 m, i.e., $n = 0.4$.

Taking the correction for altitude of 2000 m, in case of $\delta = 0.824$ and $h = 5.33$ g/m^3, the altitude correction factor is calculated as follows:

$$K_a = \frac{u_0}{u} = \left(\frac{\delta}{H}\right)^n = \left(\frac{\delta}{1 + 0.009 \times (11 - h)}\right)^n = 1.10$$

The calculation results of correction factors for other different altitudes are also listed in Table 18.10.

3. Method used in GB 311.1-1997 *Insulation Coordination for High-Voltage Transmission and Transformation Equipment*

Reference [15] provides that, for external insulation of equipment and insulation of dry-type transformers at the altitude between 1000 and 4000 m, the insulation strength is decreased by about 1% with increase in altitude by every 100 m. When conducting test at a place with altitude not more than 1000 m, the testing voltage should be calculated by multiplying the rated withstand voltage specified in the standard by the altitude correction factor as follows:

$$K_a = \frac{1}{1.1 - H \times 10^{-4}} \tag{18.23}$$

where

H is the altitude at the installation point of the equipment.

It is required to point out that the external insulation withstand rated voltage specified in the standard has taken into account the influence of atmospheric condition with altitude of 1000 m and below on external insulation discharge voltage of the equipment, so the method is deemed that it is not required to carry out correction for external insulation of the equipment at an altitude of 1000 m and below. However, the equipment insulation withstand voltage of the current UHVDC transmission systems is not determined according to the standard, so this method is not applicable for altitude correction of the air clearances in the ±800 kV UHVDC converter station.

4. Method used in the IEC 60060-1:2010 *High-Voltage Test Techniques-Part 1: General Definitions and Test Requirements*

The methods described in Refs. [16, 17] are basically identical, namely "parameter g method." The specific aspect of the former method is corrected slightly based on the researches of recent years. By this method, the discharge voltage is corrected by following equation:

$$U = U_0 K_t \tag{18.24}$$

where

U is the actual discharge voltage,
U_0 is the discharge voltage in the standard atmospheric conditions,
K_t is the atmospheric correction factor, which is the product of the correction factor k_1 for atmospheric density and density correction factor k_2, calculated as follows:

$$K_1 = k_1 k_2 \tag{18.25}$$

(1) Atmospheric density correction factor k_1

The air density has a significant influence on the breakdown voltage of the air clearances. The main cause is that, when the air density is changed, the average intermolecular distance changes and directly influences the average free travel of electrons, and indirectly influences the ionization process of the air and changes the breakdown voltage of the clearance.

As the altitude increases, the air pressure drops and its density is reduced, so the average free travel of electrons in the ionization process increases, and more energy can be accumulated in the motion process. In case of a large clearance distance, the ionization process of the gas gets more violent, so the breakdown voltage of the clearance is declined.

When the temperature rises, free travel of the electrons increases, and more kinetic energy is accumulated, being more liable to gas ionization; additionally, the thermal kinetic energy of the gas molecular increases as the temperature rises, so as to lead to increase in gas thermal ionization and decrease in breakdown voltage. Thus, when other conditions are kept the same, the higher the temperature is, the lower the breakdown voltage of the clearance is.

The relative air density is defined as follows:

$$\delta = \frac{b}{b_0} \cdot \frac{273 + t_0}{273 + t} \tag{18.26}$$

where

b is the air pressure,
b_0 is the standard atmospheric pressure, 101.3 kPa,
t is the air temperature,
t_0 is the temperature in standard atmospheric conditions, 20 °C.

The influence of air density on breakdown voltage is expressed by atmospheric density correction factor k_1, which is defined as follows:

$$k_1 = \delta^m \tag{18.27}$$

The determination of the factor m will be explained in following context:

(2) Humidity correction factor k_2

The influence of humidity on breakdown voltage is complicate. The experiment shows that the discharge voltage of the air in the uniform electric field increases with the increase in humidity, but it increases slightly. However, in a non-uniform electric field, the air humidity has an obvious effect in increasing the clearance breakdown voltage. The possible reason is that the water molecule is easy to absorb electrons to form negative ions, enabling their free travel to be decreased significantly, so that their ionizing ability in the electric field is weaken considerably. As the humidity increases, the proportion of electrons attracted by water molecules and become negative ions increases. The negative ions have a larger mass and diameter, so as to significantly weaken the ionizing ability of the electrons, and reduce the ionization process of the clearance, as well as get the breakdown voltage of the clearance increased. Additionally, the average electric field intensity is low in the extremely non-uniform electric field, so the electrons move slowly and are easily captured by the water molecular as negative ions. Based on the causes above, the increase in humidity will result in increase in breakdown voltage.

The humidity correction factor is defined as follows:

$$k_2 = k^w \tag{18.28}$$

where

k is determined jointly by h/δ and voltage type, whose relation is shown in Eq. (18.29), and determination of the factor w will be introduced in the following context.

$$\begin{cases} \text{Impulse} & k = 1 + 0.0010(h/\delta - 11) \\ \text{AC} & k = 1 + 0.0012(h/\delta - 11) \\ \text{DC} & k = 1 + 0.0014(h/\delta - 11) - 0.00022(h/\delta - 11)^2 \end{cases} \tag{18.29}$$

(3) Selection of the factors m and w

The parameter g is defined in the IEC 60060-1: 2010, which is shown in Eq. (18.30), and the parameter can be used to determine the factors m and w.

$$g = \frac{U_{50}}{500L\delta k} \tag{18.30}$$

where

L is the minimum air clearance distance,
δ is the relative air density, and
k is the parameter determined jointly by h/δ and voltage type.

The relationship between factors m & w and parameter g is shown in Fig. 18.14.

The standard IEC 60060-1: 2010 provides approximate functional relationship for the two curves, as shown in Table 18.11.

For this correction method, it is required to obtain atmospheric conditions including temperature and humidity in practical application, and to carry out iterative computations to enable the final minimum air clearance distance d to be converged. This method is applicable for air clearance design in the valve hall of the converter station.

5. Test carried out by the CEPRI for altitude correction of 50% switching impulse discharge voltage of the air clearance

CEPRI worked with Yunnan Electric Power Test Research Institute to carry out tests for 50% switching impulse discharge voltage of the outdoor busbar to fence air clearance for the ±500 kV DC converter station in the test site of Kunming, and to conduct correction for the altitude of 2000 m by use of recommended K_a = 1.11 based on the test results. For the purpose of specifically understanding the characteristics of altitude correction for external insulation of the ±800 kV UHVDC converter station and helping design the external insulation of the UHVDC

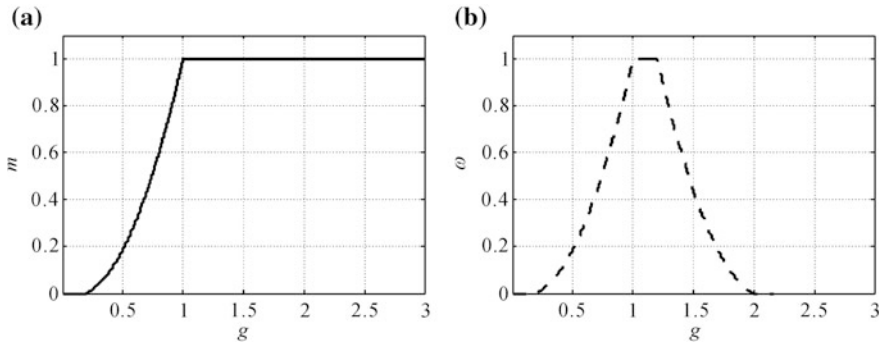

Fig. 18.14 Relationship between factors m & w and parameter g

Table 18.11 Functional relationship between m & w and parameter g

g	m	w
<0.2	0	0
0.2–1.0	$g(g - 0.2)/0.8$	$g(g- 0.2)/0.8$
1.0–1.2	1.0	1.0
1.2–2.0	1.0	$(2.2 - g)(2 - g)/0.8$
>2.0	1.0	0

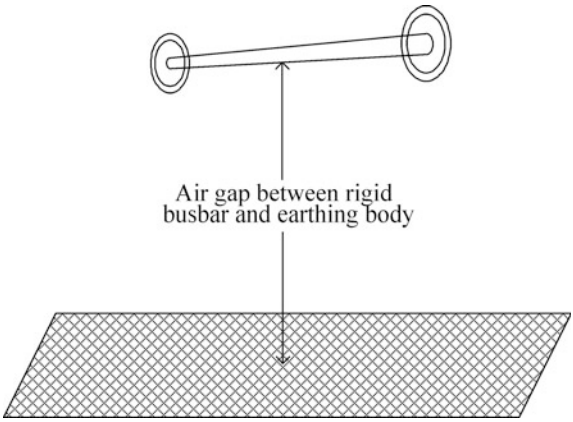

Fig. 18.15 Sketch for altitude correction test carried out by CEPRI

converter station, CEPRI worked with Yunnan Electric Power Test Research Institute to conduct relevant tests for air clearances of UHVDC busbars in Beijing, Kunming and other places again, and after analyzing the test results, put forward the correction factor for the altitude of about 2000 m [18].

In the altitude comparison tests, the pole busbar selected is an aluminum tube with a diameter of 250 mm and length of about 6 m, and a grading ring with pipe diameter of 200 mm and outer diameter of about 800 mm is provided at both ends of the busbar, respectively. During the test, the simulation ground body is a 16 m × 16 m wire net, and the air clearance distance is 3–8 m away from the aluminum tube and ground body. The test arrangement diagram in the test sites in Beijing and Kunming is shown in Fig. 18.15, and the test curves for 50% switching impulse discharge voltage obtained in two places are shown in Fig. 18.16.

The test results show that, when the air clearance distance of the busbar to grounding body is between 5 and 8 m, the difference between 50% switching impulse discharge voltage obtained at both places is about 9.6–8.0%, and considering that the consistency in test arrangement and method adopted in tests carried out at both places, it can be deemed that this difference is caused by different altitude at both test sites. The altitude for Beijing test site is about 50 m, and about 1980 m for Kunming test site. Thus, it can be approximately deemed that the 2000 m altitude correction factor for the busbar to ground air clearance is between 1.10 and 1.08 [18].

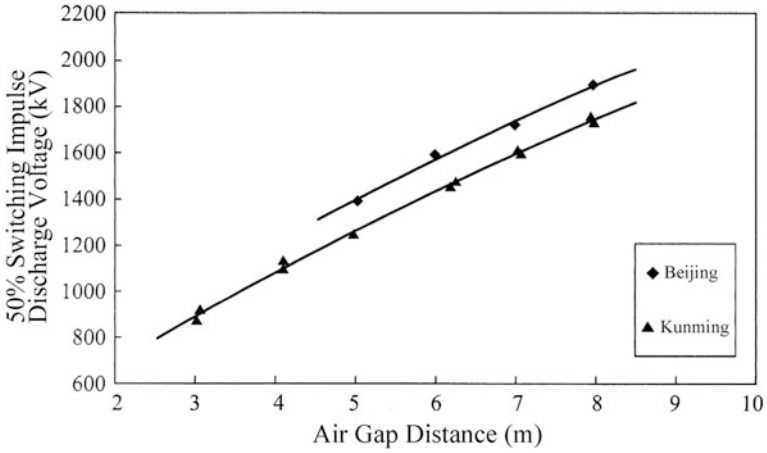

Fig. 18.16 Switching impulse discharge characteristics at different test places

Eventually, the EPRI recommends a correction factor for switching impulse discharge voltage of the air clearance in an area with an altitude of 2000 m for the ±800 kV DC project, and suggests to use an common value of 1.12 as shown in Table 18.10.

Table 18.10 lists two correction methods and test results provided by the EPRI. The test results provided by the EPRI are recommended values based on the practical tests, which are reliable, but if corrected values for different altitudes are required, it is necessary to conduct test again at other places, and the difficulty and workload are very large. With respect to the methods recommended in the IEC 60071-2:1996 *Insulation Coordination-Part 2: Application Guide* and DL/T 620-1997 *Overvoltage Protection and Insulation Coordination for AC Electrical Installations*, less parameters are required, and the methods are easy to apply, as well as the correction result for the altitude of 2000 m is consistent with the recommended value in the test used in the EPRI; therefore, the method recommended in the IEC 60071-2: 1996 can be adopted in case of being lack of actual atmospheric condition at the place where the converter station is situated.

For the reason that the correction value cannot be calculated simply by use of "parameter *g* method" proposed in the IEC 60060-1:2010 *High-Voltage Test Techniques-Part 1: General Test Requirements*, the results obtained by this method are not listed in the table above. During design of air clearance for the valve hall of the converter station, it is often required to take into consideration the influence of the atmospheric pressure, temperature, and humidity in the valve hall. Although "parameter *g* method" is calculated complicatedly, these factors can be comprehensively considered, so this method is worthwhile to be recommended in design of air clearance for the valve hall of the converter station.

18.8 Polluted External Insulation of Converter Station

The external insulation design of the converter station is mainly to select the specific creepage distance of equipment in AC switchyard, valve hall, and DC switchyard. The voltage of the UHVDC system is 60% higher than the ±500 kV HVDC transmission system, so a larger creepage distance and structural height of the post insulator is required; as the voltage level increases, the DC pollution gets more severe and a higher requirement is also made for the creepage distance; however, an excessive height of the post insulator will significantly influence its mechanical characteristic, including bending resistance and anti-seismic strength.

For the AC equipment of the converter station, the specific creepage distance can be selected according to the specific creepage distance values at individual pollution levels specified in the GB standards of China. The environmental condition in the valve hall can be controlled well and not influenced by external natural environment and pollution during operation, so the specific creepage distance of equipment can be at a lower level. The specific creepage distance of equipment in the valve hall (including external insulation and bushing of the valve) recommended in the Electric Power Industry Standard [13] should not be less than 14 mm/kV. For the DC field equipment of the converter station, the specific creepage distance is mainly designed and decided based on equivalent salt deposit density of the DC post insulators in the substation and by pollution withstand voltage method; the non-uniform rain flashover of the DC wall bushing for the converter station is one of the important issues for insulation of the DC equipment, and some auxiliary technical measures are often adopted to improve the wall bushing anti-pollution flashover performance at present.

18.8.1 Operation Experience of Polluted External Insulation of Chinese ±500 kV Converter Stations

For the reason that the knowledge for external insulation configuration of ±500 kV converter stations is lacking in early period, and the operating conditions are worsened increasingly, the converter stations worldwide were subject to external insulation flashover accidents, causing huge potential hazard to safe and stable operation of the DC systems. Summing up the experiences and lessons in operation of existing ±500 kV DC projects has an important instructive meaning for designing the external insulation of the ±800 kV UHVDC converter station.

The earliest ±500 kV DC project in China is the Gezhouba–Shanghai DC transmission project put into operation in September 1989, whose average creepage distance of equipment in the AC field of converter stations at both terminals of the project is 18–25 mm/kV, ensuring safe operation of the equipment, while the average creepage distance of DC field equipment reaches 40–50 mm/kV, external insulation accidents occurred constantly, and about 22 times/per set of external

insulation flashover took place in the first 2 years. In order to ensure safe operation of the DC system, the DC field equipment of the Gezhouba substation and Shanghai Nanqiao substation were sprayed with room temperature-vulcanized silicone rubber (RTV) from August to September in 1991. Within several years after the DC field equipment were sprayed with RTV, a satisfactory anti-flashover effect was achieved, without occurrence of any flashover accident for the DC equipment, and times of serious discharge accidents were also declined significantly. For the reason that it was restricted by technologies at that time, the quality of RTV coating was unstable, resulting in occurrence of two flashover accidents for the bushing in the Gezhouba converter station in 5 and 6 years, respectively, after spraying with the RTV; thus, the equipment were sprayed with RTV again.

The specific creepage distance for the AC 220 kV post insulator of the Guangzhou converter station for the Tianshengqiao–Guangzhou DC transmission project is 25.8 mm/kV, and the specific creepage distance of the HVDC post insulators is 41 mm/kV. Since the project was put into operation in December of 2000, no flashover accidents have taken place for the AC field equipment, and two flashover accidents took place for the DC field equipment. In 2004, for the reason that the New Baiyun Airport was put into operation, the traffic flow on the highways surrounding the Guangzhou Converter station increased significantly, resulting in further increase in pollution level of the converter station. So, all DC field equipment of the Guangzhou Converter station was sprayed with RTV. Up to now, the equipment are operated in a good condition, and the discharging sound that appeared in foggy and rainy days has disappeared almost.

The Anshun Substation as the sending end and the Zhaoqing Substation as the receiving end of the Guizhou–Guangdong Circuit I DC Transmission Project adopt the basically same specific creepage distance, the specific creepage distance is 54 mm/kV for the post insulators, and 57 mm/kV for the arresters and vertical bushings of the transformers. Since the project was put into operation, serious discharge phenomena have taken place for many times in dense fog and light intensity rain days. Especially the continuous foggy weather event covering a large area from December of 2004 to February of 2005, the post insulators of the DC field in the converter station discharged seriously, and the system had to decrease the voltage to operate. In order to improve the operation condition of the system, the insulators for the DC equipment were sprayed with RTV during the maintenance carried out at the end of December, 2005. After that, no serious discharging phenomena occur any more in rainy and foggy weather, and the system has been always operated at normal voltage level.

In addition, other ±500 kV DC projects including the Three George–Changzhou and Three George–Guangdong were sprayed with RTV after being operated for several years, achieving an excellent effect. The experiences and lessons from operation of the converter station for these ±500 kV DC projects are as follows:

(1) Main problems for operation of external insulation of the converter station lie in the DC field equipment

From operation conditions of the converter stations for the current ±500 kV DC projects, the specific creepage distance of the AC field equipment is about 20 mm/kV, which can ensure normal and safe operation of the equipment, while the specific creepage distance of the DC field equipment is between 40 and 50 mm/kV for the Gezhouba–Shanghai line, and 55 mm/kV for the Three George–Guangdong and Guizhou–Guangdong, external insulation flashover accidents or serious discharging phenomena took place. This shows that, even if the specific creepage distance of the DC field equipment is close to or even more than two times of that of the AC field equipment, it still cannot ensure their safe operation. The problem for operation of external insulation of the converter station mainly lies in operation conditions of the DC field equipment, which has to be paid particular attention to.

(2) Spraying with RTV coating is an effective measure for preventing external insulation flashover of the converter station

The DC field equipment of the converter station for several ±500 kV DC projects in China had been sprayed with RTV coating to enhance external insulation, achieving an excellent effect. Whether 40–50 mm/kV for the Gezhouba and Shanghai Nanqiao converter stations, or 41 mm/kV for the Guangzhou converter station, the creepage distance is about 30% smaller than that of insulators for other DC projects, but a satisfactory anti-pollution flashover effect is obtained after being sprayed with RTV. This shows that the post insulators with specific creepage distance of about 40 mm/kV, after being sprayed with RTV, can basically meet the requirement for external insulation of the ±500 kV DC projects in China.

In other words, the specific creepage distance of the post insulators sprayed with RTV can be reduced appropriately. This is of importance in designing external insulation of the converter station for the ±800 kV UHVDC projects. Compared to the ±500 kV DC system, the operating voltage of the UHVDC system increases by 60%, and the requirements for the creepage distance and structural height of corresponding post insulator are increased accordingly. For the DC equipment including post insulators of pole busbar and smoothing reactors directly withstanding the maximum voltage, if the same specific creepage distance (54–55 mm/kV) as the ±500 kV DC projects in later period is selected, the height of these post insulators will reach to 10 m and above. However, according to the current manufacturer's production capacity, such high pure porcelain insulator cannot ensure individual mechanical characteristics including bending resistance and anti-seismic strength. However, after being sprayed with RTV, it is possible to select a smaller specific creepage distance to reduce the insulator height, enabling it to meet the required mechanical performance.

(3) Development direction of RTV–PRTV

The RTV coating has hydrophobic nature similar to the composite external insulation material, which can improve anti-pollution flashover characteristic of the insulator effectively, and is a main means for anti-pollution flashover in the DC field

of converter stations in China, but it has some inherent problems and is improved continuously.

In the early period, the RTV coatings in China have simple manufacturing process, poor manufacturing level and unstable product quality, so the power department often takes spraying of RTV as a temporary external insulation remedial measure. As described above, the Gezhouba substation was subject to external insulation flashover accidents 5 years after spraying with RTV. This shows that the original RTV coating has been failed, and the equipment had to be sprayed with RTV again. This indicates that, after being operated for many years, the hydrophobic nature of the RTV coating will be declined, or even disappear, and re-spraying the coating can be carried out only during maintenance of the converter station, and will bring a great deal of workload.

Therefore, after many years' efforts in improvement, the Chinese manufacturers have developed a new permanent room temperature-vulcanized anti-contamination flashover composite coating (PRTV). The typical PRTV coating is a fluorosilicone copolymer formed by adding fluorine element in the original RTV silicone rubber molecular. Compared to RTV, PRTV coating has its own characteristics in aspects of hydrophobic nature, corrosion resistance, and other mechanical performances. Due to high hydrophobic nature and hydrophobic nature mobility, PRTV coating has more organic silicone-free radicals than RTV, and these organic-free radicals can continuously diffuse and wrap the pollution layer surface, so that the hydrophobic nature can move to the polluted surface to obtain an excellent hydrophobic nature at the whole polluted surface; it has superior aging resistance and longer service life which can be more than 20 years, significantly reducing workload for re-spraying the coating.

At present, the PRTV coating has been widely applied in the 110–500 kV AC systems. The operation experience shows that the insulators covered with PRTV coating have excellent anti-pollution performance, and the performance parameters of PRTV coatings are obviously superior to the RTV coating. The State Grid Corporation's company standard [19] provides that, for the power transformation equipment in polluted areas and heavily polluted areas, the insulation configuration can be realized by applying RTV or PRTV; for the transformation equipment of the newly built projects, application of RTV or PRTV coating onto the insulators with a smaller creepage distance can be taken as an effective design when the manufacturer cannot provide insulators with a larger creepage distance.

However, the specific creepage distance of the insulators sprayed with PRTV coating for the DC projects can often be selected by making a reference to the method for selecting the creepage distance of the composite insulators. The specifications of equipment for several ±500 kV DC projects in China specify that the creepage distance of the composite external insulation can be 2/3–3/4 of that of the porcelain insulators, ensuring a good operation condition of the external insulation. The Electric Power Industry Standard [13] recommends that the specific creepage distance of porcelain insulators sprayed with PRTV coating is not lower than 75% of that of corresponding porcelain insulators. To sum up, it is usually recommended that the specific creepage distance of insulators sprayed with PRTV coating is

selected based on 80% of that of corresponding porcelain insulators, so as to ensure enough insulation margin.

In a word, the PRTV coating is not considered as a temporary remedial measure taken during operation, but a new anti-pollution flashover design technique similar to composite insulators with respect to their functions. The external insulation for the ±800 kV DC converter stations should be designed by introducing such technique.

18.8.2 Selection of Post Insulators in Converter Stations

At present, the DC post insulators for the ±800 kV UHVDC converter stations can be selected from the following options: the first one is the traditional pure porcelain insulator; the second one is the composite insulator, which can be further divided into composite hollow core post insulator and composite porcelain core post insulator; the third one is the porcelain insulator sprayed with PRTV coating. This section gives a brief introduction to the advantages and disadvantages of these three kinds of DC post insulators with reference to the characteristics of the ±800 kV UHV projects.

(1) Pure porcelain insulator

We have accumulated rich experience in operation of pure porcelain insulators for the AC substation and ±500 kV DC converter station at various voltage levels; however, there is still some problems to solve when the pure porcelain insulators are applied in the ±800 kV converter station at higher voltage level.

As described above, if a specific creepage distance of about 54–55 mm/kV is selected for the post insulators of pole busbar and smoothing reactor, the height of these post insulators will reach over 10 m. The DC post insulators put into operation do not only withstand a pressure from the live part of high voltage, but also a huge torque, especially the post insulators of the knife switch. In terms of manufacturers' ability worldwide, the pure porcelain post insulators with height more than 10 m can meet the requirements for external insulation of the system, however, due to restriction by equipment conditions and technological level, manufacturing is difficult, the pass rate of large-size porcelain insulators is low and it is very difficult to ensure that the requirements for mechanical strength of finished products are met. So, there is low possibility to manufacture ±800 kV pure porcelain insulators meeting the external insulation and mechanical strength requirements.

It should be noted that this does not means that the pure porcelain insulator is useless for the UHVDC converter station. In fact, many post insulators are required in the DC converter station, and are highly different in operating voltage, for example, the operating voltage of post insulators for ±400 kV busbar, converter transformer busbar, neutral busbar, neutral busbar smoothing reactor is lower, and the creepage distance and structural height of the insulators are also lower, so the manufacturer is able to manufacture pure porcelain post insulators meeting

mechanical strength. We have accumulated rich experience in actual operation of the porcelain insulators, so the solutions adopting the pure porcelain insulators can be considered for the post insulator with low requirements.

(2) Composite insulator

In recent years, companies and research institutes in China adopt new materials and crafts to develop ±800 kV composite post insulators with internationally advanced technology, mainly including composite hollow core post insulator and composite porcelain core post insulator. With respect to the structure, the former one adopts epoxy glass fiber-reinforced plastic tube as the internal insulation, and such insulating materials as SF_6 gas or foam are filled in the tube to improve the insulation strength; the latter one adopts porcelain mandrel. Both of their external insulations are organosilicon rubber. New type composite post insulators have excellent properties such as explosion proof, aseismatic, anti-failure, pollution resistance, anti-aging, small volume, light weight and no need to clean.

Although these new products have advantages described above, they are still not used widely in view of being lack of experience in actual operation of the DC projects at voltage of ±500 kV and above, and it is required to carry out further demonstration and analysis.

(3) Porcelain insulator sprayed with PRTV coating

The characteristics and operation condition of porcelain insulators sprayed with PRTV coating are introduced in detail in the previous section, so they are neglected here. In view of its rich operating experience, economic and favorable price, smaller technical risk and other advantages, it can be recommended as the preferred solution for post insulators in DC field.

To sum up, pure porcelain insulators and porcelain insulations sprayed with PRTV coating are useful for the post insulators of DC field in the UHVDC converter station, but it is different that the pure porcelain insulators are suitable for the parts having higher requirements for creepage distance and structural height, while the porcelain insulations sprayed with PRTV coating are suitable for such parts having higher requirements for creepage distance and structural height, such as post insulators for pole busbar and pole line smoothing reactors. The composite post insulator has many advantages, but for the reason that no operation experience is available, its widely practical application still requires demonstration by long-time trial operation.

18.8.3 External Insulation Design of Post Insulators in Converter Station

The external insulation design of the post insulators for the converter station mainly means the selection of specific creepage distance of the post insulators in DC field

for the converter station. From the analysis made in the previous two sections, a rational-specific creepage distance can not only ensure normal and safe operation of the equipment in the converter station but also reduce the manufacturing difficulty of the post insulators.

In the design process of the specific creepage distance for the post insulators, it is required to first determine the pollution level of the converter station, and based on the predicted pollution level and insulator flashover characteristics, determine the required specific creepage distance by pollution withstand voltage method. In this process, the pollution level of the converter station is the basis for the whole design, and it is required to predict the actual pollution level at the place where the converter station is situated; the pollution withstand voltage method adopts the actual flashover characteristics of the post insulator to determine the specific creepage distance of the insulators, being a core for design of the whole external insulation. The following gives an introduction to the prediction of the converter station's pollution level and determination of the specific creepage distance of the post insulator by pollution withstand voltage method.

1. Predication of pollution level of converter station

For the newly built UHVDC project, if the environmental and geological conditions of the converter station are similar to other DC projects put into operation, it is possible to adopt the actual pollution data accumulated from the existing projects, but there may be only AC transmission lines in the vicinity of the newly built DC project, so it is required to collect equivalent salt deposit density and dust density data of the AC transmission projects and carry out prediction. If no AC lines in adjacent areas exist, the prediction and analysis can be carried out only based on the local meteorological data and pollution source data. Here gives a brief introduction to such prediction method.

The pollution model proposed by such method includes two parts: the first one is the existing atmospheric pollutant diffusion model; the second one is the relational model that expressing the relation between the atmospheric pollutant and the contamination degree on the insulator surface built by laboratory simulation tests. Through combining these two parts together and through examination of on-site detection data, the pollution degree of the insulator surface is calculated by use of the emission data of the pollution sources. The model calculation mainly takes into the consideration of industrial pollution sources on the converter station, so main pollutants are selected as SO_2 and dust.

According to the data on meteorological, environmental and pollution sources and after carrying out calculation of the models mentioned above, it is able to obtain the pollution accumulation and equivalent salt deposit density value. And through conversion of the equivalent salt deposit density ratio of conventional post insulators and suspension insulators under influence of AC voltage and DC/AC equivalent salt deposit density ratio of post insulators for the converter station, the equivalent salt deposit density of the final DC post insulators can be obtained, so as to basically complete prediction of the converter station. In fact, this method requires relatively detailed pollution data in the area where the converter station is

located, but these data are often acquired difficultly, so that use of this method is limited to some extent.

In addition, a DC natural pollution accumulated test station is built in the vicinity of the proposed converter station to carry out natural pollution test of the insulators and help to know the environmental pollution degree of the proposed DC converter station and pollution characteristics of different insulators, so as to provide such basic data as salt deposit density, dust deposit density, and meteorological data for design of external insulation for the equipment of the converter station, and meet the requirements for design and operation of the DC transmission projects. In fact, the DC natural pollution test station has its own advantages in aspects of accurately characterizing and estimating the pollution of the converter station and determining the external insulation configuration, which is also a powerful supplement to the aforementioned method (namely a method used to calculate the pollution level by use of the pollutant diffusion model), and will be widely used in China.

2. Determination of specific creepage distance of post insulator by pollution withstand voltage method

The pollution withstand voltage method is based on the anti-pollution flashover voltage curve of DC post insulators in the converter station at different pollution degrees, so that the anti-pollution flashover voltage of the given insulator is higher than the maximum operating voltage, and a certain margin is reserved. For this method, the first step is to obtain the pollution level data of the converter station, the second step is to determine the design withstand voltage of the insulators, the third step is to calculate the specific creepage distance of the insulators, and the fourth step is to calculate creepage distance required for insulators and individual porcelain bushings with different diameter, as shown in Fig. 18.17. During the selection of the creepage distance of post insulators by pollution withstand voltage method, the Xiangjiaba–Shanghai ±800 kV UHVDC transmission project is still taken as an example to explain the design process of the whole pollution withstand voltage method.

(1) Determination of equivalent salt deposit density value of DC post insulators in converter station

The sending end of the UHVDC project is Fulong Converter Station situated in Yibin, Sichuan, and the receiving end is Fengxian Converter Station situated in Fengxian, Shanghai. The prediction value of the equivalent salt deposit density at the insulator surface of the converter station is obtained by China Electric Power Research Institute using the method above, as shown in Table 18.12 [20].

The ratio of the equivalent salt deposit density of the conventional post insulators to that of conventional suspension insulators in the converter station can be determined according to surrounding environment of the converter station and relevant results of natural pollution test station. In case of being lack of such data, it is also able to obtain the pollution degree of the AC post insulators from the pollution degree of the AC suspension insulator shown in Table 18.12 temporarily by use of recommended value of 0.5 provided in Ref. [21].

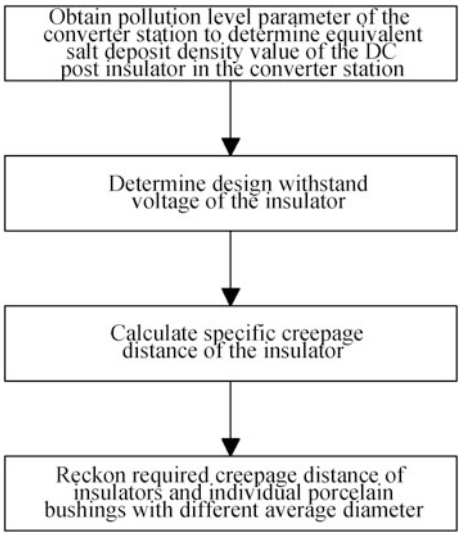

Fig. 18.17 Process of pollution withstand voltage method

Table 18.12 Prediction values of equivalent salt deposit densities in converter stations

Converter station	Fulong	Fengxian
Equivalent salt deposit density of conventional AC suspension insulator (mg/cm^2)	0.030	0.060
Equivalent salt deposit density of conventional AC post insulator (mg/cm^2)	0.015	0.030
Ratio of DC/AC equivalent salt deposit density	2.4	2.14
Equivalent salt deposit density of DC post insulator (mg/cm^2)	0.036	0.064

When the pollution degree of the AC equipment for the converter station is determined, it is able to determine the pollution degree of the DC equipment through DC/AC equivalent salt deposit density ratio (DC/AC ratio for short). The DC/AC ratio should be selected by considering many factors. On one hand, the DC/AC ratio differs as the meteorological and environmental conditions are varied; on the other hand, different types of insulators with different shapes have different pollution characteristics. No. 22-03 working group of the CIGRE has published a curve with DC/AC equivalent salt deposit density ratio decreased as the salt deposit density increases on "ELECTRA" (1992), as shown in Fig. 18.18. This curve is obtained by making a reference to measurement data of four test stations in total, of which three stations are located in Japan (distributed in coastal area) and one is located in Sweden [18]; however, conditions of such four test stations, including environmental and meteorological data, pollution components and insulators for test, are different from each other, and measurement data obtained from the same station are dispersed significantly, and the curve in the figure does not have any

referential meaning, so that only a qualitative conclusion can be proposed that the DC/AC equivalent salt deposit density ratio decreases as the pollution is aggravated. In fact, however, because the factors influencing the DC/AC equivalent salt deposit density ratio are too complicated such as environment, weather, pollution components, and insulators' type, no conclusions being similar to such curve are obtained through tests carried out in more areas. For example, the DC/AC ratio is 3.4 when the salt deposit density of the AC field in polluted areas in Sweden is 0.08 mg/cm^2, this indicates that the DC/AC equivalent salt deposit density ratio is still large when the salt deposit density is heavy; also, the test data from several DC natural pollution stations in China show that, when the insulator is heavily polluted, the DC/AC equivalent salt deposit density ratio does not tend to decrease. Therefore, selection of the DC/AC ratio still requires further research, and at present, there is not a mature theory for concluding the determination of such value, so it is preferred that the value is determined based on the actual condition of the project. For the Xiangjiaba–Shanghai UHVDC project, the DC/AC ratio of the Fulong and Fengxian Stations is 2.4 and 2.14, respectively.

After the DC/AC ratio is determined, it is able to obtain the equivalent salt deposit density of the DC post insulators through calculation of pollution degree of the AC post insulators, which is taken as a basis for the design of the external insulation by pollution withstand voltage method.

(2) Determination of design withstand voltage U_{wd} of insulators

The EPRI carried out an artificial DC pollution test under the influence of different salt deposit density for equivalent diameter deep-edge post insulators and large and small umbrella-type post insulators, with test results as shown in Fig. 18.19. In the design of external insulation for the converter stations, the dust density at surfaces

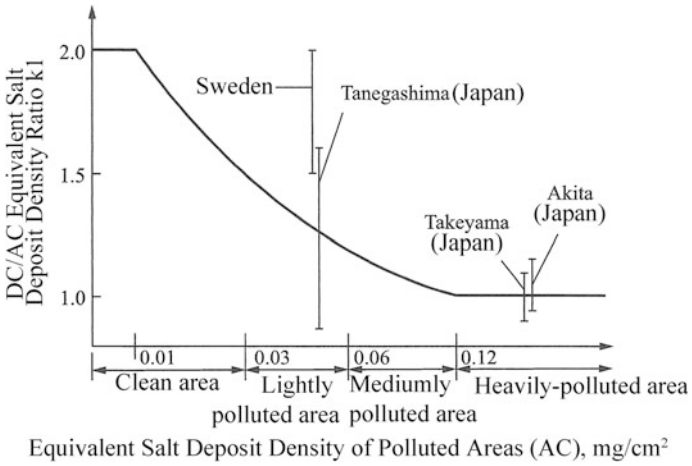

Fig. 18.18 DC/AC equivalent salt deposit density ratio curve published by CIGRE Working Group 22-03 for reference

of the DC post insulators and bushing is usually 6 times of the salt deposit density, and the pollution at the upper and lower surfaces is considered in terms of uniform distribution, so the curve in the figure is also obtained by test in the conditions above [18].

Generally, the withstand voltage of the insulators can be calculated by the following equation:

$$U_{\mathrm{wd}} = U_{50}(1 - n\sigma) \tag{18.31}$$

where

U_{50} is 50% discharge voltage of the insulator string,
σ is the standard deviation of the discharge voltage, which is usually 7% in the test,
n is the safety coefficient, which is usually taken as three in the engineering design.

Because the equivalent salt deposit density in Fengxian Converter Station is 0.064 mg/cm^2 and higher than that in Fulong Converter Station, the Fengxian Station is taken as an example. From the test curve, it can be known that, when the salt deposit density is 0.064 mg/cm^2, U_{50} of the large and small umbrella-type post insulators and equivalent diameter deep-edge post insulators is 76.9 and 86.2 kV/m, respectively, and the withstand voltage U_{wd} calculated from Eq. (18.31) is 60.7 and 68.1 kV/m, respectively.

(3) Determination of specific creepage distance λ of insulators

According to the structural parameters of these two kinds of insulators shown in Table 18.13, it is possible to calculate and obtain the specific creepage distance of

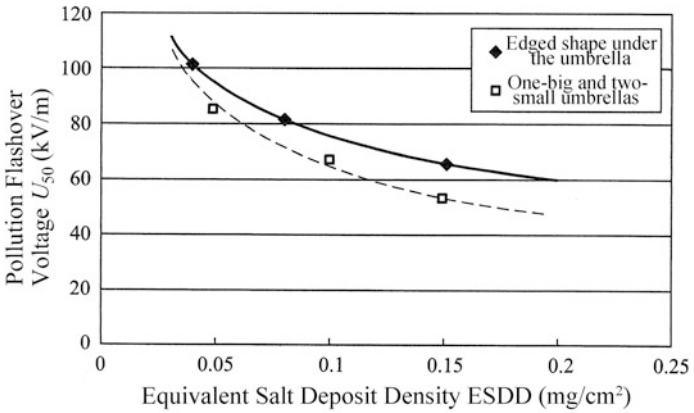

Fig. 18.19 50% flashover voltage of insulators of unit height

Table 18.13 Umbrella types and main structural parameters of post insulators

Model	Umbrella	Single section or whole unit	Umbrella (mm)	Nominal height d (mm)	Creepage distance 1 (mm)
One-large and two-small umbrella		1st section	375/305	2000	6960
		2nd section	371/312	2000	6955
		3rd section	403/333	2000	6750
		4th section	425/357	2000	6655
		Whole unit	–	8000	27320
Equivalent diameter and deep-edge umbrella	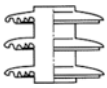	1st section	370	2000	7050
		2nd section	392	2000	7040
		3rd section	420	2000	7020
		4th section	445	2000	6700
		Whole unit	–	8000	27,810

the post insulators, and a 1.1 times of safety design margin is considered in calculation which is shown in Eq. (18.32).

$$\lambda = \frac{u}{U_{\mathrm{wd}}} \times \frac{l}{d} \times 1.1/u = \begin{cases} \dfrac{1}{60.7} \times \dfrac{27{,}320}{8} \times 1.1 = 61.9\ (\mathrm{mm/kV}) \\ \dfrac{1}{68.1} \times \dfrac{27{,}320}{8} \times 1.1 = 56.1\ (\mathrm{mm/kV}) \end{cases} \tag{18.32}$$

That is to say, the specific creepage distance for the large and small umbrella post insulators and equivalent diameter deep-edge post insulators of the UHVDC converter station is 61.9 and 56.1 mm/kV, respectively.

According to the discussion given in the previous sections above, it can be known that the equipment that directly withstand the maximum voltage, including post insulators for pole busbars and smoothing reactors, may be faced with the manufactured difficultly due to excessive height, so it is able to adopt the solution that the porcelain insulators are sprayed with PRTV coating, and that the specific creepage distance of the porcelain insulators sprayed with PRTV coating is selected based on 80% of that of the corresponding porcelain insulators. Thus, the specific creepage distance of the large and small umbrella and equivalent diameter deep-edge post insulators sprayed with PRTV coating in the DC field can be 49.5 and 44.9 mm/kV, respectively, which are shown in Table 18.14.

(4) Calculating the creepage distance required for insulators with different average diameters and various porcelain bushings

According to the relationship between the pollution characteristics of insulators with different average diameters and the creepage distance required for insulators with different diameters, it is able to calculate the creepage distance required for various categories of porcelain bushings

Table 18.14 Specific creepage distance of DC post insulators

Equivalent salt deposit density (mg/cm^2)	Umbrella	U_{50} (kV)	U_{wd} (kV)	Specific creepage distance λ (mm/kV)	Specific creepage distance λ after being sprayed with PRTV (mm/kV)
0.064	One-large and two-small umbrella	76.9	60.7	61.9	49.5
	Equivalent diameter deep-edge umbrella	86.2	68.1	56.1	44.9

Reference [22] recommends the following correction factor K_{ad} characterizing the creepage distance relation of the insulators with different diameters:

$$\begin{cases} K_{ad} = 1 & D_a < 300 \text{ mm} \\ K_{ad} = 0.0005D_a + 0.85 & D_a \geq 300 \text{ mm} \end{cases} \tag{18.33}$$

where

D_a is the average diameter of the insulators.

To sum up, the specific creepage distance of the vertical bushings with different diameters is shown in Table 18.15.

18.8.4 Creepage Distance of DC Wall Bushing in Converter Station

(1) Non-uniform rain flashover of the wall bushings

The non-uniform rain flashover of the wall bushings is one of the important accidents occurred of DC equipment external insulation in the converter station. The so-called non-uniform rain means that sheltering provided by walls of the valve hall in the converter station results in non-uniformity in moisture of the surfaces of the wall bushings installed horizontally, and the terminal far from the wall is wet by rain, and the terminal close to the wall still keeps dry.

In case of occurrence of non-uniform rain flashover, the following characteristics often appear: the salt deposit density value of the wall bushing surface is too low; the minimum flashover voltage is often lower than the operating voltage of the bushing. Therefore, it cannot be deemed that the flashover is mainly caused by the pollution, and in fact, the flashover problem of the wall bushing cannot be solved by means of solving the flashover, namely simply adding the creepage distance of

Table 18.15 Specific creepage distance of vertical bushings with different diameters

Insulation scheme	Post insulators (mm/kV)			
	Average diameter 250–300 mm		Average diameter 400 mm	
	One-large and two-small umbrella	Equivalent diameter deep-edge umbrella	One-large and two-small umbrella	Equivalent diameter deep-edge umbrella
Pure porcelain with external insulation	61.9	56.1	65.0	58.9
Sprayed with RTV/PRTV	49.5	44.9	52.0	47.1
Insulation scheme	Vertical bushings (mm/kV)			
	Average diameter 500 mm		Average diameter 600 mm	
	One-large and two-small umbrella	Equivalent diameter and deep-edge umbrella	One-large and two-small umbrella	Equivalent diameter and deep-edge umbrella
Pure porcelain with external insulation	68.1	61.7	71.2	64.5
Sprayed with RTV/PRTV	54.5	49.4	57.0	51.6

the bushing. For example, the specific creepage distance of the wall bushings for the Nelson River ±500 kV DC Project in Canada is increased to 44 mm/kV from 33 mm/kV for the ±400 kV voltage level, and the measured specific creepage distance of the wall bushings for the Gezhouba–Shanghai DC Project in China has been up to 60 mm/kV, which cannot prevent flashover accidents.

At present, the on-site technical measures that preventing wall bushings from non-uniform rain flashover include the following:

- installing a boost shed, especially the silicone rubber boost shed has best effect, and has the longest service life;
- spraying RTV coating;
- spraying silicone grease;
- periodically wipe manually or flush with water;
- temporarily reduce the operating voltage and other temporary preventive measures.

The practice proves that the measures listed above are effective, e.g., installation of a boost shed in the Dorsey Converter station in Canada, spraying with RTV coating in the Sylmar Converter station in America, and use of silicone grease in two converter stations in Itaipu of Brazil and Dadri Converter station in India, all of these stations achieve success. The wall bushings of the Gezhouba and Nanqiao converter stations in China were adopt sprayed with RTV coating, and no flashover

occurred until 1997. Service life of the silicone grease is usually not more than 3 years; after the RTV is used for several years, the hydrophobic nature of the surfaces will be reduced, for example, flashover accidents occurred in the wall bushings of the Sylmar Converter station in America and Gezhouba Converter station in China, so it is required to strengthen monitoring during operation.

(2) Common measures for solving non-uniform rain flashover

Since people have reached a common sense for flashover of the wall bushings, the newly built DC projects in individual countries adopt many designs for controlling non-uniform rain flashover, mainly including the following:

- use dry-type silicone rubber synthetic bushings in place of traditional porcelain bushing;
- use dry-type oil-immersed smoothing reactors without wall bushings;
- directly use HVDC thyristor valve outdoor;
- the wall bushing extends from the top of the valve hall vertically; and
- the wall bushing is installed with a fixed water flushing device.

The designs listed above have successful operation experience and have their respective specialties. From the perspective of operation, the use of dry-type silicone rubber synthetic bushings can significantly improve the flashover voltage to avoid the occurrence of flashover because the surface hydrophobicity improves the voltage distribution of the bushing surfaces.

References

1. GB 11032-2010. Metal-oxide arresters without clearances for A.C. systems; 2010.
2. DL/T 620-1997. Overvoltage protection and insulation coordination for AC electrical installations; 1997.
3. IEC 60099-4. Metal-oxide arresters without clearances for A.C. systems; 2009.
4. IEC 60099-5. Arresters selection and application recommendations; 2013.
5. DL/T 613-1997. Specification and technical requirement for import AC clearanceless metal oxide arresters; 1997.
6. GB/T 311.3-2007. Insulation coordination—Part 3: procedures for high-voltage direct current (HVDC) converter stations; 2007.
7. Q/GDW 276-2009. Technical specifications for metal-oxide arresters of ±800 kV converter stations; 2009.
8. Q/GDW 144-2006. Guide for overvoltage protection and insulation coordination of ±800 kV UHV DC converter station; 2006.
9. Sun Z, Liao W, Ding Y, Li Q. Air clearance flashover characteristics and selection of clearance distances for ±800 kV UHVDC transmission project. Power Syst Technol. 2008;32 (22):8–12.
10. Liu Z. Overvoltage and insulation coordination of UHV DC system. Beijing: China Electric Power Press; 2009.
11. Application guide of insulation coordination and arrester protection of HVDC converter stations. CIGRE; 1984.
12. HVDC converter station for voltage above ±600 kV. EPRI; 1985.

13. DL/T 5426-2009. System design standard for ±800 kV HVDC system; 2009.
14. IEC 60071-2:1996. Insulation coordination—Part 2: application guide; 1996.
15. GB 311.1-1997. Insulation coordination for high voltage transmission and transformation equipment; 1997.
16. IEC 60060-1:2010. High-voltage test techniques—Part 1: general definitions and test requirements; 2010.
17. GB/T 16927.1-2011. High-voltage test techniques—Part 1: general definitions and test requirements; 2011.
18. Liu Z. External insulation of UHVDC transmission system. Beijing: China Electric Power Press; 2009.
19. Q/GDW 152-2006. Pollution classification and external insulation selection for electric power system; 2006.
20. Guo X, Su Z, Le B. Design of post insulator for UHVDC converter station. Power Syst Technol. 2007;31(24):1–6.
21. GB/T 26218.1-2010. Selection and dimensioning of high-voltage insulators intended for use in polluted conditions—Part 1: definitions, information and general principles; 2010.
22. IEC/TS 60815-2:2008. Selection and dimensioning of high-voltage insulators intended for use in polluted conditions—Part 2: ceramic and glass insulators for A.C. systems; 2008.

Chapter 19
Insulation Coordination of UHVDC Transmission Line

Jidong Shi, Hao Zhou and Xu Deng

Up to august 2017, nine ±800kV UHVDC power transmission lines have been built and put into operation. There are still the other four ±800kV UHVDC power transmission lines will be put into operation at the end of 2017. Moreover, one ±1100kV UHVDC power transmission line is being built and will be put into operation in 2018. The area where these lines pass by is complicated and under severe conditions, such as pollution, acidic rain, and high altitude. All of these will have very huge impacts over the insulation coordination of DC lines, therefore, the insulation coordination of UHVDC lines is a key technology in the design of ±800 kV DC transmission project.

The insulation coordination of UHVDC lines mainly includes the following two aspects: selection of type and number of DC line insulators, and air clearance determination of DC line. Due to the particularity of UHVDC transmission system, the insulation coordination of DC lines has characteristics that differ from AC lines to some extent, for example, the insulators of DC line bear for a long time is the DC voltage with polarity remaining unchanged, its pollution accumulation is more severe than that of the insulators of AC line. Since pollution accumulation is serious, the number of insulators selected based on the requirements of working voltage is large; however, the flashover voltage of polluted insulator strings is

J. Shi (✉)
State Grid Jiangsu Maintenance Branch Company, Nanjing, Jiangsu People's Republic of China
e-mail: 838380475@qq.com

H. Zhou
College of Electrical Engineering, Zhejiang University, Xihu District, Hangzhou, Zhejiang, People's Republic of China
e-mail: zhouhao_ee@zju.edu.cn

X. Deng
Guangzhou Municipal Commission of Commerce, Guangzhou, Guangdong, People's Republic of China
e-mail: dengxu926@163.com

© Zhejiang University Press, Hangzhou and Springer-Verlag GmbH Germany 2018

H. Zhou et al. (eds.), *Ultra-high Voltage AC/DC Power Transmission*, Advanced Topics in Science and Technology in China,
https://doi.org/10.1007/978-3-662-54575-1_19

reduced very little under lightning effect, so what need to be considered is just the requirements of switching overvoltage when design the insulation coordination of air clearance for the tower head. Therefore, the insulation coordination design should be carried out for UHVDC transmission line in combination with these characteristics.

19.1 Selection of Type and Number of Insulators for UHVDC Transmission Line

The UHVDC line is normally very long, the pollution in the areas where it passes by is complicated, and the pollution accumulation on the DC lines is more serious than that of AC lines. Therefore, it is of vital importance on how to select the material, string type, and number of insulators for ensuring the safe operation of line.

The selection of the material, string type, and number of UHVDC line insulators will be introduced in the following chapters.

19.1.1 Selection of Material and Umbrella Type of Insulators

1. Material selection of insulators

At present, the applied insulators on the UHVDC transmission line mainly include porcelain insulators, glass insulators, and composite insulators.

Material selection of insulators is normally considered comprehensively in terms of its expected service life, failure rate, detection rate as well as electrical and mechanical properties, etc. The expected service life, failure rate, and detection rate of 3 types of insulators have already been discussed in detail in the insulation coordination of UHVAC transmission line. So, in this section, discussions will focused on the electrical property of insulators under DC voltage, and recommendations are given on the type selection of insulators for UHVDC line.

In order to compare the anti-pollution flashover properties of insulators in 3 kinds of materials, Tsinghua University conducted pollution flashover tests [1] by selecting 300 kN glass bell-type insulators, 300 kN porcelain bell-type insulators, and composite insulators; the curves of test results are shown in Fig. 19.1.

As shown in Fig. 19.1, the composite insulator has the strongest capability of resisting flashover, and under the same pollution conditions, its pollution flashover voltage is far higher than those of porcelain insulator and glass insulator.

For UHVDC line, the anti-pollution flashover capability is particularly important, so, under the most of circumstances, its suspended-string insulators are of

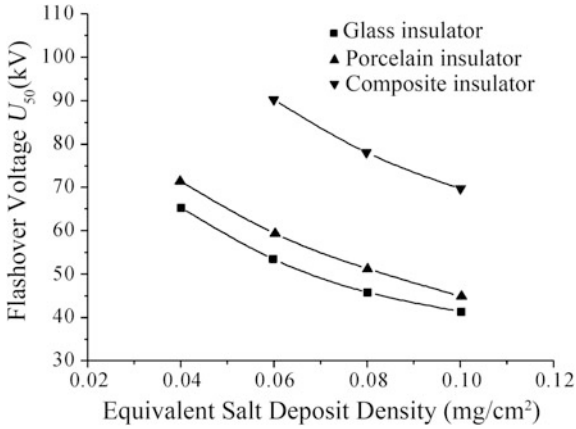

Fig. 19.1 Comparison of pollution flashover voltage of insulator string of unit length (1 m) with different materials. *Note* The test altitude is 1970 m

composite insulators normally at priority, especially in the areas of high altitude. In fact, on the several ±800 kV UHVDC lines that were already built in China at present, most of the suspended strings are of composite insulators, except for those in the heavy icing areas.

The porcelain- and glass-type insulators are mostly applied on the strain strings of UHVDC lines, and most of them are bell jar-type, double-umbrella-type, and three umbrella-type porcelain insulators. At present, the glass insulators are also developed and applied.

2. Umbrella type selection of insulator

Besides related to the materials of insulators, the insulation property of insulators has big relationship with the umbrella type of insulators. At present, the insulators applied on the UHVDC lines include two categories: disk-type insulator and composite insulator, where the disk-type insulator mainly includes bell jar (ordinary) type, double-umbrella type, and three umbrella type; their structure parameters and shed shapes are shown in Fig. 19.2. The composite insulator is mainly the long rod suspension insulator.

As for the strain string insulators of UHVDC transmission line, since they are placed in a nearly horizontal way, considering that the composite insulators cannot withstand the action of strong gravity, only disk-type insulators (bell jar-type, double-umbrella-type, and three umbrella-type insulators) are normally used as the strain string insulators. In addition, under the circumstance of heavy icing areas, since the gap between the sheds of composite insulators is small, ice that connects with shed can be easily formed, this will cause bigger impact over its insulation property. Therefore, in the heavy icing areas, disk-type insulators (bell jar-type, double-umbrella-type, and three umbrella-type porcelain insulators) are more preferred for suspension V-type strings.

At present, bell jar-type, double-umbrella-type, and three umbrella-type insulators are all applied on the UHVDC transmission lines. Generally speaking, the

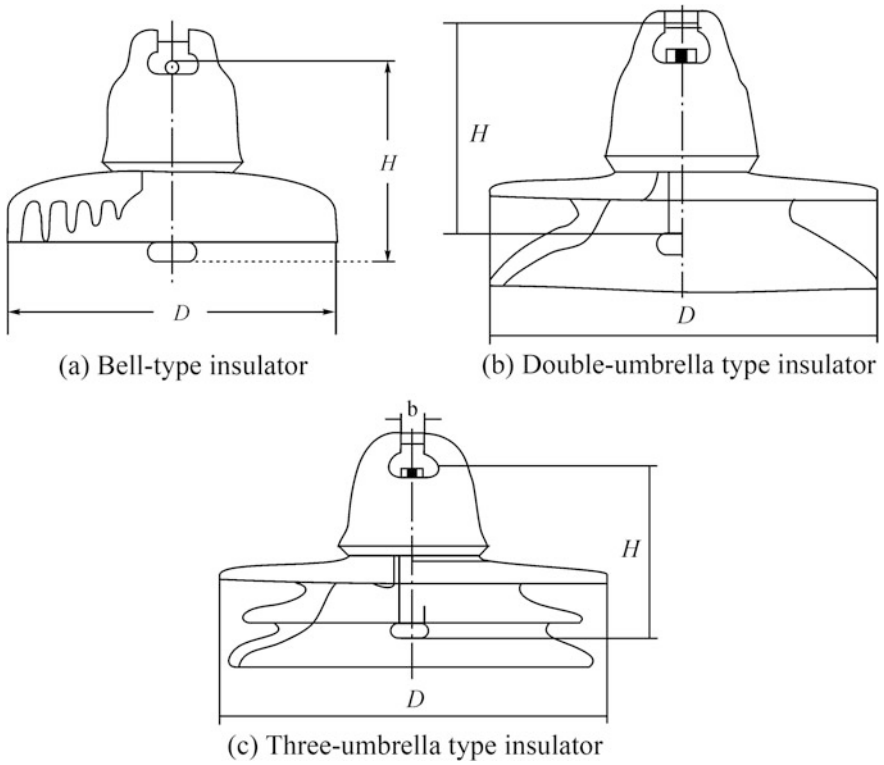

Fig. 19.2 Type structure of disk-type insulator, reprinted from Ref. [3], copyright 2004, with permission from China Electrical Power Press

bell-type insulators are more suitable for the areas having abundant rainfall, while the double-umbrella- and three umbrella-type insulators are more suitable for the areas having industrial pollution and powder pollution in the inland.

What should be emphasized is that such insulators applied on the UHVDC lines, of course, must be specially manufactured insulators for DC lines. Their biggest difference with the insulators of AC lines is that they are provided with zinc sleeves so as to resolve the phenomena of electrochemical corrosion during operation.

In several UHVDC transmission projects in China, bell-type insulators are more applied (mainly on the strain strings); however, the application of double-umbrella- and three umbrella-type insulators becomes more and more at present, and has the tendency of exceeding the bell-type insulators. First of all, this is because the former has better self-cleaning effect, good anti-pollution property, with actual operating results better than the latter; secondly, as its production process becomes more and more mature, the production cost is decreasing day by day, making it competitive with the bell-type insulators in terms of price.

19.1.2 Type Selection of Insulator Strings

The type selection of insulator strings needs to consider comprehensively such influencing factors as the impacts of electromagnetic environment, gap of tower head, insulation strength, corridor width, scope of relocation, height of towers, and its own weight.

At present, the suspension strings of EHVAC and UHVAC lines are of I-type string and V-type string in most countries. In the ±800 kV UHVDC line projects, V-type strings are normally adopted and the specific reasons are as follows:

1. Adoption of V-type strings can reduce the width of corridors significantly

For the ±800 kV UHVDC transmission line projects, as compared to I-type strings, when straight line towers with V-type insulator strings are adopted, the distance between pole conductors can be reduced by about 8 m; this will play a significant role in improving the electromagnetic environment of lines and reducing the line corridors.

2. Adoption of V-type strings can reduce the height of towers

Even if the number of V-type string insulators will increase by one time as compared to I-type strings, however, in terms of the same insulation configuration, the suspension length of V strings of ±800 kV DC lines will be shortened by about 4 m as compared to I-type strings, so, under the circumstance of same span, the straight line towers with V-type string can reduce the height by about 4 m as compared to towers with I-type string, and reduce the weight of towers by 7–9%.

3. Anti-pollution property of V-type strings is significantly better than that of I-type strings

The pollution withstand voltage of V-type strings is higher than that of single I-type strings. The reasons are:

First of all, since the included angle of V-type string insulators is approximately 90°, and arranged in a tilting way, its self-cleaning capability is obviously better than that of I-type string insulators; Secondly, the particular arrangement pattern of V-type strings has improved the capacitance of insulator strings to the ground, and reduced the impacts of capacitive current over the insulator strings, leading to increase in the pollution flashover voltage; In addition, as compared to a single I-type string, the electric arc of V-type strings can float easily on the surface of insulator strings, and is different from the pattern that a single I-type string's electric arc is very close to the insulator strings; so, the electric arc of V-type strings can be extinguished easier. Therefore, under the condition of same length of strings, the pollution flashover voltage of V-type string insulators will be higher than that of I-type string insulators. Relevant experiments show that the pollution flashover withstand voltage of V-type strings can be higher than that of I-type strings by 10–20%, or even more.

In summary, as V-type strings compared to I-type strings of straight line towers, even if the investment in both tower bodies is almost the same, but, considering the comprehensive investment after the corridors are relocated, the straight line towers with V-type string takes the advantages obviously. Therefore, at present, V-type strings are adopted on the straight line towers of UHVDC lines those have already been constructed or under construction in China.

19.1.3 Determination of the Insulators' Number

19.1.3.1 Some Important Principles for Determining the Number of Insulators in a String on UHVDC Transmission Line

1. Methods for determining the number of insulators in a string on UHVDC transmission line

As for the number of insulators in a string on the UHV transmission line, it is determined directly using specific creepage distance method or pollution withstand voltage method based on the rated DC operating voltage and pollution conditions; normally the verification of the switching overvoltage and lightning overvoltage is not required.

In fact, since key constraints are exercised on the switching overvoltage in the ±800 kV UHVDC system, the switching overvoltage level on the line normally does not exceed 1.7 times of the rated operating voltage (≤ 1.7 p.u.). However, according to the test verification by US EPRI, under the same pollution condition, the switching withstand voltage of the insulator with the same type is 2.2–2.3 times of its DC withstand voltage. Also lots of tests and researches have proven that when DC voltage is pre-applied, 50% of the switching impulse voltage is 1.7–2.3 times of DC pollution flashover voltage. Therefore, the switching overvoltage does not play a controlling role in selecting the number of insulators.

In addition, due to pollution, the number of insulators for ±800 kV DC lines is more than that for 1000 kV AC lines, its insulation margin is big under lightning impulse voltage, and the lightning withstand level of back flashover exceeds 200 kA, so, the lightning overvoltage does not play a controlling role in selecting the number of insulators at all [2].

2. Relationship between DC pollution flashover voltage and length of ±800 kV UHV insulator strings

In the previous design of insulation pollution for AC 500–1100 kV line and DC ±500 to ±600 kV line in most countries, the power frequency voltage or DC pollution flashover voltage of insulator strings and the length of strings was basically dealt with using a linear relation. In this way, based on the parameters of a single piece of insulator, the number of required insulator strings can be obtained

directly through calculating the rated operating voltage using specific creepage distance method or pollution withstand voltage method.

However, in the ±800 kV UHVDC transmission system, it is an issue worthwhile to be noted that, whether or not a linear relation can be almost maintained between DC pollution flashover voltage and length of string. It is a precondition for whether or not the specific creepage distance method or pollution withstand voltage method can be used continuously and effectively in the ±800 kV UHVDC transmission system.

Reference [3] points out, relevant test results show that 50% flashover voltage of DC suspension insulator strings in large tonnage is in proportional to the number of pieces. American General Electric Company conducted a DC pollution flashover test on the anti-fog insulators under a voltage of 200–1000 kV and a ESDD of 0.01–0.04 mg/cm^2 at Pittsfield test field, based on the results it is believed that when the number of insulators in a string is within 50 (a length of about 8 m), its DC flashover voltage is in linear relation with the length of strings. The central research institute under Japan Power conducted a test on the DC insulators with disk diameter of 420 mm under a voltage of 500 kV and a ESDD of 0.01–0.3 mg/cm^2; it is concluded that its DC pollution flashover voltage is in proportional to the length of strings, and believed that when a length of insulator strings reaches 14 m, such linear relation still exists. Therefore, for the DC disk-type insulators, even if they are applied in ±800 kV UHVDC transmission system, we can still believe that a linear relation is almost maintained between its DC pollution flashover voltage and the length of strings.

Reference [4] has given the relation curves of composite insulators' DC pollution flashover voltage of long strings versus the length of insulator strings, which are shown in Fig. 19.3.

As shown in Fig. 19.3, when the ESDD is 0.05–0.1 mg/cm^2 and the length of insulator string is 10 m, the DC pollution flashover voltage of composite insulator has a good linear relation with its length.

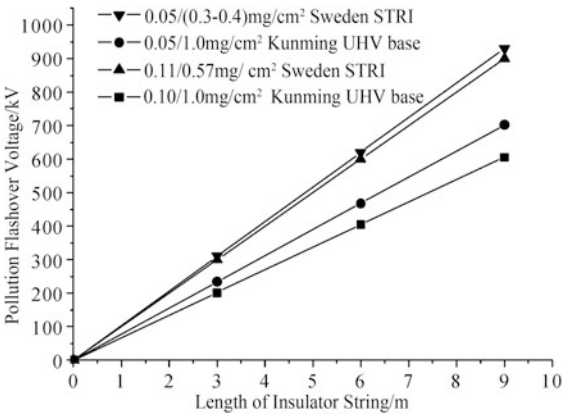

Fig. 19.3 Relationship between DC pollution flashover voltage and length of composite insulator

All in all, the long string insulators' pollution flashover characteristic, which is estimated using the pollution flashover voltage or pollution withstand voltage of a single piece of insulator or short string insulators, is still applicable in the ±800 kV UHVDC projects. It is generally believed that such linear relation can be expanded to ±800 kV UHVDC scope. The specific creepage distance method or pollution withstand voltage method can still be used to calculate the required number of insulator strings under rated DC operating voltage.

3. Anti-pollution design principles for insulator strings of DC transmission line

According to the national standard GB50790-2013, the anti-pollution design for ±800 kV UHVDC transmission lines shall be carried out by selecting proper types and number of insulators in accordance with the pollution withstand voltage characteristic of insulators, by referring to the latest approved polluted area distribution map and DC/AC pollution accumulation ratio, and combining the actual pollution investigation results at site. As for the insulators that do not have reliable pollution withstand voltage characteristic parameters, proper types, and number of insulators can also be selected by referring to the specific creepage distance method in accordance with the pollution degree.

In addition, it is stipulated in standard Q/GDW181-2008 that the specific creepage distance of DC lines should not be less than 2.0 times of the specific creepage distance of AC lines in the same areas [5]; this is mainly based on the following two reasons:

(1) In the calculation of specific creepage distance, regardless of AC system or DC system, the nominal voltage of system is adopted, but, what really plays a role in the pollution flashover is the working voltage applied on the insulator strings, the nominal voltage and the working voltage are different from each other. In the calculation of specific creepage distance of AC system, the nominal voltage of AC system U_N (that is, line voltage) is adopted, but, the working voltage actually applied on the insulator strings is phase voltage (that is, $U_N/\sqrt{3}$); in the calculation of specific creepage distance of DC system, the nominal voltage of DC system U_N is adopted, but, it is also the working voltage actually applied on the insulator strings.
(2) The manual pollution withstand voltage tests on the insulators in most countries have proven that under the same ESDD, the pollution withstand voltage value under DC condition is lower than that under AC condition by 15–20% [2].

In conclusion, the specific creepage distance of DC system is normally 2 times or above of that of AC system (that is, $\sqrt{3} \times 1.2 = 2.08$).

4. Classification of polluted areas along DC line and DC equivalent salt deposit density (ESDD) thereof

In making comparison to the anti-pollution design of AC line, the difficulties of anti-pollution design of DC line lie in determining the ESDD (DC) of polluted areas

reasonably. At present, considerations are firstly given to the actually measured degree of pollution at site when determining ESDD of polluted areas for DC line.

Considerations should be given to the fact that there are not usually the measured ESDD (DC) values for the routes where the newly built UHVDC transmission lines, but there are normally the measured ESDD (AC) values and corresponding classification of polluted areas. According to the tests conducted by the research institutes in most countries, such as China Electric Power Research Institute, the results show that the pollution accumulation quantity on DC insulators is about 2 times of that on AC insulators under the same conditions. Therefore, by referring to GB/T16434-1996 *Standard for Classification of Environmental Polluted Area and Selection of External insulation for HV Overhead Lines, Power Plants and Substations*, ESDD (AC) and NSDD (AC) can be selected according to the classification of polluted areas along AC lines, and corresponding ESDD (DC) of polluted areas can be calculated using the 2.0 pollution accumulation ratio of DC and AC, which are shown in Table 19.1 [5].

19.1.3.2 Specific Creepage Distance Method

1. Calculation method for specific creepage distance

The specific creepage distance method is mainly used to determine the relation between specific creepage distance and ESDD of polluted area based on the operating experience. In all over the world, only China has several UHVDC lines in operation, since lacking of the actual long-term operating experience, the fitting of the specific creepage distance is mainly based on the operating experience of ±500 kV DC lines; Ref. [5] recommends that the relation between specific creepage distance and ESDD of polluted area is as shown in Eq. (19.1).

$$\lambda = 6.2606 + 0.8891 \ln(\text{ESDD}) \tag{19.1}$$

Table 19.1 Classification of polluted areas along DC line and DC equivalent salt deposit density (ESDD) thereof

Polluted area classification	ESDD (AC) (mg/cm^2)	NSDD (AC) (mg/cm^2)	ESDD (DC) (mg/cm^2)	ESDD pollution accumulation ratio of upper and lower surfaces (CUR)
Clean area	0.03	0.18	0.06	1:3
Lightly polluted area	0.05	0.30	0.10	1:5
Mediumly polluted area	0.08	0.48	0.16	1:8
Heavily polluted area	0.15	0.90	0.30	1:10

where

λ is the required specific creepage distance (cm/kV);
ESDD is the equivalent salt deposit density of DC (mg/cm^2).

The specific creepage distances under different polluted areas are calculated using this method, with results as shown in Table 19.2.

2. Selection of the number of porcelain and glass insulators

For porcelain and glass-type insulators, the number of insulators determined using the specific creepage distance method is as follows:

$$n \geq \frac{\lambda U_{\mathrm{m}}}{K_{\mathrm{e}} L_0} \tag{19.2}$$

where

n is the number of each string of insulators;
L_0 is the geometric creepage distance of each piece of insulator, cm;
λ is the specific creepage distance, cm/kV;
U_{m} is the nominal voltage of system, 800 kV;
K_{e} is the effective coefficient of creepage distance of insulator.

At present, the national standard does not set forth the effective coefficient for the creepage distance of DC insulator, the insulators XP-70 and XP1-160 are normally used as the standard insulators, and its effective coefficient is 1. The effective coefficient for the rest of porcelain insulators is normally in the range of 0.84–0.92. In this section, the selected effective coefficient of creepage distance for insulator is 0.9–1.

Using the bell-type insulator CA756EZ as an example, the steps for determining the number of insulators using specific creepage distance method are as follows:

Nominal voltage U_{m} = 800 kV;
Degree of pollution II (lightly polluted area), the specific creepage distance λ = 4.21;
Insulator is CA756EZ, the geometric creepage distance L_0 = 63.5 cm;
Effective coefficient K_{e} = 0.9;
So, the number of insulators n satisfies:

Table 19.2 Specific creepage distances in different polluted areas

Polluted area classification	Clean area	Lightly polluted area	Mediumly polluted area	Heavily polluted area
ESDD (AC) (mg/cm^2)	0.03	0.05	0.08	0.15
ESDD (DC) (mg/cm^2)	0.06	0.10	0.16	0.30
Specific creepage distance (cm/kV)	3.76	4.21	4.63	5.19

$$n \geq \frac{\lambda U_{\mathrm{m}}}{K_{\mathrm{e}} L_0} \Rightarrow n \geq \frac{4.21 \times 800}{0.9 \times 63.5} = 58.9$$

By rounding up, we get $n = 59$, therefore, in class II pollution area (lightly polluted area), when bell-type insulators with creepage distance of 63.5 cm are adopted, the number of insulators for UHV line $n = 59$ pieces.

For different sizes of insulators, the required number of insulators for ±800 kV DC transmission line can be obtained through calculation using Eq. (19.2), which is shown in Table 19.3.

3. Verification of specific creepage distance for composite insulators

The pollution flashover tests conducted in most countries (including STRI tests) have proven that [2]: Under the same pollution conditions, the pollution flashover voltage of composite insulators can be higher than those of porcelain and glass insulators by 50% or above. This means that under the same operating voltage, the creepage distance of composite insulators requires only 2/3 of the creepage distances of porcelain and glass insulators. In fact, according to the actual configuration and operating of ±500 kV EHVDC transmission lines at present, the creepage distance of composite insulators is set at 3/4 or above of the creepage distance of porcelain insulators, which has considerable margin.

All in all, the required creepage distance of composite insulators can be determined by referring to the required creepage distance of porcelain insulators under the relevant pollution conditions, as long as the required specific creepage distance of composite insulators is longer than 75% of that of porcelain insulators. However, in practice, since the size of iron tower head is mainly controlled by inter-pole distance, in order to ensure certain inter-pole distance (meet the requirements of radio interference and audible noise), longer size of composite insulators are normally adopted for V-type suspension strings in the projects; the creepage distance of composite insulators is even approaching to the required creepage distance of porcelain insulators. Therefore, the actual composite insulators can normally meet the requirements of required creepage distance under system operating voltage.

4. Altitude correction

(1) Disk-type insulator

It is stipulated in the standards that in the areas where altitude exceeds 1000 m, the number of insulators should be corrected as follows:

$$n_{\mathrm{H}} = n\mathrm{e}^{m_1(H-1000)/8150}, \tag{19.3}$$

where

n_{H} is the required number of each string of insulators in the high-altitude areas;
H is the altitude, m ($H \geq 1000$ m);

Table 19.3 Results of insulators' number selected as per specific creepage distance (in the area with altitude below 1000 m)

Polluted area classification	ESDD (AC) (mg/cm^2)	Required specific creepage distance (cm/kV)	Characteristics of insulators			Number of insulators required for ±800 kV line
			Size (kN)	Geometric creepage distance (mm)	Effective coefficient	
Clean area	0.03	3.76	160	545	1.0	56
			210	545	1.0	56
			300	635	0.90	53
			400	560	0.90	60
Lightly polluted area	0.05	4.21	160	545	1.0	62
			210	545	1.0	62
			300	635	0.90	59
			400	560	0.90	67
Mediumly polluted area	0.08	4.63	160	545	1.0	68
			210	545	1.0	68
			300	635	0.90	65
			400	560	0.90	74
Heavily polluted area	0.15	5.19	160	545	1.0	77
			210	545	1.0	77
			300	635	0.90	73
			400	560	0.90	83

m_1 the characteristic factor, it reflects the degree of impacts of air pressure on the pollution flashover voltage, which is determined through tests.

The m_1 values of various insulators in Eq. (19.3) should be determined based on the actual test data. Table 19.4 has given the reference values for m_1 of part of insulator types.

(2) Composite insulator

Relevant researches conducted by China Electric Power Research Institute show the anti-pollution flashover capability of composite insulators decreases by 6.4% per each increase in altitude by 1000 m.

19.1.3.3 Pollution Withstand Voltage Method

When pollution withstand voltage method is used, the most important is to obtain test data of the reliable pollution withstand voltage for insulators in a test environment with actual pollution conditions to be simulated as far as possible. At present, lots of pollution flashover tests were carried out on AC insulators, from which the curves of relation between the pollution flashover voltage of insulators' different types and ESDD were obtained, but, the pollution withstand voltage tests carried out on DC insulators were few, using the pollution flashover data of insulators provided by Japanese NGK company as an example; the calculation examples using pollution withstand voltage method are given in this section.

1. Process for pollution withstand voltage test of DC insulators

The process for determining the number of insulators using the pollution withstand voltage method is as follows:

(1) Determination of ESDD (DC) and NSDD (DC) in polluted area

It is better to obtain the measured values of ESDD (DC) and NSDD (DC) in polluted areas for carrying out the manual pollution flashover tests so as to determine 50% flashover voltage $U_{50\%}$ of insulators. If it is unable to obtain the measured values, ESDD (AC) and NSDD (AC) can be determined according to the polluted area grade of AC, then the estimated value of ESDD (DC) can be obtained using ESDD (AC) multiplied by 2, and see Table 19.1 for detail.

Table 19.4 Reference values for m_1 of some types of insulators

Type of insulator	Standard type	Double-umbrella anti-pollution type	Three umbrella anti-pollution type
m_1	0.5	0.38	0.31

(2) Determination of pollution withstand voltage of single piece of insulator

First of all, carry out the manual pollution flashover tests on the insulators according to ESDD (DC) and NSDD in polluted areas, and obtain 50% flashover voltage $U_{50\%}$ of insulators.

After that calculate the pollution withstand DC voltage of insulators. The pollution withstand voltage of a single piece of insulator is expressed as follows:

$$U_{\max 1} = U_{50\%}(1 - 3\sigma_s), \tag{19.4}$$

where

σ_s is the variable coefficient of pollution flashover voltage of insulator, and is recommended to take 7%.

(3) Correction of non-soluble deposit density (NSDD)

In the natural pollution, the kinds of non-soluble substances and deposits density will have impacts on the pollution flashover voltage of insulators. Therefore, the test results carried out manually on pollution need to be corrected in terms of NSDD.

NGK puts forward that the correction factor of 50% flashover voltage $U_{50\%}$ is:

$$K_1 = (\mathrm{NS}_1/\mathrm{NS}_2)^{-0.12} \tag{19.5}$$

where

NS_1 is the NSDD in target polluted area, mg/cm^2, as shown in Table 19.1;
NS_2 is the NSDD for manual pollution tests, it is normally 0.1 or 1.0 mg/cm^2 (the NSDD value for manual pollution test when the insulator manufacturer carries out manual pollution flashover tests on insulators).

The withstand voltage of a single piece of insulator is corrected as follows:

$$U_{\max 2} = K_1 U_{\max 1} \tag{19.6}$$

(4) Correction of non-uniform contamination on upper and lower surfaces

The non-uniform contamination on upper and lower surfaces of insulators will have impacts on the pollution flashover voltage, so, it needs to be corrected. The unevenness of contamination on upper and lower surfaces of different polluted areas can be expressed by the ESDD ratio of upper and lower surfaces on DC insulator sheds. The results shown in Table 19.5 can be used for Ref. [2].

The correction factor obtained by Electric Power Research Institute of America (EPRI) through relevant tests is as follows:

Table 19.5 Contamination uniformity ratio of general DC insulator

ESDD (AC) (mg/cm^2)	0.03	0.05	0.08	0.15
Pollution accumulation ratio	1/3	1/5	1/8	1/10

$$K_2 = 1 - 0.38 \lg(T/B) \tag{19.7}$$

where

(T/B) is the pollution accumulation ratio of upper and lower surfaces (ESDD ratio).

The withstand voltage of a single piece of insulator is corrected as follows:

$$U_{\max 3} = K_2 U_{\max 2} \tag{19.8}$$

(5) Determination of pollution withstand voltage U_s

For UHVDC transmission lines, rated voltage U_N is 800 kV, the maximum working voltage U_s = 1.02 U_N, so, the maximum working voltage on insulator strings U_s = 816 kV.

(6) Determination of the number of insulators

Substitute the corrected parameters into the following equation, and get the number of line insulators N as follows:

$$N = U_s / U_{\max 3} \tag{19.9}$$

2. Calculation example of pollution withstand voltage method for DC insulators

In 1988, NGK gave in its design for Gezhouba-Nanqiao, Shanghai transmission line, the pollution withstand voltage value of a single piece of insulator CA-735EZ, which is shown in Table 19.6 [2].

Then by using the pollution withstand voltage value of a single piece of insulator CA-735EZ shown in Table 19.6 as an example, and using the correction method for NSDD provided by NGK to get the number of insulators on ±800 kV UHV transmission line at ESDDs under different polluted areas, the calculation process is shown in Table 19.7.

Table 19.6 Pollution withstand voltage value of single piece of insulator CA-735 EZ (NSDD is 0.1 mg/cm^2)

ESDD (mg/cm^2)	0.03	0.05	0.08	0.15
Pollution withstand voltage value (kV)	17.8	15.2	13.2	10.7

Note The data are for design of Gezhouba-Nanqiao, Shanghai transmission line provided by NGK in 1988

Table 19.7 Calculation process for selecting the number of ±800 kV line insulators by NGK's method

Degree of pollution	Clean area	Lightly polluted area	Mediumly polluted area	Heavily polluted area
ESDD (AC) (mg/cm^2)	0.03	0.05	0.08	0.15
ESDD (DC) (mg/cm^2)	0.06	0.10	0.16	0.30
Pollution accumulation ratio on upper and lower surfaces of insulator	1/3	1/5	1/8	1/10
NS_1 (mg/cm^2)	0.18	0.3	0.48	0.9
Single piece $U_{50\%}$ (kV) provided by test. NS_2 = 0.1 mg/cm^2	17.8	15.2	13.2	10.7
Required withstand voltage U_{max1} (kV) $U_{max1} = U_{50\%}(1 - 3\sigma_s)$	14.1	12.0	10.4	8.5
Correction factor for NSDD $K_1 = (NS_1/NS_2)^{-012}$	0.932	0.876	0.828	0.768
After NSDD is corrected, $U_{max2} = K_1 U_{max1}$ (kV)	13.1	10.5	8.6	6.5
Correction factor for pollution accumulation ratio on upper and lower surfaces $K_2 = 1 - 0.381\ {}_g(T/B)$	1.181	1.266	1.343	1.380
After pollution accumulation ratio is corrected (kV), $U_{max} = K_2 U_{max2}$ (kV)	15.5	13.3	11.6	9.0
Max operating voltage of line $U_s = 1.02\ U_N$ (kV)	816			
Required number of insulators $N = U_s/U_{max3}$	53	62	71	92

19.1.4 Selection of Insulators in Icing Area

Icing on the insulator surface includes 3 types—glaze, rime, and mixed-phase ice.

Glaze is an icing layer in glass shape with rough surface that is transparent or lack luster, which is formed during the time when the cooled rainfall encounters the surface of an object with temperature equal or lower than 0 °C. Glaze has strong depositing capability, and water drops occur during formation, and can form ice run easily, which belongs to wet growth.

Rime is a result of numerous unfrozen fog drops with temperature below 0 °C which are accumulated and frozen with wind unceasingly on the objects, like branches, etc. It shows as white and opaque sediments in granular structure. The adhesive force is small, no water drops occur during formation, no ice run will generate, which belongs to dry growth.

The mixed-phase ice is an ice body formed by combining the wet growth of glaze and dry growth of rime. It has some adhesive force.

There will be water drops occurring during formation of glaze and mixed-phase ice. The formed ice run may bridge the sheds of insulators, causing the withstand voltage property of insulators to decrease. Therefore, the most serious impact on the electrical property of insulators is glaze.

In China, the UHVDC transmission line is long, the situation in the areas where it passes by is complicated, the ice damage in part of areas is serious, and the flashover phenomena of insulators often occur due to icing. The factors that affect the ice flashover voltage of insulators are mainly related to the umbrella types and materials of insulators, pollution degree of insulators prior to icing, conductivity of frozen water, and amount of icing. Through the study on the icing flashover of insulators, suggestions can be put forward on the design of insulator strings of lines in the icing areas.

19.1.4.1 Type Selection of Insulators in Icing Area

Generally speaking, the umbrella types and materials of insulators will have impacts on the ice flashover voltage of insulators, and such impacts are achieved through impacts on the icing of insulators (such as icing location and bridging of ice column). Below are the discussions respectively on the impacts of materials and umbrella types over the ice flashover voltage of insulators.

1. Comparison of ice flashover voltage of insulators with different materials

By selecting porcelain bell-type insulator XZP-210, glass bell-type insulator F210P/C, and composite insulator. Reference [6] studied the DC flashover characteristics when the insulators of above three types of materials are ice covered, and the results are as shown in Fig. 19.4.

It is seen that among the three types of insulators, the porcelain insulator has the highest ice flashover voltage, glass insulator's ice flashover voltage is slightly lower than that of porcelain insulator, there is little difference between the two, but the

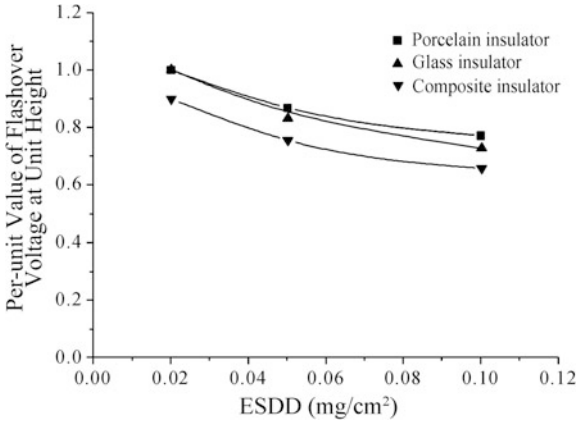

Fig. 19.4 Comparison of ice flashover voltage of insulators with three different materials. *Note* The reference value is the ice flashover voltage of the porcelain bell-type insulators

composite insulator has the lowest ice flashover voltage. This is mainly because that the porcelain insulator and glass insulator are bell jar-type insulators, their shed diameters are big, the distance between two adjacent sheds is far, and the shed edges will not be bridged by ice run completely during icing. However, the composite insulator has smaller shed diameter, under the same amount of icing, the shed can be bridged more easily or even covered by ice run completely, causing the ice flashover voltage of composite insulator to decrease. In addition, under low temperature and humid environment in a long term, the hydrophobicity of composite insulator is weakened significantly, and the insulator surface is covered by ice in the end, causing its hydrophobicity unable to play a role.

2. Comparison of ice flashover voltage of insulators with different umbrella types

By selecting three umbrella-type insulator CA-774EZ, double-umbrella-type insulator XZWP-210 and bell-type insulator XZP-210 (all of the types of insulators are 210 kN). Reference [6] made a comparison to the pollution flashover characteristics of the three types of umbrella-type insulators after they were covered by ice, the results are as shown in Fig. 19.5.

Among the three types of umbrella-type insulators, double-umbrella-type insulator has the highest ice flashover voltage, the three umbrella-type insulator the second, the bell-type insulator the lowest, but there is little difference in pollution flashover voltage of the three types of umbrella-type insulators. It is believed through analysis that the three types of insulators are suspension disk-type insulators, so, the insulator strings have little difference in the overall icing. Under the same structural height, the distance between the adjacent sheds of three umbrella-type insulator is smaller, which causes the bridging of ice column to be more serious than that of double-umbrella-type insulator; therefore, the ice flashover voltage of double-umbrella-type insulator is slightly higher than that of three umbrella-type insulator.

In conclusion, the composite insulator has a small shed, under the same amount of icing, the ice run can be bridged more easily as compared to the disk-type

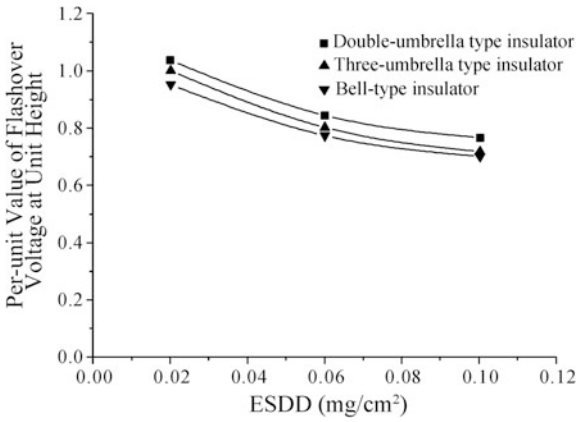

Fig. 19.5 Curve of relationship between flashover voltage and ESDD of ice-covered insulators with different umbrella types

insulator, under low temperature and humid environment, the composite insulator can lose its hydrophobicity easily, causing the flashover voltage of insulator to decrease a lot after being covered by ice, but, the porcelain insulator and glass insulator can still maintain higher insulating property after being covered by ice. As compared to the three types of umbrella-type insulators, double-umbrella-type insulator has the best pollution resistant flashover property after being covered by ice. Therefore, it is suggested that double-umbrella-type insulators be adopted in the icing areas.

19.1.4.2 Selection of the Number of Insulators in Icing Area

In the heavy icing areas, the surfaces of insulators are normally covered with thick ice layer, or even bridged by ice columns between sheds, in case of serious icing, the entire insulator is covered by ice completely, and the difference in the umbrella types and materials of insulators will become small. In this case, the icing withstand voltage gradient (that is, ice flashover voltage of insulator string at unit length) is normally used to describe the ice flashover property of ice-covered insulators.

The icing withstand voltage gradient is mainly related to the conductivity of frozen water and the amount of icing. At present, as for study on the icing flashover of DC insulators, there is no proven icing test standard, subject to limitation by its own conditions, the difference in test results conducted by different labs is big. The

Table 19.8 Withstand voltage gradients of ice-covered insulators given by different labs

Labs	Size of insulator (mm)	Number of each string	Conductivity of frozen water (μs/cm)	Voltage gradient (kV/m)	Remarks
China Electric Power Research Institute	Φ320/$H$170	26 19 19	51 108 450	95 86.6 52.6	Mini discharge voltage, outdoor
Chongqing University	Φ320/$H$170	9–21	100–200	78.7–81	Mini discharge voltage, indoor
BPA, USA	Φ320/$H$165	20	10 15.6 238	108 96 61	Mini discharge voltage, outdoor
EPRI, USA	Φ320/$H$170	38	32	68	Withstand voltage, outdoor
CRIEPI, Japan	Φ320/$H$165	10	>25	80	Withstand voltage, outdoor

icing withstand voltage gradients of DC insulators given by each lab are shown in Table 19.8 [7]. It can be seen that when there is little difference in the conductivities of frozen water, the difference in the voltage gradients obtained by different labs is very large.

As for heavy icing area, it is suggested in Ref. [8] that the design can be carried out according to the minimum value 67 kV/m of icing withstand voltage gradient of insulator, so, the length of insulator string L can be calculated using Eq. (19.10):

$$L = U_s/67 \tag{19.10}$$

where

U_s is the maximum working voltage of insulator string, 816 kV.

Besides the requirements of ice flashover voltage are met, the insulator string should also ensure that its pollution flashover voltage can meet the requirements of pollution withstand voltage in local polluted area. As for composite insulator, since lack of its operating experience and data under icing for reference, it is suggested that the composite insulators not adopted in the heavy icing areas for the time being.

19.2 Determination of Air Clearance for UHVDC Transmission Line

The air clearance that requiring insulation coordination on the UHVDC transmission line mainly refers to the gap between conductor and tower. What is different from AC line is that for all the straight line towers along the entire UHVDC line, a suspension mode by V-type insulator string is normally adopted, as compared to I-type string, under the suspension mode by V-type string, the operation of conductors is not affected by wind swing, so the operation is more stable, the verified voltage does not require considering the impacts of wind swing angle, moreover, the V string of insulators have good self-cleaning result, and the pollution accumulation is also relatively minor than that on I-type string. Therefore, a suspension mode by V-type insulator string is adopted for all the towers along the entire UHVDC line. The typical towers of UHVDC transmission line is shown in Fig. 19.6.

Similar to the UHVDC line, the insulation coordination of air clearance on UHVDC line also requires considering the impacts of the following factors.

1. Lateral width of tower

The lateral width of tower at air clearance and the wave front time of the test voltage will have significant impacts over the discharge voltage of air clearances at the towers of UHV lines. When the lateral width of tower is increased, the switching impulse discharge voltage of air clearances at towers will decrease accordingly. It is believed through analysis that the breakdown model of

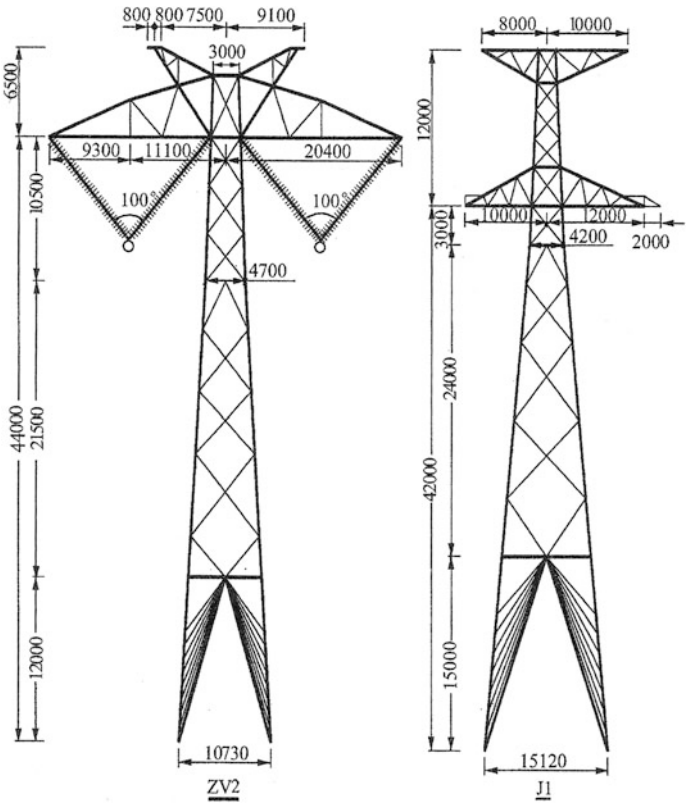

Fig. 19.6 Typical UHVDC transmission towers (mm)

conductor's impulse on the tower can be described using rod plate model to some extent. The tower is equivalent to a plate in the rod plate model. For the rod-plane gap, when the area of plate is increased, the uneven level of electric field for rod plate is intensified, causing the gap breakdown voltage to decrease. The former USSR believed that the relation between tower width and discharge voltage is as follows [9]:

$$U_{50}(\omega) = U_{50}(1)\,(1.03 - 0.03\omega) \tag{19.11}$$

where

$U_{50}(\omega)$ is discharge voltage when the width of tower body is ω(m), kV;
$U_{50}(1)$ is the discharge voltage when the width of tower body is 1 m, kV;
ω is width of tower body, m.

As for the discharge tests of the air clearance on UHVDC lines, since the width of tower body will affect the discharge voltage directly, real model tower is

normally adopted so as to ensure the discharge characteristic obtained through tests is same as the actual discharge characteristic.

2. Impact of altitude on discharge voltage of air clearance

It is stipulated in the national standard GB 50790-2013 *Code for Designing of ±800 kV DC Overhead Transmission Line* that the discharge voltage of air clearance needs to be corrected in case of altitude greater than 1000 m. For the external insulation in the areas with altitude of H (m), its discharge voltage (U_{P_H}) can be corrected using Eq. (19.12) [10].

$$U_{P_H} = k_a \cdot U_{P_0} \tag{19.12}$$

where

U_{P_H} is the required value of external insulation discharge voltage or withstand voltage when altitude is H (m), kV;
U_{P_0} is the required value of external insulation discharge voltage or withstand voltage when altitude is 0 m, kV;
k_a is the correction factor for altitude

The correction factor k_a is calculated as shown in Eq. (19.13).

$$k_a = e^{m(H/8150)} \tag{19.13}$$

where

H is the altitude (1000 m $\leq H \leq$ 2000 m), m

The values of m are selected as follows: for DC and lightning impulse voltage, m = 1.0; for switching impulse voltage, the value of m is to be selected by referring to Fig. 19.7 [10].

Then by using the correction of breakdown characteristic of air clearance on UHVDC line under switching impulse at altitude of 2000 m as an example, describe the steps how the altitude is corrected.

Assume the times of max switching overvoltage on the lines is 1.85, the required value of 50% switching impulse discharge voltage of air clearance under standard atmospheric pressure condition is as follows (Eq. (19.20) in Sect. 19.2.2 can be referenced):

$$U_{50} = \frac{k_3'}{(1-2\sigma)} U_N = \frac{1.85}{1-2\times 0.06} \times 816 = 1715\,(\text{kV})$$

The m value can be determined according to Fig. 19.7. The air clearance of line is the gap between conductor and tower, which belongs to the phase to ground insulation. By selecting curve a, the discharge voltage is at 1700 kV or above, it can be known that the m value is in a range between 0.4 and 0.45, in order to reserve some margin, select m = 0.45.

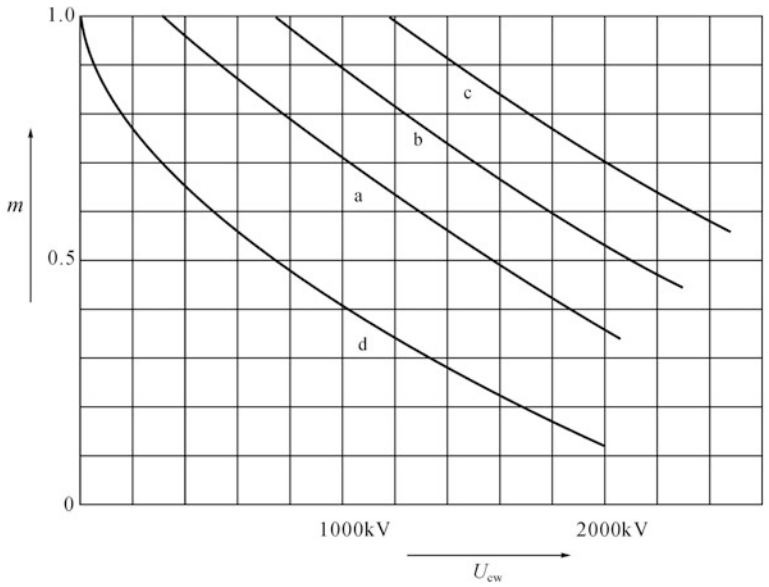

Fig. 19.7 Values of m under various voltages, reprinted from Ref. [10], copyright 1996, with permission from China Standards Press. *Note* **a** is the phase-to-ground insulation, **b** is the longitudinal insulation, **c** is the phase-to-phase insulation, **d** is the rod-plane gap (standard gap)

Without considering the impact of air humidity (that is, the correction factor of air humidity is (1), the correction factor of altitude k_a reflects, in fact, the impact of air density changes over discharge voltage. In this case, the reciprocal of altitude correction factor is the correction factor of air density, as shown in Eq. (19.14).

$$k_1 = 1/k_a \tag{19.14}$$

When the altitude is 2000 m, the calculated correction factor of altitude under DC voltage is as follows:

$$k_a = e^{m(H/8150)} = e^{1\times 2000/8150} = 1.278 \tag{19.15}$$

When the altitude is 2000 m, the correction factor of air density under DC voltage is as follows:

$$k_1 = 1/k_a = 0.782 \tag{19.16}$$

When the altitude is 2000 m, the calculated correction factor of altitude under switching impulse is as follows:

$$k_a = e^{m(H/8150)} = e^{0.45\times 2000/8150} = 1.116 \tag{19.17}$$

When the altitude is 2000 m, the correction factor of air density under switching impulse is as follows:

$$k_1' = 1/k_a = 0.896 \tag{19.18}$$

Chinese Electric Power Research Institute carried out the switching impulse discharge tests on the air clearances of tower heads for real model UHV towers in Beijing and Kunming (the difference in altitude is about 2000 m). The insulators were in V-type arrangement, the included angle was 90°, under different lengths of insulators and different air clearance distances of tower heads, comparison tests were carried out on the 50% switching impulse discharge voltage of 6-bundle conductors toward the cross arms of towers as well as toward tower bodies, the obtained test characteristic curves are shown in Fig. 19.8 [11].

On the precondition that the consistency of test samples arrangement and test methods is maintained as far as possible, the two tests on the 50% switching impulse discharge voltage of conductors toward towers were carried out, with the results showing the difference is 12.1–10.4% (the gap distance is in the range between 6.5 and 8.5 m). Therefore, it is believed that the difference in the amplitudes of discharge voltage in these two tests is the impact caused by altitude. When the altitude is 2000 m, the correction factor of atmospheric pressure is in a range between 1.12 and 1.10, the calculated correction factor of altitude obtained through Eq. (19.17) is 1.116, and the difference is small as compared to the test results. Therefore, it is believed that such method for altitude correction adopted in this book is reliable.

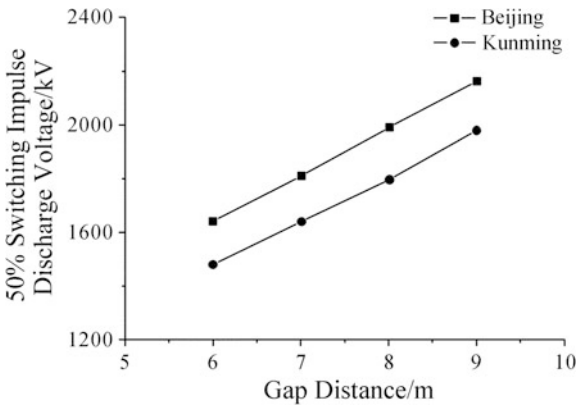

Fig. 19.8 Results of 50% switching impulse discharge voltage test on air clearance at ±800 kV tower head

19.2.1 Determination of Air Clearance Under DC Voltage

By referring to Ref. [12], the relation between 50% DC discharge voltage and rated working voltage U_N is as shown in the equation below.

$$U_{50} = \frac{k_2 k_3}{(1 - 3\sigma)k_1} U_N \tag{19.19}$$

where

k_1 is the correction factor of air density;
k_2 is the correction factor of air humidity, k_2 is 1 under the standard condition;
k_3 is the safety factor, 1.1–1.15 is selected;
σ is the variation factor of discharge voltage of air clearance under DC condition, 0.9 is selected;
U_N is the rated operating voltage, 800 kV

When the altitude is not considered, select $k_1 = 1$, $k_2 = 1$, $k_3 = 1.15$, then $U_{50} = 945$ kV. The DC discharge voltage curve of conductor toward the tower is as shown in Fig. 19.9 [2], the required air clearance distance corresponding to it is about 2.1 m. When the altitude is 2000 m, $k_1 = 0.782$, select $k_2 = 1$, $k_3 = 1.15$, then $U_{50} = 1209$ kV. According to Fig. 19.9, we can obtain a required air clearance distance of about 2.7 m.

In the UHVDC transmission line, V-type insulator string is adopted for straight line tower, the distance of conductor to the tower is fixed, and not affected by wind swing; moreover, the gap distance is at least 6–7 m or above. Therefore, DC voltage does not play a controlling role in the correction to the air clearance distance of tower.

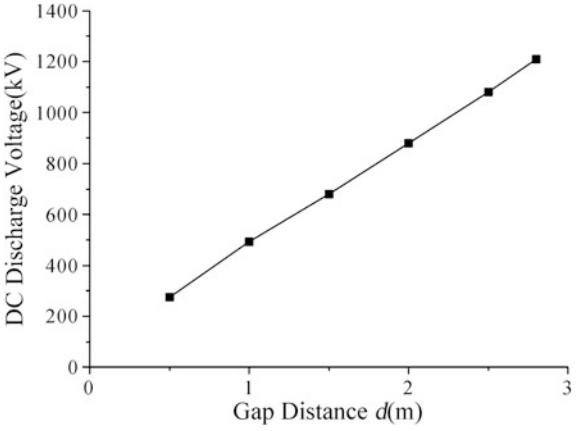

Fig. 19.9 Curve of positive DC discharge voltage of bundled conductor-to-tower body gap

19.2.2 Determination of Air Clearance Under Switching Impulse

By referring to DL/T 436-2005 *Technical Guide for HVDC Overhead Transmission Lines*, the relation between 50% switching impulse discharge voltage of air clearance for DC line and the max system voltage U_m is as shown in Eq. (19.20).

$$U_{50} = \frac{k_2' k_3'}{(1 - 3\sigma) k_1'} U_m \tag{19.20}$$

where

k_1' is the correction factor of air density;
k_2' is the correction factor of air humidity, $k_2' = 1$ under the standard condition; k_3' the times of switching overvoltage, select k_3' = 1.7–1.8;
σ is the variation factor of switching voltage of air clearance, select σ = 5%. In addition, according to the *Report on HVDC Converter Stations for Voltage above ±600 kV* published by CIGRE in 2002, this parameter is selected as 6%;
U_m is the max system voltage, 816 kV.

When the altitude is not considered, select $k_1' = 1$, $k_2' = 1$, $k_3' = 1.7$, then U_{50} = 1541 kV. The DC breakdown characteristic curve of conductor toward the air clearance of tower is as shown in Fig. 19.10 [2], the required air clearance distance corresponding to it is about 5.3 m. When the altitude is 2000 m, $k_1' = 0.896$, select $k_2' = 1$, $k_2' = 1.7$, then U_{50} = 1720 kV. According to Fig. 19.10, we can obtain a required air clearance distance of about 6.2 m.

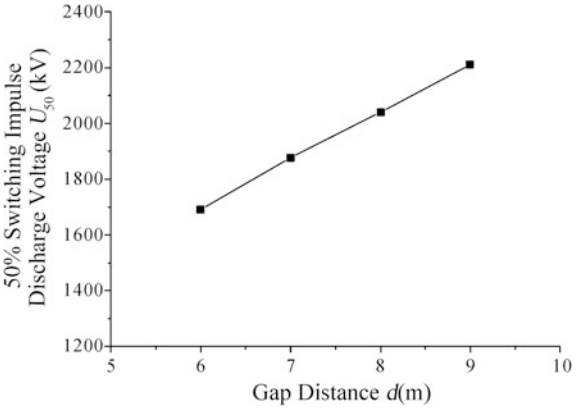

Fig. 19.10 Switching impulse discharge characteristics of air clearance for 800 kV UHVDC transmission tower

19.2.3 Determination of Air Clearance Under Lightning Impulse

When determining the air clearance under lightning impulse, there should be some differences for DC line and AC line.

As for AC line, normally the ratio of 50% impulse breakdown voltage $U_{50\%(l)}$ of air clearance to 50% impulse flashover voltage of insulator string U_{CFO} (the so-called coordination ratio) is maintained at 0.85 or so, that is, $U_{50\%(l)} = 0.85U_{\mathrm{CFO}}$. The operating practice for many years has shown that the operating experience with the AC lines designed according to the above method is satisfactory. In the UHVAC line, its coordination ratio is normally 0.8. However, in the DC line, the number of insulators is selected based on the requirement that no flashover occurs under DC operating voltage, since the DC line has stronger dust collecting effect, which causes the DC flashover voltage to decrease a lot, under the same conditions, the selected number, creepage distance, and string length of DC insulators are greater than those of the insulators of AC transmission line [13]. If the air clearance of DC line is still determined using the coordination ratio of 0.85 or 0.8, the air clearance of DC line so determined will be too big.

For the UHVDC line, if using the same method as 1000 kV UHVAC line to determine the air clearance, when the altitude is 1000 m or below, the required air clearance under lightning impulse is about 7.0–8.7 m [14], but, the required air clearance under DC working voltage is about 2.1–2.7 m, the required air clearance under switching impulse is about 5.3–6.2 m. According to the insulation coordination method for the air clearance of AC line, the required air clearance under lightning impulse should be selected and used as the design value for air clearance of DC line. However, in practice, the air clearance under lightning impulse is normally not selected; instead, the air clearance under switching impulse is selected. The concrete analysis is as follows.

For the UHVDC line, the impact of lightning overvoltage over the DC system is different from that of AC line. First of all, in the DC line, there is no DC circuit breaker, and there is no such maintenance or repair issue similar to AC system, which is caused by tripping of circuit breaker due to multiple lightning strikes. When flashover occurs due to lightning strike, the DC converter valve will act rapidly, and change quickly from rectification state to inversion state, causing the electric arc at the line fault point to extinguish rapidly, after that, the DC system will restart quickly, the duration of whole process is very short, normally in 100–300 ms, so, the whole lightning strike flashover and restart process almost does not affect the continuous operation of line. Secondly, when flashover occurs under lightning strike, due to the rapid regulating of DC control system, the value of fault current flowing through the DC line and the time of duration are smaller than the short-circuit current of AC line; therefore, the damage to the insulators is much lighter than that caused by AC line. In addition, since it is affected by the working voltage of DC line, the DC line has the natural unbalanced insulation characteristic against lightning, lightning strike normally occurs on the pole conductor which is

opposite to the polarity of thundercloud, but lightning flashover almost does not occur on another pole conductor, so, another pole can still supply power properly; furthermore, the DC system can operate at an overload of 1.4–1.5 times in a short period of time after the fault pole is blocked. Therefore, such extremely serious situation which the two poles of DC system are shut down will normally not occur. In summary, the impulse flashover on the DC line resulting from the lightning overvoltage and its consequences are far minor than that on AC line. Moreover, the occurrence of probability is not big, so, when determining the air clearance of DC line, there is normally no need to consider the requirement of lightning impulse overvoltage.

However, as for the switching overvoltage of DC line, it is different from lightning overvoltage, it has many varieties, under some faults, it is possible to cause serious accidents, for example, two poles of DC system are shut down, consequently causing significant impacts on the system's normal power supply. Therefore, when determining the air clearance of DC line, normally the key is to consider the requirements of switching impulse overvoltage.

In conclusion, as for the air clearance verification and tower size design of the UHVDC line, the lightning impulse normally does not play a controlling role, instead, the switching overvoltage is a key controlling factor.

19.2.4 Code-Recommended Value and Engineering-Applied Value for Air Clearance of UHVDC Line

The national standard GB50790-2013 *Code for Designing of ±800 kV DC Overhead Transmission Line* has given the minimum gaps between the energized parts and tower structural members (including guys and shackles, etc.) for ±800 kV line under corresponding wind swing conditions, as shown in Table 19.9.

Reference [2] has given the minimum gaps between energized parts and tower structural members for ±800 kV Yunnan-Guangdong, Xiangjiaba-Shanghai, Jinping-Southern Jiangsu UHVDC transmission lines, as shown in Table 19.10.

Table 19.9 Minimum gaps recommended by standard between energized parts and tower structural members (m)

Nominal voltage (kV)	±800				
Altitude (m)	500	1000	2000	3000	3700
Minimum gap under working voltage	2.1	2.3	2.5	2.85	3.1
Minimum gap under switching overvoltage (1.6 p.u.)	5.3	5.7	6.4	7.1	7.6
Minimum gap under lightning overvoltage	–				

Table 19.10 Minimum gaps applied in engineering between energized parts and tower structural members (m)

Nominal voltage (kV)	±800					
Altitude (m)	Times of switching overvoltage	500	1000	2000	3000	3700
Required minimum gap for switching overvoltage	1.6 p.u.	5.3	5.7	6.4	7.1	7.6
	1.7 p.u.	5.5	6.3 (5.55)	6.9 (6.2)	–	–
Required minimum gap for working voltage		2.1 (2.55)	2.3 (2.7)	2.5 (3.05)	2.85 (–)	3.1 (–)
Required minimum gap for lightning overvoltage	–					

Note The data in the brackets are the design values of ±800 kV UHVDC line from Yunnan to Guangdong, and the other data are the design values of ±800 kV UHVDC lines from Xiangjiaba to Shanghai and from Jinping to South Jiangsu

References

1. Guan Z, Zhang F, Wang X, Wang L. Consideration on external insulation design and insulator selection of UHVDC transmission lines. High Volt Eng. 2006;32(12):122–3.
2. GB 50790-2013. Code for designing of ±800 kV DC overhead transmission line; 2013.
3. Wanjun Z. High-voltage DC transmission engineering technology. Beijing: China Electric Power Press; 2004.
4. Yongli Y, Zhang F, Li R, Guoli Wang. Research on several problems in external insulation design of UHVDC transmission line. South Power Syst Technol. 2013;7(1):39–43.
5. Q/GDW 181-2008. Technical code for design of ±500 kV DC overhead transmission line; 2008.
6. Liu Z. External insulation of UHVDC transmission system. Beijing: China Electric Power Press; 2009.
7. Zhou G, Li L, Liu Z. Design of ±800 kV insulation DC transmission lines. High Volt Eng. 2009;35(2):231–5.
8. Li Y, Zhou K, Li L, He J. Design of ±800 kV DC UHV transmission line. High Volt Eng. 2009;35(7):1518–25.
9. Alexandrov ГН, et al. Design of EHV transmission line. Beijing: Water Resources and Electric Power Press; 1987.
10. IEC 60071-2. Insulation coordination—part 2: application guide; 1996.
11. Sun Z, Liao W, Su Z, Zhang X. Test study on the altitude correction factors of air clearances of ±800 kV UHVDC projects. Power Syst Technol. 2008;32(22):13–6.
12. DL/T 436-2005. Technical guide for HVDC overhead transmission lines; 2005.
13. Zhao Z. High voltage engineering (Rev. 3). Beijing: China Electric Power Press; 2013. p. 293–4.
14. Peihong Zhou, Xiu Muhong Gu, Dingxie Dai Min, Ying Lou. Study on overvoltage protection and insulation coordination for ±800 kV HVDC transmission system. High Volt Eng. 2006;32(12):125–32.

Chapter 20
Overvoltage Characteristics and Insulation Coordination of UHVDC Converter Valves

Kunpeng Zha, Xiaoguang Wei and Jie Liu

Under the action of transient voltage, such as operation, lightning, and steep wave, and during the transitions of turn-off, turn-on, and blocking under the operating condition, the UHVDC converter valves will generate various types of overvoltage. This chapter puts forward the analysis methods for the impulse overvoltage and operating overvoltage of converter valve, and based on this, studied the configuration methods for overvoltage protection, and introduced the protection of metallic oxide arrester as well as the protection of gate electron in order to ensure that the converter valves can withstand the worst steady-state operating conditions as well as various transient overvoltage. In addition, this chapter has also introduced the strategies for insulation coordination of converter valve system for determining the creepage distance and air clearance based on the level of overvoltage in the design of converter valves.

K. Zha (✉) · X. Wei
State Grid Smart Grid Research Institute, Changping District, Beijing, People's Republic of China
e-mail: zhakp@epri.sgcc.com.cn

X. Wei
e-mail: weixiaoguang@sgri.sgcc.com.cn

J. Liu
China Electric Power Research Institute, Haidian District, Beijing, People's Republic of China
e-mail: liujie1@sgcc.com.cn

© Zhejiang University Press, Hangzhou and Springer-Verlag GmbH Germany 2018

H. Zhou et al. (eds.), *Ultra-high Voltage AC/DC Power Transmission*, Advanced Topics in Science and Technology in China,
https://doi.org/10.1007/978-3-662-54575-1_20

20.1 Analysis on Overvoltage Characteristics of Converter Valves Under the Effect of Impulse Voltage

When the converter valves withstand such high-frequency transient overvoltage as lightning overvoltage and steep front overvoltage, the roles of the parasitic capacitance between metallic conductors with different potentials and the distributed capacitance of metallic conductors to the ground in the converter valve system should not be neglected any more. In order to estimate the impacts of these parameters reasonably, these distributed capacitances need to be extracted, and connected to the main circuit according to its electrical relation in the converter valves so as to establish their impulse transient analysis models and study the overvoltage characteristic of converter valves.

20.1.1 Extraction of Parasitic Capacitance of Converter Valve System

The metallic conductors in the converter valve system have big sizes and complicated structures; all these need to consume a lot of calculation resources. The boundary element method is used to perform calculations; in this method, only the conductor surface is selected and used as the calculation domain; this will improve the calculation efficiency significantly.

The boundary element method is an integral method for solving the boundary value problems; its basic theory is to convert the differential equation into the boundary integral equation, then discretize the equation into the algebraic equations, and obtain the numerical solutions to the problems by solving the algebraic equations [1–3].

Given that the boundary of spatial region V consists of curved surfaces S_1 and S_2, the electric charge density in the region is $\rho(\boldsymbol{r}')$; $\boldsymbol{r}$ and $\boldsymbol{r}'$ are used to express field point and source point, respectively, where $\boldsymbol{R} = \boldsymbol{r} - \boldsymbol{r}'$. When the boundary conditions and the electric charge distribution in the region are given, the problem of solving the distribution of electric potentials and electric field intensity in the region and at the boundary can be expressed as the boundary value problem as follows:

$$\begin{aligned} &\nabla^2\phi = -\frac{\rho}{\varepsilon} \\ &\phi = \phi_0, \quad \phi \in S_1 \\ &-\frac{\partial\phi}{\partial n} = E_0, \quad \phi \in S_2 \end{aligned} \tag{20.1}$$

where

ϕ is the electric potential;
e_n the dielectric constant of media in the region;
ε the outer normal direction of boundary;
ϕ_0 the electric potential at boundary S_1;
E_0 is the normal electric field intensity at boundary S_2.

By using Green's identities, the equations above are converted into:

$$\phi(\boldsymbol{r}) = \frac{1}{4\pi\varepsilon}\iiint_V \frac{\rho(\boldsymbol{r}')}{R}\mathrm{d}V + \frac{1}{4\pi}\iint_S \left[\frac{1}{R}\frac{\partial\phi}{\partial n} - \phi\frac{\partial}{\partial n}\left(\frac{1}{R}\right)\right]\mathrm{d}S \tag{20.2}$$

where

$\boldsymbol{r}$ is the field point in the region.

When the field point is moved to the boundary of region, the Eq. (20.2) is converted into

$$\frac{1}{2}\phi(\boldsymbol{r}) = \frac{1}{4\pi\varepsilon}\iiint_V \frac{\rho(\boldsymbol{r}')}{R}\mathrm{d}V + \frac{1}{4\pi}\iint_S \left[\frac{1}{R}\frac{\partial\phi}{\partial n} - \phi\frac{\partial}{\partial n}\left(\frac{1}{R}\right)\right]\mathrm{d}S \tag{20.3}$$

Considering the Laplace's equation of no volume charge distributed in the region, the Eq. (20.3) can be simplified as

$$\frac{1}{2}\phi(r) = \frac{1}{4\pi}\iint_S \left[\frac{1}{R}\frac{\partial\phi}{\partial n} - \phi\frac{R\cdot e_{\boldsymbol{n}}}{R^3}\right]\mathrm{d}S, \tag{20.4}$$

By discretizing the boundary and using Galerkin weighted residual approach, the Eq. (20.4) is converted into

$$\begin{aligned}\frac{1}{2}\sum_e\sum_j\sum_i\iint_{S_e} N_jN_i\phi_i\mathrm{d}S = {} & \frac{1}{4\pi}\sum_e\sum_{e'}\sum_j\sum_i\iint_{S_e} N_j\iint_{S_{e'}}\frac{N_i}{R}\frac{\partial\phi_i}{\partial n}\mathrm{d}S'\mathrm{d}S \\ & - \frac{1}{4\pi}\sum_e\sum_{e'}\sum_j\sum_i\iint_{S_e} N_j\iint_{S_{e'}} N_i\frac{R\cdot e_n}{R^3}\phi_i\mathrm{d}S'\mathrm{d}S\end{aligned} \tag{20.5}$$

where

e is the number of field unit;
e' is the number of source unit;
S_e is the integral region of field unit;
$S_{\mathrm{e}'}$ is the integral region of source unit.

Given that the vector $\boldsymbol{E} = \left[-\frac{\partial\phi_1}{\partial n}, \frac{\partial\phi_2}{\partial n}, \cdots\right]^{\mathrm{T}}$, $\boldsymbol{u} = [\phi_1, \phi_2, \ldots]^{\mathrm{T}}$, and given the matrices

$$A_{ij} = 2\pi \sum_e \iint_{S_e} N_j N_i \mathrm{d}S \tag{20.6}$$

$$C_{ij} = -\sum_e \sum_{e'} \iint_{S_e} N_j \iint_{S_{e'}} \frac{N_i}{R} \mathrm{d}S' \mathrm{d}S \tag{20.7}$$

$$D_{ij} = \sum_e \sum_{e'} \iint_{S_e} N_j \iint_{S_{e'}} N_i \frac{R \cdot e_n}{R^3} \phi_i \mathrm{d}S' \mathrm{d}S \tag{20.8}$$

Equation (20.5) is written as a form of matrix:

$$\boldsymbol{CE} = (\boldsymbol{A} + \boldsymbol{D})\boldsymbol{u} = \boldsymbol{Bu} \tag{20.9}$$

Therefore, when the boundary electric potential vector u is known, the vector E of boundary electric field intensity can be solved through the Eq. (20.9), and then the surface charge density σ can be obtained.

Now take the electrostatic independent system consisting of $n + 1$ conductors into consideration; the total electric charge carried by each conductor is zero. Given the sequential number of conductors is 0, 1, 2, …, n, the electric charges carried by them are q_0, q_1, q_2, …, q_n. According to the definition of electrostatic independent system, there is

$$q_0 + q_1 + q_2 + \cdots q_n = 0. \tag{20.10}$$

For the above linear electrostatic independent system, given conductor #0 is a reference conductor and its electric potential is zero, there is

$$\begin{cases} q_1 = C_{10}U_{10} + C_{12}U_{12} + \cdots + C_{1j}U_{1j} + \cdots + C_{1n}U_{1n} \\ q_2 = C_{21}U_{21} + C_{20}U_{20} + \cdots + C_{2j}U_{2j} + \cdots + C_{2n}U_{2n} \\ q_i = C_{i1}U_{i1} + C_{i2}U_{i2} + \cdots + C_{ij}U_{ij} + \cdots + C_{in}U_{in} \\ q_n = C_{n1}U_{n1} + C_{n2}U_{n2} + \cdots + C_{nj}U_{nj} + \cdots + C_{n0}U_{n0} \end{cases} \tag{20.11}$$

Assume conductor #i is in a high electric potential, and the electric potentials of the rest of conductors in the system are zero, according to the above Eq. (20.11), there is

$$\begin{cases} C_{21} = \frac{q_2}{U_{21}}\Big|_{U_{20}=U_{22}=\cdots=U_{2j}=\cdots=U_{2n}=0} \\ C_{i1} = \frac{q_i}{U_{i1}}\Big|_{U_{i0}=U_{i2}=\cdots=U_{ij}=\cdots=U_{in}=0} \\ C_{n1} = \frac{q_n}{U_{n1}}\Big|_{U_{n0}=U_{n2}=\cdots=U_{nj}=\cdots=U_{nn}=0} \end{cases} \tag{20.12}$$

It can be seen from Eq. (20.12), under the assumed conditions, as long as the electric charge carried by the conductor with 0 potential is obtained by calculation, the capacitance parameters between the assumed high-potential conductor and other conductors can be obtained.

Calculating by boundary element method, the electric field intensity E_n of each node can be obtained. Then from $D_n = \varepsilon_0 E_n$ and $\sigma = D_n$, the equation $\sigma = \varepsilon_0 E_n$ can be got, where σ is the surface charge density. After obtaining the electric charge density of node, carry out the interpolation of units, and then integration, and thus obtain the total electric charge of conductors. For line model, what is obtained by boundary element method is the line charge density τ of nodes; then we can obtain the total electric charge through interpolation by this method.

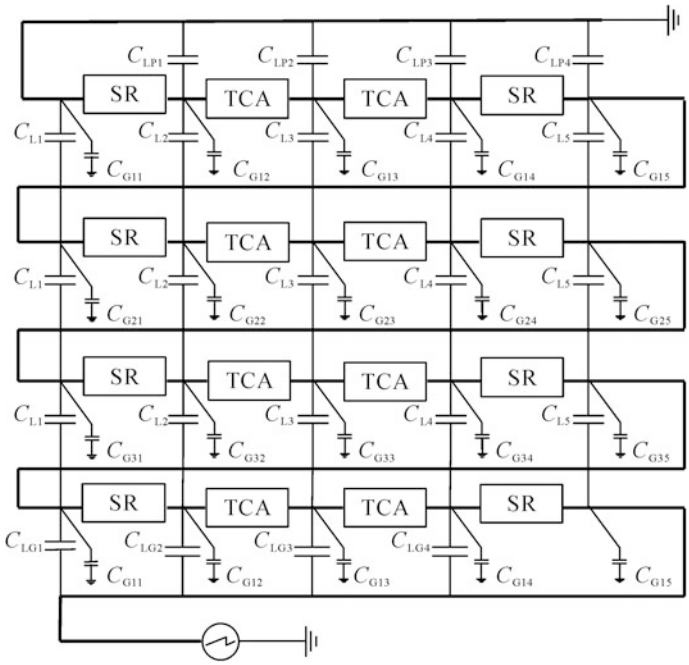

Fig. 20.1 Equivalent circuit of valve tower under impulse voltage. *Note* C_G Stray capacitance of each layer of module shields to the ground, C_{LG} Stray capacitance of bottom layer of modules to the bottom shields, C_{LP} Stray capacitance of top layer of modules to the top shields, C_L Stray capacitance of shield layer

20.1.2 Analysis Model for Impulse Transient of Converter Valve System

The component-level simplified circuits can be used for analyzing the level voltage distribution of valve module and thyristor. For the converter valve that has n layers, each layer has m groups of components, each component has l pieces of thyristors, and the equivalent circuits of valve towers under impulse voltage are shown, respectively, in Fig. 20.1.

The equivalent circuits to which beam parasitic capacitance and shield parasitic capacitance are added are shown in the figure. For the purpose of convenience, the equivalent parameters of saturation reactor and thyristor are expressed in SR and TCA, respectively.

20.1.3 Characteristics of Impulse Transient Overvoltage of Converter Valve System

By using the converter valves of ±800 kV UHVDC transmission line from Jinping to South Jiangsu as an example, each valve module is provided with 9-level thyristors. Double-valve towers consist of 4 valve layers and 8 modules; each module protects 4 shields that are insulated with each other; the top and bottom

Fig. 20.2 Structure of UHV converter valve tower

shields are provided, respectively, at the top and bottom of valve tower; and the specific structure is shown in Fig. 20.2.

Due to the impact of stray capacitances, the voltage between different valve layers and different modules are not equal. Under the extreme conditions, the module close to the incident wave will cause abnormal action of the forward overvoltage protection due to excessive high voltage stressed on it. Therefore, in the design of converter valves, the impulse overvoltage borne by different modules need to be calculated accurately, and the grading capacitance of components shall be designed to achieve the voltage sharing between different modules and valve layers [4–6].

In order to obtain the reference value, specific to the lightning overvoltage and steep front overvoltage, without considering the parameters of capacitance to the ground, calculations were performed, respectively, on the voltage of thyristors on the 1st valve module and 16th valve module, which were shown in Fig. 20.3. As it can be seen from the figures, the two peak voltages are approximately the same; therefore, in the calculations, the unbalance factor of thyristor voltage is adopted based on this.

Calculations were performed on the voltage of thyristors on 1st valve module that was close to the incident wave end; the range of grading capacitance was 0–10 nF, which is shown in Fig. 20.4. Under the action of lightning overvoltage, the change law of thyristor voltage drop is reduced as the grading capacitance is increased from 0 to 3 nF, and it is reduced as the capacitance value is increased over 3 nF. Under the action of steep front overvoltage, the maximum value of the thyristor voltage drop is reduced as the grading capacitance is increased, and when the capacitance value is greater than 5 nF, the unevenness coefficients are below 1.2.

Specific to lightning overvoltage and steep front overvoltage, calculations were performed on the unevenness coefficients of each layer of converter valves, and the range of grading capacitance is 0–10 nF, as shown in Fig. 20.5. As we can see from the figures, under the action of these two kinds of overvoltage, the voltage gradients

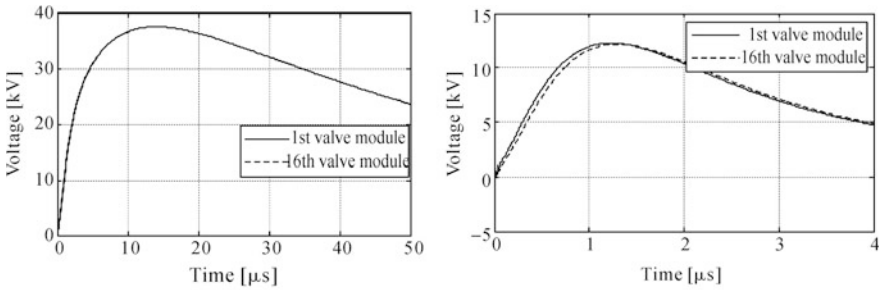

Fig. 20.3 Voltage of thyristors in the 1st valve module and 16th valve module without considering the capacitance to ground

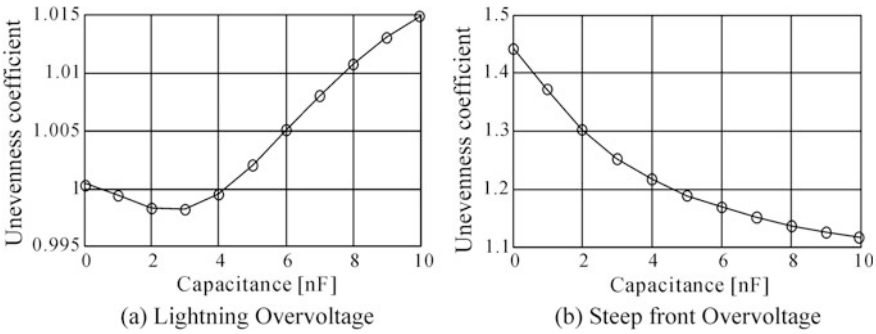

Fig. 20.4 Relationship between maximum voltage drop of thyristor in valve module close to incident wave end and compensation capacitance

of valve layers are reduced as the grading capacitance is increased, but, when the grading capacitance value was greater than 5 nF, its voltage sharing or compensating effect was relatively weak. In addition, in order to ensure that its unevenness coefficient is below 1.2, by taking into consideration comprehensively, the grading capacitance value should be larger than 5 nF.

20.2 Analysis on Overvoltage Characteristics of Converter Valve Under Operating Condition

The power electronic devices, like thyristor, are not the ideal switching elements, and there are strict limitations to their withstanding capabilities for voltage, current, etc. During operation, they can be classified as four states, i.e., turn-on, on state, turn-off, and off state. It is normally believed that turn-on and turn-off are transient processes in the cycle, and among them the overvoltage borne under turn-off state is the highest [6].

The UHV converter valve consists of numerous components which form a chain circuit. With respect to overshooting of reverse recovery voltage of the thyristor valve, its front time is about dozens of microseconds to 100 μs, which is equivalent to the switching impulse voltage, but the amplitude is normally lower than its insulation test level. The voltage of thyristor valve is almost in even distribution; much of stray capacitance to the ground can be neglected. In addition, the smoothing reactors and DC transmission lines can be expressed by constant DC sources. The stray capacitances of DC switchyard busbars, wall bushings and reactors, etc. to the ground are expressed by C_y. The stray capacitances of transformer windings at AC side to the ground, and the stray capacitances of busbars and wall bushings, etc. to the ground are expressed by C_t.

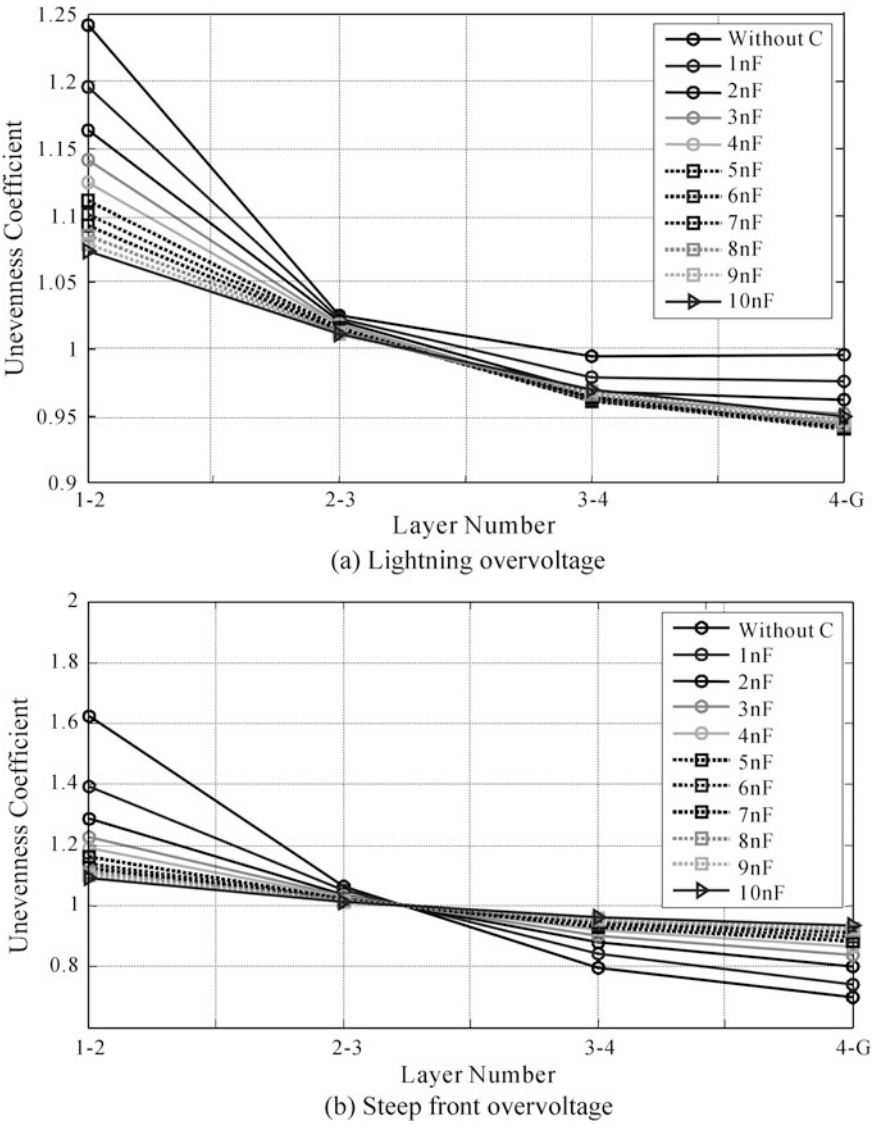

Fig. 20.5 Relationship between valve layer voltage gradient and compensation capacitance

The converter of HVDC transmission normally consists of 12-pulse bridges. With respect to the voltage stress on the turn-off valve, the impact between two bridges is very small; thus, the analysis on 6-pulse bridges is sufficient. The circuit topology is shown in Fig. 20.6.

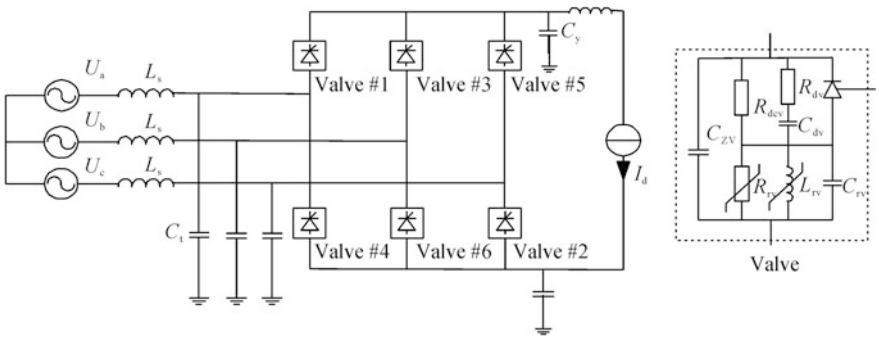

Fig. 20.6 Circuit topology of converter. *Note* L_s Leakage reactance of converter transformer, C_t Stray capacitance at AC side, C_{zv} Capacitance at valve end, R_{dcv} DC equalizing resistance of valve, R_{dv} Damping resistance of valve, C_{dv} Damping capacitance of valve, R_{rv} Reactor resistance of valve, L_{rv} Reactor inductance of valve, C_{rv} Reactor capacitance of valve, C_y Stray capacitance at DC side

20.2.1 Analysis on Turn-off Transient Overvoltage of Converter Valve

When the converter valves are turned off, due to the impact of stored electric charge of thyristors, reverse overshooting will occur at the valves; the thyristors will withstand serious reverse voltage stress; and the RC damping circuits connected in parallel on the thyristors can limit the reverse overshooting and play a role of protecting the thyristors. Hence, the turn-off process of converter valves determines the values of damping capacitance and damping resistance, which must ensure that the maximum reverse voltage stress withstood by the thyristors is within the safety margin. Moreover, only the range of parameters for damping circuit is determined; calculations and analyses can be performed on the loss of damping circuit.

The coordination of valves with the external circuits is pretty sensitive to the average stored charge characteristic of thyristors in the valves. At the interior of valves, the difference between each single thyristor will generate very important partial effect. During the reverse recovery, when the charges stored by different thyristors are different, it will have impacts on the waveforms of overvoltage applied on the thyristors on the valves. Simply speaking, the valve consists of $(n-1)$ level thyristors that have the same charging charges and one thyristor have different charging charges. If this thyristor has smaller stored charges, it will recover first, and withstand a voltage higher than other thyristors mentioned previously. On the another hand, if this thyristor has bigger stored charges, it will recover very slowly, and withstand a recovery voltage lower than other thyristors.

If no controls are carried out, there will be a very big deviation in the voltage distribution (maybe a deviation of several hundreds of volts). However, by matching the thyristor parameters, these impacts can be reduced. Controls can be

achieved by selecting thyristors or on the manufacturing process, or selecting proper damping capacitances.

In addition, what needs to be noted is that the uneven voltage distribution resulting from different stored charges is mutually independent with the accuracy matched with the valve damping circuit elements. For example, even if the damping circuit is in good condition, the phenomenon of uneven voltage distribution still exists. The unevenness of voltage distribution resulting from different stored charges can be corrected only in several milliseconds (depending upon the time constant of damping circuit). As a result, such unevenly distributed voltage is maintained in the converter till the voltage becomes positive. This means that many thyristors in the valve (those having the maximum stored charges) will have voltage crossing zero too early; on the coordinate axis, they are dozens of microseconds, or even a hundred microseconds more than the voltage at valve ends (it is often used as a reference for time delay triggering). The thyristor's characteristic of turning-off time and minimum trigger delay angle of converter should be determined by such mode that allows for such effect.

The modern DC transmission converter valve consists of dozens of, or even a hundred of thyristors connected in series. Due to the impacts of such factors as manufacturing process, it is impossible that the parameters of thyristor elements are consistent completely; hence, it is impossible to ensure that each thyristor turns on or turns off at the same time. So, when the valve is turned on or turned off, if there are no capacitances connected in parallel at both ends of thyristors, the valve voltage will be completely applied on the thyristors that act in the last. If there are capacitances connected in parallel at both ends of thyristors, the capacitance voltage will not change abruptly, which can play a role of protecting the thyristors. In addition, in order to limit the discharge current of capacitances connected in parallel with the thyristors when the thyristors are turned on, damping resistances need to be connected in series to the capacitances. Due to the impacts of such factors as stored charges of thyristors, commutation angle μ, and commutation inductance, when the valves are turned off, the reverse voltage stresses withstood by the thyristors are usually higher than the forward voltage stresses withstood by the thyristors when the valves are opened; therefore, selection of the damping parameters should be determined through studying the impacts of damping circuits over the reverse voltage stresses of thyristors.

Generally speaking, the physical simulation method and classical method are adopted for analyzing the transient process of valve turn-off. The physical simulation method is to simulate the thyristors into a group of switches that have different breaking time. When the integral of thyristor's reverse recovery current to time is equal to the stored charge Q_{rr} of such thyristor, the switch breaks off. Such method is simple and practical. The classical method is to conduct solution by solving the linear differential equation with constant coefficients, or convert the circuits into operational circuits through integral transformation. As the mature development of time-domain simulation technologies on a large scale establish the electromagnetic transient model for the turn-off process of converter valves, calculation of the electrical stress of converter valves during turn-off process can be

obtained through simulation, and such calculation is high in efficiency, and the calculation result is accurate, which is widely applied in the design of converter valve currently. In this book, this method is called as time-domain circuit method.

Next, introductions are given to these three methods, respectively [7].

20.2.2 Physical Simulation Method

The stored charges Q_{rr} of thyristor components that constitute the converter valve are not all the same; the thyristors having the same stored charges are classified as a group, and each group of thyristors is regarded approximately as an ideal switch, when the integral of reverse current flowing through the switch to time is equal to the stored charges of a group of thyristors. Such group of switches will break off, and in this way, the equivalent circuit of valve turn-off is converted into the equivalent circuit as shown in Fig. 20.7. By calculating step by step using this circuit, the maximum reverse voltage stress withstood by the thyristor that is turned off in the last can be calculated approximately.

During the reverse recovery of thyristor, the resistance of thyristor will increase; however, it is believed that by the physical simulation method during the reverse recovery of thyristor, the resistance value is always zero, and when blocking is restored, the resistance value of thyristor is stepped from zero to infinity. This is not in conformity with the reality, and there will be a very big deviation in the

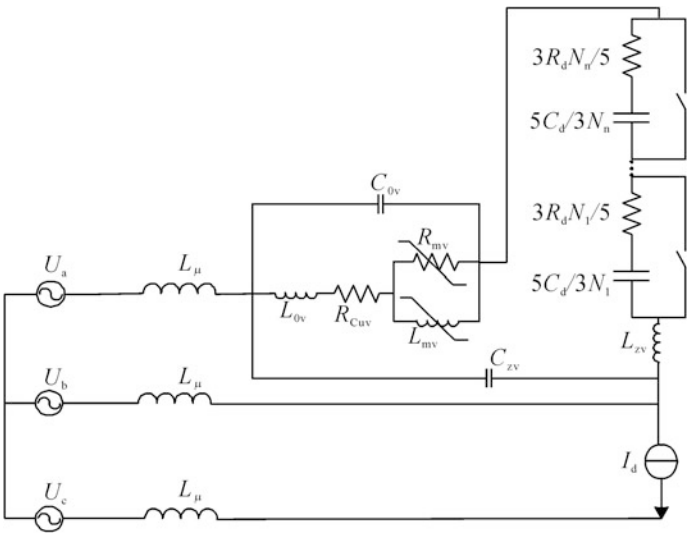

Fig. 20.7 Circuit model for calculating turn-off overvoltage of valve by physical simulation method

calculation result as compared to the reality; it is thus clear that the practical value of physical simulation method is not big.

20.2.3 Classical Method

The classical method is to solve the relation between the valve reverse voltage and time by solving the linear differential equation with constant coefficients, or convert the circuits into operational circuits through integral transformation. By using the classical method, the equivalent circuit of valve turn-off can be converted into the equivalent circuit as shown in Fig. 20.8. The converter valves that are in the process of being turned off can be substituted by current source; the exponential model of reverse recovery current or the double-curve secant model can be used to describe the relation between the reverse recovery current I_{off} and time.

By using the point when the valve current crosses zero as a starting point for timing, the KVL equation of circuit can be listed out as shown in Fig. 20.8; if the peak value of valve's reverse voltage is U_{RM}, the AC voltage sharing coefficient of valve is k_{ac}, the tolerance of damping capacitance is k_{cd}, the difference in the stored charges of thyristors connected in series with valves is ΔQ_{rr}, then the maximum reverse voltage $U_{thy-Rmax}$ of thyristors is as follows:

$$U_{thy-Rmax} = \frac{U_{RM}}{N_t} k_{ac} + \frac{\Delta Q_{rr}}{C_d} k_{Cd}, \tag{20.13}$$

where

C_d is the damping capacitance;
N_t is the number of thyristors connected in series.

The valve's reverse voltage can be calculated more accurately using the classical method; however, the components in the circuit must be linear components, otherwise the linear differential equation with constant coefficients cannot be written out, and the solutions cannot be done through the operational circuits.

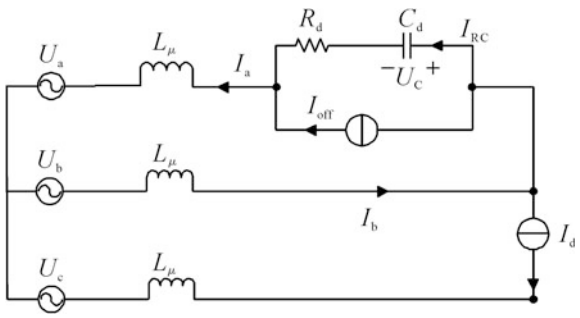

Fig. 20.8 Circuit model for calculating turn-off overvoltage of valve by classical method

The exponential model of reverse recovery current cannot truly reflect the recovery process of reverse blocking of thyristors, and it will be very difficult in determining the parameters of double-curve secant model. Moreover, the equivalent circuit has neglected the stray parameters and changes to the inductance resistance of saturation reactor with the current. Therefore, the results calculated through the classical method will also have deviations.

20.2.4 Time-Domain Circuit Method

For applying the time-domain circuit method, the transient analysis model for turning off of the converter valves needs to be established first. The Ref. [6] adopts the exponential model to simulate the reverse recovery current, and calculates the reverse recovery voltage of converter valves. The turn-off duration time of converter valve is about 200 μs only; hence, the voltage at each winding of transformer can be expressed using DC voltage source. Analyses were carried out using the turn-off of valve #6 as an example, and when valve #6 is turned off, valves #1 & 2 have already been conducted, and the reactors are saturated. It can be expressed using short circuits. The other valves #3, 4, & 5 that have already been turned off can be expressed using damping circuits; the reactors of these valves can be neglected. Valve #6 is expressed using valve reactor, damping branch, and current source, among them the current source shows the turning off process of thyristors. During turning off, the valve reactor will flow through the small-amplitude reverse current, which is almost shown as a linear inductance. Since the resistance and capacitance of valve reactors as well as the DC voltage sharing resistance have weak impacts over the turn-off overshooting of valves, they can be neglected. The simplified circuit is shown in Fig. 20.9.

The current during the reverse recovery of thyristors can be expressed as follows:

$$i_{\mathrm{r}}(t) = I_{\mathrm{RM}} \mathrm{e}^{-\frac{t-t_0}{\tau}} \tag{20.14}$$

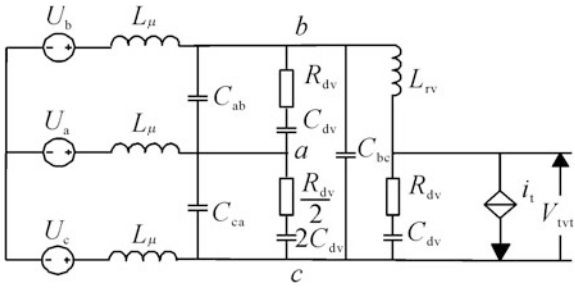

Fig. 20.9 Analysis circuit of turn-off voltage stress for converter valve

where

t_0 is the moment that thyristor crosses zero;
τ is the time constant;
I_{RM} is the thyristor's peak value of reverse current.

The voltage stress of valve turn-off itself is also affected by multiple circuit parameters, for example, damping capacitance C_d and damping resistance R_d. When $\gamma = 90°$, the turn-off voltage stress of valve is the most serious, and the overshoot coefficient is the highest. Analyses will be carried out on this item by item. The impact of damping circuit parameters on the turn-off voltage stress of valve is also very big. When the trigger delay angle $\alpha = 83°$ ($\gamma = 90°$), other parameters are fixed; C_{dv} and R_{dv} are adjusted, respectively, and the time-domain waveform U_{tvt} of valve's turn-off voltage is shown in Fig. 20.10.

By adopting the plant growth curve, Ref. [8] simulated the reverse recovery current of thyristors and performed the similar work. Changes to the peak value of reverse voltage for thyristors with the damping parameters are shown in Fig. 20.11. As it can be seen, when the damping resistance is fixed, the bigger the damping capacitance is, the smaller the reverse recovery voltage of valve is, but the loss of turn-off is increased accordingly. However, when the damping capacitance is fixed, the sole damping resistance value always exists, which causes the reverse recovery voltage to be minimum. At other trigger delay angles, the impact of damping parameters on the turn-off voltage stress is similar to this.

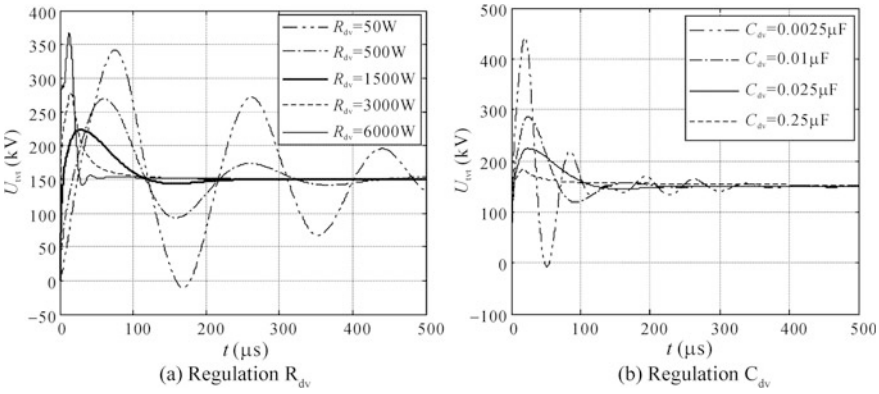

Fig. 20.10 Time-domain waveform of U_{tvt} under different damping parameters

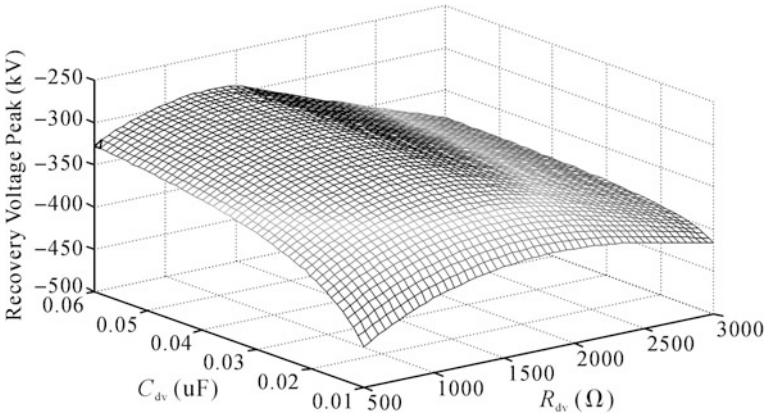

Fig. 20.11 Damping parameter and peak value of recovery voltage

20.3 Overvoltage Protection of DC Transmission Converter Valve and Its Design

The operating conditions of converter valve are complicated. It is unavoidable to have such situation that exceeds the withstand values of thyristors, for example, occurrence of various overvoltages, lightning impulse overvoltage, and transient overvoltage. Therefore, a comprehensive and sufficient protection should be provided for it, so that it can withstand the worst stable operating conditions as well as various types of transient operating conditions. In case of serious transient overvoltage, it is normally required that the converter valve can maintain its proper operation, or can resume its proper operation as soon as possible without the protections being activated. In case of worse conditions, even if the proper operation of converter valve is interrupted, it is also required that each device be protected from being damaged. The protection of converter valve includes passive protection and active protection. The passive protection conducts the overvoltage protection, for example, through arresters; the active protection is to adjust the trigger pulses, including the blocking of temporary or long-term valves or valve sets as well as the protective trigger valves. Based on the location of protections, it can be classified as the protection based on valve electric potential and the protection based on the ground electric potential. The former normally responds fast, which can provide the protection for valve's voltage directly; the latter normally cannot constitute the direct protection, and it regulates the development of faults through the coordination of trigger logics of converter valve so as to adjust the overvoltage or overcurrent to a reasonable range. Introductions will focused on the protection based on the valve electric potential in this section, including the protection of metallic oxide arresters as well as the protective trigger protection of gate electron.

20.3.1 Strategy Selection for Insulation Coordination of Converter Valves

Normally metallic oxide arresters are connected in parallel besides each single valve, which provides the overvoltage protection for converter valve by utilizing its good non-linear characteristic and strong energy-releasing capability. The commonly used strategies for insulation coordination of converter valves include mainly two. The first strategy is to use the arrester as the main protection of converter valve so as to limit the bidirectional overvoltage, while the protective trigger acts when the voltage distribution of each thyristor inside the converter valve is too uneven or the forward voltage rises up too fast. When such strategy is applied, the number of protective trigger action is less, but the required number of thyristors connected in series is more than the number of those required for the reverse test voltage. This is because the protective trigger is almost only used to deal with the worst situation; its action threshold is set at a level higher than the protection level of arrester, but lower than the level of valve's withstand voltage.

Another strategy believes that it is allowable to some extent to have the protective trigger due to irregular voltage distribution (but such trigger still does not occur frequently). The arrester is to limit the reverse overvoltage, while the protective trigger is to protect the forward overvoltage mainly. The main advantage of this strategy is that the number of thyristors connected in series can be reduced; this will reduce the cost and improve the efficiency of converter valve. When this strategy is applied, detail analyses are required on the system conditions, for example, the overvoltage caused by system failure and switch operation, for determining the minimum acceptable level for protective trigger so as to avoid the repeated actions of protective trigger.

In addition, there is a strategy that is not widely used. According to such strategy, an arrester is connected in parallel with each thyristor. In this case, the protection coordination design and fault development are different from the above two strategies. No detailed descriptions are provided herein.

20.3.2 Overvoltage Protection Function of Gate Electronic Circuit

The thyristor is a relatively weak switching component; in particular, during its turn-on and turn-off process, it can be damaged quite easily by various overvoltage and overcurrent stresses. If positive voltage is applied when the thyristor is not turned off completely, the thyristor will be re-conducted without being triggered, and can be damaged quite easily. Even if there are strict requirements for extinction angles in the control of converter valve, but, under various transient and abnormal conditions, such situation still occurs sometimes. Generally there should be a protective trigger of gate electronic circuit for performing coordination.

The gate electronic circuit not only executes the normal trigger optical signals transmitted by the valve-based electronic equipment, but also monitors and protects the thyristors, in which the protective trigger function of gate electronic circuit is included. By monitoring on the real-time signals of thyristors, such as voltage, current, and temperature, when the voltage is abnormal, the protective trigger signal is sent out to provide voltage protection.

Each thyristor of the converter valve is provided with the forward protection through forward overvoltage protection (FOP) of the electronic circuit. When the thyristor is turned off, even if the blocking capability of thyristor has recovered completely, its capability of withstanding voltage is still limited. If the forward voltage withstood by the thyristor is too high, the thyristor will be damaged by conduction due to forced breakdown. When the forward voltage at both ends of thyristor exceeds the action threshold of FOP, the thyristor will be triggered and conducted so as to avoid the thyristor being destructively broken down.

In addition, the gate electronic circuit is also provided with the following protective trigger functions:

- dv/dt protection

A fault in the converter station may cause very steep waveforms of forward transient dv/dt at both ends of the converter valve. At this moment, the thyristor may also be damaged due to forced breakdown. Therefore, thyristor triggering and monitoring (TTM) has provided the dv/dt protection function. When dv/dt at both ends of thyristor exceeds the thresholds, TTM will protect and trigger the thyristors, having them conducted so as to avoid the thyristors being destructively broken down.

- Recovery protection

During the recovery period after the thyristor has been turned off, if the thyristor withstands excessive high forward voltage, damage may be caused. In this case, even if lower forward voltage is withstood, the thyristor may also be damaged due to forced breakdown. TTM has provided the recovery protection function. During the recovery period of thyristor, when the forward voltage is greater than the protection level, TTM will protect and trigger the thyristor, having it conducted again so as to avoid the thyristor being destructively broken down.

- Current interruption protection

When the current of converter valve is small, the converter valve may have current interruption in its zones that should be conducted. At this moment, TTM will send out the trigger pulses again in order to maintain the thyristor in a conducting state, and avoid the thyristor being cut off within the time that should be conducted, or being damaged due to the forward voltage withstood directly upon cut-off.

20.4 Study on Insulation Coordination for DC Transmission Converter Valves

In the design of valve modules of the converter valves, the design of insulation coordination between components needs to be taken into consideration. The basic targets of insulation coordination are as follows: ① Determine the overvoltage levels that different equipment in the system can actually withstand under maximum stable state, transient state, and temporary overvoltage conditions; ② Select the insulation strength and characteristics of equipment in order to ensure that the converter valves can operate safely, economically, and reliably under the above voltage.

The First target is given in the electrical design of converter valve. The structure design of valve module for converter valve is to mainly consider the 2nd target. The valve module has two types of insulations: air insulation (self-recovery insulation) and solid insulation (non-self-recovery insulation). In the DC application, considerations should be given to the insulation characteristics for these types of insulations under the action of DC, AC, and impulse (including positive and negative polarities) voltage. As for the air insulation, what we need to consider mainly is the air clearance; the minimum air clearance must be determined, which is normally based on the required switching impulse withstand voltage. As for the solid insulation, what we need to consider mainly is the creepage distance; the minimum creepage distance must be determined, which is normally based on the continuous operating voltage (DC and AC) [9].

20.4.1 Calculation Method for Creepage Distance

The specific creepage distance should be selected according to the national standard GB/T311.3. Considering that under the DC voltage, the pollution accumulation on the surface of insulating materials is more serious than that under AC voltage, and therefore, the specific creepage distance should be higher than the recommended values under the clean indoor environment.

According to the electrical characteristics of converter valve, the effective value of AC voltage that the converter valve withstands for long term can be selected to determine the creepage distance. Since the effective value of AC voltage that the converter valve withstands for long term is lower than the 90% of line voltage at the secondary side of converter transformer, from the conservative design point of view, and so the line voltage at the secondary side windings of converter transformer is used to calculate the creepage distance:

$$d = U_{\mathrm{V0m}}/n_{\min} \times d_{\mathrm{u}} \tag{20.15}$$

where U_{v0m} is the line voltage at the secondary side winding of converter transformer, n_{min} the minimum number of thyristor connected in series for single valve, excluding redundancy, and d_u is the specific creepage distance.

20.4.2 Calculation Method for Air Clearance

The air clearance should be determined based on the impulse voltage. When determining the air clearance corresponding to the DC voltage level, the switching impulse is a more important decisive factor than the lightning impulse. As for a standard gap, the positive breakdown voltage under lightning impulse is higher than the positive breakdown voltage under switching impulse by 30%. When calculating the air clearance for converter valve, calculations should be done based on the switching impulse, and meanwhile, considerations should be given that lightning impulse is used to conduct verification.

The determination of air clearance can be referred to the following standards:

GB/T311.3-2007 *Insulation Coordination, Part 3: Procedures for High-voltage Direct Current (HVDC) Converter Stations*
GB/T16935.1-2008 *Insulation Coordination for Equipment within Low-voltage Systems, Part 1: Principles, Requirements and Tests*

References

1. Shili L, Xiaoguang W, Junzheng C, Guangfu T, Kunpeng Z, Gaoyong W. UHVDC converter valve shielding case surface electric field calculation using hybrid-weight-function bondary element method. Proc CSEE. 2013;33(25):180–6.
2. Kunpeng Z, Yuan L, Gaoyong W, Shili L. Study of DC test method of ±1100 kV UHVDC valve. Trans China Electrotech Soc. 2013;28(1):87–93.
3. Huan G, Guangfu T, Kunpeng Z, Xiaoguang W. Calculation on stray capacitances and impulse voltage distribution of HVDC converter valve. Proc CSEE. 2011;31(10):116–22.
4. Wenliang Z, Guangfu T. Study on wide-band model and voltage distribution of ±800 kV/4750 a UHVDC valves. Proc CSEE. 2010;30(31):1–6.
5. Hexun X. Non-linear modelling and dynamic characteristics of UHVDC converter valve. Beijing: China Electric Power Research Institute; 2012.
6. Huan G, Jialiang W, Guangfu T, Jianchao Z. Analysis of the turn-off voltage stress on HVDC thyristor valve. Proc CSEE. 2010;30(12):1–6.
7. Jing Z. Preliminary study on electrothermal characteristics of converter valve. Beijing: China Electric Power Research Institute; 2009.
8. Haifeng S, Xiang C, Qi QLW, Xiaolin L. Overvoltage distribution in HVDC converter valves and analysis of influencing factors. Proc CSEE. 2010;30(22):120–6.
9. Study on Structural Characteristics of ±1100 kV 5000 a UHVDC converter valve. China Electric Power Research Institute; 2011.

Chapter 21
UHVDC Electrical Equipment

Xu Deng, Anwen Xu and Yuting Qiu

UHVDC equipment is the base of whole UHVDC transmission project. Since UHVDC system differs from conventional EHVDC system in terms of rating voltage, wiring configuration, etc., higher requests are proposed on design, manufacture, transport, and cost control of the equipment, which results in a quantity of new problems and difficulties to be solved in engineering. UHVDC equipment mainly includes converter valve, converter transformer, smoothing reactor, AC/DC filter, DC arrester, bushing, switchgear, and DC measuring equipment. In general, DC equipment used in UHV project has characteristics of dramatically increased weight and volume, improved insulation level, and higher reliability.

21.1 Arrangement of UHVDC Equipment

The principle of HVDC transmission system is described as follows: electric energy of AC system is transmitted to rectifier through converter transformer in rectifier station, where the AC power is converted into DC power. Then, the DC power is

X. Deng (✉)
Guangzhou Municipal Commission of Commerce, Guangzhou, Guangdong, People's Republic of China
e-mail: dengxu926@163.com

A. Xu
College of Electrical Engineering, Zhejiang University, Xihu District, Hangzhou, Zhejiang, People's Republic of China
e-mail: 254051219@qq.com

Y. Qiu
State Grid Shanghai Power Supply Company, Shanghai, People's Republic of China
e-mail: ytqiu0927@163.com

© Zhejiang University Press, Hangzhou and Springer-Verlag GmbH Germany 2018

H. Zhou et al. (eds.), *Ultra-high Voltage AC/DC Power Transmission*,
Advanced Topics in Science and Technology in China,
https://doi.org/10.1007/978-3-662-54575-1_21

transmitted to the inverter station through DC line, where the DC power is inverted into AC power, which is transferred to AC system at the receiving end through converter transformer in inverter station [1]. It is obvious that DC transmission system mainly consists of rectifier station, DC line, and inverter station, and converter station is the major integral part in DC transmission system. In UHVDC system, most of DC equipment is in converter station except for DC line. The main DC equipment in converter station includes converter valves, converter transformers, smoothing reactors, AC/DC filters, and switchgears, as well as AC/DC arresters, insulators, bushings, and DC measuring equipment that are used to ensure safe and stable operation of the system. Figure 21.1 is a schematic diagram of arrangement of critical equipment of one pole in converter station. Because of the symmetrical arrangement of UHV converter station, equipment of another pole is generally same as those of this pole. Arrangement of equipment in converter station in a ±800 kV UHVDC transmission project is shown in Fig. 21.2, mainly comprising the relevant equipment in AC field, valve hall, and DC field.

As shown in Fig. 21.2, UHV converter station mainly consists of three parts, namely AC field, valve hall, and DC field.

The AC field accommodates multiple banks of AC filters and reactive power compensators, parallel connected to AC busbar.

The valve hall is a major integral part of converter station. There are two valve halls in UHVDC converter stations, i.e., HV valve hall (800 kV) and LV valve hall (400 kV). It is shown in Fig. 21.2 that the LV valve hall (400 kV) locates in the center of the converter station, while the HV valve halls (800 kV) of two poles are arranged symmetrically on both sides. Converter valve modules and the associated control and protective equipment are suspended in valve hall, where constant temperature and humidity are kept all the year round. Converter valves are the core equipment in UHVDC transmission system.

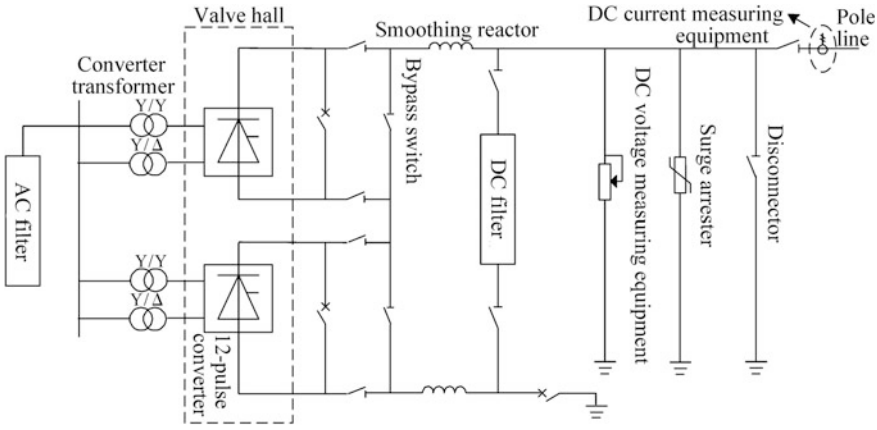

Fig. 21.1 Sketch for arrangement of key equipment of single pole in UHVDC converter station

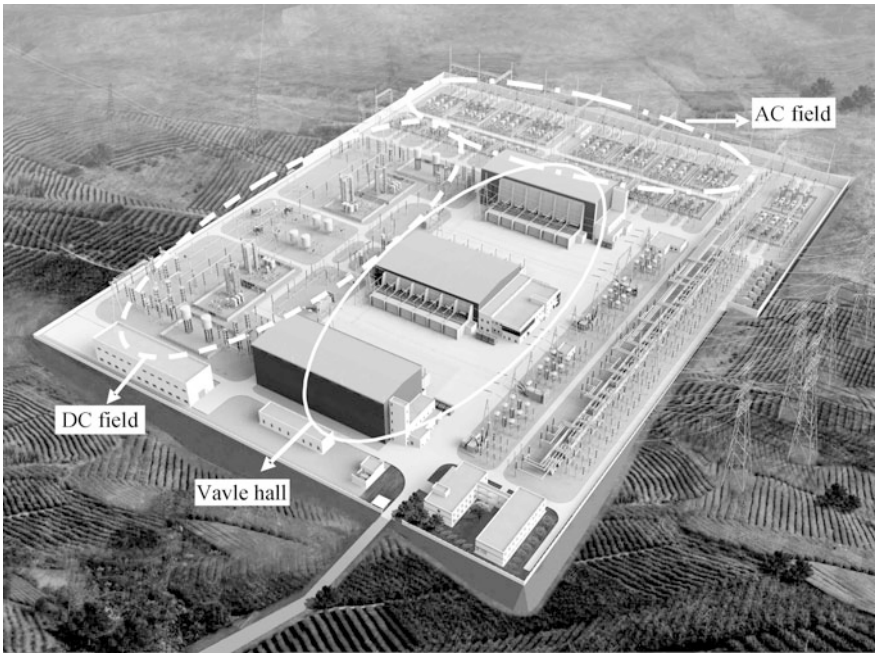

Fig. 21.2 The design sketch for arrangement in converter station of ±800 kV UHVDC transmission project

The UHVDC field locates the rear part of converter station, comprising mainly converter transformers, DC smoothing reactors, DC filters, DC switchgears, DC measuring equipment, DC arresters. Since UHVDC system is usually of two-pole, equipment in DC field is usually arranged symmetrically according to positive and negative poles.

In the yard, converter transformers are arranged at outside of HV/LV valve halls, respectively, according to their nominal working voltage, and separated by fire protection walls from each other. The HV and LV valve halls locate closely beside the transformers, and connect with the fire protection walls of the transformers to form a structural unit. As shown in Fig. 21.3, the converter transformers are installed outside of the valve halls, and three banks of transformers constitute three-phase converter transformer. The figure shows the fan of the transformer. Close to the valve hall, the transformers are connected with converter valves through valve-side lead-out bushing penetrating through the wall of the valve hall. Different converter transformers are separated with fire protection wall to enhance safety in operation.

HV direct current after conversion is transferred to outside of valve hall through wall bushing, then to DC pole line. Smoothing reactors locate on DC pole line at the exit of valve hall, in series connection with DC pole line to filter and stabilize voltage. In UHVDC transmission system, DC smoothing reactors usually adopt

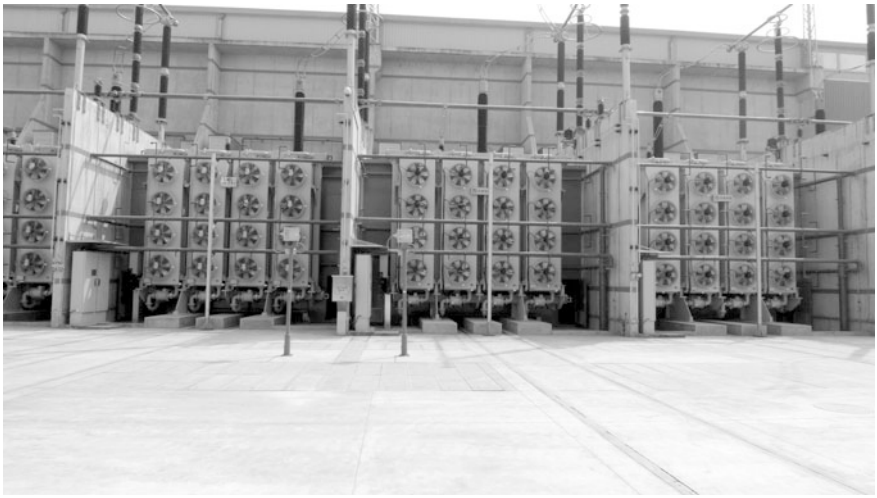

Fig. 21.3 Arrangement of converter transformers outside valve hall

separate arrangement of split smoothing reactor, i.e., half reactors are arranged on HV-side DC pole line (800 kV pole) and half reactors are arranged on neutral busbar.

DC filter is a major equipment in DC field in converter station, connected between DC pole line and neutral busbar, and locates in the center of the yard. DC filter consists of two series-connected capacitors, ancillary resistors, inductors, etc.

Arrangement of other equipment in DC field: all UHV arresters are installed near the equipment to be protected; current transformers and DC voltage dividers are installed at different measuring points in converter station.

21.2 UHV Converter Valve

The function unit to realize DC conversion in converter station is referred to as three-phase bridge converter, in which each bridge arm is a converter valve. Converter valves are the core equipment in converter station, accounting for 1/4 total investment of all equipment in converter station [2]. With the development of manufacturing technology of high-power semi-conductor, mercury arc valve, thyristor valve, GTO valve and IGBT valve, and other products come out in succession. With respect to current manufacturing technology, thyristor is still an electronic apparatus that is highest in voltage resisting level and output capacity. Therefore, thyristor valve is widely used in high-voltage, large-capacity DC transmission project because of its superior performance and mature manufacturing technology. In current UHVDC systems, all converter valves use thyristor valves.

21.2.1 Structure of UHV Converter Valve

Conventional EHVDC system usually adopts single 12-pulse converter wiring, while UHVDC system usually adopts two series-connected 12-pulse converters, i.e., each pole is made up of two series-connected 12-pulse converters. Each 12-pulse converter is arranged in an individual valve hall, so UHVDC converter valves differ in terms of HV and LV valve hall. Refer to Fig. 21.4 for schematic diagram of main circuit of double 12-pulse converters of one pole, and refer to Fig. 21.5 for detailed arrangement of the corresponding monopolar converter valve.

Same as conventional EHVDC system, the UHVDC converter valve consists of converter valve module, control, and protection system, as well as cooling system of the converter valve. They are introduced in details as follows.

(1) Converter valve module

In UHVDC system, the converter valve is designed modularly. Converter valve module is the core element to constitute UHV converter valve. One valve comprises 2 converter valve modules. Each converter valve module comprises 2 identical valve modules. Each valve module is made up of several thyristor units, 2 series-connected saturable reactors, and 1 grading capacitor [3]. Each thyristor unit is made up of thyristor, damping circuit, and DC grading resistor. The composition structure of converter valve is shown in Fig. 21.6.

In order to realize grading, control, protection, heat dissipation, and other functions of thyristor to ensure safe and reliable operation of the converter valve, the converter valve module comprises corresponding electronic circuit, saturable reactor, grading damping circuit, and other equipments. Among them, there is one-to-one relationship between trigger circuit and thyristor. The thyristor is mainly triggered photoelectrically or by direct light. At present, both trigger methods can be found in engineering. Compared with conventional and cost-saving photoelectric trigger method, thyristor triggered directly by light is much simpler in structure and higher in reliability of the whole converter, and it has great room for development.

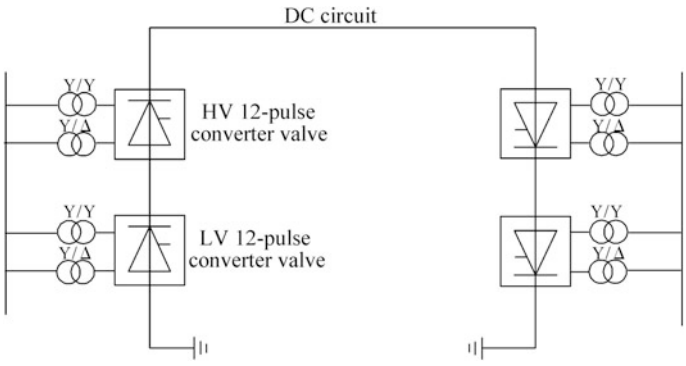

Fig. 21.4 Sketch for main circuit of 12-pulse converter of single pole of converter station

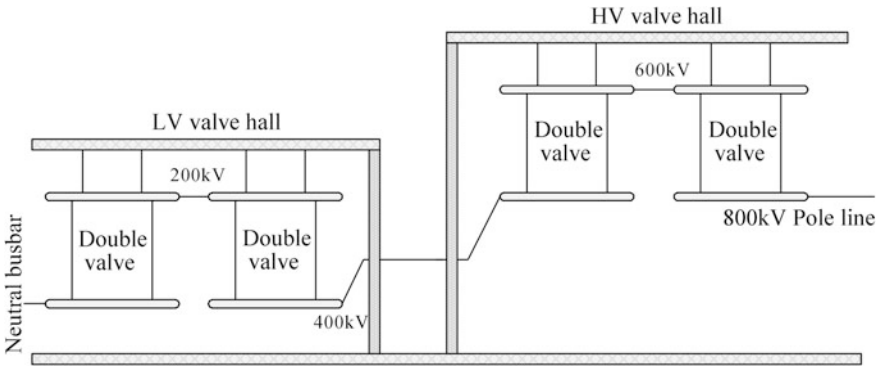

Fig. 21.5 Arrangement of converter valves of single pole of converter station

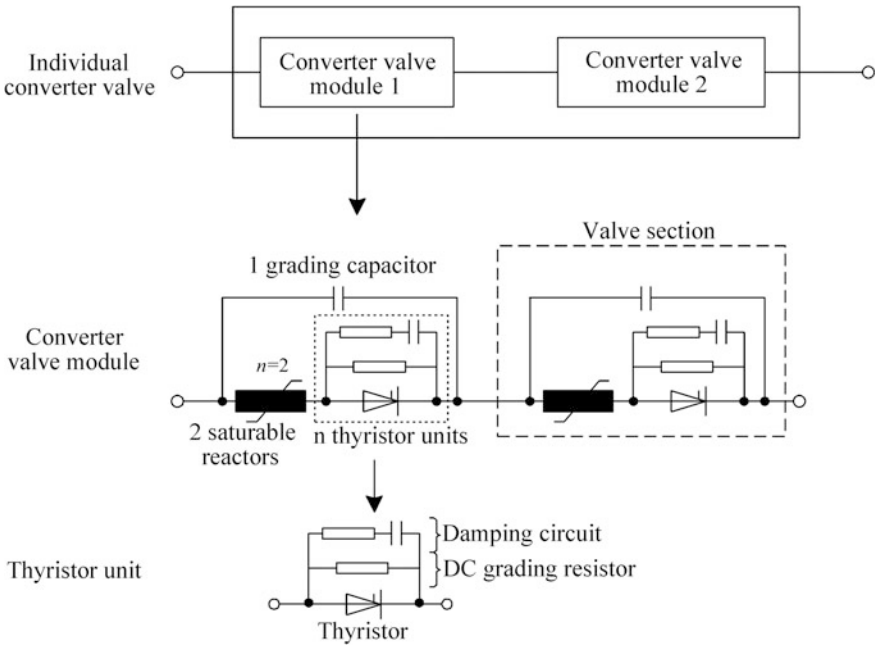

Fig. 21.6 Sketch for structure of UHV converter valve

Saturable reactor is connected in series with several thyristor units to restrain the peak voltage and current and to assist in voltage equalization. Because of the existence of stray capacitance in valve tower, the voltage distribution of valve module under very fast front impulse voltage is not balanced, so each valve module is connected in parallel with a grading capacitor at each end to equalize the voltage between valve modules. Grading damping circuit comprises damping circuit and

DC grading resistor, and is connected in parallel with each thyristor element one by one, thus guaranteeing linear distribution of voltage across thyristor valve levels under power-frequency voltage and switching impulse surge voltage, so as to achieve voltage grading and protection functions.

Arrangement of converter valves used in Fulong Station in ±800 kV Xiangjiaba-Shanghai UHVDC Transmission Project is shown in Fig. 21.7. This converter valve is of air insulation, pure water cooling, and suspended double-valve structure, arranged according to two 12-pulse valve wiring configuration. The two 12-pulse bridges are installed in LV valve hall (400 kV) and HV valve hall (800 kV), respectively, and the two halls are connected in series to ultimately supply 800 kV DC to DC transmission line. In the project, each converter valve is made of 60 thyristor units (2 for redundancy) and 8 valve reactors are connected in series. The project adopted modularization technology. One valve consists of a few of valve modules, and each valve module is connected to 15 thyristor units with 2 valve reactors in series and then with 1 grading capacitor connected in parallel. Please refer to Table 21.1 for parameters of each element in detail [3].

(2) Control and protection system of converter valve

Control and protection system of thyristor is also called Gate Unit (GU). It can respond to the initiating pulses from Valve Base Electronics (VBE), and then send trigger pulses. It can also provide protective trigger in case of overvoltage or other abnormal conditions. In addition, GU feed backs the component-monitoring signal in real time to VBE, while VBE carries out statistics on operating status of various

Fig. 21.7 Suspended converter valve used in Fulong Station

Table 21.1 Parameters of single converter valve in Fulong Converter Station

Components of converter valve	Value
Thyristor type	T4161 N80T S34 (6″ ETT)
Total number of thyristors	60
Number of redundant thyristors	2
Number of thyristors of each valve module	15
Number of reactors	8
Number of reactors of each valve module	2
Number of valve modules	4
Damped capacitance (μF)	1.6
Damped resistance (Ω)	36
Grading capacitance (nF)	4
Structure of valve tower	Double valve

components, du/dt overvoltage protection, negative voltage detection, etc., and sends the data to thyristor-monitoring equipment, which is connected with valve control and substation control systems to realize fault detection, fault locating, and other high-level functions.

(3) Cooling system of converter valve

Cooling system of converter valve usually adopts air-insulated water-cooling method, designed to keep the junction temperature of thyristor components within 60–90 °C normal temperature range, and ensure that the converter valve can run stably and continuously under nominal or even overload operating conditions.

21.2.2 Characteristics of UHV Converter Valve

Although UHVDC converter valve and conventional EHVDC converter valve have many common characteristics in aspects such as structure of valve, trigger system of thyristor, control, and protection system of converter valve and cooling system, UHVDC converter valve has its own special characteristics because the voltage level of UHVDC system is higher and the valve module adopted is somewhat different. It is manifested as follows:

(1) Throughflow capacity is higher because 6-in. thyristor is adopted. 5-in. thyristors are widely used in EHVDC transmission project, throughflow capacity of which is only 3000 A. UHVDC transmission requires higher capacity, so the 5-in. thyristor cannot meet the requirement of UHV project. For the purpose of meeting UHVDC transmission demands, the relevant equipment manufacturers developed 6-in. thyristor, which is about 50% more than 5-in.

thyristor in chip area, with 8000 V peak blocking voltage, 4000 A or more throughflow capacity. In UHVDC transmission project, the converter valve made up of 6-in. thyristor can meet the requirement of current transmission capacity without parallel connection, and is provided with higher short-circuit current and overload capacity. In ±800 kV Xiangjiaba-Shanghai UHVDC Transmission Project, which requires 6400 MW nominal transmission capacity and 4000 A nominal current, 6-in. thyristor can satisfy the transmission requirements completely. With further development of UHVDC transmission technology, in order to meet the requirement of UHVDC transmission of higher capacity, in 2010, China Electric Power Research Institute researched and developed ±800 kV/4750 A UHV converter valve independently, which has passed relevant type test and been used in ±800 kV Jinping-Southern Jiangsu UHVDC Transmission Project [4]. In 2012, China Xi'an XD Power Systems Co., Ltd. successfully designed and manufactured ±1100 kV/5000 A UHVDC converter valve which has independent intellectual property right. It also successfully researched and developed ±1100 kV converter valve module for the first time in the world, raising the throughflow capacity of the thyristor valve to 5000 A or even higher.

Improvement of thyristor technology has important effect on HVDC transmission of high capacity. It provides solutions to higher short-circuit current capacity and overload capacity of the DC transmission system, facilitating improvement of optimized design and dynamic performance of the whole system.

(2) Structure of multiple valve banks is adopted. Multiple Valve bank (MVU) structure is usually adopted in arrangement of UHVDC converter valve. The MVU made up of two or four series-connected valves is referred to as double valve and quadruple valve, respectively. As shown in Fig. 21.7, one MVU with electronic field shielding components is suspended—installed at the top of valve hall to form a valve tower.
(3) Operating condition of equipment is more rigorous. In UHVDC system, the converter valve has to face more rigorous operating condition because of the rise of system operating voltage. Special care shall be taken in the design of converter valve's external insulation. With respect to the highest voltage converter valve, insulation of air flowing to wall, ceiling, and floor shall be reconsidered on the basis of EHV converter valve design experience, and type of external electrode of the converter valve shall be chosen appropriately, thus reducing the insulation requirement through reasonable insulation coordination.
(4) Electromagnetic interference and noise become more severe. Turning on or off the converter valve can cause intense electromagnetic interference and persistent annoying noise, which will affect valve hall and DC switchgear yard negatively. Noise propagation is reduced usually by installing sound barrier, etc.

21.2.3 Tests of UHV Converter Valve

According to test purpose and content, tests of UHV converter valve can be categorized into three types, namely type test, factory test, and special test.

(1) Type test of UHV converter valve

Type test includes mainly two items, i.e., insulation test and operating test. Insulation test includes insulation type test of multiple valve, insulation type test of suspending/supporting structure of converter valve, and insulation type test of converter valve; operating test includes operating characteristics type test of converter valve, e.g., maximum operating load test, loss test of converter valve, short-circuit current test, and electromagnetic compatibility test.

(2) Factory test of UHV converter valve

Factory test of UHV converter valve includes two items, i.e., routine test and sampling test, to verify if the product is manufactured properly. Contents of the routine test include function test, AC voltage resisting test, waterway test, repeated high-voltage trigger test, thermal operation test, pressure test, water discharge, seal and valve module switching impulse test, and repeated function test. Contents of sampling test mainly include operating test of converter and sampling test of the thyristor disk.

(3) Special test of UHV converter valve

Special test of UHV converter valve is agreed between the customer and the manufacturer through negotiation, e.g., long-term aging test and in-site test.

21.2.4 Manufacturing Level of UHV Converter Valve

Up to 2015, there were only six UHVDC transmission lines put into operation in the world, i.e., Yunnan-Guangdong, Xiangjiaba-Shanghai, Jinping-Southern Jiangsu, Nuozadu-Guangdong, South Hami-Zhengzhou, and Xiluodu-Zhexi ±800 kV UHVDC transmission projects. For a long time, China had no independent research and manufacturing capability in the field of Researching and Development (R&D) of DC converter valves, which were always imported. Seizing the opportunity of construction of Yunnan-Guangdong ±800 kV UHVDC Transmission Project, Siemens Company was the first one to research and manufacture ±800 kV UHVDC converter valve in the world. Then, ABB Company acquired the research and manufacturing capability of UHVDC converter valve by the construction of Xiangjiaba-Shanghai ±800 kV UHVDC Transmission Project. Xi'an Electric Machinery Manufacture Co., Ltd. (China Xian XD Power Systems Co., Ltd. at present, or XD Group for short) and XJ Group, supported

technically by ABB Company, manufactured 6-in. thyristor (4000 A) and completed converter valve equipment for UHVDC transmission project.

With the rapid development of UHVDC transmission in China, it is imperative to realize independent research and development of UHVDC converter valve. In recent years, some Chinese manufacturers and institutes devote themselves to the research and manufacture of converter valve. In 2010, the UHV converter valve (4750 A) researched and developed independently by China Electric Power Research Institute passed all tests specified in IEC standards successfully. This converter valve had the highest level of throughflow capacity in the world and has been used in Jinping-Southern Jiangsu ±800 kV UHVDC Transmission Project. China Electric Power Research Institute became the third enterprise in the world that masters and holds the technology of design, manufacture, and test of UHVDC converter valve following ABB and Siemens. In 2012, China XD Group Co., Ltd. searched and manufactured successfully ±1100 kV/5000 A UHVDC converter valve that has independent intellectual property right, and designed and researched ±1100 kV converter valve module successfully for the first time in the world. So the thyristor valve has throughflow capacity of 5000 A or more and will be used in ±1100 kV UHVDC transmission project. Relying on our own progress in technology and advantage in cost, in the future, Chinese converter valve manufacturers will break the monopolistic status of multinational companies in market and strengthen the development of converter valve manufacturing industry in China.

21.3 UHV Converter Transformer

Converter transformer is one of the most important equipment in converter station in UHVDC project. The converter transformer is connected between the converter valve and AC system to realize connection between converter valve and AC busbar [5]. It is similar to common transformer in basic working principle, i.e., transferring energy between two windings at both sides through electromagnetic coupling. In UHVDC system, because 12-pulse converter is used as basic converter unit, two sets of commutation voltage which are ungrounded in neutral point, identical in amplitude, and different by 30º in phase angle can be supplied to converter by applying different wiring configurations of winding of the converter transformer. In addition, the short-circuit impedance of converter transformer can also restrict short-circuit fault current at DC side. Consequently, because the voltage level of the UHVDC is high, the operating voltage at valve side of HV converter transformer is also high, and reliability of the converter transformer has critical effect on safe and stable operation of the whole DC transmission system. Therefore, UHV converter transformer is much higher than EHV converter transformer in difficulties in design and manufacturing technology, and more expensive in its equipment. It is the second most important equipment next to the converter valve in UHVDC system.

21.3.1 Structure of UHV Converter Transformer

Compared with conventional EHVDC converter transformer, UHV converter transformer is massive in weight and size, and expensive in cost. Taking the case of UHV converter transformer produced by ABB, the total transport mass reaches approximately 300 t and transport size is 4.9/3.7/12.7 (height/width/length, expressed in m), almost the limit of railway transport. Meanwhile, the cost of converter transformer is much higher, and the equipment cost usually accounts for 16% of total cost of the converter station. At present, the series-connection method of two 12-pulse valve groups (400 kV + 400 kV) is adopted in UHVDC project. In such wiring method, the HV converter transformer will withstand a voltage of 800 kV or higher. Thus, the UHV converter transformer is required to be massive in capacity, high in insulation level, etc. Restricted by production capacity and transport condition of a single-phase three-winding transformer, currently, UHVDC system usually adopts single-phase double-winding transformer. Since UHVDC system usually adopts the wiring configuration of two 12-pulse converters connected in series, in UHVDC system, each converter station is usually provided with 24 converter transformers, additionally 4 as standby.

Figure 21.8 shows the ABB UHV converter transformer used in a UHVDC transmission project in China. With respect to its external view, the transformer adopts single-phase double-winding type. It is connected with converter valve through valve-side bushing. It is provided with oil conservator and HV bushing to be connected with AC system on the top of transformer housing, provided with fan of cooler at the back of housing. The housing accommodates winding, iron core, HV shielding bushing, and insulation material. Its nominal capacity is 297.1 MVA, and has the structure of single-phase four-limb iron core, so that the capacity of the transformer is distributed on two groups of posts. Direct outgoing wire structure is adopted, i.e., lead wires at valve side are connected in parallel after they are led out from two posts and then laid in oil conservator. Such design facilitates installation, improves safety performance of the product, and is cost efficient.

(a) Converter transformer to be installed (b) Installed converter transformer

Fig. 21.8 UHV converter transformer

21.3.2 Characteristics of UHV Converter Transformer

UHV converter transformer has two characteristics: one is substantial increase of insulation requirement; and another is the particularity of valve-side winding's operating environment. Therefore, in design and manufacture of UHV converter transformer, insulation design and DC magnetic bias must be taken into sufficient consideration; meanwhile, it is required to choose short-circuit impedance carefully, increase the number of taps, and take some measures to restrain the high-order harmonic component to improve general working performance of the converter transformer. Similar to conventional EHVDC, UHV converter transformer also suffers DC magnetic bias, high-order harmonic current, and other problems. It is worth noting that UHV converter transformer differs from conventional EHV converter transformer in terms of insulation design, short-circuit impedance, and on-load voltage regulating range.

1. Characteristics of insulation design

Insulation design is an important part in the design of converter transformer. Insulation structure of converter transformer's line-side winding can follow the mature technology used in 500 kV converter transformers directly, but the operating environment of its valve-side winding is special. The valve-side winding is required to not only withstand certain AC voltage but also endure DC bias voltage. Under the combined action of AC voltage and DC voltage, the valve-side winding has a significant high potential to the ground. Besides, when power reversion happens in DC transmission system, the polarity of DC voltage will change quickly, and the polarity of DC voltage withstood by valve-side winding will change correspondingly. The insulation at valve-side winding is apt to discharge during polarity reversal. Therefore, the main and longitudinal insulation structure of valve-side winding of converter transformer shall be studied and designed specially.

(1) Design of main insulation of converter transformer

Main insulation structure of converter transformer determines the basic structure of the whole converter transformer, and is concerned closely with impedance, loss, mass, and overall view of the transformer. If the insulation level of winding is raised, the main insulation distance between the windings and insulation at end can be increased appropriately, e.g., by increasing the number of angle rings, wraps, and spacer ring appropriately. With respect to UHV converter transformer, in addition to the increase of thickness of insulation layer and quantity of material, higher technology of equipment manufacture as well as higher operation and maintenance level is also required.

Currently, the internal insulation of UHV converter transformer is of oil/pressboard composite insulation structure. The insulation characteristics are different under AC voltage and DC voltage. The distribution of AC voltage is determined by the ratio of material's dielectric coefficient, and generally, the strength of electric field that oil clearance withstands is higher. The distribution of

DC voltage is determined by the material's resistance ratio, and generally, the strength of electric field that insulation cellulose and pressboard withstand is higher. In addition, change of temperature and humidity can also result in change of resistivity, and further in change of the distribution of DC voltage. With respect to the insulation of converter transformer, it withstands AC voltage that is distributed according to the dielectric coefficient and DC bias voltage that is distributed according to resistance ratio during normal stable operation. Its particular characteristic is that when the polarity of DC voltage reverses, the strength of electric field in oil–paper insulation will present capacitive distribution, i.e., similar to AC voltage distribution. At that moment, oil clearance where dielectric strength is relatively lower will suffer great voltage stress, but the strength of electric field that transformer oil withstands is relatively lower; so the oil clearance, prone to internal insulation discharge or breakdown, is the weak insulation part in transformer.

(2) Design of longitudinal insulation of converter transformer

The longitudinal insulation of converter transformer includes winding inter-turn insulation and section insulation. It determines the structure type and impulse voltage withstanding capability of the winding. Effect of both long-term operating voltage and impulse overvoltage shall be taken into consideration in the design of longitudinal insulation of converter transformer. For the long-term operating voltage, the voltage of winding shall be guaranteed to be <3 kV/mm to avoid ionization. For the effect of impulse overvoltage, lightning impulse overvoltage, switching impulse overvoltage, etc., shall be taken into consideration, and overvoltage withstanding capability shall be improved by adjusting the structure of winding and decreasing inter-turn gradient voltage. Besides, in UHVDC transmission system, because of the increase of DC voltage and increase of the number of series-connected converter units, steep wave overvoltage in the system shall also be considered in the design of longitudinal insulation. Steep wave overvoltage of high amplitude can result in longitudinal insulation breakdown of converter transformer's valve-side winding and other serious consequences. Therefore, longitudinal insulation structure shall be determined by taking all the above-mentioned aspects into consideration. Winding inter-turn gradient voltage shall be improved by means of sectionalized compensation to increase the capability of the winding to withstand impulse voltage.

2. Characteristics of short-circuit impedance

The short-circuit impedance is determined on the basis of tradeoff between two aspects: larger short-circuit impedance can reduce the short-circuit current, protect thyristor against the impact of overload, and restrain harmonic current, while smaller short-circuit impedance can reduce reactive loss and nominal capacity requirement of converter transformer. Therefore, short-circuit impedance shall be determined by taking the maximum short-circuit current level of thyristor valve, permitted reactive loss of the converter, harmonic current, and manufacturing cost of equipment into consideration.

(1) Maximum short-circuit current level of thyristor valve

When determining the short-circuit impedance of converter transformer, it is required first to ensure that the converter valve can operate safely, which is the decisive factor in parameter selection of short-circuit impedance. Short-circuit impedance u_k determines the leakage reactance of the converter transformer, so the increase of short-circuit impedance u_k can reduce the current that flows through converter valve in malfunction. If the maximum short-circuit current that the converter valve can withstand is I_M, the maximum impulse current I_s that flows through converter valve in most serious malfunction must satisfy the following expression $I_s(u_k) \leq I_M$, i.e., the impulse current in malfunction shall not exceed the withstanding capability of the converter valve. Therefore, in order to protect valve component from being damaged by significant impulse current in valve short-circuit, the short-circuit impedance u_k of converter transformer shall be as larger as possible.

(2) Reactive loss of converter transformer

Converter transformer can generate certain reactive loss, which rises with the increase of the transformer's short-circuit impedance, so the reactive power compensators in the converter station must provide more compensation margin, which will raise overvoltage due to excessive reactive power in load rejection. Therefore, for reactive consumption, the short-circuit impedance of converter transformer shall be as small as possible.

(3) Harmonic current

Increasing the short-circuit impedance can reduce the amplitude of harmonic current and reduce the number of AC filter banks to be installed, thus decreasing the cost of the filter banks.

(4) Manufacture cost of equipment

Under the condition of same DC nominal power, if short-circuit impedance increases, the capacities of both converter transformer and reactive power compensator shall be increased, thus elevating the manufacturing cost of the corresponding equipment. However, the larger short-circuit impedance reduces equipment cost of filters in the converter station because the harmonic current is restrained by the impedance.

In general, because of the dramatic increase of transmission capacity, the short-circuit impedance (about 18%) of UHV converter transformer is somewhat larger than that (15–16%) of EHV converter transformer.

3. On-load voltage regulating range

UHV converter transformer is much more than common electric transformer in terms of number of steps of on-load voltage regulating tap and wider in terms of regulating range, which is usually −5 to +23%. The step size of tap is relatively low, usually 1–2%, which deals with the rise and drop of valve-side voltage of the

converter transformer due to load change and meets step-down operation of DC system. For example, in Xiangjiaba-Shanghai ±800 kV UHVDC Transmission Project, the voltage regulating range of converter transformer is about −5 to +23%, and step size of tap is 1.25%.

21.3.3 Tests of UHV Converter Transformer

1. Test items

Type test items of UHV converter transformer include lightning carrier impulse test, short-duration AC induction voltage test, measurement of noise level, oil flow electrification test, and measurement of radio interference level.

The routine test items of UHV converter transformer can be categorized into three classes:

(1) Measurements of basic parameters: measurement of DC resistance of winding, polarity measurement, transformer ratio measurement on each tap position, no-load loss and no-load current measurement, load loss and short-circuit impedance measurement, harmonic loss test, temperature rise test, oil flow electrification test, long-duration no-load test, 1-h excitation test, High-frequency (HF) impedance measurement, frequency response test, and stray capacitance measurement.
(2) Insulation tests: iron core and relevant insulation test, insulation resistance measurement, insulation oil test, lighting impulse test, switching impulse test, bushing test, applied DC voltage withstand test including partial discharge measurement, polarity reversal test, applied AC voltage withstand test, and long-duration AC induction voltage withstand test.
(3) Auxiliary equipment tests: insulation test of auxiliary circuit, function control test of all accessories and protection equipment, power measurement of fan and oil pump, current transformer test of bushing, act test of on-load voltage regulating switch, mechanical strength test of oil tank, oil tank vacuum test, and oil tank seal test.

In order to guarantee successful equipment handover on site, the customer and the manufacturer shall make agreement on field test, which includes the following items:

(1) Measurement and inspection of basic parameters: DC resistance and insulation resistance of winding together with bushing, insulation resistance of iron core to ground, tan δ and capacitance of winding together with bushing, DC leakage current, LV no-load current, tap ratio and lead-out polarity of converter transformer, inspection and test of on-load tap switch, partial discharge measurement of winding together with bushing;

(2) Inspections of auxiliary equipment: insulation oil test, bushing test, bushing current transformer test, seal test, temperature distribution test on surface of oil tank, operation test of cooler, oil pump test, wiring check of control and auxiliary equipment circuits, power-frequency voltage withstand test, or insulation resistance measurement, check of auxiliary equipment;
(3) Others: impulse of closing test, frequency response test, noise measurement.

2. Characteristics of tests

It is known from the above-mentioned analysis that compared with the conventional electric transformer, UHV converter transformer has its particularities in tests.

(1) In addition to type test and routine test same as those of ordinary transformer, the UHV converter transformer must be subjected to some DC tests, e.g., DC voltage test, partial discharge test of DC voltage, and DC voltage polarity reversal test. Insulation requirement of valve-side winding of UHV converter transformer is higher than that of conventional converter transformer, particularly, the voltage of long-duration applied AC voltage withstand level test, DC voltage withstand level test, and DC polarity reversal test rises sharply.
(2) Result of load loss test of ordinary electric transformer does not contain effect of harmonic component. However, the work method of converter determines that there is a large harmonic current component in AC side current of converter transformer, so effect of harmonic current must be taken into consideration in load loss measurement of converter transformer.
(3) Affected by the different work methods of connected converter valve, the temperature rise test may be different for converter transformers with the same type. Therefore, different from ordinary electric transformer, temperature rise test of UHV converter transformer is not type test any more, but a routine test that must be done for each transformer.

21.3.4 Manufacturing Level of UHV Converter Transformer

The main technology of UHV converter transformer originates in companies such as ABB and Siemens. In recent years, Chinese companies such as Xi'an XD and TBEA are absorbing actively advanced technology from foreign companies through various cooperation projects to improve the manufacturing level of converter transformer made in China. On 23rd February, 2010, the first UHV converter transformer ZZDFPZ-250000/500-800, which is manufactured in China, passed all tests in Xi'an XD Transformer Company, and is the first converter transformer at HV end in UHVDC system made in China.

In the UHVDC transmission projects that have been put into operation, most of the converter transformers are made in China, except for transformers at HV end, which are designed and manufactured by Siemens and ABB. In Yunnan-Guangdong ±800 kV UHVDC Transmission Project, three quarters of transformers at LV end are 400 kV converter transformers manufactured by XD and other Chinese enterprises, while 800 kV transformers at HV end are all designed and manufactured by Siemens. In Xiangjiaba-Shanghai ±800 kV UHVDC Transmission Project, 400 kV converter transformers at LV end are manufactured by TBEA Shenyang Transformer Group Co., Ltd., Xi'an XD Transformer Co., Ltd., and other Chinese enterprises, while 800 kV converter transformer at HV end is manufactured by ABB. In Jinping-Southern Jiangsu ±800 kV UHVDC Transmission Project, 800 kV converter transformers at HV end are mainly manufactured by ABB, while converter transformers at LV end are mainly manufactured by TBEA Shenyang Transformer Group Co., Ltd.

21.4 UHV Smoothing Reactor

Smoothing reactor is one of the important equipment in HVDC converter station, also referred to as DC reactor and usually series-connected between converter valve and DC line. It is used to prevent intermittence of current when facing light load, and work with DC filter to constitute DC harmonic filter circuit of converter station, which reduces harmonic voltage and current generated during current conversion, as well as facilitates improvement of electromagnetic environment of the line. Meanwhile, it can also prevent steep wave impulse generated by DC line or DC switch from entering valve hall, inhibit rapid increase of DC fault current, and decrease the probability of failure of commutation of inverter; thus, it can protect converter valve from being damaged by overvoltage and over current to certain extent. At present, in conventional HVDC projects, DC smoothing reactors are all arranged on DC pole line, whereas in UHVDC projects, half of smoothing reactors are arranged on DC pole line and half on neutral busbar; this arrangement is referred to as separate arrangement of split smoothing reactor (SASSR).

21.4.1 Structure of UHV Smoothing Reactor

In terms of different structures of insulation and magnetic circuit of reactors, at present, two types of smoothing reactors are available, i.e., dry-type and oil immersion type. Dry-type smoothing reactors adopt coils made of multi-layer compressed aluminum winding, and it is poured with epoxy for insulation. The whole coil and protective insulation structure are supported in air by post insulator. The structure of oil-immersed smoothing reactor is similar to that of transformer, i.e., iron core and coil structure supply inductance, oil–paper composite insulation

is adopted, and the whole equipment is placed on the ground. The two types of smoothing reactors have been used successfully in UHVDC transmission projects both in China and foreign countries. Please refer to Table 21.2 for their advantages, respectively.

Since the voltage level of UHV transmission system is higher than that of conventional EHVDC project, requirement of insulation level for smoothing reactor is increased dramatically. But oil–paper insulation structure of oil-immersed smoothing reactor makes the insulation level of reactor hard to improve further through design and manufacture, so there is no mature UHV oil-immersed smoothing reactor product available. With respect to dry-type smoothing reactor, since the main insulation is supplied by post insulators, it is relatively easy to improve the insulation level; moreover, because the ground capacitance of dry-type smoothing reactor is lower, the impulse insulation level required is relatively lower. In general, dry-type smoothing reactor is recommended for UHVDC project because of its advantages such as simple structure, low technical risk, and low operating cost. Yunnan-Guangdong, Xiangjiaba-Shanghai, Jinping-Southern Jiangsu ±800 kV UHVDC Projects that have been put into operation adopt dry-type smoothing reactors.

Series-connected structure of dry-type smoothing reactor used in Xiangjiaba-Shanghai ±800 kV UHVDC Transmission Project is shown in Fig. 21.9. Each reactor provides 75 mH in nominal inductance and 4000 A nominal DC current, and can withstand 40 kA short-duration current peak. In design of the substation, the smoothing reactor is required to provide 150 mH inductance. However, because the dry-type reactor is of coreless structure, it is difficult to increase inductance of one reactor, so the engineering requirement is met by two 75 mH smoothing reactors connected in series.

Table 21.2 Comparison between characteristics of dry-type and oil-immersed smoothing reactors

Dry-type smoothing reactor	Oil-immersed smoothing reactor
Simple insulation to ground, main insulation supplied by post insulator	Oil-paper insulation system is complicated in design, but since main insulation is sealed in oil tank, it can operate reliably and has higher ability to withstand pollution
Low capacitance to ground, relatively low transient overvoltage	There is iron core, so it is easier to increase inductance than dry-type coreless smoothing reactor
Compared with oil-immersed reactor, it is free of oil, does not need auxiliary operating system. It is free of fire risk and requires low maintenance cost	Electromagnetic radiation is shielded by oil tank, so it has less effect on the surroundings
Light weight, easy to transport. It has good flexibility in arrangement	It adopts dry bushing to penetrate into valve hall, so there is no non-uniform wet flashover problem of horizontal wall bushing
In same inductance situation, equipment cost of dry-type smoothing reactor is about half of that of oil-immersed one	It is installed on the ground, low gravity center and good vibration resisting performance

Fig. 21.9 Dry-type smoothing reactors in Fengxian Station of Xiangjiaba-Shanghai ±800 kV DC project

21.4.2 Characteristics of UHV Smoothing Reactor

DC smoothing reactor in UHVDC system differs from that in conventional EHVDC system in adoption of separating arrangement of split smoothing reactor (SASSR), i.e., half of DC smoothing reactors are arranged on DC pole line, and half on neutral busbar, while in conventional EHVDC system, smoothing reactors are all arranged on DC pole line. Advantages of SASSR have been analyzed in Separate Arrangements of Split Smoothing Reactor in Chap. 18 *Insulation Coordination of UHVDC Converter station*.

Moreover, compared with common AC reactor, care shall be taken to the following points in design of UHV dry-type smoothing reactor.

(1) Temperature rise of winding

DC current differs from AC current in distribution in multi-layer shunt winding. DC current is distributed according to the conductance ratio of shunt winding, while AC current is distributed according to the inductance of each layer and inter-layer mutual inductance. Different current flowing through windings will result in different temperature rise distributions. Since both DC current and AC harmonic current will flow through the smoothing reactor at the same time, the current composition must be taken into consideration in advance to adjust winding parameters to distribute the current uniformly.

In addition, harmonic current can result in energy loss on winding too, which comprises three components: ① resistance loss of current, determined by resistance distribution; ② circulating current loss, i.e., circulating current occurs between windings due to deviation of technology; and ③ eddy current loss, a loss when eddy effect occurs in current, especially in HF harmonic current, which is several dozen times or even hundred times of resistance loss. Therefore, in order to reduce the loss generated by harmonic current, the eddy current loss and circulating current loss must be reduced by optimizing winding pattern and improving conductor quality of the winding. Correspondingly, in temperature rise test, thermal effect of harmonic loss shall be taken into consideration and DC test current shall be increased to obtain equivalent temperature rise.

(2) Design of external insulation

In case that voltage level is increased dramatically, special attention shall be paid to the external insulation design of UHV smoothing reactor. In the past, through type surface flashover and partial surface discharge under wet polluted condition emerged on many imported reactors, presenting creepage tracking. Therefore, special attention must be paid to surface insulation design of reactor, appropriately increase the surface insulation dimension, and resort to measures to prevent from rain and pollution, and restrain surface leakage current density to guard against pollution flashover and partial surface discharge.

(3) Corona design

It is known from tests that if UHV smoothing reactor is not provided with electric field shielding apparatus, tip effect of metallic bracket surely generates visible corona, presenting serious radio interference to the surroundings. Therefore, both terminals of the reactor must be installed with electric field shielding apparatus of large curvature, respectively.

(4) Noise control

Electromagnetic noise of smoothing reactor differs from that of common AC reactor in produce reason. With respect to the noise of smoothing reactor, the main factor to be controlled in fact is electromagnetic noise produced by the interaction between AC and DC, which comes from two origins: one is the alternating magnetic force produced by constant magnetic field (generated by DC current) acting on harmonic

current in the winding; and another is the alternating magnetic force produced by magnetic field of harmonic current acting on DC current in the winding. Because harmonic current is much lower than DC current, the magnetic force produced by harmonic magnetic field acting on harmonic current can be ignored. According to the simulation calculation, noise pressure level measured at point 3 m away from the coil surface of smoothing reactor without control measures is 83.2 dB, higher than technical requirement by 13.2 dB. Because the coil of smoothing reactor is designed according to the requirements of temperature rise, insulation, and dynamic thermal stability, it is very difficult to adjust its structure further according to the requirement of noise reduction. So it is recommended to envelop the reactor body with resistance noise attenuating device to guarantee that the noise around the reactor is kept within the technically required range.

21.4.3 Tests of UHV Smoothing Reactor

(1) Type tests

Type test items of UHV dry-type smoothing reactor include:

Insulation test: full lightning impulse test, chopped lightning impulse test, switching impulse test, applied DC voltage wet-withstand voltage test.

Others: temperature rise test, radio interference level.

(2) Routine tests

Routine test items of UHV dry-type smoothing reactor include:

Measurement of basic parameters: DC resistance measurement of winding, impedance measurement, inductance measurement.

Insulation test: full lightning impulse test, switching impulse test.

Operating test: loss measurement, load current test.

(3) Field test

Field test items of UHV dry-type smoothing reactor include winding resistance measurement, inductance measurement, and noise measurement.

21.4.4 Manufacturing Level of UHV Smoothing Reactor

At present, the manufacture of UHV dry-type smoothing reactor is highly mature. Since Beijing Electrical equipment General Factory (BPEG) developed ±800 kV dry-type coreless smoothing reactor that passed successfully all tests in 2008 for the first time, many factories in China have been participating actively in development of UHV smoothing reactor manufacturing technology. Currently, the manufacturers

such as Xi'an XD Transformer Co., Ltd., TBEA Shenyang Transformer Co., Ltd., and Shanghai MWB have possessed the capability to manufacture dry-type smoothing reactor of 500 kV and higher voltage level. The dry-type smoothing reactors made in China have been used widely in UHV and EHV projects. However, the structure of dry-type smoothing reactor determines that it has some disadvantages that are difficult to solve, such as large coverage area, inferior electromagnetic environment, and difficult vibration resistance.

Oil-immersed reactor is mainly used in HVDC transmission projects, which covers less area, has less impact on the surroundings, and is superior in vibration-resistant performance. In UHVDC projects, which require reactor of higher insulation level, the insulation structure of reactor that is qualified for UHV voltage level is difficult to design, and its manufacturing technology has not been mature yet. In the future, with the development of product design and manufacturing capability, oil-immersed smoothing reactor is expected to be used in UHVDC projects. But the oil-immersed smoothing reactor of oil-paper insulation is so heavy that it could be used in UHVDC projects to substitute current dry-type smoothing reactor only when transportation condition permits.

21.5 UHVAC and DC Filters

In DC transmission system, during the conversion between AC and DC by the converter, its AC side and DC side generate harmonics, respectively. At DC side, the harmonics will result in additional heat from other DC equipment, thus raising the nominal rating requirement and operation cost of equipment; at AC side, the harmonics will result in drop of operating performance of the system. Besides, overhead DC line can generate harmonic potential on adjacent communication line through electromagnetic induction, thus interfering the communication system.

At present, the main methods used in UHVDC system to restrain harmonics are that the AC side is fitted with AC filter while the DC side is fitted with smoothing reactor and DC filter. AC and DC filters can control the harmonic level in the system very well and ensure that the whole DC transmission system operates stably and effectively.

21.5.1 UHVAC Filter

AC filter is connected in parallel with AC system to realize two functions: one is to keep low impedance status of series resonance under harmonic frequency, thus providing bypass channel for the harmonics; and another is to provide reactive power required by commutation of converter.

The projects mostly adopt passive AC filter, which is characterized by simple control, highly mature design and manufacturing technology, and China's high degree of localization. In terms of structure, the AC filter consists of three components, i.e., inductor, capacitor, and resistor, and can be categorized into tuned, high-pass, or tuned high-pass type. The modern DC transmission projects usually adopt tuned high-pass (HP) filter. Table 21.3 shows circuit structure and filtering characteristics of three common tuned HP filters. It can be seen that components of tuned HP AC filter include HV and LV capacitors, reactors, and resistors. Among them, the HV capacitor must have high withstand voltage, high requirement for dielectric material, and is required to work in harsh conditions. Moreover, the HV capacitor is the most important, most expensive component with highest failure rate in AC filter. It is the critical issue in reliable operation of the whole filter. AC filter in an actual UHVDC project is shown in Fig. 21.10.

Table 21.3 Typical tuned HP filters

Description	Single tuned HP filter	Double tuned HP filter	Triple tuned HP filter
Structure of filter	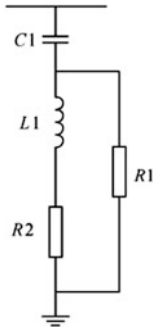	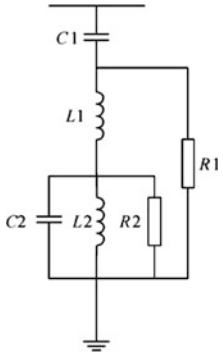	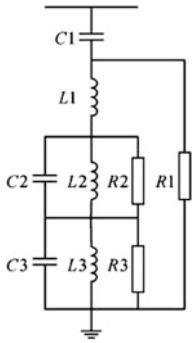
Characteristics	Simple structure. Good restraint of single-order harmonic component. Quantity of banks must be installed. Reactive balance is difficult in light load	Restrain two kinds of harmonics. High-order harmonics can be restrained in broad frequency band by adjusting damping resistor. But it is sensitive to tune-out, and high in momentary setting value of LV component	It is easy to achieve reactive balance in light load. But it is prone to tune-out, and it is hard to tune in field

Fig. 21.10 Installed AC filters

21.5.2 UHVDC Filter

1. Structure of UHVDC filter

In UHV transmission system, the harmonics at DC side mainly comprise $12n$-order (n = 1, 2, 3,…) characteristic harmonics generated by 12-pulse converters, and a small quantity of uncharacteristic harmonics produced by asymmetric parameters between AC system and equipment in converter station. Compared with ±500 kV EHVDC projects, each pole of UHVDC project is made up of two series-connected 12-pulse converter bridges, so UHV system has higher voltage level and generates harmonics that are larger in amplitude and more serious in condition. These harmonics at DC side may interfere with the communication line adjacent to the transmission line and affect the safe and stable operation of the system negatively. Therefore, DC filters, smoothing reactors, and neutral busbar surge capacitors shall be installed to restrict the interference to acceptable level.

Similar to AC filter's structure, DC filter also consists of HV and LV capacitors, reactors, etc. The main electric stress parameters include voltage stress at both terminals of HVDC filter capacitor, the voltage that determines the creepage distance between both terminals of capacitor and reactor as well as that of HV/LV wiring end to ground, stress of current flowing through various components, and current that produces audible noise. With rise of withstand voltage, UHVDC filter is huge in external dimension, for example, the UHVDC filter provided by ABB for Xiangjiaba-Shanghai ±800 kV UHVDC Transmission Project is more than 20 m high and weighs more than 80 t. Figure 21.11 shows a DC filter installed in an actual UHVDC project. The design scheme for the DC filters adopted in Xiangjiaba-Shanghai ±800 kV UHVDC Transmission Project is as shown in Fig. 21.12, in which one bank of 2/12/39 three-tuned filters is installed on each pole of each substation, respectively, between DC pole busbar and neutral busbar, with tuning frequency of 100/600/1950 Hz.

The indicator to measure up DC filter's performance is the equivalent interference current I_{eq} on DC pole line and ground electrode conductor, i.e., the

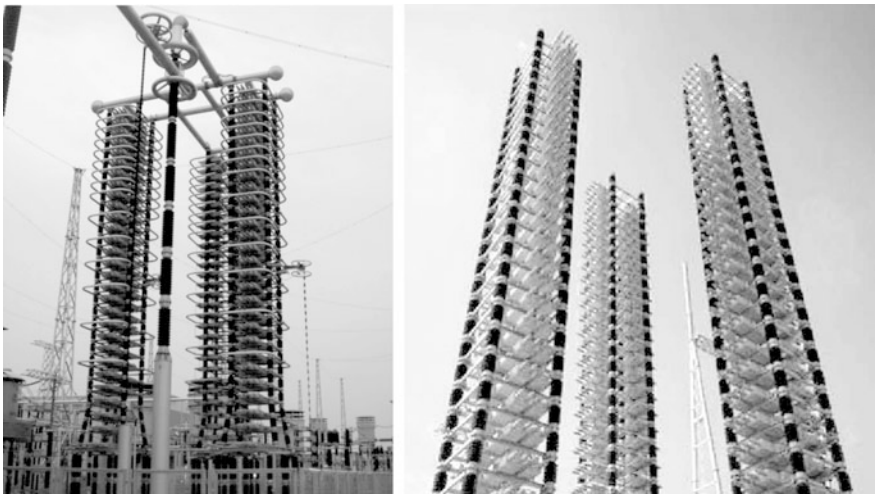

Fig. 21.11 Installed DC filter banks

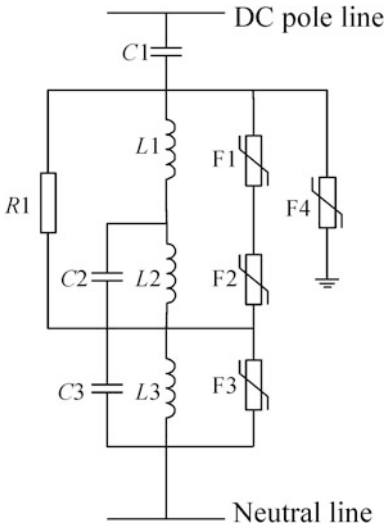

Fig. 21.12 Design scheme for DC filters of Xiangjiaba-Shanghai ±800 kV UHVDC transmission project

comprehensive interference of harmonic current of all frequencies in the line on adjacent parallel or crossing communication line is equivalent to an interference caused by the harmonic current of one frequency. Such harmonic current is referred to as the equivalent interference current. The equivalent interference current is an

important factor in DC filter, concerned with the equipment performance, operating safety of the system, and even overall manufacturing cost. It is specified in UHVDC transmission projects that the equivalent interference current shall not exceed 3000 mA when all DC filters are put into operation in bi-polar operation [6], taking the most unfavorable combination of 1–50-order harmonic current into consideration.

2. Characteristics of UHVDC filter

Differing from AC filter and EHVDC filter, UHVDC filter has the following characteristics:

(1) DC filter does not require reactive compensation as AC filter, so reactive capacity is not required to be higher than its filtering performance, and nominal parameters of the capacitor is dependent on line voltage, filtering requirements, and economy of the project, instead of reactive power.
(2) Resonance may arise in AC filter when status of AC system changes, so damping measures must be taken. But in the converter station, because of the constant impedance at DC side, DC filters that are precise in tuning are permitted to use.
(3) Harmonic voltage withstood by UHVDC filter is much higher than that in EHV project. Provided that the limit of equivalent interference current is same, capacitance of the corresponding HV capacitor shall be increased dramatically. Consequently, the HV capacitor of UHVDC filter is elevated in both cost and manufacturing difficulty. In order to decrease the manufacturing cost, on the premise of that filtering requirements are met and low-frequency (LF) resonance is prevented at DC side, it is required to reduce the number of circuits of DC filter as much as possible, and to reduce the capacitance of the HV capacitor in the branch of DC filter, or to use double- or multi-tuning filter circuits that have common HV capacitor. In addition, if permitted by actual condition, e.g., there is no communication line that may be affected, it is recommended to ease the restrictions on the equivalent interference current I_{eq}, which also facilitates reducing the cost of DC filters in converter station.
(4) Both terminals of the HV capacitor in UHVDC filter must withstand a DC voltage that is higher than that in ±500 kV DC transmission project, and its average working field intensity is about 90–110 kV/mm. In DC filter, voltage distribution is allied to the distribution non-uniformity of resistance that leaks along the porcelain insulation bushing at the end of capacitor unit as well as the impact of harmonic voltage, so parallel-connected grading resistor shall be installed inside the capacitor unit.
(5) In configuration of DC filters in actual project, the DC filters on two poles shall be configured identically in view of symmetry of the converter station.

21.5.3 Tests of UHVAC/DC Filters

1. Tests of UHVAC filter

(1) Type test of UHVAC filter

Measurement of basic parameters: high-temperature loss tangent measurement, capacitance frequency and temperature characteristic measurement, power-frequency withstand voltage test of post insulator, lightning impulse voltage test of post insulator.

Insulation tests: pole-to-enclosure power-frequency withstand voltage test, lightning impulse withstand voltage test, short-circuit discharge test.

Others: thermal stability test; isolation test, endurance test, husk destruction test, and vibration resistance test of fuse.

(2) Routine tests of UHVAC filter

Basic tests: visual inspection, loss angle tangent measurement, leak lightness test, sampling test in batch, etc.;

Insulation tests: pole-to-pole withstand voltage test, partial discharge test of single capacitor, pole-to-enclosure power-frequency withstand voltage test, discharge test, internal discharge element inspection, power-frequency withstand voltage test of post insulator.

2. Tests of UHVDC filter

Test items of UHVDC filter include nominal value measurement, withstand voltage test, thermal stability, and temperature rise test of capacitor, reactor, and resistor.

21.5.4 Manufacturing Level of UHVAC/UHVDC Filters

AC filters in UHVDC project are mostly passive AC filters, which are characterized by simple control, highly mature design and manufacturing technology, and China's higher degree of localization. In Xiangjiaba-Shanghai ±800 kV UHVDC Transmission Project and Yunnan-Guangdong ±800 kV UHVDC Transmission Project, the AC filters are mainly supplied by domestic manufacturers, such as XJ Group.

It is difficult to manufacture UHVDC filter, especially to design and manufacture HV capacitor. In Yunnan-Guangdong ±800 kV UHVDC Transmission Project, the UHVDC filters are all supplied by Siemens Company; in Xiangjiaba-Shanghai ±800 kV UHVDC Transmission Project, the UHVDC filters are all supplied by ABB Company; in Jinping-Southern Jiangsu ±800 kV UHVDC Transmission Project, relevant components of the UHVDC filters are supplied by ABB and some Chinese manufacturers together.

21.6 UHVDC Arrester

UHVDC arrester is the key equipment of overvoltage protection of UHVDC transmission system, having essential effect on the insulation level of the whole project. A reasonably arrester configuration not only increases the operating reliability of the system effectively, but also reduces the operating cost of the equipment, thus achieving optimization technically and economically. Compared with conventional EHVDC system, because of high-voltage level of UHV system and much less insulation coordination coefficient, the arrester is required to have higher non-linear coefficient to enable its residual voltage as lower as possible. Moreover, UHV projects require that the arrester possesses higher capacity of energy absorption; thus, its overall design and manufacture are more difficult.

21.6.1 Type of UHVDC Arrester

UHVDC arresters are various in types and high in performance parameters; and various arresters differ greatly in some parameters such as continuous operating voltage, chargeability. Up to 2015, there were only 6 ± 800 kV UHVDC transmission projects put into operation in the world, and all in China. There are two layouts for arresters in converter station: Xiangjiaba-Shanghai and Jinping-Southern Jiangsu ± 800 kV UHVDC Transmission Project adopting the concept recommended by ABB, while Yunnan-Guangdong ±800 kV UHVDC Transmission Project adopted the concept recommended by Siemens [7]. Please refer to Sect. 18.3 for determination of performance parameters of UHVDC arresters.

The layout of arresters in converter station in Xiangjiaba-Shanghai ±800 kV UHVDC Transmission Project to describe the concept recommended by ABB is shown in Fig. 21.13 and the protection function of all arresters in the figure is described in Table 21.4.

Arrester layout recommended by Siemens is applied in Yunnan-Guangdong ±800 kV UHVDC Project, as shown in Fig. 21.14. It is generally similar to the scheme recommended by ABB, so description of the positions and functions of various arresters in the scheme are not repeated here.

It can be found by comparing layouts of arresters depicted in Figs. 21.13 and 21.14 that the two schemes differ in protection of the winding at valve side of HV converter transformer. In Xiangjiaba-Shanghai Project, protection of series-connected MH and V arresters is adopted, so each pole of each substation requires only one MH arrester. Such concept is characterized by less arresters and relatively simple layout of arresters; its disadvantage lies in higher insulation level of the winding at valve side of converter transformer. In Yunnan-Guangdong Project, arrester A2 directly protects the winding at valve side of HV converter transformer, consequently decreasing insulation level of the equipment.

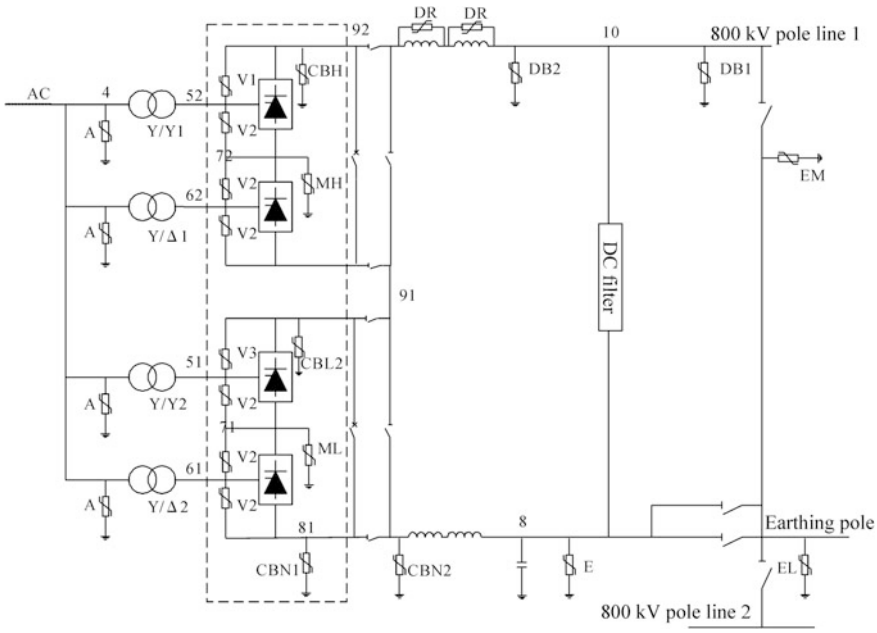

Fig. 21.13 Layout of arresters of Xiangjiaba-Shanghai ±800 kV UHVDC transmission project

Its disadvantage lies in that each pole of each substation requires three arresters, occupying larger space in the valve hall. In conclusion, the two layout schemes of arresters recommended by Siemens and ABB, respectively have their own advantages and disadvantages.

21.6.2 Characteristics of UHVDC Arrester

UHVDC system is high in voltage level, complicated in structure, various in overvoltage under fault condition, and rigorous in operating condition of arrester, so the arresters used in UHVDC system are more than those in converter station of conventional DC system in terms of type and quantity. Compared with the arresters in AC system and conventional DC system, UHVDC arrester has its distinct characteristics.

(1) Various types, great difference in performance parameters

According to different installation positions, UHVDC arresters fall into several categories, i.e., valve arrester, DC busbar arrester, DC line arrester, and neutral bus arrester, and there are some unique arresters in UHV system, e.g., DC busbar arrester between upper/lower 12-pulse converter units.

Table 21.4 Protection functions of arresters

Arrester	Designation	Protection functions
A	AC bus arrester	It is installed on AC bus and AC side of converter transformer, and mainly used to restrict switching overvoltage arising from various reasons
V1/V2/V3	Valve arrester	They are connected in parallel on both terminals of the valve to protect the converter valve from the switching overvoltage passing by converter transformer from AC side or the overvoltage arising from various reasons at DC side. The valve arresters at different positions have different requirements of energy absorption. High capability to absorb energy can be realized by parallel-connecting multiple columns
MH/ML	6-Pulse bridge arrester for upper/lower 12-pulse converter unit	They protect the DC bus between 6-pulse converter bridges
CBH	DC busbar arrester of upper 12-pulse converter unit	It is installed on DC bus at the valve side of pole smoothing reactor. It is used to protect the DC bus, bushing, and other equipment at valve side of pole smoothing reactor
CBL2	DC busbar arrester between 12-pulse converter units	It is installed in the middle of the bus between upper and lower 12-pulse converters. It is used to protect intermediate DC bus and connect wall bushing and isolator of upper/lower converter units
CBN1/CBN2	Arrester at low voltage end of converter	CBN1 is installed inside the valve hall, while CBN2 is installed outside the hall. CBN1 is used to limit lightning overvoltage intruding into the valve hall. CBN2 is high-energy arrester formed by parallel-connected multiple columns to protect relevant equipment at the valve side of neutral smoothing reactor
DB1/DB2	DC busbar/line arrester	They are installed on DC pole, mainly used to limit lightning and switching overvoltage in DC switchgear yard
DR	Parallel arrester for smoothing reactor	It is connected in parallel to both terminals of DC pole smoothing reactor, mainly used to guard against lighting inrush wave to protect the smoothing reactor from end-to-end reverse lightning overvoltage
E	Neutral busbar arrester	It is installed on neutral bus, mainly used to protect the neutral bus and equipment connected to the bus from being damaged by overvoltage. In ground fault, the energy impulse is significant, so multiple arresters connected in parallel are required to increase the discharge capacity

(continued)

Table 21.4 (continued)

Arrester	Designation	Protection functions
EM, EL	Metal return and electrode line arrester	They are used to limit lightning impulse and switching impulse from metallic return and ground electrode line, and work with arrester CBN2 to absorb switching impulse on neutral bus

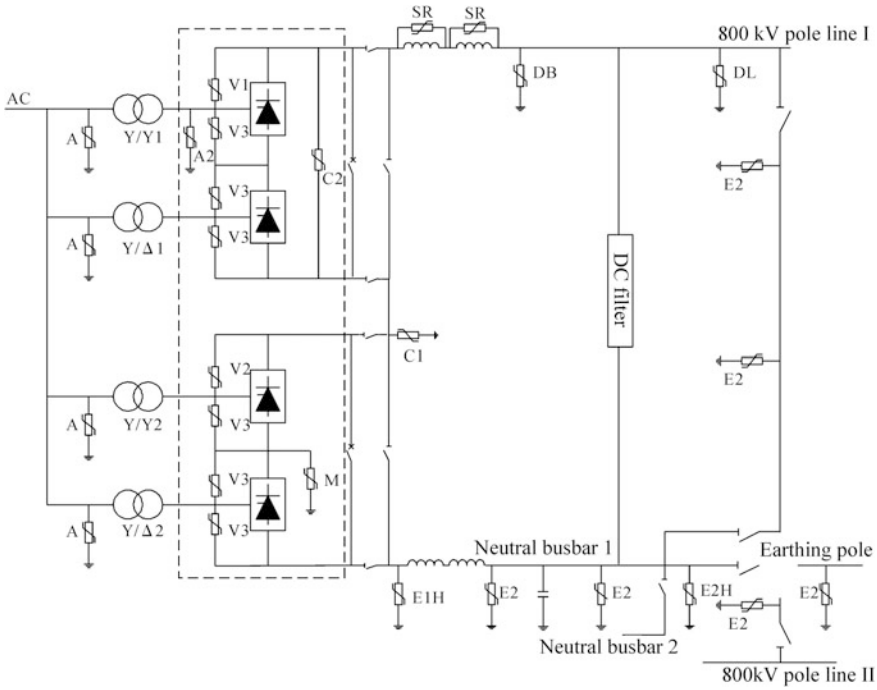

Fig. 21.14 Layout of arresters in converter station of Yunnan-Guangdong ±800 kV UHVDC transmission project

(2) Complicated continuous operating voltage

The structure of UHVDC system is more complicated. The continuous operating voltage on DC arrester comprises DC component, fundamental frequency component, and harmonic component, and the voltage that the system has to withstand is complicated in waveform. For example, when converter valve is turned off, commutation overshoot will be presented at both terminals of valve arrester, which has seriously irregular waveform.

(3) Higher discharge capacity required

The arresters on some positions in UHVDC system need to discharge a large amount of energy, so multiple column arresters connected in parallel are usually used to meet the energy requirements. When multiple columns are connected in parallel, the current sharing characteristic of arrester shall be taken into consideration.

(4) Prominent pollution problem

DC pollution deposit of DC arrester is much more serious than that of AC system. In addition, the higher the voltage level of UHVDC system is, the higher the external insulation requirement of DC arrester is. In order to ameliorate the pollution resisting performance, UHVDC arresters generally adopt silicone rubber polymeric housing and shed structures that are staggered-arranged according to their sizes, and the designed specific creepage distance is much larger than that in AC system. Silicone rubber has superior hydrophobicity transfer property, whose surface is hard to accumulate pollution, and it is light in weight and reliable in pressure relief. Meanwhile, staggered-arranged shed structures according to their size can prevent continuous conductive layer produced on the surface and increase the ratio of overall creepage distance to the whole length meanwhile.

21.6.3 Tests of UHVDC Arrester

Test of UHVDC arrester is also a difficult problem. The continuous operating voltage of different arresters differs greatly in waveform and it is hard to estimate in advance. In particular, in operating duty test, accelerated aging test, etc., real operating condition shall be simulated as much as possible. These problems challenge the insulation coordination calculation of converter station and test level of UHV arrester.

Basic tests of UHVDC arrester comprise the following items:

(1) Basic parameter measurement: visual inspection, specific creepage distance check, resistance current test, residual test, power-frequency reference voltage test, DC reference voltage test, leakage current test under 0.75 times DC reference voltage, current distribution test.
(2) Insulation test: operating duty test, external insulation withstand voltage test, radio interference and partial discharge test, test of resistance of electrical insulation material to electrochemical erosion and creepage tracking, artificial pollution test.
(3) Safety performance test: pressure relief test, seal performance test, husk destruction test, heavy current impulse withstand test, thermal cycling and boiling water test, mechanical performance test.

21.6.4 Manufacturing Level of UHVDC Arrester

Because HVDC arresters are various in types and difficult in manufacture, at present, the DC arresters used in HVDC transmission in China are mostly supplied by foreign companies, and only a fraction of the arresters are supplied by Chinese companies. Table 21.5 lists the suppliers of arresters used in some UHVDC and EHVDC transmission projects in China up to 2015, from which it can be found that the arresters used in HVDC projects are mainly supplied by foreign companies, who are still leading in manufacture of arresters. At the same time, in recent years, some Chinese arrester manufactures have also been participating in research and development of DC arresters. For instances, XD Company Xi'an Electric Porcelain Institute supplied neutral busbar arresters to Gezhouba-Shanghai Nanqiao ±500 kV DC Project, supplied pole busbar arresters to Three Gorges-Changzhou ±500 kV DC Project, and supplied all the DC arresters required by Lingbao Back-to-Back DC Project. The companies accumulate a wealth of experience in these actual projects, demonstrating that Chinese arrester manufacturers have been in possession of the capability to research and manufacture DC arresters.

In UHVDC projects, all the three projects that are put into operation at present adopt the DC arresters supplied by foreign manufacturers. The DC arresters used in Yunnan-Guangdong ±800 kV UHVDC Transmission Project are all supplied by Siemens, while those used in Xiangjiaba-Shanghai and Jinping-Southern Jiangsu ±800 kV UHVDC transmission projects are mainly supplied by ABB. In recent years, arresters made in China are also being improved both in research and manufacturing levels, and Xi'an XD and other companies have developed ±800 kV DC arresters successfully.

21.7 UHV Bushing

Bushing is used to isolate HV conductor and objects that have a potential different from the conductor, serving as insulation and support. The bushings fall into two categories, i.e., electrical bushing and wall bushing. The former is used for HV conductor to pass through diaphragm that has different potential, while the latter is used for conductor or busbar to penetrate building or wall. UHV bushing plays a key role in the entire UHVDC transmission project. Once a bushing fails, the pole must be shut down immediately, which will affect the electric system negatively. According to statistics of State Grid, HV electrical equipment accidents in 500 kV substations in China caused by bushing accounted for 35.4% total accidents by the end of 2002, which demonstrates the importance of bushing in maintaining safe and reliable operation of the system.

Table 21.5 Manufacturers of arresters selected in some EHVDC and UHVDC projects in China

Project name	DC arrester supplier	Year of placement into operation
Gezhouba-Shanghai Nanqiao ±500 kV DC transmission project	BBC (present ABB)	1989
Tianshengqiao-Guangdong ±500 kV DC transmission project	Siemens	2000
Three Gorges-Changzhou ±500 kV DC transmission project	ABB	2002
Three Gorges-Guangdong ±500 kV DC transmission project	Siemens	2004
Guizhoug-Guangdong ±500 kV DC transmission project	ABB	2004
Lingbao ±550 kV back-to-back DC transmission project	XD Xi'an Electric Porcelain Institute	2005
Yunnan-Guangdong ±800 kV UHVDC transmission project	Siemens	2010
Xiangjiaba-Shanghai ±800 kV UHVDC transmission project	ABB	2010
Jinping-Southern Jiangsu ±800 kV UHVDC transmission project	ABB	2012
Southern Hami-Zhengzhou ±800 kV UHVDC transmission project	Nanyang, Jinguan, et al.	2014
Xiluodu-Zhexi ±800 kV UHVDC transmission project	XD Xi'an Institute, China Electric Power Equipment and Technology CO.	2014

21.7.1 Structure of UHV Bushing

The basic structure of UHV bushing consists of one electrode which is inserted into the center of another electrode with a different potential. Taking the case of bushing produced by ABB, SF_6 gas and insulating paper are used as the insulating dielectric for its internal insulation, while aluminum foil is used as inter-electrode dielectric. In this way, the thin aluminum foils covered on inter-layer insulating papers form a string of coaxial cylindrical capacitors, which have high electric strength and more uniform distribution of electric field. Composite insulators at both terminals of the bushing are made of glass fiber-reinforced epoxy resin tube and silicone rubber, and coordinated with the design of stress cone, electrode shielding, and grading ball to ameliorate the distribution of electric field and potential. With respect to external insulation, long and short alternate silicone rubber sheds are arranged alternately to increase the creepage instance and improve the performance of rain resistance and

pollution resistance. UHV bushings fall into two types by their applications, i.e., UHV transformer bushing and UHV wall bushing.

(1) UHV transformer bushing

The UHV transformer bushing produced by ABB is taken as an example to introduce the structure and technical procedure of UHVDC converter transformer bushing briefly. In Xiangjiaba-Shanghai ±800 kV UHVDC Transmission Project, the converter transformer bushing in Fulong Station is shown in Fig. 21.15.

It can be seen from Fig. 21.15, that the outgoing bushing provides a channel for the converter transformer to connect with the converter valves and the wall of the hall at the valve side of UHV highest-voltage-end converter transformer. Because the operating environment at valve side of converter transformer is complicated, and the operating voltage contains DC and more harmonic component, it is sharp upon the insulation design of the bushing at the valve side.

(2) UHV wall bushing

UHV wall bushing is used to support the DC busbar in valve hall penetrating wall to connect with DC pole line installed outdoors. Its highest voltage reaches 800 kV, so it is required to have higher insulation level. In engineering, the wall bushings are installed at 10º angle to the horizontal line to improve water resisting performance of the bushing to guarantee creepage distance. In view of clean and dry environment in valve hall, the creepage distance can be reduced relatively, so the indoor section of the bushing is generally shorter than the outdoor section. Figure 21.16 shows an external view of a ±800 kV DC pole wall bushing, and Table 21.6 describes its technical procedures [8].

(a) Complete bushing structure (b) Internal part in valve hall of installed busing

Fig. 21.15 Converter transformer bushing in Fulong Converter Station of Xiangjiaba-Shanghai ±800 kV UHVDC transmission project

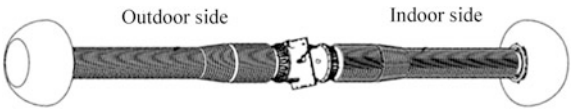

Fig. 21.16 Diagram for outline of 800 kV DC pole line wall bushing, reprinted from ref. [2], copyright 2009, with permission from China Electrical Power Press

Table 21.6 Technical parameters of 800 kV DC pole line wall bushing

Type of bushing	SF6 gas insulation, composite material
Nominal DC voltage (kV)	±800
Rated peak voltage (kV)	816
Rated current (A)	4000
Specific creepage distance (indoor) (mm/kV)	>14
Specific creepage distance (outdoor) (mm/kV)	>45
Dimensions	Indoor section about 8.3 m, outdoor section about 9.9 m
Installation angle	At 10º angle to horizontal direction

21.7.2 Characteristics of UHV Bushing

UHV bushings are large in dimensions, e.g., length of some wall bushings is nearly 19 m, and complicate in its insulation structure, which is divided into internal and external insulation. Moreover, the internal and external electric field stress shall keep balanced. The bushings are operating in harsh environment, which have to be subject to not only rain, pollution, and other environmental factors externally, but also high electric, thermal, and mechanical stress in the same time. The UHV bushings have the following characteristics in terms of material and insulation structure:

1. External insulation feature of UHV bushing

Unlike bushings used in ±500 kV DC transmission projects, silicon rubber is usually used as the external insulation of UHV bushing. The traditional pure porcelain bushing, restricted by the manufacturing technology, cannot meet the bushing thickness required by insulation of UHV system. Silicone rubber is superior in hydrophobicity transfer property, wide in temperature withstanding range, and good in dielectric property; so compared with the porcelain bushing, the silicon rubber bushing has considerably reduced the creepage distance and air clearance, and less weight. Therefore, silicone rubber is used for UHVDC bushing as its external material. Water- and pollution-resistant properties of silicone rubber

can basically solve many problems that may arise on pure porcelain bushing in ±500 kV DC transmission projects, such as non-uniform rain flashover and pollution flashover, and eliminate the explosion risk of pure porcelain bushing completely, clearing up the jeopardy to adjacent equipment caused by bushing break.

2. Distribution feature of electric field of UHV bushing

The distribution of electric field of UHV bushing is very complicated. The electric field component vertical to the dielectric surface is relatively intense, and the surface voltage distributes considerably unevenly. Because of the high strength of electric field near the intermediate flange and that between flange and guide rod, it is apt to breakdown by discharge. In insulation layer of the bushing, there are many non-concentric spots on which molecular positive and negative charges are acting. These spots may become local trap to attract space charges gathering. If it is analyzed in terms of distribution of space charges, the insulation design of DC bushing is more complicated than that of AC bushing, because the attracted space charges will not be neutralized and dissipated by time-varying electric field. In addition, the dielectric property of medium under intense electric field is different from that under applied field of lower strength. The space charges do not mainly ionize, but there are a large amount of carriers of same polarity injecting into negative and positive poles, respectively, thus increasing the distortion ratio of the field strength significantly. The intensity of some distorted field even reaches 8–10 times of original intensity. Therefore, the space charges can result in distortion of internal electric field of insulation material, which is an important factor to lead to material aging and electric breakdown.

3. Harsh operating environment of UHV bushing

UHV bushing suffers not only long-duration AC/DC operating voltage, but also the impact of other factors such as switchover of operating method of the system and change of ambient temperature. It is shown in operating experience of DC transmission system that most malfunctions of HV equipment occur during the reversal of polarity. The evident feature of the reversal of polarity is instantaneous heteropolar accumulation of the space charges, so that the electric fields of local areas are centralized on composite dielectric interface. Under this condition, flashover and breakdown are apt to happen on both AC and DC bushings. Meanwhile, with respect to DC bushings, because its electric field distributes according to resistivity, it is highly vulnerable to the impact of temperature change. The insulation resistance of polymer usually presents negative temperature characteristic. The carriers are apt to concentrate at low-temperature side because the conductivity of this side is low, thus resulting in distortion of field intensity at low-temperature side. The greater the temperature difference is the more the quantity of heteropolar charges is, and the more serious the distortion of field strength distribution is.

21.7.3 Tests of UHV Bushing

In type test of UHVDC bushing, it will suffer a combined strength that is higher than that in practical condition to look for possible damage. The test items include dry power-frequency withstand voltage test, dry lightning impulse withstand voltage test, dry or wet switching impulse withstand voltage test, temperature rise test, and bending load withstanding test.

The routine test items of UHVDC bushing are listed in their sequence:

(1) Dielectric loss angle tangent and capacitance measurement, dry lightning impulse withstand test, dry power-frequency withstand voltage test.
(2) Repeated measurement of dielectric loss angle tangent and capacitance, measurement of partial discharge under DC withstand voltage.
(3) Third measurement of dielectric loss angle tangent and capacitance, insulation test of terminal, internal pressure test of gas filled, gas insulated and gas-impregnated bushings.

In addition, according to the agreement between the manufacturer and the customer, the outdoor bushing may also be subjected to artificial pollution test, uniform and non-uniform rain DC voltage test, test of resistance of shed material to electrochemical erosion and creepage tracking, and other special tests.

21.7.4 Manufacturing Level of UHV Bushing

Nowadays, the main technologies of ±800 kV electrical bushing and wall bushing in the world are mainly monopolized by ABB and Siemens. The former mainly produces HVDC oil–paper bushing while the latter mainly produces HVDC epoxy-impregnated dry bushing. The Chinese companies, such as XJ Group and Nanjing Electric, are researching UHVDC wall bushing by means of technical introduction to acquire gradually its core technology and realize participation in relevant equipment.

21.8 UHVDC Switchgear

UHVDC system has a variety of operating modes. Because of different structures of DC transmission system under different operating modes, the operating modes shall be changed over with the help of different DC switchgears. Besides, the switchgears are also used to cut out and isolate faults in malfunction and maintenance of DC system. Therefore, there are a variety of UHVDC switchgears, which fall into several categories according to their functions in the system, i.e., HVDC transfer switch, UHVDC disconnector, and grounding switch and UHVDC bypass switch.

Typical layout of UHVDC switchgear is shown in Fig. 21.17, in which marker 1 represents UHVDC transfer switch, marker 2 represents UHVDC disconnector, and marker 3 represents UHVDC bypass switch. The disconnector is usually fitted with grounding switch beside it, which is not shown in the figure.

21.8.1 UHVDC Transfer Switch

1. Type of transfer switches

UHVDC transfer switch is the important equipment in UHVDC transmission system, mainly used to change over between various operating modes and between

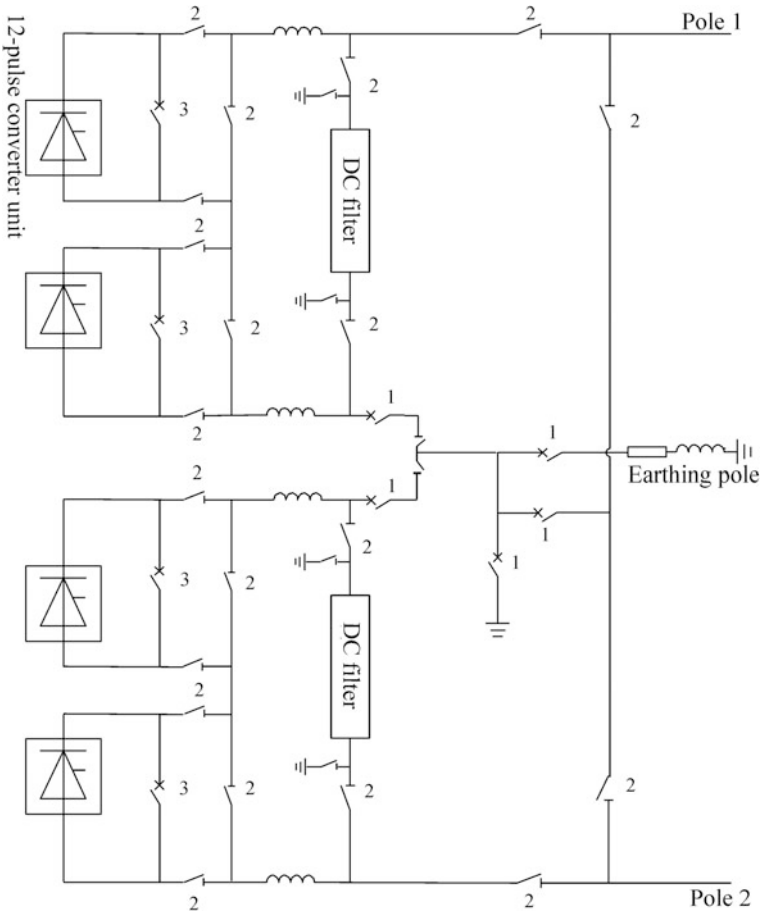

Fig. 21.17 Layout of switches in UHVDC converter station

grounding systems of the DC transmission system to ensure safe and stable operation of the DC system. Similar to those in conventional EHVDC system, UHVDC transfer switches fall into two types according to their functions, i.e., operating mode changeover and projection function. The former includes Metallic Return Transfer Breaker (MRTB) and Ground Return Transfer Switch (GRTS); the latter includes Neutral Bus Switch (NBS) and Neutral Bus Ground Switch (NBGS), and positions of the various switches in UHVDC converter station are shown in Fig. 21.18. It can be found that MRTB and GRTS locate between DC pole line and ground electrode, mainly used to change over between monopolar ground return and monopolar metallic return operation and guarantee the uninterrupted power transfer of the DC system during changeover. NBS is located on the grounding conductor inside the converter station and connected in series to neutral busbar, serving for two functions: In monopolar planned outage, the current through converter drops to zero, and then NBS is used to disconnect the shutdown converter from neutral bus; in bi-polar operation of DC system, where internal ground fault happens in one pole, the failed pole is bypassed and blocked, and then NBS is used to transfer the current injected by normal pole into failed ground point to ground electrode line [9, 10]. NBGS locates between neutral line and grounding grid inside the converter station, mainly used to provide temporary grounding for the substation.

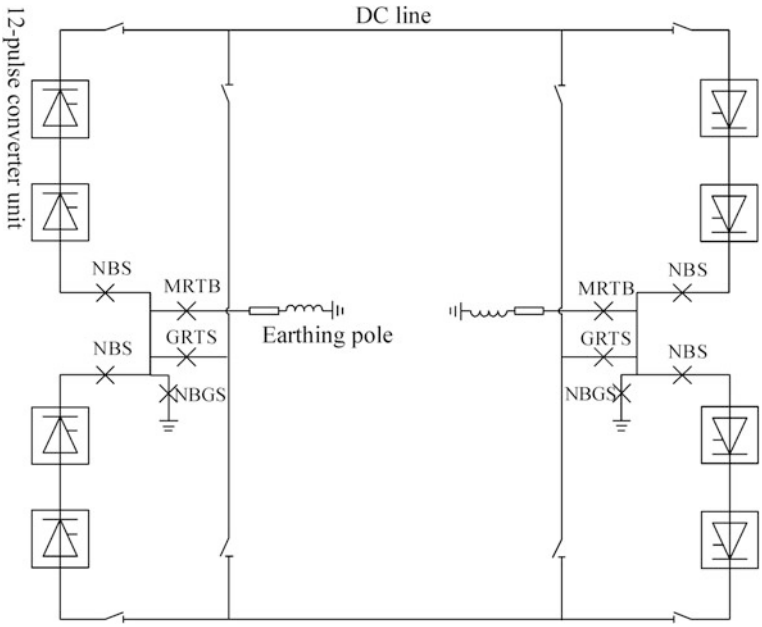

Fig. 21.18 Layout of transfer switches in UHV converter station

2. Working principle of transfer switch

Different to AC circuit breaker, no zero-crossing point is available for DC current, so it is difficult to extinguish arc. Moreover, inductance in DC circuit is high and the cut-off DC current when the transfer switch acts is large, so the DC transfer switch will absorb a large amount of energy. Meanwhile, high overvoltage may be produced in action of the transfer switch, causing re-arcing between open contacts. Because of these characteristics, the DC breaker is more difficult to manufacture than AC breaker. In the UHVDC projects in China that are put into operation, the UHVDC transfer switches generally fall into two types according to their work principles, i.e., active type and passive type [11]. Refer to Fig. 21.19 for their work principles. Among them, the structure of the passive DC transfer switch is shown in Fig. 21.20 [12].

In terms of structure, passive DC transfer switch generally consists of one SF6 breaker, one LC oscillating circuit made up of one reactor and one capacitor, and one arrester R. Among them, LC oscillating circuit is mainly used to form zero-crossing point; SF6 breaker is used to make and break the circuit, similar to AC breaker in working principle; arrester R is used to absorb the energy stored in the DC circuit. Work principle of the passive type DC transfer switch is described

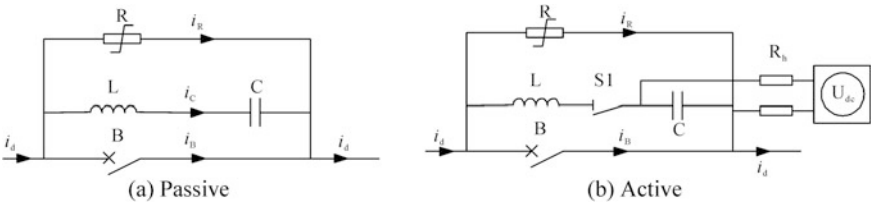

Fig. 21.19 Work Principle of UHVDC transfer switch

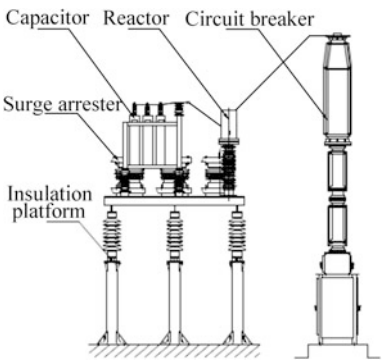

Fig. 21.20 Sketch for structure of passive DC transfer switch, reprinted from Ref. [2], copyright 2009, with permission from China Electrical Power Press

as follows: when the contacts of SF_6 breaker are opened, arc voltage generates oscillating current in the loop made of SF_6 breaker and LC branch. When the reverse peak of the oscillating current is equal to the DC current, the current flowing through SF_6 breaker crosses zero, and then the arc is extinguished. After that, the DC current flowing through SF_6 breaker is transferred to LC branch and charge the capacitor C. When the charge voltage reaches the level that arrester R acts, the energy stored in the circuit is released through the arrester R.

Compared with passive transfer switch, the active DC transfer switch is provided additionally with one disconnector S1 and one DC charging device U_{dc} that are mainly used to pre-charge capacitor C before act and break of the switch. The working principle of the active DC transfer switch is described as follows: before the transfer switch acts, the capacitor is pre-charged by charging device to a voltage. When the contacts of SF_6 breaker are opened, disconnector S1 is put into operation, and capacitor C discharges intermittently to the arc between the open contacts of SF_6 breaker through reactor L. The consequent oscillating current is superposed on the arc current of the breaker, thus forming the forced current. After the current drops to zero, arc extinguishes, and then the energy stored in DC circuit is released by arrester R. After that, the active DC transfer switch works same as the passive one in principle.

It can be seen from the working principle of these switches that in active DC transfer switch, the current flowing through the contacts of the breaker is forced by voltage of the charging device to drop to zero, while in passive DC transfer switch, the current flowing through contacts of breaker is decreased by the oscillating voltage generated by oscillating circuit to drop to zero.

In general, passive DC transfer switch is applicable to convert DC current of moderate amplitude, while active DC transfer switch can convert DC current of larger amplitude.

3. Characteristics of transfer switch

In UHVDC system, the DC transfer switches differ somewhat in their composition structure because they differ in amplitude of switching current. Each transfer switch is described in detail as follows.

(1) MRTB: It can convert current of large amplitude, during which the reverse voltage of 100–150 kV is required, so the switch is to be supported by a special active auxiliary circuit, which usually adopts active DC transfer switch.
(2) GRTS: It is similar to MRTB both in structure and work pattern, but the converted current and the reverse voltage (lower than 50 kV) required in the conversion are relatively low, so it adopts passive auxiliary circuit.
(3) NBGS and NBS: Because it can restrict the converted current and the reverse voltage required in the conversion below 2500 A and within 20–50 kV, respectively, through the blocking function of DC system, it is similar to GRTS in structure, and also adopts the passive auxiliary circuit. But it is particular that NBGS shall close rapidly to provide temporary grounding when ground electrode is open and neutral bus voltage increases out of control, so its first circuit

breaker branch actually consists of one transfer breaker and one high-speed disconnector connected in series. The transfer breaker closes and high-speed disconnector opens under normal condition; the high-speed disconnector closes when stuck-open fault arises on ground electrode; after the fault is remedied, the operating consequence is as follows: transfer breaker opens, high-speed disconnector opens, and finally transfer breaker closes again.

For these transfer switches, the DC transfer switches that perform protective function can be designed on the basis of single conversion. But the transfer switches that perform changeover of operating modes need to actualize changeover between operating modes without interruption of power transfer, and they can be designed on the basis of two consecutive conversions, i.e., reclosing after failure of opening and then opening again.

21.8.2 UHVDC Disconnector and Grounding Switch

UHVDC disconnector and grounding switch are mainly used to implement electrical isolation for the DC equipment that is out of operation effectively, thus facilitating test and service on the equipment. As shown in Fig. 21.17, marker 2 represents the disconnectors and grounding switches in UHVDC converter station, which are installed in valve hall, on DC busbar, neutral busbar, DC filter, etc.. UHVDC disconnector and grounding switch are similar to the disconnector in AC system in work principle, so it is unnecessary to go into the details. Disconnector on neutral line in Fulong Station in Xiangjiaba-Shanghai ±800 kV UHVDC Transmission Project is shown in Fig. 21.21.

21.8.3 UHVDC Bypass Switch

As UHVDC system adopts two series-connected 12-pulse converters, compared with ±500 kV DC system, a piece of switchgear is added, i.e., 12-pulse converter bypass switch, represented by marker 3 in Fig. 21.17. Installation of 12-pulse converter bypass switch makes the operation modes of UHVDC system more various and flexible, and also can reduce the loss caused by equipment failure. When any one of valve bank fails, the bypass switch bypasses the valve bank and puts it out of operation, thus ensuring that the sound converter valve banks keep operating stably. Because the bypass switch only transfers small DC current instead of breaking fault current, the broken current is relatively low. It does not need to install oscillating circuit. Figure 21.22 shows the bypass switch of LV valve in Fulong Station in Xiangjiaba-Shanghai ±800 kV UHVDC Transmission Project.

Fig. 21.21 Disconnectors on neutral line in Fulong Station of Xiangjiaba-Shanghai ±800 kV UHVDC transmission project

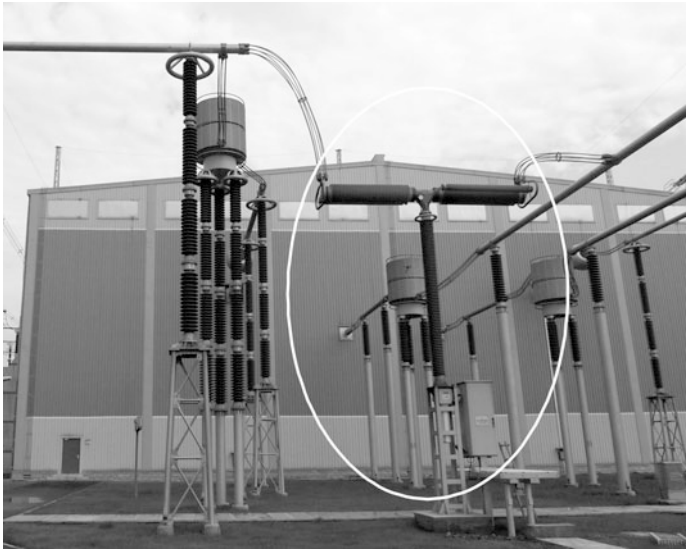

Fig. 21.22 Bypass switch of LV valve in Fulong Station of Xiangjiaba-Shanghai ±800 kV UHVDC transmission project

21.8.4 Tests of UHVDC Switchgear

UHVDC switchgear tests comprise type test, routine test, field test, etc. Among them, test items of UHVDC switchgear are based on GBT 25309-2010 *High-voltage Direct Current Transfer Switches*; test items of UHVDC disconnector and grounding switch are based on GBT 25091-2010 *High-voltage Direct Current Disconnectors and Grounding Switches*; test items of HUVDC bypass switch are based on GBT 25307-2010 *High-voltage Direct Current By-pass Switches*.

21.9 UHVDC Measuring Equipment

In order to meet the requirements of control, regulation, and protection of the system in UHV converter station, it is required to measure voltage and current of the system. In terms of UHVDC measuring equipment, they are basically same as the common voltage and current measuring equipment in general structure and type, except that their requirement of insulation level is highly raised.

21.9.1 UHVDC Voltage Measuring Equipment

UHVDC voltage measuring equipment is generally with the structure of resistor voltage divider coordinating with DC amplifier, in which the resistor voltage divider is the main mechanism of voltage sensor. Voltage at HV end can be calculated by measuring the voltage at both terminals of LV arm if the resistances of HV arm and LV arm are known, respectively. Since the resistance of HV arm resistor is usually about hundreds of megohms, the ohmic current flowing through the voltage divider under nominal voltage is generally only at milliampere level. Figure 21.23 shows a DC voltage measuring equipment in Fulong Station in Xiangjiaba-Shanghai ±800 kV UHVDC Transmission Project.

In addition, because the stray capacitance to ground varies with the position of resistor divider, the voltage on the resistor divider distributes unevenly greatly when lightning impulse happens. The resistance component at HV end suffers the impulse voltage much higher than that resistance component at the intermediate and lower end suffer. In view of this, compensating capacitors are parallel-connected at both terminals of the resistance component of the resistor voltage divider to ameliorate the electric field distribution of divided voltage.

Compared with EHVDC system, UHVDC system has higher voltage level, so the corresponding insulation level of the equipment is higher. Consequently, special care shall be taken to the insulation at the end of voltage measuring equipment and to corresponding compensator in design.

Fig. 21.23 Pole line voltage measuring equipment in Fulong Station of Xiangjiaba-Shanghai ±800 kV UHVDC transmission project

Type tests of DC voltage divider comprise measurement of capacitance and electric loss angle, measurement of HV resistance, insulation test, voltage division ratio test, transient-state response test, and frequency response test.

21.9.2 UHVDC Current Measuring Equipment

There are two types of DC current measuring equipment, i.e., electromagnetic-type zero magnetic flux DC current transformer and optical current transformer (OTA). The former is a saturated reactor employing principle of Equal Ampere-turn to obtain secondary current signals on load resistors that are in proportion to primary current. The latter collects voltage signals generated by the current flows through acquisition coils, converts the signals to digital signals through A/D converter, and then the signals of clock and current data are transferred to the receivers by light-emitting diode (LED) through optical fiber. Xiangjiaba-Shanghai ±800 kV UHVDC Transmission Project adopts electromagnetic-type DC current transformer manufactured by ABB, while Yunnan-Guangdong ±800 kV UHVDC Transmission Project adopts OTA manufactured by Siemens. Figure 21.24 shows a current transformer on neutral line of Fulong Station in Xiangjiaba-Shanghai ±800 kV UHVDC Transmission Project.

Fig. 21.24 Current transformer on neutral line in Fulong Station of Xiangjiaba-Shanghai ±800 kV UHVDC transmission project

Type tests of electromagnetic-type zero magnetic flux DC current transformer comprise calibration of measuring precision, step change response test, frequency response test, dry thermal test, measurement of electric loss and capacitance, transient-state anti-interference performance test, short-duration current test, temperature rise test, lightning impulse wave test, insulation test, etc. Type tests of OTA comprise calibration of measuring precision, step change response test, frequency response test, dry thermal test, impulse test at primary side, insulation test, etc.

References

1. DC Transmission Research Group of Zhejiang University. DC power transmission. Beijing: Electric Power Industry Press; 1982.
2. Liu Z. UHVDC electrical equipment. Beijing: China Electric Power Press; 2009.

3. Li X, Sachs G, Uder M. 6 inch high-power thyristor valves for ±800 kV UHVDC transmission. High Volt Appar. 2010;46(6):1–5.
4. Xi H, Tang G, Liu J, Wei X, Zha K. Development of the ±800 kV/4750 A ultra high voltage direct current converter valve. Proc CSEE. 2012;32(24):15–22.
5. Li Y. UHV power transmission technology. Beijing: China Water & Power Press; 2011.
6. Liu Z. Album of research achievements on UHVDC (2006). Beijing: China Electric Power Press; 2008.
7. Zhou H, Wang D. Overvoltage protection and insulation coordination for ±1100 kV UHVDC converter station. Power Syst Technol. 2012;36(9):1–8.
8. GB/T 26166-2010. Wall Bushings for ±800 kV DC power systems; 2010.
9. Bangtian W. Technology of HVDC circuit breaker. High Volt Appar. 2010;46(09):61–4.
10. Peng C, Wen J, Wang W, Liu Z, Yu K. Development of DC transfer switch for ultra high voltage DC transmission systems. Proc CSEE. 2012;32(16):151–6.
11. Binbin L, Gou R, Zhang W. Study on DC circuit breaker for ±800 kV UHVDC system. Electr Equip. 2007;8(3):8–11.
12. Wen G. Development and structure analysis of the switchgear applied to UHVDC transmission system. High Volt Appar. 2012;48(11):134–8.

Chapter 22
Electromagnetic Environment of UHVDC System

Yiru Wan, Xiao Zhang and Jiyuan Li

The impacts of UHVDC transmission project on the environment consist of several aspects, such as synthetic electric field, ions flow, magnetic field, radio interference, and audible noise, which are the major technical problems that must be considered in the engineering design, construction, and operation of power transmission projects.

Because of the characteristic of UHVDC line, its corona effect and electromagnetic environmental effect are quite different from AC and EHVDC transmission line. Electric field effect of UHVDC transmission line is one of the important differences from UHVAC transmission line. When the conductor of AC transmission line produces corona, due to the alternation of voltage, most of the ions generated by the corona are restricted to the vicinity of the conductor or neutralized, and the movements away from the conductor basically do not exist, so only nominal electric field generated by the charge on the conductor exists; however, the ions generated by the corona of UHVDC transmission line will move to the reverse polarity conductors and ground under the influence of the electric field, forming an additional electric field, so the electric field intensity is formed by both the nominal field and the additional electric field.

Y. Wan (✉)
State Grid Hangzhou Power Supply Company, Hangzhou, Zhejiang, People's Republic of China
e-mail: 15652264@qq.com

X. Zhang
State Grid Weifang Power Supply Company, Weifang, Shandong, People's Republic of China
e-mail: 154476875@qq.com

J. Li
College of Electrical Engineering, Zhejiang University, Xihu District, Hangzhou, Zhejiang, People's Republic of China
e-mail: lijiyuan_ee@zju.edu.cn

© Zhejiang University Press, Hangzhou and Springer-Verlag GmbH Germany 2018

H. Zhou et al. (eds.), *Ultra-high Voltage AC/DC Power Transmission*,
Advanced Topics in Science and Technology in China,
https://doi.org/10.1007/978-3-662-54575-1_22

The radio interference and audible noise of DC transmission lines are mainly produced by corona discharge of conductors, insulators, and line fittings, etc. The corona discharge will be affected by weather conditions, so the radio interference and the audible noise of the lines will also change with the weather conditions and be different in the intensity. For AC transmission lines, the corona discharge phenomenon is more serious in rainy days, thus the radio interference and the audible noise under heavy rain conditions are the strongest, but the corona characteristics of DC lines are contrary to the AC lines; they are in the trend of being reduced with the increased humidity, namely the radio interference and audible noise in sunny days are stronger than those in rainy days.

22.1 Electromagnetic Environmental Issues of UHVDC Transmission Line

Electromagnetic environment parameters of ±800 kV HVDC transmission lines consist of ground synthetic electric field intensity, ion flow density, DC magnetic field, radio interference and audible noise. The following detailed explanations are given for the definitions of these five parameters [1].

(1) Ground synthetic electric field: the electric field intensity synthesized by both the electric field produced by the charge on DC charged conductor and the electric field produced by the space charge due to conductor corona, in units of kV/m. The value of the synthesized electric field intensity at the earth surface is the ground electric synthetic field intensity.
(2) Ion flow density: with DC conductor corona, the spatial movement of the ions formed by the ionization under the action of the electric force form an ion flow. The ion flow intercepted per ground unit area is called ion flow density, in nA/m^2.
(3) DC magnetic field: the magnetic field generated around the conductor due to the DC current flowing through the conductor is referred as DC magnetic field, which is expressed with magnetic induction intensity, in mT.
(4) Radio interference: the electromagnetic noise generated by power lines with radio frequency components is called as radio interference, in dB (V/m).
(5) Audible noise: a-weighted noise component generated by power line corona is called as audible noise, in dB (A).

The characteristics, limit values, and calculation methods of these five electromagnetic environment parameters will be introduced, respectively, in this chapter, because the electric field intensity at the surface of conductor is the basis of calculating the radio interference and audible noise, the calculation methods of the electric field intensity at the surface of conductor will also be introduced in this chapter, and finally a brief introduction to the corona loss will be made too.

22.1.1 Electric Field Intensity and Ion Flow Density

22.1.1.1 The Characteristics of Synthetic Electric Field and Ion Flow Density

The electric field intensity of UHVDC transmission line is formed under the joint action of the nominal electric field and the additional electric field, which is a unique phenomenon of UHVDC transmission lines, as well as one of the important differences from UHVAC transmission lines.

The generation mechanism of the synthesis electric field of UHVDC transmission line is complex. Without considering the impact of corona and the resulting ions on the electric field, the charge carried by the conductor itself will generate an electrostatic field around the conductor and above the ground, which is called as the nominal electric field. Considering the impact of the corona and the resulting ions on electric field, when the UHVDC transmission line conductor surface electric field intensity is stronger than the corona inception field intensity, the air near the conductor surface will be ionized, resulting in space charge and the corona. Under the action of electric field force, the ions move toward the conductors and ground of opposite polarity to form an ion flow. The ions intercepted per unit area of the ground are called as the ion flow density. The ion flow will lead to the space charge being distributed between the two conductors as well as the conductor and the ground, forming an additional electric field.

The nominal electric field and the additional electric field, through vector superposition, form into a synthetic electric field of which the horizontal component near the ground is very small, while the vertical component is very large. Thus, the synthetic electric field is mainly determined by vertical components. Because the additional electric field is much larger than the nominal electric field, the magnitude of the synthetic electric field mainly depends on the additional electric field. The magnitude of the additional electric field depends on the severity of the corona discharge on the conductor surface. The severities of corona discharge on the conductor surface vary in different weather conditions, and different conductor surface properties such as roughness and radius of the conductor can also affect the severity of the corona discharge on the conductor surface.

By comparison, when corona occurs on the UHVAC transmission line, due to the alternation of voltage, the majority of ions generated by the corona are limited in the vicinity of the conductor or neutralized, so that the ion movement away from the conductor basically does not exist; therefore, no ion flow and additional electric field will be produced. This is the biggest difference between the electric fields generated by UHVDC transmission line and UHVAC transmission line.

It is pointed out by International Commission on Non-Ionizing Radiation Protection (ICNIRP) that, when the electric field intensity is 25 kV/m or less, it will not produce the discomfort caused by surface charge for most people. It is shown in the test of ±500 kV DC transmission line by American Bonneville Power Authority that, for the people who wear ordinary shoes, when the electric field is

30 kV/m, they may begin to feel stabbing pain on their hair and in their skin. From the studies on DC field intensity made by the former Soviet Union, it is considered that the allowable electric field under DC transmission line may be up to 50 kV/m.

In China, it is shown through human direct feeling test under the DC transmission line made by China Electric Power Research Institute that hair and skin are most sensitive to DC electric field. In the place where the ground synthetic electric field intensity is less than 30 kV/m, part of the test participants have their hair erected upwardly, but no obvious discomfort in the skin; in the place with the synthetic electric field intensities of 30, 35, 38 V/m, and 44 kV/m, respectively, the feelings of exposed skin are divided into faint sense of stimulation, the relatively obvious sense of stimulation, and clear and very strong sense of stimulation. After the test participants left the high-field region, the skin stimulation feeling disappeared immediately, without any discomfort. It is shown by the above tests that, under the DC transmission line, when the synthetic electric field exceeds 30 kV/m, the human body begins to have significant discomfort.

In addition to the effects of the DC synthetic electric field, the feeling of human body intercepting the ions flow is also one of the factors to be considered in the electromagnetic environment of DC transmission line. Studies have shown that, to get the same degree of feeling, the DC current flowing through the body should be five times larger than AC current, while the current intercepted by the person standing under the DC transmission line is less than the critical value that can be felt by two orders of magnitude, so the people standing under the line generally do not have any feeling, namely the ion flow density has little effect on the human body.

22.1.1.2 Limit Standard of Synthetic Electric Field and Ion Flow Density

The nominal electric field cannot be monitored in practice, and in the vicinity of HVDC transmission lines, the synthetic electric field under the joint action of the nominal electric field and the additional electric field has an impact on the human body, so the synthetic electric field is used as the limit indicator of DC transmission project.

Currently, there are not uniform regulations for the limits of the ground synthetic electric field and ion flow density under DC transmission lines worldwide:

(1) U.S.: the limits of ground synthetic electric fields under lines specified by Department of Energy and the North Dakota state are 30 and 33 kV/m, respectively; the occupational exposure limit of DC field specified by Industrial Hygiene Association is 25 kV/m; if the electric field is less than 15 kV/m, it is not necessary to consider the transient electric shock.
(2) Canada: the limits of ground synthetic electric field under line and ion flow density are 25 kV/m and 100 nA/m^2, respectively; the nominal electric field limit at corridor edge is 2 kV/m.
(3) Brazil: the limit of the ground synthetic electric field under Itapúa ±600 kV DC transmission line is 40 kV/m.

(4) The Soviet Union: the limit of the ground synthetic electric field under ±750 kV DC transmission line was taken as 25 kV/m for non-residential areas, and taken as 10 kV/m for residential areas.
(5) Germany: the occupational exposure limit of DC field is 40 kV/m; if the exposure time is 2 h per day, the allowable limit may be up to 60 kV/m.
(6) EU: the occupational exposure limit of DC field is 42 kV/m, and public exposure limit is 14 kV/m.
(7) China: it is specified in the power industry standard DL/T 436-2005 "*Technical Guidelines of HVDC Overhead Transmission Lines*" implemented from June 1, 2006 that the maximum ground field intensity under ±500 kV DC transmission lines should not exceed 30 kV/m, and the maximum ion flow density should not exceed 100 nA/m^2, and the maximum synthetic ground electric field in the places where residential houses are located should not exceed 15 kV/m.

For UHVDC transmission lines, it is specified in the power industry standard DL/T 1088–2008 "*The Limits of Electromagnetic Environment Parameters of* ±800 kV *UHVDC Transmission Lines*" implemented from November 2008 that if ±800 kV DC transmission lines are near the residential houses, the ground synthetic field limit should be 25 kV/m, and the 80% measured value should not exceed 15 kV/m (the 80% measured value refers to the 81st measurement result by assuming 100 groups of measurement data and arranging the measurement results obeying ascending order), and the limit of ground synthetic field intensity in the areas with the lines crossing over the farmland, roads and other areas where people are easy to reach is 30 kV/m, and the limit of ground synthetic field intensity of the lines in the mountains and other areas where people are difficult to reach should be checked based on the electrical safety distance. The limit of ion flow density under ±800 kV DC overhead transmission lines is taken as 100 nA/m^2.

22.1.1.3 Calculation Method of Synthetic Electric Field

The synthetic electric field of UHVDC transmission line is formed by superposing the nominal electric field generated by DC voltage and the additional electric field generated by space ions. Its mathematical model is shown as follows, and it is usually calculated using the finite element method or finite difference method.

$$\begin{cases} \nabla E = (\rho_{\mathrm{p}} - \rho_{\mathrm{n}})/\varepsilon_0 \\ \nabla J_{\mathrm{p}} = -R_{\mathrm{i}}\rho_{\mathrm{p}}\rho_{\mathrm{n}}/q_{\mathrm{e}} \\ \nabla J_{\mathrm{n}} = R_{\mathrm{i}}\rho_{\mathrm{p}}\rho_{\mathrm{n}}/q_{\mathrm{e}} \\ J_{\mathrm{p}} = M_{\mathrm{p}}\rho_{\mathrm{p}}E - D_{\mathrm{p}}\nabla\rho_{\mathrm{p}} + v\rho_{\mathrm{p}} \\ J_{\mathrm{n}} = M_{\mathrm{n}}\rho_{\mathrm{n}}E - D_{\mathrm{n}}\nabla\rho_{\mathrm{n}} + v\rho_{\mathrm{n}} \\ J = J_{\mathrm{p}} + J_{\mathrm{n}} \\ \nabla J = 0 \\ E = -\nabla U \end{cases} \tag{22.1}$$

where

E synthetic field intensity, V/m;
ρ_p, ρ_n positive and negative charge density, C/m^3;
q_e the charge amount of one electron, i.e., 1.602×10^{-19} C;
R_i ion recombination rate, taken as 2×10^{-12} m^3/s;
J_p, J_n positive and negative current density, A/m^2;
M_p positive ion migration rate, taken as 1.5×10^{-4} m^2/V s;
M_n negative ion migration rate, taken as 1.9×10^{-4} m^2/V s;
D_p positive ion diffusion coefficient, taken as 3.8×10^{-6} m^2/s;
D_n negative ion diffusion coefficient, taken as 4.2×10^{-6} m^2/s;
v wind speed, m/s, in case of wind, it is assumed as perpendicular to the line;
U potential to ground, V.

22.1.2 DC Magnetic Field

22.1.2.1 Characteristics of DC Magnetic Field

The magnetic field generated by DC transmission lines has the same principle with the power frequency magnetic field of AC lines, i.e., both are generated by current, and the magnetic field of DC transmission lines is generated by the positive and negative current in both directions. Starting from the ground upward, the magnetic field will be increased with the increasing distance from the ground, and rapidly decayed with the increasing horizontal distance between the two conductors. The maximum magnetic induction intensity is at micro-Tesla (μT) level.

22.1.2.2 Limit Standard of DC Magnetic Field

For the magnetic field intensity, other countries besides China have not specifically developed the standards to limit the magnetic field of DC transmission line at present. It is recommended by International Commission on Non-Ionizing Radiation Protection (ICNIRP) that the public exposure limit to the magnetic field lower than 1 Hz should be taken as 40 mT. The maximum magnetic induction intensity near the ground under ±800 kV DC transmission line is only about 1/600 of the public exposure limit recommended by ICNIRP, which is lower than the earth's magnetic field by an order of magnitude. This level of magnetic field to which people have long been accustomed will not affect people's health [2].

For ±800 kV UHVDC transmission lines, it is specified in Chinese power industry standard DL/T 1088–2008 "*The Limits of Electromagnetic Environment Parameters of* ±800 kV *UHVDC Transmission Lines*" that the limit of the magnetic induction intensity under ±800 kV DC transmission lines is 10 mT.

Since the magnetic induction intensity under ±800 kV DC transmission lines is far less than the limit of 10 mT, it is unnecessary to consider the DC magnetic field during the investigation of the electromagnetic environment of transmission lines.

22.1.2.3 Calculation Method of DC Magnetic Field

The calculation method of magnetic field is relatively mature and accurate. The calculation method of DC line is as follows:

$$H=\frac{I}{2\pi}\left[\frac{h-h_1}{(h-h_1)^2+(x-S/2)^2}+\frac{h-h_1}{(h-h_1)^2+(x+S/2)^2}\right], \tag{22.2}$$

where

I the current of each pole, in A;
h the average height of the conductor (defined as the minimum distance to ground + 1/3 sag), in m;
h_1 the height of observation point above the ground, in m;
x the horizontal distance to the center of the column, in m;
S the interpolar distance, in m.

22.1.3 Surface Electric Field Intensity of Conductor

The surface electric field intensity of conductor directly affects the level of radio interference and audible noise. The calculation of conductor surface field intensity is the basis of calculating radio interference and audible noise. Maxwell potential coefficient method, charge simulation method, and CDEGS can be used for calculating the surface electric field intensity of the conductor.

1. Maxwell potential coefficient method

When Maxwell potential coefficient method is used for the calculation, for the transmission lines with each phase being composed of a single conductor, the conductor surface electric field can be expressed with the line charge concentrated in the center of each conductor; for the transmission lines being composed of bundled conductors, the surface electric field can be calculated approximately using the equivalent single conductor instead of bundled conductors:

(1) The equivalent radius of bundled conductors is calculated as follows:

$$R_{\mathrm{eq}}=R(\sqrt[N]{Nr/R}), \tag{22.3}$$

where

N the number of bundled conductors;
R the radius of the circle where the sub-conductors are located, in m;
r the radius of the sub-conductors, in m.

(2) the charge Q on each pole can be obtained by Maxwell potential coefficient method as follows:

$$[V] = [P] \cdot [Q] \tag{22.4}$$

(3) The average potential gradient on the surface of conductor is as follows:

$$E_{\text{av}} = \frac{Q}{2\pi\varepsilon r N}. \tag{22.5}$$

(4) The maximum potential gradient on the surface of the conductor is as follows:

$$E = E_{\text{av}}\left[1 + (N-1)\frac{r}{R}\right]. \tag{22.6}$$

The solution process of the maximum potential gradient on the surface of the conductor of DC bipolar line is described in detail as below. In Fig. 22.1, conductors 1 and 2 stand for the ground wires, and conductors 3 and 4 are bipolar transmission lines, and 1′, 2′, 3′, and 4′ are, respectively the mirror images of the conductors 1, 2, 3, and 4 to the ground. It is assumed that the ground line 1 and 2 have charge $+Q_1$ and $-Q_1$, respectively, and no voltage on the ground wires; it is assumed that the transmission lines 3 and 4 are charged with $+Q$ and $-Q$, and the conductor voltages are $+U$ and $-U$, respectively.

Thus, the expression $[V] = [P] \cdot [Q]$ in step 2 may be specifically written as:

$$\begin{bmatrix} 0 \\ 0 \\ U \\ -U \end{bmatrix} = \begin{bmatrix} p_{11} & p_{12} & p_{13} & p_{14} \\ p_{21} & p_{22} & p_{23} & p_{24} \\ p_{31} & p_{32} & p_{33} & p_{34} \\ p_{41} & p_{42} & p_{43} & p_{44} \end{bmatrix} \begin{bmatrix} Q_1 \\ -Q_1 \\ Q \\ -Q \end{bmatrix} \tag{22.7}$$

Because the Eq. (22.7) contains two unknowns Q_1 and Q, so only two equations are needed to solve the charge Q on the pole conductor, and one equation must be

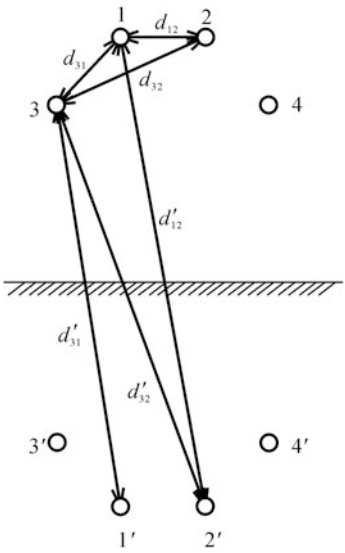

Fig. 22.1 Maxwell potential coefficient method

selected from the first and second rows, and the other equation must be selected from the third and fourth rows. Here, the first and third rows are set for simultaneous equations as follows.

$$\begin{cases} (p_{11} - p_{12})Q_1 + (p_{13} - p_{14})Q = 0 \\ (p_{31} - p_{32})Q_1 + (p_{33} - p_{34})Q = U \end{cases} \tag{22.8}$$

According to the corresponding P matrix coefficients, the relational expression between the amount of pole conductor charge Q and the pole conductor voltage U can be obtained, and the P matrix is related to such factors as the average height of pole conductor h, the average height of ground wire h_1, the radius of ground wire r_1, the equivalent radius of pole conductor R_{eq}, the spacing between pole conductors S, and the distance between each two conductors d. The P matrix coefficients required here are calculated as follows:

$$\begin{cases} p_{11} = \frac{1}{2\pi\varepsilon}\ln\frac{2h_1}{r_1}, p_{12} = \frac{1}{2\pi\varepsilon}\ln\frac{d'_{12}}{d_{12}}, p_{13} = \frac{1}{2\pi\varepsilon}\ln\frac{d'_{13}}{d_{13}}, p_{14} = \frac{1}{2\pi\varepsilon}\ln\frac{d'_{14}}{d_{14}} \\ p_{31} = \frac{1}{2\pi\varepsilon}\ln\frac{d'_{31}}{d_{31}}, p_{32} = \frac{1}{2\pi\varepsilon}\ln\frac{d'_{32}}{d_{32}}, p_{33} = \frac{1}{2\pi\varepsilon}\ln\frac{2h}{\mathrm{R}_{eq}}, p_{34} = \frac{1}{2\pi\varepsilon}\ln\frac{\sqrt{(2h)^2 + S^2}}{S} \end{cases} \tag{22.9}$$

After the P matrix coefficients are substituted into Eq. (22.8), the relational expression between pole conductor charge Q and conductor voltage U can be obtained as follows:

$$Q = \frac{2\pi\varepsilon U}{K}, K = \ln\frac{2h}{(NrR^{N-1})^{\frac{1}{N}}\sqrt{\left(\frac{2h}{S}\right)^2+1}} - \frac{\ln\frac{d'_{13}d_{32}}{d_{13}d'_{32}}\ln\frac{d'_{13}d_{14}}{d_{13}d'_{14}}}{\ln\frac{2h_1d_{12}}{r_1d'_{12}}} \tag{22.10}$$

Then Q is substituted into Eq. (22.5) in step 3, the following can be obtained

$$E_{\text{av}} = \frac{U}{rNK} \tag{22.11}$$

Finally, E_{av} is substituted into Eq. (22.6) in step 4, the following can be obtained

$$E = \frac{U}{rNK}\left[1 + (N-1)\frac{r}{R}\right]. \tag{22.12}$$

The parameters used in the above calculation process are as follows:

h_1 the average height of ground wire (defined as the minimum distance to ground + 1/3 sag), in cm;
r_1 the radius of ground wire, in cm;
U the conductor-to-ground voltage, in kV;
h the average height of conductor (defined as the minimum distance to ground + 1/3 sag), in cm
r the radius of sub-conductor, in cm;
N the number of bundled conductors;
R the radius of the circle where the sub-conductors are located, in cm;
S the interpolar distance, in cm;
d_{kj} the distance between the conductor j and conductor k, in cm;
d'_{kj} the distance between the conductor k and the ground mirror image j' of the conductor j, in cm.

2. Charge simulation method

Charge simulation method is a common method of calculating the conductor surface electric field, and it is composed on the basis of the extension of the mirror method. This method is suitable for the calculation of the electric field with infinite field domain, thus avoiding the errors due to the sealed edge, making the dimensions of the calculation being reduced by one dimension, so we can use the direct method to solve the equations. Because the field intensity at any point in the domain can be solved directly according to the charge, no electric potential numerical differentiation is required for the solution, so the calculation accuracy of field intensity is higher. However, the charge simulation method can only approximately simulate the given boundary conditions in the problem, so the solution to the electrostatic field problem obtained by this method is also the approximate solution, and there are some errors from the real solution. By optimizing the position,

electricity, and number of the simulation charge in the invalid field domain, the errors can be reduced and the equivalent accuracy of the simulation charge can be improved.

When the charge simulation method is used for calculating the electrostatic field, the charging charge on the surface of the live body or the bound charge appearing on the boundary surface of different media can be replaced by the equivalent charge located at the invalid region, which is called simulation charge. The so-called equivalence means the potential or electric field formed by these simulation charges at the original field boundary can meet the given boundary conditions. So the linear equations taking these analog electricity charges as unknowns can be written. After the electricity of these simulation charges is obtained, according to the superposition principle, the potential and electric field distribution within the field domain can be obtained. Based on uniqueness theorem of electromagnetic field, the free charges continuously distributed on the electrode surface or the bound charges continuously distributed on the media boundary surface can be equivalent to a set of discrete analog charges using the charge simulation method; then based on the principle of superposition, the electric field generated by the discrete analog charge in the space is calculated for vector superposition, and the approximate distribution of the electric field generated by the original charge distributed continuously is obtained.

For the electric field of a long straight charged round conductor in single homogeneous medium, the solving steps using the charge simulation method are as follows:

(1) Outside the calculation field domain, n pieces of analog charges Q_j (j = 1, 2, … n) are assumed as line charges $\tau_1, \tau_2, \ldots \tau_n$, to replace equivalently the charges continuously distributed on the conductor.
(2) On the conductor surface, assume the matching points M_i (i = 1, 2, … n) with the number equal to the number of analog charges, and the potential φ_i at each match point is known.

The layout of simulation charges and the match points have a great influence on the calculation accuracy. The simulation charge should be placed in alignment with the match point and it should be better to fall on the perpendicular line of the border. Assuming the vertical distance from the simulation charge to the boundary surface is "a" and the distance between the adjacent two matching points from left to right is "b", the arrangement of simulation charges and matching points is shown in Fig. 22.2. According to the experience, the value of $f = a/b$ is taken as 0.2–1.5, usually as 0.75. When the match points are distributed sparsely, a small value should be taken for f; when the match points are distributed densely, a big value should be taken for f. If the simulation charge is taken too less or too much, it will result in the situation that the equipotential surface of synthetic potential can not be approximate with the surface shape of electrode.

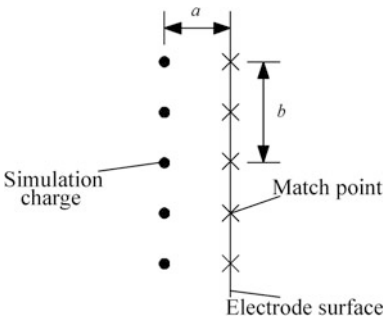

Fig. 22.2 Layout of simulation charges and match points

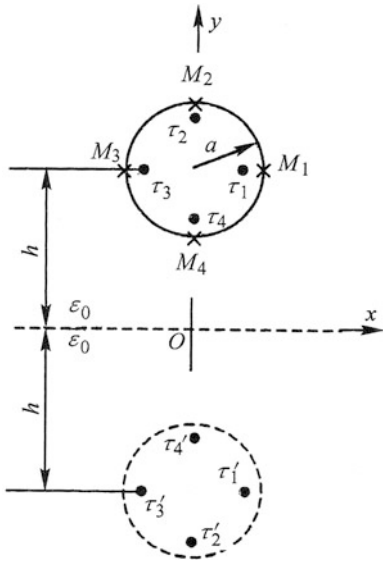

Fig. 22.3 Application of charge simulation method

(3) In order to maintain the ground potential as 0, an equivalent charged round conductor in mirror symmetry with the charged round conductor should be introduced. The simulation charge of the equivalent charged round conductor has the same setting as the original conductor, but the equivalent negative values $\tau_1', \tau_2', \ldots \tau_n'$ are taken for n pieces of analog line charges, as shown in Fig. 22.3.

(4) According to the principle of superposition, the potential generated by the simulation charge on the matching point i is as follows:

$$\varphi_i = P_{i1}Q_1 + P_{i2}Q_2 + \cdots + P_{in}Q_n - P_{i1'}Q_1 - P_{i2'}Q_2 - \cdots - P_{in'}Q_n \quad (22.13)$$

For each match point M_i of the original conductor, the potential expressions established by the analog charges can be listed as follows:

$$\begin{cases} \varphi_1 = P'_{11}Q_1 + P'_{12}Q_2 + \cdots + P'_{1n}Q_n \\ \varphi_2 = P'_{21}Q_1 + P'_{22}Q_2 + \cdots + P'_{2n}Q_n \\ \vdots \\ \varphi_n = P'_{n1}Q_1 + P'_{n2}Q_2 + \cdots + P'_{nn}Q_n \end{cases} \tag{22.14}$$

The linear algebraic equations in n-order, namely charge simulation equations are composed.

$$[\varphi] = [P][Q] \tag{22.15}$$

In the above equation, the element $P'_{ij} = P_{ij} - P_{ij'}$ of potential coefficient matrix $[P]$ stands for the potential value generated by No. j unit analog charge source on the No. i matching point, and is called as potential coefficient. P'_{ij} is related to the relative positions of the analog charge and the match point, the dielectric constant of media and the type of simulation charge, and not related to the amount of the simulation charge.

(5) Calculation of the potential coefficient matrix $[P]$

The key to calculate the electric field using the charge simulation method is the calculation of potential coefficient matrix $[P]$, which is directly determined by the type of simulation charge to be used. The analog charges set above are a pair of infinite long line charges with the same values, but the opposite polarity. Assuming the line charges $+\tau$ and $-\tau$ are placed symmetrically along the xOz plane in the rectangular coordinate system, their positions are as shown in Fig. 22.4.

Taking $y = 0$, i.e., x-axis is taken as the reference point of potential, the potential generated by this pair of line charges at any field point $A(x, y)$ is as follows:

$$\varphi = \frac{\tau}{2\pi\varepsilon}\ln\frac{\rho_2}{\rho_1}, \tag{22.16}$$

where $\rho_1 = \sqrt{(x-x_1)^2 + (y-y_1)^2}$ and $\rho_2 = \sqrt{(x-x_2)^2 + (y-y_2)^2}$ are the distances from the line charge $+\tau$ and $-\tau$ to the site point A, respectively. The corresponding potential coefficient can be obtained as follows:

$$P = \frac{1}{2\pi\varepsilon}\ln\frac{\rho_2}{\rho_1} \tag{22.17}$$

(6) Solve the charge simulation equations, then each simulation charge value $[Q]$ can be obtained.

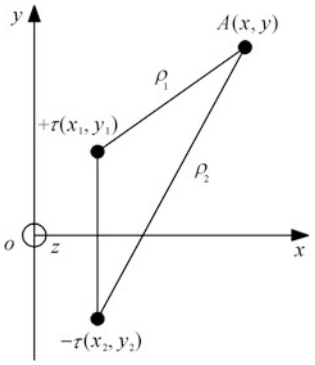

Fig. 22.4 One pair of unlimited long line charges

(7) Take several checking points at the electrode surface additionally to verify the calculation accuracy. If it does not meet the requirement, then the position, number or shape of the analog charge is to be corrected, until it meets the requirement of calculation accuracy.
(8) Based on the calculated ultimately discrete solution of analog charge [Q] at last, the electric field intensity of the conductor surface can be calculated.

For a calculating point on the surface of the conductor, at first, the electric field intensity generated in the x direction and the y direction of the point by each pair of simulation charges $\pm Q_i$ are to be calculated, respectively, the gradient relationship between the electric field intensity and the potential can be obtained as follows:

$$\overrightarrow{E} = -\nabla\varphi = -\left(\frac{\partial\varphi}{\partial x}\overrightarrow{i} + \frac{\partial\varphi}{\partial y}\overrightarrow{j}\right) = f_x\tau\overrightarrow{i} + f_y\tau\overrightarrow{j} \tag{22.18}$$

In the equation, $\overrightarrow{i}$, $\overrightarrow{j}$ are the unit vectors in x and y-axis direction, respectively. Therefore, the electric field intensity coefficients are as follows:

$$\begin{aligned} f_x &= -\frac{\partial P}{\partial x} = \frac{1}{2\pi\varepsilon}\left(\frac{x-x_1}{\rho_1^2} - \frac{x-x_2}{\rho_2^2}\right) \\ f_y &= -\frac{\partial P}{\partial y} = \frac{1}{2\pi\varepsilon}\left(\frac{y-y_1}{\rho_1^2} - \frac{y-y_2}{\rho_2^2}\right) \end{aligned} \tag{22.19}$$

The electric field intensities in the x direction and y direction are as follows:

$$\begin{aligned} E_{xi} &= f_x Q_i \\ E_{yi} &= f_y Q_i \end{aligned} \tag{22.20}$$

It can be known from Step 3 that n pairs of analog charges with the same size, opposite polarity, showing mirror symmetry are set up in total, and the electric field intensities of these n pairs of analog charges at the calculation points are decomposed

into x and y directions, and they are added, respectively, in the x direction and the y direction, i.e., $E_x = \sum_{i=1}^{n} E_{xi}, E_y = \sum_{i=1}^{n} E_{yi}$, and $E = \sqrt{E_x^2 + E_y^2}$ is the total electric field intensity of the calculated point. The very dense calculation points with the same spacing on the surface of each conductor should be taken to calculate the total field intensity, of which the maximum value of the electric field intensity is taken as the maximum electric field intensity of the surface of the conductor.

For each sub-conductor of the positive and negative conductor bundles and two ground wires of UHVDC transmission line, if the pole conductor uses 6 bundled conductor, then a total of 14 conductors are required. A model should be set up according to the above method for the calculation, through which the maximum electric field intensity on the surface of each sub-conductor can be obtained; for monopolar conductors, the average of the maximum electric field intensities on the surface of sub-conductors should be taken as the maximum electric field intensity on the surface of the pole conductor. The larger value of the maximum surface electric field intensities of positive and negative conductors should be taken as the maximum surface electric field intensity of the conductors of UHVDC lines.

3. Calculating the maximum surface electric field intensity of the conductor with CDEGS

Enviro module of CDEGS adopts the principle of continuous mirroring method. The idea of this principle lies in the fact that, in a system consisting of multiple conductors, each conductor is to be replaced by a series of image charges disposed in the conductor to maintain the equipotential on the surface, and then the conductor surface and spatial electric fields are calculated based on these image charges.

4. Calculation and comparison of maximum electric field intensities on conductor surface of UHVDC transmission lines

In order to study the differences in calculating the maximum surface electric field intensities of the conductors with the above three methods, Maxwell potential coefficient method, charge simulation method, and CDEGS will be used, respectively, as below to calculate the maximum surface electric field intensity of conductors on typical towers of Yunnan–Guangdong UHVDC transmission line. The operating voltage of the line is 800 kV, the pole conductor height above the ground is 18 m, the interpolar distance is 22 m, the conductor mode is 6×LGJ-630/45, the ground wire mode is LBGJ-180-20AC, and the bundled conductor spacing is 0.45 m. The results are shown in Table 22.1.

Table 22.1 Comparison of the maximum surface electric field intensities of conductor calculated with different methods

Calculation method	Maxwell potential coefficient method	Charge simulation method	CDEGS
The maximum electric field intensity on the surface of conductor, kV/cm	23.71	23.72	23.73

It is shown in Table 22.1 that there is a very small error among the conductor surface electric field intensities calculated, by Maxwell potential coefficient method, charge simulation method and CDEGS. The charge simulation method requires programming for the calculation, so it is complex relatively. The application penetration rate of CDEGS is not high. Therefore, under normal circumstances, Maxwell potential coefficient method can be used to calculate the maximum surface electric field intensity of UHVDC conductors, because this method is more simple and convenient, and the accuracy is higher.

22.1.4 Radio Interference

22.1.4.1 Characteristics of Radio Interference

The radio interference of UHVDC transmission line is mainly generated by the corona discharge of conductors, insulators, and line fittings etc., and its frequency is within the 30 MHz. In the low-frequency band, the field intensity of radio interference for DC transmission line is higher; while in the high frequency band, the field intensity of radio interference is lower. When the frequency is higher than 10 MHz, the interference intensity can be neglected.

Because the intensity of corona discharge is affected by different weather conditions, the field intensity of radio interference for the lines will change with different weather conditions. For AC transmission lines, the corona discharge phenomenon is more serious in rainy days; therefore, the radio interference under heavy rain condition is the strongest and higher than the situations in drizzle or sunny days. However, the radio interference characteristics of DC transmission lines are opposite to AC transmission lines, they are reduced with the increased humidity, namely, the radio interference under sunny days is greater than that in rainy days by about 3 dB.[1] This phenomenon may be explained as follows: the corona inception electric field intensity of conductor in rainy days is lower than that in sunny days, and the ions around the conductor are more than that in the sunny days, so at early stage of raining, when the ion concentration on the conductor surface is not high, the corona discharge is slightly stronger than that in sunny days; but after a period of raining time, the corona inception electric field intensity of conductor is further reduced, the ions on the surface of conductor increase, so that the irregular surface of the conductor is surrounded by more charges, thereby reducing the intensity of the corona discharge, so the radio interference in rainy days has been reduced compared to that in sunny days. Meanwhile, the radio interference of DC transmission line will increase with the increase of temperature. As the seasons change, the radio interference in late autumn and early winter is

[1]The unit of radio interference is in μV/m, usually expressed in dB, and 1 μV/m corresponds to 0 dB.

lower and is at maximum in summer. It is shown from the above analysis that the radio interference of DC transmission line is most serious in sunny days of summer.

For the lines with the same structure, the radio interference would increase with the increase of altitude. Researches show that the radio interference will be increased by about 1 dB every increment of altitude of 300 m. In addition, the radio interference of DC transmission line has the lateral attenuation trend that is almost symmetrical to the positive conductor, and it will rapidly decay with the increasing distance from the conductor.

22.1.4.2 Limit Standard of Radio Interference

Because of different national circumstances, the voltage levels of DC transmission lines are different, and the parameters of the transmission lines are also different, so there are still no uniform international standards on the radio interference limits of the DC transmission lines.

Canada uses different limits for different voltage levels. For the transmission lines of 600 kV or above, at 15 m away from the ground projection of side conductors, the radio interference limit of 0.5 MHz is 63 dB. Converted to 20 m away from the ground projection of side conductors, it is about 61 dB.

According to Chinese GB 15707-1995 "*Radio Interference Limits of High Voltage AC Overhead Transmission Lines*" and HJ/T 24–1998 "*Technical Specifications of Environmental Impact Assessment of Electromagnetic Radiation of* 500 kV *EHV Transmission and Substation Projects,*" 55 dB is taken as the limit standard, and the reference point is set at 20 m away from the ground projection of side phase conductors. For the evaluation criteria of radio interference of Chinese 1000 kV UHVAC lines, the limit standard is taken as 58 dB, with reference frequency of 0.5 MHz, and the reference point is set at 20 m away from the ground projection of side phase conductors.

For ±800 kV UHVDC transmission lines, it is specified in Chinese power industry standard DL/T 1088–2008 "*Electromagnetic Environment Parameter Limits of* ±800 kV *UHVDC Transmission Lines*" that: at 20 m away from the ground projection of positive polarity conductors of DC overhead transmission lines, the radio interference limit at frequency of 0.5 MHz should be taken as 58 dB (μV/m), and the measurement value under good weather conditions should not be larger than 55 dB (μV/m); when the altitude is higher than 1000 m, the radio interference limits should be linear corrected in accordance with 3 dB/1000 m.

22.1.4.3 Calculation Methods of Radio Interference

IEC International Special Committee on Radio Interference (CISPR) recommended the equation as below:

$$\mathrm{RI} = 38 + 1.6(g_{\max} - 24) + 46\log(r) + 5\log(N) + \Delta E_{\mathrm{f}} + 33\log\left(\frac{20}{D}\right) + \Delta E_{\mathrm{w}}, \tag{22.21}$$

where

RI the calculated value of radio interference, in dB;
$g_{\max}$ maximum potential gradient on conductor surface, in kV/cm;
r the radius of sub-conductor, in cm;
N the number of sub-conductors;
D the distance from the calculation point to the positive conductor, in m;
ΔE_{w} meteorological correction item, taking the altitude of 500 m as the benchmark, 3.3 dB should be added with each increment of 1000 m;
ΔE_{f} interference frequency correction item, $\Delta E_{\mathrm{f}} = 5[1 - 2(\log(10f))^2]$;
f the frequency required for calculations, in MHz.

What is calculated using the above equation at the reference frequency of 0.5 MHz is the 50% radio interference value at 20 m away from the positive conductor in sunny days. After the addition of 3 dB, it becomes the 80%//80% value.

In addition, there are many other methods to calculate the level of radio interference. In 1960s, BPA and EPRI had studied the bipolar DC line at Dallas ±600 kV test site and obtained the calculation equation of radio interference in sunny days as follows:

$$\mathrm{RI} = 214\lg\frac{E_{\mathrm{m}}}{E_0} - 278\left(\lg\frac{E_{\mathrm{m}}}{E_0}\right)^2 + 40\lg r + 27\lg\frac{834}{f} + 40\lg\frac{30.5}{D}, \tag{22.22}$$

where

RI the radio interference level at 30.5 m away from the positive conductor, in dB;
E_0 assumed as 14 kV/cm in the EPRI test;
r the radius of the sub-conductors, in cm;
f the frequency measurement, in MHz;
D the radial distance from the measured point to the positive conductor, in m.

The calculation equation of BPA based on the short-term test data is as follows:

$$\mathrm{RI} = \mathrm{RI}_0 + 1.5(E_{\mathrm{m}} - 20.9) + 10\lg\frac{n}{2} + 40\lg\frac{d}{4.577} - 33\lg\frac{f}{0.834}, \tag{22.23}$$

where

RI the peak value of radio interference, in dB;
d the diameter of sub conductor, in cm;
RI_0 the interference value of 51 dB at 15.2 m horizontal distance from the positive conductor, or the interference value of 40 dB at 30.5 m horizontal distance from the positive conductor.

Through a lot of long-term and short-term tests on the ±750–1200 kV test line, EPRI had obtained the empirical equation as follows:

$$RI = 63.0 + 86 \lg \frac{E_m}{25} + 10 \lg \frac{n}{3} + 40 \lg \frac{d}{4.57} + 20 \lg \frac{2}{1+f^2} + 40 \lg \frac{15}{D}. \quad (22.24)$$

Generally, the equation recommended by IEC International Special Committee on Radio Interference (CISPR) is used in most cases.

22.1.5 Audible Noise

22.1.5.1 Characteristics of Audible Noise

The audible noise generated by DC transmission line corona is a kind of broadband noise with higher frequency, and can be extended from a few hundred Hertz to ten thousands of Hertz. The attenuation of normal ambient noise is started at low frequencies, while the attenuation of DC transmission line audible noise is started at high frequencies. In addition, the audible noise of DC transmission line does not include low-frequency pure tone, so the attenuation of DC transmission line audible noise is very slow, especially in the case of low ambient noise; it is easy to distinguish them. Compared with AC transmission lines, when the audible noise is lower than 50 dB, the audible noise of DC and AC transmission lines will bring the same degree of annoyance to people, but after it is higher than 50 dB, the audible noise of DC transmission line will bring more irritable feeling to people. Therefore, the audible noise of DC transmission line is easier to bring people with irritable hearing feeling, which becomes the focus of complaints.

The audible noise of DC transmission line is distributed by taking the positive conductor as the center, forming into a basically symmetrical lateral attenuation trend. With the increase of the horizontal distance from the pole conductor, the attenuation speed of audible noise is slower than that of synthetic electric field and radio interference. Meanwhile, the wind also has some impacts on the distribution of audible noise.

For AC transmission lines, the corona discharge phenomenon in rainy days is more serious, and thus audible noise under heavy rain conditions is the strongest, and higher than the situations in sunny or drizzle days. However, the audible noise characteristics of DC transmission lines are opposite to those of AC transmission

lines. It is in a reduction trend with the increase of humidity, i.e., the audible noise under sunny conditions is stronger than that under rainy conditions. This phenomenon can be explained as that: the corona inception electric field intensity of conductor in rainy days is lower than that in sunny days, and the ions surrounding the conductor is more than those in sunny days, so at the early stage of the rain period, the ion concentration on the conductor surface is not high, and the corona discharge is slightly stronger than that in sunny days. However, after the rain continues for some time, the corona inception electric field intensity of conductor is further reduced, the ions on the surface of conductor increase, so that the irregular surfaces of the conductor are surrounded by denser charges, reducing the intensity of corona discharge, so the audible noise in rainy days is lower than those in sunny days.

In summer, there are more falling objects in the air which will cause local surface field intensity to increase by attaching to the conductor, leading to the increase of audible noise, so the audible noise of DC transmission lines is at maximum in summer.

According to the above characteristics, when determining the audible noise limits of DC transmission line, the reference point should be normally selected outside the positive conductor, and the case of summer sunny days should be considered as the focus. For the lines with the same structure, the audible noise will increase with the increasing altitude. Researches show that the audible noise will be increased by about 1 dB (A) with every increment of altitude of 300 m.

22.1.5.2 Limit Standard of Audible Noise

Operating experiences show that basically there will be no complaints if the audible noise of transmission lines is lower than 52.5 dB (A), a small amount of complaints within the range of 52.5–59 dB (A), and a large number of complaints after it reaches 59 dB (A) or above. It is shown by the studies that when the noise is at 40 dB (A) or below, people can maintain normal sleep; if it is more than 50 dB (A), about 15% of people's sleep will be affected. The audible noise of DC transmission lines should be controlled so that people under the line will not feel annoyance and it will not affect the rest of the nearby residents, so as to ensure no complaints.

In Chinese GB 3096-2008 "*Acoustic Environmental Quality Standards,*" the different standards for transmission lines are divided to be applicable to different regions:

Class 0 acoustic environment functional area: refers to the area that needs to keep quiet especially, such as rehabilitation and wellness areas.
Class 1 acoustic environment functional area: refers to the area that needs to keep quiet and is mainly functioned as residential, health, culture, education, scientific research and design, and administrative office areas.
Class 2 acoustic environment functional area: refers to the area that take commercial finance, fair trade as the main function, or mixed with residential, commercial, industrial areas that needs to maintain quiet.

Table 22.2 Urban regional environmental noise standards (unit: dB)

Category		Daytime	Nighttime
0		50	40
1		55	45
2		60	50
3		65	55
4	4a	70	55
	4b	70	60

Class 3 acoustic environment functional area: refers to the area that is mainly functioned as industrial production, warehousing and logistics areas, and needs to prevent from serious impact on the surrounding environment due to industrial noise.
Class 4 acoustic environment functional area: refers to the area that is within certain distance at both sides of the traffic trunk, and needs to prevent from serious impact on the surrounding environment due to AC noise, including two types of classes, i.e., Class 4a and 4b. Class 4a includes the regions at both sides of highway, Class I highway, Class II highway, urban expressways, urban trunk roads, urban sub-distributors, urban rail transportation (ground sections), inland waterways; Class 4b includes the regions at both sides of the railway trunk.

The environmental noise equivalent sound level limits specified for various types of sound environment functional areas are as shown in Table 22.2.

The environmental noise standards are divided into two different levels, i.e., daytime and nighttime, but the line is operating day and night, so the audible noise should meet the standards both in the daytime and nighttime. Because the standard of environmental noise at night time is lower than the daytime standard, so when the nighttime standard is taken as the limits of audible noise, the audible noise at daytime can definitely meet the environmental noise standards. Chinese ±800 kV DC transmission line may pass through Category 1, 2, 3 areas, so the audible noise must meet the environmental noise standards in different regions where the line is passing by.

The audible noise limit of DC transmission line is taken as 40–45 dB (A) in America, taken as 40 dB (A) in Japan, and the limit at the edge of corridor of DC transmission line in Brazil is taken as 40 dB (A). It can be seen that the international audible noise limit of DC transmission line is normally between 40 and 45 dB (A).

For ±800 kV UHVDC transmission line, it is specified in Chinese power industry standard DL/T 1088–2008 "*Electromagnetic Environment Parameter Limits of* ±800 kV *UHVDC Transmission Line*" that, at 20 m away from the ground projection of the positive conductor of DC overhead transmission line, 50% audible noise (L_{50}) generated by corona in sunny days must not exceed 45 dB (A); for non-residential areas at altitude of higher than 1000 m, the audible noise limits should be linear corrected in accordance with 3 dB/1000 m.

When determining the audible noise limits of DC transmission line, the environmental noise standards of local country should be met at first, and appropriate consideration should be given to the construction investment of the line while referring to the international limits at the same time.

22.1.5.3 Calculation Method of Audible Noise

The EPRI empirical equation and BPA empirical equation are more common and accurate methods to calculate the audible noise of DC lines.

(1) EPRI equation

EPRI proposed an equation to calculate the annual average corona noise in 1993:

$$\mathrm{AN} = 56.9 + 124\lg\frac{g_{\max}}{25} + 24\lg\frac{d}{4.45} + 18\log\frac{N}{2} - 10\lg D - 0.02D, \quad (22.25)$$

where

$g_{\max}$ the maximum potential gradient on the surface of the conductor, in kV/cm;
d the diameter of sub-conductor, in cm;
N the number of bundled sub-conductors;
D the distance from the calculation point to the positive conductor, in m.

(2) BPA equation

U.S. Bonneville Power Authority (BPA) recommended the following equation:
Measurement conditions: L_{50} in sunny day
Applicable scope: $4 \le N \le 8$, $r \le 2.5\,\mathrm{cm}$

$$\mathrm{AN} = -133.4 + 86\lg(g_{\max}) + 40\lg(d_{\mathrm{eq}}) - 11.4\lg D, \quad (22.26)$$

where

AN the audible noise at the probability value of L_{50}, in dB;
$g_{\max}$ the maximum potential gradient on the surface of the conductor, in kV/cm;
d_{eq} $1.32N^{0.64}r$;
r the radius of sub-conductor, in mm;
N the number of bundled sub-conductors;
D the distance from the calculation point to the positive conductor, in m.

Similarly, this value should be increased by 3.3 dB with every increment of altitude of 1000 m.

22.1.6 Corona Loss

22.1.6.1 Characteristics of Corona Loss

When the surface potential gradient of the conductor exceeds a certain critical value, causing the air ionization around the conductor, and the movement of charged ions forming into the corona current on the line, resulting in energy loss which is called as the corona loss. Corona loss increases the power loss and transmission costs and is one of the important economic and technical indicators for assessment of transmission lines [3, 4].

Compared with the AC transmission line, the corona loss of DC transmission line has its own characteristics:

(1) Under AC or DC voltage, the corona discharges almost begin at the same voltage value (of equal amplitude), but as the voltage is further increased, the increase of corona loss under DC voltage is much lower than that under AC voltage. This is one of important advantages of the DC line, and the more the applied voltage exceeds the corona starting voltage, the more significant this advantage is.
(2) Compared with AC corona, the correlation of DC corona loss with the voltage is smaller, and the correlation with the climate conditions is much smaller, and almost has no relationship with the size of the conductor diameter and whether the bundled conductors are used or not.
(3) For monopolar corona loss, the negative polarity is approximately equal to the twice of positive polarity. Bipolar corona loss is much larger than the sum of the monopolar corona loss of both the polarities.
(4) Contrary to the case of AC line, the annual corona loss of the DC line basically depends on the value under the good weather. When the conductor surface electric field intensity is the same, the annual average corona loss of bipolar DC line is only 50–65% of AC line.

22.1.6.2 Calculation Method of Corona Loss

The calculation methods that are applicable for the corona loss of ±800 kV DC transmission line are IREQ equation and Corbellini and Pelacchi equation. The applicable margin of IREQ equation is ±600–1200 kV and is obtained based on the test data of the test line sections and corona cage, with a certain representation, so it is normally recommended to use this equation. In addition, the applicable scope of Corbellini and Pelacchi equation is ±230–1200 kV, and this equation can also be applied to estimate the corona loss of ±800 kV DC transmission line.

1. IREQ equation

The corona loss estimation equation of IREQ Canada is as follows:

$$P = k_1 + k_2(g - g_0) + k_3 \lg\left(\frac{d}{d_0}\right) + k_4 \lg\left(\frac{n}{n_0}\right) [\text{dB}(1\ \text{W/m})], \tag{22.27}$$

where

g the surface electric field intensity of the conductor (kV/cm);
d the diameter of sub conductor (cm);
n the number of bundled sub-conductors;
g_0 equals to 25 kV/cm;
d_0 equals to 4.064 cm;
n_0 equals to 6.

For k_1–k_4, based on the measurement data of test line sections, the specific values can be obtained as shown in Table 22.3.

Selecting k_1–k_4 according to Table 22.3, the applicable scope of Eq. (22.27) is as follows:

Voltage: ±600–1200 kV;
Sub-conductor diameter: 2–6 cm;
Maximum conductor surface field intensity <35 kV/cm;
Number of bundled sub-conductors: 1–8.

For k_1–k_4 in Eq. (22.27), based on the measurement data of corona cage, specific values can be obtained as shown in Table 22.4.

Table 22.3 Calculation coefficients of corona loss

Season	Weather	k_1	k_2	k_3	k_4
Summer	Good weather	13.71	0.80	20	28.1
	Bad weather	19.25	0.63	20	9.7
Spring/autumn	Good weather	12.28	0.88	20	36.9
	Bad weather	17.87	0.72	20	12.8
Winter	Good weather	9.56	1.00	20	44.3
	Bad weather	14.87	0.85	20	10.2
Good weather days throughout the year		11.85	0.89	20	36.4
Bad weather days throughout the year		16.91	0.73	20	8.0

Table 22.4 Coefficients applicable to IREQ equation

Weather	k_1	k_2	k_3	k_4
Good weather days	18.52	1.12	21.83	14.46
Bad weather days	25.12	0.75	23.81	14.35

After k_1–k_4 are selected according to Table 22.4, the scope of application of Eq. (22.27) is as follows:

Voltage: ±600–1200 kV;

Sub-conductor diameter: 2–6 cm;

Maximum conductor surface field intensity <32 kV/cm;

Number of bundled sub-conductors: 1–8.

The parameters k_1–k_4 in Table 22.3 are obtained based on the measurement data of the test line sections, while the parameters k_1–k_4 in Table 22.4 are obtained based on the measurement data of corona cages, the estimated result of corona cage is greater than that of the test line section by about 20–30%.

2. Corbellini and Pelacchi equation

Italian scholars summed up the following corona loss estimation equations by summarizing the DC corona measuring results from the test and actual running line sections that have been published:

For good weather:

$$P = P_0 \cdot \left(\frac{g}{g_0}\right)^5 \cdot \left(\frac{d}{d_0}\right)^3 \cdot \left(\frac{n}{n_0}\right)^2 \cdot \left(\frac{H}{H_0}\right)^{-1} \cdot \left(\frac{D}{D_0}\right)^{-1}, \tag{22.28}$$

where

P_0 equals to 2.9, in dB (1 kW/km is taken as the benchmark);

For bad weather:

$$P = P_0 \cdot \left(\frac{g}{g_0}\right)^4 \cdot \left(\frac{d}{d_0}\right)^2 \cdot \left(\frac{n}{n_0}\right)^{1.5} \cdot \left(\frac{H}{H_0}\right)^{-1} \cdot \left(\frac{D}{D_0}\right)^{-1}, \tag{22.29}$$

where

P_0 equals to 11, in dB (1 kW/km is taken as the benchmark);
g the electric field intensity on the conductor surface, in kV/cm;
d the diameter of sub conductor, in cm;
n the number of bundled sub-conductors;
H the height of the conductor to ground, in m;
g_0 equals to 25 kV/cm;
d_0 equals to 3.05 cm;
n_0 equals to 3;
H_0 equals to 15 cm;
S_0 equals to 15 m.

Applicable scope of the equation: voltage of ±230–1200 kV.

In addition, Pique equation, Buck Cove equation, Oneida Castle equation and EPRI equation, and other equations are also available for estimating the corona loss. But it is more difficult to select the parameters required for Pique equation and Buck

Cove equation, so their applications are very difficult. Oneida Castle equation and EPRI equation are developed, respectively, for ±750 and ±600 kV DC transmission lines, so they do not apply to the corona loss estimation of ±800 kV DC transmission lines.

22.2 Electromagnetic Environmental Assessment of UHVDC Transmission Lines

In order to learn the characteristics of electromagnetic environment of UHVDC transmission line, taking Yunnan–Guangdong (Chuxiong-Suidong) ±800 kV UHVDC transmission lines as the example in this section, the SES-Enviro module in CDEGS software package of Canadian SES Company is used to simulate the environmental impact of ±800 kV DC transmission lines [5, 6].

A typical tower of Yunnan–Guangdong HVDC transmission lines is as shown in Fig. 22.5. The parameters of bipolar ±800 kV DC transmission lines are as follows: the pole conductor height above the ground is 18 m, the interpolar distance is 22 m, the conductor model is 6×LGJ-630/45, the ground wire model is

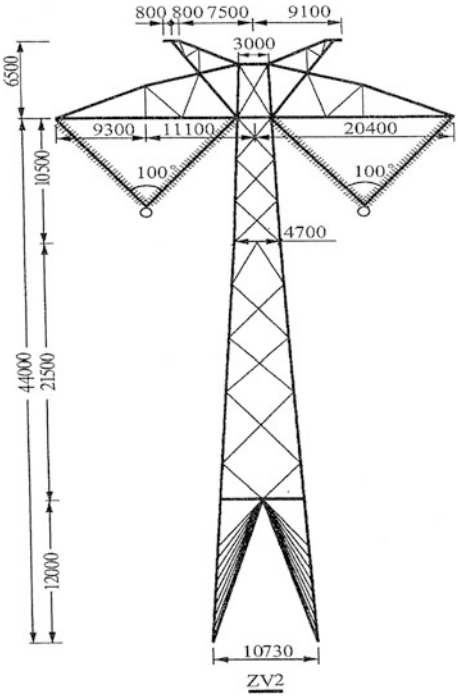

Fig. 22.5 The schematic diagram of typical tower of Yunnan–Guangdong ±800 kV UHVDC transmission line (mm)

LBGJ-180-20AC, and the spacing of bundled conductors is 0.45 m. The maximum operating voltage of the line is 825 kV, the economic operating current is 3125 A; during the calculation, the soil resistivity at the area where the line passes by is taken as 100 Ω·m, the ground altitude is taken as 0 m, the atmospheric pressure is taken as 760 mm Hg, and the temperature is taken as 25 °C.

It is normally believed that the corona inception electric field intensity of conductor of DC line has the same peak value with that of AC line, and Peek equation can be converted into the DC form:

$$E_c = 30m\delta\left(1 + \frac{0.3}{\sqrt{r\delta}}\right) (\text{kV/cm}), \tag{22.30}$$

where

- m the conductor surface roughness coefficient. $m \approx 1$ for smooth conductor; according to a large number of theories and summarized experiences, currently the values of surface roughness coefficient m under sunny and rainy conditions are taken as 0.49 and 0.38, respectively; it is taken as 0.49 under sunny days in this book;
- r the radius of the sub-conductor, in cm;
- δ the relative density of the air, and can be calculated by the equation $\delta = \frac{p}{T}\frac{T_s}{p_s}$ ($p_s = 101.3\,\text{kPa}$, $T_s = 293\,\text{K}$);

Through calculation, the corona inception electric field intensity of conductor in this example is 18.11 kV/cm.

22.2.1 Electric Field Intensity and Ion Flow Density

Figure 22.6 shows the lateral distribution of the ground synthetic electric field of transmission lines under bipolar operation mode, with pole conductor height above the ground of 18.0 m (the minimum pole conductor height above the ground of the conductors in normal non-resident areas is specified as 18 m in the procedure), and with the line operating voltage of 800 kV and the maximum operating voltage of 825 kV. Table 22.5 shows the maximum values of the ground nominal electric field and the synthetic electric field under these two operating voltages.

It can be known from Fig. 22.6 and Table 22.5 that the nominal electric field generated on the ground by the electric charge on line conductor itself is about 14 kV/m, considering the influence of the ion flow caused by the corona, the ground synthetic electric field is greater than the nominal electric field. Under the operating voltage of 800 kV, with the pole conductor height above the ground of 18.0 m, the maximum ground synthetic electric field in sunny days is still lower than the limit standard of 30 kV/m, and the synthetic electric field value can satisfy

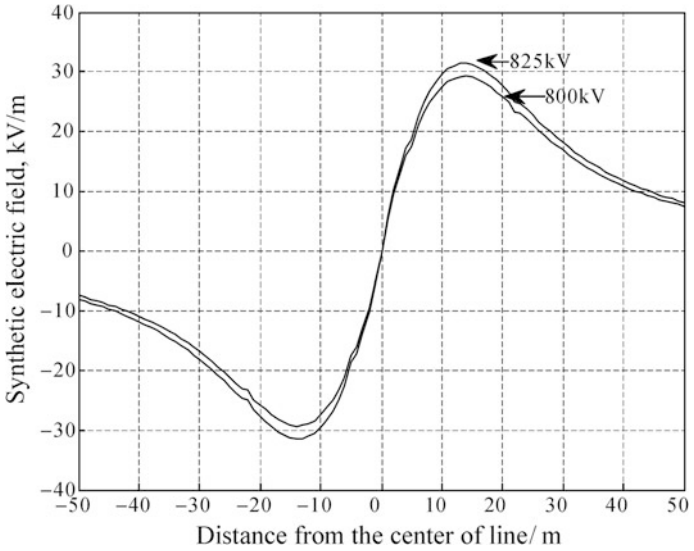

Fig. 22.6 Lateral distribution of ground synthetic electric field under UHVDC transmission line

Table 22.5 Maximum values of nominal electric field and synthetic electric field under UHVDC lines

Operating voltage (kV)	Nominal electric field intensity (kV/m)	Synthetic electric field intensity (kV/m)
825	14.50	31.40
800	14.06	29.24

the standards. Under the operating voltage of 825 kV, the maximum ground synthetic electric field in sunny days exceeds the limit standard of 30 kV/m, and the synthetic electric field value can not satisfy the standards.

Under the operating voltage of 825 kV, in order to make the ground synthetic electric field satisfy the standards, the measures such as raising the pole conductor height, increasing the cross-sectional area of the conductor, and increasing the number of bundled sub-conductors need to be taken to reduce the synthetic electric field of the lines. The calculated results show that, if 6× LGJ-630/45 conductor is used, the minimum pole conductor height above the ground is required as 19.0 m (considering the maximum sag); if conductors with modes of 6× LGJ-720/45 and 7× LGJ-630/45 are used, when the pole conductor height above the ground is 18.0 m, the ground synthetic electric field can meet the standards. At this time, the ion flow density of the line can also meet the standards. In general, if the synthetic field intensity of the line can meet the standards, the ion flow density will meet the standards too.

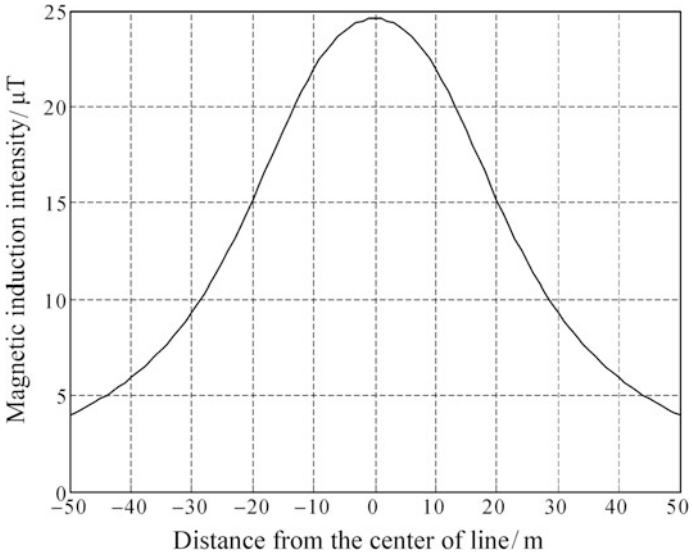

Fig. 22.7 Lateral distribution of magnetic induction intensity under the lines with economic operation current operating mode

22.2.2 Magnetic Induction Intensity

Figure 22.7 shows the lateral distribution of ground magnetic induction intensity of the transmission lines under bipolar operation mode and with pole conductor height above the ground of 18.0 m. As the magnetic induction intensity is independent of the line voltage, when the line operating voltages are 800 and 825 kV, respectively, the maximum values of magnetic induction are the same. The economic operation current of ±800 kV UHVDC transmission line is 3125 A.

It can be known from Fig. 22.7 that, for ±800 kV UHVDC transmission line, under the economic operating current mode, the maximum ground magnetic field intensity is 24.59 μT, which is far less than the limit standard of 10 mT for UHVDC line, and it is shown through calculations that even if the line is at the maximum operating current mode, the magnetic induction intensity of the line can still meet the standard. Therefore, the magnetic field effect of ±800 kV UHVDC transmission lines can be ignored.

22.2.3 Radio Interference

Figure 22.8 shows the lateral distribution of the radio interference at 20 m away from the ground projection of the positive conductors of transmission lines under

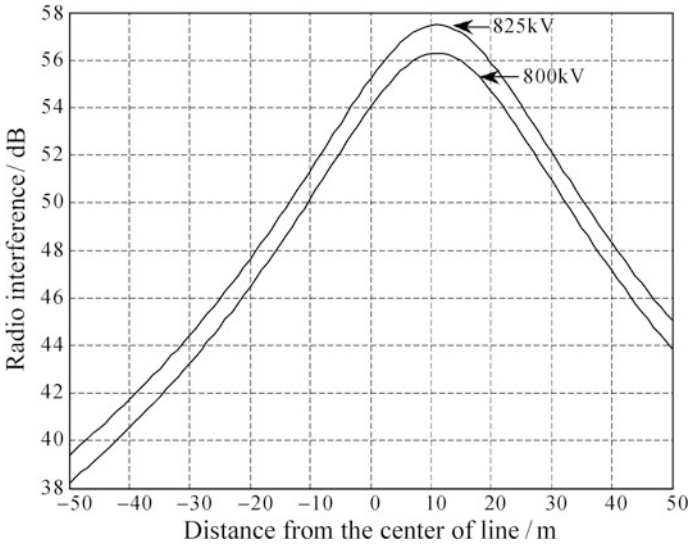

Fig. 22.8 Lateral distribution of radio interference under UHVDC Lines

Table 22.6 Maximum ground radio interference under UHVDC transmission lines

Operating voltage (kV)	RI at 20 m from the positive conductor (dB)
825	51.72
800	50.54

bipolar operation mode, at altitude of 0 m, with the pole conductor height above the ground of 18.0 m, and under line operating voltage of 800 and 825 kV, respectively. Table 22.6 shows the maximum values of ground radio interference under these two operating voltages.

It can be seen that, no matter in the operating voltage of 800 or 825 kV, at the altitude of 0 m, with the pole conductor height above the ground of 18.0 m, the radio interference at 20 m away from the ground projection of the positive conductors is less than the limit standard of 58 dB and the radio interference value can meet the standards. As the altitude increases, the radio interference value will increase. Taking the altitude of 1000 m as the basis, the radio interference limit standard will be increased by 1 dB for every increment of altitude of 300 m. It is proved through calculation that the radio interference value at high altitude is still within the limit standard.

22.2.4 Audible Noise

Figure 22.9 shows the lateral distribution of the audible noise at 20 m away from the ground projection of the positive conductors of transmission lines under bipolar operation mode, with the pole conductor to ground height of 18.0 m, and with line operating voltage of 800 and 825 kV, respectively. Table 22.7 shows the maximum values of the audible noise at 20 m away from the ground projections of the positive conductors under two operating voltages.

It can be seen that, under the operating voltage of 800 kV, at the altitude of 0 m, with the pole conductor height above the ground of 18.0 m, the audible noise at 20 m away from the ground projection of positive conductor is less than the limit standard of 45 dB and audible noise level can meet the standard. However, under the operating voltage of 825 kV, the audible noise exceeds the limit standard of 45 dB and audible noise value fails to meet the standard.

To make audible noise meet the standard, it is necessary take some measures such as raising the conductor height above the ground, increasing the cross-sectional area of the conductor, and increasing the number of bundled sub-conductors to reduce the audible noise of the line. The calculated results show

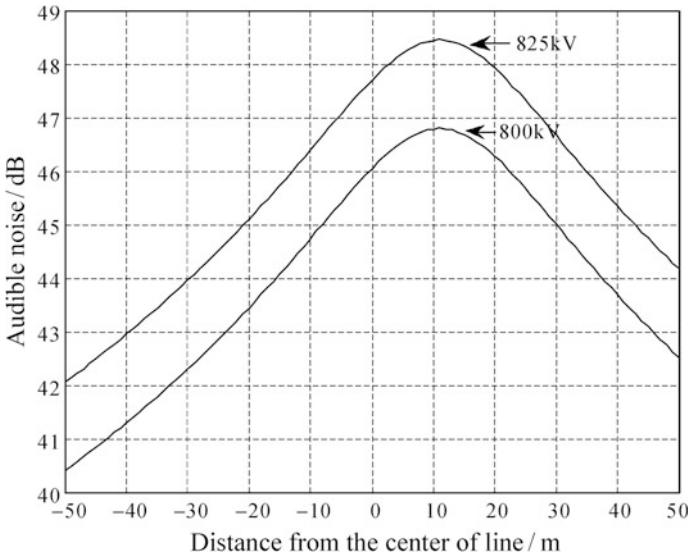

Fig. 22.9 Lateral distribution of audible noise under UHVDC transmission lines

Table 22.7 Maximum values of audible noise on ground under UHVDC transmission lines

Operating voltage (kV)	AN at 20 m from the positive conductor (dB)
825	46.52
800	44.87

that, if the conductor with the mode of 6× LGJ-630/45 is used, the minimum conductor height above the ground is required as 19.0 m (considering the maximum sag); if conductors with the mode of 6× LGJ-720/45 and 7× LGJ-630/45 are used, with the pole conductor height above the ground of 18.0 m, the audible noise can meet the standard.

With the increase of altitude, the audible noise will increase. Taking the altitude of 1000 m as the basis, the audible noise limit standard will be increased by 3 dB for every increment of altitude of 1000 m. It is proved through calculations that, if the audible noise can meet the standard at low altitudes, the audible noise of the same line at high altitudes will be still within the limit standard.

22.3 Analysis on Electromagnetic Environmental Impact Factors of UHVDC Transmission Line

22.3.1 Influence of the Pole Conductor Height Above the Ground

Figure 22.10a–c illustrate the lateral distribution of the ground synthetic electric field, radio interference and audible noise in sunny days under bipolar operation mode with the pole conductor height above the ground of 16, 18, 20 m, respectively. Table 22.8 shows the maximum values of the corresponding ground synthetic electric fields with the different conductor heights, and the radio interference and audible noise values at 20 m away from the ground projections of the positive conductors.

It can be seen from Fig. 22.10 that the ground synthetic electric field within 30 m from the center of line will decrease with the increase of the conductor height above the ground and almost has no impact in the place 30 m away. The peak values of radio interference and audible noise appear under the positive conductor, so raising the pole conductor can reduce the value of radio interference and audible noise within the entire area under the line. Therefore, raising the pole conductor height above the ground is an effective measure to reduce the synthetic electric field, radio interference, and audible noise.

22.3.2 Influence of the Interpolar Distance

Figure 22.11a–c illustrate the lateral distribution of the ground synthetic electric field, radio interference and audible noise in sunny days under bipolar operation mode with the interpolar distance of 21, 22, 23 m, respectively. Table 22.9 shows the maximum values of the corresponding ground synthetic electric fields with the different interpolar distances, and the radio interference and audible noise values at 20 m away from the ground projections of the positive conductors.

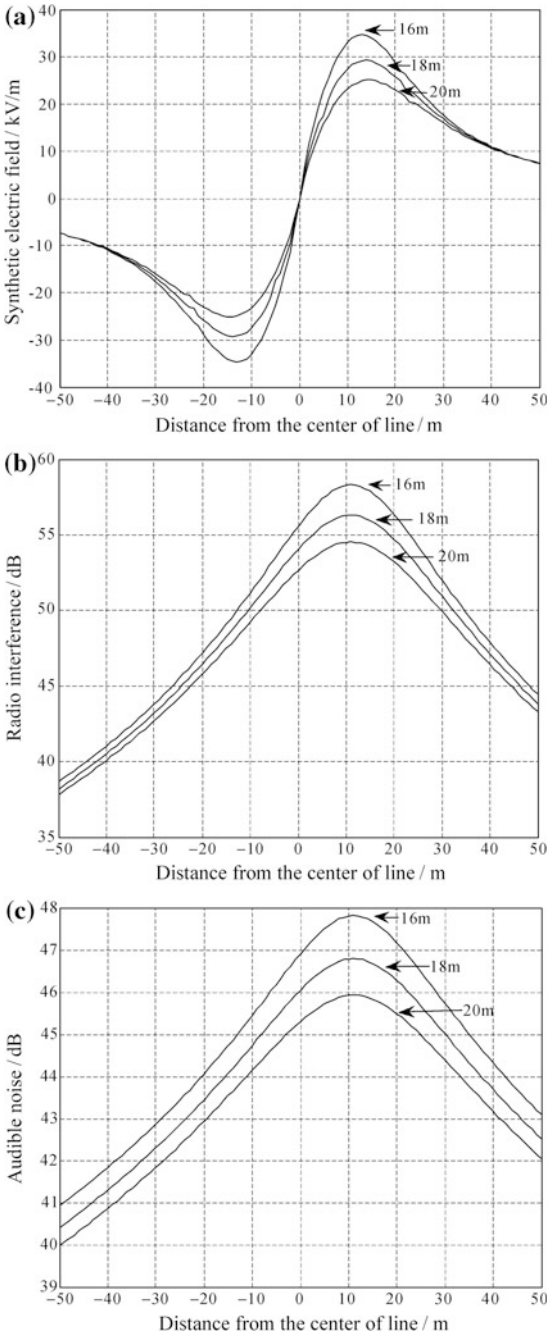

Fig. 22.10 Lateral distribution of ground electromagnetic environment factors corresponding to different pole conductor heights above the ground

Table 22.8 Values of electromagnetic environment factors of different pole conductor height above the grounds

Pole conductor height above the ground (m)	16	18	20
Maximum synthetic electric field (kV/m)	34.73	29.24	25.06
RI at 20 m from the positive conductor (dB)	51.58	50.54	49.57
AN at 20 m from the positive conductor (dB)	45.58	44.87	44.26

It is shown in Fig. 22.11 that, with the increase of interpolar distance, the ground synthetic electric field is slightly increased, but the increase magnitude is small, while both the radio interference and the audible noise will be reduced with the increase of interpolar distance. Therefore, under the premise of ensuring that all electromagnetic environment parameters will not exceed the standards, the interpolar distance should be appropriately increased to optimize the value of radio interference and audible noise, while the increased economic investment due to increased length of cross-arm as well as the increased line corridors and other issues should also be taken into consideration.

22.3.3 Influence of Bundling Spacing of Pole Conductors

Figure 22.12a–c illustrate the lateral distribution of the ground synthetic electric field, the radio interference and audible noise in sunny days under bipolar operation mode with bundling spacing of pole conductors of 0.40, 0.45, 0.50 m, respectively. Table 22.10 shows the maximum values of ground synthetic electric fields corresponding to different bundling spacing of pole conductors and the radio interference and audible noise values at 20 m away from the ground projections of the positive conductors.

Figure 22.12 shows that, with the increase of bundled conductor spacing, the ground synthetic electric field, radio interference, and audible noise were slightly increased, and the increasing trend of audible noise is the most obvious. Therefore, appropriately reducing the bundled conductor spacing can reduce the ground synthetic electric field, radio interference, and audible noise.

22.3.4 Influence of the Number of Bundled Sub-conductors

Figure 22.13a–c illustrate the lateral distribution of the ground synthetic electric field, radio interference and audible noise in sunny days under bipolar operation mode with the number of bundled sub-conductors 6, 7 and 8, respectively. Table 22.11 shows the maximum values of the ground synthetic electric field corresponding to different number of bundled sub-conductors and the radio interference and audible noise value at 20 m away from the ground projections of the positive conductors.

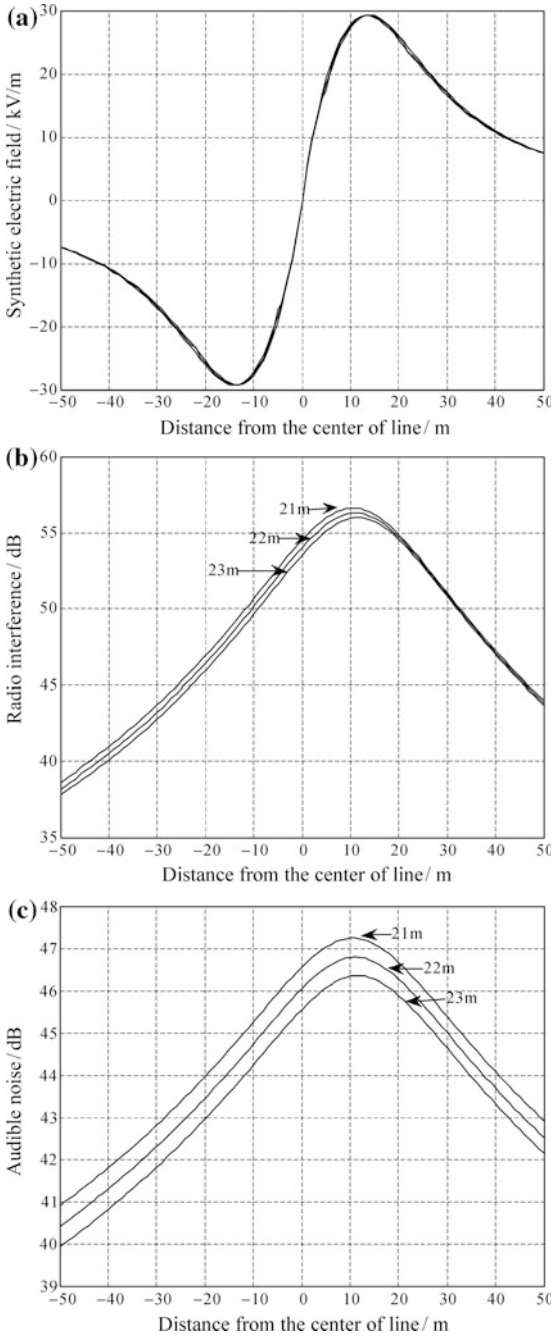

Fig. 22.11 Lateral distribution of ground electromagnetic environment factors corresponding to different interpolar distances

Table 22.9 Values of ground electromagnetic environment factors corresponding to different interpolar distances

Interpolar distances (m)	21	22	23
Maximum synthetic electric field (kV/m)	29.24	29.24	29.25
RI at 20 m from the positive conductor (dB)	50.86	50.54	50.24
AN at 20 m from the positive conductor (dB)	45.32	44.87	44.44

It can be known from Fig. 22.13 that, with the increase of the number of bundled sub-conductors, the ground synthetic electric field, radio interference and audible noise are reduced. It can be seen from the Table 22.11 that, when the number of bundled sub-conductors is increased from 6 to 8, the synthetic electric field is reduced by 3.9 kV/m (13.34%), 4.29 kV/m (16.93%); the radio interference value is reduced by 3.33 dB (6.59%), 2.59 dB (5.49%); and the audible noise is reduced by 4.27 dB (9.52%), 0.68 dB(1.67%) respectively. It is shown through the comparison of three electromagnetic environmental factors that the decrease amplitude of the synthetic electric field with the increasing number of bundled sub-conductors is larger, while the reduction of audible noise is also more obvious when the number of bundled sub-conductors is increased from 6 to 7.

Therefore, increasing the number of bundled sub-conductors can reduce the ground synthetic electric field, radio interference, and audible noise, but the construction investment of the lines and the operating losses should also be considered while selecting the number of bundled sub-conductors.

22.3.5 Influence of Cross-Sectional Area of Pole Conductors

Figure 22.14a–c illustrate the lateral distribution of the ground synthetic electric field, the radio interference and audible noise in sunny days under bipolar operation mode with cross-sectional areas of pole conductors of 630, 720, and 800 mm^2, respectively. Table 22.12 shows the maximum values of the ground synthetic electric field corresponding to different cross-sectional areas of pole conductors and the values of the radio interference and the audible noise at 20 m away from the ground projections of the positive conductors.

It can be known from Fig. 22.14 that, with the increase of the cross-sectional area of sub-conductor, the ground synthetic electric field, radio interference, and audible noise are reduced, because increasing the conductor cross-sectional area can increase the corona inception electric field intensity of conductor. Therefore, increasing the conductor cross-sectional area can be very effective in improving the electromagnetic environment but the economic factors also need to be considered during the selection of conductor cross-sectional area.

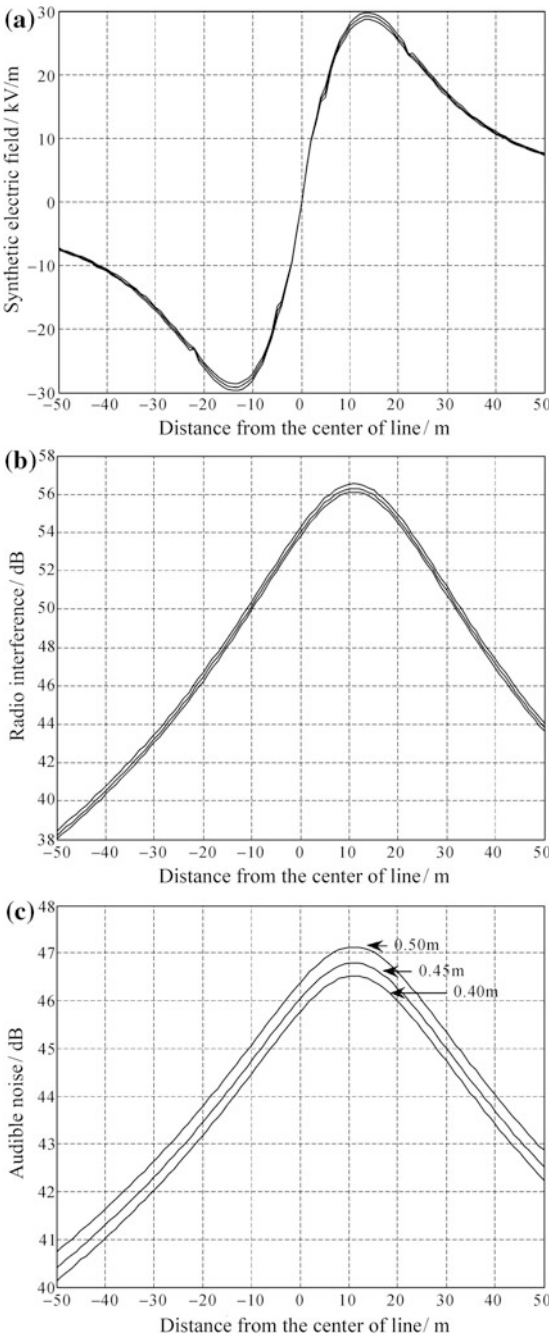

Fig. 22.12 Lateral distribution of ground electromagnetic environment factors corresponding to different bundled spacing of pole conductors

Table 22.10 Values of ground electromagnetic environment factors corresponding to different bundling spacing of pole conductors

Bundled conductor spacing (m)	0.40	0.45	0.50
Maximum synthetic electric field (kV/m)	28.71	29.24	29.81
RI at 20 m from the positive conductor (dB)	50.35	50.54	50.78
AN at 20 m from the positive conductor (dB)	44.60	44.87	45.21

22.3.6 Influence of Altitude

Figure 22.15a–c illustrate the lateral distribution of the ground synthetic electric field, radio interference and audible noise in sunny days under bipolar operation mode corresponding to the altitude of 0, 1000, and 2000 m, respectively. Table 22.13 shows the maximum values of the ground synthetic electric field corresponding to different altitudes, and the values of the radio interference and audible noise outside at 20 m away from the ground projections of the positive conductors.

It can be seen that with the increase of altitude, the corona inception electric field intensity of the conductor is reduced, the electromagnetic environment is worse and the ground synthetic electric field, radio interference, audible noise are increased.

22.4 Measures for Improving the Electromagnetic Environment of DC Transmission Lines

Based on the calculation and analysis of the influence factor for electromagnetic environment of UHVDC transmission line in the previous section, comprehensively considering the production, construction, operating experience, economic investment and other factors, reasonable design of the pole conductor height above the ground, the interpolar distance, and proper selection of conductors can effectively improve the electromagnetic environment of the lines [7, 8]:

(1) Increasing appropriately the pole conductor height above the ground is an effective measure to reduce the ground synthetic electric field, radio interference, and audible noise.
(2) Increasing the interpolar distance may reduce the radio interference and audible noise, but the degree of improvement is minimal and the effect is not as significant as increasing the conductor height above the ground appropriately.
(3) Reducing the bundled spacing of conductors can reduce the ground synthetic electric field, radio interference, and audible noise, but it will be limited by insulation coordination and corona losses.
(4) When the number of bundled conductors is increased, the ground synthetic electric field, radio interference and audible noise can be significantly improved. Making reference to the operation experience of lines, the ground

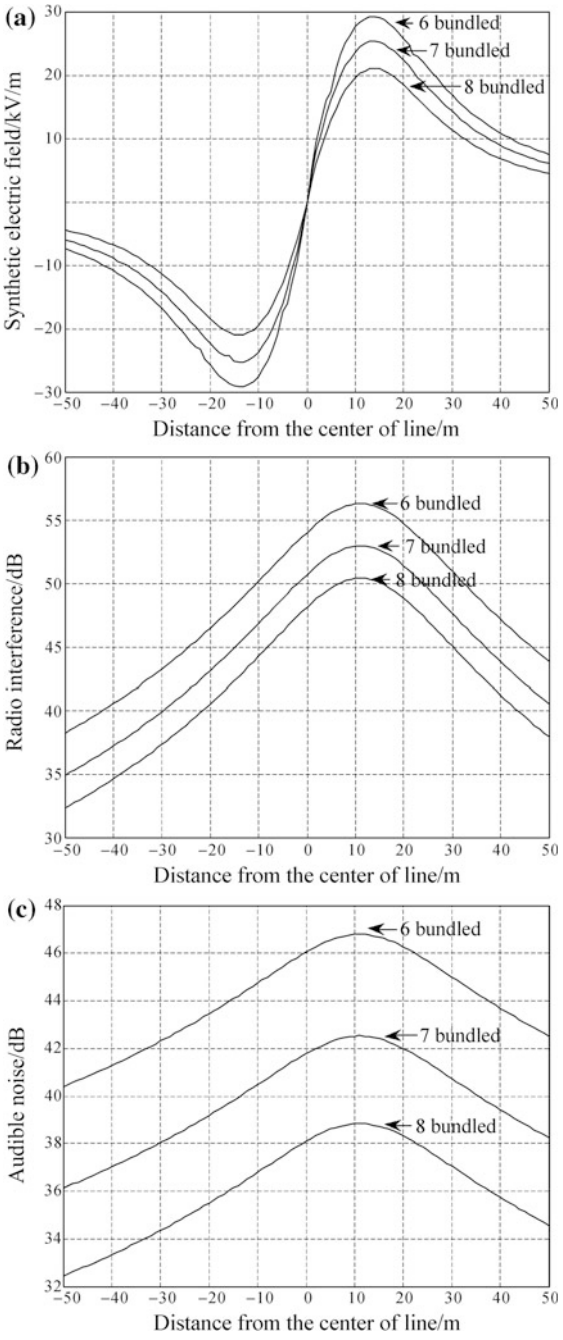

Fig. 22.13 Lateral distribution of ground electromagnetic environment factors corresponding to different numbers of bundled sub-conductors

Table 22.11 Values of ground electromagnetic environment factors corresponding to different number of bundled sub-conductors

Number of bundled sub-conductors	6	7	8
Maximum synthetic electric field (kV/m)	29.24	25.34	21.05
RI at 20 m from the positive conductor (dB)	50.54	47.21	44.62
AN at 20 m from the positive conductor (dB)	44.87	40.60	39.92

field intensity, ion flow density, audible noise, radio interference, and corona losses of 4 and 5 bundled conductors under the same arrangement are high, and often cannot meet the limit requirements at high altitudes; 6 and above bundled conductors normally can meet the requirements of various electromagnetic environment parameter limits; in addition, due to the lack of operating experience and development of ancillary fittings and other factors, 7 bundled conductors are not recommended normally.

(5) Appropriately increasing the cross-sectional area of single conductor can reduce the ground synthetic electric field, radio interference, and audible noise, but the total cross-section of conductor should not be too large and the current density must not be too low, so as to avoid excessive investment.

22.5 Electromagnetic Environment of UHVDC Converter Station

Due to numerous equipment in UHVDC converter station, the electromagnetic environment mainly consists of ground synthetic electric field, ion flow density, DC magnetic field, radio interference, and audible noise. Because the equipment in UHVDC converter station has higher voltage level and more varieties, the electromagnetic environment has some differences from ±500 kV HVDC converter station, so measures must be taken to limit it in order to meet the requirements of environmental protection [9]. Since the audible noise of converter stations is the most prominent among the electromagnetic environmental issues in UHVDC converter station, so it will be highlighted in this book. For other electromagnetic environmental indicators, their limits are to be explained. Chinese power industry standard DL/T 275–2012 "*Electromagnetic Environment Limits of* ±800 kV *UHVDC Converter Stations*" specifies the limits of the indicators as follows:

For ground synthetic electric field and ion flow densities, it is specified in the Standard that the maximum ground synthetic electric field under good weather must not exceed 30 kV/m, and the maximum ion flow density on the ground must not exceed 100 nA/m^2.

For DC magnetic field, it is specified in the Standard that the DC magnetic induction intensity at 1.5 m above the ground must not exceed 400 mT.

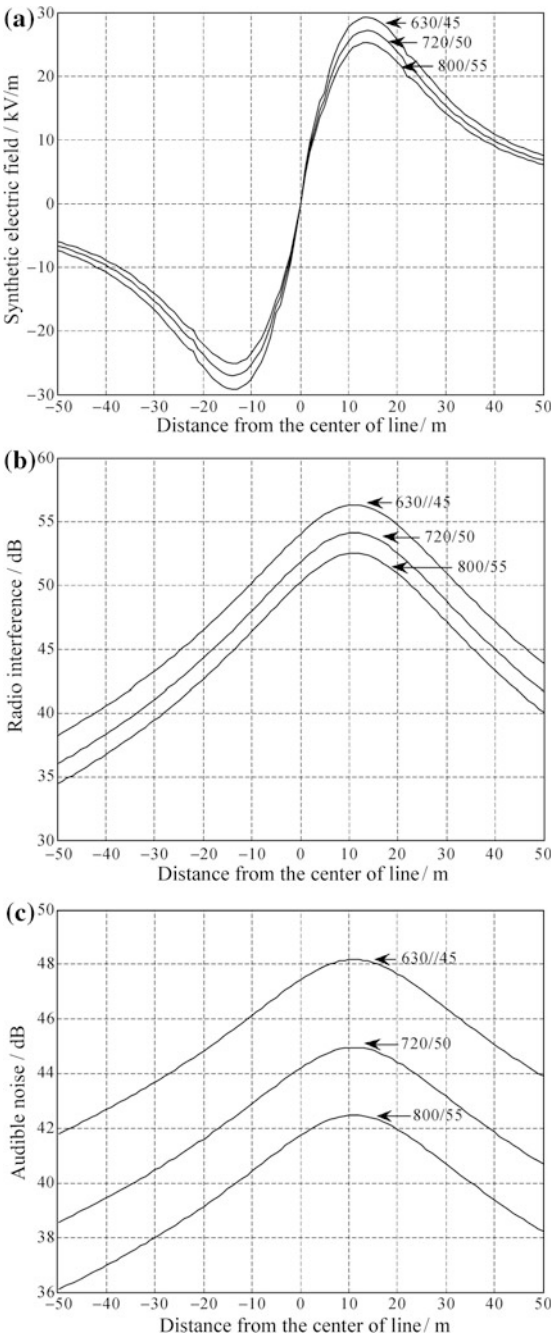

Fig. 22.14 Lateral distribution of ground electromagnetic environment factors corresponding to different cross-sectional areas of sub-conductors

Table 22.12 Maximum values of ground electromagnetic environment factors corresponding to different cross-sectional areas of sub-conductors

Cross-sectional area of sub-conductor (mm^2)	630	720	800
Maximum synthetic electric field (kV/m)	29.24	27.03	25.18
RI at 20 m from the positive conductor (dB)	50.54	49.84	49.40
AN at 20 m from the positive conductor (dB)	44.87	42.43	40.57

For radio interference, it is basically the same with ±500 kV HVDC converter station, it needs to meet the requirement that the radio interference levels at all the frequencies within 0.5–20 MHz will not exceed 40 dB (μV/m) within a specified range. Refer to the standard DL/T 275-2012 for the specific range.

Compared with AC substation, DC converter station has more noise sources, higher sound power level, and more prominent noise problem. In some ±500 kV HVDC converter stations that have already been built, the noise generated by various devices causes the noise level at and near the site exceeding the standards, which influences the surrounding residents, so the complaints of local residents come out. Therefore, the audible noise has become one of important controlled conditions in site selection, design, and construction of converter stations. The research on noise of converter station is of important reference value for improving the surrounding environment, and for the planning, construction and operation of DC transmission projects. The audible noise problems of UHVDC converter station will be introduced mainly from the aspects of noise sources, controlling indicators, and controlling measures.

22.5.1 Noise Sources of Converter Station

The noise within the converter station includes electromagnetic noise, aerodynamic noise, and mechanical vibration noise. The noise sources that causing off-spec excessive noise are converter transformers, reactors, and capacitors.

22.5.1.1 Noise of Converter Transformer

Converter transformer is a single device producing the biggest noise in the converter station, and the noise contains two aspects: the noise from transformer body and the noise from auxiliary cooling device. The noise from transformer body consists of the noise generated by the vibration of the core, winding, etc., the noise from auxiliary cooling device consists of the noise produced by fan and oil pump.

The core excitation silicon steel will produce small change in its size, i.e., the magnetostriction of silicon steel which is the main source of noise in a conventional transformer. The noise of the transformer body directly depends on the magnetostriction of silicon steel used for the core. At present, with the improvement of the

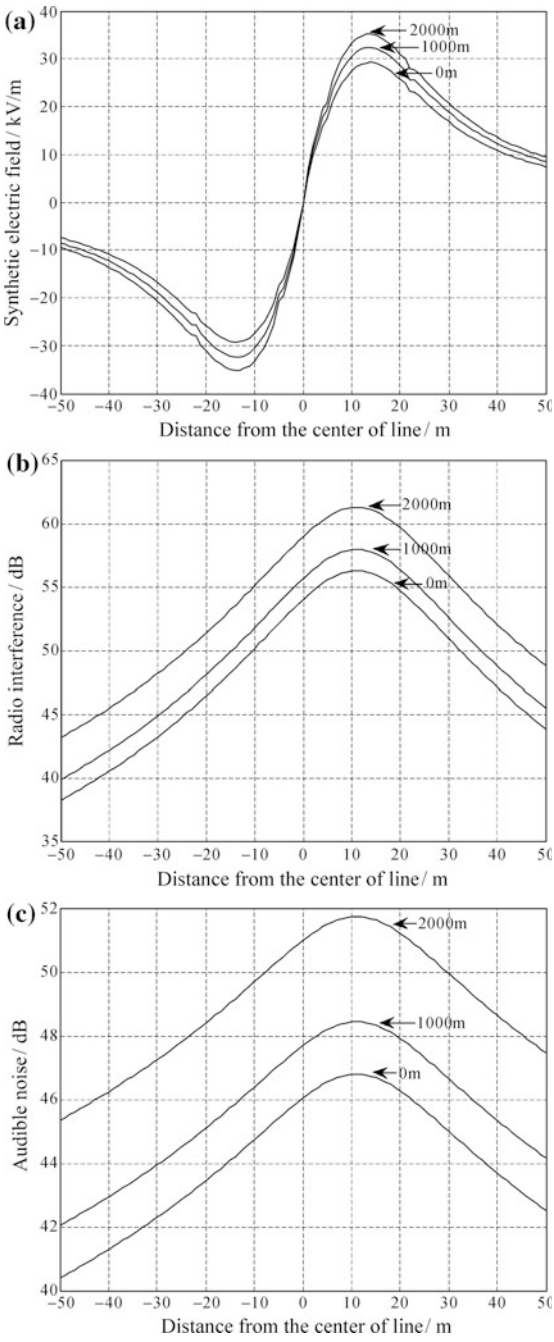

Fig. 22.15 Lateral distribution of ground electromagnetic environment factors corresponding to different altitudes

Table 22.13 Values of ground electromagnetic environment factors corresponding to different altitudes

Altitude (m)	0	1000	2000
Maximum synthetic electric field (kV/m)	29.24	32.42	35.19
RI at 20 m from the positive conductor (dB)	50.54	52.19	55.46
AN at 20 m from the positive conductor (dB)	44.87	46.52	49.82

design of core silicon steel, the noise due to magnetostriction vibration has been greatly reduced. Therefore, the noise generated by the electromagnetic force between the winding conductors or the windings become a major noise source of the converter transformer. The noise power generated by the winding will increase with the increase of transformer load. The difference between the noise levels under no load and at rated load conditions is about 20 dB (A) or even more.

The cooling device of converter transformer is also a noise source. The cooling device mainly consists of cooling fan (forced oil and air-cooled transformer), self-cooled radiator (forced oil self-cooled transformer), and pumps. The noise generated due to running of cooling fan is mainly caused by the vortex airflow generated by the blades nearby; the noise of self-cooled radiator is the vibration noise caused by the radiator, which is mainly produced by the vibration of transformer body transmitting through the oil pipelines to the radiator; the noise of transformer oil pump is mainly the friction noise generated by motor bearings, etc.

The fundamental frequency of electromagnetic noise of converter transformer is generally 100 Hz. Because the low-frequency noise has longer wavelength, with a strong diffraction and transmission capacity, will decay slowly with the increase of distance in the air, having greater impact on the surrounding environment.

22.5.1.2 Noise of Reactors

Reactor is the major noise source in the converter station, where the reactor mainly refers to the smoothing reactor and the filter reactor in AC filter field.

At present, the smoothing reactors in Chinese UHVDC system basically are dry type hollow reactors, of which the main cause of noise is the coil vibration caused by the interaction of DC current and harmonic current. At rated current, the average noise level of dry-type smoothing reactor is about 70 dB (A), the external noise radiation of the equipment is mainly the low-frequency noise, of which the sound mechanism of noise, the sound level intensity, and the frequency range are the same with converter transformers.

The reactors in AC filter field normally are dry-type hollow reactors too, of which the main cause of noise is the periodical magnetostrictive vibration of reactor excitation coil due to alternating electromagnetic field. The noise levels are usually in 65–80 dB (A), with a significant peak in the section of low frequency, and the peak in the portion of high frequency is from the response of the overall structure.

22.5.1.3 Noise of Capacitors

In addition to transformers and reactors, the capacitor is also one of the main noise sources in the converter station. The noise inside the capacitor belongs to the electromagnetic noise. Under the action of the alternating magnetic field, the electrostatic force is generated between the internal electrodes of the capacitor, so that the elements inside the capacitor produce vibration. The vibration of elements is transmitted to the housing so that the noise is formed due to the vibration of tank wall and radiated out from the housing. The noise level is about 70–90 dB (A).

22.5.2 Noise Control Indicators of Converter Station

For the audible noise of converter stations, it is specified in Chinese power industry standard DL/T 275–2012 "*Electromagnetic Environment Limits of* ±800 kV *HVDC Converter Stations*" that the noise limits at the boundary of converter station or at the boundary of noise control zone should be implemented in accordance with GB 12348-2008 "*Environmental Noise Emission Standards of Industrial Enterprises*" [10], and the noise limits at the residential houses around the converter station should be implemented in accordance with the requirements of GB 3096-2008 "*Environmental Quality Standards for Noise*" [11].

According to the test data of regional environmental noise of converter station at daytime and the relevant regulations in Chinese National Standard GB 3096-2008 "*Environmental Quality Standards for Noise*" [11], the regional environmental noise outside the fence wall of converter station after being controlled should reach the nighttime limit value specified in GB 3096-2008, namely, according to the site situations in different regions, the noise requirements should be established according to the levels specified in the standard: Level 1 as 45 dB, Level 2 as 50 dB, and so on.

Using the national standard GB 12348-2008 "*Environmental Noise Emission Standards of Industrial Enterprises*" [10] and GB 3096-2008 "Environmental *Quality Standards for Noise*" [11], the control requirements for the boundaries of converter stations are classified as Class II. Since the noise levels of converter station equipment at daytime and nighttime are basically the same, the noise control value of converter station should be based on the data values at nighttime. For the cases referred in this book, the field boundary control is required as Class II, i.e., the limit value is 50 dB.

22.5.3 Noise Control Measures of Converter Station

Noise is a mechanical vibration, which can be transmitted in the gas, liquid, and solid, and almost exists in every corner of the environment, so noise control is very

difficult. Acoustic wave system is normally composed of three aspects, i.e., the sound source, transmission route, and recipients, therefore, the noise control must be carried out from these three aspects, i.e., suppression of the sound source noise, control of transmission routes, and hearing protection of the recipients.

22.5.3.1 Suppression of Noise Source

Suppressing noise source is the most fundamental, effective, and direct measure, for which low-noise equipment should be developed and selected to reduce the noise power of sounding.

1. Converter transformer

The noise generated by the core of converter transformer is the main source of transformer noise, therefore, to reduce the noise of the core is the main way to control the noise of converter transformer. The following points are presented in this section for the noise reduction of converter transformer:

(1) The high magnetic permeability materials with small magnetostriction should be used to make core silicon steel sheets. Compared with ordinary silicon steel materials, high-quality silicon steel may reduce the noise by 4–5 dB (A).
(2) Low magnetic flux operation of core can reduce the noise. The noise can be reduced by 2–3 dB (A) for every reduction of the magnetic induction intensity of 0.1 T. Note that, with the reduction of the magnetic flux density, the cross-sectional area of the core, the volume and the cost of the transformer will be increased, and the manufacturing cost will be increased accordingly, therefore, normally the reduction amount of magnetic induction intensity should not exceed 10% of the standard magnetic induction intensity.
(3) Applying an epoxy adhesive or polyester adhesive coating on the surface of the core can increase the surface tension of the core, reducing the degree of magnetostriction, so as to suppress the noise.
(4) Install noise barriers outside the oil tank and fill the sound-absorbing material in the steel plate. These noise insulation boards can reflect back the noise transmitted from the transformer body and absorb part of the noise at the same time. The use of sound insulation board can reduce the noise by 10–15 dB (A).
(5) Advanced winding design may be utilized to reduce the winding impedance tolerances for the reduction of winding noise, and the new type low-noise cooling fan can be selected to reduce the noised of fan.
(6) Reduce DC magnetic bias of the converter transformer, and reduce the electromagnetic noise produced by it and the damage caused to the equipment, so as to avoid system safety incidents.

2. Reactor

The key point of controlling the noise of dry type hollow reactor is to limit the vibration of windings coils. The following methods can be used to reduce the noise:

① Adjusting the coil structure size, spacing rods and mechanical supports to avoid the occurrence of resonance; ② Using large conductor to increase the inertia and reduce the vibration amplitude; ③ Selecting the winding with double lays of cross-sections, to double the weight of the coil; this method can reduce the noise of reactor by about 6 dB (A).

The audible noise of oil-immersed smoothing reactor is generated by joint action of the vibration noise of the coil and the core. Except for the core, the other structures of oil-immersed smoothing reactor are similar with the converter transformer, so we can take the method of integration of iron stem to reduce the noise of reactor core. For the other noise control methods, refer to the noise reduction methods of converter transformer and hollow reactor.

3. Capacitors

Reducing the vibration of the surface elements of the capacitor is the key to reduce the capacitor noise. The following methods can be used to reduce the capacitor noise: ① Increasing the number of capacitors connected in series to reduce the dielectric stress and vibration forces in the capacitor tank; ② Improving the mechanical damping to press the stacked capacitor elements tight to increase the rigidity of the housing of the capacitor unit; ③ Considering the resonance frequency during the design of capacitor.

22.5.3.2 Control of Transmission Routes

After the use of noise control measures at sound source, if the noise of converter station still can not reach the standard, the transmission routes of noise should be controlled.

(1) Select an appropriate site which should be located away from residential areas and other noise-sensitive areas and not built in Class 0 and Class 1 areas as possible. After the site is determined, optimal layout of some equipment can also be used to control the noise.
(2) When the noise source is determined, try to increase the distance from the noise source to the noise-sensitive points as possible.
(3) In addition, the noise insulation screens filled with sound-absorbing materials can be erected for converter transformers, reactors, capacitors and other equipment, and planting trees and other measures can be taken between the noise source and the noise-sensitive points for noise insulation and noise absorption.

22.5.3.3 Hearing Protection of Recipients

After the implementation of noise reduction measures described above, the noise around the converter station normally can meet the requirements of standards, but within the converter station, especially inside the acoustic enclosures and sound barriers, the noise is relatively large and typically greater than 90 dB (A). In case of the long residence time in such an environment, the noise has a greater impact on the operation and maintenance personnel who should be stuffed with cotton in their ears or use anti-sound earplugs, anti-sound earmuffs and active noise control helmets, and other protective measures during the patrol inspection and maintenance. Meanwhile, the operating personnel should minimize the residence time in the area of high noise to reduce the health harm due to the noise.

References

1. Wan B, Xie H, Fan L, Zhang G, Liu X. Electromagnetic environment and corona control measures of UHV substation. High Volt Eng. 2010;36(1):109–15.
2. Chen R, Hu W, Qiang XC, Zhang Z. Test and evaluation of power frequency electromagnetic field of high voltage substation. J Chongqing Univ Sci Technol Nat Sci Ed. 2010;12(3):123–6.
3. Corbellini U, Pelacchi P. Corona losses in HVDC bipolar lines. IEEE Trans Power Deliv. 1996;11(3):1475–81.
4. Maruvada PS, Dallaire RD, Heroux P, et al. Corona studies for bipolar HVDC transmission at voltages between ±600 kV and ±1200 kV Part 2: special biploar line, bipolar cage and bus studies. IEEE Trans Power Appar Syst. 1981;3:1462–71.
5. Xu L, Li Y, Liu C, Hou X, Yu J. Analysis on power frequency electric and magnetic fields within 500 kV substations in chongqing area [J]. Power Syst Technol. 2008;32(2):66–70.
6. Fan Y, Degui YAO, Hui P, Wei H. Measurement and analysis of shielding effectiveness for power frequency electromagnetic field in HV substation. High Volt Appar. 2010;46(1):85–8.
7. Q/GDW 304-2009. Technical regulations for impact assessment of electromagnetic environment produced by 1000 kV transmission and transfer power engineering [S], 2009.
8. Zhao S, Shi Y. Discussion on necessity of substation electromagnetic environment protection district [J]. Electr Power Environ Prot. 2008,24(3):51–3.
9. HJ/T 24-1998. Technical regulations on environmental impact assessment of electromagnetic radiation produced by 500 kV ultrahigh voltage transmission and transfer.
10. GB 3096-2008. Environmental quality standard for noise; 2008.
11. GB 12248-2008. Emission standard for industrial enterprises noise at boundary; 2008.

Chapter 23
Comparison of Overvoltage and Insulation Coordination of ±800 kV and ±1100 kV UHVDC Systems

Wenqian Qiu, Hao Zhou and Dongju Wang

With the rapid development of ±800 kV UHVDC power transmission technology and further implementation of power transmission from west to east, the demand of the power transmission projects of longer distance and larger capacity has been gradually emergent. So it is necessary to develop the UHVDC power transmission technology with higher voltage level.

In the previous chapters, the switching overvoltage of the ±800 kV UHVDC power transmission system was introduced systematically. Based on the above-mentioned researching method on the switching overvoltage of UHVDC system, by using PSCAD/EMTDC and relying on the Zhundong–Chengdu ±1100 kV UHVDC Power Transmission Project and Xiluodu–Zhexi ±800 kV UHVDC Power Transmission Project, simulations on the overvoltage of the AC busbar, valve hall, DC pole line and neutral line in the converter stations were carried out. Finally, combining with the internal overvoltage of the Xiluodu–Zhexi ±800 kV UHVDC converter station, the internal overvoltage in the converter station of both ±1100 and ±800 kV UHVDC power transmission systems was contrasted, and the difference of overvoltage on the rectifier substation and inverter substation of UHVDC power transmission system was discussed. Based on the above results, the DC transient overvoltage at key position of ±1100 kV Zhundong converter station and the insulation level of key equipment under different arrester configuration schemes were compared, thus to propose the

W. Qiu (✉)
China Energy Engineering Group, Zhejiang Electric Power Design Institute Co., Ltd., Hangzhou, Zhejiang, People's Republic of China
e-mail: 839821641@qq.com

H. Zhou · D. Wang
College of Electrical Engineering, Zhejiang University, Xihu district, Hangzhou, Zhejiang, People's Republic of China
e-mail: zhouhao_ee@zju.edu.cn

D. Wang
e-mail: wangdongju@zju.edu.cn

© Zhejiang University Press, Hangzhou and Springer-Verlag GmbH Germany 2018

H. Zhou et al. (eds.), *Ultra-high Voltage AC/DC Power Transmission*,
Advanced Topics in Science and Technology in China,
https://doi.org/10.1007/978-3-662-54575-1_23

suggestions on insulation coordination of the converter stations in ±1100 kV UHVDC power transmission system.

In the final part of this chapter, the contrast and discussion were carried out about the combination scheme for selection of double 12-pulse converters connected in series and triple 12-pulse converters connected in series; according to the discussions, application of the double 12-pulse converters connected in series is optimum at present.

23.1 System Parameters

For the Zhundong–Chengdu ±1100 kV UHVDC Power Transmission Project, the rated bipolar transmission power is 10,450 MW. The rated voltage is ±1100 kV, and rated current is 4750 A. For the converter station at both terminals, each pole is applied with double 12-pulse converters connected in series of 550 + 550 kV, and the wiring mode is same as that of Xiluodu–Zhexi ±800 kV UHVDC Power Transmission Project and the other five ±800 kV UHVDC power transmission projects having been put into operation. The basic operation parameters of the converter station for Zhundong–Chengdu ±1100 kV UHVDC Power Transmission Project and Xiluodu–Zhexi ±800 kV UHVDC Power Transmission Project are, respectively, as shown in Tables 23.1 and 23.2 [1].

The technical parameters of the converter transformer at both sides of Zhundong–Chengdu ±1100 kV UHVDC Power Transmission Project and Xiluodu–Zhexi ±800 kV UHVDC Power Transmission Project are as shown in Tables 23.3 and 23.4 respectively.

Table 23.1 Basic operation parameters for Zhundong–Chengdu ±1100 kV UHVDC Power Transmission Project

Parameters	Zhundong	Chengdu
Rated AC operating voltage U_{acN}/kV	770	525
Max. AC operating voltage U_{acmax}/kV	800	550
Extremely lowest AC operating voltage U_{acmin}/kV	713	475
Max. DC operating voltage U_{dmax}/kV	1122	1122
Max. DC operating current I_{dmax}/A	5367	5367
Max. ideal no-load voltage of the converter $U_{di0absmax}$/kV	338.0	325.7

Table 23.2 Basic operation parameters for Xiluodu–Zhexi ±800 kV UHVDC Power Transmission Project

Parameters	Xiluodu	Zhexi
Rated AC operating voltage U_{acN}/kV	530	510
Max. AC operating voltage U_{acmax}/kV	550	550
Extremely lowest AC operating voltage U_{acmin}/kV	475	475
Max. DC operating voltage U_{dmax}/kV	809	809
Max. DC operating current I_{dmax}/A	4687.5	4687.5
Max. ideal no-load voltage of the converter $U_{di0absmax}$/kV	238.9	220

Table 23.3 Design parameters for converter transformer of Zhundong–Chengdu ±1100 kV UHVDC Power Transmission Project

Converter station	Zhundong	Chengdu
Rated capacity/MVA	542.11	521.59
Rated line voltage at grid side/kV	770	525
Rated line voltage at valve side/kV	242.11	232.94
Short circuit impedance when tap is at zero position/%	24	24
Number of tap positions	+35/−5	+25/−5
Step size of tap changer/%	0.86	1.25

Table 23.4 Design parameters for converter transformer of Xiluodu–Zhexi ±800 kV UHVDC Power Transmission Project

Converter station	Xiluodu	Zhexi
Rated capacity/MVA	378.5	358.4
Rated line voltage at grid side/kV	535	510
Rated line voltage at valve side/kV	171.4	162.2
Short circuit impedance when tap is at zero position/%	19	19
Number of tap positions	+21/−6	+24/−4
Step size of tap changer/%	1.25	1.25

23.2 Configuration and Parameters of Arresters in Converter Station

23.2.1 Configuration of Arresters in Converter Station

In the overvoltage research on the converter station of Zhundong–Chengdu ±1100 kV UHVDC Power Transmission Project in this chapter, the configuration of arresters in the converter station is temporarily considered to adopt the same scheme as the arrester configuration of Xiluodu–Zhexi ±800 kV UHVDC Power Transmission Project, as shown in Fig. 23.1. The descriptions of each arrester in Fig. 23.1 are as shown in Table 23.5.

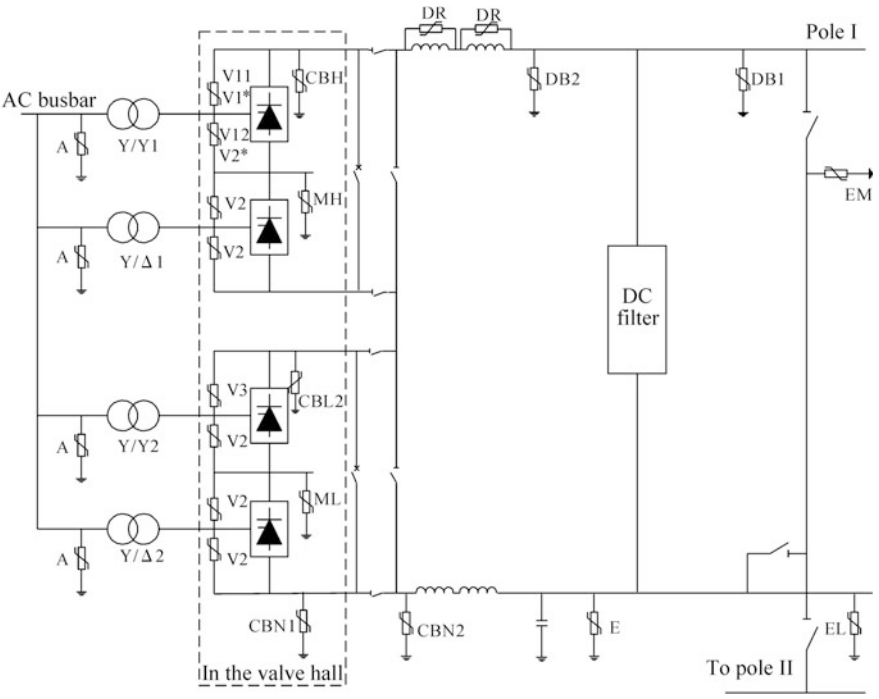

Fig. 23.1 Configuration of arresters in converter station of Zhundong–Chengdu ± 1100 kV UHVDC Power Transmission Project. *Note* In the figure, *V*1 and *V*2 with *asterisk* are the valve arresters in the inverter substation; *V*11 and *V*12 are the valve arresters in the rectifier substation

Table 23.5 Description of arresters in converter station

Arrester	Description
A	AC busbar arrester
V11/V12/V2/V3	Valve arrester
MH/ML	6-pulse bridge arrester of upper/lower 12-pulse unit
CBH	HV-end arrester of converter
CBL2	DC bus arrester between the two 12-pulse converter units
CBN1/CBN2	Neutral bus arrester at the valve side of smoothing reactor
DB1/DB2	DC pole line/busbar arrester
DR	Parallel arrester of smoothing reactor
E	Neutral busbar arrester
EM	Metallic return arrester
EL	Ground electrode line arrester

23.2.2 Basic Parameters of Arresters

The technical parameters of the arrester in the converter station for both Zhundong–Chengdu ±1100 kV UHVDC Power Transmission Project and Xiluodu–Zhexi ±800 kV UHVDC Power Transmission Project are as shown in Tables 23.6 and 23.7 [1–3], respectively.

23.3 Analysis and Contrast of Overvoltage in Converter Station

23.3.1 Overvoltage at AC Side

The equipment at AC side in the converter station is mainly protected by AC busbar arrester A; the arrester is mounted on the busbar closely adjacent to converter transformer and each major AC filter bank. In case of various types of faults occurred to the AC system or operations to be executed in the AC system, for example, single-phase ground fault occurred to the AC system, fault clearing after three-phase ground fault, and switching on and off AC filters, overvoltage with a high amplitude will be generated on the relevant equipment at AC side; the most severe condition of AC busbar arrester A is the three-phase ground fault occurred to the AC system.

When three-phase ground fault is occurred to the AC busbar, the energy stored in the AC filter bank (including capacitor bank) will be released through the fault point; in the following process of fault clearing, power supply of the system will charge the AC filter bank through the system impedance (be inductive generally); thus, the transient oscillation process will generate overvoltage on the busbar at AC side. The simplified equivalent schematic diagram of the fault is as shown in Fig. 23.2.

The calculation results of such overvoltage for both Zhundong–Chengdu ±1100 kV UHVDC Power Transmission Project and Xiluodu–Zhexi ±800 kV UHVDC Power Transmission Project are as shown in Table 23.8. For the sending end of ±1100 kV UHVDC Power Transmission Project, namely Zhundong converter station, the rated AC voltage is 770 kV, and in case of such fault, the overvoltage on the AC busbar is 1113 kV and the maximum energy flowing through arrester A is 2.52 MJ; for the receiving end, namely Chengdu converter station, the rated AC voltage is 525 kV, the maximum overvoltage on the AC busbar is 760 kV and the maximum energy flowing through arrester A is 1.03 MJ. For the sending end of ±800 kV UHVDC Power Transmission Project, namely Xiluodu converter station, the rated AC voltage is 535 kV, the maximum overvoltage on the AC busbar is 760 kV, and the maximum energy flowing through arrester A is 0.91 MJ; for the receiving end, namely Zhexi converter station, the

Table 23.6 Parameters of arresters in converter station of Zhundong–Chengdu ±1100 kV UHVDC Power Transmission Project

Arrester	CCOV/kV (Zhundong/Chengdu)	PCOV/kV (Zhundong/Chengdu)	U_{ref}/kV (Zhundong/Chengdu)	Energy/MJ (Zhundong/Chengdu)
V11/V1	354/341	410/407	410/407	16.2/14.6
V12	354/–	410/–	410/–	7.2/–
V2	354/341	421/407	421/407	7.5/7.2
V3	354/341	421/407	421/407	7.5/7.2
DB1	1122/1122	–/–	1320/1320	24.5/24.5
DB2	1122/1122	–/–	1320/1320	24.5/24.5
CBH	1234/1209	1288/1261	1505/1474	26.7/26.7
MH	915/902	981/957	1116/1100	20.5/20
CBL2	611/604	685/682	761/737	13.8/13.5
ML	404/604	–/–	493/493	4.5/4.5
CBN1	167/107	222/160	333/333	3.1/3.1
CBN2	167/107	222/160	304/304	21.7/8.5
E	55/55	–/–	304/219	2.8/2.0
EL	20/20	–/–	202/202	5.6/5.6
EM	55/55	–/–	278/219	46.6/36
DR	44/44	–/–	483/483 (rms)	3.3/3.3
A	462/318	–/–	576/397	5.0/3.5

CCOV maximum amplitude of continuous operating voltage, not including the commutation overshoot, *PCOV* maximum peak of continuous operating voltage, including the commutation overshoot, U_{ref} the rated voltage of the arrester

Table 23.7 Parameters of arresters in converter station of Xiluodu–Zhexi ±800 kV UHVDC Power Transmission Project

Arrester	CCOV/kV (Xiluodu/Zhexi)	PCOV/kV (Xiluodu/Zhexi)	U_{ref}/kV (Xiluodu/Zhexi)	Energy/MJ (Xiluodu/Zhexi)
V11/V1	250/238	291/284	291/284	10.5/7.6
V12	250/–	291/–	291/–	5.2/–
V2	250/238	297/284	297/284	5.4/3.8
V3	250/238	297/284	297/284	5.4/3.8
DB1	816/816	–/–	960/960	18.55/18.55
DB2	816/816	–/–	960/960	18.55/18.55
CBH	878/877	915/910	1070/1065	19.0/19.0
MH	660/650	725/708	806/821	22.6/14.9
CBL2	443/442	496/478	553/539	10.3/10.1
ML	295/253	–/–	359/362	3.4/3.4
CBN1	123/77	160/112	333/333	3.1/3.1
CBN2	123/77	160/112	304/304	8.7/8.7
E	95/20	–/–	304/219	2.8/2.1
EL	20/20	–/–	202/202	1.9/1.9
EM	95/20	–/–	278/219	34.2/2.1
DR	44/44	–/–	483/483 (rms)	3.3/3.3
A	318/318	–/–	398/398	3.5/3.5

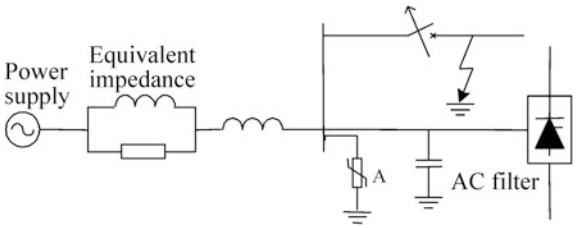

Fig. 23.2 Simplified schematic of overvoltage for three-phase AC ground fault clearing

Table 23.8 Calculation results of overvoltage on arrester A

DC voltage level (kV)	Arrester	Maximum overvoltage/kV	Maximum energy/MJ
±1100	Arrester A in the rectifier substation	1113	2.52
	Arrester A in the inverter substation	760	1.03
±800	Arrester A in the rectifier substation	758	0.91
	Arrester A in the inverter substation	758	0.78

rated AC voltage is 510 kV, the maximum overvoltage on the AC busbar is 758 kV, and the maximum energy flowing through arrester A is 0.78 MJ.

According to the calculation results as shown in Table 23.8, the following analysis is presented [3–5]:

(1) In the both ±1100 kV system and ±800 kV system, the amplitude of overvoltage on the AC busbar in Chengdu converter station (for which AC rated voltage is 525 kV), Xiluodu converter station (for which AC rated voltage is 535 kV) and Zhexi converter station (for which AC rated voltage is 510 kV) is basically identical, the ratio between overvoltage and rated voltage is, respectively, 760/525 = 1.45, 758/535 = 1.42 and 758/510 = 1.49; in Zhundong converter station (for which AC rated voltage is 770 kV), the ratio between overvoltage and rated voltage on the AC busbar is 1113/770 = 1.44. It can be seen that the amplitude of overvoltage is irrelevant to DC voltage level, however, proportional to the rated voltage of AC system.
(2) In Chengdu converter station, Xiluodu converter station and Zhexi converter station for which AC rated voltage is approximate, the overvoltage energy flowing through arrester A is also approximate; in Zhundong converter station for which AC rated voltage is 770 kV, the overvoltage energy flowing through arrester A is larger than that of other three converter stations. The overvoltage energy is mainly related to the voltage level of AC system and the short circuit impedance parameters.
(3) The overvoltage amplitude and energy of such fault are not serious. The overvoltage energy is far less than the capacity of the arresters as shown in Tables 23.6 and 23.7. From the perspective of overvoltage generation mechanism, the overvoltage is resulted from internal voltage oscillation of the system due to transient fault; the conventional AC equipment design and manufacturing have considered such oscillation overvoltage situation. Therefore, on the precondition that design procedures of AC system are met, such overvoltage will not pose threat to the equipment in the converter station generally.

23.3.2 Overvoltage in Valve Hall

From the configuration of arresters in the converter station as shown in Fig. 23.1, it can be seen that, the arresters in the valve hall of the converter station mainly include: valve arresters V11/V1, V12, V2, and V3 paralleled on the valve, converter busbar arresters CBH, MH, CBL2, and ML, and neutral line arrester CBN1. CBN1 is mainly used to prevent the lightning invasion wave overvoltage invading the valve hall along the neutral busbar; therefore, it will not be discussed in this chapter. Here, these arresters will be, respectively, discussed and analyzed according to their respective decisive overvoltage conditions.

The thyristor valves are mainly protected by the valve arresters (V11/V1, V12, V2, and V3) paralleled on them, according to their respective decisive overvoltage

conditions, it can be divided into three groups, namely V11/V1, V12/V2, and V3; the analysis is as shown below.

23.3.2.1 Valve Arresters V11/V1

In case of ground fault occurred between the HV Y/Y converter transformer and converter valve, it is necessary to release energy of the DC line and DC filter; such energy is mainly applied to the valve arresters V11/V1 on the uppermost layer of the 12-pulse converter. Such fault is also the decisive working condition of valve arresters V11/V1. The calculation results of maximum overvoltage on the valve arresters V11/V1 and the energy flowing through them under such condition are as shown in Table 23.9. It can be seen that, the maximum overvoltage on the valve arrester V11 in Zhundong converter station (the sending end of the ±1100 kV system) is 541 kV and the maximum energy is 14.64 MJ; the maximum overvoltage on the valve arrester V1 in Chengdu converter station (the receiving end of the ±1100 kV system) is 540 kV and the maximum energy is 14.3 MJ; the maximum overvoltage on the valve arrester V11 in Xiluodu converter station (the sending end of the ±800 kV system) is 379 kV and the maximum energy is 7.49 MJ; the maximum overvoltage on the valve arrester V1 in Zhexi converter station (the receiving end of the ±800 kV system) is 375 kV and the maximum energy is 6.73 MJ.

The overvoltage amplitude and energy of the valve arresters V11/V1 for both ±1100 and ±800 kV UHVDC power transmission projects, as shown in Table 23.9, are compared and analyzed as follows [2, 6, 7]:

(1) The ratio of the overvoltage amplitude of the valve arresters V11/V1 for both ±1100 and ±800 kV systems is 541/349 = 1.43 and 540/375 = 1.44, respectively; however, the ratio of rated DC voltage of the system is 1100/800 = 1.375; it can be seen that, the increased proportion of the overvoltage amplitude is slightly larger than that of rated voltage level.
(2) The ratio of the energy flowing through the valve arresters V11/V1 for both ±1100 and ±800 kV systems is 14.64/7.49 = 1.96 and 14.3/6.73 = 2.12;

Table 23.9 Calculation results of overvoltage on valve arresters V11/V1

DC voltage level (kV)	Arrester	Maximum overvoltage/kV	Maximum energy/MJ
±1100	Arrester V11 in the rectifier substation	541	14.64
	Arrester V1 in the inverter substation	540	14.3
±800	Arrester V11 in the rectifier substation	379	7.49
	Arrester V1 in the inverter substation	375	6.73

Table 23.10 Contrast of valve arrester conditions for both ±1100 and ±800 kV UHVDC Power Transmission Systems

DC voltage level/kV	1100	800
CCOV of valve arrester (at rectifier substation side)/kV	354	250
DC line length/km	2400	1728
Difference between CCOV of arrester and DC rated voltage/kV	746	550
Overvoltage energy flowing through valve arrester/MJ	14.6	7.5

however, the ratio of square of rated DC voltage of the system is $1100^2/800^2 = 1.89$; it can be seen that the increased proportion of the overvoltage energy is slightly larger than that of square of rated voltage level.

(3) According to the overvoltage mechanism introduced in Chap. 16 (Switching overvoltage in the DC system), such overvoltage is generated under the influence of DC line voltage and transformer outgoing line voltage; therefore, the amplitude of such overvoltage has certain relation with the DC rated voltage and operating voltage of arrester. The overvoltage energy is the energy of residual charges on the distributed capacitance of the DC line; the energy is directly related to the development process of the overvoltage (approximately proportional to the square of DC voltage), and influenced by the line length. Several important parameters of the UHVDC power transmission projects with different voltage levels (namely ±1100 and ±800 kV) are as shown in Table 23.10. It can be seen that the difference between CCOV of arresters V11/V1 and rated voltage of the ±1100 kV system is 746 kV and the difference between CCOV of arresters V11/V1 and rated voltage of the ±800 kV system is 550 kV. The line length is 2400 km for the ±1100 kV system and 1728 km for the ±800 kV system. So the increased proportion of overvoltage on arresters V11/V1 along with the increase of voltage level in the UHVDC power transmission system is slightly larger than that of voltage level, and the increased proportion of overvoltage energy is also slightly larger than that of the square of voltage level.

23.3.2.2 Valve Arresters V12/V2

During the occurrence of fault and switching operation, the AC system of converter station will be subject to interphase switching overvoltage impulse. Such overvoltage impulse will be transmitted to the valve hall through the winding of the converter transformer, and act on the converter valve, thus to generate relatively large overvoltage. The simplified schematic diagram of the fault is as shown in Fig. 23.3. The switching impulse wave is generated between phase A and phase C, when the impulse wave is transmitted to the valve hall (supposing valve arresters VT1 and VT6 are turned on), thus the valve arrester $V2_5$ will bear switching impulse overvoltage generated between phase A and phase C; such condition is the

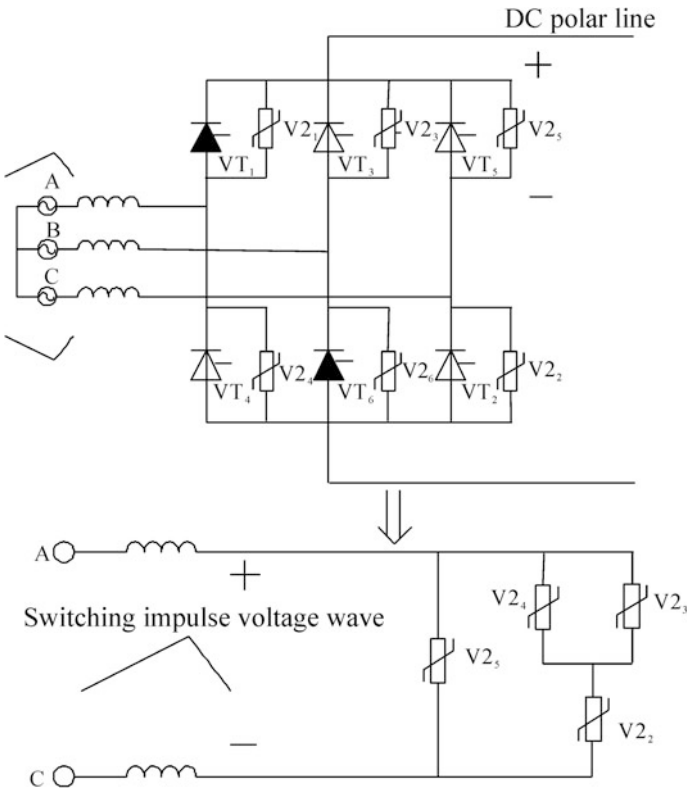

Fig. 23.3 Schematic for transmission of switching overvoltage from AC system into valve hall

decisive operating condition of the valve arresters V12/V2. The calculation results are as shown in Table 23.11. It can be seen that the maximum overvoltage on the valve arrester V2 in Zhundong converter station (namely the sending end of the ±1100 kV system) is 522 kV, and the overvoltage on the valve arrester V2 in Chengdu converter station (namely the receiving end of the ±1100 kV system) is 521 kV; the maximum overvoltage on the valve arrester V2 in Xiluodu converter station (namely the sending end of the ±800 kV system) is 376 kV, and the overvoltage on the valve arrester V2 in Zhexi converter station (namely the receiving end of the ±800 kV system) is 375 kV. Under such fault, the energy flowing through the valve arrester V2 is not large.

After comparing the overvoltage for both ±1100 and ±800 kV UHVDC power transmission systems, it can be seen that the ratio of the amplitude of overvoltage is 522/376 = 1.39 and 521/375 = 1.3, respectively, approximately equal to the ratio of rated voltage of the system (1100/800 = 1.375); therefore, the amplitude of such overvoltage is basically increased proportionally along with the increase of voltage level.

Table 23.11 Calculation results of overvoltage and energy of valve arresters V2

DC voltage level (kV)	Arrester	Maximum overvoltage/kV	Maximum energy/MJ
±1100	Arrester V2 in the rectifier substation	522	0.43
	Arrester V2 in the inverter substation	521	0.40
±800	Arrester V2 in the rectifier substation	376	0.30
	Arrester V2 in the inverter substation	375	0.30

Although the energy flowing through the valve arrester under decisive overvoltage operating condition is relatively low, the scheme of multiple column arresters connected in parallel is also adopted in the actual engineering; for example, V12 in Zhundong converter station is applied with 4 column arresters connected in parallel, and thus its capability to absorb the overvoltage energy is far more than actual energy under such decisive overvoltage condition. The converter valve is the core equipment of the UHVDC power transmission system; the overvoltage on the converter valve needs to be controlled at a relatively low level. Such overvoltage has less energy but large amplitude, and the reference voltage of the arrester is already close to the maximum voltage under normal operation. Thus, it is unable to reduce the overvoltage level by reducing the reference voltage. Therefore, the scheme of multi-column arrester connected in parallel shall be used to reduce the current on each column of arrester, thus to reduce the amplitude of overvoltage and the manufacturing cost of the converter valve.

23.3.2.3 Valve Arrester V3

When converter station is under operation with bipolar unbalanced (for example, for pole I, only the lower 12-pulse converter is put into operation and the upper 12-pulse converter is shut down; for pole II, it is under complete double 12-pulse operation), in case of single-phase ground fault occurred to the valve side of LV Y/Y converter transformer of pole I in the converter station, it will generate large overvoltage on the valve arrester V3 of pole I; such fault is the decisive operating condition of the valve arrester V3. Such overvoltage condition is similar to that of valve arresters V11/V1, and the calculation results are as shown in Table 23.12. The maximum overvoltage on the valve arrester V3 in Zhundong converter station (namely the sending end of the ±1100 kV system) is 555 kV, and the maximum energy flowing through it is 6.36 MJ; and the overvoltage on the valve arrester V3 in Chengdu converter station (namely the receiving end of the ±1100 kV system) is 547 kV; and the maximum energy flowing through it is 5.76 MJ. The maximum overvoltage on the valve arrester V3 in Xiluodu converter station (namely the

Table 23.12 Calculation results of overvoltage and energy of valve arrester V3

DC voltage level (kV)	Arrester	Maximum overvoltage/kV	Maximum energy/MJ
±1100	Arrester V3 in the rectifier substation	555	6.36
	Arrester V3 in the inverter substation	547	5.47
±800	Arrester V3 in the rectifier substation	385	2.93
	Arrester V3 in the inverter substation	373	2.84

sending end of the ±800 kV system) is 385 kV, and the maximum energy flowing through it is 2.93 MJ; and the overvoltage on the valve arrester V3 in Zhexi converter station (namely the receiving end of the ±800 kV system) is 373 kV; and the maximum energy flowing through it is 2.84 MJ.

After comparing the amplitude and energy of the overvoltage on the valve arrester V3 for both ±1100 and ±800 kV UHVDC power transmission systems in the table, the following analysis results are obtained.

(1) The ratio of the amplitude of overvoltage on the valve arrester V3 for both ±1100 and ±800 kV UHVDC power transmission systems is, respectively, 555/385 = 1.44 and 547/373 = 1.47, and 6.36/2.93 = 2.17 and 5.76/2.84 = 2.03 for the maximum energy flowing through it; the ratio of rated voltage of the system and the ratio of square are, respectively, 1100/800 = 1.38 and $1100^2/800^2$ = 1.89. This is similar to the overvoltage on the valve arresters V11/V1, the increased proportion of the amplitude of overvoltage is larger than that of rated voltage level, and the increased proportion of the overvoltage energy is larger than that of square of rated voltage level.
(2) In addition, the rated voltage on the DC busbar where the valve arrester V3 is located is half of the rated voltage of the system; according to the overvoltage generation mechanism, the overvoltage energy flowing through the valve arrester shall be within 1/3 to 1/2 of maximum energy flowing through the valve arresters V11/V1 in the same converter station. From the calculation results as shown in Tables 23.9 and 23.12, it can be seen that 6.36/14.64 = 0.434, 5.76/14.3 = 0.403, 2.93/7.49 = 0.391, and 2.84/6.73 = 0.422, and the simulation results are corresponding to above analysis.

23.3.2.4 Converter Busbar Arrester

As shown in Fig. 23.1, in the upper and lower 12-pulse converters, the busbars between two 6-pulse bridges are, respectively, protected by arresters MH and ML; the DC busbar between upper and lower 12-pulse converters is directly protected by

Table 23.13 Calculation results of overvoltage and energy on converter busbar arresters in valve hall

DC voltage level (kV)	Converter station	Arrester	Maximum overvoltage/kV	Maximum energy/MJ
±1100	Rectifier substation	CBH	1824	2.43
		MH	1293	0.98
		CBL2	901	0.02
		ML	485	≈0
	Inverter substation	CBH	1808	2.02
		MH	1337	≈0
		CBL2	894	≈0
		ML	517	≈0
±800	Rectifier substation	CBH	1350	0.69
		MH	973	≈0
		CBL2	693	≈0
		ML	354	≈0
	Inverter substation	CBH	1326	0.10
		MH	958	≈0
		CBL2	632	≈0
		ML	385	≈0

arrester CBL2; the upper 12-pulse converter HV DC busbar and penetrating bushing and other equipment on the converter are directly protected by arrester CBH. In case of full voltage startup fault, high overvoltage will be generated on the arresters such as DB, CBH, MH, CBL2, and ML, the calculation results are as shown in Table 23.13.

Compare the ratio of the amplitude of overvoltage on arresters CBH, MH, CBL2, and ML for both ±1100 and ±800 kV UHVDC power transmission projects: the ratio at rectifier side is, respectively, 1824/1350 = 1.35, 1293/973 = 1.33, 901/693 = 1.30, and 485/354 = 1.37 and the ratio at inverter side is respectively 1808/1326 = 1.36, 1337/958 = 1.40, 894/632 = 1.41, and 517/385 = 1.34. It can be seen that the proportion of the amplitude of overvoltage is close to the proportion of voltage level, and the amplitude of overvoltage is increased proportionally along with the increase of voltage level. In addition, these overvoltage energies are not large, and the reference voltage of these arresters is already close to the maximum voltage under normal operation. Therefore, in order to reduce the overvoltage at installation place, arrester with multiple column design is adopted to reduce its protection level; thus, the capability to absorb the overvoltage energy is far more than the overvoltage energy that it actually bears.

23.3.3 Overvoltage at DC Line Side

The switchgear at the line side of DC pole smoothing reactor in the converter station is mainly protected by DC pole line arrester DB1 and DC busbar arrester DB2, both of which are jointly used to restrict the overvoltage resulted from lightning and switching impulse in the DC switching yard.

When DC system starts normally, the inverter substation will be unlocked firstly and the rectifier substation will be unlocked subsequently; both DC voltage and current are controlled by means of regulating system and increased to the rated values with flat slope. In normal circumstance, high overvoltage will not be generated. However, in case fault is occurred to the control system, the inverter substation is still under locked state and the rectifier substation is deblocked in manner of minimum trigger angle, the DC system will start with full voltage. At this time, the locked inverter substation is equivalent to an open circuit; after arriving at the line end, the full voltage transmission wave will be subject to open circuit reflection, thus to generate very high overvoltage on the DC line, DC busbar, and relevant equipment; such fault is the decisive operating condition of arresters DB1/DB2. The overvoltage and energy on the arresters DB under full voltage starting fault are as shown in Table 23.14. The maximum overvoltage on the arresters DB in Zhundong converter station (namely the sending end of the ±1100 kV system) is 1824 kV, and the maximum energy is 16.03 MJ; and the overvoltage on the arresters DB in Chengdu converter station (namely the receiving end of the ±1100 kV system) is 1807 kV, and the maximum energy is 13.7 MJ. The maximum overvoltage on the arresters DB in Xiluodu converter station (namely the sending end of the ±800 kV system) is 1350 kV, and the maximum energy is 5.61 MJ, and the overvoltage on the arresters DB in Zhexi converter station (namely the receiving end of the ±800 kV system) is 1330 kV, and the maximum energy is 4.35 MJ.

Table 23.14 Calculation results of overvoltage and energy on valve arresters DB

DC voltage level (kV)	Arrester	Maximum overvoltage/kV	Maximum energy/MJ
±1100	Arrester DB in the rectifier substation	1824	16.03
	Arrester DB in the inverter substation	1807	13.7
±800	Arrester DB in the rectifier substation	1350	5.61
	Arrester DB in the inverter substation	1330	4.35

After comparing the amplitude of overvoltage and energy on the arresters DB for both ±1100 and ±800 kV UHVDC power transmission projects, the following analysis results are obtained:

(1) The ratio of the amplitude of overvoltage on the arresters DB for both ±1100 and ±800 kV UHVDC power transmission projects is 1824/1350 = 1.351 and 1807/1330 = 1.359, respectively, basically proportional to the rated voltage of the system.
(2) According to overvoltage generation mechanism, such overvoltage energy is mainly the charging energy on the DC line; such charging energy is related to the DC line voltage and line length, and the energy released on the DB is the energy released in the process that the maximum voltage of the DC line is reduced to the protection level voltage of the arrester. The amplitude of such overvoltage is proportionally increased along with the increase of voltage level and its energy is proportionally with the multiplication of square of voltage level and line length.

23.3.4 Neutral Busbar Overvoltage

23.3.4.1 Arrester at the Valve Side of Neutral Busbar Smoothing Reactor

In case of monopolar operation with metallic return, when single-phase ground fault is occurred to the valve side of the highest voltage Y/Y converter transformer outgoing bushing during power transmission from the rectifier to the inverter station, large overvoltage will be generated on arrester CBN2. After occurrence of the fault, the DC power supply of the entire fault pole will be applied to the arrester, and subsequently, the lowermost converter valve will be turned off. However, the energy stored on the metallic return has not been released completely; such residual energy will also be released by CBN2, and then the overvoltage on the neutral line will be in the reverse direction. The calculation results are as shown in Table 23.15.

Table 23.15 Calculation results of overvoltage and energy on valve arrester CBN2

DC voltage level (kV)	Arrester	Maximum overvoltage/kV	Maximum energy/MJ
±1100	Arrester CBN2 in the rectifier substation	443	20.76
	Arrester CBN2 in the inverter substation	426	6.31
±800	Arrester CBN2 in the rectifier substation	432	7.51
	Arrester CBN2 in the inverter substation	424	2.69

The maximum overvoltage at the valve side of the neutral busbar smoothing reactor in Zhundong converter station (namely the sending end of the ±1100 kV system) is 443 kV, and the maximum energy flowing through arrester CBN2 is 20.76 MJ; the maximum overvoltage on arrester CBN2 in Chengdu converter station (namely the receiving end of the ±1100 kV system) is 426 kV, and the maximum energy flowing through arrester CBN2 is 6.31 MJ. The maximum overvoltage on arrester CBN2 in Xiluodu converter station (namely the sending end of the ±800 kV system) is 432 kV, and the maximum energy flowing through arrester CBN2 is 7.51 MJ; the maximum overvoltage on arrester CBN2 in Zhexi converter station (namely the receiving end of the ±800 kV system) is 424 kV, and the maximum energy flowing through arrester CBN2 is 2.69 MJ.

From calculation results as shown in Table 23.15, it can be seen that [2, 8]:

(1) The overvoltage on the arrester CBN2 for both ±1100 and ±800 kV UHVDC power transmission projects is approximately identical, because the protection level of the arrester CBN2 selected for these two voltage levels is basically identical.
(2) The overvoltage energy flowing through the arrester CBN2 for ±1100 kV UHVDC power transmission system is much higher than that for ±800 kV UHVDC power transmission system, and the ratio is 20.76/7.51 = 2.76 and 6.31/2.69 = 2.35, respectively. Such overvoltage is mainly formed due to the circuit applied on the CBN2 which is established through ground fault point by two 12-pulse converters at fault pole, so the overvoltage energy is related to the DC voltage level and the protection level of the arrester CBN2, and under influence of such factors as system transmission capacity and line length.

23.3.4.2 Arrester at the Line Side of Neutral Busbar Smoothing Reactor

In case of monopolar operation with metallic return, when ground fault is occurred to the outlet of DC pole line, large overvoltage will be generated on the metallic return in the converter station, this is the decisive operating condition of metallic return arrester EM in the converter station at sending end. After the occurrence of such fault, the DC differential undervoltage protection will be actuated, the trigger angle of fault pole will be immediately shifted to above 90°, the rectifier will change to inverter operation, the DC line will discharge through both inverter substation and rectifier substation, and DC current will be soon reduced to zero; when the DC system restarts after some time of de-ionization, the transmission power will be resumed. For the converter station at receiving end, the neutral busbar is always grounded, the arrester EM is always connected in the system, and the actuating voltage of EL is lower than EM; therefore, in the converter station at receiving end, the arrester EL will be used to absorb the overvoltage energy. The simulation calculation results are as shown in Table 23.16; under the fault, the overvoltage on arrester EM in Zhundong converter station (namely the sending end of

Table 23.16 Calculation results of overvoltage and energy on valve arresters of neutral line

DC voltage level (kV)	Arrester	Maximum overvoltage/kV	Maximum energy/MJ
±1100	Arrester EM in the rectifier substation	378	22.9
	Arrester EL in the inverter substation	279	0.56
±800	Arrester EM in the rectifier substation	377	16.8
	Arrester EL in the inverter substation	260	≈0

the ±1100 kV system) is 378 kV, and the maximum energy is 22.9 MJ; the overvoltage on arrester EL in Chengdu converter station (namely the receiving end of the ±1100 kV system) is 279 kV, and the maximum energy is very small and only 0.56 MJ. The overvoltage on arrester EM in Zhundong converter station (namely the sending end of the ±800 kV system) is 377 kV, and the maximum energy is 16.8 MJ; the overvoltage on arrester EL in Chengdu converter station (namely the receiving end of the ±800 kV system) is 260 kV, and the maximum energy is very small.

According to the calculation results, it can be seen that [2, 8]:

(1) The overvoltage on arrester EM for both ±1100 and ±800 kV UHVDC power transmission projects is respectively 378 and 377 kV and approximately equal, because the protection level of the valve arrester EM selected for these two voltage levels is basically identical.
(2) The ratio of energy flowing through arrester EM for both ±1100 and ±800 kV UHVDC power transmission projects is 22.9/16.8 = 1.36. Such overvoltage is divided into two stages: first stage is formed due to the circuit applied on EM which is established through ground fault point by two 12-pulse converters at fault pole; second stage is formed through release of energy stored on the metallic return distributed capacitance by means of EM. These two stages jointly establish the overvoltage on the arrester EM, the overvoltage energy of the first stage is related to the system transmission capacity, and the overvoltage energy of the second stage is related to the line length. For these two projects, the ratio of transmission power is 10,450/7500 = 1.39 and the ratio of line length is 2400/1728 = 1.39; the energy is related to both system capacity and line length.
(3) In addition, according to the protection characteristics of DC system, for ground fault of the line, after protection is started, the DC system will be restarted after some time of de-ionization. In case the ground fault is a permanent fault, the relevant arresters will bear the overvoltage for another time. Based on the above conditions, when designing the maximum energy capacity of the arrester EM, the maximum energy flowing through the arrester EM can be considered as two times of calculated value under such fault, that is to say, for both ±1100

and ±800 kV UHVDC power transmission projects, the maximum energy flowing through arrester EM is, respectively, 45.8 and 33.6 MJ.

(4) For the arrester EL on the neutral line at receiving end which is always under grounded operation, both the overvoltage stressed on it and the energy flowing through it are very small generally.

23.4 Insulation Coordination of ±1100 kV UHVDC Power Transmission System

According to the previous engineering experiences and implementation of the ±800 kV UHVDC power transmission project, when voltage level is up to ±1100 kV, the equipment volume and weight will be increased, for example, for wall penetrating bushing in ±1100 kV system, the length will be up to about 25 m and the weight is approximate to 18 tons. The equipment cost and insulation level will present very intense non-linear characteristic relationship, when the insulation level of ±1100 kV UHV equipment is reduced slightly, it is able to achieve great reduction in equipment volume, manufacturing cost, test cost, and transportation difficulties, thus to obtain perfect technical and economic benefit.

For ±1000 kV UHVDC project, the insulation coordination method of converter station equipment is basically the same with ±800 kV UHVDC project. Because the arrester layout schemes for converter station directly influence the insulation level of the converter station equipment, it can be considered by optimizing the arrester arrangement to control the insulation level of ±1100 kV UHVDC converter station equipment. In addition, the short circuit impedance of the converter transformer will also affect the insulation level of converter station equipment. The influence of converter station arrester layout schemes and short circuit impedance of converter transformer on the insulation level of ±1100 kV UHVDC converter station equipment will be analyzed in the below.

23.4.1 Configuration Scheme for Arresters in Converter Station

23.4.1.1 Configuration Scheme for Arresters of ±800 kV/±1100 kV UHVDC Power Transmission Projects

At present, the Xiangjiaba–Shanghai ±800 kV UHVDC power transmission project and the Jinping–South Jiangsu ±800 kV UHVDC power transmission project having been put into operation are both applied with the arrester configuration scheme as shown in Fig. 23.4. In such scheme, the ground insulation protection of

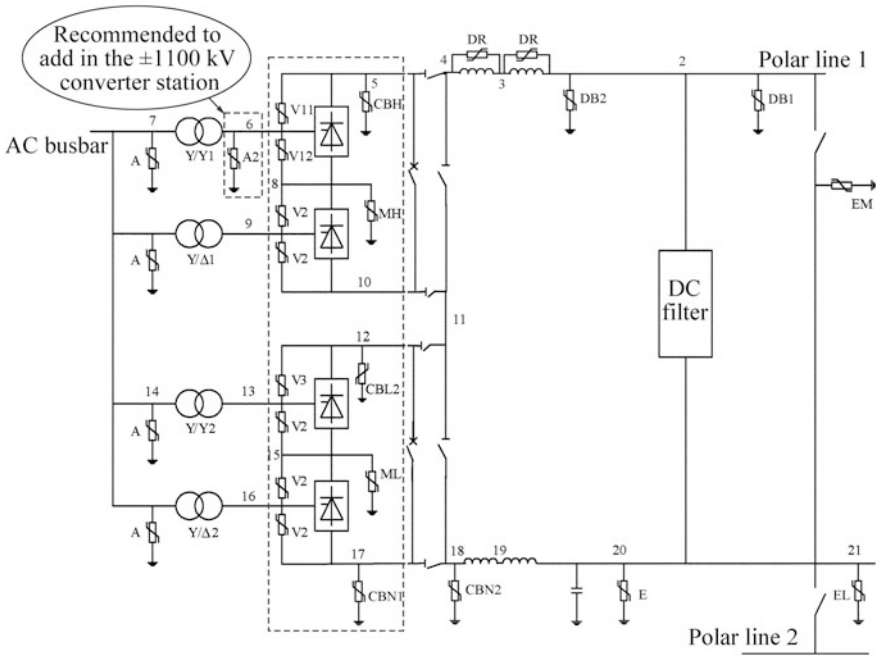

Fig. 23.4 Configuration scheme for arresters in converter station of ±800 kV/±1100 kV UHVDC Power Transmission Projects. *Note A* AC busbar arrester, *A2* arrester at the valve side of highest voltage Y/Y converter transformer, *V11/V12/V2/V3* valve arresters, *MH/ML* 6-pulse bridge arresters of upper/lower 12 converter unit, *CBH* DC bus arrester of upper 12-pulse converter group, *CBL2* DC bus arrester between the two 12-pulse converter group, *CBN1/CBN2* arrester at the bottom of the converter, *DB1/DB2* DC pole line/busbar arrester, *DR* parallel arrester of smoothing reactor, *E* neutral busbar arrester, *EM* metallic return arrester, *EL* ground electrode line arrester

the bushing at the valve side of the HV Y/Y converter transformer is achieved by series connection of the arrester MH and the arrester V12.

The bushing at the valve side of the HV Y/Y converter transformer in the converter station is protected in manner of MH + V12. The advantages are: only one arrester MH is required for each pole and each substation; in addition, the rated voltage is low, the arrangement in the valve hall is simple and the occupied space is less. The disadvantages are: the protection level after series connection of the arrester MH and the arrester V12 is high, and thus it has higher requirements on insulation level of bushing and winding at the valve side of converter transformer [9–11]. Considering that the insulation problem will be most severe after voltage level is up to ±1100 kV, in case the insulation level of the bushing at the valve side of the HV converter transformer is very high, the design and manufacturing difficulties will be very large and the cost will be very high. Thus, suitable reduction in insulation level will achieve apparent economic and technical benefits. Therefore, for ±1100 kV converter station, it is able to consider that add arrester A2 at the

valve side of HV converter transformer based on the arrester configuration scheme in the ±800 kV UHVDC converter station, thus to directly protect the bushing at the valve side of the HV converter transformer, the scheme is as shown in the dashed frame in Fig. 23.4. The arrester is able to inhibit the overvoltage transmitted from AC side through the converter transformer, thus to reduce the insulation level of the bushing at the valve side of the HV converter transformer.

The advantages for application of the arrester A2 are as follows: it is directly paralleled between the HV converter transformer valve side and ground, thus the protection effect is apparent and visual. Secondly, arrester A2 is not under high voltage during the entire power frequency period and it is only under high voltage when the converter valve at upper layer on the same phase is turned on. Therefore, the entire arrester can be applied with high chargeability, thus to obtain relatively low protection level. In addition, the arrester A2 is also favorable to reduce the insulation level of equipment at the top of the highest voltage converter valve (such as HVDC ±1100 kV wall penetrating bushing).

Addition of the arrester A2 will increase some investments, it needs to add three arresters A2 for each pole at each station, thus to occupy larger space in the valve hall. However, considering the particularity of the ±1100 kV UHVDC power transmission project, in comparison with economic benefit generated from the reduced insulation level at converter transformer valve side, the slight increase of investment on the arrester and valve hall is not worth to mention. Therefore, such scheme is worth to consider.

23.4.1.2 Contrast of Insulation Level of Key Equipment Under the Two Schemes

Relying on Zhundong–Chengdu ±1100 kV UHVDC Power Transmission Project, the overvoltage simulation for these two arrester configuration schemes (namely the ±1100 kV UHVDC converter station is applied with A2 or not applied with A2) is carried out, thus to determine the insulation level of key equipment. The calculation results are as shown in Table 23.17.

From the results as shown in Table 23.17, it can be seen that, when the arrester configuration scheme without arrester A2 is adopted, the insulation level of the bushing at the valve side of the HV converter transformer is up to 2250 kV, and the insulation level of wall penetrating bushing in ±1100 kV HVDC system is up to 2250 kV; however, when the arrester configuration scheme with arrester A2 is adopted, the insulation level of the bushing at the valve side of the HV converter transformer can be reduced to 2100 kV and the insulation level of wall penetrating bushing in ±1100 kV HVDC system can be reduced to 2150 kV. Therefore, application of the arrester configuration scheme with arrester A2 can achieve effective restriction on insulation level of equipment at these two key positions (converter transformer and wall penetrating bushing), thus to greatly reduce the equipment manufacturing difficulties and economic cost.

Table 23.17 Insulation level of equipment at different key positions in Zhundong converter station under different arrester arrangement schemes

Position	Arrester configuration scheme	Protection arrester	Arrester SIPL/kV	Recommended value of SIWL/kV	Insulation allowance/ %
DC pole line (2)	Without arrester A2	Max (DB1, DB2)	1859	2150	15.6
	With arrester A2	Max (DB1, DB2)	1859	2150	15.6
Bushing at the valve side of HV converter transformer (6)	Without arrester A2	V12 + MH	1945	2250	15
	With arrester A2	A2	1819	2100	15.4
DC 1100 kV wall penetrating bushing (5)	Without arrester A2	CBH	1946	2250	15.6
	With arrester A2	Max (A2, DB2)	1859	2150	15.6

SIPL the switching impulse protection level, *SIWL* switching impulse withstand level

23.4.2 *Influence of Short Circuit Impedance on Insulation Level of Equipment*

In ±1100 kV UHVDC project, due to the capacity of converter transformer is greater, the maximum short circuit current of valve side withstand by valves is higher than that of ±800 kV DC system when a fault occurred to the DC system. In order to limit the short circuit current of valve side, short circuit impedance of ±1100 kV DC system is general larger than that of ±800 kV DC system. However, if the short circuit impedance of the converter transformer is too large, the reactive power consumption of the converter will be increased, and the loss of converter transformer is increased, so the short circuit impedance cannot be too large. In addition, the short circuit impedance is also restricted by the manufacturing and transportation condition of converter transformer. The site-assembly of converter transformer is one of the schemes to reduce short circuit impedance and solve the limit of transport condition. The short circuit impedance of UHVDC converter transformer should be comprehensively determined after considering the above factors. The short circuit impedance of converter transformer in ±1100 kV UHVDC system is generally larger than that of ±800 kV converter transformer, which is generally about 24%, while the short circuit impedance of converter transformer in ±800 kV UHVDC project is generally 18–20% [12]. The difference of short circuit impedance of converter transformer will affect the insulation level of converter station equipment.

Because the short circuit impedance of converter transformer and the maximum ideal no-load DC voltage of converter station are basically the proportional linear relationship [13], combined with Sect. 18.3.3 (calculation of arrester parameters) in

this book, the maximal ideal no-load DC voltage of the arrester will determine arrester continuous operating voltage CCOV/PCOV, while arrester continuous operating voltage CCOV/PCOV will determine the protection level of the arrester, so the short circuit impedance of converter transformer is basically linear related with the protection level of arrester. After considering a certain safety factor, the insulation level of the equipment can be calculated by the protection level of the arrester. For ±1100 kV UHVDC project, the insulation level of HV side of the Y/Y converter transformer has become restriction for manufacturing of converter transformer. The insulation level of converter transformer can be reduced by reducing short circuit impedance of converter transformer in a certain extent. Therefore, viewing from insulation coordination, the short circuit impedance of converter transformer should be reduced as far as possible with conditions permitted. However, in order to limit the maximum short circuit current of valve side and limited by transport conditions, the short circuit impedance of the converter transformer cannot be too small. Therefore, in the practical engineering, the selection of short circuit impedance of converter transformer should be considered comprehensively.

23.4.3 Insulation Level of Equipment

It is the 750 kV AC system at AC side in Zhundong converter station; according to relevant insulation coordination standards and data concerning to AC system [9, 14–19], both lightning impulse insulation level and switching impulse insulation level for the 750 kV AC busbar and equipment in the converter station will be taken as 1950/2100 kV (transformer and other equipment) and 1550 kV, respectively.

According to the arrester protection level and equipment insulation allowance as obtained via the above discussion, it is able to obtain the insulation level at different protection positions at DC side in Zhundong converter station. The calculation results are as shown in Table 23.18.

In summary, when the scheme without the arrester A2 is adopted, the lightning impulse insulation level and switching impulse insulation level of the equipment at the line side of 1100 kV DC pole line smoothing reactor in Zhundong converter station will be selected, respectively, as allowance of 20 and 15%, the values are 2594 and 2138 kV, respectively, and the final recommended design values are 2600 and 2150 kV, respectively; the lightning impulse insulation level and switching impulse insulation level of the equipment at the valve side of DC pole line smoothing reactor are 2446 and 2338 kV, respectively, and the final recommended design values are 2500 and 2250 kV, respectively; the lightning impulse insulation level and switching impulse insulation level of the equipment at the valve side of HV Y/Y converter transformer are 2500 and 2250 kV, respectively, corresponding to that of the equipment at the valve side of the DC pole line smoothing reactor.

When the scheme with the arrester A2 is adopted, the lightning impulse insulation level and switching impulse insulation level of the equipment at the line side

Table 23.18 Insulation level of equipment in Zhundong converter station

Position	Protection arrester	LIPL/kV	LIWL/kV	Insulation allowance/%	LIPL/kV	LIWL/kV	Insulation allowance/%
Position	Max (V11, V12, V2, V3)	546	601	10	579	637	10
Between valves	A	1364	2100	54	1105	1550	40
AC busbar	CBH (scheme without A2)	2038	2446	20	1946	2238	15
DC busbar to earth on valve side	Max (A2, DB2) (scheme with A2)	2038	2446	20	1859	2138	15
DC busbar to earth on line side	Max (DB1, DB2)	2162	2594	20	1859	2138	15
Between smoothing reactors	DR	900	1080	20	–	–	–
Between HV 12-pulse converter bridges	Max (V11, V12) + V2	1079	1295	20	1143	1314	15
HV YY converter transformer phase to earth, valve side	V12 + MH (scheme without A2)	2037	2444	20	1945	2237	15
	A2 (scheme with A2)	1943	2332	20	1819	2092	15
HV YY converter transformer neutral point	A + MH	–	–	–	1797	2067	15
Upper 12-pulse bridge neutral point	MH	1504	1805	20	1436	1651	15
HV YD converter transformer phase to earth, valve side	V2 + CBL2	1577	1892	20	1563	1797	15
12-pulse bridge neutral point	CBL2	1031	1237	20	984	1132	15
LV YY converter transformer phase to earth, valve side	V2 + ML	1227	1472	20	1230	1415	15
LV YY converter transformer neutral point	A + ML	–	–	–	1012	1164	15
Lower 12-pulse bridge neutral point	ML	681	817	20	651	749	15

(continued)

Table 23.18 (continued)

Position	Protection arrester	LIPL/kV	LIWL/kV	Insulation allowance/%	LIPL/kV	LIWL/kV	Insulation allowance/%
LV YD converter transformer phase to earth, valve side	Max (V2 + CBN1, V2 + CBN2)	1004	1205	20	1011	1163	15
YY converter transformer phase-to-phase, valve side	2A′	–	–	–	722	830	15
YD converter transformer phase-to-phase, valve side	$\sqrt{3}$A′	–	–	–	625	719	15
Neutral busbar, valve side	Max (CBN1, CBN2)	458	550	20	432	497	15
Neutral busbar, line side	Max (E, EL, EM)	478	574	20	380	437	15
Earthing electrode busbar	EL	336	403	20	303	348	15
Metallic return busbar	EM	395	474	20	380	437	15
Neutral busbar smoothing reactor	CBN2 + E	892	1070	20	–	–	–

LIWL/SIWL refer to lightning/switching impulse insulation level respectively

of 1100 kV DC pole line smoothing reactor in Zhundong converter station will be selected, respectively, as allowance of 20 and 15%, the values are 2594 and 2138 kV respectively, and the final recommended design values are 2600 and 2150 kV, respectively; the lightning impulse insulation level and switching impulse insulation level of the equipment at the valve side of DC pole line smoothing reactor are 2446 and 2138 kV, respectively, and the final recommended design values are 2500 and 2150 kV, respectively; the lightning impulse insulation level and switching impulse insulation level of the equipment at the valve side of HV Y/Y converter transformer are 2332 and 2092 kV, respectively, and the final recommended design values are 2400 and 2100 kV, respectively. Therefore, it can be seen that the insulation level required at both the valve side of the smoothing reactor and the valve side of HV Y/Y converter transformer are reduced to certain extent.

23.5 Discussion on Converter Combination for ±1100 kV UHVDC System

For the ±1100 kV UHVDC power transmission system, there are two types of wiring schemes for converters: wiring scheme of two 12-pulse converters connected in series for each pole (double 12-pulse) and wiring scheme of three 12-pulse converters connected in series for each pole (triple 12-pulse). When the voltage of UHVDC power transmission system is increased from ±800 to ±1100 kV, in case the wiring scheme of two 12-pulse converters in series is still used, the capacity and volume of the converter transformer must be increased, thus to cause large difficulties in manufacturing and transportation. Therefore, it is necessary to discuss the converter wiring scheme of the ±1100 kV UHVDC power transmission system. In this section, the wiring schemes for both double 12-pulse converters and triple 12-pulse converters are, respectively, analyzed technically.

23.5.1 Discussion on Combination of ±1100 kV Converters

23.5.1.1 Contrast of Advantages and Disadvantages Between Double 12-Pulse Converter and Triple 12-Pulse Converter

The advantages of the ±1100 kV system applied with double 12-pulse converters connected in series (550 + 550 kV) are as shown below:

- The control system is similar to that of the ±800 kV system, and it can be used only after minor change;
- The strategy that smoothing reactor is separately arranged can be used, thus to reduce he amplitude of harmonic voltage on the DC busbar.

The disadvantages of the ±1100 kV system applied with double 12-pulse converters connected in series (550 + 550 kV) are as shown below:

- Both capacity and volume of the converter transformer are larger than that of the ±800 kV system, and the overall transportation has exceeded the limit available for current land transportation. Such problem can be solved in manner of site assembly.

The advantages of the ±1100 kV system applied with triple 12-pulse converters connected in series (367 + 367 + 367 kV) are as shown below:

- Both capacity and volume of the converter transformer are smaller than that of the double 12-pulse converters connected in series, so that the transportation of converter transformer is relatively easier.

The combination of triple 12-pulse converters connected in series also has many disadvantages:

- The converter structure is more complex; therefore, the control protection system corresponding to the UHVDC power transmission system and available operating modes are also more complex;
- The entire converter station requires 36 converter transformers and three types of converter valve halls (namely HV, MV, and LV); therefore, the converter station requires larger space;
- In case of combination of triple 12-pulse converters connected in series, the protection level of valve arrester is lower in comparison with the rated voltage of the system, and the voltage withstand level of the converter valve is also lower than that of the double 12-pulse converters. Therefore, the converter is easier to undertake various types of overvoltage during operation;
- The number of both arresters and paralleling columns required for the converter valve is much larger than that of double 12-pulse converters. Therefore, stricter requirements are presented for manufacturing and pairing of the valve arresters and reserved space of the valve arresters on the converter valve tower;
- In case of combination of triple 12-pulse converters connected in series, the equipment with higher insulation level required is more than that of double 12-pulse converters and the insulation level is also higher.

23.5.1.2 Number of Both Arresters and Paralleling Columns Required for Converter Valve Under Series Combination of Triple 12-Pulse Converters

In case of combination of triple 12-pulse converters connected in series, the protection level of arrester for the converter valve is about 370 kV, while it is 550 kV for the double 12-pulse converters connected in series. In comparison with 1100 kV rated voltage of the system, the proportion of the former is lower, in case the

converter valve is subject to serious overvoltage, the current and energy flowing through the valve arrester will be larger. According to the simulation, in case of ground fault at the valve side of the highest voltage converter transformer as shown in Fig. 23.5, the current and energy flowing through the valve arrester V11 paralleled on the converter valve at uppermost layer for the upper 12-pulse converter will be as shown in Table 23.19.

From the simulation results, it can be seen that in case combination of triple 12-pulse converters connected in series is used, the protection level of the valve arrester will be lower than that of combination of double 12-pulse converters

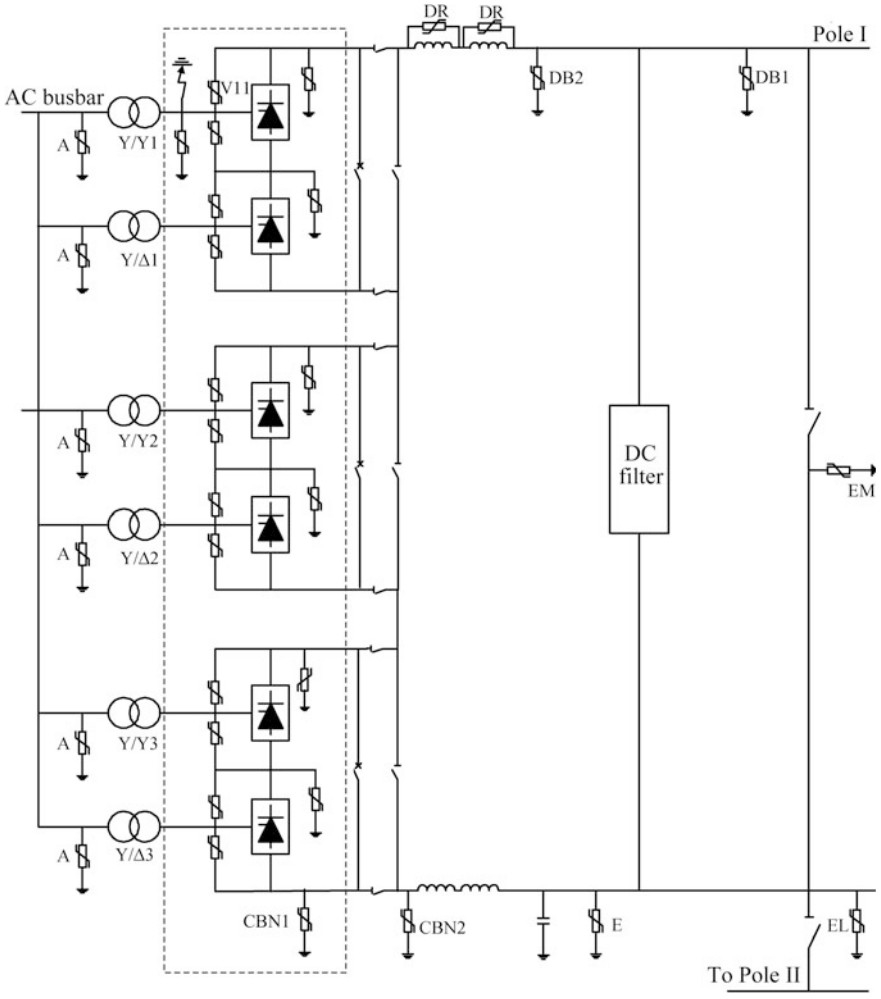

Fig. 23.5 Schematic for ground fault of outgoing line at the valve side of highest voltage converter transformer under combination of triple 12-pulse converters

Table 23.19 Calculation results of overvoltage and energy on the uppermost layer valve arrester V11 under different converter combinations

Combination	Amplitude of overvoltage/kV	Current flowing through arrester/kA	Energy flowing through/MJ	Least paralleling columns required for valve arrester
Double 12-pulse converters connected in series	541	3.61	14.64	8
Triple 12-pulse converters connected in series	365	4.03	16.03	14

connected in series. However, the energy flowing through the valve arrester V11 will be higher than that of combination of double 12-pulse converters connected in series. Thus, it requires more paralleling columns for the valve arrester. The converter valve arrester at the uppermost layer in combination of double 12-pulse converter connected in series is applied with 8 paralleling columns; thus, in case combination of triple 12-pulse converters connected in series is used, it requires at least 14 paralleling columns for the valve arrester. This will present stricter requirements on the manufacturing and pairing of the valve arresters, and need more reserved space of the valve arresters on the converter valve tower.

In case combination of triple 12-pulse converters connected in series is used, apart from significant increase of paralleling columns for the valve arrester at uppermost layer, the paralleling columns for the valve arrester at the uppermost layer in the middle 12-pulse converter (namely the second stage) are also very much. The ground fault occurred to the outgoing line at valve side of Y/Y converter transformer in the middle 12-pulse converter is as shown in Fig. 23.6. Under such fault, the calculation results of overvoltage undertaken by the valve arrester V3 at the uppermost layer in the middle 12-pulse converter are as shown in Table 23.20.

According to the calculation results, in order to meet the requirements, the valve arrester at the uppermost layer in the middle 12-pulse converter shall be configured with 8 columns at least.

In summary, it can be seen that, in case of combination scheme of both double 12-pulse converters connected in series and triple 12-pulse converters connected in series, the number of paralleling columns required for the valve arrester at the uppermost layer in each stage of 12-pulse converter are as shown in Table 23.21.

Thus, it can be seen that, in case of combination scheme of triple 12-pulse converters, the number of paralleling columns required for the valve arrester is far more than that of combination scheme of double12-pulse converters, and the configuration is also more complex.

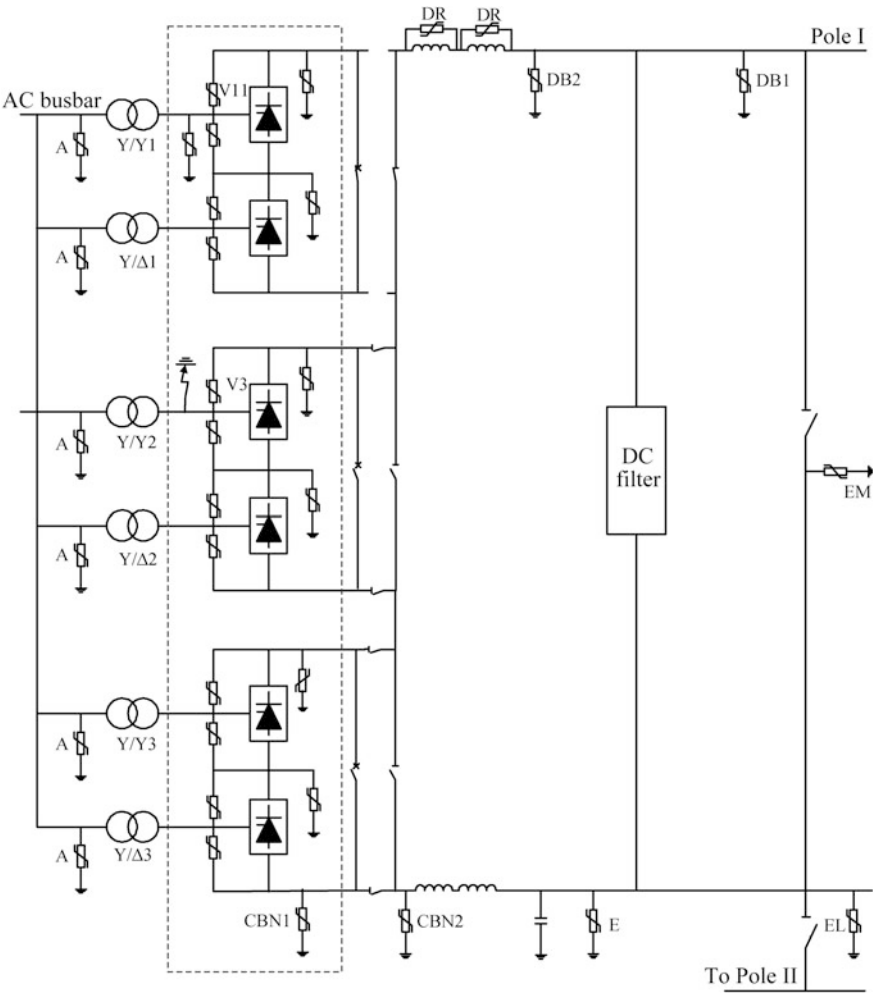

Fig. 23.6 Schematic for ground fault of outgoing line at the valve side of Y/Y converter transformer in the middle 12-pulse converter

Table 23.20 Calculation results of overvoltage and energy on the valve arrester V3 at the uppermost layer in the middle 12-pulse converter

Combination	Amplitude of overvoltage/kV	Current flowing through arrester/kA	Energy flowing through/MJ	Least paralleling columns required for valve arrester
Valve arrester V3	357	2.62	9.06	8

Table 23.21 Number of paralleling columns required for valve arrester under different protection levels of valve arrester

Combination	Protection level (kV)	Upper 12-pulse	Middle 12-pulse	Lower 12-pulse
Double 12-pulse	About 550	8	–	4
Triple 12-pulse	About 370	14	8	3

Table 23.22 Number of main equipment required under different combination of converters

Voltage level (kV)	Scheme of triple 12-pulse			Scheme of double 12-pulse		
	12-pulse converter	Wall penetrating bushing	Converter transformer	12-pulse converter	Wall penetrating bushing	Converter transformer
367	2	4	12	–	–	–
550	–	–	–	2	4	12
733	2	4	12	–	–	–
1100	2	2	12	2	2	12

23.5.1.3 Contrast of Main Equipment Required for Combination of Both Double 12-Pulse Converters and Triple 12-Pulse Converters

The contrast of converter transformers at all voltage levels and main equipment required for combination of both double 12-pulse converters and triple 12-pulse converters are as shown in Table 23.22.

From the table, it can be seen that, in case of combination scheme of triple 12-pulse converters, the number of equipment with high insulation level required will be larger than that of combination scheme of double 12-pulse converters, and the insulation will also be higher. Apparently, in case of combination scheme of triple 12-pulse converters, the investment for equipment and insulation will be much higher.

23.5.2 Selection of Combination Scheme for Converters of ±1100 kV UHVDC System

From above analysis, it can be seen that, for the ±1100 kV UHVDC system, the combination scheme of double 12-pulse converters connected in series will be apparently better than the combination scheme of triple 12-pulse converters connected in series. Therefore, after considering based on the above factors, the ±1100 kV UHVDC system shall be applied with the combination scheme of double 12-pulse converters connected in series.

References

1. Zhou H, Wang D. Overvoltage protection and insulation coordination for ±1100 kV UHVDC converter station. Power Syst Technol. 2012;36(9):1–8.
2. Wang D, Deng X, Zhou H, Chen X, Shen Y, Sun K. On the DC transient overvoltage in the converter stations of ±800 kV Xiluodu–Zhexi HVDC project. South Power Syst Technol. 2012;6(2):6–13.
3. Chen X, Zhou H, Wang D, Shen Y, Qian F, Zhou Z, Qiu W. Study on transient overvoltage of Zhexi converter station of ±800 kV DC power transmission project. Power Syst Technol. 2012;36(3):22–7.
4. Chen X, Tian J, Wang D, Yuan S, Zhou H. Analysis on overvoltage in renovated control and protection system for HVDC power transmission project from Tianshengqiao to Guangzhou. Power Syst Technol. 2011;35(6):101–6.
5. Chen X, Zhou H, Wang D, Shen Y, Ding J, Qian F, Zhou Z, Qiu W. Insulation coordination for Zhexi converter station of ±800 kV DC power transmission project from Xiluodu to Zhexi. Power Syst Technol. 2012;36(2):7–12.
6. Wang D, Deng X, Zhou H, Chen X, Xu A, Shen Y. Research on converter valve overvoltage mechanism and calculation conditions of ±800 kV converter station (English Version). High Volt Eng. 2012;12:3189–97.
7. Chen X, Zhou H, Yuan S, Wang D, Tian J, Huang Z, Lu Y. Overvoltage mechanism of converter valves for HVDC power transmission project from Tianshengqiao to Guangzhou. Power Syst Technol. 2012;36(3):88–94.
8. Yuan S, Wang D, Chen X, Huang Z, Lu Y, Tian J, Chen W, Sun K, Zhou H. Study on neutral-bus overvoltage mechanism of ±500 kV DC power transmission project from Tianshengqiao to Guangdong. Power Syst Technol. 2011;35(5):216–22.
9. Nie D, Ma W, Zheng J. Insulation coordination for ±800 kV UHVDC converter stations. High Volt Eng. 2006;9:75–9.
10. Zhou H, Chen X, Chen R, Wang D, Yuan S, Sun K. Analysis on insulation coordination scheme for ±800 kV DC converter station. Power Syst Technol. 2011;35(11):18–24.
11. Deng X, Wang D, Shen Y, Zhou H, Chen X, Sun K. DC switching overvoltage of ±1100 kV UHVDC converter station. Electric Power Autom Equip. 2014;34(1):141–7.
12. Deng X, Wang D, Shen Y, Zhou H, Chen X, Sun K. Main circuit parameter design of Zhundong-Sichuan ±1100 kV UHVDC power transmission project. Electric Power Autom Equip. 2014;34(4):133–40.
13. Zhou P, He H, Dai M, Wan L. Selection of arresters arrangement, parameters and apparatuses insulation levels for μ1 100 kV DC converter station. High Volt Eng. 2014;40(9):2871–84.
14. Nie D, Yuan Z. Research on insulation coordination for converter stations of ±800 kV UHVDC project from Xiangjiaba to Shanghai. Power Syst Technol. 2007;31(14):1–5.
15. Zhou P, Xiu M, Gu D, Dai M, Lou Y. Study on overvoltage protection and insulation coordination for ±800 kV HVDC transmission system. High Volt Eng. 2006;32(12):125–32.
16. Q/GDW 101-2003. Provisional technical code for design of 750 kV substations. 2003.
17. Huang Y, Li X, Rao H, Wen K, Tian F. Discussion on the insulation margin of thyristor valves for ±800 kV power transmission. South Power Syst Technol Res. 2006;2(6):23–7.
18. Nie D, Ma W, Li M. Insulation coordination for converter stations of UHVDC Project from Jinping to South Jiangsu. High Volt Eng. 2010;36(1):92–7.
19. Zhou H, Deng X, Wang D, Shen Y, Chen X, Sun K. Overvoltage Protection and insulation coordination for ±1100 kV UHVDC converter station (English Version). High Volt Eng. 2013;39(10):2477–84.

Chapter 24
Principles and Configurations of UHVDC Protection

Taoxi Zhu

The UHVDC transmission system mainly consists of the DC lines and the converter stations at both the terminals, and the equipment in the station includes equipment in AC field, equipment in the valve hall, and equipment in DC field [1, 2].

During the operation of UHVDC transmission system, measures shall be taken to avoid the abnormal operation of the system as far as possible, eliminate or reduce the possibility of fault occurrence, and avoid any threats to the safety of system or equipment. Once the system or equipment has any faults or operates abnormally, the types and severity of faults shall be quickly identified by detecting the fault features. The most reasonable strategy will be selected to eliminate the faults rapidly by cooperating with the control system.

24.1 Overview of UHVDC Protection

24.1.1 Basic Requirements of UHVDC Protection

Same with the AC relay protection, the UHVDC protection shall generally meet the basic requirements of "four principles," i.e., selectivity, speedy, sensitivity, and reliability [3, 4].

The "four principles" of UHVDC protection is a whole that interacts with each other. It is normally difficult to meet the above four requirements at the same time. The improvement on one performance is often at the sacrifice of other performances. Therefore, in the design, configuration and setting of DC protection, the key points of "four principles" should be identified according to the fault type and

T. Zhu (✉)
Power Dispatching and Communication Center of CSG, Guangzhou, Guangdong Province, People's Republic of China
e-mail: taoxi-zhu@hotmail.com

© Zhejiang University Press, Hangzhou and Springer-Verlag GmbH Germany 2018

H. Zhou et al. (eds.), *Ultra-high Voltage AC/DC Power Transmission*, Advanced Topics in Science and Technology in China,
https://doi.org/10.1007/978-3-662-54575-1_24

hazards which may caused by the fault. In view of the structure and operating characteristics of UHVDC transmission system and its importance in the electric power system, the coordination between "four principles" shall follow the principle of reducing the range of faults as far as possible, reducing the impulse on AC and DC systems on the basis of guaranteeing the safety of primary equipment.

What differs from the AC protection is that the DC protection has particular close coordination with the control system. The DC protection must coordinate closely with the control system to select the most reasonable strategy. Under the slight fault condition, the UHVDC system can generally return to normal operation through the handling of the control system; under the serious fault condition, the faulty equipment shall be shut down and the fault points be isolated as soon as possible by the control system. In such a way, the safety of the faulty primary equipment can be ensured and other sound equipment can operate properly so as to minimize the impacts of faults and abnormal operation on the entire system.

24.1.2 Action Result of UHVDC Protection

The close coordination of the DC protection system with the DC control system can restrict the severity of harm to the DC system, AC systems at both terminals, and relevant equipment caused by faults and abnormal operation to a greatest extent. For the instantaneous slight fault or general abnormal operation of the system, the DC protection can make the DC system to continue operating stably by carrying out relevant operations of pole control, group control, or valve control system; for the serious faults or permanent faults, the DC protection can inhibit the development of faults rapidly by the control system and isolate the faulty equipment rapidly by operating the circuit breaker directly or by controlling the trigger pulse to act quickly on the converter valve [5].

The common action strategies of UHVDC protection are as follows:

1. Alarming

The action setting of alarming is normally low, which is used for the circumstances that have potential threats to the safety of equipment and system operation. It utilizes the means of lamplights, audios, and etc. to remind the operator to take measures timely to restore the equipment status or system operation back to normal status.

2. Phase shift

Once the valve control system receives a phase shift order, it sends out the next trigger pulse with a time delay to enlarge the trigger angle. At the rectifier side, the trigger angle can be enlarged to 90° or above through phase shift operation which can turn the rectifier very quickly from the rectifying status to the inverting status and then extinguish the DC fault current. At the inverter side, the inverter can operate under a minimum commutation margin status by enlarging the trigger angle so as to restrict the fault current that flows through the thyristor of inverter.

3. Switching-in of bypass pair

Switching-in of bypass pair is normally carried out at the inverter side. The trigger pulse of the last conducted valve is maintained by the valve control system, meanwhile, the trigger pulse of another valve in the same phase is sent out to block the trigger pulses of other valves so as to drop the DC voltages of the converter rapidly to 0.

The switched in bypass pair provides the DC bypass circuit of converter, which isolates the AC and DC systems, allowing the circuit breaker at AC side to trip quickly and shortening the time for DC current component to flow through the converter transformer. Meanwhile, it can reduce the circuit impedance of the entire DC system, allowing for rapid phase shift and blocking at the rectifier side. In case the communication system fails, switching-in of bypass pair will drop the voltage at the rectifier side and provides significant fault features for the action of relevant protections.

4. Prohibition of switching-in of bypass pair

Under some particular faults condition, switching-in of bypass pair is not good for fault clearing, or even enlarges the fault, e.g., the DC pole busbar differential protection at the inverter side. Therefore, it is necessary to prohibit switching-in of the bypass pair under such condition.

5. Restart in case of fault

Restart in the case of fault is mainly used for clearing the instantaneous faults of the DC transmission line, ground electrode line, and etc. For restart in case of fault, first of all, the trigger angle of the rectifier needs to be increased to 120°–160° and changed the rectifier to an inverter status so that the energy stored in the DC system can release to the AC system very quickly, the DC current can drop to zero rapidly, and the DC line voltage can also drop to an extremely low level. When the short-circuit fault has eliminated by de-ionization, the trigger angle of the rectifier shall be reduced gradually until the DC system has restored its normal operation.

6. Decrease of power/current

The power or current of the pole is decreased to the preset value through the pole control system to reduce the overstress borne by the equipment, and clear the instantaneous faults.

7. Switching of control system

Switch the current pole control system in operation to a standby system in order to prevent the relay protection from malfunctioning due to the failure of pole control system.

8. Pole balance

When the DC transmission system operates with bipolar balance or the degree of bipolar unbalance is small, the current flowing through the ground electrode or the

grounding grid inside the station will be very small. When any faults occur or under the abnormal operation, the degree of unbalance of two poles will be larger which may cause large current flowing through the ground electrode or the grounding grid inside the station and consequently threatens the safety of equipment and operator. At this time, the bipolar balance operation can be adopted by the control system to eliminate or reduce such unbalance current.

9. Converter blocking/pole blocking

When the converter is blocked, it means the trigger pulse to the thyristor has stopped, after that, when the DC current crosses zero point, the thyristor will stop conducting. Besides blocking the trigger pulse, blocking of the converter is often accompanied with the operations of phase shift, switching-in of bypass pair, and etc. Blocking of the converter always ensures the rectifier is blocked before the inverter in order to prevent generating overvoltage due to superposition of reflected wave at the end of line caused by prior blocking at the inverter side. When the converter is blocked, the energy in the DC system will release to the AC system through the converter valve still under conduction. At this time, in order to prevent overvoltage on the AC busbar, the AC filter shall be generally removed out of service when the fault pole is blocked.

10. Isolation of faulty unit

When a valve group (pole) is removed out of service due to a fault, the faulty valve group (pole) needs to be isolated completely to avoid affecting the normal operation of the sound valve group (pole) and conduct the maintenance work on the DC equipment of the valve group (pole) that has been shut down.

When isolating the faulty valve group, it can be achieved by closing the bypass switch of faulty valve group; when isolating the faulty pole, the HV busbar disconnector and neutral busbar switches of corresponding units need to be disconnected.

11. Emergency switch off

When any severe or permanent faults happen to the AC and DC systems while the regulation of control system has reached its limit, the DC protection will act and send out an emergency switch off order to the rectifier station and inverter station. Its operation shall achieve two goals: first, eliminate the DC arc at the faulty point rapidly; second, disconnect the AC circuit breaker so as to isolate the converter from the AC system.

When the emergency switch off order is sent out, the two stations will drop the DC currents and DC voltages to zero one after another by means of phase shift, blocking the trigger pulse, switching-in bypass pair, and etc. Meanwhile, the two stations will have the AC and DC systems isolated with each other by disconnecting the AC incoming line switch of converter transformer. At the same time of emergency switch off, the AC filter is normally removed out of service by linkage in order to prevent overvoltage on the AC busbar. Similar to the blocking of converter,

emergency switch off operation must be carried out on the rectifier station before the inverter station to prevent overvoltage due to reflect of the traveling wave.

Among all the protection action strategies and orders for system operation, the emergency switch off has the highest priority level.

12. Tripping of AC circuit breaker

The grid side of converter transformer is connected to the AC system through the AC circuit breaker. Tripping of the AC circuit breaker allows to cut-off the voltage source, restrict the current of faulty circuit, and protect the converter transformer and converter valve when the valve side of converter transformer has a ground fault. Tripping of the AC circuit breaker can also prevent the converter valve from bearing unnecessary voltage stress; in particular, this is of great importance under the condition of severe overcurrent on the converter valve.

13. Closing of neutral busbar grounding switch

When an open circuit occurs to the ground electrode line, the neutral busbar grounding switch needs to be closed so that the converter can be connected to the grounding grid inside the station to avoid the equipment with lower voltage level inside the station being damaged due to the high voltage borne by these equipment.

14. Start of circuit breaker failure protection

An order for starting the circuit breaker failure protection will be normally sent when a breaking order is sent to the AC circuit breaker and DC switch. If the AC circuit breaker and DC switch fail to extinguish the arc within the preset time efficiently, the AC circuit breaker and DC switch will be reclosed for protecting the safety of switching equipment.

15. Prohibition of breaking of DC switch

When the monopolar metallic return is changed to the mode of monopolar ground return, or when the monopolar ground return is changed to the mode of monopolar metallic return, it is prohibited to break the DC switch of the original channel if the preset current does not flow through the target channel after a certain period of time. Otherwise, the DC switch may be damaged because the arc cannot be extinguished for long time due to lack of freewheeling current channel.

24.1.3 Zone of UHVDC Protection

By referring to the equipment characteristics and fault characteristics of UHVDC transmission system, the UHVDC protection can be divided into protection of converter area, protection of polar area, protection of bipolar area, protection of DC line area, protection of DC filter area, and protection of DC switch. See the dashed areas as shown in Fig. 24.1 for these zones [6, 7].

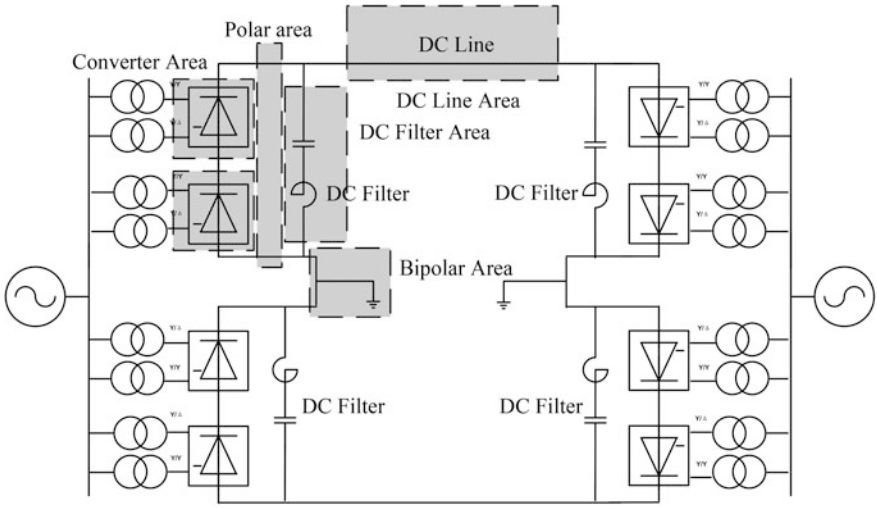

Fig. 24.1 Schematic diagram of zones of UHVDC protection

During the engineering realization, the protection of polar area, protection of DC line area, protection of bipolar area, and protection of DC switch shall be integrated in the same device. An independent protection device shall be provided for the protection of converter area for each 12-pulse converter. An independent protection device is preferred for the protection of DC filter.

24.1.4 Measuring Points of UHVDC Protection

24.1.4.1 Comparison for Measuring Point Configuration of UHVDC Protection and Conventional EHVDC Protection

The measuring point configurations of conventional EHVDC protection and UHVDC protection are shown in Figs. 24.2 and 24.3, respectively. Compared to the measuring points of EHVDC protection, since the structure of double 12-pulse converters connected in series is adopted in the UHVDC system, its measuring points has some differences which are mainly reflected in the following aspects:

(1) Bypass switches are provided in the UHVDC system, and the bypass switches are also provided with current transformers, which are used for detecting the DC current flowing through the bypass switches;
(2) In the UHVDC system, voltage transformers are provided between the HV valve group and LV valve group, which are used for measuring the voltage of neutral point;

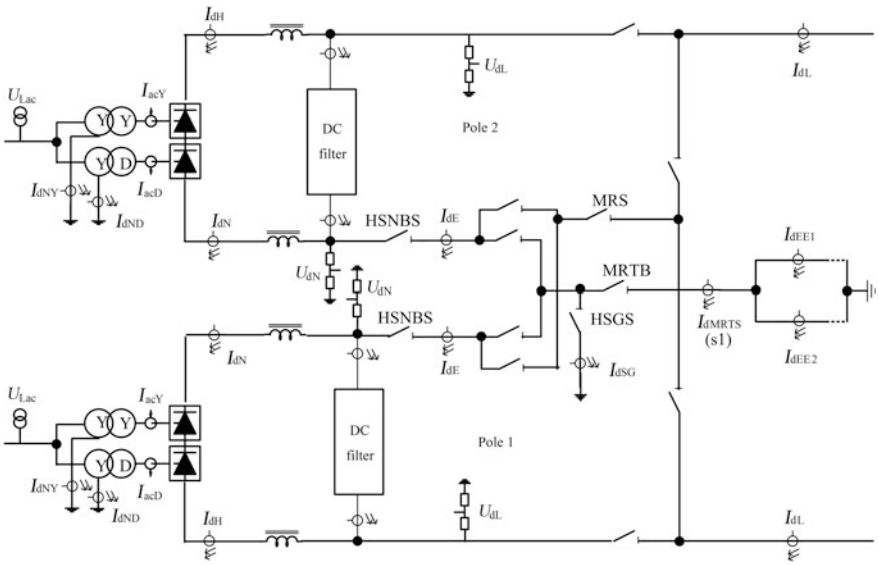

Fig. 24.2 Schematic diagram of measuring points configuration for conventional EHVDC protection

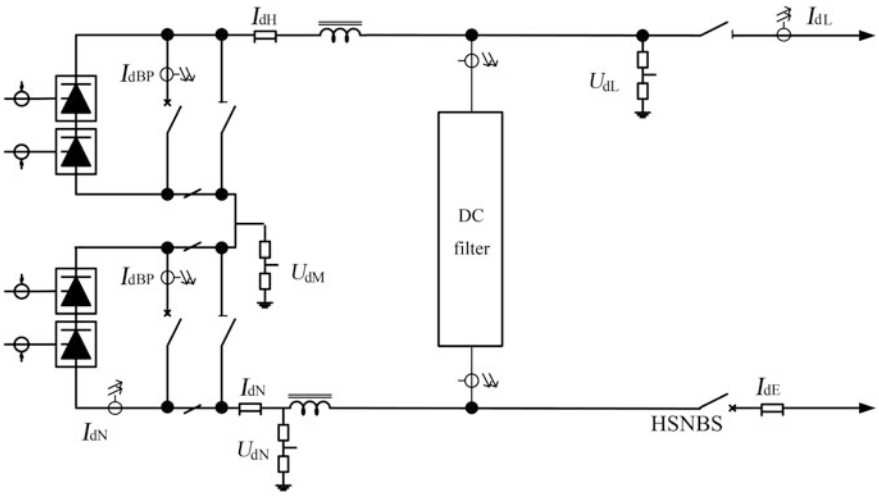

Fig. 24.3 Schematic diagram of measuring points configuration for UHVDC protection (single pole)

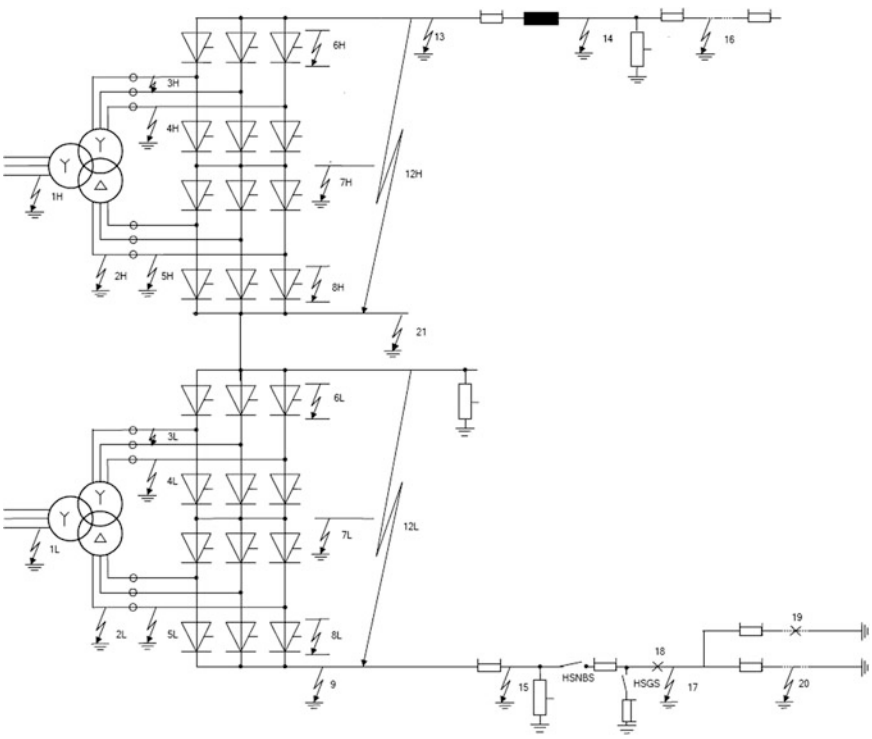

Fig. 24.4 Distribution of UHVDC fault points

(3) Since the structure of double 12-pulse converter is adopted, a complete set of voltage and current measuring equipment is provided for each HV valve group, LV valve group, and converter transformer.

The distribution of UHVDC fault points is shown in Fig. 24.4.

24.1.4.2 Input of Analog Quantity of UHVDC Protection

1. AC current circuit

For the UHVDC system adopting the structure of double 12-pulse converters connected in series, increases the AC current at the star side of converter transformer valve and that at the triangle side of converter transformer valve to corresponding quantity.

(1) Three-phase current at the star side of valve: I_{acY};
(2) Three-phase current at the triangle side of valve: I_{acD}.

2. AC voltage circuit

For the UHVDC system adopting the structure of double 12-pulse converters connected in series, increase the voltage at the AC side of converter transformer, the AC voltage at the star side of converter transformer valve, and the AC voltage at the triangle side of converter transformer valve in corresponding quantity.

(1) Three-phase voltage at the AC side U_{AC};
(2) Three-phase voltage at the valve side of star-type converter transformer U_{VY};
(3) Three-phase voltage at the valve side of triangle-type converter transformer U_{VD}.

3. DC current circuit

(1) DC busbar current I_{dH};
(2) Neutral line current of converter I_{dN};
(3) DC line current I_{dL};
(4) Neutral busbar current I_{dE};
(5) Ground electrode current I_{dEE1}, I_{dEE2};
(6) High-speed grounding switch current I_{dSG};
(7) Metallic return transfer breaker current I_{dMRTB};
(8) Bypass switch current I_{dBPS} (peculiar in the UHVDC system adopting the structure of double 12-pulse converters connected in series);
(9) DC current of neutral point at star-type converter transformer I_{dNY};
(10) DC current of neutral point at triangle-type converter transformer I_{dND}.

4. DC voltage circuit

(1) DC line voltage U_{dL};
(2) DC neutral busbar voltage U_{dN};
(3) Voltage of connection line between HV and LV valve groups U_{dM} (peculiar in the UHVDC system adopting the structure of double 12-pulse converters connected in series).

24.2 Principles and Configurations for UHVDC Protection

24.2.1 Protection of Converter Area

The protection scope of the converter area shall cover such areas as the 12-pulse converter and the AC connection at the valve side of converter transformer. Types of faults include the short-circuit and ground faults of converter and its bridge arm;

inter-phase faults and ground faults at the valve side winding of converter transformer and at the valve side connection; commutation faults and equipment abnormality caused by the fault or disturbance of AC system, abnormality of control system, and so on.

24.2.1.1 Fault Characteristics of Converter Area

The main characteristics of various faults at converter area are as follows:

1. Short-circuit fault of converter valve

Valve short circuit is a fault due to damage or short circuiting of the internal or external insulation of converter valve. This is one of the most serious faults of converter. When a valve short-circuit fault happens at the rectifier side and inverter side, the fault characteristic has some differences.

(1) Short-circuit fault at the rectifier valve

When a rectifier valve is in blocking status, it bears reverse voltage in most of time; when a valve short-circuit fault occurs, the valve can be conducted under the action of forward voltage or reverse voltage.

The fault process is briefed by taking the example of that valve V1 completes reverse conduction immediately when the commutation of valve V1 to valve V3 is over, as shown in Fig. 24.5.

When pulse P3 is sent out, valve V3 starts conducting and the equivalent circuit forms a two-phase short circuit, based on which, the short-circuit current of valve V3 can be calculated. When the commutation is completed, valve V1 starts conducting reversely, the current continues developing at two-phase short circuit current, $i3$ continues increasing and $i1$ starts to increase in negative direction. When valve V4 is commutated to valve V2, a three-phase short circuit is formed and $i3$ current is calculated by three-phase short circuit; when the commutation is completed, a two-phase short circuit is formed again; when valve V3 is commutated with valve V5, a three-phase short circuit is formed again. In such a way, a two-phase short circuit and a three-phase short circuit formed alternatively.

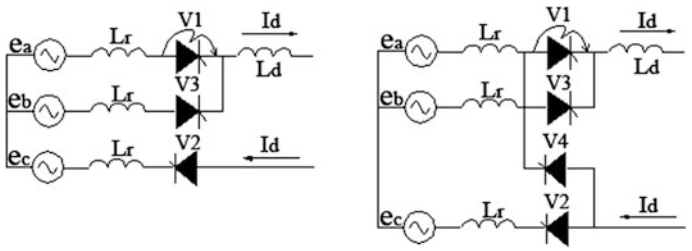

Fig. 24.5 Equivalent circuit diagram at two-phase short circuit and three-phase short circuit due to short circuit of bridge arm

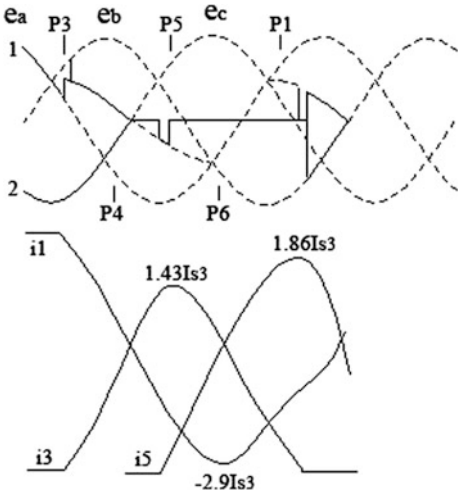

Fig. 24.6 Voltage waveform and current waveform in case of bridge arm short circuit

According to the analysis, $i3$ reaches its maximum value when it approaches to nearby 150°. The current changes of $i1$, $i3$, and $i5$ are shown in Fig. 24.6. The short-circuit characteristics of bridge arm can be summarized as when a bridge arm short-circuit fault occurs at the rectifier bridge, it causes a two-phase short circuit and a three-phase short circuit to occur alternatively at the AC side; the current flowing through the faulty valve reverses and increases severely, causing the converter bridge valve and converter transformer to bear much higher current than that during normal operation; the current at the AC side increases rapidly to several times higher than the normal working current and the DC busbar voltage of converter bridge drops.

The 12-pulse rectifier consists of two 6-pulse rectifiers connected in series. When a valve short circuit occurs at a 6-pulse rectifier, the short-circuit current at the AC side will cause the commutation voltage to reduce, consequently affecting another 6-pulse rectifier. Therefore, the current of 12-pulse rectifier will reduce, leading to the decrease of the DC transmission power.

(2) Short circuit at the inverter valve

The biggest difference between the short-circuit fault of inverter valve and the short-circuit fault of rectifier valve is that complicated commutation failure phenomena will occur at the initial stage of the former. At the later period of fault, due to the action of control system, the current decreases and the commutation failure phenomena will disappear.

When a valve of the inverter is in a blocking state, it bears the forward voltage in most of time. When the voltage is too high or the voltage goes up too rapidly, a short circuit can occur easily due to the damage of valve insulation. For example, when valve V1 of the inverter is shut off and short circuit occurs after stressing forward voltage which equals to that valve V1 is re-conducted, valve V1

commutates backward with valve V3. However, when valve V4 is conducted, V1 and V4 form a short circuit at the DC side, and the process is same as the commutation failure process. What is different is that the commutation failure will occur periodically due to short circuit and bidirectional conduction of valve V1. In addition, when the DC current is under control, the two-phase short-circuit alternating current will be larger than the DC current during the commutation of valve V1 with valve V3.

2. Commutation failure

Commutation failure is the most common fault in inverter. When the commutation between two bridge arms is completed, if the valve which is just removed out of conduction does not restore its blocking capability within the time under the action of reverse voltage, or the commutation is not completed during the period of voltage is reverse, the commutated valve will commutate backward with those valves that are originally intended to be removed out of conduction when the valve voltage is changed to forward direction. This is called as commutation failure.

Take the commutation process of valve V1 with valve V3 as an example, as shown in Fig. 24.7, when valve V3 is triggered, if the advance angle is not big or if the commutation angle is relatively big, there will be residual carrier on valve V1 after crossing the zero point. Therefore, under the action of forward voltage, valve V1 will be re-conducted without trigger pulse being added, causing valve V3 to be commutated backward to valve V1, and when arriving at moment A, valve V3 is shut off. Sometimes, since the advance angel is too small or the commutation angle is too big at the time of triggering, the commutation process of valve V1 to valve V3 is not completed yet even when arriving at moment C6, instead, valve V3 will be commutated backward to valve V1. Upon completion of commutation, valve V1 and valve V2 are conducted. In case of no fault to be controlled, each valve will be triggered subsequently according to the original order, and the conducted valve V4 will be triggered to form a DC short circuit. In case of P5, valve V5 cannot be conducted by the reason of bearing the reverse voltage. When valve V4 is commutated to valve V6, the DC short circuit disappears. If commutation failure does

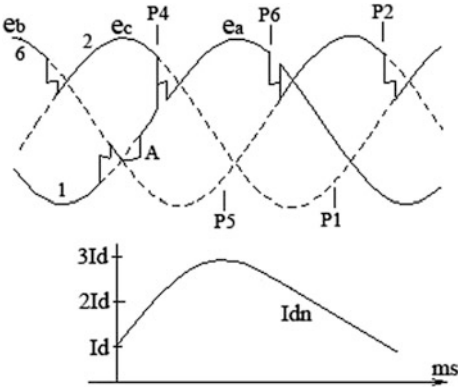

Fig. 24.7 Voltage waveform and current waveform in the commutation failure process of inverter

not occur any longer, it can restore its normal operation by itself. During the fault process, it takes 240°, about 13.3 ms for the reverse voltage of inverter to drop, and it takes 120°, about 6.7 ms for a DC short circuit.

Commutation failure mainly has the following characteristics: DC voltage drops and DC current increases.

3. DC busbar short-circuit fault of converter bridge

The DC busbar short circuit of converter bridge refers to the short-circuit fault occurring from the converter outlet to the reactors of the DC line. Such fault will also cause a short circuit at the bridge side of converter transformer. It is similar to the short circuit of bridge arm in many aspects, but in case of short circuit on the DC busbar, the six valves will keep conducted in single phase.

Below is a brief analysis on the DC busbar short-circuit process of converter bridge, as shown in Fig. 24.8. It is assumed that the converter is operating under an ideal no-load condition. When the commutation of valve V1 and valve V3 is completed, a short circuit occurs at the time of valve V2 conducting with valve V3. At this moment, a two-phase short circuit occurs in phase A and phase C at the AC side, and $i2$ and $i3$ of valve V2 and valve V3 are calculated based on two-phase short circuit. In case of $\omega t = 60^{\circ}$, valve V4 is conducted, an AC three-phase short circuit is formed, and $i2$ and $i3$ are calculated based on three-phase short circuit. In case of $\omega t = 120^{\circ}$, pulse P5 is triggered, but due to a DC short circuit, valve V5 cannot be conducted as it is under the action of very small reverse voltage, and it can be conducted only after $i2 = 0$ and valve V2 is shut off, but a three-phase short circuit will still be formed, and the current of valve V3 will continue changing in the same way as valve V5. In case of $\omega t = 180^{\circ}$, pulse P6 is triggered, but valve V6 cannot be conducted until valve V3 is shut off, while valve V3 can be shut off only when $\omega t = 300^{\circ}$. In fact, valve V6 cannot be conducted. In case of $\omega t = 300^{\circ}$, valve V3 is shut off, only valves V4 and V5 are conducted, and three-phase short circuit is changed to a two-phase short circuit. In case of $\omega t = 360^{\circ}$, $i4 = i5 = 0$, the

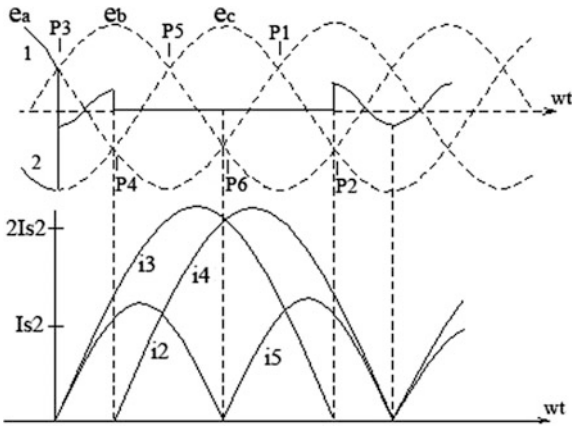

Fig. 24.8 Voltage waveform and current waveform in case of busbar short circuit of converter bridge

short-circuit current of valve bridge is all 0. If the fault remains, the rectifier bridge will change again to the two-phase short-circuit state with valve V2 and valve V3 being conducted.

The characteristics of the DC busbar short-circuit fault of converter bridge can be concluded from above as follows: when a two-phase short circuit occurs at the AC side, a three-phase short circuit will follow; the current of the conducted valve increases sharply and the current at the AC side increases sharply, which will be twice more than the current during normal operation respectively; the converter valve is kept under the forward conduction state; the current of DC busbar drops to zero.

4. Short circuit of the outlet at inverter DC side

For the fault points of the short circuit of the outlet at inverter DC side, see #13 in Fig. 24.4. The current of the DC line increases, which is similar to the short circuit at the end of the DC line, however, due to the action of the DC smoothing reactor, its fault current goes up slowly and the short-circuit current is relatively small. When the inverter has a short circuit at the DC side, the current flowing through the inverter valve will drop to zero very quickly. So the fault will not cause a threat to the inverter and converter transformer. In fact, under the action of trigger pulse of inverter, the instantaneous charge current still exists when each of the valves is triggered. Generally, under the action of current regulator of rectifier station, the fault current can be controlled, but the short circuit cannot be cleared.

As for the 12-pulse inverter, the two 6-pulse inverters with a difference of 30° are connected in series. The characteristic of short circuit at the outlet of inverter DC side is that the phenomena of current increase at the DC side and decrease at AC side of converter is same as that of the 6-pulse inverter.

5. Inter-phase short circuit at the AC side of converter

The inter-phase short circuit at the AC side of converter will directly cause a two-phase short circuit of the AC system. See #3H and 3L in Fig. 24.4 for the fault points. The AC system will generate a two-phase short-circuit current, which is somewhat different for the rectifier and inverter.

(1) Inter-phase short circuit at the AC side of rectifier

When an inter-phase short circuit happens at the AC side of rectifier, a two-phase short-circuit current will occur at the AC side, causing the rectifier to lose a two-phase commutation voltage, its DC current and voltage as well as the transmission power will drop quickly. As for the 12-pulse rectifier, although the AC voltage of the non-faulty 6-pulse converter drops a little due to the action of reactance of converter transformer, its DC voltage and DC current will also drop.

(2) Inter-phase short circuit at the AC side of inverter

When an inter-phase short circuit occurs at the AC side of inverter, commutation failure occurs to the inverter since the inverter has lost the two-phase commutation

voltage and phases are not normal. In such case, the current of DC circuit goes up, and the current at the AC side drops. In addition, it means a 2-phase short-circuit fault occurs to the AC system at the receiving end, and a 2-phase short-circuit current will be generated. When the DC fault current is controlled by the current regulator at the rectifier side, the instantaneous 2-phase short-circuit current at the AC side of each frequency will be larger than the current at the DC side. For the 12-pulse inverter, the non-faulty 6-pulse inverter is affected by the dropped commutation voltage and increased DC current which is caused by the commutation failure occurring to the faulty 6-pulse inverter. This causes the increase in the commutation angle, and as a result, commutation failure will occur.

6. Phase-to-ground short circuit at the AC side of converter

For the 6-pulse converter, the phase-to-ground short-circuit fault at the AC side of converter is similar to the valve short circuit. For the 12-pulse converter, the phase-to-ground short circuit at the AC side of the 6-pulse converter at the HV end forms a circuit through the 6-pulse converter at the LV end. See #4H, 4L, 5H, and 5L in Fig. 24.4 for the fault points.

(1) Phase-to-ground short circuit at the AC side of rectifier

The phase-to-ground short circuit at the AC side of rectifier forms a corresponding valve short circuit by passing through the station grounding grid and the DC ground electrode (it will not pass through the ground electrode when the grounding switch is closed inside the station) to arrive at the DC neutral end. Therefore, the resistance of short-circuit return will increase accordingly, and its short-circuit current is slightly smaller than that of valve short circuit. At this moment, the current at the DC neutral end is almost same as that at the AC end; however, the current at another end of DC almost remains unchanged.

For the 12-pulse rectifier, no matter a single-phase-to-ground short circuit occurs on which 6-pulse converter, the DC neutral busbar is always a part of the short-circuit return. Since the AC short-circuit return of the 6-pulse converter at the HV end needs to be formed through the 6-pulse converter at the LV end, the short-circuit current at the AC side is relatively small.

It should be noted that the secondary harmonic component will enter into the DC side during occurrence of phase-to-ground short circuit at the AC side of rectifier. If the natural frequency of DC circuit is close to this frequency, it may cause resonance to the DC circuit.

(2) Phase-to-ground short circuit at the AC side of inverter

Similarly, the phase-to-ground short circuit at the AC side of inverter forms a corresponding valve short circuit by passing through the station grounding grid and the DC ground electrode (it will not pass through the ground electrode when the grounding switch is closed inside the station) to arrive at the DC neutral end. Its fault process is similar to the valve short circuit and will cause the inverter to have commutation failure. At the initial stage of the fault, the DC current will increase

and the AC current will reduce. When the DC current is controlled by the current regulator at rectifier side and the DC short circuit is removed by the commutation of inverter station, the reverse voltage is established abruptly, causing the DC current at the HV end of converter to reduce instantly (even to zero), and the current at the AC side and the current at the DC neutral end due to the two-phase short circuit formed by the phase-to-ground short circuit will increase. At last, the converter is blocked and the circuit breaker at the AC side is tripped out by the action of corresponding protections.

For the 12-pulse inverter, since the commutation failure occurs to the faulty 6-pulse inverter, the DC current increases. This may also cause the non-faulty 6-pulse inverter to have commutation failure. Similarly, no matter a single-phase-to-ground short circuit occurs on which 6-pulse converter, the two-phase short circuit formed by the ground return will cause the current at the AC side and the current at the DC neutral end to increase, and the DC current at another end of converter will decrease sharply. After that, the current is controlled at its setting by the current regulator at rectifier side.

7. False firing fault

In most of the time during blocking period, the inverter valve bears the forward voltage. At this moment, if the inverter suffers from the action of excessive high forward voltage or if a fault occurs on the trigger circuit of valve's control electrode, a false firing fault of bridge and valve will be caused. The developing process of false firing of the inverter is similar to the primary commutation failure and it can be restored normal as long as it is controlled. The possibility for the rectifier to have false firing is little. A false firing can be deemed as an early firing, which will not cause big vibration to the normal operation.

False firing has the following characteristics: when a false firing occurs at rectifier side, the DC voltage will go up slightly; when a false firing occurs at inverter side, the DC voltage will go down, and DC current will increase.

8. No-firing fault

No-firing fault of the valve is caused by the loss of trigger pulse or the fault of gate control circuit. No-firing of the inverter causes the previously conducted valves to continue conducting. The process is similar to the commutation failure except that there will be no backward commutation, and it can be restored normal through control. When a no-firing occurs to the rectifier, for example, a no-firing fault occurs on valve V3 at the time of commutation, it causes valve V1 to continue conducting, the DC voltage of rectifier drops; when valve V4 is conducted, the DC voltage drops to zero and will not be restored until valve V5 is conducted. However, if control is carried out, the DC voltage will be restored in advance.

The no-firing fault has the following characteristics: the DC voltage and DC current will drop when ano-firing occurs to the rectifier; when a no-firing occurs to the inverter, the DC voltage will drop and the DC current will increase.

24.2.1.2 Protection Principles and Configurations of Converter Area

1. Converter short-circuit protection

(1) Main functions and principles

For some time after a short-circuit fault, the current at the AC side of converter goes up and is larger than the rated value, while the current at the DC side drops and is less than the rated value. By utilizing such characteristic, a short-circuit protection can be constituted to detect the short-circuit fault of converter and protect the safety of converter equipment. In theory, the short-circuit protection can protect almost all of the short-circuit faults on the main connection circuit of the rectifier, in addition, can protect the short-circuit fault of inverter valve, the inter-phase short-circuit fault at the AC side and the phase-to-ground short-circuit fault at the AC side.

The short-circuit protection measures the currents I_{acY} and I_{acD} on the AC connection lines of converter transformer and converter valve and the currents I_{dH} and I_{dN} at the DC side of converter. Under normal conditions, these currents are balanced. However, the balance is broken at the time of fault occurrence.

(2) Criteria for protection

$$I_{acY} > \mathrm{Min}[I_{dH}, I_{dN}] > \Delta, \quad I_{acD} > \mathrm{Min}[I_{dH}, I_{dN}] > \Delta, \tag{24.1}$$

where

I_{acY} and I_{acD} are the equivalent AC currents,
Δ is the setting value. When one of the equivalent AC currents is larger than the setting, the overcurrent protection will act.

(3) Handling strategies of faults

When the protection acts, operate the emergency switch off immediately, trip the AC circuit breaker, and isolate the faulty unit; when the protection at the inverter side acts, it is prohibited to switch in the bypass pair.

(4) Suggestions on setting

If braking characteristics are not adopted for the converter short-circuit protection, normally the fast-speed section and slow-speed section are provided. The fast-speed section shall evade the max. unbalanced current of measuring circuit at the time of fault occurring outside the area. The setting of the current is determined through simulation test, and the action time of protection is 0 ms. The slow-speed section is switched in at the inverter side only. It is determined through simulation test on condition that the measuring error under the system overload in a short period of time is evaded. The protection time delay is determined by the performance of valve group and the recommended value is 30 ms.

2. Overcurrent protection

(1) Main functions and principles

The overcurrent protection is used to detect the short-circuit faults control failures or overload under short period of time at the rectifier side and inverter side. The AC/DC overcurrent protection is used to detect such parameters as the currents at the AC side and DC side of converter and cooling water temperature of converter valve to prevent the relevant converter equipment, especially the thyristors from being damaged due to overheating.

The faults that may lead to overheating of the converter include the following: short circuit of converter valve; short circuit of the outlet at the DC side of converter; ground fault at the HV end of converter DC side, and ground fault of converter neutral point; inter-phase short circuit and phase-to-ground short circuit at the AC side of converter; sustained false firing and no-firing faults of converter valve; overload of converter, etc.

The principles for overcurrent protection include the following: detecting the currents I_{acY} and I_{acD} at the AC side of converter. When one of them is larger than the setting, the overcurrent will act.

(2) Criteria for protection

Double 12-pulse converter:

$$\text{Max } [I_{ACY}, I_{ACD}] > \Delta, \tag{24.2}$$

where

Δ is a setting value.

Four sections can be arranged: Section I is the main protection of valve group fault; Section II is the backup protection of valve group fault; Section III coordinates with the transient overload capacity (overload for 3 s); and Section IV coordinates with the continuous overload capacity (overload for 2 h).

(3) Handling strategies of fault

After the protection acts, switch over the control systems, operate the emergency switch off, trip the AC circuit breaker, and isolate the faulty unit.

(4) Suggestions on setting

The overcurrent protection is a backup protection for valve short-circuit fault and its setting, and action time shall be determined through simulation calculation. The number of protection sections shall coordinate with the overload capacity of the valve, which shall not be less than the number of the sections that are overloaded. The action setting shall not be less than 1.1 times the current value of overload coordination sections, and the setting of time delay shall coordinate with the corresponding overload capacity. When the commutation fails or the DC line and the

AC system have a fault, the section with max. setting in the overcurrent protection should not act.

3. Commutation failure protection

(1) Main functions and principles

The commutation failure protection achieves the detection and protection of the commutation failure faults by subtracting the currents I_{dH}/I_{dN} at the inverter DC side, and the currents I_{acY}/I_{acD} on the AC connection line between the converter transformer and converter valve. Under the normal conditions and external fault conditions, we have $I_{dH} = I_{dN} = I_{acY} = I_{acD}$. When the commutation fails, the two converter valves in the same bridge arm constitute a bypass pair. In such case, the AC side of converter valve is open circuit; the current on the AC connection line drops to zero, and the current flowing through the non-faulty bridge and the DC side of converter goes up significantly. Considering the impact of the transmission error of transformer, we subtract the current on the AC connection line with the larger one of I_{dH} and I_{dN}.

(2) Criteria for protection

At the star side of the converter transformer:

$$\mathrm{Max}(I_{dH}, I_{dN}) - I_{ACY} > \Delta \quad \text{and} \quad \mathrm{Max}(I_{dH}, I_{dN}) > I_{ACY} \times k \tag{24.3}$$

At the triangle side of the converter transformer:

$$\mathrm{Max}(I_{dH}, I_{dN}) - I_{ACD} > \Delta \quad \text{and} \quad \mathrm{Max}(I_{dH}, I_{dN}) > I_{ACD} \times k \tag{24.4}$$

The commutation failure protection acts when the commutation failure is detected continuously and after some time delay (timing principle) or some number of times (number counting principle).

(3) Handling strategies of fault

After the commutation failure protection at the inverter side acts, it is requested to switch over the pole control system at the first time limit, operate the emergency switch off, trip the AC circuit breaker, and isolate the faulty unit at the second time limit.

4. Suggestions on setting

The commutation failure protection setting shall be able to evade the measuring error corresponding to the max. fault current reliably. The action value and the action time delay shall ensure no malfunction occurs in case of single-phase fault at the AC side.

(4) Group differential protection

(1) Main functions and principles

The faults to be detected by valve group differential protection include the following: all the DC faults of converter that can bypass the entire inverter, including the commutation failure fault, converter valve short-circuit fault, short circuit of the outlet of HV end at converter DC side to the converter neutral point as well as the short circuit of converter neutral point to the neutral end, short circuit of the converter neutral point to the ground, sustained false firing fault, and no-firing fault of the converter valve, etc.; those types of faults that can have the inverter short circuited directly includes the short circuit of the HV end at inverter DC side to the ground and short circuit of the HV end to the neutral end.

When these faults occur, the current at the inverter DC side will overshoot. Since the inverter is bypassed or short circuited, the current on the AC connection line will be very small. The common criteria for valve group differential protection can be formed according to this electrical characteristic.

(2) Criteria for protection

$$I_{\mathrm{D}} - I_{\mathrm{ACY}} > \Delta, \quad I_{\mathrm{D}} - I_{\mathrm{ACD}} > \Delta, \tag{24.5}$$

where

I_{D} is the DC current, which can be Max (I_{dH}, I_{dN}) or Min (I_{dH}, I_{dN}).

Two sections shall be provided for such protection. Section I is the protection for valve area faults. Section II is a backup protection for valve area faults, and also serves as a backup protection for the AC faults.

(3) Handling strategies of fault

When Section I acts, operate the emergency switch off, trip the AC circuit breaker and isolate the faulty unit immediately. When Section II acts, it is requested to switch over the pole control system at the first time limit, operate the emergency switch off immediately, trip the AC circuit breaker, and isolate the faulty unit at the second time limit.

(4) Suggestions on setting

The setting of group differential protection shall be able to evade the measuring error corresponding to the max. fault current reliably. It is recommended that the action time delay be 30 ms for fast-speed section. The action value and action time delay for slow-speed section shall ensure no malfunction occurs in case of single-phase fault at the AC side, and the recommended action time delay is no less than 2.3 s.

5. Bridge differential protection

(1) Main functions and principles

The protection indicates that sustained trigger abnormality and commutation failure fault occur on the converter valve. During normal operation, the current I_{ACY} and I_{ACD} flowing on the AC connection line between bridge Y and bridge D are equal. When the relevant faults occur, the symmetrical characteristic between bridge Y and bridge D disappears due to other branches, and the currents I_{ACY} and I_{ACD} will not be equal any longer. The faults to be detected by bridge differential protection include the following: commutation failure fault and valve short-circuit fault; short circuits of the outlet of HV end and neutral end at converter DC side to the converter neutral point; short circuit of the converter neutral point to the ground; inter-phase short circuit at the AC side of converter; phase-to-ground short circuit at the AC side of converter; false firing and no-firing faults of converter valve.

(2) Criteria for protection

$$I_{AC} - I_{ACD} > \Delta, \quad I_{AC} - I_{ACY} > \Delta, \tag{24.6}$$

where

I_{AC} Max (I_{ACY}, I_{ACD}).

Normally, two sections are adopted. Section I is a high setting section; Section II is a low setting section and also serves as a backup protection for AC faults.

(3) Handling strategies of fault

When Section I protection acts, operate the emergency switch off, trip the AC circuit breaker and isolate the faulty unit. When Section II protection acts, it is request to switch over the pole control system at the first time limit, operate the emergency switch off, trip the AC circuit breaker, and isolate the faulty unit at the second time limit.

(4) Suggestions on setting

The action setting of Section I of bridge differential protection shall be able to evade the measuring error corresponding to the max. fault current. The reliability factor shall not be less than 1.3–1.5. Meanwhile, sufficient sensitivity shall be guaranteed when a valve false triggering occurs at the rectifier side and inverter side, and the recommended factor is 0.4 p.u. The action time delay must meet the requirement that when the continuous commutation failure occurs under high load, the action time is not as fast as the action time of pole control switchover, and the recommended value is 200 ms. For the action time delay of Section II, the time delay setting only needs to evade the system switchover time when the AC voltage is normal. When the AC voltage becomes abnormal, the time delay setting needs to

evade the action time of local backup protection for AC system and the recommended value is 2.3 s.

6. Neutral point shift protection at the valve side of converter transformer

(1) Main functions and principles

The winding ground fault monitoring at the AC valve side is mainly used to detect the ground fault on the connection line at the AC side of converter valve when the converter valve is in a blocking status. On one hand, it can prevent the overcurrent of converter valve and converter transformer caused by the ground fault of the AC connection line when the converter valve is deblocked; on the other hand, it can also avoid large zero sequence current flowing through the neutral line of converter transformer for long time when the converter valve is in a blocking status, causing damage to the converter transformer. The winding ground fault monitoring at the AC valve side also measures the vector sum of three-phase voltage on the connection line at AC side of converter valve. When the converter is deblocked, the protection is removed out of service automatically.

(2) Criteria for protection

$$U_{\mathrm{VYa}} + U_{\mathrm{VYb}} + U_{\mathrm{VYc}} > \Delta \quad \text{or} \quad U_{\mathrm{VDa}} + U_{\mathrm{VDb}} + U_{\mathrm{VDc}} > \Delta \tag{24.7}$$

The converter is not deblocked.

(3) Handling strategies of fault

When the protection acts, a signal for prohibiting deblocking is sent out, which prohibits the control system to deblock the converter.

(4) Suggestions on setting

The action time delay shall not be less than 2 s.

7. AC low-voltage protection

(1) Main functions and principles

As a backup protection for the fault of AC system, the AC low-voltage protection is mainly used to prevent the abnormal operation of DC system due to too low AC voltage for long time. It detects the AC voltage at one phase or several phases and handles the voltage to obtain the input voltage for protection U_{AC}. When U_{AC} is lower than the setting, the protection acts.

The AC low-voltage protection can act only when the low voltage of the AC system caused by some circumstance cannot be restored. The action setting shall be so selected to evade the action time delay and coordinate with the clearing time of AC system protection and AC system faults.

(2) Criteria for protection

$$U_{AC} < \Delta \tag{24.8}$$

(3) Handling strategies of fault

When the protection acts, carry out the emergency switch off and trip the AC circuit breaker immediately.

(4) Suggestions on setting

The voltage setting normally can be 0.3–0.5U_n. The action time delay shall be longer than the time of duration of the AC system faults, and coordinate with the time for the Section II of AC system backup distance protection to clear the faults. The recommended value is 3–4 s.

8. AC overvoltage protection

(1) Main functions and principles

The AC/DC overvoltage protection is used to detect the overvoltage of converter due to AC and DC system faults or the abnormal operation in order to protect the safety of converter equipment. The common AC/DC overvoltage protections include DC overvoltage protection, AC overvoltage protection, and voltage overstress protection of converter valve. Similar to the overcurrent protection, since the converter has different withstand time for different overvoltage, the setting of AC/DC overvoltage protection is normally divided into several sections and each section has different action time delay and action strategies. The section with smaller start value has longer time delay, and the section with larger start value has shorter time delay.

(2) Criteria for protection

$$U_{AC} > \Delta \tag{24.9}$$

(3) Handling strategies of fault

When the protection acts, carry out the emergency switch off and trip the AC circuit breaker immediately.

(4) Suggestions on setting

The setting and action time delay of AC overvoltage protection shall coordinate with the withstand voltage of AC system equipment, the overvoltage level of AC field after tripping of last circuit breaker (inverter station only), and the overvoltage control requirements for island operating mode, and also coordinate with the setting of AC system overvoltage protection. The recommended values are 1.3 p.u. and 300 ms, respectively.

9. DC overvoltage protection

(1) Main functions and principles

The DC overvoltage protection is mainly used to detect the overvoltage caused by accidental disconnection of DC line, abnormal blocking of inverter, and control system fault. The protection scope is the entire pole, including the converter, DC line, HVDC busbar, etc.

The DC overvoltage protection can be achieved by detecting the voltage U_{dL} of the DC line to ground or the voltage $U_{dL} - U_{dN}$ of the DC line to the converter LV side.

(2) Criteria for protection

Section I:

$$|U_{dL} - U_{dM}| > \Delta \quad \text{and} \quad I_{dH} < \Delta \quad \text{or} \; |U_{dM} - U_{dN}| > \Delta \quad \text{and} \quad I_{dH} < \Delta \tag{24.10}$$

Sections II and III:

$$|U_{dL} - U_{dM}| > \Delta \quad \text{or} \quad |U_{dM} - U_{dN}| > \Delta \tag{24.11}$$

(3) Handling strategies of fault

When the protection acts, carry out emergency switch off and trip the AC circuit breaker immediately.

(4) Suggestions on setting

The setting of DC overvoltage protection shall be determined according to the insulation coordination report of specific works, and normally 1.03–1.2 p.u. is selected. The time setting of each section of protection shall coordinate with the overvoltage withstand capability of equipment provided by the system parameters design.

10. DC saturation protection for neutral point of converter transformer

(1) Main functions and principles

It is used to prevent the thermal damage to the converter transformer due to large DC current flowing through the neutral point of converter transformer.

(2) Criteria for protection

$$I_{dNY} > \Delta \quad \text{or} \quad I_{dND} > \Delta \tag{24.12}$$

(3) Handling strategies of fault

Alarm and request to switch over the control system.

(4) Suggestions on setting

The setting of DC saturation protection for the neutral point of converter transformer can be determined according to the withstand capability of converter transformer, and normally 10–20 A is selected. The time delay is 30–60 s for alarming.

24.2.2 Protection of Polar Area

24.2.2.1 Fault Characteristics of Polar Area

1. Fault of the HVDC busbar or fault of the neutral DC busbar

The short circuit of the DC HV end of the 12-pulse rectifier to the ground forms a short circuit at the DC end of 12-pulse converter by passing through the station grounding grid and the DC ground electrode (when the grounding switch is closed inside the station, it will not pass through the ground electrode) to arrive at the DC neutral end. Please see #14 in Fig. 24.4 for its fault points. The short circuit causes the resistance of DC circuit to reduce and the currents at the valve and AC side to increase; while the current on the pole line at the DC side drops to zero quickly.

The short circuit of the DC HV end of the 12-pulse inverter to the ground leads to the DC end grounded directly and forms a short circuit at the inverter DC end by passing through the station grounding grid and DC ground electrode. The fault process is similar to the outlet short circuit at the inverter DC side. The fault causes the current at the DC side to increase, while the current flowing through the inverter drops to zero quickly and the current at the neutral end also drops.

For the short circuit of the DC neutral end of the 12-pulse rectifier to ground, see #15 in Fig. 24.4 for its fault points. Since the neutral end is normally at ground potential, it does not have big impact on the normal operation of converter. However, since the short-circuit resistance is connected in parallel with the ground electrode resistance, the DC current flowing through the neutral point will be redistributed.

For the short circuit of the DC neutral end of the 12-pulse inverter to the ground, since the neutral end is normally at ground potential, it does not have big impact on the normal operation of inverter. However, since the short-circuit resistance is connected in parallel with the ground electrode resistance, the DC current flowing through the neutral point will be redistributed.

The fault characteristics are as follows:

(1) When the HVDC busbar has a fault to the ground or has a fault to the neutral DC busbar, I_{dH} and I_{dL} show different change law, namely one increases, and another decreases. However, under other faults conditions, I_{dH} and I_{dL} will

increase or reduce at the same time. Based on such characteristic, the HVDC busbar faults can be distinguished from the faults outside the area exactly.

(2) Similarly, when a short circuit occurs on the neutral DC busbar of HVDC busbar, I_{dN} will increase, while I_{dE} will decrease. Under other faults conditions, I_{dN} and I_{dE} will increase or decrease at the same time.

2. Disconnection or open-circuit fault of the DC line

During the operation of the DC system, the power transmission line is disconnected due to such factor as external force, pole collapse, tower collapse, too heavy ice covering of the line, etc.

Disconnection of the DC transmission line causes an open circuit to the DC transmission system and the DC current to drop to zero. As the current drops rapidly, the trigger angle a at the rectifier side will reduce quickly. Since the tap changer of the converter transformer is at a high position at this moment, the voltage at the rectifier side goes up quickly.

3. Open-circuit fault of ground electrode

In order to avoid the impact of DC earth current on the station grounding grid and the converter transformer, the ground electrode is usually built in a place tens of kilometers away from the converter station. Therefore, a ground electrode line is required for the connection between the converter station and ground electrode. When an open-circuit fault occurs on the ground electrode line, the current flowing through the ground electrode is zero and the voltage on the neutral busbar will go up due to losing of reference potential inside the station.

24.2.2.2 Principles and Configurations of Polar Area Protection

1. DC low-voltage protection

(1) Main functions and principles

The DC low-voltage protection normally serves as a general backup for short-circuit protection, valve group differential protection, DC differential protection, and DC line protection, which is achieved by detecting the DC line voltage U_{dL}. The DC low-voltage protection can be used to detect the inter-station communication faults, meanwhile, detect the short circuits of HVDC busbars at the DC sides of rectifier and inverter to the ground, or to the neutral lines as well as the ground faults of DC line when the bypass pair is switched in at the inverter side for some reasons.

(2) Criteria for protection

Section I:

$$\Delta_2 < |U_{dL}| < \Delta_1 \tag{24.13}$$

Section II:

$$|U_{dL}| < \Delta \tag{24.14}$$

(3) Handling strategies of fault

When Section I acts, the valve group at the HV end ($|U_{dL} - U_{dM}| < \Delta$) or the valve group at the LV end ($|U_{dM} - U_{dN}| > \Delta$) shall be blocked. When Section II acts, both valve groups shall be blocked.

(4) Suggestions on setting

The recommended action setting of DC low-voltage protection is 0.25–0.50 p.u. The configurations shall be carried out according to the system design. In case of an inter-station communication fault, when this protection is required to shut down the rectifier after the inverter side is shut down, the action time of the rectifier side shall evade the local backup action time of the AC system. The action time delay of the protection shall coordinate with the current withstanding capability during bypassing of the valve and the recommended time is 1 s. If this protection is configured as a general backup for the system, the protection action time shall be longer than the action time of remote backup protection and the low-voltage protection for the AC system. The action time shall not be less than 4 s.

2. 50 Hz protection

(1) Main functions and principles

By referring to the 50 Hz component of the current on DC line, the 50 Hz protection detects the commutation failure fault, short-circuit fault of converter valve, phase-to-ground short-circuit fault at the AC side of converter, false firing and no-firing faults of converter valve, and serves as a backup protection for commutation failure and abnormal valve triggering.

(2) Criteria for protection

$$I_{dL}50\ \text{Hz} > \Delta \tag{24.15}$$

(3) Handling strategies of fault

Block the converter after the protection acts.

(4) Suggestions on setting

The protection setting shall ensure that all the abnormal trigger cases are included. The time setting shall be set by referring to the overstress withstood by the valve in case of abnormal valve firing and the overstress withstanding capability of valve group. The recommended time is not less than 1.5 s.

3. 100 Hz protection

(1) Main functions and principles

The main cause of generating 100 Hz component in the current of DC line is that the AC voltage of converter station contains negative sequence component. By referring to the 100 Hz component in the current of DC line, the 100 Hz protection detects the inter-phase short-circuit fault at the AC side of converter, and the phase-to-ground short-circuit fault at the AC side of converter, and serves as a backup protection for the AC system in case of fault.

(2) Criteria for protection

$$I_{\mathrm{dL}}100\ \mathrm{Hz} > \Delta \tag{24.16}$$

(3) Handling strategies of fault

Block the converter after the protection acts.

(4) Suggestions on setting

The final setting shall be determined in such a way that a simulation test could be carried out to simulate the 100 Hz component of current on the DC line when a single-phase metallic ground fault occurs at the AC system under the max. condition and mini. condition of AC system and under the min. current to max. current condition during normal operation of the DC current. The recommended value is 0.02–0.03 p.u. The time delay of protection action shall coordinate with the action time of Section II of distance protection of AC line protection which shall not be less than 3 s.

4. Open-circuit protection of ground electrode

(1) Main functions and principles

When two ground electrode lines are disconnected at the same time, or when the metallic returns are disconnected under the operation mode of monopolar metallic return, the potential at the neutral point will go up quickly due to losing of the potential reference point, causing a threat to the safety of converter equipment. According to the significant change characteristics of the potential at the neutral point, the overvoltage protection for ground electrode can be formed to protect the safety of converter equipment.

(2) Criteria for protection

$$|U_{dN}| > \Delta \tag{24.17}$$

(3) Handling strategies of fault

Bipolar connection mode	when the protection acts, close the high-speed grounding switch, and operate in the bipolar balanced mode;
Non-bipolar connection mode	when the protection acts, close the high-speed grounding switch, and block this pole.

(4) Suggestions on setting

The voltage setting shall coordinate with the withstand level of equipment, which shall lower than the action voltage of arrester, and larger than the max. voltage at the non-grounding side during the operation of metallic return. The action time delay shall coordinate with the duration time of the transient overvoltage for earth electrode when the operation mode is changed, and calibrate the overvoltage withstanding capability of equipment.

5. DC differential protection

(1) Main functions and principles

The DC differential protection is used to detect the currents I_{dH} and I_{dN} on the HV busbar and neutral line at the DC side of converter. Under the normal condition, these two currents are equal. When a ground fault occurs on the converter (including the grounding at the HV end of converter DC side, grounding at the neutral end, grounding at the neutral point of converter, single-phase grounding at the AC side of converter), these two currents are not equal any longer since the grounding branch is introduced. By subtracting I_{dH} and I_{dN}, the DC differential protection can be formed to protect the safety of the converter valve.

(2) Criteria for protection

$$|I_{dH} - I_{dN}| > \Delta \tag{24.18}$$

Two sections are configured for the protection. Section I is a fast-speed protection for valve area faults, and Section II is a backup protection with high sensitivity.

(3) Handling strategies of fault

When the protection acts, operate the emergency switch off, isolate the pole (or trip the neutral busbar switch), and trip the AC circuit breaker. When Section I protection at the inverter side acts, it is prohibited to switch in bypass pair.

(4) Suggestions on setting

When a fault occurs in the DC differential protection area, the fault current is normally large. The start setting can be larger, but the final start setting shall be confirmed by a simulation test. The recommended value is 0.3–0.4 p.u. The action time of the protection shall coordinate with the control characteristics of DC system, which shall be confirmed by a simulation test. The time setting of fast-speed section shall normally not exceed 10 ms.

6. Pole busbar differential protection

(1) Main functions and principles

The pole busbar differential protection is achieved by detecting the current I_{dH} of the outlet of HV end at converter DC side and the current I_{dL} on the overhead line. Under the normal condition or in case of a fault outside the HVDC busbar area, these two currents are almost equal. When a short circuit to the ground or to the neutral DC busbar occurs in the HVDC busbar area, there is very large difference value between these two currents.

(2) Criteria for protection

$$|I_{dH} - I_{dL}| > \Delta \tag{24.19}$$

(3) Handling strategies of fault

When the protection acts, operate the emergency switch off, isolate the pole (or trip the neutral busbar switch, open the disconnecting switch of DC line), and trip the AC circuit breaker.

(4) Suggestions on setting

The final protection setting shall be confirmed by a simulation test and the recommended value is not less than 0.2 p.u. The action time of the protection shall coordinate with the control characteristics of the DC system, which shall be confirmed by a simulation test. The recommended time setting of fast-speed section is 5 ms.

7. Neutral busbar differential protection

(1) Main functions and principles

The neutral busbar differential protection is achieved by detecting the current I_{dN} at neutral line of converter and the current I_{dE} of the neutral busbar. Under the normal condition or in case of a fault outside the neutral DC busbar area, these two currents

are almost equal. When a short-circuit fault to the ground occurs on the neutral DC busbar, the current at opposite end forms a circuit with this end through the fault channel. The ground electrode line is short circuited and big difference will generate in these two currents.

(2) Criteria for protection

$$|I_{\mathrm{dN}} - I_{\mathrm{dE}}| > \Delta \tag{24.20}$$

Two sections are usually adopted. Section I is a high setting section, and Section II is a low setting section.

(3) Handling strategies of fault

When the protection acts, operate the emergency switch off, isolate the pole (or trip the neutral busbar switch, open the disconnecting switch of DC line), and trip the AC circuit breaker.

(4) Suggestions on setting

The final protection setting shall be confirmed by a simulation test. The action time delay of Section II shall evade the transient process of DC line fault and internal fault of DC filter which shall normally not be less than 500 ms.

8. DC backup differential protection

(1) Main functions and principles

It is used to detect the ground faults on the converter, pole busbar, and pole neutral busbar.

The DC backup differential protection is used to protect all the ground faults on the converter, pole busbar, and pole neutral busbar by detecting the current I_{dL} on the overhead line and the current I_{dE} of the neutral busbar. It normally serves as a general backup differential protection for the grounding of DC field.

(2) Criteria for protection

$$|I_{\mathrm{dL}} - I_{\mathrm{dE}}| > \Delta \tag{24.21}$$

Two sections are usually adopted. Section I is a high setting section, and Section II is a low setting section.

(3) Handling strategies fault

When the protection acts, operate the emergency switch off, isolate the pole (or trip the neutral busbar switch, open the disconnecting switch of DC line), and trip the AC circuit breaker.

(4) Suggestions on setting

Section I is a fast-speed section, which shall be set by evading the max. differential current of the fault outside the area, or by approximately referring to the measuring error under the 2.5–3.5 times of the rated current, but the final setting shall be determined through simulation test. Its coordination grade difference with the differential protection for converter, pole busbar differential protection, and neutral busbar differential protection shall not be less than 10 ms. Section II is a slow-speed section, which shall evade the measuring error under the operating condition of short-period overload (1.5 p.u. approximately), and shall be less than the minimum operating current. Its coordination grade difference with the slow-speed section of neutral busbar differential protection shall not be less than 200 ms.

24.2.3 Bipolar Area Protection

24.2.3.1 Fault Characteristics of Bipolar Area

1. Fault of ground electrode line

The grounding resistance of ground electrode consists of the electrode line resistance and electrode resistance. In normal operating condition, the grounding resistance of the two ground electrodes is basically the same, thus the current flowing through the two electrode lines is basically equivalent. When a ground fault occurs to one of the electrode lines, the grounding resistance will change and the current in the two electrode lines will not be equivalent any more [8].

Similar to the short-circuit fault of ground electrode busbar area, the consequence of short-circuit fault of the ground electrode line is also related to the bipolar unbalance degree. A high bipolar unbalance degree will endanger the safety of persons and animals nearby the fault point.

In the monopolar ground return mode, each of the electrode lines withstands 1/2 of the rated current, respectively. When fault occurs to one of the electrode lines, especially the fault is near the converter station, the entire rated current will flow through the fault line and into the ground at the fault point. This will have severe impact on the thermal stability of the fault line and the safety of persons nearby the fault point.

2. Fault of ground electrode busbar

(1) The fault of grounding busbar area in bipolar double-ended grounding mode

In the bipolar double-ended grounding mode, the fault of grounding busbar area is shown in Fig. 24.4 (17), and in this case, the current circuit is shown in Fig. 24.9.

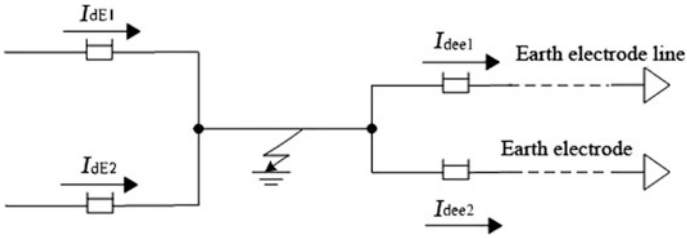

Fig. 24.9 Schematic diagram of busbar area fault of ground electrode in bipolar operation mode

Now the superimposed summation of the current into the ground in the fault point of the converter station is $I_{dE1} + I_{dE2} - I_{dee1} - I_{dee2}$, which is approximately 0 in normal condition, or equivalent to the unbalanced current of the two poles in fault condition. The consequence resulting from the fault is mainly dependent on the unbalance degree of the two poles. When the two poles are basically balanced, there will be little impact on normal operation of the DC system. If the bipolar unbalance degree is relatively high, the overcurrent inside the earth mat may occur and endanger the safety of operating personnel.

(2) The fault of grounding busbar area in monopolar ground return mode

In the monopolar ground return mode, the current circuit of the fault of grounding busbar area is shown in Fig. 24.10.

Now the superimposed summation of current into the ground in the fault point of converter station is $I_{dE1} - I_{dee1} - I_{dee2}$, which is approximately 0 in normal condition and above 0 in fault condition, approximately equivalent to the rated DC current under monopolar ground operation. The rated DC current is generally far beyond the permissible value of current into the ground in the station, which will have severe threat to equipment and personal safety in the converter station.

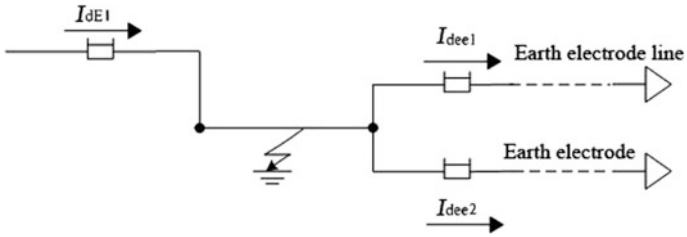

Fig. 24.10 Schematic diagram of busbar area fault of ground electrode in monopolar ground return mode

(3) The fault of grounding busbar area in the monopolar metallic return mode

In the monopolar metallic return mode and in normal condition, the converter station only has one station grounded through the station grounding grid, thus no current passes through HSGS.

When ground fault occurs to the DC system, a path is formed between the fault point and the station grounding grid. As the ground resistance is far lower than the metallic line resistance, there will be some current flowing through the HSGS and fault point.

Short circuit of metallic return will occur to the station grounding grid and the fault grounding point of another station, as a result the grounding grid in the two stations will have fault current approximate to the rated value passed through. This will have severe threat to the safety of equipment and operating personnel.

(4) Disconnection fault of ground electrode line

In case of disconnection of double lines, the ground return opens and no more current will flow through, meantime the DC system will lose potential reference point, the neutral potential increases rapidly and overvoltage appears accordingly, which will lead to insulation damage of equipment.

In the monopolar ground operation mode, the fault electrical characteristics are similar. However, if single line is disconnected, the current flowing through the sound line will be far greater than that in bipolar operation mode, and the entire bipolar unbalanced current will flow into the ground through the sound line.

3. Short-circuit fault for metallic return

In the metallic return operation mode and in normal operation, since the two converter stations only has one grounded, no current circuit is formed. In fault condition, a current circuit is formed between the station grounding grid and the short-circuit point. In the case of metallic return ground fault, relatively high current will flow through the grounding grid in the converter station and fault point, which may endanger the equipment and personal safety.

24.2.3.2 Principles and Configurations of Bipolar Area Protection

1. Differential protection of ground electrode busbar

(1) Main functions and principles

In the differential protection of ground electrode busbar, fault identification is realized based on the difference between the current on DC neutral busbar and the ground electrode line. In normal operation, the difference is zero; when ground fault occurs to the ground electrode busbar area, the difference value will increase significantly under the shunting effect of the station grounding grid. Under different operation modes, operation criteria for differential protection of ground electrode busbar are different.

(2) Criteria for protection

Bipolar operation:

$$|I_{\mathrm{dE}} - I_{\mathrm{dE_OP}} - (I_{\mathrm{dEE1}} + I_{\mathrm{dEE2}} + I_{\mathrm{dSG}})| > \Delta \tag{24.22}$$

Monopolar metallic operation:

$$|I_{\mathrm{dE}} - I_{\mathrm{dE_OP}} - I_{\mathrm{dSG}}| > \Delta \tag{24.23}$$

Monopolar ground operation:

$$|I_{\mathrm{dE}} - (I_{\mathrm{dEE1}} + I_{\mathrm{dEE2}} + I_{\mathrm{dSG}})| > \Delta \tag{24.24}$$

(3) Handling strategies of fault

In bipolar operation mode, after the protection acts, the pole balance is requested in the first time limit and the pole blocking is requested in the second time limit; in monopolar operation mode, after the protection acts, pole blocking is requested.

(4) Suggestions on setting

In bipolar operation mode, the requested pole balance delay is longer than the maximum restart time of DC line fault, and the pole blocking delay is longer than the time in which the requested pole balance operation can be succeeded, with at least 1 s grading difference reserved; in monopolar operation mode, the protection action delay shall be longer than the maximum restart time of DC line fault, with at least 200 ms reserved.

2. Overcurrent protection of station grounding grid

(1) Main functions and principles

In order to prevent excessive current flowing into the station grounding grid, leading to damage to the grid and endangering the safety of operating personnel, the overcurrent protection of station grounding grid is set by measuring the current I_{dSG} flowing through the high-speed grounding switch (HSGS) so as to identify the overcurrent condition of the grounding grid.

(2) Criteria for protection

$$|I_{\mathrm{dSG}}| > \Delta \tag{24.25}$$

In non-metallic-return (non-MR) operation mode, the protection is generally designed with two sections, including the low setting Section I and high setting Section II.

In MR operation mode, protection is designed for one section.

(3) Handling strategies of fault

In non-MR operation mode, an alarm is given out after operation of the Section I. In bipolar operation mode, the pole balance may be started; the pole blocking is done after the operation of Section II. In MR operation mode, the pole blocking is done after the protection acts.

(4) Suggestions on setting

In bipolar operation mode, bipolar current balance is regulated in the first time limit of protection and the action time shall evade the duration time of the process of restarting after the DC line fault. For pole blocking in the second time limit, the protection action time needs to consider an entire process of restart after the DC line fault, and the action grading difference from the first time limit shall be not less than the time required for the DC control system to regulate the bipolar power balance.

In monopolar ground operation mode, the protection action time may be defined as the second time limit of protection in bipolar operation mode.

In monopolar metallic operation mode, the protection action time shall coordinate with the operating time of the protections that can detect metallic return fault, such as the metallic return longitudinal differential protection and the DC line transverse differential protection, with grading difference of not less than 300 ms.

3. Grounding system protection

(1) Main functions and principles

In bipolar operation mode and when the station grounding switch operates temporarily as the grounding point, in order to keep the safety of station grounding grid, the grounding system protection which is realized by measuring the difference of bipolar DC neutral busbar current is provided in addition to the overcurrent protection of station grounding grid.,

This protection only operates when it is in bipolar operation mode and when the HSGS is closed.

(2) Criteria for protection

$$|I_{\mathrm{dE}} - I_{\mathrm{dE_OP}}| > \Delta \tag{24.26}$$

(3) Handling strategies of fault

Block the pole after the protection acts.

(4) Suggestions on setting

The action setting of protection shall be less than the minimum working current, and shall be less than the maximum DC current that the grounding grid is able to withstand. The action setting of protection shall be longer than the action time delay of Section II of the ground electrode overcurrent protection.

4. Unbalanced current protection of ground electrode

(1) Main functions and principles

In normal condition, the currents flowing through the two ground electrodes are the same. When ground fault or disconnection fault occurs to one of the electrodes, the current will no longer be the same. Through comparison of currents in these two electrode lines, the unbalanced current protection of ground electrode is provided.

(2) Criteria for protection

$$|I_{\mathrm{dEE1}} - I_{\mathrm{dEE2}}| > \Delta \tag{24.27}$$

(3) Handling strategies of fault

In bipolar operation mode	the pole balance starts after the first time limit of protection acts, and the pole blocking starts after the second time limit acts;
In monopolar operation mode	restart after the first time limit of protection acts, and the pole blocking starts after the second time limit acts.

(4) Suggestions on setting

In bipolar operation mode, the bipolar power balance is regulated in the first time limit of protection, and the action time delay is longer than the time required for the entire process of the restart of DC line. The pole blocking is completed in the second time limit. The action grading difference between Sections I and II shall be longer than the time required for regulating the pole balance by pole control, which shall not be less than 2 s.

In monopolar ground operation mode, the DC restart is done in the first time limit of protection, and the action time delay shall be longer than the time required for switching the operation mode. The pole blocking is completed in the second time limit. The action grading difference between Sections I and II shall be longer than the time required for restart process, which shall not be less than 2 s.

5. Overcurrent protection of ground electrode

(1) Main functions and principles

In order to prevent excessive current from flowing into the ground electrode, the overcurrent protection of ground electrode line is designed according to the withstanding ability of ground electrode or ground electrode line, which is realized by measuring the current on ground electrode line.

(2) Criteria for protection

$$|I_{\mathrm{dEE1}}| > \Delta \quad \text{or} \quad |I_{\mathrm{dEE2}}| > \Delta \tag{24.28}$$

(3) Handling strategies of fault

The current drops after the protection of first time limit acts, and the pole blocks after the protection of second time limit acts.

(4) Suggestions on setting

The setting shall be set according to the overload capacity of ground electrode and other equipment and the action time shall not be less than 3 s.

6. Transverse differential protection of metallic return

(1) Main functions and principles

In metallic return operation mode, if ground fault occurs out of the inverter station, a current circuit is formed between the grounding point and ground potential holding point (generally at the inverter side) of metallic return, which results in the differential current between the two pole lines at the inverter side. Such fault can be detected by monitoring the differential current between the two pole lines at the inverter side.

This protection serves as backup protection and only operates in the metallic return operation.

(2) Criteria for protection

$$|I_{\mathrm{dL}} - I_{\mathrm{dL_OP}}| > \Delta \tag{24.29}$$

(3) Fault handling strategies

Block the pole after the protection acts.

(4) Suggestions on setting

This protection serves as backup protection of ground fault under the metallic return operation mode and the setting of action time shall not be less than 2 s.

24.2.4 Protection of DC Line Area

24.2.4.1 Fault Characteristics of DC Line Area

1. Ground fault of the DC transmission line

When the DC line fault occurs, the voltage and current fluctuate violently and the DC control system will also operate quickly to eliminate the fault and protect the equipment. According to the characteristic of the DC fault current and the operation of control system after the fault, the fault process may be divided into three stages: initial traveling wave stage, transient stage, and steady stage [9, 10].

(1) The initial traveling wave stage is a period from the moment of fault occurrence to the moment before startup of control system, in which the electric field and magnetic field distributed along the line switch mutually to develop the fault current traveling wave and fault voltage traveling wave. The amplitude of fault current traveling wave is dependent on the line wave impedance and the fault voltage, but is irrelevant to the control system. In this stage, the control systems at both sides have made no response to the fault yet.
(2) In the transient stage, the fixed current control in the control system begins to function, the trigger angles at the rectifier side and inverter side increase rapidly to suppress the current injected to the fault point from both ends of line. In this case, the current at the rectifier side drops significantly and the current at the inverter side drops continuously. The fault current is composed of forced component and free component.
(3) In the steady stage, the currents at the rectifier side and inverter side are limited to respective current reference values and both sides are designed with fixed current control. The current flowing into the control point at both sides is opposite in direction, and the current flowing through fault point is the difference between the above two values, i.e., the current margin set between the DC side and the inverter side.

2. Crossing between the DC transmission line and the AC transmission line

As for the long-distance HVDC transmission lines, the crossing with the AC transmission lines of different voltage levels in different places is inevitable. Therefore, during long-time operation, the cross fault between the DC transmission line and the AC transmission line will possibly happen. If such fault occurs, because direct contact exists between the AC line and the DC line, there will be AC component of power frequency in the current of DC transmission line.

24.2.4.2 Principles and Configurations of Protection for DC Line Area

1. Traveling wave protection of DC line

(1) Main functions and principles

The traveling wave protection is designed to detect the metallic ground fault of the DC line, which is realized based on the following two principles.

In one method, the change rate of transmission line voltage du/dt, the line voltage variation ΔU, and the line current variation ΔI are used as the main criteria, to detect and identify the drastic change of the electric quantity at the end of line produced when the fault traveling wave reaches the end of line.

In the other method, when ground fault occurs to the DC line, the fault traveling wave will be propagated from the fault point to both ends of the line, so detection of DC line fault can be realized through detecting the change of pole wave. In addition, impulse current will be produced, respectively, on the overvoltage absorption capacitors on two ground electrode busbars in the case of fault. Ground wave will be developed with this impulse current and the change of DC voltage in two poles, and the fault pole is determined based on the polarity of ground wave.

(2) Criteria for protection

Criteria for protection 1:

$$\mathrm{d}U_{\mathrm{dL}}/\mathrm{d}t > \Delta 1, \quad \text{and} \quad \mathrm{Delta}U_{\mathrm{dL}} > \Delta 2, \quad \text{and} \quad \mathrm{d}I_{\mathrm{dL}}/\mathrm{d}t > \Delta 3 \tag{24.30}$$

Criteria for protection 2:

$$\begin{aligned}\text{The zero mode amplitude} &> \Delta 1, \text{the zero mode steepness} \\ &> \Delta 2, \text{and the aerial mode amplitude} > \Delta 3\end{aligned} \tag{24.31}$$

(3) Handling strategies of fault

Execute the restart for the DC line fault.

(4) Suggestions on setting

The traveling wave protection is the main protection of line fault generally without the outlet of time-delay action; the setting shall be determined through simulation calculation and simulation test, and the final setting shall be checked and determined through field test. In order to make sure the protective range under reduced voltage operation is basically the same as that under normal voltage operation, the settings shall be adjusted according to the current voltage during voltage reduction.

2. Fault component protection of DC line voltage

(1) Main functions and principles

The protection is designed to detect the metallic ground fault occurred to the DC line, for which two criteria of voltage fault component and low voltage are established according to the DC line voltage: when ground fault occurs to the DC line, the DC voltage drops quickly to a low value, which will be detected by the voltage break-variable criteria; in order to evade the disturbance impact during operation, the low-voltage level is also detected at the same time.

(2) Criteria for protection

$$\mathrm{d}U_{\mathrm{dL}}/\mathrm{d}t > \Delta 1, \quad \text{and} \quad U_{\mathrm{dL}} < \Delta 2 \tag{24.32}$$

(3) Handling strategies of fault

Execute the restart for the DC line fault.

(4) Suggestions on setting

The setting is determined through simulation calculation and simulation test. The final setting shall be checked and determined through field test. In order to make sure the protective range under reduced voltage operation is basically the same as that under normal voltage operation, the settings shall be adjusted automatically according to the current voltage during voltage reduction. The protection action time shall coordinate with the fault clearing time of the AC system main protection, which is typically not less than 100 ms.

3. Low-voltage protection of DC line

(1) Main functions and principles

The high-impedance ground fault of DC line is detected based on the voltage decreased level of the DC line; the blocking fault at inverter side can also be detected when there is no communication. The protection shall have perfect auxiliary criteria to prevent the misoperation of protection due to outside fault.

(2) Criteria for protection

$$U_{\mathrm{dL}} < \Delta \tag{24.33}$$

(3) Handling strategies of fault

When there is communication, execute the restart for the DC line fault; when there is no communication, operate the emergency switch off and trip the AC circuit breaker.

(4) Suggestions on setting

When the communication is normal, the protection action time shall be at least 20 ms longer than the maximum channel delay. In case of a communication interruption, if it is in bipolar operation mode, the time for the station to detect the normal DC voltage of the other pole shall be at least 20 ms, and the action time of protection shall be longer than this time. When the station detects low DC voltage of the other pole, the action time of protection shall be longer than the action time of local backup protection of the AC system of corresponding station. In case of a communication interruption, the action time of protection in monopolar operation mode shall be at least 100 ms longer than the action time of local backup protection of the AC system of corresponding station. In reduced voltage operation mode, the setting shall be adjusted automatically according to the current voltage.

4. DC line longitudinal differential protection

(1) Main functions and principles

The high-impedance ground fault of the DC line is detected based on the difference in the DC line currents of rectifier station and inverter station. It is used as the backup protection of traveling wave protection and voltage fault component protection. The protection will stop automatically in the case of inter-station communication fault.

(2) Criteria for protection

$$|I_{\mathrm{dL}} - I_{\mathrm{dL_OS}}| > \Delta \tag{24.34}$$

(3) Handling strategies of fault

Execute the restart for the DC line fault.

(4) Suggestions on setting

The protection action delays shall evade the AC system fault and fault clearing, the quick adjustment of DC transmission power and the transient state process of neighboring line fault during bipolar or metallic return operation. The protection action time may be extended when the inter-station communication is relatively slow, which is preferred not less than 500 ms.

5. AC and DC transmission line crossing protection

(1) Main functions and principles

The AC and DC line cross fault is detected according to the 50 Hz component in the DC line current and DC line voltage.

(2) Criteria for protection

Including two operation logics:

$$I_{\mathrm{dL50\,Hz}} > \Delta 1, \quad \text{and} \quad I_{\mathrm{dL}} > \Delta 2; \quad \text{or} \quad U_{\mathrm{dL50\,Hz}} > \Delta 1, \quad \text{and} \quad I_{\mathrm{dL50\,Hz}} > \Delta 2 \tag{24.35}$$

(3) Handling strategies of fault

Block the pole.

(4) Suggestions on setting

The protection setting and the delay setting shall be determined through simulation test. It is recommended there shall be no outlet of time delay after the protection acts.

6. Longitudinal differential protection of metallic return

(1) Main functions and principles

In the metallic return operation mode, the ground fault occurred to metallic return is detected based on the difference in the line currents of the rectifier station and inverter station of metallic return. This protection only operates under the metallic return operation mode. The protection will exit automatically when the inter-station communication is abnormal.

(2) Criteria for protection

$$|I_{\mathrm{dL_OP}} - I_{\mathrm{dL_OP_OS}}| > \Delta \tag{24.36}$$

(3) Handling strategies of fault

The protection is realized in two sections: restart after Section I (short-time delay) acts, and pole blocking after Section II (long-time delay) acts.

(4) Suggestions on setting

The protection action time shall evade the transient state process of the AC system fault, which may be set by referring to the longitudinal differential protection of DC line.

24.2.5 Protection of DC Filter Area

24.2.5.1 Fault Characteristics of DC Filter Area

The DC filter faults and hazards mainly include five aspects.

1. Capacitive component damage

A capacitor is typically composed of several capacitive components in series or parallel. When some of these capacitive components are damaged, the voltage stress is withstood by the remained sound capacitive components. With the increase of the number of damaged capacitive components, the voltage stress withstood by the sound capacitive components also increases gradually. When the number of damaged capacitive components reaches a certain value, the breakdown of residual sound capacitive components may be caused due to withstanding excessive voltage stress, or avalanche may even happen and lead to the damage of the entire capacitor. In addition, the damage of capacitive component will also result in change of capacitor parameters and degrade the filtering performance of filter.

2. Short-circuit fault

The short-circuit fault of DC filter may be classified into three types: short circuit of the main wiring of DC filter to ground or to the neutral DC busbar; ground fault of bodies of capacitor, reactor, and resistor, etc. or short circuit to the neutral DC busbar; short circuit inside the devices, such as the inter-turn short circuit of reactor, short circuit between the capacitive components of capacitor. With respect to the electrical characteristics of fault, the short circuit of device body to ground or to the neutral DC busbar may be deemed as a special case of short circuit of main wiring to ground or to neutral DC busbar.

The short-circuit fault of filter, if occurred, will possibly result in the change of parameters of devices and the change of preset harmonic channel which will make the filter unable to achieve the preset filtering effect. The short-circuit fault of filter may even cause overvoltage or overcurrent damage of several components and devices of filter, or overcurrent of other parts of the DC system.

3. Capacitor overvoltage caused by faults inside or outside the filter area or by abnormal operation

The rise of converter output voltage or relatively large number of damaged capacitive components will lead to overvoltage of capacitor. The HV capacitor withstands the most of busbar voltage during operation and the operating environment is harsh, thus the overvoltage tends to appear. The LV capacitor only withstands a small part of busbar voltage and the operating environment is much better than that of HV capacitor, generally no overvoltage will occur.

4. Reactor and resistor overheating resulting from faults inside or outside the filter area or abnormal operation

In case of faults inside or outside the filter area or abnormal operation, the content and amplitude of harmonic current flowing through the resistor and reactor will possibly exceed the design values. In this case, the heat generated by resistor and reactor exceed the handling capacity of cooling system. The heat quantity accumulates continuously, and after a period of time, the reactor and resistor will be damaged by overheating. The superheat degree of reactor and resistor is in the inverse time-limit relation with the harmonic current. The higher the harmonic content is, the higher the amplitude will be, and the shorter the time required for reaching the same superheat degree will be; otherwise the time is longer.

5. Filter detuning

A filter detuning refers to a condition that the actual resonance frequency of filter deviates from the expected resonance frequency. It will be impossible to achieve an ideal filtering effect after filter detuning. The filter detuning possibly occurs in the following cases: frequency deviation of the AC network; deviation of device parameters to the design values caused by temperature variation, manufacturing process error, aging of components, and other factors; change of capacitor parameters due to damage of capacitive components. If no fault clearing or isolation is carried out immediately after the DC filter fault occurs, it will result in damage of the filter devices and other primary equipment of converter station and cause sharp decrease of filtering performance. It can further lead to misoperation of the DC relay protection causing unnecessary shutdown of the DC system.

24.2.5.2 Principles and Configurations of Protection for DC Filter Area

Different wiring mode of the DC filter will lead to slightly different protection setting of the DC filter area, as shown in Figs. 24.11 and 24.12:

1. Differential protection

(1) Main functions and principles

Differential protection of DC filter is the main protection of the DC filter which operates reliably in the case of ground fault inside the DC filter or short circuit to neutral line. The protection is realized through detecting the currents at the busbar side and ground side.

The protection is designed with brake characteristic to prevent the misoperation of protection under fault outside its area and the function to prevent the protection misoperation due to impulse current. I_{diff} is the difference between the currents at the busbar side and ground side, I_{cdqd} is the minimum action current of differential protection, and I_{res} is the braking current. The through current is used as the braking

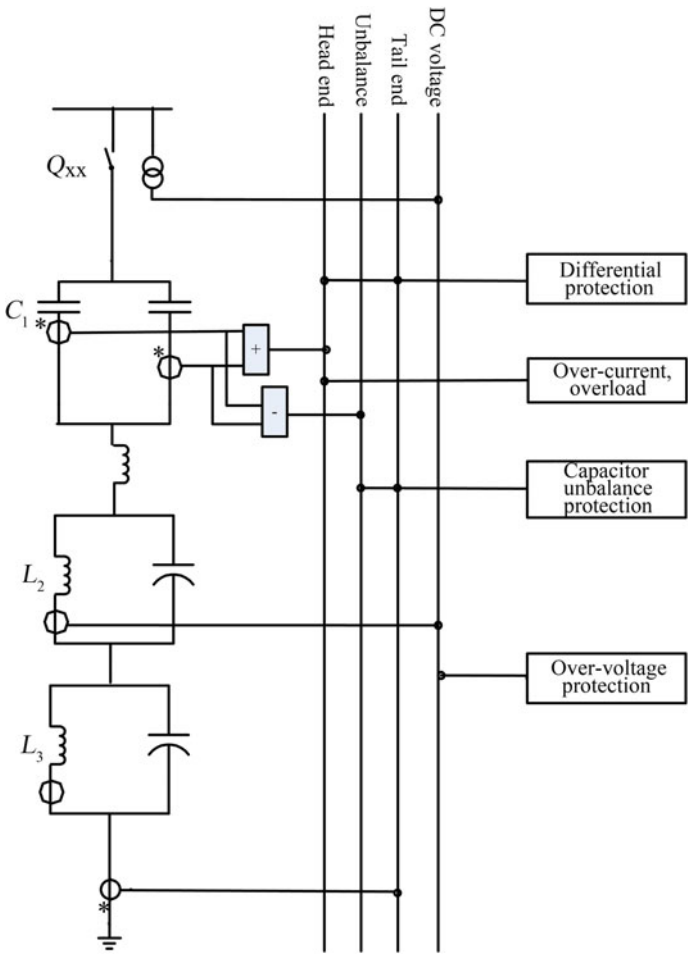

Fig. 24.11 Protection configuration diagram of π-shaped wired DC filter

current, which will decrease after the ground fault and this will help to improve the sensitivity of differential protection.

(2) Criteria for protection

$$|I_{\text{diff}}| > \max(I_{\text{cdqd}}, K \times I_{\text{res}}) \tag{24.37}$$

(3) Handling strategies of fault

After the protection acts, emergency switch off order shall be sent to the pole control system and pole isolation shall be executed.

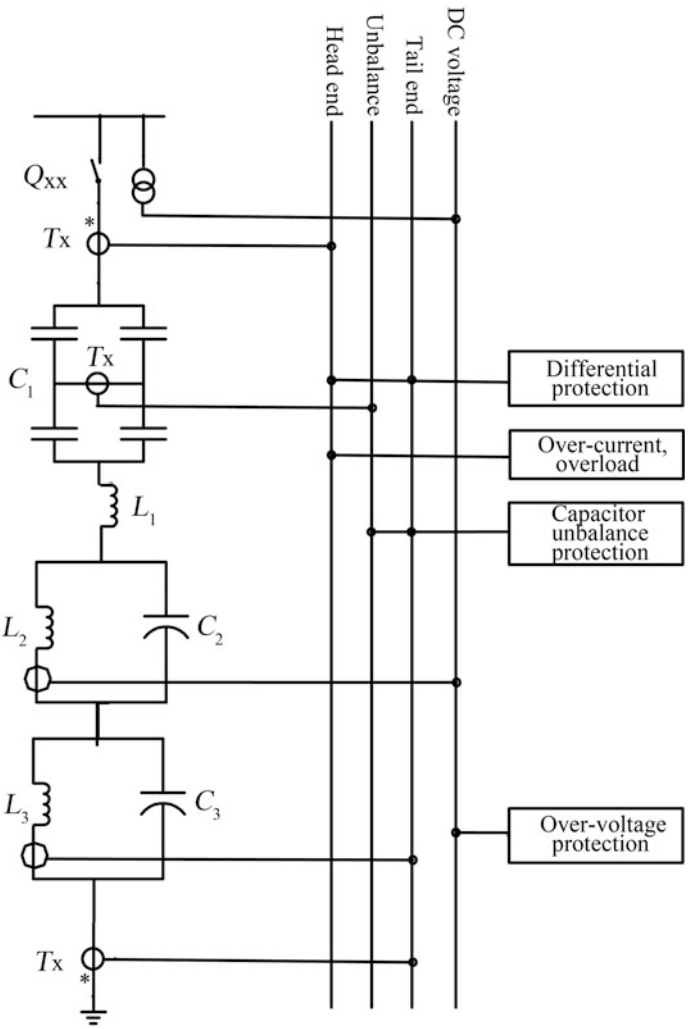

Fig. 24.12 Protection configuration diagram of H-shaped wired DC filter

(4) Suggestions on setting

I_{cdqd} shall be set to evading the maximum unbalanced current of the normal DC filter with rated load. The protection action time shall be able to prevent the misoperation of protection due to measurement disturbance and the recommended value is 15–20 ms.

2. Overcurrent (overload) protection

(1) Main functions and principles

DC filter may be designed with two protection sections, including a definite time-limit overcurrent protection and an inverse time-limit overcurrent protection. The characteristic harmonic effective value of the filter head-end current is used. The definite time-limit overcurrent protection is designed for protecting the DC filter from damage by excessive current; the inverse time-limit overcurrent protection mainly serves as the backup protection for the internal heat of DC harmonic filter and is designed to protect the entire DC filter and HV reactor $L1$ from damage by overheat or overstress. Generally, three sections are so designed as Section I for alarming and Section II and III for tripping.

(2) Criteria for protection

First, the reactor current flowing through the reactor of the filter is converted to equivalent power frequency thermal effect current based on the equivalent power frequency factor of sub-harmonic currents. The criterion for definite time-limit overcurrent protection is as follows:

$$I_{\text{hot}} > \Delta, \tag{24.38}$$

where

I_{hot} is the equivalent power frequency thermal effect current.

After the equivalent power frequency factor of sub-harmonic currents is converted to equivalent power frequency thermal effect current, the inverse time-limit overcurrent protection curve is developed based on the overload curve provided by the manufacturer established during power frequency overcurrent of the reactor.

(3) Handling strategies of fault

After the section for tripping of protection acts, the emergency switch off order and pole isolation order shall be sent out.

(4) Suggestions on setting

The setting and time of protection action shall be set according to the overload curve of the primary equipment provided by the manufacturer.

3. Capacitor overvoltage protection

(1) Main functions and principles

In the DC filter, the HV capacitor $C1$ withstands the total DC voltage and the operating environment is relatively harsh. The purpose of the HV capacitor overload protection of DC filter is the same as that of the AC filter, i.e., to prevent excessive high voltage of the pole line from decreasing the capacitor insulation property and causing damage to the capacitor.

Based on different levels of capacitor overload, the capacitor overload protection of the DC filter is generally designed with alarming and tripping.

(2) Criteria for protection

In the HV capacitor overload protection of the DC filter, the DC line voltage U_{dL} is generally measured directly using the DC measuring device. The DC line voltage and voltage-time characteristic are used to reflect the capacitor overload capacity.

$$I_{Dl} > \Delta \tag{24.39}$$

(3) Handling strategies of fault

After the tripping section of protection acts, the emergency switch off order and pole isolation order shall be sent out.

(4) Suggestions on setting

The setting is generally made based on the inverse time-limit characteristic and the overvoltage characteristic curve of capacitor provided by the equipment manufacturer.

4. Capacitor unbalance protection

(1) Main functions and principles

The capacitor is typically designed with π-shaped or H-shaped wiring. When the capacitor is damaged, the different bridge arms will have different currents. In the π-shaped wiring, the operating condition of capacitor is monitored based on the unbalanced current of two bridge arms. In the H-shaped wiring, the unbalanced current is measured directly to detect the operating condition of the capacitor.

(2) Criteria for protection

$$\frac{I_{ub}}{I_{tro}} > \Delta \quad \text{and} \quad I_{ub} > I_{ubqd}, \tag{24.40}$$

where

I_{ub} is the unbalanced current of the DC filter,
I_{tro} is the through current of the DC filter,
I_{ubqd} is the unbalance starting value.

(3) Handling strategies of fault

After the protection tripping section acts, it shall be possible to open the HV disconnector of the DC filter or send out the emergency switch off order and pole isolation order according to the head-end current of the DC filter.

(4) Suggestions on setting

The time delay of the capacitor unbalance protection shall consider the bearing capacity of capacitor in the DC filter. The time that capacitor can withstand at different voltages (involved in the capacitor parameters) is used as the setting of time delay.

24.2.6 Protection of DC Switch

24.2.6.1 Fault Characteristics of DC Switch

The DC high-speed switch is used to switch the DC current quickly from a current path to another path, so as to realize the switching of operation mode of the DC system, or isolate the fault point, keep the equipment safe, and maintain continuous operation for the sound part of system. In the UHVDC system, high-speed DC switches consist of the high-speed neutral bus switch (HSNBS), high-speed grounding switch (HSGS), metallic return transfer breaker (MRTB), ground return transfer switch (MRS), and bypass switch (BPS), in which the bypass switch (BPS) is specially in the UHVDC system.

1. Function of DC switch

The HSNBS is installed on the DC neutral bus at the side close to the ground electrode line which is used to isolate the neutral DC busbar of stopped pole from that of operating pole, so as to maintain continuous and stable operation of the normal operating pole.

The MRS is installed on the common neutral line of pole 1 and pole 2, which is used to switch the current from monopolar metallic return to monopolar ground return. In the process of switching, first close the MRTB, then two current paths will appear, i.e., metallic return circuit with higher resistance value and ground return circuit with lower resistance. When the steady-state condition is reached, the current flowing through the two paths will be in inverse relation with the resistance value. Through the opening of the MRS, the total current is transferred into the ground return.

The MRTB is installed on the common ground electrode busbar of poles 1 and 2, which is used to switch the current from monopolar ground circuit to monopolar metallic return circuit. In the process of switching, first close the MRS to develop two current paths, i.e., metallic return circuit with higher resistance value and ground return circuit with lower resistance, and then through the opening of MRTB, the total current is transferred into the metallic return.

The HSGS is installed between the common ground electrode busbar of poles 1 and 2 and the station grounding grid. In the monopolar metallic return operation, HSGS is normally in closed state and mainly used to provide the potential reference

point for the DC system. Under the bipolar operation mode and monopolar ground operation mode, the HSGS is normally in open state.

The BPS is specially equipped in the UHVDC transmission system and crossed over on the converter. When the converter is removed out of operation, it is short circuited through closing the BPS, and the current is transferred into the converter valve when the converter is put into operation.

2. DC switch failure and abnormal breaking

A DC switch failure refers to a failure in which arc extinguishing fails to be done within a safe time after the protection or control system trips the high-speed switch. If the arc cannot be extinguished normally, the energy in the arcing chamber will accumulate gradually and after a period of time, will exceed the bearing capacity of arcing chamber, or even cause an explosion of high-speed switch. Therefore, once a failure occurs, be sure to reclose the arc-extinguishing breaker immediately to protect the high-speed switch.

An abnormal breaking of DC switch refers to a breaking condition beyond the design condition of high-speed switch. For example, when switching from the monopolar ground return mode to monopolar metallic return mode, close the MRS first; until part of the ground return current has been transferred successfully to the metallic return, and a relatively stable state is achieved, disconnect the MRTB to transfer the residual current into the metallic return. This residual current is the current actually to be broken by the MRTB, and the MRTB is designed generally based on this current. However, if due to certain reasons, the MRS fails to close after the control system sends out the closing order, or even though the MRS is closed but there is no current flowing through the metallic return, when the MRTB is opened now, all energy in the DC system will be unable to be transferred to the other paths, but continue to discharge along the ground return. This may very likely cause damage to the MRTB and accordingly lead to overvoltage of other converter equipment. When switching from the monopolar metallic return mode to the monopolar ground return mode, the MRS faces with the same problem.

24.2.6.2 Principles and Configurations of DC Switch Protection

1. Bypass switch protection

(1) Main functions and principles

This protection is designed to detect the bypass switch failure, including the opening failure and closing failure.

After the trip of bypass switch, if the bypass switch fails to be disconnected reliably due to the circuit breaker failure, the bypass switch protection (opening failure section) acts to reclose the switch so as to protect the equipment from damage, and close the bypass switch after receiving the signals of the valve block emergency switch off and pole emergency switch off. If due to the failure of circuit

breaker, the bypass switch fails to close reliably and the DC current is unable to transfer from the converter to the bypass switch, this pole shall be blocked after the action of bypass switch protection (reclosing failure section).

(2) Criteria for protection

Section I (opening failure): bypass switch is at the opening position and meet the equation below:

$$I_{\mathrm{dBPS}} > \Delta \tag{24.41}$$

Section II (closing failure): after receiving the signals of valve block emergency switch off and pole emergency switch off:

$$I_{\mathrm{dBPS}} < \Delta \quad \text{and} \quad I_{\mathrm{dH}} > \Delta \tag{24.42}$$

(3) Handling strategies of fault

Reclose this switch by Section I and block this pole in Section II.

(4) Suggestions on setting

The setting shall evade the measurement error reliably and the setting of time shall coordinate with the operating time of bypass switch (BPS). The operating time is provided by the switch manufacturer.

2. Neutral bus switch protection

(1) Main functions and principles

This protection is designed to protect the failure of neutral busbar switch. After the neutral bus switch trips, if the DC switch fails to be disconnected reliably due to the circuit breaker failure, the high-speed neutral bus switch protection acts and the switch shall be closed so as to protect the equipment from damage.

(2) Criteria for protection

After opening of the neutral bus switch:

$$I_{\mathrm{dE}} > \Delta \tag{24.43}$$

(3) Handling strategies of fault

Reclose the neutral bus switch.

(4) Suggestions on setting

The setting shall evade the measurement error reliably and the setting of time shall coordinate with the operating time of bypass switch (BPS). The operating time is provided by the switch manufacturer.

3. HSGS protection

(1) Main functions and principles

This protection is designed to protect the failure of HSGS. After the HSGS trips, if the DC switch fails to disconnect reliably due to the circuit breaker failure, the HSGS protection acts and the switch shall be closed so as to protect the equipment from damage.

(2) Criteria for protection

After opening of HSGS:

$$I_{\mathrm{dSG}} > \Delta \tag{24.44}$$

(3) Handling strategies of fault

Reclose the HSGS.

(4) Suggestions on setting

The setting shall evade the measurement error reliably and the setting of time shall coordinate with the operating time of bypass switch (BPS). The operating time is provided by the switch manufacturer.

4. Protection of metallic return transfer breaker

(1) Main functions and principles

This protection is designed to protect the failure of metallic return transfer breaker. After the metallic return transfer breaker is disconnected, if the DC switch fails to be disconnected reliably due to the circuit breaker failure, the switch shall be reclosed after the protection acts so as to protect the equipment from damage.

In the sequential control operation, after the ground return transfer breaker is closed, if $I_{\mathrm{dL_OP}} < \Delta$, the metallic return transfer breaker shall not be opened. This function is preferred to be realized in the DC station control system.

(2) Criteria for protection

After the disconnection of metallic return transfer breaker:

$$I_{\mathrm{dEE1}} + I_{\mathrm{dEE2}} > \Delta \quad \text{or} \quad I_{\mathrm{dMRTB}} > \Delta \tag{24.45}$$

(3) Handling strategies of fault

Reclose the metallic return transfer breaker.

(4) Suggestions on setting

The setting shall evade the measurement error reliably and the setting of time shall coordinate with the operating time of bypass switch (BPS). The operating time is provided by the switch manufacturer.

5. Protection of ground return transfer breaker

(1) Main functions and principles

This protection is designed to protect the failure of ground return transfer breaker. After the ground return transfer breaker is disconnected, if the DC switch fails to be disconnected reliably due to the circuit breaker failure, the switch shall be reclosed after the protection acts so as to protect the equipment from damage.

In the sequential control operation, after the metallic return transfer breaker is closed, if $I_{\mathrm{dMRTB}} < \Delta$, the ground return transfer breaker shall not be opened. This function is preferred to be realized in the DC station control system.

(2) Criteria for protection

After the ground return transfer breaker opens:

$$|I_{\mathrm{dL_OP}}| > \Delta \tag{24.46}$$

(3) Handling strategies of fault

Reclose the ground return transfer breaker.

(4) Suggestions on setting

The setting shall evade the measurement error reliably and the setting of time shall coordinate with the operating time of bypass switch (BPS). The operating time is provided by the switch manufacturer.

24.2.7 Coordination Relation of DC Protection

The overall coordination relation of DC protection is listed in Table 24.1.

Table 24.1 The overall coordination relation of DC protection

S. no.	Protected areas	Function name	Range of protection	Function
1	Protection of converter area	Converter short-circuit protection	Converter fault	Main protection
2		Overcurrent protection	Converter fault	Backup protection
3		Commutation failure protection	Converter fault	Backup protection
4		Group differential protection	Converter fault	Backup protection
5		Bridge differential protection	Converter fault	Backup protection
6		Neutral point shift protection at the valve side of converter transformer	Converter fault	Alarm monitoring
7		AC low-voltage protection	Monitoring the AC system fault	Backup protection
8		AC overvoltage protection	Monitoring the AC system fault	Backup protection
9		DC overvoltage protection	Unexpected DC line break, abnormal blocking of inverter, and overvoltage resulting from control system fault	Main protection
10		Neutral DC saturation protection of converter transformer		Alarm monitoring
11	Protection of pole area	DC undervoltage protection	DC-to-ground fault	Backup protection
12		50 Hz protection	Commutation failure, valve firing anomaly	Backup protection
13		100 Hz protection	AC system fault	Backup protection
14		Open-circuit protection of ground electrode	Disconnection fault at the grounding point of DC system	Main protection
15		DC differential protection	Converter ground fault	Main protection
16		Pole busbar differential protection	DC HV busbar ground fault	Main protection
17		Neutral busbar differential protection	DC neutral busbar ground fault	Main protection
18		DC backup differential protection	Ground fault in the converter, pole busbar, pole neutral busbar	Backup protection

(continued)

Table 24.1 (continued)

S. no.	Protected areas	Function name	Range of protection	Function
19	Protection of bipolar area	Differential protection of ground electrode busbar	Ground fault of ground electrode busbar area	Main protection
20		Overcurrent protection of station grounding grid	Excessive current flowing into the station grounding grid	Main protection
21		Earthed system protection	Excessive current flowing into the station grounding grid	Backup protection
22		Unbalanced current protection of ground electrode	Ground electrode line ground fault	Main protection
23		Overcurrent protection of ground electrode	Ground electrode line fault	Backup protection
24		Transverse differential protection of metallic return	Ground fault under the metallic return mode	Backup protection
25	Protection of DC line area	Traveling wave protection	Metallic ground fault of the line	Main protection
26		Voltage break-variable protection	Metallic ground fault of the line	Main protection
27		Low-voltage protection of DC line	High-impedance ground fault of the line	Backup protection
28		Longitudinal differential protection of DC line	High-impedance ground fault of the line	Backup protection
29		AC/DC cross protection	AC/DC cross fault	Main protection
30		Longitudinal differential protection of metallic return	Metallic return ground fault	Main protection
31	Protection of DC switch	Bypass switch protection	Bypass switch fault	Main protection
32		Protection of neutral busbar switch	Neutral busbar switch fault	Main protection
33		HSGS protection	HSGS fault	Main protection
34		Protection of metallic return transfer breaker	Metallic return transfer breaker fault	Main protection
35		Protection of ground return transfer breaker	Ground return transfer breaker fault	Main protection
36	Protection of DC filter	Differential protection	DC harmonic filter ground fault	Main protection
37		Overcurrent (overload) protection	DC harmonic filter equipment fault	Backup protection
38		Capacitor overvoltage protection	Capacitor fault	Main protection
39		Capacitor unbalance protection	Capacitor fault	Main protection

24.3 Difference Between UHVDC Protection and Conventional DC Protection

The difference between the UHVDC protection and conventional DC protection mainly covers the following aspects.

24.3.1 Configuration of Protective Devices

In the UHVDC transmission system, since the structure of bipolar 12-pulse converters connected in series, each group of 12-pulse converter can be out of service without affecting the normal operation of the other group. Therefore, in the UHVDC transmission system, the pole protection, DC line protection, and protection of bipolar area shall be realized using the same device, and the converter protection shall be arranged based on the valve block; while in the conventional DC protection system, the converter protection, pole protection, DC line protection, and protection of bipolar area shall be realized using the same device.

24.3.2 Protection Configuration and Principle

The structure of the UHVDC transmission system is basically the same as that of the conventional DC transmission system, thus the protection configurations and principles of polar area, bipolar area, DC line area, and DC filter area of the two systems are basically the same; the protection of converter area and DC switch are also basically similar. However, the UHVDC system is provided with bypass switch protection which is rare in the conventional DC system. In addition, the UHVDC system only needs to block one faulty valve block instead of the entire pole when the protection starts to block the converter, while the conventional DC system generally block the entire pole. The differences between the two systems are described as follows:

1. Configuration of bypass switch protection

Bypass switch is specially equipped in the UHVDC transmission system. When the converter stops operation, it is short circuited through closing the bypass switch; and the current is transferred to the converter valve by disconnecting the bypass switch when the converter is put into operation.

In order to prevent the failure in closing of bypass switch when the converter is removed out of operation, or failure in disconnection of bypass switch when the converter is put into operation, the bypass switch protection is provided in the

UHVDC protection, which is designed to detect the bypass switch failure, including the opening failure and closing failure.

In the conventional DC protection system, as no bypass switch is equipped, no bypass switch protection is designed.

2. Several principles of protection are different

(1) DC overvoltage protection

In the UHVDC protection, the DC overvoltage protection is provided for each converter, and is realized by monitoring the U_{dL}, U_{dM}, and U_{dN}, respectively:

Section I:

$$|U_{dL} - U_{dM}| > \Delta \quad \text{and} \quad I_{dH} < \Delta; \quad \text{or} \quad |U_{dM} - U_{dN}| > \Delta \quad \text{and} \quad I_{dH} < \Delta \tag{24.47}$$

Sections II and III:

$$|U_{dL} - U_{dM}| > \Delta \text{ or } |U_{dM} - U_{dN}| > \Delta \tag{24.48}$$

In the conventional DC protection, the DC overvoltage protection is provided for the entire pole and is realized by monitoring the U_{dL} or $U_{dL} - U_{dN}$:

Section I:

$$|U_{dL}| > \Delta \quad \text{and} \quad I_{dH} < \Delta; \quad \text{or} \quad |U_{dL} - U_{dN}| > \Delta \quad \text{and} \quad I_{dH} < \Delta \tag{24.49}$$

Sections II and III :

$$|U_{dL}| > \Delta \quad \text{or} \quad |U_{dL} - U_{dN}| > \Delta \tag{24.50}$$

(2) DC low-voltage protection

In the UHVDC protection, after the DC low-voltage protection acts, the U_{dM} can be monitored at the same time so as to identify the fault coverage. If only the HV valve block or LV valve block fault is identified, only the faulty valve block shall be blocked after the protection acts, otherwise the pole has to be blocked.

Section I:

$$\Delta_2 < |U_{dL}| < \Delta_1 \tag{24.51}$$

Section II:

$$|U_{dL}| < \Delta \tag{24.52}$$

After Section I acts, the HV valve ($|U_{dL} - U_{dM}| < \Delta$) or LV valve ($|U_{dM} - U_{dN}| > \Delta$) blocks; after Section II acts, both valves block. For the monopolar 12-pulse converter structure, the converter shall be blocked immediately after the protection acts.

3. Consequences of some protection actions are different

For the protection of the converter area of the UHVDC system, the consequence of converter short-circuit protection, overcurrent protection, commutation failure protection, group differential protection, bridge differential current protection, AC low-voltage protection, and AC overvoltage protection is to stop the corresponding valve groups; while in the conventional DC system, the consequence of these protections is to stop the corresponding poles.

References

1. Xijie D. Fundamentals of direct current transmission. Beijing: Water Resources and Electric Power Press; 1990.
2. Zhenya L. An album of research accomplishments of UHVDC power transmission technology. 1st ed. Beijing: China Electric Power Press; 2008.
3. China Southern Power Grid-EHV Power Transmission Company, SCUT School of Electric Power. Relay protection principle and technology of HVDC transmission system. Beijing: China Electric Power Press; 2013.
4. Wanjun Z. HVDC transmission project technology. Beijing: China Electric Power Press; 2004.
5. Zheng X. AC/DC power system-dynamic behavior analysis. Beijing: China Machine Press; 2004.
6. Shengshi Z. Principle and technique of relay protection of high voltage network. Beijing: China Electric Power Press; 1995.
7. Xingyuan L. HVDC transmission operation and control. Beijing: China Electric Power Press; 1988.
8. Aimin L, Zexiang C, Dayong R, Xiaohua L. Analysis on the dynamic performance characteristics of HVDC control and protections for the HVDC line faults. Autom Electric Power Syst. 2009;33(11):72–5.
9. Haiyun L, Chuang F. Discussion of the voltage change rate setting value in travelling wave based protection of GGII HVDC line. Southern Power Syst Technol. 2008;2(1):14–7.
10. Gang W, Jianbin L, Haifeng L, Zhikeng L. Transient Energy Protection for ±800 kV UHVDC transmission lines. Autom Electric Power Syst. 2010;34(1):28–31.

Part IV
Design of UHV Power System

The design, leading the whole UHV engineering construction, plays a very important role in both provide guidance for the practical engineering implementation and to ensure the safety and economy during the project life cycle. Compared with the EHV power transmission project, the UHV power system have the characteristics of high voltage level, large transmission capacity, long transmission distance, high reliability requirements, etc., so higher requirements are also put forward for the design of UHV power transmission system.This section will focus on the content and requirements of design for UHV power transmission system include UHVAC substation, UHVDC converter station, UHVAC power transmission line, and UHVDC transmission line.

Chapter 25
Design of Ultra-High-Voltage Alternating Current (UHVAC) Substation

Feng Qian, Wenqian Qiu, Jian Ding, Chunxiu An, Hongbo Liu, Jianhua Chen and Yang Shen

The successful operation of 1000 kV Southeast Shanxi-Nanyang-Jingmen UHVAC Demonstration Project marks that the development of China's power grid has entered the ultra-high-voltage era. The construction of ultra-high-voltage (UHV) power grid has a substantial influence on the sustainable development of China's electric power industry, improvement of technical equipment level of power grid, and impetus to industrial upgrade of electrotechnical equipment manufacturing industry in China. The design, leading the whole UHV engineering construction, plays a very important role in both digestion and utilization of scientific achievements and guidance to the practical engineering implementation.

F. Qian (✉) · W. Qiu · J. Ding · C. An · H. Liu · J. Chen · Y. Shen
China Energy Engineering Group, Zhejiang Electric Power Design Institute Co., Ltd., Hangzhou, Zhejiang, People's Republic of China
e-mail: qianfeng@163.com

W. Qiu
e-mail: 839821641@qq.com

J. Ding
e-mail: ding_jian_hz@139.com

C. An
e-mail: 497094889@qq.com

H. Liu
e-mail: 1564832794@163.com

J. Chen
e-mail: 13575758055@139.com

Y. Shen
e-mail: shenyangzju@21cn.com

© Zhejiang University Press, Hangzhou and Springer-Verlag GmbH Germany 2018

H. Zhou et al. (eds.), *Ultra-high Voltage AC/DC Power Transmission*,
Advanced Topics in Science and Technology in China,
https://doi.org/10.1007/978-3-662-54575-1_25

This chapter, based on the electrical connection and layout of UHV substation, deals with the issues that need to be particularly considered in such aspects as site selection, main electrical connection, model selection of distribution equipment, and general layout.

25.1 Design Depth Requirements and Main Standards

25.1.1 Design Depth Requirements

To implement the requirement of "Collectivized Operation, Intensive Development, Lean Management and Standardized Construction," standardize the design work for the UHV engineering, adapt to the requirements for the UHV substation construction, enhance the quality and level of UHV substation construction and control the cost reasonably, State Grid Corporation of China has formulated Q/GDW 11216-2014 *Code of Content Profundity for Preliminary Design for* 1000 kV *Substation* and Q/GDW 11217-2014 *Code of Content Profundity for Working Drawing Design for* 1000 kV *Substation* in combination with the experience in the deign of the UHV substation demonstration projects, specifying the content and depth for design.

25.1.2 Main Standards

After the UHVAC demonstration project was put into operation, the State Grid Corporation of China organized the preparation of some standards of UHV substations, among which the following procedures and codes are mainly relevant to the design:

GB 50697-2011 *Code for Design of* 1000 kV *Substation*
GB/Z 24842-2009 *Overvoltage and Insulation Coordination of* 1000 kV *UHVAC Transmission Project*
Q/GDW 294-2009 *Technical Code for Design of* 1000 kV *AC Substations (Electrical Section)*
Q/GDW 286-2009 *Technical Guide on* 1000 kV *System Voltage and Reactive Power*
Q/GDW 323-2009 *Standards for Environmental Pollution Classification for* 1000 kV *System*
Q/GDW 278-2009 *Technical Specification for Grounding of* 1000 kV *Substation*
Q/GDW 304-2009 *Technical Regulations for Impact Assessment of Electromagnetic Environment Produced by* 1000 kV *Transmission and transfer Power Engineering*

Q/GDW 318-2009 *Overvoltage and Insulation Coordination for* 1000 kV *Transmission and Transformation Project*
Q/GDW 319-2009 *Guide for Overvoltage and Insulation Coordination of* 1000 kV *AC Transmission System*
*Power Transmission and Transformation Project General Design of State Grid Corporation of China (*1000 kV *Substation Booklet) (Version 2013)*
*Power Transmission and Transformation Project General Equipment of State Grid Corporation of China (*1000 kV *Substation Booklet) (Version 2013).*

25.1.3 Key and Difficult Issues of Design

The UHV frames and supports are featured by large tension force, wide span, high height, etc. The selection of calculation wind velocity, determination of economic sag, and selection of type of the frames and supports (including determination of section form of beams and columns and selection of main and auxiliary materials, etc.) are all difficult points in design.

A large amount of calculation and optimization is needed to determine the bay width of UHV distribution equipment, height of equipment supports, height of busbar frames, height of incoming (outgoing) line frames, longitudinal dimensions, road planning for distribution equipment, etc., while there are few calculation equations and mathematic models that can be used directly in calculation of wire tension and wind swing, etc. for UHV voltage level.

25.2 Site Selection and General Layout

25.2.1 Site Selection

The site selection of UHV substation is a job strongly based on policy and technology, and therefore, needs to be completed by the joint effort of a number of units and disciplines. Since the UHV substation covers a large area of land, has a high requirement on technology, and greatly affects the surrounding environment, it is more difficult than the common substation in site selection. Special attention shall be taken to the following aspects during the site selection of UHV substation:

1. Stick to the principle of optimal land utilization

The basic national policy of land conservation in China shall be followed strictly during site selection. The substation shall utilize wasteland or barren land as far as possible and shall not occupy or occupy as less as possible farmland to conserve arable land. In general, the UHV substation covers a land of more than 12 ha. In case HGIS or AIS distribution equipment is adopted, the land area occupied by the

Table 25.1 Parameters of heavy-duty transport equipment

S/N	Designation of equipment	Manufacturer	Transport dimension	Transport weight (t)
			Length (m) × width (m) × height (m)	
1	Main transformer	TBEA (Tebian Electric Apparatus Stock Co., Ltd.) Shenyang Transformer Co., Ltd.	11.5 × 5.11 × 4.97	397
		Baoding Tianwei Baobian Electric Co., Ltd.	11.05 × 4.95 × 4.99	388
		Xi'an XD Transformer Co., Ltd.	8.81 × 4.59 × 5.00	346
2	HV reactor	/	6.6 × 3.685 × 4.65	173

substation may sometimes be up to 40 hectares, which will consume substantial land resources.

In general, distribution equipment of UHV projects is of the outdoor GIS type, having a good result of land resource saving. With the ceaseless promotion of UHV projects and continual optimization of electrical layout, the land area required by substations is decreasing constantly.

2. Pay attention to the implementation scheme for heavy-duty equipment transport and traffic problem

The large-scale over-limit equipment used in UHV substation is mainly the main transformer and the 1000 kV HV reactor. The transport parameters of some manufacturers' equipment subject to heavy-duty transport are shown in Table 25.1. It can be seen from the table that the transport of a single phase of the main transformer is comparable to that of a 500 kV three-phase compact transformer in weight and dimension, and, compared with the common transformer, has much higher requirements on the roads and bridges on the way and requires much higher transport cost correspondingly. Compared with the transformer, the problem of limitation by transport requirements on the UHV reactor is not severe. The route of transport is mainly restricted by the dimension and weight of main transformer.

3. Reduce the environmental impact as far as possible

The environmental impact includes two aspects, i.e., the impact of surroundings on the substation and the impact of substation construction on the surroundings. The former mainly includes a variety of pollutants in the dirty area. So the site shall be selected as far from the area where air is polluted severely and where there is heavy salt mist as possible. If it is inevitable to select the site in unfavorable conditions as above-mentioned, the selected site shall preferably be located on the windward side of pollution source, or, alternatively, measures such as composite apparatus, indoor distribution equipment and dust-proof coating shall be taken. During the construction of UHV substation, special attention shall be paid to the impact of the substation on the surroundings, mainly including the following aspects:

(1) Noise pollution. The noise source of UHV substation mainly comes from the audible noise generated by corona on wires and the noise of electrical equipment. China has not yet specified the limit standard for the audible noise of substation, which can refer to the relevant 750 kV standards. In design of 1000 kV distribution equipment, the limit standard for audible noise, as same as that for corona radio interference, can be specified to a level not exceeding the line level at the boundary wall of the substation (in case of 750 kV, the control standard is 60 dB (A), corresponding to Category II zone as specified in China's standard GB 12348-2008: *Emission Standard for Industrial Enterprises Noise at Boundary*).
(2) Visual impact. The UHV substation covers a large area of land and the frames and supports inside the substation and the iron towers outside the substation are evidently higher than those of other voltage grades, which cause obvious visual impact to the people. So the site shall be selected away from the residential area as far as possible, away from natural reserves, scenic spots, etc. The substation shall be constructed in such a way that the substation and the iron towers blend harmoniously with the surrounding environment.
(3) Water system change and water pollution. The construction of UHV substation usually changes the original water system. Rainwater of the substation area and other areas segregated is changed into organized drainage, which may affect local irrigation to a certain extent. Meanwhile, the wastewater and sewage discharged during the operation of the substation also affect the local water quality to a certain extent if they are not treated properly. Therefore, the site selected for the substation shall not locate upstream of drinking water reservoir. The issue to be addressed during design is that the discharged wastewater and emergency oil must be subject to rigorous treatment to such an extent that they will not pollute the surroundings. Water drainage outside of the substation shall be planned by comprehensively taking the local original water system into consideration so that the drained water will have no negative effect on the irrigation ability of adjacent river courses and water channels.

25.2.2 General Planning and Layout

The general planning and layout consists of two aspects, i.e., the general layout inside the boundary wall and the layout of general plane on landform. The former needs comprehensive coordination of the members of engineering team, and shall be subject to full discussion and argumentation by taking landform and geological conditions of the site into consideration. The latter shall be carried out mainly by the major in civil construction, which shall analyze the field of the site selected according to the general layout determined preliminarily, incorporate the land area, road connection, earthworks, foundation treatment, compensation for demolition and relocation, flood control in the site, environmental impact and others together to

implement repeated comprehensive discussion and argumentation, to obtain the layout of the general plane of the substation on the construction site and finally complete the general planning and layout of the substation.

On the basis of the feature of large occupancy area of UHV substation, in case of general planning and layout of the substation under complicated landform or geological conditions, the influence of minor adjustment to the substation site on the project (e.g., the design schemes for side slope retaining wall and drainage outside the substation) and the influence of vertical layout design on total coverage area, earthwork volumes, and foundation treatment, etc. shall be fully considered. The more sufficiently and comprehensively the planning and layout is discussed and argued in early stage, the less the repeats of design will occur in later stage and the simpler the project implementation and investment control will become.

25.3 Main Electrical Connection

Japan and the Former Soviet Union have performed certain research in the UHV power transmission field and successfully built up several 1000 kV UHV power transmission lines which, however, are basically used just for step-down operation at present. The UHV substations in Japan adopt double-busbar four-section connection, while the UHV substations in the Former Soviet Union adopt 4/3 circuit breaker connection (the load-center substation) and other connection methods. In the twentieth century, the developed countries in Europe and America also carried out large amount of researches in the UHV field. The double-circuit-breaker connection is commonly used for 765 kV UHV substation in the countries in South America [1].

After the 1000 kV Southeast Shanxi-Nanyang-Jingmen UHVAC Demonstration Project was put into production, State Grid Corporation of China, on the basis of the summarized experience of the Demonstration Project, published the enterprise standard Q/GDW 294-2009 *Technical Code for Design of* 1000 kV *AC Substations (Electrical Section),* which set forth the following stipulations for 1000 kV main electrical connection:

> With regard to the final connection method for 1000 kV distribution equipment, the 3/2 circuit breaker connection shall preferably be used in case the total number of such connecting components as lines and transformers is of five or more circuits.
>
> If the connecting components such as lines and transformers are relatively few in initial, the polygonal connection or other simplified connection forms using relatively few circuit breakers can be adopted in accordance with the actual total number of connecting components. But such connection form shall be easy to be changed to the final connection form.
>
> When 3/2 circuit breaker connection is adopted, the homonymous circuits shall be configured in different strings, and the power supply circuit and load circuit shall preferably be paired in string. If connection is restricted by the conditions, the homonymous circuits can be connected to the busbar on the same side.

The connection scheme, when used in specific projects, shall also comprehensively take the equipment manufacturing capability and electrical layout into consideration.

According to *Electrical Engineering Electrical Design Manual*, with regard to one-and-a-half breaker connection, consideration shall be given to the possibility that a circuit may carry the maximum load current of another circuit when the circuit breaker fails or is under maintenance. Therefore, the continuous working current of a circuit shall be twice normal load current of adjacent circuits [2]. If calculation is carried out on the basis that the transmission power of each circuit is 5000 MW, with the power factor considered at around 0.95, the working current of one circuit will reach 3039 A. If one-and-a-half breaker connection is adopted, the working current thereof will reach 6078 A. A circuit breaker having 6300 A rated current shall be considered to choose.

In the early phase of the 1000 kV Southeast Shanxi-Nanyang-Jingmen UHVAC Demonstration Project, the research and development situation of 1000 kV equipment is that the rated current of all 1000 kV circuit breakers produced by manufactures in China is not higher than 4000 A. Therefore, in the current phase of the Project, the main connection scheme at 1000 kV side of 1000 kV substations in Southeast Shanxi and Jingmen adopts the double-circuit-breaker connection. In the future phase, the equipment manufacturing capability will be improved in accordance with the needs of the system, and the one-and-a-half breaker connection (the circuit breaker with rated current of 6300–8000 A) will be adopted.

From the research and development of equipment, the companies such as Henan Pinggao Electric Co., Ltd., New Northeast Electric (Shenyang) High Voltage Switchgear Co., Ltd. and Xi'an XD Switchgear Electric Co., Ltd. have possessed relatively mature 1000 kV GIS products with rated current of 6300 A. From the prospect of development of equipment manufacturing capability, the 1000 kV system can satisfy the requirements of current-carrying capacity of UHV lines by adopting the one-and-a-half breaker connection scheme.

25.4 Overvoltage Protection

As per the conclusions of relevant reports from some scientific study [3], the overvoltage control level for 1000 kV power system are shown as follows:

1. Overvoltage control level for 1000 kV power system

(1) Power frequency temporary overvoltage

At the substation side of outgoing breaker: 1.3 p.u.; at the line side of outgoing breaker: 1.4 p.u.

(2) 2% statistical switching overvoltage of the substation

Phase-to-ground overvoltage at the substation side: 1.6 p.u.; phase-to-ground overvoltage at the line side: 1.7 p.u.

Phase-to-phase overvoltage at substation side: 2.8 p.u.; phase-to-phase overvoltage at line side: 2.8 p.u.

2. Overvoltage protection for 1000 kV power system

(1) Power frequency overvoltage

The charging reactive power of the 1000 kV line is high, so capacitance effect of the no-load line, asymmetrical ground fault, load shedding and other causes can result in power frequency temporary overvoltage in the 1000 kV system. It is an effective measure to limit power frequency overvoltage in the system by installing HV shunt reactors at the outlet of the 1000 kV line. For example, in the Huainan-Shanghai UHVAC Demonstration Project in China to Transmit Power from Anhui to Eastern China, a set of HV shunt reactors with capacity of 3×240 Mvar is installed, respectively, at the outlets of the double-circuit line between Huainan and South Anhui; a set of HV shunt reactors with capacity of 3×200 Mvar is installed diagonally at the outlets of the double-circuit line between South Anhui and North Zhejiang; a set of HV shunt reactors with capacity of 3×240 Mvar is installed diagonally at the outlets of the double-circuit line between North Zhejiang and West Shanghai. In such a way, the overvoltage control requirement of the system is met.

The neutral point of UHV shunt reactors is grounded by the small reactor to limit the non-full phase resonance overvoltage in non-full phase operation.

(2) Switching overvoltage

1000 kV switching overvoltage mainly consists of closing overvoltage, single-phase reclosing overvoltage, no-load line breaking overvoltage and ground fault clearing overvoltage. The most effective measure to limit such overvoltage is to install the closing resistor on the circuit breaker.

For example, in the Huainan-Shanghai UHVAC Demonstration Project to Transmit Power from Anhui to Eastern China, the circuit breakers are mounted with 600 Ω closing resistors and the lines are additionally mounted with arresters at the outlets to limit the switching overvoltage level of 1000 kV lines.

(3) Lightning overvoltage

The lightning overvoltage is caused by direct lightning striking or back striking on phase conductors, or by induction resulting from lightning striking on the ground near the lines. China Electric Power Research Institute and State Grid Electric Power Research Institute have conducted analog calculation for the lightning protection of 1000 kV Southeast Shanxi Substation, Nanyang Switch Station and Jingmen Substation with the aid of electro-magnetic transient programs (ATP and EMTP) [4]. The calculated result shows that both the transformer side and the line

side shall be equipped with arresters, and whether the busbar, the wire in strings, and the shunt reactor side shall be equipped with arresters is contingent closely on whether to consider single-line operation and the protection angle of incoming section of the line. The value of 1000 kV equipment insulation level also affects the distance between the arrester and the equipment to be protected. The calculated result of Power Transmission Project from Anhui to Eastern China shows that under rigorous conditions such as single-line operation, some lines with HV shunt reactors need to be installed with a set of arresters, respectively, at the outlets of the line and near the HV shunt reactor bushings to meet the insulation requirements of equipment.

Therefore, the arrester configuration of 1000 kV system in specific project shall be determined on the basis of lightning overvoltage prediction, switching overvoltage calculation or simulation test.

(4) Secondary arc current and recovery voltage

The valve of the phase-to-phase capacitance and the inductance in 1000 kV line are high, so special attention must be taken to the secondary arc current and recovery voltage during reclosure in order to enhance the success rate of single-phase reclosure. The secondary arc current and recovery voltage can be limited by installing additionally the neutral small reactor in HV shunt reactors to realize 100% full compensation for line phase-to-phase capacitance. In Japan, the secondary arc current and recovery voltage are limited by separately installing high-speed ground switches on lines.

3. Parameters of 1000 kV arrester

(1) Selection of rated voltage of arrester

The temporary overvoltage of the system determines the rated voltage of the arrester. The relation between rated voltage U_r of the arrester and the maximum working line voltage U_m can be expressed as $U_r = \beta U_m/\sqrt{3}$, where β is multiple of temporary overvoltage. Calculated by the equation, the rated voltage of the arrester at the busbar side of substation is 828 kV, while that of the arrester at the line side of substation is 888 kV. Since the duration of power frequency overvoltage with amplitude between 1.3 and 1.4 p.u. is short, the arrester with rated voltage of 828 kV can withstand the overvoltage absolutely and has sufficient margins. Therefore, the whole line can adopt arresters with rated voltage of 828 kV.

(2) Selection of continuous operating voltage of the arrester

In accordance with the guideline for selection of arresters, the continuous operating voltage of arresters must be greater than or equal to the continuous operating voltage of the system at the working positions thereof. Since the arresters are installed phase-to-ground, its continuous operating voltage is determined to be 638 kV (see Table 25.2).

(3) Main parameters of the arrester

Table 25.2 Main technical parameters of the arrester used in 1000 kV system

Item	Substation side/line side
Nominal voltage of system (kV)	1000
Maximum voltage of system (kV)	1100
Temporary overvoltage of system (p.u.)	1.3
Rated voltage of arrester (kV)	828
Continuous operating voltage of arrester (kV)	≥ 638
2 kA switching impulse current residual voltage (kV, peak value)	≤ 1460
20 kA lightning impulse current residual voltage (kV, peak value)	≤ 1620

Table 25.3 List of minimum air clearances of 1000 kV distribution equipment (at altitude of 1000 m)/unit: m

S/N	Discharge voltage type	A_1		A_2
		A_1'	A_1''	
1	Power frequency discharge voltage	4.20		6.80
2	Positive switching impulse voltage wave	Quad-bundled conductor-ground tubular busbar-ground: 6.80	Grading ring-ground: 7.5	Between quad-bundled conductors: 9.2
				Between grading rings: 10.1
				Between tubular busbars: 11.3
3	Positive lightning impulse voltage wave	5.00		5.50

Note $A_1(A_1', A_1'')$—the minimum phase-to-ground air clearance. A_1' is the clearance between bundled conductor and grounding part and the clearance between tubular conductor and grounding part; A_1'' is the clearance between grading ring and grounding part; A_2—the minimum phase-to-phase air clearance

25.5 Minimum Air Clearance

The air clearances of 1000 kV distribution equipment are shown in Table 25.3.

25.6 Insulation Level of Electrical Equipment

Insulation coordination shall be performed in accordance with the principle specified in the national standard GB 50697-2011 *Code for Design of* 1000 kV *Substations* and GB/Z 24842-2009 *Overvoltage and Insulation Coordination of* 1000 kV *UHV AC Transmission Project*, i.e., the coordination coefficient of

lightning impulse is taken as 1.33 (for the transformer and shunt reactor) and 1.45 (for equipment such as the high-voltage electrical apparatus, current transformer, bushing, etc.), and the general coordination coefficient of switching impulse is taken as 1.15 [3, 5]. The rated insulation levels of 1000 kV equipment are shown in Table 25.4.

Table 25.4 Rated insulation levels of 1000 kV equipment

Designation of equipment	Peak value of equipment test voltage (kV)			
	Lightning impulse withstand voltage		Switching impulse withstand voltage	Power frequency withstand voltage
	Full wave internal and external insulation	Chopped wave	Internal and external insulation dry and wet condition	Dry and wet condition
Auto transformer	2250	2400	1800	1100 (5 min)
Shunt reactor	2250	2400	1800	1100 (5 min)
Capacitor voltage transformer	2400	–	1800	1100 (5 min)
Switchgear	2400	–	1800	1100 (1 min)
Between open contacts of switchgear	2400 + 900	–	1675 + 900	1100 + 635 (1 min)
Post insulator	2400	–	1800	1100 (1 min)

Designation of equipment	Coordination Coefficient of Protection Level	
	Lightning impulse protection level	Switching impulse protection level
	kV (peak)	kV (peak)
Auto transformer	20 kA residual voltage of arrester: 1620	2 kA switching wave residual voltage of arrester: 1460
	Full wave coordination coefficient: 2250/1620 = 1.39	Actual coordination coefficient:
	20 kA residual voltage of arrester: 1620	1800/1460 = 1.23 1.15
Shunt reactor	2250/1620 = 1.39	1800/1460 = 1.23, 1.15
Capacitor voltage transformer	2400/1620 = 1.48 1.33	1800/1460 = 1.23 1.15
Switchgear	2400/1620 = 1.48 1.45	1800/1460 = 1.231.15
Between open contacts of switchgear	–	–
Post insulator	2400/1620 = 1.48 1.45	1800/1460 = 1.23 1.15

Note The value of reverse test voltage between open contacts of switchgear is taken as 1.0 time the peak value of the maximum phase-to-ground power frequency voltage of the system for switching, while taken as 1.0 time the peak of the maximum phase-to-ground power frequency voltage of the system for lightning

25.7 Selection of Main Electrical Equipment

The main electrical equipment shall be selected in such a way that the requirements under normal running, maintenance, short-circuit, and overvoltage can be met. The equipment shall also be appropriate to the development and expansion in the future and verified in accordance with the local environmental conditions.

25.7.1 Electrical Calculation

The selection of the main electrical equipment mainly involves the following calculations and verifications:

(1) Calculation of short-circuit current
(2) Long-term working conditions (voltage, current, and mechanical load)
(3) Short-circuit steady condition
(4) Insulation level.

25.7.2 Main Transformer

The 1000 kV main transformer is crucial equipment in UHV project. The main transformer put into operation in the 1000 kV Southeast Shanxi-Nanyang-Jingmen UHVAC Demonstration Project has single-phase capacity of 1000 MVA with voltage of 1000 kV.

The main transformer is of three-phase or single-phase, which mainly depends on a variety of factors including manufacturing condition, reliability, and transport condition of the transformer. Because the single-phase transformer is more cost-efficient than the three-phase transformer, the single-phase transformer is mainly adopted in UHV project. Compared with common transformers of the same capacity, the autotransformer has many advantages, including low manufacturing cost due to small material consumption; high efficiency due to small active and reactive loss; low impedance because of self-coupling relation of high-voltage and medium-voltage coils, which can improve stability of the system to a certain extent; able to increase the extreme manufacturing capacity of transformer to facilitate transport and installation. Based on the current manufacturing level and transport condition of main transformer in China, the UHVAC transformers used in the Demonstration Project and the Power Transmission Project from Anhui to Eastern China are all of single-phase, self-coupling, and off-circuit voltage regulating transformer, with rated capacity of 1000 MVA, voltage ratio of $\frac{1050}{\sqrt{3}}/\frac{520}{\sqrt{3}} \pm 2 \times 2.5\%/110\,\text{kV}$ and short-circuit impedance of $U_{1-2}\% = 18\%$.

The main transformer consists of main body and voltage-regulating transformer. The voltage-regulating transformer is mounted outside the oil tank of the main body which comprises the bodies of voltage regulator and compensator and change-over voltage regulating switch. The voltage regulating part is independent of the main body so that the main body can keep operating even if the voltage-regulating part fails. In addition, the method simplifies the design of the transformer and improves its reliability, thus facilitates long-term safe and stable operation.

In order to avoid the technical problems caused by oil flow electrification, the 1000 kV transformer shall be cooled by OFAF (oil forced air forced) cooling method; moreover, the air fans and oil pumps can be stopped appropriately under light load to achieve change-over between OFAF/ONAF/ONAN cooling methods to reduce loss and consumption of auxiliary machines.

It shall be determined in design according to conditions of the system and equipment whether the standby phase shall be installed. Alternatively, it can be considered to set up one standby phase in one area according to the conditions such as parameters of transformer, transport condition, and status of the system.

To adapt to the requirements for large-capacity power transmission of the UHV substations under planning, the 1000 kV main transformer manufacturers, through the development activities carried out based on the previous experience in the design and development of the UHV substation transformers, have been equipped with the capability to produce the single-phase 1000 kV/1500 MVA main transformers. According to the investigation and survey on the major manufacturers of 1000 kV main transformers in China, including Xi'an XD Transformer Co., Ltd. (hereinafter referred to as Xi'an Transformer), Baoding Tianwei Baobian Electric Co., Ltd. (hereinafter referred to as Baobian) and TBEA Shenyang Transformer Co., Ltd. (hereinafter referred to as Shenyang Transformer), the overall dimension of the 1500 MVA large-capacity main transformer is as shown in the following Table 25.5.

For the 1000 MVA transformer, the distance between the main transformer's incoming line framework and the main transformer framework is 41 m. Based on a comprehensive consideration in the overall dimension of the 1500 MVA large-capacity transformer, the distance between the main transformer's incoming line framework and the main transformer framework shall be increased by 2–43 m (see Table 25.6; Figs. 25.1, 25.2 and 25.3).

Table 25.5 Overall dimension of 1500 MVA transformer

S/N	Manufacturer	Depth (m)	Width (m)	Bushing height (m)
1	Xi'an transformer	17.65	13.04	18.85
2	Baobian	16.55	12.92	17.73
3	Shenyang transformer	16.2	15.1	19

Table 25.6 Main parameters of 1000 kV transformer

S/N	Voltage ratio	Rated capacity	Connection symbol
1	$\frac{1050}{\sqrt{3}}/\frac{525(520.515)}{\sqrt{3}}$ $\pm 4\times 1.25\%(\pm 10\times 0.5\%)/110$	1000/1000/334	Ia0i0
2	$\frac{1050}{\sqrt{3}}/\frac{525(520.515)}{\sqrt{3}}$ $\pm 4\times 1.25\%(\pm 10\times 0.5\%)/110$	1500/1500/500	

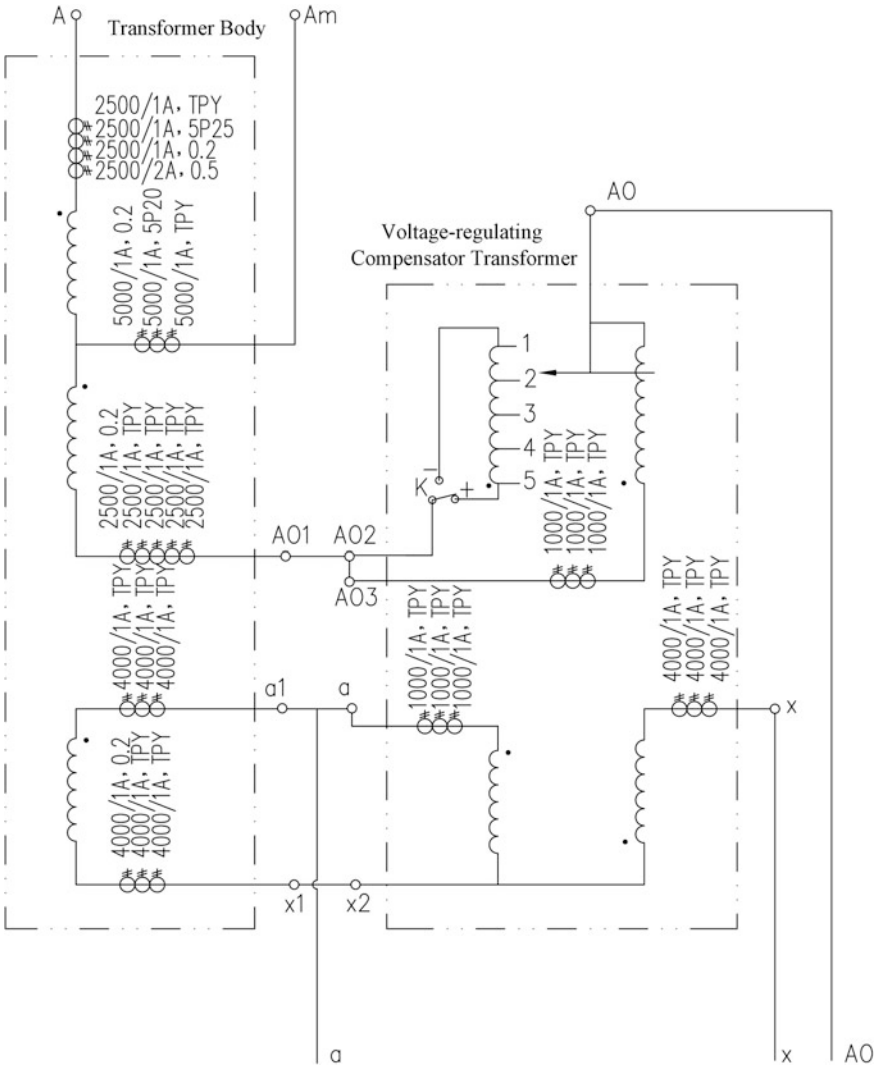

Fig. 25.1 Wiring sketch for A-phase of 1000 kV main transformer

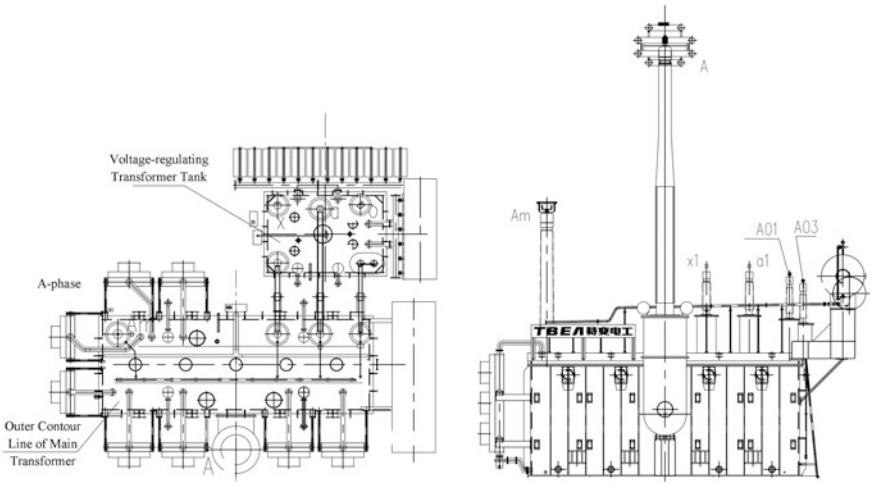

Fig. 25.2 Sketch for A-phase layout of 1000 kV transformer

25.7.3 Switchgear

At present, three types of switchgears are optional for 1000 kV voltage class, namely, AIS, HGIS and GIS. The 1000 kV voltage transformer and arrester adopt air-insulated switchgear (AIS) that independent of HGIS and GIS.

The type of switchgears shall be selected on the basis of practical condition of the project, equipment manufacturing and supply conditions, and the relevant industrial policies in China. After sufficient argument, the 1000 kV switchgear of Southeast Shanxi Substation in Southeast Shanxi-Nanyang-Jingmen Demonstration Project adopted GIS, while the 1000 kV switchgears of Nanyang Switch Station and Jingmen Substation adopted HGIS. AIS was ever considered to be used as the 1000 kV switchgear in Nanyang Switch Station, but HGIS substituted AIS after comprehensive consideration in manufacturing capacity of the equipment manufacturers in China, safe operation of the equipment, construction period, and conservation of land resources. The 1000 kV switchgears of the four UHV substations in Huainan-Shanghai UHVAC Demonstration Project to Transmit Power from Anhui to Eastern China all adopted GIS switchgears.

25.7.4 Voltage Transformer

In order to facilitate commissioning and test, outdoor independent 1000 kV voltage transformer adopts non-superposition CVT, i.e., the capacitor voltage divider is separated from electromagnetic unit.

Fig. 25.3 Photo of 1000 kV main transformer

25.7.5 UHV Shunt Reactor

The single-phase reactors are used as UHV shunt reactors, which have rated voltage of $1050/\sqrt{3}$ kV and are in star-connection arrangement. The capacity of UHV shunt reactor shall be selected according to the line length. The capacity of compensation varies with the line length. The series recommended for the three-phase capacity of UHV shunt reactors of State Grid Corporation in China are 1080 MVA/960 MVA/840 MVA/720 MVA/600 MVA.

Since the capacity and loss of 1000 kV UHV shunt reactors are much higher than those of previous 500 kV shunt reactors, the oil natural air forced (ONAF) method is used for cooling of the shunt reactors. The insulation level of neutral point of UHV shunt reactors is considered as 145 kV level.

It shall be determined in design according to conditions of the system and equipment whether the standby phase shall be installed. Alternatively, it can be considered to set up one standby phase in one area according to the conditions such as parameters of reactor, transport condition, and status of the system.

25.8 UHV Distribution Equipment

25.8.1 Classification and Design Principle of UHV Distribution Equipment

25.8.1.1 Classification of UHV Distribution Equipment

The main equipment of 1000 kV distribution equipment can be categorized into three types, i.e., conventional air-insulated switchgear (AIS), hybrid gas-insulated switchgear (HGIS), and gas-insulated metal enclosed switchgear (GIS). GIS is usually adopted in consideration of the more and more nervous land resources, which is emphatically introduced as the following.

For one-and-a-half breaker connection, layout scheme of GIS equipment has three options, i.e., three-column layout, straight-line layout and single-column layout. The single-column layout can be divided into typical connection single-column layout, conventional obliquely connected single-column layout and elevated obliquely connected single-column layout [2]. These layouts will be introduced in the following text and can be chosen in design according to practical condition of project.

(1) Three-column layout

Three-column layout is the most typical arrangement of air-insulated equipment of one-and-a-half breaker connection. It is characterized by precise simulation of main connection and convenient operation. The whole distribution equipment is large in its longitudinal dimension and relatively small in its width.

(2) Straight-line layout

Straight-line layout is a configuration of distribution equipment that has the smallest longitudinal dimension. It is characterized by the shortest longitudinal dimension, cross connection, flexible direction of incoming and outgoing lines and shortest branch busbar between circuit breakers. Its disadvantages include long main busbar, long transverse dimension and the blur of the inter-string device. Figure 25.4 shows the straight-line layout.

(3) Single-column layout

(a) Typical connection single-column layout

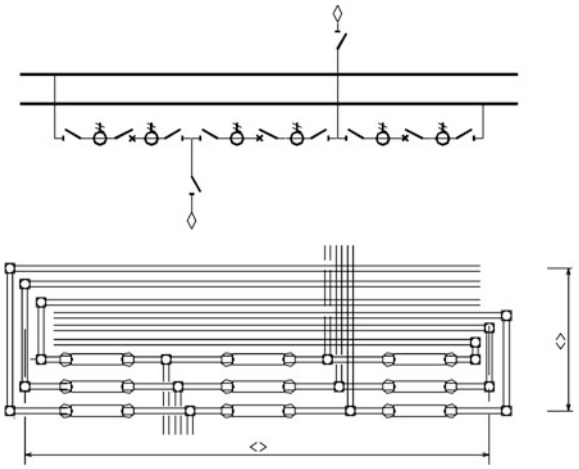

Fig. 25.4 Straight-line layout

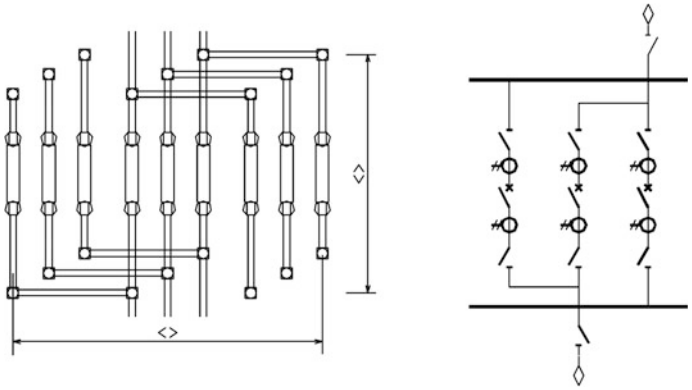

Fig. 25.5 Single-column layout

Typical connection single-column layout is difficult to realize cross connection, but is appropriate to outgoing lines at both sides and to the connection method in which number of incoming lines is comparable to that of outgoing lines. In one-and-a-half breaker connection, two elements in one string have to be outgoing in two different directions, and branch busbar between the circuit breaker and busbar is relatively long. As shown in Fig. 25.5.

(b) Conventional obliquely connected single-column layout

Conventional obliquely connected single-column layout is developed on the basis of typical connection single-column layout, which is characterized by easy realization of cross connection and flexible outgoing direction. However, branch busbar

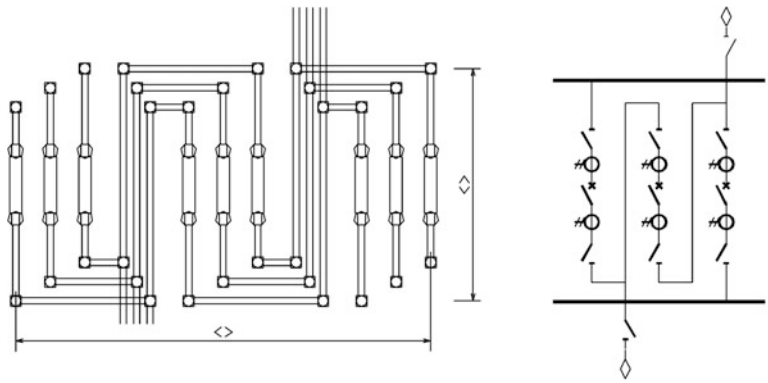

Fig. 25.6 Conventional obliquely connected single-column layout

between circuit breakers is longer and manufacturing cost of the equipment is higher. As shown in Fig. 25.6.

(c) Elevated obliquely connected single-column layout

Elevated obliquely connected single-column layout evolves from conventional obliquely connected single-column layout. It is characterized by the same arrangement as conventional obliquely connected single-column layout, easy realization of cross outgoing lines and flexible outgoing directions. However, branch busbar between circuit breakers is longer and equipment-manufacturing cost increases. Compared with conventional obliquely connected single-column layout, the elevated one has its unique arrangement: the obliquely connected branch busbar of circuit breaker is in elevated layout and does not occupy transverse space, so the layout is less than conventional obliquely connected single-column layout in transverse dimension. The whole GIS equipment is high, causing maintenance and inspection inconvenient. Some obliquely connected branch busbars also need to be removed when dismantling the equipment. Figure 25.7 shows the elevated obliquely connected single-row layout.

(4) Folding layout

The folding layout refers to that, on the basis of the straight-line layout, as the overall transverse length of GIS is limited by the general layout, the circuit breakers at an end of GIS may be arranged in a folding manner. Such folding layout applies only in the bay at the end. Although it reduces the transverse line dimension, it blocks the possibility for future expansion at such end. Refer to Fig. 25.8 for the folding layout.

The main characteristics of all layout patterns are as shown in Table 25.7.

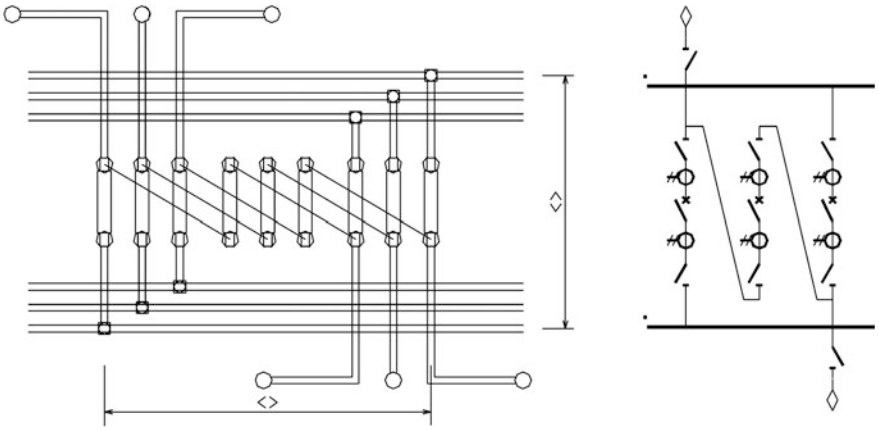

Fig. 25.7 Elevated obliquely connected single-row layout

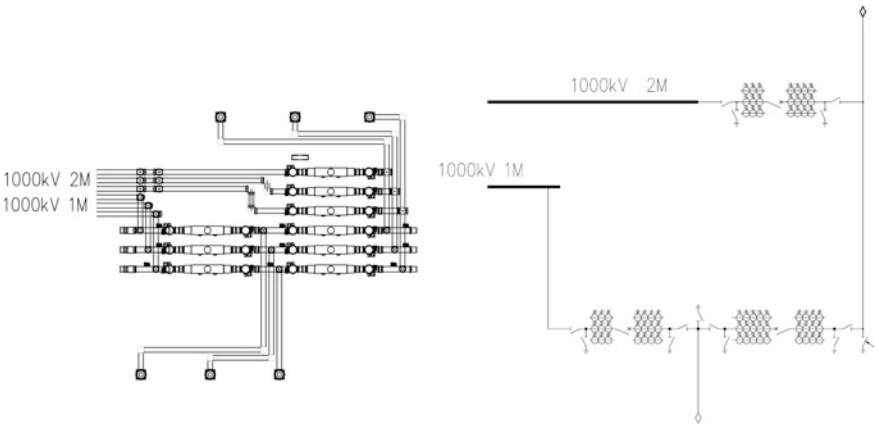

Fig. 25.8 Folding layout

25.8.1.2 Design Principles of UHV Distribution Equipment

The design principles of 1000 kV distribution equipment can be preliminarily summarized as the following:

1. Minimize the occupied land

The occupied land area of open-type distribution equipment (AIS) is roughly proportional to the square of the voltage grade. For example, in case of the same form of main connection and the same number of incoming and outgoing circuits, the area of 500 kV distribution equipment is about four times that of 220 kV, and

Table 25.7 Characteristics of GIS layout patterns

Layout pattern	Advantages	Disadvantage
Three-column layout	It is precise in simulation of main connection and convenient for operation	The whole distribution equipment, being large in longitudinal dimension and small in transverse dimension, is uncoordinated with the general layout and inconvenient for cross connection
Typical connection single-column layout	The branch busbars connecting the devices in a string are short	It is difficult to realize cross connection
Conventional obliquely connected single-column layout	It is easy to realize cross connection and flexible in incoming and outgoing line directions	The branch busbars in a string are long, leading to increased cost
Elevated obliquely connected single-column layout	It is easy to realize cross connection and flexible in incoming and outgoing line directions	The branch busbars in a string are long; the whole GIS is tall and thus inconvenient for overhaul and maintenance
Straight-line layout (separated phase layout of busbars)	It is small in longitudinal dimension and flexible in cross connection and incoming and outgoing line directions as well as short in connecting busbars in a string	A large-tonnage crane need be used to lift the circuit breakers across the main busbars which are high above the ground and lead to reduced seismic resistance
Straight-line layout (layout of busbars concentrated at the incoming line side)	It is small in longitudinal dimension and flexible in cross connection and incoming and outgoing line directions; besides, the branch busbars of outgoing line do not cross with the main busbars	It is inconvenient for equipment lifting and operator patrol inspection
Straight-line layout (layout of busbars concentrated at the outgoing line side)	It is small in longitudinal dimension and flexible in cross connection and incoming and outgoing line directions; besides, it is convenient for equipment lifting and operator patrol inspection	The branch busbars of the outgoing line cross with the main busbars and the branch busbars are long in length
Folding layout	It reduces the transverse line dimension	The possibility for future expansion is limited

the occupied land area of 1000 kV distribution equipment is also around four times that of 500 kV.

In 1000 kV substation, only the occupied land area of 1000 kV distribution equipment is up to 30–35 hm^2 (AIS device, 10-circuit 1000 kV outgoing lines), accounting for 70% of the area of the whole substation. Therefore, in the design of

1000 kV distribution equipment, how to reduce the occupied land area has become a very important issue.

2. Minimize the effect of electrostatic induction

The minimum safety clearance of high-voltage distribution equipment for 220 kV and below is decided by the requirements of insulation coordination, but in the UHV distribution equipment, the affect of electrostatic induction is gradually increased. In the design of UHV distribution equipment, the protective measures against electrostatic induction shall be taken into full consideration for the layout.

The restriction measures against electrostatic induction of distribution equipment mainly include two aspects:

On one hand, the protective measures to be considered for human bodies:

(1) When maintenance equipment with high altitude, wear conductive shoes and shield clothing should be considered to prevent maintenance personnel from the accident caused by electrostatic induction;
(2) During the equipment maintenance, consider to set up movable metal meshes to isolate the area with high electric field intensity;
(3) With reference to the methods of Former Soviet Union, set forth the allowable residence time under various electric field intensities;
(4) Designate safe inspection routes and maintenance climbing paths.

On the other hand, in the design of UHV distribution equipment, the measures to be considered for arrangement:

(1) Try the best to avoid the presence of flexible conductors above the electrical equipment. For the distribution equipment of one-and-a-half breaker connection, simply in terms of the impact level of electrostatic induction, the flat-ring layout is better than three-column layout, because it eliminates the overhead flexible conductors above all circuit breakers, thereby greatly reducing the space electric field intensity near the circuit breaker. However, if from the perspective of comprehensive technical and economic considerations, an alternative method is to change the geometric parameters of conductors, for example, increase the height of conductors above ground, reduce the phase-to-phase distance of conductors and reduce the number of conductor bundles;
(2) It is required that each circuit shall have the same phase sequence to avoid the existence of the same phase region in two adjacent circuits with opposite phase sequences. Because the electric fields in the vicinity of the same phase region are directly superimposed, leading to the increase of electric field intensity, when the side phases of adjacent spans are of different phases (ABC-ABC), the electric field intensity between the spans is lower and the electric field intensity of the side phase on the outside is higher. When the side phases of adjacent spans are of the same phase (ABC-CBA), the electric field intensity between the spans is increased significantly;

(3) In order to limit the value of ground electric field intensity, the value of the safety clearance C from conductor to ground shall meet the requirements of electrostatic induction and the requirements of overvoltage, and the C value of 1000 kV distribution equipment is 17.5 m;
(4) Set up simple shielding measures. Set up simple shielding measures beside the equipment with electric field intensity greater than 10 kV/m;
(5) The ground electric field intensity in the area near the series compensation devices is high, so it may be considered to use 2 m-high fence to surround it, to make the area outside the fence at a lower electric field intensity;
(6) Since the threshold of feeling of electrostatic induction in a high electric field is not the same as that of electric shock at low voltage, even if the induced current is only 100–200 μA, as discharge has already occurred when it is not contacted completely, resulting in clear acanthesthesia at the moment of contacting, the electric field intensity in the positions of oil drain valves, tap changer, circuit breaker terminal boxes, etc. shall not be too high, so that the operating personnel and maintenance personnel may access to them;
(7) The induced currents of vehicles in the substation are relatively high, with most exceeding 100 μA. The current outside the conductor's side phase is, in particular, greater than the current between phases. Therefore, considered from the perspective of electrostatic induction, the vehicles shall preferably be driven between phases. Usually, in order to avoid unnecessary interferences and prevent the occurrence of secondary accidents when the handheld equipment and appliances are loaded on and off the vehicles, the vehicles need to be properly grounded when entering the substation. For lift maintenance vehicles, it is necessary to ground the vehicle body and the working platform to keep them at the same potential with the device.

Based on the actual experience over the years, most countries deem that the area with ground electric field intensity lower than 5 kV/m is a non-affected zone and the allowable electric field intensity for distribution equipment is 7.0–10 kV/m. In the distribution equipment with electric field intensity not exceeding the permitted values, electrostatic induction has no pathological influence on human bodies. However, when working in the area with electric field intensity more than 5 kV/m, since there are electrostatic induction and even spark discharge, the worker will have feeling of tingling, prickling, and uneasiness. For this reason, the protective measures are needed. In particular, when maintenance is carried out at height, the protective measures shall be taken all the more, otherwise, the secondary accident of high falling may be caused, leading to a serious consequence. In the design of UHV distribution equipment, various protective measures mentioned above shall be given full attention to minimize the impact of electrostatic induction.

3. Minimize corona radio interference

In UHV distribution equipment, to limit corona radio interference, the use of expanded hollow conductors and multi-bundled conductors as well as the application of large-diameter aluminum tubes and combined aluminum tubes for

conductors are effective ways. For electrical devices, the grading rings or shields with different numbers and shapes are normally provided at the device terminals in order to improve the distribution of electric field and to limit the electric field intensity at the surface of the conductors and the porcelains within a certain values, so that they will basically not produce corona discharge at certain voltage, and meanwhile, the allowable radio interference value shall be specified for the device. According to IEC standard, under 1.1 times the maximum working phase voltage, the radio interference voltage at 1 MHz is not greater than 2500 μV, and at the fine night under 1.1 times the maximum working phase voltage, there shall be no visible corona on the device. China's current allowable value of radio interference for 500 and 750 kV electrical equipment is no more than 500 μV; the allowable radio interference value specified by Canadian Standards Association and the US's AEP standards is not greater than 2000 μV; during the calculation of the integrated interference level of a 1000 kV distribution equipment, the allowable radio interference value for 1000 kV electrical equipment shall be considered as not greater than 2000 μV tentatively.

4. Control the noise

In design of 1000 kV distribution equipment, the reasonable selection of equipment and general layout will be able to limit the noise of the substation. The measures to limit the substation noise are as follows:

(1) The noise sources such as main transformers and reactors shall be arranged reasonably, trying to take advantage of the end wall of the building for the role of sound insulation, so that the noise cannot be directly emitted but diffracted;
(2) The noise sources shall be arranged downwind of the largest wind frequency side;
(3) In case, there are anti-noise requirements for the environment of the area near the substation, the noise sources shall not be arranged close to walls;
(4) The noise level limits shall be specified for 1000 kV equipment, which can be referred to requirements of the voltage grade of 750 kV. The noise level limits for 750 kV equipment: continuous noise level of transformers, reactors and other equipment shall be 80 dB, and the non-continuous noise level of SF_6 circuit breakers shall be 110 dB.

5. Avoid the crossing of 1000 kV outgoing lines

The height of 1000 kV overhead lines from the ground is normally more than 20 m, and the tower height is very high, for example, the height of towers in United States, Russia, and Italy is within 40–60 m, and the vertical double-circuit tower in Japan is up to 108 m, it will be difficult to achieve the design if the crossing of outgoing lines occurs. When using one-and-a-half breaker connection scheme, the relatively effective method is to use three-column-type layout scheme. The outgoing lines in two opposite directions shall be paired into strings according to the actual geological locations, and in case that they cannot be paired into strings, the method of increasing spacing can only be used to meet the needs of actual outgoing

direction. For the GIS scheme, the strings can be paired in a relative flexible manner, but the quantity of tubular busbars also needs to be increased due to the needs for pairing strings. The layout shall be optimized in the design as much as possible.

6. Simple structure and clear layout

The successful experience of the current layout and structural design of 330–750 kV distribution equipment in China shall be fully absorbed, making use of medium-sized single-layer framework, and avoid double-layer frames.

7. Have good transport conditions, convenient for operation and maintenance

To facilitate the maintenance and operation, set phase-to-phase transport roads like 500 kV, enabling the transport and repair machinery can reach the vicinity of the jobsite of every single-phase electrical device along the phase-to-phase road, which is a very convenient way. Because of the larger *C* value of 1000 kV, when the height of equipment support is considered under the premise of ensuring the C value, it can be guaranteed that the lift truck and maintenance vehicle transporting equipment can safely pass through the phases.

25.8.2 Minimum Safety Clearance Values A, B, C, *and* D

The minimum safety clearance of 1000 kV outdoor distribution equipment shall not be less than the values in Table 25.8.

When flexible conductors are used for outdoor distribution equipment, under the different overvoltage conditions with altitude not more than 1000 m, the minimum safety clearances from live parts to ground parts and between live parts of different phases shall be verified in accordance with Table 25.9, and the largest value shall be used.

1. The electrostatic induction electric field intensity 1000 kV outdoor distribution equipment (the space electric field intensity at 1.5 m above the ground) shall not be more than 10 kV/m and a small part of the regions can be allowed to reach 15 kV/m.
2. The following measures can be taken to reduce the electrostatic induction electric field intensity in the design:
   (1) Reduce crossing-over of the same phase busbars and the arrangements in the same phase angles;
   (2) Reduce or avoid adjacent arrangements with the same phase;
   (3) The operating devices including control boxes shall be arranged in the area of lower electric field intensity;
   (4) If necessary, the shielded cable and shielding rings can be added appropriately for the equipment;
   (5) Increase the mounting height of equipment and leads.

Table 25.8 Minimum safety clearances of 1000 kV outdoor distribution equipment (m)

Symbol	Scope of application		Safety clearance
A_1'	Quad-bundled conductor—ground		6.80
	Tubular busbar—ground		
A_1''	Ring—ground		7.50
A_2	Between phases of live conductors	Quad-bundled conductor—quad-bundled conductor	9.20
		Grading ring—grading ring	10.10
		Tubular busbar—tubular busbar	11.30
B_1	(1) Live conductor to barrier (2) Transport equipment outside contour to live conductor (3) Between the vertical crossing conductors not for power outage maintenance at the same time		8.25
B_2	Between the mesh cover fences and the live parts		7.60
C	Live conductor to ground	Single tubular busbar	17.50
		Quad-bundled overhead conductor	19.50
D	(1) The horizontal distance between two parallel circuits not for power outage maintenance at the same time		9.50
	(2) Live conductor to the top of the wall		
	(3) Live conductor to the edge of the building		

Note The data in the table is the safety clearance at the altitude of 1000 m; the data between crossing conductors needs to meet the requirements of both A_2 and B_1; when considering live operations, the radius of human body activities shall be taken as 0.75 m

Table 25.9 Minimum safety clearances under different conditions with flexible conductors being used (m)

Overvoltage category	Lightning overvoltage	Switching overvoltage	Power frequency overvoltage
Conductor to ground part (A_1)	5.00	6.80	4.00
		7.50 (ring–ground)	
Conductor to conductor (A_2)	5.50	9. 20	6.80
		10.10 (ring–ring)	

3. In order not to limit the maintenance operation mode, the busbar and crossover lines set for 1000 kV outdoor distribution equipment shall be able to withstand the weight of human body, and their load values are as follows:

   (1) For single-phase maintenance operations, the total weight of human, tools, and insulated rope ladder acting on the conductor of each phase may be designed as 350 kg and the total weight of human and tools acting on the beam may be considered as concentrated load of 200 kg.

(2) For three-phase power outage maintenance, the total weight of human and tools acting on each phase conductor can be designed as 200 kg, and the total weight of human and tools acting on the beam is also considered as 200 kg.
(3) Nobody is allowed to step on the connecting wires of equipment.

4. Appreciate requirements shall be raised for the construction methods of hanging on wires, and the over traction value shall be limited, so that the over traction force will not become the control conditions for structural framework strength.
5. 1000 kV outdoor open-type distribution equipment shall be provided with phase-to-phase transport routes, and according to the requirements of electrical connection, equipment layout, and safety distance, the phase-to-phase distance, height of equipment support, and road turning radius shall be determined, in order to meet the requirements of transport vehicles and maintenance machinery driving along the routes with the electrical equipment energized.

25.8.3 Main Features of UHV Distribution Equipment

Due to high voltage and large capacity of 1000 kV distribution equipment, its main features are as follows:

(1) Internal overvoltage plays the control role in the insulation coordination;
(2) Internal overvoltage and electrostatic induction voltage have a significant impact on determination of the safety air clearance distance;
(3) The protective measures against harms to human body due to electrostatic induction must be considered;
(4) The requirements of the allowable standards of corona and radio interference shall be satisfied;
(5) Expanded diameter hollow conductors, multi-bundled conductors, and large-diameter or modular tubes shall be used;
(6) The issue of land conservation becomes more prominent;
(7) The measures to facilitate the operation and maintenance such as mechanization shall be considered;
(8) The noise shall be limited.

25.8.4 Size Determination of 1000 kV Distribution Equipment

Currently, the major manufacturers of the 1100 kV GIS are Henan Pinggao Electric Co., Ltd. (hereinafter referred to as Pinggao), New Northeast Electric Group High

Voltage Switchgear Co., Ltd. (hereinafter referred to as NHVS) and Xi'an XD Switchgear Electric Co., Ltd. (hereinafter referred to as Xi'an Switchgear). The circuit breaker manufactured by Pinggao adopts the hydraulic operating mechanism with double breaks connected in series and is configured in the same housing with the closing resistor. Such circuit breaker adopts the straight-line layout with its center line overlapped with the center lines of other equipment in a string. The disconnector manufactured by Pinggao adopts the vertical break and electric spring operating mechanism and may be installed with damping resistor; besides, whether to install switching resistor on the disconnector or not will have no influence on the layout of GIS. The busbar disconnector and grounding switch are provided with separate air chambers. Each complete string of the GIS manufactured by Pinggao is 74.5 m in length. The scheme has been applied at the Southeast Shanxi Substation and Huainan Substation. The circuit breaker manufactured by NHVS has two types: double breaks connected in series or four breaks connected in series. In the two types, the circuit breaker with double breaks is configured in the same housing with the closing resistor and is of straight-line layout, with the key components and parts imported from other countries; the circuit breaker with four breaks, configured in a housing independent from the housing of the closing resistor, is of π-type layout and is completely independently produced. The disconnector manufactured by NHVS adopts the vertical break and electric spring operating mechanism and may be installed with damping resistor. The circuit breaker manufactured by Xi'an Switchgear, adopting the hydraulic operating mechanism with four beaks connected in series, is configured in a housing independent from the housing of the closing resistor and is of π-type layout. The disconnector manufactured by Xi'an Switchgear has two types: with and without damping resistor. The GIS disconnectors manufactured by Xi'an Switchgear as applied at Wannan Substation are not installed with switching resistors, but the longitudinal dimension of the body is large due to the limitation by the structure of connection between the disconnectors and CTs. For the GIS where the disconnector is installed with switching resistor, Xi'an Switchgear has improved the GIS's structural form. In the improved GIS, the disconnector is changed to the vertical structure from the horizontal structure and, as a result, the structure of connection with CT may be changed to 0° connection from 90° connection. In such case, the longitudinal dimension may be reduced while the transverse dimension is increased to some extent. Moreover, Xi'an Switchgear has also carried out research on the optimization of GIS where the disconnector is not installed with switching resistor, and the optimization scheme is similar to that for the GIS where the disconnector is installed with switching resistor (see Table 25.10).

(1) Determination of transverse dimension of distribution equipment

The transverse dimension of the distribution equipment is determined by two factors. One factor is the width and number of bays of the distribution equipment, and the other is the length and number of circuit breakers in the GIS subject to straight-line layout, which finally determines the overall length of the GIS. The

Table 25.10 Overall dimension of 1500 MVA transformer

	Pinggao	Xi'an switchgear (before improvement)	Xi'an switchgear (after improvement)	NHVS Double-break type	NHVS Four-break type
Phase-to-phase spacing of circuit breaker (m)	2.5	5.5	3.75	2.5	3.7
Phase-to-phase spacing of busbar (m)	1.6	1.335	1.335	1.6	1.6
Spacing from side-phase circuit breaker to side-phase busbar outer contour (m)	16.4	24.0	19.3	16.4	21.3
Complete string length (m)	74.5	51	64.5	72	69.4
Circuit breaker structure	Straight-line layout	π-type layout	π-type layout	Straight-line layout	π-type layout

width and number of bays determine the overall length of the outgoing line framework. The bigger one of the two lengths is a control condition for the field of the complete distribution equipment.

(2) Determination of longitudinal dimensions of distribution equipment

In terms of the layout, the optimization of the longitudinal dimensions of the GIS focuses on the following two aspects: ① optimization of the longitudinal dimension at the incoming line side, i.e., optimization of the distance from incoming line bushing to equipment body; ② optimization of the longitudinal dimension at the outgoing line side, i.e., optimization of the distance from outgoing line bushing to equipment body. The longitudinal dimension of the equipment body is determined by the manufacturer's structural design.

(3) Typical dimension of distribution equipment

Based on the optimization mentioned above, the framework and equipment spacing under the single-column layout scheme for the 1000 kV circuit breakers are shown in Table 25.11.

The framework and equipment spacing under the double-column layout scheme for the 1000 kV circuit breakers are shown in Table 25.12.

The longitudinal dimensions of the 1000 kV distribution equipment are shown in Table 25.13.

Table 25.11 List of framework and equipment spacing under the single-column layout scheme for 1000 kV circuit breakers

Framework form	Framework width (m)	Phase-to-phase central spacing (m)	Phase-to-ground central spacing (m)	Conductor attachment point height (m)
Steel pipe lattice framework	Incoming line 49	13.2	11.3	41
	Outgoing line 51	14.2	11.3	
Steel pipe herringbone column framework	Incoming line 47	13.2	10.3	41
	Outgoing line 49	14.2	10.3	

Note
(1) The phase-to-phase spacing is taken as 14.2 m as controlled by the size of the arrester grading ring and 13.2 m as controlled by the size of the capacitor voltage transformer grading ring
(2) As controlled by the section size of the framework column, the phase-to-ground spacing is taken as 11.3 m when the steel pipe lattice framework is adopted and 10.3 m when the steel pipe herringbone column framework is adopted

Table 25.12 List of framework and equipment spacing under the double-column layout scheme for 1000 kV circuit breakers

Framework form	Framework width (m)	Phase-to-phase central spacing (m)	Phase-to-ground central spacing (m)	Conductor attachment point height (m)
Portal framework (outgoing line)	51	14.2	11.3	41
π-type framework (incoming line)	Column spacing 14.4, beam width 26.4	13.2	–	32

25.9 Connection and Layout of Shunt Compensation Device

The reactive power and voltage control of UHV power grid is much more difficult than that of the 500 kV power grid. Because the charging power of UHV transmission line is about 4–5 times that of the 500 kV lines, the reactive power has great fluctuations when transmission power changes, and therefore, the reactive power and voltage control must be performed by adjusting the reactive power compensation device, thereby reducing the reactive transmission of the transmission lines, reducing network losses and ensuring the voltage operating at a reasonable level. The voltage and reactive power control measures of the UHV system mainly consist of adjusting transformer taps and installing high-voltage reactors,

Table 25.13 List of longitudinal dimensions of 1000 kV distribution equipment

S/N	Item	Layout dimension (m)
1[a]	Longitudinal dimension between incoming and outgoing line bushings in GIS	49
2[a]	Longitudinal dimension between incoming and outgoing line frameworks	54
3	Longitudinal dimension from main transformer transportation road to capacitor voltage transformer	8
4	Longitudinal dimension from capacitor voltage transformer to incoming line framework	5
5	Longitudinal dimension from outgoing line framework to arrester	5
6	Longitudinal dimension from arrester to the road before 1000 kV shunt reactor	4
7	Longitudinal dimension from the road before 1000 kV shunt reactor to capacitor voltage transformer	4.5
8	Longitudinal dimension from capacitor voltage transformer to 1000 kV shunt reactor bushing	4
9	Longitudinal dimension from 1000 kV shunt reactor bushing to transportation road	22.25/20.75

Note [a]The spacing between the incoming and outgoing line bushings shall be in accordance with the dimension listed when the circuit breaker adopts the single-column layout, and shall be determined according to the equipment conditions when the circuit breaker adopts the double-column layout but not according to the dimension listed

series compensation devices, low-voltage capacitor banks, low-voltage reactor banks, etc.

To limit 1000 kV power frequency overvoltage, reducing the voltage level of light load lines, it needs to install a certain proportion of high-voltage reactors for 1000 kV transmission lines. However, when the line overloaded, if the compensation is too high, the high-voltage reactor has an adversely affect on the balance of reactive power, as well as causes the decrease of voltage level. The main contents of reactive power and voltage control of UHV power grid are as follows: rational allocation of line high-voltage reactors and low-voltage reactive power compensation devices, maintaining balance of reactive power by switching over low-voltage reactive power compensation devices when the transmission power of line changes, as well as meeting the requirements of the operating voltage. The principles to be followed in configuration of reactive power compensation are as follows [6]:

(1) The low-voltage reactive power compensation device is used for balancing the reactive power on the transmission lines at the time when it transfers different active power, so that the terminal voltage of UHV transmission lines keeps within a reasonable range. Reactive configuration shall satisfy the principle of hierarchical partitioning balance, and the UHV busbar voltage shall be controlled between 1000 and 1100 kV.

(2) UHV transmission line has a large charging power and the voltage of transmission line is very high during no-load, so the low-voltage reactive power compensation configuration shall be able to meet the requirements of switching no-load lines, that is to ensure that the voltage at both ends of the line is lower than 1100 kV.
(3) The grouping capacity of low-voltage reactive power compensation device shall meet the requirements of voltage fluctuation, and the voltage fluctuations at the medium-voltage side caused by switching shall not exceed 2.5% of the rated voltage.
(4) The low-voltage reactive power compensation capacity shall not exceed the third winding capacity.
(5) The configuration of the low-voltage reactive power compensation device shall be combined with the position adjustment of transformer taps, to ensure that the busbar voltage will not exceed the limits when the reactive power balance requirements are satisfied.

25.9.1 Classification of Shunt Compensation Devices

UHV compensation devices can be divided into two categories: series compensation device and shunt compensation device. The series compensation devices are rarely in use and currently applied only in UHV expansion project. Shunt compensation devices can be classified into three categories, i.e., shunt capacitor compensation device, shunt reactors compensation device and UHV shunt reactors, of which the shunt capacitor compensation devices and the shunt reactors compensation devices are switched by using circuit breakers, while the UHV shunt reactor is connected directly to the line. Classification and functions of various types of compensation devices are shown in Table 25.14.

25.9.2 Grouping Capacity of Shunt Compensation Devices

Currently, the voltage of the busbar installed at low-voltage side reactive power compensation device of 500 kV substations in China is mainly at 35 and 66 kV. The maximum grouping compensation capacity of shunt capacitor banks is 60–80 Mvar for each group, and the capacity of single capacitor is 334 or 500 kVar. Neutral non-grounded double-star connection mode is adopted in most of the capacitor banks, and there is a small number of delta connection too. The series reactor in shunt capacitor banks is dry-type air-core reactor. Under normal conditions, for inhibition of 5 times and more harmonic waves, series reactance rate of 5–6% shall be selected, for inhibition of 3 times harmonic waves, series reactance rate

Table 25.14 Classification and functions of compensation devices

Type		Function
Series capacitor compensation device		Enhancing system stability and improving transmission capacity
Shunt compensation device	Shunt capacitor compensation device	Providing the grid with capacitive reactive power that can be adjusted in steps, to compensate the excessive inductive reactive power and to reduce the power loss of the grid and improve the voltage
	Shunt reactor compensation device	Providing the grid with inductive reactive power that is adjustable in steps, to compensate the residual capacitive reactive power of the grid and to ensure the voltage keeping within the allowable range
	UHV shunt reactors	Connected to UHV lines in parallel for compensating the charging power of transmission lines, reducing the power frequency overvoltage level of the system, and reducing the secondary arc current, to facilitate system synchronization, and to improve the reliability of power transmission and other functions

of 12–13% shall be selected. Dry-type air-core reactor shall be selected as the shunt reactor at priority, and the maximum single capacity shall be 20 Mvar.

The grouping capacity of low-voltage reactive power compensation device of UHV substation may affect the voltage fluctuations after switching over. Referring to the provisions of DL 5014-92 *Technical Regulation for Designing of Reactive Power Compensation Devices for* 330–500 kV *Substation* [7], the grouping capacity of shunt capacitor banks and low-voltage shunt reactor banks shall meet the following requirements:

(1) When the grouping devices are switching in different combination methods, it must not cause high harmonic resonance and hazardous harmonics enlargement;
(2) The change in the value of busbar voltage at transformer medium-voltage side caused by switching a group of compensation devices shall not be more than 2.5% of its rated voltage;
(3) It shall be consistent with the capacity of the circuit breaker switching capacitor banks;
(4) It shall not exceed the blasting capacity of a single capacitor and the explosion-resistant energy of a fuse.

To simplify the connection and reduce the investment, the grouping capacity shall be increased and the number of groups shall be reduced. The UHV substation will temporarily adopt the relevant provisions of reactive power compensation devices of 500 kV substations, grouping capacity of low-voltage capacitor shall be considered as 240 Mvar per single group, with rated voltage of 120 kV; low-voltage capacity reactors shall be considered as 240 Mvar per single group, with rated voltage of 105 kV.

25.9.3 Shunt Compensation Devices

25.9.3.1 Selection of Shunt Capacitor

1. Selection of rated voltage of shunt capacitor

In the UHV network, it is required that the maximum operating voltage of shunt capacitors is 126 kV, while the nominal voltage is 110 kV, with a big difference between these two values, so an appropriate margin shall be kept in selection of the rated voltage of the shunt capacitors. If a capacitor with low rated voltage, it will cause a high voltage on the capacitor dielectric, and then the performance and life of the capacitors will be adversely affected. While if you choose a capacitor with too high rated voltage, which is with too large safety margin, it will cause the reduced output capacity of capacitor bank. Thus, in order to meet the requirements of such output capacity, the installed capacity must be very high, which will increase the investment.

For the selection of rated voltage of shunt capacitors in China, there are some differences among the standards. The main difference lies in the overvoltage multiplier of the capacitor over the long run. Considering both technical and economic aspects comprehensively, the rated voltage of shunt capacitor banks recommended for UHV project over the long run shall be designed in accordance with that the long-term operating voltage is 1.05 times the rated voltage of the capacitor. The maximum operating voltage of the system is 126 kV, and the long-term operating voltage is taken as 120 kV. This will not only ensure the long-term stable operation of the capacitor in 126 kV, but also reduce the investment.

2. Selection of rated capacity of shunt capacitors

It shall be noted that China's current standard does not specify the selected standard value of the rated voltage and the rated capacity of a single capacitor; in the capacitor banks at the levels of 10 and 35 kV, the rated voltages, rated capacities, and the number of capacitor units in series and in parallel selected by manufacturers are comparatively consistent, while in the capacitor bank at the level of 66 kV, the differences exist in these values selected by manufacturers, which is mainly due to the capacity of the capacitor bank becomes higher and higher and the maximum operating voltages of the third winding of the main transformer are different depending on substations; in order to ensure the capacitor banks can adequately output the reactive power, the calculations and values selected by manufacturers are different. Therefore, in the UHV projects, each manufacturer shall be required to provide the conventional and mature products of capacitors, and try to select the products used in the capacitor banks at levels of 10, 35, and 66 kV.

25.9.3.2 Selection of Shunt Reactors

The rated voltage of 110 kV shunt reactors is selected as 105 kV, the maximum operating voltage as 115 kV, and the rated capacity as 240 Mvar. Currently, there are two types of 110 kV shunt reactors: one type is of oil-immersed, single phase, and self-cooled; the other is dry-type air-cored reactor. The manufacturing experience in oil-immersed reactors is richer, having higher technical level, and there is no problem in production conditions and test equipment. However, on the current level of China's manufacturing process, some problems such as oil seepage, oil leakage, possible localized overheating, and higher noise inevitably exist in the oil-immersed reactor, so it will need larger workload of maintenance. Dry-type air-cored reactor is complied with the development direction of oil-free substation. The dry-type air-cored reactor is featured with high mechanical strength, high resistance to short-circuit capacity, less maintenance, and no strict fire safety measures required, but due to its larger capacity, thus the absolute value of the loss is higher, resulting in a higher heat source for the reactor, of which the heat balance problems need to be solved. Additionally, the dry-type air-cored reactor has the phenomena such as the presence of dendritic discharge and the cracking of resin encapsulation on the surface of reactor. Because many dry-type shunt reactors are used in engineering with good operation condition, and for the devices at voltage level of 110 kV, the adoption of dual-coil in series per phase does not have greater difficulty in manufacturing the devices, and therefore, the dry-type reactor is recommend for UHV projects.

25.9.4 Layout of Shunt Compensation Devices

25.9.4.1 Layout of Shunt Capacitors

There are three types of layouts for capacitor device, i.e., outdoor, semi-open, and indoor. In case of the capacitor installed in the open air outside the house, minimum civil work is required; the construction duration can be shortened; the installation costs can be saved; particularly the ventilation and heat dissipation conditions are very good, and wind and rain can wash the capacitor naturally. The main disadvantage of this layout is the large impact of weather and environmental pollution, but with the improvement of product quality of capacitors, the annual damage rate of capacitor banks installed in the open air is declined significantly. Outdoor layout is recommended for capacitor bank of UHV projects.

25.9.4.2 Layout of Shunt Reactors

The low-voltage air-core shunt reactors used in 1000 kV substations are featured by its higher single-phase capacity, heavier single-phase weight, and larger volume. In

order to reduce the floor space, it shall be designed with medium-sized layout. In addition, to further reduce the floor space and facilitate leading lines for reactors, three-phase reactors shall be laid out in triangle arrangement.

25.10 Connection and Layout of Station-Service Power

25.10.1 Main Design Principles

For the design principles of station-service power of UHV substation, make reference to DL/T 5155-2002 *Technical Code for Designing AC Station Service of* 220–500 kV *Substation* [8], in which the design requirements for station power of 500 kV substations are as follows: "The number of station-service operating transformer units connected at the LV side of the main transformer shall not be less than two, and a dedicated standby transformer shall be set up with a reliable power supply outside the station."

When 2 groups of main transformers are put in service for Phase I UHV substation, the station-service operating power supply shall be connected from the low-voltage busbar side of the main transformer (110 kV) and meanwhile a circuit of standby power shall be connected from outside the station. When only one group of transformer was put in service for the Phase I substation, it needs to be connected to two circuits of reliable standby power from outside the station, in order to ensure the reliability of the station-service power supply of the substation.

25.10.2 Connection of Station-Service Power

The connection of the 380 V station-service power system of UHV substation shall be made with single-busbar segment, the LV side of two station-service operating transformers, through automatic air switch taps is connected to I, II section busbars, and the LV side of standby station transformer can be connected as needed to the busbar I or busbar II. During normal operation, these two sections of busbar are operated alternatively, that is, when any station-service operating transformer fails or quits running, standby station transformer will put in the low-voltage busbar which is connected from the faulty operating transformer.

25.10.3 Station-Service Equipment and Layout

Low-voltage station transformer is arranged outdoor in the center of the station area, close to the 380 V station-service central distribution room. Station

transformers are separated from each other by a firewall. The cable entry is used at the HV side of station transformer, and the busbar bridge is used between the low-voltage side outlet and the 380 V central distribution panel. Each local protection room shall be installed with low-voltage sub-panels.

The low-voltage drawout-type switchgear cabinet may be used as low-voltage distribution panel. Low-voltage electrical equipment may be selected in accordance with short-circuit current level at LV side of station transformer.

25.10.4 Lighting and Maintenance

25.10.4.1 Lighting Power System

Lighting power systems shall be determined based on the demands of operation and the importance of illumination when dealing with incidents, and its power system is divided into AC power and DC power. The AC power is from the AC power distribution panel or sub-panel of station-service power and the main function is for normal lighting; the DC power source is powered by batteries, and mainly for emergency lighting in important places such as main control and communication building, protection room, and site of main transformer.

25.10.4.2 Lighting Mode

The fluorescent lights shall mainly be used for lighting inside the buildings; the efficient metal halide floodlights shall be used for outdoor distribution equipment, and the garden lights shall be used for road lighting.

25.10.4.3 Maintenance System

According to the needs of different equipment maintenances, the maintenance room and spare parts warehouse shall be set. Meanwhile, the maintenance boxes shall be installed in the main transformer area and the outdoor distribution equipment area.

25.11 General Plan and Vertical Layout

25.11.1 General Layout Plan

The general plane of UHV substation includes a variety of equipment areas, such as the areas for 1000 and 500 kV distribution equipment, 1000 kV main transformer,

1000 kV shunt reactors, and low-voltage reactive compensation devices, besides it is provided with production and living buildings (structures), such as main control and communication building, electrical maintenance room, and multipurpose building, much more complex than the substations at voltage grade of 500 kV and below. The typical general layout plan of the 1000 kV substation is as shown in Fig. 25.9. First, 1000 kV high-voltage distribution equipment and 1000 kV main transformer and the shunt reactors have a series of characteristics, such as high-voltage level, large capacity, complex structure, large sizes, and large floor space; the corona radio interference, noise and electrostatic induction level produced by these equipment are comparatively higher, and large buildings such as maintenance rooms and spare parts rooms are normally required for maintenance of main electrical equipment. Secondly, in order to compensate the reactive power losses of 1000 kV main transformer with large capacity and meet the requirements of the power system voltage quality, large capacity reactive power compensation device must be set up. These factors greatly increased the complexity of 1000 kV substation general layout. In addition, the operation and maintenance personnel required for 1000 kV substation are much more than the ones for 500 kV substation.

All of the above production and living facilities compose a whole of 1000 kV substation. Normally, the layout design of 1000 kV substation buildings (structures) shall be in accordance with the following requirements:

(1) Scientific and reasonable function zoning, smooth and concise production process flow, and easy operation and management;
(2) Adapted to local conditions, making full use of the space in the substation, and flexibly arranging buildings (structures);
(3) Compaction of the floor space at the substation front area;
(4) Combined with the station site optimization and water-soil conservation schemes to protect the ecological environment and promote the harmonious development between man and nature;
(5) Generally, the main control and communication building shall be arranged in the main entrance of the substation, with good visual effects, far away from noise sources such as high-voltage reactors and the main transformer as possible, to create a comfortable operating environment for the operating personnel. Generally, the main control and communication building shall be combined with multipurpose building so that they can be arranged as a main control and multipurpose building, to improve the utilization rate of buildings. They may also be built separately based on the operating needs, or the multipurpose building may be set in other areas outside the walls;
(6) The small protection chambers at all levels shall be arranged in a central location for equipment protection to ensure that the length of the secondary cable is the shortest;
(7) The fire fighting houses including foam sprinkler rooms shall be arranged in the place close to the corresponding equipment, to ensure that the distance of foam pipe is the shortest and that the response time of the firefighting is the fastest;

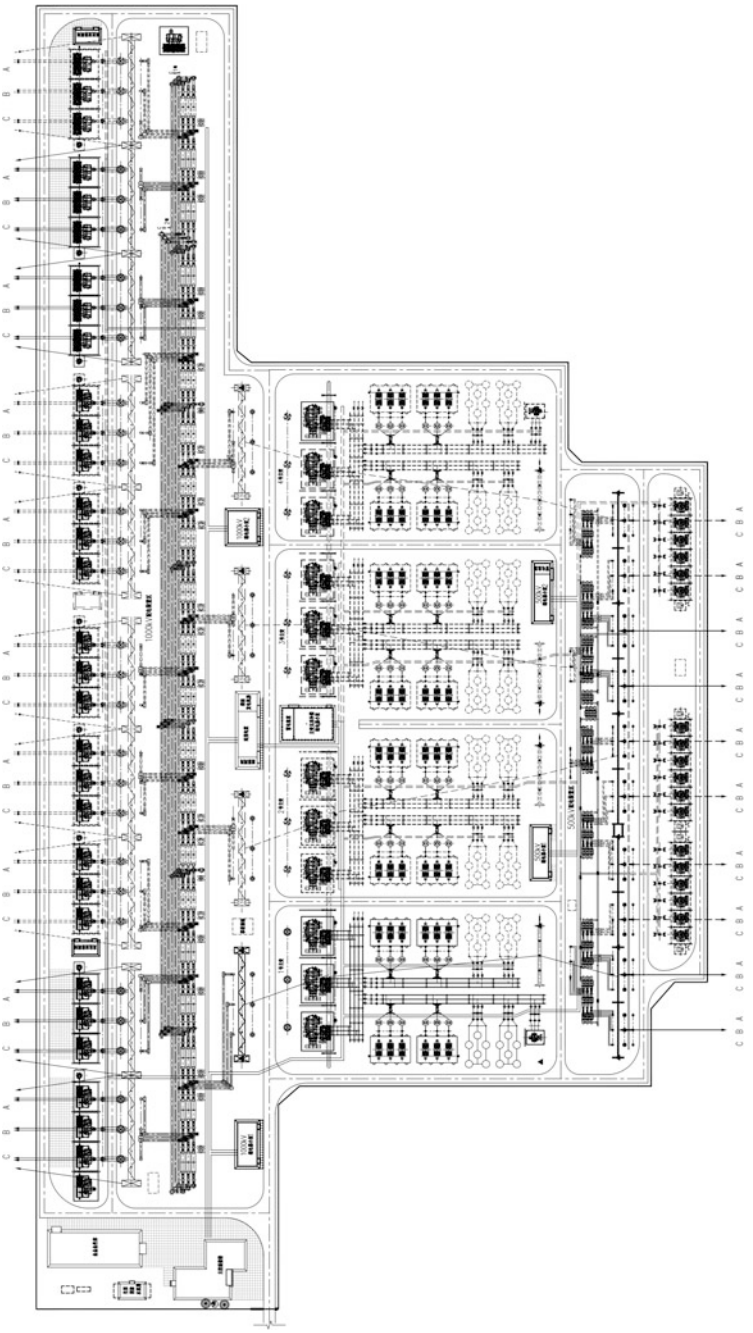

Fig. 25.9 General layout plan

(8) The station-service power room shall be arranged in the center of the total substation, so that optimal service efficiency can be achieved;
(9) Because of the large sizes of spare parts room, it shall be arranged in a relatively concealed location under the premise of meeting the transport passage requirements.

25.11.2 Vertical Layout

Vertical layout design means that the planning and design of ground elevations of the sites in the vertical direction is carried out by making use of natural terrain, according to the comprehensive consideration of technical requirements, considering transport and earthworks balance, etc. The main vertical design principles of substation are as follows:

(1) The site shall meet the requirements of flood control; the design elevation must not be lower than the flood level at frequency of 1%, and appropriate flood protection measures shall be taken when these requirements cannot be satisfied;
(2) If the site is not impacted by the high water level, the site elevation shall be designed in the principle of balancing the total amount of earthworks and backfilling inside and outside the station;
(3) In case that the natural terrain of the construction site has a larger slope or when the substation is to be built on complex mountainous terrain, the feasibility of using the step arrangement shall be demonstrated.

Since the 1000 kV substation project site covers a large area, the determination of design elevation has a direct influence to the amount of earthwork and engineering method of foundation, and thus the progress, investment, and quality of the substation construction may be affected, so the vertical design is very critical. For the substation constructed on the mountainous area, generally it will not be affected by the flood level and waterlogging water level, but because of big ups and downs of the site topography, there will be not only a tremendous amount of earthwork and backfilling, but also the technical problems of high slope and high retaining wall and so on. For the substation built in such sites, a better vertical layout pattern conforming to the engineering terrain shall be selected by means of investigation.

When flat slope design is used for the site, the design slope shall be determined based on equipment layout, soil conditions, drainage patterns and road longitudinal slope, normally considered as 0.5–2%; while it may be less than 0.5% when with reliable drainage measures, the local maximum gradient should not be more than 6%, and the anti-erosion measures shall be provided if necessary. In case of the stepped arrangement, in addition to the close relationship with the terrain, the height of the steps must also take full account of the process layout, equipment, transportation, geological stability, and convenient construction and other factors.

It shall be particularly noted that, due to the large area occupied by 1000 kV substation, the original river system in that area will be inevitably changed. After the completion of the substation in the mountainous area, it will often form into the main body intercepting the flood together with the mountains where it is located, so the vertical design shall be done by working closely with other disciplines such as drainage outside the station, in order to achieve the best economic indexes.

25.11.3 Roads of Substation

The roads shall be planned and designed based on the requirements of transport, maintenance, and fire control, combined with the general layout, vertical layout, natural conditions outside the station and local development plans and other factors.

The plane curve radius and longitudinal slope of the roads accessing to the station shall meet the requirements of transporting large equipment within the station. The roads accessing to 1000 kV substation shall be of the highway type, with road width of 6 m, and the turning radius meets the transport requirements of the main transformer, normally considered as not less than 25 m. The longitudinal slope of road shall be controlled as less than 8%. If the road accessing to the station is long, the method of setting passing bays can be used to reduce the indexes of occupied land area. The access road in front of the gate of the station area shall be set as straight section of road, and the length of straight section shall be determined according to the terrain conditions.

In addition to meeting the requirements of operation, maintenance, and equipment installation, the layout of station roads shall also meet the relevant provisions of safety, fire protection, and land conservation. The trunk roads of substation shall be arranged in rings to meet the requirements of lifting equipment, maintenance, etc. The patrol roads in the substation shall be set according to the needs of operation and operational inspection, and the inspection route shall be determined in combination with the layout of cable channels on ground.

The in-station road for transporting main transformer shall have a width of 5.5 m and turning radius of 25 m, the transport road for high-voltage reactors shall have a width of 4.5 m and turning radius of 18 m, and all the in-station roads shall adopt asphalt road pavement or concrete pavement of highway type.

25.12 Main Buildings (Structures)

25.12.1 Buildings of Substation

According to the characteristics of technological operation, the buildings of 1000 kV substation mainly consist of production buildings such as main control

and communication building, 1000 kV relay room, main transformer and reactive power relay room, 500 kV relay room and station-service power room, and auxiliary buildings such as spare parts warehouse and multipurpose building, as well as dependent buildings such as fire pump house and boiler house. Various buildings shall be combined in functions based on the general layout, and the joint architect shall be adopted as far as possible.

The building design follows the same concept of conventional substation. The following is a detail introduction to the key design points of buildings related to the voltage level of 1000 kV substation.

(1) Main control and communication building and multipurpose building

Rooms of main control building of the 1000 kV substation are configured based on the design principles of attended operation substation. Rooms of main control and communication building include production rooms (e.g., main control room, relay rooms, and communication machine rooms), auxiliary rooms (e.g., maintenance room and pump house) and subsidiary rooms (e.g., rest rooms).

Building can be single-floor, two-floor, or three-floor building depending on the scale and size of site. Main control and communication building is better to be arranged in the section convenient for perambulation inspection and observation of outdoor equipment by operators, minimization of cable length, avoiding the impact of noise, and forming an excellent opposite scenery with the access road. Main control room shall have good orientation. Main control room in the heating zone should face the sunny side, which in hot area should face prevailing wind direction in summer.

For substation located in the mountainous area with large quantity of excavation and backfilling, the design of main control and communication building and multipurpose building should be of vertical arrangement combined with the site conditions and take local conditions into account so that optimized use functions and architectural effect can be realized and excellent economic benefit can be obtained. Figures 25.10 and 25.11 show the design idea of plane vertical arrangement of the main control and communication building and substation front area of a certain mountainous area substation.

(2) Spare parts warehouse

For 1000 kV substation, it is generally considered that all the spare equipment, spare parts, and maintenance machines and tools are put within the substation. According to the configuration of Southeast Shanxi Substation, all the spare equipment, spare parts, and maintenance machines and tools are placed in the spare parts warehouse except for spare coils used for 110 kV shunt reactor.

The largest object in the warehouse is 1000 kV bushing (about 15 m×2 m×3 m), which is horizontally placed. For dimension of spare parts warehouse, main consideration is the requirement for loading and unloading of 1000 kV bushing so that the bushing carrying vehicle can enter the warehouse and 2 sets of 10 t bridge crane in the warehouse can be used for loading and unloading. Other equipment can be carried into

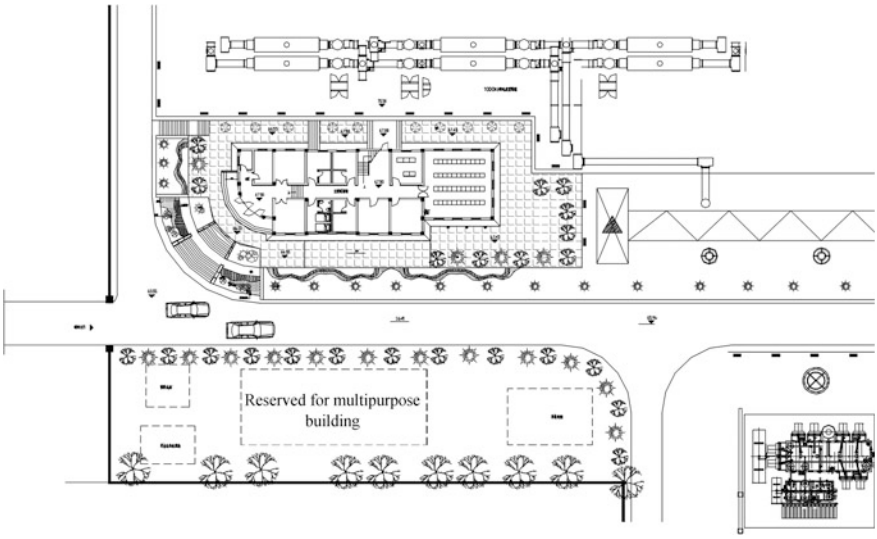

Fig. 25.10 Planar graph of substation front area

Fig. 25.11 Effect drawing of main control building

the warehouse with vehicles for the convenience of loading and unloading. In addition, in case no separate garage is designed, placement and storage of large size crane (about 7 m long × 4 m wide × 4 m high) and tools will be considered.

Size and dimension of building should conform to the quantity and dimension of all spare parts and meanwhile storage and taking of spare equipment should be considered. According to general layout, one spare parts warehouse or several warehouses can be provided depending on the dimension of spare parts and the requirement of transportation and lifting of spare parts. Prior to design, all the spare equipment, spare parts, and maintenance machines and tools to be placed and stored in the substation should be verified and balanced according to the technological requirement, and the size of building should be determined combined with corresponding general layout.

Figure 25.12 shows the plane layout and in-place transport plan of the 1000 kV spare parts warehouse of a certain UHV substation. The spare parts warehouse is arranged separately in the southeast corner of the substation, side by side with the boiler house. Since the site is small in size and the length of bushing-carrying vehicle is over 20 m, which has to adjust to the direction when entering the warehouse, the spare parts warehouse is arranged to the east-most side so that the vehicle can enter the warehouse. With equipment, machines and tools to be placed in the warehouse, transportation corridor, maintenance access, and lifting height taking into account, the spare parts warehouse of the project is determined as 36 m long and 15 m wide, elevation of the roof lab is determined as 11.40 m, and the elevation of the top of the angle-table under the crane beam is determined as 7.80 m.

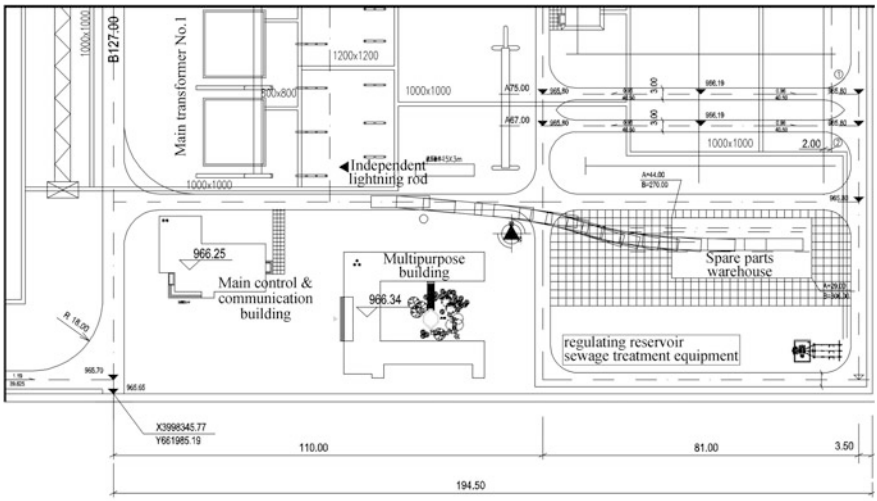

Fig. 25.12 Southeast Shanxi 1000 kV spare parts warehouse layout and in-place transport plan

25.12.2 UHV Substation Framework

UHV substation framework is the important structure of UHV substation, of which the withstand loads, the height and span are significantly increased as compared with those of other voltage level, and featured by high height, large span, and heavy load. The research on structure selection, economic root span, load combination, wind load, seismic action, temperature impact, etc. of 1000 kV substation framework is an important task in the design of UHV substation.

1. Structural forms of UHV framework around the world

In America, the former Soviet Union, Japan, Italy, the research on UHV power transformation and transmission technologies began in the end of 60' and early 70' in the last century and constructed some UHVAC power transmission projects and test projects. UHV substation framework in countries outside China all uses lattice structure, of which Japan uses angle steel structure while other countries use steel pipe structure.

China began the feasibility study of UHV power transformation and transmission projects in 2005. The three substations of UHV demonstration project (Southeast Shanxi 1000 kV substation, Nanyang 1000 kV switch station, Jingmen 1000 kV substation) were put into operation in July 2009. The 1000 kV distribution equipment of the demonstration project used HGIS or GIS scheme, respectively. The designer made large amount of research work for 1000 kV substation framework. For distribution equipment, lattice steel pipe structure was selected (see Fig. 25.13).

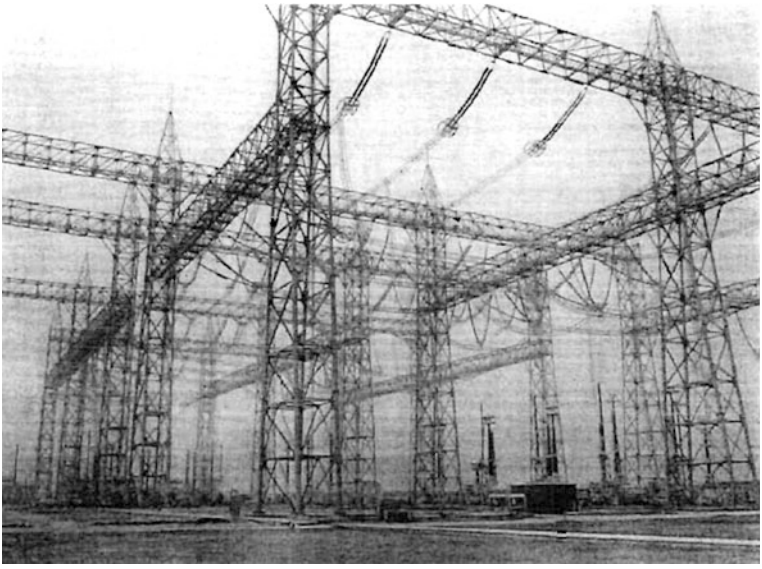

Fig. 25.13 1000 kV lattice framework of Nanyang switch station

In the subsequent projects such as the Project to Transmit Power from Anhui to Eastern China, the designer borrowed the successful experiences of substation framework developed around the world, especially the research results of test and demonstrative projects, and developed the framework type meeting the requirement of project construction combined with the practical conditions of the project through rational type selection and elaborate design. The design personnel optimized the sectional dimension and node structures of the lattice steel pipe framework, minimized the steel quantity used in the framework, and reduced the dimension of the site used for 1000 kV distribution equipment. In the North Zhejiang 1000 kV substation, herringbone column structure was selected for 1000 kV framework after demonstration and real model test. Some designers also carried research on various subjects for steel pipe concrete frame structure and aluminum alloy materials (see Figs. 25.14 and 25.15).

2. Determination of framework dimension

(1) The width of framework

The width of framework is determined by the bay width of the electrical specialty. Generally speaking, the width of incoming (outgoing) line portal framework is equal to bay width. To determine electrical bay width, consideration is required from two aspects: the first consideration is about the electrical distance of the overhead flexible conductors on the top layer of the bay. First, when the flexible conductors in the middle of the span have maximum inter-phase swing, phase conductors must not discharge. Secondly, when the side-phase jumpers have maximum swing within the incoming (outgoing) line portal framework, there must

Fig. 25.14 1000 kV lattice framework of Southeast Shanxi substation

Fig. 25.15 1000 kV herringbone column framework of North Zhejiang substation

be no discharge to civil framework column. The other consideration is the electrical equipment to be installed on the ground in the circuit. Firstly, phase-to-phase distance of electrical equipment should meet the requirement of minimum phase-to-phase electrical distance and the electrical distance when equipment is transported between phases. Secondly, the side-phase electrical equipment arranged below and near the portal framework must not discharge to framework columns.

For distribution equipment design, the maintenance distance of side-phase electrical equipment between two adjacent circuits must be guaranteed. Since the distance between center lines of two sets of side-phase electrical equipment in adjacent circuits of 1000 kV distribution equipment may reach 20 m and above, this condition does not have control action, and hence it is generally not considered in the determination of the bay width of 1000 kV distribution equipment. In addition, structural width of civil framework columns that can bear the upper part load should be considered in the calculation of phase-to-ground distance.

In UHV demonstration project, phase-to-phase distance of conductors was taken as 15 m and phase-to-ground distance was taken as 12 m (for 4 m wide of lattice framework column). Therefore, the width of 1000 kV framework was taken as 54 m. Through optimization of safe electrical distance and the framework column width, the width of 1000 kV framework has been designed as 51 m at present. When steel pipe herringbone columns are used or when the section of framework columns is re-optimized, the width of framework can be further reduced.

(2) The height of framework

When 1000 kV bushing are placed below the framework, since 1000 kV bushing is the longest installation unit in GIS equipment or high-voltage shunt reactor, the height of framework is mainly determined by the non-live lifting height of GIS bushing and high-voltage shunt reactor bushing. The length of 1000 kV GIS bushing is generally about 15 m and its outline dimension is as shown in Fig. 25.16. For calculation of the lifting height of bushing, the several factors such

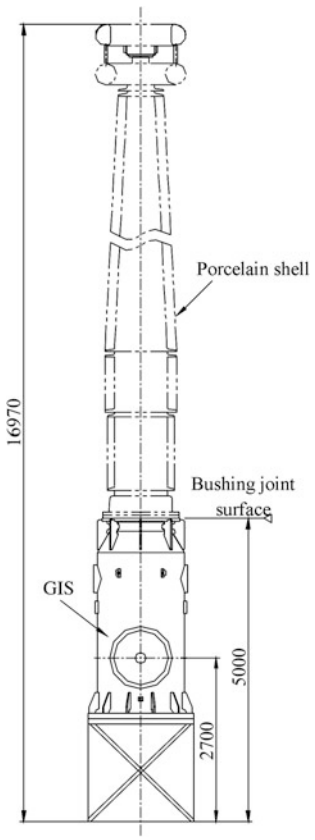

Fig. 25.16 Outline of bushing (mm)

as the height of GIS foundation above the ground, height of elevated base of bushing, height of bushing, lifting height, length of bushing lifting rope, length of hook and lifting rope of crane and the length of insulator chain on the framework in vertical direction must be considered. Then 1–2 m margin must be considered to obtain the final height of 1000 kV incoming (outgoing) line framework. In the demonstration project of China, the height of outgoing line framework and the incoming line framework was taken as 45 and 43 m up to the beam bottom, respectively, which, at present, have been optimized as 41 and 38 m for the project. Based on the practical project, it can be further optimized according to the equipment arrangement so as to reduce the height of framework and steel quantity to be used in the framework (see Fig. 25.17).

For 1000 kV outgoing line framework, line-to-equipment crossing requirement must also be met. In case the height difference between the terminal tower position and the outgoing framework is too large, the height of outgoing line framework must be raised or lowered accordingly.

In addition to meeting lifting requirement of main transformer bushing, the height of main transformation framework must also meet the safety air clearance

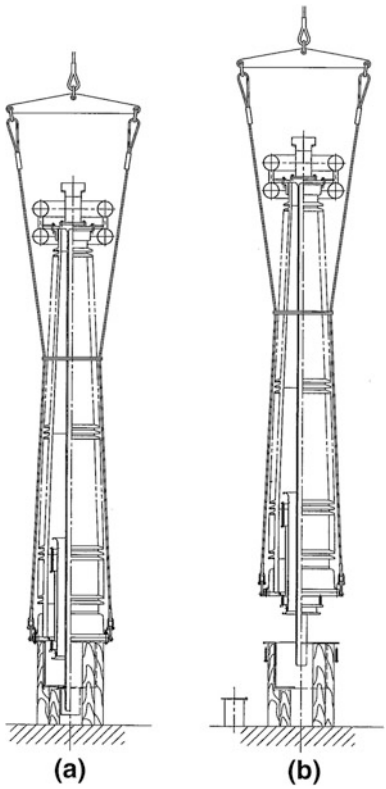

Fig. 25.17 Sketch for protection cover removal process after erection of bushing

distance requirement for withstanding voltage test of main transformer. Height of main transformer framework is generally taken as 32 m.

(3) Selection of economic root span

In 1000 kV framework design, research on framework column root span is very important. Design of framework root span has to meet the requirement of ultimate bearing capacity condition and the ultimate condition in normal operation at the same time. Generally speaking, the wider the root span is, the lesser the steel quantity of main material used for framework column will be, steel quantity of auxiliary materials will be increased, and width of electrical bay will be increased accordingly. On the contrary, when the root span is decreased, steel quantity of the main materials used for framework columns will be increased while steel quantity of the auxiliary materials will be decreased and the land requisition index of framework will be decreased accordingly. During design, a rational root span will be searched out through analysis and comparison for different root span sequence so that on the premise of meeting requirement of bearing capacity and deformation, the framework design will be economically rational and have fluent streamline and meet phase-to-ground electrical distance requirement.

For rectangular lattice framework columns, chord members are the main stressed bar members; the internal force is high, and its sectional dimension is dominated by strength. Web members are the secondary stressed bar members. Its sectional dimension is determined by structure rigidity requirement. In the calculation of sectional dimension, the strength does not play a full role. Under the same load condition, it shows from the large amount of calculation result of lattice framework: the wider the root span, the smaller displacement of column top is, however with not much influence on the displacement in the framework plane. The size of root span is closely related to the steel quantity used for the column. When the root span changes from small to large, the steel quantity used will first change from high to low, and then will be increased on the contrary when a certain extent is reached. This is because that, though the stress of chord members is reduced, but most of the web members have to increase construction section due to the increase of dimension, causing increase of steel quantity on the whole.

When the above frameworks are designed, the safety grade of 1000 kV framework is grade 1 and importance factor is 1.1. The calculated stress ratio of bar members is controlled at no more than 0.9 and deformation is controlled at no more than $H/200$ (H is the height above the ground at the position where deformation occurs) under the condition that the construction requirements are met.

For framework column with the height of the hanging point of conductors at about 45 m and bay width at about 54 m, it is better that the root span outside the plane varies in the range of 3–5 m and that the root span within the plane varies in the range of 7–11 m. For a particular project, the root span of framework column should be determined through adequate verification based on the actual conductor load, deflection angle, wind pressure, and electrical live distance.

(4) Load and load combination

Loads acted on the framework include the dead weight of structures, conductor tension under various operating conditions, wind pressure acted on structures, temperature action and seismic action. When the members have relatively large sections, the influence of load action of icing on structure on the internal force of members will also be considered. Load and load combination can be referred to *Substation Framework Design Manual* [9].

Conductor tension is closely related to electrical arrangement, model of conductors, sag and downlead, wind velocity, position of outgoing line tower, which will be provided through technological calculation, of which different types of electrical arrangement will lead to relatively large difference in conduction span hence also causing a large influence on conductor tension variation. When AIS equipment is used, for one-and-a-half circuit breaker connection, when the main transformer uses low vertical overhead incoming lines, the longitudinal dimension of 1000 kV distribution equipment will be as long as 120 m and the conductor tension acted on framework will be about 100 kN for each phase. When GIS straight-line layout is used, span of conductors on incoming line framework is generally at about 50 m and conductor tension is within 70 kN. Therefore, selection

Table 25.15 Conductor load on the line side (unit: kN)

Design operating condition	Ice coating	Strong wind	Installation	Low temperature	High temperature
Horizontal tension	120	120	108	110	100
Vertical load	56	41.5	55	55	55
Lateral wind pressure	6.3	30	6.3	6.3	6.3

Table 25.16 Ground wire load (unit: kN)

Design operating condition	Ice coating	Strong wind	Installation	Low temperature	High temperature
Horizontal tension	20	20	20	20	20
Vertical load	4.9	3.3	4.9	3.3	4.9
Lateral wind pressure	0.7	2.7	2	2.7	0.7

Table 25.17 Conductor load inside the substation (unit: kN)

Design operating condition	Ice coating	Strong wind	Installation	Low temperature	High temperature
Horizontal tension	70	66	61.9	20	70
Vertical load	35.8	32.8	34.27	35.8	35.8
Lateral wind pressure	1.5	13.2	1.5	1.5	1.5

of suitable electrical arrangement can also reduce the force acted on the framework, reduce the steel quantity index to be used in the project and obtain good economic and social benefits in addition to realizing the purpose of land saving. Conductor load of 1000 kV framework of a certain 1000 kV substation is as shown in Tables 25.15, 25.16 and 25.17.

(5) Wind load and wind vibration

The height of conductor hanging point of 1000 kV framework is 45 m and is up to 70 m when the height of lightning rod is added. Length-width ratio of section is generally over 2.0. Basic natural vibration period is at about 0.9 s. It is featuring in high flexibility, low damping, and low natural vibration frequency, very sensitive to wind load which often becomes a main load dominating structure design. Recurrence interval of wind load is increased from 50 to 100 years in the framework design due to the importance of UHV substation, that is, the basic wind pressure is considered as once in a century.

It is pointed out in the load code that vibration caused by wind is significant for high-rise structure with height larger than 30 m, length-width ration more than 1.5 and basic natural vibration period of structure T1 larger than 0.25 s, and that the vibration will increase with the natural vibration period of structure. Wind vibration impact caused by fluctuating wind pressure on the structure should be considered in

the design. Wind vibration coefficient β_z is an important coefficient affecting the wind load acted on substation framework.

Wind vibration coefficient β_z can be calculated in sections according to the requirement in load code and its weighted value can be taken prior to wind load calculation. Or wind load can be calculated in sections based on the said value obtained by calculation in sections. However, the results of these two methods obtained have a certain influence on the internal stress of framework beams and columns. For present tower framework, β_z value calculated in sections is within the range of 1.05–2.06 and the weighted value is at about 1.5. When weighted value is used in the unified internal stress calculation, the internal stress obtained for the upper section of column and framework beam will be 6–8% lower than that obtained in sectional calculation, and is obviously on the unsafe side. Therefore, special research on the value taking of wind vibration coefficient for 1000 kV framework design was carried out in the design of demonstration project and it was concluded that wind vibration coefficient was taken as 1.65. This conclusion was basically accepted in the subsequent projects. It is pointed out in the industrial standard "*Technical Code for the Design of Tower and Pole Structures of Overhead Transmission Line*" [10]: when overall height of tower and pole is more than 60 m, β_z will use values that increased gradually from bottom to top according to *Load Code for the Design of Building Structures* [11], and, however, its weighted value will not be less than 1.6. It is presented in *Code for Design of* 1000 kV *Substation* [5] that wind vibration coefficient is better to use segmented design. It should be point out that though the calculation is tedious, but the result is closer to the practical condition.

(6) Temperature effect

In order to prevent the temperature effect from causing high effects of action within structural system, the codes and standards have defined the temperature zones according to their own structural features. In the above temperature zones, the influence of temperature on structures can be disregarded. It is defined in *Code for Design of Steel Structures* [12] that "Calculation of effect of temperature can be cancelled for open air structure with temperature zone less than 120 m." *Technical Code for the Design of Substation Buildings and Structures* [13] requires that "For continuous bent with no rigid support on both ends and with overall length exceeding 150 m or continuous rigid frame structure with overall length exceeding 100 m, impact of the effect of temperature should be considered."

It can be seen through comparison of different codes and standards that the type of structure has a high impact on the length of temperature zones. The vertical support structure with high horizontal rigidity and strong restraint function on lateral horizontal members has large temperature effects. Therefore, the length of temperature zones is defined relatively short. For structure that exceeding the length of temperature zones, the effect of temperature should be considered.

In the UHV demonstration project, temperature stress was researched. It was considered that when 1000 kV framework is arranged as continuous two-span

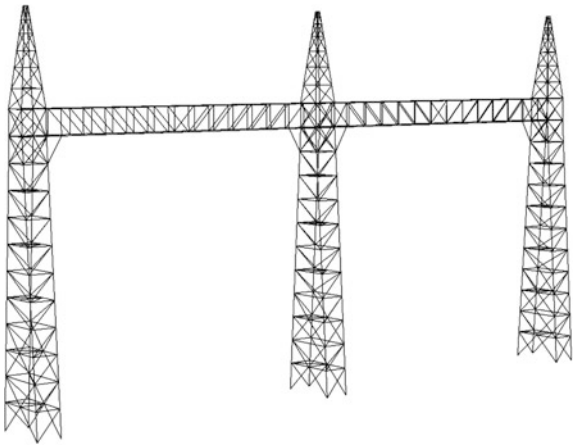

Fig. 25.18 Two-span model

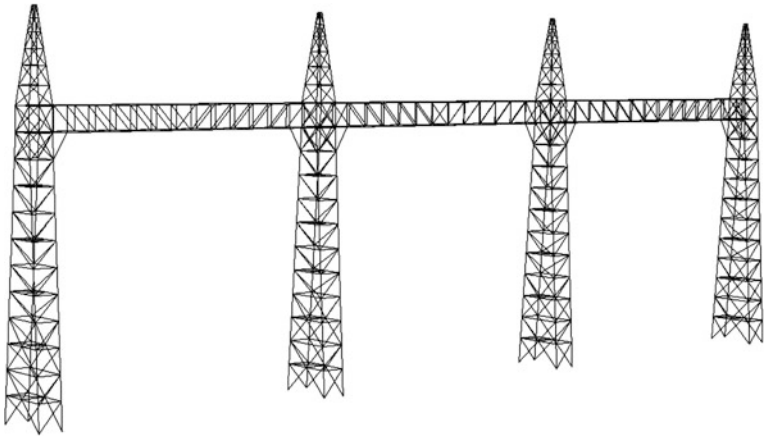

Fig. 25.19 Three-span model

form, temperature action has relatively small impact on the overall structure of framework. Therefore, it was recommended that the effect of temperature action may not be considered for continuous two-span outgoing line framework with single-span of 54 m. When 1000 kV framework uses continuous three-span or four-span arrangement, temperature action will have a relatively large impact on the overall structure of the framework. The overall impact of temperature action should be taken into account.

In a certain project, a universal structure analysis software ANSYS was used to analyze the temperature action of framework with different numbers of span and make calculation for continuous two-span, three-span, and four-span frameworks, respectively. The calculation models are as shown in Figs. 25.18, 25.19 and 25.20.

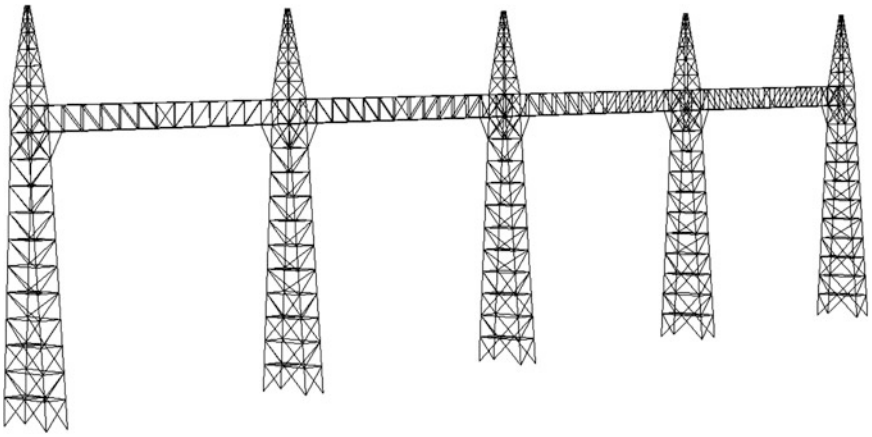

Fig. 25.20 Four-span model

Table 25.18 Internal force and displacement of framework columns under load combinations

Length of framework	Control mode	Maximum internal force (kN)		Maximum displacement Y (mm)
		Colum foot pressure	Column foot tension	
Two-span	Temperature action mode	1710	1416	130.1
	Other control mode	1960	1680	86.6
Three-span	Temperature action mode	1914	1675	162.6
	Other control mode	1980	1750	91.6
Four-span	Temperature action mode	2120	1910	199.4
	Other control mode	2027	1765	98.3

The calculation results in comparison of maximum internal force and the displacement on the top of columns under different operating conditions are shown in Table 25.18.

It can be seen from the above table that temperature action increases with the number of continuous span of framework. When the framework is arranged in three spans and below, temperature stress has no control function to bearing capacity, and, however, it is the control mode of the ultimate limit state of framework under normal operation. In case of four-span framework, the temperature action becomes the control mode of framework design; both stress and deformation reach the maximum values. In the meantime, the displacement on the top of column is

already close to the upper limit value. And steel quantity used for framework is totally determined by temperature action.

Therefore, for 54 m span lattice framework, when it is arranged in three spans under different temperature operating conditions, the internal force of bar members is smaller than other control mode (generally strong wind operating condition), and temperature stress does not have much influence. However, deformation calculation will be based on relevant load combinations. In addition, rational construction method will be used at beam-column node to reduce restraint to beam deformation and mitigate the impact of temperature stress on the structure.

When the framework is arranged in continuous four and above spans, the continuous framework will be segmented so that it will meet requirement of limit value of the codes. However, excessive segmentation will increase longitudinal floor space of framework, hence resulting in increase of the number of column and steel consumption. Therefore, it is possible to seek for adding roller support or provide temperature expansion joints to effectively release temperature stress without increasing floor space. At present, there are some design institutes having already completed theoretical study and laboratory test work on roller support and sliding support for the framework of large size substation. These economical and effective new structures wait to be applied in subsequent UHV project.

(7) Seismic effect

In view of the importance of UHV substation, site selection should avoid high intensity seismic region. However, with continuous development of UHV power grid, it is inevitable that 1000 kV substation will be constructed in M7 and M8 seismic regions. Therefore, for framework located in M7 and M8 seismic regions, seismic analysis shall be carried out in the design.

According to the design experiences of previous projects, because the steel pipe framework is of high-rise structure with relatively long natural vibration period, thus seismic does not often have any control function to the framework section design. It is also definitely concluded in *Code for Design of* 1000 kV *UHV Substation* that seismic may not be considered in framework calculation. In practical project, design personnel should be better to make analysis based on the category of construction site to make clear that whether seismic analysis should be made or not.

25.12.3 UHV GIS Equipment Foundation

In order to implement the state policy on land saving, the use of GIS equipment arrangement in UHV substation has become a trend. Based on the structural features and connection type of GIS equipment, GIS equipment is very sensitive to foundation deformation. Manufactures have different requirement on civil-work foundation, and, however, their requirement is very rigorous. In the foundation

design of UHV substation buildings and structures, importance has been attached to the optimization of design schemes of GIS equipment foundation by design personnel. It is necessary to explore the control of deformation, cracking, levelness of embedded parts, positioning accuracy of reserved terminals, etc. of GIS equipment foundation.

In UHV projects already finished or still under construction at present, suppliers of GIS equipment include Henan Pinggao Electric Co., Ltd., New Northeast Electric (Shenyang) High Voltage Switchgear Co., Ltd. and Xi'an XD Switchgear Electric Co., Ltd. Requirement of the manufacturers on the equipment foundation includes foundation bearing capacity, foundation deformation, top elevation, accuracy of embedded parts of foundation, cable trench arrangement in coordination with ground grid, and meeting field assembly and maintenance requirement.

(1) Requirement on bearing capacity of foundation

Load transmitted to foundation by equipment includes dead weight and operating force of equipment, horizontal force and vertical force on the top of foundation caused by wind load and earthquake. It is concluded from data analysis of different manufacturers that stress of GIS foundation is characterized by point loads on the upper part of foundation distributed in a disperse manner in different magnitudes with maximum stress point located at circuit breaker unit at about 300 kN, relatively small load at remaining equipment unit and busbar supporting load, and basically the same load distribution between strings. In addition, all the manufacturers require that 10–15 kN/m^2 live load be considered within the scope of foundation slab.

(2) Requirement on foundation deformation

Deformation of foundation will affect connection strength between equipment units. Excessive foundation deformation will increase leak probability of the sealing system, in worse case, causing GIS fault hence affecting safety in power grid operation. Manufacturers provide expansion joints to adjust deformation caused by foundation in the manufacture and design of upper part equipment. Even so, the requirement on foundation deformation is still very rigorous. Generally, it is only allowed that deformation joint of foundation is in consistent with the setup position of upper part expansion joint.

The requirement on foundation deformation includes that in horizontal direction and that in vertical direction. The 1000 kV GIS equipment of most manufacturers uses a complete string as a unit. Expansion joint is provided on busbar bushing between each string to coordinate foundation deformation. It is required that each unit is located on the same independent slab foundation and expansion joint can be provided between the units. Equipment to foundation deformation is mainly controlled between independent slabs, between embedded parts on the same slab, and between slab body and incoming line and outgoing line bushing foundations. To sum up the present technical parameters of the current manufacturers, in the design of GIS foundation, the foundation and embedded part deformation limit values are

Table 25.19 Limits of GIS foundation deformation

	Horizontal direction (mm)	Vertical direction (mm)
Between two independent slab foundations	20	20
Between foundation proper and incoming and outgoing line bushings	4	15

Table 25.20 Limits of deformation between embedded parts on slab foundation

Distance between embedded parts d (m)	Differential settlement (mm)
$d \leq 5$	≤ 5
$d > 5$	≤ 30 and $\leq 0.1\%$

controlled in accordance with Tables 25.19 and 25.20, and this will meet the engineering requirement.

(3) Requirement of equipment on site

Manufacturers require a certain degree of cleanliness within GIS slab, and that the site ground is in flush with equipment foundation surface, and that the site can be used as field assembly and maintenance site. Designs of the previous project all use slab foundation with top elevation meeting the requirement of manufacturers. However, direct placement of foundation in open air environment or on mass volume concrete has brought some trouble to civil work design and certain difficulty to cable trench arrangement, construction of earth mat of GIS equipment and accuracy control of embedment of ground terminals.

(4) Structural forms of GIS equipment foundation

Foundation construction of the built substations at present includes slab foundation with plate thickness of about 2 m and raft foundation jointed with grade beam with plate thickness around 300 mm. These foundations are all open air structures subjecting to significant temperature influence. In addition, when the structure is constructed, cable trench, ground copper bars, and up-lead terminals must be completed together with the main structure. For this, some design institute recommended the use of buttress type GIS foundation design, i.e., use buttress to fix the equipment and transmit the load to the bottom slab, and the remaining site uses paved floor. This design avoids direct placement of foundation in open air environment, effectively eliminates GIS mass volume concrete construction and subsequent cracking phenomenon, facilitating flexible arrangement of cable trench and grounding construction as well as subsequent adjustment while meeting requirement of field assembly (see Fig. 25.21).

The section of buttress type GIS foundation is shown in Fig. 25.22.

Fig. 25.21 Photo of slab raft foundation

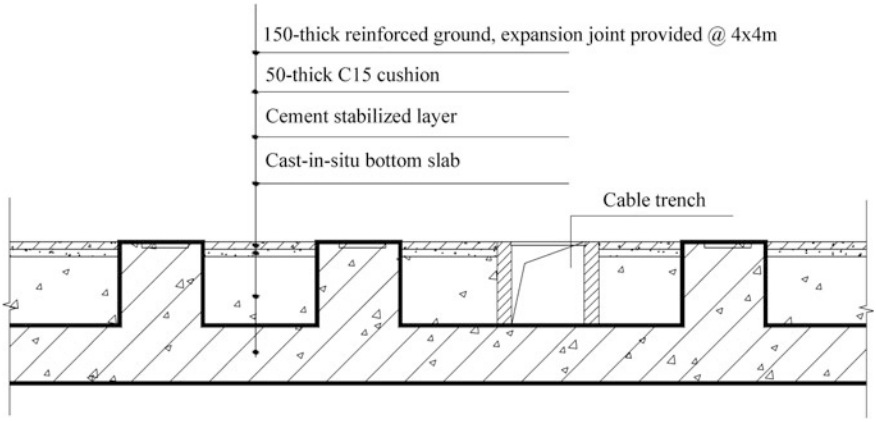

Fig. 25.22 Section of buttress-type GIS foundation

25.13 Secondary Electrical Connection

25.13.1 Main Design Principles

Secondary connection design of 1000 kV substation seeks for safety, reliability, technically advancement, economical in use, and compliance with national conditions, continuously sums up experiences, actively and carefully uses and promotes appraised new technology and new products. The computer supervisory and control

system are used in 1000 kV substation. Substation operator on duty is always attended. Remote control, telemetering, telesignalisation, and teleregulation are realized by relevant dispatching office. Monitoring and control devices and relay protection devices of the computer supervisory and control system are transferred to lower level according to objects and functions and are placed in local protective chambers. Main principles of secondary electrical connection are as follows:

(1) Follow the principle of "safety, reliability, technically advancement, economical and rational and in compliance with national conditions." Use mature, advanced and reliable computer supervisory and control system with good openness, expansibility, high anti-interference capability, and meeting project requirement.
(2) The substation will use the computer supervisory control system. No additional conventional control and mimic panel will be provided. The substation uses strong current one-to-one control connection. Rated voltage of DC power supply can use 110 or 220 V.
(3) Protective chambers are provided near the position where primary equipment is relatively concentrated and the control cable length between primary equipment and secondary equipment can be shortened as much as possible, with such factors as cable length, number of common facilities, and convenience in operation and maintenance comprehensively considered. Environmental conditions of protective chambers should meet safety and reliability requirement of relay protection device and control device, and available with excellent electromagnetic shielding measures, with position avoiding equipment possible generating high electromagnetic field.
(4) For circuit breaker with two independent tripping systems, the two tripping systems should be powered by two battery DC power sources respectively. The two sets of exit relay of the protection should also be connected to two sets of tripping windings respectively.
(5) Transient characteristics of current transformer and voltage transformer should meet the requirement of relay protection.
(6) Circuit with operating voltage of 250 V and above is not suitable to connect to control and protection panels.

25.13.2 Computer-Based Monitoring System

The UHV substation is provided with 1 set of technically advanced and functionally perfect computer-based monitoring system to perform such functions as normal control, monitoring, signaling, measurement, data statistics and analysis, etc. The control building of substation is provided with independent control duty room used for operation management of 1000, 500, and 110 kV equipment in the substation.

The substation uses layered, distributed open-type computer-based monitoring system. Conventional control panel and signal panel are cancelled. Bay-level

control and protection device are transferred to lower level and arranged according to objects and functions. Using DL/T860 (IEC 61850) communication standard, the system is modeled and networked together with relay protection equipment and shares the same information platform.

According to the current practical conditions of the application of substation computer-based monitoring system in China, with such features as large quantity of information, many measuring points, frequent emergency event, and complicated electromagnetic environment of 1000 kV UHV substation taken into account and in view of the current development condition and the trend of the computer-based monitoring system, the principles with which the design of the computer-based monitoring system is determined for UHV substation are as follows:

(1) Computer-based monitoring system is of open-type layered and distributed network architecture. Station-level network uses double fiber-optic Ethernet. Bay-level equipment uses distributed arrangement.
(2) Data of substation are collected and processed in a unified manner. The resource is shared.
(3) Host machine, operator stations, and telecontrol workstations use the UNIX operating system.
(4) Bay-level equipment is provided with I/O measuring and control devices according to step-down and step-up phase engineering scales, and is dispersedly arranged in control building and different voltage grade relay chambers in distributed manner according to the control area. I/O units are provided strictly in accordance with unit, and can quit operation with maintenance of primary equipment electrical bay.
(5) Electrical analog quantity acquisition of the computer-based monitoring system uses AC sampling, with conventional transmitters cancelled. Digital quantity signal including status of primary equipment is sampled in a point-to-point manner. General electrical energy meter is provided at non-gateway point. Electrical energy gateway measuring meter is provided at electric energy charging gateway and respectively connected to the electric charging system.
(6) Fault recording does not occupy network resources of the monitoring system. Fault recording information can use separate network.
(7) Provide two sets of telecontrol data transmission equipment in redundancy configuration, which communicate with different types of measuring, control, and protection devices through fiber-optic Ethernet, send the data collected by measuring and control units to the database of telecontrol equipment, and, after protocol conversion, upload to different dispatching terminals. Information resources are shared by main station of the computer-based monitoring system and telecontrol data transmission equipment without repeated data collection so as to save investment.
(8) Computer-based monitoring system has anti-error locking function. Five-prevention workstation is provided. Anti-misoperation uses in-bay anti-misoperation combined with station-level anti-misoperation method.

Measuring and control unit is configured as per bay, which can realize anti-misoperation inside the bay. Message exchange between measuring and control unit and station-level anti-misoperation system can realize the whole anti-error locking function.

(9) Computer-based monitoring system has interface with electric power dispatching data network, and is available with electric power data network interface. Its hardware and software configuration should be able to support the future networked communication technology and communication protocol requirement.

(10) Substation's training simulation workstations are provided to perform software simulation for bay level of substation, substation level, and main electrical equipment level.

(11) Network safety protection of the computer-based monitoring system should be strictly in accordance with the requirement of relevant provisions. Isolation and protection measures are provided.

(12) It is considered to use substation communication network and system standard DL/T-860 (IEC 61850).

25.13.3 Element Protection

25.13.3.1 Protection of Main Transformer

1. 1000 kV main transformer consists of main body and voltage regulating transformer. Voltage regulating transformer contains low-voltage compensation. Transformer protection includes main body protection and protection of voltage regulating transformer and compensation transformer.
2. Protection of main transformer uses microcomputer-based main and standby dual protection. Main protection uses 2 sets of differential protection using different operation principles. In addition, it shall also be provided with split-phase differential protection and non-electricity protection on the high- and medium-voltage sides.
3. Protection of 1000 kV main transformer should be able to rapidly and sensitively eliminate faults or give alarm signals in case of phase-to-phase fault and ground fault occurred with transformer windings and their outgoing lines, turn-to-turn fault of windings, over-current and overvoltage, over-excitation, over-load faults caused by external phase-to-phase fault and ground fault and other abnormal operation mode, and be able to avoid excitation surge based on excitation flux characteristics at the time of switching. It also has measures to prevent transformer protection malfunction caused by saturation of current transformer and non-consistent transient characteristics.

4. Split-phase differential protection on HV and LV sides is provided, which is connected with the current transformer from the HV, LV, and common windings of main transformer. The advantages are as follows:
   (1) It is not subject to the influence of excitation surge and over-excitation. Simple ratio-restrained differential protection can be used.
   (2) Protection can be set only in accordance with the unbalanced current produced by current transformer under transformer load, which features in low set value and high sensitivity.
   (3) The current transformers on all sides can adopt the star connection mode, without need to make deviation angles, enhancing the sensibility in ground short-circuit faults.
   (4) Protection device is installed phase by phase. As long as protection device acts, the fault phase is known immediately, hence, reducing fault correction time.
5. Overvoltage protection is provided. The transformer trips at delayed time when closing of unloaded transformer produces resonance overvoltage.

25.13.3.2 Protection of High-Voltage Reactor

Protection of high-voltage reactor should be able to rapidly and sensitively eliminate faults or give alarm signals in case of single-phase-to-ground short and turn-to-turn short with reactor windings, phase-to-phase short and single-phase ground short with outgoing lines, low oil level, temperature rise and cooling system fault, over-load, and other abnormal operations.

(1) Main protection of shunt reactors should use microcomputer-based current differential protection device.
(2) Protection device should not be subject to the influence of transient current leading to malfunction. In case of TA secondary circuit fault, protection device shall be able to lock up reliably and give alarm signal. In case of fault occurs on the circuit during full-phase oscillation or non-full-phase oscillation, reactor protection device should not be misoperation.
(3) The operation time of differential instantaneous trip protection is ≤ 20 ms (1.5 times of the set value). The operation time of differential protection is ≤ 30 ms (twice the set value). The protection action value is continuously adjustable, and the protection should be sensitive to the faults in the whole differential range.
(4) Turn-to-turn short protection: in case reactor has $\geq 5\%$ turn-to-turn fault, turn-to-turn short protection device will act instantaneously. When circuit breaker is operating in non-full-phase mode and turn-to-turn short occurs with healthy phase, the protection device will operation correctly.

(5) Over-current protection: over-current protection device consists of 3-phase current element having definite time-lag and inverse time-lag characteristics. The protection will break 1000/500 kV line circuit breaker in delayed time.
(6) Over-load protection: it consists of current element having definite time-lag and inverse time-lag characteristics. The protection sends out alarm signal in delayed time.
(7) Non-electricity protection such as gas and pressure release of shunt reactor: non-electricity protection includes severe gas, slight gas, pressure release, low oil level, high oil temperature protections. Protection of severe gas, slight gas, high oil temperature, high coil temperature breaks 1000/500 kV line circuit breaker and send out alarm signal through independent tripping output unit. Protection of slight gas and low oil level gives out alarm signal. Non-electricity protection will not start circuit-fail protection.
(8) Neutral reactor protection uses ground current protection device having definite time-lag and inverse time-lag characteristics. Protection act and gives out alarm signal in delayed time. Besides, neutral reactor should be provided with non-electricity protections such as gas and pressure release.
(9) Tripping output unit: each set of main protection and standby protection is provided with one set of output unit. Non-electricity protection is provided with one set of output unit. Protective tripping output unit connector is provided. Protection is able to provide two sets of tripping coils for the circuit breaker on the tripping side and provide circuit breaker on the opposite side of tripping circuit of the contact.

25.13.4 System Protection

25.13.4.1 Protection of 1000 kV Lines

Each 1000 kV line is provided with 2 sets of whole line quick action main protection. Each set of protection is provided with dual 2 Mbit/s optic-fiber communication interfaces. Channels are transmitted by using direct or roundabout 2 Mbit/s OPGW optic-fiber communication circuit. In normal condition, the first set of main protection uses point-to-point direct pass optic-fiber communication channel. The other set of main protection uses roundabout optic-fiber communication channels. For the double-circuit line on the same tower, phase-segregated current differential protection should be preferentially considered.

Each set of main protection has complete backup protection function. Main protection and backup protection are realized using the same set of protection device. Backup protection is provided with complete multi-section phase-to-phase and grounding distance protection, and one set of definite time-lag or inverse time-lag zero sequence directional over-current protection is provided to reflect high resistance ground fault.

For full-phase oscillation of the line, the protection should not have malfunction. Repeated fault of the line during full-phase oscillation or non-full-phase oscillation, the protection should be act reliably as possible. The protection should be able to reflect fault of relatively serious ground fault resistor. Under the influence of steady state, transient state harmonic component and direct current component caused by distributed capacitance of line, shunt reactor, transformer (excitation surge), high-voltage DC power transmission equipment and series compensation capacitors, the protection device should not have malfunction.

Phase-segregated current differential protection should be suitable to use in the circumstance where current transformers on both sides of the circuit have different transformation ratio.

Protection device should use computer-based quick action protection with low power consumption, perfect function and having mature operation experience. The protection uses single-phase tripping method. Quick action main protection should have phase selection function. Each set of computer-based protection device should have fault locating and fault recording and event logging functions at the same time.

25.13.4.2 Overvoltage Protection of 1000 kV Lines

On both sides of 1000 kV lines, dual overvoltage protection and transferred tripping in situ discriminating elements are provided. Overvoltage protection is installed as per phase. Criterion of transferred tripping in situ discriminating element should use integrated current variation element, zero-sequence current element, integrated voltage element having compensation function, and low power element. Overvoltage protection should have no malfunction under normal operation of system or under interference by system transient state process. The protection's action time and setting value should in accordance with the overvoltage protection of primary equipment, and should be able to use in capacitive potential transformer.

After overvoltage protection action, transferred tripping signal will be sent to the main protection of the opposite side through the channel of main protection of the line.

The two sets of overvoltage protection and transferred tripping in situ discriminating elements are placed in the same cabinet with corresponding two sets of line protections.

The two sets of protection of each line are located in independent cabinets respectively and are powered by different DC battery bank respectively. AC voltage circuit, current circuit, DC power supply, digital input, tripping circuit, startup transferred tripping and remote signal transmission channel of line main protection, backup protection and overvoltage protection in dual-configuration lines should all be independent from each other and have no electrical relation. Each set of protection should have independent split-phase output which only acts on one set of tripping coil of circuit breaker.

25.13.4.3 Protection of 1000 kV Circuit Breaker

1000 kV circuit breaker protection is provided as per circuit breaker. Circuit breaker failure protection is also included. Circuit breaker relating to line circuit is provided with auto-reclosing function. Each set of circuit protection is located in a separate cabinet.

Circuit breaker failure protection only considers single-phase failure condition of circuit breaker and is able to detect the fault in dead zone. The starting circuit of circuit breaker failure protection uses series connection of protective single-phase tripping outlet contact with phase current element. It should be considered that phase current element has adequate sensitivity when there is a fault at the end of the circuit.

When circuit breaker failure protection is started, it will re-trip the circuit breaker once instantaneously, and, for a period of delay, it will trip the three phases of the circuit breaker and the adjacent circuit breaker. At the same time, the line circuit breaker failure output sends a tripping signal to the opposite line circuit through the channel of main protection. The circuit breaker failure output at the side of busbar trips relevant circuit breakers on the busbar of failed circuit breaker through busbar protection output.

There are two sets of transferred tripping signal, which are sent to the main protection of line on the opposite side through the channels of the two sets of main protection respectively.

Auto-reclosure only realizes one reclosure. No multiple reclosure should take place under any circumstances. Auto-reclosure uses single-phase reclosure. However, it can realize three-phase reclosure, integrated reclosure, and reclosure shutdown modes. Reclosure startup modes include protection startup and uncorresponding startup. Reclosure device provides single-phase and three-phase tripping startup respectively. For reclosure of the two circuit breakers on the circuit side, it should be able to flexibly select and determine "Reclosing circuit breaker first" and "reclosing circuit breaker next." First closing and next closing relation of the two circuit breakers uses time priority principle.

25.13.4.4 1000 kV Remote Tripping Protection

Each 2 M optic-fiber communication interface of each set of main protection for the line should be able to receive and transmit one inter-tripping command and one remote tripping command. Remote/inter-tripping channels should be able to switching in and off.

Inter-tripping function: when there is a fault on the circuit leading to protection action on one side tripping three phases, the protection device will send a transfer three-phase tripping signal to the opposite side. When the circuit protection device of the opposite side receives three-phase inter-tripping signal, it will avoid retransmit the three-phase inter-tripping signal. In order to avoid malfunction of the protection device due to receiving signal by mistake, the circuit protection will trip

the three phases of the circuit breaker after receiving three-phase inter-tripping signal and the protection in this side has acted.

Remote tripping function: when the overvoltage protection, circuit breaker failure protection and high-voltage shunt reactor protection act, the remote tripping signal will be sent to the main protection of the line on the opposite side through the main protection channel. Only when the opposite side receives the remote tripping signal and the in situ discriminating element acts, circuit breaker three-phase tripping operation is allowed.

25.13.4.5 Protection of 1000 kV Busbar

Each section of 1000 kV busbar is provided with 2 sets of complete, independent busbar differential protection and according to the prospective capacity, differential measuring element of the protection should be split-phase type. For one-and-a-half-circuit breaker main connection, busbar protection configuration is considered as that of single busbar, i.e., each section of 1000 kV busbar is provided with 2 sets of busbar protection, and total of 4 sets.

Busbar protection has no special requirement on CT characteristics, and the CT saturation has no influence on its action accuracy. The anti-CT saturation performance should adjust to the requirement of short-circuit current level of 1000 kV system. Elements are allowed to use CT with different transformation ratio. It is possible to use TPY secondary CT, P secondary CT, or TPY/P secondary CT. For a busbar protection using one-and-a-half circuit breaker connection, no composite voltage locking is provided.

Busbar protection in dual configuration is installed in their respective cabinets. AC current circuit, DC power supply, digital input, tripping circuit are independent to each other and have no electrical relation. Each set of busbar protection only acts on one set of tripping coil of circuit breaker. When circuit breaker failure protection trips the circuit breaker on busbar side, it will be realized by starting busbar protection.

25.13.4.6 1000 kV Fault Oscillograph

In order to analyze AC current, voltage, and the action of relay protection device when the power system has a fault, the substation is provided with a separate fault oscillograph to record the current and voltage of 1000 kV circuit and the main transformer, action of protection device (including high-voltage shunt reactor protection) and the operating conditions of the protection channel. In addition, in order to accurately record the current on circuit breakers at the 1000 kV busbar side within the busbar section when there is an internal/external fault, it is necessary to record circuit breaker current on busbar side and the busbar voltage.

For main connection of one-and-a-half circuit breaker, fault oscillograph of recording circuit and main transformer recording quantity is provided according to

relay chamber. The whole station is provided with one set of 1000 kV busbar fault oscillograph.

Fault oscillograph is of digital type, and includes fault locating and accident analysis functions. Fault oscillograph should be able to be networked separately to communicate with relay protection and fault information management system substation through Ethernet interface. Recorded information can be remotely transmitted to dispatching department of all levels for accident analysis and processing through the substation.

25.13.4.7 1000 kV Line Fault Location Device

Both sides of 1000 kV transmission line is provided with separate double-ended fault location device that using traveling wave principle. Data exchange between both sides uses 2 M channel. Each substation is provided with one set.

Line fault location device is of digital type, has independent starting element and has the function of outputting the recorded information locally and transmitting it to remote place. Line fault location device uses high-speed acquisition technology, GPS synchronization technology, matched filtering technology and wavelet technology to realize double-ended traveling wave fault location supported by single-ended traveling wave fault location. Line fault location device should be able to communicate with dispatching center through power data net or special channel.

25.13.5 System Communication

Substation uses optic-fiber communication, and has dual optical cable router to organize information service communication channels from substation to relevant communication stations. The substation should be provided at least with 3-level transmission net equipment and connect the same to state-level, regional-level and provincial-level communication transmission net as required. Critical boards of equipment are provided in redundancy. Service boards relating to dispatching and automation service are provided in redundancy. Transmission rate of optical fiber transmission trunk circuit is 2.5–10 Gbit/s, transmission rate of branch circuit is 622 Mbit/s–2.5 Gbit/s. Optical Cable is OPGW optical cable. Optic-fiber core is mainly G.652 optic-fiber. Number of optic-fiber cores is generally 24. When the optical cable is shared by regional net and provincial net, the number of optic-fiber core will be properly increased.

Substation is provided with dispatching telephone and administrative telephone exchange equipment, which are connected to the power system dispatching telephone exchange net and administrative telephone exchange net respectively for voice communication of dispatching and management. Also it is considered to install telecom local telephone for communication with local telephone office.

Integrated data network equipment is provided which is connected to power system data network for communication of electric power production and management data.

Substation is provided with 2 sets of complete communication power supply system. System capacity is configured in accordance with specific engineering calculation. The required AC power is supplied by AC power supply of different station service power busbar sections. Communication equipment room and communication battery room are provided. The area of equipment room is considered in accordance with final stage capacity of the substation. Meanwhile, the panel position should be reasonably arranged according to practical condition. Power environment monitoring system in communication equipment room is established to realize telesignalisation and remote control for communication equipment room, communication power supply and battery room environment, power system and air conditioning.

25.13.6 Dispatching Automation System

To meet the needs of substation automation management, the substation is provided with 1 set of technically advanced and functionally perfect computer-based monitoring system to realize supervision and control over the operating conditions of substation electrical equipment. In order to avoid repeated configuration of remote control and secondary equipment, the station computer-based monitoring system and remote control system share 1 set of I/O unit which communicate with dispatching through remote control data processing and communication equipment.

25.13.7 Electric Energy Metering and Billing System

Substation gateway metering point should be provided on both sides of 1000 kV lines, HV side of ex-substation power supply, 500 kV outgoing line side, main transformer intermediate voltage side in principle. Gateway check point is provided on the HV side of main transformer.

Technical requirements for gateway electric energy meters are as follows:

(1) Precision: the active energy is better than grade 0.2S, and the reactive energy is better than grade 1;
(2) With bi-directional metering function;
(3) With RS485 serial output port;
(4) Able to store 7 days' electric energy when resolution is set as 1 min.

The substation is provided with special electric energy acquisition and processing device to collect real data of electric energy on the site, and transmits

electric energy data to dispatching electric energy metering main stations through data network or MODEM dial-up program controlled exchange network respectively. The communication protocol is IEC 60870-5-102.

Technical requirements for electric energy acquisition and processing equipment are as follows:

(1) It should be able to accept energy meter RS485 series port, and have time-sharing accumulative storage capability for electric energy data by automatically or manually setting multiple time intervals.
(2) Adequate communication ports should be provided. It can communicate at least two main station systems through power dispatching data network, power program-control exchange network or special line channel to realize transmission of electric energy data.
(3) Communication should use DL/T719 or DL/T645 communication protocol and TCP/IP network communication protocol.
(4) When storage data resolution is set as 1 min and electric energy input reaches maximum quantity allowed by electric energy processing device, electric energy device will be able to store electric energy data collected for 14 days.

25.13.8 Operating Power Supply System and Others

25.13.8.1 DC System

1. DC system configuration

(1) The UHV substation generally uses 2 sets of DC system. Each set of DC system is provided with 2 sets of battery and 3 sets of charging unit. DC voltage can be 220 or 110 V. Service area of the first set of DC system includes 1000 kV main transformer and reactive protection cells and main control building (including emergency inverter panel of the whole substation). Service area of the second set of DC system is 500 kV protection cells.
(2) Battery: valve regulated lead acid (VRLA) batteries are used. They are generally rack-mounted. Capacity of battery of the first and second set of DC system is selected respectively in accordance with load statistics and 2 h emergency discharge time.
(3) Charging unit: each set of DC system is provided with 3 sets of charging unit. High frequency switching power supply is used. Output voltage regulating range is 198–260 V.

2. Connection of DC system

(1) Busbar connection: use single-busbar sectional connection. Storage battery banks are connected to different busbar sections respectively. Connecting knife switch is provided between two busbar sections. 2 battery banks are allowed to be in parallel during switching between two busbar sections.
(2) Connection of charging unit: the two charging units are connected to the two busbar sections respectively through DC circuit breaker to charge these two battery banks and provide the required capacity of frequent load. The third charging unit is connected to the two battery banks by switching over the knife switch. When any of the charging unit quit operation due to failure, the third charging unit will be switched in.
(3) Test discharge circuit: each battery bank is provided with a dedicated test discharge circuit.
(4) DC network: protection cells is provided with DC split screen respectively, which is powered with main and split screen in radial arrangement.
(5) DC distribution panel: connection is made up with two busbar sections inside the power distribution cabinet. 2 circuits of DC power come from different battery banks and are connected to busbar through knife switch. Locking should be available to prevent parallel operation of two battery banks.

25.13.8.2 AC Uninterrupted Power Supply (UPS) System

Substation is provided with 1 set of AC UPS system to provide uninterrupted power for important loads of computer-based monitoring system including host machine, network equipment, remote control workstation, GPS and fire alarm device. Dual main machine redundancy configuration is used. Capacity load rate is considered as 60% according to relevant procedures, and for normal condition, 2×7.5 kVA is selected. Each cell is provided with 1 UPS panel to provide uninterrupted power for important loads in the cells including network equipment, gateway watt hour meters, electric energy acquisition devices, GPS split screens and so on. Dual redundancy configuration is used.

UPS has no built-in batteries. DC power is supplied by batteries with the DC system in the substation.

25.13.9 Equipment Status On-Line Monitoring System

In order to realize condition-based maintenance of electrical equipment, implement early monitoring and fault diagnosis and prevent accident spreading of electrical equipment, substation is provided with 1 set of on-line monitoring system for electrical equipment, including functions such as oil on-line monitoring of main transformer and high-voltage reactor, partial discharge, break-close time of circuit

breakers of GIS combination electric apparatus, SF_6 gas monitoring, partial discharge and arrester on-ling monitoring.

Detect internal initial failure and its development tendency through acquisition and analysis of relevant parameters and information. Maintenance people can carry out comprehensive analysis according to the detected data, diagnose conditions of equipment so as to reduce loss, avoid occurrence of fatalities and improve safe and economical operation of power grid.

References

1. Liu Z. UHV power grid. Beijing: China Economic Press; 2005.
2. Yi D. Electric engineering electrical design manual. Beijing: Water Resources and Electric Power Press; 1989.
3. GB/Z24842-2009. Overvoltage and insulation coordination of 1000 kV UHV AC Transmission Project; 2009.
4. Liao X, Lin F, Sui J, et al. Improved reactive compensation strategy for 1000 kV UHV system. Mod Electr Power. 2008;25(6):45–8.
5. GB 50697-2011. Code for design of 1000 kV substation; 2011.
6. Chen H, Fan Y, Chen H. 1000 kV GIS layout types for Southern Anhui UHV substations. East China Electr Power. 2008;36(7):59–63.
7. DL/T 5014-2010. Technical rules for designing of reactive power compensation equipment in 330–500 kV substations; 2010.
8. DL/T 5155-2002. Technical code for designing AC station service of 220–500 kV substation; 2002.
9. Central Southern China Electric Power Design Institute. Electric substation framework design manual. Wuhan: Hubei Changjiang Publishing Group; 2006.
10. DL/T 5154-2012. Technical code for the design of tower and pole structures of overhead transmission line; 2012.
11. GB 50009-2012. Load code for the design of building structures; 2012.
12. GB 50017-2003. Code for design of steel structures; 2003.
13. DL/T5457-2012. Technical code for the design of substation buildings and structures; 2012.

Chapter 26
Design of UHVDC Converter Station

Zhichao Zhou, Xiaofei Ding, Wenqian Qiu, Jianhua Chen, Chunxiu An and Sheng Liu

In China, the energy resources and energy demands are distributed contrarily, so objectively, the configuration of the energy resources shall be optimized in a large scale. For the development of the electric power industry, it is an inevitable trend to develop new large-scale coal-based power generation bases in Shanxi, Shanxi, Inner Mongolia, and Ningxia, and develop large-scale hydropower bases in the places in Southwest China which are rich in hydropower, to transmit electric power to Mid-East China that is short of energy resources by means of the long-distance, large-capacity, and low-loss power transmission. Besides, for the purpose of maintaining the national energy security and improving the energy guarantee level, the energy cooperation and international power transmission shall be performed actively. As the Yunnan–Guangdong UHVDC Power Transmission Project, Xiangjiaba–Shanghai UHVDC Power Transmission Project, and other UHVDC transmission projects are completed and put into operation, the construction of the UHVDC power transmission in China has stepped into the high-speed development stage. At present, China has completed 7 ± 800 kV DC power transmission projects, and is planning and designing a fair number of ±800 kV DC power transmission projects and the first ±1100 kV DC power transmission project, becoming the world's biggest country in the field of DC power transmission. This chapter discusses the engineering design of the UHVDC converter station.

26.1 Site Selection and General Layout

26.1.1 General Requirements

The coverage area of UHV converter station inside the boundary may vary from 15 to 25 ha depending on its scale and layout. Similar to the UHVAC substation, the converter station shall also be sited in a location adjacent to the load center, and shall occupy as less land as possible by following the state's guidelines and

© Zhejiang University Press, Hangzhou and Springer-Verlag GmbH Germany 2018

H. Zhou et al. (eds.), *Ultra-high Voltage AC/DC Power Transmission*,
Advanced Topics in Science and Technology in China,
https://doi.org/10.1007/978-3-662-54575-1_26

policies, with all conditions to build the substation available. In addition, the site selection of UHVDC converter station is generally same as that of UHVAC substation in construction field, line corridor, and geological conditions. The site selection of the converter station shall be subject to comprehensive and detailed discussion in general layout, heavy-duty equipment transport, water resource supplied to the substation, environmental protection, etc., thus to determine the site of the converter station scientifically and reasonably [1, 2].

26.1.2 General Layout

The site selection and general layout of the converter station shall implement the principles of reasonable land use and economically intensive land use. In general planning of the site area, such factors as the geographic location, landform and terrain, geological conditions, system planning, construction scale, water supply and drainage conditions, outbound traffic, and heavy-duty equipment transport shall be jointly considered. Meantime, the outgoing line direction, road access to the substation, routes of water supply, and drainage shall be planned as a whole, considering both near-term and long-term development, the technological requirements, outgoing corridor planning, construction and living requirements, planned capacity, so as to achieve the optimized and regulated land use to harmonize the substation with its surroundings.

The main buildings and structures (e.g., valve hall and control building) and large-sized equipment (e.g., converter transformer and smoothing reactor) should be located in the zones where the geological conditions are relatively good. In different sites, especially in the site where the terrain undulates dramatically and elevation differs greatly, the partial adjustment of the general layout affects significantly the converter station in total coverage, road connection, foundation treatment, land indemnification, and so on. Therefore, it is very important to verify the general layout in site selection [3].

26.1.3 Heavy-Duty Equipment Transport

The site of converter station should be near the existing or planned railways, highways, or waterways for reducing the investment in traffic and transport, expediting the construction progress and minimize the transport cost.

The equipment in UHVDC converter station subject to heavy-duty equipment transport is mainly converter transformer and smoothing reactor. According to the data of heavy-duty equipment used in the converter stations that are built or under construction, parameters of equipment subject to heavy-duty equipment transport are shown in Tables 26.1 and 26.2.

It can be seen from the table above that the heavy-duty equipment in UHV converter station has a large increase in terms of dimensions and weights of transport than the equipment used in previous substation, so they can be loaded on the special vehicles or the transport separately and assembly on site. Because more equipment is subject to heavy-duty equipment transport and longer time span of transportation, the waterway plus highway transport is the preferable method in transport selection, to reduce the effect to remove the obstructions and reinforce the bridges along the transport route, reduce the possible crossings, and mitigate the impact of frequent transport on road traffic. When considering the bridge reinforcement solution and rent of port, the influence caused by transport cycle shall also be taken into consideration.

26.1.4 Water Supply to Converter Station

The water to be used in the converter station includes production water, domestic water, fire-fighting water, etc.

Table 26.1 Parameters of equipment subject to heavy-duty equipment transport used in the ±800 kV converter station

S/N	Equipment name	Transport dimension Length (m) × width (m) × height (m)	Transport weight (t)	Quantity (set)
1	HV converter transformer	13.0 × 4.0 × 5.0	~360	12 + 2
2	LV converter transformer	10.5 × 4.0 × 5.0	~260	12 + 2
3	Smoothing reactor	5.3 × 5.3 × 4.5	~85	12 + 1

Table 26.2 Parameters of equipment subject to heavy-duty equipment transport used in the ±1100 kV converter station

S/N	Equipment name	Transport dimension Length (m) × width (m) × height (m)	Transport weight (t)	Quantity (set)
1	HV converter transformer	15.5 × 5.0 × 6.0	~550	12 + 2
2	LV converter transformer	14.0 × 4.5 × 5.5	~460	12 + 2
3	Smoothing reactor	6 × 6 × 4.6	~110	12 + 1

Operation of the converter station needs continuous supply of production water; therefore, the reliable water supply is a guarantee of safe operation of the converter station. There should be two reliable water supplies for the substation. If only one water supply is available, a reservoir of production water that sustains three days of production should be built up.

When selecting the station site, it is necessary to comprehensively calculate the water demand of the converter station first, and then carry out extensive investigation on water source around the planned site to determine the reliable water supply. In investigation of water source, attention shall be paid to following points:

1. Priority shall be given to running water or underground water. If it is difficult to acquire running or underground water, surface water can be adopted as water supply, but the influence caused by change of quality and amount of the water source shall be taken into sufficient consideration.
2. Water plant shall be subject to intensive investigation, including the name and capacity of the water reservoir supplying water to the plant, water supply capacity of running water pipe network, planned capacity of the plant, current water supply scope and margin of water supply, planned water consumption demand of surrounding consumers, etc.
3. It is necessary to investigate if the pipe size and water pressure of the running water pipe network satisfy the requirement to connect the water to the converter station and verify the distance of connection and the technical measures to be taken.
4. It is required to acquire the written commitment from the local running water company to supply water for the converter station.

It shall be noted that, if the water supply to two water plants comes from the same reservoir, the two plants cannot be deemed as two independent water supplies of the converter station even if the two plants have their own pipe networks, respectively. The quality of the water supply shall meet the current national standard *Standards for Drinking Water Quality*. The solution for water source and supply for the converter station shall be recommended finally after comprehensive technical and economic comparison.

26.1.5 Environmental Impact

The environmental impact involves two aspects, i.e., the impact of surroundings on the substation and the impact of substation construction on the surroundings.

1. The impact of surroundings on the converter station

Various pollutants in dirty area have negative effect on the operation reliability of electrical equipment in the substation. The intensity of the negative effect depends greatly on the conductivity, water absorbing quality and adhesive force of the

pollutants, the meteorologic conditions, the quantity of the pollutants, and the distance away from the pollution sources. If a substation locates in seriously dirty area, it may have negative effect on the DC equipment. As for the equipment of large creepage distance, the existing production capacity of the DC equipment manufacturer cannot well satisfy the outdoor conditions. Though the equipment arranged indoors can lead to fewer equipment manufacturing difficulties, the construction investment and operating cost are high; therefore, the site shall be selected in such a way to keep away from the area where the air is polluted seriously or there is heavy salt fog as far as possible.

2. The impact of converter station on the surroundings

The UHVDC converter station is large in scale. In addition to its impact on local planning, other issues including the control of the substation noise, regional water and soil conservation, harmonization of lines and iron towers with ambient environment, and discharged water quality shall be stressed in construction.

With the rapid development of Chinese DC transmission projects, multiple DC transmission projects have been constructed or put into operation. Because of many noise sources and higher sound power level in the UHV converter station, in view of the existing HV converter station in China, there is higher sound pressure level at the boundary and adjacent sensitive areas. Some converter stations had affected the neighborhood already.

In order to prevent the passive situation of mitigating the noise after construction of the substation, the measures to reduce noise must be taken into consideration in site selection and layout design of ±800 kV converter station. The site must be selected in such a way to keep as far away from the residential zone as possible and the layout of buildings and structures in the substation shall be reasonable. Meanwhile, the noise shall be reduced to the permissible level by fully making use of the buildings and structure to alleviate and absorb the noise and installing sound barriers. Ensure the converter station is harmonic with the environment and can be developed continuously.

26.2 Main Electrical Connection

The main electrical connection of the converter station, including mainly connection of converter unit, DC switchyard, AC switchyard, AC filter, reactive power compensation equipment, and substation-service power system, shall be determined according to the requirements of connected systems and the construction scale of the substation. Typical main electrical connections are shown in Fig. 26.1.

The scales of some UHVDC projects which are built or under construction are shown in Table 26.3.

26.2.1 Connection of Converter Unit

On the premise that the requirements of the system are met, the connection of converter unit shall be determined by considering the manufacturing capacity of thyristor, manufacturing level of converter transformer, and transport condition.

Because the transmission power of UHV converter station is quite large, the manufacture and transportation limit of converter transformer are the decisive factor that limit the unit connection of converter. According to the current manufacture capacity, the UHV converter station adopts series connection of two 12-pulse valve groups at each pole. The voltage of each pole of converter is configured as 400 kV (550 kV) + 400 kV (550 kV). To reduce the probability of the monopolar outage caused by the fault of single 12-pulse converter valve set, to raise the availability of DC system, and to reduce the impact on AC system, the DC switchyard shall be connected in such a way that when one 12-pulse valve group is out of operation, the other valve groups can keep operating. Each 12-pulse valve group shall be equipped with bypass switch and other equipment at its DC side.

26.2.2 Connection of DC Switchyard

26.2.2.1 Principles for Connection

The connection of DC switchyard shall have following functions [1, 2]:

1. To realize the basic connection for operation, such as bipolar and monopolar ground returns, monopolar metallic returns, etc.;
2. Isolation and grounding can be performed when any pole or any converter unit in the substation is overhauled;
3. Isolation and grounding can be performed when any pole of the DC line is overhauled;
4. Isolation and grounding can be performed when one or two ends of ground electrode of the DC system and their lead wires are overhauled during operation of complete or incomplete monopolar metallic circuit;
5. Isolation and grounding can be performed when one or two ends of ground electrode and their lead wires are overhauled during complete or incomplete bipolar operation;
6. When any one of the two poles is in operation, if changing the ground circuit operation to metallic circuit operation or vice versa, the DC power transmission shall not be interrupted and the DC transmission power shall not be decreased generally;
7. Cut-off and overhaul of faulty pole or converter unit shall not affect the power transmission of sound pole or converter unit.

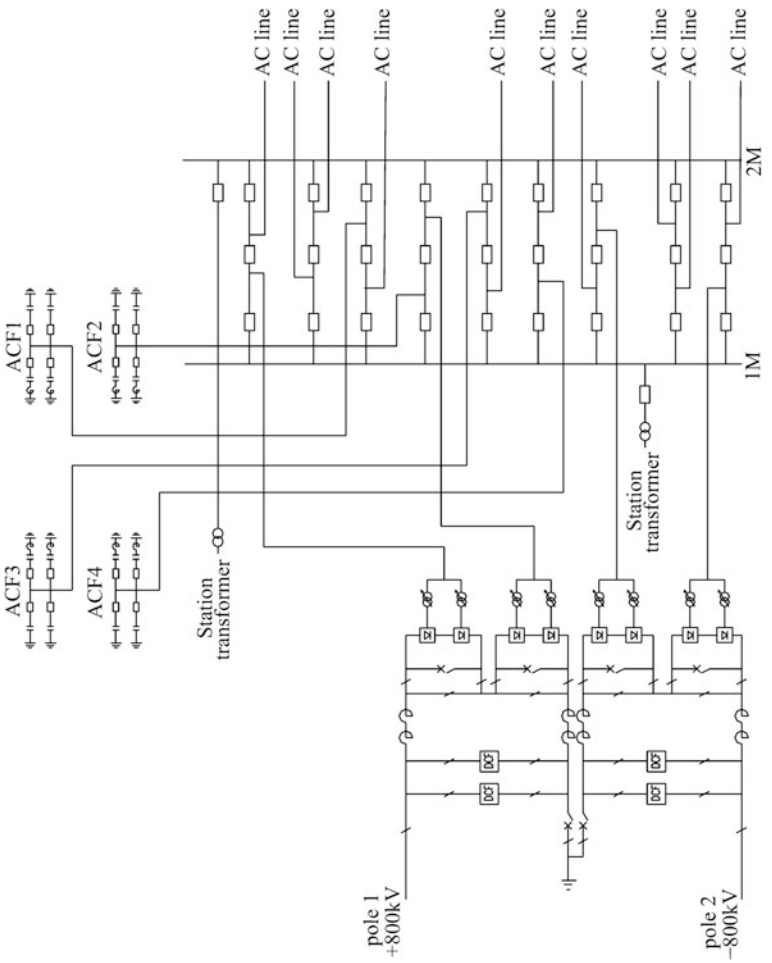

Fig. 26.1 Typical main electrical connection

Table 26.3 Scales of some UHVDC projects have been built or under construction

Items		Unit	Yunnan–Guangdong ±800 kV	Xiangjiaba–Shanghai ±800 kV	Jinping–South Jiangsu ±800 kV	South Hami–Zhengzhou ±800 kV	Left bank of Xiluodu–Zhejiang Jinhua ±800 kV	Zhundong–South Anhui ±1100 kV
Rated DC voltage		kV	800	800	800	800	800	1100
Rated transmission power		MW	5000	6400	7200	8000	8000	12,000
Rated DC current		A	3125	4000	4500	5000	5000	5455
Main connection	–	Including two complete single poles. Each complete single pole consists of two series-connected 12-pulse converters which having ±400 kV DC voltage						
DC bipolar line	Cross section	mm^2	6 × 630	6 × 720	6 × 900	6 × 1000	6 × 900	6 × 1250
	Distance	km	1373	1907	2090	2210	1680	3305
Nominal voltage at AC line side		kV	500	500	500	500	500	750
AC outgoing line	Sending end	Circuit	7	10	9	8	8	10
	Receiving end	Circuit	8	7	6	8	10	2/8[a]
Converter transformer	Sending end	MVA	(24 + 4) × 250	(24 + 4) × 321	(24 + 4) × 363	(24 + 4) × 405	(24 + 4) × 404	(24 + 4) × 608
	Receiving end	MVA	(24 + 4) × 244	(24 + 4) × 297	(24 + 4) × 341	(24 + 4) × 377	(24 + 4) × 382	(24 + 4) × 587
Smoothing reactor	Unipolar line	Set	2	2	2	3	3	3
	Unipolar neutral	Set	2	2	2	3	3	3

(continued)

Table 26.3 (continued)

Items		Unit	Yunnan–Guangdong ±800 kV	Xiangjiaba–Shanghai ±800 kV	Jinping–South Jiangsu ±800 kV	South Hami–Zhengzhou ±800 kV	Left bank of Xiluodu–Zhejiang Jinhua ±800 kV	Zhundong–South Anhui ±1100 kV
DC filter	Set of each pole	Set	2	1	1	1	1	1
	Tuning frequency	–	12/24/45	2/12/39	12/24 + 2/39	12/24 + 2/39	12/24 + 2/39	2/12
Filter and capacitor	Sending end	Mvar	11 × 187 (ACF) + 7 × 187(SC)	9 × 220 (ACF) + 5 × 220(SC)	9 × 215 (ACF) + 5 × 215(SC)	12 × 230 (ACF) + 5 × × 270 (SC)	10×239(ACF) + 10 × 290(SC)	12 × 305 (ACF) + 8 × 380(SC)
	Receiving end	Mvar	7 × 190 (ACF) + 8 × 210 (SC)	9 × 260 (ACF) + 6 × 260 (SC)	8 × 270 (ACF) + 8 × 270 (SC)	10 × 260 (ACF) + 9 × 260 (SC)	9 × 287 (ACF) + 8 × 287 (SC)	12 × 340 (ACF) + 9 × 285 (ACF) + 5 × 285 (SC)
Area within boundary	Sending end	hm^2	22.48	16.91	17.29	24.6	15.896	27.98
	Receiving end	hm^2	23.65	15.06	15.83	16.38	15.73	27.701

[a]The converter station at receiving end adopts the hierarchical access. LV valves are connected to the 1000 kV system, and the HV valves are connected to the 500 kV system. The number upon the "/" is the number of outgoing line in the 1000 kV system, and the number below the "/" is the number of outgoing line in the 500 kV system

26.2.2.2 Connection Method

The equipment of DC switchyard mainly consists of smoothing reactor, DC filter, DC measuring equipment, arrester, impulse capacitor, switchgear, etc. Considering the current equipment manufacturing capacity and by analyzing and comparing the connection method of DC yard in ±800 kV DC converter station, the connection method of DC yard shall adopt following methods.

1. The DC switchyard adopts the typical connection method of bipolar DC with ground electrode line. The DC filters, smoothing reactors, and other equipment are installed between pole lines. The smoothing reactors are series-connected to the polar busbar and neutral busbar, respectively, and installed closely to the valve group. The quantity of the smoothing reactor series-connected depends on the actual situation of the project, equipment manufacturing capacity, and limited conditions for heavy-duty equipment transport. The DC filter is connected to the pole line and the neutral line connected with valve group after the smoothing reactor to filter out the harmonic wave on the DC side, reducing the interference of the DC transmission lines on the adjacent communication lines. The DC filter shall be connected in such a way that the DC transmission power will not be interrupted or decreased when any one set of the filters is put into or out of operation. Therefore, a disconnector is provided on both HV and LV sides of the filter, and the disconnector on the HV side shall be capable of switching in normal operation. For the purpose of facilitating maintenance, an earth switch is installed on both sides of the filters.
2. In order to realize the most basic operating mode, i.e., bipolar and monopolar operation, in addition to the construction of the two pole lines, each pole shall be equipped with independent neutral busbar. In order to decrease the insulation level of equipment and reduce the investment, the bipolar neutral busbar shall be connected and grounded. During the monopolar ground return operation, a part of the current will return via the neutral point and the AC transmission line on the AC side of converter transformer; therefore, if the AC and DC systems share a grounding grid, high DC current will flow through the transformer, causing damage to the transformer, and interfering with the communication severely; furthermore, after such large DC current flows into the ground, it will corrode the objects buried underground seriously. For the purpose of reducing the impact of the DC current on the AC system and the equipment in the converter station, a ground electrode is set far away from the station and a neutral busbar is connected to such ground electrode via overhead line; besides, the neutral grounding is considered under various operating modes. In the converter station, a temporary ground electrode is set, serving as a standby ground electrode under the bipolar operating mode and the monopolar metallic return operating mode, so as to avoid the impact on the DC transmission in case of the maintenance or failure of the ground electrode line. In addition, for realization of the monopolar metallic return operating mode, the neutral points on the rectifier side and the inverter side need be connected via neutral line and grounded on either side.

However, considering that the projects are generally of bipolar lines, i.e., during the monopolar operation, the pole line of the other pole may be used as neutral line, so one of the neutral lines need not be constructed, which will save the investment and is technically feasible and considered by most of the projects as well, with mature operation experience.

3. The neutral busbar is equipped with corresponding high-speed transfer switch to adapt to the transfer between various operating modes. Furthermore, both the pole busbar and neutral busbar are equipped with corresponding disconnector and earthing switch to realize the safe maintenance under various operating modes and of the equipment.
4. In order to mitigate the impact of the high-frequency stray current on the pole line-ground return and pole line-metallic return, surge capacitor (C1) is installed on the neutral line side.

26.2.2.3 Connection of DC Deicing Operation

When the lines pass through heavily icing area, DC deicing operation shall be considered for the DC switchyard to increase the reliability of the lines. The operation method is to produce about two times of rated current on the DC lines by changing the connection pattern of the DC system, thus heating the DC lines up rapidly in short time to melt the ice adhered to the conductors, guaranteeing the safe operation of grid.

The connection of DC deicing operation method requires to change the connection pattern at the DC side, i.e., bypassing the LV 12-pulse valve groups of each pole and parallel-connecting the HV 12-pulse valve groups of each pole (with the parallel-connecting point arranged at the outlet of DC yard pole line) to generate two times of DC nominal current on the DC line, and to ensure the current flowing through the DC equipment is no higher than the rated current.

The connection of DC deicing operation is realized by the following measures:

1. Since the converter valve is unilaterally conductive, in order to realize the parallel connection of HV converter valve groups at both poles, the deicing connection shall be added to the bypass circuit of HV converter valve group of Pole 2 to turn over the voltage of the valve groups in case of deicing.
2. In order to provide the path to the current of HV converter valve group of Pole 2, the deicing circuits are added to the neutral busbar of Pole 2 and the metallic return from the outlet of the pole busbar of Pole 2.
3. The deicing connection shall be equipped with conversion device to fulfill the changeover between the normal operation and deicing operation.

The schematic diagram of DC yard connection with the deicing connection is shown in Fig. 26.2. Additionally installed deicing connection is represented by dashed lines.

The DC current direction in deicing operation is shown in Fig. 26.3. In the figure, Circuit 1 indicates the flow direction of the DC current passing through HV valve groups at Pole 1, and the amplitude of the current is that of the rated direct current; Circuit 2 indicates the flow direction of the DC current passing through HV valve groups at Pole 2, and the amplitude of the current is that of the rated direct current. The amplitude of current of the DC circuit is two times of that of the rated direct current.

26.2.3 AC Switchyard Connection

The connection method of the AC switchyard is determined through an economic comparison according to the position of converter station in the electric power system, the number of AC lines going into and out from the converter station, load characters, performance parameters of equipment and other conditions, and in combination with a comprehensive consideration in the reliability of power supply, flexibility of operation, convenience of operation and maintenance, facilitation of extension, reasonable investment, land saving, and other requirements. Moreover, the connection method shall also conform to the relevant requirements specified in DL/T *5218 Technical Code for the Design of* 220–750 kV *Substation*. Since the

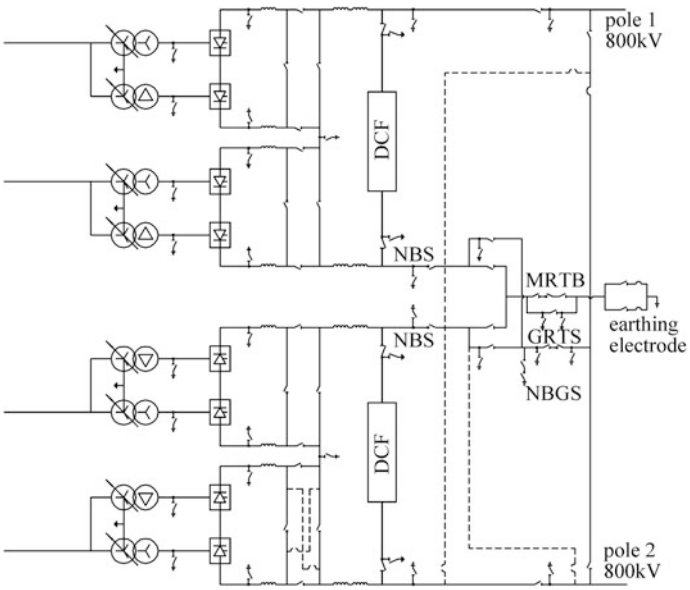

Fig. 26.2 Connection for DC-based deicing solution

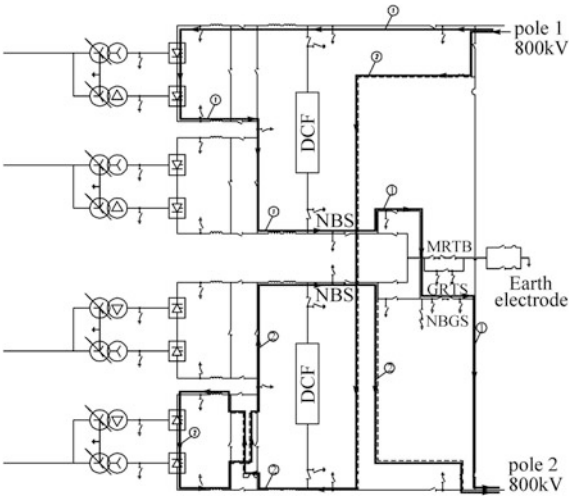

Fig. 26.3 Schematic diagram of DC current direction in deicing operation

voltage of the AC system to which the UHV converter station is connected is always 500 kV or higher, the connection of the AC switchyard of all UHV converter stations under construction and completed is of 3/2 connection pattern which is highly reliable and flexible in operation.

26.2.4 AC Filter Connection

The connection of AC filter shall be determined by comprehensively taking into consideration the DC system requirements as well as the influence of AC filter switching on the AC and DC system. The AC filters in the UHV converter station always have 16–26 sub-banks. If the AC filters are connected to the AC busbar in the way of sub-bank, the switchers in the AC switchyard will be quite a lot. Due to frequent operation of circuit breaker of filter sub-bank, the reliability of AC busbar will reduce. So, the AC filters are usually connected to the AC busbar of converter unit in the way of grouping into banks. 4–5 AC filter banks are usually set in the UHV converter station, and every bank is connected with 4–6 AC filter sub-banks. The AC filter bank adopts single bus connection.

26.3 Overvoltage Protection of Converter Station

Overvoltage can be divided into two types, i.e., internal and external overvoltage. For the internal overvoltage, the dynamic, operating, and transient overvoltage shall be considered, but the resonance overvoltage is generally left out of account.

Generation of resonance overvoltage shall be avoided in design and operation of the converter station. If the resonance overvoltage is inevitable, appropriate measures shall be taken, such as installation of phase-selection closing device or closing resistor.

The external overvoltage refers mainly to the lightning strike on the AC and DC lines and ground electrode lines, including direct lightning stroke and shielding failure. Considering the damping effect of the smoothing reactor on the lightning invasion wave, the overvoltage caused by the lightning strike on line generally does not impact the relevant equipment on the valve side of smoothing reactor. The internal overvoltage includes the overvoltage on the AC side and DC side. The overvoltage on the AC side is mainly caused by load rejection in DC system, AC system to ground fault, switching of AC filter, etc., while the overvoltage on the DC side is mainly caused by ground fault in DC system, short circuit, and failure of control, etc. The said overvoltage will be transferred to converter valve or pole line.

The purpose of overvoltage protection and insulation coordination is to seek for a solution of arrester configuration and parameter selection so as to ensure the safety of all equipment (including arrester itself) in the substation in normal operation, during fault period, and after fault; and achieve the most economic effect of the whole substation.

The basic principles of overvoltage protection and arrester configuration of the substation are as follows [1]:

(1) The overvoltage generated at AC side shall be restricted by the arresters at AC side.
(2) The overvoltage generated at DC side shall be restricted by the arresters at DC side.
(3) The key equipment in the substation shall be protected by the arresters near the equipment.
(4) The winding at the valve side of converter transformer can be protected by the combination of the arresters protecting other equipment. The winding at the valve side of converter transformer with the maximum potential voltage can be directly protected by the arresters closest to it.
(5) The arresters of multi-column parallel structure can be adopted. The parallel dispersion configuration of multiple arresters can also be adopted.
(6) The DC neutral busbar shall be equipped with impulse capacitor.

Other overvoltage protection measures include:

(1) In order to protect the thyristors against damage by positive overvoltage, in addition to installing arresters on the valve arm, positive overvoltage protective trigger device shall be installed on the valve arm of each thyristor as backup protection of overvoltage on the valve.
(2) The incoming circuit breaker of converter transformer shall be mounted with closing resistor to damp the impulse voltage when closing the no loaded converter transformer and to restrict the inrush current in closing.

(3) Each circuit breaker of AC filter sub-bank shall be equipped with phase-selection closing device to limit the inrush current in closing, decrease the interference on the system caused by the AC filter putting into and out of operation and by operation of capacitor, and guard against the overvoltage on internal elements at the LV side of AC filter in closing.

The typical configurations of the arresters on the DC side of the ±800 kV UHV converter station of State Grid and Southern Power Grid are shown in Figs. 26.4 and 26.5, respectively, while those of the arresters on the DC side of the ±1100 kV UHV converter station are shown in Fig. 26.6. The AC-side outgoing line, station transformer, and filter bank busbar are also equipped with arresters, respectively.

It can be seen from Figs. 26.4 and 26.5 that the arrester on the LV 12-pulse converter unit is basically same as that on the neutral busbar in terms of configuration in the ±800 kV converter stations of State Grid and Southern Power Grid, but that on the HV 12-pulse converter unit is greatly different. In the projects of Southern Power Grid, A2 arrester is provided on the converter transformer valve side at the highest end, and C2 arrester is provided for the whole HV 12-pulse converter unit, eliminating the MH and CBH arresters as used in the projects of China Sate Grid. Each of the two protection modes has its own advantages and disadvantages. A particular analysis shall be made on the basis of the particular conditions to determine which scheme is more appropriate.

The following is an expatiation of ±800 kV converter stations, in which Fengxian Station of State Grid and Pu'er Station of Southern Power Grid are taken as examples, and of ±1100 kV converter stations, in which Zhundong Station is taken as an example. The protection level of each arrester used at Fengxian, Pu'er, and Zhundong converter stations is listed in Tables 26.4, 26.5 and 26.6.

26.4 Insulation Levels of Equipment

The insulation levels of electrical equipment are determined through insulation coordination, i.e., determined from the aspects of safe operation, technical reasonability, and economic reasonability according to the possible overvoltage level on the equipment of the system and taking the protection level of the corresponding arresters into consideration. The insulation coordination method of the DC substation is same as that of the AC system, which is a usual practice, i.e., the lightning impulse withstand level (LIWL), switching impulse withstand level (SIWL), or steep-front impulse withstand level (SFIWL) are determined by multiplying the protection level of the arrester by a certain coefficient.

Withstand levels of each point at DC side in Fengxian, Pu'er, Zhundong converter station are shown in Tables 26.7, 26.8 and 26.9.

The lightning impulse protection level (LIPL) and switching impulse protection level (SIPL) of arresters and their corresponding coordination current shall be studied on the basis of lightning and switching digital simulation, and taking into consideration the discharge capacity of the arrester and the number of internal

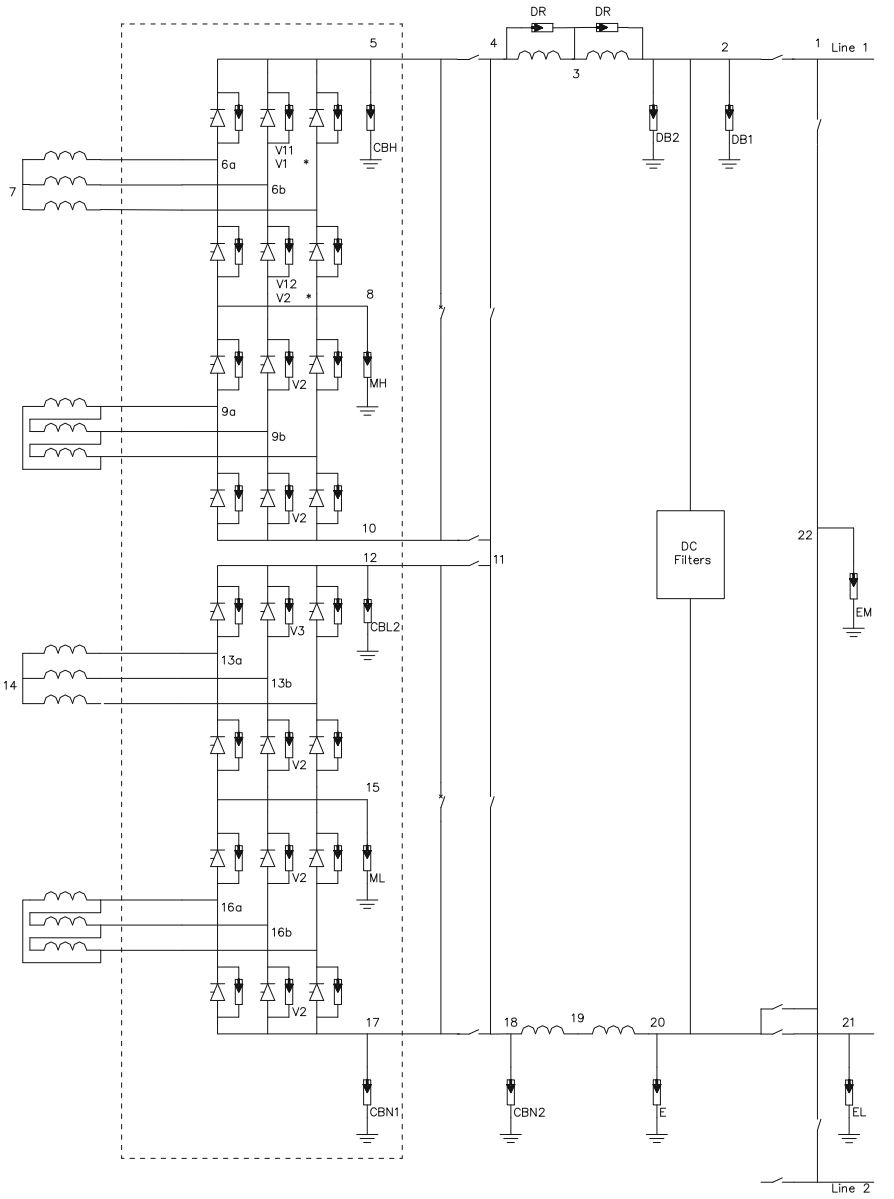

Fig. 26.4 Typical arrester configuration of ±800 kV UHV converter station of state grid

parallel columns. The 8/20 and 30/60 μs lightning and switching impulse current characteristics of the arrester are generally used for the digital simulation calculation.

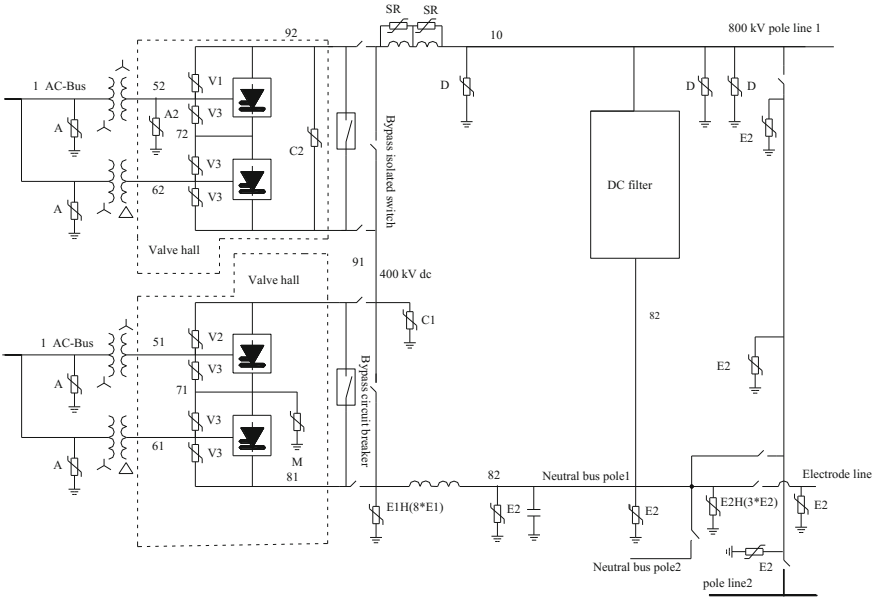

Fig. 26.5 Typical arrester configuration of ±800 kV UHV converter station of southern power grid

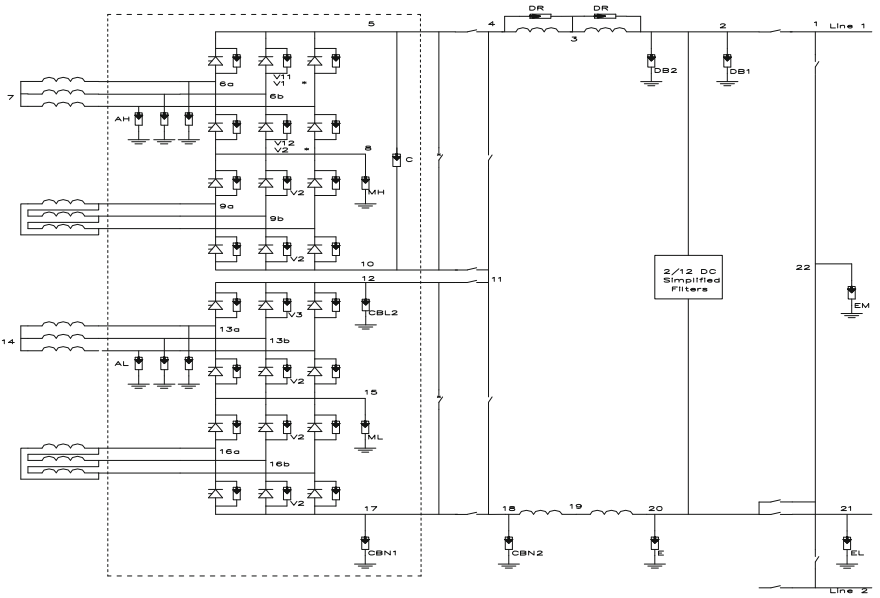

Fig. 26.6 Typical arrester configuration of ±1100 kV UHV converter station

Table 26.4 Protection levels of each arrester in ±800 kV Fengxian converter station

Arrester	CCOV (kV)	PCOV (kV)	LIPL (kV)	SIPL (kV)	Column number	Energy (MJ)
V1	233.2	278.2	361	386	6	7.5
V2	233.2	278.2	368	386	3	3.7
V3	233.2	278.2	368	386	3	3.7
DB1	824	–	1625	1391	3	13.3
DB2	824	–	1625	1391	3	13.3
CBH	859	895	1397	1356	4	19.0
MH	637.7	672.2	1058	1009	4	14.2
CBL2	433.6	468.7	719	685	4	9.7
ML	250	285	495	485	2	3.3
CBN1	77	112	458	–	3	3.1
CBN2	77	112	419	437	6	8.5
E	20	–	345	–	2	2.0
EL	20	–	311	303	6	5.6
EM	20	–	386	341	2	2.0
DR	44	–	900	–	1	3.3
A	$550/\sqrt{3}$	–	942	761	1	41.0

Table 26.5 Protection levels of each arrester in ±800 kV Pu'er converter station

Arrester	MCOV/CCOV (kV)	LIPL (kV)	SIPL (kV)	Column number	Energy (MJ)
A	318ac	907	776	1	4.5
A2	885	1344	1344	2	9
V1	245	395	395	8	10
V2	245	395	395	4	5
V3	245	395	395	2	2.6
M	245	500	500	2	3.4
C1	477	791	706	2	4.6
C2	477	791	706	2	4.6
D	816	1579	1328	2	9
E1	52dc + 80ac	320	269	4	3.6
E2	52dc	320	269	4	3.6
SR	>40ac	719	641	1	2

The pollution level at the DC side of the substation shall be determined according to the study result of pollution predication. Appropriate umbrella structure shall be chosen according to the pollution characteristics in external insulation design of the DC equipment. When designing the external insulation of converter station in high-altitude area, the impact of high altitude on flashover of external insulation shall be considered, and corrected properly.

Table 26.6 Protection levels of each arrester in ±1100 kV Zhundong converter station

Arrester	PCOV (kV)	CCOV (kV)	LIPL (kV)	SIPL (kV)	Column number	Energy (MJ)
V11	399.3	344.5	520.7/2[a]	534.1/4[a]	8	21
V12	399.3	344.5	534.1/2[a]	552.2/4[a]	4	8.5
V2	409.3	344.5	550.6/2[a]	569.3/4	4	9
V3	409.3	344.5	550.6/2[a]	569.3/4[a]	4	9
ML	–	400	701.7/2[a]	661.6/0.5[a]	2	5.3
MH	970	906	1536/2[a]	1425/0.2[a]	4	22
CBL2	718	641	1094/2[a]	1026/0.2[a]	4	14.9
AH	1298	1204	1913/2[a]	1820/0.5[a]	4	38.7
AL	718	641	1081/2[a]	1028/0.5[a]	4	21.8
DB1	–	1170	2125/20[a]	1826/1[a]	8	32
DB2	–	1170	2125/10[a]	1826/1[a]	8	32
CBN1	212	165	476/2[a]	/	2	4.4
CBN2	212	165	426/2[a]	448/14[a]	20	60
E	–	90	478/5[a]	/	2	4.1
EL	–	20	311/10[a]	303/8[a]	6	8.3
EM	–	90	431/20[a]	398/7[a]	16	110
A	–	462	1380/20[a]	1142/20[a]	1	
A′				365		
DR	–	50	1276/0.5[a]	–	1	5

[a]The number behind the "/" is corresponding current, in kA

26.5 Minimum Air Clearance Distance

When designing the air clearance distance at DC side of the converter station, the impact of combination of DC, AC, lighting, and switching impulse voltages shall be thought over mainly. Because the live conductors of equipment in the substation are mainly fixed poles, the air clearance distance is determined largely by lightning and switching impulse. In order to calculate the air clearance distance at the DC side precisely, the discharge characteristic curve of overhead flexible conductor, tubular rigid busbar versus frame, electrical equipment (grading ring) versus frame, and tubular busbar versus valve hall's steel column are needed.

In terms of lightning impulse, there is a linear relationship between its flashover voltage and clearance length. In terms of switching impulse, there is a non-linear relationship between the flashover voltage and clearance length. The discharge voltage presents a non-linear saturation trend with the increase of voltage level, and 1600 kV is a very obvious inflection point position. Because of the saturation characteristic of the clearance under switching impulse, the air clearance distance required under switching voltage in the valve hall is usually greater than the clearance distance determined by the lightning impulse. Therefore, the greater one

Table 26.7 Withstand levels of each point at DC side in ±800 kV Fengxian converter station

	Protection equipment	LIPL (kV)	LIWL (kV)	Margin (%)	SIPL (kV)	SIWL (kV)	Margin (%)
Both sides of valve	Max(V1, V2, V3)	368	405	10	386	425	10
AC busbar	A	942	1550	64	761	1175	54
DC busbar (line side)	Max(DB1, DB2)	1625	1950	20	1391	1600	15
DC busbar (valve side)	CBH	1397	1800	28	1356	1600	18
Both ends of smoothing reactor on pole bus	DR	900	1080	20	–	–	–
Across the HV 12-pulse bridge	Max (V1 + V2) + V2	736	884	20	772	888	15
Phase-to-ground on valve side of HV Yy converter transformer	V2 + MH*	1426	1712	20	1360	1564	15
Neutral point on valve side of HV Yy converter transformer	A′ + MH	–	–	–	1261	1451	15
Busbar at middle point on HV 12-pulse bridge	MH	1058	1270	20	1009	1161	15
Phase-to-ground on valve side of HV Yd converter transformer	V2 + CBL2	1087	1305	20	1071	1232	15
Middle point between HV and LV 12-pulse bridges	CBL2	719	863	20	685	788	15
Phase-to-ground on valve side of LV Yy converter transformer	V2 + ML	863	1036	20	871	1002	15
Neutral point on valve side of LV Yy converter transformer	A′ + ML	–	–	–	737	848	15
Busbar at middle point of LV 12-pulse bridge	ML	495	594	20	485	558	15
Phase-to-ground on valve side of LV Yd converter transformer	Max(V2 + CBN1, V2 + CBN2)	826	996	20	823	947	15
Phase-to-phase on valve side of Yy converter transformer	2*A′	–	–	–	504	580	15
Phase-to-phase on valve side of Yd converter transformer	$\sqrt{3}$*A′	–	–	–	436	502	15

(continued)

Table 26.7 (continued)

	Protection equipment	LIPL (kV)	LIWL (kV)	Margin (%)	SIPL (kV)	SIWL (kV)	Margin (%)
Valve side of neutral busbar	Max(CBN1, CBN2)	458	550	20	437	503	15
Line side of neutral busbar	Max(E, EL, EM)	386	464	20	341	393	15
Ground electrode busbar	EL	311	374	20	303	349	15
Metallic return busbar	EM	386	464	20	341	393	15
Both ends of smoothing reactor on neutral bus	CBN2 + E	–	764	917	20	–	–

Table 26.8 Withstand levels of each point at DC side in ±800 kV Pu'er converter station

	Protection equipment	LIPL (kV)	LIWL (kV)	Margin (%)	SIPL (kV)	SIWL (kV)	Margin (%)
AC busbar	A	907	1550	71	776	1175	51
Phase-to-ground on valve side of LV Yy converter transformer	M + V3	–	1300	–	895	1050	17
Phase-to-ground on valve side of LV Yd converter transformer	V3 + E1	–	950	–	641	750	17
Busbar at middle point of LV 12-pulse bridge	M	500	750	50	500	600	20
Neutral point on valve side of HV Yy converter transformer	A2	1344	1800	34	1344	1600	19
Phase-to-ground on valve side of HV Yd converter transformer	C1 + V3	–	1550	–	1101	1300	18
Busbar at middle point of HV 12-pulse bridge	C1 + V3	–	1550	–	1101	1300	18
Valve side of neutral busbar	E1	320	450	41	269	325	21
Line side of smoothing reactor on neutral bus	E2	320	450	41	269	325	21
Middle point between HV and LV 12-pulse bridges	C1	791	1175	49	706	950	35
DC busbar (valve side)	A2	–	1800	–	1344	1600	19
DC busbar (line side)	D	1579	1950	23	1328	1600	20
Between outgoing line of LV Yy and Yd converter transformer	A′	–	750	–	473	650	37

(continued)

Table 26.8 (continued)

	Protection equipment	LIPL (kV)	LIWL (kV)	Margin (%)	SIPL (kV)	SIWL (kV)	Margin (%)
Between the middle points of two 6-pulse converter bridge of LV 12-pulse converter bridge	2V	–	1175	–	790	950	20
Across the LV 12-pulse bridge	C1E1	–	1175	–	706	950	35
Between outgoing line of HV Yy and Yd converter transformer	A′	–	750	–	473	650	37
Between the middle points of two 6-pulse converter bridge of HV 12-pulse converter bridge	2V	–	1175	–	790	950	20
Across the HV 12-pulse bridge	C2	740	1175	59	706	950	35
Both sides of smoothing reactor on pole line	SR	719	1050	46	641	950	48
Both sides of smoothing reactor on neutral bus	E1E2	–	450	–	269	375	39
Valves	V	395	454	15	395	454	15

Table 26.9 Withstand levels of each point at DC side in ±1100 kV Zhundong converter station

	Protection equipment	LIPL (kV)	LIWL (kV)	Margin (%)	SIPL (kV)	SIWL (kV)	Margin (%)
Both sides of valve	Max (V11/V12/V2/V3)	551	606	10	569	627	10
AC busbar (HV end)	A	1380	2100	52.2	1142	1550	35.8
DC busbar (smoothing reactor side)	Max(DB1, DB2)	2125	2550	20	1826	2100	15
Both sides of smoothing reactor	DR	1276	1532	20	–	–	15
Across the HV 12-pulse bridge	Max(V1, V2) + V2	1085	1302	20	1122	1290	15

(continued)

Table 26.9 (continued)

	Protection equipment	LIPL (kV)	LIWL (kV)	Margin (%)	SIPL (kV)	SIWL (kV)	Margin (%)
Phase-to-ground on valve side of HV Yy converter transformer	AH	1913	2295	20	1820	2093	15
Neutral point on valve side of HV Yy converter transformer	A′ + MH	/	/	20	1790	2059	15
Busbar at middle point of HV 12-pulse bridge	MH	1536	1845	20	1425	1639	15
Phase-to-ground on valve side of HV Yd converter transformer	V2 + CBL2	1645	1974	20	1596	1835	15
Middle point between HV and LV 12-pulse bridges	CBL2	1094	1313	20	1026	1180	15
Phase-to-ground on valve side of LV Yy converter transformer	AL	1081	1297	20	1028	1182	15
Neutral point on valve side of LV Yy converter transformer	A′ + ML	/	/	20	1027	1181	15
Busbar at middle point of LV 12-pulse bridge	ML	701.7	842	20	661.6	761	15
Phase-to-ground on valve side of LV Yd converter transformer	Max(V2 + CBN1, V2 + CBN2)	1027	1233	20	1018	1171	15
Phase-to-phase of Yy at valve side	2*A′	/	/	20	730	840	15
Phase-to-phase of Yd at valve side	$\sqrt{3}$*A′	/	/	20	632	727	15
Valve side of neutral busbar	Max(CBN1, CBN2)	476	571	20	448	516	15
Line side of neutral busbar	Max(E, EL, EM)	478	574	20	398	458	15
Ground electrode busbar	EL	311	373	20	303	348	15
Metallic circuit busbar	EM	431	517	20	398	458	15
Both sides of smoothing reactor on neutral bus	CBN2 + E	904	1085	20	/	/	15

of the calculated results of lightning impulse and switching impulse shall be taken as the minimum clearance distance.

It can be known from the above analysis that the air clearance is bound up with the insulation coordination of converter station. Therefore, the converter station's arrester configuration and insulation coordination need to be made clear first to determine LIWL and SIWL at each point based on which the calculation can be conducted according to the environmental conditions.

The minimum clearances at various points in the valve halls at Fengxian, Pu'er, and Zhundong converter stations are given in Tables 26.10, 26.11, 26.12 and 26.13. The minimum clearances at the DC switchyards of Fengxian and Pu'er Converter Stations are given in Tables 26.14 and 26.15. The minimum clearances at various points in indoor DC switchyard of Zhundong converter station are given in Table 26.16.

26.6 Selection of Main Electrical Equipment

26.6.1 Calculation of Short-Circuit Current

26.6.1.1 Short-Circuit Current Level of AC Busbar of the Converter Station

The DC project's bipolar operation design level year and far-seeing development design level year are predominantly chosen for the short-circuit current calculation, and the minimum short-circuit current of DC project's monopolar operation level year shall be subject to verification. The minimum short-circuit level of the AC busbar of the substation shall be determined according to the calculation and analysis of short-circuit current of the design level year. Then the AC filters and capacitors shall be banked and selected on the basis of the minimum short-circuit level. The maximum short-circuit current level of the AC busbar of the substation shall be determined on the basis of the calculation and analysis of short-circuit current of far-seeing level year, to provide a reference for the selection of equipment such as circuit breaker.

26.6.1.2 Short-Circuit Current at DC Side

With respect to the short-circuit current at DC side of the converter station, the decisive fault conditions generally include the following types:

1. For the busbars in thyristor valve and thyristor valve bridge: short-circuit current generated when both ends of a single valve are short-circuited.

Table 26.10 Minimum air clearances in valve hall at ±800 kV Fengxian converter station

Position	Insulation level (kV)	Minimum air clearance (mm)
	SIWL	
+800 to +400 kV or −800 to −400 kV	950	4216
+800 to 6-pulse neutral point of HV valve group or −800 to 6-pulse neutral point of HV valve group	550	1765
+400 to 6-pulse neutral point of HV valve group or −400 kV to 6-pulse neutral point of HV valve group	550	1765
+400 kV to DC neutral busbar or −400 kV to DC neutral busbar	950	4216
+400 kV to 6-pulse neutral point of LV valve group or −400 kV to 6-pulse neutral point of LV valve group	550	1765
DC neutral busbar to 6-pulse neutral point of LV valve group	550	1765
+800 or −800 kV on valve side of smoothing reactor to ground	1600	9327
6-pulse neutral point of HV valve group to ground	1300	6722
+400 or −400 kV to ground	950	4101
6-pulse neutral point of LV valve group to ground	550	1747
DC neutral busbar on valve side of smoothing reactor to ground	504	1529
HV Yy—A/B/C to ground	1600	9327
HV Yy—x/y/z to ground	1600	9327
HV Yd phase-to-ground	1300	6722
LV Yy—A/B/C to ground	1050	4801
LV Yy—x/y/z to ground	950	4101
Phase-to-ground of LV Yd	1050	4801
Phase-to-phase on valve side of HV Yy	750	2885
Phase-to-neutral point on valve side of HV Yy	350	897
Phase–to-phase on valve side of HV Yd	550	1765
Between lead wires of valves sides of HV Yy and Yd	1050	4956
Phase–to-phase on valve side of LV Yy	750	2885
Phase-to-neutral point on valve side of LV Yy	350	897
Phase–to-phase on valve side of LV Yd	550	1765
Between lead wires of valves sides of LV Yy and Yd	1050	4956
HV Yy—A/B/C to +800 or −800 kV	550	1765
HV Yy—A/B/C to 6-pulse neutral point of HV valve group	550	1765
HV Yd to 6-pulse neutral point of HV valve group	550	1765
HV Yd to +400 or −400 kV	550	1765
LV Yy—A/B/C to +400 or −400 kV	550	1765
LV Yy—A/B/C to 6-pulse neutral point of LV valve group	550	1765
LV Yd to 6-pulse neutral point of LV valve group	550	1765
LV Yd to DC neutral busbar	550	1765
HV Yy—A/B/C to +400 or −400 kV	1050	4956
HV Yy—x/y/z to +400 or −400 kV	1050	4956
LV Yy—A/B/C to DC neutral busbar	1050	4956
LV Yy—x/y/z to DC neutral busbar	1050	4956
Between HV and LV 12-pulse bridges	950	4216

Note As the lightning current is not the dominant factor in the determination of minimum air clearance, the LIWL is not required, the same below

Table 26.11 Minimum air clearances in HV valve hall at ±800 kV Pu'er converter station

				LIWL (kV)	SIWL (kV)	Coefficient	Minimum air clearance (mm)
52	Bushing of Y converter transformer	Phase–to-ground	Ring-plate	1800	1613	1.2	7026
52–52	Bushing of Y converter transformer	Phase-to-phase	Ring-ring	750	568	1.3	1654
52N–52	Bushing of Y converter transformer	Phase-to-phase	Ring-ring	550	328	1.3	1213
52N	Neutral point of Y converter transformer	Phase-to-ground	Ring-plate	1675	1446	1.2	5932
52N	Neutral point of Y converter transformer	Phase-to-ground	Rod-plate	1675	1446	1.15	6289
62	Bushing of Δ converter transformer	Phase-to-ground	Ring-plate	1550	1321	1.2	5166
62	Bushing of Δ converter transformer	Phase-to-phase	Ring-ring	750	568	1.3	1654
52–62	Bushing of Y converter transformer—bushing of Δ converter transformer	Phase-to-phase	Ring-ring	1175	948	1.3	2901
52–72	Bushing of Y converter transformer—HV 6-pulse neutral point	Phase-to-phase	Ring-ring	494	474	1.3	1090
52–92	Bushing of Y converter transformer—800 kV busbar	Phase-to-phase	Ring-ring	494	474	1.3	1090
52N–92	Neutral point of Y converter transformer—800 kV busbar	Phase-to-phase	Ring-ring	950	802	1.3	2302
52–91	Bushing of Y converter transformer—800 kV busbar	Phase-to-phase	Ring-rod	988	948	1.15	3314
52N–91	Neutral point of Y converter transformer—800 kV busbar	Phase-to-phase	Ring-rod	950	802	1.15	2600
62–91	Bushing of Δ converter transformer—neutral 400 kV	Phase-to-phase	Ring-ring	494	474	1.3	1090
72	HV 6-pulse neutral point	Phase-to-ground	Rod-plate	1550	1321	1.15	5466
92	800 kV valve group—ground	Phase-to-ground	Structural block-plate	1800	1613	1.2	7026
92	800 kV valve group—wall	Phase-to-ground	Structural block-plate	1800	1613	1.15	7463
92	800 kV busbar—ground	Phase-to-ground	Rod-plate	1800	1613	1.15	7463
92	800 kV wall bushing	Phase-to-ground	Ring-plate	1800	1613	1.2	7026
91–92	800 kV busbar—400 kV busbar	Phase-to-phase	Rod-rod	1175	847	1.3	2592

Table 26.12 Minimum air clearances in LV valve hall at ±800 kV Pu'er converter station

				LIWL (kV)	SIWL (kV)	Coefficient	Minimum air clearance (mm)
51	Bushing of Y converter transformer	Phase-to-ground	Ring-plate	1300	1074	1.2	3787
51–51	Bushing of Y converter transformer	Phase-to-phase	Ring-ring	750	568	1.3	1654
51N–51	Bushing of Y converter transformer	Phase-to-phase	Ring-ring	550	328	1.3	1213
51N	Neutral point of Y converter transformer	Phase-to-ground	Ring-plate	1050	928	1.2	3060
51N	Neutral point of Y converter transformer	Phase-to-ground	Rod-plate	1050	928	1.15	3212
61	Bushing of Δ converter transformer	Phase-to-ground	Ring-plate	950	797	1.2	2466
61	Between bushings of Δ converter transformer	Phase-to-phase	Ring-ring	750	568	1.3	1654
51–61	Bushing of Y converter transformer to bushing of Δ converter transformer	Phase-to-phase	Ring-ring	1175	948	1.3	2901
51–71	Bushing of Y converter transformer—LV 6-pulse neutral point	Phase-to-phase	Ring-ring	494	474	1.3	1090
51–91	Bushing of Y converter transformer—400 kV busbar	Phase-to-phase	Ring-ring	494	474	1.3	1090
51N–91	Neutral point of Y converter transformer—400 kV busbar	Phase-to-phase	Ring-ring	950	802	1.3	2302
61–81	Bushing of Δ converter transformer—neutral busbar	Phase-to-phase	Ring-ring	494	474	1.3	1090
71	LV 6-pulse neutral point	Phase-to-ground	Rod-plate	750	600	1.15	1722
91	400 kV valve group to ground	Phase-to-ground	Structural block-plate	1175	847	1.2	2687
91	400 kV busbar to ground	Phase-to-ground	Rod-plate	1175	847	1.15	2813
91	400 kV wall bushing	Phase-to-ground	Ring-plate	1175	847	1.2	2687
81–91	400 kV busbar to neutral busbar	Phase-to-phase	Rod-rod	1175	847	1.3	2592
81	Neutral wall bushing	Phase-to-ground	Ring-plate	450	323	1.2	1019

Table 26.13 Minimum air clearances in indoor valve hall at ±1100 kV Zhundong converter station

Typical clearance	SIWL (kV)	Coefficient	Minimum air clearance (mm)
Valve side of pole line smoothing reactor (5-0)	2100	1.35	11,000
Both sides of valve (5–6a/6a–8…)	656	1.3	1700
Both sides of 12-pulse converter	1290	1.2	5300
Phase-to-ground on valve side of HV Yy converter transformer (6a–0)	2100	1.35	11,000 (to ground) 1300 × to ground = 15,000 (to side wall)
Phase-to-phase on valve side of HV Yy converter transformer (6a–6b)	840	1.3	2400
Phase to neutral point on valve side of HV Yy converter transformer (6a–7)	420	1	1400
Neutral point to ground on valve side of HV Yy converter transformer (7-0)	2059	1.35	10,300
Valve side of Yy converter transformer to valve side of Yd converter transformer (6a–9a, 13a–16a)	1290	1.2	5300
Yy neutral point to valve side of Yd converter transformer (7–9a, 14–16a)	1081	1.2	4000
HV 12-pulse Yy neutral point to 550 kV busbar (7–10)	1081	1.35	3300
Busbar at middle point of HV 12-pulse bridge (8-0)	1639	1	12,000
Phase-to-ground on valve side of HV Yd converter transformer (9a-0)	1835	1.2	10,400 (to ground) 1300 × to ground = 13,600 (to side wall)
Phase-to-phase on valve side of HV Yd converter transformer (9a–9b)	727	1.3	2000
Middle point between HV and LV 12-pulse bridges (10-0)	1180	1.1	5300
550 kV busbar to neutral point of 12-pulse Yy converter transformer (12–14)	420	1	1400
Phase-to-ground on valve side of LV Yy converter transformer (13a-0)	1182	1.2	4600
Phase-to-phase on valve side of LV Yy converter transformer (13a–13b)	840	1.3	2400
Phase to neutral point on valve side of LV Yy converter transformer (13a–14)	420	1	1400
Neutral point on valve side of LV Yy converter transformer (14-0)	1181	1.2	4600
Busbar of middle point of LV 12-pulse bridge (15-0)	761	1	3100
Phase-to-ground on valve side of LV Yd converter transformer (16a-0)	1158	1.2	4400 (to ground) 1300× to ground = 5800 (to side wall)
Phase-to-phase on valve side of LV Yd converter transformer (16a–16b)	727	1.3	2000
Valve side of neutral busbar smoothing reactor	503	1	1700

Table 26.14 Minimum air clearances in DC Switchyard at ±800 kV Fengxian converter station (mm)

Clearance characteristics	Conductor to plane	Conductor to equipment support or parallel conductor	Conductor to conductor
Pole busbar to ground	7220	6030	5218
Neutral busbar to ground	340	277	245
Pole busbar to pole busbar	15,787	12,314	12,535
Pole busbar to neutral busbar	9279	7209	6301
Neutral to neutral	1082	882	779

Table 26.15 Minimum air clearances in DC Switchyard at ±800 kV Pu'er converter station

	LIWL (kV)	SIWL (kV)	Minimum air clearance (mm) (coefficient k = 1.15)
10-pole busbar to neutral busbar	1950	1600	8000
8–10-pole busbar to neutral busbar	NA	NA	–
91 valve group busbar to ground	1175	950	3600
8 neutral busbar to ground	450		1000

2. For the busbar connected with the bushing at valve side of converter transformer: short-circuit current generated when there is three-phase short circuit between converter transformer and thyristor valve bridge.
3. For the DC wall bushing and DC pole busbar at valve side of smoothing reactor: short-circuit current generated when the DC pole busbar between thyristor valve bridge and smoothing reactor has a ground fault.
4. For the smoothing reactor and DC pole busbar at DC line side of smoothing reactor: short-circuit current generated when the pole busbar on the DC line side of smoothing reactor has a ground fault.
5. For the neutral busbar equipment and neutral busbar: short-circuit current generated when the neutral point of converter transformer has a ground fault and that generated when the DC pole busbar between thyristor valve bridge and smoothing reactor has a ground fault.

Table 26.16 Minimum air clearances in indoor DC Switchyard at ±1100 kV Zhundong converter station

Typical clearance	SIWL (kV)	Clearance coefficient	Minimum air clearance (mm)
±1100 kV main air clearance	2100	1.25	13,000
±1100 kV air shunt clearance	2100	1.2	15,000
±1100 kV grading ring to grading ring	2100	1.3	12,000
±1100 kV grading ring to steel structure	2100	1.2	15,000
±1100 kV grading ring to support (including adjacent support)	2100	1.25	13,000
±1100 kV grading ring to fence, protective cage, and ground	2100	1.25	13,000
±1100 kV tubular busbar to ground	2100	1.25	13,000
±1100 kV tubular busbar to steel structure	2100	1.2	15,000
±1100 kV tubular busbar to support (including adjacent support)	2100	1.25	13,000
±1100 kV tubular busbar to protective cage	2100	1.25	13,000
Smoothing reactor to ground	2100	1.25	13,000
Smoothing reactor to steel structure	2100	1.2	15,000
±1100 kV HV capacitor C1 to pole busbar	2100	1.2	15,000
Maintenance of ±1100 kV HV capacitor C1 to 1100 kV grading ring not considered	2100	1.2	15,000
±1100 kV HV capacitor C1 to 1100 kV live grading ring in case of half-voltage maintenance	1265	1.0	13,200 (10,200 + 3000)
±1100 kV HV capacitor C1 to 550 kV live grading ring in case of half-voltage maintenance	1200	1.0	12,200 (9200 + 3000)
±1100 kV HV capacitor C1 to live grading ring in case of full-voltage maintenance	2100	1.0	33,000
±1100 kV pole busbar to ±550 kV bypass busbar	1290	1.0	6,000
Between two smoothing reactors	–	–	13,000
Isolating distance of disconnector	2100	To be determined by manufacturer	8000
±1100 kV smoothing reactor to grading ring	TBD	–	–
±1100 kV bushing grading ring to wall	2100	1.25	13,000
±1100 kV bushing grading ring to steel structure	2100	1.2	15,000
±1100 kV bushing grading ring to ground	2100	1.2	15,000
C1 HV capacitor tower grading ring to ceiling	2100	1.25	13,000
C1 HV capacitor tower grading ring to structure	2100	1.2	15,000
C1 HV capacitor tower grading ring to ground	2100	1.2	15,000
±1100 kV flexible conductor to ground	2100	1.0	18,000
±1100 kV conductor to steel structure	2100	1.0	18,000
±1100 kV conductor to support (including adjacent support)	2100	1.0	18,000

(continued)

Table 26.16 (continued)

Typical clearance	SIWL (kV)	Clearance coefficient	Minimum air clearance (mm)
±1100 kV conductor to fence and protective cage	2100	1.0	18,000
Grading ring to support of multi-column parallel equipment (such as disconnector, RI capacitor, and reactor)	2100	1.25	13,000
±1100 kV outdoor grading ring of wall bushing to people	2100	1.0	28,000

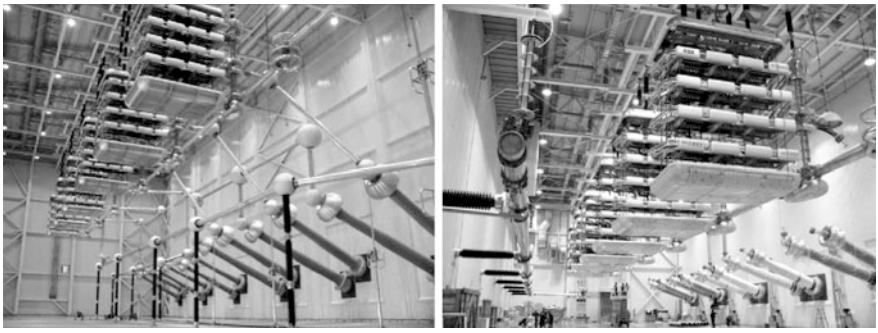

Fig. 26.7 Completed converter valves

26.6.2 Converter Valve

The converter valve is a basic unit equipment of converter, and the key equipment to convert the current. The converter valve system shall satisfy the requirements of less loss, easy installation and maintenance, and saving investment. The completed valves are shown in Fig. 26.7.

1. Requirements of the system for converter valve

The continuous operating rating and over-load capability shall be determined in accordance with the system requirements.

The long-term over-load capability of the DC system can be considered as 1.0–1.05 times the rated transmission capacity.

In accordance with the experience obtained from the previous DC projects, current manufacturing level of thyristors and performance level of firing control system, the rated rectifier trigger angle is generally taken as 15°, and the rated inverter extinction angle is generally taken as 17°.

2. Voltage of valve group

It is recommended to adopt the bipolar configuration for the UHVDC transmission system, in which two 12-pulse converter valve groups are connected in series at each pole, so there are four groups of 12-pulse valve groups at each station

(400 + 400 kV) or (550 + 550 kV) voltage combination scheme for HV 12-pulse converter valve groups and LV 12-pulse converter valve groups shall be adopted.

3. Electrical performance and parameters selection of valve

(1) Electrical performance of valve and characteristics of elements

The performance of converter valve is directly bound up with the characteristics of thyristor elements. Viewed from the fundamental requirements for the design of converter valve, the optimization of valve is a complicated problem to be considered comprehensively in terms of technology and economy. The minimization of series-connected thyristor and selection of element parameters is an important target in design of the valve.

The Yunnan–Guangdong DC Project and Pu'er–Jiangmen DC Project with rated current of 3150 A both adopt thyristors of 5 in. The Xiangjiaba–Shanghai DC Project with rated current of 4000 A, the Jinping–South Jiangsu DC Project with rated current of 4500 A, the Left bank of Xiluodu–Zhejiang Jinhua Project and the South Hami–Zhengzhou Project with rated DC current of 5000 A, the Zhundong–South Anhui DC Project with rated current of 5455 A, and the Xilin Gol League–Taizhou Project and the Shanghaimiao–Shandong Project with rated DC current of up to 6250 A all adopt thyristor converter valves of 6 in.

(2) Requirement for voltage withstand performance of the valve

The thyristor valve shall be capable of withstanding various overvoltages. The protection margin shall be taken into consideration during the design of voltage withstand capability of the valve. Refer to the insulation level of electrical equipment for voltage withstand margin of the valve and multiple valve unit. The redundancy of converter valves should not be less than 3%.

(3) Current characteristics requirement of the valve

The thyristor valve shall not only be capable of bearing DC current under rated load, continuous over-load, and short-term over-load conditions, which is determined by normal operating plan of DC system, but also be provided with certain transient overcurrent capability, which is determined by fault condition of the system.

(4) Loss characteristics of valve

Loss of converter valve is the important base of performance guarantee values of HVDC transmission system, an important indicator to evaluate performance of converter valve. It is found in experience of DC projects that loss of converter station under rated load accounts of 1% or less transmission power, while loss of thyristor valve accounts of 25% loss of the whole station. Therefore, minimization of the valve loss is one of major tasks in design of thyristor valve.

After determining parameters of thyristor and auxiliary elements, loss of the valve can be calculated. The loss depends largely on the DC rated current, on-state resistance, forward voltage drop, recovery charge and trigger angle of thyristor,

damping capacitance, damping resistance, etc. On the premise of meeting the requirements of normal operation, parameter of elements in the valve shall be selected in such a way that the loss is minimized.

4. Thermal properties of valve

In accordance with current manufacture level of elements of thyristor, the junction temperature under normal condition shall not exceed 90 °C. Rated capacity of cooling system shall be chosen to satisfy such requirement.

A variety of transient fault currents is decisive to the maximum permissible junction temperature of thyristor elements. As for thyristor elements, the process that converter valve bears fault current could be assumed to be adiabatic, in which cooling system and heat radiator do not work generally. The process is presented by sharp rise of junction temperature of thyristor. Evaluation of capability of the valve to withstand fault current focuses on the junction temperature in the end stage of fault, and on the maximum junction temperature when it withstands forward operating voltage immediately after the fault is cleared. The maximum actual junction temperature shall be LV than the ultimate junction temperature that may cause permanent damage on thyristor elements, and certain margin shall be considered. At present, manufacture level in the world is as below:

Ultimate junction temperature resulting in permanent damage: 300–400 °C
Maximum junction temperature after suffering the most severe fault current: 190–250 °C

5. Trigger of valve

With regard to the DC transmission projects in operation in the world, the valve is fired by means of photovoltaic conversion triggering and direct light triggering.

Photovoltaic conversion triggering is the most common approach used at present. In Xiangjiaba–Shanghai Project, the converter valves produced by ABB and SIEMENS are all of photovoltaic conversion triggering.

6. Control and protection of valve

For the thyristor valve triggered by photovoltaic conversion, its control and protection is realized by electronic equipment of the valve, including thyristor control unit, valve interface unit, and thyristor element monitoring equipment. Valve control system is responsible mainly for operation control of valve group.

Protection of converter valve comprises internal and external portions.

Internal protection measures of the valve include arrester protection and Break Over Diode (BOD). BOD protection is used to prevent that the thyristor elements suffer forward overvoltage when there is no normal control pulse. The protection of backward overvoltage is realized by valve arrester. Protection of the valve also includes control protection of cooling system.

External protection measures of the valve consist mainly of overcurrent protection of valve group and pole protection zone, differential protection of valve bridge, pole differential protection, and overvoltage protection at converter station.

7. Structure, cooling method, and insulation method of valve

The structure of converter valve is designed according to the cooling method and insulation method. In view of the insulation method, the valve can be provided with air insulation, oil insulation, and SF6 insulation. In view of the cooling method, the valve can be provided with water cooling, air cooling, oil cooling, Freon cooling, etc. There are four types of coordination between insulation and cooling of the valve.

In the UHVDC projects completed and under construction, 6 inches' thyristor valves are provided with air insulation and water cooling, while the valve towers are equipped with dual valves and suspension-installed. The converter valve tower is of multi-level structure and each level comprises valve modules. The levels are series-connected to form a complete valve tower. The valve tower is equipped with valve interface unit (VBE/VCU) beside it, which is connected with the thyristors inside the tower via optic fiber cable to send trigger pulses and supervise operating condition of each thyristor. The tower is provided with cooling water tubes from top to bottom and with leakage monitoring and protection device, which is connected with VBE/VCU via optic fiber cable.

8. Requirement of converter valve for valve hall

In order to ensure safe and reliable operation of the converter valve, valve hall of converter station of DC projects shall be provided with following conditions:

(1) The valve hall shall be fully metallic-shielded to prevent against external electromagnetic interference (EMI) and against interference produced by valve commutating operation. The shielding effect (difference between internal and external radio signal measurements of the valve hall) shall be greater than 17 dB (10.76–21 MHz).
(2) The valve hall shall be equipped with air conditioning system to regulate temperature and humidity to specified scope, thus ensuring that there will not be condensate and overheating on insulation elements of the valve under various operating conditions. Temperature of the hall under normal operation is restricted to 10–50 °C, and extreme temperature does not exceed 60 °C.
(3) Micro-positive pressure shall be maintained in the hall to guard against dust intrusion to keep air clean in the hall.
(4) The valve hall shall be equipped with advanced and reliable fire prevention system, including flame retardant structure and material, sensitive fire detector, and extinguishing system as well as effective fire-fighting devices [4].

26.6.3 Converter Transformer

The converter transformer is the core equipment to realize the mutual conversion between AC and DC, which, together with the converter valves, achieves the mutual conversion between AC and DC. Converter transformers that are installed and being installed are shown in Fig. 26.8.

Fig. 26.8 Converter transformers that are installed and being installed

1. Capacity of converter transformer

It is recommended to adopt bipolar configuration for UHVDC transmission system, in which two 12-pulse converter valve groups are connected in series in each pole. On the basis of experience of UHVDC projects and difficulty in manufacture and transportation of equipment, it is recommended to adopt 24 single-phase dual-winding converter transformers in UHVDC projects, and another 4 transformers for standby. Capacity of the transformer shall be determined according to rated transmission capacity and over-load requirement of DC system.

2. Configuration group

In UHV converter station, each 12-pulse valve group is equipped with 6 single-phase dual-winding transformers, three of them in Y-configuration on valve side, and another three in Δ-configuration. The winding on valve side of 3 Y-configured transformers is in high potential, while the winding on valve side of 3 Δ-configured transformers is in low potential.

Winding at line side of converter transformer shall be Y-connected, and neutral point is led out and grounded directly. Configuration groups of the dual windings of single phase are YNy12 and YNd11, respectively.

3. Requirement of tolerance range of main parameter

Difference between the short-circuited resistances of windings, phases, and converter transformers must be kept as minimum as possible; otherwise, it will result in great difference between commutation time of the valves, so that larger non-characteristic harmonics are produced at AC side, causing heating of the equipment, and overvoltage, overcurrent, and other problems. In accordance with the requirements specified in IEC standards about converter transformer, and based on characteristics of the converter transformer, the difference between impedances of the transformers shall be controlled within ±2%, while the difference between short-circuited resistances of principal taps shall be within ±5% of guaranteed impedance. Where scope of tapping is less than 30% adjustable range, the short-circuited resistance corresponding to the scope shall not exceed ±5% of

impedance of principal tap in general, and the short-circuited resistance corresponding to other scope of tapping shall not exceed ±10% impedance of principal tap. Meanwhile, tolerance of transformation ratio of each converter shall be controlled within ±0.5%.

4. Requirement for DC bias

Because of unbalance of trigger angle, power frequency current flows through the DC line, so that positive-sequence 2-order harmonic voltage is produced on AC busbar of converter station; in addition, during monopolar ground return operation, because current is injected into ground electrode, DC current will be produced in windings of the converter transformer. Capability of the converter transformer to withstand DC-biased current is considered not lower than 10 A (converted into the value on winding at line side of the transformer) generally.

26.6.4 Smoothing Reactor

The converter realizes the mutual conversion between AC and DC and also generates the harmonics and injects them into the DC lines. These harmonics will interfere with the adjacent communication lines. Smoothing reactors can restrain the harmonics effectively, and limit the rise rate and the amplitude of the DC current under the condition of failure or interference; moreover, it can also reduce the AC pulsation components at DC side and ensure the current uninterrupted under minimum DC current operating conditions. Smoothing reactors installed are shown in Fig. 26.9.

The most important parameter of smoothing reactor is the inductance. Inductance of smoothing reactor shall be optimized on the premise of meeting following all conditions:

1. The requirement to limit rate of rise of fault current;
2. The requirement to guard against intermittent current in case of low DC load;

Fig. 26.9 Installed smoothing reactor

3. The requirement to stabilize DC current ripples;
4. Technical and economic comparison between configurations of smoothing reactor and DC filters;
5. Inductance of smoothing reactor does not result in resonance with DC filter, DC line, converter transformer, neutral capacitor, and other equipment at low frequencies such as 50, 100 Hz.

The type of smoothing reactor is selected comprehensively according to the valve group connection and DC yard configuration. In ±500 kV DC projects, oil-immersed type smoothing reactors are used because its maximal advantage is that it is installed near the valve hall, the dry-type bushing at valve side can be inserted into valve hall directly to substitute the horizontal wall bushing. Dry-type bushing is also used for the vertical bushing, which can reduce the probability of pollution flashover. In UHV converter station, the DC yard is equipped with bypass circuit, so the smoothing reactor cannot be installed directly near the valve hall, and then the maximal advantage of oil-immersed type smoothing reactor does not exist anymore, while the dry-type smoothing reactor has more advantages in reliable operation and redundancy. The main insulation of dry-type smoothing reactor is borne by the post insulators, which are not apt to causing failure of main insulation even when failure of turn-to-turn insulation occurs, and the failure can be detected in time. If one reactor in one bank has to be put out of operation due to failure, it can be short-circuited by its two ends, then be put into operation again, replaced later in overhaul so as to reduce the power outage hours.

For the purpose of reducing the insulation level of HV valve tower to ground, the reactors can be arranged half in the pole line and half in the neutral busbar, and the dry-type reactor can facilitate the realization of such connection, which will not increase the investment.

In conclusion, the smoothing reactors in the UHV project shall be dry-type and be arranged half in the pole line and half in the neutral busbar.

26.6.5 AC Filter and Shunt Capacitor

The DC system will absorb the capacitive reactive power from AC system no matter if the converter station is in rectifier operation or in inverter operation; therefore, the substation shall be provided with reactive power compensators after the reactive capacity that can be provided by the AC system is considered. In general, the substation is provided with AC filters and shunt capacitors for reactive power compensation. In addition, the AC filters are also used to restrain the harmonic component. Installed AC filters and shunt capacitors are shown in Fig. 26.10.

Single-tuned, double-tuned, triple-tuned, high-pass, or tuned high-pass AC filter can be used. The rated parameters of filter elements shall be determined by considering the harmonic current and voltage generated by both the converter and

Fig. 26.10 Installed AC filters and shunt capacitors

background harmonics. The AC filters and HV capacitors of shunt capacitors are installed vertically on supports, and of dual-tower structure.

The HV capacitor of AC filter adopts internally fused capacitor, while the LV capacitor adopts fuseless capacitor. The capacitor is of stainless steel in its enclosure, of non-PCB in impregnant, good in sealing property, and easy for installation and removal.

The AC filters and HV capacitors of shunt capacitors are installed vertically on supports, and of dual-tower structure.

26.6.6 DC Filter

The harmonic voltage at the DC side of the substation will generate AC current. If such AC current is superimposed on the DC current of transmission line, it will interfere with adjacent communication system and deteriorate the communication quality. And the low-frequency harmonic current may endanger the personal and equipment safety via induced voltage, DC filters can be used to solve these problems effectively. When selecting DC filters, the low-frequency resonance of fundamental frequency or double frequency shall be avoided at DC side besides the function of eliminating the harmonic wave.

There are two types of DC filters available, i.e., passive filter and active filter. In view of the operating experience and reliability, passive filters with mature operating experience are used in all UHVDC transmission projects. The installed DC filter banks are shown in Fig. 26.11.

26.6.7 Other DC Equipment

In DC system, most of faults can be controlled by limiting the fault current in short time by the control system. Generally, the fault current can be limited to the

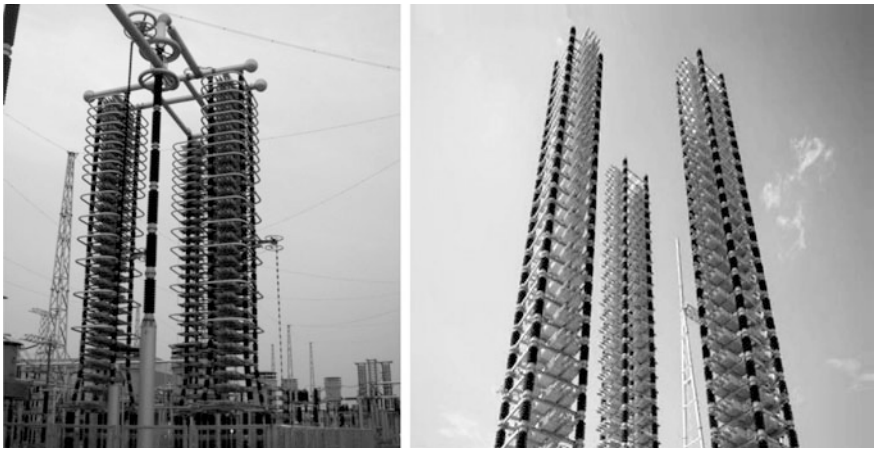

Fig. 26.11 Installed DC filter bank

magnitude comparable to the rated current. Therefore, DC circuit breaker need to cut-off the fault current of magnitude comparable to the rated current and cut-off normal load current.

1. DC bypass circuit breaker
   The DC bypass circuit breakers are adopted on purpose that when one of the two series-connected converters on each pole is put into or out of operation, the operation of another converter should not be affected.
   Following factors shall be taken into consideration when selecting DC bypass circuit breaker:

   (1) Breaking capacity: when the second converter in the two converters connected in series in one pole starts up with high current, the maximum current stress will be produced on the bypass circuit breaker.
   (2) Closing capacity: closing current is the maximum short duration DC current when the circuit breaker functions.
   (3) Capability to withstand voltage: the voltage means operating voltage, impulse withstand voltage, and recovery voltage;
   (4) Operating duration: the main requirement is that the closing time of circuit breaker (from receipt of making command to closure of contacts) shall not exceed 100 ms.

The DC bypass circuit breakers shall be parallelly connected with each 12-pulse valve group of each pole, respectively. Two circuit breakers are needed by the HV and LV groups, respectively, in each substation. The grounding insulation of HV bypass circuit breaker is DC 800 kV, while the insulation between open contacts is DC 400 kV. The grounding insulation of LV end bypass circuit breaker and the insulation between open contacts are DC 400 kV, respectively. Therefore, the bypass circuit breaker can be modified from the EHVAC SF6 circuit breaker.

DC bypass circuit breaker is in breaking position when it is in normal state: its function is to short circuit the valve group and operate the disconnector corresponding to the valve group when a 12-pulse valve group and its ancillary system have a fault, or when maintenance is planned to be conducted, so as to keep the normal 12-pulse valve group operating. In such a way, it is not required to block single pole, thus reducing impact on the system, keeping higher energy availability of the DC system, and isolating the faulted valve group to facilitate maintenance. After maintenance of the faulted valve group, break the bypass circuit breaker and operate the ancillary disconnector to put the remedied valve group into operation. The bypass circuit breaker ensures automatic completion of the above process through design of control and protection system.

2. DC high-speed switch

For the purpose of changeover between different DC operating ways, the substation is generally equipped with one DC high-speed metallic return transfer breaker (MRTB) and one DC high-speed ground return transfer switch (GRTS) in the rectifier converter station. Two neutral busbar switches (NBS) and one neutral busbar grounding switch (NBGS) shall be installed on the neutral busbar of DC yard of each pole in the rectifier and inverter converter station.

The MRTB is used to transfer the DC operating current from ground return to metallic return, while the GRTS is used to transfer the DC operating current from metallic return to ground return. The resistance of ground return is generally small while that of metallic return is large. Because the ground and metallic returns operate in parallel during transfer of current, the MRTB requires to switch on/off higher DC current due to small resistance of the return, while the GRTS requires to switch off smaller DC current due to large resistance of the return.

It is the function of NBS that in monopole planned outage, or if fault other than ground fault occurs inside the converter, the NBS can be used to isolate the blocked pole from the faulty pole rapidly. In normal bipolar operation, if ground fault occurs inside any pole, the NBS is used to transfer the DC current injected into faulty earthing point by normal pole to earthing pole circuit.

The NBGS is used as the standby ground electrode when the ground electrode is overhauled or fails in bipolar operation. When the ground electrode line breaks, the unbalanced current will increase the voltage on neutral busbar. The NBGS closure is used to establish the connection between neutral busbar and the ground to guarantee the continued bipolar operation and prevent the bipolar blocking and DC transmission deterioration. When the ground electrode line resumes its normal state, the NBGS must be able to transfer the current that flows through it to the grounding grid of the substation to the ground electrode line. In addition, when the transfer cannot be realized by the NBS, the NBGS must be able to provide temporary grounding channel to reduce the transfer current of NBS.

There is no natural zero-crossing point for DC current. With respect to the DC projects that require higher absorption of current commutation energy, measures must be taken to force the DC current crossing zero to transfer it. The available measures include self-excitation (passive) and separate-excitation (active)

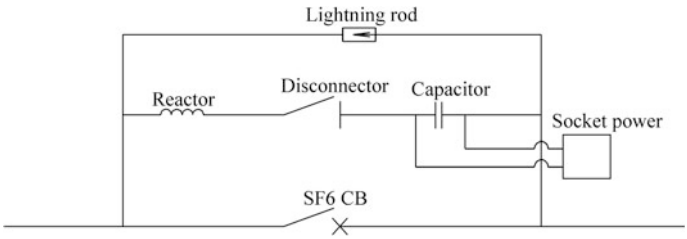

Fig. 26.12 Structure of DC high-speed switch of separate-excitation oscillation

oscillation. Compared with separate-excitation (active) oscillation, the self-excitation oscillation requires less investment and maintenance work while increasing the operation reliability of the system. So the DC switch is usually of self-excitation oscillation. The structure of DC high-speed switch of separate-excitation oscillation is shown in Fig. 26.12.

3. DC measuring devices

The DC measuring devices include a variety of current transformers installed on the DC pole, neutral line, and DC filter bank. All DC current-measuring devices have specified measuring precision, and have sufficiently good transient response and frequency response characteristics to ensure that the measuring signal is still in scope of precision required by function of the control and protection system even in case of maximum error. Measurement error of the current-measuring device shall not exceed 0.5% under rated current, not exceed 1.5% under 3 times of rated current, and not exceed 10% under 6 times of rate current. There are two types of DC current-measuring devices, i.e., conventional zero-flux DC current transformer and optical current transformer. With respect to the former, the measuring element is installed in the oil-filled porcelain insulator, and it is mature in manufacturing technology and rich in operating experience, but its measuring signal is vulnerable to interference, and the element is large in size and heavy in mass. For the HV current-measuring devices, if insulator of large diameter is used, the flashover accident occurs sometimes, causing negative effect on safe operation of the substation. For the optical fiber DC current-measuring device, it has advantages as follows:

(1) High-precision shunt is used to measure the DC current.
(2) Luminous energy-based electronic equipment in case of high potential.
(3) The optical signal transmission system is free of EMI.
(4) Influence of pollution can be reduced effectively by the surface made of silicone rubber.
(5) Light in structure, simple in foundation.
(6) Good in insulation performance, and safe and reliable.

(7) Small in volume, light in weight, reduction of transportation cost, and installation time.
(8) Good in environmental protection, not filled with oil or SF6 gas.

Because optical CT is low in maintenance cost, moving parts need no maintenance, change of insulation foil or paper as well as live cleaning is not needed, so it is usually used as the HVDC current-measuring device, while optical CT or zero-flux CT can be used as the LV current-measuring device.

The DC voltage-measuring devices include a variety of potential transformers installed on the DC pole and neutral line, which provide the signals to the control and protection system. The devices can be divided into two types according to their operating principles, i.e., DC CT type and resistance divider voltage plus DC amplifier type. The measuring device adopting the latter principle is usually used as the HVDC voltage-measuring device. Moreover, in order to satisfy the requirement of time response, the resistance voltage divider can be substituted by resistance–capacitance voltage divider. The internal resistance of DC voltage-measuring devices has sufficient thermal stability. Deviation of the precision of measurement does not exceed 0.5% within variation scope of 50 °C ambient temperature. When the voltage to be measured changes between zero and maximum stable DC voltage, measurement precision of the DC voltage-measuring device shall be ±1% rated DC voltage, which is with respect to the signal at inlet of control and protection system connected with PT. Measurement scope of DC PT shall be so large that DC voltage up to 1.5 p.u. can be measured, and precision of measurement must be kept within ±10% rated DC voltage. DC PT shall have good transient response and frequency response characteristics to ensure that the voltage measured under maximum tolerance is still within the precision required by control and protection system. Quality of output signal shall be good enough to ensure that as for the DC voltage to be measured of different levels (positive and negative polarity), i.e., the scope from 0.1 to 1.5 p.u., the output signals are all available and can satisfy the requirement of precision corresponding to the scope of measurement.

26.6.8 Wall Bushing

Because of increase of voltage level, difficulty in design and manufacture of ±800 kV wall bushing aggravates further. The main critical technology about ±800 kV wall bushing is to improve the capability against non-uniform rain flashover. It is demonstrated by the operating experience both in China and other countries that the dry-type wall bushing of synthetic silicone rubber not only solves non-uniform rain flashover and pollution flashover on the bushing, but also eliminates the possibility of damage of broken porcelain bushing on adjacent equipment, as well as the possibility of fire hazard in valve hall caused by oil leakage. Such wall bushing is the major direction of development of wall bushing.

Fig. 26.13 Installed wall bushing

Because UHVDC project is equipped with circuit of bypass switch valve group, and adopts dry-type smoothing reactor, it is recommended to adopt dry-type synthetic bushing as the wall bushing. Because the silicon rubber surface of dry-type composite bushing possesses water repellent behavior and recover capacity of water repellent behavior, uneven wet flashover accident can be prevented effectively without auxiliary measures taken in operation. Moreover, the sheath surface of silicon rubber shed can be cleaned at much longer intervals, reducing the work quantities of operators largely. Wall bushing shall be installed at 5° horizontally tilt. The installed wall bushing is shown in Fig. 26.13.

26.7 Vertical Layout Design

26.7.1 Main Tasks and Design Principles

The vertical layout design of DC substation is same as that of AC substation in tasks and principles generally, in which the designer shall also take advantage of the natural terrain of the site to perform vertical layout design for different ground elevations, determine the design elevations of different function zones so as to satisfy the requirements of technology and application. Since a substation covers large area, the determination of design elevation directly influences the quantities of earthwork and foundation treatment method, further influences the schedule, investment, and quality of construction of the project.

The vertical layout design of the field shall meet relevant provisions in DL/T 5056 *Technical Code of General Plan Design for Substation*. The layout includes the vertical layout with slight slope and vertical layout with terrace. The main design principles are explained as follows:

(1) The flood control requirement is in the first place to be met in vertical design of the substation. The design elevation of the site shall be higher than the flood stage of 1% probability. Where the design elevation cannot live up to the requirement above-mentioned, reliable flood control measures shall be taken in the site.
(2) The landform shall be utilized reasonably in vertical layout of the site. The vertical layout shall be determined by adapting to the local conditions and taking the technological requirements, traffic and transport, earthwork balancing, noise control, and drainage route into comprehensive consideration. If the local earthwork balancing will increase the difficulty and cost of the project, the waste disposal area or borrow pit satisfying requirements shall be designated.
(3) The function zones shall be arranged according to the contour lines to facilitate the adoption of sloping or stepping layout vertically in different zones.

26.7.2 Vertical Layout with Slight Slope and Slope Selection

The design slope of the site shall be determined according to the equipment arrangement, soil conditions, drainage method, and road gradient, which should be 0.5–2%. If reliable drainage measures are taken, the design slope can be less than 0.5%. The maximum local slope should not be greater than 6% and measures against scouring should be taken if necessary. The design slope of the field where the outdoor distribution device is parallel with busbar direction should not be greater than 1% and other technological requirements shall be satisfied.

26.7.3 Vertical Layout with Terrace

When the slope of natural landform of the site is greater than 5–8% and there is evident slope trend in original landform, during the vertical layout design of the site, an optimal vertical layout shall be recommended after particular assessment is conducted on the feasibility of layout with terrace through combination of elevations in different zones and the earthwork calculation on the basis of landform and terrain of the site, technical processes, traffic organization, noise control and foundation treatment, etc. In assessment of the layout with terrace, full consideration should be given to the relationship between the propagation direction of noise source in site and the natural landform outside the site to avoid such result that the earthwork cost is saved moderately but the noise control cost increases greatly.

The elevation of terrace has close relation with the landform; in addition, full consideration should be given to the feasibility and safety of technological arrangement, easy transport, geological stability of rock and soil, and convenient construction, so as to reduce the earthwork quantities and guarantee the safe

operation. Each terrace should not be too high and controlled within 2–3 m in general. If the site covers large area, the height of the terrace can be increased appropriately on the basis of that the longitudinal gradient of road in the site is not greater than 6%.

26.7.4 Vertical Layout of Buildings and Structures

It is specified according to engineering practices of existing UHV converter stations that the floor elevation of the important structures in the site such as valve hall, control building, valve external cooling equipment room should be 0.45 m higher than the ground elevation of converter transformer transport yard, while the ground elevation of transport yard is 0.1 m higher than the site elevation. The floor elevation of relay house, multifunctional building, and GIS house should be 0.45 m higher than the outdoor ground elevation, while that of spare parts warehouse, multifunctional fire-fighting pump house, etc. should be 0.30 m higher than the outdoor ground elevation. The center elevation of road in the site should be 0.1 m higher than the outdoor ground elevation.

26.8 Power Distribution Device of UHVDC Converter Station

The electrical general layout shall be arranged according to the sequence of DC switchyard to valve hall, and converter transformer to AC power distribution device. The incoming lines shall be designed comprehensively by combining the landform of the site, AC and DC outgoing line direction, and type of power distribution devices, so as to achieve unobstructed technical process, advanced technique, convenient operation, construction, maintenance, overhaul, and expansion, optimized cost, etc., as possible. Following design principles shall be complied with as possible:

1. The corridors of incoming and outgoing lines meet the requirements of urban planning.
2. The converter transformer and smoothing reactor shall be arranged as far away from the dwelling buildings as possible.
3. The AC and DC filters shall be arranged far away from dwelling buildings and multifunctional building.
4. Demolition of dwelling buildings is needed as less as possible.
5. The occupancy area is minimized. In case of complicated landform, the earthwork quantities in the site shall be as reduced as possible. Earthwork balancing shall be achieved in the site to reduce the quantities of foundation treatment.

6. Road to the substation is convenient and reasonable.
7. The noise pollution in the site is alleviated as low as possible so as to reduce the influence on the surroundings.
8. Keep expansion of the substation as much as possible.

26.8.1 Converter Area Layout

The safe operation of valve hall (valve) and converter transformer in converter area is critical to guarantee the DC transmission and produce benefit, and the investment of valve hall and transformer accounts for most of the total investment of substation construction. Therefore, in the layout design of the area, safe operation of converter transformer and valve hall (valve) takes first priority over any other aspects, and the investment takes second priority.

In the UHV substations completed and under construction, each 12-pulse valve group is installed in a valve hall. Each pole is equipped with one HV and one LV valve hall, respectively, so the whole substation is equipped with 4 halls. The 800 kV valve tower is mounted in the HV valve hall, while the 400 kV valve tower is mounted in the LV valve hall. Refer to Fig. 26.14 for the typical converter area layout, and refer to Table 26.17 for dimensions of converter areas of some UHVDC projects.

26.8.1.1 Valve Hall Layout

There are four valve halls in the UHV converter station. The layout of valve hall decides the layout of converter area. There are various layouts of valve hall based on the types of valve tower. In case of duplex valve tower, the converter

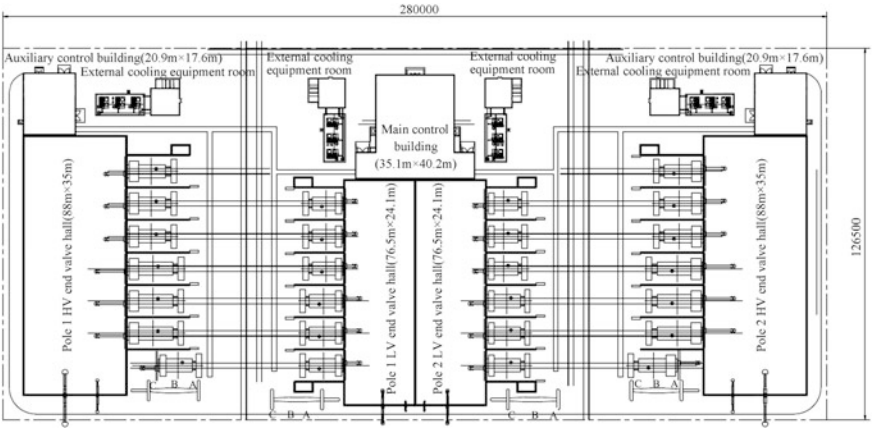

Fig. 26.14 Typical converter area layout

Table 26.17 Dimension of converter area of some UHVDC projects (m)

Project	East Guangzhou	Fengxian	Fulong	Tongli	Yulong	Jinhua	Shuanglong
Length × width (m)	298 × 129.5	290 × 116	298 × 116	292 × 127	292 × 125	280 × 127	280 × 126

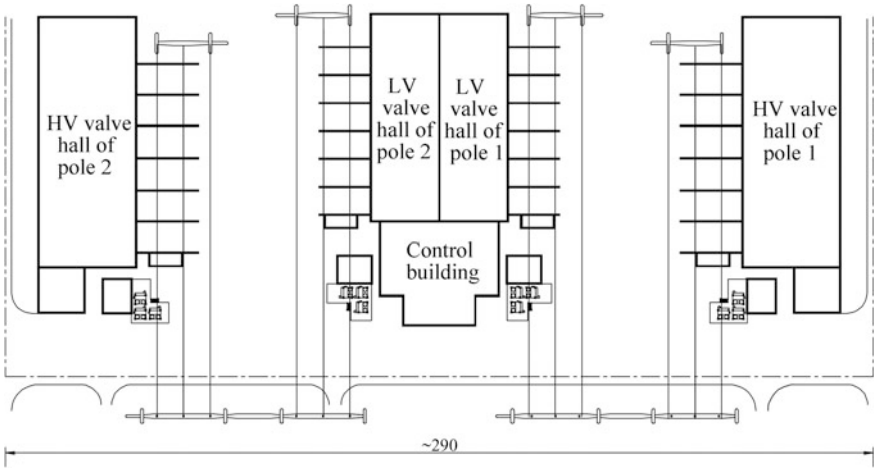

Fig. 26.15 Solution 1 for valve hall layout (m)

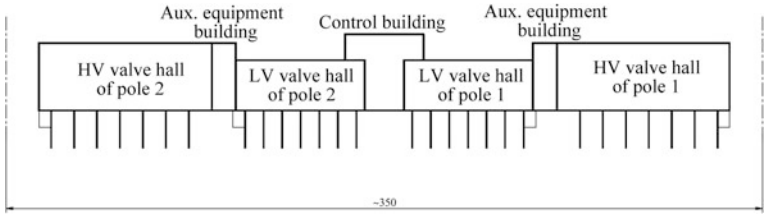

Fig. 26.16 Solution 2 for valve hall layout (m)

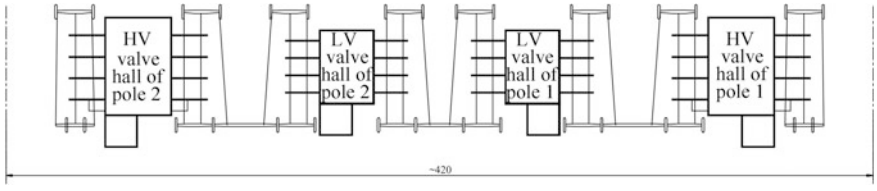

Fig. 26.17 Solution 3 for valve hall layout (m)

transformers are lined up closely against the valve hall, and the HV and LV valve halls can be arranged oppositely or lined up. In case of quadruple valve tower, 6 converter transformers in each valve hall are divided into two groups, then arranged against both sides oppositely (Fig. 26.15) or lined up against the same side of a hall. But the arrangement at same side in valve hall will increase the connection difficulties of the valve hall greatly, and bring hidden trouble to electrical safety. Moreover, the length of the hall is subject to arrangement of the transformer, so the space of valve hall has to be increased greatly, causing difficulties in design of the construction, structure, heating, ventilating, and air conditioning. So line-up arrangement is not adopted in general. Refer to Table 26.18 for the comparison of the characteristics of the three layout schemes for duplex valve tower and quadruplex valve tower.

All of the three schemes above can meet the requirements, though they are different from each other in assembly and maintenance of converter transformer. Based on different arrangements, the three schemes are different greatly in noise transmission. Combining landform characteristics of the site and distribution of surrounding residents, the noise of converter station shall be controlled to transmit westward and northward, thus reducing influence on the residents. In Solution 1, the layout is neat and attractive, simple in busbar connection and occupies relatively small area. But the direction has to be changed when replacing the auxiliary phase of the converter transformer. In Solution 2, the layout is identical with ±500 kV converter station in pattern and practice. The connection in the valve hall is simple, but there are many leads above the assembling yard of the converter transformer, affecting negatively on the visual effect. Solution 3 is based on the quadruple valve, the valve hall covers relatively small area, the connection is clear, but specific busbar shall be installed additionally, so the total occupancy area is large.

Above all, any one of the three schemes in the valve hall has its own advantages and disadvantages. Among them, Scheme 1 and Scheme 2 are equal generally in coverage area, so both schemes have been adopted in UHV projects. Scheme 3 has distinct disadvantages in reduction of noise and land use, so it has not been used in UHVDC projects yet.

26.8.1.2 Determination of Valve Hall Dimensions

Suspension installation method is adopted in the valve towers in UHVDC projects that have been completed in China. Compared with the valve tower of supporting type, the suspension-installed valve tower is suspended on steel beam of valve hall through its suspension insulator string, thus satisfying effective seismic requirement, avoiding the danger that the pillar insulator suffers stress due to poor installation, and reducing the height of the valve hall to some extent.

The dimensions of valve hall are associated with such factors as the dimension of valve body, air clearance distance in valve hall, layout type of converter transformer, width of converter transformer, bushing length at valve side of converter transformer.

Table 26.18 Comparison of characteristics of three layout patterns of valve hall

S/N	Compared item	Layout pattern of valve hall		
		Scheme 1 (refer to Fig. 26.15)	Scheme 2 (refer to Fig. 26.16)	Scheme 3 (refer to Fig. 26.17)
1	Applicability	Applicable to double valve unit and single-phase dual-winding converter transformer	Applicable to double valve unit and single-phase dual-winding converter transformer	Applicable to quadruple valve unit and single-phase dual-winding converter transformer
2	Arrangement	The HV and LV valve halls of each pole are arranged face to face. The two LV valve halls are arranged back to back. The six converter transformers corresponding to a valve hall are arranged in line-up pattern, intermediately against the valve hall	The 4 valve halls in the whole station are arranged in line-up pattern. 24 converter transformers are arranged in line-up pattern at the same side of the hall, intermediately against valve hall	The 4 valve halls in whole substation are arranged separately face to face. The six converter transformers corresponding to a valve hall are divided into two groups, arranged at both sides of the hall, three transformers of Yy configuration at one side and three transformers of Yd configuration at the other side
3	Configuration of main control building	Set up 1 main control building and two auxiliary equipment rooms	Set up 1 main control building and two auxiliary equipment rooms	Set up 2 main control buildings (principal one and ancillary one) and two auxiliary equipment rooms
4	Configuration of busbar	No jumper wire above assembling yard. Trim arrangement. Connection of busbar of converter transformer is simple. Large span and high tension of busbar	There is multi-span busbar above assembling yard of converter transformer. Busbar connection of converter transformer is complicated. Short span and low tension of busbar	Busbar of every six converter transformers is connected to AC switchyard through the high-crossover conductor set above the converter transformer. Busbar connection of converter transformer is complicated. Short span and low tension of busbar
5	Wiring inside valve hall	DC wall bushings are introduced from same side of the valve halls. LV valve tower of each valve hall is far away from the wall bushing, and outgoing line of the valve tower is perpendicular to direction of the wall bushing. The outgoing line shall be routed around the valve hall	Connection inside the valve hall is simple and configuration of the connection is mature	Connection inside the valve hall is simple. The valve hall is small in area, but is increased in height

(continued)

Table 26.18 (continued)

S/N	Compared item	Layout pattern of valve hall		
		Scheme 1 (refer to Fig. 26.15)	Scheme 2 (refer to Fig. 26.16)	Scheme 3 (refer to Fig. 26.17)
6	Size of valve hall	The valve hall is large in area and low in height	The valve hall is small in area and low in height	The valve hall is small in area and increased in height
7	Replacement of standby transformer	Proper of the converter transformer needs turning sometimes	Proper of the converter transformer does not needs turning	Proper of the converter transformer needs turning sometimes
8	Noise	Noise transmits to DC switchyard and AC switchyard	Noise propagates to AC switchyard and its both sides. The noise is high acoustically, and extensive in coverage, so it is difficult to control	The noise transmits to DC switchyard, AC switchyard, and both sides
9	Coordination with DC switchyard	Small longitudinal size of DC switchyard	Relatively large longitudinal size of DC switchyard	Large longitudinal size of DC switchyard
10	Coordination with AC switchyard	It is much smoother for the converter transformer connected in series. The angle between busbar and AC GIS incoming line is appropriate	Angle of lead wire of converter transformer connected in series is large. The busbar is large in span and complicated in wiring	Busbar shall be set in AC switchyard. The connection is complicated
11	Assembly of converter transformer	It is permitted that the converter transformers are assembled back to back and transport distance is reserved for other converter transformers. The all 24 converter transformers can be assembled at the same time	Assembly of the converter transformer is low in mutual influence. The 24 converter transformers can be assembled at the same time	It is considered that transport of other converter transformers is permitted when only one converter transformer is assembled. It is not permitted to assemble the converter transformers that are configured back to back

Among the factors, the dimensions of valve tower and other key equipment in the valve hall and electrical safety distance are the most principal and direct factors affecting the dimension of valve hall. In case of the LV valve hall, since the air clearance distance between bushings at the valve side of the converter transformer is relatively small, the dimension of the valve hall depends greatly on the width of the transformer body and its fan or the air clearance distance of interphase at AC side.

Dimensions of valve hall vary significantly with the different arrangements of converter transformer in the valve hall. A reasonable and cost-efficient arrangement is as below: in case of scheme of duplex valve unit, the 6 converter transformers corresponding to a valve hall shall be arranged in line-up pattern at the same side of the hall, intermediately against the hall; in case of scheme of quadruple valve unit, the six converter transformers corresponding to a valve hall are divided into 2 groups according to configuration, which shall be arranged at both sides of valve hall, intermediately against the hall.

The bushing at valve side of the transformer extending into the hall could be arranged horizontally or up-and-down. The converter transformers produced by ABB usually adopt horizontal arrangement, while those produced by Siemens usually adopt up-and-down arrangement. The arrangement of bushing may influence the dimension of valve hall. The influence can be analyzed by clearance distance calculation in practical engineering.

Figures 26.18 and 26.19 indicate the critical dimensions which decide the overall dimensions of valve hall, while Table 26.19 lists the critical dimensions and corresponding influencing factors that decide the overall dimensions of valve hall.

Viewed from information collected from manufacturers of converter valve and converter transformer, for ±800 kV converter station, HV valve hall with the dimension of 86.2 × 33.5 m and LV valve hall with the dimension of 76.5 × 23.1 m can accommodate arrangement of equipment produced by any manufacturer currently. The dimensions of valve hall in some UHVDC projects are shown in Table 26.20.

26.8.1.3 Arrangement of Converter Transformer

The connection of converter transformer with valve hall can be divided into two types, namely close arrangement and separate arrangement. In order to reduce the occupancy area of the converter station and save the land resource, the converter transformers are arranged closely against the valve hall, i.e., 6 converter transformers corresponding to each valve hall are lined up and arranged against one side of the valve hall, separated by fire-retardant walls from each other. The bushing at the DC side of the transformer is inserted into the valve hall and Y or Δ connection is accomplished inside the valve hall. Arrangement of converter transformer bushing being inserted in valve hall has the following advantages:

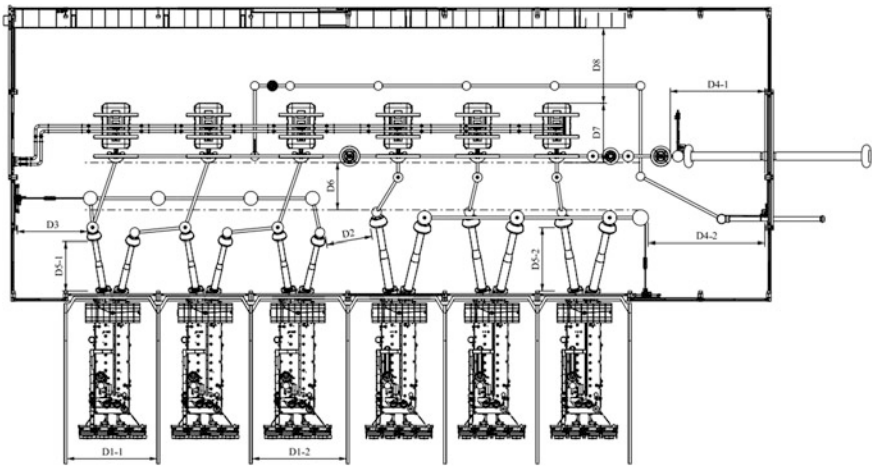

Fig. 26.18 Key dimensions which decide the length and width of valve hall

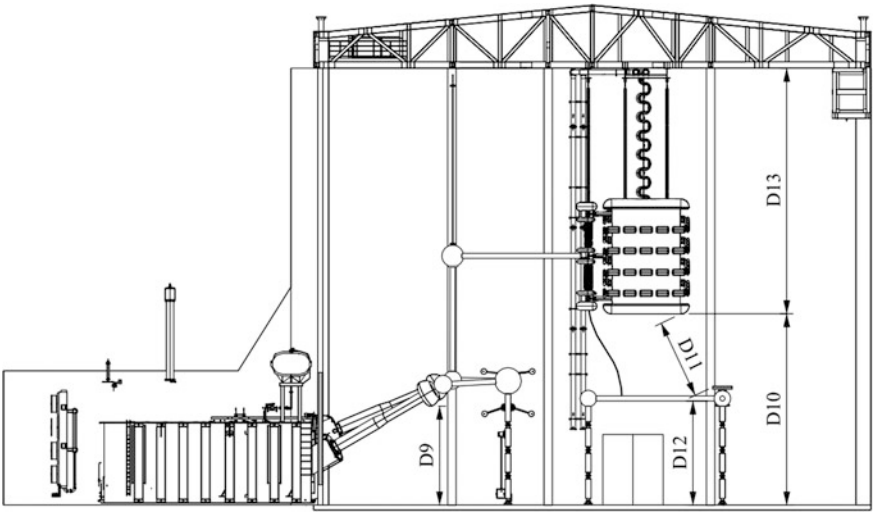

Fig. 26.19 Key dimensions which decide the height of valve hall

1. The favorable operating environment in valve hall could be utilized to reduce creepage distance of converter transformer bushing;
2. Non-uniform wet flashover of converter transformer bushing can be prevented;
3. 12 separate wall bushings can be omitted in each pole;

Table 26.19 Critical dimensions and corresponding influencing factors that decide the overall dimensions of valve hall

Critical dimensions	Influence on overall dimensions of valve hall	Remarks
D1-1	Length of valve hall	1. It is determined based on width of fans at tail of converter transformer 2. It is determined based on air clearance of phase-to-ground/phase-to-phase at line side of converter transformer
D1-2		1. Same as influences of D1-1 2. Where the fan at tail of converter transformer is the influencing factor, D2 shall be taken into consideration to determine if the converter transformer shall be eccentric
D2		1. It is determined based on phase-to-phase clearance on valve side of converter transformer of Yy and Yd configuration 2. Air clearances at Pole 1 and Pole 2 are different, and the larger one shall be taken as input to determine D1-2
D3		1. It is determined based on air clearance between Yd converter transformer to side wall. Air ducts of air conditioner, pillars on the side wall shall be taken into consideration 2. Since requirement of clearance between terminals on valve side of converter transformer and the third side wall is more rigorous than the clearances related to two side walls, in the three clearances D3/D5-1/D9, at least one clearance shall be 20–30% larger than another two, so as to eliminate influence on the third wall. Generally speaking, the scheme is increase of D3
D4-1		1. It is determined based on distance between DC wall bushing and wall 2. Influences of occupation area of optical CT and arrester shall be taken into consideration at the same time 3. The dimension is appropriate to valve hall of back-to-back arrangement
D4-2		1. It is determined based on distance between connecting busbar on valve side of Yy converter transformer and wall. 2. Influence on the third wall is same as that in D3. 3. The dimension is appropriate to valve hall of line-up pattern.
D5-1	Width of valve hall	1. It is determined by Yd converter transformer manufacturer. It is arranged in such a way to satisfy requirement of air clearance of the terminals on valve side to zero potentials, such steel columns, profiled steel plate, and ground disconnector 2. Influence of different phase-to-phase air clearances of Yd configuration shall be taken into consideration in arrangement

(continued)

Table 26.19 (continued)

Critical dimensions	Influence on overall dimensions of valve hall	Remarks
D5-2		1. It is determined by Yy converter transformer manufacturer. It is arranged in such a way to satisfy requirement of air clearance of the terminals on valve side to zero potentials, such steel columns, profiled steel plate, and ground disconnector
D6		1. It is determined by air clearance requirement of busbar of Yd or Yy to valve tower 2. Space for travel and operation of maintenance trolley shall be taken into consideration
D7		1. As for width of valve tower, generally speaking, the valve towers produced by Xuji, China Epri, and ABB are not different greatly in width, but the tower produced by Siemens is narrower in width
D8		1. It is determined by the air clearance of valve group on Y side related to walkway 2. When determining the clearance, the clearance between grading shield at top of valve tower and walkway (based on insulation level of middle point of 12-pulse unit), and the clearance between middle section of the tower and the walkway (based on insulation level of valve side of Yy transformer to ground) shall be taken into consideration. The larger one shall be taken as control factor 3. Since walkway involves personal safety, the air clearance here in case of 800 kV HV valve hall shall be calculated according to 5 standard deviations (generally 2 standard deviations) 4. Dimensions of the walkway shall not be greater than 0.9 m width $\times$ 2.2 m height
D9	Height of valve hall	1. Requirement of air clearance of converter transformer to ground: under normal circumstance, the requirement shall be met by adjusting height of foundation of converter transformer. It does not affect height of the valve hall normally
D10		1. Requirement of air clearance of converter valve to ground 2. With respect to HV valve hall, influences of air clearance of valve tower to ground, air clearance of valve tower bottom at Y side to 400 kV busbar (D11), and air clearance of 400 kV busbar to ground (D12) shall be taken into consideration. The largest one shall be taken as height of the valve tower above the ground 3. Space for driving and operating lift of the valve hall shall also be taken into consideration
D11		1. Air clearance of valve tower bottom at Y side of HV valve hall to 400 kV busbar
D12		1. Air clearance of 400 kV busbar to ground
D13		1. As for height of valve tower, the converter valve produced by different manufacturers are not different greatly in height, except for the one produced by Siemens, which is higher

Table 26.20 Dimension of valve hall in some UHVDC projects (m)

Project	East Guangzhou	Fengxian	Fulong	Tongli	Yulong	Jinhua	Shuanglong
HV valve hall (length × width/m)	81.5 × 31.6	79.7 × 32.8	80 × 32.8	86.2 × 33.05	88 × 35	88 × 35	88 × 35
LV valve hall (length × width/m)	61 × 20.8	63.1 × 23.1	70.5 × 23.1	76.5 × 23.1	75.5 × 24.1	76.5 × 24.1	76.5 × 24.1

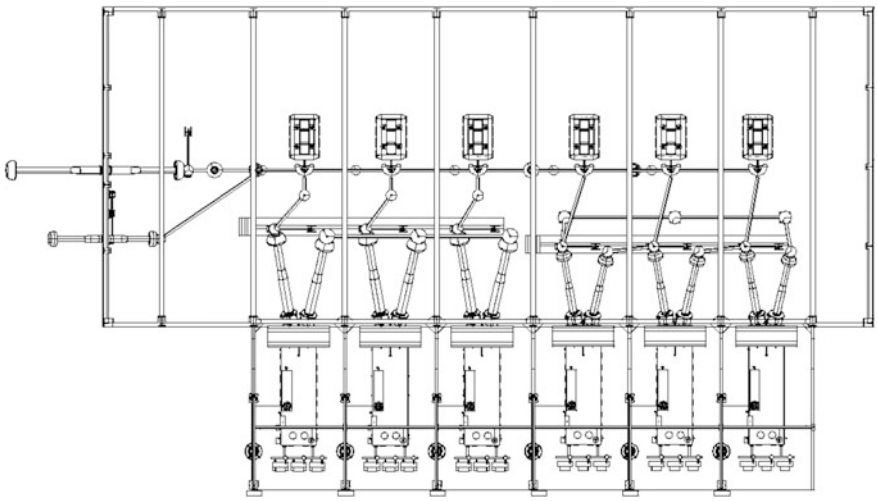

Fig. 26.20 Layout of converter transformers in HV valve hall

4. Coverage area of converter transformer can be reduced (Fig. 26.20).

HV and LV standby converter transformers can be considered to be arranged in the outdoor open space in DC switchyard or AC PLC area. Direction of 4 standby converter transformer bushings shall be kept consistent with the adjacent working transformer to facilitate replacing the near standby phase. Such arrangement has the following characteristics:

1. The distance between standby converter transformer and working transformer is shorter, so the converter transformer moves by shorter distance when replacing it.
2. If the direction of standby converter transformer bushing is perpendicular to that of the working transformer, both of them have to be turned in replacement, which results in more works.

26.8.1.4 Determination of Assembling Yard of Converter Transformer

The determination of assembling yard of the converter transformer is closely associated with the layout of the valve hall. Requirements and dimensions of the assembling yard of the converter transformer vary with different layouts. The assembling yard of converter transformer shall be determined by taking transportation, assembly method, occupation area of maintenance, and requirement of construction organization of converter transformer into consideration, based on the following principles:

1. When the converter station is in normal operation, all the standby converter transformers can be removed easily;
2. The place where failed converter transformer that is put out of operation is placed temporarily shall not impede that the standby one is moved into assembling yard;
3. During installation, when a converter transformer is being assembled, transport passage for other converter transformers is not considered.

Dimensions of assembling yard of converter transformer in valve hall of face-to-face arrangement (i.e., Scheme 1) shall be determined in accordance with diagram as shown in Fig. 26.21:

Value "A" in the diagram is length of fire wall of HV converter transformer, and value "B" is safe distance between HV (Yy) converter transformer bushing and fire wall, which is 1–1.5 m normally. Value "C" is the distance from HV converter transformer bushing to the center of transformer body. Value "D" is the distance from LV (Yy) converter transformer bushing to the center of transformer body. Value "E" is the distance between LV (Yy) converter transformer bushing and fire wall, which is 1–1.5 m normally. Value "F" is length of LV converter transformer's fire wall.

Dimensions of assembling yard of converter transformer in valve hall of line-up pattern (i.e., Scheme 2) are determined according to the diagram shown in (Fig. 26.22):

Value "A" in the diagram is length of fire wall of HV converter transformer. Value "B" is the safe distance between HV (Yy) converter transformer bushing and

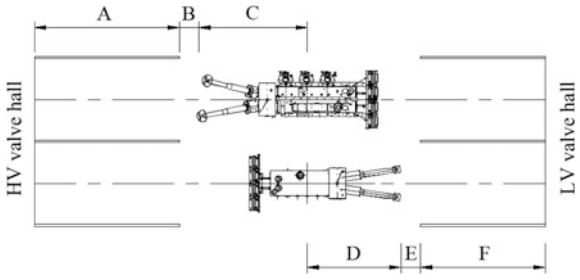

Fig. 26.21 Schematic diagram of determination for assembling yard's dimensions in valve hall of face-to-face arrangement

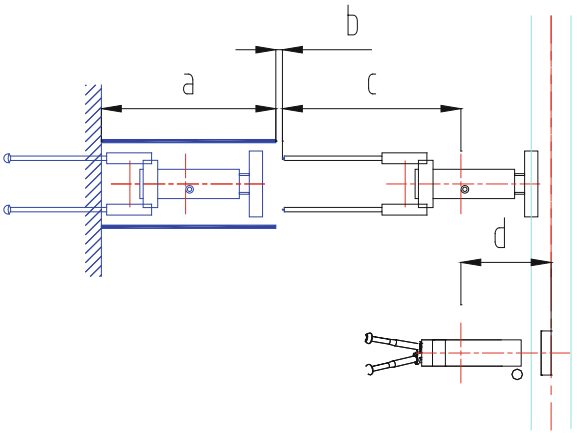

Fig. 26.22 Diagram of determination for assembling yard's dimensions in line-up valve hall

Table 26.21 Dimensions of assembling yard of converter transformer in some UHVDC projects

Projects	East Guangzhou	Fengxian	Fulong	Tongli	Yulong	Jinhua	Shuanglong
Width (m)	85.1	77	81.3	77	80.1	75	73.5

fire wall, which is 1–1.5 m normally. Value "C" is the distance from HV converter transformer bushing to the center of transformer body. Value "D" is the largest distance from transformer radiator to the center of transformer body (Table 26.21).

26.8.2 DC Switchyard Arrangement

The DC switchyard can be arranged indoors or outdoors. The type of DC switchyard is selected mainly on the basis of the pollution level in the substation site and the manufacturing capacity of DC equipment. Indoor arrangement can solve the problem that creepage distance of DC equipment is increased because of severe pollution in the station site, and the problem that arcing distance between electrodes has to be increased because of damage of electrode shape by rainwater. However, the indoor yard needs higher investment and higher operating cost. The ±800 kV UHVDC converter stations which are existing or under construction in China are all of outdoor arrangement, and ±1100 kV UHVDC converter stations which are being planned and designed are of indoor arrangement.

26.8.2.1 Outdoor DC Switchyard

The typical low-type tubular busbar arrangement is adopted for the outdoor DC switchyard, and the tubular busbars are arranged symmetrically along the pole in

general. The DC neutral equipment is arranged in the center of DC switchyard, and the DC filter banks, encircled by fence, are arranged between the DC pole line and the DC neutral line. Since many HV capacitors of 800 kV DC filters have to be used, duplex or triple tower arrangement is recommended. The installation method of the tower includes the supporting and suspension installation. The smoothing reactors (dry-type insulation) are series-connected to the pole busbar and neutral busbar, respectively, and installed by means of support installation. In order to lower the height of equipment, smoothing reactor of pole line and HV capacitor of DC filter adopt the low-type arrangement, encircled by fence. Outdoor switchyard is connected with the valve hall via outdoor wall bushing. The DC yard is equipped with lead towers of DC pole line at both sides, which are connected to the DC lines outside the substation. There is a ground electrode line tower in the center of the yard to lead the ground electrode line outside the substation.

The outdoor DC yard requires large area to adapt to the transverse dimensions of valve hall and transformer area. Proper adjustment of relative position of the equipment could reduce the longitudinal dimension of the outdoor DC yard to a certain extent. Refer to Fig. 26.23 for the typical outdoor DC yard arrangement and to Table 26.22 for the dimensions of outdoor DC yards of some UHV converter stations.

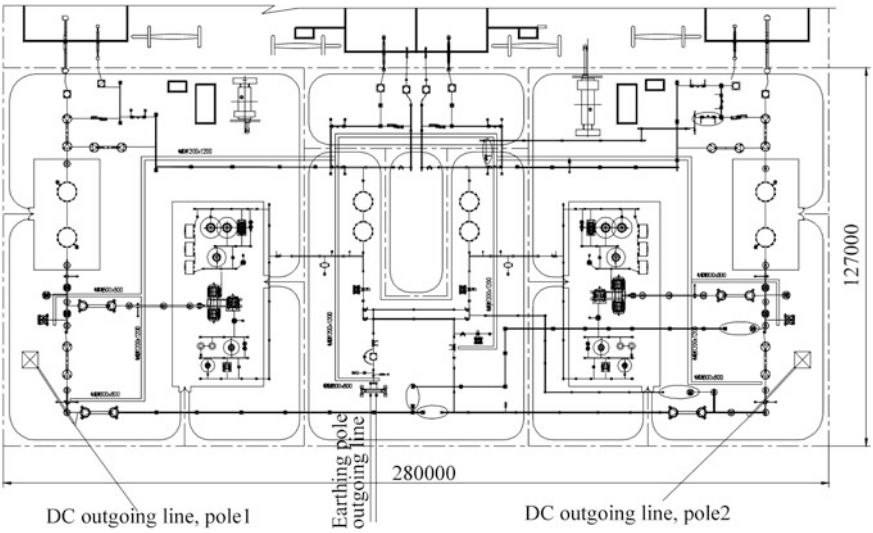

Fig. 26.23 Typical outdoor UHVDC switchyard (mm)

Table 26.22 Dimensions of outdoor DC switchyards of some UHVDC converter stations (m)

Project	East Guangzhou	Fengxian	Fulong	Tongli	Yulong	Wuyi	Shuanglong
Length × width (m)	299 × 132.5	290 × 130	298 × 134.5	292 × 130	292 × 148	280 × 127	280 × 130

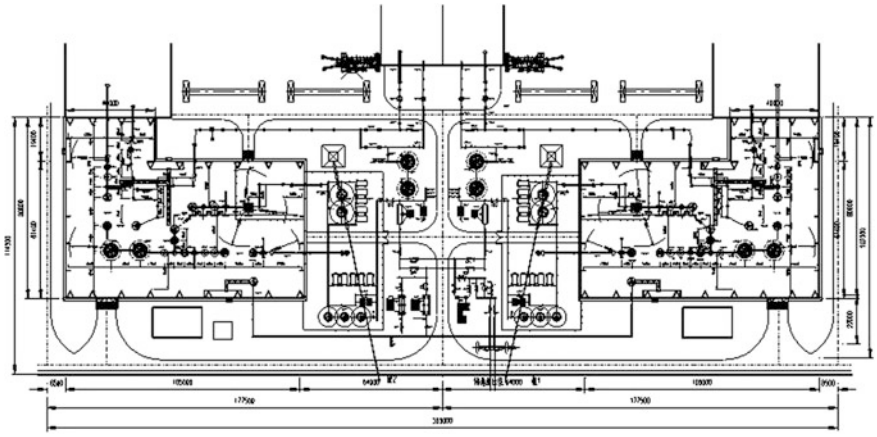

Fig. 26.24 Arrangement of indoor DC switchyard in Zhundong station (mm)

26.8.2.2 Indoor DC Switchyard

Design principle of indoor DC switchyard is to minimize area and height of construction of DC switchyard, make every effort to make the DC switchyard simple in structure and clear in connection, and guarantee good operating environment to reduce creepage distance of equipment and reduce difficulty in equipment manufacture. Therefore, the indoor DC switchyard adopts indoor arrangement of pole line equipment and a part of intermediate busbar equipment, and outdoor arrangement of neutral busbar and LV circuit of DC filter. The equipment to be arranged indoors includes pole line disconnector, smoothing reactor, DC voltage divider, optic fiber cable current transformer, arrester, surge capacitor, bypass switch of HV valve group, HV capacitor tower of DC filter. The whole DC switchyard is arranged symmetrically in general on pole, and the structure in the indoor yard is arranged in L shape to minimize longitudinal dimensions of DC switchyard. The structures in indoor yard are arranged closely against valve hall, and connected with valve hall through indoor wall bushing. LV outgoing line of capacitor C1 of DC filter is connected to the equipment at LV part of filter through wall bushing, while pole busbar is connected to outdoor DC line through outdoor wall bushing. LV equipment of DC filter, bypass equipment of LV valve group, and neutral equipment are arranged between the structures in the indoor yard of Pole 1 and Pole 2. Refer to Fig. 26.24 for arrangement of indoor DC switchyard of Zhundong Station.

26.8.2.3 DC Deicing Scheme

For the purpose of accommodating with the connection of DC-based deicing operation, the DC yard shall be provided with more tubular busbars. In order not to

affect the layout and occupancy area of equipment of the DC yard, the additionally installed tubular busbars shall be segregated from other DC yard equipment in respect of their altitudes. Sufficient air clearance distance shall be ensured for the busbars.

26.8.3 Layout of AC Filter Yard

AC filter banks are key integral parts of a converter station. The AC filter yard covers 1/4–1/3 of the whole UHV converter station site. In order to decrease the equipment investment, increase the connection reliability, and fulfill the requirements of reactive switching and voltage control of the system, the AC filter sub-banks and shunt capacitor sub-banks are integrated into larger banks, respectively, then connected to the AC distribution devices. Such s connection pattern has such advantages as high reliability and flexible switching of filters, and satisfies the harmonics standard and system requirement. It can not only keep the bipolar operation, but also switch conveniently off the filter banks corresponding to another pole in monopolar operation. In addition, it facilitates the mutual backup between the two poles, so it has good applicability [5].

26.8.3.1 Layout of AC Filter Banks

At present, the AC filter yard of UHVDC converter station can be laid out by arranging some filter banks into a pattern which contains the line-up pattern, checkerboard pattern, and improved checkerboard pattern.

1. Line-up pattern

The line-up pattern is characterized by that the sub-banks in a bank are arranged at the same side of the busbar. The typical line-up layout of the 500 kV AC filter yard is shown in Fig. 26.25, while its profile is shown in Fig. 26.26.

Interphase roads are provided between 500 kV power distribution equipment, and roads for maintenance, handling, and patrol inspection are constructed before and behind the fence of AC filter sub-banks and shunt capacitor sub-banks.

Currently, the line-up layout of AC filter yard is widely adopted in the ±500 and ±660 kV converter stations under the administration of State Grid Corporation and ±800 kV converter stations under the administration of South Grid Corporation. The line-up layout has such advantages as easy maintenance, convenient arrangement, and good adaption to the general layout if the number of sub-banks in a bank is odd. Its disadvantage is that the filter is arranged on the same side of the busbar, and the dimension of fence of filter varies greatly with different tuning of the filter, decreasing utilization rate of the land, and occupying large area of ground.

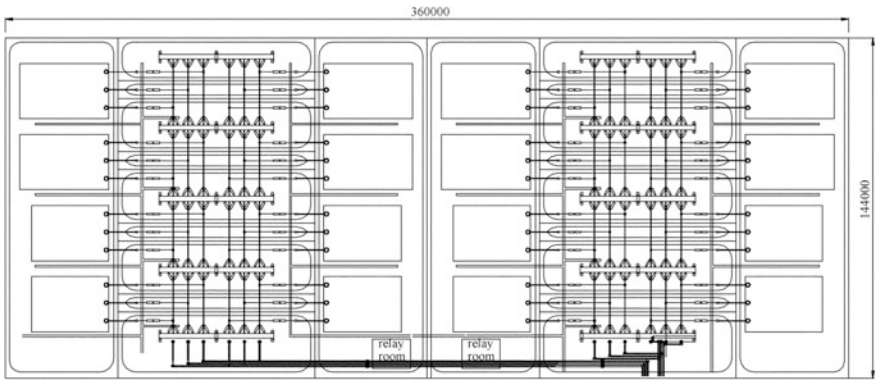

Fig. 26.25 Typical line-up layout plan (mm)

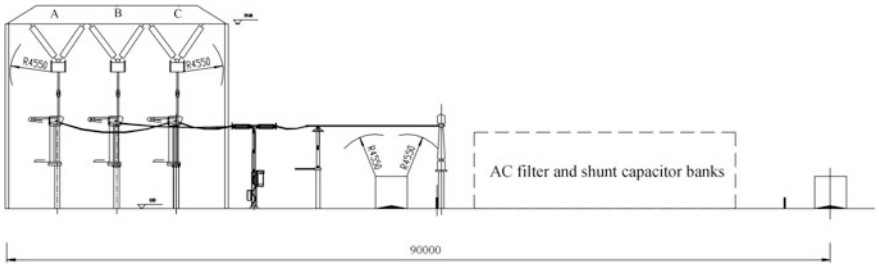

Fig. 26.26 Typical profile of line-up layout (mm)

2. Checkerboard pattern

It is the features of checkerboard pattern that four sub-banks in a bank are arranged symmetrically on both sides of the busbar to form a checkerboard pattern, like Chinese pictographic character "田". The typical checkerboard-pattern layout plan of AC filter yard is shown in Fig. 26.27, while the profile of the layout is shown in Fig. 26.28. It is characterized by:

(1) In line-up layout, the longitudinal dimension of the fence of AC filter banks is different from that of the shunt capacitor banks and the banks are lined up in one row, so the longitudinal dimension of the banks depends on the dimension of the fence of AC filter banks, which cannot be decreased. In checkerboard-pattern layout, the AC filter banks and shunt capacitor banks are separately arranged in two rows. In such a way, the longitudinal dimension of the row of shunt capacitor banks is decreased, thus reducing the overall dimensions.
(2) Since both sides of the busbar shall be connected with the AC filter banks or shunt capacitor banks, the original single-column vertical break disconnector is

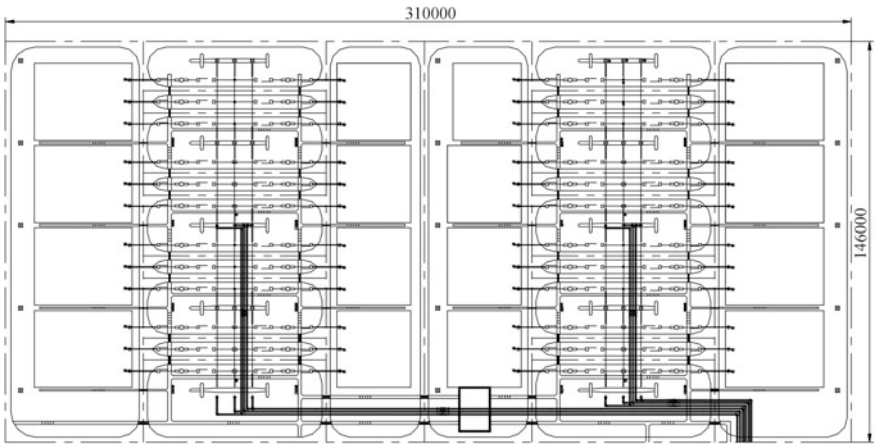

Fig. 26.27 Typical checkerboard-pattern layout plan (mm)

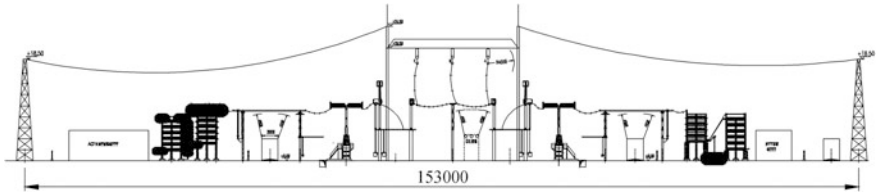

Fig. 26.28 Typical profile of checkerboard-pattern layout (mm)

canceled and substituted by double-column single-earth horizontal break disconnector. The original independent busbar earthing switch can be canceled and substituted by the earthing switch at the busbar side of the two-column disconnector of one sub-bank in each bank. Meanwhile, the capacitive potential transformer beneath the busbar of each bank is also used as the transition connection of the busbar down leads, thus reducing the number of support insulators. The busbar shall also be changed into flexible busbar correspondingly.

(3) Though the longitudinal dimension of sub-bank is increased due to substitution of double-column single-earthing disconnector which breaks horizontally for disconnector which breaks vertically, the transverse dimension of the AC filter yard is decreased greatly as a whole and the longitudinal width is not increased because the busbar is shared by both rows and the GIL tubular busbar conduction is adopted. The advantage is significant when there are many banks in the converter station.

(4) If the number of the filter sub-banks is even, the checkerboard-pattern layout can save about 14% occupancy area compared with the line-up layout of same scale. But, if the number of filter sub-banks is odd, the checkerboard pattern

occupies larger area due to the limitation by the band busbar, resulting in lower land utilization rate.

The checkerboard-pattern layout is adopted for the ±800 kV converter stations of Xiangjiaba–Shanghai and Jinping–South Jiangsu lines [7].

3. Improved checkerboard-pattern layout

The improved checkerboard-pattern layout is developed by optimizing the checkerboard-pattern and line-up pattern layouts. Its overall layout is like the checkerboard-pattern layout, i.e., four sub-banks in a bank are arranged symmetrically at both sides of bank busbar to form a checkerboard pattern, like Chinese pictographic character "田". The optimized feature is that in the improved checkerboard pattern wire is introduced from GIS bushing through the high-level jumper wire, and then connected to the filter sub-banks via the low-level jumper wire. The typically improved checkerboard-pattern layout of the AC filter yard is shown in Fig. 26.29, while the profile is shown in Fig. 26.30.

Height of double-level busbar of improved checkerboard pattern of 500 kV AC filter shall be determined by applying following methods (Fig. 26.31):

- Height of lower-level busbar

Clearance between top of 500 kV circuit breaker and lower-level tubular busbar is verified against value "D" temporarily.

In the diagram,

$$H \geq HT + B1 + R/2 + \Delta R,$$

where H is the height of centerline of tubular busbar (mm); HT is the height of top of 500 kV circuit breaker (mm); according to previous projects: HT = 10,500 mm;

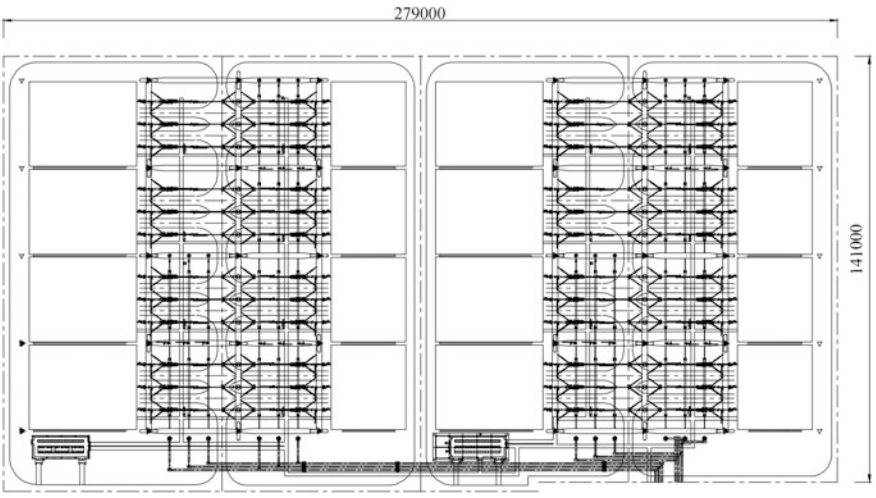

Fig. 26.29 Typical improved checkerboard-pattern layout plan (mm)

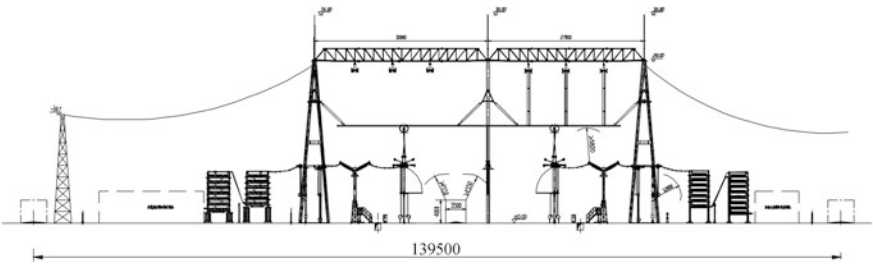

Fig. 26.30 Typical profile of improved checkerboard-pattern layout (mm)

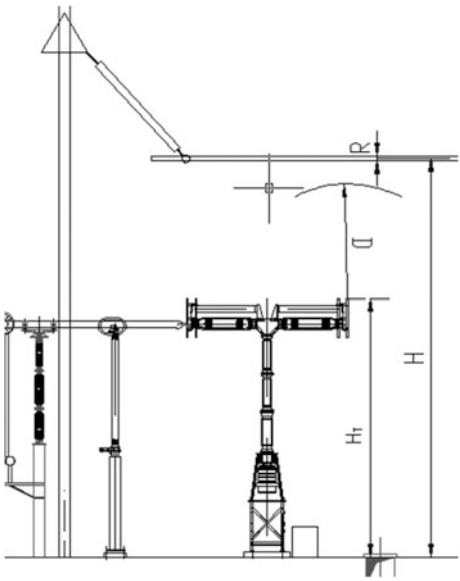

Fig. 26.31 Verification of height of lower-level busbar

D is between the fenceless live parts that are paralleled and will not be in outage in the same time for maintenance; *D* is made to be 5800 mm; *R* is the diameter of tubular busbar, $R = 250$ mm; and ΔR is the flexibility of tubular busbar, for high-capacity or important switchgears; the permissible flexibility in a span is normally lower than $D/2$, $\Delta R = D/2$;

$H \geq 10{,}500 + 5800 + 125 + 125 = 16{,}550$.

Considering some safety margin, height of centerline of the tubular busbar is 16.8 m.

It shall be noted that outage of single group, removal of circuit breaker, and maintenance of withdrawn arc extinguish chamber are not considered in the method of verification. In such condition, crane shall be maneuvered for lifting. In accordance with safety rules, height of the tubular busbar shall be raised by 7–8 m. It has been confirmed by the operating organization that the possibility that circuit breaker of filter yard shall be removed and maintained is relatively low, so maintenance of

the breaker is generally arranged in overhaul of the whole station, or outage of AC filter bank is considered.

- Determination of height of high-level jumper wire frame

Principle of height of high-level frame: distance between live part of tubular busbar of lower-level filter sub-bank and down conductor of high-level jumper wire shall satisfy requirement of Value "B1" (Fig. 26.32).

In accordance with the diagram above, the distance between live part of tubular busbar of side phase filter sub-bank (V-shaped string of grading ring) and jumper of high-level cross circuitry, and distance between high-level cross circuitry beam and tubular bus bar can be 9.3 m to a minimum. Considering some safety margin and conventional dimensions of switchgear, the distance between high-level cross circuitry beam and tubular busbar is determined to be 11.2 m, while height of the beam is determined to be 28 m.

For the improved checkerboard-pattern layout, there is a road for maintenance between the AC filter sub-bank and shunt capacitor sub-bank, which connects with the local interphase roads and extends to the fences of AC filter sub-banks and shunt capacitor sub-banks to facilitate the maintenance, handling, and patrol inspection of the equipment of sub-banks. The improved pattern has following advantages (Table 26.23):

(1) The length of GIL tubular busbar of filter bank is reduced to some extent, compared with both the line-up layout and checkerboard-pattern layout.
(2) Because the disconnectors of filter sub-bank adopt the vertical break type and are lined up, the space between the fence and disconnector can be reduced greatly. One road for maintenance set up between the two sub-banks, combined with the local interphase roads, is sufficient to satisfy the requirements for operation, repair, and maintenance of the filter sub-banks; therefore, the dedicated road for maintenance before fence can be canceled further to reduce the space between two filter sub-banks.

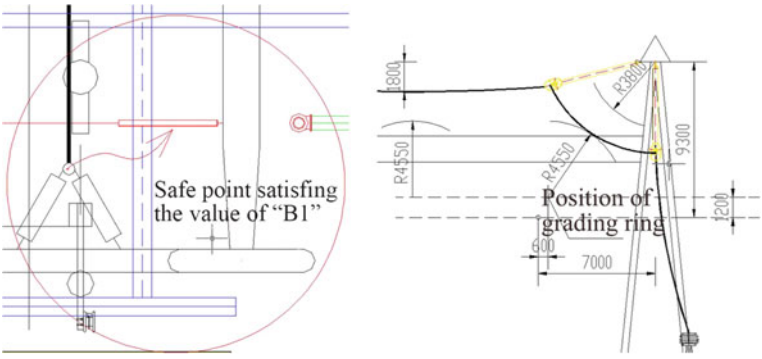

Fig. 26.32 Check diagram of height of high-level jumper wire frame (mm)

Table 26.23 Layout dimensions of AC filter yards in some UHVDC converter stations (m)

Project	East Guangzhou	Fengxian	Fulong	Tongli	Yulong	Jinhua	Shuanglong
Occupancy area	135*280.5	145*309	2*146*180	146*311	148*356	141*279	173.5*288
Layout	Line-up	Checkerboard pattern	Checkerboard pattern	Checkerboard pattern	Checkerboard pattern	Improved checkerboard pattern	Improved checkerboard pattern
Scale	15 sub-banks	15 sub-banks	14 sub-banks	16 sub-banks	14 sub-banks	17 sub-banks (note)	20 sub-banks

Note No. 17 sub-bank is arranged specially, the occupancy area does not include the area of No. 17 sub-bank

(3) Overhead grounding wire column is set up on the structure for lightning protection of the AC filter yard, so one row of overhead grounding wire columns in the middle of checkerboard-pattern layout can be canceled.
(4) The improved layout is applicable for any bank no matter if it contains sub-banks of odd number or of even number because of the reasonable connection led from high-level and low-level busbars.

The improved checkerboard-pattern layout is adopted for the ±800 kV converter stations in Left Bank of Xiluodu–Zhejiang Jinhua and South Hami–Zhengzhou UHVDC Projects.

4. Layout dimensions of AC filter yard.

26.8.3.2 Determination of Dimensions Inside the Fence of AC Filter Sub-banks

The equipment enclosed by the fence of AC filter sub-banks mainly consists of capacitor towers, reactors, current transformers, arresters, etc. The dimensions inside the fence shall be so determined to facilitate the installation, maintenance, and patrol inspection of the equipment and meet the requirement on air clearance distance of regulations.

For the 500 kV AC filter banks, the tower top at the HV side of capacitor shall be subject to the verification of 500 kV and the bottom subject to the verification of 330 kV. The equipment from the tower bottom at the LV side of capacitor to the HV side connection terminals of reactors shall be subject to the verification of 110 kV. Other equipment can be subject to the verification of 35 kV. The fence of sub-banks is generally 28 m wide. The length of the fence varies greatly according to the filtering characteristics, and the length is 26–43 m in existing projects.

For the 750 kV AC filter banks, the tower top at the HV side of capacitor shall be subject to the verification of 750 kV and the bottom subject to the verification of 330 kV. The equipment from the tower bottom at the LV side of capacitor to the HV side connection terminals of reactors shall be subject to the verification of 150 kV. Other equipment can be subject to the verification of 35 kV. The fence of sub-banks is generally 36.5 m wide. The length of the fence varies greatly according to the filtering characteristics, and the length is 21.5–45 m in existing projects.

For the 1000 kV AC filter banks, the tower top at the HV side of capacitor shall be subject to the verification of 1000 kV and the bottom subject to the verification of 500 kV. The equipment from the tower bottom at the LV side of capacitor to the HV side connection terminals of reactors shall be subject to the verification of 220 kV. Other equipment can be subject to the verification of 35 kV. The fence of sub-banks is generally 50 m wide. The length of the fence varies greatly according to the filtering characteristics, and the length is 28–50 m in existing projects.

26.8.4 Layout of AC Power Distribution Devices

The layout of AC power distribution devices in UHVDC converter station is generally same as that in conventional ±500 kV converter station, which also adopts 3/2 circuit breaker connection, but the number of strings is increased. Because UHV project has occupied a site of large area, the AC power distribution devices usually adopt indoor (outdoor) GIS type by considering reduction of site area, decrease of earthwork amount, convenient incoming line of converter transformer, and improvement of reliability in operation, and other factors.

26.8.5 Summary of Electrical General Layout

Electrical general layout of UHV converter station is similar to the ordinary 500 kV converter station, reflecting the technological feature of "DC switchyard-converter area-AC power distribution devices" in the overall layout [6].

Taking Fengxian converter station as an example, the 500 kV AC power distribution devices are of indoor GIS type, arranged at the east side of the substation site. The outgoing line in the phase and future extends eastward, and then turns northward. The converter transformer, valve hall, and control building are arranged in the center of the site. The 800 kV outdoor DC switchyard is arranged at west side of the site, outgoing line extending westward. Four banks of the AC filters, in checkerboard-pattern layout, are arranged collectively at the north side of the site, and introduced into the string through GIS tube. The AC protections are decentralized. The Backup on-duty building, multifunctional fire-fighting pump house, garage, etc., are designated to the southeast side of the site. The road access to the site comes from south side of the site (Fig. 26.33).

Each pole is provided with a HV and a LV valve hall, respectively, so there are 4 valve halls, 1 control building, and 2 auxiliary equipment houses in the substation in total. The high-end and LV valve halls of same pole are arranged face to face, and two low-end valve halls are arranged back to back. The valve tower is of suspension-type duplex valve. There are 6 duplex valve towers suspended in each valve hall. The converter transformer, of single-phase dual-winding type, is arranged closely to the valve hall, and the valve-side bushing is inserted into the hall directly. The main control building is arranged at the side of the LV valve hall, facing the 500 kV AC switchyard. Two auxiliary equipment houses are arranged at the side of HV hall valve, respectively.

The whole substation is laid out neatly and compactly, showing itself a standard rectangle. The converter station covers less area, being clear in zoning and reasonable in layout. The area inside the boundary is about 15.06 ha.

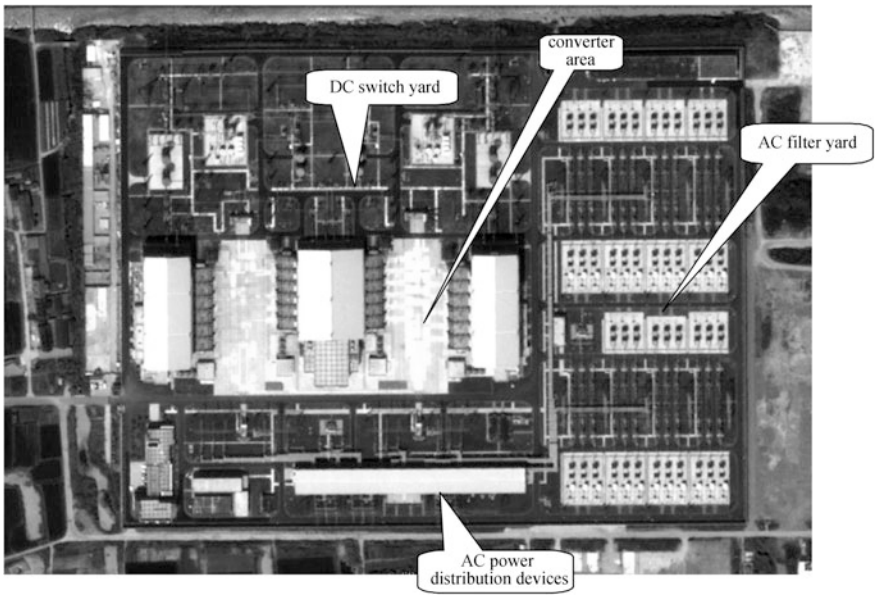

Fig. 26.33 Aerial photography of UHVDC converter station

26.9 Buildings in Converter Station

26.9.1 Main Buildings and Structures

The buildings and structures in UHVDC converter station include the main production buildings, such as valve halls, control building, relay houses, and the auxiliary (accessorial) production buildings, such as multifunctional water pump house, water intake pump house, multifunctional building, servicing spare parts warehouse, garage, security, and doorkeepers house. If the DC yard or GIS is of indoor arrangement, the main production buildings shall also include indoor DC yard and GIS house. If rest house is set up near the substation for the operators, the design of multifunctional building in the substation can be simplified into office building.

Compared with the AC substation, there are more single buildings in the DC substation, which are complicated in functions and various in structure and shape. If outdoor DC yard and indoor GIS house are adopted, the building area of the whole substation is about 27,000 m^2. Therefore, the buildings account for a large proportion of design of the substation.

26.9.2 Valve Hall

The valve hall shall ensure good sealing performance; all openings and clearances must be sealed closely to maintain micro-positive pressure inside the valve hall to prevent entry of dusts from outside, thus keeping the air clean inside the hall.

Hexahedral electromagnetic shielding is adopted in the valve hall to prevent the influence of electromagnetic wave interference.

The access of the valve hall at 0 m layer of each pole shall not be less than 2, i.e., one access leads directly outdoors, while another leads to the control building. There should be at least one access in the valve hall used as transporting path. The clearance above the access shall be sufficient to transport the maximum equipment in the valve hall and to admit the elevator used for installation and maintenance of converter valves. Doors at the access of valve halls shall be electromagnetic shielding doors, opened towards outdoors or control building.

Patrol-inspection path shall be provided at appropriate place, which can pass through to the roof truss area of valve top and connect with the controlling building, so as to satisfy the patrol-inspection requirements of operators. Doors between patrol-inspection path and control building shall be electromagnetic shielding doors, opened towards control building.

Electromagnetic shielding fireproof viewing window shall be provided at appropriate place (generally the first floor or the second floor of control building) between the valve hall and control building, so that the operators in the control building can observe the operation of electrical equipment in valve halls.

The exterior wall of the valve hall shall not be provided with daylighting windows. If installation of fire-fighting louver window or emergency exhaust fan is required by process, necessary measures for electromagnetic shielding and against leakage must be taken, and shutting device shall be mounted at the air opening to ensure that the valve hall is in close state in normal operation.

If the space between the valve hall and converter transformer, smoothing reactor does not meet the requirements of fire prevention, the wall must satisfy the requirement of 4-h fire-resistance rating. Fire-retarding coating is not necessary for steel roof truss of valve hall.

The claddings and doors of valve hall shall have good performance of sealing, temperature preservation, thermal insulation, and noise insulation. The face coat of valve hall floor shall be the building finishing material that is abrasion-resistant, dust–free, and easy to clean.

The valve hall is of complex structure. The foundation of valve hall shall be reinforced concrete-independent base slab under column. Reinforced concrete tie beams are set up between the base slabs so that the foundations can be combined to withstand the horizontal shear due to wind load and earthquake. Reinforced concrete-piled raft foundation is used under the fire-retardant walls of valve halls and converter transformers as well as the converter transformers.

26.9.3 Control Building and Auxiliary Equipment Building

For the purpose of convenient connection of process equipment and pipelines, as well as patrol inspection during operation, the control building and valve hall can be combined together.

The control building can be a two- or three-storey building. Equipment rooms such as valve-cooling equipment room, pole auxiliary equipment room, 400 V power distribution room, communication equipment room, and other equipment rooms are arranged on the ground floor. Office spaces such as main control room, equipment room, conference room, offices are arranged on the first floor.

The openings for hoist shall be provided in the control building. If it is a three-storey building and the main control room lies on the third floor, it is recommended to provide a passenger-and-freight elevator. The space for installation and maintenance of the elevator could be reserved properly on the ground floor provided that there is sufficient space in the building.

In order to prevent the influence of electromagnetic wave interference, electromagnetic shielding measures must be taken for the control building.

Passages in the control building, such as corridor, stairway, doorway, shall be organized in such a way as to meet relevant requirements as specified in current national standard *Code of Design on Building Fire Protection and Prevention*. The main doorway shall be taken into comprehensive consideration with the general layout of the substation, so that it is easy to connect with the main roads in the substation.

The control building can be provided with cable trench or underground cable corridor according to the process requirement. If underground cable corridor is adopted, the technical measures on fire prevention, evacuation, air ventilation, fume exhaust, moisture prevention, and water drainage of the building shall be taken into comprehensive consideration. The claddings, windows, and doors of the building shall possess such performance as heat preservation, thermal insulation, and noise insulation.

The main control room shall be arranged in such a way that the noise influence is reduced as low as possible, and the room possesses favorable orientation and conditions of natural ventilation and natural lighting. In the room, the equipment shall be arranged and the illumination shall be designed in such a way as to avoid glare generated on screens.

The HV valve hall of each pole shall be provided with auxiliary equipment building at its side, in which there are 400 V power distribution room, valve-cooling equipment room, and staircase connected to the patrol path in the hall. The auxiliary equipment building shall be same as the main control building in façade to keep consistent architectural style in the substation.

26.9.4 Indoor DC Yard

For indoor DC yard, the smoothing reactor shall be supported and the DC filters shall be provided with dual towers arranged completely indoors.

The yard is of single-storey steel structure, and the structure for maintenance is made of composite profiled steel sheet.

26.9.5 GIS House

The GIS house is arranged according to the electrical process. It is a single-storey steel structure building, and single-layer aluminum- and zinc-plating high strength colorful profiled steel sheets are applied as envelope material on the exterior wall surface, from 1.2 m above the ground level upwards, while wall coating is applied on the exterior wall surface from the ground level up to 1.2 m height. The roof of the house is same as that of valve hall. Reinforced concrete-independent base slab under column is adopted for GIS house, and reinforced concrete tie beams are set up between base slabs.

26.9.6 Other Buildings

The relay house, security house, garage, 35 kV power distribution house, spare parts warehouse, multifunctional pump house, fire-fighting pump house, industrial water make-up equipment house are all one-storey buildings.

26.9.7 Type of Structure

The main structure of valve hall is a combined steel-concrete frame bent structure or reinforced concrete frame bent structure. In the structure, the retardant wall between valve hall and converter transformer adopts a structure of reinforced concrete frame plus filler wall.

The roof of valve hall is a steel structure with purlin roof. The envelope structure of the roof is a light roof made of composite profiled steel sheet. In the regions vulnerable to typhoon, the envelope structure of roof can also be a combined steel-concrete structure having base mold made of profiled steel sheet. Structural system of valve hall roof shall be arranged in such a way so as to guarantee the integral rigidity and stability of the structure. The nodes shall be designed such that the structure is simple and the construction is easy.

The main structure of control building is of reinforced concrete-framed structure. The floor and roof shall be made of cast in situ-reinforced concrete slabs, and the envelope structure shall be masonry filler wall.

The fire-retardant wall between converter transformers is of structure combining cast in situ-reinforced concrete frame with filler wall. The thickness of protective coat applied on the reinforced concrete frame of the fire-retardant wall shall be such that it satisfies not only the requirements specified in concrete design codes, but also the relevant requirements specified in current national fire prevention codes.

Indoor GIS house (if exist) shall preferentially be of light steel structure. If the span is relatively small, reinforced concrete structure can also be used, and the envelope structure shall adapt to the main structure.

26.10 Connection and Layout of Substation-Service Power

As an auxiliary system of the converter station, the substation-service power system is an important guarantee for safe and reliable operation of the substation. Compared with ±500 kV converter station, ±800 kV converter station is more complicated in production system (including AC switch field, DC switch field, and AC/DC filter) and auxiliary production system (including cooling system, air conditioning system), and requires higher capacity of substation-service power. Therefore, it is especially important that the substation-service power system is reasonably designed.

In general, the substation-service power supply of UHV converter station is provided with independent three-circuit power supply, of which at least one circuit is used as internal substation-service power supply to ensure the reliability of the power supply and saving cost. In selecting external substation-service power source, first priority shall be given to the power sources whose higher-level sources come from different power supply zones instead of the same substation as possible, since the reliability of substation-service power supply directly affects the safe and reliable operation of the converter station. In addition, because the UHV converter station has high substation-service power load capacity, the external substation-service power source should be at 35 or 110 kV voltage level and supply power through dedicated lines. With respect to the internal substation-service power source, priority shall be given to the solution of feeding from the AC distribution device string and from the AC filter busbar to utilize the field in the substation sufficiently. When it is impossible to feed from positions above-mentioned, it is recommended to feed from the busbar of AC distribution device or busbar of AC filter bank by the way of T connection.

The sectionalized single-busbar configuration is usually adopted for the HV substation-service power supply system. The HV voltage transformer system consists of two working transformers and one dedicated standby transformer, and is provided with the device which can put the transformers into operation automatically. Operation in parallel should not be designed for the HV working

transformers. And capacity of each transformer shall be determined according to the load of the whole substation.

The sectionalized single-busbar configuration is adopted for the LV substation-service system. Each valve group shall be provided with two LV transformers correspondingly. The two LV transformers shall be led from two HV working busbar sections, respectively, and act as standby to each other.

26.11 Secondary System

26.11.1 Control and Protection of AC and DC Systems

26.11.1.1 Main Concept of Design

1. The converter station shall be designed as attended station. A computer-based monitoring system shall be set up in the converter station as a united common platform for the AC and DC systems to fulfill data acquisition, processing, monitoring, control, and recording of all systems and equipment of the whole station, to provide good operating interface and application functions including data statistics and analysis to the operators.
2. The computer-based monitoring system is of three-layer structure, including station level, control level, and local level. Equipment of control level and local control is fully duplicated.
3. On the basis of project characteristics that each converter unit of each pole in ±800 kV UHVDC converter station can be put into and out from operation automatically, the DC control and protection system shall keep equipment and function of control and protection of each converter unit relatively independent in configuration of equipment, control strategy, and protection zoning.
4. HVDC protection and control systems are separated and independent, and configured in duplication or multifold. As far as function and organized panel are concerned, the protection systems of two poles are independent mutually and those of two converter units of each pole are also independently mutually.
5. HVDC control and protection systems are adaptive to rectifier operation and to inverter operation.
6. The equipment of control level and local level of the AC switchyard is integrated and organized into panels according to series, and arranged collectively in local relay rooms. Control equipment of AC filter bank is configured according to banks; control equipment and protection equipment are independent mutually; and protection device of AC filter is configured in duplication according to filter bank. The equipment of control level and local level of station service power supply system is integrated to be organized into panels and

arranged in local relay rooms. The control equipment is independent from protection equipment.
7. DC control and protection system can satisfy technical requirement of ice melting and blocking in the project.

26.11.1.2 Computer-Based Monitoring System

A computer-based monitoring system shall be set up in the converter station as a united common platform for the AC and DC systems to fulfill data acquisition, processing, monitoring, control, and recording of all systems and equipment of the whole station, to provide good operating interface and application functions including data statistics and analysis to the operators.

1. Structure of system

The computer-based monitoring system adopts modularized and hierarchical distributed network structure. The whole system comprises station level, control level, and local level (I/O interface equipment of distributed data acquisition system). The equipment of station level and those of control level is connected via dual-optic fiber Ethernet, while the equipment of control level and those of local level is connected via optic fiber or high-speed fieldbus of massive capacity. Refer to Fig. 26.25 for typical configuration of computer-based monitoring system of converter station.

2. Function of system

(1) Control mode

Control mode of converter station is designed according to requirement of hierarchical control. And under any circumstances, only one control mode of the control position is able to function in the system. The control mode includes control by remote dispatching center, control by operator in operating and control room of the converter station, local control by equipment panel of control level of the monitoring system, and control by equipment of local level (i.e., field manual or electric manipulation on equipment proper or control panel of adjacent secondary system).

(2) Operating function

In normal operation, the operators exert real-time operating function to the equipment to be controlled and operated in the station via operator station. All the equipment in the station is interlocked in operation.

(3) Sequence control, regulation, and interlock function

The monitoring system realizes automatic sequence control, regulation, and interlock functions in accordance with requirement of changeover of operating plan and transfer of control mode of HVDC system.

(4) Supervisory function of SCADA system

This system includes single-line diagram of main connection of the system and that of connection mode for operation of UHVDC system, supervisory signals of HVDC system, supervisory signals of AC system, status signal of equipment, event sequence, central alarm record, and trend record.

(5) Data acquisition and processing function

The monitoring system realizes real-time data acquisition and processing function on primary and secondary equipment of all auxiliary systems in HVDC switchyard and AC switchyard and in the station. The local data acquisition and control system adopt hierarchical and modularized structure, comprising two levels, i.e., control system and control interface. I/O sampling unit, data transmission bus, main equipment, and control output are configured in full duplication.

(6) Communication function of inter-station SCADA system

Communication with SCADA system in opposite converter station is realized through the bridge configured redundantly in SCADA.

(7) Miscellaneous functions

These mainly include event review, report generation and print, management, simulation training for operating personnel, and simulation of the system.

3. Configuration of system equipment

(1) Station level

Highly effective real-time station control system is configured to provide the operators with station-level control, supervision, measurement, management, and other functions. Meanwhile, the station control system is connected to electric power data communication network via equipment at network interface to exert automatic dispatching of the power grid.

Equipment of station level is arranged in operating control room in main control building and station control and protection equipment room. The station control system shall be equipped with all necessary workstations, printers, etc. The operator can configure functions of the monitoring system via engineer stations, and complete normal control, opening/closure, and on–off operation of AC and DC equipment in the station, supervision, measurement, and record of operating status of the equipment, as well as processing of various information. When the system works as main control station, it can also control operation of relevant equipment in opposite station (Fig. 26.34).

(2) Control level

Equipment of control level realizes local station control of the equipment in control area, sequence/regulation control and interlock, switching synchronization, and other functions, which will be configured in duplication.

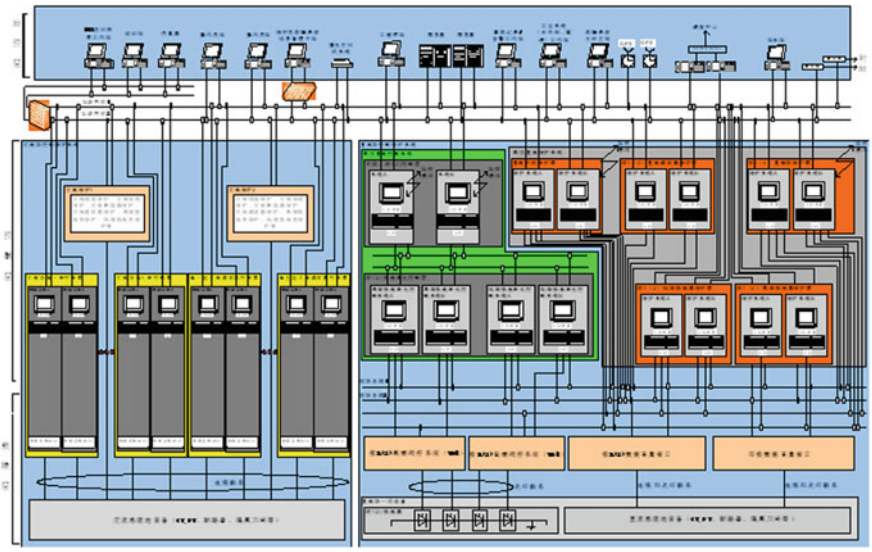

Fig. 26.34 Configuration of typical computer-based monitoring system of converter station

The equipment of control level communicates with those of station level via dual-optic fiber Ethernet, and exchange data with those of local level via high-speed field busbar or dual-optic-fiber Ethernet LAN.

Equipment of control level of DC switchyard is integrated with HVDC control system. Polar and bipolar control system shall be configured separately. Equipment of control level of each pole shall be configured individually according to pole and converter unit in terms of functions and organized panel, thus separating main machine of control from that of protection.

Valve-cooling control equipment is configured according to valve group, and integrated with equipment of local level into a panel. The control equipment is configured in duplication and installed in corresponding valve-cooling room.

Equipment of control level of AC switchyard is duplicated and arranged in the nearest local relay room by their control areas, and integrated with equipment of local level into a panel.

(3) Local level

Equipment of local level serves as connection interface with primary equipment. Its sampling module conducts filtering, segregation, A/D conversion, change of scale, and other preliminary processing to the sampled field signals, then sends the signals to all control systems of relevant control areas via high-speed field busbar or dual-optic-fiber Ethernet LAN. Meanwhile, equipment of local level receives control commands of the relevant controls system to achieve real-time control or regulation to the object to be controlled.

Equipment of local level is of modularized hierarchical structure, which is configured in full duplication from I/O sampling unit, data transmission bus, main equipment to control outlet, arranged in distributed pattern, and installed in the secondary equipment room nearest the equipment of main circuit.

Equipment of local level is configured according to two poles, pole and converter unit (valve and converter transformer), respectively, in principle, in terms of function and organized panel, to accommodate requirements of monopolar and 1/2 monopolar operating plan on each pole, and to facilitate operation, management, and maintenance of equipment under different operating plans.

Equipment of local level of AC switchyard is duplicated and arranged in the nearest local relay room by their control areas, and integrated with the equipment of control level into a panel.

26.11.1.3 HVDC Control and Protection System

There is no essential difference in design principle between control and protection system of ±800 kV UHVDC converter station and that of ±500 kV conventional DC converter station. Each pole of ±800 kV UHVDC converter station is composed of two series-connected converter units, and each converter unit is provided with independent bypass circuit breaker and disconnector to realize auto-switching function of the unit. Therefore, the control strategy, protection zoning, and equipment configuration shall be designed in such a way that the converter units can keep mutual independence in their control and protection equipment and functions. In addition, on the premise that requirements of technical performance and function under various operating conditions are met, the converter units shall be convenient for the operators and maintenance workers to debug, operate, and maintain the control and protection equipment.

DC control and protection equipment of HV converter station shall adopt standard function modules based on microprocessor and digital signal processor. The control system shall be constructed into hierarchical and distributed structure. Any hardware or software of the DC control and protection system shall be fully duplicated or multiplied and has consummate self-check function and transfer logics to ensure safety and reliability in operation of the system, thus minimizing maintenance of the equipment.

The control and protection systems of each pole and of two poles are independent mutually. In each pole, the control and protection systems of HV converter unit and LV converter unit are also independent mutually. Failure or service of any pole or any converter unit does not affect operation of another pole or another converter unit.

DC transmission protection system is bound up with control system. Only close coordination between them can restrain development of fault, ensure safety of equipment, prevent disturbance, and recover the system quickly. The control and protection systems shall segregate a faulty element with minimum disturbance in minimum time to increase the stability of operation. In Three Gorges–Changzhou

and Three Gorges–Guangdong DC transmission projects, the DC control and protection systems are designed integrally in term of their hardware and they are organized into panels in unified way [8].

In accordance with management mode and operating practices of China's power grid, control system is required to be separated from and independent of protection one. In the Three Gorges–Shanghai DC transmission project, attempt is made to make the main computers of DC control and protection separate and independent of each other, which, however, are still assembled into the same cabinet, and the connection with primary equipment is realized via unified data acquisition unit. The control system and protection systems of ±800 kV converter station are separate and independent, and are configured and organized into panel according to different principles.

1. HVDC control system

HVDC control system adopts principle of hierarchical distributed configuration. Control equipment of each converter unit of two poles and each pole is configured independent fully and duplicated from I/O sampling unit, data transmission bus, main equipment to control outlet.

It is planned that basic control mode of DC transmission system includes polar power control mode, independent control mode of pole power, emergency pole current control mode, synchronous pole current control mode, emergency power drop/rise control mode, polar full voltage/reduced voltage operation control mode, pole power backfeeding control mode, control mode of open line test control mode of pole line, reactive power control mode, low-load reactive improvement control mode, ice-melting control mode, and ice-blocking control mode.

The equipment of control level of DC control system of ±800 kV UHVDC converter station shall be configured functionally according to dual poles, pole, and valve group (converter unit). The equipment of control level of dual poles and each pole, that of single pole, and control equipment of high-end and LV valve group of each pole are totally independent physically. The control level of HVDC system comprises dual-pole control level, pole control level, and converter control level according to series-connection characteristics of valve groups of UHVDC system, and special control networks are configured between dual-pole control level and pole control level, between pole control level and converter control level, respectively.

Dual-pole control level realizes the bipolar interlock and blocking, bipolar power control, bipolar power transfer control, inter-pole current balance control, bipolar reactive power control, and other functions. Pole control level realizes start/stop of the pole, unblocking/blocking of the pole, coordinates power/current control of the pole, voltage/trigger angle control of the pole, sequence control and interlock of the pole, control of tap, troubleshooting and control, inter-station communication of the pole, inter-pole communication, and other functions. Converter unit control level realizes firing control of valve group of converter unit, generates trigger pulse of valve group, start/stop of valve group of converter unit, unlocking/blocking, engagement/disengagement of valve group of converter unit, sequence control and

interlock of converter unit layer, over-load supervision of valve group, and other functions.

2. UHVDC protection

(1) Principle for configuration of UHVDC protection

The UHVDC protection shall be configured according to the zones to be protected. Each protection zone shall be overlapped with its adjacent zones to avoid dead zone of protection.

The protection of each protection zone shall be at least of dual-configuration. In term of configuration of equipment, interface relationship between protection equipment of functional zones shall be simplified as possible, so that the interfaces are easy for maintenance to guarantee their reliability and safety. The protection of the two poles shall be configured completely independent. The protection of the faulty pole shall not affect the normal operation of the other pole during the bipolar operation. The protection of the converter unit of each pole shall be configured completely independent. The fault of any element in a converter unit shall not affect the normal operation of another converter unit of the same pole.

(2) Zoning of UHVDC protection

In accordance with the zones to be protected and functional requirements, UHVDC protection can be divided generally into following zones: AC lead protection zone of HV converter transformer (Pole 1, Pole 2), AC lead protection zone of LV converter transformer (Pole 1, Pole 2), HV converter transformer protection zone (Pole 1, Pole 2), LV converter transformer protection zone (Pole 1, Pole 2), DC line protection zone (Pole 1, Pole 2), pole DC busbar protection zone (Pole 1, Pole 2), DC filter protection zone (Pole 1, Pole 2), bipolar switchyard protection zone, and DC ground electrode line protection zone, etc.

(3) Scheme for configuration of UHVDC protection

In order to improve the safety and reliability of the UHVDC protection system, each equipment or protection zone shall be equipped with at least two independent protections, each of which shall have complete protecting functions. The two protections shall be based on different principles, measuring appliances, channels, and power supplies as much as possible. In case that it is impossible to apply different principles, the protective circuit shall be configured redundantly to ensure that when any of the main protection refuses to act, the equipment can be shut down safely, and that the standby protection can detect the failure when the main protection fails to do so. The DC protection of the two poles and of the two converter units of each pole shall be configured completely independent of each other.

The protection functions shall be configured in accordance with the influence extent of faults in a protection zone. The interface relationship between the protection equipment in various functional zones shall be simplified to facilitate the maintenance personnel to carry out maintenance and commissioning of the

equipment (including primary and secondary equipment) in the zones, so as to minimize the influence extent of the faults in the zones.

(4) DC line fault-locating system

The DC line fault-locating device is an independent equipment, installed on both ends of the DC line. It detects the transient and permanent faults of the DC line, and locates the fault through calculation.

The fault-locating device receives the common timing signal and is not equipped with special satellite clock receiver. The DC line fault-locating device is provided with independent inter-station communication channel to realize the precise locating on the DC line.

(5) DC transient fault recording system

The DC transient fault recording system is arranged in the equipment room of the station. It consists of numerous data acquisition units and is used for recording the waves of secondary measurement of all voltage transformers and current transformers in the HVDC system, including the current on the AC side of converter transformer. The system communicates with the computer-based monitoring system in the station through the fault recording and analysis master station arranged in operator control room. The main station is shared by the HVDC fault recording and AC fault recording.

26.11.1.4 AC Element Protection

The AC element protection comprises the converter transformer protection, AC filter bank protection, station transformer protection, standby station transformer, etc., of which, the converter transformer protection is included in the DC control protection system, and the AC filter protections are used to protect the lead wire zone of the AC filter bank and the equipment in sub-banks, including the AC lead protection and the filter sub-bank protection. Other element protections are similar as those in the AC substation.

26.11.1.5 Valve-Cooling Control and Protection System

The valve-cooling control and protection system is of dual-configuration, and is arranged in the valve-cooling equipment room nearby. It is mainly used to control the water pumps (including cooling water pump, make-up water pump, secondary circulating pump, and spray pump) and the temperature (including cooling fan, parallel electric valve, and electric heater). It fulfills the real-time supervision on the main operation parameters of the valve-cooling system, such as the temperature, flow rate, water level, conductivity, pressure, equipment situation. All alarm signals are transferred to the substation control system to update the alarm signal list.

The protection functions mainly include the temperature protection, flow rate protection, leakage protection, pressure protection, water level protection, conductivity protection.

26.11.1.6 Control Building and Local Relay House

According to the general electrical layout, two HV valve halls are arranged separately, while two LV valve halls are arranged back to back. The main control building locates beside the two LV valve halls. The control and protection equipment for the LV valve group of two poles and the auxiliary equipment such as valve-cooling devices, auxiliary power supply, are arranged in the control building. Passages for patrol inspection of two LV valve halls are connected directly with the main control building to facilitate operation and maintenance. The control and protection equipment of HV valve groups of two poles and the auxiliary equipment such as valve-cooling devices, auxiliary power supply, are arranged in the two auxiliary control buildings. The deployment of local relay house and the configuration of control and protection equipment of the AC equipment are similar with those in the AC substation.

26.11.1.7 Auxiliary Systems

1. DC power supply system

The 110 or 220 V DC working voltages can be adopted. The capacity of storage battery bank shall be able to sustain 2 h of emergency power supply.

Under normal operating condition, the two storage battery banks and two chargers bear partial equipment load each. The capacity of storage battery and discharger are selected according to the demand of whole equipment within the power supply scope.

On the basis of the features that all valve groups in the UHVDC converter station are relatively independent, the substation is generally equipped with 6–7 DC power source systems, of which 4 power source systems are assigned to four valve groups, one system for each; 1 power source system is assigned to the bipolar control and protection equipment and substation commonly used equipment; and 1–2 systems are assigned to the control and protection equipment in the AC yard.

2. AC uninterrupted power supply system (UPS)

The whole station is equipped with two AC uninterrupted power supply (UPS) systems, standby to each other, supplying high-quality, and reliable AC power to SCADA system's workstation, printer, telecontrol equipment, in-station fault oscillograph, electric energy metering instrument, and other important loads.

The AC UPS system is connected with the battery system of common equipment at the station. No special battery is provided.

3. Station communication

The station telephone communication system is used for the communication of dispatching, production, and management in the station. Station telephone communication and system dispatching communication share the same exchange board.

4. Intelligent auxiliary control system

In order to ensure the safe operation of the station and facilitate the operation, maintenance, and management, the whole station shall be equipped centrally with one set of intelligent auxiliary control system to fulfill all-around intelligent linkage controls, such as monitoring, fire alarm, technical prevention, illumination, environmental monitoring. Operators in the substation and remote dispatchers can monitor and manage the sub-systems in the substation via centralized management platform and HMI of the intelligent auxiliary control system, thus allowing the sub-systems implementing the functions required by the substation.

5. Online monitoring system of transformer oil–gas insulation

The monitoring and analysis system can conduct real-time online and continuous monitoring on the gases dissolved in oil, including at least hydrogen H_2, acetylene C_2H_2, ethylene C_2H_4, methane CH_4, ethane C_2H_6, carbon monoxide CO, and carbon dioxide CO_2, and on the trace water H_2O. The system comprises two parts, i.e., online detection of gas content in insulating oil and chromatographic analysis and diagnosis. The system provides the information for the decision of operation and maintenance, i.e., to decide if the equipment could keep operating or need repair and maintenance.

26.11.1.8 Design of Secondary Circuit Immune to Electromagnetic Interference (EMI)

The electromagnetic environment generated by the HV voltage of AC/DC switchyards in the converter station will cause severe interference on the secondary circuit, while the secondary circuit consists of digital equipment, which utilizes large numbers of electronic elements. In addition, the local control and data sampling equipment are decentralized into local relay house in switchyard or decentralized near primary equipment, so the secondary equipment must be immune to EMI. Effective measures against EMI shall be considered in design of the secondary circuit.

1. Software and hardware of the secondary equipment shall be designed and manufactured in such a way that they possess higher ability to resist EMI. Cables involving in HV distribution devices shall be laid in radiation pattern and

must not be laid parallel with the HV conductors. Shield cables shall be adopted for the secondary circuit, with the shield of cable being earthed properly.
2. Shielding measures shall be taken between the local relay house, main and auxiliary control buildings, and its function rooms.
3. Double-shielded control cable shall be used for the connection between the data sampling equipment and the primary equipment.
4. Optic fiber equipment shall be used for all communications between the DC control and protection systems and the computer monitoring systems.
5. Measuring and control panel and protection panel are equipped with special earthing copper busbars having cross section not less than 100 mm^2, which are connected with the grounding grid of the relay house closely. The grounding grid of relay house is connected with the main grounding grid at one point by four copper cables having cross section not less than 50 mm^2 each.
6. Copper busbars having cross section not less than 100 mm^2 are laid in cable laying direction in the cable trench from the switchyard to the relay protection house.

26.11.2 AC Protection System and Safety and Stabilizing Devices

1. 500 kV AC protection system

The AC side of the converter station is generally at 500 kV level. Protections of the AC system is generally same as that of the conventional 500 kV AC substation in configuration, but the influence of high-order harmonic components in current and voltage of the converter station on the AC system protection shall be taken into consideration. The AC protection in converter station shall have immunity to the harmonics interference. The harmonic current and voltage generated in operation of converter transformer under normal or faulty condition of the system shall not result in maloperation or misstrip of the AC system protection. The transition process under transient condition and EMI shall not affect the normal operation of the AC system protection.

2. Safety and stabilizing device

The safety and stabilizing (SS) device in the converter station is configured according to the following principles: equipping two SS control devices and each device having its cabinet. Each SS device is directed to the opposite converter station and relevant transformer substation, i.e., each SS device communicates with SS device in the opposite converter station via a direct channel with 2M band width, and also communicates with SS devices in relevant transformer substation via a special optic fiber core. Meanwhile, the communication equipment room shall be

provided with a communication interface panel, which accommodates two photo-electric converting devices with 2M band width. Each SS device shall also have the communication interface to the DC control system of the converter station itself.

26.11.3 Dispatching Automation

1. Dispatching management relation and telecontrol information transmission principle

In accordance with the nature of UHVDC transmission projects, in the converter station, the DC system equipment (including DC tie-lines), AC system equipment (including AC filter), and AC equipment that have significant impact on the safety of UHV power grid (e.g., safety and stabilizing device) shall be dispatched and administrated directly by the dispatching center of the grid.

The converter station sends the telecontrol information required directly to the grid dispatching center (including the standby dispatching center) and receives the control commands assigned by the grid dispatching center to the DC transmission system. In order to satisfy the requirement of supervision on the converter station by grid dispatching center at provincial or municipal level, the converter station is required to send the relevant telecontrol information to the local grid dispatching center, opposite area dispatching center, and the dispatching center at provincial or municipal level.

2. Telecontrol system solution

(1) Telecontrol information acquisition

The solution for telecontrol information acquisition is determined in principle according to the *Specifications for the Design of Dispatching Automation in Electric Power Systems*, and shall also meet the operation and management requirements of centralized dispatching of grid, management at different levels, and independent accounting. The converter station shall be equipped with one computer-based supervisory control and data acquisition (SCADA) system to achieve local monitoring function and telecontrol function comprehensively in the converter station. Operating system of SCADA system must adopt UNIX and LINUX, while supporting communication protocol of standard DL/T-860 (IEC61850).

Acquisition of telecontrol information of the substation is conducted by the data acquisition equipment in SCADA system. In order to avoid repeated equipment configuration, acquisition of telecontrol information of the substation and automation information in the substation are all performed by the data acquisition I/O units of computer supervisory system.

(2) Telecontrol equipment configuration

The telecontrol system shall comprise relevant data acquisition and communication device (or telecontrol work station), data network access equipment (including safety and prevention equipment), and MODEM. In view of special features of UHVDC projects, it is recommended to adopt redundant configuration in telecontrol work station to guarantee the reliability of the telecontrol system.

The telecontrol work station is connected with supervisory system LAN in the converter station via high-speed Ethernet interface, and obtains the telecontrol information required by the dispatching centers at different levels directly from the I/O units. A variety of control and regulation commands assigned by the grid dispatching centers shall be sent directly to the I/O units at bay level from the telecontrol work station.

The telecontrol work station shall be able to realize the transmission of telecontrol information through point-to-point telecontrol channel and data network.

Necessary longitudinal encryption and authentication device special for electric industry shall be set up to ensure the safety of telecontrol information transmission of converter station.

3. Electric energy metering

The converter station shall be equipped with one electric energy metering system, including electric energy meter, electric energy data acquisition terminal, to collect the data from the electric energy meter and transmit the electric energy data of corresponding gateway to dispatching center. The establishment of metering gateway and configuration principle of metering equipment shall comply with the provisions of State Grid Corporation.

4. GPS Time synchronization

There should be only one time synchronizing system in the converter station, i.e., the whole substation utilizes one GPS time synchronizing system. Time synchronizing signals of all equipment of secondary system for which time synchronization is necessary shall be controlled by such synchronizing system. Individual equipment will not be equipped with special synchronizing standard clock.

The unified GPS time synchronizing system set up in the converter station is used mainly to realize time synchronization and signal unification of the computer supervisory system, protection device, fault recorder, etc., and provide the interfaces for various time synchronizing signals required by the equipment above-mentioned.

5. Requirement of safety and protection for secondary system

In order to implement the Order No. 30 [2002] of the State Economic and Trade Commission Regulations on Security Protection of Computer-based Monitoring System and Dispatching Automation Data Network of Power Grid and Power Plant and the Order No. 5 of the State Electricity Regulatory Commission Regulations on Security Protection of Electric Secondary System, the scheme for security

protection of the secondary system of converter station is determined on the basis of Scheme for Security Protection of Electric Secondary Systems in China.

The security protection of the secondary system of converter station is mainly of "longitudinal protection" and mainly takes necessary security isolation measures between the converter station and the dispatching center.

26.11.4 System Communication

The requirements on channel by information transmission mainly involve DC control and protection system, dispatching automation information, dispatching telephone, administration communication, comprehensive data network, and AC replay protection. The configuration and channel organization for system communication shall be analyzed based on the specific projects. Main communication equipment in the converter station is introduced as follows:

1. System dispatching exchange

The converter station shall be equipped with one dispatching program-controlled exchange, dispatching console, and digital recording system. The exchange is also used for communication in the substation.

2. Integrated data communication network

The converter station is equipped with one integrated data network access equipment to connect to the dispatching node at municipal level.

3. Satellite communication system

With the development of electric system, the disaster recovery of communication for electric power system has become a problem concerned by all levels of authorities. Satellite communication has many advantages, for example, it is immune from restriction by landform and region, not susceptible to natural disaster and man-made destruction; it is easy to use, convenient in moving, less in investment, and lower in operating and maintenance cost. However, the transmission delay of satellite is relatively longer, but it can accomplish the transmission of audio information, video information, and data information basically under emergency situation. Satellite and optic fiber communication, being mutually independent of each other, are promising emergency communication methods in emergency situation, so it is considerable to set up one set of ground receiving equipment of satellite communication in the converter station.

4. Communication power supply

The converter station is equipped with two sets of 48 V/200 A power supply (including redundant rectifier modules) for communication, and each power supply is equipped with one storage battery.

5. Power environment supervisory system of communication equipment room

For the unattended case, the converter station can be equipped with one set of power environment supervisory system of communication equipment room so that the communication operation and maintenance department can know the real-time operating condition of communication equipment and the power environment in communication station.

6. Communication equipment room

The converter station can be provided with communication equipment room, in which optic fiber communication equipment, switches, equipment of integrated data network, distribution frames, protection interface cabinet, etc., are installed. The room covers about 80 m^2. In addition, an independent power supply room could be set in the converter station to accommodate the communication power supply and storage battery.

References

1. GB/T 50789-2012. Code for Design of ±800 kV DC Converter Station; 2012.
2. DL/T 5223-2005. Technical Rule for Designing HVDC Converter Station; 2005.
3. DL/T 5056-2007. Technical Code of General Plan Design for Substation; 2007.
4. GB 50016-2006. Code of Design on Building Fire Protection and Prevention; 2006.
5. Jingjun L, Dangjiu L. ±800 kV UHV DC converter station AC filter yard layout optimization [J]. Electr Power Constr. 2010;31(1):26–33.
6. China Electricity Council. Code for design of ±800 kV DC Converter Station. Beijing: China Planning Press; 2012.
7. Xiangjiaba-Shanghai ±800 kV UHVDC Transmission Project Insulation Coordination. ABB Power Systems; 2007.
8. Nuozhadu-Guangdong ±800 kV UHVDC Transmission Project Insulation Coordination. ABB Power Systems; 2013.

Chapter 27
Design of Ultra-High-Voltage Alternating Current (UHVAC) Power Transmission Lines

Jiamiao Chen, Wenqian Qiu, Feng Pan and Gang Song

As the trunk channels for power transmission with large power capacity and long transmission distance, the UHV lines, compared with the conventional EHV transmission lines, have the characteristics of high reliability requirements, high-voltage level, large transmission capacity, large conductor section, high insulation requirements, high tower height, high tower loads, etc. [1], so higher requirements are also put forward for the design of UHV power transmission lines.

The thematic technical researches, tests, and special assessments carried out at the early stage of engineering design will provide critical guidance and support for the subsequent engineering design. In addition, due to the UHV transmission line project's high importance, large tower load, wide corridor, and strict requirements in environmental impact assessment, the requirements in content and depth of engineering preliminary design, and construction drawing design are also higher than those of the EHV transmission line project. The determination of routing scheme and the design meteorological conditions is the basis for the UHV transmission line project design, and the conductor selection, insulation coordination, fitting selection, tower design, foundation selection, channel cleaning, environmental protection measures, etc., are critical for the proper engineering design.

Currently, the 1000 kV UHVAC power transmission lines mainly consist of two forms, i.e., single circuit and double circuit on the same tower. The first UHVAC

J. Chen (✉) · W. Qiu · F. Pan · G. Song
China Energy Engineering Group, Zhejiang Electric Power Design Institute Co., Ltd., Hangzhou, Zhejiang, People's Republic of China
e-mail: chenjiamiao@163.com

W. Qiu
e-mail: 839821641@qq.com

F. Pan
e-mail: qiushif@163.com

G. Song
e-mail: songgang130@sina.com

© Zhejiang University Press, Hangzhou and Springer-Verlag GmbH Germany 2018

H. Zhou et al. (eds.), *Ultra-high Voltage AC/DC Power Transmission*,
Advanced Topics in Science and Technology in China,
https://doi.org/10.1007/978-3-662-54575-1_27

line built and put into operation in China, Southeast Shanxi-Nanyang-Jingmen 1000 kV line (referred to as the Middle Route UHV) adopted the single-circuit design for the whole line; the Huainan-South Anhui-North Zhejiang-West Shanghai 1000 kV UHVAC line (referred to as the Power Transmission from Anhui to Eastern China) completed and put into operation in 2013 adopted the double circuit on the same tower design; the North Zhejiang–Fuzhou 1000 kV UHVAC line put into operation in 2014 combines both the single circuit and the double circuit, with the single circuit mainly used for lines in the mountainous areas and the double circuit on the same tower used for lines in the areas where corridors are restricted.

The UHV lines described hereunder, unless otherwise specified, refer to the 1000 kV UHVAC lines and ±800 kV UHVDC lines. This chapter will focus on the discussion in the engineering design of 1000 kV UHVAC lines (Figs. 27.1 and 27.2).

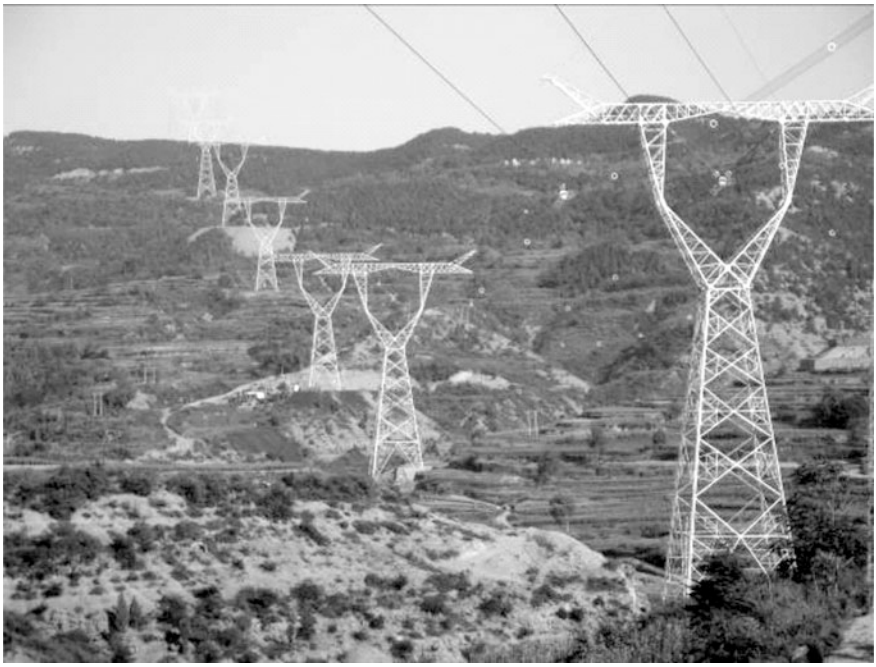

Fig. 27.1 Southeast Shanxi-Nanyang-Jingmen 1000 kV UHVAC single-circuit transmission line

Fig. 27.2 Huainan-South Anhui-North Zhejiang-West Shanghai 1000 kV UHVAC double-circuit transmission line

27.1 Design Basis

The design of UHV power transmission line shall be implemented in strict accordance with the latest effective version of the relevant laws and regulations, mandatory standards, technical standards and industry design standards, procedures, etc., that are applicable to the design of transmission line, reasonably absorbing the research results of key technologies carried out in conjunction with the project, and actively referring to the successful experience and rational proposals obtained and accumulated from the transmission line projects that have been built and put into operation.

27.2 Line Routes

The principles of the line routes are basically similar to that in EHV lines, while UHV lines need to be given special considerations when passing by the mountainous areas and icing areas.

1. When multi-circuit UHV lines are laid in parallel passing by the mountainous areas, the parallel spacing shall be appropriately increased to avoid the two circuits of UHV lines going on the same side of the slope of a mountain.
2. First, it shall avoid the severely icing area and the length of strain section of the line shall be limited based on the different ice areas. The length of strain section shall not be more than 10 km at light icing area, not be greater than 5 km at medium icing area, and not be greater than 3 km at heavy icing area. In case of long length of strain section, the preventive measures against string falling shall

be considered. For the locations with poor operating conditions, such as in the mountainous area or heavy icing area with considerable height difference or span spacing, the length of strain section shall be appropriately shortened compared with the above requirements.

27.3 Design Meteorological Conditions

27.3.1 Principles of Selection

Mathematical statistics analysis of major meteorological elements such as wind and ice shall be made in combination with field surveys along the route for determination. Under normal circumstances, the wind pressure values specified in *Load Code for the Design of Building Structures* and the design and operation experience of nearby existing lines shall also be referenced.

The basic wind speed and design ice thickness are the main meteorological conditions for the UHV power transmission line design, and the basic requirements are as follows:

1. The recurrence interval is taken as once in 100 years.
2. The basic wind speed is taken as the 10-min average strong wind value at the height of 10 m above the ground (at the height of 10 m above the average minimum water level in strong wind season over the years in case of large span).
3. The basic wind speed shall not be less than 27 m/s, and, if necessary, the calculation shall be checked on the basis of rare wind speed conditions.

27.3.2 Basic Wind Speed

1. Mathematical statistics method of wind speed

In determination of the basic wind speed, the average annual maximum wind speed of the local meteorological station at 10-min interval shall be taken as the sample, for which the probability calculation shall be made by using the recommended extreme values type I probability distribution (Gumbel) in the engineering design.

2. Correction of the height of the wind instrument

The heights of the wind instrument measuring the maximum wind speed may vary depending on the meteorological observatories (stations), and the heights of the wind instrument of the same station may be different from years, so the maximum

wind speed over the years of all meteorological stations shall be corrected as the wind speed at a height of 10 m to ground.

3. Values taken for basic design wind speed

Normally, the meteorological station is near the city, so the wind speed may be small. There may be a certain distance from the line to the meteorological station, so the records of the meteorological station cannot completely cover the strong wind at a full range of the line. In order to ensure the safety of UHV transmission lines, normally based on the wind speed statistics, comprehensively considering the wind pressure values of *Load Code for the Design of Building Structures* and the meteorological survey data along the line, by increasing certain margin of safety, it shall be selected as the basic design wind speed for engineering applications. The *Load Code for the Design of Building Structures* also gives out the minimum value of the basic wind pressure, which can be translated into the basic wind speed according to the equation $W = V^2/1600$.

For the transmission lines in mountainous areas, it shall be determined by using methods of statistical analysis and contrast observation etc., based on the maximum basic wind speed of the mountainous areas calculated by the meteorological data of the meteorological observatories or stations at neighboring regions, as well as depending on the actual operating experience. Generally, if there is no reliable data, the statistic value at nearby plains can be used after it is increased by 10%.

For the transmission lines that need to cross big section of important navigable rivers or wide water surface(generally refer to the sections with a span of 1000 m, with tower height more than 100 m), if an accident occurs, there will be a wide range of influence, and it is difficult to repair. In order to ensure the safe operation of the large crossings, the design standards shall be increased. According to the design and operation experience of large crossings in the past in China, if reliable local information is unavailable, the selection shall be made by converting the onshore wind statistics of the transmission line nearby into the wind speed at 10 m above the average minimum water level in strong wind season over the years at the place of crossing, and increased by 10%, and plus an additional 10% after the analysis of the influence of water surface [2].

4. Design wind speed for conductor tension and load calculation

When calculating the conductor tension and loads of the overhead transmission line, the wind speed at the average height of the conductor shall be taken as the design wind speed. For this reason, it is required to do the conversion of the basic wind speed at 10 m height above the ground according to Eq. (27.1).

$$V_{\mathrm{H}} = V_{10}\left(\frac{Z_{\mathrm{H}}}{10}\right)^{\alpha}, \tag{27.1}$$

where

V_{10} is the basic wind speed where 10 m height above the ground, in m/s;
Z_H is the average conductor height above the ground, in m;
V_H is the conductor line wind velocity at the corresponding average height above the ground, in m/s;
α is the factor relating to the roughness of ground surface, for instance, in area of Class B, $\alpha = 0.16$.

For the 1000 kV UHVAC line located in Class B region, its designed basic wind speed shall be 27 m/s; if the average height of the lower phase conductors is taken as 30 meters, the conductor line wind speed at the corresponding average height of conductors is $V_{30} = 27 \times (30/10)^{0.16} = 32.1$ m/s.

27.3.3 Design Icing

The icing on the conductor is formed mainly by the combined effects of atmospheric conditions, terrain, and line characteristics. According to its freezing nature, conductor icing can be divided into four kinds, i.e., glaze, rime, mixed rime, and snow cover, of which the mixed rime and the glaze have the most hazards to the overhead lines.

Since most of the local meteorological observatories (stations) along the UHV power transmission line lack complete and systematic observation records of the conductor icing, the data of icing are incomplete. Therefore, the selection of design ice thickness depends mainly on the investigation of the icing on the power lines and communication lines and other natural objects at the areas along the transmission line, and is determined comprehensively in combination with the design ice thickness and operating experience of the transmission lines that have been constructed.

Depending on ice thickness, the design ice areas can be divided into light icing area, the medium icing area, and heavy icing area; the area with ice thickness at 10 mm and below is the light icing area, the one with ice thickness more than 10 mm but less than 20 mm is the medium icing area, and the area of 20 mm and above is the heavy icing area.

The features of the lines in heavy ice area: first, the harsh operating environment and severe icing are considered as the main loading conditions for controlling the strength of line components; secondly, the lines' specific static and dynamic characteristics (such as uneven icing, ice shedding, and flashover of ice-covered insulator string) have corresponding special requirements on longitudinal torsional strength of the tower, the tower head layout, conductor, fittings, insulation, etc.; thirdly, with difficulties in operation and maintenance, once an accident occurs, due to the high altitude, steep terrain and bad weather conditions, longer outage time may be suffered frequently. Therefore, special consideration shall be given to the lines in the heavy icing area.

The principle of "avoiding the heavy and choosing the light" shall be followed in the route selection of the heavy icing areas, that is, "avoiding the severe icing sections" shall be taken as a prerequisite to consider. The basic principles of route selection: ① avoid the severe icing sections and filthy serious regions identified through surveys; ② the lines shall be laid along the undulating terrain and the span spacing shall not be too large. The lines are required as evenly as possible in the same time, to avoid the big difference between the adjacent span distances; ③ the line route shall avoid narrow mountain passes, wind passages, lakes and reservoirs, and others that may be easily subjected to icing zone; ④ the limit of used span and the corresponding height of heavy icing lines shall be paid attention to, long span shall adopt isolated span, and in principle, the used span distance shall not be more than 800 m; and ⑤ since the heavy icing line has significant load, more serious ice overload conditions would appear in the operation, so it is required to control the corner angle of lines not more than 40° during the route selection.

Based on the investigation of icing disasters of transmission line over many years, particularly the survey and analysis of the ice disaster of the grid in early 2008, under the same environmental conditions, the ice thickness on the ground line of transmission lines is normally larger than that of the conductor. For this reason, it is specified by the design procedures that, for the lines at icing region, the design ice thickness values of ground wire shall be 5 mm more than the conductor, with its main purpose of increasing the mechanical strength of the tower-ground wire brackets.

In the absence of reliable information, the design ice thickness of the line with large span shall be 5 mm larger than the general transmission line nearby.

27.4 Selection of Conductor and Ground Wire of AC Lines

The engineering investment of the UHV overhead line accounts for a larger percentage in the investment of the project, normally about 40–50%, adding the Engineering changes in the tower and foundation caused by conductor program, which has a great impact on the cost of the entire project. During the selection of conductors, the factors that shall be comprehensively considered are mainly the voltage drop, economic current density, allowable current-carrying capacity, electromagnetic environmental impact, necessary mechanical strength, annual costs, economy, etc. During the engineering design, the experience and outcomes already obtained shall be constantly summarized and used for conductor selection and demonstration, and in combination with practical engineering and with the manufacture, construction, operation, and maintenance, and other factors considered in a comprehensive way, the economic and reasonable conductor section and bundled mode that meeting the technical requirements shall be recommended.

In order to have more new technologies, new materials and new processes applied to the power grid construction, embodying the requirements of energy saving and environmental protection, in the design of UHV lines, the engineering

application of energy-saving conductors shall be actively studied in conjunction with the actual conditions of project.

27.4.1 Main Parameters for Conductor Selection

Under the normal transmission power, the selection of 1000 kV transmission lines mainly depends on the corona conditions and the radio interference and audible noise are derived from the corona effects, of which the radio interference and audible noise are the main control conditions for the selection of minimum conductor crossing section [2].

27.4.1.1 Common Conductor Types

During the conductor-type selection, it shall first be based on the matured conductor type with manufacturing experience in China. The types and features of several commonly used conductors with large section are as shown in Table 27.1.

27.4.1.2 Conductor Current Density

In the design of transmission lines, through analysis of the conductor prices, power energy costs and the characteristics of the transmission line project and other factors of each period, each country presents the most economical transmission current per unit section of the conductor, which is called as the economic current density. Since aluminum conductor steel reinforced (ACSR) is mainly used as the overhead transmission lines in China, when the maximum load utilization hours are more than 5000 h, the economic current density with aluminum as the conductive

Table 27.1 Common conductor types and characteristics

Conductor type	Stranded conductor structure Aluminum strand × single wire/steel strand × single wire (mm)	Total section (mm^2)	Conductor Outer diameter (mm)	Section ratio of steel to aluminum
JL/G2A-900/75	84 × 3.69/7 × 3.69	975.00	40.60	0.082
LGJ-800/55	45 × 4.80/7 × 3.20	870.60	38.40	0.069
ACSR-720/50	45 × 4.53/7 × 3.02	775.24	36.23	0.069
LGJ-630/45	48 × 4.12/7 × 3.20	666.55	33.60	0.069
LGJ-500/45	48 × 3.60/7 × 2.80	531.68	30.00	0.088

material shall be taken as 0.9 A/mm^2, and it is also taken as the reference value of current density for the preliminary selection of conductor in UHV transmission line project design.

27.4.1.3 Maximum Allowable Temperature of Conductor

The maximum allowable conductor temperature is the main factor for controlling the conductor ampacity. It is mainly decided in accordance with the loss in strength of conductor and the heating of connection fittings after the long-term operation. The higher the operating temperature, the longer the duration of the high temperature, and the greater the loss in strength of the conductor will be.

It is specified in China's *Code for Design* that when checking the conductor's allowable current-carrying capacity, ACSR and aluminum alloy stranded conductor steel reinforced (AACSR) shall adopt 70 °C and, if necessary, +80 °C can be used, and 90 °C shall be used for large span. However, according to the operating experience and research data overseas, the higher allowable temperature is used, i.e., 150 °C can be used for ACSR. In this case, the oxidation of conductor connectors and heating of the connection fittings shall be mainly considered.

27.4.1.4 Conductor Surface Electric Field Intensity

Conductor surface electric field intensity is the basic condition for conductor selection. If the conductor surface electric field intensity is too high, it will cause the overall corona of conductor, and not only corona loss will be increased dramatically, but also cause other problems related with electromagnetic environment, so UHV lines must be limited with the conductor surface electric field intensity.

The maximum conductor surface field intensity depends on the maximum operating voltage, sub-conductor diameter, phase conductor bundled mode, and phase-to-phase distance. It has many calculation methods, of which the successive image method with higher precision can be used for the calculation in engineering design. The conductor surface field intensity shall not exceed 80–85% of the full corona critical field intensity, in order to avoid the emergence of overall corona of conductor.

The calculated results of critical electric field intensity of various conductors by using Peek equation are as shown in Table 27.2.

27.4.1.5 Radio Interference

The radio interference of transmission line is mainly produced by the corona discharge of conductors, insulators, line fittings, etc. The limits for radio interference of 1000 kV overhead transmission lines specified in *Code for Design* are as follows: "at the areas with elevation of 500 m or below, at a distance of 20 m from the

Table 27.2 Conductor critical electric field intensity E_0 (at altitude below 1000 m)

Conductor type	Diameter (mm)	Critical electric field intensity E_0 (kV/cm)	
		Maximum value	Effective value
JL/G2A-900/75	40.69	28.22	19.95
LGJ-800/55	38.40	28.36	20.05
ACSR-720/50	36.23	28.51	20.16
LGJ-630/45	33.60	28.71	20.30
LGJ-500/45	30.00	29.02	20.52

projection on the ground of side phase conductor and at 2 m height above the ground, and with the frequency of 0.5 MHz, the design control value of radio interference shall not exceed 58 dB (μV/m)" [2]. The above values are calculated on the basis of wet conductor. With these control values, under good weather conditions, the radio interference generated by the conductor corona will not exceed the limit value of 55 dB (μV/m).

The reply by the State Environmental Protection Administration on the environmental impact report of the 1000 kV Power Transmission Project to Transmit Power from Anhui to Eastern China requires that the radio interference limits of the 1000 kV transmission line shall be "controlled to be no greater than 55 dB (μV/m) at a distance of 20 m from the projection of side phase conductor with the test frequency of 0.5 MHz under sunny conditions."

In the engineering design, for the lines which have the altitude of more than 500 m, its radio interference limits value shall be corrected for high altitude. The correction factor is as such, taking the 500 m above sea level as reference, the radio interference limit value shall be increased by 1 dB for every altitude increment of 300 m.

In addition to the bundled conductor form (sub-conductor diameter and bundled spacing), the radio interference value of UHV transmission lines also has relation to the spatial arrangement of the phase conductors. When the double-circuit UHV lines on the same tower adopt the reverse phase-sequence arrangement, the radio interference values for "I"- and "V"-type conductor suspension strings will vary to some extent, which will affect the selection result of conductors. In order to meet the limit requirements of radio interference level not greater than 55 dB, the "I"-type string arrangement shall be used, the minimum conductor cross-section can be selected as 8×630 mm^2 and its radio interference level shall be 54.88 dB; when the "V"-type string arrangement is used, the horizontal spacing between side phase conductors of double circuit line is decreased, so the minimum conductor cross-section must be selected as 8×720 mm^2, and its radio interference level shall be 54.65 dB. In this case, the level of radio interference has become a control condition for conductor selection. In terms of the reduction of investment and radio interference, the use of expanded conductor may be considered. In case the

aluminum section of expanded conductor essentially keeps the same, by increasing the diameter of the conductor, the radio interference value will be reduced, and meanwhile, its tension will be greatly reduced in comparison with the tension of conductor with the same diameter, which can save the line investment.

Audible Noise

With the development from EHV to UHV, as the rise of voltage and the increase of the number of sub-conductors, the noise problem caused by the conductor corona of transmission lines has become more and more prominent, and special attention must be paid to it, because its limit standard will directly affect the selection of sub-conductor section and bundled mode.

The international design target values of audible noise of UHV lines are basically between 50 and 58 dB (A) and most are 53 dB (A), and the audible noise of EHV transmission lines in actual operation is mostly controlled within this range.

The route of UHV transmission line is mainly in agricultural region, which is considered as Class 1 area as per China's environmental noise limits standard. With reference to this standard, the audible noise of UHV transmission line shall not exceed 55 dB (A).

It is required in *Code for Design* that, "in the areas with altitude of 500 m and below, at 20 m away from the projection of side phase conductor of the line, the design control value for audible noise of wet conductor shall not be more than 55 dB (A)" [2]. Taking into account that the 1000 kV AC transmission lines will also pass through the more economically developed and densely populated areas, in order to minimize the adverse impact on the environment when the line passes by, as well as having the economy of engineering construction taken into account, it is appropriate to have the audible noise under wet conductor conditions in the engineering design controlled at no more than 55 dB (A). For sparsely populated high-altitude areas, the noise limits shall be corrected for high altitude, and taking the altitude of 500 m as a starting point, the audible noise limit shall be increased by 1 dB (A) for every altitude increment of 300 m.

Internationally, the research institutions in many countries have conducted in-depth research on the audible noise of EHV and UHV transmission lines and presented their prediction equations, but because of different environments and conditions of their experiments, the calculation results of their prediction equations are also different. The current prediction equation for audible noise calculation that is more commonly used in engineering design is the one recommended by BPA, an American electric power company, based on the experimental studies.

27.4.2 Conductor Cross-Section and Bundled Configuration

27.4.2.1 Selection of Conductor Cross-Section

The transmission capacity of each circuit of UHVAC line is normally between 5000 and 6500 MW, and thus the calculated current of each phase is 3040–3950 A (with power factor of 0.95); in accordance with the aforementioned current density reference value of 0.9 A/mm^2, the required current-carrying conductor section shall be 3380–4390 mm^2, which can be used as the basic condition for the selection of conductor cross-section.

27.4.2.2 Number of Sub-conductors

According to the researches and engineering applications of the conductors of UHV lines around the world, in order to solve the corona problem, it is normally required to increase the number of bundled conductors and the conductor cross-section in UHV lines; at present, the eight-bundled conductors are used for the UHVAC lines that have been put into operation and under construction in China. During the engineering design, normally, in accordance with the requirements on the total current-carrying section preliminarily calculated as per the economic current density of 0.9 A/mm^2, various combinations of bundled conductor configurations shall be conducted to calculate the electrical and mechanical properties. Typical bundled configurations are shown in Table 27.3.

27.4.2.3 Bundled Conductor Spacing

For the selection of bundled conductor spacing, both the sub-span oscillation and the electrical properties of the bundled conductors shall be considered. The sub-span oscillation means the unstable vibration phenomenon of sub-conductor at the leeward side induced by the wake flow of sub-conductors at windward side. It is suggested by researches that when the ratio of the bundle spacing (S) to the sub-conductor diameter (d) $S/d > 16$–18, the sub-span oscillation may be avoided; in terms of the electrical aspect, there is an optimum bundle spacing, with which the

Table 27.3 Typical bundled configurations and cross-sections of phase conductor

S/N	Conductor type and bundled configuration	Total aluminum section (mm^2)	Current density (A/mm^2)
1	6× JL/G2A-900/75	5411	0.56–0.73
2	8× LGJ-500/45	3976	0.76–0.99
3	8× LGJ-630/45	4988	0.61–0.79
4	8× ACSR-720/50	5801	0.52–0.68

Table 27.4 Values of bundled conductor spacing

Number of sub-conductors	Sub-conductor nominal section (mm^2)	Bundle spacing that limiting sub-span oscillation *S* (mm)	Bundle spacing that meeting the electrical properties *S* (mm)	Adopted value *S* (mm)	Actual *S*/*d*
6	800–900	540–650	335–390	400, 450	10–13.1
8	500–720	430–610	<235	400	10.4–14.9
10	300–400	380–430	240–250	375	13.9–15.6

surface electric field intensity of sub-conductors is the smallest. The calculated results are shown in Table 27.4.

It can be seen from the above table that the bundle spacing required to limit sub-span oscillation is inconsistent with the bundle spacing required for the optimum electrical properties. The ratio of *S*/*d* adopted for 500 kV AC and DC EHV lines in China is 15–18.7, but for UHV lines, due to the large number of sub-conductors and the more harsh electrical requirements, the layout is much more difficult than that of the 500 kV line. From the experience of countries overseas, the bundle spacing of 18 inches, equivalent to 457 mm, is used for 345–750 kV lines in United States regardless of the size of the conductor section, and the ratio of the bundle spacing to the sub-conductor diameter is calculated as 9.57–16.9. Its *S*/*d* value has a larger range of variation, and the minimum value is smaller than the one adopted in China. The *S*/*d* value adopted for UHV lines is normally around 10–17 [1]. The *S*/*d* value of 13.3 is adopted for the Southeast Shanxi-Nanyang-Jingmen 1000 kV single-circuit UHVAC line which already built in China, and the *S*/*d* value of 11.9 is adopted for the 1000 kV double-circuit UHVAC line to transmit power from Anhui to Eastern China.

In terms of the structure of bundled conductors that has been adopted or recommended for UHV lines around the world, because the number of sub-conductors of UHV line is increased, it is difficult to ensure that $S/d > 16–18$ when conductors with a large cross-section are adopted. For this reason, the *S*/*d* value is generally controlled as not less than 10 in the engineering design. If the eight-bundled conductors with cross-section of 630 or 500 mm^2 are used, the bundled conductor spacing can be 400 mm.

27.4.3 Phase-Sequence Arrangement of the Double-Circuit Conductors

27.4.3.1 Impact on the Surface Electric Field Intensity of Conductors

The phase-sequence arrangement of conductors for the double-circuit UHV line on the same tower has an impact on their surface electric field intensity. The surface electric field intensity of conductors with the reverse phase-sequence arrangement is larger, and their ratio value of E_m (surface electric field intensity)/E_0 (critical corona inception electric field intensity) is also larger than that with the same phase-sequence arrangement. At the altitude below 1000 m, the calculated values of the maximum surface electric field intensity of the vertically arranged double-circuit conductors on the same tower with "I"-type strings are shown in Table 27.5.

It can be seen from the above table that the various conductor schemes with the reverse phase-sequence arrangement have a slightly larger surface electric field intensity compared to those with the same phase-sequence arrangement, but their E_m/E_0 ratio can be controlled at below 0.83, meeting the requirements that no full corona will occur.

27.4.3.2 Impact on the Double-Circuit Lightning Trip

The reverse phase-sequence arrangement is beneficial for prevention from lightning back flashover to avoid the simultaneous trip of both circuits. It enables the voltage acting on the insulator strings caused by lightning to be superimposed with the system working voltage, and can cause one circuit of the line to flash over first to shunt the current and reduce the voltage drop on tower body and grounding resistance as well as the inductive coupling of the failed phase shunting with the normal phase, thus to reduce the withstand voltage of insulator strings on normal phase, so as to realize that the other circuit of the line will not trip at the same time to ensure the safety of power transmission by the line. From the standpoint of prevention of simultaneous trip of both circuits caused by lightning back flashover,

Table 27.5 Maximum surface electric field intensity E_m of same tower double-circuit conductors (kV/cm)

Conductor structure	Bundle spacing (mm)	E_0 (kV/cm)	Reverse phase-sequence arrangement			Same phase-sequence arrangement		
			AC phase	BB phase	CA phase	AA phase	BB phase	CC phase
8× LGJ-500/45	400	20.52	16.80	16.93	16.92	14.78	16.93	16.02
8× LGJ-630/45	400	20.30	15.28	15.39	15.34	13.32	15.26	14.42
8× ACSR-720/50	400	20.16	14.40	14.51	14.47	12.78	14.65	13.80

the reverse phase-sequence arrangement is recommended for the double-circuit line on the same tower.

27.4.3.3 Impact on the Minimum Conductor Height Above the Ground

Through the calculation and analysis of the ground clearances under different phase-sequence arrangements, the double-circuit UHV power transmission line on the same tower with the same phase-sequence arrangement has a larger required minimum ground clearance compared with that with the reverse phase-sequence arrangement. With the maximum ground electric field intensity taken as 10 kV/m, for the double-circuit tower with "I"-type string, the minimum ground clearance of conductors arranged in the same phase sequence shall be 3–4 m larger than that of those arranged in the reverse phase sequence. In consideration of the minimum height above the ground, the same phase-sequence arrangement is not recommended for the project.

27.4.3.4 Impact on the Width of Line Corridor

The phase-sequence arrangement of the double-circuit conductors on the same tower has a certain impact on the width of the line corridor, i.e., the corridor width under the same phase-sequence arrangement is greater than that under the reverse phase-sequence arrangement. Taking the double-circuit line on the same tower with conductors of $8 \times 630\ mm^2$ section and "I"-type string as an example, under different phase-sequence arrangements, the calculated widths of line corridor controlled under the ground electric field intensity of 4 kV/m are shown in Table 27.6.

Table 27.6 Widths of double-circuit line corridor under the control of 4 kV/m electric field intensity (m)

Height above the ground	Tower type	
	Double-circuit tower with I-type string (arranged in the reverse phase sequence)	Double-circuit tower with I-type string (arranged in the same phase sequence)
18–28 m	73–66	74–71
28–30 m	66–62	71–70
30–32 m	62–56	70–68
32–34 m	56–44	68–66
34–36 m	–	66–64

27.4.3.5 Electromagnetic Environment Requirements for the Conductors with Different Phase-Sequence Arrangement

For the conductors with different phase-sequence arrangements, the electrical properties of the line will be different. The radio interference and audible noise levels of the conductors with the reverse phase-sequence arrangement are greater than those with the same phase sequence, as shown in Tables 27.7 and 27.8; in terms of compliance with the electromagnetic environment requirements, the conditions of the conductors with the reverse phase-sequence arrangement are worse than those with the same phase-sequence arrangement.

For the UHVAC double-circuit lines on the same tower, if the same phase-sequence arrangement is used, the selection of 8× LGJ-500/45 conductors can meet the requirements in transmission capacity, economic current density, electromagnetic environment, etc., of the lines, but it will lead to higher ground electric field intensity, larger minimum height above the ground, and wider corridor width, and if the lines go through the economically developed regions, it will cause a corresponding increase in house demolition. The reverse phase-sequence arrangement is beneficial to the prevention of double-circuit tripping accident due to lightning back flashover to the line, but the failure resulting from lightning back flashover has an extremely small probability because of the 1000 kV UHV line's high insulation level and high lightning withstand level. The lightning trip failure is usually caused by lightning shielding of conductors.

When the reverse phase-sequence arrangement is used for the lines, the 8× LGJ-630/45 conductors need to be selected to meet the requirements in electromagnetic environment limits. In such case, compared with 8× LGJ-500/45 conductors, the load of tower will be increased, but because the average nominal height of the tower with 8× LGJ-630/45 conductors is around 4 m lower than that of the one with 8× LGJ-500/45 conductors, and the width of the line corridor is around 2 m smaller, the economy of its overall investment is necessary to be compared in a detailed manner in combination with the actual engineering conditions.

27.4.4 Application of Expanded Conductors

Currently, there are three types of expanded conductors developed in China: the round aluminum wire space-winding type, shaped-wire supporting type, and shaped-wire space-winding type. Their structures are shown in Fig. 27.3.

The main expanded conductor currently used in the project is the round-wire expanded conductor of space-winding (strand-extracted) structure, and there is actual experience in the manufacturing and construction of conductor specifications expanded from 310 to 400 and from 630 to 720 (section). In recent years, the structure optimization of expanded conductors has begun, and the shaped-wire

Table 27.7 Calculated results of radio interference of double-circuit conductors on the same tower with different arrangement [dB (μV/m)]

Conductor structure	Bundle spacing (mm)	I-type string with the reverse phase-sequence arrangement	I-type string with the same phase-sequence arrangement	V-type string with the reverse phase-sequence arrangement	V-type string with the same phase-sequence arrangement
8× LGJ-500/45	400	56.29	53.14	57.74	52.18
8× LGJ-630/45	400	54.88	51.17	55.03	50.29
8× ACSR-720/50	400	53.07	50.28	53.15	49.74

Table 27.8 Calculated results of audible noise of double-circuit conductors on the same tower with different arrangement [dB (A)]

Conductor structure	Bundle spacing (mm)	I-type string with the reverse phase-sequence arrangement	I-type string with the same phase-sequence arrangement	V-type string with the reverse phase-sequence arrangement	V-type string with the same phase-sequence arrangement
8× LGJ-500/45	400	56.84	54.36	56.14	51.31
8× LGJ-630/45	400	54.64	52.20	54.01	49.18
8× ACSR-720/50	400	53.38	50.94	52.87	47.92

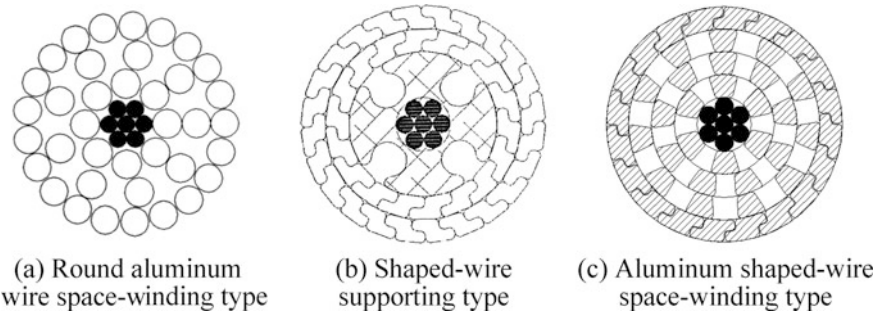

Fig. 27.3 Diagram of typical structures of space-winding (strand-extracted) expanded conductors

space-winding (strand-extracted) structure has been developed. The expanded conductor of shaped-wire supporting type is supported by high-density polyethylene, but it is not used in practical engineering application due to the high cost.

The round wire expanded conductors adopting the space-winding technology has relatively simple structure and relatively low requirements in equipment and technology, and has a better economy than the supporting-type and shaped-wire space-winding expanded conductors, and there are certain operation experience accumulated. At present, the major conductor manufacturers in China are able to produce the round-wire space-winding expanded conductors, which can meet the requirements of batch applications in UHV project. The round-wire space-winding expanded conductors are specially studied in the UHV Project to Transmit Power from Anhui to Eastern China, and have been designed and used in the wire-in ducts of substation and the jumpers of strain tower. The JLK/G1A-530(630)/45 round-wire space-winding expanded conductors (expanded from 530 to 630) are adopted for the 100 km line of the double-circuit section of the North Zhejiang–Fuzhou 1000 kV line with relatively good topographical conditions and construction conditions.

The round-wire space-winding-type expanded conductors are prone to slipping of the support layer and depression of the outer aluminum wire, and in the construction process of unfolding, it may be subject to "stacked wires," "jumping strands," and other phenomena. Therefore, the manufacturers are required to ensure the manufacturing technology, and in the process of tension stringing, the tension and speed shall be strictly controlled.

27.4.5 Selection of Ground Wire and OPGW Optical Cable

The selection of ground wire (including optical fiber composite overhead ground wire also known as OPGW optical cable) is an important part of the UHV project design. The ground wire is the first barrier against the lightning to UHV

transmission lines, while OPGW optical cable, in addition to lightning protection, shall also function as the "nerve center" of the information system for the UHV transmission line, which is required to have high operational reliability.

27.4.5.1 Selection of Ground Wire

The ground wire of UHV project shall meet the following basic requirements: ① having excellent mechanical properties and electrical properties; ② having good resistance to vibration and corrosion resistance performance; ③ the selection of ground wire shall not only meet the requirements in short-circuit current thermal capacity, but also be verified according to the conditions for corona inception; ④ OPGW optical cable shall have excellent function of optical communication, and enough performance of resistance to lightning.

27.4.5.2 Minimum Diameter of Ground Wire

For the smallest section of the ground wire of UHVAC line, it is required in *Code for Design* that, "the ground wire (including optical fiber composite overhead ground wire) shall, in addition to meet the short-circuit current thermal capacity requirements, be verified according to the conditions for corona inception, and the ratio of ground wire's surface electrostatic field intensity to corona inception electric-field intensity shall not be greater than 0.8" [2].

The UHVAC line has a rated voltage of 1000 kV and maximum operating voltage of 1100 kV. In case of the erection type of the double circuit on the same tower, depending on the tower size, the average distance from the ground wire to the conductor in the middle of the span is around 16–20 m. Since the ground wire is in the strong electric field environment of the conductor, if the surface field intensity of the ground wire is too high, it will cause the overall corona of the ground wire which will not only dramatically increase the corona loss, but also will bring a lot of other problems. In the engineering design, the minimum diameter of the ground wire shall be determined based on the ratio of the ground wire's surface electrostatic field intensity E_m to the corona inception electric field intensity E_0.

Table 27.9 shows the E_m and E_0 of several commonly used ground wires for the UHVAC double circuit, which are calculated based on the surface roughness coefficient of 0.82.

It can be seen from the calculated results that, because the vertical distance from the hanging point of the ground wire to the hanging point of the conductor at the head of straight line tower is large (usually more than 15 m), the maximum E_m/E_0 is 0.71, which is less than 0.8 required; however, the height of ground wire bracket of the tower head of strain tower is low, normally around 12.5 m, and its maximum E_m/E_0 value has reached 0.9.

The maximum surface field intensity of the ground wire may be reduced by increasing the vertical distance between the conductor and the ground wire so as to

Table 27.9 E_m/E_0 at tower head of double-circuit straight line tower and strain tower at various altitudes

Ground wire type		JLB20A-170	JLB20A-185	JLB20A-210	JLB20A-240
Diameter (mm)		17	17.5	18.75	20
Altitude (m)	Relative air density	E_0 (kV/m)			
0	1	32.93	32.81	32.54	32.3
500	0.955	32.12	32.00	31.73	31.49
1000	0.908	31.25	31.14	30.87	30.63
Tower Type		E_m (kV/m)			
Straight line tower		22.05	21.50	20.22	19.11
Strain tower		28.89	28.16	26.81	25.04

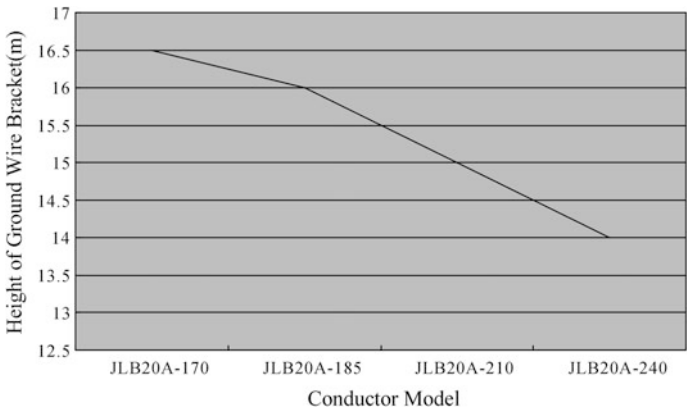

Fig. 27.4 Height of ground wire brackets for the various ground wires meeting E_m/E_0 limit requirements

reduce the E_m/E_0 value, of which the limit is normally controlled as 0.75 in engineering design. Based on the calculations of the above four ground wires, the heights of ground wire bracket meeting the limit requirements of $E_m/E_0 < 0.75$ are shown in Fig. 27.4.

27.4.5.3 Selection of OPGW

Optical fiber composite overhead ground wire (OPGW) is used for the ground wire with the new type of communication structure for high-voltage transmission system, and has dual functions of common overhead ground wire and fiber optic communication. Based on the locations where OPGW optic cable is located, it can be divided into the types of being layer stranded, armored, and with central beam

tube, of which stainless steel tube layer stranded structure is widely used in construction in recent years, and has many advantages, such as with a compact simple structure, allowing the placement of more number of fiber cable, better uniform distribution of the light unit, and sufficient length of the entire cable. Additionally, the layer stranded structure is the same with the common ground wire, and it has a good match with the common ground wire, so 90% of all OPGW in China are this kind of structured products at present.

As UHV ground wire, OPGW must meet the selection requirements of ground wire; as overhead ground wire, the primary role of OPGW is to try to make lightning that could fall on the power transmission line strike to itself in order to protect the conductor, so OPGW being struck by lightning is inevitable; however, OPGW system shall be provided with the important functions of system communication and protection of signaling function additionally. Once the fiber channel is damaged, it will endanger the safe operation of the system, which requires OPGW having a better lightning resistance. Through computational analysis and previous design experience, full aluminum clad steel products shall be selected to improve the ability of OPGW lightning resistance, and, in addition, the diameter of outer individual wire shall not be less than 3.0 mm; meanwhile, OPGW must match with the mechanical properties of the other ground wire, and their sag characteristics shall be as similar as possible.

27.5 Insulation Coordination Design of AC Transmission Line

The insulation coordination of UHV transmission line shall be designed primarily in accordance with relevant standards, referring to the research findings carried out in the early works, as well as the latest test results of scientific research units, to carrying out the coordination design of the line external insulation levels and determining the appropriate air clearance. The main tasks include the following:

(1) According to the site contamination survey, combined with operational experience and the latest provincial distribution map of polluted areas along the line, integrated with the analysis of environment, meteorology, industrial pollution, and the operation condition of the transmission and distribution equipment of the regions the line passing through, determine the division of polluted areas of the project.
(2) Compare the insulation performance, electrical and mechanical properties, weather resistance, etc., of different types of insulators, to determine the type selection of the insulators.
(3) Integrating the plan of line towers and the applicable conclusions of the selection of conductor and ground wires, determine the configuration scheme of the insulator strength, and determine the pieces of insulator strings.

(4) Propose the recommended values for tower power frequency, operations, lightning and live working air clearance, and the phase-to-phase spacing values under power frequency, and switching overvoltage required for the project.

27.5.1 Type Selection of Insulators

Because of large transmission capacity, high-voltage level, and high requirement of external insulation level of UHV line, as well as increased number of sub-conductors and increased height above the ground of the UHV transmission line, resulting in the level of external loads being greatly improved, higher demands are raised to the mechanical strength and electrical properties of insulators.

27.5.1.1 Characteristics of Various Types of Insulators

Three main types of insulators, i.e., ceramic disk insulators, glass disk insulators, and rod-type composite insulators, are commonly used for overhead transmission lines, and now the rod-type porcelain insulators having non-breakdown structure and middle to long creepage distances have also been put into operation in 500 kV line.

Porcelain disk-type, glass disk-type, and rod-type composite insulators have their advantages and disadvantages, and their mechanical and electrical properties and evaluations of operating conditions are as shown in Table 27.10.

27.5.1.2 Comparison of Pollution Flashover-Resistant Performance of Insulators

The pollution flashover-resistant performances of all types of insulators are related to the shed structure and the creepage distance of the insulators. The scientific research and experiment departments in China have conducted a lot of artificial insulator pollution flashover tests to the different types of insulators, of which the artificially flashover test results for different types of porcelain and glass disk insulators under normal voltage showed that, with the same height of structure, for the three umbrella-type suspension insulators, the more the monolithic creepage distance, the better the pollution flashover-resistant performance.

For the double-umbrella-type porcelain insulators (with creepage distance of 485 mm), the common type of porcelain insulators (with creepage distance of 505 mm), and glass insulators (with creepage distance of 485 mm) with little difference in creepage distance, there is a little difference in 50% flashover voltages of these three disk-type insulators, the pollution flashover-resistant performance of the

Table 27.10 Simplified comparisons of technical performances of porcelain, glass and composite insulators

S/N	Item	Porcelain disk insulators	Glass disk insulators	Composite insulators
1	Structure and technology	More complex	More complex	Simple
2	Unit weight	Lighter	Lighter than porcelain	Weight (whole piece)
3	Creepage distance variability	Not easy to change	Not easy to change	Easy to adjust
4	Anti-impact performance	Better	Good	Poor, must not be stepped on, nor climbing
5	Spontaneous explosion rate	Without spontaneous explosion	With spontaneous explosion	Without spontaneous explosion
6	Withstand voltage breakdown	May breakdown	May breakdown	Non-breakdown
7	Hydrophobicity	Poor	Poor	Good
8	Pollution flashover resistant voltage value	Lower	Lower	High
9	Field intensity distribution	Uneven	Even	Uneven
10	Anti-aging properties	Ordinary	Better	Poor
11	Tensile strength	Ordinary	Better	Ordinary
12	Resistance to vibration fatigue	Ordinary	Good	Ordinary
13	Thermal stability	Better	Better	Ordinary
14	Resistance to icing hazards	Better	Better	Prone to icing flashover after being iced
15	Anti-lightning performance	Poor	Better	Poor
16	Resistance to leakage and erosion	Poor	Better	Poor
17	Resistance to wind drift sand	Good	Better	Not used in desert area
18	Prevention from rodent or birds	Good	Good	Poor
19	Assembled into insulator string	More pieces required, more complex assembly	More pieces required, more complex assembly	As a whole piece, easier assembly

(continued)

Table 27.10 (continued)

S/N	Item	Porcelain disk insulators	Glass disk insulators	Composite insulators
20	Packing and shipping	Light unit weight, and flexible packaging and shipping methods	Light unit weight, and flexible packaging and shipping methods	The whole length is about 10 m, so it is difficult for transport at mountainous areas
21	Judgment for operation	Measuring zero	Self-testing	–
22	Life cycle	Longer	Long	Shorter

double-umbrella-type porcelain insulators is slightly better, and the one of common type of insulators is a bit poor.

It is shown through the AC contamination test results of the composite insulators with different umbrella structures that, the composite insulators with one big umbrella and two small umbrellas have a better pollution flashover-resistant performance than the composite insulators with one big umbrella and one small umbrella.

With the same structural height, the composite insulators have the highest pollution flashover-resistant voltage, followed by three umbrella-type disk insulators, while the bell-type structure and the rod-type porcelain insulators are almost the same.

27.5.1.3 Selection of Insulator Strength

Double- and multi-insulator strings shall be checked for the mechanical strength after one of the insulators is disconnected. The load and safety factor shall be considered based on the case of insulator disconnection.

In the engineering design, the calculation shall be made based on the actual load conditions of the used conductor. Normally, the main combination types of conductor suspension insulator strings include single 300 kN, single 420 kN, single 550 kN, double 300 kN, double 420 kN, double 550 kN, triple 420 kN, and triple 550 kN; the main combination types of conductor strain insulator strings include quadruple 420 kN, triple 550 kN, or double 760 kN.

In the design of the lines, the suitable insulators should be selected by considering the technical characteristics and mechanical strength requirements of each insulator, and the specific contaminations along the line and the economy of string assembly comprehensively.

Because of its excellent pollution flashover-resistant performance of the composite insulator, the length of the insulator string can be significantly shortened, and the size of the tower and the construction costs can be reduced. Additionally, the price of composite insulators with large tonnage is lower than the one of porcelain or glass insulators, so the use of composite insulators is more economic. In order to

avoid the accident that may be caused by brittle fracture of composite insulators, it can be solved by using double-strings in parallel, which is also technically feasible.

27.5.1.4 Opinions on Selection Recommended

The main advantages of disk-shaped insulator include high mechanical strength, good flexibility of long strings, light weight of single element, easy for transportation and construction, as well as easy to shape and with diverse selections. Because the disk-type insulators belong to the breakdown insulators, the insulation requires high electrical intensity. After the elements of porcelain insulators deteriorate, heavy workload is required for the inspection and testing; in case the disconnected strings are not timely detected, the string may break at the time of lightning of pollution flashover; the glass insulators may be suffered from spontaneous explosion phenomenon, the surface leakage current caused by heavy pollution may deteriorate the spontaneous explosion phenomenon, but the spontaneous explosion phenomenon is beneficial to line maintenance and preventing from the occurrence of line dropping accident.

The main advantages of composite insulators include the non-breakdown structure, good self-cleaning performance, and large creepage distance coefficient (the ratio of creepage distance to insulation length). The contamination of composite insulators is lower than the one of disk-shaped insulators when they are in the same environment, and can obtain a higher pollution flashover voltage. If an appropriate creepage distance is selected, a longer cleaning cycle can be achieved. The ratio of the tensile strength of composite insulator to its weight is high, so it has an excellent pollution flashover-resistant property, but there will be the possibilities of the breakdown in the interface and the "brittle fracture" of core rod, and the consensus on the service life of organic composite materials and the long-term reliability of end connectors has not been reached yet.

As it can be seen from the above description, for the line insulators with different structures and materials, the porcelain, glass, and composite insulators have their own advantages at the aspects of their materials and application features, but also have their own shortcomings. For 1000 kV UHV lines, the insulators of these three materials can meet the needs of proper operation.

In summary, the recommendations for insulator selection of 1000 kV AC transmission line are as follows:

(1) The ordinary disk-type insulators have a low 50% flashover voltage of single insulator, and with the increase of altitude, they have the maximum extent of reducing the pollution flashover voltage. Because of its ridges on the bottom surface of the insulator, with poor self-cleaning in a drought environment, easy to accumulate dirt, not easy to clean, they are only recommended for the applications in cleaner areas.
(2) The double-umbrella-type insulators have a high pollution flashover voltage, and the decrease of pollution flashover voltage is not significant with the

increase of altitude, indicating that this type of insulator has a better resistance to pollution flashover at high altitude. In addition, the insulators of this shape have been widely used in China, and have accumulated a lot of operation experience. It is proven through operation that this type of insulator has a good self-cleaning effect, less dirt accumulated, with operating results significantly better than the standard and bell-type insulators. It is recommended using such insulators in the areas of normal contamination.

(3) The three umbrella-type insulators not only have the highest average flashover voltage for each piece, but also the decrease of pollution flashover voltage is not significant with the increase of altitude. It can be seen from the pollution flashover test results of the insulators of different materials and shapes that, this insulator has the best performance. It is recommended rationally using such insulators in moderately polluted areas.

(4) For the moderate and heavily polluted areas, the use of composite insulators is proposed. The composite insulators have good pollution flashover resistance properties, and with increasing of altitude, the reduction of pollution flashover voltage is small.

27.5.2 Selection of the Number of Pieces of Insulator Strings

The insulation coordination of transmission line shall be able to maintain a safe and reliable operation under all conditions of power frequency voltage, switching overvoltage, and lightning overvoltage.

The length of insulator strings of UHV transmission lines shall be determined in accordance with the conditions of withstand power frequency operating voltage. It is shown through a lot of tests that the AC withstand voltage properties are proportional to the string length, regardless of the type of contamination (dust contamination, industrial contamination, and salt contamination), the degrees of contamination (mild contamination, heavy contamination, and extreme contamination), and the types of insulators. The contamination withstand voltage properties under the switching impulse voltage are also proportional to the length of the string approximately.

27.5.2.1 Selection of the Number of Insulators by Power Frequency Voltage

There are two methods that may be used for the selection of number of insulators by power frequency voltage, namely, creepage distance method and pollution withstand voltage method.

1. Creepage distance method

The insulator string length shall be determined based on the creepage distance. With this method, in accordance with pollution conditions the region that the transmission line goes through, the measurements of salt density and ash density, as well as the operating experience of existing transmission line, the contamination level and the corresponding creepage distance shall be first determined, then the number of insulators shall be calculated according to the creepage distance of the selected insulators.

The number of insulators per string required by the power frequency voltage creepage distance shall meet the following requirement:

$$N \geq \frac{\lambda U_{\mathrm{m}}}{K_{\mathrm{e}} L_0}, \tag{27.2}$$

where

N is the number of insulator pieces per string;
U_{m} is the rated voltage of the system, in kV;
L_0 is the geometric creepage distance for each piece of suspension insulator, in cm;
λ is the specific creepage distance, in cm/kV;
K_{e} is the effective coefficient of insulator creepage distance, which refers to the ratio of pollution flashover voltages of the tested insulator to the basic insulator at unit leakage distance and under the same natural conditions and the same pollution accumulation time, and its value shall be determined through tests.

This method is simple, easy to operate, has been widely adopted in engineering design and, after being verified by many of the practical engineering, is an acceptable engineering design method, of which the key point is to determine the creepage distance effective coefficient K_{e} of the insulators in different shapes. In case of the absence of accurate experimental data, it is recommended "taking the effective coefficient K_{e} value as 1.0 for the common-type, double-umbrella-type and triple-umbrella-type insulators in light polluted areas; the effective coefficient K_{e} value of antifouling bell-type insulators as 0.9; the effective coefficient K_{e} value of common-type disk, double-umbrella-type, and triple-umbrella-type insulators in moderate and heavy polluted areas as 0.95; and the effective coefficient K_{e} value of antifouling bell-type insulators as 0.85" [2].

2. Pollution withstand voltage method

The pollution withstand voltage method is to obtain the pollution withstand voltage of the insulators at different levels of contamination from the tests, so that the pollution withstand voltage of the selected insulator strings is greater than the maximum operating voltage of the line. The method is directly linked to the

pollution tolerance of actual insulators, so it is the better method of determining the length of insulator strings.

The steps of using pollution withstand voltage method in engineering design are as follows:

(1) Determine the degree of the site contamination SPS (salt density ESDD/ash density NSDD);
(2) Have the degree of the site contamination SPS corrected to salt deposit density SDD;
(3) Determine the maximum withstand voltage of single piece of insulator U_{max};
(4) Determine the design target voltage at pollution level of the line project U_M, which can be 1.1 times of the maximum value of operating phase voltage;
(5) Calculate the number of insulators for insulator strings N, $N = U_M/U_{max}$;
(6) Verify the number of insulator pieces according to the nature of the operating voltage (long-term operating voltage, power frequency overvoltage, and switching overvoltage).

27.5.2.2 Selection of the Number of Insulators by Switching Overvoltage

The 50% discharge voltage $U_{50\%}$ of positive polarity switching impulse voltage wave of the line insulator strings voltage required by the switching overvoltage shall be consistent with the requirement of the following equation:

$$U_{50\%} \geq K_1 \cdot U_S, \tag{27.3}$$

where

U_s is the statistical switching overvoltage of the line to ground, in kV;
K_1 is the statistical coordination factor for the switching overvoltage of the line insulator string, taken as 1.25.

Assuming that the statistical switching overvoltage multiplier of 1000 kV transmission line is taken as 1.7 p.u., and the maximum operating voltage of the system taken as 1100 kV, the 50% discharge voltage $U_{50\%}$ of positive polarity switching impulse voltage wave shall be as follows:

$$U_{50\%} \geq 1.25 \times 1.7 \times \sqrt{2} \times 1100/\sqrt{3} = 1909 \text{ kV}.$$

After considering two pieces of insulator with zero value, the numbers of insulator strings in the Grade 0 & I polluted areas of 1000 kV AC transmission line required by the switching voltage are 34 and 44, respectively (calculated based on bell-type 300 kN insulators), and when the contamination levels are greater than or equal to Grade II, the selection of the number of insulators for insulator strings

based on the switching overvoltage has become ineffective, and the number of insulators for insulator strings shall be determined by the power frequency voltage.

27.5.2.3 Checking of the Number of Insulators by the Requirement of Lightning Overvoltage

In general, the lightning overvoltage has no direct relationship with the operating voltage. In the EHV system, due to the high external insulation level of transmission lines, the lightning overvoltage is not decisive in the design of the external insulation. However, under the lightning overvoltage, the insulator string shall meet certain withstanding level. It is found through calculations that, the single-circuit tripping back striking lightning withstand level of 1000 kV double-circuit transmission line on the same tower is 208–250 kA typically, and double-circuit tripping back striking lightning withstand level is 220–281 kA typically. The probability of occurrence of such lightning current is very low (on the order of magnitude 0.1% and below), and, therefore, probability of the lightning back flashover of 1000 kV transmission line is very low.

The lightning shielding failure tripping rate is analyzed and calculated in accordance with the electrical geometric type (EGM). In Class III polluted zone, at altitude below 1000 m, the number of insulator string of 54, and with the tower grounding resistance of 10 Ω and adopt negative protection angle, the calculated lightning shielding failure tripping rate of single circuit line is far lower than the expected lightning trip rate of 0.1 times/100 km·a for 1000 kV transmission line project. The lightning overvoltage still has no control effect on the selection of the number for insulator strings.

27.5.3 Air Clearance at Tower Head

The external insulation level of EHV overhead transmission line depends primarily on the power frequency voltage, switching overvoltage, and lightning overvoltage of the overhead transmission line. For the transmission lines, the determination of insulator string length and the selection of the air clearance are the basis for the determining of tower head size and design of the tower head structure, which will directly affect the costs and operational reliability of the line project. For the UHV transmission line at the level of 1000 kV, due to the increased operating voltage, the external insulation level is normally controlled by power frequency voltage and switching overvoltage.

Table 27.11 Minimum clearance between 1000 kV single-circuit conductor and tower components (m)

Altitude (m)	500	1000	1500
Power frequency voltage	2.7	1.9	3.1
Switching overvoltage			
Side phase I-type strings	5.6	6.0	6.4
Middle phase V-type strings (to the tower body)	6.7	7.2	7.7
Middle phase V-type strings (to the upper cross arm)	7.9	8.0	8.1

Table 27.12 Minimum clearance between 1000 kV double-circuit conductor and tower components (m)

Altitude (m)	500	1000	1500
Power frequency voltage	2.7	2.9	3.1
Switching overvoltage	6.0	6.2	6.4
Lightning overvoltage	6.7	7.1	7.6

27.5.3.1 Minimum Clearance at Tower Head

The minimum air clearance from the conductors to the tower components after the wind swinging shall satisfy the requirements of power frequency voltage, switching overvoltage, and lightning overvoltage.

1. For the minimum air clearance required for the power frequency voltage and switching overvoltage, the impact of multi-clearance shunt conductors on the discharge voltage shall be considered at first to figure out the power frequency voltage and switching overvoltage under standard meteorological conditions, and the high-altitude correction shall be made for the power frequency voltage and switching overvoltage at different altitudes, and then the air clearance discharge characteristic curves shall be checked, to determine the minimum air clearance (Tables 27.11 and 27.12).
2. The lightning overvoltage clearance is determined based on the acceptable line shielding failure tripping rate.

When the suspension strings are used for the side phase of UHV single-circuit line, the air clearance under lightning impulse is not dominant to the sizing of tower head. It is mainly the clearance distance required by power frequency voltage under strong wind conditions that has dominance.

When the V-type strings are used for the middle phase of UHV single circuit line, the air clearance to the tower is mainly controlled by the clearance distance required under the switching impulse. The possibility of lightning shielding failure for middle phase conductors of UHV single circuit lines is low, even if there is a lightning shielding failure, the lightning current amplitude is very low, and will not lead to line insulation flashover, and the probability causing the shielding failure trip-out is almost zero. Therefore, for the UHV single-circuit line, the required value for the air clearance under lightning impulse may not be specified.

For UHV double-circuit transmission line on the same tower, the distance from the conductor to the lower cross arm has a significant effect on the lightning impulse

insulation level and the lightning tripping rate. The required value of air clearances under lightning impulse may be greater than the clearance distance determined by the switching overvoltage, which needs to be studied and determined.

During the selection of the insulation level for 1000 kV same tower double-circuit transmission line, the air clearance under lightning impulse shall be selected by combining the requirements of the air clearance of tower required under switching impulse. The probability of the insulation flashover of 1000 kV same tower double-circuit transmission line under the switching impulse is very low, while the probability of occurrence of insulation flashover in the lightning impulse is relatively much greater. The main cause of lightning trip for UHV double-circuit transmission line on the same tower is the lightning shielding failure. And the increase of the minimum clearance can reduce the rate of lightning shielding failure of the lines significantly. Of course, the decrease of the protection angle of ground wire can also reduce the lightning trip rate.

In order to reduce the lightning trip rate, the minimum air clearance under lightning impulse of line tower may be increased appropriately, especially for the routes in mountainous areas.

27.5.4 Lightning Protection and Grounding Design

The features of lightning protection for UHV transmission lines include that the insulation level of the line is very high and the possibility of lightning strikes on the ground wire or back flashover on tower head is very low; the tower is much higher that it is more prone to occurrence of shielding failure [3].

To improve the performance of lightning protection of UHV lines, the following aspects shall be mainly considered in the engineering design:

(1) Set up two ground wires

UHV lines shall be set up with two ground wires. When one of them uses OPGW compound optical cable, in order to improve the lightning protection performance of OPGW, the outer stranded wires with larger diameter shall be used as much as possible. By increasing the section of the outer stranded wire, the probability of strand breakage due to the lightning to OPGW can be relatively reduced.

(2) Reduce the protection angle of ground wire, to improve the lightning withstand level of shielding failure. For example, in Northern Zhejiang–Fuzhou 1000 kV transmission line, 90% mountainous terrain exist along the line, to meet the requirements of lightning protection level, the protection angle for double-circuit ground wire to the outside sub-conductor shall not be greater than minus 4° in the plains, no more than minus 6° on hills, mountains; the protection angle of single-circuit ground wire to the outside sub-conductor shall not be greater than 6°; the protection angle of ground wire to the jumpers of strain tower shall be less than 0°.

(3) Lower the tower height.
(4) Reduce the grounding resistance of tower. Each tower shall be grounded. For the normal line towers, its power frequency grounding resistance shall be limited to 30 Ω or less, and grounding conductor normally shall be Φ 10–12 round galvanized steel bar. For the mountainous areas with high soil resistivity, the physical resistance reducing agent or module can be used to further reduce the grounding resistance.

Because the copper-clad steel has excellent corrosion resistance, free replacement, and low operation and maintenance costs, it may be used in the plains, ponds, and green belts with high corrosion and difficulties of replacing the grounding conductors, and some area of mountains and hills with the difficulties of transportation.

(5) In the middle of span, the distance between the conductor and the ground wire at 15 °C, when there is no wind, shall not be less than the value calculated as follows:

$$S = 0.015L + \sqrt{2}U_{\mathrm{m}}/\sqrt{3}/500 + 2, \tag{27.4}$$

where

S is the distance from conductor to the ground wire at the center of the span, in m;
L is the span distance, in m;
U_{m} is the maximum voltage of system, in kV.

(6) Proper selection of line route in mountainous area

When the line traces in the mountains, because the slope of the ground has a greater impact on shielding failure trip-out rate, continuous line traces on the hillside, as well as too large grounding resistance of continuous towers shall be avoided as possible during the selection of line.

(7) Improvement of the tower design

In the tower design, both the protection angle of the ground wire and horizontal displacement of conductor and ground wires shall be considered for the arrangement of tower head. For the line project with the most in the hilly terrain, the lightning protection angle of ground wire shall be minimized in the tower design to enhance the level of lightning protection of the line. In addition, the conductor arrangement also has a great impact on lightning protection performance. For the double-circuit transmission line on the same tower, the lightning performance of vertically arranged drum-type tower is inferior than that of the umbrella-type tower,

the protection angle of ground wire lightning protection of the former needs to be reduced by 3–4° when compared to the latter.

(8) Installation of line arrester

For the lines in high lightning-affected areas, in order to reduce the lightning trip-out rate, line arresters shall be installed in the areas that are easily subject to lightning strike identified in the lightning density investigation along the line of the project and on the towers vulnerable to lightning strike with a large height difference, large span, and close to water. Normally, the line arrester shall be installed at the middle phase or the lower phase of double-circuit tower at downward side of the hillside or at the cross arm of the side phase conductors of single-circuit tower. During the installation of line arresters, it shall be noted that the mounting height of arrester bracket is to be adjusted according to the height of actual hanging point of the conductor.

(9) Other measures

Based on the operating experience of China's EHV transmission lines, in the lightning-sensitive points, the lightning withstand level may be improved by taking proper measures such as mounting sideward rods, coupling ground wires, by-pass ground wires, etc.

27.6 Design of AC Line Insulator Strings and Fittings

Since the 1000 kV power transmission line has large transmission capacity and high-voltage level, the corona problem is prominent. Subject to the control by the limits of electromagnetic environment, the phase conductor is normally in 8 bundles, and the cross-section of sub-conductor is 500, 630, or 720 mm^2.

Since the number of sub-conductors is numerous and the cross-section of sub-conductor is big, the conductor load borne by the insulator strings is large; meanwhile, the conductor fitting strings also face the corona problem due to high voltage. Therefore, the insulator fitting strings adopted by the UHV line shall have sufficient mechanical strength and good electrical performance so as to ensure the safe operation.

27.6.1 Basic Principles

The insulator strings of UHV line shall be configured in such a way that the requirement of mechanical strength is met first. The mechanical strength is mainly controlled by the maximum load under normal operation of the line; secondly,

economy of combining various types of strings shall be fully taken into consideration so as to ensure the safety, reliability, economy, and reasonableness of the insulator string-type design.

On the pre-condition that the safety and economy of insulator string-type design is ensured, the string type with less number of connections shall be used as far as possible. Operating experience and test researches indicate that when double- or multiple insulator strings are adopted, its insulation performance will decrease slightly as compared to single insulator string, that the fault probability of the insulator string itself is larger, that the work load on installation, operation, and maintenance is bigger, and that the load of insulator string itself will also increase substantially. Therefore, on the condition that the requirement of mechanical strength is met, and fittings and types of insulators are permitted, the string type with less number of connections shall be selected as far as possible.

Proper voltage-balancing and anti-corona measures shall be taken for insulator strings and fittings. The first fitting that is connected with the cross arm of tower shall be able to rotate flexibly, with reasonable force being borne, whose mechanical strength shall be higher by at least one grade than those of other fittings on the string. The load-carrying capability of first fitting that the insulator string is connected with cross arm is complicated. Much operating experience has proven that if the first tower-connecting fitting is not flexible enough, it is not only worn easily itself, but also it will cause damage to its adjacent fittings and further damage to the whole string. Therefore, during the selection of the first fitting, the strength, materials, and types shall be taken into consideration.

27.6.2 Safety Factor

The safety factor of mechanical strength of insulator shall not be less than the values listed in Table 27.13. Mechanical strength of the double- and multiple insulator strings shall be checked on a basis of breakage of one string, and its load and safety factors shall be taken into consideration based on insulator breakage.

Table 27.13 Safety factor of insulator mechanical strength

Case	Maximum operating load		Perennial load	Checking load	Disconnection	Insulator breakage
	Disk-type insulator	Rod-type insulator				
Safety factor	2.7	3.0	4.0	1.8	1.8	1.5

Notes The perennial load refers to the load borne by the insulator under average annual air temperature. The checking load refers to the load borne by the insulator under the checking conditions. The climate condition for disconnection and insulator breakage is that no wind but ice exists with temperature being at −5 °C

The safety factor of fitting mechanical strength shall be not less than 2.5 under the maximum operating load condition, and not less than 1.5 under disconnection and insulator breakage conditions.

27.6.3 Suspension Insulator String of Conductor

There are mainly two types of conductor suspension strings which are widely applied in the power transmission line projects around the world: I-type string and V-type string. In the early projects, I-type string was mainly adopted. This type of string has the characteristic of simple structures and reasonable load-carrying capability. Application of V-type string can inhibit wind swing of suspension string of conductor, thus to reduce the dimensions of tower head, which plays an effect of compressing the width of corridor and reducing the housing relocation. Such type is widely applied in the corridor crowded areas where houses are intensified. On the another hand, application of V-type string structure will be helpful for self-cleaning of insulators under raining, for the operating insulators are always in a tilting state of about 45°, and meanwhile, for the lines located in the heavy ice-covered areas, it is also helpful for inhibiting the formation of ice between sheds of adjacent insulators, helpful to preventing ice flashover of the line.

In the engineering design, proper type of string structure shall be selected by taking the types of towers, corridors of lines, landforms, and ice area conditions into consideration comprehensively. Generally speaking, for the single-circuit straight-line towers (cup-type towers or cat head towers) of 1000 kV line, V-type strings are adopted for the phase conductors, and I-type strings are adopted for side phase conductors; for the single-circuit straight-line towers (cup-type towers) in the heavy ice-covered areas, V-type strings are adopted for three-phase conductors; either I-type or V-type strings can be adopted for the straight-line towers of double-circuit lines on the same tower.

For 1000 kV AC double-circuit power transmission line, as compared with I-type string, although the cross arm of tower is extended when using the V-type string, since V-type string has a limitation to the offset of conductors, the phase-to-phase distance of conductors can be reduced by about 6 m, the corridor width of whole line is smaller, and this can reduce the residence relocation and reduce cutting of the trees along the corridor, etc.; from the perspective of corona, radio interference, and audible noise, when I-type string layout is adopted for the conductors of line, the conductors with cross-section of 8×630 mm^2 or above can meet the requirements of electromagnetic environment limits; when V-type string layout is adopted, the distance between side conductors is compressed, according to the requirements of controlling the audible noise indexes in the population-intensified areas strictly, the conductors with cross-section of 8×720 mm^2 or above are required, or the spacing between the upper and lower conductor layers is increased by about 2 m rather than increasing the cross-section of conductor.

The conventional I-type suspension insulator string and V-type suspension string are shown, respectively, in Figs. 27.5 and 27.6.

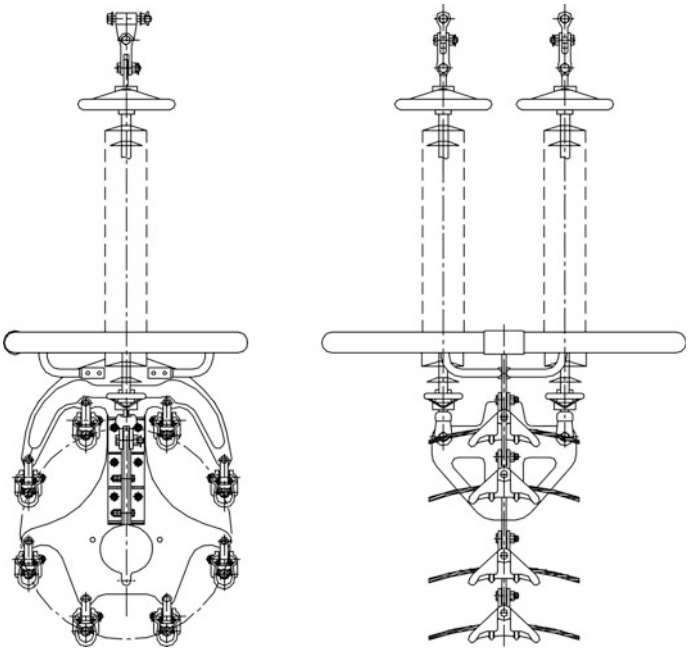

Fig. 27.5 Layout of I-type double-suspension string in 1000 kV line

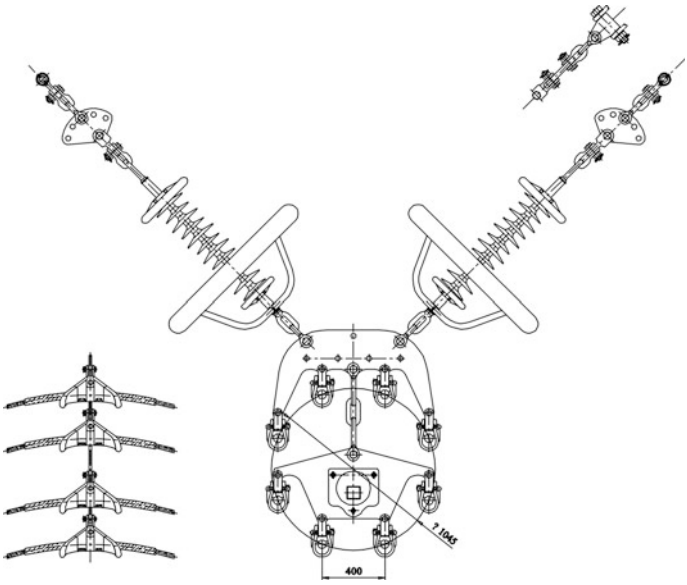

Fig. 27.6 Layout of V-type suspension string in 1000 kV line

27.6.4 Strain Insulator String of Conductor

The combination mode of strain insulator strings adopted in the power transmission line is determined based on the technical economy comparisons in terms of conductor design conditions, climate conditions, construction installation, operation, maintenance, etc. Under normal circumstances, it is ideal to adopt the combination mode of double-strain insulator string, which is not only simple in the structure, highly safe, and reliable in the operation, but also pretty convenient in the construction installation, operation, and maintenance. However, with the increasing of the total cross-section at each phase of conductor, as well as the changes to the manufacturing level of insulators and the status of supplies and sales, selection of the strain insulator strings with multiple connections combination is becoming more prominent in economy. The insulators with strength of 300–550 kN has mature manufacturing process, and rich operating experience, so it is widely applied in the UHV power transmission lines. With the development of insulator's manufacturing technologies, the manufacturing process of 760 kN insulator is becoming matured day by day, which has been demonstrated for trial in the UHV power transmission line projects in China.

The section of conductors in 1000 kV line includes 8×500 mm^2 and 8×630 mm^2, and the combination mode of tension strings to be adopted shall be selected among the combination mode of double insulator strings, triple insulator strings, quadruple insulator strings, and sextuple insulator strings, from which the best combination mode of tension string is selected; meanwhile, the number of hanging points of cross arms, types of fittings connecting with towers as well as the connection mode of tension strings with eight-bundled conductors, etc. shall be studied and discussed.

The tension strings assembled by multiple insulator strings through various fittings must meet the following 5 essential requirements:

1. Under the normal operating conditions, including the action of ice and wind loads, the tension distribution on each connected insulator shall be equal, and can meet the specified requirements of safety factor in case of any differences;
2. Under the disconnection or insulator breakage condition, the tension string can still maintain the proper operation of the line, and the rest of insulator strings can withstand the impulse loading without being damaged; meanwhile, the tension distribution on the rest of insulator string shall be equal as far as possible, or shall meet the specified requirements of safety factor;
3. In case of any differences in tension distribution on each insulator string due to any errors or changes in the length of conductor or insulator, the tension string has the possibility of being adjusted or self-restoration;
4. When the conductor generates any movement, like jumping or galloping, each connection point (including the connection points on the cross arms of towers) shall be worn resistant and fatigue resistant;

5. Convenient for construction installation and wire tightening operations, and convenient for operation and maintenance operations.

The multiple tension strings shall meet the requirements of items (1), (2), and (3) above, which is achieved by utilizing a special part, i.e., the yoke plate. Verified through relevant tests, the dedicatedly designed triple and quadruple tension strings can meet the requirements of the aforesaid 3 items. The requirements in item (4) are mainly related to the number of hanging points on the cross arms and the fittings connecting with towers, which will be described in the next section.

The layout patterns of several strain insulator strings of conductors mainly applied in the engineering design are shown in Figs. 27.7, 27.8, and 27.9.

27.6.5 Jumper Fitting String of Strain Tower

In the UHV line, as the length of strain insulator string of conductors increases, the length, sag, and wind swing of by-pass jumper will also increase. The jumper has become a control factor for the design of strain tower head. The adoption of the ordinary soft jumper will cause the increase in the dimensions of tower head.

The rigid by-pass jumper is a type of jumper which is commonly applied in the EHV lines and UHV lines in other countries besides China. It is being extensively applied gradually in China at present. For the 1000 kV AC line, the rigid jumper is used as the by-pass jumpers of strain towers. There are two commonly used types of rigid jumpers, which are the squirrel-cage and aluminum tube rigid jumpers, respectively. These two types of rigid jumpers can limit the angle of wind deflection by means of appropriate counterweight, hence achieving the goal of compressing the dimensions of strain tower heads. In addition, the impact of these two types of rigid jumpers on the height of strain tower is almost the same. What can be said is that the selection of the type of rigid jumpers mainly depends upon the technicality and economy of these two types of rigid jumpers (Table 27.14).

By taking the technical, installation, transportation, and economic factors into account comprehensively, the adoption of both squirrel-cage rigid jumpers and aluminum tube rigid jumpers as the by-pass jumpers for strain tower in the 1000 kV line can meet the requirements of engineering application. In contrast, in case of the adoption of the squirrel-cage rigid jumpers, several sections of steel tubes can be flange connected through the bracket of conductors, the installation and transportation are convenient, and, as compared to the aluminum tube rigid jumpers, it reduces the electrical connection points of conductors. In terms of the practical engineering, since crimping method is adopted at 4-bundle to 1-bundle clamps for aluminum tube rigid jumpers, the surface is not smooth, and corona result is not ideal. In addition, the adoption of squirrel-cage rigid jumpers can save about 10,000 RMBs for each phase of conductor as compared to the adoption of aluminum tube rigid jumper. Therefore, the adoption of squirrel-cage rigid jumpers has certain economy.

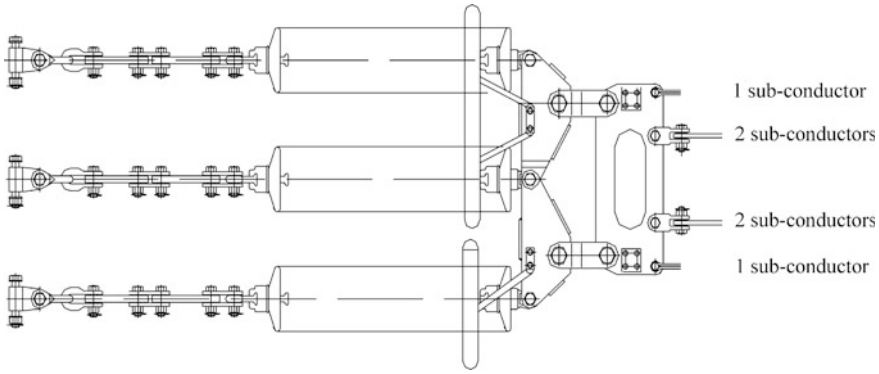

Fig. 27.7 Horizontal layout of triple tension strings (3 × 550 kN)

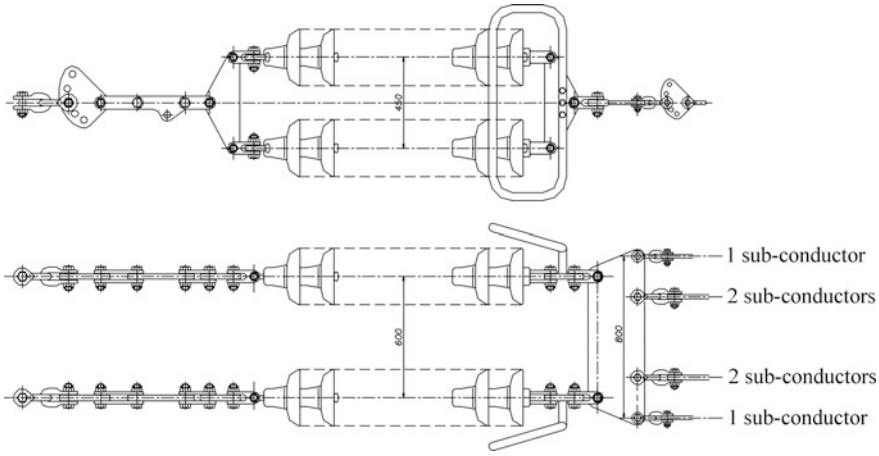

Fig. 27.8 Vertical layout of quadruple tension strings (4 × 420 kN)

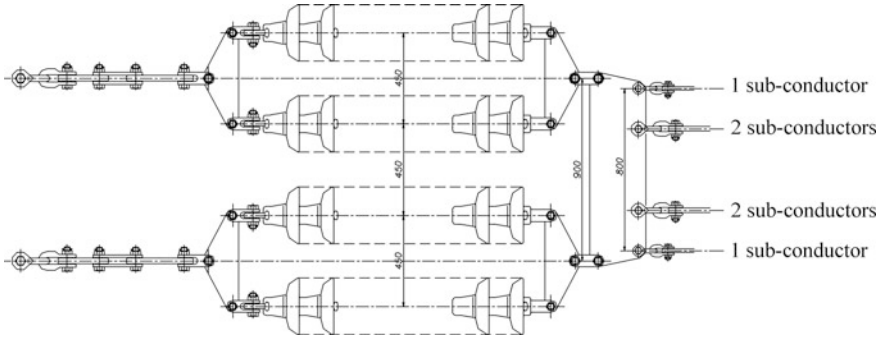

Fig. 27.9 Horizontal layout of quadruple tension strings (4 × 420 kN)

Table 27.14 Comparison of technical properties between squirrel-cage rigid jumper and aluminum tube rigid jumper

Item	Squirrel-cage rigid jumper	Aluminum tube rigid jumper
Type of connection	Steel tubes to be connected by flanges section by section	Assembled tubular busbar
Length adjustment	Convenient	The length of aluminum tubes required by each strain tower needs to be provided. If length adjustment is required, re-fabrication of aluminum tubes is required
Transportation	Convenient	Not convenient
Mechanical property	High mechanical strength, almost no deflection	Relatively lower mechanical strength, big deflection
Electrical property	In the whole jumper system, there aren't any connections except for strain clamps, good electrical property	Except for strain clamps, total 16 connections need to be added at 4-bundle to 1-bundle clamps, overcurrent susceptible to be impacted
Counterweight	Steel tube is heavy itself, so less counterweights to be added, the mode of counterweight is simple	Aluminum tube is light, many counterweights to be added, the mode of counterweight is complicated
Corona	In the whole jumper system, there aren't strong field concentrating points, the corona situation is good	Electric field concentrates at 4-bundle to 1-bundle clamps, corona can occur easily
Lifting	More convenient	Convenient
Parts and components	Few	Complicated
Appearance	Conductors are fixed onto the supports, the result is not ideal, there are laces	Neat, nice-looking

Squirrel-cage rigid jumpers are adopted for 1000 kV UHVAC Transmission Line Project to Transmit Power from Anhui to Eastern China. Jumpers are fixed onto the brackets by adding a jumper supporting device below the jumpers (at the middle section of the wound jumpers in the third span). The support brackets are suspended to the cross arms of towers through the insulator strings of jumpers. Counter weights can be added on the support brackets as required. The squirrel-cage rigid jumpers can reduce effectively the wind swing and sag of jumpers, and compress the structural dimension of towers. The result of its combination with tension strings is as shown in Fig. 27.10.

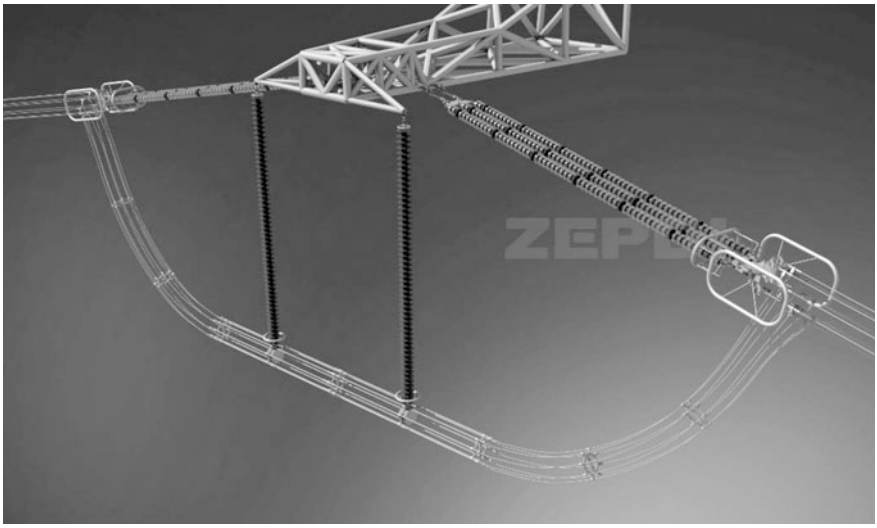

Fig. 27.10 Combination of squirrel-cage rigid jumpers of strain tower in 1000 kV line

27.6.6 Main Fittings

The fittings used in the power transmission lines mainly include clamps (suspension clamps and strain clamps), link fittings (clevises and yoke plates, etc.), protective fittings (spacers, vibration dampers, grading rings, etc.), and splicing fittings (splicing sleeves, etc.). Fitting is an important part for safe operation of the line. Even if it covers less cost in the construction of lines, it is very critical. Failure and damage of a fitting can lead to failure of the whole line. As the voltage level increases, the requirement of line fittings for reliability becomes higher.

27.6.6.1 Basic Requirements

Besides that national standards, industrial standards, and relevant specifications are met, specific to the special requirements raised for 1000 kV line, the design of the fittings for UHV power transmission lines shall also take into account the convenience for transportation, installation, maintenance, and replacement. To summarize, there are the following issues:

1. High reliability, which can meet the requirements of safe and stable operation of 1000 kV power transmission lines.
2. Reasonable structure, including the structures for fittings to be connected with insulators, conductors or fittings, as well as the own structures of fittings.
3. Materials of fittings shall be convenient for processing and manufacturing, and suitable for mass production.

4. Anti-corona design shall be adopted for fittings in order to prevent it being impacted by corona, and meet the requirements of non-occurrence of visible corona under 1.1 times maximum operating phase voltage in clear night, and of radio interference level not greater than 1000 μV [3].
5. Fittings shall be interchangeable, convenient for maintenance of the line.

27.6.6.2 Tower-Connecting Fittings

The tower-connecting fitting is a fitting used for connecting suspension insulator strings or strain insulator strings to the cross arms of towers, which is an important factor for ensuring safe operation of UHV lines. Besides sufficient mechanical strength, it must be able to rotate flexibly, and resist wearing, etc.

At present, GD clevises and trunnion clevises are commonly used as the tower-connecting fittings for tension strings and suspension strings in the UHV power transmission line projects, which can ensure flexible rotation in every direction. The disadvantage of GD-type tower-connecting fitting is that it needs to be installed in advance at the time of tower assembly, disposal of hanging points makes the structure of tower cross arm complicated, and it is not convenient to manufacture and install it.

The strength grade of tower-connecting fittings is normally higher than that of other link fittings in the strings. The tower-connecting fittings shall be processed in integrally forged way.

27.6.6.3 Eight-Bundled Suspension Yoke Plate

In China, the sub-conductors in 1000 kV UHV power transmission lines are of eight-bundled types. Adoption of either integral-type or split-type suspension yoke plates shall be determined depending upon the specific condition of the projects.

The integral-type yoke plate has good stability, small number of fittings, and simple structure, but it is heavy in weight, normally around 135–180 kg, and not convenient for handling, especially in the mountainous areas. The split-assembled-type yoke plate has many parts connected, and is light in weight of single piece, and convenient for manufacturing, transportation, and installation; besides, it also makes the suspension clamps swing more flexibly.

As can be seen from Fig. 27.11, the eight-bundled suspension yoke plate is a combination of two yoke plates. From the aspect of anti-corona, the lower yoke plate is in the interior of annular area formed by bundled conductors, whose potential gradient is zero, which will not generate visible corona. In the combined yoke plate, the swinging angle of wind deflection of upper two sub-conductors will be restricted, the maximum rotating angle of suspension clamp is 25°, and the wind swing of the other conductors will almost not be restricted.

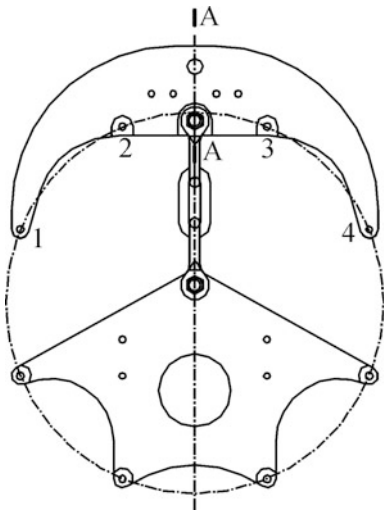

Fig. 27.11 Sketch of combined suspension Yoke Plate in 1000 kV line

27.6.6.4 Suspension Clamp

Suspension clamp is one of the critical fittings in the power transmission lines. Suspension clamp is a pivot point for conductors, which will withstand all the loads transmitted by conductors, and is susceptible to damage [1], and its property will have a direct impact on the service life of overhead line and loss of line. As for the UHV power transmission line, the requirements for mechanical strength reliability and anti-corona property of clamps are even higher.

In the UHV line, as voltage increases, the corona of fittings will become a major problem, so anti-corona design must be provided for clamps.

Since the manufacturing process of suspension clamp is complicated, according to the previous design experience in the EHV lines, the strength grade is normally 2–4. It is suggested that the strength grade of suspension clamp be graded as 80, 100, 120, and 150 kN. In case of big vertical spans, preformed armor rods are normally added, and therefore, suspension clamp of 100 kN or above shall meet the requirements of adding preformed armor rods.

Other requirements for suspension clamp are as follows:

(1) For the design of suspension clamp, besides that the normal tensile stress is taken into account, at the exit of clamp (including the interior of clamp), the bending stress and squeezing stress shall also be taken into account, and the exit angle of single side is normally in the range of 0°–25° [4].
(2) The radius of curvature of hull cable troughs shall not be less than 8–10 times of conductor diameter, and the contact part between clamp and conductor shall be kept smooth.
(3) Suspension clamp shall be able to rotate flexibly, having a swinging angle of not less than ±30°.

(4) There shall be sufficient contact surface between the suspension clamps and installed conductors in order to reduce any damage due to fault current.
(5) When the ratio of aluminum section to steel section of a conductor is greater than 11, the holding strength of suspension clamp shall not be less than 24% of the calculated breaking strength of a conductor.

The clamp materials are normally in aluminum alloy. The previous fabrication of suspension clamps was essentially done by using casting process. With the improvements of process and equipment, in the several UHV projects being constructed recently, aluminum alloy-forged clamp starts to be popularized. Such clamps utilize the advanced solid-state die forging process and have the characteristics of light weight and high mechanical strength, and in particular, remarkable effect of anti-corona and energy saving.

27.6.6.5 Spacer

The spacer damper is generally applied in the UHV lines. On one hand, it plays a role of isolation, making each sub-conductor in one phase of the conductor maintaining proper space with each other; on the another hand, it reduces the harm to the conductors arising out of aeolian vibration and sub-span oscillation through its damping characteristics [1].

Special requirements of UHV line for spacer are as follows:

(1) Good mechanical property to guarantee reliable mechanical strength. It is required that the spacer can withstand sufficiently the centripetal force arising out of short-circuit current, and in case of occurrence of maximum short-circuit current, it can support the spacing between sub-conductors, and prevent collision with each other. Besides this, the clamp is also required to have sufficient strength, and have sufficient holding strength on conductors.
(2) High requirement for anti-corona. It is required that the spacer shall be designed with the function of anti-corona. In particular, when the clamp is exposed at the outside of conductor splitting circle, corona can be easily generated, and sufficient attention must be paid during design.
(3) Good damping performance. The spacer damper obtains the required rigidity by utilizing elasticity of rubber so as to maintain the geometrical dimensions of bundled conductors, while make the conductors having sufficient movement. Damping performance is a critical parameter for studying and designing spacer dampers, which is related to the damping coefficient of rubber element materials. However, its vibration absorption effect is closely related to the structure and operating condition of the spacer, and sufficient consideration shall be given.
(4) Good fatigue-resistant property. When the transmission line has been running for long time, if the spacer cannot withstand fatigue vibration, it may cause the spacer to drop off, or cause damage to the conductors during vibration, which causes harm to the safe operation of line.

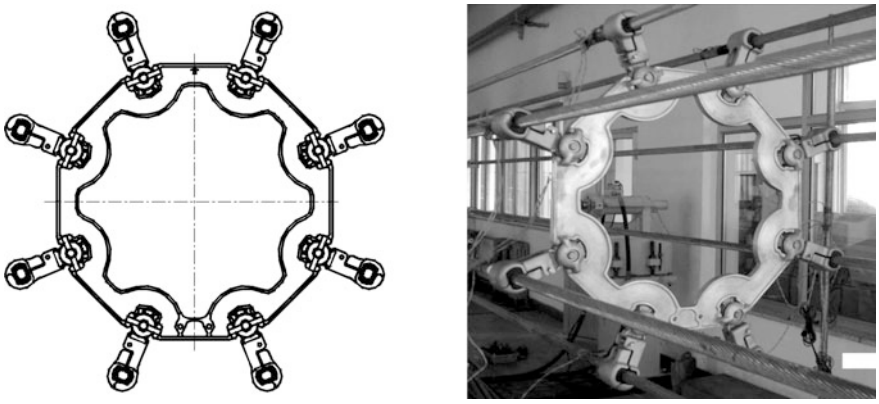

Fig. 27.12 Assembly pattern of the spacers for eight-bundled conductors in 1000 kV AC line

The assembly pattern of the spacers for eight-bundled conductors in 1000 kV AC line is as shown in Fig. 27.12.

27.7 Conductor Transposition Design for AC Line

In the power system, the balancing status of three-phase voltages is one of the important indexes for the quality of electric energy. Due to the asymmetry of three-phase parameters of the power transmission line, there is more or less deviation between three-phase voltage, current, and positive sequence quantity, which causes unbalancing of three phases, consequently bringing much unfavorable impact on the equipment of power system. In the power transmission line, the magnitude of unbalance factor of voltage and current mainly depends upon the coupling degree of negative sequence and positive sequence as well as zero sequence and positive sequence of the impedance and admittance of conductors, and the poorer the balance of power transmission line is, the bigger the sequence to sequence coupling factor is, and the corresponding unbalance factor is bigger.

The phase-to-phase coupling factor of conductors has direct relationship with the layout of three-phase conductors. At present, for the single circuit of UHVAC power transmission line, the layout of conductors is basically classified as horizontal arrangement and triangular arrangement. The balance of triangular arrangement of three-phase conductors is better than the horizontal arrangement; for double circuits, vertical arrangement is generally adopted.

By changing the position relations between three-phase conductors (that is, transposition), to reduce the phase-to-phase coupling factors, it is the most effective method for resolving the unbalance factor of power system in the long-distance EHV power transmission line. Therefore, in order to ensure the safety and stability

of power system, in the long-distance EHV power transmission line, the distance of transposition and the way of transposition must be designed well for conductors.

27.7.1 Main Content of Conductor Transposition Design

The conductor transposition is not required for DC line. The main work content of conductor transposition design for AC line includes the following:

1. Determine the limit requirement for unbalance factor of power transmission line.
2. According to the actual length of line, conductor layout pattern and dimensions of tower head to be used, calculate the electrical unbalance factor of line.
3. Analyze various factors that affect the unbalance factor of line.
4. According to the unbalance factor of line, determine the length of transposition for UHV line.
5. Carry out technical economy analysis for the way of transposition of line, and recommend the appropriate way of transposition and type of tower for transposition for UHV line.

27.7.2 Determination of Unbalance Factor Limits

In the power system, the balance of three-phase voltages is a main index for judging electric energy indexes. According to the *Quality of Electric Energy Supply Admissible Three-Phase Voltage Unbalance Factor*, "the allowable value of unbalance factor of normal voltage at the point of common coupling in the power system shall be 2% and shall not exceed 4% for short period of time." The national standard does not provide corresponding indexes for power transmission line. The point of common coupling is defined as the coupling point for more than one user in the power system. For the power transmission line as an integral part of the system, the unbalance factor generated by itself shall also be understood as being below 2%.

Therefore, in the engineering design, 2% is normally used as the limit for the electrical unbalance factor of power transmission line.

27.7.3 Calculation of Unbalance Factor for Power Transmission Line

27.7.3.1 Method for Unbalance Factor Calculation

The more practical method adopted in the engineering design is three-phase power flow program simulation method. The calculation idea is as follows: assume that the power, voltage, and current at the sending side of line are symmetrical and do not change with time, carry out processing of the wave shape data on voltage and current at the receiving side of line to get the amplitudes and phases of fundamental wave components at each phase, then take the component of each sequence through phase-sequence transformation, and calculate the unbalance factor of line.

Calculate and set up models according to the open power network to be supplied at one side, simulate the overhead lines by using π-type equivalent circuit, and calculate the equivalent load impedance value according to transmission power, transmission voltage, and power factor. The power system analysis software EMTP-ATP applied internationally is normally used to calculate the unbalance factor of overhead line.

According to the *Quality of Electric Energy Supply Admissible Three-Phase Voltage Unbalance Factor*, the limits for unbalance factor refer to the unbalance factor of voltage. Therefore, the calculation result is the unbalance factor of voltage in the general engineering design.

27.7.3.2 Calculation Conditions

The parameters required for calculation include system parameters (rated voltage, transmission power, power factor, etc.), conductor and ground wire parameters (conductor type, number of sub-conductors, bundle spacing, etc.), types of tower (single circuit or double circuit, dimensions of tower head, clearance distance of conductors and ground wires, etc.) and other parameters (average height of conductors and ground wires, resistivity of soil, etc.).

The single circuit of 1000 kV line adopts mainly two types of towers, that is, cup-type tower with three phases configured horizontally, and cat head tower with triangular arrangement. Umbrella-type tower with three phases configured vertically is adopted for double circuits. The typical structural dimensions of tower head are as shown in Fig. 27.13.

27.7.3.3 Unbalance Factor Analysis of the Line Without Transposition

The unbalance factor of power transmission line increases with the increase of the line length. This is because the unbalanced capacitance and current increases with the increase of the line length.

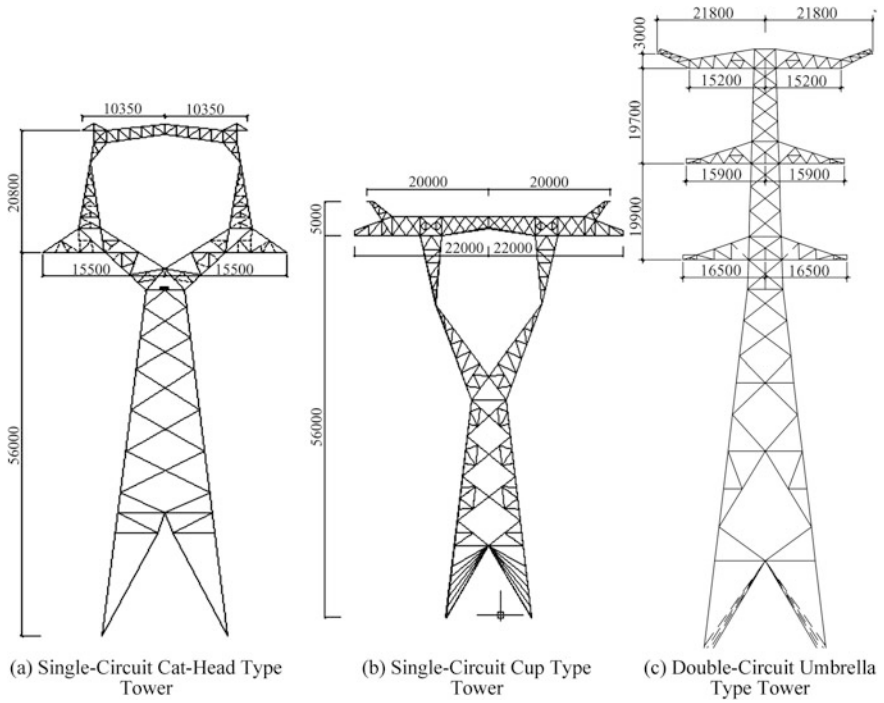

Fig. 27.13 Typical structural dimensions of 1000 kV single-circuit and double-circuit tower heads (mm)

1. Unbalance factor of single circuit

The calculation indicates that the way of conductor arrangement in the single circuit has a big impact on the unbalance factor of line. The unbalance factor of three-phase conductors configured horizontally is around two times of that configured triangularly. Under normal circumstances, the unbalance factor of single-circuit 1000 kV line configured horizontally exceeds 2% when it length reaches 130 km.

2. Unbalance factor of double circuits

Under the same conditions, the double-circuit power transmission line on the same tower has maximum unbalance factor under the operating mode of same phase sequence. The line configured out of phase sequence has medium unbalance factor, and the line with the reverse phase sequence has minimum unbalance factor. The line configured in same phase sequence requires transposition when exceeding 100 km. The line configured out of phase sequence requires transposition when exceeding 160 km. The line configured in the reverse phase sequence requires transposition when exceeding 300 km.

This is because the electric field will couple with the magnetic field in the double-circuit line on the same tower, the two circuits will interfere with each other, under the operating mode of same phase sequence, the interference between the two circuits will be enhanced, consequently causing the unbalance factor to increase, but, under the arrangement pattern in the reverse phase sequence and out of phase sequence, the interference between two circuits will be weakened each other, so the double-circuit line has smaller unbalance factor.

In the actual project, the combination of tower types with conductors in different arrangement patterns is normally adopted according to many factors, like the landforms of the project, corridor of lines, lightning arresting etc., and therefore, calculation needs to be carried out depending upon the concrete projects for determining whether transposition is required or not, and recommending the reasonable length of transposition.

27.7.4 Selection of Transposition Ways

The transposition ways of conductors mainly include two ways, i.e., straight line transposition and strain transposition.

In the straight line transposition tower, since the arrangement pattern of conductors is changed at the transposition point, this will cause the suspension insulator strings of conductors of transposition tower to have offsets. For the UHV line, since the insulator strings are longer, the offsets of insulator strings will have impacts on the straight line transposition tower, and have more impacts on the clearance of conductors. In addition, during the transposition of conductors, since the straight line tower will have the problem of conductor crossover, and can easily cause phase-to-phase discharge under the cases that the conductors are covered by ice unevenly, and removed unevenly. Therefore, transposition of the straight line tower has many restrictive operating conditions. Under normal circumstances, it is not recommended that the way of straight line transposition be adopted for single-circuit UHVAC line.

The strain transposition is to have the crossover point of phase conductor transposition controlled on the strain transposition tower. For one strain transposition tower, one crossing of the two-phase conductors can be realized, or two crossings of the three-phase conductors can be realized. The commonly used strain transposition types include strain tower transposition type with small framework, self-support strain transposition, and split-phase transposition (Figs. 27.14 and 27.15).

In the transposition of strain tower, the clearance between towers can be easily met and the performance is also reliable when the transposition by strain tower with small framework is used, but it can be restricted by the landforms in mountainous areas. However, the self-support strain transposition tower will not be restricted by landforms, and can utilize its intersecting point, that is, it does not only ensure the operating conditions of angle tower, but also gives consideration to transposition.

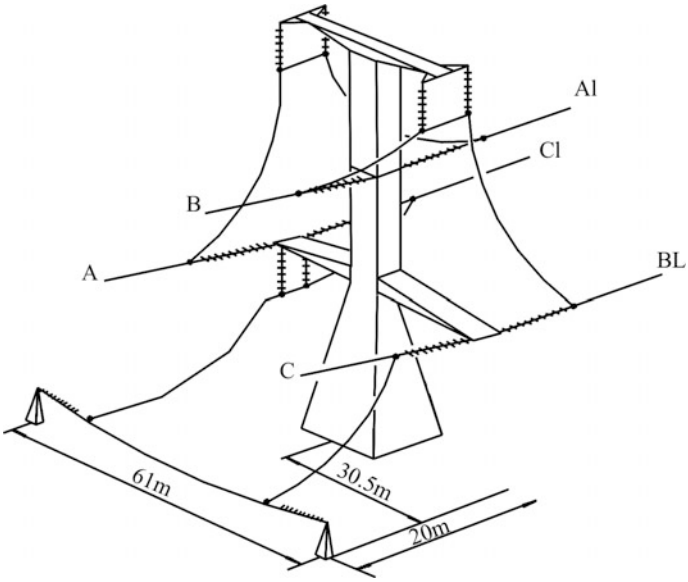

Fig. 27.14 Sketch of strain transposition tower with small framework

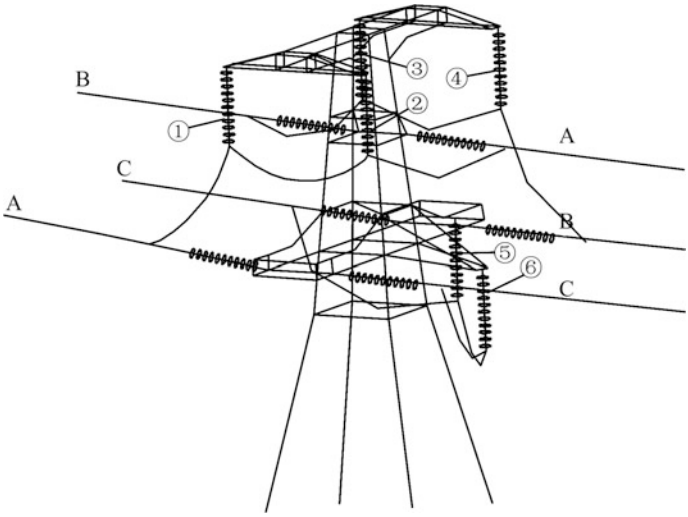

Fig. 27.15 Sketch of self-support strain transposition tower

However, since there are many conductors jumping on the body of tower, increasing the calculation difficulties of conductor clearances and construction difficulties. Therefore, under normal circumstances, it is recommended that the

strain transposition towers with small framework be used in the plain and hill zones, and self-support strain transposition towers to be used in the mountainous areas.

27.8 Tower Design for UHV Transmission Line

Towers are the structures to support the conductors and ground wires of overhead power transmission lines and make the distance among them and the distance between them and the ground meet the electrical insulation safety and electromagnetic environment limits under various possible atmospheric environmental conditions. Based on the different functions and applications, the towers can be classified as straight line tower, angle tower, terminal tower, transposition tower, and crossover tower.

The cost of tower covers about 30–50% of the investment in the UHV power transmission line, and therefore, in the UHV lines, the determination of the structure of towers, load planning, sizes of towers, operating spans, and height of towers is of vital importance to control the project investment in the UHV power transmission lines.

27.8.1 Types and Characteristics of Tower

In the UHV lines, selection of tower types shall, first of all, meet the requirements of large power transmission, safe electrical clearances, and high reliable structures, and besides that the reasonableness of technical economy of tower structures is taken into account, comprehensive considerations shall also be given to many factors, like resources along the corridors of lines, cleaning of access, impacts of space layout of conductors on the external electromagnetic environment, lightning protection, wind swing prevention, anti-pollution flashover, anti-icing flashover, anti-theft, etc., of the lines as well as the procurement, fabrication, construction installation of tower materials, and the operation and maintenance of towers after completion so on and so forth.

At present, the types of towers in the UHV lines include mainly two types, i.e., single circuit and double circuit. As the construction of UHV lines goes in-depth step by step into the eastern China coastal areas where economy is highly developed, but the resources along the corridors are scarce, such case that erection condition of multiple circuits on the same towers shared by UHV lines and EHV lines will occur, for example, the scheme for the construction of 4-circuit on the same tower shared by 1000 and 500 kV will be studied for Huainan-Nanjing-Shanghai UHVAC transmission line.

27.8.1.1 Type of Single-Circuit Tower

On the outline structure, the single-circuit straight line tower is generally classified into two types. The first type is guyed tower, which includes mainly guyed V tower, guyed portal tower, guyed cat tower, etc. The second type is self-supporting tower, for which the cup-type tower with three-phase conductors configured horizontally, and the cat head tower with three-phase conductors configured triangularly are normally adopted [1]. The single-circuit strain angle tower is basically of "干"-shaped tower configured triangularly mainly.

The structure of guyed tower is simple and single tower consumes less material, so the project cost is lower. However, the land occupation of guyed tower is large, which is easily restricted no matter in mountainous areas or in plain areas, and therefore, such tower is seldom used generally in the UHV power transmission line projects in China.

The widely used single-circuit tower type mainly includes cup-type tower and cat head tower (as shown in Fig. 27.16). These two types of towers have their own advantages and disadvantages. The three-phase conductors of cup-type tower are configured horizontally, the length of its cross arms is longer than that of cat head tower, and therefore, the corridor covered by the lines is wider. The three-phase conductors of cat head tower are configured triangularly, and its intermediate phase conductors need to be raised by nearly 20 m in height, leading to load increase of tower, thus the weight of tower is heavier about 5–10% than that of the tower configured horizontally. Therefore, selection of either cup-type tower or cat head tower shall be based on the concrete situation of the project. Generally speaking, in order to reduce the project cost, for the lines located in the mountainous areas that do not require strict corridors, and that do not require much relocation, it is better to adopt cup-type tower; for the lines located in the plain and hill areas that have

(a) Cup-type Straight Line Tower (b) Cat-head Type Straight Line Tower

Fig. 27.16 Middle route UHV 1000 kV single-circuit power transmission line already completed and put into operation

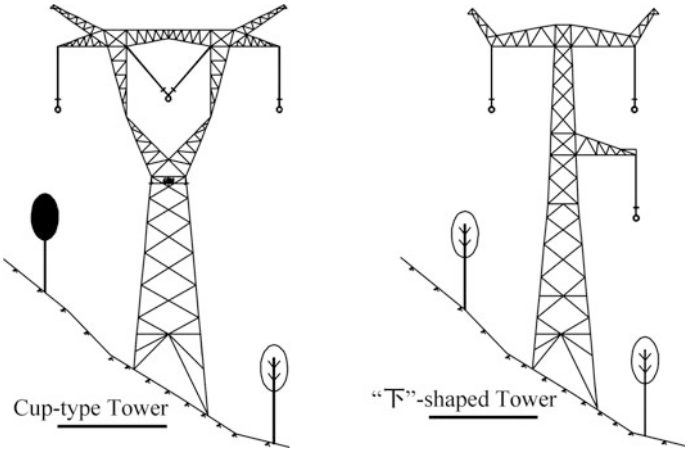

Fig. 27.17 Comparison between cup-type tower and "下"-shaped tower

relatively crowded corridors, and that require much relocation, it is better to adopt cat head tower.

By taking such factors into consideration comprehensively as impact of the line corridor width on the relocation of residence, indexes of tower materials, etc., for the single-circuit cup-type tower and cat head tower recommended in the engineering design, V-type strings are normally adopted for intermediate phase, and I-type strings for side phase in the layout pattern of the suspension insulator strings.

Considering that the lines in the mountainous areas where will pass through the areas with big slopes, the operating height of towers can be easily controlled by the distance of conductors at upward slope side to the ground, while the distance of conductors at downward slope side to ground is high, which is susceptible to lightning shielding failure, so consideration may be given to adopt the new type of side slope straight line tower of "下"-shaped, and as compared to the cup-type tower, this can decrease the height of conductors at downward slope side to the ground, and hence reduce the probability of lightning shielding failure. Such type of tower has been applied in part of sections of the North Zhejiang–Fuzhou UHVAC Line. The comparison between these two types is as shown in Fig. 27.17.

For the single-circuit strain angle tower, "干"-shaped tower is adopted in most cases. Such tower has simple structures and clear load-carrying capability, the line corridor covered by it is also narrow, and moreover, the construction installation and maintenance are also convenient. Such tower is extensively used in the lines of various voltage levels in China and other countries, from which rich operating experience has been accumulated.

27.8.1.2 Type of Double-Circuit Tower

The shape of 1000 kV double-circuit tower head can be classified as vertically configured type and triangularly configured type based on the arrangement of circuits as shown in Fig. 27.18. As compared to that configured vertically, adoption of triangular arrangement can decrease the height of tower by around 20 m, but the width of corridor will need to be increased by around 40 m. The preliminary estimates indicate that regardless of economic benefit indexes, social benefit, environmental benefit, etc., the triangular arrangement does not have any advantages, and therefore, it is normally not recommended in the projects.

The type of tower, for which three-phase conductors are configured vertically at present, includes mainly drum type (intermediate phase has the longest cross arm) and umbrella type (bottom phase has the longest cross arm), which can both meet the operating requirements of I-type suspension insulator strings and V-type strings. The I-type insulator string has the advantages of simple structures, convenient construction and operation, and moreover, the straight line tower has short length of cross arms. The V-type insulator string has a function of inhibiting windage yaw of conductors, its width of corridor is smaller than that of straight line tower of I-type string, so it can reduce relocation of residence, cutting of trees, etc., but the cross arm of its conductors is long, the spacing between tower layers will increase, and therefore, the unit weight of tower is heavier. For the 1000 kV UHV power transmission line, when V-type insulator string is adopted, the phase-to-phase distance of double-circuit line is reduced, the line corridor is compressed, but, in order to meet the requirements of electromagnetic environment, such as radio interference, audible noise, etc., it needs to be replaced with the conductors with large sections, or the distance between the conductors needs to be increased, and the distance to the ground needs to be increased, but under such circumstance, the overall investment in the project will be increased a lot. What type needs to be

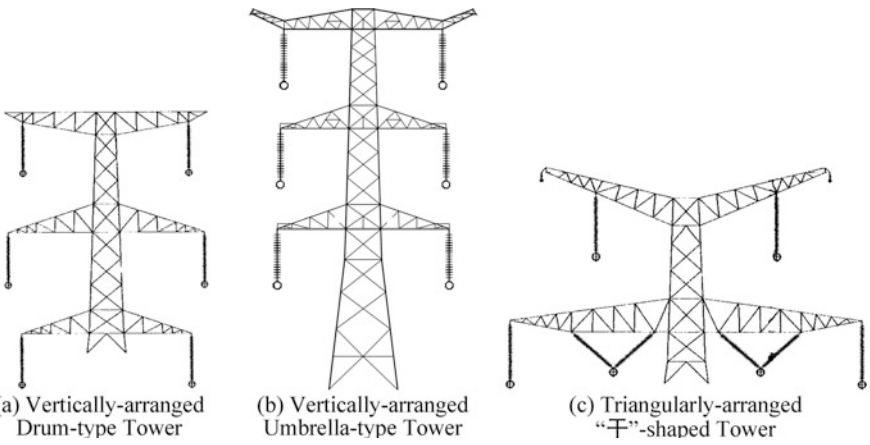

Fig. 27.18 Arrangement of double-circuit tower heads

adopted shall be determined through comprehensive technical and economy comparison based on the area where the project is located. In the 1000 kV UHVAC power transmission line projects from Anhui to eastern China, and from North Zhejiang to Fuzhou, the umbrella-type straight line towers configured vertically are adopted in the double circuits, and the insulator strings of conductors are of I-type strings.

27.8.1.3 Characteristics of Tower Structure

The structure of UHV tower is a latticed composite consisting of geometries. The essential elements to build up the geometries are structural members. The purpose of optimizing the tower structure design is to make full use of structural members on a basis of meeting the requirement of strength, stability, and deformation through selection of the reasonable layout scheme of structural members so that the tower structure can meet the requirements of nice appearance, balanced load-carrying capability, and economic cost.

According to the load-carrying capability characteristics of UHV line tower, the double-circuit tower is normally designed as per steel-tube tower, and the single-circuit tower is normally designed as per angle-steel tower. With the application of big-size angle steel (limb width 220 and 250 mm, or even 300 mm), the double-circuit tower can also be designed as per angle-steel tower; however, as compared to steel-tube tower, the weight of tower is normally heavier than steel-tube tower by 30% or above, and therefore, economic efficiency needs to be further optimized. The primary members and bracing members of double-circuit steel-tube tower body as well as the primary members of cross arms are normally of steel tubes, and for the rest of bracing members and auxiliary materials, angle steels or steel tubes may be used according to the reasonableness of structure arrangement.

When steel tubes are used in the double-circuit tower, the welding work load will be increased greatly. Adoption of the steel-tube tower structure shall take full consideration of the current status in China in the materials supply, manufacturing capacity, fabricating process, etc., and the advanced design concepts and mature structure types of steel-tube towers from other countries shall also be absorbed.

The beam-bar model is used to do calculations in the design of steel-tube tower, that is, set up models by using primary members as beam units and bracing members and other member bars as bar units. If bar system model is used to carry out the steel-tube tower design, 10–15% design margin shall be reserved for primary members in order to reflect the impact of bending moment of rod end on the strength of primary members.

The bar system model is used to do calculations in the design of angle-steel tower, that is, all the member bars bear the axial force only, without considering the bending moment of rod end. For the single-limb angle-steel tower (including big-size angle steel), carry out calculations and material selection according to conventional methods. For the primary members of combined angle-steel tower,

5–10% design margin is reserved in order to reflect the impact of branching limbs with uneven force on the stability of primary members.

27.8.2 Tower Loads and Combinations

In the UHV line project, the main factors that affect the tower and foundation indexes are the load applied on it. Therefore, the reasonable tower load and combination principle is of vital importance for reducing the project investment of the line, and ensuring the long-term safe and stable operation of the line.

27.8.2.1 Importance Factor of Structure and Load Recurrence Interval

Relative to 500 kV power transmission line, the transmission capacity of UHV line is increased by several times, and its impact on the safe and stable operation of the whole electric power grid has also been increased significantly. As a direct supporting structure of the power transmission line, the safety and reliability of tower structure are directly related to the safety of whole line. By taking into account the importance of UHV line, the recurrence interval of design load of the line is considered as 100 years, the safety class of tower structure is considered as class 1, and the importance factor of structures is considered as 1.1.

27.8.2.2 Tower Loads

The loads to be borne by the tower are normally split into horizontal load, longitudinal load, and vertical load. The horizontal load refers to the load along the cross arm direction, which comes from mainly the wind load of conductors and ground wires, wind load of tower body as well as the component of line tension in the direction of cross arms. The longitudinal load refers to the load perpendicular to the direction of cross arms, which is mainly the unbalanced tension of conductors and ground wires. The vertical load refers to the load perpendicular to the ground floor, which is mainly the dead weight of line and tower structure.

The magnitude of wind load is related to wind pressure, height variation factor of wind pressure, coefficient of structural shape, adjustment factor of wind load, and wind shield area. The calculation method for wind load specified in the code of power transmission line currently in effect is almost the same as that specified in the *Load Code for the Design of Building Structures*.

The longitudinal load includes the unbalanced tension of lines generated under the circumstances of pour tower, disconnection, string breakage, uneven ice covering or ice removal, uneven wind velocity of adjacent spans or asymmetry of wind direction, etc.

27.8.2.3 Load Combinations

The basic load combinations of tower are classified as five categories, namely, normal operating condition, uneven ice covering condition, disconnection condition, installation condition, and checking calculation condition. The normal operating condition mainly takes into account the three cases, namely basic wind velocity, maximum ice coverage, and minimum air temperature, which shall ensure that the line can withstand various climate loads under the design conditions during the operating period. The uneven ice coverage case refers to the lines located in the ice areas of 10 mm or above. According to different thicknesses of ice coverage, considerations shall be given to the bending moment, torsional moment, or the combined load of bending moment and torsional moment generated by all of the conductors and ground wires and under the uneven ice load, which the tower is able to withstand. Under the disconnection condition, the number of disconnections and the tension value of the disconnected wires shall be selected according to different categories of towers, number of circuits, and number of conductor splits in an aim to guarantee the longitudinal rigidity of towers. Under the installation condition, considerations shall be given to various installation cases which possibly occur, guaranteeing there is necessary strength when the tower is under the installation operation so as to ensure the safety of construction. The checking calculation condition normally refers to performing calculation checks on the cases which possibly occur, such as earthquake, rare strong wind, and rare ice coverage, so as to avoid fatal damage to the power transmission lines in case of occurrence of the above cases.

The combination factors of variable loads under various load conditions shall be taken by referring to Table 27.15.

27.8.3 Materials of Tower

27.8.3.1 Section Selection of Structural Members

For the section selection of tower structural members, there are mainly angle steels and steel tubes. In the 1000 kV transmission line, the maximum internal force of member bars of the single-circuit tower is around 5000 kN, the maximum internal force of member bars of double-circuit tower is around 14,000 kN, and the angle steels can meet the requirements of single-circuit tower. For the double-circuit

Table 27.15 Combination factors of variable loads

Normal operating condition	Disconnection condition	Installation condition	Uneven ice coverage condition	Checking calculation condition
1.0	0.9	0.9	0.9	0.75

Table 27.16 Advantages and disadvantages of angle-steel self-supporting tower and steel-tube self-supporting tower

Type of tower	Angle-steel self-supporting tower	Steel-tube self-supporting tower
Main advantages and disadvantages	1. Light weight of single piece, convenient fabrication, transportation and installation	Heavy weight of single piece, difficult fabrication, transportation and installation
	2. Full bolted structure, small welding work load, short fabrication period	Flange connection, big welding work load, long fabrication period
	3. Big shape coefficient, many auxiliary member bars, big wind shield area, which causes big wind load, and big steel consumption	Small shape coefficient, less auxiliary member bars, wind load is smaller than that of angle-steel self-supporting tower, steels consumption of the whole tower is smaller than that of angle-steel self-supporting tower
	4. Many connecting sections, poor overall rigidity, connection by packet angle steel, big displacement on the tower top	Less connecting sections, high overall rigidity, connection by flange disk, small displacement on the tower top
	5. Big acting force of the foundation	Wind load is smaller than that of angle-steel self-supporting tower, small acting force of foundation

crossover tower and strain angle tower with bigger load, it is more advantageous to adopt steel tubes. The section types of angle steels and steel tubes each have their own advantages and disadvantages as shown in Table 27.16.

As compared to steel-tube self-supporting tower, the angle-steel self-supporting tower has the advantages of convenient fabrication, transportation, and installation, and meanwhile, its fabrication period is also short; its disadvantage is large steel consumption. The steel consumption of angle-steel self-supporting tower is large, but the unit price is low, while the steel consumption of steel-tube self-supporting tower is small, but the unit price is high, so the overall costs of both are almost the same.

What types of sections are to be selected shall be determined in conjunction with the concrete situation of project, comprehensive considerations shall be given to the size of load as well as the construction transportation conditions, and on the premise that safety and reliability are ensured, economic efficiency and feasibility shall be taken into account.

27.8.3.2 Selection of Materials

In the design and fabrication of towers of power transmission lines in China, the two steels Q235 and Q345 are almost adopted for long term, and their yield strengths are 235 and 345 MPa, respectively, which depend upon the developing characteristics of steels in China. Steels Q235 and Q345 have the advantages of

good strength stability and lower dispersion, and their disadvantages are that the yield strengths are lower. As compared to the countries overseas that have developed power transmission lines, the materials of steels used in China for the tower structures of power transmission lines are sole, strength values are slightly low, and selectivity of materials is small, consequently causing higher steel consumption of towers. As the construction of UHV line projects goes in depth, the high-strength steels Q420 and Q460 are applied in the power transmission lines of voltage levels 500 and 750 kV (it is reported in statistics that since 2006, the towers of power transmission lines have used nearly 400,000 tons of high-strength steels Q420), certain experience has been accumulated in the application of high-strength steels.

Selection of the materials shall be determined according to the mechanical property of materials and the load-carrying capability requirement of structural members. Since high-strength steel tubes Q420 and Q460 have higher strengths, when high-strength steel tubes are used as the primary members of tower structures that have bigger load-carrying capability, the tower materials can be saved to some extent, so there is certain economic efficiency. In the design, high-strength steels are normally used as the primary members with smaller slenderness ratio, and as the structural members under the control of strength. For the steel-tube towers, selection of materials also needs to take the welding property of materials into account.

27.8.3.3 Application of Big-Size High-Strength Angle Steel

With the rapid development of power grid projects construction, the external load on the towers in the UHV multiple-circuit power transmission line projects is becoming bigger and bigger. The commonly used materials and sizes in the previous projects are still very difficult to meet the requirement of bearing capacity. The size of conventional angles is normally limited to $\angle 200 \times 24$ or below. For the towers with large load, the composite angle-steel members with double splicing and four splicing are used in most cases.

Eight-bundled conductors with big sections are used in the single circuits of UHV lines with the characteristics of large load, big dimensions of tower heads, and high tower height. The load of primary members of angle-steel towers is increased significantly, and bearing capacity requirement can only be met by using big-size angle steels or conventional composite angle steels (double splicing or four splicing). Use of the big-size high-strength angle steels can change the unreasonable section types of composite angle steels, reduce significantly the fabrication load and welding work load of double-spliced and four-spliced towers, and decrease the steel consumption indexes of towers so as to mitigate significantly the construction load and construction difficulties during erection of towers for helping the control of the costs. The use of big-size high-strength angle-steel tower can achieve stronger re-distribution capability of internal force, which will make the whole tower have better overload capability.

The bearing capacity analysis of big-size angle steels indicates that a single big-size angle steel can substitute most of the double-spliced composite angle steel

members with ordinary sizes. The big double-spliced composite angle-steel members can substitute most of the four-spliced composite angle-steel members with ordinary sizes. With equivalent area, the critical calculated length of a single big-size angle steel is smaller than that of double-spliced angle steels with ordinary sizes, and the critical slenderness ratio of double-spliced big-size angle steels is bigger than that of four-spliced angle steels with ordinary sizes [5].

In the design, use of big-size angle steels in the towers of UHV lines can reduce the weight of towers. In addition, the quantity of filler plates and bolts for big-size angle-steel towers can be reduced significantly, thus saving the costs of fabrication and assembly, which will play an active role of controlling the composite costs of towers.

27.8.4 Optimization Design of Tower Structure

The following main principles shall be abided by in the optimization design of tower structures: ① The premise is ensuring the strength, stability, rigidity, safe, and reliable operation of towers. ② Layout of the structural members is reasonable, types of structures are simple, and the force transmission route is direct, short, and clear. ③ Reduce the steel consumption of towers so as to have an economic and reasonable cost of towers. ④ Consider both the material saving property and environmental-friendly design of towers, decrease the construction difficulties of towers, and enhance maintainability of towers during operation.

On such basis, in the structure design of towers, optimization shall be normally carried out in terms of layout of tower heads, slope of tower body, layout of panel and web primary members, section shape of tower body, layout of diaphragms, design of nodes, design of long and short legs, etc.

27.8.4.1 Layout of Tower Head

On the basis of the requirement of electrical clearances being met, optimization shall be carried out in the layout of tower heads. This will not only make the tower shape more nice-looking, but also it is of vital importance for decreasing the weight of towers. In the design, the structure of tower heads shall be made compacted as far as possible, the force transmission of primary members is simple, the load-carrying capability of nodes is reliable, and the shape is nice-looking.

27.8.4.2 Layout of Tower Body

Selection of the slopes and foot distances of tower body has bigger impacts on the weight of towers, which directly affects the sizes of primary members and bracing members of tower body as well as the acting force of foundations.

In the design of towers, multiple proposals shall be combined and optimized in terms of the slopes and foot distances of tower body under the given load condition. Through comparing the calculated weights of various composite towers as well as their acting force of foundations, the best slopes of towers shall be optimized provided that sufficient strength and rigidity of towers are ensured.

27.8.4.3 Layout of Primary Member Panels and Web Members

The layout of web members of tower body and the adjustment of panels of tower body shall be taken into account at the same time. In the design, a reasonable calculation length of primary member can be determined first to make the strength and stability of primary member reach the optimum force state. On such basis, the panel length of primary member shall be determined, and the layout of web members of the tower body shall be carried out, and then the panel of tower body shall be optimized reasonably based on the layout of web members of tower body, so as to get the optimum layout of primary member panels and web members in the end.

The selection of the sizes of the structural members is not only related to the internal force to be borne by the structural members, but also related to the length of structural members. Provided that the internal force is not changed (after the slopes of tower body are determined), the sizes are in direct proportion to the length of structural members. Only after the calculation length of the primary member is determined reasonably can the panels of the primary member be laid properly.

The following main principles shall be abided by in the layout of web members: ① The load of primary members and bracing members shall be distributed reasonably. Material layout on the tower body shall be even and coordinative. The force transmission routes shall be clear, and structure layout shall be simple. ② The horizontal angles of web members shall be brought under control reasonably so that the web members can have even load-carrying capability. ③ The lengths and slopes of bracing members shall be optimized, big and small crosses shall be screened, and multiple layout proposals for parallel axles and smallest axles, etc., shall be compared so as to decrease the weight of towers. ④ By optimizing the quantity of crossover web members at the diaphragms of tower body, and by providing K-type web members at the diaphragms and other forms, prevent the web members from being applied with force at the same time.

27.8.4.4 Section Shape of Tower Body

According to the ratio of transverse horizontal load to longitudinal horizontal load, the section shapes of straight line towers normally include rectangle and square. The tower body with rectangular sections has smaller wind load. When the longitudinal load is small, the rectangular cross towers with big foot distance at front side and small foot distance at side face shall be used, thus the weight of towers can

be relatively smaller. The overall rigidity of square towers is better than that of rectangle towers, and in particular, under the condition of big span load, the longitudinal rigidity of rectangular towers looks weak. For omni-bearing towers, the connection of the long/short legs of square towers with the tower body is simpler than that of rectangular towers, both the fabrication and construction are convenient.

27.8.4.5 Layout of Diaphragm

In the design of towers, diaphragms are normally provided, and diaphragms must be of geometric invariable bodies. Generally speaking, diaphragms shall be provided at the sections where the slopes of tower body change, and where the twisting force is directly applied, and at the sections of tower top and tower leg top. Moreover, in the same slope scope of tower body, the distance of diaphragms to be provided is normally not greater than 5 times of the average width, and furthermore, it is better not greater than 4 primary member sections [6]. Through experience accumulation and unceasing optimization in the previous projects, many types of diaphragms have become the typical diaphragm types. Several commonly used diaphragm types are given in the figure below, as shown in Fig. 27.19.

In the layout of tower structures, diaphragms shall be provided reasonably so as to prevent the force transmission being disordered. The geometric shapes of diaphragms shall take into account comprehensively the dimensions of sections and the magnitude of loads. When the sections of the heads or bodies of steel-tube towers or angle-steel towers are small, types (a), (b), (c), and (d) are mainly adopted. For the portions with bigger section dimensions of tower body (for example, top surface of tower legs), types (e), (f), and (g) are mainly adopted. For the bigger diaphragms, the calculation length of structural members shall be

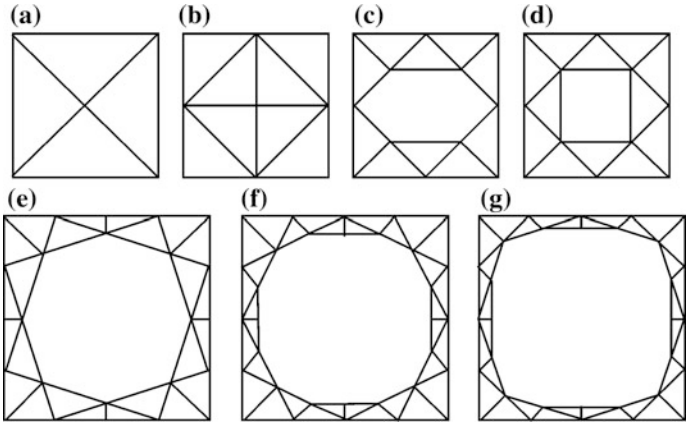

Fig. 27.19 Types of diaphragms commonly used in towers

reduced as far as possible in the layout so as to reduce the sizes of structural members and decrease the weight of diaphragms.

27.8.4.6 Node Design

The nodes shall be designed in such a way to have compacted connection and sufficient rigidity, and meanwhile, provided that the structure requirements are met, the node design shall be simplified as far as possible in order to avoid the occurrence of secondary stress and decrease the weight of towers.

Node design is an important work in the design of steel-tube towers, which is a part requiring highest welding work load in the fabrication of towers, and a major link for controlling the fabrication efficiency. Tubular joints are used in the traditional steel-tube towers, which require much welding work load. In the design of power transmission line project from Anhui to eastern China, lots of flashboards are used for connection (it is better to use cross-shaped flashboards for connecting the primary members of cross arms of steel-tube towers with its tower body), which has decreased significantly the welding work load, avoided cutting of intersecting lines, and improved the fabrication efficiency. Adoption of standardized design of flashboards can also save a great deal of tube heads design. This has improved the design efficiency and quality, and also made the batch production become possible, which is beneficial for quality control of the project.

27.8.4.7 Configuration of Long/Short Legs

Construction of the UHV line project has put forward higher requirements for environmental protection and conservation of water and soil. The lines located in the hilly landforms require a configuration mode of installing long/short legs of towers + foundations with high/low heights, and the landforms can be utilized as far as possible in order to minimize the excavation of basal plane. In combination with the impact of long/short legs on the weight of towers, from an economic perspective, the average value of maximum slopes of landforms for the tower positions along the project needs to be determined based on statistic. The control differential of long/short legs of towers shall be controlled based on the consistency of diagonal lines with the average of maximum landform slopes. In general, according to the towers with different nominal heights, the maximum differential of long/short legs is planned as 6.0–15 m, the basic differential is 1.5 m, and the maximum length of legs shall be controlled within 20.0 m. For some tower where the landform slopes are steeper, on one hand, the foundations with high/low heights are used to regulate; on the another hand, checking of calculations is carried out according to the operating conditions of towers, and the application range of the differentials for long/short legs shall be increased in such a way to achieve the goal of economic and environmental-friendly design.

27.8.5 Issues to Be Noticed in the Design of Tower Structure

27.8.5.1 Impact of Bending Moment of Rod End on Double-Circuit Steel-Tube Tower

For the UHV power transmission towers, due to the impacts of welding continuity, rigid connection of nodal plates, etc., the truss members suffer great built-in action at the nodes. This restricts to some extent the changes in the included angles between member bars, causing bending of the member bars, forming of bending moment at rod end, resulting in uneven partial stress at structural members and nodes, which easily causes damage to the member bars and nodes.

The calculation indicates that under the action of various conditions, the primary members below the lower cross arms of double-circuit towers have bigger bending moment, in particular, the primary members at tower legs and near to the tower legs, at the places of slope changes, at the nodes of primary members of lower cross arms, and furthermore, the maximum bending moment of most of the member bars occurs at the ends.

In the North Zhejiang–Fuzhou UHV transmission line project, a simulation analysis has been performed by using multi-scale modeling specific to the typical double-circuit steel-tube towers. The result indicates that for most of the structural members of steel-tube towers, since the stress generated by the bending moment of rod ends covers about 15% of all the stresses, the excellent plasticity property of steel tubes can be utilized fully to resist the unfavorable impacts of bending moment of rod ends. When the stress generated by the bending moment of rod ends exceeds 15%, the impact of the bending moment of rod ends shall be taken into account in order to avoid excessive developing of plasticity, and in the actual operation, consideration may be taken by reserving proper margin [7]. When the bending moment of rod ends is taken into account, the load-carrying capability of the primary members of steel-tube towers is stretch bending or press bending, and in the calculation, the impacts of axial force and bending moment on the load-carrying capability of the member bars shall be taken account at the same time.

27.8.5.2 Transportation of Steel-Tube Tower Members for the Lines Located in the Hilly Areas

According to the construction of double-circuit steel-tube towers in the hilly areas for the Transmission Line Project to Transmit Power from Anhui to Eastern China and the North Zhejiang–Fuzhou Transmission Line Project, the transportation of steel-tube tower members for the power transmission lines located in the hilly areas becomes an issue, to which critical attention shall be paid in the design.

For the tower located in the flat ground in front of the hills, trucks are used to transport the members of angle-steel towers and steel-tube towers, for which

Fig. 27.20 Tower member transportation by tracked vehicles

Fig. 27.21 Transportation of steel tubes by ropeways for the lines located in the Hilly areas

automobiles are mainly used for lifting and unloading. For the tower where the slopes of hilly landforms are less than 30°, and where the conditions for road construction are made available, roads may be constructed, and transportation can be carried out by using tracked vehicles (Fig. 27.20).

For the tower where the slopes of hilly landforms are greater than 30°, or where the conditions for road construction are not available, transportation can be carried out by using ropeways. Angle steels can be transported by using simple ropeways, while steel tubes need to be transported by using heavy ropeways (Fig. 27.21).

To facilitate the transportation and installation of tower members for the lines located in the hilly areas, in principle, the weight of unit piece of steel-tube tower members shall be controlled at not exceeding 3.5 tons, and the length shall be

controlled at not exceeding 9 m; the weight of single structural member of angle-steel tower members shall be controlled within 1 ton, and the length shall be controlled at not exceeding 12 m.

References

1. Hao Z, Yuhong Y. Discussion on several important problems of developing UHVAC transmission in China. Power Syst Technol. 2005;29(12):1–9.
2. GB50665-2011. Code for design of 1000 kV overhead transmission line; 2011.
3. GB/Z24842-2009. Overvoltage and insulation coordination of 1000 kV UHVAC transmission project; 2009.
4. GB/T24834-2009. Technical specification for fittings of 1000 kV AC overhead transmission line; 2009.
5. DL/T 5154-2012. Technical code for the design of tower and pole structures of overhead transmission line; 2012.
6. Central Southern China Electric Power Design Institute of China Power Engineering Consulting Group Corporation. Special Report on the Deepened Research of the Design of Single-Circuit Angle-Steel Tower of North Zhejiang–Fuzhou UHVAC Line Project. 2013.
7. Northeast Electric Power Design Institute of China Power Engineering Consulting Group Corporation. Special Report on the Type Optimization and Structure Design Research of the Double-Circuit Tower of North Zhejiang–Fuzhou UHVAC Line Project. 2013.

Chapter 28
Design of UHVDC Transmission Lines

Jiamiao Chen, Wenqian Qiu, Jia Tao, Yong Guo and Jianfei Chen

Currently, two voltage levels of ±800 and ±1100 kV are available in the UHVDC power transmission system in China to realize the transmission of long distance and large capacity. The bipolar single-circuit overhead lines are applied as the transmission lines. The completed UHVDC power transmission line projects which are now operating at the voltage level of ±800 kV include the Yunnan–Guangzhou project, Xiangjiaba–Shanghai project, Jinping–South Jiangsu project, South Hami–Zhengzhou project, and Xiluodu–Zhexi project, while the program of scientific research on the UHVDC power transmission of ±1100 kV voltage level has also been completed, and the engineering design and construction preparation are ongoing based on the Zhundong–East China (South Anhui) project.

The engineering design of UHVDC transmission line is same with that of UHVAC transmission line in terms of the principle for line route selection, determination of design meteorological condition, etc. This chapter will focus on the difference in selection of conductors, insulation configuration, tower and foundation design, and so on during engineering design between UHVDC transmission line and UHVAC transmission line (Fig. 28.1).

J. Chen (✉) · W. Qiu · J. Tao · Y. Guo · J. Chen
China Energy Engineering Group, Zhejiang Electric Power Design Institute Co., Ltd., Hangzhou, Zhejiang, People's Republic of China
e-mail: chenjiamiao@163.com

W. Qiu
e-mail: 839821641@qq.com

J. Tao
e-mail: tao_jia@zepdi.com

Y. Guo
e-mail: gy-guoyong@126.com

J. Chen
e-mail: 1204074960@qq.com

© Zhejiang University Press, Hangzhou and Springer-Verlag GmbH Germany 2018

H. Zhou et al. (eds.), *Ultra-high Voltage AC/DC Power Transmission*,
Advanced Topics in Science and Technology in China,
https://doi.org/10.1007/978-3-662-54575-1_28

Fig. 28.1 ±800 kV Xiangjiaba–Shanghai UHVDC transmission line

28.1 Selection of Conductors for DC Line

The conductor is one of the most important components of the power transmission line, and the erection of UHVDC line normally accounts for about 30% of the total investment of the project. The conductor selection and determination of bundle configuration, as the key process in the design of UHVDC transmission line, has a large influence on the line's transmission capacity, transmission performance, environmental problems (including electric field effect, radio interference, and audible noise), corridor width, technical and economic indicators, as well as scope of housing demolition and relocation. Meanwhile, the conductor scheme will directly affect the quantities of the towers, poles, and foundations along the transmission line, and is directly related to the construction cost of the whole transmission line project, and the technical characteristics and operation cost of the project after completion.

28.1.1 Main Principles for Conductor Selection

With regard to the conductor selection, the comprehensive analysis shall be carried out in terms of electrical properties, mechanical properties, and economy, so that the economically reasonable conductor section and bundle configuration meeting the technical requirements will be selected. The conductors shall meet the requirements on power transmission firstly and can ensure the safe and reliable

operation at the same time, meanwhile, meet the requirements on environmental protection and, being economically reasonable as well.

In terms of the electrical properties, due to the rise of voltage level, the UHVDC line has various prominent problems incurred by conductor corona, especially the environmental problems (radio interference, audible noise, etc.). Therefore, the corona effect is usually taken as the key control factor for conductor selection.

28.1.2 Conductor Section and Bundle Configuration

For the UHVDC lines, the economic current density is no longer a key factor for determining the conductor section. The conductor selection is mainly dependent on the corona conditions and the corona-derived effects, i.e., radio interference and audible noise. To determine the conductor, normally, the technical and economic comparative analysis will be carried out on the conductors with various sections selected according to the system transmission capacity, and then such key factors as conductor surface potential gradient, radio interference, and audible noise will be taken into consideration in terms of the electrical properties to ensure that the environmental impact will be controlled within the allowed range [1]. The bundle configuration of a conductor is mainly determined by the conductor's corona characteristics and the influence by the corona effect on the conductor's mechanical properties (including vibration, galloping, and icing), fittings, poles, and towers.

The large-section conductors and multi-bundled configuration are applied on the UHVDC line to solve the transmission capacity and corona problem. The schemes of the large-section conductors with at least 6-bundled configuration are applied can normally meet the requirements on electrical performance. China's UHVDC lines built at the early stage all adopted the 6-bundled conductors. With the increase in the rated transmission power, some new UHVDC lines begin to use the 8-bundled large-section conductors. For example, the ±800 kV Xilin Gol League–Taizhou UHVDC Line, with transmission power of 10,000 MW, adopts 8×1250 mm^2 conductors, and the ±1100 kV Zhundong–East China UHVDC Line, with transmission power of 12,000 MW, also adopts 8×1250 mm^2 conductors. During the engineering design, the factors such as construction investment, production and manufacturing, construction equipment, and operation cost shall also be considered in the determination of the bundle number and section of sub-conductors.

The conductor combinations applied in the UHVDC power transmission projects completed and under construction in China are shown in Table 28.1.

Table 28.1 List of conductor combinations applied in the UHVDC power transmission projects in China

S/N	Project name	Voltage level (kV)	Transmission power (MW)	Rated current (A)	Conductor model	Number of sub-conductors	Power transmission distance (km)
1	Yunnan–Guangdong	±800	5000	3125	LGJ-630/45	6	1412
2	Xiangjiaba–Shanghai	±800	6400	4000	ACSR-720/50	6	1891
3	Jinping–South Jiangsu	±800	7200	4500	JL/G3A-900/40	6	2058
4	Xiluodu–Zhexi	±800	8000	5000	JL/G3A-900/40	6	1669
5	South Hami–Zhengzhou	±800	8000	5000	JL/G3A-1000/45	6	2210
6	Jiuquan–Hunan	±800	8000	5000	JL1/G3A-1250/70	6	2387
7	Lingzhou–Shaoxing	±800	8000	5000	JL1/G3A-1250/70	6	1720
8	Shanxi–Jiangsu	±800	8000	5000	JL1/G3A-1250/70	6	1100
9	Xilin Gol League–Taizhou	±800	10,000	6250	JL1/G3A-1250/70	8	1619
10	Shanghaimiao–Shandong	±800	10,000	6250	JL1/G3A-1250/70	8	1228
11	Zhundong–East China	±1100	12,000	6000	JL1/G3A-1250/70	8	3330

28.1.3 Main Electrical Properties of Conductor

28.1.3.1 Transmission Efficiency of Conductor

The distance of the UHVDC power transmission line is very long, over 1000 km for the ±800 kV line in length and even over 3000 km for the ±1100 kV line in length. If the section of conductors is too small, the voltage drop of the transmission line will be very high, leading to the reduction in the line's transmission efficiency. It is generally considered that the line's transmission efficiency is uneconomic when lower than 93%. The ±1100 kV Zhundong–East China Line is about 3330 km in total; when the rated current reaches up to 6000 A, if the scheme of the 8×JL/G3A-900/40 or 10×JL/G2A-720/50 conductors is adopted, the voltage drop will be 83.7 and 82.5 kV, respectively, and the transmission efficiency will be 92.4 and 92.5%, respectively, both lower than 93%; when the scheme of the 8×JL1/G3A-1250/70 conductors is adopted, the voltage drop will be 59.3 kV and the transmission efficiency will be 94.6%, meeting the requirement of transmission efficiency.

28.1.3.2 Overload Temperature of Conductor

The conductor selection shall guarantee the safe operation of the UHV line when it is overloaded. According to the stipulations in GB50790-2013 *Code for Designing of* ±800 kV *DC Overhead Transmission Line* (referred to as the *Code for Designing of DC Transmission Line*), the conductor's maximum allowable current shall be considered as the current under 10% overload condition, i.e., 1.1 times the rated current. The overload temperature of conductor shall meet the requirements on the conductor's allowable temperature.

The overload temperature of the 6×JL1/G3A-1250/70 conductors applied on the ±800 kV DC line with rated transmission power of 8000 MW is 64.5 °C, and that of the 8×JL1/G3A-1250/70 conductors applied on the ±1100 kV DC line with transmission power of 12,000 MW is 58.2 °C, both lower than the ACSRs' maximum allowable temperature of 70 °C. During the calculation, the ambient temperature shall be taken as the maximum mean temperature of the month with the maximum temperature and, generally, the wind speed and solar radiation power density for the line calculation are, respectively, taken as 0.5 m/s and 1000 W/m^2.

28.1.3.3 Power Loss

The power loss of the DC line is divided into the resistance power loss and corona power loss, in which the resistance loss accounts for a major part and the corona loss is about 3.0–10.0% of the resistance loss but is not negligible due to its long time existence. The calculation results of the resistance power loss and corona

power loss of the ±800 kV DC line with transmission power of 8000 MW under different conductor schemes are shown in Table 28.2.

As shown in Table 28.2, the bigger the DC resistance of pole conductor, the larger the resistance power loss; under the same bundle configuration, the corona loss decreases with the increase in the diameter of sub-conductors; the higher the altitude, the larger the corona loss. The increase in the conductor's section and the number of sub-conductors is quite useful to reducing the line's power loss and the enhancing the energy utilization rate. However, the excessive increase in the conductor's section and the number of sub-conductors will lead to the great increase in engineering investment. Therefore, the selection must be carried out in a reasonable and appropriate manner.

28.1.3.4 Surface Electric Field Intensity of Conductor

When the surface electric field intensity of the DC line's conductor exceeds the air electrical breakdown strength, the conductor will generate partial discharge which will form the corona. The excessively high surface electric field intensity of conductor will cause complete corona of conductor. As a result, not only the corona loss will increase sharply, the impact on the electromagnetic environment will also be very severe. Therefore, the surface electric field intensity of conductor must be effectively controlled during the design of the UHVDC line.

1. Corona inception electric field intensity of conductor

It is generally considered that the corona inception electric field intensity of the conductor of the DC transmission line has the same peak value as that of the AC transmission line. The Peek Formula can be converted into the DC form

$$E_0 = 30\, m\delta\left(1 + \frac{0.301}{\sqrt{\delta r}}\right), \tag{28.1}$$

where

m the surface roughness factor of conductor. The surface roughness factor m of conductor in fine day and rainy day conditions are 0.49 and 0.38 respectively;
δ the relative air density;
r the radius of sub-conductor (cm).

The calculation results of corona inception electric field intensity of conventionally selected conductor in the DC transmission project are shown in Table 28.3.

2. Maximum surface electric field intensity of conductor

The surface electric field intensity of conductor is determined by the operating voltage, diameter of sub-conductor, number of sub-conductors, bundle spacing of sub-conductors, pole conductor height above the ground, and interpolar distance. Successive image method can be used in engineering design.

Table 28.2 Resistance and corona power losses of ±800 kV line under different conductor schemes

S/N	Conductor combination	Sub-conductor diameter (mm)	DC resistance of pole conductor (Ω/km)	Resistance power loss (kW/km)	Corona power loss (kW/km)		
					Altitude 0 m	Altitude 1000 m	Altitude 2000 m
1	6×JL1/G3A-1250/70	47.35	0.00382	102.866	5.255	5.575	5.910
2	6×JL/G3A-1000/45	42.10	0.00482	131.935	5.681	6.713	7.958
3	6×JL/G3A-900/40	39.90	0.00532	147.595	6.112	7.220	8.555
4	6×JL/G1A-800/55	38.40	0.00591	164.885	6.450	7.616	9.023
5	6×ACSR-720/50	36.20	0.00664	186.405	6.996	8.258	9.779

Table 28.3 Calculation results of conductor corona inception electric field intensity E_0 (kV/cm)

S/N	Type of conductor	Diameter (mm)	Corona inception electric field intensity E_0 (kV/cm) (Fine day/rainy day)		
			0 m altitude	1000 m altitude	2000 m altitude
1	JL1/G3A-1250/70	47.35	17.72/13.71	16.09/12.59	14.71/11.50
2	JL/G3A-1000/45	42.10	17.75/13.77	16.26/12.62	14.88/11.54
3	JL/G3A-900/40	39.90	17.81/13.81	16.32/12.66	14.94/11.58
4	JL/G1A-800/55	38.40	17.89/13.88	16.40/12.72	15.02/11.64
5	ACSR-720/50	36.20	17.99/13.95	16.50/12.79	15.10/11.71

Table 28.4 Average maximum electric field intensity on conductor surface

S/N	Conductor type and number of sub-conductors	Bundle spacing (cm)	Diameter of sub-conductor (mm)	Conductor surface maximum electric field intensity (kV/cm)	
				Height of conductor 18 m	Height of conductor 23 m
1	6×JL/G3A-1250/70	50	47.35	18.282	18.221
2	6×JL/G3A-1000/45	50	42.10	19.310	19.307
3	6×JL/G3A-900/40	45	39.90	20.386	20.102
4	6×JL/G1A-800/55	45	38.40	21.288	20.993
5	6×ACSR-720/50	45	36.20	22.299	21.991
6	8×ACSR-720/50	40	36.20	18.345	18.076

The calculation results of the average maximum surface electric field intensity of the conductors applied on the ±800 kV DC line adopting different conductor combination schemes (with interpolar distance of 20 m) are as shown in Table 28.4.

It can be inferred from Table 28.4 that the maximum surface electric field intensity under all pole conductor schemes is always greater than the corona inception electric field intensity E_0, which means that, at most of the time, the conductors are in corona condition. The number and diameter of sub-conductors have relatively large influence on the surface electric field intensity of conductor, while the interpolar distance, pole conductor height above the ground, and sub-conductor spacing have very small influence on the surface electric field intensity of conductor.

28.1.3.5 Total Electric Field Intensity and Ion Current Density

The existence of the total electric field intensity and ion current in the DC line will bring about certain influence on the production and life of the nearby residents, and the magnitude concerns the personal safety of the nearby residents. Therefore,

the total electric field intensity and ion current density must be limited within a certain range. It is stipulated in *Code for Designing of DC Transmission Line* that the limit value of the maximum ground total electric field intensity under the DC line is 30 kV/m, the limit value of the maximum total electric field intensity nearby the residential housing is 25 kV/m (in sunny days), and the limit value of the maximum ion current density is not more than 100 nA/m^2 in sunny days and not more than 80 nA/m^2 in rainy days. The total electric field intensity of the DC line is larger in rainy days than in sunny days. Therefore, the condition in rainy days must be considered in the determination of the minimum conductor height above the ground.

The analytical method is usually adopted to calculate the ground total electric field intensity. The calculated total electric field intensity and ion current density under the DC line are shown in Table 28.5.

As shown in Table 28.5, the magnitude of the space field intensity under the DC transmission line is related to such factors as the arrangement type, geometric position, and dimension of conductors in addition to the voltage applied. The electric field intensity under the transmission line can be reduced by the adjustment of the conductor height above the ground, interpolar distance, bundled conductor configuration and dimension, pole conductor arrangement type, etc. Among these methods, the proper increase in the conductor height above the ground is the most effective. The altitude has a large influence on the total electric field intensity and ion current density. According to the research, each increase of 1000 m in altitude will lead to about 4–5 kV/m increase of the total electric field intensity and about 10–26 nA/m^2 increase of the ion current density.

In addition to the above described factors, according to the electromagnetic environment full-scale test carried out by China Electric Power Research Institute (CEPRI) at the UHVDC test base in Beijing, it is found that the ground total electric field intensity is also related to the air quality and humidity. The theoretical calculation result of the ground total electric field intensity coincides with the test result obtained under good air quality and moderate humidity; when the air quality is poor and the dust adsorption on the conductor is severe, the ground total electric

Table 28.5 Calculation results of total electric field intensity and ion current density (0 m altitude, sunny day)

Voltage level (kV)	Conductor combination	Total electric field intensity (kV/m)	Ion current density (nA/m^2)	Remarks
±800	6×JL1/G3A-1250/70	17.16	14.4	Interpolar distance of 20 m and conductor height of 18 m
±800	6×JL/G3A-1000/45	18.92	23.09	
±800	6×JL/G3A-900/40	20.88	29.63	
±800	6×JL/G1A-800/55	22.73	37.28	
±1100	8×JL1/G3A-1250/70	20.60	11.84	Interpolar distance of 26 m and conductor height of 25 m
±1100	8×JL/G3A-1000/45	22.03	15.5	

field intensity will increase; in the north of China, when the conductor adsorbs the dust and the air is dry, the ground total electric field intensity will be even higher [2]. In the northern climatic area, compared to the southern climatic area, the proper increase in the conductor height above the ground can be used to eliminate the influence of the increased total electric field intensity.

28.1.3.6 Radio Interference

The radio interference of the DC line mainly results from the corona discharge by conductors, insulators or line fittings, etc., with the frequency basically being within 30 MHz. Meanwhile, the magnitude of the corona discharge will change as the weather changes, and the sunny or rainy day or even the different seasons will have significant influence on the corona discharge. The level of radio interference is lower in the bad weather than in the good weather, which is the biggest feature that differentiates the DC line from the AC line.

It is recommended in the *Code for Designing of DC Transmission line* that the empirical Eq. (28.2) should be used to calculate the radio interference (average value) of the bipolar DC line in sunny days. In addition, the requirements that "in the regions at an altitude of no more than 1000 m, at 20 m to the on-ground projection of the positive conductor on the DC overhead transmission line, the radio interference with frequency of 0.5 MHz shall not exceed 58 dB (μV/m) in 80% of the time and under confidence level of 80%" should be meet.

$$E = 38 + 1.6(g_{\max} - 24) + 46\log(r) + 5\log(n) + 33\log\frac{20}{D} + \Delta E_{\mathrm{W}} + \Delta E_{\mathrm{f}}, \tag{28.2}$$

where

E the radio interference electric field intensity at a distance of D to positive conductor; dB (μV/m);
$g_{\max}$ the maximum field intensity on conductor surface, kV/cm;
r the radius of sub-conductor, cm;
n the number of sub-conductors;
D the distance to positive conductor (applicable to $D < 100$ m), m;
ΔE_{w} the climate correction term;
ΔE_{f} the interference frequency correction term.

In the above equation, the interference value obtained through the calculation of the first five terms refers to the interference value at the reference frequency of 0.5 MHz with a distance of D to positive conductor in fine day. To obtain the interference values at other frequencies and other climate conditions, the calculation contents of the latter two terms (namely ΔE_{w} and ΔE_{f}) will be added. Of which, the climate correction term ΔE_{w} adopts 3 and −3 dB for summer and winter,

respectively, and 0 for spring and autumn. The interference frequency correction term can be calculated by the equation given below:

$$\Delta E_{\mathrm{f}} = 5[1 - 2(\log 10f)^2], \tag{28.3}$$

where

f the measuring frequency, in MHz, and the frequency range is 0.15–3.0 MHz.

For the line with an altitude of more than 1000 m, the altitude correction must be made. On the basis of 1000 m, the radio interference electric field intensity will increase by 1 dB with every increase of altitude by 300 m.

28.1.3.7 Audible Noise

The intensity of audible noise incurred by corona on conductor of the DC line is dependent on the conductor's geometric characteristic, operating voltage, height above the ground, and weather condition, and must be considered together with the radio interference. Besides, the intensity of audible noise controls the conductor selection under many circumstances [1]. Unlike the electric field, magnetic field, and radio interference, the audible noise is a kind of phenomenon that can be directly felt through hearing and thus is more easier to become the focused problem to be complained. The limits on the audible noise incurred by the DC line must be kept consistent with the local limits on environmental noise.

The audible noise incurred by the DC transmission line is a little lower in the rainy days than in the sunny days. Therefore, the audible noise in the sunny days is the condition to be firstly considered during the design of the DC line [3]. Two equations for the calculation of the audible noise are recommended in the *Code for Designing of DC Transmission line*, and the Eq. (28.4) is mostly applied to the engineering. The limits on the audible noise shall meet the requirements that "in the regions at an altitude of no more than 1000 m, at 20 m to the on-ground projection of the positive conductor on the DC overhead transmission line, the audible noise incurred by corona shall not exceed 45 dB (A) and shall be controlled below 50 dB (A) in the sparsely populated regions at a high altitude."

$$P_{\mathrm{dB}} = 56.9 + 124\log\frac{g_{\max}}{25} + 25\log\frac{d}{4.45} + 18\log\frac{n}{2} - 10\log R_{\mathrm{p}} - 0.02R_{\mathrm{p}} + K_n, \tag{28.4}$$

where

P_{dB} the audible noise of transmission line, dB(A);
$g_{\max}$ the maximum field intensity of conductor surface, kV/cm;
d the diameter of sub-conductor, cm; n is the number of sub-conductors;
R_{p} the distance to positive conductor, m;

K_n the correction term, when $n \geq 3$, $K_n = 0$; when $n = 2$, $K_n = 2.6$, when $n = 1$, $K_n = 7.5$.

For the line at an altitude of more than 1000 m, the altitude correction must be made. On the basis of 1000 m, the audible noise will increase by 1 dB with every increase of altitude by 300 m.

The audible noise incurred by the DC line gradually decreases as the interpolar distance increases, with average variation gradient about −0.60 dB/m. The audible noise reduces with the increase of average height of conductor, with the average variation gradient of about −0.2 dB/m. Therefore, measures of increasing interpolar distance and average height of conductors can be taken to reduce the audible noise.

28.1.4 Selection of Ground Wire Types

With regard to the UHVDC line, as the induced charge on the ground wire is large, it is possible to produce very high surface electric field intensity on the ground wire. When the surface electric field intensity exceeds the corona inception electric field intensity, the ground wire will produce the corona loss, radio interference, audible noise, etc. Therefore, in addition to meeting the requirements on the short-circuit current thermal capacity, the ground wire (including the optical fiber composite overhead ground wire) shall also be verified based on the corona inception condition, which mainly depends on the diameter of the ground wire [1]. Generally, the ratio of the ground wire's maximum surface electric field intensity to the corona inception electric field intensity shall not be more than 0.8, and the ground wire's surface electric field intensity shall be not more than 18 kV/cm.

In consideration of the advantages such as high mechanical strength and good anti-corrosion performance, the aluminum clad steel wires are generally used as the ground wire of the DC lines.

To meet the above requirements, the aluminum clad steel with section of 150 mm^2 and above are used as the ground wire of the ±800 kV DC lines and those with section of 240 mm^2 and above are used as the ground wire of the ±1100 kV DC lines.

28.2 Insulation Coordination Design of DC Line

The differences between the DC and AC insulation coordination design are mainly reflected in two aspects: on one hand, under the same pollution condition, the pollution flashover voltage of the insulator in the DC system is lower than 15–20% of that in the AC system, and on the other hand, due to the influence of the unidirectional electric field, the contamination on the surface of the DC insulator is far more than that of the AC insulator, being one time more on average [2].

The main content of insulation coordination design is to determine the classification of polluted areas and the degree of pollution along the transmission line of the project by the pollution investigation, select suitable insulator types, and determine the number of insulator and the air clearance in the insulator string so that the transmission line can operate safely and reliably under various conditions of operating voltage, operating overvoltage, and lightning overvoltage. Scientific and rational insulation configuration can save project investment and reduce pollution flashover accident rate.

28.2.1 Pollution Investigation and Polluted Area Classification

The accurate classification of pollution degree along the whole transmission line and the determination of the scope of all levels of polluted area by the pollution investigation along the line is an important premise of the rational insulation configuration of DC line.

The main principles and basis for classification of polluted areas along the DC transmission line are as follows:

(1) "Pollution measurement and investigation report along the transmission line" presented by scientific research and test institute is the important basis for polluted area classification.
(2) According to latest polluted area distribution map of electric power system in each province along the transmission line of the project, polluted area classification can be carried out by giving full consideration to atmospheric conditions and the development trend of environmental pollution and taking field investigation into account. Determination of the pollution degree of polluted areas should be proactive.
(3) Polluted areas and the degree of pollution of each area should be determined according to three elements of "operation experience, wet pollution features and site equivalent salt deposit density" based on the field investigation. When the three elements are not consistent, the operation experience shall prevail.
(4) For areas having neither operation experience nor salt deposit density measurement values, the pollution degrees along the transmission line can be determined in accordance with the latest polluted area distribution map of each province and by taking pollution accumulation ratio of DC transmission line to AC transmission line into account.

According to the design practice of DC transmission line in China, pollution is generally classified as lightly polluted area, moderately polluted area, and severely polluted area with equivalent salt deposit density taken as 0.05, 0.08, and 0.15 mg/cm^2, respectively.

28.2.2 Insulator Types

The insulator string length of the DC line is mainly determined by the pollution flashover characteristics of the whole insulators under operating voltage. At present, in the tens of operating HVDC transmission lines, ceramic insulators, toughened glass insulators, and composite insulators are all used, of which, most frequently used are toughened glass insulators and ceramic insulators. In recent years, the composite insulators began to be widely used in the engineering.

28.2.2.1 Characteristics of Various Insulators

1. Ceramic and glass disc insulators

Disc-shaped insulators include bell type, dual-umbrella type and tri-umbrella type depending on different umbrella constructures, as shown in Fig. 28.2. The dual-umbrella-type and tri-umbrella-type insulators are relatively suitable for inland industrially polluted area and dust polluted area. Taking the tri-umbrella-type insulators as an example, though its pollution withstand voltage is 5% lower than the bell-type insulators, its model has a better aerodynamic characteristic. Its pollutant deposit in moderately and severely polluted areas can be about 1/3 lower than the bell-type insulators. The characteristic parameters of typical disc-shaped suspension insulators used in the DC transmission lines are shown in Table 28.6.

The tension insulator strings on the conductors of the UHVDC line mainly adopt the disc porcelain or glass insulators. With the continuous improvement of the materials and manufacturing process, the large-tonnage DC insulators with strength levels of 760 and 840 kN have begun to be applied in the engineering.

2. Bar-type composite insulators

With the continuous aggravation of pollution degree of the environment along the transmission line, the composite insulators having excellent pollution withstand performance are widely used on the transmission lines with various voltage levels. The composite insulators can withstand very high breakdown voltage and belongs to the non-breakdown insulators, but the core bar may be subject to "brittle fracture." The composite insulator has a higher power-frequency flashover voltage than the porcelain and glass insulators, but a little lower 50% lightning impulse flashover voltage than the disc insulator string. The relevant test has shown that the 50% pollution flashover voltage of the DC composite insulator has a linear relationship with the insulator's structural height, i.e., the 50% pollution flashover voltage will proportionally increase as the structural height increases.

In addition, the overall length of the composite insulator is long and determined by the various pollution classes and altitudes, normally around 9.6–11.8 m on the ±800 kV line and around 12.3–16.6 m on the ±1100 kV line. In the UHV projects, especially when applied in the line projects in the mountainous areas,

(a) 300 kN Bell Ceramic Insulator CA-756EZ

(b) 300 kN Dual-umbrella Ceramic Insulator XZWP-300

(c) 300 kN Tri-umbrella Ceramic Insulator CA-776EZ

(d) 300 kN Bell-type Glass Insulator FC300P

Fig. 28.2 Typical outside view of disc-shaped insulators used in DC transmission lines

Table 28.6 Summary of characteristic parameters of typical disc-shaped suspension insulators used in DC transmission line

S/N	Material	Product model	Umbrella shape	Structure height (mm)	Creepage distance (mm)	Disc diameter (mm)	Rated mechanical strength (kN)
1	Electric ceramics	CA-756EZ	Bell	195	635	400	300
2		XZWP-300	Dual-umbrella	195	525	365	300
3		CA-776EZ	Tri-umbrella	195	670	400	300
4	Glass	FC300P	Bell	195	700	380	300

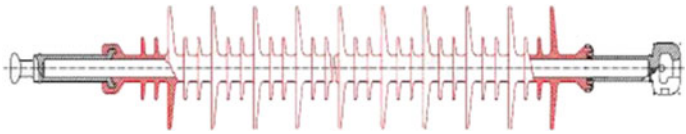

Fig. 28.3 Sketch of overall structure of UHVDC composite insulator

the increase in the structural height of the whole insulator will bring about difficulties in the processing, transportation, and installation of the composite insulators.

The composite insulators are mainly applied in the suspension insulator strings and jumper insulator strings on the UHVDC line and have outstanding technical and economic advantages when used in the seriously polluted areas. The overall structure of the typical DC composite insulator is shown in Fig. 28.3.

28.2.2.2 Comparison of Insulator String Types and Pollution Flashover Characteristics

The suspension insulator strings on the DC line mainly include the I-type string, V-type string, and Y-type string. The tension insulator string is normally of horizontal multiple string.

To study the DC pollution flashover characteristics under different string type arrangements, CEPRI carried out a large number of tests. The tests show that, under the same pollution condition, without regard to the contamination characteristics, the arrangement type of the insulator strings (I-type string, V-type string, and horizontal arrangement) has basically no influence on the pollution flashover performance. In consideration of the contamination characteristics, the contamination on the V-type insulator is about 70–80% of that on the I-type string. Therefore, the pollution flashover performance of the V-type string is better than that of the I-type string, and similar to that of the horizontally arranged string.

CEPRI also carried out test on the pollution flashover characteristics of the Y-type string. The V part of the Y-type string has 28 pcs insulators in each string

(a) Photo for Arrangement of Artificial Pollution

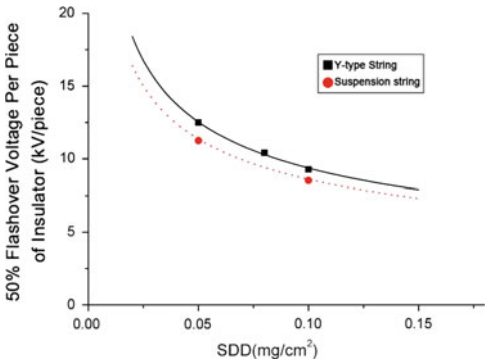

(b) Relation between Y-type String Flashover Voltage

Fig. 28.4 DC pollution flashover characteristic test of Y-type insulator string

and the I part has double 2 × 13 pcs insulators. The test object arrangement and test results are shown in Fig. 28.4.

Compared with the I-type suspension string with the same number of insulators in a single string, the difference in the flashover voltage of the Y-type string and the I-type string is within 9%. In consideration of the dispersity of the pollution flashover tests, it can be deemed that, under the same pollution and same string length, the 50% pollution flashover characteristic curves of the suspension string and the Y-type string are close to each other. It shall be noted that, for the insulators in the Y-type string, as 2/3 of the string is of V-type string arrangement, the contamination performance will be better than the insulators of the suspension I-type string. Based on the comprehensive consideration of the contamination and pollution flashover characteristics, the pollution flashover characteristic of the Y-type string is better than that of the suspension string.

Besides, the pollution flashover voltage of the double string is lower than that of the single string. In order to reduce the impact, the inter-string distance of multiple insulators shall be as large as possible. The inter-string distance is generally not shorter than 650 mm. For the transmission line in area with serious icing, the inter-string distance should be increased.

28.2.3 Selection of the Number of Insulators for the Insulator Strings

The selection of the number of insulators on DC transmission line is mainly determined by the pollution withstand voltage characteristics under operating voltage. Therefore, the number of insulators is generally selected according to the

pollution property, then checked and calculated by the switching overvoltage and lightning impulse characteristics.

Theoretically, it is relatively appropriate to select the number of insulators according to the natural contamination flashover characteristics, but this is difficult for the actual engineering. Therefore, normally, two methods are currently available for the determination of the number of insulators, which are to select the insulators according to the artificial pollution flashover characteristics (also referred to as the pollution withstand voltage method) and according to the specific leakage distance based on the operation experience (also referred to as the specific leakage distance method). The former is relatively intuitive, but the SDD value measured by the applicable and uniform measurement method must be available and, furthermore, it is also related to such factors as pollution composition and pollution uniformity ratio, and hence, in principle, it shall be adopted for the UHVDC lines [1]; the latter, which conducts calculation based on the geometric leakage distance of the insulator, is not rigorous enough in theory (without consideration of the influence on the effective leakage distance by the different insulator shapes), but is simple and easy to implement.

28.2.3.1 Linear Relationship in Insulation Design

Among the results of the DC polluted insulator tests carried out by various countries, the test by the USA shows that the pollution flashover voltage of the insulator string with no more than 80 pcs insulators is basically linear to the string length; the test by Italy shows the same linear relationship when the string length is not more than 12 m; the test by Japan shows that the linear relationship between the pollution flashover voltage and the string length still exists when the insulator string length is up to 14 m; the length of the insulator strings applied on the UHVDC lines in China is also within 10–20 m, so the linear relationship between the pollution flashover voltage of insulator string and the string length basically exists.

28.2.3.2 Selection of the Number of Insulators for the Insulator Strings Based on the Operating Voltage

As the dust absorption of constant electric field and the DC arc not easy to die out, under the identical pollution severity, the DC pollution flashover voltage of insulator is lower than the effective value of the AC pollution flashover voltage. Therefore, under the identical voltage level, the number of insulators used on the DC transmission line will be more than the number of insulators used on the AC transmission line. The insulation level is mainly determined by the DC pollution electric discharge characteristics of insulator string.

1. Select the number of insulators using pollution withstand voltage method

In the construction of the UHVDC projects, the scientific research and test organizations carried out a large number of insulator withstand voltage tests, and obtained the pollution withstand voltage values of different types of insulators under various pollution conditions. The pollutant component correction, contamination uniformity correction under different climate conditions and different types of insulators, and non-soluble deposit density (NSDD) correction are considered in the selection of the number of insulators.

According to the classification of different polluted areas, on the basis of the SDD values on the lower surface of the insulator, the calculation process of the number of insulators on ±800 kV line using the pollution withstand voltage method in the *Code for Designing of DC Transmission Line* is shown in Table 28.7.

2. Select the number of insulators using specific creepage distance method

The *Code for Designing of* ±800 kV *DC Overhead Transmission Line* has given the logarithmic fitting expression of insulator-specific creepage distance as a function of equivalent salt deposit density under conductor-to-earth voltage, as shown below:

Table 28.7 Selection of the number of insulators on ±800 kV line according to the SDD values on the lower surface of insulator

Pollution degree	Lightly polluted area	Moderately polluted area	Severely polluted area
ESDD (bottom surface) (mg/cm^2)	0.05	0.08	0.15
Top-to-bottom surface pollution deposit ratio of insulators	1:5	1:8	1:10
NSDD H_1 (mg/cm^2)	0.30	0.48	0.90
Maximum operating voltage of transmission line (kV)	816		
Withstand voltage required by insulator string $V_{\text{withstand}}$ (kV)	816/(1–3 × 0.07) = 1033		
Single piece $U_{50\%}$ (kV) provided in test (NSDD H_2 = 0.1 mg/cm^2)	15.0	12.8	10.7
NSDD correction factor $K_1 = (H_1/H_2)^{-0.12}$	0.88	0.83	0.77
After NSDD correction $U'_{50\%} = K_1 \times U_{50\%}$ (kV)	13.14	10.60	8.22
Top-to-bottom surface pollution deposit ratio correction coefficient $K_2 = 1 - 0.38\log(T/B)$	1.266	1.343	1.380
After pollution deposit ratio correction $U''_{50\%} = K_2 \times U'_{50\%}$ (kV)	16.64	14.24	11.34
Required number of insulators ($V_{\text{withstand}}/U''_{50\%}$)	62	73	91

Table 28.8 Calculated specific creepage distance required for DC transmission line

AC equivalent salt deposit density (mg/cm^2)	DC equivalent salt deposit density (mg/cm^2)	Reckoned specific creepage distance required for DC transmission line (cm/kV)
0.03	0.06	3.76
0.05	0.10	4.21
0.08	0.16	4.63
0.15	0.30	5.19

$$L = 6.2606 + 0.8891 \times \ln(\text{ESDD}), \tag{28.5}$$

where

L the required specific creepage distance, cm/kV;
ESDD the DC equivalent salt deposit density, mg/cm^2.

Test shows, under the same environmental condition in inland area, that the contaminant deposit ratio (equivalent slat deposit density) of insulator string of the DC transmission line is about 2.0 times that of the AC transmission line. The specific creepage distance of the DC transmission line calculated by using the Eq. (28.5) will meet the requirements as listed in Table 28.8.

3. Number of insulators selected for the built DC projects

For ±800 kV UHVDC transmission line, the suspension insulator strings in light and medium icing areas all use composite insulators, and the suspension strings in heavy icing area use disc-shaped insulators. No matter in light, medium, or heavy icing areas, the tension insulator strings usually use disc-shaped insulators. For selecting the number of insulators, the smaller one of the insulator number recommended by DC pollution withstand voltage method and the maximum insulator number recommended by specific DC creepage distance shall be taken.

With the areas at altitude ≤ 1000 m as an example, the insulator number of suspension insulator string selected for several ±800 kV DC lines that have been constructed or under construction is shown in Table 28.9.

28.2.3.3 Selection of the Number of Insulators for Tension Insulator Strings

Operation experience shows that, because the tension insulator string's stress is higher than the suspension insulator string's stress, and this can easily produce zero resistance insulators, the number of insulators of tension insulator strings is generally 1–2 pieces more than the number of insulators of suspension insulator strings with the same class. For horizontal arrangement of insulator strings, the pollution withstand voltage value is significantly higher than that of suspension insulator strings in the same polluted area due to relatively good self-cleaning capability.

Table 28.9 Number of insulators of suspension insulator strings (Bell V-type string)

Insulator type	Pollution degree			
	Lightly polluted area (0.5 mg/cm^2)	Moderately polluted area (0.8 mg/cm^2)	Severely polluted area (0.15 mg/cm^2)	Project
CA-745EZ (210 kN)	63	77	88	Jinping–South Jiangsu Line
CA-756EZ (300 kN)	56	70	81	Jinping–South Jiangsu Line
CA-765EZ (400 kN)	61	74	81	Jinping–South Jiangsu Line
CA-765EZ (400 kN)	65	79	86	Ningdong–Zhejiang Line in Southern Region
CA-765EZ (400 kN)	71	86	98	Ningdong–Zhejiang Line in Northern Region

In terms of economy, the number of insulators of tension insulator strings shall not be increased on the basis of that of suspension insulator strings and it is not necessary to use large creepage distance anti-pollution insulators. The tension insulator strings of EHVAC/EHVDC or UHVAC/DC transmission lines in China and other countries all use disc-shaped ceramic or glass insulators. Under the identical pollution condition and same altitudes, it is recommended that the same number of insulators be used for both tension insulator strings and suspension insulator strings and margin be reserved for insulation coordination.

Table 28.10 shows the configuration of the number of tension insulators on the ±800 kV Lingzhou–Shaoxing DC Line. The number of insulators is designed based on the differentiated design principle with the climate characteristics being taken into consideration. Table 28.11 shows the configuration of the number of tension insulators on the ±1100 kV Zhundong–East China DC Line.

28.2.3.4 Selection of Composite Insulators

The results of the pollution flashover tests carried out in China and other countries demonstrate that, under the same pollution condition and even under the hydrophilic condition, the pollution flashover voltage of the composite insulator is still above 50% higher than that of the porcelain and glass insulators. Therefore, under the same operating voltage, the creepage distance of the composite insulator only requires 2/3 of that of the porcelain and glass insulators. In the engineering design, the creepage distance of the composite insulator is normally taken as above 3/4 of that of the disc insulator.

Using the pollution withstand voltage method to design the configuration solution of composite insulators also requires pollutant component correction and

Table 28.10 Basic number of insulators of tension insulator strings on ±800 kV line at different altitudes

Pollution degree	Type of insulator	Number of insulators per string		
		Altitude of 1000 m	Altitude of 2000 m	Altitude of 2500 m
Lightly polluted area (0.05 mg/cm^2)	550 kN (Bell)	60/56	64/59	66/61
	550 kN (Tri-umbrella)	44/41	45/43	46/44
Moderately polluted area (0.08 mg/cm^2)	550 kN (Bell)	74/67	79/72	81/74
	550 kN (Tri-umbrella)	55/51	57/53	59/54
Severely polluted area (0.15 mg/cm^2)	550 kN (Bell)	85/74	90/79	93/82
	550 kN (Tri-umbrella)	73/64	76/67	78/68

Note The values on the left of "/" are the numbers with the northern climate characteristics considered, and those on the right are the numbers with the southern climate characteristics considered

Table 28.11 Basic number of insulators of tension insulator strings on ±1100 kV line at different altitudes

Pollution degree	Type of insulator	Number of insulators of each string
Lightly polluted area (0.05 mg/cm^2)	550 kN (Bell)	87/81
	550 kN (Tri-umbrella)	80/72
	840 kN (Bell)	77/70
Moderately polluted area (0.08 mg/cm^2)	550 kN (Bell)	103/92
	550 kN (Tri-umbrella)	98/79
	840 kN (Bell)	85/78
Severely polluted area (0.15 mg/cm^2)	550 kN (Bell)	113/102
	550 kN (Tri-umbrella)	103/95
	840 kN (Bell)	92/90

Note The values on the left of "/" are the numbers with the northern climate characteristics considered, and those on the right are the numbers with the southern climate characteristics considered

pollution non-uniform distribution correction just like the ceramic insulators. In addition, taking the conclusion of the report "*Research on the pollution discharge characteristics and high-altitude discharge coefficient of* ±800 kV *DC insulators*" presented by CEPRI as reference, the altitude correction coefficient of transmission line insulator is as follows: the composite insulators will be compensated by 6.4% with every 1000 m increase of altitude.

Table 28.12 Basic insulation configuration of ±800 kV DC composite insulators

Altitude (m)	Polluted area		
	Length of composite insulator string (m)/creepage distance (m)		
	Lightly polluted area (0.05 mg/cm^2)	Moderately polluted area (0.08 mg/cm^2)	Severely polluted area (0.15 mg/cm^2)
1000	9.6/36.9	9.6/36.9	10.6/40.8
1500	9.6/36.9	10.6/40.8	11.0/42.3
2000	10.6/40.8	10.6/40.8	11.8/45.4

Table 28.13 Basic insulation configuration of ±1100 kV DC composite insulators

Altitude (m)	Polluted area		
	Length of composite insulator string (m)/creepage distance (m)		
	Lightly polluted area (0.05 mg/cm^2)	Moderately polluted area (0.08 mg/cm^2)	Severely polluted area (0.15 mg/cm^2)
1000	12.3/50.4	12.3/50.4	13.9/56.9
2000	12.3/50.4	13.9/56.9	15.4/63.1
3000	13.9/56.9	15.4/63.1	16.6/68.0

The length and creepage distance of composite insulator strings used for ±800 kV DC line projects are shown in Table 28.12.

The length and creepage distance of composite insulator strings used for ±1100 kV DC Zhundong–East China DC transmission line project are shown in Table 28.13.

28.2.3.5 Check Based on Overvoltage Condition

The number of insulators and the length of insulator strings on the DC line are determined based on the pollution condition under the operating voltage and should also be checked based on the overvoltage condition. Currently, the calculation results of the switching overvoltage level of the Chinese ±800 kV DC lines are within 1.6–1.8 p.u. [1], while the calculated value of the switching overvoltage level of the ±1100 kV Zhundong–East China line is lower than 1.6 p.u.

The switching impulse flashover voltage of the polluted insulators on the DC line decreases with the increase of the pollution degree. The test carried out by America EPRI verified that, under the same pollution condition, the DC switching withstand voltage of insulator is 2.2–2.3 times the DC withstand voltage of the insulator of the same model. Furthermore, a large number of tests and researches demonstrate that, when the DC voltage is pre-applied, its 50% switching impulse voltage is 1.7–2.3 times the 50% pollution flashover operating voltage. Therefore, the switching overvoltage is not a control factor for the selection of the number of insulators.

Due to the pollution, the DC line has more insulators and longer insulator strings compared to the AC 1000 kV line; besides, it has a large insulation margin under the lightning impulse voltage and back flashover lightning current of over 200 kA. Therefore, the lightning overvoltage is not a control factor for the selection of the number of insulators.

28.2.4 Air Clearance of Tower Head

For the power transmission line, the determination of various air clearances of tower head is the basis for the determination of tower head dimension and the design of tower head structure. After the deflection by wind, the air clearance between conductor and tower member shall meet the requirements of operating voltage, switching overvoltage, and lightning overvoltage [1].

28.2.4.1 Influence of Various Overvoltages on Air Clearance

The maximum overvoltage of the UHVDC line often occurs at the midpoint of the non-faulty pole line when the ground fault occurs at the midpoint of the line, and the line's overvoltage level presents a decrease trend from the line's midpoint to the converter stations at both sides with a slight up and down.

The overvoltage distribution curve along the line is obtained through the electromagnetic transient calculation. The air clearances corresponding to different switching overvoltage multiples are listed according to the analysis of the overvoltage level. It is found that the air clearance increases as the switching overvoltage multiple increases and it is also related to the altitude at which the line is located.

With regard to the operation of the UHVDC line, since the DC converter valve acts fast, the time for restart is extremely short, basically without influence on the continuous operation of the line. Therefore, the influence of the lightning overvoltage is not considered in the clearance design of tower head, and the clearance controlling the tower head dimension is the switching overvoltage clearance.

28.2.4.2 Air Clearance of Tower Head

All the tangent towers along the UHVDC line adopt the V-type insulator strings. The operating voltage and lightning overvoltage do not play control effect on the tower head air clearance, while the switching overvoltage will directly affect the design of tower head. In the engineering design, it is necessary to carry out analysis and calculation in combination with the practical conditions of specific project, and the switching overvoltage multiple and air clearance, in particular, shall be determined based on the results of the scientific research and test organizations.

Table 28.14 Tower head air clearance of ±800 kV DC line (m)

Altitude (m)		500	1000	2000	3000	Remarks
Operating voltage		2.10	2.30	2.50	–	*Code for Designing of DC Transmission Line*
		2.10	2.30	2.50	2.85	Xiangjiaba–Shanghai Line, Jinping–South Jiangsu Line
		2.10	2.30	2.50	–	Xiluodu–Zhejiang Line, Hami–Zhengzhou Line
		2.55	2.70	3.05	–	Yunnan–Guangdong Line
Switching overvoltage	1.6 p.u.	4.90	5.30	5.90	–	*Code for Designing of DC Transmission Line*
	1.6 p.u.	5.30	5.70	6.40	7.10	Jinping–South Jiangsu Line
	1.6 p.u.	4.90	5.30	5.90	–	Xiluodu–Zhejiang Line, Hami–Zhengzhou Line
	1.7 p.u.	5.50	6.30	6.90	–	Xiangjiaba–Shanghai Line
	1.7 p.u.	5.50	5.55	6.20		Yunnan–Guangdong Line

Table 28.15 Recommended values for tower head air clearance of ±1100 kV DC line (m)

Altitude (m)	1000	2000	3000
Working overvoltage clearance (m)	3.2	3.7	4.2
Clearance S (m) when switching overvoltage is 1.5 p.u.	8.1	8.7	9.2
Clearance S (m) when switching overvoltage is 1.58 p.u.	8.9	9.5	9.9

Table 28.14 shows the values of the air clearance of several ±800 kV DC lines built in China and the comparison with the air clearances specified in the *Code for Designing of DC Transmission Line*. Table 28.15 lists the recommended values for the air clearance of the ±1100 kV Zhundong–East China DC line.

28.3 Design of Insulator Strings and Fittings of DC Line

28.3.1 Insulator String of Conductor

28.3.1.1 Suspension Insulator String of Conductor

The I-type strings and V-type strings are the suspension string types widely used on the UHV lines. When the V-type strings are used, the interpolar distance of the conductors on the DC line will be reduced, which can effectively reduce the corridor width and steel consumption of steel towers [4].

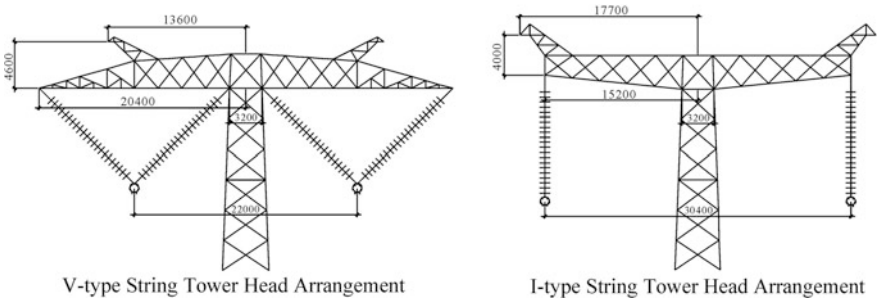

Fig. 28.5 Comparison of I-type string and V-type string tower heads of ±800 kV UHVDC line (mm)

The tower dimension of ±800 kV DC transmission line is large, occupies wide line corridor, and requires large amount of house demolition, so it is necessary to use tower type suitable for small corridor width. For the straight line towers using V-type insulator string, the interpolar distance of conductors can be reduced by about 8 m compared with that using I-type insulator strings, as shown in Fig. 28.5.

The V-type insulator strings have restriction to the offset of conductor. Although the cross arm of the conductor is longer than that of I-type string tower, the conductor point-to-tower body horizontal distance of V-type string tower is shorter than the I-type string tower. Therefore, its conductor load-to-tower body torque is smaller than the I-type string tower. For this reason, the use of V-type insulator string can reduce line corridor width, house demolition, tree felling, and project construction cost, and the consumption of steel by a single V-type string tower can reduce by 7–9% as compared with I-type string tower.

With identical insulation configuration, the suspension length of V-type string of ±800 kV DC transmission line will be 4 m shorter than I-type string. In other words, if identical span is used, the straight line tower with V-type string can lower the tower positioning height by 4 m as compared with I-type string. On the average, the straight line tower can further reduce the tower weight by about 2 tons. On the other hand, under the condition of same string length, the V-type string arrangement can effectively reduce the pollution flashover voltage of insulator strings. This provides good technical support to the safe operation of transmission line. Therefore, in the aspect of enhancing insulation, the use of V-type insulator string arrangement has significant superiority. In view of this, the straight line towers of UHVDC transmission lines that have been built or under construction in China all use V-type suspension insulator strings.

The value of included angle between two V-type suspension insulator strings has major influence on the tower head design. According to large amount research and design data collected in China and other countries, the included angle of V-type insulator strings is basically in the range of 70°–120°. In engineering design, the angle is generally selected as a half of V-type string included angle, and minus 5°–10° of the maximum calculated wind swing angle of I-type insulator strings.

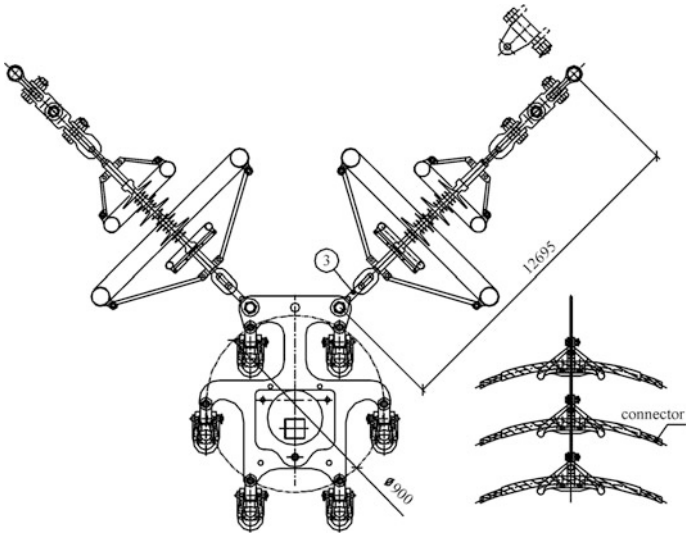

Fig. 28.6 Assembly diagram of single V-type suspension insulator strings for ±800 kV DC transmission lines (mm)

Composite insulators are mostly used for the conductor suspension insulator strings of DC transmission lines (except for transmission lines in heavy icing area) in China. The commonly used connection of composite insulator ends is the ball–bowl structure. Through operation investigation of the built EHV transmission lines, so far, several fall-off accidents of ball head or bowl head have occurred in conductor side of composite insulator in China. To effectively prevent the occurrence of similar problems, starting from Xiangjiaba–Shanghai DC transmission project, the ball head–bowl head connection structure has been reconstructed as ring–ring connection structure, thus the fall-off problems of ball head of the V-type composite insulator strings on the conductors have been solved well. Composite insulator V-type string assembly using ring–ring connection is shown in Fig. 28.6.

28.3.1.2 Conductor Tension Insulator String

Multiple bundle and large-section conductors are used for the UHV transmission lines, which have higher requirements on the mechanical strength of the conductor tension insulator strings. UHVDC transmission line generally uses six-bundle or eight-bundle conductors with sub-conductor section from 630 to 1250 mm^2. Therefore, insulators used for tension string are generally multiple columns of 550, 760, and 840 kN disc-type insulators. For example, triple 550 kN or double 760 kN insulators can be used for 6×JL/G3A-900/40 conductors, quadruple 550 kN insulators can be used for 6×JL/G3A-1250/70 conductors, and sextuple 550 kN or quadruple 840 kN insulators can be used for 8×JL1/G3A-1250/70 conductors.

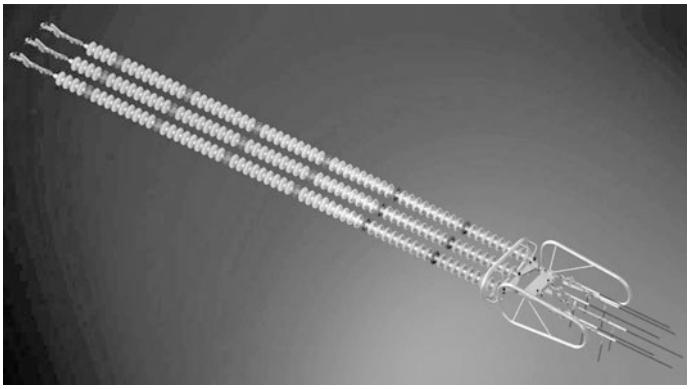

Fig. 28.7 Schematic of assembled typical six-bundle conductor with triple tension insulator strings for ±800 kV UHVDC line

A schematic of assembled typical six-bundle conductor with triple tension insulator strings is shown in Fig. 28.7.

28.3.1.3 Inter-string Spacing of Multiple Insulators

The inter-string spacing of multiple insulator strings will be determined by the electric field intensity distribution, pollution flashover voltage, and mechanical strength of the insulator strings to guarantee the electrical strength of insulator strings, and the inter-string insulators will not contact and collide with each other under operating condition.

In terms of the electrical property, according to the analysis on the results of the pollution withstand voltage test on the DC double insulator strings in high-altitude areas carried out by the scientific research organization, the parallel connection of double strings will increase the probability in flashover of the whole string. Under the heavy icing condition, the small inter-string distance will cause the ice and snow to fill the inter-string spacing, bridge the insulators, and reduce the icing withstand voltage of insulators.

In terms of the mechanical property, as the insulator string of the UHV transmission line is long, the insulator string offset caused by wind load shall also be considered in addition to the diameter of insulator disc when determining the inter-string distance, in order to guarantee that the two strings in parallel connection will have no collision.

The basic inter-string distance of 650 mm can be used for the suspension insulator string and tension insulator string of conductors on DC transmission line. When transmission line is heavy icing, the inter-string distance of multiple insulator strings should be properly increased. For Jinping–South Jiangsu and

Xiluodu–Zhejiang DC transmission line projects in the heavy icing area, 800 and 1000 mm inter-string distances are used for suspension insulator strings and tension insulator strings, respectively.

28.3.2 Selection of Main Fittings

28.3.2.1 Tower-Connecting Fittings

The tower-connecting fittings commonly used on the overhead lines include the UB-type clevises, U-type shackles, trunnion clevises, GD-type clevises. In previous projects, wear and break accidents occurred to UB-type clevises and U-type shackles connected with tower. Considering the importance of UHV transmission line, in order to avoid similar problems, it is recommended that UB-type clevises and U-type shackles no longer be used as tower connection fittings. It is recommended to use trunnion clevises and GD-type clevises to guarantee flexible rotation in each direction, and the clevises are shown, respectively, in Figs. 28.8 and 28.9.

Wearing should be considered for the top part connecting with tower, so the strength of the tower connection end should be higher than the real service strength and should be higher than the strength of other fittings in the string. Tower connection fittings are required to use overall forging method for manufacturing to provide sufficient guarantee in mechanical property.

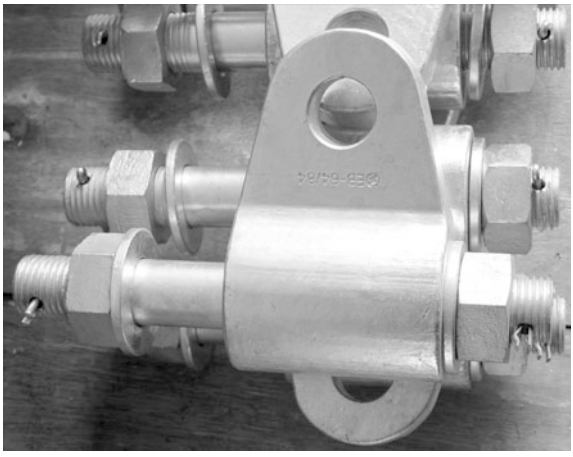

Fig. 28.8 Suspension string tower-connecting fittings-trunnion clevis

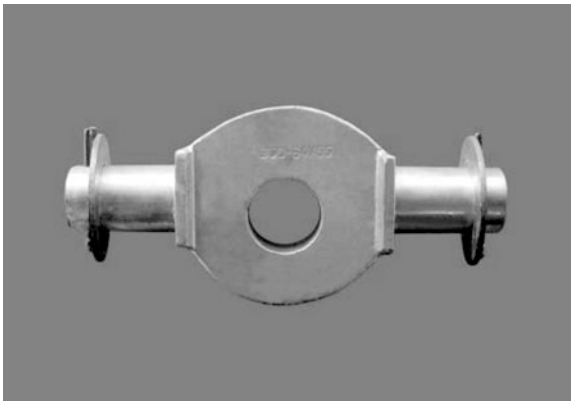

Fig. 28.9 Tension string tower-connecting fittings-GD clevis

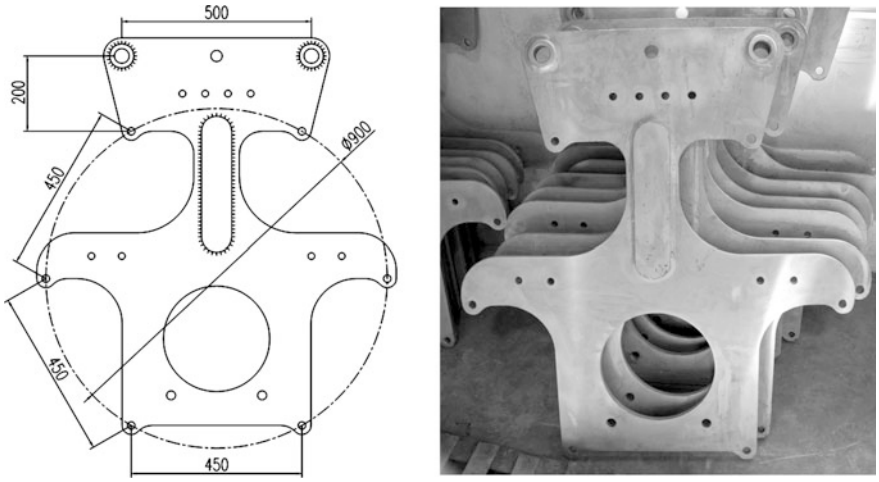

Fig. 28.10 Six-bundle integral suspension yoke plate for DC line (mm)

28.3.2.2 Suspension Yoke Plates

The yoke plates in the suspension string include two types, namely the integral yoke plate and combined yoke plate. Most of China's ±800 kV lines using six-bundled conductors basically use the integral yoke plates. In view of the design, manufacturing, construction, and installation, the application on the lines in the mountainous areas has no problem. The structure of the six-bundled integral yoke plate is shown in Fig. 28.10. The ±1100 kV line adopts the eight-bundled conductors with large section, increasing in the number of sub-conductors and load, which puts forward higher requirements on the manufacturing of the eight-bundled suspension yoke plates. For example, when the integral yoke plate structure design is adopted,

the weight of single piece will be above 300 kg, and the conditions for installation and transportation in mountainous areas need be fully considered.

28.4 Clearance of Conductor to Ground for DC Line

28.4.1 Minimum Clearance of Conductor to Ground

The DC transmission line's clearances of conductor to ground and conductor to the crossed facility are the key parameters for the design of line project. Not only is the normal insulation level need to be considered to meet the basic requirements of the large-capacity transmission, but also the influences of factors such as the electrostatic field intensity, total electric field intensity, and ion current density should be considered. The clearances of conductor to ground and conductor to the crossed facility used in the DC line design can be classified into three categories depending on the principles for value selection:

1. Clearances determined by electric field intensity

The ground electric field intensity and ion current density control values of UHVDC overhead transmission line are shown in Table 28.16.

The corona inception electric field intensity of conductors will reduce with the increase of altitude. Under the conditions of identical voltage, conductor and line structure dimension, the ground total electric field intensity, and ion current density will increase. In order to control the ground total electric field intensity and ion current density, pole conductor height should be properly increased. Under the condition of identical interpolar distance, the clearance of conductor to ground should be increased by 6% with every 1000 m increase of altitude.

2. Clearances determined by electrical insulation strength

This kind of distance refers to the distance determined by the discharge clearance of operating overvoltage.

Table 28.16 Total electric field intensity and ion current density limits

Place	Total electric field intensity (kV/m)		Ion current density (nA/m^2)	
	Fine day	Rainy day	Fine day	Rainy day
Residential area	25	30	80	100
General non-residential area	30	36	100	150
Sparsely populated non-agriculture cultivation area	35	42	150	180

Table 28.17 Clearance values of conductor to ground (m)

S/N	Area	±800 kV	±1100 kV	Calculation conditions
1	Residential area	21.0 (South of China)	30.0 (South of China)	Max. sag of conductor
		23.0 (North of China)	32.0 (North of China)	
2	Non-residential area	18.0 (South of China)	26.0 (South of China)	Max. sag of conductor
		20.0 (North of China)	28.0 (North of China)	
3	Area with poor traffic condition	15.5	21	Max. sag of conductor
4	Mountain slope accessible on foot	13.0	15.5	Max. wind deflection of conductor
5	(Net clearance for the) mountain slope, cliff and rock inaccessible on foot	11.0	13.5	Max. wind deflection of conductor

3. Clearances determined by other factors

This kind of distance is to avoid the influence of power transmission line on the facilities of other departments, and often use the values recognized by relevant organizations according to usual practice. In the current line design, the values have no relationship with voltage level.

At the altitude of 1000 m, the clearances of conductor to ground of the ±800 and ±1100 kV UHVDC lines adopting the V-type suspension insulator strings can be referred to the values as listed in Table 28.17.

28.4.2 Relation Between Clearance of Conductor to Ground and Environmental Climate

The air quality and humidity in the north and the south of China has large difference, which can produce significant influence on the ground total electric field of the DC transmission line; however, it is impossible to predict correctly by calculation at present. The research carried out by CEPRI based on Hami–Zhengzhou, Lingzhou–Shaoxing ±800 kV DC transmission line projects concludes that, for the transmission line project crossing the south and the north of China, because of large difference in climate, when the transmission line passes through residential area and

non-residential area, the minimum clearance of pole conductor to ground should be corrected according to environmental climate [5].

CEPRI carried out the full voltage test on electromagnetic environment of ±800 kV DC transmission line under different clearances of conductor to ground and different climate environments by using 6 × 720 and 6 × 900 mm^2 conductors, proposing the recommended correction value of environmental climate for the minimum clearance of conductor to ground of ±800 kV DC transmission line constructed in the south and north of China: the minimum clearance of pole conductor to ground in general areas, non-residential areas, and residential areas in the north should be increased by 11.1 and 9.5%, respectively, than that in the general areas in the south. For areas where dust absorption is serious, the minimum clearance of pole conductor to ground in residential areas and non-residential areas should be increased by 18.5 and 19.3%, respectively, as compared with that in general areas in the south.

28.5 Tower Design of DC Line

28.5.1 Tower Types of DC Line

Currently, all the UHVDC lines already built and under construction adopt the mode of bipolar single circuit. However, with increasing construction of UHVDC transmission projects, the transmission line has entered the coastal area in east China where economy is developed, residential buildings are densely concentrated, and road resources are urgently short of. The UHVDC project using the solution of double-circuit transmission line on the same tower shall also be implemented. The ±500 kV Jinmen–Fengjing transmission line of Gezhouba–Shanghai DC integrated reconstruction project put into operation in 2011 uses the solution of double-circuit transmission line on the same tower (as shown in Fig. 28.11). The construction of this transmission line has also provided a reference for UHVDC transmission line to use double-circuit transmission line on the same tower.

For viewing the tower types used for EHVDC and UHVDC transmission lines currently in China and other countries, iron towers are widely used. Depending on the construction form and stress characteristics, iron towers can be divided into two basic types: guyed tower and self-supporting tower, as shown in Fig. 28.12.

A guyed tower is light in weight, for which the steel consumption and construction cost can be reduced. This type of tower has mature experiences in mechanical analysis, processing and fabrication, tower erection, and wire installation. However, guyed towers occupy large area of land and can easily be restricted by terrain. A self-supporting tower has the advantages of small land area occupation, excellent rigidity, and suitable to various terrains. The first ±500 kV Gezhouba–Shanghai DC transmission line in China used large amount of guyed towers. At present, that line has been put out of service.

Fig. 28.11 Double-circuit DC line of ±500 kV Jinmen–Fengjing Project

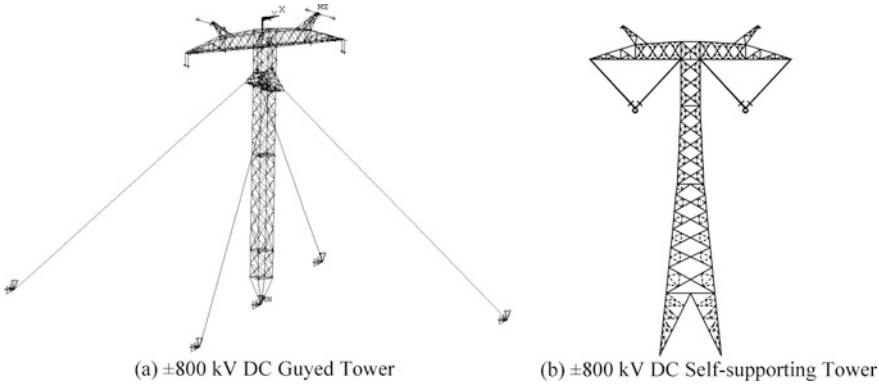

Fig. 28.12 ±800 kV DC tower types

Most of ±500 kV and above DC transmission lines in China use self-supporting towers. Depending on the functions, self-supporting towers can be divided into straight line tower, suspension angle tower, and tension angle tower.

The single-circuit DC transmission lines generally use T-type towers with bipolar conductor horizontally arranged. The straight line towers are subdivided into full "I"-string type and "V"-string type depending on the type of conductor suspension insulators. In economically developed area with crowded corridor and high corridor clearing cost, the tower type with bipolar conductor vertically

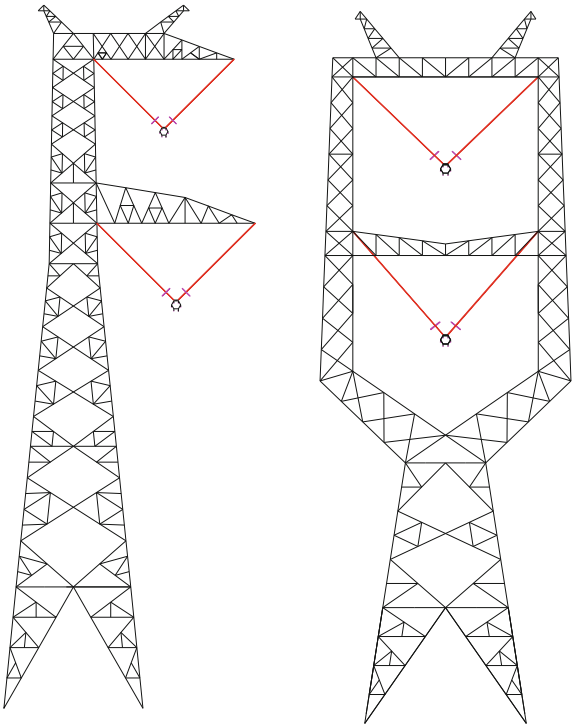

Fig. 28.13 Towers in vertical arrangement for conductors of UHVDC Line (*left* "F"-type tower; *right* cup-type tower)

arranged can also be used, like F-type tower and cup-type tower as shown in Fig. 28.13.

When a transmission line passes through a mountainous area with steep slope, the service height of tower can be easily controlled by the clearance of conductor to ground at the up-hill side, while the clearance of conductor to ground at the down-hill side is high and can easily suffer the shielding failure, so the new straight line tower with Z-type side slope can be used, which can reduce the clearance of conductor to ground at the down-hill side and the probability of shielding failure as compared with the conventional T-type tower. The T-type tower with horizontal cross arm and Z-type tower with step cross arm are shown in Fig. 28.14.

28.5.2 Structural Characteristics of Towers for DC Line

At present, the DC transmission lines mainly use bipolar self-supporting tower, as shown in Fig. 28.12b. Following will give an introduction to the design characteristics of straight line tower, straight line angle tower, and strain tower used for the DC transmission line.

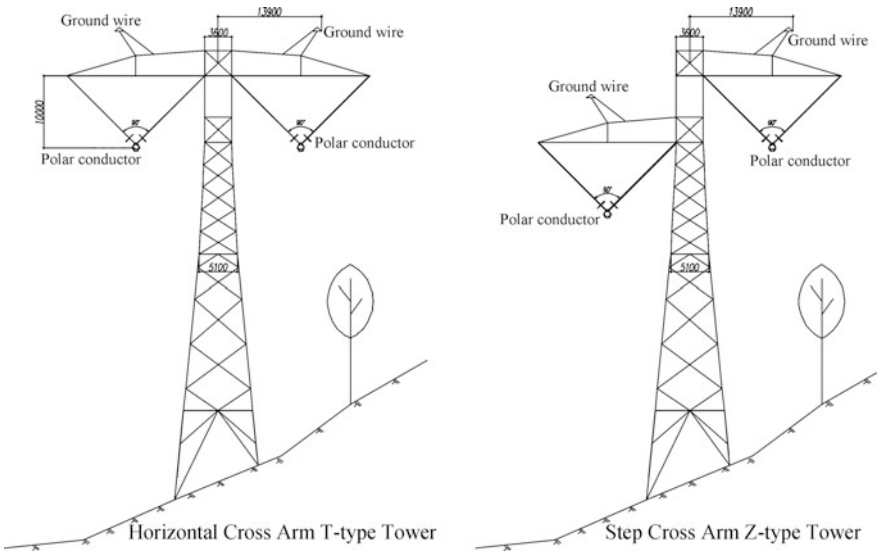

Fig. 28.14 Comparison of T-type tower with horizontal cross arm and Z-type side slope tower with step cross arm (mm)

For the straight line tower, the conductor attachment method determines the size of tower head. Since a single-circuit DC transmission tower has only two poles, the size of interpolar distance will directly affect the steel consumption of the tower and the width of line corridor. The interpolar distance approximately exhibits a linear relation with the tower weight. The tower weight will increase by about 3% with every 5% increase of interpolar distance. Minimization of the interpolar distance is a key for the horizontal arrangement of DC transmission line to control tower weight.

The straight line angle tower is mainly used in those towers where the line routing direction is changed in small angle. The angle is generally smaller than 20°. When compared with the tension angle tower, due to the releasing action to longitudinal unbalanced tensional force by attaching string, the consumption of foundation concrete and tower steel is relatively small, having significant advantage. The L-type strings are generally used on the straight line angle tower, as shown in Fig. 28.15.

The "干"-shaped strain tower is the most commonly used type of bipolar DC strain tower. Because the tension string of ±800 kV DC strain tower has a long length and the jumper can be as long as 40 m or above, the commonly used flexible jumper or I-string rigid jumper are bound to cause the increase in tower height and cross arm length due to jumper sag and wind swing, thus causing poor economic efficiency. For this reason, the V-type string shall be used for attaching the jumper string of strain tower, as shown in Fig. 28.16.

Fig. 28.15 L-type string straight line angle tower

Fig. 28.16 Type of "干"-shaped strain tower

28.5.3 Tower Load and Combination

All kinds of towers shall be calculated according to the load under normal operating condition (including basic wind speed and maximum icing), non-uniform ice load condition, disconnection condition, and installation condition. Check calculation shall be carried out for all types of rare cases that may possibly occur. In view of the importance of UHV transmission project, the importance factor γ_0 of tower structure is taken as 1.1 in all cases except for the installation condition where γ_0 is taken as 1.0.

28.5.4 Tower Materials of DC Line

The primary members of the pole and tower for power transmission line are angle steel and steel tube. Most of angle steel materials are Q235B, Q345B, and Q420B,

and most of steel tube materials are Q235B and Q345B. Compared with angle steel tower, because the drag factor of steel tube member is small, the wind load of steel tube tower body can be reduced, saving tower material, and reducing the acting force of tower on foundation. In addition, the section of steel tube members is biaxial symmetric section, having advantages of high bending rigidity and high overload resistant capacity. However, the steel tube tower is relatively difficult for fabrication and requires large amount of welding and long fabrication period. In addition, the unit weight is high and the transportation and assembly is difficult for transmission line in mountainous area.

Because the DC power transmission tower has only bipolar conductors, the load of primary members of tower will be greatly reduced as compared with the UHVAC power transmission line. The use of large size angle steel or conventional combined angle steel can meet the requirement of load bearing capacity. In view of the advantages of angle steel tower in manufacturing and construction, it is recommended to use angle steel tower for the DC power transmission line.

Large size angle steel is named mainly in contrast to conventional angle steel. The limb width of conventional equal-sided angle steel is 200 mm while the limb width of large size angle steel reaches 220 and 250 mm, with wall thickness in the range of 16–30 mm. The section bending rigidity of large size angle steel is greatly improved as compared with the conventional angle steel. The bearing capacity of primary members of tower body is controlled mainly by the section area of members. If the section and slenderness ratio of the two members are equivalent, the load bearing capacity of the two members is basically the same. Except for L200 × 24 of double-limb combined angle steel, other types can find large size angle steel with equivalent section area. Using large size angle steel as primary members avoids the connection filler plates for primary members of combined angle steel. At the same time, there is no need to consider the reduction problem of bearing capacity for the primary members of combined angle steel. The weight of large size angle steel tower is about 5–7% lighter than the conventional combination angle tower. The types of angle steel sections are shown in Fig. 28.17.

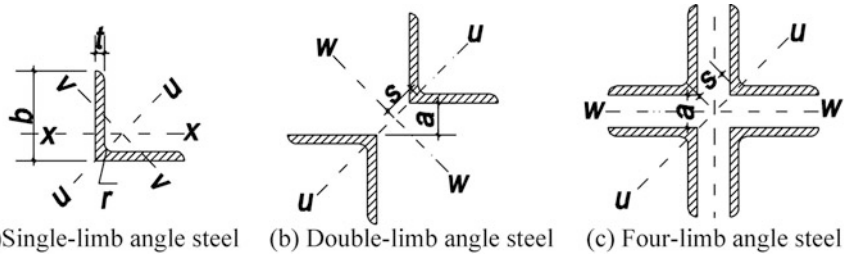

Fig. 28.17 Types of angle steel sections

28.5.5 Issues to Be Noticed in Tower Design

28.5.5.1 Reduction Hole Number of Large Size Angle Steel

For angle steel members controlled by tensile strength, due to section weakening by screwed hole, the impact of reduction hole number must be considered in the check calculation of section strength. The large size angle steel can have double-row or three-row screwed holes as required. The corresponding saw-tooth breaking sections are shown in Figs. 28.18 and 28.19. For the reduction hole number of angle steel, the maximum value of reduction hole number shall be calculated with the breaking sections.

The trial calculation is performed according to the equivalent area principle [6]. When double-row screwed holes are opened for large size angle steel, the reduction hole number is taken as 2.6. When three-row screwed holes are opened, the reduction hole number will be taken as 3.7. It can be seen that when three-row screwed holes are opened, the section of rod member will be seriously weakened. For tie rod, use of the reduction hole number shall be avoided.

28.5.5.2 Compression-Stabilized Bearing Capacity of Primary Members of Combined Angle Steel

In the past, when compression-stabilized bearing capacity was calculated for double-limb and four-limb combination sections as shown in Fig. 28.17b, c, the stabilized bearing capacity was calculated according to the solid-web members when the filler plate spacing is less than 40 i (i is the minimum rotary radius of single-limb angle steel) and the number of filler plate between every two lateral support points of primary members is not less than 2. However, the above rule is

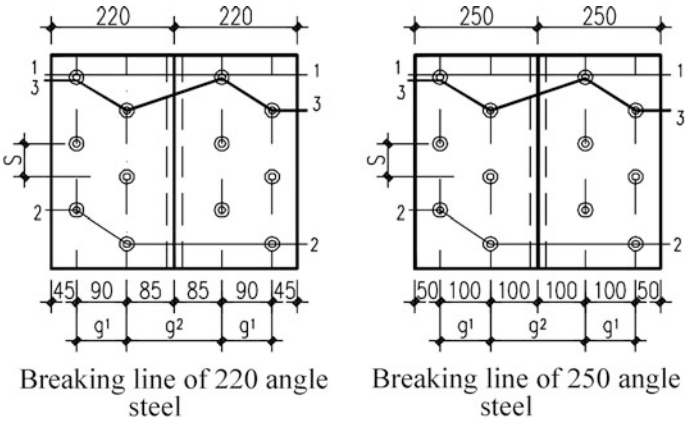

Fig. 28.18 Double-row screwed holes opened for large size angle steel (mm)

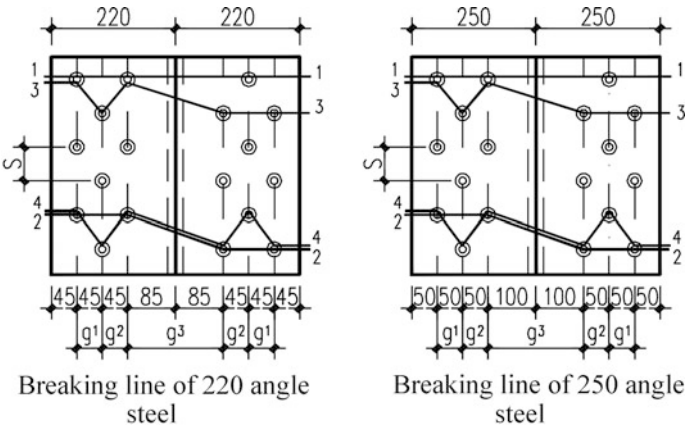

Fig. 28.19 Three-row screwed holes opened for large size angle steel (mm)

only applicable to the case where the filler plates and combined angle steel are welded or riveted together. For the primary members of angle steel tower connected with common bolts, the sliding of bolt connection will lead to uneven limb stress causing the primary members unable to reach the bearing capacity of solid-web rod, which has been demonstrated by full-scale tower test [7].

With reference to the calculation equation for the slenderness ratio of the latticed members as specified in the *Code for Design of Steel Structures*, it is recommended that the influence of combination slenderness ratio should be considered in the calculation of stabilized bearing capacity of combined angle steel members. The calculation equation is as follows:

$$\text{Double-limb angle steel}: \lambda = \sqrt{\lambda_{\mathrm{w}}^2 + \lambda_{\mathrm{v}}^2} \tag{28.6}$$

$$\text{Four-limb angle steel}: \lambda = \sqrt{\lambda_{\mathrm{w}}^2 + \lambda_{\mathrm{x}}^2} \tag{28.7}$$

where

λ_{w} the slenderness ratio of whole length member to axis *w*;
λ_{v} the slenderness ratio of single-limb angle steel to smallest axis;
λ_{x} the slenderness ratio of single-limb angle steel to parallel axis.

The calculated length will be the bolt spacing at the edge of filler plate.

28.5.5.3 Geometric Non-linearity Analysis of DC Transmission Tower

At present, most of the transmission tower calculations use linearity calculation method, namely when calculating the internal force of structure, the influence of

tower deformation is not considered. On the DC transmission tower, the interpolar distance is large, and the tower cross arm is relatively long. In addition, external load is mainly applied on the top of tower. Therefore, it is necessary to consider the influence of geometric deformation on the internal force of a member.

According to the geometric non-linear analysis on several tower types and the comparison with linearity calculation results, both the bending rigidity and twist rigidity of tower are satisfactory and are able to meet the resistance-to-deformation requirement as required by *Code for Designing of DC Transmission Line*. When compared with linearity calculation results and by referring to geometric non-linearity, the section stress ratio of primary members of cross arm and tower body has no obvious change, and is less than 5%. Therefore, the influence of non-linear effect can be neglected. However, the non-stressed auxiliary material in the reinforcement surface in the linearity calculation becomes stressed material in the non-linearity calculation. Increase of internal force of members and cross diagonal member subjecting to press at the same time will happen to the tower diagonal members, especially the diagonal members on varying slopes during the non-linearity calculation, which leads to diagonal member unable to provide effective support to the primary members of tower body. Sufficient attention should be given to this in tower design.

28.6 Foundation Design for DC Line

28.6.1 Common Foundation Types

Presently, the foundation types commonly used for the towers along the DC line mainly include excavated and backfilled foundation, undisturbed soil foundation, rock foundation, pile foundation, and other new foundations.

The heavily excavated and backfilled foundation mainly include flexible plate extension foundation, rigid foundation, and combined foundation. At present, the excavation and backfill soil foundation commonly used in power transmission line projects includes rigid foundation and flexible plate extension foundation.

The undisturbed soil foundation mainly includes excavated foundation, pile foundation, and rock foundation. Due to reduction of disturbances on undisturbed soil, the load bearing capacity of foundation soil can be given full play, and the foundation materials and construction cost can be greatly reduced, resulting in wide application in power transmission projects.

The rock foundation is applicable to tower with shallow covering layer, low rock weathering extent, and good completeness. This type of foundation gives full play the mechanical property of rock and reduces greatly the consumption of foundation material. Especially in high mountain areas where transport is difficult, this type of foundation is of obvious economic advantage. The rock foundation includes rock anchor rod foundation, rock built-in foundation.

The pile foundation is a deep foundation, mainly used in the place where the geological condition is poor and the foundation acting force is relatively large. At present, the pile foundation used for iron towers of power transmission line is mainly bored pile foundation and manually excavated pile foundation. Besides, the mini-pile (known as tree root pile) is a new pile foundation type. Due to its higher load bearing capacity, under identical load and geological condition, the mini-pile foundation used for straight line tower can save construction cost by about 20% as compared with the bored pile foundation commonly used in soft soil groundwork, about 35% as compared with the angle tower foundation [8], so it is a foundation type worthy to be promoted.

28.6.2 Issues to Be Noticed in Foundation Design

28.6.2.1 Application of High Strength Anchor Bolts

Anchor bolts or insertion type angle steel is usually used for the connection of the DC transmission tower with foundation. Anchor bolt connection has the advantage of simple and convenient construction and good maintainability. The commonly used anchor bolt number is 4 and 8. With the increase of uplift load of tower, the load bearing capacity requirement can be met by increasing the number of anchor bolts and improving the grade of anchor bolts.

At present, the anchor bolt materials commonly used for iron towers of power transmission lines include the following types: (1) Q235B grade anchor bolts: bolt size is M24–M72; design load bearing capacity of single bolt being 50.77–518.1 kN; (2) 35# anchor bolts: bolt size is M30–M72; design load bearing capacity of single bolt being 96.65–615.25 kN; and (3) 45# anchor bolts: bolt size is M30–M72; design load bearing capacity of single bolt being 109.37–696.2 kN.

The maximum uplift force of the DC power transmission tower has exceeded 6000 kN. Although increasing the number of anchor bolts can provide higher load bearing capacity, the 12- and 16-anchor bolt arrangement is very complicated, the material consumption is high, and the installation difficulty is also high. The use of high strength anchor bolts can avoid the aforementioned problem.

The design tensile strength of 42CrMo high strength anchor bolt is 300 N/mm^2 and the bolt size is M30–M72. The design load bearing capacity of single anchor bolt is 190.8–971.4 kN. Use of M72 bolts can meet the uplift load bearing capacity requirement of the DC transmission tower. This type of anchor bolt has been widely used in the DC tower design.

28.6.2.2 Calculation of Uplift Bearing Capacity for Dug Foundation and Manual-Excavated Pile Foundation

The uplift bearing capacity of dug foundation will be calculated by using shearing method [9]. This method is applicable to the foundation of which the depth-to-width ratio H/D is less than 4, meeting the assumption of rigid short piles. Manual-excavated pile foundation is generally designed according to *Technical Code for Building Pile Foundations* (JGJ94-2008). The two methods differ greatly. The embedded depth of foundation and corresponding depth-to-width ratio (H/D) increases with the increase of load. At this point, the foundation gradually exhibits the characteristics of elastic pile. When $\alpha l > 2.5$, the ultimate failure mode under the joint action of foundation and soil cannot simply use the soil failure mode of shallow foundation under the action of ultimate load. The design philosophy has been developing in the direction relating to the failure mode and pile operating behavior.

For different depth-to-width ratio conditions (identical bottom diameter and different embedded depth is taken in calculation), calculation is made using professional geotechnical finite element software Plaxis. The calculation results under the action of uplift load are shown in Fig. 28.20. It can be known from figure that with the increase of depth-to-width ratio, the influence scope of soil mass displacement reduces gradually, the failure mode becomes gradually from inverted circular truncated cone mode to vertical cylindrical slip surface mode, then local failure mode. The critical depth-to-width ratio is near $H/D = 4$. For the case where depth-to-width ratio $H/D > 4$, the conventional design method of rigid short pile bearing capacity is no longer able to meet the requirements of practical engineering design.

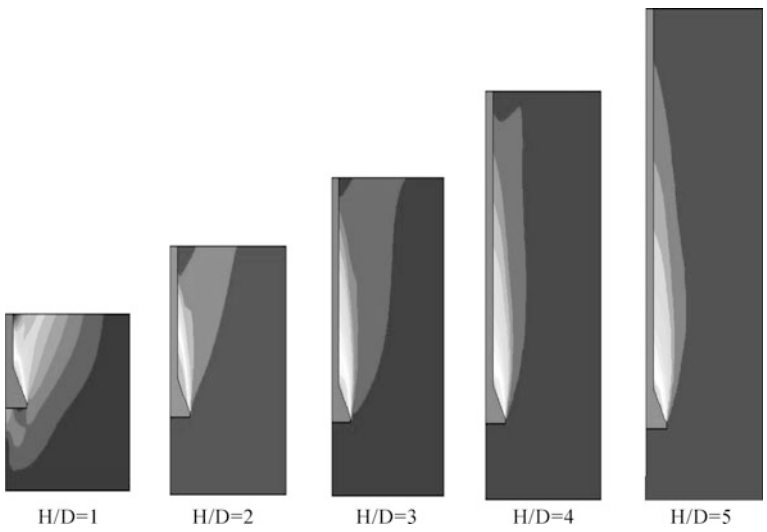

Fig. 28.20 Uplift calculation and comparison of foundations with different depth-to-width ratios

The model test shows that, in saturated (or non-saturated) silty soil foundation, the increase of embedded depth of foundation will lead to rapid increase of ultimate uplift bearing capacity of foundation. When the depth-to-width ratio H/D = 1–3, the calculation method recommended by standard (DL/T 5219-2005) *Technical Regulation for Designing Foundation of Overhead Transmission Line* can apply. When the depth-to-width ratio H/D = 5, the failure mode is similar to the failure mode assumed in (JGJ94-2008) *Code for Design of Building Pile Foundations*. The calculation can be made by referring to pile foundation design method.

28.6.2.3 Calculation of Uplift Bearing Capacity of Rock Bolt Foundation

Most of the rock bolt foundations used for transmission line are full-length bounded non-pre-stressed anchor rod foundations. They have the advantages of simple structure and convenient construction. They can use plain steel bars or deformed steel bars as the anchor rod body, which are poured into the bore-hole of rock layer using mortar with strength no less than 25 MPa. The mortar and rod jointly form the anchorage bolted in the rock. When the full-length bounded anchor rod is bearing the uplift force, there may be four failure modes:

1. the anchor rod body is pulled break off;
2. the holding force between rod and mortar is not sufficient, and the rod is pulled out;
3. there is not enough bonding force and friction force between the anchorage and rock layer. The anchorage is pulled out as a whole;
4. the rock has no enough shear-bearing capacity, and failure occurs along the inverted cone failure face.

It is found through calculation that it is usually the third failure mode that plays the control function. Calculation of this failure mode involves in selection of effective anchorage depth of anchor rod. However, at present, how to select the value of effective anchorage depth of anchor rod has no unified conclusion. There is no definite reference value in *Technical Regulation for Designing Foundation of Overhead Transmission Line* [9]. This causes a certain difficulty to the design.

Large amount of tests show that the rock anchor rod has basically no anchoring force distribution below the depth of 15–20 times the anchorage diameter. The anchoring force can only extend toward the depth when failure occurs to the rock around the top of anchor rod. This shallow stress transmission phenomenon is mainly caused by the inconsistent elastic characteristic values of anchor rod, mortar, and rock layer.

When the anchor rod is uplifted, the anchoring force is not uniformly distributed along the anchorage depth. On the contrary, the stress concentrates on the anchoring end close to the bottom of cushion cap. With the continuous increase of stress, the bond between the anchorage and the rock layer is gradually disjointed starting from

the anchoring end close to the bottom of cushion cap, and the anchoring stress develops toward the depth along the interface. With the decrease of anchoring stress, the uplift resistance of anchor rod is not directly proportional to the anchorage depth, and the failure occurs. It can be concluded that the excessive increase in the anchorage depth cannot increase the uplift resistance of anchor rod well.

Therefore, in order to guarantee that the anchor rod anchorage is safe and reliable so that the theoretical calculation result is basically consistent with the anchoring stress condition and the degree of safety required in the design is satisfied, the anchorage depth used in the design shall not exceed 15–20 times the anchorage diameter. When the calculation anchorage depth exceeds the upper limit value, such technical measures as improving the rock quality in the anchored section (for example, consolidation grouting) and expanding the anchorage diameter should be adopted to solve the problem. Also the anchorage depth shall not be less than the lower limit value (3.0 m) to avoid the case that the anchor rod is pulled out due to excessively shallow anchorage depth when the local strength of rock decreases or adverse combination structure plane exists.

28.6.3 Treatment Measures for Foundations Under Special Geological Conditions

As the UHVDC line is long in transmission distance and large in regional span, the line foundations are characterized by dispersion, independence, complexity, difficulty in transportation, etc. The unfavorable geological sections, such as the collapsible loess regions, liquefied subgrade, saline soil, worked-out section, eolian sand geology, gobi desert, karst geology, expansive soil, landslide, collapse, and gully, will exist along the line inevitably. The proper treatment of the line foundations under these geological conditions is very important to ensure the safe construction and reliable operation of the project.

When the line passes through the collapsible loess regions, the tower shall not be erected on the collapsible loess subgrade as far as possible. If it is unavoidable, the tower shall be erected at a place without water catchment, away from the irrigable land, water catchment area, gully, ponor, etc., and with smooth drainage as far as possible. If it is still unavoidable, the subgrade treatment measures shall be taken. As the subsidence of the collapsible loess results from being soaked in water, the treatment measures shall be focused on waterproofing and proper drainage of water shall be provided at the tower positions to prevent the subgrade soil from being eroded by water. When the waterproof treatment cannot meet the requirements, the corresponding subgrade treatment measures can be taken. Generally, the lime-soil cushion will be applied.

When the line passes through the regions with seismic intensity of 7° and above, where the field is of saturated sand soil and saturated silty soil, the possibility in subgrade liquefaction must be considered, and the necessary anti-seismic measures

shall be taken to stabilize the subgrade or foundation. When the liquefiable soil layer or soft soil layer is not large in thickness and its distance to the ground is small, it may be completely or partially removed and then backfilled with artificially compacted materials, such as coarse sand, gravels, rubbles, mineral slags, lime soil, clayey soil, or other non-erosive materials with stable properties; for the liquefiable layer with large thickness and deep burial depth, the bored piles are generally adopted to eliminate the influence on the foundation by the liquefiable soil layer.

The foundations of the transmission line are made of reinforced concrete. For the steel tower foundations located in the saline soil area, the salt solution will penetrate into the concrete foundation through the pore in the concrete or the capillary action. The harmful ion in the salt solution will cause electrochemical corrosion to the rebars. With the increase in the rust volume, the internal stress of the concrete will increase, and the longitudinal cracks will develop toward the direction of the main rebars, causing damage to the structure. In the saline soil corroded area, the grade of the foundation concrete need be appropriately enhanced to provide proper anti-corrosion protection for the foundation. At the tower positions where strong corrosion and liquefaction exist, the body-enwrapped bored piles shall be adopted for the foundation. Generally, the waterproofing geotechnical materials are used to enwrap the pile body to isolate the pile body materials from the surrounding soil and water to prevent corrosion.

For the DC line in the eolian sand areas, in consideration of the particularity of the eolian sand geological condition in desert, the sand soil is relatively loose and the undisturbed soil foundations shall not be adopted. The excavated foundations are recommended and commonly include the fabricated foundation, rigged stepped foundation, and flexible spread foundation. For the tower positions that may be subject to wind erosion, the straw checkerboards, gravel covering or gravel grid, and other sand fixation measures shall also be taken.

For the expansive soil, it is appropriate to mainly consider that the burial depth of foundation shall be larger than the depth of climate influenced markedly layer. Meanwhile, the drainage facilities shall be provided, and measurements of anti-seepage shall be taken on the bottom of the intercepting ditch and drainage ditch at the periphery of the tower foundation. These facilities can prevent the rainwater and surface water, etc., produced during the construction and operation from penetrating into the subgrade and eliminate the influence of expansive soil.

28.6.4 Mechanical Construction of Foundations

With the large-scale construction of the UHV line projects, the mechanical operation for the foundation construction will become more and more widely used. Compared to the traditional manual operation, the mechanical operation's advantages in such aspects as the construction efficiency and safety are increasingly prominent. The key of the mechanical foundation design is the close combination of the design proposal and the construction equipment based on the construction

capability of the existing equipment. The traffic and site conditions at the tower positions and the organic combination of the design and the construction and the construction equipment and the construction technology shall be focused on.

During the engineering design, the construction machinery applicable under different geological and topographic conditions shall be proposed based on the survey of the foundation construction machinery. For example, the medium-sized rotary drilling rig or mechanical Luoyang shovel may be applied to form holes on the excavated foundation or bored foundation in the plain and hilly areas with flat land and convenient transportation; the excavator may be applied to excavate the foundation pit of the heavily excavated foundation; while the portable drilling rig may be applied to conduct the bolt drilling construction for the rock bolt foundation in the mountainous area.

References

1. China Electricity Council. GB50790-2013. Code for designing of ±800 kV DC overhead transmission line. 2013.
2. Southwest Electric Power Design Institute Co., Ltd. of China Power Engineering Consulting Group Corporation. General specifications for preliminary line design of Lingzhou-Shaoxing ±800 kV UHVDC transmission line project. 2013-6.
3. Jiangsu Electric Power Design Institute, etc. Special report on conductor and ground wire selection research of Zhundong-East China ±1100 kV UHVDC transmission line project. 2016-1.
4. Technical Guide for HVDC Overhead Transmission Lines. DL/T 436-2005. Technical guide for HVDC overhead transmission lines. 2005.
5. Hunan Electric Power Design Institute, etc. Special report on insulation coordination and air clearance research of Zhundong-East China ±1100 kV UHVDC transmission line project. 2016-1.
6. Southwest Electric Power Design Institute Co., Ltd. of China Power Engineering Consulting Group Corporation, et al. DL/T5154-2012. Technical code for the design of tower and pole structures of overhead transmission line. 2012.
7. Yong G, Jianguo S, Jianguo Y. Stability analysis on the multiple angle members of transmission towers. Steel Struct. 2012;27(1):11–6.
8. Northwest Electric Power Design Institute Co., Ltd. of China Power Engineering Consulting Group Corporation. Special report on foundation type selection and design optimization research of Xiluodu-West Zhejiang ±800 kV UHVDC transmission line project. 2012-2.
9. Northeast Electric Power Design Institute Co., Ltd. of China Power Engineering Consulting Group Corporation, et al. DL/T 5219-2005. Technical regulation for designing foundation of overhead transmission line. 2005.